PHYSICS OF ATOMS AND MOLECULES

B.H. BRANSDEN
AND
C.J. JOACHAIN

Physics of atoms and molecules

Physics of atoms and molecules

B. H. Bransden and C. J. Joachain

Longman
London and New York

Longman Group Limited
Longman House, Burnt Mill, Harlow
Essex CM20 2JE, England
Associated companies throughout the world

Published in the United States of America
by Longman Inc., New York

First published 1983
Reprinted 1984

British Library Cataloguing in Publication Data

Bransden, Brian Harold
Physics of atoms and molecules.
1. Atoms
2. Molecules
I. Title II. Joachain, Charles Jean
539 QC173 80-41903

ISBN 0-582-44401-2

Printed in Hong Kong by
Wing King Tong Co. Ltd

To Pauline, Halina, Philippe and Hélène

Contents

Preface

Modern undergraduate courses in physics invariably include a good deal of material on basic atomic physics, including discussions of atomic structure, the optical and X-ray spectra of atoms, the interaction of atoms with electric and magnetic fields, the theory of simple molecules and some atomic scattering theory. As a rule, part of this material is given in a course on quantum mechanics, and some separately. Correspondingly, most books on quantum mechanics deal with some of these topics, usually in a rather sketchy fashion, while texts on 'Atomic Spectra', 'Collision Theory' and the like, deal with individual topics at considerably greater length than the undergraduate requires.

The aim of this book is to present a unified account of the physics of atoms and molecules, from a modern viewpoint, in adequate detail, but keeping within the undergraduate framework. It is based on courses given by the authors at the Universities of Durham, Glasgow, California (Berkeley), Brussels and Louvain-la-Neuve, and is suitable for study at second or third year level of an undergraduate course following some study of elementary quantum theory.

Following a brief historical introduction in Chapter 1, Chapter 2 contains an outline of the ideas and approximation methods of quantum mechanics, which are used later in the book. This is in no sense intended as a substitute for a proper study of quantum mechanics, but serves to establish notation and as a convenient summary of results. In Chapters 3 to 8, the structure of atoms and the interaction of atoms with radiation are discussed, followed in Chapters 9 and 10 by an account of the structure and spectra of molecules. Selected topics dealing with the scattering of electrons by atoms, and of atoms by atoms, are given in Chapters 11 to 13 while in the final chapter, a few of the many important applications of atomic physics are considered. Various special topics and derivations are given in the appendices together with useful tables of units. For a full understanding, the reader should work through the problems given at the end of the chapters. Hints at the solutions of selected problems are given at the end of the book.

We wish to thank our colleagues and students for numerous helpful discussions and suggestions. It is also a pleasure to thank Mme E. Péan and Mrs M. Raine for their patient and careful typing of the manuscript.

B. H. Bransden, Durham
C. J. Joachain, Brussels
July 1980

1 Electrons, photons and atoms

The physics of atoms and molecules which constitutes the subject matter of this book rests on a long history of discoveries, both experimental and theoretical. A complete account of the historical development of atomic and molecular physics lies far outside the scope of this volume. Nevertheless, it is important to recognise the key steps which have occurred in this evolution. In the present chapter we shall briefly describe the major experiments and discuss the basic theoretical concepts which are at the root of modern atomic and molecular physics.

1.1 THE ATOMIC NATURE OF MATTER

The first recorded speculations as to whether matter is continuous, or is composed of discrete particles, were made by the Greek philosophers. In particular, following ideas of Anaxagoras (500–428 BC) and Empedocles (484–424 BC), Leucippus (*circa* 450 BC) and his pupil Democritus (460–370 BC) argued that the universe consists of empty space and of indivisible particles, the *atoms* [1], differing from each other in form, position and arrangement. The atomic hypothesis, however, was rejected by Aristotle (384–322 BC) who strongly supported the concept of the continuity of matter.

In modern times, the question was re-opened following the experimental discovery of the gas laws by R. Boyle in 1662, and the interpretation of these laws in terms of a kinetic model by D. Bernoulli in 1738. The kinetic theory of gases developed throughout the nineteenth century, notably by R. Clausius, J. C. Maxwell and L. Boltzmann, was able to explain the physical properties of gases by assuming that:

1. A gas consists of a large number of particles called *molecules* which make elastic collisions with each other and with the walls of the container.
2. The molecules of a particular substance are all identical and are small compared with the distances that separate them.

[1] The Greek word '*atomos*' (atom) means 'indivisible'.

3. The temperature of a gas is proportional to the average kinetic energy of the molecules.

In parallel with the development of the kinetic theory, the laws of chemical combination were being discovered, which again could be interpreted by making hypotheses about the atomic nature of matter. In 1801, J. L. Proust formulated the law of definite proportions which states that when chemical elements combine to form a given compound, the proportion by weight of each element is always the same. This was followed in 1807 by J. Dalton's law of multiple proportions, according to which when two elements combine in different ways, to form different compounds, then for a fixed weight of one element, the weights of the other element are in the ratio of small integers. These laws were explained by Dalton in 1808, who made the hypothesis that the elements are composed of discrete atoms. For a given element these atoms are all identical and each atom has the same weight. Compounds are formed when atoms of different elements combine in a simple ratio.

Also in 1808, J. L. Gay-Lussac discovered that when two gases combine to form a third, the volumes are in the ratio of simple integers. This result was explained by A. Avogadro in 1811. He was the first to make a clear distinction between atoms, the discrete particles of the elements, and molecules, which are the discrete particles of compounds, composed of two or more atoms bound together. Avogadro was able to show that the Gay-Lussac law is satisfied if equal volumes of different gases, at the same pressure and temperature, contain equal numbers of molecules.

It is interesting that the atomic explanation of chemistry was not fully accepted until late in the nineteenth century [2], largely because chemists tended to ignore the compelling evidence from kinetic theory [3]. In addition to the properties of gases, the kinetic theory was able to explain other phenomena, for example the random motion of small particles suspended in a fluid. This motion, discovered by R. Brown in 1827, is due to the collisions of the molecules of the fluid with the suspended particles.

From the chemical laws the relative weights of atoms can be established. Originally, Dalton proposed a scale in which hydrogen was given, by definition, the atomic weight 1. Later, this was superseded by a scale in which naturally occurring oxygen was assigned the atomic weight 16. On this scale, known as the *chemical scale*, atomic hydrogen has the atomic weight 1.008.

A *mole* is defined as a quantity of a substance weighing μ grams, where μ is the atomic (or molecular) weight of that substance. *Avogadro's number* N_A is the number of atoms (or molecules) in one mole of any substance. The first estimate of N_A was made by J. Loschmidt in 1865. In fact, N_A can be found in several ways, one of the most interesting being from observations of Brownian motion.

[2] The nineteenth-century controversies are described in an interesting book by Knight (1967), while a collection of original papers covering the early history of the atomic theory, translated into English, has been given by Borse and Motz (1966).

[3] An account of the kinetic theory and its applications can be found in the text by Morse (1966).

The number deduced in this way in 1907 by J. Perrin, who performed experiments on the motion of suspended particles, was close to the best modern value of

$$N_A = 6.022 \times 10^{23} \text{ mole}^{-1} \quad [1.1]$$

1.2 THE ELECTRON

The first experimental evidence that electric charge was not infinitely divisible, but existed in discrete units, was obtained by M. Faraday, who discovered the *laws of electrolysis* in 1833. In his experiments Faraday passed a current through conducting (electrolytic) solutions of chemical compounds. He found that the mass M of a substance (for example, hydrogen, oxygen or metals) liberated at an electrode during a certain time interval was proportional to the quantity of electricity, Q, passed through the solution during that time. He also found that a given quantity of electricity always liberated the same mass of a given substance, and that this mass was proportional to the equivalent weight of the substance, where the equivalent weight is defined as the atomic (or molecular) weight μ divided by the valency v. Faraday's laws of electrolysis can be summarised by the formula:

$$M = \frac{Q}{F}\frac{\mu}{v} \quad [1.2]$$

where F is a constant called *Faraday's constant*. Its value in SI units is given by:

$$F = 9.648\,46 \times 10^4 \text{ coulombs/mole} \quad [1.3]$$

Thus, since $M = \mu$ grams for one mole, we see from [1.2] and [1.3] that it takes 96 484.6 C (sometimes called one Faraday) to liberate for example 1.008 g of hydrogen, 107.9 g of silver, 23 g of sodium, 35.5 g of chlorine (which are all monovalent), 8 g of oxygen (having a valency of 2) and so on.

Faraday interpreted his results by assuming that a given amount of electricity is carried by each atom (or group of atoms) during electrolysis. The charged atoms (or groups of atoms) he called *ions*. In electrolysis, the electric current is the result of the motion of the ions through the solution, the positively charged ions (or cations) moving towards the cathode and the negatively charged ions (or anions) moving towards the anode. At the electrodes, the ions are converted to neutral atoms (or radicals) which are liberated or which give rise to secondary reactions.

Faraday's results implied the existence of an *elementary unit* of electricity, some types of ion carrying one unit, others two units and so on. Indeed, as H. Helmholtz emphasised in 1881 during a speech in honour of Faraday: 'If we assume the existence of atoms of chemical elements, we cannot escape from drawing the further inference that electricity also, positive as well as negative, is divided into definite elementary charges that behave like atoms of electricity'. However, at the time of Faraday's experiments the idea, that electrical charge

existed in discrete units, did not seem to agree with the evidence from other electrical phenomena, such as metallic conduction, and both Faraday and Maxwell were reluctant to accept it. In fact, the hypothesis that there is a 'natural unit of electricity' was only put forward by C. I. Stoney in 1874, who proposed that this unit should be taken to be the quantity of electricity which must pass through an electrolytic solution in order to liberate one atom of a monovalent substance. Since one Faraday (96484.6 C) liberates one mole of a monovalent substance and because one mole contains N_A atoms, where N_A is Avagadro's number, the 'natural unit of electricity', e, is given by

$$e = \frac{F}{N_A} \qquad [1.4]$$

Stoney suggested the word 'electron' for this unit, and he obtained for e an approximate value of 10^{-20} C, using the rough estimates of N_A that were available from kinetic theory. In 1880, Helmholtz pointed out that it is apparently impossible to obtain electricity in smaller amounts than e. The first *direct* measurements of this smallest possible charge were initiated by J. J. Thomson and carried out by his student J. S. Townsend in 1897, and the first accurate value was found in the famous oil-drop experiment of R. M. Millikan in 1909, to which we shall return below.

Cathode rays and Thomson's measurement of e/m

When electrodes are placed in a gas at normal atmospheric pressure no current passes and the gas acts as an insulator until the electric field is increased to above 3 or 4 MV/m when sparking takes place. In contrast, at low pressures, a steady current can be maintained in a gas. At pressures of about 1 mm of mercury, the discharge is accompanied by the emission of light, but at still lower pressures a dark region forms near the cathode. The dark region, called the Crookes dark space, increases in size as the pressure falls, filling the discharge tube at pressures of 10^{-3} mm and below. If, under these low pressure conditions, a small hole is made in the anode (see Fig. 1.1), a green glow is observed on the glass wall of the discharge tube.

The causative agents of this phenomenon were termed 'cathode rays'. The properties of these rays were studied in the latter part of the nineteenth century

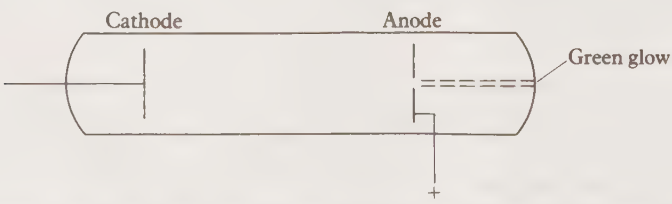

1.1 Low-pressure discharge tube. Cathode rays passing through a hole in the anode cause a green glow on the glass wall of the tube.

by W. Crookes and P. Lenard, who showed that the rays travelled in straight lines, cast 'shadows' and also carried sufficient momentum to set in motion a light paddle wheel. In 1895, J. Perrin demonstrated that the rays carried negative charge by collecting the charge on an electrometer. At that time very differing views were expressed as to the nature of the cathode rays, but J. J. Thomson set out the hypothesis that the rays consisted of a stream of particles each of mass m and charge $-e$, originating in the cathode of the discharge tube. Since the earlier investigations showed that the properties of the cathode rays were independent of the material of the cathode and of the gas in the tube, the particles could be assumed to be constituents of all matter.

In Thomson's experiments the deflection of the cathode rays by static electric and magnetic fields was investigated, which allowed the determination of the '*specific charge*', the ratio e/m, of the constituent particles. The cathode rays were passed between parallel plates, a distance D apart, to which a potential difference V could be applied, as in Fig. 1.2. The cathode rays emerging from the region of the electric field were detected on a screen S, and the deflection measured as a function of V. Neglecting end effects, the electric field strength $\mathscr{E}$ between the plates can be taken to be uniform and equal to V/D, and in this field the charged particle experiences a constant acceleration of magnitude $e\mathscr{E}/m$ in the Y direction (see Fig. 1.2). If the initial velocity of a particle is v, the time taken to traverse the region between the plates, of length x_1, is $t_1 = x_1/v$. The subsequent time to reach the screen, placed at distance x_2 from the plates, is $t_2 = x_2/v$.

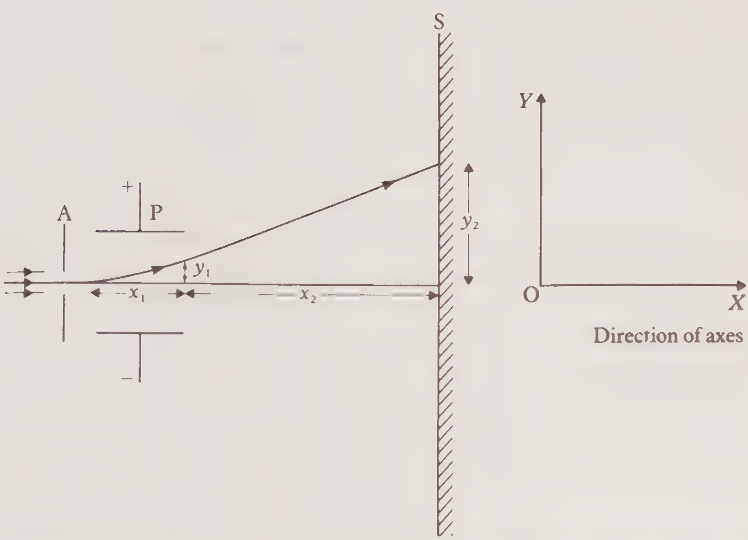

1.2 Schematic diagram of Thomson's apparatus to measure e/m. A stream of cathode rays, passing through a small hole in the anode A of a discharge tube, is deflected by being passed between the plates of a condenser P to which a potential is applied.

After the time t_1, the deflection in the Y direction is

$$y_1 = \tfrac{1}{2}\left(\frac{e\mathscr{E}}{m}\right)t_1^2 = \tfrac{1}{2}\left(\frac{e\mathscr{E}}{m}\right)\left(\frac{x_1}{v}\right)^2 \qquad [1.5]$$

On leaving the region between the plates, the component of the particle velocity in the Y direction is

$$v_y = \left(\frac{e\mathscr{E}}{m}\right)t_1 = \left(\frac{e\mathscr{E}}{m}\right)\left(\frac{x_1}{v}\right) \qquad [1.6]$$

from which the total deflection in reaching the screen is

$$y_2 = v_y t_2 + y_1 = \frac{e}{m}\frac{\mathscr{E}x_1}{v^2}\left(\tfrac{1}{2}x_1 + x_2\right) \qquad [1.7]$$

Thus, a measurement of the deflection y_2 provides a value of the combination (e/mv^2), if $\mathscr{E}$, x_1 and x_2 are known.

To determine e/m, an independent measurement is required from which v can be found. By placing the apparatus within a Helmholtz coil, Thomson could apply a constant magnetic field $\mathscr{B}$, directed in the Z direction, at right angles both to the electric field and to the undeflected path of the cathode rays. The magnetic force on the charged particles is of magnitude $ev\mathscr{B}$ and is perpendicular to the particle trajectory, being initially in the Y direction. If both electric and magnetic fields are applied simultaneously, the net force on the particles vanishes provided $\mathscr{E}$ and $\mathscr{B}$ are adjusted so that

$$ev\mathscr{B} = e\mathscr{E} \qquad [1.8]$$

Two experiments can now be performed. In the first, the values of $\mathscr{B}$ and $\mathscr{E}$ are measured for which the cathode rays are undeflected and this provides the value of v, since from [1.8] we have $v = \mathscr{E}/\mathscr{B}$. In the second, the magnetic field is switched off and the deflection due to the electric field alone is measured [4]. Knowing v, the specific charge e/m can be calculated from [1.7].

Thomson found a value for the specific charge somewhat smaller than the modern value of 1.76×10^{11} C/kg. The specific charge for the lightest known positive ion (the hydrogen ion) is smaller by a factor of approximately 1840, so either the cathode ray particles are much lighter or they carry a very large charge. Thomson assumed that the charge on a cathode ray particle was equal in magnitude (but opposite in sign) to that on the hydrogen ion, so that each particle was lighter than a hydrogen ion by a factor of about 1840. Particles with this property are now called *electrons*, thus changing the original meaning of the word electron which was applied by Stoney to the magnitude e of the charge carried by a hydrogen ion or a cathode ray particle.

[4] If the electric field is switched off the cathode rays move along an arc of a circle of radius R, where $(mv^2/R) = ev\mathscr{B}$. From this the deflection by a magnetic field extending over a region of length x, can be calculated.

Millikan and the charge of the electron

Following his determination of an accurate value for the charge to mass ratio of the electron, J. J. Thomson, together with his student J. S. Townsend, attempted to measure the electronic charge itself. The method employed was to produce clouds of charged water droplets and to estimate the number of droplets in a cloud from a knowledge of its total mass and the rate at which the cloud settles. The total charge of the cloud could be measured with an electrometer and hence the charge on each drop estimated. In an extension of the method due to H. A. Wilson, the charge on the cloud was measured by applying an electric field in the opposite direction to gravity, and adjusting the strength of the field until the cloud ceased to settle, but remained suspended at rest. Both these methods failed to provide accurate results because of the evaporation of the droplets during the experiment. However, a brilliant modification of Wilson's method, by R. M. Millikan in 1909, gave the first accurate value for the magnitude, e, of the electronic charge.

In Millikan's experiments very small oil droplets a few microns in diameter were formed by spraying mechanically from a nozzle. The droplets became charged by friction as they were formed. They also acquired charges from the surrounding air, which could be ionised by passing X-rays through the apparatus. Some droplets were allowed to fall through a small hole into a region between two parallel plates of a condenser to which an electrostatic potential V could be applied. The motion of the drops was viewed by a microscope with a micrometer eyepiece, and the velocity of fall was measured. The whole apparatus, a schematic diagram of which is shown in Fig. 1.3, was enclosed in a thermostat to avoid convection currents of the air between the condenser plates, which were 22 cm in diameter and separated by about 15 mm.

If the condenser is uncharged ($V = 0$), a droplet of effective mass M falls under gravity, reaching a terminal velocity v_1 when the gravitational force Mg is balanced by the viscous drag of the air. According to Stokes's law this occurs

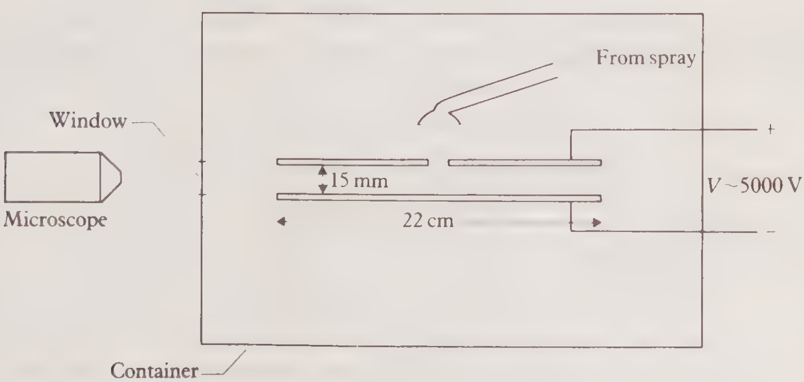

1.3 Millikan's experiment for the determination of the charge of the electron.

when

$$Mg = 6\pi\eta r v_1 \quad [1.9]$$

where η is the coefficient of viscosity of air and r the radius of the drop. The mass of the drop is $4\pi r^3 \rho_O/3$ where ρ_O is the density of the oil, and allowing for the buoyancy of the air the effective mass is

$$M = \tfrac{4}{3}\pi r^3(\rho_O - \rho_A) \quad [1.10]$$

where ρ_A is the density of the air.

The potential V (of the order of 5 kV) can now be applied. If it is sufficiently large and in the correct direction, the drop will move upwards until a new terminal velocity v_2 is reached. If D is the distance between the plates and q is the charge on the drop

$$q\frac{V}{D} - Mg = 6\pi\eta r v_2 \quad [1.11]$$

Thus, from [1.9] and [1.11], the charge on the drop is

$$q = 6\pi\eta r\left(\frac{D}{V}\right)(v_1 + v_2) \quad [1.12]$$

which can be determined by measuring v_1, v_2 and (D/V), since the radius of the drop is given by [1.9] and [1.10], provided η, ρ_O and ρ_A are known.

The same drop could be observed for a period of some hours, during which time the charge q varied because positive or negative ions were acquired from the surrounding air. From many thousands of observations, Millikan found that as q altered, it always changed in integral units of a basic charge and in general the magnitude of q was given by

$$|q| = 1.59\, n \times 10^{-19}\ \mathrm{C} \quad [1.13]$$

where n was an integer usually between 3 and 30. Thus the basic charge, which he identified with the magnitude of the electronic charge e, was found to have the value 1.59×10^{-19} C. Later measurements in which better values of the viscosity η were used gave an improved value,

$$e = 1.60 \times 10^{-19}\ \mathrm{C} \quad [1.14]$$

Combining these results with the modern value of e/m, a value for the mass of the electron is obtained,

$$m = 9.11 \times 10^{-31}\ \mathrm{kg} \quad [1.15]$$

which is approximately 1840 times lighter than a hydrogen ion, as postulated by Thomson.

1.3 BLACK BODY RADIATION

During the later part of the nineteenth century, and in the early years of this century, evidence accumulated that the classical physics, represented by Newton's laws of motion and Maxwell's electromagnetic equations, is inadequate to describe atomic phenomena. The first clues to a new physics, based on the quantisation of energy, came from a study of the properties of radiation from hot bodies. It is a matter of common experience that a hot body radiates electromagnetic energy in the form of heat. In fact, at any temperature, a body emits radiation of all wavelengths, but the distribution in wavelength, the *spectral distribution*, depends on temperature. At low temperature, most of the energy is in the form of low frequency infra-red radiation, but as the temperature increases more energy is radiated at higher frequencies, until by ~500°C radiation of visible light is observed. At still higher temperatures, such as that of an incandescent lamp filament the spectral distribution has shifted sufficiently to the higher frequencies for the body to be white hot. Not only the spectral distribution changes with temperature, but the total energy radiated also changes, increasing as a body becomes hotter.

In 1874, J. Stefan showed that the power emitted per unit area, R, from a body at the absolute temperature T (K), called the total emittance, could be represented by the empirical law

$$R = e\sigma T^4 \qquad [1.16]$$

where e is called the *emissivity* with $e \leqslant 1$. The emissivity varies with the nature of the surface, but the constant σ, known as Stefan's constant, is independent of the nature of the radiating surface and is given by

$$\sigma = 5.67 \times 10^{-8}\ \mathrm{W\ m^{-2}\ K^{-4}} \qquad [1.17]$$

When radiation falls on a body some is reflected and some is absorbed. For example, dark bodies absorb most of the radiation falling on them, while light coloured bodies reflect most of it. The *absorptivity*, a, of a surface is defined as the fraction of the energy of the radiation falling on unit area which is absorbed, and a *black body* is defined as a body with a surface having an absorptivity equal to unity, that is a body which absorbs all the radiant energy falling upon it.

If a body is in thermal equilibrium with its surroundings, and therefore is at constant temperature, it must emit and absorb the same amount of radiant energy per unit time, for otherwise its temperature would rise or fall. The radiation emitted or absorbed under these circumstances is called *thermal radiation*. By considering the thermal equilibrium between objects made of different substances G. R. Kirchhoff in 1895 proved, using the laws of thermodynamics, that the absorptivity of a surface is equal to its emissivity, $e = a$, independently of its temperature, and that this holds for radiation of each particular wavelength. Kirchhoff's law thus shows that the emissivity of a black body is unity and that a black body is the most efficient radiator of electromagnetic energy. In 1884, L. Boltzmann derived the relation [1.16] from

thermodynamics for the case of a black body ($e = 1$). It is now known as the Stefan–Boltzmann law. It follows, from the Stefan–Boltzmann law, that the energy radiated by a black body depends only on the temperature. The spectral distribution of this radiation is of a universal nature and is of particular interest.

A perfect black body is an idealisation, but it can be very closely realised in the following way. Consider a cavity kept at a constant temperature of which the interior walls are blackened. A small hole made in the wall of such a cavity behaves like a black body, because any radiation falling on the hole from outside will pass through it and after multiple reflections will eventually be absorbed by the interior surfaces and the opening has an effective absorptivity of unity. Since the cavity is in thermal equilibrium, the radiation within it and the radiation from the small opening are characteristic of the thermal radiation from a black body. This radiation was studied experimentally as a function of the temperature of the enclosure, and the spectral distribution at each temperature was measured by O. Lummer and E. Pringsheim in 1899.

The power emitted per unit area, from a black body, at wavelengths between λ and $\lambda + \mathrm{d}\lambda$ is denoted by $R(\lambda)\,\mathrm{d}\lambda$, so that the total power emitted per unit area is

$$R = \int_0^\infty R(\lambda)\,\mathrm{d}\lambda \qquad [1.18]$$

and by the Stefan–Boltzmann law $R = \sigma T^4$. The observed spectral distribution function $R(\lambda)$ is shown plotted against λ, for a number of different temperatures in Fig. 1.4. We see that, for fixed λ, $R(\lambda)$ increases with increasing T. At each temperature, there is a wavelength $\lambda_{\max}$, for which $R(\lambda)$ has its maximum value. Using general thermodynamical arguments it had been predicted in 1893 by W. Wien that $\lambda_{\max}$ would vary inversely with T and this was confirmed by the later experiments. The relation

$$\lambda_{\max} T = b \qquad [1.19]$$

is known as *Wien's displacement law*, and the constant b has the value $b = 2.898 \times 10^{-3}$ mK.

The spectral distribution function $R(\lambda)$, for the power emitted, is related by a geometrical factor to the spectral distribution function $\rho(\lambda)$ for the energy density within the cavity. In fact, if $\rho(\lambda)\,\mathrm{d}\lambda$ is defined as the energy density of the radiation with wavelengths between λ and $\lambda + \mathrm{d}\lambda$, it can be shown [5] that $\rho(\lambda) = 4R(\lambda)/c$, consequently measurements of $R(\lambda)$ determine the spectral distribution of the energy density within the cavity. It is also interesting to consider the energy density as a function of the frequency $\nu = c/\lambda$, in which case a distribution function $\rho(\nu)$ is defined so that

$$\rho(\nu) = \rho(\lambda)\left|\frac{\mathrm{d}\lambda}{\mathrm{d}\nu}\right| = \lambda^2\rho(\lambda)/c \qquad [1.20]$$

[5] The details of the calculation are given in the book by Richtmyer, Kennard and Cooper (1969).

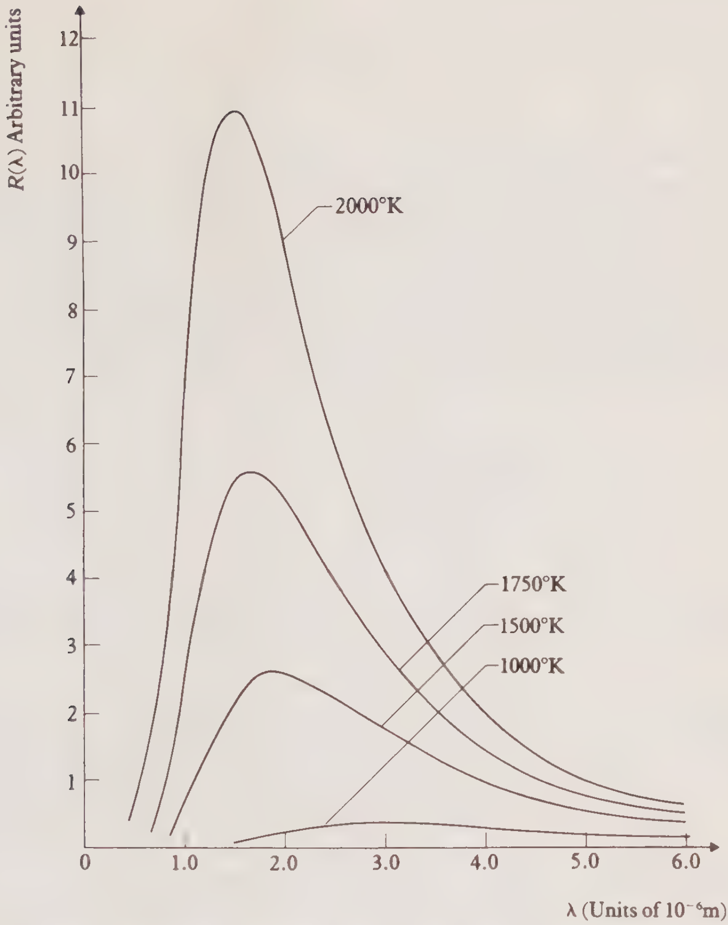

1.4 Spectral distribution of radiation from a black body at different temperatures.

Again, using very general thermodynamical arguments, Wien was able to show in 1894 that $\rho(\lambda)$ had to be of the form

$$\rho(\lambda) = \lambda^{-5} f(\lambda T) \qquad [1.21]$$

where $f(\lambda T)$ was some function, which could only be determined by going beyond thermodynamical reasoning to a more detailed theoretical model. After some attempts by Wien, Lord Rayleigh and J. Jeans derived a distribution function $\rho(\lambda)$ (and hence $f(\lambda T)$) in the following way.

The number of standing electromagnetic waves (modes) per unit volume within a cavity, with wavelengths within the interval λ to $\lambda + \mathrm{d}\lambda$, is given by $8\pi\, \mathrm{d}\lambda/\lambda^4$ (Problem 1.2). This number is independent of the size and shape of a sufficiently large cavity. The energy density can then be written as

$$\rho(\lambda) = \frac{8\pi}{\lambda^4}\,\bar{\varepsilon} \qquad [1.22]$$

or alternatively as

$$\rho(\nu) = \frac{8\pi\nu^2}{c^3}\,\bar{\varepsilon} \qquad [1.23]$$

where $\bar{\varepsilon}$ is the average energy in the mode with wavelength λ. Rayleigh and Jeans then suggested that each standing wave of radiation could be considered to be due to an assemblage of a large number of oscillating electric dipoles of frequency $\nu = c/\lambda$. The energy, ε, of each oscillator can take any value, $0 \leqslant \varepsilon < \infty$, independently of the frequency ν, but since the system is in thermal equilibrium, the average energy $\bar{\varepsilon}$ can be obtained by weighting each value of ε with the Boltzmann factor $\exp(-\varepsilon/kT)$, where k is Boltzmann's constant. Setting $\beta = 1/kT$, we have

$$\bar{\varepsilon} = \frac{\displaystyle\int_0^\infty \varepsilon e^{-\beta\varepsilon}\,d\varepsilon}{\displaystyle\int_0^\infty e^{-\beta\varepsilon}\,d\varepsilon}$$

$$= -\frac{d}{d\beta}\left[\log\int_0^\infty e^{-\beta\varepsilon}\,d\varepsilon\right] = kT \qquad [1.24]$$

Inserting this value of $\bar{\varepsilon}$ into [1.22] or [1.23] gives the Rayleigh–Jeans distribution law

$$\rho(\lambda) = \frac{8\pi}{\lambda^4}(kT) \qquad [1.25]$$

from which, using [1.21], we see that $f(\lambda T) = 8\pi k(\lambda T)$.

In the limit of long wavelengths the Rayleigh–Jeans result [1.25] approaches the experimental results, as shown in Fig. 1.5. However, as can be seen from the figure, $\rho(\lambda)$ does not show the observed maximum, and diverges as $\lambda \to 0$. This behaviour at short wavelengths is known as the 'ultra-violet catastrophe', and as a consequence the total energy per unit volume

$$\rho_{\text{tot}} = \int_0^\infty \rho(\lambda)\,d\lambda \qquad [1.26]$$

is seen to be infinite.

Planck's quantum theory

No solution to these difficulties can be found using classical physics. However, in December 1900, M. Planck presented a new form of the black body radiation spectral distribution, based on a revolutionary hypothesis. He postulated that the energy of an oscillator of a given frequency ν cannot take arbitrary values between zero and infinity, but can only take on the discrete values $n\varepsilon_0$, where n

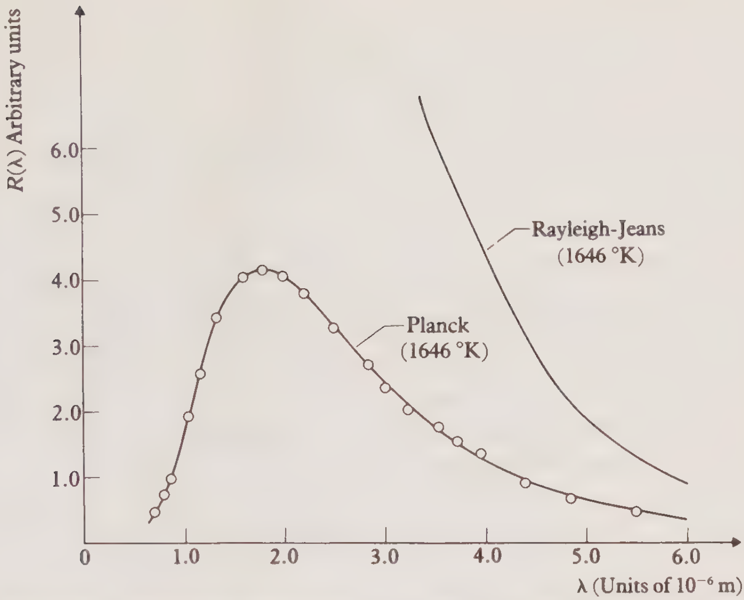

1.5 The Rayleigh–Jeans and Planck distributions at 1646 K. The dots represent the experimental points of Lummer and Pringsheim.

is a positive integer or zero, and ε_0 is a finite amount, or *quantum*, of energy, which may depend on the frequency. In this case the average energy of an assemblage of oscillators, each of frequency ν, in thermal equilibrium is given by

$$\bar{\varepsilon} = \frac{\sum_{n=0}^{\infty} n\varepsilon_0 e^{-\beta n \varepsilon_0}}{\sum_{n=0}^{\infty} e^{-\beta n \varepsilon_0}} = -\frac{d}{d\beta}\left[\log \sum_{n=0}^{\infty} e^{-\beta n \varepsilon_0}\right]$$

$$= -\frac{d}{d\beta}\left[\log\left(\frac{1}{1 - e^{-\beta\varepsilon_0}}\right)\right] = \frac{\varepsilon_0}{e^{\beta\varepsilon_0} - 1} \qquad [1.27]$$

Substituting this value of $\bar{\varepsilon}$ in [1.22], we find

$$\rho(\lambda) = \frac{8\pi}{\lambda^4}\frac{\varepsilon_0}{e^{\varepsilon_0/kT} - 1} \qquad [1.28]$$

In order to satisfy Wien's law [1.21], ε_0 must be taken to be proportional to the frequency ν:

$$\varepsilon_0 = h\nu \qquad [1.29]$$

where h is a fundamental physical constant, called *Planck's constant*. Planck's

distribution law then can be written as

$$\rho(\lambda) = \frac{8\pi hc}{\lambda^5} \frac{1}{e^{hc/\lambda kT} - 1} \qquad [1.30]$$

so that $f(\lambda T) = 8\pi hc[\exp(hc/\lambda kT) - 1]^{-1}$. In terms of frequency,

$$\rho(\nu) = \frac{8\pi h\nu^3}{c^3} \frac{1}{e^{h\nu/kT} - 1} \qquad [1.31]$$

By expanding the denominator in [1.30], it is easy to show that at long wavelengths $\rho(\lambda) \to 8\pi kT/\lambda^4$ in agreement with the Rayleigh–Jeans formula [1.25]. On the other hand, for short wavelengths, the presence of the exponential in the denominator of [1.30] ensures that $\rho(\lambda) \to 0$ as $\lambda \to 0$. The value of λ for which the Planck distribution [1.30] is a maximum can also be evaluated (Problem 1.3) and it is found that

$$\lambda_{\max} T = \frac{hc}{4.965\,k} = b \qquad [1.32]$$

where b is Wien's displacement constant.

In Planck's theory, the total energy density is finite and we find from [1.30] and [1.26] (see Problem 1.4) that

$$\rho_{\text{tot}} = aT^4 \qquad [1.33]$$

where

$$a = \frac{8\pi^5}{15} \frac{k^4}{h^3 c^3} \qquad [1.34]$$

Since ρ_{tot} is related to the emittance R by $\rho_{\text{tot}} = 4R/c$, where R is given by the Stefan–Boltzmann law [1.16], with $e = 1$, we see that Stefan's constant σ is given by

$$\sigma = \frac{2\pi^5}{15} \frac{k^4}{h^3 c^2} \qquad [1.35]$$

Equations [1.32] and [1.35] relate σ and b to the three fundamental physical constants c, h and k. In 1901, the velocity of light, c, was known accurately and the experimental values of b and σ were also known. Using this data, Planck calculated both the values of h and k, which he found to be $h = 6.55 \times 10^{-34}$ J s and $k = 1.346 \times 10^{-23}$ J K^{-1}. Not only was this the first calculation of Planck's constant, but it was, at that time, the most accurate value of Boltzmann's constant available. The modern values of h and k are given by (Appendix 11)

$$\begin{aligned} h &= 6.62618 \times 10^{-34} \text{ J s} \\ k &= 1.38066 \times 10^{-23} \text{ J K}^{-1} \end{aligned} \qquad [1.36]$$

Using his values of h and k, Planck obtained very good agreement with the experimental data for $\rho(\lambda)$ over the entire range of wavelengths (see Fig. 1.5).

The idea of quantisation of energy, in which the energy of a system can only take certain discrete values, was totally at variance with classical physics, and Planck's theory was not accepted readily. However it was not long before the quantum concept was used to explain other phenomena. Indeed in 1905, A. Einstein was able to interpret the photoelectric effect by introducing the idea of *photons*, or light quanta, and in 1907 he used the Planck formula for the average energy of an oscillator [1.27] to derive the law of Dulong and Petit concerning the specific heat of solids. Subsequently N. Bohr, in 1913, was able to invoke the idea of quantisation of atomic energy levels to explain the existence of line spectra.

1.4 THE PHOTOELECTRIC EFFECT

In the course of experiments investigating the properties of electromagnetic waves, H. Hertz discovered in 1887 that ultra-violet light falling on metallic electrodes facilitates the passage of a spark. Further work by W. Hallwachs, M. Stoletov, P. Lenard and others showed that charged particles are ejected from metal surfaces irradiated by high frequency electromagnetic waves. This phenomenon is called the *photoelectric effect*. In 1900, Lenard measured the charge to mass ratio of the charged particles in experiments similar to those of J. J. Thomson, and in this way he was able to identify the particles as electrons.

In his experiments to establish the mechanism of the photoelectric effect, Lenard used the apparatus shown in schematic form in Fig. 1.6. Electrons liberated by light striking a cathode C could pass through a small hole in an anode A and be detected by an electrometer connected to a collecting plate P. The anode current was studied as a function of the voltage difference V between anode and cathode. The variation of the photoelectric current with V is shown in Fig. 1.7. As V is increased, so that the electrons are attracted towards the anode, the current increases until it saturates when V is of the order of 20 V. If

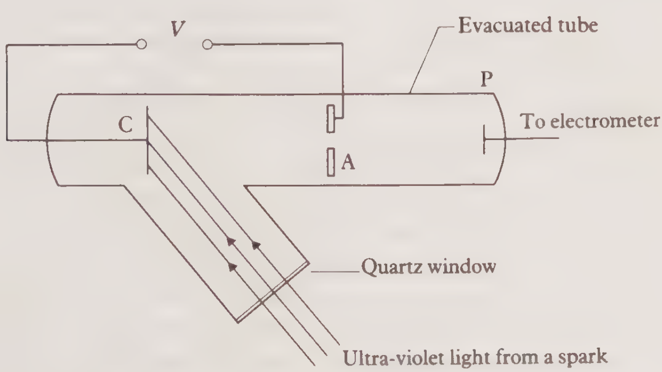

1.6 Lenard's apparatus for investigating the photoelectric effect.

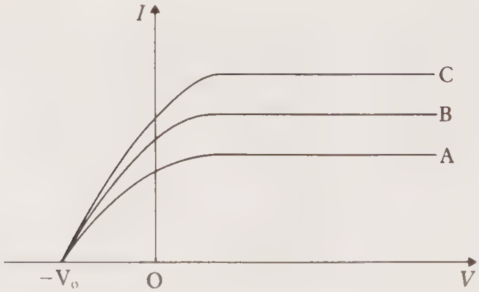

1.7 The variation of the photoelectric current with voltage, for different intensities of light, A < B < C.

V is decreased, and then reversed, so that the cathode is positive with respect to the anode, there is a definite voltage V_0 at which the current ceases and the emission of electrons from the cathode stops. From this result it follows that the electrons are emitted with velocities up to a maximum $v_{\max}$ and the stopping voltage V_0 is just enough to repel an electron with kinetic energy $\frac{1}{2}mv_{\max}^2$, giving

$$eV_0 = \tfrac{1}{2}mv_{\max}^2 \tag{1.37}$$

The most important features of the experimental data are the following:

1. There is a minimum, or threshold frequency ν_t of the radiation, below which no emission of electrons takes place, no matter what the intensity of the incident radiation, or for how long it falls on the surface.
2. Electrons emerge with a range of velocities from zero up to a maximum $v_{\max}$ and the maximum kinetic energy, $\frac{1}{2}mv_{\max}^2$, is found to depend linearly on the frequency of the radiation and to be independent of its intensity.
3. For incident radiation of a given frequency, the number of electrons emitted per unit time is proportional to the intensity of the radiation.
4. Electron emission takes place immediately the light shines on the surface, with no detectable time delay.

According to classical, pre-quantum, physics it would be natural to suppose that the maximum kinetic energy of the emitted electrons would increase with the energy density (or intensity) of the incident radiation, independently of the frequency. In fact, this is not in accord with what is observed. Another important aspect of classical theory is that the incident energy is spread uniformly over the illuminated surface. To eject an electron from an atom, this energy would have to be concentrated over an area of atomic dimensions, and to achieve such a concentration would require a certain time delay. Experiments can be arranged for which the predicted time delay is minutes, or even hours, and yet no detectable time delay is actually observed.

In 1905, Einstein offered an explanation for these seemingly strange aspects of the photoelectric effect, based on an extension of Planck's idea of the quantisation of black body radiation. In Planck's theory, the oscillators representing the source of the electromagnetic field could only vibrate with energies given by

$E = nh\nu$. In contrast, Einstein supposed that the electromagnetic field itself was quantised and that light consists of corpuscles, called *light quanta* or *photons* and that each photon travels with the velocity of light c and carries a quantum of energy of magnitude

$$E = h\nu = hc/\lambda \tag{1.38}$$

The photons are sufficiently localised, so that the whole quantum of energy can be absorbed by a single atom at one time. When a photon falls on a metallic surface, its entire energy $h\nu$ is used to eject an electron from an atom. Because of the interaction of the ejected electron with other atoms it requires a certain minimum energy to escape from the surface. The minimum energy required to escape depends on the metal and is called the *work function* W. It follows that the maximum kinetic energy of a photoelectron is given by

$$\tfrac{1}{2}mv_{\text{max}}^2 = h\nu - W \tag{1.39}$$

This relation is called Einstein's equation. The threshold frequency ν_t is determined by the work function since in this case $v_{\text{max}} = 0$, from which

$$h\nu_t = W \tag{1.40}$$

The number of electrons emerging from the metal surface per unit time is proportional to the number of photons striking the surface per unit time, but the intensity of the radiation is also proportional to the number of photons falling on a certain area per unit time, since each photon carries a fixed energy $h\nu$. It follows that the photoelectric current is proportional to the intensity of the radiation and that all the experimental observations are explained by Einstein's theory.

A series of very accurate measurements carried out between 1914 and 1916 by Millikan provided further confirmation of Einstein's theory. Combining [1.37] with [1.39], we see that the stopping voltage satisfies

$$eV_0 = h\nu - W \tag{1.41}$$

Millikan measured, for a given surface, V_0 as a function of ν, and showed that his results fell on a straight line (see Fig. 1.8) of slope h/e. Knowing e, Millikan obtained the value 6.56×10^{-34} J s for h, which agreed well with Planck's results. It is interesting that Millikan was able to use visible, rather than ultra-violet light for this experiment by using surfaces of lithium, sodium and potassium which have small values of the work function W.

Although the photoelectric effect provides compelling evidence for a corpuscular theory of light, it must not be forgotten that the existence of diffraction and interference phenomena demonstrate that light also exhibits a wave behaviour. The particle and the wave aspects of light are contained within modern quantum electrodynamics, which is capable of predicting both types of phenomena.

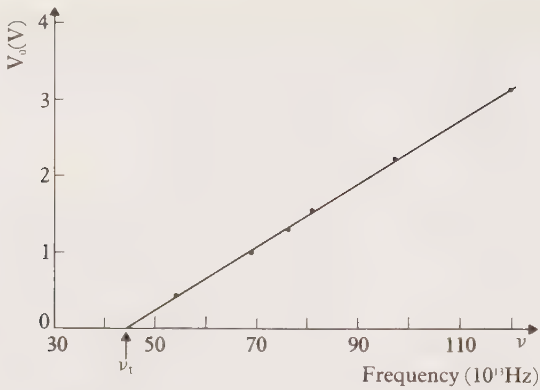

1.8 Millikan's results (dots) for the stopping potential V_0 as a function of frequency ν.

Photons and the electromagnetic spectrum

The electromagnetic spectrum extends from radio waves with low frequencies up to gamma rays of high frequency (see Fig. 1.9). At each particular frequency, the radiation consists of photons, each of energy $E = h\nu = hc/\lambda$. In Fig. 1.9 we show the photon energy corresponding to each part of the spectrum. The energies are given in electron volts (eV), which is a particularly convenient unit to use in atomic and nuclear physics. It is defined to be the energy acquired by an electron passing through a potential difference of one volt. Since the electronic charge has the absolute value $e = 1.602 \times 10^{-19}$ C, we have that

$$\begin{aligned} 1 \text{ eV} &= 1.602 \times 10^{-19} \text{ Coulomb-Volts} \\ &= 1.602 \times 10^{-19} \text{ J} \end{aligned} \qquad [1.42]$$

1.5 X-RAYS AND THE COMPTON EFFECT

The corpuscular nature of electromagnetic radiation was exhibited in a spectacular way in a quite different experiment performed in 1923 by A. H. Compton, in which a beam of X-rays was scattered through a block of material. X-rays had been discovered by W. K. Röntgen in 1895 and were known to be electromagnetic radiation of high frequency (see Fig. 1.9). The scattering of X-rays by various substances was first studied by C. G. Barkla in 1909, who interpreted his results with the help of J. J. Thomson's classical theory, developed around 1900. According to this theory, the oscillating electric field of the radiation acts on the electrons contained in the atoms of the target material. This interaction forces the atomic electrons to vibrate with the same frequency as the incident radiation. The oscillating electrons, in turn, radiate electromagnetic waves of the same frequency. The net effect is that the incident radiation is scattered with no change in wavelength and this is called *Thomson scattering*.

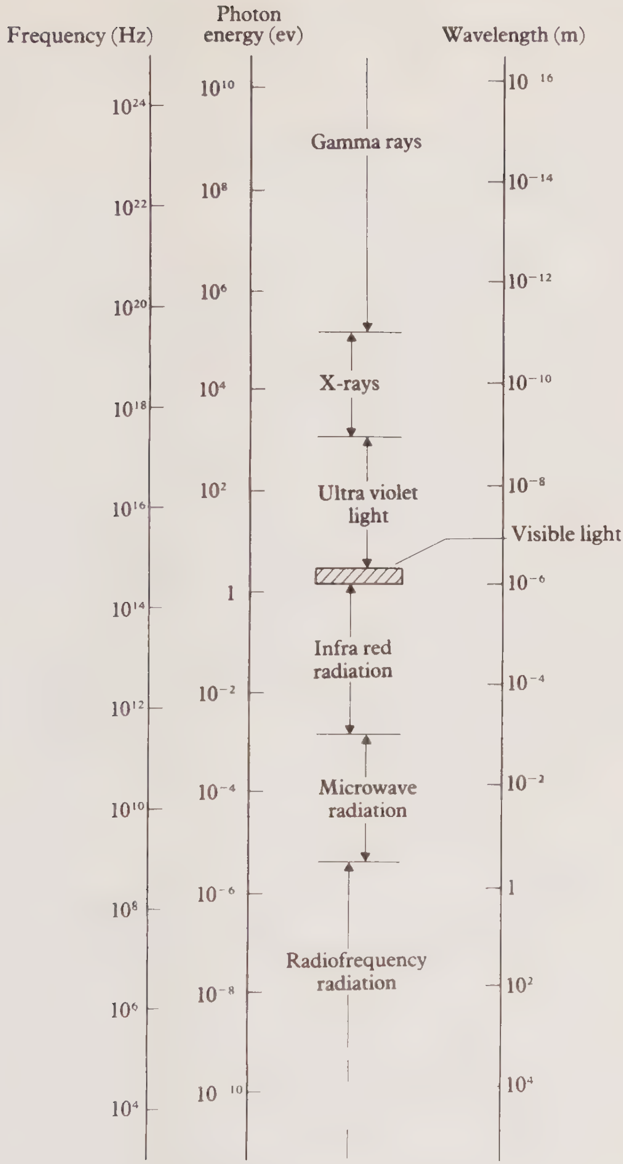

1.9 The electromagnetic spectrum.

In general, Barkla found that the scattered intensity predicted by Thomson's theory agreed well with his experimental data. However, he found that some of his results were anomalous, particularly in the region of 'hard' X-rays, which correspond to shorter wavelengths. At the time of Barkla's work, it was not possible to measure the wavelengths of X-rays and a further advance could not be made until M. von Laue in 1912, and later W. L. Bragg had shown that the

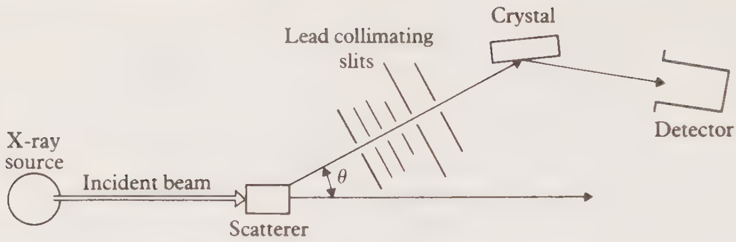

1.10 Schematic diagram of Compton's apparatus.

wavelengths could be determined by studying the diffraction of X-rays by crystals. The experiment of Compton, which we shall now describe, was only possible because a precise determination of wavelength could be made using a crystal spectrometer.

The experimental arrangement used by Compton is sketched in Fig. 1.10. He irradiated a graphite target with a nearly monochromatic beam of X-rays, of wavelength λ_0. He then measured the intensity of the scattered radiation as a function of wavelength. His results, illustrated in Fig. 1.11, show that although part of the scattered radiation had the same wavelength λ_0 as the incident radiation, there was also a second component of wavelength λ_1, where $\lambda_1 > \lambda_0$. This phenomenon, called the *Compton effect*, could not be explained by the classical Thomson model. The shift in wavelength between the incident and scattered radiation, the *Compton shift* $\Delta\lambda = \lambda_1 - \lambda_0$, was found to vary with the angle of scattering (see Fig. 1.11) and to be proportional to $\sin^2(\theta/2)$ where θ is the angle between the incident and scattered beams. Further investigation showed $\Delta\lambda$ to be independent of both λ_0 and of the material used as the scatterer, and that the value of the constant of proportionality was 0.048×10^{-10} m.

To interpret these results, Compton suggested that the modified line at wavelength λ_1 could be attributed to scattering of the X-ray photons by loosely bound electrons in the atoms of the target. In fact, such electrons can be treated as *free* since their binding energies of a few electron volts are small compared with the energy of an X-ray photon and this explains why the results are independent of the nature of the material used for the target.

Let us then consider the scattering of an X-ray photon by a free electron, which can be taken to be at rest initially. Since the energies involved in the collision may be large, we need to use relativisitic kinematics and we shall first outline the results required [6]. The total energy of a particle having a rest mass m and a velocity $\mathbf{v}$ is given by

$$E = \frac{mc^2}{\sqrt{1 - v^2/c^2}} \qquad [1.43]$$

[6] A good account of the theory of special relativity is given in the text of Taylor and Wheeler (1966).

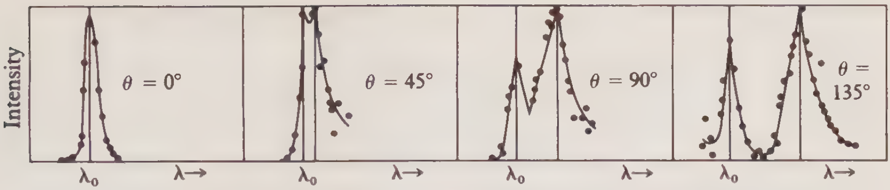

1.11 Compton's data for the scattering of X-rays by graphite.

The kinetic energy T of the particle is defined as the difference between E and the rest mass energy mc^2, so that

$$T = E - mc^2 \qquad [1.44]$$

The corresponding momentum of the particle is

$$\mathbf{p} = \frac{m\mathbf{v}}{\sqrt{1 - v^2/c^2}} \qquad [1.45]$$

and from [1.43] and [1.45] we see that the energy and momentum are related by

$$E^2 = m^2c^4 + p^2c^2 \qquad [1.46]$$

Since the velocity of a photon is c and its energy $E = h\nu = hc/\lambda$ is finite, we see from [1.43] that we must take the mass of a photon to be zero, in which case we observe from [1.46], that the magnitude of its momentum is

$$p = E/c = h/\lambda \qquad [1.47]$$

Let us now consider the situation depicted in Fig. 1.12, where a photon of energy $E_0 = hc/\lambda_0$ and momentum $\mathbf{p}_0 (p_0 = E_0/c)$ collides with an electron initially at rest. After the collision, the photon has an energy $E_1 = hc/\lambda_1$ and a momentum $\mathbf{p}_1 (p_1 = E_1/c)$ in a direction making an angle θ with the direction of incidence, while the electron recoils with a momentum $\mathbf{p}_2$ making an angle ϕ

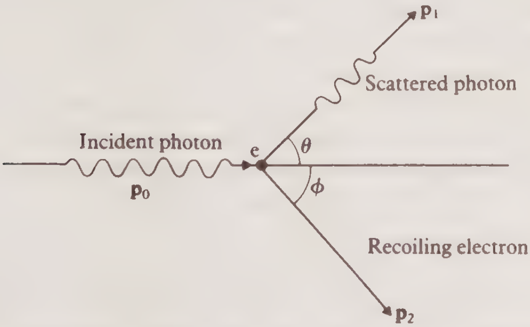

1.12 A photon of momentum $\mathbf{p}_0$ collides with a stationary electron e, and is scattered with momentum $\mathbf{p}_1$, while the electron recoils with momentum $\mathbf{p}_2$.

with the incident direction. Conservation of momentum yields

$$\mathbf{p}_0 = \mathbf{p}_1 + \mathbf{p}_2 \tag{1.48}$$

from which

$$p_2^2 = p_0^2 + p_1^2 - 2p_0p_1 \cos\theta \tag{1.49}$$

Conservation of energy then gives

$$E_0 + mc^2 = E_1 + (m^2c^4 + p_2^2c^2)^{\frac{1}{2}} \tag{1.50}$$

and defining the kinetic energy of the electron after the collision as T_2 we have

$$\begin{aligned} T_2 &= (m^2c^4 + p_2^2c^2)^{\frac{1}{2}} - mc^2 \\ &= E_0 - E_1 = c(p_0 - p_1) \end{aligned} \tag{1.51}$$

From [1.51] we have that

$$p_2^2 = (p_0 - p_1)^2 + 2mc(p_0 - p_1) \tag{1.52}$$

and combining [1.52] with [1.49] we find that

$$mc(p_0 - p_1) = p_0p_1(1 - \cos\theta) = 2p_0p_1\sin^2\theta/2 \tag{1.53}$$

Since $\lambda_0 = h/p_0$ and $\lambda_1 = h/p_1$ this can be written in the form

$$\Delta\lambda = \lambda_1 - \lambda_0 = 2\lambda_c \sin^2(\theta/2) \tag{1.54}$$

where the constant λ_c is given by

$$\lambda_c = \frac{h}{mc} \tag{1.55}$$

and is called the *Compton wavelength* of the electron. Equation [1.54] is known as the *Compton equation*. The calculated value of $(2\lambda_c)$ is 0.04852×10^{-10} m, and this agrees very well with the experimental data.

The existence of the unmodified component of the scattered radiation, which has the same wavelength λ_0 as the incident radiation, can be explained by assuming that it results from scattering by electrons so tightly bound that the entire atom recoils. In this case, the mass to be used in [1.55] is M, the mass of the entire atom, and since $M \gg m$, the Compton shift $\Delta\lambda$ is negligible. For the same reason, there is no Compton shift for light in the visible region, because the photon energy in this case is not large compared with the binding energy of even the loosely bound electrons. In contrast, for very energetic γ-rays only the shifted line is observed, since the photon energies are large compared with the binding energies of even the tightly bound electrons.

The recoil electrons predicted by Compton's theory were observed in 1923 by W. Bothe and also by C. T. R. Wilson. A little later, in 1925, W. Bothe and H. Geiger demonstrated that the scattered photon and the recoiling electron appear simultaneously. Finally, in 1927 A. A. Bless measured the energy of the ejected electrons, which he found to be in agreement with the prediction of Compton's theory.

1.6 THE NUCLEAR ATOM

By the early years of this century, the atomic nature of matter had been well established. It was known that atoms contained electrons and that an electron was much lighter than even the lightest atom. It had also been shown that electrons could be removed from atoms of a given species, producing positively charged ions, but that only a finite number of electrons could be obtained from each atom. This number is characteristic of the atoms of each element and is called the atomic number Z. In the normal state an atom is electrically neutral so that it must contain positive charge of an amount Ze, where $-e$ is the charge on the electron, and the mass of an atom must be associated with this positive charge.

Atomic sizes

Information about atomic sizes can be found from simple arguments about the nature of solids. Let us assume that in a solid the atoms are packed as closely as possible. If the diameter of each atom is D, then a length L of material contains L/D atoms, and a volume L^3 contains $(L/D)^3$ atoms. Now the number of atoms in one mole of substance is equal to Avagadro's number N_A, given by [1.1]. If the density in kg/m^3 is ρ, one mole will occupy a volume of $(10^{-3}\ \mu/\rho)$ m^3 where μ is the atomic weight. It follows that a unit volume contains $(10^3\rho/\mu)\,6 \times 10^{23}$ atoms. This is to be equated with $1/D^3$, with the result

$$D = \left[\frac{\mu}{6\rho}\,10^{-26}\right]^{1/3} \qquad [1.56]$$

In Table 1.1 some values of D obtained from this formula are shown for a number of elements. It is seen that all the atoms concerned have diameters of about 2×10^{-10} m, and this can be taken to be representative of atomic sizes, which do not vary greatly from element to element.

Table 1.1 Atomic sizes

Element	*Atomic weight* μ	ρ(in kg/m^3)	D(in m)
Lithium	7	0.53×10^3	2.6×10^{-10}
Carbon (diamond)	12	3.5×10^3	1.8×10^{-10}
Iron	26	7.8×10^3	1.8×10^{-10}
Silver	47	10.5×10^3	2.0×10^{-10}
Gold	79	19.3×10^3	1.9×10^{-10}
Lead	207	11.35×10^3	3.1×10^{-10}

The experiments of Geiger, Marsden and Rutherford

The question now arises as to how the mass and positive charge are distributed within the atom. The answer was provided by a series of experiments by H. Geiger, E. Marsden and E. Rutherford, carried out between 1906 and

1913, on the scattering of α particles by metallic foils of various thicknesses. Alpha particles are emitted by many radioactive substances, for example uranium. By measuring the deflection of α particles by electric and magnetic fields, Rutherford found that α particles had a charge to mass ratio q/M (that is, a specific charge) which was the same as that of the doubly ionised helium atom. Spectroscopic measurements subsequently confirmed that α particles were fully ionised helium atoms, with a mass about four times that of a hydrogen atom and a positive charge equal to $+2e$. The kinetic energies of the α particles employed in the experiments were several million electron volts (MeV).

A schematic diagram of the experiments of Geiger and Marsden is shown in Fig. 1.13. The α particles emitted from a source are collimated and then scattered from thin metallic foils, for example gold foils of thickness $\sim 10^{-6}$ m. Alpha particles produce scintillations in zinc sulphide and can be detected by observing a screen, coated with this substance, with a microscope. Most of the α particles are deflected through very small angles ($<1°$), but some are deflected through large angles; about 1 in 8000 being deflected through angles greater than 90°. The measurements established that:

1. For a fixed angle of scattering and fixed energy, the number of particles scattered within an element of solid angle $d\Omega$ is proportional to the thickness of the foil, except at very small angles of scattering ($<1°$).
2. At a fixed angle and for a given foil, the number of particles scattered within an element of solid angle $d\Omega$ is inversely proportional to E^2, where E is the kinetic energy of the α particles.
3. For a given energy and a given foil, the number of particles scattered within an element of solid angle $d\Omega$ is proportional to $(\sin\theta/2)^{-4}$, where θ is the angle of scattering.
4. At a fixed energy and for a foil of given thickness, the number of particles scattered within an element of solid angle $d\Omega$ in a given direction is proportional to Z^2, where Z is the atomic number of the atoms in the foil.

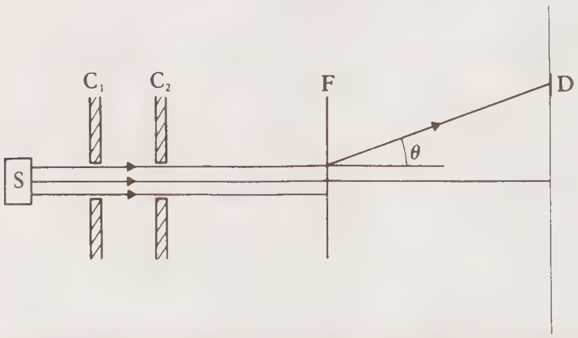

1.13 The scattering experiments of Geiger and Marsden. S represents a radioactive source emitting α particles, which are collimated by slits C_1 and C_2. The α particles fall on to a fixed foil F and those particles scattered through an angle θ are detected at D on a screen coated with a scintillating material. The apparatus is enclosed in an evacuated chamber to avoid scattering of the α particles by the air.

To understand what is meant by scattering in a certain direction, within an element of solid angle $d\Omega$ we refer to Fig. 1.14. Consider a particle travelling along the Z axis and being deflected along the direction OD after a collision with an atom situated at O. The direction OD is defined by the angle of scattering θ between OD and the Z axis and by the azimuthal angle ϕ, which is the angle between OX and the projection of OD on the XY plane. The element of solid angle $d\Omega$ subtended at O by a small area of the detecting screen, placed at D at right angles to OD is given by $d\Omega = \sin\theta \, d\theta \, d\phi$.

The number of atoms, n, encountered by a beam of particles of unit cross-sectional area, traversing a thin foil is proportional to the thickness of the foil. Since the intensity of scattering in a given direction is found to be proportional to the thickness of the foil, and hence to n, it can be inferred that each particle makes at most one collision with an atom within the foil. If multiple scattering occurred then the number of particles deflected through a certain angle would increase much more rapidly with n. The incident flux N is defined as the number of particles crossing a unit area normal to the direction of the beam, per unit time. The number of α particles scattered within an element of solid angle $d\Omega$ in the direction (θ, ϕ) (see Fig. 1.14) will be denoted by dN', and this quantity is proportional both to $n \, d\Omega$ and to the flux N. Thus

$$dN' = \left(\frac{d\sigma}{d\Omega}\right) Nn \, d\Omega \qquad [1.57]$$

The constant of proportionality $(d\sigma/d\Omega)$ is called the *differential cross-section* and determines the intensity of scattering from a single isolated atom. Clearly the cross-section is characteristic of the particular type of atom and it is a function

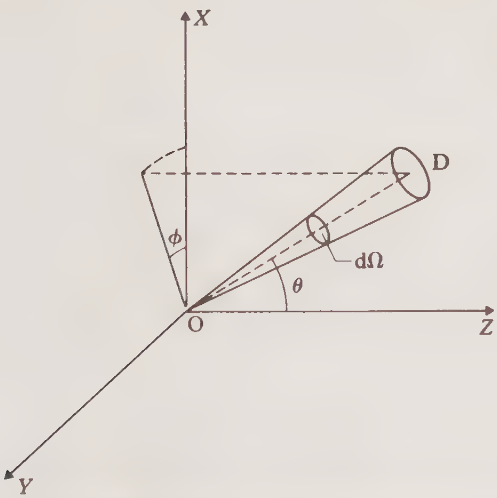

1.14 The geometry of scattering. The detector D subtends an element of solid angle $d\Omega$ at the scattering centre O. The polar coordinates of OD are (θ, ϕ). The incident beam is directed along the Z axis so that θ and ϕ are the scattering angles.

both of the energy of the incident particles and of the scattering angles. The experiments of Geiger and Marsden have axial symmetry about the direction of incidence (the Z axis), so in this case $d\sigma/d\Omega$ depends on θ only and not on the azimuthal angle ϕ.

In explaining the experimental data, we can neglect the influence of the electrons within the atom and assume that the scattering is due to the positive charge alone. This is because the α particles are about 8000 times as heavy as an electron and the kinematics of a collision with an electron will allow a maximum deflection of much less than 0.1° (see Problem 1.10). It can also be shown that if the positive charge is spread uniformly throughout the atom, as in a model proposed by J. J. Thomson, there would be no appreciable scattering at large angles, and even at 1° the number of scattered α particles would be negligible. The data can be fully explained by a model proposed in 1911 by Rutherford, who suggested that all the mass and positive charge of an atom is concentrated at the centre of the atom in a *nucleus* of very small dimensions. By treating the nucleus as a point charge, Rutherford obtained the differential scattering cross-section of a beam of α particles of charge $2e$ by the Coulomb force of a nucleus of charge (Ze). It is given in the centre of mass (CM) system by (see Appendices 1 and 2)

$$\frac{d\sigma}{d\Omega} = \left(\frac{2Ze^2}{4\pi\varepsilon_0}\right)^2 \frac{1}{4\mu^2 v^4} \frac{1}{\sin^4 \theta/2} \qquad [1.58]$$

Here v is the initial relative velocity of the α particle and the nucleus and μ is the reduced mass $\mu = M_\alpha M_N/(M_\alpha + M_N)$ where M_α and M_N are the masses of the α particle and of the nucleus, respectively. The Geiger and Marsden experiments were performed for heavy targets, in which case the CM and laboratory system nearly coincide. Since $E \sim v^2$, the formula [1.58] completely explains each of the experimental findings 2, 3 and 4.

The nucleus

The nucleus, although small compared with the atom, is finite in size. This can be demonstrated by the departure of the cross-section from the Rutherford scattering formula, at a given angle of scattering, when the energy of the incident α particle is raised to make the distance of closest approach comparable to the nuclear radius. For a head-on collision at zero impact parameter, the distance of closest approach r_0 is given by (see Appendix 1)

$$\frac{1}{2}\mu v^2 = \left(\frac{2Ze^2}{4\pi\varepsilon_0}\right)\frac{1}{r_0} \qquad [1.59]$$

Departures from Rutherford scattering occur when r_0 becomes less than $\sim 10^{-14}$ m and this distance is characteristic of nuclear sizes. The structure of the nucleus is the subject of the text by Burcham (1979), where it is shown that nuclei are composed of *protons*, of positive charge e and *neutrons* which are

uncharged. Both protons and neutrons have approximately the same mass (which is about 1840 times as large as the mass of the electron), and are referred to collectively as *nucleons*. The chemical properties of an atom are determined by the charge of the nucleus, Ze, where Z is the atomic number. It is found that, in general, several nuclei exist for each value of Z differing in the number of neutrons N they contain. Atoms with the same Z but with different mass numbers $A = N + Z$ are called *isotopes*. Many naturally occurring elements are mixtures of two or more different isotopes. For example oxygen is a mixture of three stable isotopes ^{16}O, ^{17}O and ^{18}O, where the notation is such that the superscript indicates the mass number A. The isotope ^{16}O occurs with a relative abundance of 99.759 per cent. The atomic weight of an element on the chemical scale, defined in Section 1.1, is therefore based on a mixture of oxygen isotopes. Because of this a new scale has been introduced recently, in which the isotope of carbon ^{12}C is assigned a mass of 12 atomic mass units (a.m.u. or u). The absolute value of the atomic mass unit is

$$1 \text{ a.m.u.} = 1.661 \times 10^{-27} \text{ kg} \qquad [1.60]$$

and differs very slightly from the previous unit based on the chemical scale.

Limitations of the Rutherford model

In the Rutherford model, the electrons move in the Coulomb field of the nucleus in orbits, like a planetary system. A particle moving on a curved trajectory is accelerating and an accelerating charged particle radiates electromagnetic waves and loses energy. The laws of classical physics – Newton's laws of motion and Maxwell's electromagnetic equations – if applied to the Rutherford atom, show that in a time of the order 10^{-10} s all the energy of the atom would be radiated away and the electrons would collapse into the nucleus. This is clearly contrary to experiment and is another piece of evidence to suggest that the laws of motion need to be modified when applied to phenomena on the atomic scale. Another fact not explained by the Rutherford model is the existence of atomic line spectra, to which we now turn our attention.

1.7 ATOMIC SPECTRA AND THE BOHR MODEL OF HYDROGEN

Isaac Newton was the first person to resolve white light into separate colours by dispersion with a prism, but it was not until 1752 that Th. Melvill first showed that light from incandescent gas was composed of a large number of discrete frequencies called *emission lines*. It was subsequently discovered that atoms exposed to white light can only absorb light at certain discrete frequencies called *absorption lines*. With the development of diffraction gratings, much greater resolving powers could be obtained and towards the end of the last century much progress was made in the empirial analysis of line spectra. G. R. Kirchhoff was the first to show that only certain definite frequencies can be radiated or absorbed by a given element and that the emission frequencies coincide with the

absorption frequencies. The fact that each element has its own characteristic line spectrum is of the greatest importance and is, for example, the only means by which the presence of particular elements in the sun and stars can be determined.

The most important discovery in the search for regularities in the line spectra of atoms was made by J. Balmer in 1885, who showed that the frequencies of a series of lines in the visible part of the spectrum of atomic hydrogen were among those given by the empirical formula

$$\nu_{ab} = R\left(\frac{1}{n_a^2} - \frac{1}{n_b^2}\right); \; n_a = 1, 2 \ldots \qquad n_b = 2, 3 \ldots . \tag{1.61}$$

where ν_{ab} is the frequency of either an emission or absorption line, n_a and n_b are positive integers with $n_b > n_a$ and R is a constant, known as Rydberg's constant. It is usual in the spectroscopy of the visible and ultra-violet regions to give the frequencies in terms of inverse wavelengths, or wave numbers

$$\tilde{\nu} = \frac{1}{\lambda} = \frac{\nu}{c} \tag{1.62}$$

The corresponding Rydberg constant for hydrogen then has the value

$$\tilde{R} = 109677.58 \text{ cm}^{-1} \tag{1.63}$$

However, in the infra-red or microwave region, frequencies are usually expressed in megahertz (MHz). The wave number given in units of cm^{-1} is related to the frequency given in MHz by

$$\tilde{\nu}(\text{cm}^{-1}) = \frac{10^{14}}{3}\,\nu(\text{MHz}) \tag{1.64}$$

where we have taken the velocity of light to be 3.00×10^8 m/s.

It was subsequently discovered that Balmer's formula is not only applicable to the visible region, but in fact describes the complete spectrum of atomic hydrogen. In spectroscopy, wavelengths are generally given in Ångstrom units, where 1 Å $\equiv 10^{-10}$ m, so that if the wave number $\tilde{\nu}_{ab}$ of a particular line is given in cm^{-1} the wavelength in Ångstrom units is

$$\lambda_{ab} = 10^8/\tilde{\nu}_{ab} \tag{1.65}$$

In atomic hydrogen, the series of lines with $n_a = 1$ is known as the *Lyman series* and lies in the ultra-violet part of the spectrum. The lines are labelled α, β, γ . . . in order of decreasing wavelengths; the wavelength of the Lyman α line ($n_b = 2$) is 1216 Å, while the series limit ($n_b = \infty$) is 912 Å. The Balmer series ($n_a = 2$) (the first to be discovered) lies in the visible region. The Balmer lines are denoted by H_α, H_β, H_γ . . . . The Balmer H_α line ($n_b = 3$) was first discovered by J. von Fraunhofer in the solar spectrum and was called by him the C line. It is a strong red line with a wavelength of 6563 Å. The next members of

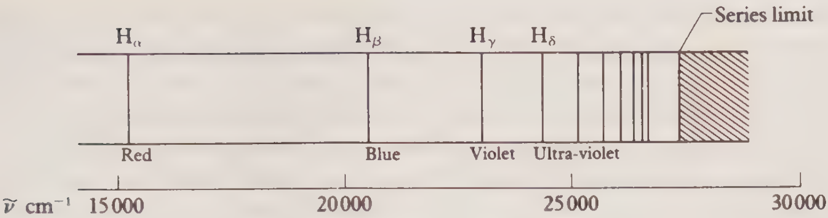

1.15 The Balmer series of atomic hydrogen.

the series ($n_b = 4$ and $n_b = 5$) at 4861 and 4340 Å are blue and violet respectively and the series limit is 3646 Å (see Fig. 1.15).

Further series of lines are found in the infra-red part of the spectrum: the Paschen series ($n_a = 3$) starts with a line at 18751 Å; the Brackett series ($n_a = 4$) starts at 40500 Å and the Pfund series ($n_a = 5$) at 74000 Å.

The set of quantities R/n_a^2, are called *terms*. J. R. Rydberg showed that for other atoms, particularly the alkalis, the frequencies of lines could be represented approximately as differences of terms T_n, where

$$T_n = R/(n + \alpha)^2, \qquad n = 1, 2, 3 \ldots \tag{1.66}$$

and where α was a constant for each particular series. Subsequently it was discovered by W. Ritz that the frequencies of all lines can be represented by the difference of terms, even if the terms cannot be represented by a simple formula such as [1.66]. This has the consequence that if lines of frequencies ν_{12} and ν_{23} can be represented as

$$\nu_{12} = T_1 - T_2; \qquad \nu_{23} = T_2 - T_3 \tag{1.67}$$

then a line of frequency ν_{13} will exist, where

$$\nu_{13} = (T_1 - T_2) + (T_2 - T_3) = T_1 - T_3 \tag{1.68}$$

This is an example of the *Ritz combination principle*, which states that if lines at frequencies ν_{ij} and ν_{jk} exist in a spectrum with $j > i$ and $k > j$ then there will usually be a line at ν_{ik} where

$$\nu_{ik} = \nu_{ij} + \nu_{jk} \tag{1.69}$$

However, not all combinations of frequencies are observed because certain selection rules operate which will be discussed in Chapters 4 and 8.

Bohr's model of the hydrogen atom

A major step forward was taken by N. Bohr in 1913. Working in Rutherford's laboratory, he was able to combine the concepts of Rutherford's nuclear atom, Planck's quanta and Einstein's photons to predict the observed spectrum of atomic hydrogen.

Bohr assumed that the electron in an atom moved in an orbit about the nucleus under the influence of the electrostatic attraction of the nucleus.

Circular or ellipitcal orbits are allowed by classical mechanics, and Bohr elected to consider circular orbits for simplicity. He then postulated that instead of the infinity of orbits which are possible in classical mechanics, only a certain set of stable orbits, which he called *stationary states* are allowed. As a result, atoms can only exist in certain allowed energy levels, with energies E_a, E_b, E_c, . . .

Bohr further postulated that an electron in a stable orbit does not radiate electromagnetic energy, and that radiation can only take place when a transition is made between the allowed energy levels. To obtain the frequency of the radiation, he made use of the idea that the energy of electromagnetic radiation is quantised and carried by photons, each photon associated with the frequency ν carrying an energy $h\nu$. Thus, if a photon of frequency ν is absorbed by an atom, conservation of energy requires that

$$h\nu = E_b - E_a \tag{1.70}$$

where E_a and E_b are the energies of the atom in the initial and final orbits, with $E_b > E_a$. Similarly, if the atom passes from a state of energy E_b to another state of lower energy E_a, the frequency of the emitted photon must be given by the *Bohr frequency relation* [1.70].

The *terms* of spectroscopy can then be interpreted as being the energies of the various allowed energy levels of an atom. It is important to note that because of the existence of the energy-frequency relationship, we can use frequency (or wave number) units of energy where convenient, and in this book we shall often use Hertz or inverse centimeters as energy units. In terms of electron volts, we have

$$\begin{aligned} 1\text{ eV} &\equiv 2.41797 \times 10^{14}\text{ Hz} \\ &\equiv 8065.48\text{ cm}^{-1} \end{aligned} \tag{1.71}$$

Other conversions of units are given in Appendix 11.

For the case of the hydrogen atom Bohr was able to modify the classical planetary model to obtain the quantisation of energy levels by making the additional postulate that the angular momentum of the electron moving in a circular orbit can only take one of the values $L = nh/2\pi = n\hbar$, where n is a positive integer, $n = 1, 2, 3, \ldots$ and the commonly occurring quantity $h/2\pi$ is conventionally denoted by $\hbar$. The allowed energy levels can then be determined in the following way.

We shall make the approximation (which we shall remove later) that the nucleus is infinitely heavy compared with the bound electron and is therefore at rest. The electron will be taken to be moving in a circular orbit of radius r, in which case the Coulomb attractive force acting on the electron, due to its electrostatic interaction with the nucleus of charge Ze, can be equated with the electron mass m times the centripetal acceleration (v^2/r):

$$\frac{Ze^2}{(4\pi\varepsilon_0)r^2} = \frac{mv^2}{r} \tag{1.72}$$

where v is the velocity of the electron. A second equation is obtained from Bohr's postulate that the orbital angular momentum is quantised:

$$L = mvr = n\hbar, \qquad n = 1, 2, 3, \ldots \tag{1.73}$$

From [1.72] and [1.73], we obtain the possible values of v and r

$$v = \frac{Ze^2}{(4\pi\varepsilon_0)\hbar n} \tag{1.74}$$

$$r = \frac{(4\pi\varepsilon_0)\hbar^2 n^2}{Ze^2 m} \tag{1.75}$$

The kinetic energy of the electron T, is then found to be

$$T = \frac{1}{2}mv^2 = \frac{m}{2\hbar^2}\left(\frac{Ze^2}{4\pi\varepsilon_0}\right)^2 \frac{1}{n^2} \tag{1.76}$$

and the potential energy V is, correspondingly,

$$V = -\frac{Ze^2}{(4\pi\varepsilon_0)r} = -\frac{m}{\hbar^2}\left(\frac{Ze^2}{4\pi\varepsilon_0}\right)^2 \frac{1}{n^2} \tag{1.77}$$

from which the total energy E_n of the system is

$$E_n = T + V = -\frac{m}{2\hbar^2}\left(\frac{Ze^2}{4\pi\varepsilon_0}\right)^2 \frac{1}{n^2} \tag{1.78}$$

Taking $Z = 1$ for atomic hydrogen and using the Bohr frequency relation [1.70], the frequencies of light emitted in a transition between two levels a and b are

$$\nu_{\mathrm{ab}} = \frac{m}{4\pi\hbar^3}\left(\frac{e^2}{4\pi\varepsilon_0}\right)^2 \left(\frac{1}{n_{\mathrm{a}}^2} - \frac{1}{n_{\mathrm{b}}^2}\right), \; n_{\mathrm{b}} > n_{\mathrm{a}} \tag{1.79}$$

in agreement with [1.61] provided R is taken to be

$$R(\infty) = \frac{m}{4\pi\hbar^3}\left(\frac{e^2}{4\pi\varepsilon_0}\right)^2 \tag{1.80}$$

Here we have written $R(\infty)$ to recall that we are using the infinite nuclear mass approximation.

If instead of frequencies we use wave numbers $\tilde{\nu}_{\mathrm{ab}}$ we have

$$\tilde{\nu}_{\mathrm{ab}} = \tilde{R}(\infty)\left(\frac{1}{n_{\mathrm{a}}^2} - \frac{1}{n_{\mathrm{b}}^2}\right), \; n_{\mathrm{b}} > n_{\mathrm{a}} \tag{1.81}$$

where

$$\tilde{R}(\infty) = \frac{m}{4\pi c\hbar^3}\left(\frac{e^2}{4\pi\varepsilon_0}\right)^2 \tag{1.82}$$

Evaluating $\tilde{R}(\infty)$ we find

$$\tilde{R}(\infty) = 109\,737 \text{ cm}^{-1} \qquad [1.83]$$

in good, but not perfect, agreement with the experimental value [1.63].

Returning to equation [1.78], we see that the energy levels of a one-electron atom are given by

$$E_n = -I_P/n^2, \qquad n = 1, 2, 3 \ldots \qquad [1.84]$$

where I_P is given by

$$I_P = \frac{1}{2}\frac{m}{\hbar^2}\left(\frac{Ze^2}{4\pi\varepsilon_0}\right)^2 = 13.6\, Z^2 \text{ eV} \qquad [1.85]$$

The level with the lowest energy is known as the ground state and has $n = 1$. If the atom absorbs an energy greater than I_P, the energy of the electron becomes positive and the electron is ejected from the atom. The quantity I_P is known as the *ionisation potential*, and the value (13.6 eV) can be verified by experiments in which hydrogen atoms are ionised either by absorbing photons or in collision processes. An energy level diagram for hydrogen, showing series of spectral lines is shown in Fig. 1.16. The quantum number n is called the *principal quantum number* to distinguish it from other quantum numbers that we shall meet later. A commonly used notation is one in which an electron in a level with $n = 1$ is said to be in the K shell. Correspondingly if $n = 2$ or $n = 3$, the electron is said to be in the L or M shells respectively.

Atomic units

The radius of the orbit of the electron in the ground state of hydrogen is known as the first Bohr radius of hydrogen and is denoted by the symbol a_0

$$a_0 = \frac{(4\pi\varepsilon_0)\hbar^2}{me^2} = 5.29 \times 10^{-11} \text{ m} \qquad [1.86]$$

In atomic physics, it has proved to be extremely useful to introduce a set of units, called *atomic units* (a.u.) in which a_0 is taken as the unit of length. Correspondingly the mass of the electron is employed as the unit of mass and $\hbar$ as the unit of angular momentum. To complete the system the unit of charge is taken to be the absolute magnitude e of the electronic charge and the permittivity of free space ε_0 is $1/4\pi$. In atomic units ($m = \hbar = e = 1$, $4\pi\varepsilon_0 = 1$), we have

$$E_n = -\tfrac{1}{2}Z^2/n^2 \text{ a.u.} \qquad [1.87]$$

The ground state energy of hydrogen ($Z = 1, n = 1$) is $-\frac{1}{2}$ a.u., from which we see that the atomic unit of energy is equivalent to 27.2 eV. The atomic unit of

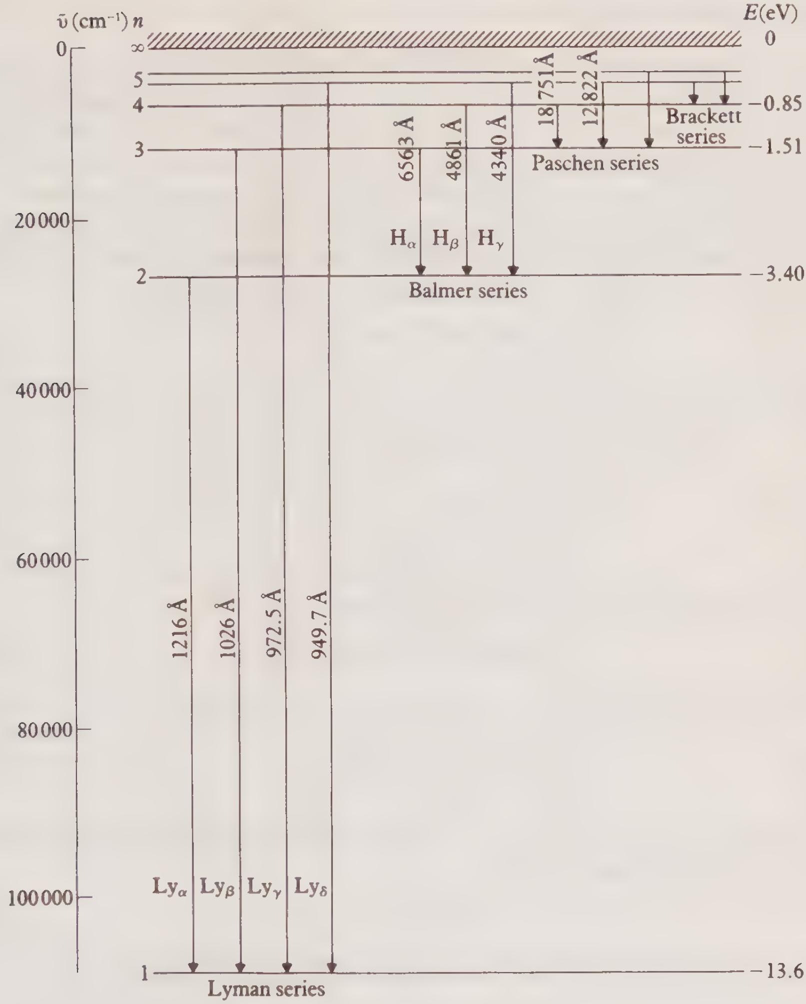

1.16 The spectrum of atomic hydrogen.

velocity is equal to the velocity v_0 of the electron in the first Bohr orbit of hydrogen. From [1.74] we see that

$$v_0 = \frac{e^2}{(4\pi\varepsilon_0)\hbar} = \alpha c \qquad [1.88]$$

where we have introduced the dimensionless constant

$$\alpha = \frac{e^2}{(4\pi\varepsilon_0)\hbar c} \qquad [1.89]$$

which is known as the *fine-structure constant* and has the value $\alpha \simeq 1/137$. Thus we see that in atomic units the velocity of light is $c \simeq 137$ a.u. Further details concerning atomic units can be found in Appendix 11.

Finite nuclear mass

Although the approximation, in which the nucleus is assumed to be infinitely heavy and at rest, is good enough for many purposes, a distinct improvement can be made if we allow the nucleus to move. In this case, both the nucleus A of mass M and the electron B of mass m rotate about the centre of mass of the system C as in Fig. 1.17. In the absence of forces external to the atom, the centre of mass will either be at rest, or in uniform motion, according to Newton's law. The distance AB is again denoted by r and the angular velocity of the line AB about an axis through C by ω. Since C is the centre of mass

$$M \times \mathrm{AC} = m \times \mathrm{CB} \qquad [1.90]$$

from which

$$\begin{aligned} \mathrm{AC} &= \left(\frac{m}{M+m}\right)r \\ \mathrm{CB} &= \left(\frac{M}{M+m}\right)r \end{aligned} \qquad [1.91]$$

The total angular momentum of the system is

$$L = m\omega \mathrm{CB}^2 + M\omega \mathrm{AC}^2 = \mu\omega r^2 \qquad [1.92]$$

where

$$\mu = \frac{mM}{m + M} \qquad [1.93]$$

is the reduced mass. Putting $r\omega = v$, where v is the velocity of the electron with respect to the nucleus, we have

$$L = \mu v r = n\hbar, \qquad n = 1, 2, 3, \ldots \qquad [1.94]$$

which is the same as equation [1.73] but with μ replacing m.

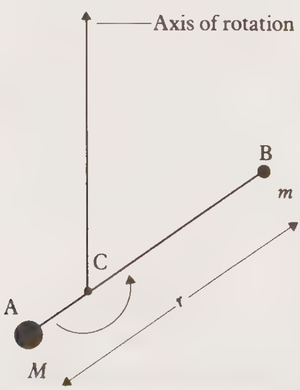

1.17 Bohr model with finite nuclear mass.

The centripetal force acting on the electron B is of magnitude

$$mCB\omega^2 = \mu\omega^2 r \tag{1.95}$$

and this is to be equated with the Coulomb force

$$\mu\omega^2 r = \frac{\mu v^2}{r} = \left(\frac{Ze^2}{4\pi\varepsilon_0}\right)\frac{1}{r^2} \tag{1.96}$$

This is the same equation of motion as before, but with μ replacing m.

The kinetic energy of the system is

$$T = \tfrac{1}{2}(M + m)v_{\mathrm{CM}}^2 + \tfrac{1}{2}\mu v^2 \equiv T_{\mathrm{CM}} + T_{\mathrm{I}} \tag{1.97}$$

where v_{CM} is the velocity of the centre of mass, and T_{I} is the internal (or relative) kinetic energy. A bound state energy E_n is defined as the difference between the total energy and the kinetic energy T_{CM} of the centre of mass,

$$E_n = T_{\mathrm{I}} + V = \tfrac{1}{2}\mu v^2 - \left(\frac{Ze^2}{4\pi\varepsilon_0}\right)\frac{1}{r} \tag{1.98}$$

so that E_n is given by [1.78] with μ replacing m

$$E_n = -\frac{\mu}{2\hbar^2}\left(\frac{Ze^2}{4\pi\varepsilon_0}\right)^2\frac{1}{n^2} \tag{1.99}$$

Similarly the allowed values of r are given by [1.75] with, again, μ replacing m

$$r = \frac{(4\pi\varepsilon_0)\hbar^2 n^2}{Ze^2\mu} = \frac{n^2}{Z}\frac{m}{\mu}a_0 = \frac{n^2}{Z}a_\mu \tag{1.100}$$

where we have defined

$$a_\mu = a_0\frac{m}{\mu} \tag{1.101}$$

The Rydberg constant for a nucleus of mass M can be written immediately in terms of $R(\infty)$ and $\tilde{R}(\infty)$ by

$$R(M) = \frac{\mu}{m}R(\infty) \quad \text{and} \quad \tilde{R}(M) = \frac{\mu}{m}\tilde{R}(\infty) \tag{1.102}$$

For hydrogen $M = M_{\mathrm{p}}$, where M_{p} is the mass of the proton and $\tilde{R}(M_{\mathrm{p}}) = 109\,681\ \mathrm{cm}^{-1}$ which agrees with the experimental value [1.63] to better than 4 parts in 10^5.

Because of the nuclear mass effect there is an *isotopic shift* between the spectral lines of different isotopes of the same atom. For example, there is such a shift between the spectrum of atomic deuterium, which has a nucleus with $Z = 1$ but containing a proton and a neutron (so that its mass $M \simeq 2M_{\mathrm{p}}$) and that of atomic hydrogen. The ratio of frequencies of corresponding lines is 1.000 27, which is easily detectable, and in fact through this the discovery of the deuteron was made.

One-electron atoms

By taking $Z = 2, 3, 4, \ldots$, the Bohr model predicts the energy levels (and hence the line spectra) of all the ions containing one electron with a nucleus of charge Ze. The observed frequencies agree closely with the Bohr formula [1.79] until Z becomes large ($Z \gtrsim 20$). The orbital velocity of the electron in the ground state divided by the velocity of light is such that (see [1.74] and [1.89])

$$\frac{v}{c} = \alpha Z \simeq \frac{Z}{137} \tag{1.103}$$

so it is to be expected that, for large Z, relativistic effects will be significant. In Table 1.2, the values of $\tilde{R}(M)$ are shown for a few hydrogenic ions together with the wavelengths of the lines corresponding to the $n = 2$ to $n = 1$ transition, which are known as *resonance lines*.

Table 1.2 Rydberg constants for some hydrogenic systems and the wavelengths of the resonance lines $n = 2 \rightarrow n = 1$

	Wavelength of the transition (Å)	$\tilde{R}(M)(\text{cm}^{-1})$
H I†	1215.664	109 677.58
D I	1215.336	109 707.19
He II	303.779	109 772.26
Li III	134.994	109 728.72
C VI	33.734	109 732.29
O VIII	18.967	109 733.54

† The Roman numeral indicates the degree of ionisation. I denotes the neutral atom, II an atom from which one electron has been ionised and so on.

The Franck and Hertz experiment

The Bohr model predicts that the energy levels of atoms are quantised and only certain discrete values of the total energy are allowed. This can be confirmed rather directly by an experiment originally devised by J. Franck and G. Hertz in 1914. A schematic diagram of the apparatus is shown in Fig. 1.18. In the first

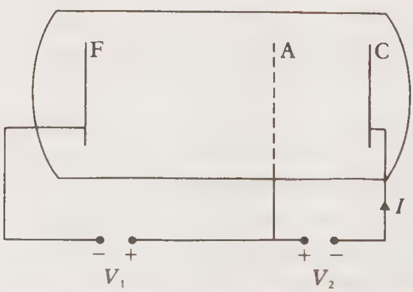

1.18 Schematic diagram of Franck and Hertz's experiment.

stage of the experiment, the apparatus is evacuated. A filament F is heated so that it emits electrons, which are attracted to and pass through a wire grid, A, which is maintained at a positive potential V_1 with respect to the filament. The electrons accelerated by the potential V_1 attain a kinetic energy $mv^2/2 = eV_1$. After passing through the grid they are collected by a plate C and cause a current I to flow in the circuit. The plate C is maintained at a small negative voltage V_2, where $|V_2| \ll V_1$, with respect to the grid A. The small voltage V_2 has the effect of reducing the kinetic energy of the electrons slightly, but not enough to stop them being collected.

The apparatus is now filled with mercury vapour. The electrons collide with the atoms of mercury, and if the collisions are elastic, so that there is no transfer of energy from the electrons to the internal structure of the atoms, the current I will be unaffected by the introduction of the gas. This follows because mercury atoms are too heavy to gain appreciable kinetic energy when struck by an electron. The electrons are deflected but retain the same kinetic energy. In contrast, if an electron makes an inelastic collision with a mercury atom in which it loses an energy E, exciting the mercury atom to a level of greater internal energy, then its final kinetic energy will be $mv_1^2/2 = (eV_1 - E)$. If eV_1 is equal to E, or is only a little larger, the retarding potential V_2 will be sufficient to prevent the electron from reaching the collecting plate and it will no longer contribute to the current I.

The experiment is carried out by gradually increasing V_1 from zero and measuring the current I as a function of V_1. The result obtained is shown diagrammatically in Fig. 1.19. The current I is seen to fall sharply at a potential V_R, which is known as the resonance potential, and which is (for Hg) 4.9 V. The results can be interpreted by supposing that for $eV_1 < 4.9$ eV the atom cannot absorb the energy of the electrons and the collisions are elastic, while exactly 4.9 eV above its ground state, mercury atoms possess another discrete energy level. When eV_1 reaches this value, a large number of the colliding electrons excite atoms to this level, losing their energy in the process, and reducing the current I sharply.

If the voltage V_1 is increased the current again increases, and further sharp falls are seen. Some of these are due to electrons having sufficient energy to

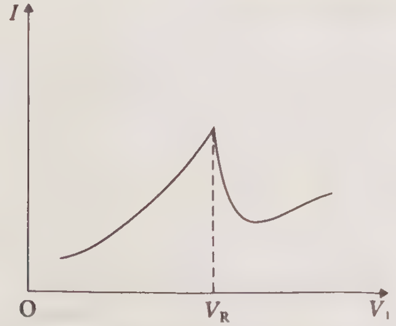

1.19 The current variation with voltage in a Franck–Hertz experiment.

excite two or more atoms to the 4.9 eV level; but others are due to the excitation of higher discrete levels. We have seen that 1 eV corresponds to a frequency of 8065 cm^{-1}, so if this interpretation is correct, a line would be expected in the mercury spectrum corresponding to a transition from the first excited state at 4.9 eV to the ground state, with a frequency of $4.9 \times 8065 \text{ cm}^{-1} \simeq 39500 \text{ cm}^{-1}$. Franck and Hertz were indeed able to verify the existence of such a line, and also to show that radiation of this frequency was only emitted from the vapour when V_1 exceeded 4.9 V.

This experiment, and corresponding experiments using other gases and vapours, provide excellent confirmation of the discrete nature of bound state energy levels. It can also be demonstrated that when sufficient energy is available to ionise an atom, the energy of the ejected electron can take any positive value, so we can say that *the energy level spectrum of an atom consists of two parts: discrete negative energies corresponding to bound states and a continuum of positive energies corresponding to unbound (ionised) states.*

Limitations of the Bohr model

Although the planetary model of the hydrogen atom is rather successful, and the idea of quantised atomic energy is correct, the model is unsatisfactory in many respects. Firstly, it cannot be generalised to deal with systems of two or more electrons. In addition, the assumptions made, and in particular, the hypothesis that only circular orbits are allowed, are inexplicable and arbitrary. Among other objections are the lack of any method to calculate the rate of transitions between the different energy levels when radiation is emitted or absorbed, and the inability to handle unbound systems. In later work, W. Wilson and A. Sommerfeld showed how to remove the restriction to circular orbits and Sommerfeld also obtained relativistic corrections to the Bohr model. However, the other objections still persisted, and the theory – called *the old quantum theory* – remained restricted in scope. It was eventually superseded by the quantum mechanics developed by E. Schrödinger, W. Heisenberg and others, following the ideas of L. de Broglie.

X-ray spectra and Moseley's law

Despite the general inability of the Bohr model to describe many-electron systems, it was able to provide an illuminating explanation of the regularities in X-ray spectra observed by H. Moseley in 1913. In an X-ray tube the radiation is emitted from a target bombarded by high energy electrons. The X-ray region may be taken to be in the range of wavelengths from 0.1 to 10 Å corresponding to photon energies from a few keV to several hundred keV (see Fig. 1.9). The spectrum observed is characteristic of the material used as the target in the tube and consists of a continuous spectrum upon which is superimposed a line spectrum. Moseley studied the line spectra of 39 elements from aluminium (the lightest) to gold (the heaviest). All the spectra were remarkably similar. In most

cases, the spectrum consisted of two groups of lines, the K series and the L series; for a given element the L lines being at lower frequencies than the K lines. For heavier elements other series of lines appeared at still lower frequencies.

Moseley found that the frequency ν_n of the nth line of each series varied smoothly with the atomic number of the target element, Z. By plotting $\sqrt{\nu_n}$ against Z, he established the law

$$\sqrt{\nu_n} = C_n(Z - \sigma) \tag{1.104}$$

where C_n is independent of Z, and σ is in the range 1 to 2 for the K series and is in the range 7.4 to 9.4 for the L series. An example is the K line of lowest frequency, the K_α line, for which the *Moseley plot* is shown in Fig. 1.20. Since plots of $\sqrt{\nu_n}$ against Z were smoother than those against the atomic weight μ, this suggested that Z had a fundamental significance. At this time the atomic number had no significance other than giving the position of an element in Mendeleev's periodic table. In the main the ordering of the elements of the table was given by their atomic weights μ, although Mendeleev found that certain pairs had to be reversed in order to preserve the periodicity of the chemical properties. For example in order of weights the 18th element is potassium ($\mu = 39.102$) and the 19th argon ($\mu = 39.948$). This arrangement puts potassium in the rare gas column and argon in the alkali metal column and to preserve the chemical periodicity argon has to be assigned the atomic number 18 and potassium 19.

An explanation of the significance of Z was given by Moseley in terms of the Bohr model, which had been published a year before. He first argued that in the high energy electron bombardment of the target atoms, the inner (tightly bound) electrons are ejected leaving vacancies. The X-rays are emitted when a less tightly bound electron makes a transition, filling a vacancy. Since the

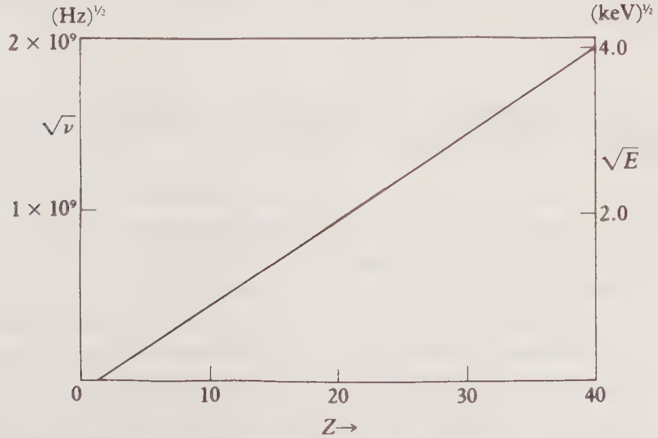

1.20 A Moseley plot of $\sqrt{\nu}$ against Z for the K_α line in the X-ray spectrum. A scale in $\sqrt{E}$, with E in keV, is shown on the right-hand side of the figure.

transitions concern tightly bound electrons in orbits close to the nucleus, the effective potential experienced by these electrons is due mainly to the Coulomb field of the nucleus, screened to a small extent by the other electrons. The atomic number Z was known to be approximately equal to $\mu/2$ and the experiments of Geiger and Marsden had shown that the nuclear charge was also approximately $\mu/2$. This suggested the identification of Z with the nuclear charge and $(Z - \sigma)$ as an effective charge, σ allowing for screening of the nucleus by other electrons. Using the Bohr formula for the energy levels of one electron moving in a Coulomb field with charge $(Z - \sigma)$, the frequencies of the spectrum are given by

$$\nu_{mn} = R(Z - \sigma)^2 \left(\frac{1}{m^2} - \frac{1}{n^2}\right) \qquad [1.105]$$

where n and m are both integers and $n > m$. The K series of lines can be attributed to transitions in which the final energy level has $m = 1$ (the K shell). The line of longest wavelength in the K series is the K_α line, and for this $n = 2$. The L series of lines are those in which the vacancy occurs in the $m = 2$ level (the L shell) and the line of longest wavelength corresponds to $n = 3$.

By interpreting the regularities he had observed in the X-ray spectra in this way, Moseley was able to establish the critical identification of Z, the atomic number, with the nuclear charge, and to show that the Bohr model could be applied to the most tightly bound inner electrons of an atom, which move in a potential dominated by the nuclear Coulomb field. It is interesting to note that in plotting his results Moseley found that to avoid breaks in his curve, he had to postulate the existence of four, hitherto unknown, elements with $Z = 43$, 61, 72 and 75. These were discovered subsequently.

A further discussion of X-ray spectra is given in Chapter 8. The optical spectra of many-electron atoms are much more complicated and cannot be interpreted so easily, since the outer electrons move in potentials which are not strongly dominated by the nuclear potential.

1.8 THE STERN–GERLACH EXPERIMENT – ANGULAR MOMENTUM AND SPIN

We shall now discuss an experiment of fundamental importance, carried out by O. Stern and W. Gerlach in 1922, to measure the magnetic dipole moments of atoms. The results demonstrated, once more, the inability of classical mechanics to describe atomic phenomena and confirmed the necessity of a quantum theory of angular momentum, which had been suggested by Bohr's model.

Let us first understand how an atom comes to possess a magnetic moment. In the Bohr model of a hydrogenic atom, an electron occupies a circular orbit, rotating with an orbital angular momentum $\mathbf{L}$. A moving charge is equivalent to an electric current, so that an electron moving in a closed orbit forms a current loop, and this in turn creates a magnetic dipole (Duffin, 1968). In fact whatever

model of atomic structure we make, the electrons can be expected to possess angular momentum and accordingly atoms possess magnetic moments.

A circulating current of magnitude I enclosing a small plane area $\mathrm{d}A$ gives rise to a magnetic dipole moment

$$\boldsymbol{\mathcal{M}} = I\,\mathrm{d}\mathbf{A} \qquad [1.106]$$

where the direction of $\mathrm{d}\mathbf{A}$ is along the normal to the plane of the current loop, as shown in Fig. 1.21.

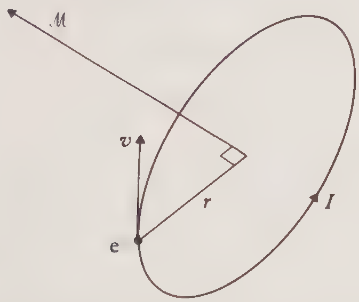

1.21 The magnetic dipole due to a current loop.

When the current is due to an electron moving with a velocity v in a circle of radius r, I is given by

$$I = \frac{ev}{2\pi r} \qquad [1.107]$$

Since the area enclosed is πr^2, we have $\mathcal{M} = evr/2 = eL/2m$, and as the direction of the current is opposite to the direction of rotation of the electron

$$\boldsymbol{\mathcal{M}} = -\left(\frac{e}{2m}\right)\mathbf{L} \qquad [1.108]$$

The Bohr quantisation rule [1.73] suggests that $\hbar$ is a natural unit of angular momentum, so we can write

$$\boldsymbol{\mathcal{M}} = -\mu_{\mathrm{B}}(\mathbf{L}/\hbar) \qquad [1.109]$$

where

$$\mu_{\mathrm{B}} = \frac{e\hbar}{2m} \qquad [1.110]$$

Because $(\mathbf{L}/\hbar)$ is dimensionless, μ_{B} has the dimensions of a magnetic moment. It is known as the *Bohr magneton* and has the numerical value

$$\mu_{\mathrm{B}} = 9.27 \times 10^{-24}\ \mathrm{JT}^{-1} \qquad [1.111]$$

Quite generally, a system of electrons possessing a total angular momentum $\mathbf{J}$ has a magnetic moment $\boldsymbol{\mathcal{M}}$ antiparallel to $\mathbf{J}$, and it is usual to write

$$\boldsymbol{\mathcal{M}} = -g\mu_B(\mathbf{J}/\hbar) \qquad [1.112]$$

where g is a dimensionless constant called a *gyromagnetic ratio*.

Interaction with a magnetic field

If an atom with a magnetic moment $\boldsymbol{\mathcal{M}}$ is placed in a magnetic field $\boldsymbol{\mathcal{B}}$, the energy of interaction (potential energy) is (see Duffin, 1968)

$$W = -\boldsymbol{\mathcal{M}} \cdot \boldsymbol{\mathcal{B}} \qquad [1.113]$$

The system experiences a torque $\boldsymbol{\Gamma}$, where

$$\boldsymbol{\Gamma} = \boldsymbol{\mathcal{M}} \times \boldsymbol{\mathcal{B}} \qquad [1.114]$$

and a net force $\mathbf{F}$, where

$$\mathbf{F} = -\boldsymbol{\nabla} W \qquad [1.115]$$

Combining [1.113] with [1.115] we see that the components of $\mathbf{F}$ are

$$F_x = \boldsymbol{\mathcal{M}} \cdot \frac{\partial \boldsymbol{\mathcal{B}}}{\partial x}; \qquad F_y = \boldsymbol{\mathcal{M}} \cdot \frac{\partial \boldsymbol{\mathcal{B}}}{\partial y}; \qquad F_z = \boldsymbol{\mathcal{M}} \cdot \frac{\partial \boldsymbol{\mathcal{B}}}{\partial z} \qquad [1.116]$$

In a magnetic field that is uniform, no net force is experienced by a magnetic dipole, which precesses with a constant angular frequency. For an orbiting electron this angular frequency is (see [1.108], [1.109] and [1.114])

$$\omega_L = \frac{\mu_B}{\hbar} \mathcal{B} \qquad [1.117]$$

It is called the *Larmor angular frequency*. On the other hand, in an inhomogeneous field an atom experiences a net force proportional to the magnitude of the magnetic moment.

The Stern–Gerlach experiment

In 1921, Stern suggested that magnetic moments of atoms could be measured by detecting the deflection of an atomic beam by such an inhomogeneous field. The experiment was carried out a year later by Stern and Gerlach. The apparatus is shown in schematic form in Fig. 1.22.

The first experiments were made using atoms ot silver. A beam is produced by heating the metallic vapour in an enclosure, which is situated in an evacuated region into which the silver atoms stream through a small hole. The beam can be collimated with a system of slits and passed between the poles of a magnet shaped to produce an inhomogeneous field, as shown in the figure. The beam is then detected by allowing it to fall on a cool plate. The density of the deposit is proportional to the intensity of the beam and to the length of time for which the beam falls on the plate.

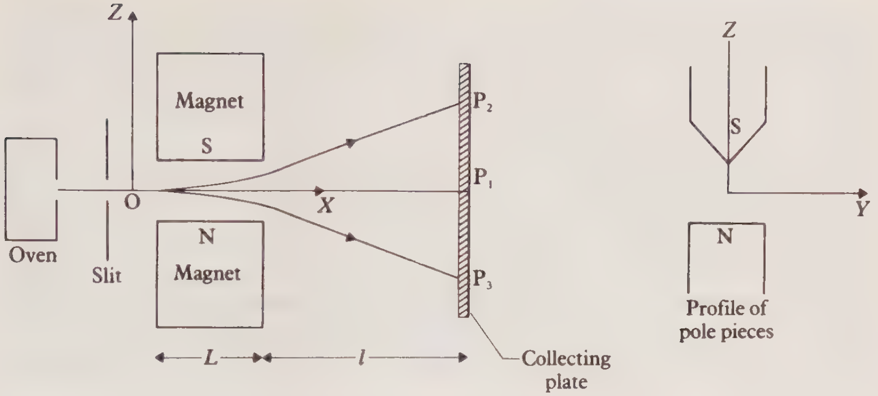

1.22 The Stern–Gerlach apparatus.

Taking the shape of the magnets as shown in Fig. 1.22, the force on each atom is given by (see [1.116])

$$F_x = \mathcal{M}_z \frac{\partial \mathcal{B}_z}{\partial x}; \qquad F_y = \mathcal{M}_z \frac{\partial \mathcal{B}_z}{\partial y}; \qquad F_z = \mathcal{M}_z \frac{\partial \mathcal{B}_z}{\partial z} \qquad [1.118]$$

The magnet is symmetrical about the XZ plane and the beam is confined to this plane. It follows that $\partial\mathcal{B}_z/\partial_y = 0$. Also, apart from edge effects, $\partial\mathcal{B}_z/\partial x = 0$, so that the only force on the atoms in the beam is in the Z direction.

In the incident beam, the direction of the magnetic moment $\boldsymbol{\mathcal{M}}$ of the atoms will be completely at random and in the Z direction it would be expected that every value of $\mathcal{M}_z$ would occur in the interval $-\mathcal{M} \leqslant \mathcal{M}_z \leqslant \mathcal{M}$, with the consequence that the deposit on the collecting plate would be spread over a region symmetrically disposed about the point of no deflection. The surprising result that Stern and Gerlach obtained in their experiments on silver, was that two distinct and separate lines were formed on the plate (see Fig. 1.23), symmetrically about the point of no deflection. Similar results were found for atoms of copper and gold, and in later work, for sodium, potassium and hydrogen.

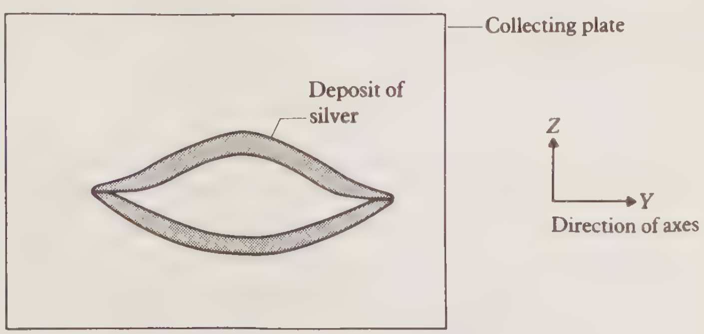

1.23 Results of the Stern–Gerlach experiment for silver.

The quantisation of the component of the magnetic moment along the direction defined by the magnetic field is termed *space quantisation*. This implies that the component of the angular momentum in a certain direction is quantised so that it can only take certain values. In general for each type of atom, the values of $\mathcal{M}_z$ will range from $(\mathcal{M}_z)_{\max}$ to $-(\mathcal{M}_z)_{\max}$ and correspondingly L_z will range from $-(L_z)_{\max}$ to $(L_z)_{\max}$. If we denote the observed multiplicity of values of $\mathcal{M}_z$ (and hence L_z) by α we can try to interpret α and to deduce the allowed values of L using the Bohr model. Indeed, the Bohr quantisation of angular momentum suggests that orbital angular momentum only occurs in integral units of $\hbar$. We may postulate that the magnitude of orbital angular momentum can only take values $L = l\hbar$, where l is positive integer or zero. Thus the maximum value of L_z is $+l\hbar$ and its minimum value $-l\hbar$. If L_z is also quantised in the form

$$L_z = m\hbar \qquad [1.119]$$

where m is a positive or negative integer or zero, then m must take on the values $-l, -l + 1, \ldots, l - 1, l$ and the multiplicity α must be equal to $(2l + 1)$. The number m is known as a *magnetic quantum number*. In fact as we shall see in the next chapter, this result turns out to be correct in quantum mechanics, with the difference that the possible values of the total orbital angular momentum are of the form $L = \sqrt{l(l+1)}\hbar$ with $l = 0, 1, 2, \ldots$ rather than of the form $L = l\hbar$ suggested by the Bohr model. However the results of Stern and Gerlach for silver do not fit with this scheme, since the multiplicity of values of the Z component of the angular momentum for silver is 2. This implies a total angular momentum $(2l + 1) = 2$ giving $l = \frac{1}{2}$, a non-integral value.

Electron spin

The explanation of this result for silver came in 1925, when S. Goudsmit and G. E. Uhlenbeck showed that the splitting of spectral lines occurring when atoms are placed in a magnetic field (the Zeeman effect) could be explained if electrons possess an *intrinsic magnetic moment* $\boldsymbol{\mathcal{M}}_s$ in addition to the magnetic moment produced by orbital motion, where the component of $\boldsymbol{\mathcal{M}}_s$ in a given direction can take the two values $\pm\mathcal{M}_s$ only. We can postulate that this magnetic moment is due to an *intrinsic angular momentum*, or *spin*, of the electron, which we denote by $\mathbf{S}$. By analogy with [1.112], we then have

$$\boldsymbol{\mathcal{M}}_s = -g_s\mu_B\mathbf{S}/\hbar \qquad [1.120]$$

where g_s is the *spin gyromagnetic ratio*. If we introduce a spin quantum number s, analogous to l, so that the multiplicity of the spin component in a given direction is $(2s + 1)$, we must have $s = \frac{1}{2}$ and the possible values of the component of the spin $\mathbf{S}$ in the Z direction are $\pm\hbar/2$, while the magnitude of the spin is $\sqrt{s(s+1)}\hbar = \sqrt{\frac{3}{4}}\hbar$. The Stern–Gerlach results are then explained if we assume that the orbital angular momentum of a silver atom is zero, but its spin angular momentum is given by $s = \frac{1}{2}$.

We have seen that the magnetic moment of an electron is due partly to its orbital angular momentum and partly to its spin angular momentum, and we can write

$$\boldsymbol{\mathcal{M}} = -\mu_B(\mathbf{L} + g_s\mathbf{S})/\hbar \qquad [1.121]$$

Measurements of the magnitude of $\boldsymbol{\mathcal{M}}$ for atomic hydrogen have shown that the electron spin gyromagnetic ratio is $g_s = 2$. The discovery of this intrinsic property of the electron is of fundamental importance. In fact, it is now known that all particles can be assigned an internal angular momentum. In some cases, such as the pion (π meson) it is zero, but in others, such as the electron, the proton, the neutron, it is one-half (i.e. $s = \frac{1}{2}$) and for other elementary particles it may be $s = 1$, $s = \frac{3}{2}$, . . .

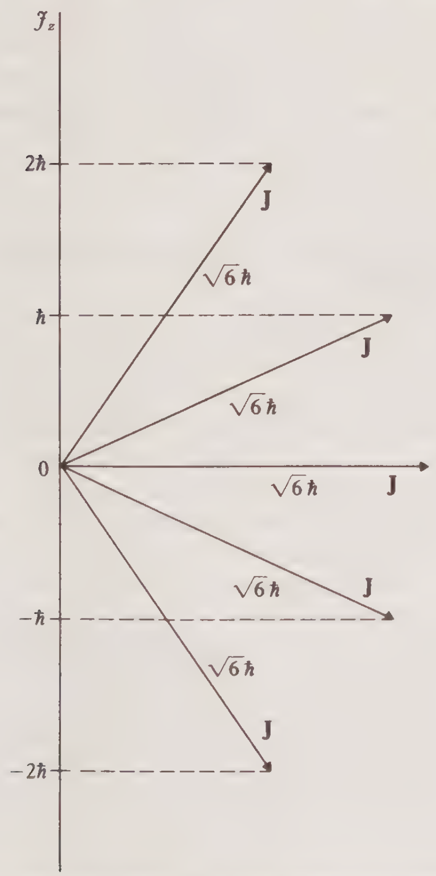

1.24 Precession of the angular momentum **J** about the axis of quantisation for the case $j = 2$.

Angular momentum

In general the total angular momentum of an atom is the result of adding vectorially all spin and orbital angular momenta of the electrons it contains. If the total angular momentum is $\mathbf{J}$, then a measurement of the component of $\mathbf{J}$ in the Z direction can only provide $(2j + 1)$ values, given by $m_j\hbar$, where the *magnetic quantum number* m_j can take the values $-j, -j + 1, \ldots j - 1, j$. It is found that j can take integral or half-integral values only; $j = 0, \frac{1}{2}, 1, \frac{3}{2} \ldots$. For an angular momentum whose component in a given direction has the multiplicity $(2j + 1)$, a measurement of the magnitude of the angular momentum produces the value $\sqrt{j(j + 1)}\hbar$. Thus, in a Stern–Gerlach experiment, a beam of atoms with angular momentum of magnitude $\sqrt{j(j + 1)}\hbar$ will produce $(2j + 1)$ spots on the detecting screen, symmetrically disposed about the point of zero deflection.

Another property of angular momentum in quantum mechanics (which will be discussed in Chapter 2), is that there is a limitation on the precision with which simultaneous measurements of two (or three) components of an angular momentum can be measured. In fact, if the value of the Z component is known precisely, the values of the x and y components are indefinite, but on the *average* are zero. This situation is often represented by *a vector model* in which the angular momentum vector $\mathbf{J}$ of length $\sqrt{j(j + 1)}\hbar$, precesses about the Z axis such that J_z has one of the $(2j + 1)$ values $m_j\hbar$. This is shown in Fig. 1.24 for the particular case $j = 2$.

1.9 DE BROGLIE'S HYPOTHESIS AND THE GENESIS OF WAVE MECHANICS

In our brief historical survey, we have seen how, as knowledge of atomic structure increased, evidence accumulated that a description in terms of classical physics – Newton's laws of mechanics and Maxwell's electromagnetic equations – was inadequate. Electromagnetic radiation displays particle as well as wave characteristics; the energy of the field being quantised, each packet of energy $h\nu$ being carried by a photon. On the other hand, the energy levels and angular momenta of bound electrons in atoms are also quantised; in contrast beams of electrons moving under electric and magnetic fields, as in Thomson's experiments, behave like classical charged particles.

In 1924, L. de Broglie made a great unifying, but speculative, hypothesis, that just as radiation has particle-like properties, electrons and other material particles possess wave-like properties. The energy of a photon is given by $E = h\nu$, where ν is the frequency and the corresponding momentum is $p = h\nu/c = h/\lambda$ where λ is the wavelength. For free material particles, de Broglie assumed that the associated wave also has a frequency ν and a wavelength λ, related to the energy E and the momentum p of the particle by

$$\nu = \frac{E}{h} \qquad [1.122]$$

and

$$\lambda = \frac{h}{p} \qquad [1.123]$$

In particular, for a particle of mass m moving at a non-relativistic speed v, one has $p = mv$ so that $\lambda = h/mv$.

This idea immediately gives a *qualitative* explanation of the quantum condition [1.73], used in the Bohr model of the hydrogen atom. Indeed, let us suppose that an electron in a hydrogenic atom moves in a circular orbit of radius r, with velocity v. If this is to be a stable stationary state, the wave associated with the electron must be a standing wave and a whole number of wavelengths must fit in to the circumference $2\pi r$. Thus

$$n\lambda = 2\pi r \qquad n = 1, 2, 3, \ldots \qquad [1.124]$$

Since $\lambda = h/p$ and $L = rp$, we immediately find the condition

$$L = nh/2\pi = n\hbar \qquad [1.125]$$

which is identical with [1.73]. Later, in 1925, these qualitative ideas were incorporated into the systematic theory of quantum mechanics developed by Schrödinger, which will be discussed in the next chapter.

When waves are scattered or pass through slits, which have dimensions comparable to their wavelength, interference and diffraction effects are observed. Now, as seen from [1.123], the *de Broglie wavelengths* associated with electrons of energy 1, 10 and 100 eV are, respectively, 12, 3.9 and 1.2 Å (where 1 Å = 10^{-10} m). Thus, in macroscopic situations, as in Thomson's experiments, the de Broglie electron wavelengths are exceedingly small compared with the dimensions of any obstacles or slits in the apparatus and no interference or diffraction effects can be observed. However, the spacing of atoms in a crystal lattice is of the order of a few angstroms and in 1927 C. J. Davisson and L. H. Germer showed that electron beams could be diffracted when scattered from crystals, and displayed the predicted wave properties.

Electron diffraction

In the Davisson and Germer experiment, a beam of monenergetic electrons is directed to strike the surface of a crystal of nickel normally, and the number of electrons $N(\theta)$ scattered at an angle θ to the incident direction are measured (see Fig. 1.25). The electron beam energy employed was 54 eV. The scattered intensity is shown in Fig. 1.26. It falls from a maximum at $\theta = 0°$ to a minimum near 35°, then rises to a peak near 50°. The strong scattering at $\theta = 0°$ is expected from either a particle or a wave theory, but the peak at 50° can only be explained by constructive interference of the waves scattered by the regular crystal lattice.

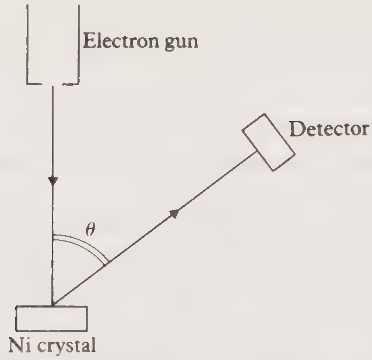

1.25 Schematic diagram of Davisson and Germer's experiment on the diffraction of electrons when scattered by a crystal of nickel.

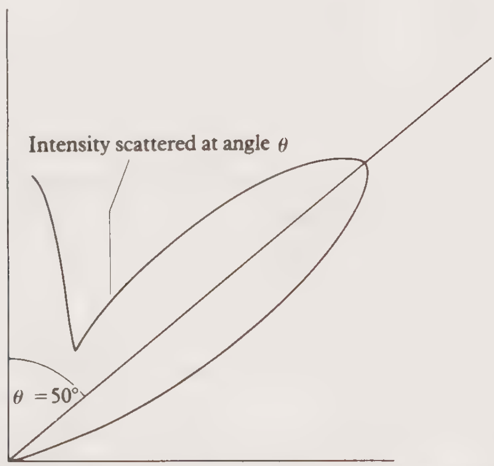

1.26 Polar diagram of the scattered intensity against angle of scattering for electrons of 54 eV in the Davisson–Germer experiment.

If the atoms in the crystal are spaced at a distance d, then the Bragg condition for constructive interference at a scattering angle θ is (see Fig. 1.27)

$$n\lambda = d \sin \theta \quad \text{with} \quad n = 1, 2, 3 \ldots \qquad [1.126]$$

Experiments in which X-rays were diffracted established that for nickel, the atomic spacing is $d = 2.15$ Å. Assuming that the peak at 50° corresponds to first-order diffraction ($n = 1$), the corresponding electron wavelength must be $\lambda = (2.15 \sin 50°)$ Å $= 1.65$ Å. The wavelength of a 54 eV electron is 1.67 Å, which agrees with the value of 1.65 Å within the experimental error.

Subsequent experiments have confirmed the variation of λ with momentum predicted by the de Broglie formula [1.123]. Diffraction has also been demonstrated when atoms and neutrons are scattered by crystals. In all cases agreement has been found with de Broglie's hypothesis.

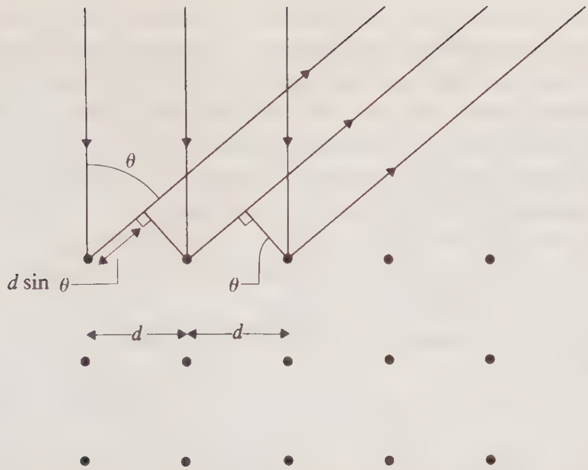

1.27 The Bragg condition. Low energy electrons are only scattered by atoms in the surface plane. The difference in path length for scattering angle θ is $d \sin \theta$ which must equal a whole number of wavelengths for constructive interference.

PROBLEMS

1.1 Consider a Thomson apparatus with the following dimensions

Length of the condenser plates: $x_1 = 0.1$ m
Distance from the plates to the screen: $x_2 = 0.45$ m
Distance between the plates: $d = 0.03$ m

When a voltage of 1500 V is applied between the plates, a deflection $y_2 = 0.2$ m is observed. This deflection is reduced to zero if a magnetic field $\mathcal{B} = 1.1 \times 10^{-3}$ T is applied.
(a) Find the velocity v of the electrons.
(b) Determine the value of e/m given by this experiment.

1.2 Show that the number $N(\lambda)\,d\lambda$ of standing electromagnetic waves (modes) in a large cube of volume V with wavelengths within the interval λ to $\lambda + d\lambda$ is given by $N(\lambda)\,d\lambda = 8\pi V\,d\lambda/\lambda^4$.

1.3 Using Planck's radiation law [1.30] for $\rho(\lambda)$, prove that

$$\lambda_{\max} T = \frac{hc}{4.965\, k}$$

where $\lambda_{\max}$ is the wavelength at which $\rho(\lambda)$ is a maximum. From this result and the values of h, c and k given in Appendix 11, obtain the constant b which occurs in Wien's displacement law [1.19].

1.4 Using Planck's radiation law [1.30] for $\rho(\lambda)$, prove that the total energy density ρ_{tot} is given by $\rho_{\text{tot}} = aT^4$, where $a = 8\pi^5 k^4/15h^3c^2$.

$$\left[\text{Hint:} \quad \int_0^\infty \frac{x^3}{e^x - 1}\,dx = \frac{\pi^4}{15}\right]$$

1.5 The photoelectric work function W for lithium is 2.3 eV.
(a) Find the threshold wavelength λ_t for the photoelectric effect.
(b) If ultraviolet light of wavelength $\lambda = 2000$ Å is incident on a lithium surface, obtain the maximum kinetic energy of the photoelectrons and the value of the stopping voltage V_0.

1.6 Consider black body radiation at absolute temperature T. Show that:
(a) The number of photons per unit volume is $N = 2.029 \times 10^7\ T^3$ photons/m^3. [Hint: $\int_0^\infty x^2(e^x - 1)^{-1}\,dx = 2.404\,11$]
(b) The average energy per photon is $\bar{E} = 3.73 \times 10^{-23}\ T$ joules $= 2.33 \times 10^{-4}\ T$ eV.

1.7 A photon of wavelength $\lambda_o = 0.708$ Å is incident on an electron which is initially at rest.
(a) What is the wavelength shift $\Delta\lambda$ at the photon scattering angle $\theta = 30°$?
(b) What is the angle ϕ (measured from the incident photon direction) at which the electron recoils?
(c) What is the kinetic energy T_2 of the recoiling electron?

1.8 Consider the Compton scattering of a photon of wavelength λ_0 by a free electron moving with a momentum of magnitude P in the same direction as that of the incident photon.
(a) Show that in this case the Compton equation [1.54] becomes

$$\Delta\lambda = 2\lambda_0 \frac{(p_0 + P)c}{E - Pc} \sin^2\frac{\theta}{2}$$

where $p_0 = h/\lambda_0$ is the magnitude of the incident photon momentum, θ is the photon scattering angle and $E = (m^2c^4 + P^2c^2)^{1/2}$ is the initial electron energy.
(b) What is the maximum value of the final electron momentum? Compare with the case $P = 0$ discussed in the text.
(c) Show that if the free electron initially moves with a momentum of magnitude P in a direction opposite to that of the incident photon, the wavelength shift is given by

$$\Delta\lambda = 2\lambda_0 \frac{(p_0 - P)c}{E + Pc} \sin^2\frac{\theta}{2}$$

1.9 Consider a photon of energy $E_0 = 2$ eV which is scattered from an electron having a kinetic energy $T = 20$ GeV (1 GeV $= 10^9$ eV) and moving initially in a direction opposite to that of the photon. What is the energy E_1 of the scattered photon? [Hint: use the result (c) of Problem 1.8]

1.10 Consider the scattering of an α particle of energy 10 MeV by an atomic electron, which we assume for simplicity to be initially at rest.
(a) What is the maximum momentum that can be transferred to the atomic electron?
(b) What is the maximum angle of deflection of the α particle?

1.11 Consider a Rutherford scattering experiment in which an α-particle of laboratory energy 10 MeV scatters from a gold nucleus ($Z = 79$).
(a) Find the distance of closest approach for a head-on collision.
(b) Using the results of Appendices 1 and 2, find the centre of mass scattering angle θ of the α particle if its impact parameter is $b = 8 \times 10^{-14}$ m.
(The mass of the α particle is $M_\alpha \simeq 4$ a.m.u. and the mass of the gold nucleus is $M_N \simeq 197$ a.m.u.)

1.12 Alpha particles of laboratory energy E are scattered by a copper nucleus ($Z = 29$) of mass $M_N \simeq 63$ a.m.u. and radius $R \simeq 5 \times 10^{-15}$ m. Find the value of E for which departures from Rutherford scattering occur for head-on collisions ($\theta = 180°$).

1.13 Using the infinite nuclear mass approximation in the Bohr model, obtain the wavelengths of the first four lines of the Lyman, Balmer and Paschen series for H, He^+, Li^{2+} and C^{5+}.

1.14 Consider a one-electron atom (or ion), the nucleus of which contains A nucleons (Z protons and $N = A - Z$ neutrons). The mass of that nucleus is given approximately by $M \simeq AM_p$, where $M_p \simeq 1.67 \times 10^{-27}$ kg is the proton mass. Using this value of M, obtain the relative correction $\Delta E/E$ to the Bohr energy levels due to the finite nuclear mass for the case of hydrogen ($A = 1$, $Z = 1$), deuterium ($A = 2$, $Z = 1$), tritium ($A = 3$, $Z = 1$), $^4He^+$ ($A = 4$, $Z = 2$) and $^7Li^{2+}$ ($A = 7$, $Z = 3$).

1.15 Calculate the difference in wavelengths $\Delta\lambda$ between the Balmer H_α lines in atomic hydrogen and deuterium.

1.16 Calculate the energy E_R with which an hydrogen atom recoils when emitting a photon in a transition from the $n = 4$ level to the $n = 1$ level, and show that E_R is negligible in comparison with the energy difference between the two levels.

1.17 Use Moseley's law [1.105] with $\sigma = 1$ for K lines and $\sigma = 7.4$ for L lines to
(a) Calculate the two longest wavelengths in the K series of Cu ($Z = 29$).
(b) Calculate the three longest wavelengths in the L series of gold ($Z = 79$).
(c) Find the element whose K_α line has the wavelength 0.723 Å.

1.18 With reference to Fig. 1.22 showing a Stern–Gerlach apparatus, calculate the distance P_2P_3 from the following data:

Field gradient: $\dfrac{\partial \mathcal{B}_z}{\partial z} = 10^3\ T/m$

Length of pole piece: $L = 0.1$ m
Distance to screen: $l = 1$ m
Atomic beam composed of silver atoms, for which $\mathcal{M}_z = \pm\mu_B$
Temperature of oven: 600 K

Assume that the velocity of the silver atoms is equal to the root mean square velocity of $(3kT/M)^{1/2}$, where k is Boltzmann's constant and M is the mass of a silver atom.

1.19 Calculate the de Broglie wavelength of:

(a) A mass of 1 kg moving at a velocity of 1 m/s.
(b) A free electron of energy $E = 200$ eV.
(c) A free α particle of energy $E = 5$ MeV.
(d) A free neutron of energy $E = 0.02$ eV.
(e) A free electron of kinetic energy $E = 1$ MeV. (Consider whether you need to use relativistic kinematics.)

2 The elements of quantum mechanics

In Chapter 1, we discussed some of the evidence for the atomic nature of matter. We also learned that the classical Newtonian form of mechanics could not describe phenomena on the atomic scale. In particular, we saw that experiments involving the diffraction of electrons or atoms by crystals demonstrate that particles exhibit wave properties. Equally, experimental evidence for the quantisation of the radiation field, from phenomena as different as black body radiation, the photoelectric effect and the Compton effect, points to a fundamental wave-particle duality which must be taken into account in satisfactory theories of both matter and radiation. For material particles, such a theory was developed in the years 1925 and 1926 by W. Heisenberg, M. Born and P. Jordan in a form known as *matrix mechanics*. An equivalent form of the theory, called *wave mechanics*, was proposed at the same time by E. Schrödinger, following the ideas put forward in 1924 by L. de Broglie. A more abstract form of quantum mechanics, which includes both matrix mechanics and wave mechanics was published by P.A.M. Dirac in 1930.

In this chapter, we shall outline the main results and approximation methods of quantum mechanics, which will be used in the detailed discussions of atomic and molecular phenomena following in later chapters. In the space available, only those aspects of the subject which find immediate application will be discussed. For detailed accounts of the fundamentals of quantum theory we refer to the standard texts of which Dicke and Wittke (1960), Messiah (1968), Schiff (1968) and Merzbacher (1970) are excellent examples.

2.1 WAVES AND PARTICLES, WAVE PACKETS AND THE UNCERTAINTY PRINCIPLE

The experiments on the corpuscular nature of the electromagnetic radiation, which we discussed in the previous chapter, require that with the electromagnetic field we must associate a particle, the photon, whose energy E and magnitude of momentum p are related to the frequency ν and wavelength λ of the electromagnetic radiation by

$$E = h\nu, \qquad p = h/\lambda \qquad [2.1]$$

On the other hand, the experiments on the wavelike properties of particles, also discussed in Chapter 1, imply that we associate with each particle a wave or

matter field, the de Broglie relations which link the frequency ν and the wavelength λ of the wave with the particle energy E and magnitude of momentum p being also given by [2.1]. As a consequence, we can assume that the relations [2.1] hold for all types of particles and field quanta. Introducing the angular frequency $\omega = 2\pi\nu$, the wave number $k = 2\pi/\lambda$ and the reduced Planck constant $\hbar = h/2\pi$, we may write the relations [2.1] in the more symmetric form

$$E = \hbar\omega, \qquad p = \hbar k \tag{2.2}$$

As a first step in formulating non-relativistic wave mechanics for material particles, let us consider a free particle of mass m, having a well defined momentum $\mathbf{p} = p_x\hat{\mathbf{x}}$ directed along the positive X direction and a non-relativistic energy $E = p_x^2/2m$. Guided by [2.2], we associate with this particle a plane wave

$$\Psi(x, t) = A\mathrm{e}^{i(kx-\omega t)} \tag{2.3}$$

where A is a constant. This plane wave travels in the positive X direction, has a wave number $k = 2\pi/\lambda = p_x/\hbar$ and an angular frequency $\omega = E/\hbar$ which we may also write as

$$\omega = \frac{\hbar k^2}{2m} \tag{2.4}$$

The function $\Psi(x, t)$ is known as a *wave function*, and we shall discuss its significance shortly. For the moment, we note that for a free particle, represented by the plane wave [2.3], we have

$$-i\hbar\frac{\partial}{\partial x}\Psi = p_x\Psi \tag{2.5}$$

and

$$i\hbar\frac{\partial}{\partial t}\Psi = E\Psi \tag{2.6}$$

This one-dimensional treatment is easily extended to three dimensions. To a free particle of mass m, having a well-defined momentum $\mathbf{p}$ and an energy $E = p^2/2m$, we now associate a plane wave

$$\Psi(\mathbf{r}, t) = A\mathrm{e}^{i(\mathbf{k}\cdot\mathbf{r}-\omega t)} \tag{2.7}$$

where the *propagation vector* $\mathbf{k}$ is related to the momentum $\mathbf{p}$ by

$$\mathbf{p} = \hbar\mathbf{k} \tag{2.8}$$

with

$$k = |\mathbf{k}| = \frac{|\mathbf{p}|}{\hbar} = \frac{2\pi}{\lambda} \tag{2.9}$$

The vector $\mathbf{r}$ is the position vector of the particle and the angular frequency ω is

still given by $\omega = E/\hbar = \hbar k^2/2m$. The equation [2.6] remains unchanged for the plane wave [2.7], while [2.5] is now replaced by its obvious generalisation

$$-i\hbar\boldsymbol{\nabla}\Psi = \mathbf{p}\Psi \tag{2.10}$$

where $\boldsymbol{\nabla}$ is the gradient operator, having Cartesian components $(\partial/\partial x, \partial/\partial y, \partial/\partial z)$. The relations [2.6] and [2.10] show that for a free particle the energy and momentum can be represented by the differential operators

$$E_{\text{op}} = i\hbar\frac{\partial}{\partial t}, \qquad \mathbf{p}_{\text{op}} = -i\hbar\boldsymbol{\nabla} \tag{2.11}$$

acting on the wave function Ψ. It is a *postulate* of wave mechanics that when the particle is not free the dynamical variables E and $\mathbf{p}$ are still represented by these differential operators.

The plane waves [2.3] or [2.7] represent particles having a definite momentum, but since their amplitude is constant, these plane waves correspond to a complete absence of localisation of the particle in space. To describe a particle which is confined in a certain spatial region, a *wave packet* can be formed by superposing plane waves of different wave numbers. For example, in order to describe a free particle which is confined in a region of the X axis, we shall superimpose plane waves of the form [2.3] to obtain the wave packet

$$\Psi(x, t) = (2\pi\hbar)^{-1/2}\int_{-\infty}^{+\infty} \mathrm{e}^{i(p_x x - Et)/\hbar}\phi(p_x)\,\mathrm{d}p_x \tag{2.12}$$

where the factor in front of the integral has been chosen for future convenience. Writing $\psi(x) \equiv \Psi(x, t = 0)$ we see that the functions

$$\psi(x) = (2\pi\hbar)^{-1/2}\int_{-\infty}^{+\infty} \mathrm{e}^{ip_x x/\hbar}\phi(p_x)\,\mathrm{d}p_x \tag{2.13a}$$

and

$$\phi(p_x) = (2\pi\hbar)^{-1/2}\int_{-\infty}^{+\infty} \mathrm{e}^{-ip_x x/\hbar}\psi(x)\,\mathrm{d}x \tag{2.13b}$$

are just *Fourier transforms* of each other. More generally, we write at time t

$$\Psi(x, t) = (2\pi\hbar)^{-1/2}\int_{-\infty}^{+\infty} \mathrm{e}^{ip_x x/\hbar}\Phi(p_x, t)\,\mathrm{d}p_x \tag{2.14a}$$

and

$$\Phi(p_x, t) = (2\pi\hbar)^{-1/2}\int_{-\infty}^{+\infty} \mathrm{e}^{-ip_x x/\hbar}\Psi(x, t)\,\mathrm{d}x \tag{2.14b}$$

so that the functions $\Psi(x, t)$ and $\Phi(p_x, t)$ are also mutual Fourier transforms. The functions $\Phi(p_x, t)$ and $\phi(p_x) \equiv \Phi(p_x, t = 0)$ are called *wave functions in momentum space*.

The Heisenberg uncertainty principle

Consider the case for which the wave function $\phi(p_x)$ is localised in a certain region of the p_x variable. As a simple example, we shall assume that $\phi(p_x)$ is the Gaussian function

$$\phi(p_x) = \mathrm{e}^{-(p_x - p_0)^2/\gamma^2} \tag{2.15}$$

We note that $\phi(p_x)$ has a maximum at $p_x = p_0$ and falls to $1/\mathrm{e}$ of its maximum value at $p_x = p_0 \pm \gamma$, so that the 'width' of the distribution represented by [2.15] is $\Delta p_x = 2\gamma$ (see Fig. 2.1). Using the known result

$$\int_{-\infty}^{+\infty} \mathrm{e}^{-\alpha u^2} \mathrm{e}^{-\beta u} \, \mathrm{d}u = \left(\frac{\pi}{\alpha}\right)^{1/2} \mathrm{e}^{\beta^2/4\alpha} \tag{2.16}$$

we find from [2.13] that

$$\psi(x) = (2\hbar)^{-1/2} \gamma \mathrm{e}^{ip_0 x/\hbar} \mathrm{e}^{-\gamma^2 x^2/4\hbar^2} \tag{2.17}$$

Apart from the factor $\exp(ip_0 x/\hbar)$ which is known as a 'phase factor' since $|\exp(ip_0 x/\hbar)|^2 = 1$, we see that the function $\psi(x)$ is again a Gaussian. It has a maximum at $x = 0$ and $|\psi(x)|$ falls to $1/\mathrm{e}$ of its maximum value at $x = \pm 2\hbar/\gamma$, so that the 'width' of the function $|\psi(x)|$ is $\Delta x = 4\hbar/\gamma$, as shown in Fig. 2.1. It is important to remark that if we increase γ so that the width Δx is decreased and the function $|\psi(x)|$ becomes more strongly localised about $x = 0$, then the width Δp_x of the distribution [2.15] becomes larger, and the function $\phi(p_x)$ gets broader. For any finite, non-zero value of γ the product of the width is $\Delta x \Delta p_x = 8\hbar$, which is independent of γ and is of the order of magnitude of $\hbar$. Similar conclusions can be derived for functions $\phi(p_x)$ having different shapes

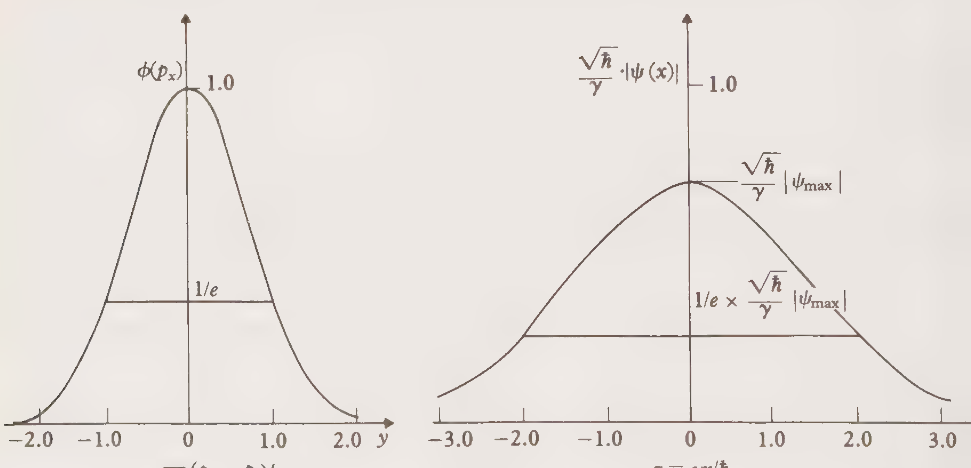

2.1 The wave packets $\phi(p_x)$ and $\psi(x)$ defined in [2.15] and [2.17]. The function $\phi(p_x)$ is plotted against $y = (p_x - p_0)/\gamma$; it falls to $1/\mathrm{e}$ of its maximum value at $y = \pm 1$, so the width of the distribution is $\Delta p_x = 2\gamma$. The function $\sqrt{\hbar}|\psi(x)|/\gamma$ is plotted against $z = \gamma x/\hbar$; it falls to $1/\mathrm{e}$ of its maximum value at $z = \pm 2$, so the width of the distribution is $\Delta x = 4\hbar/\gamma$.

(Problem 2.1). In fact, it is a general result of Fourier analysis that if $\psi(x)$ and $\phi(p_x)$ are mutual Fourier transforms as in [2.13]–[2.14], then

$$\Delta x \, \Delta p_x \gtrsim \hbar \tag{2.18}$$

This is the *Heisenberg uncertainty relation for position and momentum*, according to which the uncertainty Δx in measuring the x coordinate of a particle is related to the uncertainty Δp_x in measuring the x component of the momentum, the product of the uncertainties being larger than a quantity of order $\hbar$. A precise definition of the uncertainties Δx and Δp_x will be given below.

The foregoing discussion is readily generalised to more than one dimension. By superposing plane waves of the form [2.7] we obtain the wave packet

$$\begin{aligned} \Psi(\mathbf{r}, t) &= (2\pi\hbar)^{-3/2} \int \mathrm{e}^{i(\mathbf{p}\cdot\mathbf{r}-Et)/\hbar} \phi(\mathbf{p}) \, \mathrm{d}\mathbf{r} \\ &= (2\pi\hbar)^{-3/2} \int \mathrm{e}^{i\mathbf{p}\cdot\mathbf{r}/\hbar} \Phi(\mathbf{p}, t) \, \mathrm{d}\mathbf{p} \end{aligned} \tag{2.19}$$

where the wave functions in momentum space $\Phi(\mathbf{p}, t)$ and $\phi(\mathbf{p}) \equiv \Phi(\mathbf{p}, t = 0)$ are the Fourier transforms of $\Psi(\mathbf{r}, t)$ and $\psi(\mathbf{r}) \equiv \Psi(\mathbf{r}, t = 0)$, respectively. That is

$$\Phi(\mathbf{p}, t) = (2\pi\hbar)^{-3/2} \int \mathrm{e}^{-i\mathbf{p}\cdot\mathbf{r}/\hbar} \Psi(\mathbf{r}, t) \, \mathrm{d}\mathbf{r} \tag{2.20}$$

and

$$\phi(\mathbf{p}) = (2\pi\hbar)^{-3/2} \int \mathrm{e}^{-i\mathbf{p}\cdot\mathbf{r}/\hbar} \, \psi(\mathbf{r}) \, \mathrm{d}\mathbf{r} \tag{2.21}$$

The three-dimensional form of the Heisenberg uncertainty relations for position and momentum is now

$$\Delta x \, \Delta p_x \gtrsim \hbar, \qquad \Delta y \, \Delta p_y \gtrsim \hbar, \qquad \Delta z \, \Delta p_z \gtrsim \hbar \tag{2.22}$$

The position–momentum uncertainty relations [2.22] have been derived by using the theory of Fourier analysis. This theory may also be invoked to obtain a *time–energy uncertainty relation*. Indeed, according to Fourier analysis, a wave packet of duration Δt must be composed of plane-wave components whose angular frequencies extend over a range $\Delta\omega$ such that $\Delta t \, \Delta\omega \gtrsim 1$. Since $E = \hbar\omega$, we therefore have

$$\Delta t \, \Delta E \gtrsim \hbar \tag{2.23}$$

which is the *Heisenberg uncertainty relation for time and energy*. It connects the uncertainty ΔE in the determination of the energy of a system with the time interval Δt available for this energy determination. Thus, if a system does not stay longer than a time Δt in a given state of motion, its energy in that state will be uncertain by an amount $\Delta E \gtrsim \hbar/\Delta t$.

The Heisenberg uncertainty relations [2.22] and [2.23], which are fundamental to any wave theory of matter, are particular cases of the *uncertainty principle* formulated by W. Heisenberg in 1927. This principle states that it is impossible to specify precisely and simultaneously the values of 'complementary' dynamical variables such as x and p_x, y and p_y, z and p_z, or t and E.

The uncertainty relations [2.22] and [2.23] may be used to estimate various basic quantities which occur in quantum physics. For example, it is possible by using the position-momentum uncertainty relations [2.22] to obtain an estimate of the size and of the energy of the hydrogen atom in its ground state (Problem 2.2). On the other hand, the time–energy uncertainty relation [2.23] is very useful in studying the lifetime of unstable systems.

Interpretation of the wave function

To make progress in the theory, we need to interpret the meaning of the wave function $\Psi(\mathbf{r}, t)$. In searching for this interpretation, we must remember that $\Psi(\mathbf{r}, t)$ is in general a complex function, and that $|\Psi(\mathbf{r}, t)|$ is large where the particle is likely to be found, and small everywhere else. We also recall that diffraction patterns, made by light, depend on the intensity of the radiation determined by the Poynting vector, which can be interpreted as measuring the flux of photons, and which depends on the square of the vector potential. In a similar way, M. Born in 1926 made the fundamental postulate that if a particle is described by a wave function $\Psi(\mathbf{r}, t)$, the probability of finding the particle within the volume element $\mathrm{d}\mathbf{r} = \mathrm{d}x\,\mathrm{d}y\,\mathrm{d}z$ about the point $\mathbf{r}$ at the time t is

$$P(\mathbf{r}, t)\,\mathrm{d}\mathbf{r} = |\Psi(\mathbf{r}, t)|^2\,\mathrm{d}\mathbf{r} \tag{2.24}$$

so that

$$P(\mathbf{r}, t) = |\Psi(\mathbf{r}, t)|^2 = \Psi^*(\mathbf{r}, t)\Psi(\mathbf{r}, t) \tag{2.25}$$

is the (position) *probability density*. Born's statistical interpretation of the wave function has to be justified by the success of the theory built on it. For $P(\mathbf{r}, t)$ to be unique everywhere, one must require that the wave function $\Psi(\mathbf{r}, t)$ should be continuous and single-valued. It is also worth noting that since $|\Psi(\mathbf{r}, t)|^2$ is the physically significant quantity, two wave functions which differ from each other by a constant multiplicative factor of modulus one (that is, a constant phase factor of the form $\exp(i\alpha)$) are equivalent.

Since the probability of finding the particle somewhere must be unity, we deduce from [2.24] that the wave function $\Psi(\mathbf{r}, t)$ should be *normalised* so that

$$\int |\Psi(\mathbf{r}, t)|^2\,\mathrm{d}\mathbf{r} = 1 \tag{2.26}$$

where the integral extends over all space. Wave functions satisfying this condition are said to be *square integrable*. However, not every wave function can be normalised like this, for example the plane wave [2.7]. In this case $|\Psi(\mathbf{r}, t)|^2\,\mathrm{d}\mathbf{r}$ can be interpreted as the *relative* probability of finding the particle

at time t in a volume element $d\mathbf{r}$ centred about $\mathbf{r}$, so that the ratio $|\Psi(\mathbf{r}_1, t)|^2/|\Psi(\mathbf{r}_2, t)|^2$ gives the probability of finding the particle within a volume element centred about $\mathbf{r} = \mathbf{r}_1$, compared with that of finding it within the same volume element at $\mathbf{r} = \mathbf{r}_2$.

There are alternative methods of normalising wave functions which are not square integrable. For example, we may assume that the system is confined to a large box of volume V, in which case the normalisation condition [2.26] reads

$$\int_V |\Psi(\mathbf{r}, t)|^2 \, d\mathbf{r} = 1 \tag{2.27}$$

where the integration now extends over the volume V. It can be shown that calculated physical quantities are independent of V, provided the box is sufficiently large. Plane waves such as [2.7] can also be 'normalised' with the help of the *Dirac delta function* $\delta(x)$, which is defined by the relation

$$f(0) = \int_{-\infty}^{+\infty} f(x)\, \delta(x) \, dx \tag{2.28}$$

where $f(x)$ is an arbitrary well behaved function. There are several ways of representing the delta function, one of which is

$$\delta(x) = \lim_{\alpha \to \infty} \frac{\sin \alpha x}{\pi x} \tag{2.29}$$

When used in [2.28] the infinitely rapid oscillations of this function when $x \neq 0$ imply that the only contribution to the integral arises from the neighbourhood of $x = 0$, and

$$\begin{aligned} \int_{-\infty}^{+\infty} f(x)\, \delta(x) \, dx &= f(0) \lim_{\alpha \to \infty} \int_{-\infty}^{+\infty} \frac{\sin \alpha x}{\pi x} \, dx \\ &= f(0) \end{aligned} \tag{2.30}$$

Other useful representations of the Dirac delta function, which are readily deduced from [2.29] are

$$\delta(x) = \lim_{\beta \to 0} \frac{1 - \cos \beta x}{\pi \beta x^2} \tag{2.31}$$

and

$$\delta(x) = (2\pi)^{-1} \lim_{K \to \infty} \int_{-K}^{+K} e^{ikx} \, dk = (2\pi)^{-1} \int_{-\infty}^{+\infty} e^{ikx} \, dk \tag{2.32}$$

We see that the Dirac delta function is an unusual function (in fact a 'distribution') which is such that, in effect,

$$\delta(x) = 0 \quad \text{if} \quad x \neq 0, \qquad \int_{-\infty}^{+\infty} \delta(x) \, dx = 1 \tag{2.33}$$

Using this result, we find that the plane waves

$$\psi_{\mathbf{k}}(\mathbf{r}) = (2\pi)^{-3/2} e^{i\mathbf{k}\cdot\mathbf{r}} \qquad [2.34]$$

satisfy the relation

$$\begin{aligned}\int \psi^{\star}_{\mathbf{k}'}(\mathbf{r})\psi_{\mathbf{k}}(\mathbf{r})\,\mathrm{d}\mathbf{r} &= (2\pi)^{-3}\int_{-\infty}^{+\infty} e^{i(k_x-k'_x)x}\,\mathrm{d}x \\ &\quad\times \int_{-\infty}^{+\infty} e^{i(k_y-k'_y)y}\,\mathrm{d}y \int_{-\infty}^{+\infty} e^{i(k_z-k'_z)z}\,\mathrm{d}z \\ &= \delta(k_x-k'_x)\,\delta(k_y-k'_y)\,\delta(k_z-k'_z) \\ &= \delta(\mathbf{k}-\mathbf{k}') \qquad [2.35]\end{aligned}$$

which is known as an *orthonormality relation*. In addition, the plane waves [2.34] satisfy the *closure relation*

$$\int \psi^{\star}_{\mathbf{k}}(\mathbf{r}')\psi_{\mathbf{k}}(\mathbf{r})\,\mathrm{d}\mathbf{k} = \delta(\mathbf{r}-\mathbf{r}') \qquad [2.36]$$

Expectation values

Consider a one-dimensional system in which the normalised wave function is $\Psi(x, t)$. Since $|\Psi(x, t)|^2\,\mathrm{d}x$ is the probability of finding the particle at the position x in the interval $\mathrm{d}x$, the *average* or *expectation value* of x may be defined as

$$\langle x\rangle = \int_{-\infty}^{+\infty} x|\Psi(x, t)|^2\,\mathrm{d}x \qquad [2.37]$$

Likewise, the expectation value of any function $f(\mathbf{r})$ of the coordinates x, y, z, in a state represented by the normalised wave function $\Psi(\mathbf{r}, t)$ is

$$\langle f\rangle = \int f(\mathbf{r})|\Psi(\mathbf{r}, t)|^2\,\mathrm{d}\mathbf{r} \qquad [2.38]$$

where the integral is taken over all space.

How should we calculate the average value of the momentum of the particle? The wavelength, which determines the magnitude of the momentum of a particle through [2.1], has only a precise value for a plane wave such as [2.7]. For such a wave the momentum is obtained by operating on the wave function with the differential operator $-i\hbar\nabla$, as in [2.10]. When the wave function is not a plane wave, we shall still assume that the momentum is represented by this operator (see [2.11]) and the average value of the momentum in a state represented by a normalised wave function $\Psi(\mathbf{r}, t)$ is

$$\langle\mathbf{p}\rangle = \int \Psi^{\star}(\mathbf{r}, t)\mathbf{p}_{\mathrm{op}}\Psi(\mathbf{r}, t)\,\mathrm{d}\mathbf{r} = \int \Psi^{\star}(\mathbf{r}, t)(-i\hbar\nabla)\Psi(\mathbf{r}, t)\,\mathrm{d}\mathbf{r} \qquad [2.39]$$

In general, if an operator A depends on $\mathbf{r}$, $\mathbf{p}$ and t, its expectation value is defined as

$$\langle A \rangle = \int \Psi^\star(\mathbf{r}, t) A(\mathbf{r}, -i\hbar\nabla, t) \Psi(\mathbf{r}, t)\, d\mathbf{r} \tag{2.40}$$

The uncertainties Δx, Δp_x and so on which appeared in the uncertainty relations [2.22] can now be defined as standard deviations by the formulae

$$\Delta x = \langle (x - \langle x \rangle)^2 \rangle^{1/2}, \qquad \Delta p_x = \langle (p_x - \langle p_x \rangle)^2 \rangle^{1/2} \tag{2.41}$$

2.2 THE SCHRÖDINGER EQUATION

In order to compute the average values of functions of the position and momentum of a particle, which are the quantities determined by a series of measurements, some way is needed of calculating wave functions. We first notice that the wave packet [2.19] for a free particle satisfies the differential equation

$$i\hbar \frac{\partial}{\partial t} \Psi = -\frac{\hbar^2}{2m} \nabla^2 \Psi \tag{2.42}$$

because $E(p) = p^2/2m$, and this is called the Schrödinger equation for a free particle. What is the Schrödinger equation for a particle moving in a potential $V(\mathbf{r}, t)$? Using [2.11], the Schrödinger equation for a free particle can be written

$$E_{\text{op}}\Psi = \frac{1}{2m} (\mathbf{p}_{\text{op}})^2 \Psi \tag{2.43}$$

The operator $(\mathbf{p}_{\text{op}})^2/2m$ represents the kinetic energy T of the particle. The total energy or Hamiltonian operator of a particle is just

$$H = T + V = -\frac{\hbar^2}{2m} \nabla^2 + V \tag{2.44}$$

and the generalisation of the Schrödinger equation for a particle in a potential is

$$E_{\text{op}}\Psi = (T + V)\Psi \tag{2.45}$$

or

$$i\hbar \frac{\partial}{\partial t} \Psi = H\Psi \tag{2.46}$$

which explicitly reads

$$i\hbar \frac{\partial}{\partial t} \Psi(\mathbf{r}, t) = \left[-\frac{\hbar^2}{2m} \nabla^2 + V(\mathbf{r}, t) \right] \Psi(\mathbf{r}, t) \tag{2.47}$$

This is the *time-dependent Schrödinger equation* for a particle moving in a potential. We remark that this equation is *linear* in $\Psi(\mathbf{r}, t)$. As a result, it

satisfies the *superposition principle*, according to which a linear superposition of possible wave functions is also a possible wave function. The fact that the superposition principle applies is directly related to the wave nature of matter, and in particular to the existence of interference effects for de Broglie waves. We also note that the Schrödinger equation [2.47] is of first order in the time derivative $\partial/\partial t$, so that once the initial value of the wave function Ψ is given at some time t_0, namely $\Psi(\mathbf{r}, t_0)$, its values at all other times can be found.

The time-dependent Schrödinger equation [2.47] will now be used to obtain two important results concerning probability conservation and the time variation of expectation values.

Probability conservation

The probability of finding a particle within a fixed volume V is seen from [2.24] to be

$$\int_V P(\mathbf{r}, t)\, \mathrm{d}\mathbf{r} = \int_V |\Psi(\mathbf{r}, t)|^2\, \mathrm{d}\mathbf{r} \tag{2.48}$$

The rate of change of this probability can be obtained with the help of [2.47]:

$$\begin{aligned}\frac{\partial}{\partial t}\int_V P(\mathbf{r}, t)\, \mathrm{d}\mathbf{r} &= \int_V \left(\Psi^\star \frac{\partial \Psi}{\partial t} + \frac{\partial \Psi^\star}{\partial t}\Psi\right) \mathrm{d}\mathbf{r} \\ &= \frac{i\hbar}{2m}\int_V [\Psi^\star \nabla^2 \Psi - (\nabla^2 \Psi^\star)\Psi]\, \mathrm{d}\mathbf{r} \\ &= -\int_V \boldsymbol{\nabla} \cdot \mathbf{j}\, \mathrm{d}\mathbf{r}\end{aligned} \tag{2.49}$$

where we have introduced the vector

$$\mathbf{j}(\mathbf{r}, t) = \frac{\hbar}{2mi}[\Psi^\star \boldsymbol{\nabla} \Psi - (\boldsymbol{\nabla} \Psi^\star)\Psi] \tag{2.50}$$

Using Green's theorem, we find that

$$\frac{\partial}{\partial t}\int_V P(\mathbf{r}, t)\, \mathrm{d}\mathbf{r} = -\int_S \mathbf{j} \cdot \mathrm{d}\mathbf{S} \tag{2.51}$$

where the integral on the right-hand side is over the surface S bounding the volume V. Since the rate of change of the probability of finding the particle in the region V is equal to the probability flux passing through the surface S, the vector $\mathbf{j}$ can be interpreted as a *probability current density*. The equation

$$\boldsymbol{\nabla} \cdot \mathbf{j} + \frac{\partial P}{\partial t} = 0 \tag{2.52}$$

which follows from [2.49] is analogous to the continuity equation of electromagnetism, expressing charge conservation.

Time variation of expectation values

The rate of change of the expectation value [2.40] of an operator A is given by

$$\begin{aligned}\frac{\mathrm{d}}{\mathrm{d}t}\langle A\rangle &= \frac{\mathrm{d}}{\mathrm{d}t}\int(\Psi^\star A\Psi)\,\mathrm{d}\mathbf{r}\\ &= \int\left(\frac{\partial\Psi^\star}{\partial t}A\Psi + \Psi^\star\frac{\partial A}{\partial t}\Psi + \Psi A\frac{\partial\Psi}{\partial t}\right)\mathrm{d}\mathbf{r}\\ &= \left\langle\frac{\partial A}{\partial t}\right\rangle + \frac{1}{i\hbar}\int\Psi^\star(AH - HA)\Psi\,\mathrm{d}\mathbf{r}\end{aligned} \qquad [2.53]$$

where we have used the Schrödinger equation [2.46]. The *commutator* of two operators A and B is defined as

$$[A, B] = AB - BA \qquad [2.54]$$

and two operators are said to commute if their commutator vanishes. Using this definition [2.53] can be written as

$$\frac{\mathrm{d}}{\mathrm{d}t}\langle A\rangle = \left\langle\frac{\partial A}{\partial t}\right\rangle + \frac{1}{i\hbar}\langle[A, H]\rangle \qquad [2.55]$$

In particular, if the operator A does not depend explicitly on time (that is, $\partial A/\partial t = 0$), we have

$$i\hbar\frac{\mathrm{d}}{\mathrm{d}t}\langle A\rangle = \langle[A, H]\rangle \qquad [2.56]$$

and if A commutes with H, A is a constant of the motion ($\mathrm{d}\langle A\rangle/\mathrm{d}t = 0$).

Using the result [2.56] one can prove (Problem 2.5) *Ehrenfest's theorem*, according to which the expectation value of the variables $\mathbf{r}$ and $\mathbf{p}$ obey equations corresponding to Newton's equations of motion. That is,

$$m\frac{\mathrm{d}\langle\mathbf{r}\rangle}{\mathrm{d}t} = \langle\mathbf{p}\rangle, \qquad \frac{\mathrm{d}\langle\mathbf{p}\rangle}{\mathrm{d}t} = -\langle\nabla V\rangle \qquad [2.57]$$

Time-independent Schrödinger equation and energy eigenfunctions

When the potential does not depend on the time, the Schrödinger equation [2.47] admits *stationary state solutions* of the form

$$\Psi(\mathbf{r}, t) = \psi_E(\mathbf{r})\mathrm{e}^{-(i/\hbar)Et} \qquad [2.58]$$

where E is a constant and where $\psi_E(\mathbf{r})$ satisfies the *time-independent Schrödinger*

equation

$$\left[-\frac{\hbar^2}{2m}\nabla^2 + V(\mathbf{r})\right]\psi_E(\mathbf{r}) = E\psi_E(\mathbf{r}) \tag{2.59}$$

or

$$H\psi_E = E\psi_E \tag{2.60}$$

The significance of the constant E is seen by recognising that E is the expectation value of the total energy $H = T + V$. That is

$$E = \langle H \rangle = \int \Psi^\star(\mathbf{r}, t) H \Psi(\mathbf{r}, t)\, \mathrm{d}\mathbf{r} \tag{2.61}$$

In writing [2.61] we have assumed that the wave function Ψ is normalised to unity, so that

$$\int \psi^\star_E(\mathbf{r})\psi_E(\mathbf{r})\, \mathrm{d}\mathbf{r} = 1 \tag{2.62}$$

where the integral can be taken over all space for square integrable functions, or over a large volume V in the other cases. We shall find that only certain values of E are compatible with normalisable solutions. These values are called the *energy eigenvalues* and the corresponding solutions ψ_E are the *eigenfunctions* of the energy operator H. Equations of the type

$$A\psi_n = a_n\psi_n \tag{2.63}$$

– where A is an operator and a_n is a number – are called *eigenvalue equations*; a_n being called the *eigenvalue* and ψ_n the *eigenfunction* of the operator A. If more than one eigenfunction corresponds to a given eigenvalue, this eigenvalue is said to be *degenerate*.

It is a general postulate of quantum mechanics that each dynamical variable (such as the position, momentum, energy, . . .) can be represented by a linear operator [1] and that the result of a precise measurement of the variable can only be one of the eigenvalues of this operator. For example, the only possible result of a measurement of the energy of the system is one of the eigenvalues E of the Hamiltonian operator H.

The spectrum of the Hamiltonian

The set of all eigenvalues of the Hamiltonian is called the *energy spectrum*. It may consist of *discrete* values or a *continuous* range, or both. In general the discrete eigenvalues are associated with *bound states* (analogous to the closed orbits of classical mechanics) and the continuum with *scattering states* (corresponding to open classical orbits).

[1] For a definition of linear operators, see Byron and Fuller (1969) or Mathews and Walker (1973).

It is easy to show by integrating by parts that for any normalised eigenfunction ψ_E of H one has

$$
\begin{aligned}
E^\star = \langle H\rangle^\star &= \left[\int \psi_E^\star\left[-\frac{\hbar^2}{2m}\nabla^2 + V\right]\psi_E \,\mathrm{d}\mathbf{r}\right]^\star \\
&= \int \psi_E\left[-\frac{\hbar^2}{2m}\nabla^2 + V\right]\psi_E^\star \,\mathrm{d}\mathbf{r} = \int \psi_E^\star\left[-\frac{\hbar^2}{2m}\nabla^2 + V\right]\psi_E \,\mathrm{d}\mathbf{r} \\
&= \langle H\rangle = E
\end{aligned}
\tag{2.64}
$$

so that the eigenvalues E are *real*.

In general, if A is a linear operator and Φ and Ψ are any two wave functions, the adjoint operator $A^\dagger$ is defined by the relation

$$
\int \Phi^\star A^\dagger \Psi \,\mathrm{d}\mathbf{r} = \int (A\Phi)^\star \Psi \,\mathrm{d}\mathbf{r}
\tag{2.65}
$$

If $A^\dagger = A$, then A is said to be *self-adjoint* or *Hermitian*, in which case $\langle A\rangle = \langle A\rangle^\star$ and the eigenvalues of A are real. Operators representing physical quantities (such as H, $\mathbf{r}$ or $\mathbf{p}$) are called *observables*, and it is a postulate of quantum mechanics that observables must be Hermitian.

We shall now prove that if ψ_E and $\psi_{E'}$ are two eigenfunctions corresponding to unequal eigenvalues E and E', then

$$
\int \psi_E^\star(\mathbf{r})\psi_{E'}(\mathbf{r}) \,\mathrm{d}\mathbf{r} = 0
\tag{2.66}
$$

in which case ψ_E and $\psi_{E'}$ are said to be *orthogonal*. We first note that

$$
\psi_{E'}^\star(H - E)\psi_E = 0
\tag{2.67a}
$$

and

$$
\psi_E[(H - E')\psi_{E'}]^\star = 0
\tag{2.67b}
$$

Subtracting these two equations, and integrating we have

$$
\begin{aligned}
(E - E')\int \psi_{E'}^\star\psi_E \,\mathrm{d}\mathbf{r} &= \int [\psi_{E'}^\star H\psi_E - (H\psi_{E'})^\star\psi_E] \,\mathrm{d}\mathbf{r} \\
&= 0
\end{aligned}
\tag{2.68}
$$

where in the last step we have used the fact that H is Hermitian. Since $E \neq E'$, we see that [2.66] follows from [2.68].

When several eigenfunctions $\psi_{E,r}$, $r = 1, 2, \ldots, \alpha$ correspond to a given eigenvalue E (that is, if the eigenvalue E is degenerate) linear combinations of the eigenfunctions $\psi_{E,r}$ can always be constructed so that the resulting α eigenfunctions belonging to the eigenvalue E are mutually orthogonal. Each of these eigenfunctions is evidently orthogonal to every eigenfunction belonging to a different eigenvalue $E' \neq E$. Thus all the energy eigenfunctions can be made orthogonal to each other, even when some of the eigenvalues are degenerate.

The eigenfunctions ψ_n of an operator A are said to constitute an *orthonormal set* if they are both normalised and mutually orthogonal. That is

$$\int \psi_{n'}^{\star}(\mathbf{r})\psi_n(\mathbf{r})\,d\mathbf{r} = \delta_{nn'} \qquad [2.69]$$

where $\delta_{nn'}$ is the Kronecker symbol

$$\delta_{nn'} = \begin{cases} 1, & n = n' \\ 0, & n \neq n' \end{cases} \qquad [2.70]$$

The energy eigenfunctions ψ_E constitute such a set, and in the same way so do the eigenfunctions of an Hermitian operator representing any observable [2].

2.3 EXPANSIONS, OPERATORS AND OBSERVABLES

We shall assume that all the orthonormal eigenfunctions $\psi_n(\mathbf{r})$ of a given Hermitian operator A form a *complete set*, in the mathematical sense that an arbitrary normalised wave function $\Psi(\mathbf{r}, t)$ can be expanded in terms of them:

$$\Psi(\mathbf{r}, t) = \sum_n c_n(t)\psi_n(\mathbf{r}) \qquad [2.71]$$

Suppose now that at time t a measurement is made of the observable represented by A. Then, as we have seen above, the value obtained must be one of the eigenvalues a_n. A further postulate, due to Born, is that the probability $P_n(t)$ of obtaining the value a_n is given by

$$P_n(t) = |c_n(t)|^2 \qquad [2.72]$$

As a consequence, we are certain to obtain a particular eigenvalue a_n only when the wave function that describes the particle at time t is the corresponding eigenfunction ψ_n (apart from a constant phase factor). Immediately after a measurement in which the result a_n is obtained, the system will be found in the state represented by the wave function ψ_n.

We can calculate the *probability amplitudes* c_n from [2.71] using the orthonormal property [2.69] of the expansion functions ψ_n. Multiplying [2.71] by $\psi_{n'}^{\star}$ and integrating, we obtain

$$\begin{aligned} \int \psi_{n'}^{\star}(\mathbf{r})\Psi(\mathbf{r}, t)\,d\mathbf{r} &= \sum_n c_n(t) \int \psi_{n'}^{\star}(\mathbf{r})\psi_n(\mathbf{r})\,d\mathbf{r} \\ &= \sum_n c_n(t)\,\delta_{nn'} \\ &= c_{n'}(t) \end{aligned} \qquad [2.73]$$

[2] If n is a continuous index, then a 'delta function' normalisation analogous to [2.35] can be used. Alternatively, a 'box' normalisation of the type [2.27] can be introduced, in which case n remains discrete and the relations [2.69]–[2.70] apply without modification.

It is convenient at this point to introduce the Dirac notation

$$\langle f|g\rangle = \int f^\star(\mathbf{r})g(\mathbf{r})\,d\mathbf{r} \qquad [2.74]$$

so that the result [2.73] reads $c_{n'} = \langle\psi_{n'}|\Psi\rangle$. More generally, we define the *matrix element* of an operator A as

$$\langle f|A|g\rangle = \int f^\star(\mathbf{r})Ag(\mathbf{r})\,d\mathbf{r} \qquad [2.75]$$

so that the expectation, or average, value of A can be written as

$$\begin{aligned}\langle A\rangle &= \langle\Psi|A|\Psi\rangle \\ &= \sum_n\sum_{n'} c_{n'}^\star c_n\langle\psi_{n'}|A|\psi_n\rangle \\ &= \sum_n\sum_{n'} c_{n'}^\star c_n a_n\langle\psi_{n'}|\psi_n\rangle \\ &= \sum_n |c_n|^2 a_n \end{aligned} \qquad [2.76]$$

where we have used [2.63] and the orthonormality relation [2.69], which reads $\langle\psi_{n'}|\psi_n\rangle = \delta_{nn'}$ in Dirac's notation.

Another important relation can be proved from [2.71] and [2.73]. Indeed, since

$$\begin{aligned}\Psi(\mathbf{r}, t) &= \sum_n c_n(t)\psi_n(\mathbf{r}) \\ &= \sum_n \left[\int \psi_n^\star(\mathbf{r}')\Psi(\mathbf{r}', t)\,d\mathbf{r}'\right]\psi_n(\mathbf{r})\end{aligned} \qquad [2.77]$$

we have

$$\sum_n \psi_n^\star(\mathbf{r}')\psi_n(\mathbf{r}) = \delta(\mathbf{r} - \mathbf{r}') \qquad [2.78]$$

where $\delta(\mathbf{r} - \mathbf{r}')$ is the Dirac delta function discussed in Section 2.1. The result [2.78] (see also [2.36] for the special case of the plane waves) is known as the *closure* property of the orthonormal set of functions ψ_n.

General solution of the Schrödinger equation for a time-independent potential

Let us assume that the potential is independent of time, so that the time-dependent Schrödinger equation [2.47] admits stationary state solutions of the form [2.58]. Expanding the general solution of [2.47] in terms of energy eigenfunctions, we then write (see [2.71] and [2.73])

$$\Psi(\mathbf{r}, t) = \sum_E c_E(t)\psi_E(\mathbf{r}) \qquad [2.79]$$

where

$$c_E(t) = \int \psi_E^\star(\mathbf{r})\Psi(\mathbf{r}, t)\, \mathrm{d}\mathbf{r} \qquad [2.80]$$

Substituting [2.79] into the Schrödinger equation [2.47], and using the orthonormality of the eigenfunctions ψ_E, together with the fact that they satisfy the time-independent Schrödinger equation [2.59], we find that the coefficients $c_E(t)$ satisfy the equation

$$i\hbar \frac{\mathrm{d}}{\mathrm{d}t} c_E(t) = E c_E(t) \qquad [2.81]$$

which is readily integrated to yield

$$c_E(t) = c_E(t_0)\mathrm{e}^{-(i/\hbar)E(t-t_0)} \qquad [2.82]$$

We note that the probability P_E of obtaining the energy value E is constant, since from [2.72] and [2.82] we have

$$P_E = |c_E(t)|^2 = |c_E(t_0)|^2 \qquad [2.83]$$

Using [2.79] and [2.82], we find that

$$\Psi(\mathbf{r}, t) = \sum_E c_E(t_0)\mathrm{e}^{-(i/\hbar)E(t-t_0)}\psi_E(\mathbf{r}) \qquad [2.84]$$

or

$$\Psi(\mathbf{r}, t) = \sum_E \tilde{c}_E(t_0)\psi_E(\mathbf{r})\mathrm{e}^{-(i/\hbar)Et} \quad ; \quad \tilde{c}_E(t_0) = c_E(t_0)\mathrm{e}^{(i/\hbar)Et_0} \qquad [2.85]$$

so that the general solution $\Psi(\mathbf{r}, t)$ is a linear superposition of stationary state solutions [2.58], as we expect from the linearity of the Schrödinger equation [2.47].

These results may also be used to write down an expression for $\Psi(\mathbf{r}, t)$ at any time, once it is known at the time $t = t_0$. Indeed, from [2.80] and [2.84], we have

$$\begin{aligned}\Psi(\mathbf{r}, t) &= \sum_E \left[\int \psi_E^\star(\mathbf{r}')\Psi(\mathbf{r}', t_0)\, \mathrm{d}\mathbf{r}'\right]\mathrm{e}^{-(i/\hbar)E(t-t_0)}\psi_E(\mathbf{r}) \\ &= \int K(\mathbf{r}, t; \mathbf{r}', t_0)\Psi(\mathbf{r}', t_0)\, \mathrm{d}\mathbf{r}' \qquad [2.86]\end{aligned}$$

where

$$K(\mathbf{r}, t; \mathbf{r}', t_0) = \sum_E \psi_E^\star(\mathbf{r}')\psi_E(\mathbf{r})\mathrm{e}^{-(i/\hbar)E(t-t_0)} \qquad [2.87]$$

We see from [2.86] that K may be interpreted as the probability amplitude that a particle originally at $\mathbf{r}'$ will propagate to the point $\mathbf{r}$ in the time interval $t - t_0$. The function K is therefore called a *propagator*.

Matrix representations of wave functions and operators

Let us consider a complete orthonormal set of functions $\{\psi_j\}$. Any physically admissible wave function Ψ can be expanded in terms of them as (see [2.71] and [2.73])

$$\Psi = \sum_j c_j \psi_j, \qquad c_j = \langle \psi_j | \Psi \rangle \tag{2.88}$$

The set $\{\psi_j\}$ is called a *basis* and the coefficients c_j are the components of Ψ in that basis. Once a given basis – also called a *representation* – has been chosen, Ψ is completely specified by its components c_j. Thus the set $\{\psi_j\}$ may be thought of as a basis in a vector space [3], and Ψ as being represented by a vector in that vector space, whose components are the coefficients c_j.

The action of a linear operator A on Ψ may be specified in terms of its effect on the components c_j in a given representation. Indeed, starting from [2.88] we have

$$A\Psi = A \sum_j c_j \psi_j = \sum_j c_j A \psi_j \tag{2.89}$$

Let us express the new vectors $\psi'_j = A\psi_j$ in our basis as

$$\psi'_j = A\psi_j = \sum_i A_{ij} \psi_i \tag{2.90}$$

where

$$A_{ij} = \langle \psi_i | A | \psi_j \rangle \tag{2.91}$$

Then, if we write

$$\Psi' = A\Psi = \sum_i c'_i \psi_i \tag{2.92}$$

so that the coefficients c'_i are the components of Ψ' in our basis, we have from [2.89]–[2.92]

$$\Psi' = A\Psi = \sum_i \sum_j A_{ij} c_j \psi_i = \sum_i c'_i \psi_i \tag{2.93}$$

so that

$$c'_i = \sum_j A_{ij} c_j \tag{2.94}$$

This is a *matrix equation* which relates the components c_j of Ψ and c'_i of $\Psi' = A\Psi$ by means of the *matrix elements* A_{ij} of the linear operator A.

Thus far we have adopted a given representation (that is, a given complete orthonormal set of basis vectors $\{\psi_j\}$) in which Ψ is represented by a vector having components c_j and the operator A by a matrix whose matrix elements are

[3] Vector spaces are discussed by Byron and Fuller (1969) and Mathews and Walker (1973).

given by [2.91]. This representation, however, is not unique. Indeed, we may develop Ψ in terms of another complete orthonormal set of basis vectors $\{\varphi_k\}$ as

$$\Psi = \sum_k d_k \varphi_k, \qquad d_k = \langle \varphi_k | \Psi \rangle \tag{2.95}$$

and the coefficients d_k are the components of a vector representing Ψ in the 'new' basis $\{\varphi_k\}$. In particular, any 'old' basis vector may be expressed in the 'new' basis as

$$\psi_j = \sum_k U_{kj} \varphi_k \tag{2.96}$$

where

$$U_{kj} = \langle \varphi_k | \psi_j \rangle \tag{2.97}$$

In the same way, the reverse expansion is

$$\varphi_k = \sum_j \langle \psi_j | \varphi_k \rangle \psi_j = \sum_j U_{kj}^\star \psi_j \tag{2.98}$$

Since

$$\Psi = \sum_j c_j \psi_j = \sum_j \sum_k c_j U_{kj} \varphi_k = \sum_k d_k \varphi_k \tag{2.99}$$

we also see that

$$d_k = \sum_j U_{kj} c_j \tag{2.100}$$

The set of numbers U_{kj} can be regarded as the elements of a matrix U and the equation [2.100] written in matrix form as

$$d = Uc \tag{2.101}$$

The matrix U is readily shown to be *unitary*, namely such that

$$UU^\dagger = U^\dagger U = I \tag{2.102}$$

where I is the unit matrix. Indeed, we have

$$\begin{aligned}
(UU^\dagger)_{kn} &= \sum_j U_{kj} U_{jn}^\dagger = \sum_j U_{kj} U_{nj}^\star \\
&= \sum_j \langle \varphi_k | \psi_j \rangle \langle \varphi_n | \psi_j \rangle^\star \\
&= \int \mathrm{d}\mathbf{r}\, \varphi_k^\star(\mathbf{r}) \int \mathrm{d}\mathbf{r}'\, \varphi_n(\mathbf{r}') \sum_j \psi_j^\star(\mathbf{r}') \psi_j(\mathbf{r}) \\
&= \int \mathrm{d}\mathbf{r}\, \varphi_k^\star(\mathbf{r}) \int \mathrm{d}\mathbf{r}'\, \varphi_n(\mathbf{r}')\, \delta(\mathbf{r} - \mathbf{r}') \\
&= \int \mathrm{d}\mathbf{r}\, \varphi_k^\star(\mathbf{r}) \varphi_n(\mathbf{r}) = \delta_{kn}
\end{aligned} \tag{2.103}$$

where we have used the closure relation for the functions ψ_j. Similarly, one has

$$(U^\dagger U)_{kn} = \delta_{kn} \qquad [2.104]$$

so that the unitarity property [2.102] follows from [2.103] and [2.104]. Therefore the passage from one representation of quantum mechanics to another is effected by *unitary transformations*.

Instead of changing the representation by means of a unitary transformation, we may also apply unitary transformations directly to the wave functions (vectors) and operators. For example, let Ψ and Φ be two wave functions and A an operator (observable) such that

$$A\Psi = \Phi \qquad [2.105]$$

Let us now apply the unitary transformation U, so that

$$\Psi' = U\Psi, \qquad \Phi' = U\Phi \qquad [2.106]$$

Writing

$$A'\Psi' = \Phi' \qquad [2.107]$$

we have

$$A'U\Psi = U\Phi = UA\Psi \qquad [2.108]$$

Hence, using [2.102], we find that

$$A = U^\dagger A' U, \qquad A' = UAU^\dagger \qquad [2.109]$$

These equations imply (Problem 2.8) that if A and A' are two operators connected by a unitarity transformation:

1. If A is Hermitian, then A' is also Hermitian.
2. The eigenvalues of A' are the same as those of A.
3. One has

$$\langle\Phi'|A'|\Psi'\rangle = \langle\Phi|A|\Psi\rangle \qquad [2.110]$$

where Ψ' and Φ' are defined by [2.106]. In particular, the expectation value $\langle\Psi|A|\Psi\rangle$ remains unchanged. By choosing $A = I$ (the unit operator) we also see that the scalar (inner) product $\langle\Phi|\Psi\rangle$ is invariant under a unitary transformation. As a result, the normalisation is also preserved, since $\langle\Psi'|\Psi'\rangle = \langle\Psi|\Psi\rangle$.

Let us assume that the orthonormal functions $\{\psi_j\}$ which we use as a basis set for a matrix representation are the eigenfunctions of some quantum mechanical operator A. Then, using [2.63], we find that

$$\begin{aligned} A_{ij} &= \langle\psi_i|A|\psi_j\rangle = \langle\psi_i|a_j|\psi_j\rangle \\ &= a_j\,\delta_{ij} \end{aligned} \qquad [2.111]$$

so that the matrix which represents the operator A in this basis is *diagonal*.

Solving the eigenvalue equation [2.63] for an observable A is therefore equivalent to finding a unitary transformation which diagonalises the corresponding matrix.

The Heisenberg equations of motion

We have learned in Section 2.2 how to calculate the time rate of change of the expectation value of an operator A (see [2.55]). In a similar way, one can show that

$$\frac{\mathrm{d}}{\mathrm{d}t}\int \Phi^\star A\Psi \,\mathrm{d}\mathbf{r} = \int \Phi^\star \frac{\partial A}{\partial t}\Psi \,\mathrm{d}\mathbf{r} + \frac{1}{i\hbar}\int \Phi^\star [A, H]\Psi \,\mathrm{d}\mathbf{r} \qquad [2.112]$$

where $\Phi(\mathbf{r}, t)$ and $\Psi(\mathbf{r}, t)$ are two arbitrary wave functions. Thus we have the operator (or matrix) equation

$$\frac{\mathrm{d}A}{\mathrm{d}t} = \frac{\partial A}{\partial t} + \frac{1}{i\hbar}[A, H] \qquad [2.113]$$

where $\mathrm{d}A/\mathrm{d}t$ is the operator whose matrix elements are the time rate of change of the matrix elements of A. The equation [2.113] is known as the *Heisenberg equation of motion* of a dynamical variable.

Commuting observables

Let two different observables be represented by the operators A and B. From Born's postulate, it follows that if there is a state in which a simultaneous measurement of the two observables is certain to yield the values a_i and b_j, then a_i and b_j must be eigenvalues of A and B, respectively. The corresponding wave function, ψ_{ij}, must be an eigenfunction of both A and B. That is,

$$A\psi_{ij} = a_i\psi_{ij}; \qquad B\psi_{ij} = b_j\psi_{ij} \qquad [2.114]$$

If such eigenfunctions of A and B can be found for all the eigenvalues a_i and b_j, then the two observables are said to be *compatible*, and the ψ_{ij} form a complete set. By taking suitable linear combinations of any degenerate eigenfunctions, this set can be made orthonormal,

$$\langle \psi_{i'j'}|\psi_{ij}\rangle = \delta_{ii'}\,\delta_{jj'} \qquad [2.115]$$

From [2.114], we see that

$$[A, B]\psi_{ij} = (AB - BA)\psi_{ij} = 0 \qquad [2.116]$$

and since any wave function Ψ can be expanded in terms of the orthonormal set $\{\psi_{ij}\}$, we must have

$$[A, B] = 0 \qquad [2.117]$$

so that the two operators A and B commute with each other. Conversely, if A

and B are two operators which commute with each other, there exists a complete set of eigenfunctions which are simultaneously eigenstates of both A and B. On the other hand, if $[A, B] \neq 0$, a precise simultaneous measurement of both the observables is impossible.

As an example, let us consider the Cartesian components x, y, z of the position operator and the Cartesian components of the momentum operator, $p_x = -i\hbar\, \partial/\partial x, p_y = -i\hbar\, \partial/\partial y$ and $p_z = -i\hbar\, \partial/\partial z$. If $f(x)$ is a function of x, we have

$$\begin{aligned}[x, p_x]f(x) &= -i\hbar\left\{x\frac{\partial f}{\partial x} - \frac{\partial}{\partial x}(xf)\right\} \\ &= i\hbar\, f(x) \end{aligned} \qquad [2.118]$$

so that we may write the relation $[x, p_x] = i\hbar$. More generally, we have

$$[x, p_x] = [y, p_y] = [z, p_z] = i\hbar \qquad [2.119]$$

while all other commutators – such as $[x, p_y]$ – vanish. It follows that, for example, x and p_y have common eigenfunctions and can be measured simultaneously with arbitrary accuracy. In contrast, since x and p_x do not commute with each other, a precise simultaneous measurement of both of these observables is impossible. Indeed, as we saw in Section 2.1, the accuracy to which both x and p_x can be measured is limited by the uncertainty principle.

The above arguments can be extended to any number of observables. The greatest number of commuting observables that can be found for a given system is said to form a *complete set of commuting observables*.

Commutator algebra

It is convenient to list here some elementary rules for the calculation of commutators. These rules are easily verified (Problem 2.9) from the basic definition [2.54]. If A, B and C are three linear operators

$$[A, B] = -[B, A] \qquad [2.120a]$$
$$[A, B+C] = [A, B] + [A, C] \qquad [2.120b]$$
$$[A, BC] = [A, B]C + B[A, C] \qquad [2.120c]$$
$$[A, [B, C]] + [B, [C, A]] + [C, [A, B]] = 0 \qquad [2.120d]$$

2.4 ONE-DIMENSIONAL EXAMPLES

In this section we shall analyse the time-independent Schrödinger equation

$$-\frac{\hbar^2}{2m}\frac{\mathrm{d}^2\psi(x)}{\mathrm{d}x^2} + V(x)\psi(x) = E\psi(x) \qquad [2.121]$$

for two simple one-dimensional potentials: the infinite square well and the linear harmonic oscillator. This will allow us to illustrate the theory and to obtain several results which will be useful in further chapters.

The infinite square well

Let us consider a particle of mass m which is constrained by impenetrable walls to move in a region of width L, where the potential energy is constant. Taking this constant to be zero, and setting $a = L/2$, the potential energy for this problem is

$$V(x) = \begin{cases} 0, & |x| > a \\ \infty, & x < -a, \quad x > a \end{cases} \tag{2.122}$$

and is illustrated in Fig. 2.2(a).

Because the potential energy is infinite at $x = \pm a$, the probability of finding the particle outside the well is zero. Hence the wave function $\psi(x)$ must vanish for $|x| > a$, and we only need to solve the Schrödinger eigenvalue equation [2.121] inside the well. Moreover, since the wave function must be continuous,

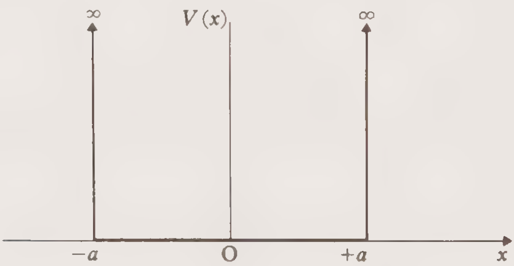

(a)

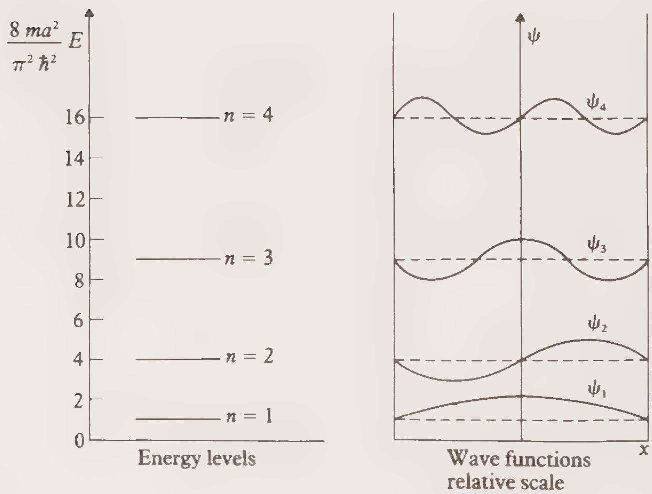

(b)

2.2 (a) The infinite square well
(b) Wave functions and eigenvalues for the infinite square well.

$\psi(x)$ must vanish at the constraining walls, namely

$$\psi(x) = 0 \quad \text{at} \quad x = \pm a \qquad [2.123]$$

We shall see shortly that it is precisely this *boundary condition* which leads to the quantisation of the energy.

The time-independent Schrödinger equation for $|x| < a$ reads

$$-\frac{\hbar^2}{2m}\frac{\mathrm{d}^2\psi(x)}{\mathrm{d}x^2} = E\psi(x) \qquad [2.124]$$

and has the general solution

$$\psi(x) = A \sin kx + B \cos kx, \qquad k = \left(\frac{2m}{\hbar^2}E\right)^{1/2} \qquad [2.125]$$

Applying the boundary condition [2.123] we find that

$$A \sin ka = 0, \qquad B \cos ka = 0 \qquad [2.126]$$

As a result, there are two possible classes of solutions. For the *first class* $A = 0$ and $\cos ka = 0$, so that the only allowed values of k are

$$k_n = \frac{n\pi}{2a} = \frac{n\pi}{L} \qquad [2.127]$$

with $n = 1, 3, 5, \ldots$ The corresponding eigenfunctions $\psi_n(x) = B_n \cos k_n x$ can be normalised so that

$$\int_{-a}^{+a} \psi_n^{\star}(x)\psi_n(x)\,\mathrm{d}x = 1 \qquad [2.128]$$

from which the normalisation constants B_n are found (within an arbitrary phase factor) to be $B_n = a^{-1/2}$. The normalised eigenfunctions of the first class may therefore be written as

$$\psi_n(x) = \frac{1}{\sqrt{a}}\cos\frac{n\pi}{2a}x, \qquad n = 1, 3, 5, \ldots \qquad [2.129]$$

Similarly, for the *second class* of solutions, such that $B = 0$ and $\sin ka = 0$, the allowed values of k are given by [2.127] with $n = 2, 4, 6, \ldots$ and the corresponding normalised eigenfunctions are

$$\psi_n(x) = \frac{1}{\sqrt{a}}\sin\frac{n\pi}{2a}x, \qquad n = 2, 4, 6, \ldots \qquad [2.130]$$

For both classes of eigenfunctions it is unnecessary to consider negative values of n, since these lead to solutions which are not linearly independent of those corresponding to positive n. The *energy eigenvalues* E_n are given by

$$E_n = \frac{\hbar^2 k_n^2}{2m} = \frac{\hbar^2}{8m}\frac{\pi^2 n^2}{a^2} = \frac{\hbar^2}{2m}\frac{\pi^2 n^2}{L^2}, \qquad n = 1, 2, 3, \ldots \qquad [2.131]$$

We see that there is an infinite number of discrete energy levels, with one eigenfunction corresponding to each energy level. The energy eigenvalues and the corresponding eigenfunctions are shown in Fig. 2.2(b) for the first few states. It is interesting to note that the lowest energy or *zero-point energy* is $E_1 = \hbar^2\pi^2/8ma^2$ so that there is no state of zero energy. This is in agreement with the requirements of the uncertainty principle. Indeed, the position uncertainty is roughly given by $\Delta x \simeq a$. The corresponding momentum uncertainty is therefore $\Delta p_x \sim \hbar/a$, leading to a minimum kinetic energy of order $\hbar^2/ma^2$, in qualitative agreement with the value of E_1.

There is an important difference between the two classes of eigenfunctions which we have obtained. That is, the eigenfunctions belonging to the first class are such that $\psi_n(-x) = \psi_n(x)$, and are therefore *even* functions of x, while those of the second class are such that $\psi_n(-x) = -\psi_n(x)$ and hence are *odd*. This division of the eigenfunctions into even and odd types is a consequence of the fact that the potential $V(x)$ is symmetric about $x = 0$, $V(-x) = V(x)$, so that the Hamiltonian is invariant under the *parity* or reflection operation $x \to -x$.

Finally, we observe that a general solution of the time-dependent Schrödinger equation [2.46] for the present problem can be written as a linear superposition of stationary solutions (see [2.85]), namely

$$\Psi(x, t) = \sum_{n=1}^{\infty} c_n\psi_n(x)\mathrm{e}^{-(i/\hbar)E_nt} \qquad [2.132]$$

where the coefficients c_n can be determined from the knowledge of the wave function Ψ at some particular time, say $t = 0$. Thus, using [2.80], we find that

$$c_n = \int_{-a}^{+a} \psi_n^\star(x)\Psi(x, t = 0)\,\mathrm{d}x \qquad [2.133]$$

The linear harmonic oscillator

We now consider the one-dimensional motion of a particle of mass m which is attracted to a fixed centre by a force proportional to the displacement from that centre. Thus, choosing the origin at the centre of force, the restoring force is given by $F = -kx$ (Hooke's law), where k is the force constant. This force can thus be represented by the potential energy

$$V(x) = \tfrac{1}{2}kx^2 \qquad [2.134]$$

which is shown in Fig. 2.3(a). Such a parabolic potential is of great importance in quantum physics as well as in classical physics, since it can be used to approximate an arbitrary continuous potential $W(x)$ in the neighbourhood of a stable equilibrium position $x = a$ (see Fig. 2.3(b)). Indeed, if we expand $W(x)$ in a Taylor series about $x = a$, we find that

$$W(x) = W(a) + (x - a)W'(a) + \tfrac{1}{2}(x - a)^2W''(a) + \cdots \qquad [2.135]$$

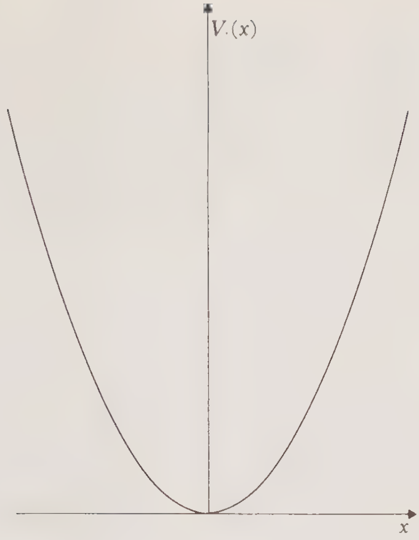

(a)

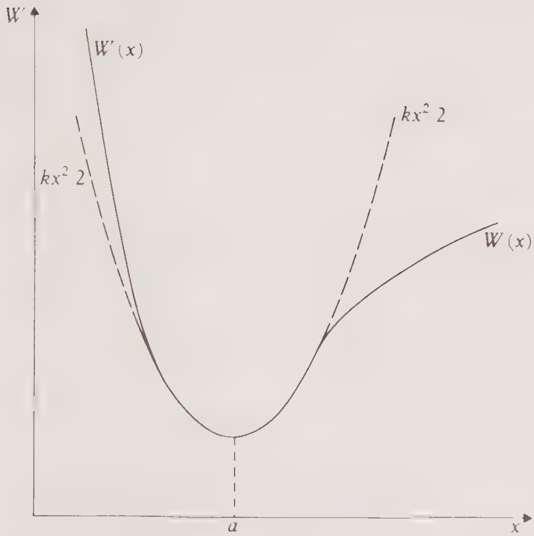

(b)

2.3 (a) The parabolic well $V(x) = \frac{1}{2}kx^2$. This is the potential of the simple harmonic oscillator. (b) A potential well $W(x)$ can be approximated by an oscillator potential near the minimum.

where $W'(a) = (\mathrm{d}W/\mathrm{d}x)_{x=a}$ and $W''(a) = (\mathrm{d}^2W/\mathrm{d}x^2)_{x=a}$. Since $W(x)$ has a minimum at $x = a$, we have $W'(a) = 0$ and $W''(a) > 0$. Choosing a as the coordinate origin and $W(a)$ as the origin of the energy scale, we see that the harmonic oscillator potential [2.134] is the first approximation to $W(x)$. Hence the linear harmonic oscillator is the prototype for systems in which there exist small vibrations about a point of stable equilibrium. This will be illustrated in Chapters 9 and 10, where we shall study the vibrational motion of nuclei in molecules.

The one-dimensional Schrödinger equation [2.121] becomes, for the linear harmonic oscillator

$$-\frac{\hbar^2}{2m}\frac{\mathrm{d}^2\psi(x)}{\mathrm{d}x^2} + \frac{1}{2}kx^2\psi(x) = E\psi(x) \qquad [2.136]$$

It is convenient to rewrite this equation in terms of dimensionless quantities. To this end we introduce the dimensionless variable

$$\xi = \alpha x, \qquad \alpha = \left(\frac{mk}{\hbar^2}\right)^{1/4} \qquad [2.137]$$

and the dimensionless eigenvalue

$$\lambda = \frac{2E}{\hbar\omega} \qquad [2.138]$$

where

$$\omega = \left(\frac{k}{m}\right)^{1/2} \qquad [2.139]$$

is the angular frequency of the corresponding classical oscillator. The Schrödinger equation [2.136] then becomes

$$\frac{\mathrm{d}^2\psi}{\mathrm{d}\xi^2} + (\lambda - \xi^2)\psi = 0 \qquad [2.140]$$

Let us first analyse the behaviour of ψ in the asymptotic region $|\xi| \to \infty$. We may then neglect the term λ compared to ξ^2, and the resulting equation is readily seen to have solutions of the form $\xi^n \exp(\pm\, \xi^2/2)$, where n is finite. The physically acceptable solution must contain only the minus sign in the exponent. This suggests looking for solutions to [2.140] of the form

$$\psi(\xi) = \mathrm{e}^{-\xi^2/2}H(\xi) \qquad [2.141]$$

where $H(\xi)$ are functions which must not affect the asymptotic behaviour. Substituting [2.141] into [2.140] we obtain for $H(\xi)$ the equation

$$\frac{\mathrm{d}^2H}{\mathrm{d}\xi^2} - 2\xi\frac{\mathrm{d}H}{\mathrm{d}\xi} + (\lambda - 1)H = 0 \qquad [2.142]$$

Energy levels

Solutions of [2.142] which satisfy the above requirement and are finite everywhere are only found for $\lambda = 2n + 1$, where $n = 0, 1, 2, \ldots$. They are called *Hermite polynomials* $H_n(\xi)$. The energy spectrum of the linear harmonic oscillator is therefore given by (see [2.138])

$$\begin{aligned} E_n &= \hbar\omega\left(n + \frac{1}{2}\right) \\ &= h\nu\left(n + \frac{1}{2}\right), \qquad n = 0, 1, 2, \ldots \end{aligned} \tag{2.143}$$

where $\nu = \omega/2\pi$.

The infinite sequence of discrete, equally spaced energy levels [2.143] is similar to that discovered in 1900 by Planck for the radiation field modes (see Section 1.3). This is due to the fact that a decomposition of the electromagnetic field into normal modes is essentially a decomposition into uncoupled harmonic oscillators. We note, however, that according to [2.143] the linear harmonic oscillator, even in its lowest energy state, $n = 0$, has the energy $\hbar\omega/2$. On the other hand the lowest energy of a classical harmonic oscillator is zero. The finite value $\hbar\omega/2$ of the ground state energy level, which is called the *zero-point energy*, is therefore a purely quantum mechanical effect, and is directly related to the uncertainty principle (Problem 2.11). The eigenvalues [2.143] of the linear harmonic oscillator are *non-degenerate*, since for each eigenvalue there exists only *one* eigenfunction, apart from an arbitrary multiplicative factor.

Hermite polynomials

The Hermite polynomials $H_n(\xi)$, which are the physically acceptable solutions of [2.142] corresponding to the eigenvalues $\lambda = 2n + 1$, are polynomials of order n, having the parity of n, which are uniquely defined except for an arbitrary multiplicative constant. This constant is traditionally chosen so that the highest power of ξ appears with the coefficient 2^n in $H_n(\xi)$. This is consistent with the following definition of the Hermite polynomials:

$$H_n(\xi) = (-1)^n e^{\xi^2} \frac{d^n e^{-\xi^2}}{d\xi^n} \tag{2.144}$$

The first few Hermite polynomials, obtained from [2.144], are

$$\begin{aligned} H_0(\xi) &= 1 \\ H_1(\xi) &= 2\xi \\ H_2(\xi) &= 4\xi^2 - 2 \\ H_3(\xi) &= 8\xi^3 - 12\xi \\ H_4(\xi) &= 16\xi^4 - 48\xi^2 + 12 \\ H_5(\xi) &= 32\xi^5 - 160\xi^3 + 120\xi \end{aligned} \tag{2.145}$$

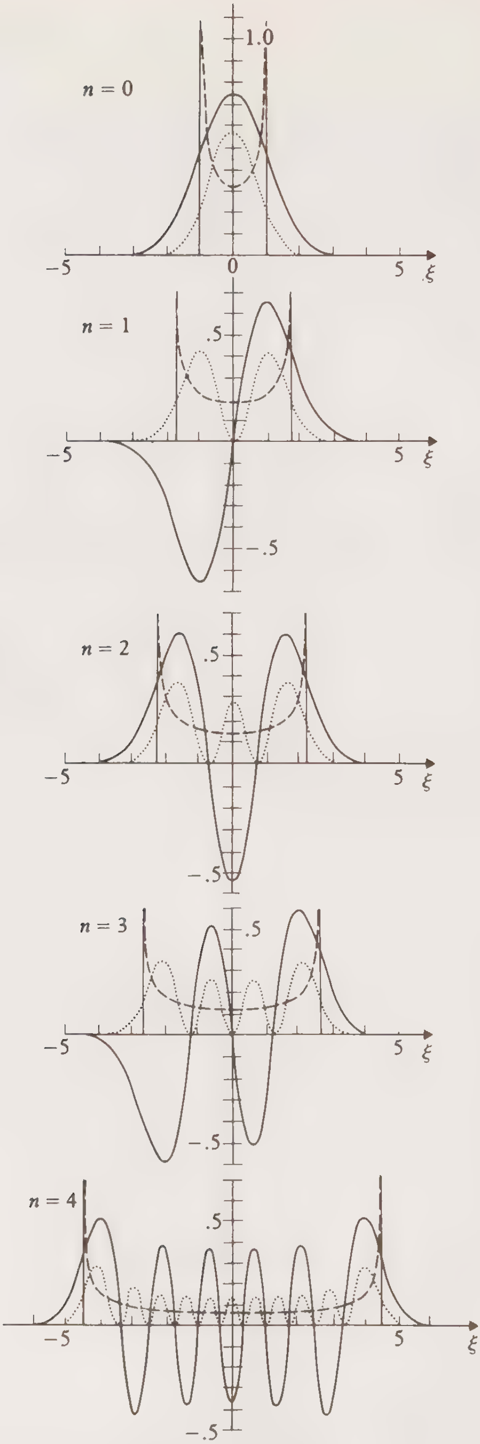

2.4 Wave functions for the simple harmonic oscillator

—— $\psi_n(\xi)/\sqrt{\alpha}$ with $\xi = \alpha x$, see [2.148] and [2.137]

----- $|\psi_n(\xi)|^2/\alpha$

--- The probability distribution for a classical oscillator with energy E_n. The classical motion is confined to the region between the vertical lines.

Another definition of the Hermite polynomials $H_n(\xi)$, which is equivalent to [2.144], involves the use of a *generating function* $G(\xi, s)$. That is

$$G(\xi, s) = e^{-s^2+2s\xi}$$

$$= \sum_{n=0}^{\infty} \frac{H_n(\xi)}{n!} s^n \qquad [2.146]$$

The relation [2.146] means that if the function $\exp[-s^2 + 2s\xi]$ is expanded in a power series in s, the coefficients of successive powers of s are just $1/n!$ times the Hermite polynomials $H_n(\xi)$. Using the generating function [2.146] it may be shown that the Hermite polynomials satisfy the recurrence relation

$$H_{n+1}(\xi) - 2\xi H_n(\xi) + 2nH_{n-1}(\xi) = 0 \qquad [2.147]$$

The wave functions for the linear harmonic oscillator

Using [2.141], we see that to each of the discrete values E_n of the energy, given by [2.143], there corresponds one, and only one physically acceptable wave function, namely

$$\psi_n(x) = N_n e^{-\alpha^2x^2/2} H_n(\alpha x) \qquad [2.148]$$

where we have returned to our original variable x, and N_n is a constant which (apart from an arbitrary phase factor) is determined by requiring that the wave function [2.148] be normalised to unity. That is

$$\int_{-\infty}^{+\infty} |\psi_n(x)|^2 \, dx = \frac{|N_n|^2}{\alpha} \int_{-\infty}^{+\infty} e^{-\xi^2} H_n^2(\xi) \, d\xi = 1 \qquad [2.149]$$

The integral on the right is evaluated in Appendix 3 by using the generating function [2.146]. It is found (see equation [A3.10]) that the normalisation constant N_n can be chosen to be

$$N_n = \left(\frac{\alpha}{\sqrt{\pi} 2^n n!} \right)^{1/2} \qquad [2.150]$$

so that the normalised linear harmonic oscillator wave functions are given by

$$\psi_n(x) = \left(\frac{\alpha}{\sqrt{\pi} 2^n n!} \right)^{1/2} e^{-\alpha^2x^2/2} H_n(\alpha x) \qquad [2.151]$$

It is also shown in Appendix 3 that the wave functions $\psi_n(x)$ and $\psi_m(x)$ are orthogonal if $n \neq m$, in agreement with the fact that they correspond to non-degenerate energy eigenvalues.

Because the Hamiltonian of the linear harmonic oscillator,

$$H = -\frac{\hbar^2}{2m} \frac{d^2}{dx^2} + \frac{1}{2} kx^2 \qquad [2.152]$$

is invariant under the *parity* operation $x \to -x$, the eigenfunctions $\psi_n(x)$ are either *even* functions of x(for $n = 0, 2, 4, \ldots$) or *odd* functions of x (for $n = 1, 3, 5, \ldots$). This is apparent in Fig. 2.4 where plots of the first few harmonic oscillator wave functions are shown, together with the corresponding probability densities $|\psi_n|^2$. It is also clear from this figure that for small values of n the quantum mechanical probability densities are very different from the corresponding densities for the classical harmonic oscillator. However, the agreement between the classical and quantum-mechanical probability densities quickly improves with increasing values of n. This is an illustration of Bohr's *correspondence principle*, according to which the predictions of quantum physics must correspond to those of classical physics in the limit in which the quantum numbers specifying the state of the system become large.

2.5 ANGULAR MOMENTUM

The classical orbital angular momentum of a particle is

$$\mathbf{L} = \mathbf{r} \times \mathbf{p} \tag{2.153}$$

where $\mathbf{r}$ and $\mathbf{p}$ are the position and momentum vectors of the particle, respectively. Using the fact that $\mathbf{p}$ is represented in wave mechanics by the vector operator $-i\hbar\boldsymbol{\nabla}$, we see that $\mathbf{L}$ is represented by the vector operator $-i\hbar(\mathbf{r} \times \boldsymbol{\nabla})$. Its Cartesian components are given by

$$\begin{aligned} L_x &= yp_z - zp_y = -i\hbar\left(y\frac{\partial}{\partial z} - z\frac{\partial}{\partial y}\right) \\ L_y &= zp_x - xp_z = -i\hbar\left(z\frac{\partial}{\partial x} - x\frac{\partial}{\partial z}\right) \\ L_z &= xp_y - yp_x = -i\hbar\left(x\frac{\partial}{\partial y} - y\frac{\partial}{\partial x}\right) \end{aligned} \tag{2.154}$$

Using the rules [2.120] of commutator algebra and the basic commutation relations [2.119] one finds that

$$[L_x, L_y] = i\hbar L_z, \qquad [L_y, L_z] = i\hbar L_x, \qquad [L_z, L_x] = i\hbar L_y \tag{2.155}$$

so that the operators L_x, L_y and L_z do not mutually commute. As a consequence, it is impossible to find a representation that diagonalises more than one of them, and the components of the orbital angular momentum cannot in general [4] be assigned definite values simultaneously. However, each of the three components of $\mathbf{L}$ is easily seen to commute with the operator

[4] An exception occurs when the angular momentum is zero ($L_x = L_y = L_z = 0$). In this case any function which only depends on the magnitude r of the position vector $\mathbf{r}$ is a simultaneous eigenfunction of L_x, L_y and L_z.

$\mathbf{L}^2 = L_x^2 + L_y^2 + L_z^2$. For example,

$$\begin{aligned}[L_z, \mathbf{L}^2] &= [L_z, L_x^2] + [L_z, L_y^2] \\ &= [L_z, L_x]\, L_x + L_x[L_z, L_x] + [L_z, L_y]\, L_y + L_y[L_z, L_y] \\ &= i\hbar(L_yL_x + L_xL_y) - i\hbar(L_xL_y + L_yL_x) = 0 \end{aligned} \qquad [2.156]$$

Thus it is possible to construct simultaneous eigenfunctions of $\mathbf{L}^2$ and one component of $\mathbf{L}$, so that $\mathbf{L}^2$ and this component can be simultaneously defined precisely. In what follows we shall choose this component to be L_z.

It is convenient to express L_z and $\mathbf{L}^2$ in spherical polar coordinates (r, θ, ϕ), which are related to the Cartesian coordinates (x, y, z) of the vector $\mathbf{r}$ by

$$\begin{aligned} x &= r \sin\theta \cos\phi \\ y &= r \sin\theta \sin\phi \\ z &= r \cos\theta \end{aligned} \qquad [2.157]$$

with $0 \leqslant r \leqslant \infty$, $0 \leqslant \theta \leqslant \pi$, $0 \leqslant \phi \leqslant 2\pi$ (see Fig. 2.5). It is found that (Problem 2.12)

$$L_z = -i\hbar \frac{\partial}{\partial\phi} \qquad [2.158]$$

and

$$\mathbf{L}^2 = -\hbar^2 \left[\frac{1}{\sin\theta} \frac{\partial}{\partial\theta}\left(\sin\theta \frac{\partial}{\partial\theta} \right) + \frac{1}{\sin^2\theta} \frac{\partial^2}{\partial\phi^2} \right] \qquad [2.159]$$

The eigenfunctions $\Phi(\phi)$ of L_z satisfy the eigenvalue equation

$$L_z\Phi(\phi) = m\hbar\Phi(\phi) \qquad [2.160]$$

where the eigenvalues have been written as $m\hbar$ for convenience. The normalised

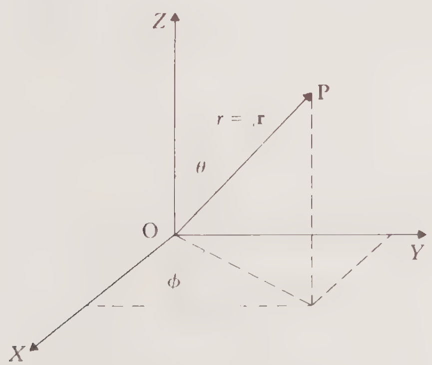

2.5 Polar coordinates (r, θ, ϕ) of a point P.

solutions of [2.160] are

$$\Phi_m(\phi) = \frac{1}{\sqrt{2\pi}} e^{im\phi} \qquad [2.161]$$

Since the functions Φ_m must be single-valued, we have $\Phi_m(2\pi) = \Phi_m(0)$, so that m, which is called the *magnetic quantum number*, is restricted to positive or negative integers, or zero ($m = 0, \pm 1, \pm 2, \ldots$). We also note that the functions [2.161] are orthonormal,

$$\int_0^{2\pi} \Phi^\star_{m'}(\phi)\Phi_m(\phi)\, d\phi = \delta_{mm'} \qquad [2.162]$$

The simultaneous eigenfunctions of $\mathbf{L}^2$ and L_z are called the *spherical harmonics* and are denoted by $Y_{lm}(\theta, \phi)$. They satisfy the eigenvalue equations

$$\mathbf{L}^2 Y_{lm}(\theta, \phi) = l(l+1)\hbar^2 Y_{lm}(\theta, \phi) \qquad [2.163]$$

and

$$L_z Y_{lm}(\theta, \phi) = m\hbar Y_{lm}(\theta, \phi) \qquad [2.164]$$

where the eigenvalue of $\mathbf{L}^2$ has been written as $l(l+1)\hbar^2$. The quantum number l is known as the *orbital angular momentum quantum number*. Setting

$$Y_{lm}(\theta, \phi) = \Theta_{lm}(\theta)\Phi_m(\phi) \qquad [2.165]$$

substituting into [2.163] and using [2.159], we find that the functions $\Theta_{lm}(\theta)$ satisfy the equation

$$\left[-\frac{1}{\sin\theta}\frac{\partial}{\partial\theta}\left(\sin\theta\frac{\partial}{\partial\theta}\right) + \frac{m^2}{\sin^2\theta}\right]\Theta_{lm}(\theta) = l(l+1)\Theta_{lm}(\theta) \qquad [2.166]$$

The physically acceptable solutions of this equation that remain finite over the range $0 \leqslant \theta \leqslant \pi$ exist only when $l = 0, 1, 2, \ldots$ and $m = -l, -l+1, \ldots, +l$. They can be expressed in terms of *associated Legendre functions* $P_l^m(\cos\theta)$, which are defined in the following way. Introducing the variable $w = \cos\theta$, we first define the *Legendre polynomials* $P_l(w)$ of degree l by the relation

$$P_l(w) = \frac{1}{2^l l!}\frac{d^l}{dw^l}(w^2 - 1)^l \qquad [2.167]$$

An equivalent definition of $P_l(w)$ can be given in terms of a generating function, namely

$$\begin{aligned} T(w, s) &= (1 - 2sw + s^2)^{-1/2} \\ &= \sum_{l=0}^{\infty} P_l(w)s^l, \qquad |s| < 1 \end{aligned} \qquad [2.168]$$

The Legendre polynomials satisfy the differential equation

$$\left[(1-w^2)\frac{\mathrm{d}^2}{\mathrm{d}w^2} - 2w\frac{\mathrm{d}}{\mathrm{d}w} + l(l+1)\right]P_l(w) = 0 \qquad [2.169]$$

which is readily shown to be equivalent to [2.166], with $m = 0$. One has the recurrence relation

$$(2l+1)wP_l - (l+1)P_{l+1} - lP_{l-1} = 0 \qquad [2.170]$$

which is also valid for $l = 0$ if one defines $P_{-1} = 0$. The orthogonality relations read

$$\int_{-1}^{+1} P_l(w)P_{l'}(w)\,\mathrm{d}w = \frac{2}{2l+1}\delta_{ll'} \qquad [2.171]$$

One also has the closure relation

$$\frac{1}{2}\sum_{l=0}^{\infty}(2l+1)P_l(w)P_l(w') = \delta(w-w') \qquad [2.172]$$

Important particular values of the Legendre polynomials are

$$P_l(1) = 1, \qquad P_l(-1) = (-1)^l \qquad [2.173]$$

For the lowest values of l one has explicitly

$$\begin{aligned} P_0(w) &= 1 \\ P_1(w) &= w \\ P_2(w) &= \tfrac{1}{2}(3w^2 - 1) \\ P_3(w) &= \tfrac{1}{2}(5w^3 - 3w) \\ P_4(w) &= \tfrac{1}{8}(35w^4 - 30w^2 + 3) \\ P_5(w) &= \tfrac{1}{8}(63w^5 - 70w^3 + 15w) \end{aligned} \qquad [2.174]$$

The associated Legendre functions $P_l^m(w)$ are now defined by the relations

$$P_l^m(w) = (1-w^2)^{m/2}\frac{\mathrm{d}^m}{\mathrm{d}w^m}P_l(w), \qquad m = 0, 1, 2, \ldots l \qquad [2.175]$$

They satisfy the recurrence relations

$$(2l+1)wP_l^m = (l+1-m)P_{l+1}^m + (l+m)P_{l-1}^m \qquad [2.176a]$$

$$(2l+1)(1-w^2)^{1/2}P_l^{m-1} = P_{l+1}^m - P_{l-1}^m \qquad [2.176b]$$

and the orthogonality relations

$$\int_{-1}^{+1} P_l^m(w)P_{l'}^m(w)\,\mathrm{d}w = \frac{2}{2l+1}\frac{(l+m)!}{(l-m)!}\delta_{ll'} \qquad [2.177]$$

The first few associated Legendre functions are given explicitly by

$$\begin{aligned}
P_1^1(w) &= (1 - w^2)^{1/2} \\
P_2^1(w) &= 3(1 - w^2)^{1/2}w \\
P_2^2(w) &= 3(1 - w^2) \\
P_3^1(w) &= \tfrac{3}{2}(1 - w^2)^{1/2}(5w^2 - 1) \\
P_3^2(w) &= 15w(1 - w^2) \\
P_3^3(w) &= 15(1 - w^2)^{3/2}
\end{aligned} \qquad [2.178]$$

The functions $\Theta_{lm}(\theta)$, normalised so that

$$\int_0^\pi \Theta^\star_{l'm}(\theta)\Theta_{lm}(\theta) \sin\theta \, d\theta = \delta_{ll'} \qquad [2.179]$$

are given in terms of the associated Legendre functions P_l^m by

$$\begin{aligned}
\Theta_{lm}(\theta) &= (-1)^m \left[\frac{(2l+1)(l-m)!}{2(l+m)!}\right]^{1/2} P_l^m(\cos\theta), \qquad m \geqslant 0 \\
&= (-1)^{|m|}\Theta_{l|m|}(\theta), \qquad m < 0 \quad [2.180]
\end{aligned}$$

Using [2.165], [2.161] and [2.180], the spherical harmonics are given by

$$Y_{lm}(\theta, \phi) = (-1)^m \left[\frac{(2l+1)(l-m)!}{4\pi(l+m)!}\right]^{1/2} P_l^m(\cos\theta)e^{im\phi}, \qquad m \geqslant 0 \quad [2.181a]$$

$$Y_{l,-m}(\theta, \phi) = (-1)^m Y^\star_{lm}(\theta, \phi) \qquad [2.181b]$$

They satisfy the orthonormality relations

$$\begin{aligned}
\int Y^\star_{l'm'}(\theta, \phi)Y_{lm}(\theta, \phi)\, d\Omega &= \int_0^{2\pi} d\phi \int_0^\pi d\theta \sin\theta \, Y^\star_{l'm'}(\theta, \phi)Y_{lm}(\theta, \phi) \\
&= \delta_{ll'}\,\delta_{mm'}
\end{aligned} \qquad [2.182]$$

where we have written $d\Omega = \sin\theta \, d\theta \, d\phi$. The closure relation reads

$$\sum_{l=0}^{\infty}\sum_{m=-l}^{+l} Y^\star_{lm}(\theta, \phi)Y_{lm}(\theta', \phi') = \delta(\Omega - \Omega'),$$

$$\delta(\Omega - \Omega') = \frac{\delta(\theta - \theta')\,\delta(\phi - \phi')}{\sin\theta} \qquad [2.183]$$

The first few spherical harmonics are listed in Table 2.1. Polar plots of the probability distributions

$$|Y_{lm}(\theta, \phi)|^2 = (2\pi)^{-1}|\Theta_{lm}(\theta)|^2 \qquad [2.184]$$

are shown in Fig. 2.6. Additional useful formulae involving the Legendre polynomials and the spherical harmonics are given in Appendix 4. In that appendix we also discuss *matrix representations* of angular momentum operators,

Table 2.1 The first few spherical harmonics $Y_{lm}(\theta, \phi)$

l	m	*Spherical harmonic* $Y_{lm}(\theta, \phi)$
0	0	$Y_{0,0} = \dfrac{1}{(4\pi)^{1/2}}$
1	0	$Y_{1,0} = \left(\dfrac{3}{4\pi}\right)^{1/2} \cos\theta$
	± 1	$Y_{1,\pm 1} = \mp\left(\dfrac{3}{8\pi}\right)^{1/2} \sin\theta\, e^{\pm i\phi}$
2	0	$Y_{2,0} = \left(\dfrac{5}{16\pi}\right)^{1/2} (3\cos^2\theta - 1)$
	± 1	$Y_{2,\pm 1} = \mp\left(\dfrac{15}{8\pi}\right)^{1/2} \sin\theta\cos\theta\, e^{\pm i\phi}$
	± 2	$Y_{2,\pm 2} = \left(\dfrac{15}{32\pi}\right)^{1/2} \sin^2\theta\, e^{\pm 2i\phi}$
3	0	$Y_{3,0} = \left(\dfrac{7}{16\pi}\right)^{1/2} (5\cos^3\theta - 3\cos\theta)$
	± 1	$Y_{3,\pm 1} = \mp\left(\dfrac{21}{64\pi}\right)^{1/2} \sin\theta\,(5\cos^2\theta - 1) e^{\pm i\phi}$
	± 2	$Y_{3,\pm 2} = \left(\dfrac{105}{32\pi}\right)^{1/2} \sin^2\theta\cos\theta\, e^{\pm 2i\phi}$
	± 3	$Y_{3,\pm 3} = \mp\left(\dfrac{35}{64\pi}\right)^{1/2} \sin^3\theta\, e^{\pm 3i\phi}$

and define the *raising* and *lowering* operators

$$L_{\pm} = L_x \pm iL_y \qquad [2.185]$$

These operators are such that (see [A4.21])

$$L_{\pm} Y_{lm}(\theta, \phi) = \hbar[l(l+1) - m(m \pm 1)]^{1/2} Y_{l,m\pm 1}(\theta, \phi) \qquad [2.186a]$$

or

$$L_{\pm}|lm\rangle = \hbar[l(l+1) - m(m \pm 1)]^{1/2}|lm \pm 1\rangle \qquad [2.186b]$$

where in the last line we have used the *Dirac ket notation*, in which the eigenfunctions Y_{lm} are written in the form $|lm\rangle$.

Let us assume that the particle is in the orbital angular momentum state $|lm\rangle$ such that $\mathbf{L}^2|lm\rangle = l(l+1)\hbar^2|lm\rangle$ and $L_z|lm\rangle = m\hbar|lm\rangle$ (see [2.163] and [2.164]). Although two components of the orbital angular momentum cannot in general be assigned precise values simultaneously, it is nevertheless possible to say something about the components L_x and L_y. Indeed, one can readily show

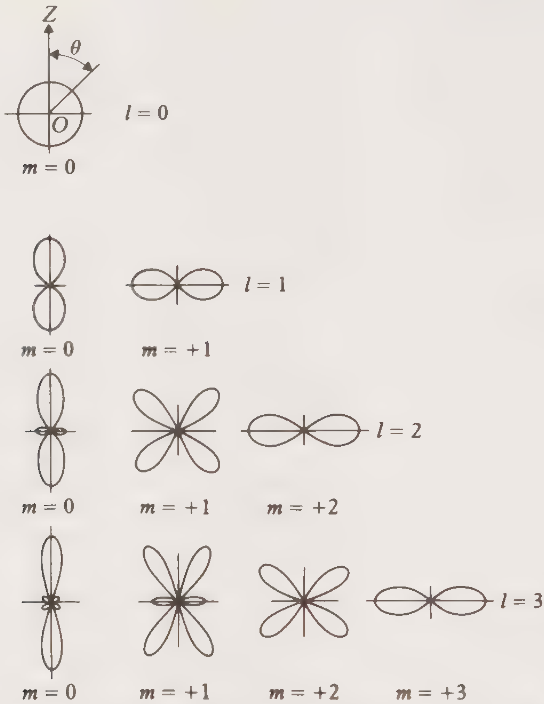

2.6 Polar plots of the probability distributions $|Y_{lm}(\theta, \phi)|^2 = (2\pi)^{-1}|\Theta_{lm}(\theta)|^2$

(Problem 2.13) that

$$\langle lm|L_x|lm\rangle = \langle lm|L_y|lm\rangle = 0 \qquad [2.187]$$

and

$$\langle lm|L_x^2|lm\rangle = \langle lm|L_y^2|lm\rangle = \tfrac{1}{2}\,[l(l+1) - m^2]\hbar^2 \qquad [2.188]$$

We note that when $m = +l$ or $m = -l$, so that the orbital angular momentum is respectively 'parallel' or 'antiparallel' to the Z-axis, its x and y components are still not zero. It is helpful to visualise these results in terms of the *vector model* introduced in Section 1.8 (see Fig. 1.24). According to this model, the orbital angular momentum vector $\mathbf{L}$, of length $\sqrt{l(l+1)}\hbar$, precesses about the Z-axis, the $(2l + 1)$ allowed projections of $\mathbf{L}$ on the Z-axis being given by $m\hbar$, with $m = -l, -l + 1, \ldots +l$.

Spherical harmonics in real form

In some applications it is convenient to use an alternative set of eigenfunctions of $\mathbf{L}^2$, which are the *real forms of the spherical harmonics*. That is,

$$\begin{aligned} Y_{l,\cos}(\theta, \phi) &= N\Theta_{l|m|}(\theta)\cos|m|\phi \\ Y_{l,\sin}(\theta, \phi) &= N\Theta_{l|m|}(\theta)\sin|m|\phi \end{aligned} \qquad [2.189]$$

where the normalisation constant N is equal to $\pi^{-1/2}$, except for $m = 0$ for which $N = (2\pi)^{-1/2}$. For $m = 0$, the function $Y_{l,\cos}$ is clearly identical to the spherical harmonic $Y_{l,0}$. On the other hand, for $m \neq 0$ we have

$$\begin{aligned} Y_{l,\cos} &= \frac{1}{\sqrt{2}}(Y_{l|m|} + Y^{\star}_{l|m|}) \\ Y_{l,\sin} &= -\frac{i}{\sqrt{2}}(Y_{l|m|} - Y^{\star}_{l|m|}) \end{aligned} \qquad [2.190]$$

The spherical harmonics in real form are eigenfunctions of $\mathbf{L}^2$ and L_z^2, but not of L_z (except, of course, when $m = 0$). They behave like simple functions of the Cartesian coordinates, and for this reason are well suited for describing the directional properties of chemical bonds (see Chapter 9).

The first few spherical harmonics in real form are listed in Table 2.2. We have used in this table the so-called 'spectroscopic' notation, in which the value of the orbital angular momentum quantum number l is indicated by a letter,

Table 2.2 The first few spherical harmonics in real form

l	$\lvert m\rvert$	*Spherical harmonic in real form*
0	0	$s = \frac{1}{(4\pi)^{1/2}}$
1	0	$p_z = \left(\frac{3}{4\pi}\right)^{1/2} \cos\theta$
	1	$p_x = \left(\frac{3}{4\pi}\right)^{1/2} \sin\theta\cos\phi$ $p_y = \left(\frac{3}{4\pi}\right)^{1/2} \sin\theta\sin\phi$
2	0	$d_{3z^2-r^2} = \left(\frac{5}{16\pi}\right)^{1/2} (3\cos^2\theta - 1)$
	1	$d_{xz} = \left(\frac{15}{4\pi}\right)^{1/2} \sin\theta\cos\theta\cos\phi$ $d_{yz} = \left(\frac{15}{4\pi}\right)^{1/2} \sin\theta\cos\theta\sin\phi$
	2	$d_{x^2-y^2} = \left(\frac{15}{4\pi}\right)^{1/2} \sin^2\theta\cos 2\phi$ $d_{xy} = \left(\frac{15}{4\pi}\right)^{1/2} \sin^2\theta\sin 2\phi$

according to the correspondence

Value of l	0	1	2	3	4	5	
	$\updownarrow$	$\updownarrow$	$\updownarrow$	$\updownarrow$	$\updownarrow$	$\updownarrow$	
Code letter	s	p	d	f	g	h	, . . .

These code letters are remnants of the spectroscopist's description of various series of spectral lines, the letters s, p, d and f being the first letters of the adjectives 'sharp', 'principal', 'diffuse' and 'fundamental', respectively. For values of l greater than three the letters follow in alphabetical order (g for $l = 4$, h for $l = 5$, and so on). The subscripts z, x, y, xz, yz, etc. used in Table 2.2 indicate the behaviour of the real spherical harmonic in terms of Cartesian coordinates. Polar graphs of the s, p_x, p_y and p_z functions are given in Fig. 2.7. We also remark that while the probability distributions [2.184] corresponding to the 'genuine' spherical harmonics are independent of the azimuthal angle ϕ, those corresponding to the spherical harmonics in real form (that is, $|Y_{l,\cos}|^2$ and $|Y_{l,\sin}|^2$) depend on ϕ in the same way as the functions $\cos^2 |m|\phi$ and $\sin^2 |m|\phi$, as seen from [2.189].

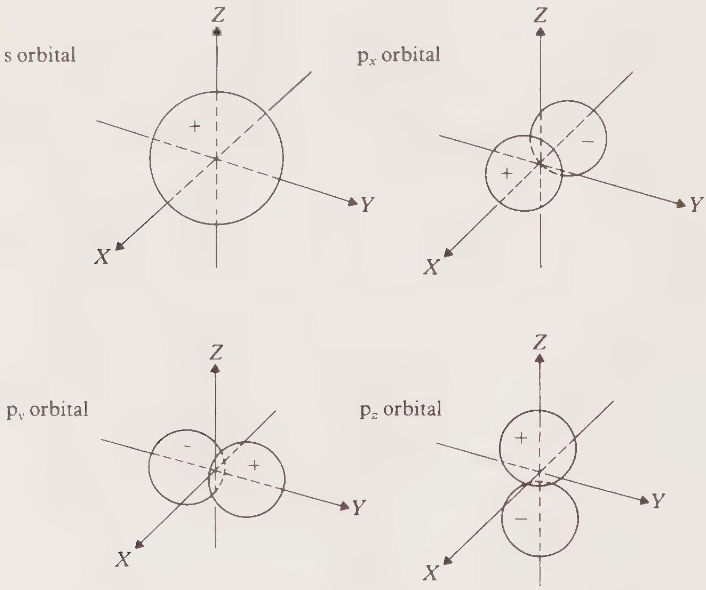

2.7 Polar diagrams of the real spherical harmonics s, p_x, p_y and p_z.

The rigid rotator

As an example of the use of the operator $\mathbf{L}^2$ and of its eigenfunctions, consider the motion of a particle of mass m, constrained to remain at a given distance R_0 from a fixed point, which we choose as the origin of coordinates. Denoting by $I = mR_0^2$ the moment of inertia, the Hamiltonian of this system, which is known

as a (three-dimensional) *rigid rotator*, is

$$H = \frac{\mathbf{L}^2}{2I} \qquad [2.191]$$

Using the expression [2.159] of $\mathbf{L}^2$ in spherical polar coordinates, the Schrödinger eigenvalue equation reads

$$\frac{\mathbf{L}^2}{2I}\psi(\theta, \phi) \equiv -\frac{\hbar^2}{2I}\left[\frac{1}{\sin\theta}\frac{\partial}{\partial\theta}\left(\sin\theta\frac{\partial}{\partial\theta}\right) + \frac{1}{\sin^2\theta}\frac{\partial^2}{\partial\phi^2}\right]\psi(\theta, \phi) = E\psi(\theta, \phi) \qquad [2.192]$$

Thus, we see from [2.163] that the eigenfunctions are just the spherical harmonics $Y_{lm}(\theta, \phi)$, and the energy eigenvalues are

$$E = \frac{\hbar^2}{2I}l(l+1), \qquad l = 0, 1, 2, \ldots \qquad [2.193]$$

Spin angular momentum

We saw in Chapter 1 that the Stern–Gerlach experiment can be interpreted as showing that the electron possesses an internal degree of freedom, the *spin*, which behaves like an angular momentum in the way it couples with a magnetic field. The z component of this spin angular momentum can only take on two values $m_s\hbar$, where $m_s = \pm 1/2$. Therefore, the electron spin cannot be described by the orbital angular momentum operator $\mathbf{L}$ we have considered thus far, since the z component of $\mathbf{L}$ only takes on the values $m\hbar$, with $m = -l, -l+1, \ldots +l$, and $l = 0, 1, 2, \ldots$. We shall assume, however, that *all* angular momentum operators, whether orbital or spin, satisfy commutation relations of the form [2.155]. Thus, if S_x, S_y and S_z are the three Cartesian components of the electron spin angular momentum operator $\mathbf{S}$, they must satisfy the commutation relations

$$[S_x, S_y] = i\hbar S_z, \qquad [S_y, S_z] = i\hbar S_x, \qquad [S_z, S_x] = i\hbar S_y \qquad [2.194]$$

Using the results of Appendix 4, we may readily obtain the properties of the spin angular momentum and of the spin eigenfunctions. Denoting by χ_{s,m_s} the simultaneous eigenfunctions of $\mathbf{S}^2$ and S_z, we have

$$\mathbf{S}^2\chi_{s,m_s} = s(s+1)\hbar^2\chi_{s,m_s} \qquad [2.195]$$

and

$$S_z\chi_{s,m_s} = m_s\hbar\chi_{s,m_s} \qquad [2.196]$$

Since $m_s = \pm 1/2$ for an electron, we must have $s = 1/2$, and we say that the electron has spin one-half. There are only two different normalised spin eigenfunctions χ_{s,m_s}, namely

$$\alpha \equiv \chi_{1/2,1/2}; \ \beta \equiv \chi_{1/2,-1/2} \qquad [2.197]$$

and we see from [2.195] and [2.196] that

$$\mathbf{S}^2\alpha = \tfrac{3}{4}\hbar^2\alpha; \qquad \mathbf{S}^2\beta = \tfrac{3}{4}\hbar^2\beta \tag{2.198}$$

and

$$S_z\alpha = \frac{\hbar}{2}\alpha; \qquad S_z\beta = -\frac{\hbar}{2}\beta \tag{2.199}$$

The spin eigenfunctions α and β are said to correspond respectively to *spin up* ($\uparrow$) and *spin down* ($\downarrow$) states. A general spin-1/2 function χ is an arbitrary linear superposition of the two basic spin states α and β. That is,

$$\chi = \chi_+\alpha + \chi_-\beta \tag{2.200}$$

where χ_+ and χ_- are complex coefficients such that $|\chi_+|^2$ is the probability of finding the electron in the 'spin up' state α, while $|\chi_-|^2$ is the probability of finding it in the 'spin down' state β. The normalisation condition $\langle\chi|\chi\rangle = 1$ gives

$$|\chi_+|^2 + |\chi_-|^2 = 1 \tag{2.201}$$

provided that the basic spin states α and β are orthonormal, namely

$$\begin{aligned} \langle\alpha|\alpha\rangle &= \langle\beta|\beta\rangle = 1 \\ \langle\alpha|\beta\rangle &= \langle\beta|\alpha\rangle = 0 \end{aligned} \tag{2.202}$$

We note from [2.198] and [2.200] that for an arbitrary spin-1/2 function χ we have $\mathbf{S}^2\chi = (3\hbar^2/4)\chi$, so that we may write

$$\mathbf{S}^2 = \tfrac{3}{4}\hbar^2 \tag{2.203}$$

Introducing the raising and lowering operators

$$S_\pm = S_x \pm iS_y \tag{2.204}$$

and using the general relations [A4.15]–[A4.16] of Appendix 4, with $j = 1/2$ and $m = \pm 1/2$, we have

$$\begin{aligned} S_+\alpha &= 0; \qquad & S_+\beta &= \hbar\alpha \\ S_-\alpha &= \hbar\beta; \qquad & S_-\beta &= 0 \end{aligned} \tag{2.205}$$

From [2.199], [2.204] and [2.205] we may construct a table which tells us how the components of $\mathbf{S}$ act on α and β. That is,

$$\begin{aligned} S_x\alpha &= \frac{\hbar}{2}\beta; \qquad & S_x\beta &= \frac{\hbar}{2}\alpha \\ S_y\alpha &= \frac{i\hbar}{2}\beta; \qquad & S_y\beta &= -\frac{i\hbar}{2}\alpha \\ S_z\alpha &= \frac{\hbar}{2}\alpha; \qquad & S_z\beta &= -\frac{\hbar}{2}\beta \end{aligned} \tag{2.206}$$

Using [2.200] and the results of this table, we remark that if χ is an arbitrary spin-1/2 function one has $S_x^2\chi = (\hbar^2/4)\chi$, with a similar result for S_y^2 and S_z^2.

Thus we have

$$S_x^2 = S_y^2 = S_z^2 = \frac{\hbar^2}{4} \qquad [2.207]$$

Since there are only two basic spin states α and β, a *matrix representation* of the spin operators will only require two-by-two matrices. It is apparent from [2.195]–[2.199] that the matrices representing the operators $\mathbf{S}^2$ and S_z may be taken to be the two-by-two diagonal matrices

$$\mathbf{S}^2 = \frac{3}{4}\hbar^2\begin{pmatrix}1 & 0\\ 0 & 1\end{pmatrix}; \qquad S_z = \frac{\hbar}{2}\begin{pmatrix}1 & 0\\ 0 & -1\end{pmatrix} \qquad [2.208]$$

The normalised spin-1/2 eigenfunctions α and β are given by the two-component column vectors (also called spinors)

$$\alpha = \begin{pmatrix}1\\ 0\end{pmatrix}; \qquad \beta = \begin{pmatrix}0\\ 1\end{pmatrix} \qquad [2.209]$$

and may be considered as the basis vectors of a two-dimensional 'spin space'. The orthonormality relations [2.202] can then be written in the form

$$\begin{aligned}\alpha^\dagger\alpha &= \beta^\dagger\beta = 1\\ \alpha^\dagger\beta &= \beta^\dagger\alpha = 0\end{aligned} \qquad [2.210]$$

where the dagger denotes the adjoint. Thus $\alpha^\dagger$ and $\beta^\dagger$ are the row vectors

$$\alpha^\dagger = (1 \quad 0); \qquad \beta^\dagger = (0 \quad 1) \qquad [2.111]$$

and according to the rules of matrix multiplication, we have explicitly

$$\alpha^\dagger\alpha = (1 \quad 0)\begin{pmatrix}1\\ 0\end{pmatrix} = 1 \qquad [2.212]$$

$$\alpha^\dagger\beta = (1 \quad 0)\begin{pmatrix}0\\ 1\end{pmatrix} = 0, \quad \text{etc} \ldots$$

It is also readily verified that the equations [2.205] are satisfied if

$$S_+ = \hbar\begin{pmatrix}0 & 1\\ 0 & 0\end{pmatrix} \qquad S_- = \begin{pmatrix}0 & 0\\ 1 & 0\end{pmatrix} \qquad [2.213]$$

whence

$$S_x = \frac{\hbar}{2}\begin{pmatrix}0 & 1\\ 1 & 0\end{pmatrix} \qquad S_y = \frac{\hbar}{2}\begin{pmatrix}0 & -i\\ i & 0\end{pmatrix} \qquad [2.214]$$

The results [2.208] and [2.214] can also be written as

$$\mathbf{S} = \frac{\hbar}{2}\boldsymbol{\sigma} \qquad [2.215]$$

where

$$\sigma_x = \begin{pmatrix} 0 & 1 \\ 1 & 0 \end{pmatrix} \qquad \sigma_y = \begin{pmatrix} 0 & -i \\ i & 0 \end{pmatrix} \qquad \sigma_z = \begin{pmatrix} 1 & 0 \\ 0 & -1 \end{pmatrix} \tag{2.216}$$

are called the *Pauli spin matrices*. Their principal properties, which can readily be verified (Problem 2.14) are summarised by the equations

$$\sigma_x^2 = \sigma_y^2 = \sigma_z^2 = 1 \tag{2.217a}$$

$$\sigma_x\sigma_y = -\sigma_y\sigma_x = i\sigma_z; \quad \sigma_y\sigma_z = -\sigma_z\sigma_y = i\sigma_x; \quad \sigma_z\sigma_x = -\sigma_x\sigma_z = i\sigma_y \tag{2.217b}$$

$$\mathrm{Tr}\ \sigma_x = \mathrm{Tr}\ \sigma_y = \mathrm{Tr}\ \sigma_z = 0 \tag{2.217c}$$

$$\det \sigma_x = \det \sigma_y = \det \sigma_z = -1 \tag{2.217d}$$

where Tr means the trace and det the determinant. Moreover, the three Pauli matrices σ_x σ_y σ_z and the unit two-by-two matrix form a complete set of 2×2 matrices, in the sense that an arbitrary 2×2 matrix can be expressed in terms of them. Finally, one can prove (Problem 2.14) the identity

$$(\boldsymbol{\sigma} \cdot \mathbf{A})(\boldsymbol{\sigma} \cdot \mathbf{B}) = \mathbf{A} \cdot \mathbf{B} + i\boldsymbol{\sigma} \cdot (\mathbf{A} \times \mathbf{B}) \tag{2.218}$$

where **A** and **B** are any two vectors, or two vector operators whose components commute with those of the spin **S** (that is with those of $\boldsymbol{\sigma}$). In the latter case the order of **A** and **B** on both sides of [2.218] must be respected.

Using the explicit form [2.209] of the basic spinors α and β, an arbitrary spin 1/2 function [2.200] may be written as the spinor

$$\chi = \begin{pmatrix} \chi_+ \\ \chi_- \end{pmatrix} \tag{2.219}$$

and the normalisation condition [2.201] becomes

$$\chi^\dagger \chi = 1 \tag{2.220}$$

where $\chi^\dagger$ denotes the adjoint of the spinor χ, namely

$$\chi^\dagger = (\chi_+^\star\ \chi_-^\star) \tag{2.221}$$

It is worth noting that if the electron is in a pure 'spin up' state α or a pure 'spin down' state β, the expectation values of S_x and S_y vanish, $\langle S_x \rangle = \langle S_y \rangle = 0$ while $\langle S_x^2 \rangle = \langle S_y^2 \rangle = \hbar^2/4$ (see Problem 2.13). Thus, even when the spin angular momentum **S** is said to be 'up' ($m_s = +1/2$) or 'down' ($m_s = -1/2$), its x and y components are still not zero. As in the case of the orbital angular momentum **L**, these results can be visualised with the help of a vector model. According to this model, the spin vector **S**, of length $\sqrt{3/4}\hbar$, precesses about the Z axis, the only allowed projections of **S** on the Z axis being $m_s\hbar$, with $m_s = \pm 1/2$. This is illustrated in Fig. 2.8.

Thus far we have only considered the spin of the electron. Other particles, such as the atomic nuclei, may also possess a spin angular momentum **S**, for which the quantum number s (see [2.195]) can be either integral or half-integral.

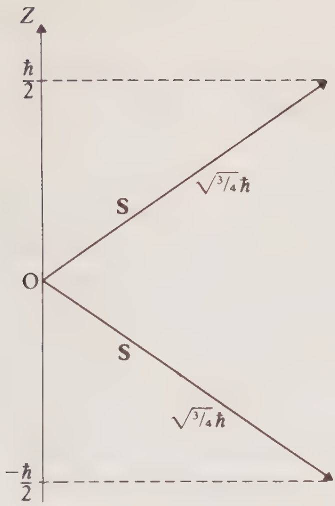

2.8 The vector model of the spin, for a spin one-half particle.

From the results of Appendix 4, with $j = s$ and $m = m_s$, we see that the quantum number m_s takes on the $2s + 1$ values $-s, -s + 1, \ldots s - 1, s$. The matrices representing the spin operators S_x, S_y, S_z and $\mathbf{S}^2$ then have dimensions $2s + 1$; they can be written explicitly by using the methods of Appendix 4 (see Problem 2.15).

Total angular momentum

The total angular momentum of a particle can be written as

$$\mathbf{J} = \mathbf{L} + \mathbf{S} \qquad [2.222]$$

The orbital angular momentum $\mathbf{L} = \mathbf{r} \times \mathbf{p}$ operates only in 'ordinary' space and satisfies the commutation relations [2.155]. On the other hand, the spin angular momentum $\mathbf{S}$ satisfies the commutation relations [2.194] and operates only in 'spin space'. All its components therefore commute with those of $\mathbf{r}$ and $\mathbf{p}$, and hence with all those of $\mathbf{L}$. As a result, the total angular momentum $\mathbf{J}$ satisfies the commutation relations

$$[J_x, J_y] = i\hbar J_z, \qquad [J_y, J_z] = i\hbar J_x, \qquad [J_z, J_x] = i\hbar J_y \qquad [2.223]$$

which characterise an angular momentum operator.

It is shown in Appendix 4 that the simultaneous eigenfunctions of $\mathbf{J}^2 = J_x^2 + J_y^2 + J_z^2$ and J_z satisfy the eigenvalue equations

$$\mathbf{J}^2\psi_{jm_j} = j(j+1)\hbar^2\psi_{jm_j} \qquad [2.224]$$

and

$$J_z\psi_{jm_j} = m_j\hbar\psi_{jm_j} \qquad [2.225]$$

where j is a non-negative integer or half-integer ($j = 0, 1/2, 1, 3/2, \dots$) and $m_j = -j, -j+1, \dots j-1, j$.

Since all the components of $\mathbf{L}$ commute with all those of $\mathbf{S}$, the operators $\mathbf{L}^2$, L_z, $\mathbf{S}^2$ and S_z mutually commute, and have the simultaneous eigenfunctions

$$\psi_{lsm_lm_s} = Y_{lm_l}(\theta, \phi)\chi_{s,m_s} \qquad [2.226]$$

where we have written $m_l \equiv m$ [5]. It can be shown (Problem 2.16) that the four operators $\mathbf{L}^2$, $\mathbf{S}^2$, $\mathbf{J}^2$ and $\mathcal{J}_z$ also form a commuting set of operators. Their simultaneous eigenfunctions are linear combinations of the functions $\psi_{lsm_lm_s}$ and are often denoted by the symbol $\mathcal{Y}_{ls}^{jm_j}$ (see Appendix 4). For a given value of l and s the possible values of j are given by

$$|l - s|, |l - s| + 1, \dots l + s \qquad [2.227]$$

For a given j the quantum number m_j can take on the $2j+1$ values $-j$, $-j + 1, \dots j - 1, j$, as we have seen above.

Wave functions for a spin-1/2 particle

Thus far in this section we have focused our attention on the angular and spin parts of the wave functions. In general, the wave functions also depend on the radial coordinate r and on the time t. For example, in the case of a spin-1/2 particle (e.g. an electron), a general expression for the wave function is

$$\Psi(q, t) = \Psi_+(\mathbf{r}, t)\alpha + \Psi_-(\mathbf{r}, t)\beta \qquad [2.228]$$

where q denotes the ensemble of the (continuous) spatial variables $\mathbf{r}$ *and* the (discrete) spin variable ($m_s = \pm 1/2$) of the particle. The probability density for finding at time t the particle at $\mathbf{r}$ with 'spin up' is $|\Psi_+(\mathbf{r}, t)|^2$, and with 'spin down' it is $|\Psi_-(\mathbf{r}, t)|^2$. Using [2.209] we may also write the wave function Ψ as a two-component or spinor wave function, namely

$$\Psi = \begin{pmatrix} \Psi_+ \\ \Psi_- \end{pmatrix} \qquad [2.229]$$

2.6 CENTRAL FORCES

Let us now return to the Schrödinger equation [2.59] describing the motion of a spinless particle of mass m in a time-independent potential $V(\mathbf{r})$. We shall consider in this section the important case of *central* potentials, that is potentials $V(r)$ which depend only upon the magnitude $r = |\mathbf{r}|$ of the vector $\mathbf{r}$. Since $V(r)$ is spherically symmetric, it is natural to use the spherical polar coordinates defined

[5] In general we shall use the notation m for a magnetic quantum number, but where it is important to distinguish between different kinds of angular momenta, we shall use the notation m_l, m_s, m_j, as necessary.

in [2.157]. The Hamiltonian of the system is then given by

$$H = -\frac{\hbar^2}{2m}\nabla^2 + V(r)$$
$$= -\frac{\hbar^2}{2m}\left[\frac{1}{r^2}\frac{\partial}{\partial r}\left(r^2\frac{\partial}{\partial r}\right) + \frac{1}{r^2\sin\theta}\frac{\partial}{\partial\theta}\left(\sin\theta\frac{\partial}{\partial\theta}\right) + \frac{1}{r^2\sin^2\theta}\frac{\partial^2}{\partial\phi^2}\right] + V(r) \qquad [2.230]$$

Using the expression [2.159] of $\mathbf{L}^2$, we may also write

$$H = -\frac{\hbar^2}{2m}\left[\frac{1}{r^2}\frac{\partial}{\partial r}\left(r^2\frac{\partial}{\partial r}\right) - \frac{\mathbf{L}^2}{\hbar^2 r^2}\right] + V(r) \qquad [2.231]$$

so that the Schrödinger equation [2.59] reads

$$\left\{-\frac{\hbar^2}{2m}\left[\frac{1}{r^2}\frac{\partial}{\partial r}\left(r^2\frac{\partial}{\partial r}\right) - \frac{\mathbf{L}^2}{\hbar^2 r^2}\right] + V(r)\right\}\psi(\mathbf{r}) = E\psi(\mathbf{r}) \qquad [2.232]$$

Now $\mathbf{L}^2$ and L_z only operate on angular variables, and in addition $[\mathbf{L}^2, L_z] = 0$. Therefore, we see from [2.231] that

$$[H, \mathbf{L}^2] = [H, L_z] = 0 \qquad [2.233]$$

We may thus look for solutions of the Schrödinger equation [2.232] which are simultaneous eigenfunctions of the operators H, $\mathbf{L}^2$ and L_z. Since the spherical harmonics $Y_{lm}(\theta, \phi)$ are simultaneous eigenfunctions of $\mathbf{L}^2$ and L_z (see [2.163] and [2.164]) we can write a particular solution as

$$\psi_{E,l,m}(r, \theta, \phi) = R_{E,l}(r)Y_{lm}(\theta, \phi) \qquad [2.234]$$

Substituting [2.234] into [2.232], and using [2.163], we obtain for the radial function $R_{E,l}(r)$ the equation

$$\left\{-\frac{\hbar^2}{2m}\left[\frac{1}{r^2}\frac{\mathrm{d}}{\mathrm{d}r}\left(r^2\frac{\mathrm{d}}{\mathrm{d}r}\right) - \frac{l(l+1)}{r^2}\right] + V(r)\right\}R_{E,l}(r) = ER_{E,l}(r) \qquad [2.235]$$

which shows that $R_{E,l}$ does not depend on the magnetic quantum number m.

The radial equation [2.235] can be simplified by introducing the new radial function

$$u_{E,l}(r) = rR_{E,l}(r) \qquad [2.236]$$

The new radial equation which we obtain for $u_{E,l}(r)$ is then

$$\left[-\frac{\hbar^2}{2m}\frac{\mathrm{d}^2}{\mathrm{d}r^2} + \frac{l(l+1)\hbar^2}{2mr^2} + V(r)\right]u_{E,l}(r) = Eu_{E,l}(r) \qquad [2.237]$$

For potentials which are less singular than r^{-2} at the origin, a power series expansion of $u_{E,l}(r)$ can be made for small r, and the examination of the indicial

equation shows that

$$u_{E,l}(r) \underset{r\to 0}{\sim} r^{l+1} \qquad [2.238]$$

The equation [2.237] is similar to the one-dimensional Schrödinger equation [2.121] for an *'effective potential'*

$$V_{\text{eff}}(r) = V(r) + \frac{l(l+1)\hbar^2}{2mr^2} \qquad [2.239]$$

which contains the repulsive *centrifugal barrier* term $l(l+1)\hbar^2/2mr^2$ in addition to $V(r)$. We remark, however, that the variable r is confined to positive values $0 \leqslant r \leqslant \infty$, in contrast to the variable x in [2.121].

Parity

The *parity* operator $\mathcal{P}$ is defined by the relation

$$\mathcal{P}f(\mathbf{r}) = f(-\mathbf{r}) \qquad [2.240]$$

where $f(\mathbf{r})$ is an arbitrary function. Thus the parity operator corresponds to an inversion of the position coordinate $\mathbf{r}$ through the origin. It is a Hermitian operator since, for any two wave functions $\phi(\mathbf{r})$ and $\psi(\mathbf{r})$, we have

$$\begin{aligned}\int \phi^\star(\mathbf{r})\mathcal{P}\psi(\mathbf{r})\, d\mathbf{r} &= \int \phi^\star(\mathbf{r})\psi(-\mathbf{r})\, d\mathbf{r} \\ &= \int \phi^\star(-\mathbf{r})\psi(\mathbf{r})\, d\mathbf{r} \\ &= \int [\mathcal{P}\phi(\mathbf{r})]^\star\psi(\mathbf{r})\, d\mathbf{r} \qquad [2.241]\end{aligned}$$

Let us now consider the eigenvalue equation for $\mathcal{P}$, which we write as

$$\mathcal{P}\psi_\alpha(\mathbf{r}) = \alpha\psi_\alpha(\mathbf{r}) \qquad [2.242]$$

From the definition [2.240] of $\mathcal{P}$ and the fact that $\mathcal{P}f(-\mathbf{r}) = f(\mathbf{r})$, we deduce that

$$\mathcal{P}^2 = I \qquad [2.243]$$

where I is the unit operator. Hence

$$\mathcal{P}^2\psi_\alpha(\mathbf{r}) = \alpha\mathcal{P}\psi_\alpha(\mathbf{r}) = \alpha^2\psi_\alpha(\mathbf{r}) = \psi_\alpha(\mathbf{r}) \qquad [2.244]$$

so that $\alpha^2 = 1$ and the eigenvalues of $\mathcal{P}$ are $\alpha = \pm 1$. Denoting the corresponding eigenfunctions by ψ_+ and ψ_-, we have

$$\mathcal{P}\psi_+(\mathbf{r}) = \psi_+(\mathbf{r}), \qquad \mathcal{P}\psi_-(\mathbf{r}) = -\psi_-(\mathbf{r}) \qquad [2.245]$$

or

$$\psi_+(-\mathbf{r}) = \psi_+(\mathbf{r}), \qquad \psi_-(-\mathbf{r}) = -\psi_-(\mathbf{r}) \qquad [2.246]$$

Thus $\psi_+(\mathbf{r})$ is an *even* function of $\mathbf{r}$, and $\psi_-(\mathbf{r})$ is an *odd* function of $\mathbf{r}$. The eigenfunctions ψ_+ are said to have *even parity*, while the eigenfunctions ψ_- have *odd parity*. We note that ψ_+ and ψ_- are orthogonal. They also form a complete set, since any function $\psi(\mathbf{r})$ can always be written as

$$\psi(\mathbf{r}) = \psi_+(\mathbf{r}) + \psi_-(\mathbf{r}) \qquad [2.247]$$

where

$$\psi_+(\mathbf{r}) = \tfrac{1}{2}[\psi(\mathbf{r}) + \psi(-\mathbf{r})] \qquad [2.248]$$

has obviously even parity, while

$$\psi_-(\mathbf{r}) = \tfrac{1}{2}[\psi(\mathbf{r}) - \psi(-\mathbf{r})] \qquad [2.249]$$

has odd parity.

Let us now return to the central force problem. Under the parity operation $\mathbf{r} \to -\mathbf{r}$, the spherical polar coordinates (r, θ, ϕ) become $(r, \pi - \theta, \phi + \pi)$. The central force Hamiltonian [2.230] is clearly unaffected by this operation, or in other words the parity operator $\mathcal{P}$ commutes with the Hamiltonian [2.230]

$$[\mathcal{P}, H] = 0 \qquad [2.250]$$

As a result, simultaneous eigenfunctions of the operators $\mathcal{P}$ and H can be found. Applying the parity operator on the wave function $\psi_{E,l,m}(r, \theta, \phi) = R_{E,l}(r)Y_{lm}(\theta, \phi)$ (see [2.234]), we have

$$\mathcal{P}[R_{E,l}(r)Y_{lm}(\theta, \phi)] = R_{E,l}(r)Y_{lm}(\pi - \theta, \phi + \pi) \qquad [2.251]$$

Now, from the definition [2.181] of the spherical harmonics, it can be shown that

$$Y_{lm}(\pi - \theta, \phi + \pi) = (-1)^l Y_{lm}(\theta, \phi) \qquad [2.252]$$

so that Y_{lm} has the parity of l. Thus

$$\mathcal{P}[R_{E,l}(r)Y_{lm}(\theta, \phi)] = R_{E,l}(r)(-1)^l Y_{lm}(\theta, \phi) \qquad [2.253]$$

and the wave function $\psi_{E,l,m}$ itself has the parity of l (even for even l, odd for odd l).

The free particle

We shall discuss at length various applications involving central potentials in subsequent chapters. For further reference, we consider here the (very) special case of the free particle, for which $V(r) = 0$. Writing $k = \sqrt{2mE}/\hbar$, the radial equation [2.235] becomes

$$\left[\frac{\mathrm{d}^2}{\mathrm{d}r^2} + \frac{2}{r}\frac{\mathrm{d}}{\mathrm{d}r} - \frac{l(l+1)}{r^2} + k^2\right] R_{E,l}(r) = 0 \qquad [2.254]$$

It is convenient to set $\rho = kr$ and to write $R_l(\rho) \equiv R_{E,l}(r)$, so that the above equation reads

$$\left[\frac{d^2}{d\rho^2} + \frac{2}{\rho}\frac{d}{d\rho} + \left(1 - \frac{l(l+1)}{\rho^2}\right)\right] R_l(\rho) = 0 \qquad [2.255]$$

This equation is known as the *spherical Bessel differential equation*. The solutions of [2.255] which are regular and finite everywhere are given (up to a multiplicative constant) by the spherical Bessel functions $j_l(\rho)$, defined by

$$j_l(\rho) = \left(\frac{\pi}{2\rho}\right)^{1/2} \mathcal{J}_{l+\frac{1}{2}}(\rho) \qquad [2.256]$$

where $\mathcal{J}_\nu(\rho)$ is a Bessel function of order ν. The first few spherical Bessel functions are given explicitly by

$$j_0(\rho) = \frac{\sin\rho}{\rho}$$

$$j_1(\rho) = \frac{\sin\rho}{\rho^2} - \frac{\cos\rho}{\rho}$$

$$j_2(\rho) = \left(\frac{3}{\rho^3} - \frac{1}{\rho}\right)\sin\rho - \frac{3}{\rho^2}\cos\rho \qquad [2.257]$$

Additional properties of the functions $j_l(\rho)$ will be discussed in Chapter 11.

The eigenvalues k^2 of [2.254] can take on any positive real value. As a result, the energy $E = \hbar^2k^2/2m$ can assume any value in the interval $(0, \infty)$, giving an example of a *continuous spectrum*. Thus, returning to [2.234] and using the foregoing results, we see that for every positive value of E there exists an eigenfunction of the free particle Schrödinger equation labelled by the orbital angular momentum quantum numbers (l, m), namely

$$\psi_{E,l,m}(r, \theta, \phi) = Cj_l(kr)Y_{lm}(\theta, \phi) \qquad [2.258]$$

where C is a constant. It can be shown that the ensemble of *spherical waves* [2.258] forms a complete set.

On the other hand, we have seen in Section 2.1 that a free particle of momentum $\hbar\mathbf{k}$ and energy $E = \hbar^2k^2/2m$ is represented by the plane wave $\exp(i\mathbf{k}\cdot\mathbf{r})$. Since the spherical waves [2.258] form a complete set, we may expand the plane wave $\exp(i\mathbf{k}\cdot\mathbf{r})$ in terms of them. That is,

$$e^{i\mathbf{k}\cdot\mathbf{r}} = \sum_{l=0}^{\infty}\sum_{m=-l}^{+l} c_{lm}(\mathbf{k})j_l(kr)Y_{lm}(\theta, \phi) \qquad [2.259]$$

If we choose the Z axis to be along the wave vector $\mathbf{k}$, then the left hand side of [2.259] reads $\exp(i\mathbf{k}\cdot\mathbf{r}) = \exp(ikr\cos\theta)$, which is independent of ϕ. Setting $w = \cos\theta$, the expansion of $\exp(i\mathbf{k}\cdot\mathbf{r})$ reduces to an expansion in terms of Legendre polynomials $P_l(w)$. A straightfoward calculation (Problem 2.17) then

yields

$$e^{i\mathbf{k}\cdot\mathbf{r}} = \sum_{l=0}^{\infty} (2l + 1)i^l j_l(kr)P_l(\cos\theta) \qquad [2.260]$$

Using the addition theorem of the spherical harmonics (see the equation [A4.23] of Appendix 4) we can also write the above formula in the form of equation [2.259]. That is

$$e^{i\mathbf{k}\cdot\mathbf{r}} = 4\pi \sum_{l=0}^{\infty} \sum_{m=-l}^{+l} i^l j_l(kr) Y^{\star}_{lm}(\hat{\mathbf{k}}) Y_{lm}(\hat{\mathbf{r}}) \qquad [2.261]$$

where $\hat{\mathbf{x}}$ denotes the polar angles of a vector $\mathbf{x}$. Upon comparison of [2.259] and [2.261] we see that the coefficients $c_{lm}(\mathbf{k})$ are given by $c_{lm}(\mathbf{k}) = 4\pi i^l Y^{\star}_{lm}(\hat{\mathbf{k}})$.

2.7 SEVERAL-PARTICLE SYSTEMS

Until now we have only discussed the motion of a single particle. In this section we shall generalise our results to N-particle systems. We begin by considering a system of N non-relativistic *spinless* particles having masses m_i, position coordinates $\mathbf{r}_i$ and momenta $\mathbf{p}_i$ ($i = 1, 2, \ldots N$). The classical Hamiltonian function of this system is

$$H(\mathbf{r}_1, \ldots \mathbf{r}_N, \mathbf{p}_1, \ldots \mathbf{p}_N, t) = \sum_{i=1}^{N} \frac{p_i^2}{2m_i} + V(\mathbf{r}_1, \ldots \mathbf{r}_N, t) \qquad [2.262]$$

where V is the potential energy. The total classical energy E of the system is

$$E_{\text{tot}} = H(\mathbf{r}_1, \ldots \mathbf{r}_N, \mathbf{p}_1, \ldots \mathbf{p}_N, t) \qquad [2.263]$$

The Schrödinger equation for the wave function $\Psi(\mathbf{r}_1, \ldots \mathbf{r}_N; t)$ which describes the dynamical state of the system is obtained by considering E_{tot} and $\mathbf{p}_i$ to be the differential operators (compare with [2.11])

$$E_{\text{op}} = i\hbar \frac{\partial}{\partial t}, \qquad (\mathbf{p}_i)_{\text{op}} = -i\hbar \nabla_{r_i} \qquad [2.264]$$

and writing that E_{op} and $H_{\text{op}} \equiv H(\mathbf{r}_1, \ldots \mathbf{r}_N, -i\hbar\nabla_{r_1}, \ldots -i\hbar\nabla_{r_N}, t)$ give identical results when acting on Ψ. That is

$$i\hbar \frac{\partial}{\partial t} \Psi = H_{\text{op}}\Psi = \left[\sum_{i=1}^{N} \left(-\frac{\hbar^2}{2m_i} \nabla^2_{r_i} \right) + V(\mathbf{r}_1, \ldots \mathbf{r}_N, t) \right] \Psi \qquad [2.265]$$

The normalisation condition [2.26] now takes the form

$$\int |\Psi(\mathbf{r}_1, \ldots \mathbf{r}_N, t)|^2 \, d\mathbf{r}_1 \ldots d\mathbf{r}_N = 1 \qquad [2.266]$$

The total orbital angular momentum $\mathbf{L}$ of the system is the sum of the individual orbital angular momenta $\mathbf{L}_i = \mathbf{r}_i \times \mathbf{p}_i$

$$\mathbf{L} = \sum_{i=1}^{N} \mathbf{L}_i \qquad [2.267]$$

It is also worth noting that all the components of the position $\mathbf{r}_i$ and momentum $\mathbf{p}_i$ of particle i commute with all those pertaining to particle j provided that $i \neq j$, so that the fundamental commutation relations read

$$[x_i, p_{xj}] = i\hbar\,\delta_{ij}, \qquad [y_i, p_{xj}] = 0, \text{ etc.} \tag{2.268}$$

Two-body systems

Of particular interest is a system of two particles, of masses m_1 and m_2, interacting via a time-independent potential $V(\mathbf{r}_1 - \mathbf{r}_2)$ which depends only upon the relative coordinate $\mathbf{r}_1 - \mathbf{r}_2$. The classical Hamiltonian of the system is therefore given by

$$H = \frac{\mathbf{p}_1^2}{2m_1} + \frac{\mathbf{p}_2^2}{2m_2} + V(\mathbf{r}_1 - \mathbf{r}_2) \tag{2.269}$$

Making the substitutions $\mathbf{p}_1 \to -i\hbar\boldsymbol{\nabla}_{r_1}$ and $\mathbf{p}_2 \to -i\hbar\boldsymbol{\nabla}_{r_2}$ in [2.269], we obtain the quantum mechanical Hamiltonian operator, and the corresponding Schrödinger equation reads

$$i\hbar\frac{\partial}{\partial t}\Psi(\mathbf{r}_1, \mathbf{r}_2, t) = \left[-\frac{\hbar^2}{2m_1}\nabla_{r_1}^2 - \frac{\hbar^2}{2m_2}\nabla_{r_2}^2 + V(\mathbf{r}_1 - \mathbf{r}_2)\right]\Psi(\mathbf{r}_1, \mathbf{r}_2, t) \tag{2.270}$$

Because the potential V only depends on the difference of coordinates $\mathbf{r}_1 - \mathbf{r}_2$, an important simplification can now be made. We introduce the relative coordinate

$$\mathbf{r} = \mathbf{r}_1 - \mathbf{r}_2 \tag{2.271}$$

together with the vector

$$\mathbf{R} = \frac{m_1\mathbf{r}_1 + m_2\mathbf{r}_2}{m_1 + m_2} \tag{2.272}$$

which determines the position of the centre of mass (CM) of the system. Changing variables from the coordinates $(\mathbf{r}_1, \mathbf{r}_2)$ to the new coordinates $(\mathbf{r}, \mathbf{R})$ one finds that the Schrödinger equation [2.270] becomes

$$i\hbar\frac{\partial}{\partial t}\Psi(\mathbf{R}, \mathbf{r}, t) = \left[-\frac{\hbar^2}{2M}\nabla_R^2 - \frac{\hbar^2}{2\mu}\nabla_r^2 + V(\mathbf{r})\right]\Psi(\mathbf{R}, \mathbf{r}, t) \tag{2.273}$$

where

$$M = m_1 + m_2 \tag{2.274}$$

is the total mass of the system and

$$\mu = \frac{m_1 m_2}{m_1 + m_2} \tag{2.275}$$

is the reduced mass of the two particles. The Schrödinger equation [2.273] may

also be obtained by introducing the relative momentum

$$\mathbf{p} = \frac{m_2\mathbf{p}_1 - m_1\mathbf{p}_2}{m_1 + m_2} \qquad [2.276]$$

together with the total momentum

$$\mathbf{P} = \mathbf{p}_1 + \mathbf{p}_2 \qquad [2.277]$$

Since

$$\frac{\mathbf{p}_1^2}{2m_1} + \frac{\mathbf{p}_2^2}{2m_2} = \frac{\mathbf{P}^2}{2M} + \frac{\mathbf{p}^2}{2\mu} \qquad [2.278]$$

the classical Hamiltonian [2.269] can be written as

$$H = \frac{\mathbf{P}^2}{2M} + \frac{\mathbf{p}^2}{2\mu} + V(\mathbf{r}) \qquad [2.279]$$

Performing the substitutions $\mathbf{P} \to -i\hbar\nabla_R$ and $\mathbf{p} \to -i\hbar\nabla_r$ in [2.279], we then obtain the quantum mechanical Hamiltonian operator leading to the Schrödinger equation [2.273].

Two separations of the equation [2.273] can now be made. The time dependence can first be separated as in [2.58] since the potential is time-independent. Secondly, the spatial part of the wave function can be separated into a product of functions of the centre of mass coordinate $\mathbf{R}$ and of the relative coordinate $\mathbf{r}$. Thus the Schrödinger equation [2.273] admits solutions of the form

$$\Psi(\mathbf{R}, \mathbf{r}, t) = \Phi(\mathbf{R})\psi(\mathbf{r})e^{-i(E_{CM}+E)t/\hbar} \qquad [2.280]$$

where the functions $\Phi(\mathbf{R})$ and $\psi(\mathbf{r})$ satisfy respectively the equations

$$-\frac{\hbar^2}{2M}\nabla_{\mathrm{R}}^2\,\Phi(\mathbf{R}) = E_{\mathrm{CM}}\,\Phi(\mathbf{R}) \qquad [2.281]$$

and

$$\left[-\frac{\hbar^2}{2\mu}\nabla_r^2 + V(\mathbf{r})\right]\psi(\mathbf{r}) = E\psi(\mathbf{r}) \qquad [2.282]$$

We see that the equation [2.281] is a time-independent Schrödinger equation describing the centre of mass as a free particle of mass M and energy E_{CM}. The second time-independent Schrödinger equation [2.282] describes the relative motion of the two particles; it is the same as the equation corresponding to the motion of a particle having the reduced mass μ in the potential $V(\mathbf{r})$. The total energy of the system is clearly

$$E_{\mathrm{tot}} = E_{\mathrm{CM}} + E \qquad [2.283]$$

We have therefore 'decoupled' the original two-body problem into two one-body problems, that of a free particle (the centre of mass) and that of a single

particle of reduced mass μ in a potential $V(\mathbf{r})$. We remark that if we elect to work in the centre of mass system of the two particles, we need not be concerned with the motion of the centre of mass, the coordinates of which are eliminated.

Systems of particles with spin. Addition of angular momenta

Let us now consider a system of particles which may possess spin. We shall denote by q_i the ensemble of space and spin coordinates of the particle i. The angular momentum $\mathbf{J}_i$ of that particle is the sum of its orbital angular momentum $\mathbf{L}_i$ and its spin angular momentum $\mathbf{S}_i$,

$$\mathbf{J}_i = \mathbf{L}_i + \mathbf{S}_i \qquad [2.284]$$

The total orbital angular momentum $\mathbf{L}$ of the system is given by [2.267]. The total spin angular momentum is

$$\mathbf{S} = \sum_{i=1}^{N} \mathbf{S}_i \qquad [2.285]$$

Finally, the total angular momentum of the system is the sum of the individual angular momenta $\mathbf{J}_i$,

$$\mathbf{J} = \sum_{i=1}^{N} \mathbf{J}_i \qquad [2.286]$$

In many problems of quantum physics the Hamiltonian H of the system is rotationally invariant. As a consequence, it may be shown [6] that H commutes with the components of the total angular momentum $\mathbf{J}$, so that we can look for the eigenfunctions of H among the simultaneous eigenfunctions of $\mathbf{J}^2$ and $\mathcal{J}_z$. On the other hand, we know in general how to obtain the eigenfunctions of the individual angular momentum operators $\mathbf{J}_i^2$, $\mathcal{J}_{iz}$ (see Appendix 4). The problem of the *addition of angular momenta* consists in obtaining the eigenvalues and eigenfunctions of $\mathbf{J}^2$ and $\mathcal{J}_z$ in terms of those of $\mathbf{J}_i^2$ and $\mathcal{J}_{iz}$. The simplest addition problem, namely that of adding *two* angular momenta is discussed in Appendix 4.

Indistinguishable particles

Many systems considered in further chapters of this book contain a number of particles (notably electrons) which are all *identical*. In this case the Hamiltonian must be symmetric with respect to any interchange of the space *and* spin coordinates of the particles. Thus an interchange operator P_{ij} that permutes the variables q_i and q_j of particles i and j commutes with the Hamiltonian:

$$[P_{ij}, H] = 0 \qquad [2.287]$$

[6] See Messiah (1968) or Merzbacher (1970).

As a consequence, if $\psi(q_1, \ldots q_i, \ldots q_j, \ldots q_N)$ is an eigenfunction of H with eigenvalue E, so is also $P_{ij}\psi$, where

$$P_{ij}\psi(q_1, \ldots q_i, \ldots q_j, \ldots q_N) = \psi(q_1, \ldots q_j, \ldots q_i, \ldots q_N) \quad [2.288]$$

Since two successive interchanges of q_i and q_j bring the particles back to their initial configurations, we have

$$P_{ij}^2 = I \quad [2.289]$$

so that the eigenvalues of the operator P_{ij} are $\varepsilon = \pm 1$. Wave functions corresponding to the eigenvalue $\varepsilon = +1$ are such that

$$\begin{aligned} P_{ij}\psi(q_1, \ldots q_i, \ldots q_j, \ldots q_N) &= \psi(q_1, \ldots q_j, \ldots q_i, \ldots q_N) \\ &= \psi(q_1, \ldots q_i, \ldots q_j, \ldots q_N) \end{aligned} \quad [2.290]$$

and are said to be *symmetric* under the interchange P_{ij}. On the other hand, wave functions which correspond to the eigenvalue $\varepsilon = -1$ are such that

$$\begin{aligned} P_{ij}\psi(q_1, \ldots q_i, \ldots q_j, \ldots q_N) &= \psi(q_1, \ldots q_j, \ldots q_i, \ldots q_N) \\ &= -\psi(q_1, \ldots q_i, \ldots q_j, \ldots q_N) \end{aligned} \quad [2.291]$$

and are said to be *antisymmetric* under the interchange P_{ij}.

More generally, there are $N!$ different permutations of the variables $q_1, \ldots q_N$. Defining P as the permutation that replaces q_1 by q_{P1}, q_2 by $q_{P2}, \ldots q_N$ and q_{PN} and noting that P can be obtained as a succession of interchanges, we have

$$[P, H] = 0 \quad [2.292]$$

A permutation P is said to be *even* or *odd* depending on whether the number of interchanges leading to it is even or odd. If we let the operator P act on a wave function $\psi(q_1, \ldots q_N)$, we have

$$P\psi(q_1, \ldots q_N) = \psi(q_{P1}, \ldots q_{PN}) \quad [2.293]$$

It is worth stressing that except for the case $N = 2$ the $N!$ permutations P do *not* commute among themselves. This is due to the fact that the interchange operators P_{ij} and P_{ik} $(k \neq j)$ do not mutually commute. Therefore, the eigenfunctions $\psi(q_1, \ldots q_N)$ of H are not *in general* eigenfunctions of all the $N!$ permutation operators P. However, there are *two* exceptional states which *are* eigenstates of H and of the $N!$ permutation operators P. The first one is the *totally symmetric state* $\psi_S(q_1, \ldots q_N)$ satisfying [2.290] for *any* particle interchange P_{ij}, so that for all P

$$\begin{aligned} P\psi_S(q_1, \ldots q_N) &= \psi_S(q_{P1}, \ldots q_{PN}) \\ &= \psi_S(q_1, \ldots q_N) \end{aligned} \quad [2.294]$$

The other one is the *totally antisymmetric* state $\psi_A(q_1, \ldots q_N)$, which satisfies

[2.291] for *any* interchange P_{ij}. Hence, for all P

$$P\psi_A(q_1, \dots q_N) = \psi_A(q_{P1}, \dots q_{PN}) = \begin{cases} \psi_A(q_1, \dots q_N) & \text{for an even permutation} \\ -\psi_A(q_1, \dots q_N) & \text{for an odd permutation} \end{cases} \quad [2.295]$$

We also remark that the equation [2.292] implies that P is a constant of the motion, so that a system of identical particles represented by a wave function of a given symmetry (S or A) will keep that symmetry at all times.

According to our present knowledge of particles occurring in nature, the two types of states ψ_S and ψ_A are thought to be sufficient to describe all systems of identical particles. This is called the *symmetrisation postulate*. Particles having states described by totally symmetric wave functions are called *bosons*. They can be shown [7] to obey Bose–Einstein statistics. Experiment shows that particles of *zero* or *integral* spin, such as the photon ($s = 1$) are bosons. On the other hand, particles having states described by totally antisymmetric functions are called *fermions*. They satisfy Fermi–Dirac statistics [7]. It is found that particles having *half-integral* spin values such as the electron and the proton ($s = 1/2$) are fermions. The statement that the wave function of a system of identical fermions must be totally antisymmetric in the combined space and spin coordinates of the particles is the generalised version of the *Pauli exclusion principle*.

If the system is composed of different kinds of bosons (fermions), then its wave function must be separately totally symmetric (antisymmetric) with respect to permutations of each kind of identical particles. For example, in the case of the hydrogen molecule H_2, the total wave function must be antisymmetric under the interchange of the two electrons and also antisymmetric under the interchange of the two protons.

2.8 APPROXIMATION METHODS

As in the case of classical mechanics, there are relatively few physically interesting problems in quantum mechanics which can be solved exactly. Approximation methods are therefore of great importance in discussing the application of quantum theory to specific systems, such as the atomic and molecular ones considered in this book. In this section we shall review several approximation methods which will be used extensively in further chapters.

Time-independent perturbation theory

Perturbation theory deals with the changes induced in a system by a 'small' disturbance. Although we shall also apply perturbation methods to scattering problems at a later stage (see Chapters 11–13) we shall start here by discussing the *Rayleigh–Schrödinger perturbation theory*, which is concerned with the

[7] See Dicke and Wittke (1960) or Messiah (1968).

modifications in the *discrete* energy levels and corresponding eigenfunctions of a system when a perturbation is applied.

Let us assume that the time-independent Hamiltonian H of a system may be separated in two parts,

$$H = H_0 + \lambda H' \qquad [2.296]$$

where the 'unperturbed' Hamiltonian H_0 is sufficiently simple so that the corresponding Schrödinger eigenvalue equation

$$H_0\psi_k = E_k\psi_k \qquad [2.297]$$

may be solved, and the term $\lambda H'$ is a small perturbation. The parameter λ will be used below to distinguish between the various orders of the perturbation calculation. We assume that the (known) eigenfunctions ψ_k corresponding to the (known) eigenvalues E_k of H_0 form a complete orthonormal set (which may be partly continuous). Thus, if ψ_i and ψ_j are two members of that set, we have

$$\langle\psi_i|\psi_j\rangle = \delta_{ij} \quad \text{or} \quad \delta(i-j) \qquad [2.298]$$

where the symbol $\delta(i-j)$ should be used when both ψ_i and ψ_j correspond to continuous states. In what follows we shall simplify the notation by extending the meaning of δ_{ij} to cover both possibilities in [2.298]. The eigenvalue problem which we want to solve is

$$H\Psi_k = \mathscr{E}_k\Psi_k \qquad [2.299]$$

where we have used the notation $\mathscr{E}_k$ and Ψ_k to denote the perturbed energy levels and eigenfunctions, respectively.

(a) Non-degenerate case

Let us focus our attention on a particular unperturbed, discrete energy level E_k, which we assume to be *non-degenerate*. We suppose that the effect of the perturbation $\lambda H'$ is small enough so that the perturbed energy level $\mathscr{E}_k$ is much closer to E_k than to any other unperturbed level. It is then reasonable to expand both Ψ_k and $\mathscr{E}_k$ in powers of λ, namely

$$\Psi_k = \sum_{n=0}^{\infty} \lambda^n \psi_k^{(n)} \qquad [2.300]$$

and

$$\mathscr{E}_k = \sum_{n=0}^{\infty} \lambda^n E_k^{(n)} \qquad [2.301]$$

where the index n refers to the order of the perturbation. Substituting the expansions [2.300] and [2.301] in [2.299], and using [2.296] we have

$$(H_0 + \lambda H')(\psi_k^{(0)} + \lambda\psi_k^{(1)} + \lambda^2\psi_k^{(2)} + \cdots)$$
$$= (E_k^{(0)} + \lambda E_k^{(1)} + \lambda^2 E_k^{(2)} + \cdots)(\psi_k^{(0)} + \lambda\psi_k^{(1)} + \lambda^2\psi_k^{(2)} + \cdots) \qquad [2.302]$$

Let us now equate the coefficients of equal powers of λ. Beginning with λ^0, we see that

$$H_0\psi_k^{(0)} = E_k^{(0)}\psi_k^{(0)} \qquad [2.303]$$

so that

$$\psi_k^{(0)} \equiv \psi_k, \qquad E_k^{(0)} \equiv E_k \qquad [2.304]$$

as expected. The coefficient of λ then gives

$$H_0\psi_k^{(1)} + H'\psi_k = E_k\psi_k^{(1)} + E_k^{(1)}\psi_k \qquad [2.305]$$

while that of λ^2 yields

$$H_0\psi_k^{(2)} + H'\psi_k^{(1)} = E_k\psi_k^{(2)} + E_k^{(1)}\psi_k^{(1)} + E_k^{(2)}\psi_k \qquad [2.306]$$

and so on.

In order to obtain the first energy correction $E_k^{(1)}$, we premultiply [2.305] by $\psi_k^\star$ and integrate over all space. This gives

$$\langle\psi_k|H_0 - E_k|\psi_k^{(1)}\rangle + \langle\psi_k|H' - E_k^{(1)}|\psi_k\rangle = 0 \qquad [2.307]$$

Using [2.297] together with the fact that H_0 is Hermitian, so that $\langle\psi_k|H_0|\psi_k^{(1)}\rangle = \langle H_0\psi_k|\psi_k^{(1)}\rangle = E_k\langle\psi_k|\psi_k^{(1)}\rangle$, we find from [2.307] the very simple but important result

$$E_k^{(1)} = \langle\psi_k|H'|\psi_k\rangle \equiv H'_{kk} \qquad [2.308]$$

Similarly, we deduce from [2.306] that

$$\langle\psi_k|H_0 - E_k|\psi_k^{(2)}\rangle + \langle\psi_k|H' - E_k^{(1)}|\psi_k^{(1)}\rangle - E_k^{(2)}\langle\psi_k|\psi_k\rangle = 0 \qquad [2.309]$$

and therefore

$$E_k^{(2)} = \langle\psi_k|H' - E_k^{(1)}|\psi_k^{(1)}\rangle \qquad [2.310]$$

An equivalent expression of $E_k^{(2)}$ may be obtained by starting from [2.305], and is given (Problem 2.18) by

$$E_k^{(2)} = -\langle\psi_k^{(1)}|H_0 - E_k|\psi_k^{(1)}\rangle \qquad [2.311]$$

Expressions for higher order corrections $E_k^{(n)}$, $n \geqslant 3$ can be obtained in a similar way. For example, one has (Problem 2.18)

$$E_k^{(3)} = \langle\psi_k^{(1)}|H' - E_k^{(1)}|\psi_k^{(1)}\rangle - 2E_k^{(2)}\langle\psi_k|\psi_k^{(1)}\rangle \qquad [2.312]$$

Let us now return to [2.305]. The Rayleigh–Schrödinger method attempts to obtain the solution $\psi_k^{(1)}$ of that equation in the following way. First, the 'unperturbed' equation [2.297] is solved for all eigenvalues and eigenfunctions (including those belonging to the continuous part of the spectrum, if there exists one). The unknown function $\psi_k^{(1)}$ is then expanded in the basis set of the unperturbed eigenfunctions. That is,

$$\psi_k^{(1)} = \sum_m a_m^{(1)}\psi_m \qquad [2.313]$$

where the sum over m means a summation over the discrete part of the set and an integration over its continuous part. Substituting [2.313] into [2.305], we obtain

$$(H_0 - E_k)\sum_m a_m^{(1)}\psi_m + (H' - E_k^{(1)})\psi_k = 0 \qquad [2.314]$$

Premultiplying by $\psi_l^{\star}$, integrating over all space and using the fact that $H_0\psi_l = E_l\psi_l$ and $\langle\psi_l|\psi_k\rangle = \delta_{kl}$, we find that

$$a_l^{(1)}(E_l - E_k) + \langle\psi_l|H'|\psi_k\rangle - E_k^{(1)}\,\delta_{kl} = 0 \qquad [2.315]$$

For $l = k$ this reduces to our basic result [2.308]. On the other hand, for $l \neq k$ we have

$$a_l^{(1)} = \frac{H'_{lk}}{E_k - E_l}, \qquad l \neq k \qquad [2.316]$$

where we have set $H'_{lk} \equiv \langle\psi_l|H'|\psi_k\rangle$. We note that the equation [2.305] does not determine the coefficient $a_k^{(1)}$, which is the 'component' of $\psi_k^{(1)}$ along ψ_k. We can thus require without loss of generality that

$$a_k^{(1)} = \langle\psi_k|\psi_k^{(1)}\rangle = 0 \qquad [2.317]$$

and rewrite [2.313] as

$$\begin{aligned}\psi_k^{(1)} &= \sum_{m\neq k} a_m^{(1)}\psi_m \\ &= \sum_{m\neq k} \frac{H'_{mk}}{E_k - E_m}\,\psi_m\end{aligned} \qquad [2.318]$$

Substituting this result in [2.310] we obtain

$$\begin{aligned}E_k^{(2)} &= \sum_{m\neq k} \frac{H'_{km}H'_{mk}}{E_k - E_m} \\ &= \sum_{m\neq k} \frac{|H'_{km}|^2}{E_k - E_m}\end{aligned} \qquad [2.319]$$

The third-order correction $E_k^{(3)}$ may be obtained in a similar way from [2.312] and [2.318].

(b) Degenerate case

Thus far we have assumed that the perturbed eigenfunction Ψ_k differs slightly from a given function ψ_k, solution of the 'unperturbed' equation [2.297]. When the level E_k is α-fold degenerate, there are *several* 'unperturbed' wave functions $\psi_{kr}(r = 1, 2, \ldots \alpha)$ corresponding to this level and we do not know *a priori* to which functions the perturbed eigenfunctions tend when $\lambda \to 0$. This means

that the above treatment – and in particular the basic expansion [2.300] – must be modified to deal with the degenerate case.

The α unperturbed wave functions ψ_{kr} corresponding to the level E_k are orthogonal to the unperturbed wave functions ψ_l corresponding to *other* energy levels $E_l \neq E_k$. Although they need not be orthogonal among themselves, it is always possible to construct from linear combinations of them a new set of α unperturbed wave functions which are mutually orthogonal and normalised to unity. We may therefore assume without loss of generality that this has already been done, so that

$$\langle \psi_{kr} | \psi_{ks} \rangle = \delta_{rs} \qquad (r, s = 1, 2, \ldots \alpha) \tag{2.320}$$

Let us now introduce the correct zero-order functions χ_{kr} which yield the first term in the expansion of the exact wave function Ψ_{kr} in powers of λ. That is

$$\Psi_{kr} = \chi_{kr} + \lambda \psi_{kr}^{(1)} + \lambda^2 \psi_{kr}^{(2)} + \cdots \tag{2.321}$$

We shall also write the perturbed energy $\mathscr{E}_{kr}$ as

$$\mathscr{E}_{kr} = E_k + \lambda E_{kr}^{(1)} + \lambda^2 E_{kr}^{(2)} + \cdots \tag{2.322}$$

with $E_k \equiv E_{kr}$ ($r = 1, 2, \ldots \alpha$) since the level E_k is α-fold degenerate. Using the above expansions in [2.299] and equating the coefficients of λ we find that

$$H_0 \psi_{kr}^{(1)} + H' \chi_{kr} = E_k \psi_{kr}^{(1)} + E_{kr}^{(1)} \chi_{kr} \tag{2.323}$$

Since the functions χ_{kr} are linear combinations of the unperturbed wave functions ψ_{kr}, we may write

$$\chi_{kr} = \sum_{s=1}^{\alpha} c_{rs} \psi_{ks} \qquad (r = 1, 2, \ldots \alpha) \tag{2.324}$$

where the coefficients c_{rs} are to be determined. Similarly, expanding $\psi_{kr}^{(1)}$ in the basis set of the unperturbed wave functions, we have

$$\psi_{kr}^{(1)} = \sum_m \sum_s a_{kr,ms}^{(1)} \psi_{ms} \tag{2.325}$$

where the indices r and s refer explicitly to the degeneracy. Substituting the above expressions of χ_{kr} and $\psi_{kr}^{(1)}$ in [2.323] and using the fact that $H_0 \psi_{ms} = E_m \psi_{ms}$, we find that

$$\sum_m \sum_s a_{kr,ms}^{(1)} (E_m - E_k) \psi_{ms} + \sum_s c_{rs} (H' - E_{kr}^{(1)}) \psi_{ks} = 0 \tag{2.326}$$

Premultiplying by $\psi_{ku}^{\star}$ and integrating over all space, we obtain

$$\sum_m \sum_s a_{kr,ms}^{(1)} (E_m - E_k) \langle \psi_{ku} | \psi_{ms} \rangle + \sum_s c_{rs} [\langle \psi_{ku} | H' | \psi_{ks} \rangle - E_{kr}^{(1)} \delta_{us}] = 0$$

$$(u = 1, 2, \ldots \alpha) \tag{2.327}$$

where we have used [2.320]. Since $\langle \psi_{ku} | \psi_{ms} \rangle = 0$ when $k \neq m$ and $E_k = E_m$ if

$k = m$, we see that [2.327] reduces to

$$\sum_{s=1}^{\alpha} c_{rs}[\langle\psi_{ku}|H'|\psi_{ks}\rangle - E_{kr}^{(1)}\,\delta_{us}] = 0$$

$$(u = 1, 2, \ldots \alpha) \quad [2.328]$$

This is a linear, homogeneous system of equations for the α unknown quantities $c_{r1}, c_{r2}, \ldots c_{r\alpha}$. A non-trivial solution is obtained if the determinant of the quantity in square brackets vanishes,

$$\det|\langle\psi_{ku}|H'|\psi_{ks}\rangle - E_{kr}^{(1)}\,\delta_{us}| = 0 \qquad (s, u = 1, 2, \ldots \alpha) \qquad [2.329]$$

This equation yields α real roots $E_{k1}^{(1)}, E_{k2}^{(1)}, \ldots E_{k\alpha}^{(1)}$. If all these roots are *distinct* the degeneracy is *completely removed* to first order in the perturbation. On the other hand, if some or all roots of [2.329] are identical the degeneracy is only *partially* (or *not at all*) *removed.* The residual degeneracy may then be either removed in higher order of perturbation theory, or it may persist to all orders. The latter case occurs when the operators H_0 and H share symmetry properties.

For a given value of r, the coefficients c_{rs} $(s = 1, 2, \ldots \alpha)$ which determine the 'correct' unperturbed zero-order wave function χ_{kr} via [2.324] may be obtained by substituting the value of $E_{kr}^{(1)}$ in the system [2.328] and solving for the coefficients $c_{r1}, c_{r2}, \ldots c_{r\alpha}$ in terms of one of them. The last coefficient is then obtained (up to a phase) by requiring the function χ_{kr} to be normalised to unity. It is clear that this procedure does not lead to a unique result when two or more roots $E_{kr}^{(1)}$ of equation [2.329] coincide, since in this case the degeneracy is not fully removed.

Time-dependent perturbation theory

We shall now discuss the perturbation theory of a system whose total Hamiltonian H may be split as

$$H = H_0 + \lambda H'(t) \qquad [2.330]$$

where the 'unperturbed' Hamiltonian H_0 is time-independent and $H'(t)$ is a small *time-dependent* perturbation. The method which we outline below is known as *Dirac's method of variation of constants.*

Let us suppose that we know the eigenvalues E_k of the unperturbed Hamiltonian H_0, together with the corresponding stationary eigenfunctions ψ_k, which we assume to be orthonormal and to form a complete set. Thus, since $H_0\psi_k = E_k\psi_k$, the general solution of the time-dependent Schrödinger equation

$$i\hbar\frac{\partial\Psi_0}{\partial t} = H_0\Psi_0 \qquad [2.331]$$

is given by

$$\Psi_0 = \sum_k c_k^{(0)}\psi_k e^{-iE_kt/\hbar} \qquad [2.332]$$

where the coefficients $c_k^{(0)}$ are *constants* and the sum is over the entire set of eigenfunctions ψ_k. Because the functions ψ_k form a complete set, the general solution Ψ of the time-dependent Schrödinger equation

$$i\hbar \frac{\partial \Psi}{\partial t} = H\Psi \tag{2.333}$$

can be expanded as

$$\Psi = \sum_k c_k(t)\psi_k e^{-iE_k t/\hbar} \tag{2.334}$$

where the unknown coefficients $c_k(t)$ clearly *depend on the time*. Since the wave functions ψ_k are orthonormal, and provided Ψ is normalised to unity, we can interpret the quantity $|c_k(t)|^2$ as the probability of finding the system in the state labelled k at the time t, and $c_k(t)$ as the corresponding probability amplitude. Upon comparison of [2.332] and [2.334] we see that if $H'(t) = 0$ the coefficients c_k reduce to the constants $c_k^{(0)}$ which are therefore the *initial values* of the c_k. Thus, as we expect from [2.332] the quantity $|c_k^{(0)}|^2$ gives the probability of finding the system in the stationary state ψ_k before the perturbation is applied.

To find equations for the coefficients $c_k(t)$ the expansion [2.334] is inserted into the Schrödinger equation [2.333]. From [2.330] and the fact that $H_0\psi_k = E_k\psi_k$, we then have

$$i\hbar \sum_k \dot{c}_k(t)\psi_k e^{-iE_k t/\hbar} = \sum_k c_k(t)\lambda H'(t)\psi_k e^{-iE_k t/\hbar} \tag{2.335}$$

where the dot indicates a derivative with respect to the time. Taking the scalar product with a particular function ψ_b belonging to the set $\{\psi_k\}$ and using the fact that $\langle\psi_b|\psi_k\rangle = \delta_{bk}$, we then find from [2.335] the set of coupled equations

$$\dot{c}_b(t) = (i\hbar)^{-1} \sum_k \lambda H'_{bk}(t)c_k(t)e^{i\omega_{bk}t} \tag{2.336}$$

where

$$H'_{bk}(t) = \langle\psi_b|H'(t)|\psi_k\rangle \tag{2.337}$$

and where the *Bohr angular frequency* ω_{bk} is defined by

$$\omega_{bk} = \frac{E_b - E_k}{\hbar} \tag{2.338}$$

The system of coupled differential equations [2.336] is completely equivalent to the original time-dependent Schrödinger equation, and no approximation has been made thus far. However, if the perturbation $\lambda H'$ is weak, we can expand the coefficients c_k in powers of the parameter λ as

$$c_k = c_k^{(0)} + \lambda c_k^{(1)} + \lambda^2 c_k^{(2)} + \cdots \tag{2.339}$$

Substituting this expansion into the system [2.336] and equating the coefficients

of equal powers of λ, we find that

$$\dot{c}_b^{(0)} = 0 \qquad [2.340a]$$

$$\dot{c}_b^{(1)} = (i\hbar)^{-1} \sum_k H'_{bk}(t) e^{i\omega_{bk}t} c_k^{(0)} \qquad [2.340b]$$

$$\vdots \quad \vdots \quad \vdots$$

$$\dot{c}_b^{(s+1)} = (i\hbar)^{-1} \sum_k H'_{bk}(t) e^{i\omega_{bk}t} c_k^{(s)} \qquad s = 0, 1, \ldots \qquad [2.340c]$$

Thus the original system [2.336] has been decoupled in such a way that the equations [2.340] can now in principle be integrated successively to any given order.

The first equation [2.340a] simply confirms that the coefficients $c_k^{(0)}$ are time-independent. As we have seen above, the constants $c_k^{(0)}$ define the initial conditions of the problem. In what follows, we shall assume for the sake of simplicity that the system is initially (that is, for $t \leqslant t_0$) in a well-defined stationary state ψ_a of energy E_a. Thus

$$c_k^{(0)} = \begin{cases} \delta_{ka} & \text{for discrete states} \\ \delta(k-a) & \text{for continuous states} \end{cases} \qquad [2.341]$$

We note that this statement is not in contradiction with the uncertainty relation $\Delta E \, \Delta t \geqslant \hbar$ since we have essentially an 'infinite' amount of time available to prepare our initial state. Upon substitution of [2.341] into [2.340b] we then have

$$\dot{c}_b^{(1)}(t) = (i\hbar)^{-1} H'_{ba}(t) e^{i\omega_{ba}t} \qquad [2.342]$$

where $\omega_{ba} = (E_b - E_a)/\hbar$. This equation is readily solved to give

$$c_b^{(1)}(t) = (i\hbar)^{-1} \int_{t_0}^{t} H'_{ba}(t') e^{i\omega_{ba}t'} \, dt' \qquad [2.343]$$

where the integration constant has been chosen in such a way that $c_b^{(1)}(t)$ vanishes at $t = t_0$, namely, before the perturbation is applied. To first order in the perturbation the transition probability for the transition $a \to b$ is then given by

$$P_{ba}(t) = |c_b^{(1)}(t)|^2 \qquad [2.344]$$

If H' is independent of time, except for being 'turned on' at the time $t_0 = 0$ and 'turned off' at time t, we have

$$c_b^{(1)}(t) = -\frac{H'_{ba}}{\hbar\omega_{ba}} (e^{i\omega_{ba}t} - 1) \qquad [2.345]$$

and the first-order *transition probability* from state a to a state $b \neq a$ is given by

$$P_{ba}(t) = |c_b^{(1)}(t)|^2 = \frac{2}{\hbar^2} |H'_{ba}|^2 F(t, \omega_{ba}) \qquad [2.346]$$

where

$$F(t, \omega) = \frac{1 - \cos \omega t}{\omega^2} \qquad [2.347]$$

The function $F(t, \omega)$ is shown in Fig. 2.9 for fixed t. We see that it exhibits a sharp peak about the value $\omega = 0$. The height of this peak is proportional to t^2, while its width is approximately $2\pi/t$. Setting $x = \omega t/2$, we also note that

$$\int_{-\infty}^{+\infty} F(t, \omega) \, d\omega = t \int_{-\infty}^{+\infty} \frac{\sin^2 x}{x^2} \, dx = \pi t \qquad [2.348]$$

where we have used a standard integral. We remark that this result allows us also to write for large t (see [2.31])

$$F(t, \omega) \underset{t \to \infty}{\simeq} \pi t \, \delta(\omega) \qquad [2.349]$$

Let us first analyse [2.346] for a fixed value of t. Since the function $F(t, \omega_{ba})$ has a sharp peak of width $2\pi/t$ about the value $\omega_{ba} = 0$, it is clear from [2.346] that transitions to those final states b for which ω_{ba} does not deviate from zero by more than $\delta\omega_{ba} \simeq 2\pi/t$ will be strongly favoured. Therefore the transitions $a \to b$ will occur mainly towards those final states whose energy E_b is located in a band of width

$$\delta E \simeq 2\pi\hbar/t \qquad [2.350]$$

about the initial energy E_a, so that the unperturbed energy is conserved to within $2\pi\hbar/t$. This result may easily be related to the time–energy uncertainty

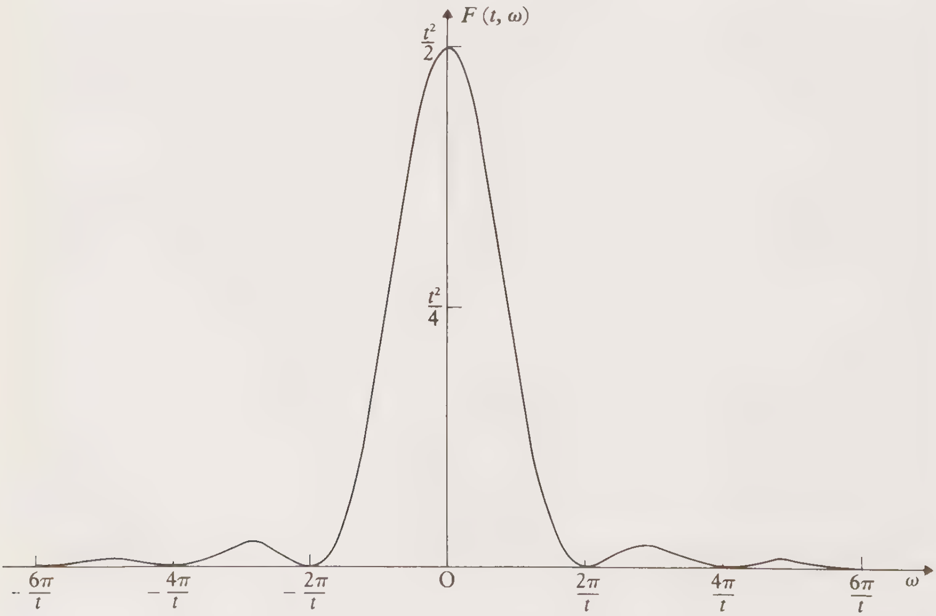

2.9 The function $F(t, \omega)$ for fixed t.

relation $\Delta E \, \Delta t \gtrsim \hbar$. Indeed, since the perturbation gives a way of measuring the energy of the system by inducing transitions $a \to b$, and because this perturbation acts during a time t, the uncertainty related to this energy measurement should be approximately $\hbar/t$, in qualitative agreement with [2.350].

We now study the transition probability [2.346] as a function of t. For a transition to a *given state* b we must distinguish two cases:

1. If the transition is such that the unperturbed energy is strictly conserved ($\omega_{ba} = 0$), then we see from [2.346] that

$$P_{ba}(t) = \frac{|H'_{ba}|^2}{\hbar^2} t^2 \qquad [2.351]$$

so that the transition probability increases as t^2.

2. If on the contrary one has $\omega_{ba} \neq 0$, then one sees from [2.346] that the function $F(t, \omega_{ba})$ oscillates between the values 0 and $2/\omega_{ba}^2$ with a frequency $\omega_{ba}/2\pi$. As a result, $P_{ba}(t)$ will oscillate with the same frequency about the average value

$$\bar{P}_{ba} = \frac{2|H'_{ba}|^2}{\hbar^2 \omega_{ba}^2} = \frac{2|H'_{ba}|^2}{(E_b - E_a)^2} \qquad [2.352]$$

Instead of considering transitions to a particular state b, it is often necessary to deal with transitions involving a *group of states* b' whose energy $E_{b'}$ lies within a given interval $(E_b - \eta, E_b + \eta)$ centred about the value E_b. If we denote by $\rho_{b'}(E_{b'})$ the *density of levels* $E_{b'}$, namely the number of states b' per unit energy, then the first-order transition probability P_{ba} from the initial state a to the group of final states b' is given by

$$\bar{P}_{ba}(t) = \frac{2}{\hbar^2} \int_{E_b - \eta}^{E_b + \eta} |H'_{b'a}|^2 F(t, \omega_{b'a}) \rho_{b'}(E_{b'}) \, \mathrm{d}E_{b'} \qquad [2.353]$$

Assuming that η is small enough so that $H'_{b'a}$ and $\rho_{b'}$ are nearly constant within the integration range, we have

$$P_{ba}(t) = \frac{2}{\hbar^2} |H'_{ba}|^2 \rho_b(E_b) \int_{E_b - \eta}^{E_b + \eta} F(t, \omega_{b'a}) \, \mathrm{d}E_{b'} \qquad [2.354]$$

We shall also assume that t is large enough so that the quantity η satisfies the condition

$$\eta \gg 2\pi\hbar/t \qquad [2.355]$$

It is clear that the overwhelming part of the integral on the right of [2.354] arises from transitions which conserve the energy (within $\delta E = 2\pi\hbar/t$). Since $\eta \gg 2\pi\hbar/t$, we may write

$$\int_{E_b - \eta}^{E_b + \eta} F(t, \omega_{b'a}) \, \mathrm{d}E_{b'} \simeq \hbar \int_{-\infty}^{+\infty} F(t, \omega_{b'a}) \, \mathrm{d}\omega_{b'a} = \pi t \qquad [2.356]$$

where we have used [2.348]. Thus [2.354] reduces to

$$P_{ba}(t) = \frac{2\pi}{\hbar} |H'_{ba}|^2 \rho_b(E) t \qquad [2.357]$$

with $E = E_a = E_b$, so that the transition probability increases linearly with t for those transitions which conserve the energy. We may therefore introduce a *transition probability per unit time* (or transition rate)

$$W_{ba} = \frac{\mathrm{d}P_{ba}}{\mathrm{d}t} \qquad [2.358]$$

and we see from [2.357] that to first order in perturbation theory, we have

$$W_{ba} = \frac{2\pi}{\hbar} |H'_{ba}|^2 \rho_b(E) \qquad [2.359]$$

This formula, first obtained by Dirac, is also often referred to as *Fermi's Golden Rule*. We recall that we have proved it here for a perturbation H' which is independent of time, except for being 'turned on' at $t = 0$ and 'turned off' at time t. However, the Golden Rule can be generalised to other time-dependent processes, and we shall return to it when discussing the interaction of atoms with electromagnetic fields. We simply remark at this point that [2.359] is only valid if the time t during which the perturbation acts is sufficiently large so that the condition [2.355] is satisfied, and yet small enough so that first-order perturbation theory is justified, namely if

$$P_{ba}(t) = W_{ba} t \ll 1 \qquad [2.360]$$

so that there is little change in the initial state a for times t of physical interest.

The variational method

We shall now discuss an approximation method, known as the *variational method*, which is very useful in obtaining the bound state energies and wave functions of a time-independent Hamiltonian H. We denote by E_n the eigenvalues of this Hamiltonian and by ψ_n the corresponding orthonormal eigenfunctions, and assume that H has at least one discrete eigenvalue. Let ϕ be an arbitrary normalisable function, and let $E[\phi]$ be the functional

$$E[\phi] = \frac{\langle \phi | H | \phi \rangle}{\langle \phi | \phi \rangle}$$

$$= \frac{\displaystyle\int \phi^\star H \phi \,\mathrm{d}\tau}{\displaystyle\int \phi^\star \phi \,\mathrm{d}\tau} \qquad [2.361]$$

where the integration is extended over the full range of all the coordinates of the system.

It is clear that if the function ϕ is identical to one of the exact eigenfunctions ψ_n of H, then $E[\phi]$ will be identical to the corresponding exact eigenvalue E_n. Moreover, it will now be shown that any function ϕ for which the functional $E[\phi]$ is stationary is an eigenfunction of the discrete spectrum of H. Thus, if ϕ and ψ_n differ by an arbitrary infinitesimal variation $\delta\phi$,

$$\phi = \psi_n + \delta\phi \qquad [2.362]$$

then the corresponding first-order variation of $E[\phi]$ vanishes:

$$\delta E = 0 \qquad [2.363]$$

and the eigenfunctions of H are solutions of the variational equation [2.363].

To prove this statement, we note that upon clearing the fractions and varying, we have from [2.361]

$$\delta E \int \phi^\star \phi \,\mathrm{d}\tau + E \int \delta\phi^\star \phi \,\mathrm{d}\tau + E \int \phi^\star \,\delta\phi \,\mathrm{d}\tau = \int \delta\phi^\star H \phi \,\mathrm{d}\tau + \int \phi^\star H \,\delta\phi \,\mathrm{d}\tau \qquad [2.364]$$

Since $\langle\phi|\phi\rangle$ is assumed to be finite and non-vanishing, we see that the equation [2.363] is equivalent to

$$\int \delta\phi^\star (H - E)\phi \,\mathrm{d}\tau + \int \phi^\star (H - E)\,\delta\phi \,\mathrm{d}\tau = 0 \qquad [2.365]$$

Although the variations $\delta\phi$ and $\delta\phi^\star$ are not independent, they may in fact be treated as such, so that the individual terms in [2.365] can be set equal to zero. To see how this comes about, we replace the arbitrary variation $\delta\phi$ by $i\,\delta\phi$ in [2.365] so that we have

$$-i \int \delta\phi^\star (H - E)\phi \,\mathrm{d}\tau + i \int \phi^\star (H - E)\,\delta\phi \,\mathrm{d}\tau = 0 \qquad [2.366]$$

Upon combining [2.366] with [2.365] we then obtain the two equations

$$\int \delta\phi^\star (H - E)\phi \,\mathrm{d}\tau = 0$$

$$\int \phi^\star (H - E)\,\delta\phi \,\mathrm{d}\tau = 0 \qquad [2.367]$$

which is the desired result. Using the fact that H is Hermitian, we see that the two equations [2.367] are equivalent to the Schrödinger equation

$$(H - E[\phi])\phi = 0 \qquad [2.368]$$

Thus any function $\phi = \psi_n$ for which the functional [2.361] is stationary is an

eigenfunction of H corresponding to the eigenvalue $E_n \equiv E[\psi_n]$. Conversely, if ψ_n is an eigenfunction of H and E_n the corresponding energy, we have $E_n = E[\psi_n]$ and the functional $E[\psi_n]$ is stationary because ψ_n satisfies the equations [2.367]. It is worth stressing that if ϕ and ψ_n differ by $\delta\phi$, the variational principle [2.363] implies that the leading term of the difference between $E[\phi]$ and the true eigenvalue E_n is *quadratic* in $\delta\phi$. As a result, errors in the approximate energy are of *second order* in $\delta\phi$ when the energy is calculated from the functional [2.361].

We also remark that the functional [2.361] is independent of the normalisation and of the phase of ϕ. In particular, it is often convenient to impose the condition $\langle\phi|\phi\rangle = 1$. The above results may then be retrieved by varying the functional $\langle\phi|H|\phi\rangle$ subject to the condition $\langle\phi|\phi\rangle = 1$, namely

$$\delta \int \phi^\star H \phi \, \mathrm{d}\tau = 0, \qquad \int \phi^\star \phi \, \mathrm{d}\tau = 1 \tag{2.369}$$

The constraint $\langle\phi|\phi\rangle = 1$ may be taken care of by introducing a Lagrange multiplier [8] which we denote by E, so that the variational equation reads

$$\delta\left[\int \phi^\star H \phi \, \mathrm{d}\tau - E \int \phi^\star \phi \, \mathrm{d}\tau\right] = 0 \tag{2.370}$$

or

$$\int \delta\phi^\star (H - E)\phi \, \mathrm{d}\tau + \int \phi^\star (H - E) \, \delta\phi \, \mathrm{d}\tau = 0 \tag{2.371}$$

This equation is identical to [2.365], and we see that the Lagrange multiplier E has the significance of an energy eigenvalue.

An important additional property of the functional [2.361] is that it provides an *upper bound* to the exact ground state energy E_0. To prove this result, we expand the arbitrary, normalisable function ϕ in the complete set of orthonormal eigenfunctions ψ_n of H. That is

$$\phi = \sum_n a_n \psi_n \tag{2.372}$$

Substituting [2.372] into [2.361], we find that

$$E[\phi] = \frac{\sum_n |a_n|^2 E_n}{\sum_n |a_n|^2} \tag{2.373}$$

where we have used the fact that $H\psi_n = E_n\psi_n$ and $\langle\phi|\phi\rangle = \Sigma_n |a_n|^2$. If we now subtract E_0, the lowest energy eigenvalue, from both sides of [2.373] we have

$$E[\phi] - E_0 = \frac{\sum_n |a_n|^2 (E_n - E_0)}{\sum_n |a_n|^2} \tag{2.374}$$

[8] Lagrange multipliers are discussed for example in Byron and Fuller (1969).

Since $E_n \geqslant E_0$, the right-hand side of [2.374] is non-negative, so that

$$E_0 \leqslant E[\phi] \qquad [2.375]$$

and the functional $E[\phi]$ gives an upper bound – or in other words a *minimum principle* for the ground state energy.

The property [2.375] constitutes the basis of the *Rayleigh–Ritz variational method* for the approximate calculation of E_0. This method consists in evaluating the quantity $E[\phi]$ by using *trial functions* ϕ which depend on a certain number of *variational parameters*, and then to minimise $E[\phi]$ with respect to these parameters in order to obtain the best approximation of E_0 allowed by the form chosen for ϕ.

The Rayleigh–Ritz variational method can also be used to obtain an upper bound for the energy of an excited state, provided that the trial function ϕ is made orthogonal to all the energy eigenfunctions corresponding to states having a lower energy than the energy level considered. Indeed, let us arrange the energy levels in an ascending sequence: $E_0, E_1, E_2, \ldots$ and let the trial function ϕ be orthogonal to the energy eigenfunctions $\psi_n (n = 0, 1, \ldots i)$, namely

$$\langle \psi_n | \phi \rangle = 0, \qquad n = 0, 1, \ldots i \qquad [2.376]$$

Then, if we expand ϕ in the orthonormal set $\{\psi_n\}$ as in [2.372] we have $a_n = \langle \psi_n | \phi \rangle = 0$ $(n = 0, 1, \ldots i)$ and the functional $E[\phi]$ becomes

$$E[\phi] = \frac{\sum\limits_{n=i+1} |a_n|^2 E_n}{\sum\limits_{n=i+1} |a_n|^2} \qquad [2.377]$$

so that

$$E_{i+1} \leqslant E[\phi] \qquad [2.378]$$

As an example, suppose that the lowest energy eigenfunction ψ_0 is known, and let ϕ be a trial function. The function

$$\tilde{\phi} = \phi - \psi_0 \langle \psi_0 | \phi \rangle \qquad [2.379]$$

is orthogonal to ψ_0 (that is, $\langle \psi_0 | \tilde{\phi} \rangle = 0$) and can therefore be used to obtain an upper limit of E_1, the exact energy of the first excited state.

In many practical situations the lower energy eigenfunctions ψ_n $(n = 0, 1, \ldots i)$ are not known exactly and one only has approximations (obtained for example from a variational calculation) of these functions. In this case the orthogonality condition [2.376] cannot be achieved exactly, and the relation [2.378] is violated. For example, let us suppose that the (normalised) function ϕ_0 is an approximation to the true ground state eigenfunction ψ_0. If ϕ_1 is a trial function orthogonal to ϕ_0 (that is, if $\langle \phi_0 | \phi_1 \rangle = 0$) it may be shown (Problem 2.23) that

$$E_1 - \varepsilon_0 (E_1 - E_0) \leqslant E[\phi_1] \qquad [2.380]$$

where ε_0 is the positive quantity

$$\varepsilon_0 = 1 - |\langle\psi_0|\phi_0\rangle|^2 \tag{2.381}$$

Thus $E[\phi_1]$ does not provide a rigorous upper bound to E_1. However, if ϕ_0 is a good approximation to ψ_0, then ε_0 will be small and the violation of the relation $E_1 \leqslant E[\phi_1]$ will be mild.

The application of the variational method to excited states is greatly facilitated if the Hamiltonian of the system has certain *symmetry properties*, since in this case the orthogonality condition [2.376] can be satisfied exactly for certain states. For example, if the excited state in question is of different parity or angular momentum than the lower states, then the orthogonality condition is automatically satisfied.

Particularly useful trial functions ϕ can be constructed by choosing a certain number (N) of linearly independent functions $\chi_1, \chi_2, \ldots \chi_N$ and forming the linear combination

$$\phi = \sum_{n=1}^{N} c_n \chi_n \tag{2.382}$$

where the coefficients $c_1, c_2, \ldots c_N$ are linear variational parameters which must be determined by minimising the functional $E[\phi]$ in order to obtain the best approximation to E_0. Substituting [2.382] in [2.361] we find that

$$E[\phi] = \frac{\sum_{n=1}^{N} \sum_{n'=1}^{N} c_{n'}^{\star} c_n H_{n'n}}{\sum_{n=1}^{N} \sum_{n'=1}^{N} c_{n'}^{\star} c_n \Delta_{n'n}} \tag{2.383}$$

where we have set

$$\begin{aligned} H_{n'n} &= \langle\chi_{n'}|H|\chi_n\rangle \\ \Delta_{n'n} &= \langle\chi_{n'}|\chi_n\rangle \end{aligned} \tag{2.384}$$

We remark that if the functions χ_n are orthonormal, then $\Delta_{n'n} = \delta_{n'n}$.

In order to find the values of the variational parameters $c_1, c_2, \ldots c_N$ which minimise $E[\phi]$, we first rewrite [2.383] as

$$E[\phi] \sum_{n=1}^{N} \sum_{n'=1}^{N} c_{n'}^{\star} c_n \Delta_{n'n} = \sum_{n=1}^{N} \sum_{n'=1}^{N} c_{n'}^{\star} c_n H_{n'n} \tag{2.385}$$

Differentiating with respect to each c_n or $c_{n'}^{\star}$, expressing that $\partial E/\partial c_n = 0$ (or $\partial E/\partial c_{n'}^{\star} = 0$), we obtain a system of N linear and homogeneous equations in the variables $c_1, c_2, \ldots c_N$, namely

$$\sum_{n=1}^{N} c_n (H_{n'n} - \Delta_{n'n} E) = 0; \qquad n' = 1, 2, \ldots N \tag{2.386}$$

The necessary and sufficient condition for this system to have a non-trivial solution is that the determinant of the coefficients vanishes. That is,

$$\det|H_{n'n} - \Delta_{n'n}E| = 0 \qquad [2.387]$$

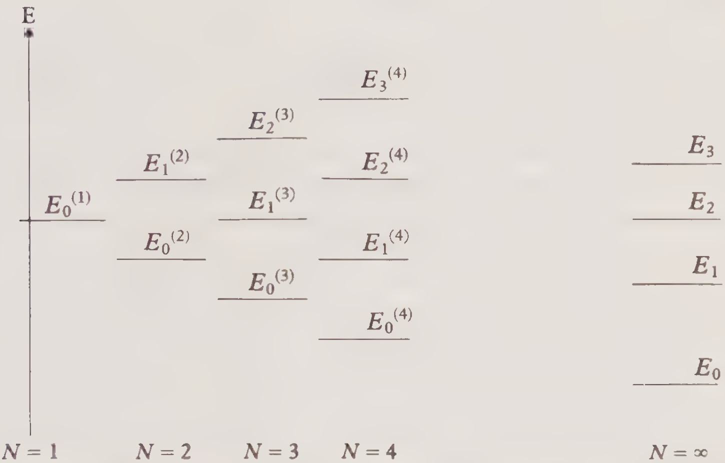

2.10 Approximate eigenvalues given by the Rayleigh–Ritz variational method with linear trial functions. Each root $E_i^{(N)}$ of the determinantal equation [2.387] is an upper bound on the corresponding exact eigenvalue E_i.

Let $E_0^{(N)}, E_1^{(N)}, \ldots E_{N-1}^{(N)}$ be the N roots of this equation, arranged in an ascending sequence; the superscript (N) indicates that we are dealing with a $N \times N$ determinant. The lowest root $E_0^{(N)}$ is of course an upper bound to the ground state energy E_0. Upon substituting $E_0^{(N)}$ in the system of equations [2.386] and solving for the coefficients c_n in terms of one of them (for example c_1, which may be used as a normalisation factor), we then obtain the corresponding 'optimum' approximation ϕ_0 to the ground state wave function ψ_0. It may also be shown that the other roots $E_i^{(N)}$ of [2.387], with $i = 1, 2, \ldots N - 1$, are upper bounds to excited state energies of the system. In particular, if the Hamiltonian commutes with a Hermitian operator A and the trial function [2.382] has been constructed from eigenfunctions corresponding to a given eigenvalue α of A, then the roots $E_i^{(N)}$, with $i = 1, 2, \ldots N$ are upper bounds to the energies E_i associated with excited states belonging to the eigenvalue α of A (for example a given value of the angular momentum or the parity). The 'optimum' approximations $\phi_0, \phi_1, \ldots \phi_{N-1}$ to the true wave functions, obtained by the above method, may also be shown to be mutually orthogonal. Moreover, if we construct a new trial function ϕ' containing an additional basis function χ_{N+1}, namely

$$\phi' = \sum_{n=1}^{N+1} c_n \chi_n \qquad [2.388]$$

it can be proved that the 'new' $(N + 1)$ roots $E_0^{(N+1)}, E_1^{(N+1)}, \ldots E_N^{(N+1)}$ of the determinantal equation [2.387] are separated by the 'old' roots $E_0^{(N)}$, $E_1^{(N)}, \ldots E_{N-1}^{(N)}$. This property, which is illustrated in Fig. 2.10, is known as the *Hylleraas–Undheim theorem.*

The variation–perturbation method

We have seen in our discussion of perturbation theory that according to the Rayleigh-Schrödinger method the solution $\psi_k^{(1)}$ of [2.305] (for the non-degenerate case) or the solution $\psi_{kr}^{(1)}$ of [2.323] (for the degenerate case) are obtained by expanding these functions in the basis set $\{\psi_m\}$ of the unperturbed eigenfunctions. The coefficients of this expansion and the second- and third-order corrections to the energy are then given in terms of matrix elements of H' between unperturbed eigenfunctions (see for example [2.316] and [2.319]). Unfortunately, in many cases the evaluation of all the necessary matrix elements of H' and of the required summations is very difficult. In these cases, however, it is possible to obtain *approximations* to $\psi_k^{(1)}$, $E_k^{(2)}$ and $E_k^{(3)}$ by using the *variation–perturbation method*, which we shall now describe for the non-degenerate case.

Let us assume that the unperturbed eigenfunction ψ_k as well as the corresponding energy E_k and the first-order energy correction $E_k^{(1)} = \langle\psi_k|H'|\psi_k\rangle$ are known for a given state k. Let $\phi_k^{(1)}$ be an arbitrary trial function and $F_1[\phi_k^{(1)}]$ the functional

$$F_1[\phi_k^{(1)}] = \langle\phi_k^{(1)}|H_0 - E_k|\phi_k^{(1)}\rangle + 2\,\langle\phi_k^{(1)}|H' - E_k^{(1)}|\psi_k\rangle \qquad [2.389]$$

We now express that this functional is *stationary* for variations of $\phi_k^{(1)}$ around the correct first-order wave function $\psi_k^{(1)}$. Proceeding as in the case of the variational method studied above, we find that the variational equation

$$\delta F_1 = 0 \qquad [2.390]$$

implies that

$$(H_0 - E_k)\phi_k^{(1)} + (H' - E_k^{(1)})\psi_k = 0 \qquad [2.391]$$

so that the function $\phi_k^{(1)}$ which makes the functional F_1 stationary is a solution $\psi_k^{(1)}$ of the equation [2.305]. Moreover, by comparing [2.305], [2.310] and [2.389] we see that $F_1[\phi_k^{(1)}]$ reduces to the correct value of $E_k^{(2)}$ when $\phi_k^{(1)} \equiv \psi_k^{(1)}$.

Let us now consider the particular case of a state k for which E_k is the *lowest* eigenvalue of H_0 corresponding to a given symmetry. It is then straightforward to show that (compare with [2.375])

$$E_k^{(2)} \leqslant F_1[\phi_k^{(1)}] \qquad [2.392]$$

One can then proceed in a way similar to that followed in the Rayleigh–Ritz method. First, a trial function $\phi_k^{(1)}$ is chosen containing a certain number of variational parameters. One then inserts that trial function in the functional

$F_1[\phi_k^{(1)}]$, which is minimised with respect to the variational parameters. Because of [2.392] this minimum value of $F_1[\phi_k^{(1)}]$ gives an *upper bound* to $E_k^{(2)}$. The corresponding 'optimum' function $\phi_k^{(1)}$ can also be used to calculate an approximate value of $E_k^{(3)}$ by replacing $\psi_k^{(1)}$ by $\phi_k^{(1)}$ in [2.312].

The method can be extended to calculate approximate values of $\psi_k^{(2)}$, $E_k^{(4)}$ and $E_k^{(5)}$. To this end, we consider a trial function $\phi_k^{(2)}$ and the functional

$$F_2[\phi_k^{(2)}] = \langle\phi_k^{(2)}|H_0 - E_k|\phi_k^{(2)}\rangle + 2\langle\phi_k^{(2)}|H' - E_k^{(1)}|\psi_k^{(1)}\rangle - 2E_k^{(2)}\langle\phi_k^{(2)}|\psi_k\rangle \tag{2.393}$$

where $\psi_k^{(1)}$ is now assumed to be known. Let us express that this functional is stationary with respect to variations of $\phi_k^{(2)}$. The condition

$$\delta F_2 = 0 \tag{2.394}$$

yields the equation

$$(H_0 - E_k)\phi_k^{(2)} + (H' - E_k^{(1)})\psi_k^{(1)} - E_k^{(2)}\psi_k = 0 \tag{2.395}$$

so that the function $\phi_k^{(2)}$ which makes the functional F_2 stationary is a solution $\psi_k^{(2)}$ of [2.306]. In addition, it is easily shown that when $\phi_k^{(2)} \equiv \psi_k^{(2)}$ the functional F_2 gives the exact value of $E_k^{(4)}$, apart from terms which are independent of $\phi_k^{(2)}$. Moreover, F_2 yields a minimum principle (upper bound) for $E_k^{(4)}$ when the state k is the lowest eigenvalue of H_0 corresponding to a given symmetry. The function $\phi_k^{(2)}$ determined from the variational principle [2.394] can also be used to calculate the energy correction $E_k^{(5)}$. By constructing functionals $F_3[\phi_k^{(3)}]$, $F_4[\phi_k^{(4)}]$, and so on, the variation–perturbation method can be used to calculate higher order perturbation corrections to the wave functions and the energy eigenvalues.

PROBLEMS

2.1 Consider the momentum space wave function $\phi(p_x) = 0$, $|p_x - p_0| > \gamma$ $\phi(p_x) = C$, $|p_x - p_0| \leq \gamma$ where p_0, C and γ are constants. Find the corresponding wave function $\psi(x)$ in configuration space and determine the constant C, so that $\psi(x)$ satisfies the normalisation condition

$$\int_{-\infty}^{\infty} \mathrm{d}x|\psi(x)|^2 = 1.$$

Using a reasonable definition of the 'width' Δx of $|\psi(x)|$, show that $\Delta x\, \Delta p_x > \hbar$.

2.2 Consider an electron of momentum $\mathbf{p}$ in the Coulomb field of a proton. The total energy is

$$E = \frac{p^2}{2m} - \frac{e^2}{(4\pi\varepsilon_0)r},$$

where r is the distance of the electron from the proton. Assuming that the

uncertainty Δr of the radial coordinate is $\Delta r \simeq r$ and that $\Delta p \simeq p$, use Heisenberg's uncertainty principle to obtain an estimate of the size and the energy of the hydrogen atom in the ground state.

2.3 Consider the normalised Gaussian wave packet $\psi(x) = N \exp(-\lambda^2 x^2)$ where $N = (2\lambda^2/\pi)^{1/4}$. Using [2.16], calculate the uncertainties Δx and Δp_x from [2.41] and show that $\Delta x \, \Delta p_x = \hbar/2$.

2.4 Starting from [2.39] show that

$$\langle \mathbf{p} \rangle = \int \Phi^\star(\mathbf{p}, t)\mathbf{p}\Phi(\mathbf{p}, t) \, d\mathbf{p}$$

where $\Phi(\mathbf{p}, t)$ is the normalised momentum space wave function corresponding to $\Psi(\mathbf{r}, t)$ (see [2.20]).

2.5 A particle of mass m moving in a potential $V(\mathbf{r})$ has the Hamiltonian $H = -(\hbar^2/2m)\nabla^2 + V(\mathbf{r})$. Using the result [2.56] prove Ehrenfest's theorem [2.57].

2.6 (a) Using the definition of an adjoint operator [2.65] prove that if A and B are two operators then $(AB)^\dagger = B^\dagger A^\dagger$.
(b) Suppose that A and B are two non-commuting Hermitian operators. Determine which of the following operators are Hermitian (i) AB (ii) $[A, B]$ (iii) $AB + BA$ (iv) ABA (v) A^n where n is a positive integer.

2.7 Let E_n denote the energy eigenvalues of a one-dimensional system and $\psi_n(x)$ the corresponding energy eigenfunctions. Suppose that the normalised wave function of the system at $t = 0$ is given by

$$\Psi(x, t = 0) = \frac{1}{\sqrt{2}} e^{i\alpha_1}\psi_1(x) + \frac{1}{\sqrt{3}} e^{i\alpha_2}\psi_2(x) + \frac{1}{\sqrt{6}} e^{i\alpha_3}\psi_3(x)$$

where the α_i are constants.
(a) Write down the wave function $\Psi(x, t)$ at time t.
(b) Find the probability that at time t a measurement of the energy of the system gives the value E_2.
(c) Does $\langle x \rangle$ vary with time? Does $\langle p_x \rangle$ vary with time? Does $E = \langle H \rangle$ vary with time?

2.8 If U is a unitary operator and $A' = UAU^\dagger$ where A is a Hermitian operator, show that:
(a) A' is Hermitian.
(b) The eigenvalues of A' are the same as those of A
(c) $\langle \Phi' | A' | \Psi' \rangle = \langle \Phi | A | \Psi \rangle$ where Ψ' and Φ' are connected with Ψ and Φ by [2.106].

2.9 Verify the equations [2.120].

2.10 Consider a particle of mass m moving in one dimension in the infinite square well [2.122]. Suppose that at time $t = 0$ its wave function is given by

$$\Psi(x, t = 0) = A(a^2 - x^2)$$

(a) Find the probability P_n that a measurement of the energy will give the value E_n, where E_n is given by [2.131].
(b) Obtain the average value of the energy.

2.11 Classically the simple harmonic oscillator having the total energy $E = p^2/2m + m\omega^2x^2/2$ could have $x = p = 0$ and hence $E = 0$. In quantum mechanics, there will be uncertainties $x = 0 + \Delta x$, $p_x = 0 + \Delta p_x$ such that $\Delta_x \Delta p_x \gtrsim \hbar$. Show that because of this condition the minimum total energy cannot be zero and must be of the order of $\hbar\omega$.

2.12 Starting from the definitions [2.154] show that L_x, L_y and L_z can be expressed in spherical polar coordinates (see [2.157]) as

$$L_x = i\hbar\left(\sin\phi \frac{\partial}{\partial\theta} + \cot\theta\cos\phi\frac{\partial}{\partial\phi}\right)$$

$$L_y = i\hbar\left(-\cos\phi \frac{\partial}{\partial\theta} + \cot\theta\sin\phi\frac{\partial}{\partial\phi}\right)$$

$$L_z = -i\hbar\frac{\partial}{\partial\phi}$$

and verify that $\mathbf{L}^2 = L_x^2 + L_y^2 + L_z^2$ is given by [2.159]. Using these results show that $[\mathbf{L}, f(r)] = 0$ and $[\mathbf{L}^2, f(r)] = 0$ where $f(r)$ is an arbitrary function of the radial coordinate r. Show also that $[\mathbf{L}, \mathbf{p}^2] = 0$, where $\mathbf{p}^2 = -\hbar^2\nabla^2$.

2.13 Obtain the results [2.187] and [2.188], and show that for $s = \frac{1}{2}$ $\langle S_x^2\rangle = \langle S_y^2\rangle = \hbar^2/4$.

2.14 Verify equations [2.217] and [2.218].

2.15 Write down explicitly the matrices representing the operators S_x, S_y, S_z, S_+, S_- and $\mathbf{S}^2$ for $s = 1$ and $s = 3/2$.

2.16 Prove that $\mathbf{L}^2$, $\mathbf{S}^2$, $\mathbf{J}^2$ and J_z form a commuting set of operators, and that $[(\mathbf{L}\cdot\mathbf{S}), J_z] = 0$.

2.17 Assuming that the expansion of a plane wave in a series of Legendre polynomials is of the form

$$\exp(ikr\cos\theta) = \sum_{l=0}^{\infty} c_l j_l(kr) P_l(\cos\theta)$$

find the coefficients c_l.
Hint: Use the fact that $j_l(kr) \underset{r\to\infty}{\longrightarrow} (kr)^{-1}\sin(kr - l\pi/2)$.

2.18 Show that $E_k^{(2)}$ and $E_k^{(3)}$ are given by [2.311] and [2.312] respectively.

2.19 Consider a linear harmonic oscillator for which the Hamiltonian is

$$H_0 = -\frac{\hbar^2}{2m}\frac{\mathrm{d}^2}{\mathrm{d}x^2} + \frac{1}{2}kx^2$$

If this oscillator is perturbed by an additional potential of the form $H' = \frac{1}{2}k'x^2$, find the first and second order corrections to the energy levels using perturbation theory. Also find the first order correction to the

wave function. Compare your results with the exact solution

$$E_n = \hbar\omega\left(n + \frac{1}{2}\right)\left(1 + \frac{k'}{k}\right)^{1/2}$$

where $\omega = (k/m)^{1/2}$. Hint: Obtain first the matrix elements:

$$x_{ij}^2 = \langle\psi_i|x^2|\psi_j\rangle$$

$$= \begin{cases} (2\alpha^2)^{-1}[(j+1)(j+2)]^{1/2} & i = j+2 \\ (2\alpha^2)^{-1}\,(2j+1) & i = j \\ (2\alpha^2)^{-1}[j(j-1)]^{1/2} & i = j-2 \end{cases}$$

where $\quad \alpha = \left(\dfrac{mk}{\hbar^2}\right)^{1/4}$

2.20 A two-dimensional isotropic harmonic oscillator has the Hamiltonian

$$H = -\frac{\hbar^2}{2m}\left(\frac{\partial^2}{\partial x^2} + \frac{\partial^2}{\partial y^2}\right) + \frac{1}{2}k(x^2 + y^2)$$

(a) Show that the energy levels are given by

$$E_{n_x n_y} = \hbar\omega\,(n_x + n_y + 1); \quad n_x = 0, 1, 2 \ldots \quad n_y = 0, 1, 2 \ldots, \qquad \omega = (k/m)^{1/2}$$

What is the degeneracy of each level?

(b) If the oscillator is perturbed by an interaction of the form $H' = \lambda xy$, where λ is a constant, find the first-order modification of the energy of the first excited level.

2.21 Consider a particle of charge q and mass m, which is in simple harmonic motion along the X axis with force constant k. An electric field $\mathscr{E}(t)$, directed along the X axis, is switched on at time $t = 0$ so that the system is perturbed by an interaction

$$H'(t) = -qx\mathscr{E}(t)$$

If $\mathscr{E}(t)$ has the form

$$\mathscr{E}(t) = \mathscr{E}_0 \exp(-t/\tau)$$

where $\mathscr{E}_0$ and τ are constants, and if the oscillator is in the ground state for $t \leqslant 0$, find the probability that the oscillator will be found in an excited state as $t \to \infty$.

2.22 (a) By varying the parameter a in the trial function

$$\begin{aligned} \phi_0(x) &= (a^2 - x^2)^2, & |x| &< a \\ &= 0 & |x| &\geqslant a \end{aligned}$$

obtain an upper bound for the ground state energy of a linear harmonic

oscillator having the Hamiltonian

$$H = -\frac{\hbar^2}{2m}\frac{\mathrm{d}^2}{\mathrm{d}x^2} + \frac{1}{2}m\omega^2 x^2$$

(b) Show that the function $\phi_1(x) = x\phi_0(x)$ is a suitable trial function for the first excited state and obtain a variational estimate of the energy of this level.

2.23 Prove the result given in equation [2.380].

2.24 Let $E_{n,l}$ denote the discrete energy levels of a particle of mass m in a central potential $V(r)$, corresponding to a given orbital angular momentum quantum number l, and let $E_{n,l}^{\min}$ be their minimum value. Prove that $E_{n,l}^{\min} < E_{n,l+1}^{\min}$

Hint: Write the Hamiltonian of the particle as

$$H = H_r + \frac{\mathbf{L}^2}{2mr^2}, \; H_r = -\frac{\hbar^2}{2m}\frac{1}{r^2}\frac{\partial}{\partial r}\left(r^2\frac{\partial}{\partial r}\right) + V(r)$$

and note that H_r is a purely radial operator.

3 One-electron atoms

In this chapter we begin our quantum mechanical study of atomic structure by considering the simplest atom, namely the hydrogen atom, which consists of a proton and an electron. Apart from small corrections, which we shall discuss in Chapter 5, the hydrogen atom may be considered as a non-relativistic system of two particles interacting by means of an attractive Coulomb potential. Other similar one-electron systems, called hydrogenic atoms, include the isotopes of hydrogen (deuterium, tritium) and the hydrogenic ions (He^+, Li^{++}, etc.) which we have already encountered in our study of the Bohr model. These hydrogenic systems will also be discussed in the present chapter.

Our starting point is the Schrodinger equation for one-electron atoms. After separating the centre of mass motion, we solve the eigenvalue equation for the relative motion in spherical polar coordinates, and obtain the energy levels and wave functions of the discrete spectrum. We then consider the expectation values of various operators, prove the virial theorem and conclude this chapter with a discussion of 'special' hydrogenic systems such as muonium, positronium, muonic and hadronic atoms, and Rydberg atoms.

3.1 THE SCHRÖDINGER EQUATION FOR ONE-ELECTRON ATOMS

Let us consider a hydrogenic atom containing an atomic nucleus of charge Ze and an electron of charge $-e$ interacting by means of the Coulomb potential

$$V(r) = -\frac{Ze^2}{(4\pi\varepsilon_0)r} \qquad [3.1]$$

where r is the distance between the two particles. We denote by m the mass of the electron and M the mass of the nucleus. Since the interaction potential [3.1] only depends on the relative coordinate of the two particles, we may use the results of Section 2.7 to separate the motion of the centre of mass. Remembering that $\mathbf{P}$ is the total momentum associated with the motion of the centre of mass and $\mathbf{p}$ the relative momentum, the total energy of the atom can be split into two parts. The first one is the kinetic energy $P^2/2(M+m)$ corresponding to the motion of the centre of mass, and the second one is the (internal) energy of the

relative motion, governed by the Hamiltonian

$$H = \frac{p^2}{2\mu} - \frac{Ze^2}{(4\pi\varepsilon_0)r} \qquad [3.2]$$

where

$$\mu = \frac{mM}{m + M} \qquad [3.3]$$

is the reduced mass of the two particles. Thus, working in the centre of mass system (where $P = 0$) and in the position representation, we must solve the one-body time-independent Schrödinger equation

$$\left[-\frac{\hbar^2}{2\mu}\nabla^2 - \frac{Ze^2}{(4\pi\varepsilon_0)r}\right]\psi(\mathbf{r}) = E\psi(\mathbf{r}) \qquad [3.4]$$

Instead of using the position representation, as we shall do below, it is also possible to solve the Schrödinger equation for one-electron atoms in momentum space. This is carried out in Appendix 5, where the hydrogenic wave functions in momentum space are obtained.

Solution in spherical polar coordinates

Because the interaction potential [3.1] is central, the wave equation [3.4] may be separated in spherical polar coordinates (see Section 2.6). Thus we write a particular solution of this equation as

$$\psi_{E,l,m}(r, \theta, \phi) = R_{E,l}(r)Y_{lm}(\theta, \phi) \qquad [3.5]$$

where $Y_{lm}(\theta, \phi)$ is a spherical harmonic corresponding to the orbital angular momentum quantum number l and to the magnetic quantum number m (with $m = -l, -l + 1, \ldots +l$). The function $R_{E,l}(r)$ satisfies the radial Schrödinger equation

$$\left\{-\frac{\hbar^2}{2\mu}\left[\frac{1}{r^2}\frac{\mathrm{d}}{\mathrm{d}r}\left(r^2\frac{\mathrm{d}}{\mathrm{d}r}\right) - \frac{l(l+1)}{r^2}\right] - \frac{Ze^2}{(4\pi\varepsilon_0)r}\right\}R_{E,l}(r) = ER_{E,l}(r) \qquad [3.6]$$

which we have obtained by substituting into [2.235] the expression [3.1] of the Coulomb potential. As we remarked in Section 2.6, we can simplify [3.6] by introducing the new unknown function

$$u_{E,l}(r) = rR_{E,l}(r) \qquad [3.7]$$

Thus, using [2.239] we find that $u_{E,l}(r)$ satisfies the equation

$$\frac{\mathrm{d}^2u_{E,l}}{\mathrm{d}r^2} + \frac{2\mu}{\hbar^2}[E - V_{\mathrm{eff}}(r)]u_{E,l}(r) = 0 \qquad [3.8]$$

where

$$V_{\text{eff}}(r) = -\frac{Ze^2}{(4\pi\varepsilon_0)r} + \frac{l(l+1)\hbar^2}{2\mu r^2} \qquad [3.9]$$

is the effective potential. Figure 3.1 shows $V_{\text{eff}}(r)$ for the case $Z = 1$ and $\mu = m$ (corresponding to a hydrogen atom with an 'infinitely heavy' proton) and for the values $l = 0, 1, 2$.

The problem of solving the Schrödinger equation [3.4] therefore reduces to that of solving the radial one-dimensional equation [3.8] corresponding to a particle of mass μ moving in an effective potential V_{eff} made up of the Coulomb potential [3.1] plus the 'centrifugal barrier' potential $l(l+1)\hbar^2/2\mu r^2$. It is clear that since $V_{\text{eff}}(r)$ tends to zero for large r, the solution $u_{E,l}(r)$ for $E > 0$ will have an oscillatory behaviour at infinity and will be an acceptable eigenfunction for any positive value of E. We therefore have a continuum spectrum for $E > 0$.

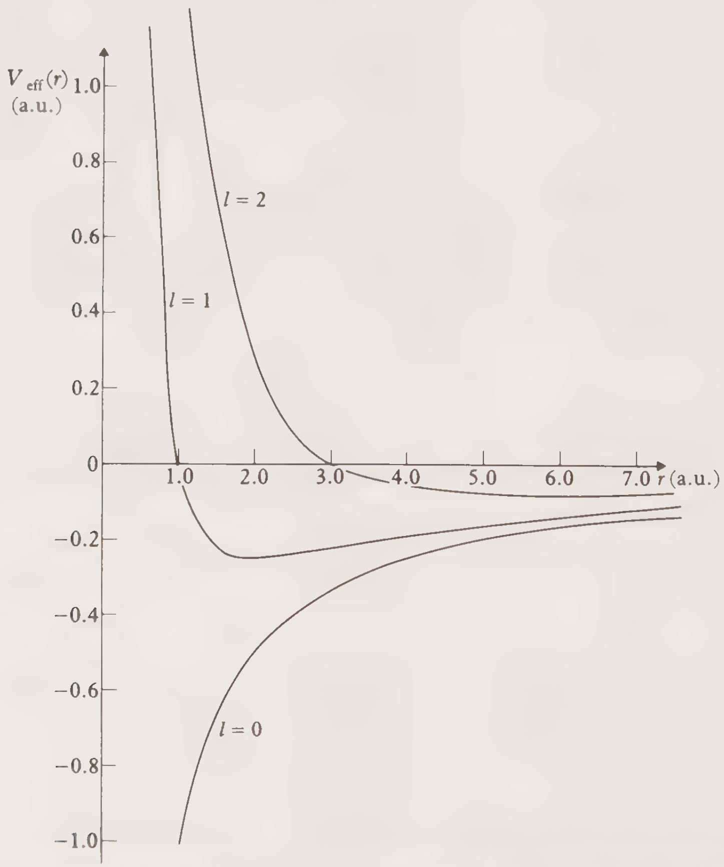

3.1 The effective potential $V_{\text{eff}}(r)$ given by [3.9], for the case $Z = 1$ and $\mu = m$, and the values $l = 0, 1, 2$. Atomic units are used (see Appendix 11), so that $V_{\text{eff}}(r)$ is expressed in units $e^2/(4\pi\varepsilon_0 a_0)$ and r in units of a_0, where a_0 is the Bohr radius [1.86].

The corresponding unbound states play an important role in the analysis of the scattering of electrons by ions; we shall return to such collision phenomena in Chapter 11. For the moment, however, we will only be concerned with the bound states of hydrogenic atoms, corresponding to the case $E < 0$.

Let us return to the radial equation [3.8]. We shall look for solutions which vanish at $r = 0$, i.e.

$$u_{E,l}(0) = 0 \tag{3.10}$$

so that the radial function $R_{E,l}(r)$ – and hence the full wave function $\psi_{E,l,m}(\mathbf{r})$ given by [3.5] – remains finite at the origin [1]. It is convenient to introduce the dimensionless quantities

$$\rho = \left(-\frac{8\mu E}{\hbar^2}\right)^{1/2} r \tag{3.11}$$

and

$$\lambda = \frac{Ze^2}{4\pi\varepsilon_0\hbar}\left(-\frac{\mu}{2E}\right)^{1/2} = Z\alpha\left(-\frac{\mu c^2}{2E}\right)^{1/2} \tag{3.12}$$

where $\alpha = e^2/(4\pi\varepsilon_0\hbar c) \simeq 1/137$ is the fine structure constant and we recall that $E < 0$. In terms of the new quantities ρ and λ, the equation [3.8] now reads

$$\left[\frac{\mathrm{d}^2}{\mathrm{d}\rho^2} - \frac{l(l+1)}{\rho^2} + \frac{\lambda}{\rho} - \frac{1}{4}\right]u_{E,l}(\rho) = 0 \tag{3.13}$$

As in the case of the harmonic oscillator (see Section 2.4) we first analyse the asymptotic behaviour of $u_{E,l}(\rho)$. To this end, we remark that when $\rho \to \infty$ the terms in $1/\rho$ and $1/\rho^2$ become negligible with respect to the constant term $(-1/4)$, so that [3.13] reduces to the equation

$$\left[\frac{\mathrm{d}^2}{\mathrm{d}\rho^2} - \frac{1}{4}\right]u_{E,l}(\rho) = 0 \tag{3.14}$$

whose solutions are $\exp(\pm\rho/2)$. Therefore, using the fact that the function $u_{E,l}(r)$ must be bounded everywhere, including infinity, we keep only the exponentially decreasing function and we have

$$u_{E,l}(\rho) \underset{\rho\to\infty}{\sim} \mathrm{e}^{-\rho/2} \tag{3.15}$$

[1] The finiteness of the wave function $\psi_{E,l,m}(\mathbf{r})$ is not really a necessary requirement. In fact, mildly singular wave functions are encountered in some cases, for example in the Dirac relativistic theory of one-electron atoms. The correct boundary condition is obtained by requiring that all the possible physical states are described by a complete, orthogonal set of wave functions. However, for a large class of potentials including the Coulomb potential [3.1], this condition may be shown to lead to the simpler requirement [3.10].

This result suggests that we should search for a solution of the radial equation [3.13] having the form

$$u_{E,l}(\rho) = \mathrm{e}^{-\rho/2} f(\rho) \tag{3.16}$$

where we have written $f(\rho) \equiv f_{E,l}(\rho)$ to simplify the notation. Substituting [3.16] in [3.13], we obtain for $f(\rho)$ the equation

$$\left[\frac{\mathrm{d}^2}{\mathrm{d}\rho^2} - \frac{\mathrm{d}}{\mathrm{d}\rho} - \frac{l(l+1)}{\rho^2} + \frac{\lambda}{\rho}\right] f(\rho) = 0 \tag{3.17}$$

We now write a power series expansion for $f(\rho)$ in the form

$$f(\rho) = \rho^{l+1} g(\rho) \tag{3.18}$$

where

$$g(\rho) = \sum_{k=0}^{\infty} c_k \rho^k, \qquad c_0 \neq 0 \tag{3.19}$$

and we have used the fact (see Section 2.6) that $u_{E,l}(\rho)$ – and therefore $f(\rho)$ – behaves like ρ^{l+1} for all central potentials $V(r)$ which are less singular than r^{-2} at the origin. Upon substitution of [3.18] into [3.17] we find that the function $g(\rho)$ satisfies the differential equation

$$\left[\rho \frac{\mathrm{d}^2}{\mathrm{d}\rho^2} + (2l + 2 - \rho)\frac{\mathrm{d}}{\mathrm{d}\rho} + (\lambda - l - 1)\right] g(\rho) = 0 \tag{3.20}$$

Moreover, using the expansion [3.19] to solve the equation [3.20], we find that

$$\sum_{k=0}^{\infty} [k(k-1)c_k\rho^{k-1} + (2l + 2 - \rho)kc_k\rho^{k-1} + (\lambda - l - 1)c_k\rho^k] = 0 \tag{3.21}$$

or

$$\sum_{k=0}^{\infty} \{[k(k+1) + (2l+2)(k+1)]c_{k+1} + (\lambda - l - 1 - k)c_k\}\rho^k = 0 \tag{3.22}$$

so that the coefficients c_k must satisfy the recursion relation

$$c_{k+1} = \frac{k + l + 1 - \lambda}{(k+1)(k + 2l + 2)} c_k \tag{3.23}$$

If the series [3.19] does not terminate, we see from [3.23] that for large k

$$\frac{c_{k+1}}{c_k} \sim \frac{1}{k} \tag{3.24}$$

a ratio which is the same as that of the series for $\rho^p \exp(\rho)$, where p has a finite value. Thus in this case we deduce from [3.16] and [3.18] that the

function $u_{E,l}(r)$ has an asymptotic behaviour of the type

$$u_{E,l}(\rho) \underset{\rho \to \infty}{\sim} \rho^{l+1+p} \mathrm{e}^{\rho/2} \qquad [3.25]$$

which is clearly unacceptable.

The series [3.19] must therefore terminate, or in other words $g(\rho)$ must be a polynomial in ρ. Let us assume that the highest power of ρ in $g(\rho)$ is ρ^{n_r}, where the *radial quantum number* $n_r = 0, 1, 2, \ldots$ is a positive integer or zero. Then the coefficient $c_{n_r+1} = 0$, and from the recursion relation [3.23] we deduce that

$$\lambda = n_r + l + 1 \qquad [3.26]$$

Let us introduce the *principal quantum number*

$$n = n_r + l + 1 \qquad [3.27]$$

which is a positive integer ($n = 1, 2, \ldots$) since n_r and l can take on positive integer or zero values. Thus, from [3.26] and [3.27], we see that the eigenvalues of [3.13] are given by

$$\lambda = n, \qquad n = 1, 2, \ldots \qquad [3.28]$$

3.2 ENERGY LEVELS

Replacing in [3.12] the parameter λ by its value [3.28] we obtain the energy eigenvalues

$$\begin{aligned} E_n &= -\frac{1}{2n^2}\left(\frac{Ze^2}{4\pi\varepsilon_0}\right)^2 \frac{\mu}{\hbar^2} \\ &= -\frac{e^2}{(4\pi\varepsilon_0)a_0} \frac{\mu}{m} \frac{Z^2}{2n^2} \\ &= -\frac{e^2}{(4\pi\varepsilon_0)a_\mu} \frac{Z^2}{2n^2} \end{aligned} \qquad [3.29]$$

where $a_0 = 4\pi\varepsilon_0\hbar^2/me^2$ is the Bohr radius [1.86] and $a_\mu = 4\pi\varepsilon_0\hbar^2/\mu e^2 = a_0 m/\mu$ is the modified Bohr radius [1.101]. We may also write

$$E_n = -\frac{1}{2}\mu c^2 \frac{(Z\alpha)^2}{n^2} \qquad [3.30]$$

where $\alpha = e^2/(4\pi\varepsilon_0\hbar c)$ is the fine structure constant. The first form [3.29] which does not contain the velocity of light c clearly shows that the energy levels E_n have been obtained by solving a non-relativistic equation. The second form [3.30], in which the energies E_n are expressed in terms of the rest mass energy μc^2, will be useful at a later stage when we shall discuss the relativistic corrections to the energy levels of one-electron atoms (see Chapter 5). Using

atomic units (a.u.) defined in Appendix 11, we also have

$$E_n = -\frac{Z^2}{2n^2}\left(\frac{\mu}{m}\right) \tag{3.31}$$

where we have written explicitly the electron mass (which is equal to unity in a.u.) for future convenience.

The energy values E_n, which we have obtained here by solving the Schrödinger equation for one-electron atoms, agree exactly with those found in Section 1.7 from the Bohr model. The agreement of this energy spectrum with the main features of the experimental spectrum was pointed out when we analysed the Bohr results. This agreement, however, is not perfect and we shall discuss in Chapter 5 various corrections (such as the fine structure arising from relativistic effects and the electron spin, the Lamb shift and the hyperfine structure due to nuclear effects) which must be taken into account in order to explain the details of the experimental spectrum.

We note from [3.31] that since n may take on all integral values from 1 to $+\infty$, the energy spectrum corresponding to the Coulomb potential [3.1] contains an infinite number of discrete energy levels extending from $-(Z^2/2n^2)(\mu/m)$ to zero. This is due to the fact that the magnitude of the Coulomb potential falls off slowly at large r. On the contrary, short-range potentials such as the square well have a finite (sometimes zero) number of bound states.

Another striking feature of the result [3.31] is that the energy eigenvalues depend only on the principal quantum number n, and are therefore degenerate with respect to l and m. Indeed, for each value of n the orbital quantum number l may take on the values $0, 1, \ldots n-1$ and for each value of l the $(2l+1)$ possible values of the magnetic quantum number m are $-l, -l+1, \ldots, +l$. The total degeneracy of the energy level E_n is therefore given by

$$\sum_{l=0}^{n-1}(2l+1) = 2\,\frac{n(n-1)}{2} + n = n^2 \tag{3.32}$$

As we have already pointed out in Section 2.6, the degeneracy with respect to m is present for any central potential $V(r)$. On the other hand, the degeneracy with respect to l is characteristic of the Coulomb potential; it is removed if the dependence of the potential on r is modified. For example, we shall see in Chapters 7 and 8 that many properties of the alkali atoms can be understood in terms of the motion of a single 'valence' electron in a potential which is central, but which deviates from the $1/r$ Coulomb behaviour because of the presence of the 'inner' electrons. As a result, the energy of this valence electron does depend on l and the degeneracy with respect to l is removed, leading to n distincts levels E_{nl} for a given principal quantum number n. Finally, if an external magnetic field is applied to the atom, we shall see in Chapter 5 that the $(2l+1)$ degeneracy with respect to the magnetic quantum number m is removed.

Figure 3.2 shows an energy-level diagram for the hydrogen atom; it is similar to that displayed in Fig. 1.16 except that the degenerate energy levels with the

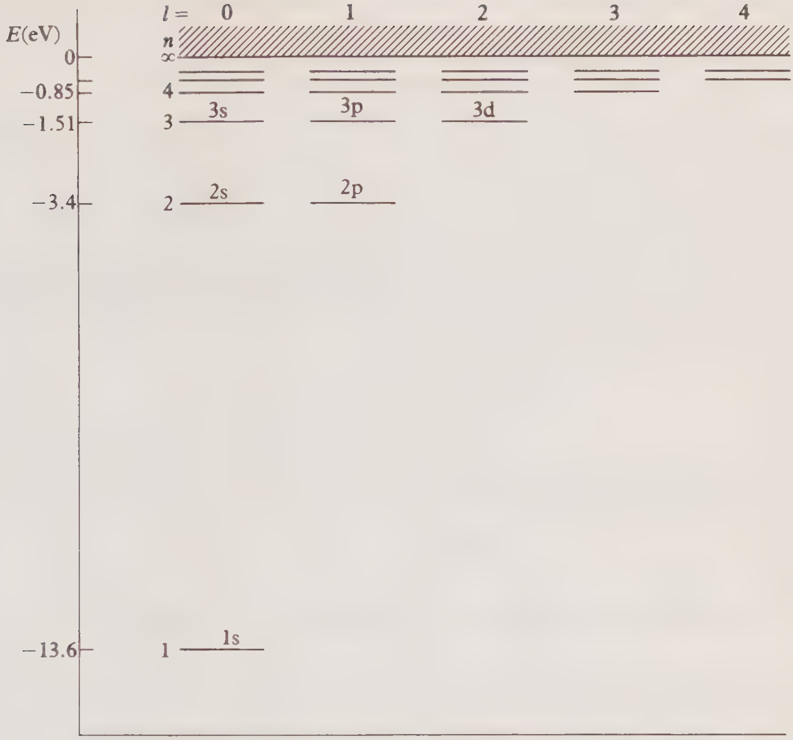

3.2 Energy-level diagram for atomic hydrogen.

same n but different l are shown separately. Following the usual spectroscopic notation, these levels are labelled by two symbols. The first one gives the value of the principal quantum number n and the second one indicates the orbital quantum number l according to the correspondence discussed in Section 2.5, namely

Value of l	0	1	2	3	4	5
	$\updownarrow$	$\updownarrow$	$\updownarrow$	$\updownarrow$	$\updownarrow$	$\updownarrow$
Code letter	s	p	d	f	g	h

Looking at the hydrogen atom spectrum (Fig. 3.2), we see that the ground state is a 1s state, the first excited state is fourfold degenerate and contains a 2s state and three 2p states (with $m = -1, 0, +1$), etc.

Having obtained the energy levels of one-electron atoms within the framework of the Schrödinger non-relativistic theory, we may now ask about the spectral lines corresponding to transitions from one level to another. This problem will be discussed in detail in the next chapter, where we shall study the interaction of one-electron atoms with electromagnetic radiation. In particular, we shall calculate the transition rates for the most common transitions, the so-called electric dipole transitions, and we shall prove that these transitions

obey the selection rules

$$\begin{aligned} \Delta l &= l - l' = \pm 1 \\ \Delta m &= m - m' = 0, \pm 1 \end{aligned} \qquad [3.33]$$

while $\Delta n = n - n'$ is arbitrary. Here the symbols n, l, m refer to the quantum numbers of the upper state and n', l', m' to those of the lower state of the transition. Since the bound state energies E_n depend only on n, and because transitions can occur between states with any two values of n, it is clear that the Bohr frequency rule [1.70] can still be applied to obtain the frequencies of the spectral lines corresponding to transitions between the energy levels. Thus, using atomic units, we have

$$\nu_{n'n} = Z^2 R(M) \left(\frac{1}{n'^2} - \frac{1}{n^2} \right) \qquad [3.34]$$

where $R(M)$ is defined by [1.102] and where $n = 2, 3, 4, \ldots, n' = 1, 2, 3, \ldots$ with $n > n'$.

3.3 THE EIGENFUNCTIONS OF THE BOUND STATES

So far we have seen that the energy levels predicted by the Schrödinger theory for one-electron atoms agree with those already obtained in Section 1.7 by using the Bohr model. However, the Schrödinger theory has much more predictive power than the old quantum theory since it also yields the *eigenfunctions* which will enable us to calculate probability densities, transition rates, and so on.

The radial eigenfunctions of the bound states

In order to obtain these eigenfunctions explicitly, let us return to [3.20]. We shall now show that the physically acceptable solutions of this equation, corresponding to $\lambda = n$, may be expressed in terms of *associated Laguerre polynomials*. To this end we first define the *Laguerre polynomials* $L_q(\rho)$ by the relation

$$L_q(\rho) = e^{\rho} \frac{d^q}{d\rho^q} (\rho^q e^{-\rho}) \qquad [3.35]$$

and we note that these Laguerre polynomials may also be obtained from the generating function

$$\begin{aligned} U(\rho, s) &= \frac{\exp[-\rho s/(1-s)]}{1-s} \\ &= \sum_{q=0}^{\infty} \frac{L_q(\rho)}{q!} s^q, \qquad |s| < 1 \end{aligned} \qquad [3.36]$$

Differentiation of this generating function with respect to s yields the recurrence formula

$$L_{q+1}(\rho) + (\rho - 1 - 2q)L_q(\rho) + q^2 L_{q-1}(\rho) = 0 \tag{3.37}$$

Similarly, if we differentiate $U(\rho, s)$ with respect to ρ we find that

$$\frac{\mathrm{d}}{\mathrm{d}\rho} L_q(\rho) - q\frac{\mathrm{d}}{\mathrm{d}\rho} L_{q-1}(\rho) + qL_{q-1}(\rho) = 0 \tag{3.38}$$

Using [3.37] and [3.38] it is a simple matter to prove that the lowest order differential equation involving only $L_q(\rho)$ is given by

$$\left[\rho\frac{\mathrm{d}^2}{\mathrm{d}\rho^2} + (1-\rho)\frac{\mathrm{d}}{\mathrm{d}\rho} + q\right]L_q(\rho) = 0 \tag{3.39}$$

Next, we define the associated Laguerre polynomials $L_q^p(\rho)$ by the relation

$$L_q^p(\rho) = \frac{\mathrm{d}^p}{\mathrm{d}\rho^p} L_q(\rho) \tag{3.40}$$

Upon differentiation of [3.39] p times, one finds that $L_q^p(\rho)$ satisfies the differential equation

$$\left[\rho\frac{\mathrm{d}^2}{\mathrm{d}\rho^2} + (p+1-\rho)\frac{\mathrm{d}}{\mathrm{d}\rho} + (q-p)\right]L_q^p(\rho) = 0 \tag{3.41}$$

Setting $\lambda = n$ in [3.20] and comparing with [3.41] we see that the physically acceptable solution $g(\rho)$ of [3.20] is given by

$$g(\rho) = N_{nl}L_{n+l}^{2l+1}(\rho) \tag{3.42}$$

where N_{nl} is a constant which will be determined below (apart from an arbitrary phase factor) by the normalisation condition. We note that $L_{n+l}^{2l+1}(\rho)$ is a polynomial of order $(n + l) - (2l + 1) = n - l - 1 = n_r$ in agreement with the discussion following [3.25]. We also note from [3.11] and [3.29] that

$$\begin{aligned}\rho &= \frac{2Z}{na_0}\left(\frac{\mu}{m}\right)r \\ &= \frac{2Z}{na_\mu}r\end{aligned} \tag{3.43}$$

where we recall that $a_\mu = a_0 m/\mu$ is the modified Bohr radius. In atomic units ($a_0 = 1$) we have

$$\rho = \frac{2Z}{n}\left(\frac{\mu}{m}\right)r \tag{3.44}$$

We may also obtain a generating function for the associated Laguerre polynomials by differentiating [3.36] p times with respect to ρ. That is,

$$U_p(\rho, s) = \frac{(-s)^p \exp[-\rho s/(1-s)]}{(1-s)^{p+1}}$$

$$= \sum_{q=p}^{\infty} \frac{L_q^p(\rho)}{q!} s^q \qquad [3.45]$$

An explicit expression for $L_{n+l}^{2l+1}(\rho)$ is given by

$$L_{n+l}^{2l+1}(\rho) = \sum_{k=0}^{n_r} (-1)^{k+1} \frac{[(n+l)!]^2}{(n_r-k)!(2l+1+k)!} \frac{\rho^k}{k!},$$

$$n_r = n - l - 1 \qquad [3.46]$$

and is readily verified by substitution into [3.45], with $q = n + l$ and $p = 2l + 1$.

Using [3.7], [3.16], [3.18] and [3.42] we may now write the full hydrogenic radial function as

$$R_{nl}(r) = N_{nl} \mathrm{e}^{-\rho/2} \rho^l L_{n+l}^{2l+1}(\rho),$$

$$\rho = \frac{2Z}{na_\mu} r \qquad [3.47]$$

where we have used the notation R_{nl} (which displays explicitly the quantum numbers n and l) instead of the symbol $R_{E,l}$ introduced at the beginning of this chapter.

Hydrogenic wave functions of the discrete spectrum

Using [3.5], we see that the complete eigenfunctions of the discrete spectrum for a one-electron atom may be written as

$$\psi_{nlm}(r, \theta, \phi) = R_{nl}(r) Y_{lm}(\theta, \phi) \qquad [3.48]$$

where the radial functions R_{nl} are given by [3.47] and the spherical harmonics Y_{lm} provide the angular part of the wave functions. We require that the eigenfunctions [3.48] be normalised, namely

$$\int_0^\infty \mathrm{d}r\, r^2 \int_0^\pi \mathrm{d}\theta \sin\theta \int_0^{2\pi} \mathrm{d}\phi\, |\psi_{nlm}(r, \theta, \phi)|^2 = 1 \qquad [3.49]$$

Since the spherical harmonics are already normalised on the unit sphere (see [2.182]), the normalisation condition [3.49] shows that the radial functions $R_{nl}(r)$ are normalised as

$$\int_0^\infty |R_{nl}(r)|^2 r^2 \,\mathrm{d}r = 1 \qquad [3.50]$$

Using [3.47] we see that [3.50] becomes

$$|N_{nl}|^2 \left(\frac{na_\mu}{2Z}\right)^3 \int_0^\infty \mathrm{e}^{-\rho}\rho^{2l}[L_{n+l}^{2l+1}(\rho)]^2\rho^2\,\mathrm{d}\rho = 1 \qquad [3.51]$$

It is shown in Appendix 3 that the integral over ρ can be evaluated by using the generating function [3.45]. The result is (see [A3.26])

$$\int_0^\infty \mathrm{e}^{-\rho}\rho^{2l}[L_{n+l}^{2l+1}(\rho)]^2\,\rho^2\,\mathrm{d}\rho = \frac{2n[(n+l)!]^3}{(n-l-1)!} \qquad [3.52]$$

so that the normalised radial functions for the bound states of one-electron atoms may be written as [2]

$$R_{nl}(r) = -\left\{\left(\frac{2Z}{na_\mu}\right)^3 \frac{(n-l-1)!}{2n[(n+l)!]^3}\right\}^{1/2} \mathrm{e}^{-\rho/2}\rho^l L_{n+l}^{2l+1}(\rho)$$

$$\rho = \frac{2Z}{na_\mu}r, \qquad a_\mu = \frac{4\pi\varepsilon_0\hbar^2}{\mu e^2} \qquad [3.53]$$

As an illustration of the above formulae, we shall consider the case of an 'infinitely heavy' nucleus, so that a_μ reduces to $a_0 = 4\pi\varepsilon_0\hbar^2/me^2$, the first Bohr radius. The first few radial eigenfunctions are then given explicitly by

$$R_{10}(r) = 2(Z/a_0)^{3/2}\exp(-Zr/a_0)$$

$$R_{20}(r) = 2(Z/2a_0)^{3/2}(1 - Zr/2a_0)\exp(-Zr/2a_0)$$

$$R_{21}(r) = \frac{1}{\sqrt{3}}(Z/2a_0)^{3/2}(Zr/a_0)\exp(-Zr/2a_0)$$

$$R_{30}(r) = 2(Z/3a_0)^{3/2}(1 - 2Zr/3a_0 + 2Z^2r^2/27a_0^2)\exp(-Zr/3a_0)$$

$$R_{31}(r) = \frac{4\sqrt{2}}{9}(Z/3a_0)^{3/2}(1 - Zr/6a_0)(Zr/a_0)\exp(-Zr/3a_0)$$

$$R_{32}(r) = \frac{4}{27\sqrt{10}}(Z/3a_0)^{3/2}(Zr/a_0)^2\exp(-Zr/3a_0) \qquad [3.54]$$

In order to express these functions in atomic units (a.u.) one just sets $a_0 = 1$ in [3.54]. To take into account the reduced mass effect, we should replace a_0 by $a_\mu = a_0(m/\mu)$.

Using the radial wave functions [3.53] together with the explicit expressions of the spherical harmonics given in Table 2.1, we display in Table 3.1 the complete normalised bound state hydrogenic eigenfunctions $\psi_{nlm}(r, \theta, \phi)$ for the first three shells (i.e. the K, L and M shells corresponding respectively to the values $n = 1$, 2 and 3 of the principal quantum number) for the case of an

[2] In writing [3.53] we have used the fact that the radial eigenfunctions $R_{nl}(r)$ may be taken to be real without loss of generality.

Table 3.1 The complete normalised hydrogenic wave functions corresponding to the first three shells, for an 'infinitely heavy' nucleus. The quantity $a_0 = 4\pi\varepsilon_0\hbar^2/me^2$ is the first Bohr radius. In order to take into account the reduced mass effect one should replace a_0 by $a_\mu = a_0(m/\mu)$

Shell	*Quantum numbers* n	l	m	*Spectroscopic notation*	*Wave function* $\psi_{nlm}(r, \theta, \phi)$
K	1	0	0	1s	$\frac{1}{\sqrt{\pi}}(Z/a_0)^{3/2}\exp(-Zr/a_0)$
L	2	0	0	2s	$\frac{1}{2\sqrt{2\pi}}(Z/a_0)^{3/2}(1 - Zr/2a_0)\exp(-Zr/2a_0)$
	2	1	0	$2p_0$	$\frac{1}{4\sqrt{2\pi}}(Z/a_0)^{3/2}(Zr/a_0)\exp(-Zr/2a_0)\cos\theta$
	2	1	± 1	$2p_{\pm 1}$	$\mp\frac{1}{8\sqrt{\pi}}(Z/a_0)^{3/2}(Zr/a_0)\exp(-Zr/2a_0)\sin\theta\exp(\pm i\phi)$
M	3	0	0	3s	$\frac{1}{3\sqrt{3\pi}}(Z/a_0)^{3/2}(1 - 2Zr/3a_0 + 2Z^2r^2/27a_0^2)\exp(-Zr/3a_0)$
	3	1	0	$3p_0$	$\frac{2\sqrt{2}}{27\sqrt{\pi}}(Z/a_0)^{3/2}(1 - Zr/6a_0)(Zr/a_0)\exp(-Zr/3a_0)\cos\theta$
	3	1	± 1	$3p_{\pm 1}$	$\mp\frac{2}{27\sqrt{\pi}}(Z/a_0)^{3/2}(1 - Zr/6a_0)(Zr/a_0)\exp(-Zr/3a_0)\sin\theta\exp(\pm i\phi)$
	3	2	0	$3d_0$	$\frac{1}{81\sqrt{6\pi}}(Z/a_0)^{3/2}(Z^2r^2/a_0^2)\exp(-Zr/3a_0)(3\cos^2\theta - 1)$
	3	2	± 1	$3d_{\pm 1}$	$\mp\frac{1}{81\sqrt{\pi}}(Z/a_0)^{3/2}(Z^2r^2/a_0^2)\exp(-Zr/3a_0)\sin\theta\cos\theta\exp(\pm i\phi)$
	3	2	± 2	$3d_{\pm 2}$	$\frac{1}{162\sqrt{\pi}}(Z/a_0)^{3/2}(Z^2r^2/a_0^2)\exp(-Zr/3a_0)\sin^2\theta\exp(\pm 2i\phi)$

'infinitely heavy nucleus'. We have also indicated in Table 3.1 the spectroscopic notation, introduced in our discussion of the energy levels. We shall often refer to one-electron orbital wave functions such as the hydrogenic wave functions ψ_{nlm} as *orbitals*. In accordance with the spectroscopic notation, orbitals corresponding to $l = 0$ will be called s orbitals, those with $l = 1$ will be denoted as p orbitals, and so on.

In some applications it is convenient to consider a different set of hydrogenic wave functions, in which the *real form* of the spherical harmonics is used for the angular part. As we saw in Section 2.5, the spherical harmonics in real form exhibit a directional dependence and behave like simple functions of Cartesian coordinates. Orbitals using the real form of the spherical harmonics for their angular part are therefore particularly convenient to discuss some properties such as the directed valence characteristic of chemical bonds. We recall that the spherical harmonics in real form are not eigenfunctions of L_z (expect, of course, for $m = 0$ where they coincide with the usual spherical harmonics). For a given n and l the hydrogenic wave functions obtained by using the real form of the spherical harmonics are distinguished by the symbols $x, y, z, 3z^2 - r^2, xz, yz, xy$, etc. which have been introduced in Section 2.5. As an example, let us consider the three 2p wave functions (for which $n = 2, l = 1$ and $m = 0, \pm 1$). Using the real forms of the spherical harmonics given in Table 2.2, together with the radial function $R_{21}(r)$ from [3.54], we see that the corresponding normalised hydrogenic wave functions are given by

$$\psi_{2\mathrm{p}_x} = \psi_{2,1,\cos\phi} = \frac{1}{4\sqrt{2\pi}}(Z/a_0)^{3/2}(Zr/a_0)\exp(-Zr/2a_0)\sin\theta\cos\phi \qquad [3.55a]$$

$$\psi_{2\mathrm{p}_y} = \psi_{2,1,\sin\phi} = \frac{1}{4\sqrt{2\pi}}(Z/a_0)^{3/2}(Zr/a_0)\exp(-Zr/2a_0)\sin\theta\sin\phi \qquad [3.55b]$$

$$\psi_{2\mathrm{p}_z} = \psi_{2\mathrm{p}_0} = \psi_{2,1,0} = \frac{1}{4\sqrt{2\pi}}(Z/a_0)^{3/2}(Zr/a_0)\exp(-Zr/2a_0)\cos\theta \qquad [3.55c]$$

In what follows, unless otherwise stated, we shall always use the usual (complex) form of the spherical harmonics.

Discussion of the hydrogenic bound state wave functions. Probability density. Parity

Let us return to the hydrogenic wave functions [3.48]. First of all, we note that

$$|\psi_{nlm}(r, \theta, \phi)|^2 \mathrm{d}\mathbf{r} = \psi^{\star}_{nlm}(r, \theta, \phi)\psi_{nlm}(r, \theta, \phi)r^2\,\mathrm{d}r\sin\theta\,\mathrm{d}\theta\,\mathrm{d}\phi \qquad [3.56]$$

represents the probability of finding the electron in the volume element $\mathrm{d}\mathbf{r}$ (given in spherical polar coordinates by $\mathrm{d}\mathbf{r} = r^2\,\mathrm{d}r\sin\theta\,\mathrm{d}\theta\,\mathrm{d}\phi$ when the system is in the stationary state specified by the quantum numbers (n, l, m). The quantity $|\psi_{nlm}|^2 = \psi^{\star}_{nlm}\psi_{nlm}$ is the *probability density*. Using [3.48] and [2.184],

we see that

$$|\psi_{nlm}(r, \theta, \phi)|^2 = |R_{nl}(r)|^2|Y_{lm}(\theta, \phi)|^2$$
$$= |R_{nl}(r)|^2(2\pi)^{-1}|\Theta_{lm}(\theta)|^2 \qquad [3.57]$$

so that the probability density does not depend on the coordinate ϕ. In fact, we see from [3.57] that the behaviour of $|\psi_{nlm}|^2$ is completely specified by the product of the quantity $|R_{nl}(r)|^2$, which gives the *electron density* as a function of r *along a given direction*, and the *angular factor* $(2\pi)^{-1}|\Theta_{lm}(\theta)|^2$.

The spherical harmonics $Y_{lm}(\theta, \phi)$ and the angular factors $(2\pi)^{-1}|\Theta_{lm}(\theta)|^2$ have been studied in detail in Section 2.5. In particular, we refer the reader to polar plots shown in Fig. 2.6. We also recall that if the real form of the spherical harmonics is used (i.e. if the sine and cosine functions of ϕ are used), then the probability density will depend on ϕ, the dependence being through the functions $\sin^2 m\phi$ and $\cos^2 m\phi$. Polar representations of the angular dependence of the probability density for s and p orbitals (in the real form) are given by Fig. 2.7.

We now turn our attention to the properties of the radial eigenfunctions $R_{nl}(r)$. We have already seen that the quantity $|R_{nl}(r)|^2$ represents the electron density as a function of r along a given direction. On the other hand, the *radial distribution function*

$$D_{nl}(r) = r^2|R_{nl}(r)|^2 \qquad [3.58]$$

gives the probability per unit length that the electron is to be found at a distance r from the nucleus. Indeed, by integrating [3.56] over the polar angles θ and ϕ and using [3.48], we see that

$$D_{nl}(r)\,\mathrm{d}r = r^2|R_{nl}(r)|^2\,\mathrm{d}r \int_0^{\pi} \mathrm{d}\theta \sin\theta \int_0^{2\pi} \mathrm{d}\phi\, |Y_{lm}(\theta, \phi)|^2$$
$$= r^2|R_{nl}(r)|^2\,\mathrm{d}r \qquad [3.59]$$

represents the probability of finding the electron between the distances r and $r + \mathrm{d}r$ from the nucleus, regardless of direction. The appearance of the factor of r^2 on the right side of [3.59] is because the volume enclosed between two spheres of radii r and $r + \mathrm{d}r$ is proportional to that factor. The first few radial eigenfunctions [3.53] are plotted in Fig. 3.3, together with the corresponding radial distribution functions $D_{nl}(r)$.

Several interesting features emerge from the examination of the eigenfunctions $R_{nl}(r)$ and the radial distribution functions $D_{nl}(r)$.

1. Only for s-states ($l = 0$) are the radial wave functions different from zero at $r = 0$. We also note that since $Y_{00} = (4\pi)^{-1/2}$ is independent of θ and ϕ, one has from [3.53]

$$|\psi_{n00}(0)|^2 = \frac{1}{4\pi}|R_{n0}(0)|^2 = \frac{Z^3}{\pi a_\mu^3 n^3} \qquad [3.60]$$

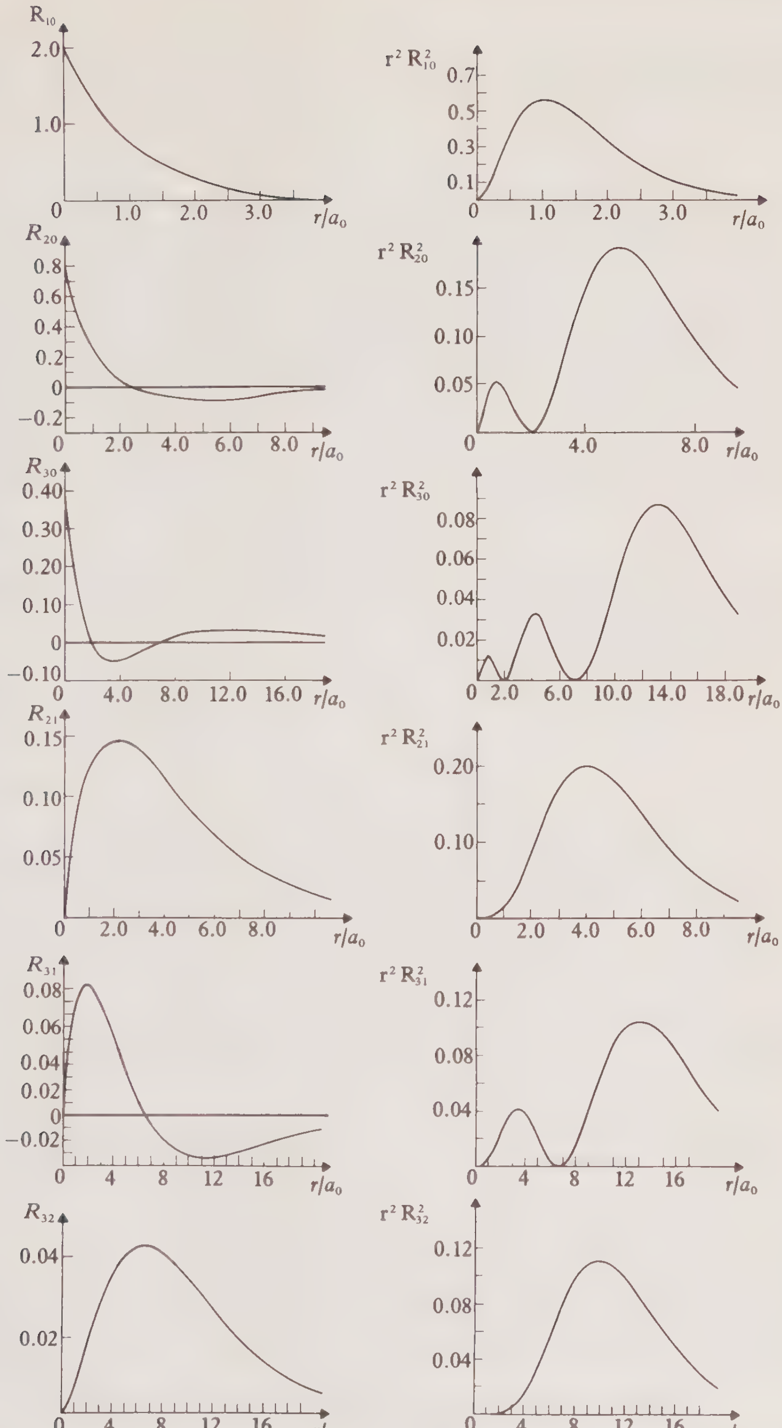

3.3 Radial functions $R_{nl}(r)$ and radial distribution functions $r^2R^2_{nl}(r)$ for atomic hydrogen.

a result which plays an important role in the theory of hyperfine structure (see Chapter 5). Moreover, each of the s-state eigenfunctions $\psi_{n00} \equiv \psi_{ns}$ is such that $\mathrm{d}R_{n0}/\mathrm{d}r \neq 0$ at $r = 0$. This peculiar behaviour is because the potential energy [3.1] is infinite at the origin.

2. For $l \neq 0$ the fact that R_{nl} is proportional to r^l for small r forces the wave function to remain small over distances from the nucleus which increase with l. This is because the effective potential [3.9] contains the centrifugal barrier term $l(l+1)\hbar^2/(2\mu r^2)$ which prevents the electron from approaching the nucleus. Among the eigenfunctions which have the same n, the one with the lowest value of l has the largest amplitude in the vicinity of the nucleus.
3. The associated Laguerre polynomial $L_{n+l}^{2l+1}(\rho)$ is a polynomial of degree $n_r = n - l - 1$ having n_r radial nodes (zeros). Thus the radial distribution function $D_{nl}(r)$ will exhibit $n - l$ maxima. We note that there is only one maximum when, for a given n, the orbital quantum number l has its largest value $l = n - 1$. In this case $n_r = 0$, and we see from [3.46] and [3.53] that

$$R_{n,n-1}(r) \sim r^{n-1}\mathrm{e}^{-Zr/na_\mu} \tag{3.61}$$

Hence, $D_{n,n-1}(r) = r^2 R_{n,n-1}^2(r)$ will have a maximum at a value of r obtained by solving the equation

$$\frac{\mathrm{d}D_{n,n-1}}{\mathrm{d}r} = \left(2nr^{2n-1} - \frac{2Z}{na_\mu} r^{2n}\right)\mathrm{e}^{-2Zr/na_\mu} = 0 \tag{3.62}$$

i.e. at

$$r = \frac{n^2 a_\mu}{Z} \tag{3.63}$$

which is precisely the value [1.100] appearing in the Bohr model. However, in contrast to the Bohr model, the diffuseness of the electron cloud implies that the concept of size is less precise in the quantum mechanical theory, so that the value [3.63] should be interpreted as 'a most probable distance'. We see from [3.63] that this most probable distance is proportional to n^2 and inversely proportional to Z. More generally, the maximum value of $D_{nl}(\mathrm{r})$ recedes from the nucleus with increasing values of n (see Fig. 3.3) and becomes closer to the nucleus by a factor of Z^{-1} when Z increases.

To conclude our study of the hydrogenic bound state wave functions [3.48] we now discuss their *parity*. Since we have reduced the study of hydrogenic atoms to the problem of a particle of mass μ in a central field, we may use directly the results of Section 2.6. Thus the parity operation $\mathbf{r} \to -\mathbf{r}$ (i.e. $(r, \theta, \phi) \to (r, \pi - \theta, \phi + \pi)$ in spherical polar coordinates) leaves the radial part $R_{nl}(r)$ of the hydrogenic wave function unaffected, while the angular part $Y_{lm}(\theta, \phi)$ has the parity of l, as shown by [2.252]. As a result, under the parity operation $\mathcal{P}\mathbf{r} = -\mathbf{r}$ the hydrogenic wave functions [3.48] transform according to

$$\begin{aligned}\mathcal{P}[R_{nl}(r)Y_{lm}(\theta, \phi)] &= R_{nl}(r)Y_{lm}(\pi - \theta, \phi + \pi) \\ &= R_{nl}(r)(-1)^l Y_{lm}(\theta, \phi)\end{aligned} \tag{3.64}$$

We see that for l *even* the hydrogenic wave functions $\psi_{nlm}(r, \theta, \phi) = R_{nl}(r)Y_{lm}(\theta, \phi)$ are unaffected by the parity operation: they are said to be of *even parity*. For l *odd* the wave functions ψ_{nlm} change sign under the parity operation and are said to be of *odd parity*.

3.4 EXPECTATION VALUES. THE VIRIAL THEOREM

Using normalised hydrogenic wave functions $\psi_{nlm}(\mathbf{r})$ we can calculate the expectation (or average) values of various operators. As a simple example, let us consider the average value of the distance r when the hydrogenic atom is in the ground state, that is the quantity $\langle\psi_{100}|r|\psi_{100}\rangle \equiv \langle r\rangle_{100}$. Taking into account the reduced mass effect, we have $\psi_{100} = (Z^3/\pi\, a_\mu^3)^{1/2}\exp(-Zr/a_\mu)$ and therefore

$$\begin{aligned}\langle r\rangle_{100} &= \int \psi_{100}^\star(r) r \psi_{100}(r)\,\mathrm{d}\mathbf{r}\\ &= \int |\psi_{100}(r)|^2 r\,\mathrm{d}\mathbf{r}\\ &= \frac{Z^3}{\pi a_\mu^3}\int_0^\infty \mathrm{d}r\, r^3 \mathrm{e}^{-2Zr/a_\mu}\int_0^\pi \mathrm{d}\theta\,\sin\theta\int_0^{2\pi}\mathrm{d}\phi\end{aligned} \qquad [3.65]$$

The angular integral has the value 4π and the radial integral is readily performed to give

$$\langle r\rangle_{100} = \frac{3a_\mu}{2Z} \qquad [3.66]$$

For a general hydrogenic eigenstate $\psi_{nlm}(\mathbf{r})$ we may calculate in the same way

$$\begin{aligned}\langle r\rangle_{nlm} &= \int \psi_{nlm}^\star(\mathbf{r}) r \psi_{nlm}(\mathbf{r})\,\mathrm{d}\mathbf{r}\\ &= \int_0^\infty |R_{nl}(r)|^2 r^3\,\mathrm{d}r\end{aligned} \qquad [3.67]$$

Using the normalised radial eigenfunctions [3.53] it is found that

$$\langle r\rangle_{nlm} = a_\mu \frac{n^2}{Z}\left\{1 + \frac{1}{2}\left[1 - \frac{l(l+1)}{n^2}\right]\right\} \qquad [3.68]$$

which is seen to agree with [3.66] when $n = 1$ and $l = 0$. We remark from [3.68] that $\langle r\rangle_{nlm}$, which we may interpret as the 'size' of the atom, is inversely proportional to Z and roughly proportional to n^2, in agreement with the discussion following [3.63]. In fact, we see that for s-states ($l = 0$) $\langle r\rangle_{nlm}$ is directly proportional to n^2; for states with $l \neq 0$ the deviations from this proportionality are small.

It is also interesting to evaluate the average values of r^k, where k is a positive or a negative integer, since the quantities $\langle r^k\rangle_{nlm}$ clearly exhibit the differences

between the radial eigenfunctions. For example, one has

$$\langle r^2\rangle_{nlm} = a_\mu^2 \frac{n^4}{Z^2}\left\{1 + \frac{3}{2}\left[1 - \frac{l(l+1) - 1/3}{n^2}\right]\right\} \quad [3.69]$$

$$\langle r^3\rangle_{nlm} = a_\mu^3 \frac{n^6}{Z^3}\left\{1 + \frac{27}{8}\left[1 - \frac{1}{n^2}\left(\frac{35}{27} - \frac{10}{9}(l+2)(l-1)\right)\right.\right.$$
$$\left.\left. + \frac{1}{9n^4}(l+2)(l+1)l(l-1)\right]\right\} \quad [3.70]$$

$$\left\langle \frac{1}{r}\right\rangle_{nlm} = \frac{Z}{a_\mu n^2} \quad [3.71]$$

$$\left\langle \frac{1}{r^2}\right\rangle_{nlm} = \frac{Z^2}{a_\mu^2 n^3(l + 1/2)} \quad [3.72]$$

$$\left\langle \frac{1}{r^3}\right\rangle_{nlm} = \frac{Z^3}{a_\mu^3 n^3 l(l + 1/2)(l + 1)} \quad [3.73]$$

We note from [3.68]–[3.73] that $\langle r^k\rangle_{nlm} \sim (a_\mu/Z)^k$, a result which is easily explained since the Z dependence can be 'factored out' of the problem by defining a new reference length $\tilde{a}_\mu = a_\mu/Z$. We also remark that the expectation values of positive powers of $r (k > 0)$ are controlled by the principal quantum number n, while those corresponding to negative powers of r are strongly dependent on l for $k < -1$. This is due to the fact that for positive powers $(k > 0)$ the important contributions to the integral

$$\langle r^k\rangle_{nlm} = \int_0^\infty |R_{nl}(r)|^2 r^{k+2}\,\mathrm{d}r \quad [3.74]$$

arise from large values of r, for which R_{nl} behaves essentially like r^{n-1} $\exp(-Zr/na_\mu)$. On the other hand, for negative powers such that $k < -1$ the main contributions to the integral [3.74] come from the region of small r, where R_{nl} is proportional to r^l.

Using the result [3.71] we may immediately obtain the average value of the potential energy $V(r) = -Ze^2/(4\pi\varepsilon_0)r$. The result is

$$\begin{aligned}\langle V\rangle_{nlm} &= -\frac{Ze^2}{4\pi\varepsilon_0}\left\langle\frac{1}{r}\right\rangle_{nlm}\\ &= -\frac{e^2}{(4\pi\varepsilon_0)a_\mu}\frac{Z^2}{n^2}\\ &= 2E_n\end{aligned} \quad [3.75]$$

where we have also used the equation [3.29] which gives the energy eigenvalues E_n. From [3.75] we can also deduce the average value of the kinetic energy operator $T = -(\hbar^2/2\mu)\nabla^2$. That is,

$$\langle T\rangle_{nlm} = E_n - \langle V\rangle_{nlm} = -E_n \quad [3.76]$$

so that

$$2\langle T\rangle = -\langle V\rangle \qquad [3.77]$$

where we have dropped the subscripts. The result [3.77] is a particular case of the *virial theorem*, which we shall now prove.

The virial theorem

Let us denote by H the Hamiltonian of a physical system and by Ψ its state vector, solution of the time-dependent Schrödinger equation [2.46]. We have proved in Section 2.3 that the time rate of change of the expectation value $\langle A\rangle \equiv \langle\Psi|A|\Psi\rangle$ of an operator which does not depend explicitly on t satisfies the equation

$$i\hbar \frac{\mathrm{d}}{\mathrm{d}t}\langle\Psi|A|\Psi\rangle = \langle\Psi|[A, H]|\Psi\rangle \qquad [3.78]$$

where $[A, H] = AH - HA$ is the commutator of the operators A and H.

Let us further assume that H is time-independent and denote respectively by E_n and ψ_n its eigenenergies and eigenfunctions. For a *stationary state* $\Psi_n = \psi_n \exp(-iE_nt/\hbar)$ and a time-independent operator A it is clear that the expectation value $\langle\Psi_n|A|\Psi_n\rangle = \langle\psi_n|A|\psi_n\rangle$ does not depend on t so that [3.78] reduces in this case to

$$\langle\psi_n|[A, H]|\psi_n\rangle = 0 \qquad [3.79]$$

We now apply this result to the particular case of the non-relativistic motion of a particle of mass μ in a potential $V(\mathbf{r})$, the corresponding time-independent Hamiltonian being

$$H = \frac{p^2}{2\mu} + V = T + V \qquad [3.80]$$

where $T = p^2/2\mu = -\hbar^2\nabla^2/2\mu$ is the kinetic energy operator. Moreover, we choose A to be the time-independent operator $\mathbf{r}\cdot\mathbf{p}$. We then have from [3.79]

$$\langle\psi_n|[(\mathbf{r}\cdot\mathbf{p}), H]|\psi_n\rangle \equiv \langle[(\mathbf{r}\cdot\mathbf{p}), H]\rangle = 0 \qquad [3.81]$$

Using the algebraic properties [2.120] of the commutators, together with the fundamental commutation relations [2.119] and the fact that $\mathbf{p} = -i\hbar\boldsymbol{\nabla}$, we find that

$$\begin{aligned}
[(\mathbf{r}\cdot\mathbf{p}), H] &= \left[(xp_x + yp_y + zp_z), \frac{1}{2\mu}(p_x^2 + p_y^2 + p_z^2) + V(x, y, z)\right] \\
&= \frac{i\hbar}{\mu}(p_x^2 + p_y^2 + p_z^2) - i\hbar\left(x\frac{\partial V}{\partial x} + y\frac{\partial V}{\partial y} + z\frac{\partial V}{\partial z}\right) \\
&= 2i\hbar T - i\hbar(\mathbf{r}\cdot\boldsymbol{\nabla}V)
\end{aligned} \qquad [3.82]$$

From [3.81] and [3.82] we therefore obtain the relation

$$2\langle T\rangle = \langle \mathbf{r}\cdot\nabla V\rangle \qquad [3.83]$$

which is known as the virial theorem [3]. It is worth noting that this result may also be obtained by choosing the operator A to be $\mathbf{p}\cdot\mathbf{r}$ instead of $\mathbf{r}\cdot\mathbf{p}$. Indeed, the difference between $\mathbf{r}\cdot\mathbf{p}$ and $\mathbf{p}\cdot\mathbf{r}$ is a constant, and therefore commutes with H.

If the interaction potential is spherically symmetric and proportional to r^s, and if the expectation values exist, we deduce from [3.83] that

$$\begin{aligned} 2\langle T\rangle &= \left\langle r\frac{\partial V}{\partial r}\right\rangle \\ &= s\langle V\rangle \end{aligned} \qquad [3.84]$$

For example the case $s = 2$ corresponds to the harmonic oscillator, for which $\langle T\rangle = \langle V\rangle$. On the other hand the case $s = -1$, corresponding to the hydrogenic atom, yields the relation $2\langle T\rangle = -\langle V\rangle$, in agreement with our result [3.77], which is therefore seen to be a direct consequence of the virial theorem.

3.5 SPECIAL HYDROGENIC SYSTEMS: MUONIUM; POSITRONIUM; MUONIC AND HADRONIC ATOMS; RYDBERG ATOMS

Let us recall some of the key results we have obtained for hydrogenic systems. The energy eigenvalues are given by [3.29] and the frequencies of the transitions by [3.34]. In particular, the ionisation potential $I_P = |E_{n=1}|$ is just

$$I_P = \frac{e^2}{(4\pi\varepsilon_0)a_\mu}\frac{Z^2}{2} \qquad [3.85]$$

and the 'extension' a of the wave function describing the relative motion of the system is roughly given in the ground state (see [3.63]) by

$$a = \frac{a_\mu}{Z} = \frac{(4\pi\varepsilon_0)\hbar^2}{Z\mu e^2} \qquad [3.86]$$

where $\mu = mM/(m + M)$ is the reduced mass.

[3] We recall that in classical mechanics the *virial* of a particle is defined as the quantity $-(1/2)\overline{\mathbf{F}\cdot\mathbf{r}}$, where $\mathbf{F}$ is the force acting on the particle and the bar denotes a *time average*. If the motion is periodic (or even if the motion is not periodic, but the coordinate and velocity of the particle remain finite) and $\bar{T}$ denotes the time average of the kinetic energy of the particle, one has (Goldstein, 1962).

$$\bar{T} = -\tfrac{1}{2}\overline{\mathbf{F}\cdot\mathbf{r}}$$

and this relation is known as the *virial theorem*. If the force is derivable from a potential V the virial theorem becomes

$$2\bar{T} = \overline{\mathbf{r}\cdot\nabla V}$$

which is the classical analogue of [3.83].

The hydrogenic systems we have considered so far correspond to an atomic nucleus of mass M and charge Ze and an electron of mass m and charge $-e$ interacting by means of the Coulomb potential [3.1]. The 'normal' hydrogen atom, containing a proton and an electron is the prototype of these hydrogenic systems. The hydrogenic ions He^+ ($Z = 2$), Li^{++} ($Z = 3$), Be^{3+} ($Z = 4$), etc. are also examples of such systems. As we have already noted in Chapter 1, and as we can see again from the above formulae, the value of a for these ions is reduced with respect to that of the hydrogen atom by a factor of Z and their ionisation potential is increased by a factor of Z^2 (neglecting small reduced mass effects).

The (neutral) isotopes of atomic hydrogen, deuterium and tritium, also provide examples of hydrogenic systems. Here the proton is replaced by a nucleus having the same charge $+e$, namely a deuteron (containing one proton and one neutron) in the case of deuterium or a triton (containing one proton and two neutrons) in the case of tritium. Since $M_d \simeq 2M_p$ and $M_t \simeq 3M_p$, where M_p is the mass of the proton, M_d the mass of the deuteron and M_t the mass of the triton, we see that the reduced mass μ is slightly different for hydrogen, deuterium and tritium, the relative differences being of the order of 10^{-3}. Thus the quantities I_P and a are nearly identical for the three atoms, the small differences in the value of μ giving rise to *isotopic shifts* of the spectral lines (of the order of 10^{-3}) which we have already discussed in Chapter 1.

Positronium, muonium

In addition to deuterium and tritium, there exist also other 'less conventional' isotopes of hydrogen, in which the role of the nucleus is played by another particle. For example, *positronium* (e^+e^-) is a bound hydrogenic system made of a positron e^+ (the antiparticle of the electron, having the same mass as the electron, but the opposite charge) and an electron e^-. *Muonium* (μ^+e^-) is another non-conventional isotope of hydrogen, in which the proton has been replaced by a positive muon μ^+, a particle which is very similar to the positron e^+, except that it has a mass $M_\mu \simeq 207\, m$ and that it is unstable, with a lifetime of about 2.2×10^{-6} s. Both positronium and muonium may thus be considered as light isotopes of hydrogen. Positronium was first observed in 1951 and muonium in 1960. Table 3.2 gives the values of the reduced mass μ, the 'radius' a and the ionisation potential I_P for positronium and muonium, compared with those of the hydrogen atom.

Positronium and muonium have attracted a great deal of interest because they only contain *leptons* (i.e. particles which are not affected by the strong interactions) and hence are particularly suitable systems to verify the predictions of quantum electrodynamics. We remark that both positronium and muonium are *unstable*. Indeed, muonium has a lifetime of 2.2×10^{-6} s (which is the lifetime of the muon μ^+ itself) while in positronium the electron and the positron may annihilate, their total energy including their rest mass energy being completely converted into electromagnetic radiation (photons).

Muonic atoms

In all the hydrogenic systems we have considered until now the negative particle is an electron. In 1947 J. A. Wheeler suggested that other negative particles could form a bound system with a nucleus. These negative particles can be *leptons* such as the negative muon μ (which is a kind of 'heavy electron' having the same mass and lifetime as the positive muon μ^+, but a negative charge $-e$) or *hadrons* (particles which can have strong interactions). The unusual 'atoms' formed in this way are sometimes called 'exotic atoms'. We shall return shortly to hadronic atoms and examine for the moment the muonic atoms which are formed when a negative muon μ is captured by the Coulomb attraction of a nucleus of charge Ze as the muon is slowing down in bulk matter.

As a first example, let us consider the simplest muonic atom $(\mathrm{p}\mu)$ which contains a proton p and a muon μ. Since the muon has a mass which is about 207 times that of the electron, the reduced mass of the muon with respect to the proton is approximately 186 times the electron mass. As a result, the 'radius' a of the muonic atom $(\mathrm{p}\mu)$ is 186 times smaller than that of the hydrogen atom, the ionisation potential I_{P} of $(\mathrm{p}\mu^-)$ being 186 times larger than the corresponding quantity for atomic hydrogen (see Table 3.2). The frequencies of the spectral lines corresponding to transitions between the energy levels of $(\mathrm{p}\mu^-)$ may thus be obtained from those of the hydrogen atom by multiplying the latter by a factor of 186. For transitions between the lowest energy levels of $(\mathrm{p}\mu^-)$ the spectral lines are therefore lying in the X-ray region.

Let us now assume that the negative muon μ is captured by the Coulomb field of a nucleus $\mathcal{N}$ of charge Ze. Assuming that we are dealing with a heavy nucleus, so that we may neglect the reduced mass effect, we see that equation [3.86] would then yield for the bound system $(\mathcal{N}\mu^-)$ the value $a \simeq a_0/(207\,Z)$, while [3.85] would give an ionisation potential I_{P} larger than that of hydrogen by a factor of $207\,Z^2$. Thus for the case of muonic lead (corresponding to a nucleus

Table 3.2 The reduced mass μ, 'radius' a and ionisation potential I_{P} of some 'unconventional' hydrogenic systems, compared with the corresponding quantities for the hydrogen atom (pe). Atomic units are used. The masses of the particles considered are $M_{\mathrm{p}} = M_{\bar{\mathrm{p}}} \simeq 1836$, $M_{\mu} = M_{\mu^+} \simeq 207$, $M_{\pi^-} \simeq 273$, $M_{\mathrm{K}^-} \simeq 966$, $M_{\Sigma^-} \simeq 2343$, the unit of mass being the electron mass m.

System	*Reduced mass* μ	*'Radius'* a	*Ionisation potential* I_{P}
(pe^-)	$\dfrac{1836}{1837} \simeq 1$	$\simeq a_0 = 1$	$\simeq \dfrac{e^2}{(4\pi\varepsilon_0)2a_0} = 0.5$
$(\mathrm{e}^+\mathrm{e}^-)$	0.5	2	0.25
$(\mu^+\mathrm{e}^-)$	$\dfrac{207}{208} \simeq 1$	$\simeq a_0 = 1$	$\simeq 0.5$
$(\mathrm{p}\mu^-)$	$\simeq 186$	$\simeq 5.4 \times 10^{-3}$	$\simeq 93$
$(\mathrm{p}\pi^-)$	$\simeq 238$	$\simeq 4.2 \times 10^{-3}$	$\simeq 119$
(pK^-)	$\simeq 633$	$\simeq 1.6 \times 10^{-3}$	$\simeq 317$
$(\mathrm{p}\bar{\mathrm{p}})$	$\simeq 918$	$\simeq 1.1 \times 10^{-3}$	$\simeq 459$
$(\mathrm{p}\Sigma^-)$	$\simeq 1029$	$\simeq 9.7 \times 10^{-4}$	$\simeq 515$

with $Z = 82$) we would have $I_P \simeq 19$ MeV (1 MeV $= 10^6$ eV) and $a \simeq 3 \times 10^{-15}$ $m = 3$ Fermi. In fact this value of a is smaller than the radius R of the lead nucleus, which is given by $R \simeq 6.7$ Fermi, so that the expressions [3.85]–[3.86] cannot be used any more! Indeed, they have been derived on the assumption that the two particles of the hydrogenic system interact by means of the Coulomb potential [3.1] for *all values* of the relative distance r, i.e. that both particles are considered to be *point-like*. This assumption is an excellent one for 'usual' (electronic) atoms or ions such as hydrogen, deuterium, tritium, He^+, Li^{2+}, etc., where the finite extension of the nucleus gives rise to very small effects such as the *volume effect* which will be shown in Chapter 5 to yield tiny shifts of the energies associated with low-lying s-states. However, for muonic atoms with large values of Z (such as muonic lead) the volume effect may lead to important shifts of the low-lying levels (in particular of the 1s and 2s states). Nevertheless the main *qualitative* features predicted by [3.85]–[3.86] are correct: the ionisation potential I_P is of the order of several MeV, the spectral lines corresponding to transitions between the lowest energy levels lie at the limit of the X-ray and γ-ray regions, and in the 1s state the muon spends a significant fraction of its time within the nucleus. The fact that the muon acts as a probe of the nucleus and that the energy spectrum of muonic atoms is therefore sensitive to the internal structure of the nucleus constitutes one of the major interests of the study of muonic atoms.

We conclude this brief discussion of muonic atoms by three remarks. Firstly, muonic atoms are unstable, since the negative muon μ^- has a finite lifetime $\tau \simeq 2.2 \times 10^{-6}$ s (which is the same as that of its antiparticle, the positive muon μ^+). Secondly, muonic atoms usually keep an electron cloud, but the influence of the electrons on the hydrogenic system (nucleus + muon μ^-) is almost always negligible, since the muon μ^- remains on the average much closer to the nucleus than the electrons. Thirdly, the muon is often captured into an excited state of the (nucleus + muon) system. It will then 'cascade' down to the ground state, either by emitting radiation in the form of X-rays or by means of radiationless transitions known as *Auger transitions*, in which electrons from the cloud are ejected.

Hadronic atoms

In contrast with the leptons (such as the electron e^-, the positron e^+ and the muons μ^- and μ^+) which participate only in the electromagnetic and weak interactions, the hadrons participate in the *strong* (nuclear-type) interactions in addition to the electromagnetic and weak interactions. There are two kinds of hadrons, the *baryons* (such as the proton p, the neutron n, the antiproton $\bar{p}$, the antineutron $\bar{n}$, the hyperons Σ, Ξ, . . .) which have half-integer spin ($\frac{1}{2}$, $\frac{3}{2}$, . . .) and are therefore fermions, and the *mesons* (such as the π-mesons, the K-mesons, etc.) which have integral spin (0, 1, . . .) and hence are bosons. Among the hadrons, those having a negative charge can form with a nucleus $\mathcal{N}$ a 'hydrogenic-type' system which is referred to as a *hadronic atom*. In particular,

the system $(\mathcal{N}\pi^-)$ is called a *pionic atom*, $(\mathcal{N}K^-)$ is known as a *kaonic atom* while $(\mathcal{N}\bar{p})$ is called an *antiprotonic atom*. Hydrogenic-type systems containing a nucleus and a negative hyperon – for example $(\mathcal{N}\Sigma^-)$ – are known as *hyperonic atoms*. All these hadronic atoms are unstable, but their lifetime is long enough so that some of their spectral lines have actually been observed.

Since hadrons interact strongly with nuclei, it is clear that the theory of hydrogenic systems which we have developed in this chapter – and which only takes into account the Coulomb interaction [3.1] – cannot be directly applied to hadronic atoms. Thus the values of a and I_P listed in Table 3.2 only give a rough estimate of the 'radius' and of the ionisation potentials of the hadronic atoms $(p\pi^-)$, (pK^-), $(p\bar{p})$ and $(p\Sigma^-)$. However, because the strong interactions have a short range, *excited states* of hadronic atoms and in particular those with $l \neq 0$ for which the wave function is very small in the vicinity of the origin can essentially be studied by using the theory of this chapter. The energies of these excited states are thus given by

$$E_n \simeq -\frac{1}{n^2} I_P \qquad [3.87]$$

and their 'radii' by

$$a_n \simeq n^2 a \qquad [3.88]$$

where I_P and a are given respectively by [3.85] and [3.86].

Rydberg atoms

A highly excited atom (or ion) has an electron with a large principal quantum number n. The electron (or the atom) is said to be in a 'high Rydberg state' and the highly excited atom is also referred to more simply as a 'Rydberg atom'.

Several characteristic quantities of the hydrogen atom are compared in Table 3.3 for $n = 1$, arbitrary n and $n = 100$. It is clear from the examination of this table that highly excited hydrogen atoms with $n \sim 100$ exhibit some remarkable properties. For example, *their size is enormous* on the atomic scale. Indeed, with electron orbital radii of the order of 10^{-7} m, such atoms are as big as simple bacteria! Also, their geometrical cross-section being proportional to n^4 is therefore 10^8 larger when $n = 100$ than in the ground state $n = 1$. On the other hand, the electron in a high Rydberg state is *very weakly bound*, its binding energy being smaller than the binding energy of the ground state by a factor n^2. For example the energy required to ionise a hydrogen atom with $n = 100$ is only 1.36×10^{-3} eV. We also remark that the energy separation ΔE between adjacent levels is given for large n by

$$\begin{aligned}\Delta E = E_{n+1} - E_n &= I_P^H\left(\frac{1}{n^2} - \frac{1}{(n+1)^2}\right) \\ &\simeq 2I_P^H/n^3\end{aligned} \qquad [3.89]$$

where $I_P^H \simeq 13.6$ eV is the ionisation potential of the hydrogen atom. Thus for $n = 100$ this energy separation is given by $\Delta E \simeq 2.7 \times 10^{-5}$ eV ($\simeq 0.22$ cm^{-1}

Table 3.3 Comparison of some characteristic quantities of the hydrogen atom for different values of the principal quantum number n

Quantity	$n = 1$	*Arbitrary* n	$n = 100$
Radius a_n of Bohr orbit (in m)	$a_0 \simeq 5.3 \times 10^{-11}$	$\simeq n^2 a_0$	5.3×10^{-7}
Geometric cross-section πa_n^2 (in m^2)	$\pi a_0^2 \simeq 8.8 \times 10^{-21}$	$\simeq n^4 \pi a_0^2$	8.8×10^{-13}
Binding energy $\lvert E_n \rvert$ (in eV)	$I_P^H \simeq 13.6$	I_P^H/n^2	1.36×10^{-3}
Energy separation ΔE between adjacent levels (in eV)		$\simeq 2I_P^H/n^3$ (n large)	2.7×10^{-5}
Root-mean-square velocity of electron v_n (in ms^{-1})	$v_0 \simeq c\alpha \simeq 2.2 \times 10^6$	$\simeq v_0/n$	2.2×10^4
Period T_n (in s)	$T_0 = 1.5 \times 10^{-16}$	$\simeq n^3 T_0$	1.5×10^{-10}

in units of reciprocal centimetres), so that the selective excitation of atoms in highly excited states requires experimental techniques with extremely high resolution. A highly excited hydrogen atom left to itself has a relatively long lifetime, increasing roughly as n^3 for a fixed angular momentum quantum number l. However, even thermal collisions can transfer enough energy to the atom to ionise it, although it is possible that a neutral system passing through the (very large) Rydberg atom will leave it undisturbed.

Many of the studies concerning Rydberg atoms also deal with excited states of atoms other than hydrogen. However, for a large enough n, a Rydberg atom of any kind may be considered as an 'ionic core' plus a single highly excited electron. If this electron has enough angular momentum, so that it does not significantly penetrate the core, it will essentially move in a Coulomb field corresponding to an effective charge $Z_{\text{eff}} = 1$ (in atomic units). Such Rydberg atoms are therefore very similar to highly excited (Rydberg) hydrogen atoms.

Rydberg atoms have attracted much attention in recent years. In addition to their intrinsic interest they are also important in such diverse areas as radioastronomy, plasma physics and laser physics.

PROBLEMS

3.1 Using the explicit expressions of the hydrogenic wave functions given in Table 3.1, calculate the expectation values $\langle r \rangle$, $\langle r^2 \rangle$, $\langle 1/r \rangle$, $\langle p \rangle$ and $\langle p^2 \rangle$ for the following states: (i) 1s, (ii) 2s, (iii) 2p. Verify that the virial theorem [3.77] is satisfied.

3.2 Any region of space in which the kinetic energy T of a particle would become negative is forbidden for classical motion. For a hydrogen atom in the ground state, of total energy $E_{1s} = -\frac{1}{2}$ a.u.

(a) Find the classically forbidden region.

(b) Using the ground state wave function $\psi_{1s}(r)$, calculate the probability of finding the electron in this region.

3.3 Consider a hydrogen atom of which the wave function at $t = 0$ is the following superposition of energy eigenfunctions $\psi_{nlm}(\mathbf{r})$

$$\Psi(\mathbf{r}, t = 0) = \frac{1}{\sqrt{14}}[2\psi_{100}(r) - 3\psi_{200}(r) + \psi_{322}(\mathbf{r})]$$

(a) Is the wave function an eigenfunction of the parity operator?
(b) What is the probability of finding the system in the ground state (100)? In the state (200)? In the state (322)? In another eigenstate?
(c) What is the expectation value of the energy? Of the operator $\mathbf{L}^2$? Of the operator L_z?

3.4 Consider a tritium atom, containing a nucleus, ^{3}H (the triton) and an electron. The triton nucleus, which consists of one proton ($Z = 1$) and two neutrons, is unstable, since by beta emission it decays to ^{3}He, which contains two protons ($Z = 2$) and one neutron. This decay process occurs very rapidly with respect to characteristic atomic times, and will be assumed here to take place instantaneously. As a result, there is a sudden doubling of the Coulomb attraction between the atomic electron and the nucleus when the tritium nucleus ^{3}H decays by beta emission into ^{3}He. Assuming that the tritium atom is in the ground state when the decay takes place, and neglecting recoil effects ($M = \infty$) find the probability that immediately after the decay the He$^+$ ion can be found:
(a) In its ground state 1s?
(b) In any state other than the ground state? (Total probability for excitation or ionisation.)
(c) In the 2s state?
(d) In a state with $l \neq 0$?

3.5 The electron and the proton of an hydrogen atom interact not only through the electrostatic potential [3.1], but also by means of the gravitational interaction. Using perturbation theory (Section 2.8), obtain the relative energy shift $\Delta E/E_{1s}$, where ΔE is the energy change due to the gravitational force and E_{1s} is the ground state energy of hydrogen, as given by [3.29] with $Z = 1$ and $n = 1$.
(Note: The gravitational constant is $G = 6.672 \times 10^{-11}$ N m^2 kg^{-2}.)

3.6 Using the definition [2.21], obtain the momentum space wave functions of the hydrogen atom for the 1s, 2s and 2p states. Compare your results with those of Appendix 5.
(Hints: Use the expansion [2.261] of a plane wave in spherical harmonics, and the known integral

$$\int_0^\infty e^{-ax} j_l(bx) x^{l+1}\, dx = \frac{(2b)^l l!}{(a^2 + b^2)^{l+1}}$$

Note that integrals involving higher powers of x can be obtained by differentiating this result with respect to the parameter a.)

4 Interaction of one-electron atoms with electromagnetic radiation

In this chapter, we shall first discuss the interaction of hydrogenic atoms with electromagnetic radiation and show how spectral lines arise, and at a later stage we shall study the photoelectric effect. In considering the interaction of an atom with radiation, there are three processes to analyse. First, just as a classical oscillating charge will radiate spontaneously, an atom can make a spontaneous transition from an excited state to a state of lower energy, emitting a photon which is the quantum of the electromagnetic field. This process is called spontaneous emission. Second, an atom can absorb a photon from a beam of radiation, making a transition from a state of lower to a state of higher energy. The rate of absorption is proportional to the intensity of the applied field. Finally, atoms can also emit photons under the influence of an applied radiation field. This is called stimulated emission and it is distinguished from spontaneous emission because the transition rate, like that for absorption, is proportional to the intensity of the applied field. Stimulated emission finds an important practical application in the *laser* which produces intense beams of coherent radiation and which will be discussed in Chapter 14.

In a rigorous treatment, we would have to start by studying quantum electrodynamics, in which the electromagnetic field is expressed in terms of its quanta – the photons. Each photon corresponding to a field of frequency ν carries an amount of energy $h\nu$. Even in comparatively weak fields the photon density can be very high (see Problem 4.1) and under these circumstances the number of photons can be treated as a continuous variable and the field can be described classically by the usual Maxwell equations. We shall proceed by using a semi-classical model in which the radiation field is treated classically, but the atomic system is described by quantum mechanics. The approximation will also be made that the influence of the atom on the external field can be neglected. Clearly these assumptions do not hold in the case of spontaneous emission, because only one photon is concerned – and one is not a large number! The proper treatment of spontaneous emission is well understood, but is beyond the scope of this book. However, in this case, we shall be able to find the transition rate indirectly using a statistical argument due to Einstein.

4.1 THE ELECTROMAGNETIC FIELD AND ITS INTERACTION WITH CHARGED PARTICLES

The classical electromagnetic field *in vacuo* is described by electric and magnetic field vectors $\mathcal{E}$ and $\mathcal{B}$, which satisfy Maxwell's equations [1]. We shall express these and other electromagnetic quantities in rationalised MKS units, which form part of the standard SI system. The electric field $\mathcal{E}$ and magnetic field $\mathcal{B}$ can be generated from scalar and vector potentials ϕ and $\mathbf{A}$ by

$$\mathcal{E}(\mathbf{r}, t) = -\nabla\phi(\mathbf{r}, t) - \frac{\partial}{\partial t}\mathbf{A}(\mathbf{r}, t) \tag{4.1}$$

$$\mathcal{B}(\mathbf{r}, t) = \nabla \times \mathbf{A}(\mathbf{r}, t) \tag{4.2}$$

The potentials are not completely defined by [4.1] and [4.2]. In particular, $\mathcal{E}$ and $\mathcal{B}$ are unaltered by the substitutions $\mathbf{A} \to \mathbf{A} + \nabla\chi$, $\phi \to \phi - \partial\chi/\partial t$, where χ is any scalar field. This property of *gauge invariance* allows us to impose a further condition on $\mathbf{A}$, which we shall choose to be

$$\nabla \cdot \mathbf{A} = 0 \tag{4.3}$$

When $\mathbf{A}$ satisfies this condition, we are said to be using the Coulomb gauge. From Maxwell's equations (without sources) we can show that $\mathbf{A}$ satisfies the wave equation (as do ϕ, $\mathcal{E}$ and $\mathcal{B}$)

$$\nabla^2\mathbf{A} - \frac{1}{c^2}\frac{\partial^2\mathbf{A}}{\partial t^2} = 0 \tag{4.4}$$

In what follows we shall set the scalar potential $\phi = 0$ since in empty space the most general solution of Maxwell's equations for a radiation field can always be expressed in terms of potentials such that $\nabla \cdot \mathbf{A} = 0$ and $\phi = 0$.

A monochromatic plane wave solution of equations [4.3]–[4.4] corresponding to the angular frequency ω (i.e. to the frequency $\nu = \omega/2\pi$) is one that represents a real vector potential $\mathbf{A}$ as

$$\begin{aligned}\mathbf{A}(\omega; \mathbf{r}, t) &= 2\mathbf{A}_0(\omega)\cos(\mathbf{k}\cdot\mathbf{r} - \omega t + \delta_\omega) \\ &= \mathbf{A}_0(\omega)[\exp[i(\mathbf{k}\cdot\mathbf{r} - \omega t + \delta_\omega)] + \text{c.c.}]\end{aligned} \tag{4.5}$$

Here $\mathbf{A}_0$ is a vector which, as we shall see shortly, describes both the intensity and the polarisation of the radiation, $\mathbf{k}$ is the propagation vector, δ_ω is a real phase and c.c. denotes the complex conjugate. We note that [4.3] is satisfied if

$$\mathbf{k}\cdot\mathbf{A}_0(\omega) = 0 \tag{4.6}$$

so that $\mathbf{A}_0(\omega)$ is perpendicular to $\mathbf{k}$ and the wave is *transverse*. Equation [4.4] is satisfied provided that $\omega = kc$, where k is the magnitude of the propagation vector $\mathbf{k}$.

[1] Useful texts on electromagnetism are those by Duffin (1968) and Jackson (1975).

The electric and magnetic fields associated with the vector potential [4.5] are given respectively from [4.1] and [4.2] by

$$\begin{aligned} \mathscr{E} &= -2\omega A_0(\omega)\hat{\boldsymbol{\varepsilon}} \sin(\mathbf{k}\cdot\mathbf{r} - \omega t + \delta_\omega) \\ \mathscr{B} &= -2A_0(\omega)(\mathbf{k}\times\hat{\boldsymbol{\varepsilon}}) \sin(\mathbf{k}\cdot\mathbf{r} - \omega t + \delta_\omega) \end{aligned} \qquad [4.7]$$

where we have written $\mathbf{A}_0(\omega) = A_0(\omega)\hat{\boldsymbol{\varepsilon}}$. The direction of the electric field $\mathscr{E}$ is along the real unit vector $\hat{\boldsymbol{\varepsilon}}$, which specifies the *polarisation* of the radiation, and is called the polarisation vector. From [4.6] we note that $\hat{\boldsymbol{\varepsilon}}$ must lie in a plane perpendicular to the propagation vector $\mathbf{k}$ and can therefore be specified by giving its components along two linearly independent vectors lying in this plane. We also see from [4.7] that both $\mathscr{E}$ and $\mathscr{B}$ are perpendicular to the direction of propagation $\mathbf{k}$, and to each other.

The expressions [4.7] describe a *linearly polarised* plane wave, namely a plane wave with its electric field vector $\mathscr{E}$ always in the direction of the polarisation vector $\hat{\boldsymbol{\varepsilon}}$. A general state of polarisation for a plane wave propagating in the direction $\hat{\mathbf{k}}$ can be described by combining two independent linearly polarised plane waves with polarisation vectors $\hat{\boldsymbol{\varepsilon}}_\lambda(\lambda = 1, 2)$ perpendicular to $\hat{\mathbf{k}}$, where the phases in the two component waves are in general different.

In a quantum description of the electromagnetic field the energy in each mode of angular frequency ω, in some region of volume V [2], is carried by a number $N(\omega)$ of photons, each of energy $\hbar\omega$. The total energy in the mode is therefore given by $N(\omega)\hbar\omega$ and the energy density by $N(\omega)\hbar\omega/V$. In order to relate this quantum description with the classical approach we are using here, we first construct the energy density of the field, which is given by

$$\tfrac{1}{2}(\varepsilon_0\mathscr{E}^2 + \mathscr{B}^2/\mu_0) = 4\varepsilon_0\omega^2 A_0^2(\omega)\sin^2(\mathbf{k}\cdot\mathbf{r} - \omega t + \delta_\omega) \qquad [4.8]$$

where ε_0 and μ_0 are respectively the permittivity and permeability of free space [3]. The average energy density over a period $(2\pi/\omega)$ is

$$\rho(\omega) = 2\varepsilon_0\omega^2 A_0^2(\omega) \qquad [4.9]$$

Equating this result with $N(\omega)\,\hbar\omega/V$, we have

$$A_0^2(\omega) = \frac{\hbar}{2\varepsilon_0\omega V}N(\omega) \qquad [4.10]$$

Similarly, the magnitude of the Poynting vector $(\mathscr{E}\times\mathscr{B})/\mu_0$ is the rate of energy flow through a unit cross-sectional area normal to the direction of propagation $\mathbf{k}$. Averaged over a period, this quantity defines the intensity of the

[2] Provided V is taken to be much larger than atomic dimensions, the physical results are independent of this quantity.

[3] Numerical values of ε_0 and μ_0 are given in Appendix 11.

radiation, which is given by

$$
\begin{aligned}
I(\omega) &= 2\varepsilon_0\omega^2 c A_0^2(\omega) \\
&= \left[\frac{N(\omega)\hbar\omega}{V}\right] c \\
&= \rho(\omega)c
\end{aligned}
\qquad [4.11]
$$

A general pulse of radiation can be described by taking $\phi = 0$ and representing $\mathbf{A}(\mathbf{r}, t)$ as a superposition of the plane waves $\mathbf{A}(\omega; \mathbf{r}, t)$. Taking each plane wave component to have the same direction of propagation $\hat{\mathbf{k}}$ and adopting a given direction of linear polarisation $\hat{\boldsymbol{\varepsilon}}$, so that

$$\mathbf{A}_0(\omega) = A_0(\omega)\hat{\boldsymbol{\varepsilon}} \qquad [4.12]$$

we write

$$\mathbf{A}(\mathbf{r}, t) = \int_{\Delta\omega} A_0(\omega)\hat{\boldsymbol{\varepsilon}}[\exp[i(\mathbf{k}\cdot\mathbf{r} - \omega t + \delta_\omega)] + \text{c.c.}]\,\mathrm{d}\omega \qquad [4.13]$$

We shall be concerned with the case in which the radiation is nearly monochromatic, so that the amplitude $A_0(\omega)$ is peaked about some angular frequency ω_0, differing from zero in a region of width $\Delta\omega$.

In a naturally occurring pulse the radiation arises from many atoms emitting photons independently, which implies that the phases δ_ω are distributed at random, as a function of ω; in other words, the radiation is *incoherent* [4]. It follows that the average energy density in a pulse of the form [4.13] is

$$\bar{\rho} = \int_{\Delta\omega} 2\varepsilon_0\omega^2 A_0^2(\omega)\,\mathrm{d}\omega = \int_{\Delta\omega} \rho(\omega)\,\mathrm{d}\omega \qquad [4.14]$$

As seen by comparing with [4.9], the contributions from each mode are summed, with no interference terms. Similarly the average intensity is

$$\bar{I} = \int_{\Delta\omega} I(\omega)\,\mathrm{d}\omega \qquad [4.15]$$

where the intensity per unit angular frequency range $I(\omega)$ is given by [4.11].

Charged particles in an electromagnetic field

The Hamiltonian of a spinless particle of charge q and mass m in an electromagnetic field is

$$H = \frac{1}{2m}(\mathbf{p} - q\mathbf{A})^2 + q\phi \qquad [4.16]$$

[4] This remark does not apply to radiation from lasers, which exhibits a high degree of coherence.

where $\mathbf{p}$ is the generalised momentum of the particle. The steps leading to [4.16] are given in Appendix 6. Ignoring for the present small spin-dependent terms, the Hamiltonian of an electron of mass m in an electromagnetic field is given by [4.16], with $q = -e$.

In order to describe a hydrogenic atom in an electromagnetic field we must also take into account the presence of the nucleus, of charge Ze and mass M. Since M is very large compared to the electron mass m (we are considering here 'ordinary' one-electron systems such as H, He^+, . . .) the interaction between the radiation field and the nucleus can be ignored to a high degree of accuracy. In the same spirit we shall also neglect reduced mass effects and take the nucleus to be the origin of the coordinates. However, we must include in the Hamiltonian the electrostatic Coulomb potential $-Ze^2/(4\pi\varepsilon_0)r$ between the electron and the nucleus. It is convenient to regard this electrostatic interaction as an additional potential energy term, while the radiation field which perturbs the atom is described in terms of a vector potential $\mathbf{A}$ alone, as discussed above. The time-dependent Schrödinger equation for a hydrogenic atom in an electromagnetic field then reads

$$i\hbar \frac{\partial}{\partial t} \Psi(\mathbf{r}, t) = \left[\frac{1}{2m}(-i\hbar\nabla + e\mathbf{A})^2 - \frac{Ze^2}{(4\pi\varepsilon_0)r}\right]\Psi(\mathbf{r}, t) \qquad [4.17]$$

where we have written $\mathbf{p} = -i\hbar\nabla$. Because of the gauge condition [4.3], we have

$$\begin{aligned}\nabla \cdot (\mathbf{A}\Psi) &= \mathbf{A} \cdot (\nabla\Psi) + (\nabla \cdot \mathbf{A})\Psi \\ &= \mathbf{A} \cdot (\nabla\Psi) \qquad [4.18]\end{aligned}$$

so that ∇ and $\mathbf{A}$ commute. Making use of this fact, we may rewrite the Schrödinger equation [4.17] as

$$i\hbar \frac{\partial}{\partial t} \Psi(\mathbf{r}, t) = \left[-\frac{\hbar^2}{2m}\nabla^2 - \frac{Ze^2}{(4\pi\varepsilon_0)r} - \frac{i\hbar e}{m}\mathbf{A} \cdot \nabla + \frac{e^2}{2m}\mathbf{A}^2\right]\Psi(\mathbf{r}, t) \qquad [4.19]$$

We shall treat the weak field case in which the term in $\mathbf{A}^2$ is small compared with the term linear in $\mathbf{A}$ [5]. Accordingly we shall drop the term in $\mathbf{A}^2$ and treat the linear term as a small perturbation. In terms of photons, this means that we shall only treat the emission or absorption of one photon at a time. The simultaneous emission or absorption of two photons is generally negligible. An exception to this arises in the very strong coherent fields generated by lasers.

[5] Although we are treating the case for which $\mathbf{A}^2$ is small compared with $\mathbf{A}$, the photon density is assumed to be high enough for the radiation field to be treated classically. Both conditions are well satisfied in the emission and absorption processes we shall describe.

4.2 TRANSITION RATES

Having neglected the term in $\mathbf{A}^2$, we see that the time-dependent Schrödinger equation [4.19] may be written as

$$i\hbar \frac{\partial \Psi}{\partial t} = [H_0 + H'(t)]\Psi \qquad [4.20]$$

where

$$H_0 = -\frac{\hbar^2}{2m}\nabla^2 - \frac{Ze^2}{(4\pi\varepsilon_0)r} \qquad [4.21]$$

is the time-independent hydrogenic Hamiltonian describing the one-electron atom in the absence of external fields and

$$H'(t) = -\frac{i\hbar e}{m}\mathbf{A}\cdot\boldsymbol{\nabla} \qquad [4.22]$$

is a perturbation which depends explicitly on the time variable through the vector potential $\mathbf{A}$.

We shall study this problem by using the time-dependent perturbation theory given in Chapter 2. The unperturbed eigenfunctions ψ_k, solutions of

$$H_0\psi_k = E_k\psi_k \qquad [4.23]$$

are normalised hydrogenic wave functions. Because the set of functions ψ_k (including both the discrete set studied in Chapter 3 and the continuous set corresponding to unbound states) is complete, the general solution Ψ of the time-dependent Schrödinger equation [4.20], which we assume to be normalised, can be expanded as

$$\Psi = \sum_k c_k(t)\psi_k(\mathbf{r})\mathrm{e}^{-iE_kt/\hbar} \qquad [4.24]$$

where the sum is over both the discrete set and the continuous set of hydrogenic eigenfunctions ψ_k. The coefficients $c_k(t)$ satisfy the coupled equations [2.336] with $\lambda = 1$,

$$\dot{c}_b(t) = (i\hbar)^{-1}\sum_k H'_{bk}(t)c_k(t)\mathrm{e}^{i\omega_{bk}t} \qquad [4.25]$$

where

$$\begin{aligned} H'_{bk}(t) &= \langle\psi_b|H'(t)|\psi_k\rangle \\ &= \int \psi_b^*(\mathbf{r})H'\psi_k(\mathbf{r})\,\mathrm{d}\mathbf{r} \end{aligned} \qquad [4.26]$$

and

$$\omega_{bk} = (E_b - E_k)/\hbar \qquad [4.27]$$

Let us suppose that the system is initially in a well-defined stationary bound state of energy E_a described by the wave function ψ_a and that the pulse of radiation is switched on at the time $t = 0$. Thus the initial conditions are given by

$$c_k(t \leqslant 0) = \delta_{ka} \tag{4.28}$$

and, to first order in the perturbation H', we have (see [2.343])

$$\begin{aligned} c_b^{(1)}(t) &= (i\hbar)^{-1} \int_0^t H'_{ba}(t') \mathrm{e}^{i\omega_{ba}t'} \, \mathrm{d}t' \\ &= -\frac{e}{m} \int_0^t \langle \psi_b | \mathbf{A} \cdot \boldsymbol{\nabla} | \psi_a \rangle \, \mathrm{e}^{i\omega_{ba}t'} \, \mathrm{d}t' \end{aligned} \tag{4.29}$$

where $\omega_{ba} = (E_b - E_a)/\hbar$ and

$$\langle \psi_b | \mathbf{A} \cdot \boldsymbol{\nabla} | \psi_a \rangle = \int \psi_b^\star(\mathbf{r}) \mathbf{A} \cdot \boldsymbol{\nabla} \psi_a(\mathbf{r}) \, \mathrm{d}\mathbf{r} \tag{4.30}$$

To proceed further, we use the vector potential $\mathbf{A}(\mathbf{r}, t)$ given by [4.13] to obtain

$$\begin{aligned} c_b^{(1)}(t) = -\frac{e}{m} \int_{\Delta\omega} \mathrm{d}\omega A_0(\omega) \Bigg[& \mathrm{e}^{i\delta_\omega} \langle \psi_b | \mathrm{e}^{i\mathbf{k}\cdot\mathbf{r}} \, \hat{\boldsymbol{\varepsilon}} \cdot \boldsymbol{\nabla} | \, \psi_a \rangle \int_0^t \mathrm{d}t' \mathrm{e}^{i(\omega_{ba} - \omega)t'} \\ & + \mathrm{e}^{-i\delta_\omega} \langle \psi_b | \mathrm{e}^{-i\mathbf{k}\cdot\mathbf{r}} \, \hat{\boldsymbol{\varepsilon}} \cdot \boldsymbol{\nabla} | \psi_a \rangle \int_0^t \mathrm{d}t' \mathrm{e}^{i(\omega_{ba} + \omega)t'} \Bigg] \end{aligned} \tag{4.31}$$

In general, the duration of the pulse will be much larger than the periodic time $(2\pi/\omega_{ba})$ which is for example $\sim 2 \times 10^{-15}$ s for the yellow sodium D line at 5890 Å. It follows that the first integral over t' will be negligible unless $\omega_{ba} \simeq \omega$, i.e. unless $E_b \simeq E_a + \hbar\omega$. Thus we see that in this case the final state of the atom has greater energy than the initial state and one photon of energy $\hbar\omega$ has been *absorbed* from the radiation. On the other hand, the second integral over t' in [4.31] will be negligible unless $\omega_{ba} \simeq -\omega$, that is unless $E_b \simeq E_a - \hbar\omega$. In this case the initial state of the atom has greater energy than the final state and one photon of energy $\hbar\omega$ is *emitted*. Since only one of these conditions can be satisfied for a pair of states a and b, we can deal with the two terms separately.

We shall assume for the moment that both the initial and final atomic states are *discrete*. The photoelectric effect, which corresponds to transitions from a discrete initial state to final states lying in the continuum, will be studied in Section 4.8.

Absorption

We start with the first term of [4.31], describing absorption. Using the fact that the radiation is incoherent – so that no interference terms occur – we find that

the probability for the system to be in the state b at time t is

$$|c_b^{(1)}(t)|^2 = 2\int_{\Delta\omega} \mathrm{d}\omega \left[\frac{eA_0(\omega)}{m}\right]^2 |M_{ba}(\omega)|^2 F(t, \omega - \omega_{ba}) \qquad [4.32]$$

where we have defined the matrix element M_{ba} as

$$\begin{aligned} M_{ba} &= \langle \psi_b | \mathrm{e}^{i\mathbf{k}\cdot\mathbf{r}} \hat{\boldsymbol{\varepsilon}} \cdot \boldsymbol{\nabla} | \psi_a \rangle \\ &= \int \psi_b^\star(\mathbf{r}) \mathrm{e}^{i\mathbf{k}\cdot\mathbf{r}} \hat{\boldsymbol{\varepsilon}} \cdot \boldsymbol{\nabla}\psi_a(\mathbf{r})\, \mathrm{d}\mathbf{r} \end{aligned} \qquad [4.33]$$

and we recall that $\omega = kc$. Upon setting $\bar{\omega} = \omega - \omega_{ba}$, the function $F(t, \bar{\omega})$ which appears in [4.32] is seen to be the same as the function $F(t, \omega)$ introduced in Chapter 2. That is (see [2.347])

$$F(t, \bar{\omega}) = \frac{1 - \cos \bar{\omega} t}{\bar{\omega}^2}, \qquad \bar{\omega} = \omega - \omega_{ba} \qquad [4.34]$$

The properties of $F(t, \omega)$ discussed in Section 2.8 may therefore be used directly here, provided that we make the substitution $\omega \to \bar{\omega}$. In particular, since for large t the function $F(t, \bar{\omega})$ has a sharp maximum at $\bar{\omega} = 0$ (see Fig. 2.9), i.e. at $\omega = \omega_{ba}$, we can set $\omega = \omega_{ba}$ in the slowly varying quantities $A_0^2(\omega)$ and $|M_{ba}(\omega)|^2$, take these factors outside the integral in [4.32] and extend the limits of integration on ω to $\pm\infty$. Hence we have

$$|c_b^{(1)}(t)|^2 = 2\left[\frac{eA_0(\omega_{ba})}{m}\right]^2 |M_{ba}(\omega_{ba})|^2 \int_{-\infty}^{+\infty} F(t, \bar{\omega})\, \mathrm{d}\omega \qquad [4.35]$$

and using the result [2.348], we obtain

$$|c_b^{(1)}(t)|^2 = 2\pi\left[\frac{eA_0(\omega_{ba})}{m}\right]^2 |M_{ba}(\omega_{ba})|^2 t \qquad [4.36]$$

Thus the probability $|c_b^{(1)}(t)|^2$ increases linearly with time and a *transition rate for absorption* W_{ba} can be defined as

$$W_{ba} = \frac{\mathrm{d}}{\mathrm{d}t}|c_b^{(1)}(t)|^2 = 2\pi\left[\frac{eA_0(\omega_{ba})}{m}\right]^2 |M_{ba}(\omega_{ba})|^2 \qquad [4.37]$$

In terms of the intensity per unit angular frequency range, $I(\omega)$, which is given by [4.11], we have

$$W_{ba} = \frac{4\pi^2}{m^2 c}\left(\frac{e^2}{4\pi\varepsilon_0}\right)\frac{I(\omega_{ba})}{\omega_{ba}^2} |M_{ba}(\omega_{ba})|^2 \qquad [4.38]$$

The rate of absorption of energy from the beam, per atom, is $(\hbar\omega_{ba})W_{ba}$. It is convenient to define an *absorption cross-section* σ_{ba} which is the rate of absorption of energy (per atom) divided by $I(\omega_{ba})$. That is,

$$\sigma_{ba} = \frac{4\pi^2 \alpha \hbar^2}{m^2 \omega_{ba}} |M_{ba}(\omega_{ba})|^2 \qquad [4.39]$$

where $\alpha = (e^2/4\pi\varepsilon_0)/\hbar c \sim 1/137$ is the fine structure constant. Since the incident flux of photons of angular frequency ω_{ba} is obtained by dividing the intensity $I(\omega_{ba})$ by $\hbar\omega_{ba}$, we see that the cross-section σ_{ba} may also be defined as the transition probability per unit time and per unit atom, W_{ba}, divided by the incident photon flux. The cross-section σ_{ba} has the dimensions of an area and can be regarded as the area of a disc of absorbing material that, placed at right angles to the beam, would absorb the same number of photons per second, each of energy $\hbar\omega_{ba}$, as the atom under consideration.

Stimulated emission

To calculate the transition rate for stimulated emission, we return to [4.31] and in particular to the second term in the expression for $c_b^{(1)}(t)$, which corresponds to a downward transition ($E_b \simeq E_a - \hbar\omega$) in which a photon of energy $\hbar\omega$ is emitted. It is convenient to interchange the labels of the states a and b so that the state b is again the one with higher energy. The transition $b \to a$ corresponding to stimulated emission may then be viewed as the reverse transition of the absorption process $a \to b$ which we have just studied. Carrying out the same manipulations as we did for absorption, we find that the *transition rate* for stimulated emission, $\bar{W}_{ab}$ is given by

$$\bar{W}_{ab} = \frac{4\pi^2}{m^2 c}\left(\frac{e^2}{4\pi\varepsilon_0}\right)\frac{I(\omega_{ba})}{\omega_{ba}^2}|\bar{M}_{ab}(\omega_{ba})|^2 \qquad [4.40]$$

where

$$\begin{aligned}\bar{M}_{ab} &= \langle\psi_a|e^{-i\mathbf{k}\cdot\mathbf{r}}\,\hat{\boldsymbol{\varepsilon}}\cdot\boldsymbol{\nabla}|\psi_b\rangle \\ &= \int \psi_a^{\star}(\mathbf{r})e^{-i\mathbf{k}\cdot\mathbf{r}}\,\hat{\boldsymbol{\varepsilon}}\cdot\boldsymbol{\nabla}\psi_b(\mathbf{r})\,d\mathbf{r}\end{aligned} \qquad [4.41]$$

On integration by parts, and using the fact that $\hat{\boldsymbol{\varepsilon}}\cdot\mathbf{k} = 0$, one has

$$\bar{M}_{ab} = -M_{ba}^{\star} \qquad [4.42]$$

and comparing [4.38] and [4.40], we find that

$$\bar{W}_{ab} = W_{ba} \qquad [4.43]$$

Thus we see that under the same radiation field the number of transitions per second exciting the atom from the state a to the state b is the same as the number de-exciting the atom from the state b to the state a. This is consistent with the *principle of detailed balancing*, which says that in an enclosure containing atoms and radiation in equilibrium, the transition probability from a to b is the same as that from b to a, where a and b are any pair of states.

A *stimulated emission cross-section* $\bar{\sigma}_{ab}$ can be defined in analogy with the absorption cross-section [4.39] by dividing the rate at which energy is radiated

by the atom, $(\hbar\omega_{ba})\bar{W}_{ab}$, by the intensity $I(\omega_{ba})$. From [4.43] we have

$$\bar{\sigma}_{ab} = \sigma_{ba} \tag{4.44}$$

Despite the fact that the transition rates W_{ba} and $\bar{W}_{ab}$ are equal, stimulated emission is usually much less intense than absorption. Indeed, under equilibrium conditions the initial population of the upper level b is smaller than that of the lower level a because of the Boltzmann factor $\exp(-\hbar\omega_{ba}/kT)$. However, if a *population inversion* is achieved between the two levels a and b, then stimulated emission becomes the dominant process. This is the case in the MASER (an acronym for Microwave Amplification by Stimulated Emission of Radiation) and the LASER (Light Amplification by Stimulated Emission of Radiation) where stimulated emission enables atomic or molecular systems to amplify incident radiation. Masers and lasers will be discussed in Chapter 14.

Spontaneous emission

In quantum electrodynamics (QED), the part of the vector potential describing the *absorption* of a single photon from an N photon state has the form [6]

$$\mathbf{A}_1 = \hat{\boldsymbol{\varepsilon}}\left[\frac{N(\omega)\hbar}{2V\varepsilon_0\omega}\right]^{1/2} \mathrm{e}^{i(\mathbf{k}\cdot\mathbf{r} - \omega t + \delta_\omega)} \tag{4.45}$$

and it can be shown that the QED transition rate for absorption is given in first-order perturbation theory by

$$W_{ba} = \frac{4\pi^2}{m^2}\left(\frac{e^2}{4\pi\varepsilon_0}\right)\frac{N(\omega_{ba})\hbar}{V\omega_{ba}}|M_{ba}|^2\,\delta(\omega - \omega_{ba}) \tag{4.46}$$

Using [4.11] and integrating over a range of angular frequencies about ω_{ba}, this result is seen to be identical with [4.38].

The corresponding part of the vector potential describing the *creation* of a photon, adding a single photon to a N photon state, is

$$\mathbf{A}_2 = \hat{\boldsymbol{\varepsilon}}\left[\frac{(N(\omega) + 1)\hbar}{2V\varepsilon_0\omega}\right]^{1/2} \mathrm{e}^{-i(\mathbf{k}\cdot\mathbf{r} - \omega t + \delta_\omega)} \tag{4.47}$$

and the transition rate for emission is given by

$$\bar{W}_{ab} = \frac{4\pi^2}{m^2}\left(\frac{e^2}{4\pi\varepsilon_0}\right)\frac{[N(\omega_{ba}) + 1]\hbar}{V\omega_{ba}}|M_{ba}|^2\,\delta(\omega - \omega_{ba}) \tag{4.48}$$

After integrating over ω, this expression is seen to be identical to the semi-classical result [4.40], *provided* $N(\omega_{ba}) + 1$ *is replaced by* $N(\omega_{ba})$. The semi-classical approximation amounts to the neglect of 1 compared with $N(\omega_{ba})$,

[6] A detailed discussion can be found in Sakurai (1967).

and this is the same as neglecting the possibility of spontaneous emission. In the absence of external field one has $N = 0$ and the *transition rate* for the spontaneous emission of a photon, W^{s}_{ab}, is given from [4.48] by

$$W^{s}_{ab} = \frac{4\pi^2}{m^2}\left(\frac{e^2}{4\pi\varepsilon_0}\right)\frac{\hbar}{V\omega_{ba}}|M_{ba}|^2\,\delta(\omega - \omega_{ba}) \qquad [4.49]$$

What can be observed is the emission of a photon in a particular direction (θ, ϕ) within an element of solid angle $\mathrm{d}\Omega$. In order to obtain the physical transition rate we must therefore sum [4.49] over the number of allowed photon states in this interval. To do this we need to calculate the density $\rho_a(\omega)$ of the final photon states, in accordance with the Golden Rule [2.359].

Density of states

Let the volume V be a cube of side L. (In fact the shape does not matter provided V is large.) We can impose periodic boundary conditions [7] on the function $\exp(-i\mathbf{k}\cdot\mathbf{r})$ which is contained in the expression [4.47] representing the wave function of the emitted photon. That is,

$$k_x = \frac{2\pi}{L}n_x, \qquad k_y = \frac{2\pi}{L}n_y, \qquad k_z = \frac{2\pi}{L}n_z \qquad [4.50]$$

where n_x, n_y, n_z are positive or negative integers, or zero. Since L is very large, we can treat n_x, n_y and n_z as continuous variables, and the number of states in the range $\mathrm{d}\mathbf{k} = \mathrm{d}k_x\,\mathrm{d}k_y\,\mathrm{d}k_z$ is

$$\begin{aligned}\mathrm{d}n_x\,\mathrm{d}n_y\,\mathrm{d}n_z &= \left(\frac{L}{2\pi}\right)^3 \mathrm{d}k_x\,\mathrm{d}k_y\,\mathrm{d}k_z \\ &= \left(\frac{L}{2\pi}\right)^3 k^2\,\mathrm{d}k\,\mathrm{d}\Omega \end{aligned} \qquad [4.51]$$

Expressed in terms of $V = L^3$ and $\omega = ck$, the number of states in the angular frequency interval $\mathrm{d}\omega$ with directions of propagation within $\mathrm{d}\Omega$ is

$$\rho_a(\omega)\,\mathrm{d}\omega\,\mathrm{d}\Omega = \frac{V}{(2\pi)^3}\frac{\omega^2}{c^3}\,\mathrm{d}\omega\,\mathrm{d}\Omega \qquad [4.52]$$

Using [4.49] and integrating over the angular frequency ω, the transition rate for the emission of a photon into the solid angle $\mathrm{d}\Omega$ is then given by

$$W^{s}_{ab}(\Omega)\,\mathrm{d}\Omega = \frac{\hbar}{2\pi m^2 c^3}\left(\frac{e^2}{4\pi\varepsilon_0}\right)\omega_{ba}|M_{ba}(\omega_{ba})|^2\,\mathrm{d}\Omega \qquad [4.53]$$

[7] The imposition of periodic boundary conditions amounts to assuming that all space can be divided into identical large cubes of volume L^3, each containing an identical physical system. The vector potential $\mathbf{A}$ must then be periodic with period L along each of the three Cartesian axes.

The total transition rate is found by summing over each of the two independent polarisations of the photon, corresponding to polarisation vectors $\hat{\boldsymbol{\varepsilon}}_\lambda(\lambda = 1, 2)$ and integrating over all angles of emission. That is

$$W^{\mathrm{s}}_{ab} = \frac{\hbar}{2\pi m^2 c^3}\left(\frac{e^2}{4\pi\varepsilon_0}\right)\int \mathrm{d}\Omega \sum_{\lambda=1}^{2} \omega_{ba}|M^{\lambda}_{ba}(\omega_{ba})|^2 \qquad [4.54]$$

where M^{λ}_{ba} is given by [4.33], with $\hat{\boldsymbol{\varepsilon}}$ replaced by $\hat{\boldsymbol{\varepsilon}}_\lambda$.

4.3 THE DIPOLE APPROXIMATION

In many cases of practical interest the matrix element M_{ba} defined in [4.33] can be simplified by expanding the exponential $\exp(i\mathbf{k}\cdot\mathbf{r})$ as

$$\mathrm{e}^{i\mathbf{k}\cdot\mathbf{r}} = 1 + (i\mathbf{k}\cdot\mathbf{r}) + \frac{1}{2!}(i\mathbf{k}\cdot\mathbf{r})^2 + \cdots \qquad [4.55]$$

Consider for example the case of optical transitions. The atomic wave functions extend over distances of the order of the first Bohr radius of the atom, i.e. about 1 Å (= 10^{-8}cm). On the other hand, the wavelengths associated with optical transitions are of the order of several thousand Ångströms, so that the corresponding wave number $k = 2\pi/\lambda$ is of the order of 10^5 cm^{-1}. Thus the quantity (kr) is small for $r < 1$ Å and we can replace $\exp(i\mathbf{k}\cdot\mathbf{r})$ by unity in [4.33], which amounts to *neglecting retardation* across the atom. This is known as the *electric dipole approximation* [8]. In this approximation, [4.33] becomes

$$\begin{aligned} M_{ba} &= \hat{\boldsymbol{\varepsilon}}\cdot\langle\psi_b|\boldsymbol{\nabla}|\psi_a\rangle \\ &= \hat{\boldsymbol{\varepsilon}}\cdot\frac{i}{\hbar}\langle\psi_b|\mathbf{p}|\psi_a\rangle \\ &= \hat{\boldsymbol{\varepsilon}}\cdot\frac{im}{\hbar}\langle\psi_b|\dot{\mathbf{r}}|\psi_a\rangle \end{aligned} \qquad [4.56]$$

since $\mathbf{p} = m\dot{\mathbf{r}} = -i\hbar\boldsymbol{\nabla}$. Now, applying the Heisenberg equation of motion [2.113] to the dynamical variable $\mathbf{r}$, we have

$$\dot{\mathbf{r}} = (i\hbar)^{-1}[\mathbf{r}, H_0] \qquad [4.57]$$

where we have replaced H by H_0 since we are working in perturbation theory. Therefore

$$\begin{aligned} \langle\psi_b|\dot{\mathbf{r}}|\psi_a\rangle &= (i\hbar)^{-1}\langle\psi_b|\mathbf{r}H_0 - H_0\mathbf{r}|\psi_a\rangle \\ &= (i\hbar)^{-1}(E_a - E_b)\langle\psi_b|\mathbf{r}|\psi_a\rangle \end{aligned} \qquad [4.58]$$

or, in a more compact notation,

$$\mathbf{p}_{ba} = im\omega_{ba}\mathbf{r}_{ba} \qquad [4.59]$$

[8] The dipole approximation becomes less accurate as the frequency of the radiation increases, and is inadequate for X-ray transitions.

where

$$\mathbf{p}_{ba} = \langle\psi_b|\mathbf{p}|\psi_a\rangle = m\langle\psi_b|\dot{\mathbf{r}}|\psi_a\rangle \tag{4.60}$$

and

$$\mathbf{r}_{ba} = \langle\psi_b|\mathbf{r}|\psi_a\rangle \tag{4.61}$$

This allows us to express M_{ba} in the form

$$M_{ba} = -\frac{m\omega_{ba}}{\hbar}\,\hat{\boldsymbol{\varepsilon}}\cdot\mathbf{r}_{ba} \tag{4.62}$$

The transition rate for absorption in the electric dipole approximation may now be obtained by substituting [4.62] into [4.38]. That is,

$$W_{ba} = \frac{4\pi^2}{c\hbar^2}\left(\frac{e^2}{4\pi\varepsilon_0}\right)I(\omega_{ba})|\hat{\boldsymbol{\varepsilon}}\cdot\mathbf{r}_{ba}|^2 \tag{4.63}$$

It is convenient at this point to introduce the *electric dipole moment*

$$\mathbf{D} = -e\mathbf{r} \tag{4.64}$$

and its matrix element

$$\mathbf{D}_{ba} = -e\mathbf{r}_{ba} \tag{4.65}$$

in terms of which [4.63] reads

$$W_{ba} = \frac{4\pi^2}{c\hbar^2}\left(\frac{1}{4\pi\varepsilon_0}\right)I(\omega_{ba})|\hat{\boldsymbol{\varepsilon}}\cdot\mathbf{D}_{ba}|^2 \tag{4.66}$$

We note that the quantity $\hat{\boldsymbol{\varepsilon}}\cdot\mathbf{D}_{ba}$ is the component of the electric dipole moment in the direction $\hat{\boldsymbol{\varepsilon}}$, between the states b and a. If $\mathbf{D}_{ba}$ (or $\mathbf{r}_{ba}$) is non-vanishing, the transition is said to be *allowed*; if $\mathbf{D}_{ba}$ vanishes the transition is *forbidden*. When the transition is forbidden, higher terms in the series [4.55], which correspond to *magnetic dipole*, *electric quadrupole* transitions, and so on, may be non-vanishing, but the transition rate will be much smaller than for allowed transitions. If M_{ba} in its unapproximated form [4.33] vanishes, the transition is said to be *strictly forbidden*, but it may still occur through the simultaneous emission (or absorption) of two photons or by processes of even higher order in perturbation theory.

Let us now return to [4.63]. If we define θ as the angle between the vectors $\hat{\boldsymbol{\varepsilon}}$ and $\mathbf{r}_{ba}$, we may write

$$W_{ba} = \frac{4\pi^2}{c\hbar^2}\left(\frac{e^2}{4\pi\varepsilon_0}\right)I(\omega_{ba})|\mathbf{r}_{ba}|^2\cos^2\theta \tag{4.67}$$

where

$$|\mathbf{r}_{ba}|^2 = |x_{ba}|^2 + |y_{ba}|^2 + |z_{ba}|^2 \tag{4.68}$$

For unpolarised isotropic radiation, the orientation of $\hat{\boldsymbol{\varepsilon}}$ will be at random, and $\cos^2\theta$ can be replaced by its average of 1/3 (see Problem 4.4), giving

$$\begin{aligned} W_{ba} &= \frac{4\pi^2}{3c\hbar^2}\left(\frac{e^2}{4\pi\varepsilon_0}\right) I(\omega_{ba})|\mathbf{r}_{ba}|^2 \\ &= \frac{4\pi^2}{3c\hbar^2}\left(\frac{1}{4\pi\varepsilon_0}\right) I(\omega_{ba})|\mathbf{D}_{ba}|^2 \end{aligned} \qquad [4.69]$$

It is worth noting that because of [4.43] the expression [4.69] also represents the transition rate for *stimulated emission in the dipole approximation* corresponding to the transition $b \to a$, i.e. the dipole approximation to $\bar{W}_{ab}$. On the other hand, the transition rate for *spontaneous emission* of a photon into the solid angle $\mathrm{d}\Omega$ is given *in the dipole approximation* by substituting [4.62] into [4.53]. That is,

$$\begin{aligned} W^{\mathrm{s}}_{ab}(\Omega)\,\mathrm{d}\Omega &= \frac{1}{2\pi\hbar c^3}\left(\frac{e^2}{4\pi\varepsilon_0}\right)\omega_{ba}^3|\hat{\boldsymbol{\varepsilon}}\cdot\mathbf{r}_{ba}|^2\,\mathrm{d}\Omega \\ &= \frac{1}{2\pi\hbar c^3}\left(\frac{1}{4\pi\varepsilon_0}\right)\omega_{ba}^3|\hat{\boldsymbol{\varepsilon}}\cdot\mathbf{D}_{ba}|^2\,\mathrm{d}\Omega \\ &= \frac{1}{2\pi\hbar c^3}\left(\frac{e^2}{4\pi\varepsilon_0}\right)\omega_{ba}^3|\mathbf{r}_{ba}|^2\cos^2\theta\,\mathrm{d}\Omega \end{aligned} \qquad [4.70]$$

where we recall that θ is the angle between $\hat{\boldsymbol{\varepsilon}}$ and $\mathbf{r}_{ba}$. By summing this expression with respect to the two polarisation directions of the photon and integrating over the angles one obtains the full transition rate for spontaneous emission of a photon in the dipole approximation, namely

$$\begin{aligned} W^{\mathrm{s}}_{ab} &= \frac{4}{3\hbar c^3}\left(\frac{e^2}{4\pi\varepsilon_0}\right)\omega_{ba}^3|\mathbf{r}_{ba}|^2 \\ &= \frac{4}{3\hbar c^3}\left(\frac{1}{4\pi\varepsilon_0}\right)\omega_{ba}^3|\mathbf{D}_{ba}|^2 \\ &= \frac{4}{3c^2}\,\alpha\,\omega_{ba}^3|\mathbf{r}_{ba}|^2 \end{aligned} \qquad [4.71]$$

4.4 THE EINSTEIN COEFFICIENTS

We shall verify that [4.71] is the correct expression for the rate of spontaneous emission by using the treatment of emission and absorption or radiation given by Einstein in 1916. Consider an enclosure containing atoms (of a single kind) and radiation in equilibrium at absolute temperature T, and let a and b denote two non-degenerate atomic states, with energy values E_a and E_b such that $E_b > E_a$. We denote by $\rho(\omega_{ba})$ the energy density of the radiation at the angular frequency $\omega_{ba} = (E_b - E_a)/\hbar$. The number of atoms making the transition from a to b per unit time by absorbing radiation, $\dot{N}_{ba}$, is proportional to the total

number N_a of atoms in the state a and to the energy density $\rho(\omega_{ba})$. That is

$$\dot{N}_{ba} = B_{ba} N_a \rho(\omega_{ba}) \tag{4.72}$$

where B_{ba} is called the *Einstein coefficient for absorption*. Since $\rho = I/c$ (see [4.11]) and the transition rate for absorption (per atom) is W_{ba}, we have from (4.69)

$$B_{ba} = \frac{W_{ba}}{\rho} = \frac{4\pi^2}{3\hbar^2}\left(\frac{e^2}{4\pi\varepsilon_0}\right)|\mathbf{r}_{ba}|^2 \tag{4.73}$$

where in the last step we have used the dipole approximation [4.69] for W_{ba}.

On the other hand, the number of atoms making the transition $b \to a$ per unit time, $\dot{N}_{ab}$, is the sum of the number of spontaneous transitions per unit time, which is independent of ρ, and the number of stimulated transitions per unit time, which is proportional to ρ. Thus

$$\dot{N}_{ab} = A_{ab} N_b + B_{ab} N_b \rho(\omega_{ba}) \tag{4.74}$$

where N_b is the total number of atoms in the state b, A_{ab} is the *Einstein coefficient for spontaneous emission* and B_{ab} is the *Einstein coefficient for stimulated emission.* In our notation $A_{ab} = W^{\mathrm{s}}_{ab}$. At equilibrium we have $\dot{N}_{ba} = \dot{N}_{ab}$, so that from [4.72] and [4.74] we deduce that

$$\frac{N_a}{N_b} = \frac{A_{ab} + B_{ab}\rho(\omega_{ba})}{B_{ba}\rho(\omega_{ba})} \tag{4.75}$$

We also know that at thermal equilibrium the ratio N_a/N_b is given by [9]

$$\frac{N_a}{N_b} = \mathrm{e}^{-(E_a - E_b)/kT} = \mathrm{e}^{\hbar\omega_{ba}/kT} \tag{4.76}$$

where k is Boltzmann's constant. From [4.75] and [4.76] we thus find for $\rho(\omega_{ba})$ the expression

$$\rho(\omega_{ba}) = \frac{A_{ab}}{B_{ba}\mathrm{e}^{\hbar\omega_{ba}/kT} - B_{ab}} \tag{4.77}$$

Since the atoms are in equilibrium with the radiation at temperature T, the energy density $\rho(\omega)$ is given by the Planck distribution law discussed in Section 1.3. Using [1.31] together with the fact that $\rho(\omega)\,\mathrm{d}\omega = \rho(\nu)\,\mathrm{d}\nu$, with $\omega = 2\pi\nu$, the energy density at the particular angular frequency ω_{ba} is

$$\rho(\omega_{ba}) = \frac{\hbar\omega_{ba}^3}{\pi^2 c^3}\frac{1}{\mathrm{e}^{\hbar\omega_{ba}/kT} - 1} \tag{4.78}$$

In order for [4.77] and [4.78] to be identical, the three Einstein coefficients must

[9] See for instance the text by Kittel (1958).

be related by the two equations

$$B_{ba} = B_{ab} \quad [4.79a]$$

$$A_{ab} = \frac{\hbar \omega_{ba}^3}{\pi^2 c^3} B_{ab} \quad [4.79b]$$

The relation [4.79a] expresses the principle of detailed balancing discussed previously. Using [4.73] and [4.79], we verify that W_{ab}^{s} ($= A_{ab}$) is indeed given in the dipole approximation by the expression [4.71]. It is a simple matter to generalise the above results to the case in which the energy levels E_a and (or) E_b are degenerate. Denoting by g_a and g_b the degeneracy of these levels, one finds (Problem 4.5) that [4.79a] becomes

$$g_a B_{ba} = g_b B_{ab} \quad [4.80]$$

while the relation [4.79b] remains unchanged.

4.5 SELECTION RULES AND THE SPECTRUM OF ONE-ELECTRON ATOMS

In the last section, we found the probability of a radiative transition between two levels a and b, in the electric dipole approximation. For stimulated emission or absorption of radiation with a particular polarisation vector $\hat{\varepsilon}$, the basic expression is given by [4.63] and for spontaneous emission by [4.70]. In each case the transition rate depends on the key quantity $|\hat{\varepsilon} \cdot \mathbf{r}_{ba}|^2$. In order to study this expression it is convenient to introduce the *spherical components* of the vectors $\hat{\varepsilon}$ and $\mathbf{r}$. According to the definition [A4.45] of Appendix 4 the spherical components $\varepsilon_q (q = 0, \pm 1)$ of $\hat{\varepsilon}$ are given in terms of its Cartesian components $(\hat{\varepsilon}_x, \hat{\varepsilon}_y, \hat{\varepsilon}_z)$ by

$$\varepsilon_1 = -\frac{1}{\sqrt{2}}(\hat{\varepsilon}_x + i\hat{\varepsilon}_y), \qquad \varepsilon_0 = \hat{\varepsilon}_z, \qquad \varepsilon_{-1} = \frac{1}{\sqrt{2}}(\hat{\varepsilon}_x - i\hat{\varepsilon}_y) \quad [4.81]$$

As we shall see later, if the direction of propagation of the radiation is along the Z axis ($\hat{\varepsilon}_z = 0$), ε_1 and ε_{-1} describe states of circular polarisation.

Similarly, the spherical components $r_q (q = 0, \pm 1)$ of the vector $\mathbf{r}$ are given by

$$\begin{aligned} r_1 &= -\frac{1}{\sqrt{2}}(x + iy) = -\frac{1}{\sqrt{2}} r \sin\theta \, e^{i\phi} = r\left(\frac{4\pi}{3}\right)^{1/2} Y_{1,1}(\theta, \phi) \\ r_0 &= z = r\cos\theta = r\left(\frac{4\pi}{3}\right)^{1/2} Y_{1,0}(\theta, \phi) \\ r_{-1} &= \frac{1}{\sqrt{2}}(x - iy) = \frac{1}{\sqrt{2}} r \sin\theta \, e^{-i\phi} = r\left(\frac{4\pi}{3}\right)^{1/2} Y_{1,-1}(\theta, \phi) \end{aligned} \quad [4.82]$$

The scalar product $\hat{\boldsymbol{\varepsilon}} \cdot \mathbf{r}_{ba}$ can be expressed in terms of spherical components as

$$\begin{aligned}\hat{\boldsymbol{\varepsilon}} \cdot \mathbf{r}_{ba} &= \sum_{q=0,\pm 1} \varepsilon_q^\star (\mathbf{r}_{ba})_q \\ &= -\varepsilon_1^\star \frac{1}{\sqrt{2}}(x_{ba} + iy_{ba}) + \varepsilon_0^\star z_{ba} + \varepsilon_{-1}^\star \frac{1}{\sqrt{2}}(x_{ba} - iy_{ba}) \quad [4.83]\end{aligned}$$

or

$$\hat{\boldsymbol{\varepsilon}} \cdot \mathbf{r}_{ba} = \sum_{q=0,\pm 1} \varepsilon_q^\star I^q_{n'l'm';nlm} \quad [4.84]$$

where

$$\begin{aligned}I^q_{n'l'm';nlm} &= \left(\frac{4\pi}{3}\right)^{1/2} \int_0^\infty \mathrm{d}r\, r^3 R_{n'l'}(r) R_{nl}(r) \\ &\times \int \mathrm{d}\Omega\, Y^\star_{l'm'}(\theta, \phi) Y_{1,q}(\theta, \phi) Y_{lm}(\theta, \phi) \quad [4.85]\end{aligned}$$

and where we have written the quantum numbers of the levels a and b of the hydrogenic atom as nlm and $n'l'm'$, respectively. The radial integral in [4.85] is always non-zero, but the angular integrals are only non-zero for certain values of (l, m) and (l', m'), giving rise to *selection rules* which we shall now investigate.

Parity

Under the reflection $\mathbf{r} \to -\mathbf{r}$ we have shown in Section 3.3 that the hydrogenic wave functions behave like (see [3.64])

$$\begin{aligned}R_{nl}(r) Y_{lm}(\theta, \phi) &\to R_{nl}(r) Y_{lm}(\pi - \theta, \phi + \pi) \\ &= R_{nl}(r)(-1)^l Y_{lm}(\theta, \phi) \quad [4.86]\end{aligned}$$

and the parity of the wave function is even or odd according to whether l is even or odd. By making the coordinate transformation $\mathbf{r} \to -\mathbf{r}$ in [4.85] we see that

$$I^q_{n'l'm';nlm} = (-1)^{l+l'+1} I^q_{n'l'm';nlm} \quad [4.87]$$

Hence the quantity $I^q_{n'l'm';nlm}$ is only non-vanishing if $(l + l' + 1)$ is even. In other words, *the electric dipole operator only connects states of opposite parity.*

Magnetic quantum numbers

The integral over ϕ which must be performed in [4.85] is of the form

$$\mathcal{J}(m, m', q) = \int_0^{2\pi} \mathrm{e}^{i(m+q-m')\phi}\, \mathrm{d}\phi \quad [4.88]$$

We shall consider separately the two cases $q = 0$ and $q = \pm 1$, which correspond respectively to radiation polarised *parallel* to the Z axis and *perpendicular* to the Z axis.

1. $q = 0$ (polarisation vector $\hat{\varepsilon}$ in the Z direction).

In this case the integral [4.88] – and therefore the matrix element [4.85] – vanishes unless

$$m' = m \quad \text{i.e.} \quad \Delta m = 0 \tag{4.89a}$$

2. $q = \pm 1$ (propagation vector k in the Z direction).

Here the ϕ integration in [4.88] yields for the matrix element [4.86] the selection rule

$$m' = m \pm 1 \quad \text{i.e.} \quad \Delta m = \pm 1 \tag{4.89b}$$

In a given transition, only one of the conditions $\Delta m = 0$ or $\Delta m = \pm 1$ can be satisfied, and hence only one of the matrix elements z_{ba} and $(x \pm iy)_{ba}$ will be non-zero.

Orbital angular momentum

The integral over the angles in [4.85], which we call $\mathscr{A}(l, m; l', m'; q)$, can be evaluated by the methods of Appendix 4. The result, expressed in terms of Clebsch-Gordan coefficients, is

$$\begin{aligned} \mathscr{A}(l, m; l', m'; q) &= \int \mathrm{d}\Omega \; Y^{\star}_{l'm'}(\theta, \phi) Y_{1,q}(\theta, \phi) Y_{lm}(\theta, \phi) \\ &= \left(\frac{3}{4\pi} \frac{2l + 1}{2l' + 1} \right)^{1/2} \langle l100|l'0\rangle \langle l1mq|l'm'\rangle \end{aligned} \tag{4.90}$$

From the properties of the Clebsch–Gordan coefficients we note that $\mathscr{A}(l, m; l', m'; q)$ vanishes unless $m' = m + q$, which is in agreement with the selection rules [4.89] we have just obtained for the magnetic quantum numbers. In addition, the properties of the Clebsch–Gordan coefficients also imply that $\mathscr{A}(l, m; l', m'; q)$ vanishes unless

$$l' = l \pm 1, \quad \text{i.e.} \quad \Delta l = \pm 1 \tag{4.91}$$

This is the orbital angular momentum selection rule for electric dipole transitions. This rule can also be deduced in a more elementary fashion by using the recurrence relations satisfied by the associated Legendre functions $P_l^m(\cos \theta)$. Indeed, using the expressions [2.181] for the spherical harmonics, together with the selection rules [4.89] for the magnetic quantum numbers, we

see that the θ integration in [4.90] can be written, apart from numerical factors

$$\int_{-1}^{+1} \mathrm{d}(\cos\theta) P_l^m(\cos\theta)\, P_{l'}^m(\cos\theta) \cos\theta \quad \text{for} \quad q = 0 \qquad [4.92a]$$

$$\int_{-1}^{+1} \mathrm{d}(\cos\theta) P_l^m(\cos\theta) P_{l'}^{m\pm1}(\cos\theta) \sin\theta \quad \text{for} \quad q = \pm 1 \qquad [4.92b]$$

From the recurrence relations [2.176],

$$(2l+1)\cos\theta\, P_l^m(\cos\theta) = (l+1-m)\, P_{l+1}^m(\cos\theta) + (l+m) P_{l-1}^m(\cos\theta) \qquad [4.93a]$$

and

$$(2l+1)\sin\theta\, P_l^{m-1}(\cos\theta) = P_{l+1}^m(\cos\theta) - P_{l-1}^m(\cos\theta) \qquad [4.93b]$$

together with the orthogonality relation [2.177]

$$\int_{-1}^{+1} \mathrm{d}(\cos\theta) P_l^m(\cos\theta) P_{l'}^m(\cos\theta) = \frac{2}{2l+1}\frac{(l+m)!}{(l-m)!}\delta_{ll'} \qquad [4.94]$$

we find that $l' = l \pm 1$, in accordance with [4.91]. Using either of the above methods one can also obtain the explicit forms of the quantities $\mathscr{A}(l, m; l', m'; q)$, which is left as an exercise for the reader (Problem 4.6).

Electron spin

We note that the electric dipole operator does not depend in any way on the spin of the electron. It follows that the component of the electron spin in the direction of quantisation remains unaltered by the absorption or emission of dipole radiation.

The spin of the photon

The selection rules for electric dipole transitions have a simple interpretation in terms of the spin of the photon. To discuss this point, we must first explore in more detail the possible states of polarisation of an electromagnetic wave. In Section 4.1 we saw that a general state of polarisation for a plane wave propagating in the direction $\hat{\mathbf{k}}$ can be described by combining two independent *linearly polarised* plane waves (having in general different phases) with polarisation vectors $\hat{\boldsymbol{\varepsilon}}_\lambda$ ($\lambda = 1, 2$) orthogonal to $\hat{\mathbf{k}}$. The resulting polarisation vector $\hat{\boldsymbol{\varepsilon}}$ lies in a plane perpendicular to $\hat{\mathbf{k}}$, so that a state of arbitrary polarisation can always be represented as

$$\hat{\boldsymbol{\varepsilon}} = a_1\hat{\mathbf{e}}_1 + a_2\hat{\mathbf{e}}_2; \qquad a_1^2 + a_2^2 = 1 \qquad [4.95]$$

where $\hat{\mathbf{e}}_i (i = 1, 2)$ are fixed mutually orthogonal real unit vectors in a plane perpendicular to $\hat{\mathbf{k}}$. We shall take $\hat{\mathbf{e}}_1$, $\hat{\mathbf{e}}_2$ and $\hat{\mathbf{k}}$ to form a right-handed system, so

that (see Fig. 4.1)

$$\hat{\mathbf{k}} = \hat{\mathbf{e}}_1 \times \hat{\mathbf{e}}_2; \qquad \hat{\mathbf{e}}_1 \cdot \hat{\mathbf{e}}_2 = 0 \tag{4.96}$$

The foregoing discussion may of course be directly generalised to pulses of the form [4.13], for which the polarisation vector $\hat{\varepsilon}$ is independent of ω.

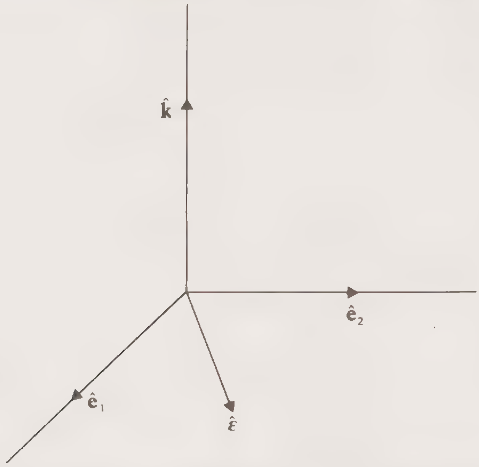

4.1 The vectors $\hat{\mathbf{e}}_1$, $\hat{\mathbf{e}}_2$ and $\hat{\mathbf{k}}$, forming a right-handed set of mutually orthogonal unit vectors. Also shown is the polarisation vector $\hat{\varepsilon}$ which lies in the plane of $\hat{\mathbf{e}}_1$ and $\hat{\mathbf{e}}_2$.

An alternative description of a general state of polarisation of an electromagnetic wave may be given in terms of two *circularly polarised waves*. Let us first consider the particular case in which the direction of propagation is along the Z axis. In place of the vector potential [4.5], we consider the potentials $\mathbf{A}^{\mathrm{L}}(\omega; \mathbf{r}, t)$ and $\mathbf{A}^{\mathrm{R}}(\omega; \mathbf{r}, t)$ defined by

$$\begin{aligned} A_x^{\mathrm{L}} &= A_x^{\mathrm{R}} = \sqrt{2}A_0(\omega)\cos(kz - \omega t + \delta_\omega) \\ A_y^{\mathrm{L}} &= -A_y^{\mathrm{R}} = -\sqrt{2}A_0(\omega)\sin(kz - \omega t + \delta_\omega) \\ A_z^{\mathrm{L}} &= A_z^{\mathrm{R}} = 0 \end{aligned} \tag{4.97}$$

The corresponding electric field vectors $\boldsymbol{\mathscr{E}}^{\mathrm{L}}$ and $\boldsymbol{\mathscr{E}}^{\mathrm{R}}$ are such that

$$\begin{aligned} \mathscr{E}_x^{\mathrm{L}} &= \mathscr{E}_x^{\mathrm{R}} = -\sqrt{2}\omega A_0(\omega)\sin(kz - \omega t + \delta_\omega) \\ \mathscr{E}_y^{\mathrm{L}} &= -\mathscr{E}_y^{\mathrm{R}} = -\sqrt{2}\omega A_0(\omega)\cos(kz - \omega t + \delta_\omega) \\ \mathscr{E}_z^{\mathrm{L}} &= \mathscr{E}_z^{\mathrm{R}} = 0 \end{aligned} \tag{4.98}$$

On facing into the oncoming wave, the vector $\boldsymbol{\mathscr{E}}^{\mathrm{L}}$ is seen to be of constant magnitude and to be rotating in an anticlockwise way in the (X, Y) plane at a frequency ω (see Fig. 4.2(a)), while the vector $\boldsymbol{\mathscr{E}}^{\mathrm{R}}$ is of the same magnitude but rotates at a frequency ω in a clockwise way (see Fig. 4.2(b)). The radiation described by $\boldsymbol{\mathscr{E}}^{\mathrm{L}}$ is said to be left-hand circularly polarised and that corresponding to $\boldsymbol{\mathscr{E}}^{\mathrm{R}}$ is right-hand circularly polarised. By forming the combination

$$a_{\mathrm{L}}\boldsymbol{\mathscr{E}}^{\mathrm{L}} + a_{\mathrm{R}}\boldsymbol{\mathscr{E}}^{\mathrm{R}}$$

4.2 In circularly polarised radiation the electric field vectors $\mathscr{E}^L$, and $\mathscr{E}^R$ rotate in anticlockwise and clockwise directions when facing into the oncoming wave.

where a_L and a_R are complex coefficients, radiation in any state of polarisation can be produced. For example, if $a_L = a_R = 1$, we obtain linearly polarised radiation, with the electric field vector oriented along the X axis.

In terms of complex exponentials, $\mathbf{A}^L$ and $\mathbf{A}^R$ can be written as

$$\begin{aligned}\mathbf{A}^L &= A_0(\omega)[\hat{\mathbf{e}}^L e^{i(kz-\omega t+\delta\omega)} + \text{c.c.}]\\ \mathbf{A}^R &= A_0(\omega)[\hat{\mathbf{e}}^R e^{i(kz-\omega t+\delta\omega)} + \text{c.c.}]\end{aligned} \qquad [4.99]$$

where $\hat{\mathbf{e}}^L$ and $\hat{\mathbf{e}}^R$ are two complex orthogonal unit vectors such that

$$\hat{\mathbf{e}}^L = \frac{1}{\sqrt{2}}(\hat{\mathbf{x}} + i\hat{\mathbf{y}}); \qquad \hat{\mathbf{e}}^R = \frac{1}{\sqrt{2}}(\hat{\mathbf{x}} - i\hat{\mathbf{y}}) \qquad [4.100]$$

and describing respectively the states of left-hand and right-hand circularly polarised radiation. An arbitrary state of polarisation can be specified by a complex vector $\hat{\mathbf{n}}$ such that

$$\hat{\mathbf{n}} = a^L\hat{\mathbf{e}}^L + a^R\hat{\mathbf{e}}^R; \qquad |a^L|^2 + |a^R|^2 = 1 \qquad [4.101]$$

and this description is as general as the one given by [4.95]. We note that if the direction of propagation is not along the Z axis, then we can write more generally

$$\hat{\mathbf{e}}^L = \frac{1}{\sqrt{2}}(\hat{\mathbf{e}}_1 + i\hat{\mathbf{e}}_2); \qquad \hat{\mathbf{e}}^R = \frac{1}{\sqrt{2}}(\hat{\mathbf{e}}_1 - i\hat{\mathbf{e}}_2) \qquad [4.102]$$

where $\hat{\mathbf{e}}_1$ and $\hat{\mathbf{e}}_2$ are the unit vectors introduced in [4.95].

We have already seen in Section 4.2 that the terms in $\mathbf{A}$ associated with $\exp[i(kz - \omega t)]$ give rise to the absorption of photons (see [4.45]) and those with $\exp[-i(kz - \omega t)]$ to the emission of photons (see [4.47]). From [4.49], [4.42], [4.63] and [4.70] we see that, in the electric dipole approximation, we should use the expressions $\hat{\mathbf{e}}^L \cdot \mathbf{r}_{ba}$ or $\hat{\mathbf{e}}^R \cdot \mathbf{r}_{ba}$ to describe the *absorption* of a left-hand or a right-hand circularly polarised photon, respectively, while the expressions $\hat{\mathbf{e}}^{L\star} \cdot \mathbf{r}^\star_{ba}$ $(=\hat{\mathbf{e}}^{L\star} \cdot \mathbf{r}_{ab})$ or $\hat{\mathbf{e}}^{R\star} \cdot \mathbf{r}^\star_{ba}$ $(=\hat{\mathbf{e}}^{R\star} \cdot \mathbf{r}_{ab})$ must be used to describe the *emission* of the corresponding circularly polarised photons. Thus, if a left-hand circularly polarised photon is emitted in the Z direction, the appropriate

expression is

$$\hat{\mathbf{e}}^{\mathrm{L}\star} \cdot \mathbf{r}_{ab} = \frac{1}{\sqrt{2}}(\hat{\mathbf{x}} - i\hat{\mathbf{y}}) \cdot \mathbf{r}_{ab}$$

$$= \frac{1}{\sqrt{2}}(x_{ab} - iy_{ab}) \qquad [4.103]$$

If we denote by $m\hbar$ the Z component of the angular momentum for the initial (upper) state b, we see from [4.82] and [4.89] that the matrix element [4.103] vanishes unless the final (lower) state a of the atom has a component $(m - 1)\hbar$ of angular momentum in the Z direction. A similar reasoning leads to the conclusion that the emission of a right-hand circularly polarised photon increases the component of the angular momentum of the atom along the Z axis by $\hbar$.

By conservation of angular momentum, each photon must have a component of angular momentum parallel to the Z axis (the direction of propagation) of $\pm\hbar$. Since photons travelling parallel to the Z axis cannot have a component of *orbital* angular momentum in the Z direction, the angular momentum carried by the photons in this case can only be due to their intrinsic spin. Further, for electric dipole radiation, the orbital angular momentum of the photon must be zero, since the wave function (the vector potential) is spherically symmetrical (we have replaced $\exp(i\mathbf{k} \cdot \mathbf{r})$ by 1). From these remarks, and from the selection rule $\Delta l = \pm 1$, we infer that the photon has spin of unit magnitude, that is $\mathbf{S}^2 = s(s + 1)\hbar^2$ with $s = 1$. The components of the spin in the direction of propagation are $S_z = m_s\hbar$ with $m_s = \pm 1$. The component of the spin along the direction of the propagation is called the *helicity* of a particle. In this case, only two helicity states are possible, because the electromagnetic wave is transverse and the case $m_s = 0$ is excluded. From the definition of helicity it is clear that a photon with helicity $+\hbar$ is always left-hand circularly polarised and one with helicity $-\hbar$ is always right-hand circularly polarised, and this is independent of any particular choice of axes.

Beth's experiment

If a beam of light, propagating parallel to the positive Z axis, is left circularly polarised, each photon in the beam will have a positive angular momentum $+\hbar$ along the Z axis. If the beam contains N photons per unit volume, the energy density of the beam, ρ, will be $\rho = N\hbar\omega$, where ω is the angular frequency of the radiation, and a unit volume will possess an angular momentum $L_z = N\hbar$. The ratio $\rho/\omega = N\hbar$ is independent of frequency and is equal in magnitude to the angular momentum L_z. Similarly, for a right-hand circularly polarised beam $\rho/\omega = -L_z$ (a plane polarised beam carries no angular momentum). These facts are consistent with the results of a remarkable experiment carried out in 1936 by R. A. Beth.

In Beth's experiment an anisotropic crystalline plate is prepared, which has the property that (at a certain wavelength), it converts left-hand circularly polarised light passing through it, to right-hand circularly polarised light, acting as a half-wave plate. Because of this, the plate must be subjected to a couple of magnitude Γ_z per unit area, where

$$\Gamma_z = 2cL_z = 2\rho c/\omega \tag{4.104}$$

The angle is measured by suspending the plate from a quartz fibre and measuring the angle through which the plate rotates. The effect can be doubled by reflecting the light which has passed through the plate, so it passes through the plate a second time. A fixed quarter-wave plate must be inserted, so that the polarisation of the light is in the correct sense to reinforce the couple (see Fig. 4.3). The angle of deflection is extremely small, but the constancy of the

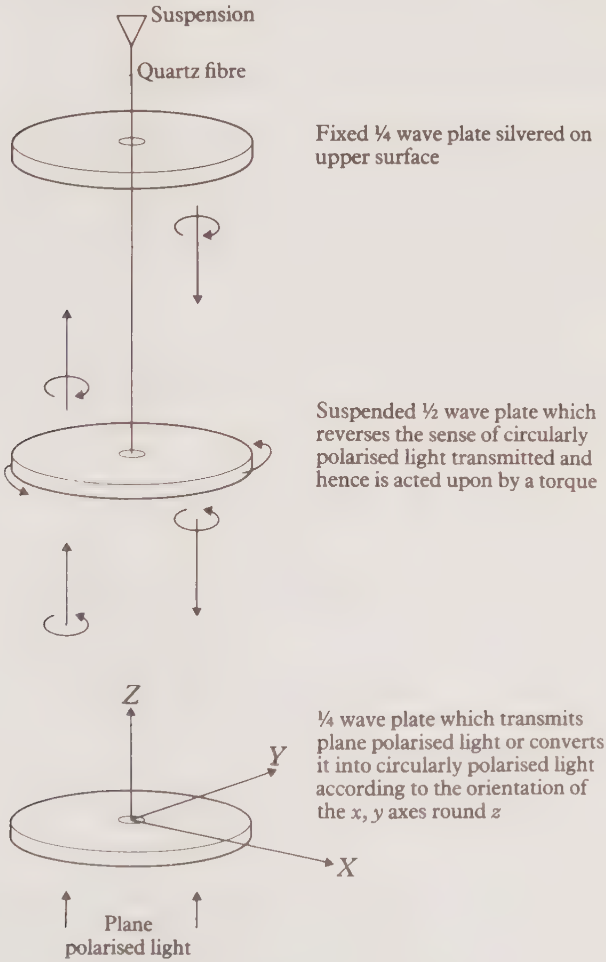

4.3 Schematic diagram of Beth's experiment.

ratio ρ/ω can be observed, and a result of the expected order of magnitude obtained provided the experiment is carried out with due precautions. For example, the whole apparatus must be in a vacuum to avoid the effect of currents in the air, and the power of the source of illumination must be known accurately.

Parity of the photon

Provided tiny effects due to the weak nuclear interactions are neglected, a system of electrons interacting with the electromagnetic field conserves parity [10]. From the behaviour of the vector potential **A** under reflections, it can be inferred that the photon carries negative parity, which is consistent with the selection rule [4.87] showing that an electric dipole transition causes a change in parity of the atom.

Magnetic dipole and electric quadrupole transitions

When the electric dipole matrix elements vanish, the transition may still occur through higher order terms in the expansion [4.55]. The next order of approximation retains the term $i(\mathbf{k}\cdot\mathbf{r})$. If we take the direction of propagation $\hat{\mathbf{k}}$ to be along the Z axis, and the polarisation vector $\hat{\varepsilon}$ to be along the X axis the part $\tilde{M}_{ba}$ of the matrix element M_{ba} arising from this term is (see [4.33])

$$\tilde{M}_{ba} = -\frac{m\omega_{ba}}{\hbar c}\langle\psi_b|z\dot{x}|\psi_a\rangle \qquad [4.105]$$

With a little manipulation, $\tilde{M}_{ba}$ can be written as the sum of two terms (Problem 4.8), namely

$$\tilde{M}_{ba} = -\frac{\omega_{ba}}{2\hbar c}\langle\psi_b|L_y|\psi_a\rangle - \frac{im\omega_{ba}^2}{2\hbar c}\langle\psi_b|zx|\psi_a\rangle \qquad [4.106]$$

where L_y is the y component of the orbital angular momentum operator $\mathbf{L}$.

Both terms in [4.106] are of the same order of magnitude. The first is proportional to the matrix element of the component of the *orbital magnetic moment* of the atom in the y direction, $\mathcal{M}_y = -eL_y/2m$ and the second is proportional to the *electric quadrupole moment* of the atom. Both terms are smaller than the electric dipole contribution to M_{ba} (when this does not vanish) by a factor of the order of the fine structure constant α.

To obtain the complete expression for *magnetic dipole radiation*, the magnetic moment due to the electron *spin* must be added to the orbital magnetic moment.

[10] Very small parity-violating terms in the electromagnetic interaction, involving the so-called 'neutral currents' have been discovered in 1978 in the deep inelastic scattering of polarised electron by protons and deuterons. These neutral currents, which are a consequence of a unified description of electromagnetic and weak interactions imply very small parity-violating effects in atomic transitions.

The selection rules are found to be

$$\begin{aligned}\Delta l &= 0\\ \Delta j &= 0, \pm 1\\ \Delta m_j &= 0, \pm 1\end{aligned} \qquad [4.107]$$

where j and m_j denote the quantum numbers associated respectively with the operators $\mathbf{J}^2$ and $\mathcal{J}_z$, $\mathbf{J} = \mathbf{L} + \mathbf{S}$ being the total angular momentum of the electron. An example of magnetic dipole transition is that occurring between hyperfine levels of the ground state of atomic hydrogen at the wavelength of 21 cm, which we shall study in Chapter 5.

It is easy to see that the matrix elements of the products (xy), (yz) and (xz) vanish unless a and b are states of the same parity. The selection rules for *electric quadrupole radiation* are then given by

$$\begin{aligned}\Delta l &= 0, \pm 2 \qquad (l = 0 \leftrightarrow l' = 0 \text{ forbidden})\\ \Delta m &= 0, \pm 1, \pm 2\end{aligned} \qquad [4.108]$$

We note that for $\Delta l = \pm 2$ the contribution to M_{ba} is coming only from the electric quadrupole part, so that we have a pure electric quadrupole transition.

The spectrum of one-electron atoms

In Chapter 3 it was shown that in the non-relativistic approximation, and neglecting spin-orbit coupling, the bound states of a one-electron atom were degenerate in the quantum numbers l and m and the energy of a level depended only on the principal quantum number n. That is (see [3.29] and [3.31])

$$\begin{aligned}E_n &= -\frac{1}{2n^2}\left(\frac{Ze^2}{4\pi\varepsilon_0}\right)^2\frac{\mu}{\hbar^2}\\ &= -\frac{Z^2}{2n^2}\left(\frac{\mu}{m}\right) \qquad \text{in a.u.}\end{aligned} \qquad [4.109]$$

where μ is the reduced mass, given in terms of the mass of the nucleus M and the mass of the electron m by $\mu = mM/(m + M)$ (see [3.31]). Since there is no selection rule limiting n, the hydrogenic spectrum contains all frequencies given by the expression [3.34] which we recall here, namely

$$\nu_{n'n} = Z^2 R(M)\left(\frac{1}{n'^2} - \frac{1}{n^2}\right) \qquad [4.110]$$

where $n = 2, 3, 4, \ldots, n' = 1, 2, 3 \ldots$ with $n > n'$ and $R(M)$ is given by [1.102]. The gross structure of the spectra of one-electron atoms, described in Chapter 1 within the framework of the Bohr model, agrees with this formula. The foregoing discussion in this chapter gives a consistent derivation of the result [4.110]. However, it is important to note that the selection rules [4.89]

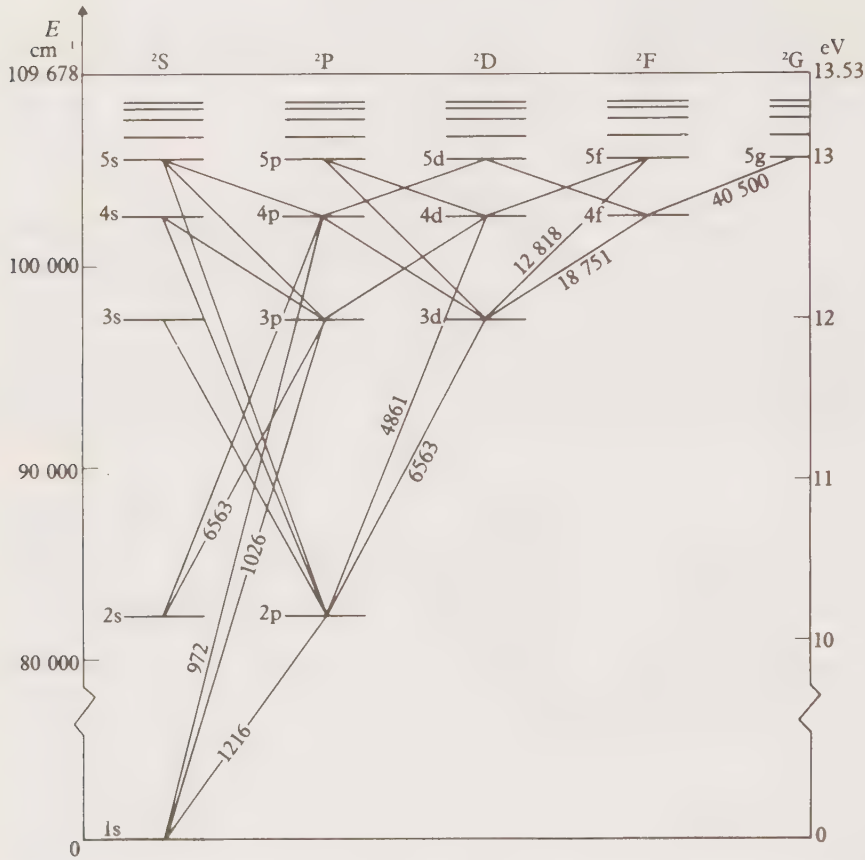

4.4 Term, or Grotrian diagram for atomic hydrogen. The ordinate shows the energy above the 1s ground state in cm^{-1} ($8065\ cm^{-1} = 1$ eV) on the left and in eV on the right and the energy levels are shown plotted against the orbital angular momentum. Transitions obeying the $\Delta l = \pm 1$ selection rule are indicated by solid lines. The numbers against the lines indicate the wavelength in angström units (1 Å $= 10^{-8}$ cm). For clarity, only transitions between the lower-lying levels are shown, and the wavelengths are shown only for a selection of lines. The splitting due to fine structure is too small to be shown on a diagram of this scale.

and [4.91] limit the values of the quantum numbers m and l of the level concerned. This is illustrated in Fig. 4.4 for the case of the orbital angular momentum quantum number l.

4.6 LINE INTENSITIES AND THE LIFETIMES OF EXCITED STATES

As we have seen in Section 4.3, the intensity of a transition between a pair of states a and b is proportional, in the dipole approximation, to the quantity $|\mathbf{r}_{ba}|^2$. Thus the relative intensities of a series of transitions from a given initial state a to various final states k are determined by the quantities $|\mathbf{r}_{ka}|^2$.

Oscillator strengths and the Thomas–Reiche–Kuhn sum rule

In discussions of intensities it is customary to introduce a related dimensionless quantity f_{ka}, called the *oscillator strength*. It is defined as

$$f_{ka} = \frac{2m\omega_{ka}}{3\hbar}|\mathbf{r}_{ka}|^2 \qquad [4.111]$$

with $\omega_{ka} = (E_k - E_a)/\hbar$. We note that this definition implies that $f_{ka} > 0$ for absorption, where $E_k > E_a$. On the other hand we have $f_{ka} < 0$ for emission processes.

The oscillator strengths [4.111] obey the sum rule, due to Thomas, Reiche and Kuhn

$$\sum_k f_{ka} = 1 \qquad [4.112]$$

where the sum is over all levels, including the continuum. This sum rule can be proved as follows. Let f_{ka}^x be defined as

$$\begin{aligned} f_{ka}^x &= \frac{2m\omega_{ka}}{3\hbar}|x_{ka}|^2 \\ &= \frac{2m\omega_{ka}}{3\hbar}\langle a|x|k\rangle\langle k|x|a\rangle \end{aligned} \qquad [4.113]$$

where we have used the simplified notation $\langle a|x|k\rangle \equiv \langle\psi_a|x|\psi_k\rangle$. From [4.59], we have

$$x_{ka} = \langle k|x|a\rangle = -\frac{i}{m\omega_{ka}}\langle k|p_x|a\rangle \qquad [4.114a]$$

$$x_{ak} = \langle a|x|k\rangle = \frac{i}{m\omega_{ka}}\langle a|p_x|k\rangle \qquad [4.114b]$$

and hence

$$f_{ka}^x = \frac{2i}{3\hbar}\langle a|p_x|k\rangle\langle k|x|a\rangle \qquad [4.115a]$$

$$= -\frac{2i}{3\hbar}\langle a|x|k\rangle\langle k|p_x|a\rangle \qquad [4.115b]$$

$$= \frac{i}{3\hbar}\{\langle a|p_x|k\rangle\langle k|x|a\rangle - \langle a|x|k\rangle\langle k|p_x|a\rangle\} \qquad [4.115c]$$

where the last line has been obtained by taking half the sum of the two expressions [4.115a] and [4.115b].

We can now use the closure property of the hydrogenic wave functions which form a complete set, namely $\Sigma_k |k\rangle\langle k| = 1$ to find from [4.115c] that

$$\sum_k f_{ka}^x = \frac{i}{3\hbar} \langle a|p_x x - xp_x|a\rangle \qquad [4.116]$$

But since $[x, p_x] = i\hbar$, we have the sum rule

$$\sum_k f_{ka}^x = \frac{1}{3} \qquad [4.117]$$

The same argument holds for f_{ka}^y and f_{ka}^z, which proves the sum rule [4.112].

The oscillator strengths and transition probabilities can be easily calculated for one-electron atoms and ions, because the hydrogenic wave functions are known exactly. The labels a and k in f_{ka} include all the quantum numbers of the initial and final states, and in particular f_{ka} depends on the magnetic quantum numbers. It is convenient to define an *average oscillator strength* for the transition $nl \to n'l'$, which is independent of the magnetic quantum numbers and hence of the polarisation of the radiation by

$$\bar{f}_{n'l',nl} = \frac{1}{2l+1} \sum_{m'=-l'}^{l'} \sum_{m=-l}^{l} f_{n'l'm',nlm} \qquad [4.118]$$

It is easy to see that the average oscillator strengths also obey the sum rule [4.112]. Some calculated values of $\bar{f}_{n'l',nl}$ for hydrogenic atoms (or ions) are given in Table 4.1.

The transition rates for spontaneous emission in the dipole approximation are given in terms of oscillator strengths (see [4.71] and [4.111]) by

$$W_{ka}^s = \frac{2\omega_{ka}^2}{mc^3}\left(\frac{e^2}{4\pi\varepsilon_0}\right)|f_{ka}| \qquad [4.119]$$

For hydrogenic atoms the oscillator strengths and transition probabilities decrease as the principal quantum number n of the upper level increases, W_{ka}^s decreasing like n^{-3} for large n.

Table 4.1 Average oscillator strengths for some transitions in hydrogenic atoms and ions†

Initial level	*Final level*	*Discrete spectrum* $n = 1$	$n = 2$	$n = 3$	$n = 4$	$\sum_{n=5}^{\infty}$	*Continuum spectrum*
1s	*np*	—	0.416	0.079	0.029	0.041	0.435
2s	*np*	—	—	0.435	0.103	0.111	0.351
2p	*ns*	−0.139	—	0.014	0.003	0.003	0.008
2p	*nd*	—	—	0.696	0.122	0.109	0.183

† More complete tabulations can be found in Bethe and Salpeter (1957).

Atomic lifetimes

If $N(t)$ atoms are in an excited state b at a particular time t, the rate of change of $N(t)$ is

$$\dot{N}(t) = -N(t) \sum_k W^{s}_{kb} \qquad [4.120]$$

where W^{s}_{kb} is the transition rate for spontaneous emission and the sum is over all states k, of lower energy, to which decay is allowed by the selection rules. On integration, $N(t)$ can be expressed in terms of $N(t = 0)$ by

$$N(t) = N(t = 0)\mathrm{e}^{-t/\tau} \qquad [4.121]$$

where τ is called the *lifetime* or *half-life* of the level b, and

$$\tau^{-1} = \sum_k W^{s}_{kb} \qquad [4.122]$$

In the absence of external fields, the lifetime of an atomic level cannot depend on the orientation of the atom, and hence cannot depend on the magnetic quantum number m of the level b. This property can also be verified by evaluating [4.122] explicitly in the dipole approximation, and remembering that the sum over k includes all the magnetic substates of the final levels k to which the atom can decay. The lifetimes τ of some of the lower levels of atomic hydrogen are shown in Table 4.2. The corresponding lifetimes of hydrogenic ions, with nuclear charge Z, are shorter and are given by

$$\tau(Z) = Z^{-4}\tau(Z = 1) \qquad [4.123]$$

Table 4.2 Lifetime of some levels of atomic hydrogen (in 10^{-8} s)

Level	2p	3s	3p	3d	4s	4p	4d	4f
Lifetime	0.16	16	0.54	1.56	23	1.24	3.65	7.3

In general the lifetime of a highly excited state is longer than that of a low-lying level. It is also interesting to note that the 2s level has an infinite lifetime in the dipole approximation. In fact the 2s level has a lifetime of 1/7 s, the dominant decay process, 2s → 1s, occurring by the emission of two photons (i.e. through higher order in the interaction between the atom and the electromagnetic field). The lifetime of 1/7 s is very long on the atomic time-scale, and the 2s level is said to be *metastable*.

4.7 LINE SHAPES AND WIDTHS

In the approximation used in Section 4.2 to calculate transition rates, we found that the angular frequency of the radiation emitted or absorbed between two atomic levels of energies E_a and E_b (with $E_b > E_a$) was exactly $\omega_{ba} = (E_b - E_a)/\hbar$, so that the spectral line was infinitely sharp. This cannot be completely accurate for the following reason. All atomic levels, except the

ground state, decay with a finite lifetime τ. By the uncertainty principle, the energy of such a level cannot be precisely determined, but must be uncertain by an amount of order $\hbar/\tau$. Therefore there is a finite probability that photons will be emitted with energies in an interval about $(E_b - E_a)$ of width $(\hbar/\tau_a + \hbar/\tau_b)$, where τ_a and τ_b are the lifetimes of the states a and b, respectively.

Let us consider for example the spontaneous decay of an excited state b of the atom to the state a which we choose to be the ground state. We return to the coupled equations [4.25] – with the perturbation H' given by [4.22] – and retain only those terms which contain the two atomic states a and b. The initial state of the system is characterised by an amplitude $c_b(t)$, while the final state consists of a photon of angular frequency ω, emitted in a direction (θ, ϕ) with a polarisation $\boldsymbol{\varepsilon}_\lambda$, in addition to the ground state atom. The corresponding amplitude depends on ω, (θ, ϕ) and λ, but we will write it in shortened form as $c_a(\omega, t)$. When summing over the possible final states, we must make use of the density of states factor [4.52]. Using [4.22], the expression [4.13] of $\mathbf{A}(\mathbf{r}, t)$ and remembering that M_{ba}^λ is given by [4.33], with $\hat{\varepsilon}$ replaced by $\hat{\varepsilon}_\lambda$, the equation [4.25] for $\dot{c}_b(t)$ can be written in explicit form as

$$\dot{c}_b(t) = -\frac{e}{m}\frac{V}{(2\pi)^3 c^3}\sum_{\lambda=1}^{2}\int \mathrm{d}\omega\, \omega^2 \int \mathrm{d}\Omega A_0(\omega) M_{ba}^\lambda(\omega) \mathrm{e}^{i(\omega_{ba}-\omega)t+i\,\delta_\omega}\, c_a(\omega, t) \tag{4.124}$$

where we have only retained the part of $\mathbf{A}(\omega)$ that corresponds to the emission of a photon. Since a single photon is emitted $A_0(\omega)$ is found from [4.47] with $N(\omega) = 0$, namely

$$A_0(\omega) = \left(\frac{\hbar}{2V\varepsilon_0\omega}\right)^{1/2} \tag{4.125}$$

The equation for the time derivative of the amplitude $c_a(\omega, t)$ is again given by [4.25], with the same value of $A_0(\omega)$. We find that

$$\dot{c}_a(\omega, t) = -\frac{e}{m} A_0(\omega) \bar{M}_{ab}^\lambda(\omega) \mathrm{e}^{i(\omega-\omega_{ba})t-i\,\delta_\omega}\, c_b(t) \tag{4.126}$$

Since there is only a single amplitude $c_b(t)$, there is no sum over states on the right-hand side of [4.126].

In our previous treatment we solved the coupled equations by making the approximation $c_b(t) = 1$ on the right-hand side of [4.126], but we now allow for the decay of the upper level by writing

$$\begin{aligned} c_b(t) &= 1 \qquad & t < 0 \\ c_b(t) &= \mathrm{e}^{-t/2\tau} \qquad & t \geqslant 0 \end{aligned} \tag{4.127}$$

This is still an approximation, but it has been shown that the departure from exponential decay is exceedingly small. We can now integrate [4.126] over t to

find $c_a(\omega, t)$,

$$c_a(\omega, t) = -\frac{e}{m} A_0(\omega)\bar{M}^{\lambda}_{ab}(\omega)\mathrm{e}^{-i\delta_\omega}\int_0^t \mathrm{e}^{i(\omega-\omega_{ba})t'}\mathrm{e}^{-t'/2\tau}\,\mathrm{d}t'$$

$$= -\frac{e}{m} A_0(\omega)\bar{M}^{\lambda}_{ab}(\omega)\mathrm{e}^{-i\delta_\omega}\frac{\mathrm{e}^{i(\omega-\omega_{ba})t}\mathrm{e}^{-t/2\tau}-1}{i(\omega-\omega_{ba})-1/2\tau} \qquad [4.128]$$

At times $t \gg \tau$ the probability that a photon has been emitted is given by $|c_a(\omega, t)|^2$, which is proportional to

$$\left|\frac{1}{i(\omega-\omega_{ba})-1/2\tau}\right|^2 = \frac{1}{(\omega-\omega_{ba})^2+1/4\tau^2} \qquad [4.129]$$

The intensity of the emitted radiation therefore reaches a maximum when $\omega = \omega_{ba} = (E_b - E_a)/\hbar$, and decreases to one-half of the maximum value at

$$\begin{aligned}\omega &= \omega_{ba} \pm 1/(2\tau)\\ &= (E_b - E_a \pm \Gamma/2)/\hbar\end{aligned} \qquad [4.130]$$

where

$$\Gamma = \frac{\hbar}{\tau} \qquad [4.131]$$

is the *width* of the line. The intensity distribution given by [4.129] is said to be *Lorentzian* in shape (see Fig. 4.5). We note that this intensity distribution may

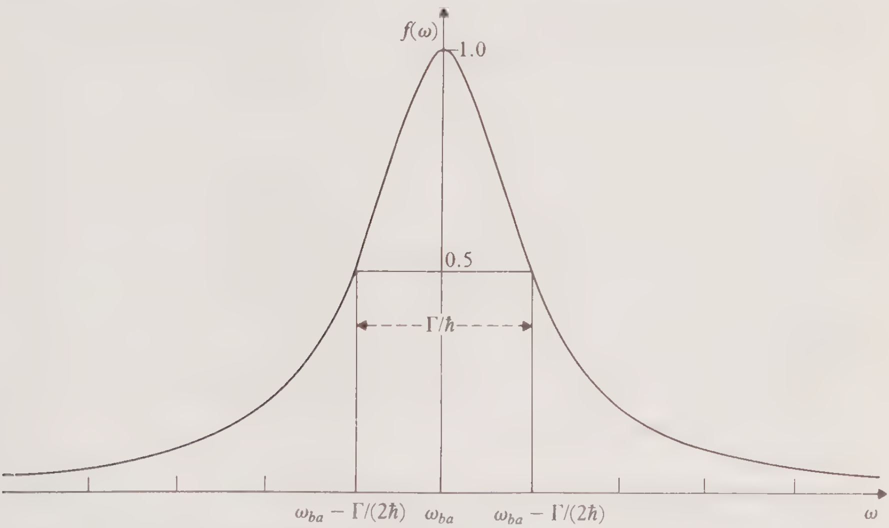

4.5 A plot of the Lorentzian intensity distribution

$$f(\omega) = \frac{\Gamma^2/4\hbar^2}{(\omega-\omega_{ba})^2+\Gamma^2/4\hbar^2}$$

Note that $f(\omega_{ba}) = 1$ and $f(\omega) = 1/2$ when $\omega = \omega_{ba} \pm 1/(2\tau) = \omega_{ba} \pm \Gamma/(2\hbar)$.

also be written as

$$\mathcal{I}(\omega) = \mathcal{I}_0 \frac{\Gamma^2/4}{(\hbar\omega + E_a - E_b)^2 + \Gamma^2/4}, \qquad \mathcal{I}_0 = \text{const} \qquad [4.132]$$

To calculate the lifetime τ, we insert the expression [4.128] for $c_a(\omega, t)$ into [4.124]. Using [4.125] for $A_0(\omega)$ we find that

$$\dot{c}_b(t) = -\left(\frac{e^2}{4\pi\varepsilon_0}\right) \frac{\hbar}{4\pi^2 m^2 c^3} \sum_{\lambda=1}^{2} \int d\Omega \int d\omega\, \omega |M_{ba}^{\lambda}(\omega)|^2 \left[\frac{e^{-t/2\tau} - e^{i(\omega_{ba} - \omega)t}}{i(\omega - \omega_{ba}) - 1/2\tau}\right] \qquad [4.133]$$

The function in square brackets is sharply peaked about $\omega = \omega_{ba}$. The term $\omega|M_{ba}^{\lambda}(\omega)|^2$ is slowly varying, and so can be evaluated at $\omega = \omega_{ba}$. The range of integration can then be taken from $\omega_{ba} - \eta$ to $\omega_{ba} + \eta$, with $\eta \to +\infty$. Using [11].

$$\lim_{\eta \to +\infty} \int_{-\eta}^{+\eta} \frac{1}{x - \alpha + i\beta} dx = -i\pi \qquad [4.134a]$$

$$\int_{-\infty}^{+\infty} \frac{e^{-ixt}}{x - \alpha + i\beta} dx = -2\pi i e^{-i(\alpha - i\beta)t} \qquad [4.134b]$$

with $x = \omega$, $\alpha = \omega_{ba}$ and $\beta = 1/2\tau$, we find that

$$\dot{c}_b(t) = -\left(\frac{e^2}{4\pi\varepsilon_0}\right) \frac{\hbar}{4\pi m^2 c^3} \int d\Omega \sum_{\lambda=1}^{2} \omega_{ba} |M_{ba}^{\lambda}(\omega_{ba})|^2 e^{-t/2\tau} \qquad [4.135]$$

This is consistent with [4.127], from which we see that

$$\dot{c}_b(t) = -\frac{1}{2\tau} e^{-t/2\tau}, \qquad t \geqslant 0 \qquad [4.136]$$

The transition rate is given by $W_{ab}^{s} = \tau^{-1}$ and we have therefore

$$W_{ab}^{s} = \frac{1}{\tau} = \frac{\hbar}{2\pi m^2 c^3} \left(\frac{e^2}{4\pi\varepsilon_0}\right) \int d\Omega \sum_{\lambda=1}^{2} \omega_{ba} |M_{ba}^{\lambda}(\omega_{ba})|^2 \qquad [4.137]$$

which agrees with our previous result [4.54].

The intensity distribution of the spectral lines corresponding to absorption and stimulated emission can be shown, in the same way, to have the Lorentzian shape [4.132]. By using the identity

$$\lim_{\Gamma \to 0} \frac{\Gamma/2}{(\hbar\omega + E_a - E_b)^2 + \Gamma^2/4} = \pi\delta(\hbar\omega + E_a - E_b) \qquad [4.138]$$

it may also be verified that the total absorption cross-section σ_{ba} (integrated over all angular frequencies ω) has the value previously found in [4.39].

[11] The second integral can be evaluated by using contour integration.

As the uncertainty principle suggests, a more complete treatment demonstrates that the width of a line from one excited level b to another excited level a is given by

$$\Gamma = \frac{\hbar}{\tau_a} + \frac{\hbar}{\tau_b} \qquad [4.139]$$

where τ_a and τ_b are the half-lives of each of the levels, taking into account all possible ways in which the levels can decay.

When the final state a is the ground state (in which case $\tau_a = \infty$) the width $\hbar/\tau_b$ is called the *natural width* of the level b. From Table 4.2 we see that the half-life of the 2p level of atomic hydrogen is 1.6×10^{-9} s, giving a width of $\Gamma \simeq 4.11 \times 10^{-7}$ eV $\simeq 3.32 \times 10^{-3}$ cm^{-1}. In general the natural widths of spectral lines are very small and are usually masked by other effects, which contribute to the broadening of spectral lines. Among the most important of these are the pressure broadening effect and the Doppler effect.

Pressure broadening

The atoms emitting or absorbing radiation in a gas undergo collisions. In each collision there is a certain probability that an atom initially in an excited state b will make a radiationless transition to a lower state, so that the lifetime of the excited state b will be decreased. If the number of collisions per second removing atoms from the state b is W_c, the total number of transitions out of the state b, per second, is $W_c + 1/\tau_b$, where τ_b is the natural lifetime of the state b. The total observed breadth of the line will then be

$$\Gamma = \hbar\left(W_c + \frac{1}{\tau_b}\right) \qquad [4.140]$$

The shape of the line remains Lorentzian. The number of collisions per second depends on the pressure of the gas, and this effect is therefore called pressure broadening. Thus, in order to observe experimentally the natural line width it is essential that the pressure in the spectral source should be low. By changing the pressure and observing the corresponding change in line width, information about the collisions occurring in a gas can be obtained.

Doppler broadening

The wavelength of the light emitted by a moving atom is shifted by the Doppler effect. If the gas atoms are moving at non-relativistic speeds, and the radiation is viewed in the X direction, the wavelength λ of light emitted by an atom with a component of velocity v_x in the x direction is

$$\lambda = \lambda_0\left(1 \pm \frac{v_x}{c}\right) \qquad [4.141]$$

where $\lambda_0 = c/\nu_0$ is the natural wavelength of the line and ν_0 the natural frequency. The plus sign in [4.141] corresponds to an atom receding from the observer and the minus sign to an atom approaching the observer. The frequency $\nu = c/\lambda$ of the light emitted by the moving atom is thus related to the natural frequency ν_0 by

$$\nu = \frac{\nu_0}{1 \pm \dfrac{v_x}{c}} \simeq \nu_0\left(1 \mp \frac{v_x}{c}\right) \qquad [4.142]$$

The Maxwellian velocity distribution of the gas atoms is

$$\mathrm{d}N(v_x) = N_0 \exp(-Mv_x^2/2kT)\,\mathrm{d}v_x \qquad [4.143]$$

where M is the atomic mass, k is Boltzmann's constant, T is the absolute temperature and N_0 is a constant.

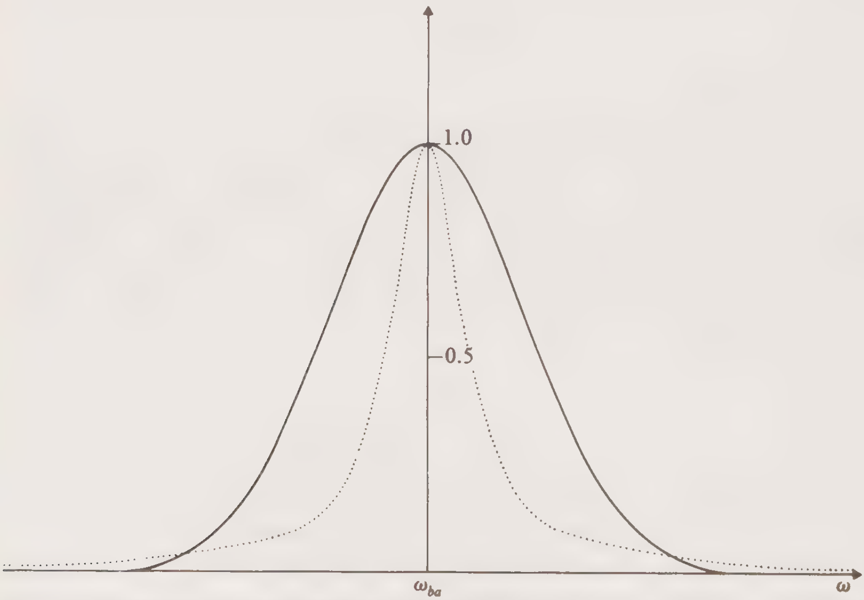

4.6 A comparison of a Gaussian distribution (solid line) of form $F(\omega) = \exp[-\alpha(\omega - \omega_{ba})^2]$, with a Lorentzian distribution (dotted line)

$$f(\omega) = \frac{\Gamma^2/4\hbar^2}{(\omega - \omega_{ba})^2 + \Gamma^2/4\hbar^2}$$

The intensity $\mathcal{I}(v)$ of light emitted in the frequency interval $(\nu, \nu + \mathrm{d}\nu)$, with ν close to ν_0, is proportional to the number of atoms emitting light of frequency between ν and $\nu + \mathrm{d}\nu$, i.e. having a velocity component v_x between v_x and $v_x + \mathrm{d}v_x$. Using [4.142] and [4.143], we then have

$$\mathcal{I}(\nu) = \mathcal{I}(\nu_0)\exp\left[-\frac{Mc^2}{2kT}\left(\frac{\nu - \nu_0}{\nu_0}\right)^2\right] \qquad [4.144]$$

The width $\Delta\nu$ of the curve $\mathcal{I}(v)$ at half-maximum is given by $2(\nu_0 - \nu_1)$, where ν_1 is the frequency at which the exponential is equal to 1/2. Thus

$$\Delta\nu = \frac{2\nu_0}{c}\left[\frac{2kT\log 2}{M}\right]^{1/2} \qquad [4.145]$$

This quantity is usually much greater than the natural width of the line. It is clear that since $\Delta\nu$ is proportional to $T^{1/2}$ one should work at low temperatures to decrease the importance of Doppler broadening. We also note from [4.145] that the Doppler broadening is proportional to the frequency ν_0 and inversely proportional to the square root of the atomic mass M.

Although pressure broadening does not alter the line shape, which remains Lorentzian, the Gaussian shape produced by the Doppler effect is quite different. However, the Gaussian decrease exhibited by [4.144] is so rapid that for $(\nu - \nu_0)$ greater than a few times the width $\Delta\nu$, the observed intensity is due to the 'tail' of the Lorentzian intensity distribution, as shown in Fig. 4.6.

4.8 THE PHOTOELECTRIC EFFECT

If electromagnetic radiation of sufficiently high frequency is absorbed by an atomic system A the final state may lie in the continuum and one or several electrons will be ejected from A. This is known as *photoionisation* and is the process responsible for the photoelectric effect (see Section 1.4).

In this section we shall obtain the cross-section for a particular (single) photoionisation process, in which the electron is ejected from a hydrogenic atom (ion). We assume that this atom (ion) is initially in the ground state (1s), described by the wave function $\psi_a(\mathbf{r}) \equiv \psi_{1s}(r)$ and having the energy E_{1s}. We denote by $E = h\nu = \hbar\omega$ the energy of the absorbed photon. Let $\mathbf{k}_f$ be the wave vector of the electron in the final state and $\mathbf{p}_f = \hbar\mathbf{k}_f$ its momentum. Assuming that the ejected electron is non-relativistic, its kinetic energy in the final state is given by $\hbar^2k_f^2/2m$, and energy conservation yields

$$\hbar\omega + E_{1s} = \frac{\hbar^2k_f^2}{2m} \qquad [4.146]$$

a relation which is valid in the non-relativistic regime, for which

$$\hbar\omega(\text{or } \hbar^2k_f^2/2m) \ll mc^2 \qquad [4.147]$$

The final state $\psi_b(\mathbf{k}_f, \mathbf{r})$ represents a continuum state corresponding to an electron with a wave vector $\mathbf{k}_f$ and a (positive) energy $\hbar^2k_f^2/2m$ moving in the field of a nucleus of charge Ze (which we assume to be infinitely heavy). Thus $\psi_b(\mathbf{k}_f, \mathbf{r})$ is a (positive energy) Coulomb wave function satisfying the equation

$$\left(-\frac{\hbar^2}{2m}\nabla^2 - \frac{Ze^2}{(4\pi\varepsilon_0)r} - \frac{\hbar^2k_f^2}{2m}\right)\psi_b(\mathbf{k}_f, \mathbf{r}) = 0 \qquad [4.148]$$

For sufficiently high energies of ejection (i.e. when $\hbar^2 k_f^2/2m \gg |E_{1s}|$) the interaction with the nucleus can be neglected and $\psi_b(\mathbf{k}_f, \mathbf{r})$ can be represented by a plane wave:

$$\psi_b(\mathbf{k}_f, \mathbf{r}) = V^{-1/2} e^{i\mathbf{k}_f \cdot \mathbf{r}} \qquad [4.149]$$

where we have normalised the system in a box of large volume V.

The photoelectric cross-section can be obtained from [4.39] by summing over the continuous states of the ejected electron, in a manner analogous to the one described in Section 2.8. Thus we find that

$$\sigma = \frac{4\pi^2 \alpha \hbar^2}{m^2 \omega} \tilde{\rho}_b \int |M_{ba}(\omega)|^2 \, d\Omega \qquad [4.150]$$

where $\Omega \equiv (\theta, \phi)$ denotes the angular coordinates of the ejected electron (see Fig. 4.7) and $\tilde{\rho}_b = (2\pi)^{-3} Vm\, k_f \hbar^{-1}$ is the density of final states (see Problem 4.11). The differential cross-section for an electron to be ejected within the solid angle $d\Omega$ in the direction (θ, ϕ) is therefore

$$\frac{d\sigma}{d\Omega} = (2\pi)^{-3} \frac{4\pi^2 \hbar \alpha}{m} \left(\frac{k_f}{\omega}\right) |V^{1/2} M_{ba}(\omega)|^2 \qquad [4.151]$$

From [4.33] and using [4.149] the matrix element M_{ba} is given by

$$M_{ba} = V^{-1/2} \int e^{-i\mathbf{k}_f \cdot \mathbf{r}} e^{i\mathbf{k} \cdot \mathbf{r}} \hat{\boldsymbol{\varepsilon}} \cdot \nabla \psi_{1s}(r) \, d\mathbf{r} \qquad [4.152]$$

Upon integration by parts, we find that

$$V^{1/2} M_{ba} = -i\hat{\boldsymbol{\varepsilon}} \cdot (\mathbf{k} - \mathbf{k}_f) \int e^{i(\mathbf{k} - \mathbf{k}_f) \cdot \mathbf{r}} \psi_{1s}(r) \, d\mathbf{r} \qquad [4.153]$$

Since $\mathbf{k} \cdot \hat{\boldsymbol{\varepsilon}} = 0$, we have

$$\hat{\boldsymbol{\varepsilon}} \cdot (\mathbf{k} - \mathbf{k}_f) = -k_f \cos \gamma \qquad [4.154]$$

where γ is the angle between the direction of ejection and the direction of polarisation (see Fig. 4.7). The integral appearing in [4.153] is proportional to the Fourier transform of the ground state wave function $\psi_{1s}(r)$, namely

$$\int e^{i\mathbf{K} \cdot \mathbf{r}} \psi_{1s}(r) \, d\mathbf{r} = 8\pi \left(\frac{Z^3}{\pi a_0^3}\right)^{1/2} \frac{Z/a_0}{[(Z/a_0)^2 + K^2]^2} \qquad [4.155]$$

where we have introduced the vector

$$\mathbf{K} = \mathbf{k} - \mathbf{k}_f \qquad [4.156]$$

From [4.151] and [4.153] – [4.156], the differential cross-section is seen to be given by

$$\frac{d\sigma}{d\Omega} = 32\alpha \left(\frac{\hbar}{m}\right) \left(\frac{k_f^3}{\omega}\right) \frac{Z^5 a_0^3 \cos^2 \gamma}{[Z^2 + K^2 a_0^2]^4} \qquad [4.157]$$

Without loss of generality we can take the direction of propagation, $\hat{\mathbf{k}}$, of the radiation to be along the Z axis and the direction of the polarisation vector $\hat{\varepsilon}$ to be the X direction. Then, as $\mathbf{k}_f$ is in the direction $\Omega \equiv (\theta, \phi)$, we have (see Fig. 4.7)

$$\cos \gamma = \sin \theta \cos \phi \qquad [4.158]$$

and

$$K^2 = k^2 + k_f^2 - 2k\, k_f \cos \theta \qquad [4.159]$$

At incident photon energies well in excess of the ionisation threshold ($\simeq$13.6 eV for atomic hydrogen), i.e. when $\hbar\omega \gg |E_{1s}|$, we have from [4.146]

$$\hbar\omega \simeq \frac{\hbar^2 k_f^2}{2m} \qquad [4.160]$$

so that

$$\frac{k}{k_f} \simeq \frac{\hbar k_f}{2mc} = \frac{v_f}{2c} \qquad [4.161]$$

where v_f is the velocity of the ejected electron. In the non-relativistic regime, for which $v_f/c \ll 1$, we use this result to write

$$K^2 \simeq k_f^2\left(1 - \frac{v_f}{c} \cos \theta\right) \qquad [4.162]$$

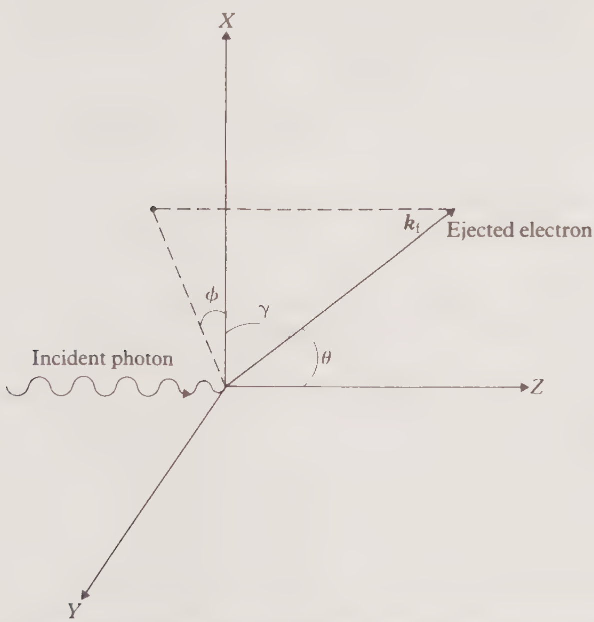

4.7 The angles employed in the discussion of the photoelectric effect. The incident radiation is in the Z direction, with polarisation vector in the X direction. The momentum of the ejected electron is $\hbar\mathbf{k}_f$.

Moreover, since $\hbar\omega \simeq \hbar^2 k_f^2/2m \gg |E_{1s}|$ and $E_{1s} = -Z^2(e^2/4\pi\varepsilon_0)/2a_0$, we have

$$k_f^2 a_0^2 \gg \frac{2m}{\hbar^2} |E_{1s}| a_0^2 = Z^2 \qquad [4.163]$$

so that

$$Z^2 + K^2 a_0^2 \simeq k_f^2 a_0^2 \left(1 - \frac{v_f}{c} \cos \theta\right) \qquad [4.164]$$

and the differential cross-section [4.157] reads

$$\frac{d\sigma}{d\Omega} = 32\alpha\left(\frac{\hbar}{m}\right) \frac{Z^5}{\omega(k_f a_0)^5} \frac{\sin^2 \theta \cos^2 \phi}{\left(1 - \frac{v_f}{c} \cos \theta\right)^4} \qquad [4.165]$$

We note that the ejected electrons have a cosine-squared distribution with respect to the polarisation vector $\hat{\varepsilon}$ of the incident radiation. For an *unpolarised* photon beam an average must be made over the polarisations of the photon, so that we have in that case

$$\left(\frac{d\sigma}{d\Omega}\right)_{\text{unpol}} = 16\alpha\left(\frac{\hbar}{m}\right) \frac{Z^5}{\omega(k_f a_0)^5} \frac{\sin^2 \theta}{\left(1 - \frac{v_f}{c} \cos \theta\right)^4} \qquad [4.166]$$

We remark that both cross-sections [4.165] and [4.166] exhibit a sine-squared distribution in the angle θ, which favours the ejection of the electrons at right angles to the incident photon beam. The quantity $(1 - v_f \cos \theta/c)^{-4}$ also affects the angular distribution, but since $v_f/c \ll 1$ it only yields a small correction to the $\sin^2 \theta$ distribution. In fact, since

$$\left(1 - \frac{v_f}{c} \cos \theta\right)^{-4} = 1 + 4\frac{v_f}{c} \cos \theta + \cdots \qquad [4.167]$$

we see that if we drop terms of order $(v_f/c)^2$ we may write the differential cross-section [4.166] as

$$\left(\frac{d\sigma}{d\Omega}\right)_{\text{unpol}} = 16\alpha\left(\frac{\hbar}{m}\right) \frac{Z^5}{\omega(k_f a_0)^5} \sin^2 \theta \left(1 + 4\frac{v_f}{c} \cos \theta\right) \qquad [4.168]$$

Upon integration over the angles (θ, ϕ) of the ejected electron, the total cross-section (for an unpolarised incident photon beam) is given by

$$\sigma = \frac{128\pi}{3} \alpha\left(\frac{\hbar}{m}\right) \frac{Z^5}{\omega(k_f a_0)^5} \qquad [4.169]$$

Using [4.160] and the fact that $E_{1s} = -Z^2(e^2/4\pi\varepsilon_0)/2a_0 = -(1/2)\, mc^2(Z\alpha)^2$, we may also write [4.169] as

$$\sigma = \frac{256\pi}{3} \alpha Z^{-2} \left(\frac{|E_{1s}|}{\hbar\omega}\right)^{7/2} a_0^2 \qquad [4.170]$$

or

$$\sigma = \frac{16\sqrt{2}\pi}{3}\alpha^8 Z^5 \left[\frac{mc^2}{\hbar\omega}\right]^{7/2} a_0^2 \qquad [4.171]$$

We note from [4.171] that the photoelectric cross-section σ decreases like $(\hbar\omega)^{-7/2}$ with increasing photon energy and increases like Z^5 with increasing nuclear charge. This formula can be applied not only to the ionisation of one-electron atoms and ions, but also (approximately) to the ejection of electrons from the inner shell of atoms by X-rays, although the dipole approximation worsens with increasing photon energy.

PROBLEMS

4.1 Calculate how many photons per second are radiated from a monochromatic source, 1 watt in power, for the following wavelengths (a) 10 m (radio wave) (b) 10 cm (microwave) (c) 5890 Å (yellow sodium light) (d) 1 Å (soft X-ray). At a distance of 10 m from the source, calculate the number of photons passing through unit area, normal to the direction of propagation, per unit time and the density of photons, in each case.

4.2 Show that the Schrödinger equation [4.17] representing a hydrogenic atom in an external electromagnetic field, can be transformed to the form

$$i\hbar\frac{\partial\Phi}{\partial t} = \left[-\frac{\hbar^2}{2m}\nabla^2 - \frac{Ze^2}{(4\pi\varepsilon_0)r} + e(\mathcal{E}\cdot\mathbf{r})\right]\Phi$$

provided the vector potential $\mathbf{A}$ does not vary over the atom (the electric dipole approximation) and where

$$\Psi = \Phi\exp\left[-\frac{ie}{\hbar}\mathbf{A}(t)\cdot\mathbf{r}\right] \quad \text{and} \quad \mathcal{E} = -\frac{\partial\mathbf{A}}{\partial t}.$$

4.3 Starting from the transformed Schrödinger equation of Problem 4.2 and taking $\mathcal{E} = 2\omega A_0 \sin(\omega t)$, use first-order perturbation theory to obtain the transition rate for absorption in the electric dipole approximation given by [4.66].

4.4 (a) Establish the result [4.69] starting from equation [4.67].

(b) The full transition rate for spontaneous emission of a photon from an atom is obtained from [4.70], by integrating over all angles of emission and summing over two independent polarisation directions $\hat{\boldsymbol{\varepsilon}}_1$, $\hat{\boldsymbol{\varepsilon}}_2$:

$$W_{ab}^{s} = \frac{1}{2\pi\hbar c^2}\left(\frac{e^2}{4\pi\varepsilon_0}\right)\omega_{ba}^3\int d\Omega\,\{|\hat{\boldsymbol{\varepsilon}}_1\cdot\mathbf{r}_{ba}|^2 + |\hat{\boldsymbol{\varepsilon}}_2\cdot\mathbf{r}_{ba}|^2\}$$

Starting from this expression obtain the result [4.71].

4.5 Generalise the results of Section 4.4 to the case in which the level E_a is g_a times degenerate and the level E_b is g_b times degenerate, and show that the Einstein coefficients satisfy the relations

$$g_a B_{ba} = g_b B_{ab}; \qquad A_{ab} = \frac{\hbar \omega_{ba}^3}{\pi^2 c^3} B_{ab}$$

4.6 Obtain the explicit forms of the coefficients $\mathscr{A}(l, m; l', m'; q)$, either by using a table of Clebsch–Gordan coefficients, or by using the recurrence relations [4.93].

4.7 Show that

$$\sum_{m'} |\mathscr{A}(l, m; l', m'; m' - m)|^2 = \frac{3}{4\pi} \frac{l+1}{2l+1}$$

if $l' = l + 1$ and

$$\sum_{m'} |\mathscr{A}(l, m; l', m'; m' - m)|^2 = \frac{3}{4\pi} \left(\frac{l}{2l+1}\right)$$

if $l' = (l - 1)$; find the transition rate for absorption of unpolarised isotropic radiation by a hydrogenic atom from a level (nl) to the $(2l' + 1)$ degenerate levels $(n'l')$ and show that it is independent of the magnetic quantum number of the initial sublevel.

4.8 Show that the matrix element $\tilde{M}_{ba}$ given by [4.105], can be obtained from [4.33] and deduce [4.106].

4.9 Calculate the oscillator strength for the $2p \to 1s$ transition in a hydrogenic atom, and find the half-life of the 2p level, checking the answer against Table 4.1.

4.10 For a given initial level a, of a hydrogen atom, show that

$$\sum_b \sigma_{ba} - \sum_b{}' \bar{\sigma}_{ba} = 2\pi^2 r_0 c,$$

where σ_{ba} is the absorption cross-section, in the electric dipole approximation, and the sum Σ_b is over all states (including continuum states) with $E_b > E_a$, and $\bar{\sigma}_{ba}$ is the corresponding cross-section for stimulated emission and the sum Σ_b' is over all states with $E_b < E_a$. On the right-hand side r_0 is the classical electron radius, $r_0 = e^2/(4\pi\varepsilon_0 mc^2)$.

4.11 Show that the number of states of a free electron moving in a direction (θ, ϕ) within a solid angle $d\Omega$ in a large cubical box of volume V, with energy between E and $E + dE$ is given by

$$\rho_b(E)\, d\Omega = (2\pi)^{-3}\, V\, mk\, d\Omega/\hbar^2$$

where $E = \hbar^2 k^2/2m$. In terms of the angular frequency $\omega = E/\hbar$ we have $\tilde{\rho}(\omega)\, d\omega = \rho(E)\, dE = \hbar\rho(E)\, d\omega$

5 One-electron atoms: fine structure, hyperfine structure and interaction with external electric and magnetic fields

Our discussion of the energy levels and wave functions of one-electron atoms in Chapter 3 was based on the simple, non-relativistic Hamiltonian

$$H = \frac{p^2}{2\mu} - \frac{Ze^2}{(4\pi\varepsilon_0)r} \qquad [5.1]$$

where the first term represents the (non-relativistic) kinetic energy of the atom in the centre of mass system, and the second term is the electrostatic (Coulomb) interaction between the electron and the nucleus. Although the energy levels obtained in Chapter 3 from the Hamiltonian [5.1] are in good qualitative agreement with experiment, the very precise measurements carried out in atomic physics demonstrate the existence of several effects which cannot be derived from the Hamiltonian [5.1] and require the addition of correction terms to [5.1]. In this chapter we shall discuss several of these corrections and we shall also consider the problem of the interaction of one-electron atoms with external (static) electric and magnetic fields.

We begin by analysing the relativistic corrections to [5.1], which give rise to a splitting of the energy levels known as fine structure. Next, we discuss the effect of an external magnetic field (the Zeeman effect) or electric field (the Stark effect) on the spectra of one-electron atoms. We then describe a subtle effect called the Lamb shift, which displaces certain of the fine structure components and is therefore responsible for additional splittings of the energy levels. Finally, we consider various small corrections such as the hyperfine structure splitting and the volume effect, which take into account the fact that the nucleus is not simply a point charge, but has a finite size, and may possess an intrinsic angular momentum (spin), a magnetic dipole moment, an electric quadrupole moment, and so on.

5.1 FINE STRUCTURE OF HYDROGENIC ATOMS

The fine structure of the energy levels of hydrogenic atoms is due to relativistic effects. In order to analyse these effects we therefore need for the electron a basic wave equation which satisfies the requirements of special relativity as well as those of quantum mechanics. This is the Dirac equation, which is discussed briefly in Appendix 7, and which provides the correct relativistic wave equation for electrons.

The most rigorous way of obtaining the relativistic corrections to the Schrödinger (Bohr) energy levels of one-electron atoms is to solve the Dirac equation for an electron in the central field $V(r) = -Ze^2/(4\pi\varepsilon_0)r$ of the nucleus which is assumed to be of infinite mass and at the origin of the coordinates. It turns out that the Dirac equation for a central field can be separated in spherical polar coordinates and that the resulting radial equations can be solved exactly for the Coulomb potential $V(r) = -Ze^2/(4\pi\varepsilon_0)r$ [1]. However, these calculations are rather lengthy and since the relativistic corrections are very small (provided that Z is not too large), it is convenient to use perturbation theory, keeping terms up to order v^2/c^2 in the Dirac Hamiltonian. We shall therefore start from the Hamiltonian [A7.65] of Appendix 7 which we rewrite as

$$H = H_0 + H' \tag{5.2}$$

where

$$H_0 = \frac{p^2}{2m} - \frac{Ze^2}{(4\pi\varepsilon_0)r} \tag{5.3}$$

is simply the Hamiltonian [5.1] with $\mu = m$ [2] and

$$H' = H'_1 + H'_2 + H'_3 \tag{5.4}$$

with

$$H'_1 = -\frac{p^4}{8m^3c^2} \tag{5.5}$$

$$H'_2 = \frac{1}{2m^2c^2}\frac{1}{r}\frac{\mathrm{d}V}{\mathrm{d}r}\mathbf{L}\cdot\mathbf{S} \tag{5.6}$$

and

$$H'_3 = \frac{\pi\hbar^2}{2m^2c^2}\left(\frac{Ze^2}{4\pi\varepsilon_0}\right)\delta(\mathbf{r}) \tag{5.7}$$

The physical interpretation of the three terms which constitute H' is discussed in Appendix 7. We simply note here that H'_1 is a relativistic correction to the kinetic energy, H'_2 represents the spin-orbit interaction and H'_3 is the Darwin term.

Before we proceed to the evaluation of the energy shifts due to these three terms by using perturbation theory, we remark that the Schrödinger theory

[1] See for example Bethe and Salpeter (1957).

[2] For the sake of simplicity we shall ignore all reduced mass effects in discussing the fine structure calculations. It is of course straightforward to incorporate the reduced mass effect in H_0 and in the corresponding unperturbed energy levels E_n by replacing the electron mass m by its reduced mass μ. On the other hand, the reduced mass effects arising in H' cannot be obtained by just replacing m by μ in the results of the perturbation calculation. Fortunately, these latter reduced mass effects are very small since H' is already a correction to H_0.

discussed in Chapter 3 does not include the spin of the electron. In order to calculate corrections involving the spin operator – such as those arising from H'_2 – we start from the 'unperturbed' equation

$$H_0\psi_{nlm_lm_s} = E_n\psi_{nlm_lm_s} \tag{5.8}$$

where E_n are the Schrödinger eigenvalues [3.29] (with $\mu = m$) and the zero order wave functions $\psi_{nlm_lm_s}$ are modified (two-component) Schrödinger wave functions (also referred to as Pauli wave functions or 'spin-orbitals') given by

$$\psi_{nlm_lm_s}(q) = \psi_{nlm_l}(\mathbf{r})\chi_{1/2,m_s} \tag{5.9}$$

where q denotes the space and spin coordinates collectively. The quantum number m_l which can take the values $-l, -l+1, \ldots, +l$ is the magnetic quantum number previously denoted by m [3], $\psi_{nlm_l}(\mathbf{r})$ is a one-electron Schrödinger wave function (see [3.48]) such that

$$H_0\psi_{nlm_l}(\mathbf{r}) = E_n\psi_{nlm_l}(\mathbf{r}) \tag{5.10}$$

and $\chi_{1/2,m_s}$ are the spin eigenfunctions for spin one-half ($s = 1/2$) introduced in Section 2.5, with $m_s = \pm 1/2$. We recall that $\chi_{1/2,m_s}$ is a two-component spinor and that the normalised spinors corresponding respectively to 'spin up' ($m_s = +1/2$) and 'spin down' ($m_s = -1/2$) are conveniently denoted by

$$\alpha \equiv \begin{pmatrix} 1 \\ 0 \end{pmatrix} \quad \text{and} \quad \beta \equiv \begin{pmatrix} 0 \\ 1 \end{pmatrix} \tag{5.11}$$

Since H_0 does not act on the spin variable the two-component wave functions [5.9] are separable in space and spin variables. It is also worth noting that we now have *four* quantum numbers (n, l, m_l, m_s) to describe a one-electron atom, the effect of the spin on the 'unperturbed' solutions being to double the degeneracy, so that each Schrödinger energy level E_n is now $2n^2$ degenerate.

Energy shifts

We now calculate the energy corrections due to the three terms [5.5]–[5.7], using the Pauli wave functions as our zero-order wave functions.

1. $H'_1 = -\dfrac{p^4}{8m^3c^2}$ (*relativistic correction to the kinetic energy*)

Since the unperturbed energy level E_n is $2n^2$ degenerate, we should use the degenerate perturbation theory discussed in Section 2.8. However, we first note that H'_1 does not act on the spin variable. Moreover, it commutes with the components of the orbital angular momentum (see Problem 2.12) so that the

[3] When no confusion is possible, we shall continue to write m instead of m_l for the magnetic quantum number associated with the operator L_z.

perturbation H_1' is already 'diagonal' in l, m_l and m_s. The energy correction ΔE_1 due to H_1' is therefore given in first-order perturbation theory by

$$\begin{aligned}\Delta E_1 &= \left\langle \psi_{nlm_lm_s} \left| -\frac{p^4}{8m^3c^2} \right| \psi_{nlm_lm_s} \right\rangle \\ &= \left\langle \psi_{nlm_l} \left| -\frac{p^4}{8m^3c^2} \right| \psi_{nlm_l} \right\rangle \\ &= -\frac{1}{2mc^2} \langle \psi_{nlm_l} | T^2 | \psi_{nlm_l} \rangle \end{aligned} \qquad [5.12]$$

where $T = p^2/2m$ is the kinetic energy operator. From [5.3] we have

$$T = H_0 + \frac{Ze^2}{(4\pi\varepsilon_0)r} \qquad [5.13]$$

and therefore

$$\begin{aligned}\Delta E_1 &= -\frac{1}{2mc^2} \left\langle \psi_{nlm_l} \left| \left(H_0 + \frac{Ze^2}{(4\pi\varepsilon_0)r} \right) \left(H_0 + \frac{Ze^2}{(4\pi\varepsilon_0)r} \right) \right| \psi_{nlm_l} \right\rangle \\ &= -\frac{1}{2mc^2} \left[E_n^2 + 2E_n \left(\frac{Ze^2}{4\pi\varepsilon_0} \right) \left\langle \frac{1}{r} \right\rangle_{nlm_l} + \left(\frac{Ze^2}{4\pi\varepsilon_0} \right)^2 \left\langle \frac{1}{r^2} \right\rangle_{nlm_l} \right] \end{aligned} \qquad [5.14]$$

where we have used [5.10]. From the results [3.30], [3.71] and [3.72] (with $\mu = m$) we finally obtain

$$\begin{aligned}\Delta E_1 &= -\frac{1}{2mc^2} \left\{ \left[\frac{mc^2(Z\alpha)^2}{2n^2} \right]^2 - 2\left(\frac{Ze^2}{4\pi\varepsilon_0} \right) \frac{mc^2(Z\alpha)^2}{2n^2} \frac{Z}{a_0 n^2} \right. \\ &\qquad \left. + \left(\frac{Ze^2}{4\pi\varepsilon_0} \right)^2 \frac{Z^2}{a_0^2 n^3 (l + 1/2)} \right\} \\ &= \frac{1}{2} mc^2 \frac{(Z\alpha)^2}{n^2} \frac{(Z\alpha)^2}{n^2} \left[\frac{3}{4} - \frac{n}{l + 1/2} \right] \\ &= -E_n \frac{(Z\alpha)^2}{n^2} \left[\frac{3}{4} - \frac{n}{l + 1/2} \right] \end{aligned} \qquad [5.15]$$

2. $H_2' = \dfrac{1}{2m^2c^2} \dfrac{1}{r} \dfrac{dV}{dr} \mathbf{L} \cdot \mathbf{S}$ ***(spin–orbit term)***

We shall first rewrite this term more simply as

$$H_2' = \xi(r) \mathbf{L} \cdot \mathbf{S} \qquad [5.16]$$

where we have introduced the quantity

$$\xi(r) = \frac{1}{2m^2c^2} \frac{1}{r} \frac{dV}{dr} \qquad [5.17]$$

In our case $V(r) = -Ze^2/(4\pi\varepsilon_0)r$, so that

$$\xi(r) = \frac{1}{2m^2c^2}\frac{Ze^2}{4\pi\varepsilon_0}\frac{1}{r^3} \tag{5.18}$$

Since the operator $\mathbf{L}^2$ does not act on the radial variable r nor on the spin variable, and commutes with the components of $\mathbf{L}$, we see from [5.16] that $\mathbf{L}^2$ commutes with H_2'. It follows that the perturbation H_2' does not connect states with different values of the orbital angular momentum l. For a given value of n and l there are $2(2l + 1)$ degenerate eigenstates of H_0 (the factor of 2 arising from the two spin states), so that the calculation of the energy shift due to H_2' requires the diagonalisation of $2(2l + 1) \times 2(2l + 1)$ submatrices.

This diagonalisation is greatly simplified by using for the zero-order wave functions a representation in which $\mathbf{L} \cdot \mathbf{S}$ is diagonal. It is clear that the functions $\psi_{nlm_lm_s}$ given by [5.9], which are simultaneous eigenfunctions of the operators H_0, $\mathbf{L}^2$, $\mathbf{S}^2$, L_z and S_z are not adequate because $\mathbf{L} \cdot \mathbf{S}$ does not commute with L_z or S_z. However, we shall now show that satisfactory zero-order wave functions may be obtained by forming certain linear combinations of the functions $\psi_{nlm_lm_s}$. To this end, we introduce the total angular momentum of the electron

$$\mathbf{J} = \mathbf{L} + \mathbf{S} \tag{5.19}$$

and we note that

$$\mathbf{J}^2 = \mathbf{L}^2 + 2\mathbf{L} \cdot \mathbf{S} + \mathbf{S}^2 \tag{5.20}$$

so that

$$\mathbf{L} \cdot \mathbf{S} = \tfrac{1}{2}(\mathbf{J}^2 - \mathbf{L}^2 - \mathbf{S}^2) \tag{5.21}$$

Consider now wave functions ψ_{nljm_j} which are eigenstates of the operators H_0, $\mathbf{L}^2$, $\mathbf{S}^2$, $\mathbf{J}^2$ and $\mathcal{J}_z$, the corresponding eigenvalues being E_n, $l(l + 1)\hbar^2$, $s(s + 1)\hbar^2$, $j(j + 1)\hbar^2$ and $m_j\hbar$. In this particular case we have $s = 1/2$ and therefore (see Section 2.5)

$$\begin{aligned} j &= l \pm 1/2, \qquad l \neq 0 \\ j &= 1/2, \qquad\quad\; l = 0 \end{aligned} \tag{5.22}$$

and

$$m_j = -j, -j + 1, \ldots + j \tag{5.23}$$

By using the methods of Section 2.5 and Appendix 4, we can form the functions ψ_{nljm_j} from linear combinations of the functions $\psi_{nlm_lm_s}$ [4]. Since $\mathbf{L} \cdot \mathbf{S}$ commutes with $\mathbf{L}^2$, $\mathbf{S}^2$, $\mathbf{J}^2$ and $\mathcal{J}_z$ it is apparent that the new zero-order wave functions ψ_{nljm_j} form a satisfactory basis set in which the operator $\mathbf{L} \cdot \mathbf{S}$ (and

[4] Specifically, if we use the Dirac notation so that the ket $|nlsm_lm_s\rangle$ corresponds to the wave function $\psi_{nlm_lm_s}$ and the ket $|nlsjm_j\rangle$ to the wave function ψ_{nljm_j} (with $s = 1/2$), we have

$$|nlsjm_j\rangle = \sum_{m_l, m_s} \langle lsm_lm_s|jm_j\rangle\, |nlsm_lm_s\rangle$$

The Clebsch–Gordan coefficients $\langle lsm_lm_s|jm_j\rangle$ are not needed in the present calculation since we are only interested in expectation values.

hence the perturbation H_2') is diagonal. Using [5.16] and [5.21], we see that for $l = 0$ the energy shift due to the term H_2' is given by

$$\begin{aligned}\Delta E_2 &= \left\langle \psi_{nljm_j} \left| \frac{1}{2}\,\xi(r)[\mathbf{J}^2 - \mathbf{L}^2 - \mathbf{S}^2] \right| \psi_{nljm_j} \right\rangle \\ &= \frac{\hbar^2}{2}\langle \xi(r) \rangle \left[j(j+1) - l(l+1) - \frac{3}{4} \right] \qquad [5.24]\end{aligned}$$

where $\langle \xi(r) \rangle$ denotes the average value of $\xi(r)$ in the state ψ_{nljm_j}. From [5.17] and [3.73], we have

$$\begin{aligned}\langle \xi(r) \rangle &= \frac{1}{2m^2c^2}\left(\frac{Ze^2}{4\pi\varepsilon_0}\right)\left\langle \frac{1}{r^3} \right\rangle \\ &= \frac{1}{2m^2c^2}\left(\frac{Ze^2}{4\pi\varepsilon_0}\right)\frac{Z^3}{a_0^3 n^3 l(l+1/2)(l+1)} \qquad [5.25]\end{aligned}$$

Thus, for $l \neq 0$, we obtain from [5.24] and [5.25]

$$\begin{aligned}\Delta E_2 &= \frac{mc^2(Z\alpha)^4}{4n^3 l(l+1/2)(l+1)} \times \begin{cases} l & \text{for } j = l + 1/2 \\ -l-1 & \text{for } j = l - 1/2 \end{cases} \\ &= -E_n \frac{(Z\alpha)^2}{2nl(l+1/2)(l+1)} \times \begin{cases} l & \text{for } j = l + 1/2 \\ -l-1 & \text{for } j = l - 1/2 \end{cases} \qquad [5.26]\end{aligned}$$

For $l = 0$ the spin–orbit interaction [5.16] vanishes and therefore $\Delta E_2 = 0$ in that case.

3. $H_3' = \dfrac{\pi\hbar^2}{2m^2c^2}\left(\dfrac{Ze^2}{4\pi\varepsilon_0}\right)\delta(\mathbf{r})$ (*Darwin term*)

This term does not act on the spin variable, is diagonal in l, m_l and m_s and applies only to the case $l = 0$. Calling ΔE_3 the corresponding energy correction and using the result [3.60], we have

$$\begin{aligned}\Delta E_3 &= \frac{\pi\hbar^2}{2m^2c^2}\frac{Ze^2}{4\pi\varepsilon_0}\langle \psi_{n00}|\delta(\mathbf{r})|\psi_{n00}\rangle \\ &= \frac{\pi\hbar^2}{2m^2c^2}\frac{Ze^2}{4\pi\varepsilon_0}|\psi_{n00}(0)|^2 \\ &= \frac{1}{2}mc^2\frac{(Z\alpha)^2}{n^2}\frac{(Z\alpha)^2}{n} \\ &= -E_n\frac{(Z\alpha)^2}{n}, \qquad l = 0 \qquad [5.27]\end{aligned}$$

We may now combine the effects of H_1', H_2' and H_3' to obtain the total energy shift $\Delta E = \Delta E_1 + \Delta E_2 + \Delta E_3$ due to relativistic corrections. From [5.15],

[5.26] and [5.27] we have for all l

$$\Delta E_{nj} = -\frac{1}{2} mc^2 \frac{(Z\alpha)^2}{n^2} \frac{(Z\alpha)^2}{n^2} \left(\frac{n}{j + 1/2} - \frac{3}{4} \right)$$
$$= E_n \frac{(Z\alpha)^2}{n^2} \left(\frac{n}{j + 1/2} - \frac{3}{4} \right) \qquad [5.28]$$

where the subscripts nj indicate that the correction depends on both the principal quantum number n and the total angular momentum quantum number j, with $j = 1/2, 3/2, \ldots n - 1/2$. To each value of j correspond two possible values of l given by $l = j \pm 1/2$, except for $j = n - 1/2$ where one can only have $l = j - 1/2 = n - 1$.

Adding the relativistic correction ΔE_{nj} to the non-relativistic energies E_n, we find that the energy levels of one-electron atoms are now given by

$$E_{nj} = E_n \left[1 + \frac{(Z\alpha)^2}{n^2} \left(\frac{n}{j + 1/2} - \frac{3}{4} \right) \right] \qquad [5.29]$$

so that the binding energy $|E_{nj}|$ of the electron is slightly increased with respect to the non-relativistic value $|E_n|$, the absolute value $|\Delta E_{nj}|$ of the energy shift becoming smaller as n or j increases, and larger as Z increases. The formula [5.29] is easily shown to agree through order $(Z\alpha)^2$ with the result

$$E_{nj}^{\text{exact}} = mc^2 \left\{ \left[1 + \frac{Z\alpha}{n - j - 1/2 + [(j + 1/2)^2 - Z^2\alpha^2]^{1/2}} \right]^{-1/2} - 1 \right\} \qquad [5.30]$$

obtained by solving the Dirac equation for the potential $V(r) = -Ze^2/(4\pi\varepsilon_0)r$ [1]

Fine structure splitting

Starting from non-relativistic energy levels E_n which are $2n^2$ times degenerate (the factor of two arising from the spin) we see that in the Dirac theory this degeneracy is partly removed. In fact, a non-relativistic energy level E_n depending only on the principal quantum number n splits into n different levels in the Dirac theory, one for each value $j = 1/2, 3/2, \ldots n - 1/2$ of the total angular momentum quantum number j. This splitting is called *fine structure splitting*, and the n levels $j = 1/2, 3/2, \ldots n - 1/2$ are said to form a *fine structure multiplet*. We note that the dimensionless constant $\alpha \simeq 1/137$ controls the scale of the splitting, and it is for this reason that it has been called the fine structure constant.

The fine structure splitting of the energy levels corresponding to $n = 1, 2, 3$ is illustrated in Fig. 5.1. We have used in that figure the spectroscopic notation

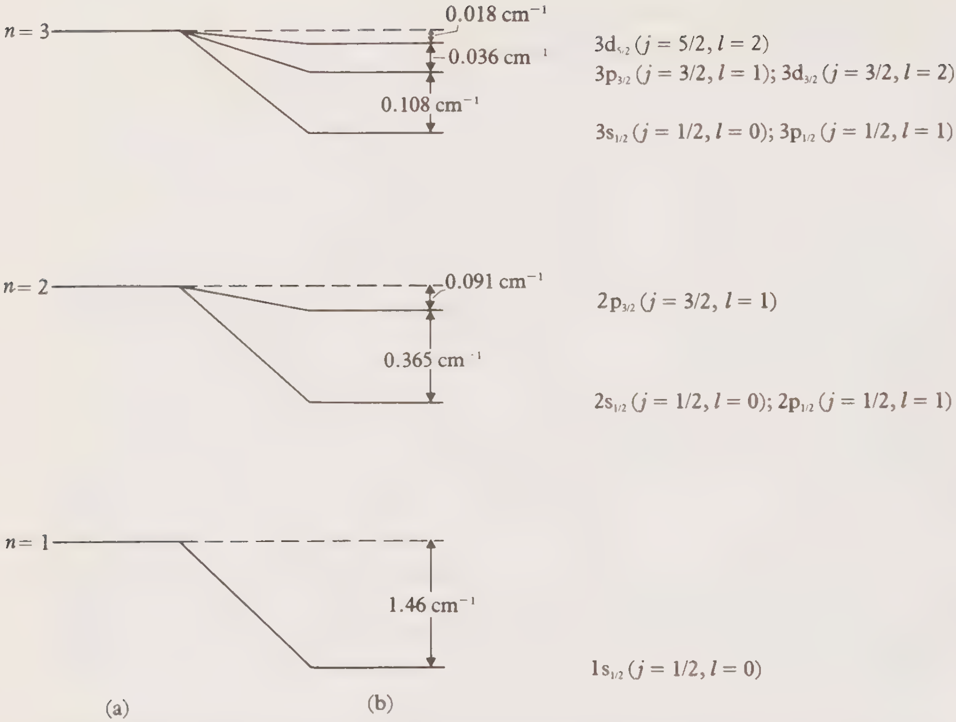

5.1 Fine structure of the hydrogen atom. The non-relativistic levels are shown on the left in column (a) and the split levels on the right in column (b), for $n = 1$, 2 and 3. For clarity, the scale in each diagram is different.

nl_j (with the usual association of the letters s, p, d, . . . with the values $l = 0, 1, 2, \ldots$ and an additional subscript for the value of j) to distinguish the various spectral terms corresponding to the Dirac theory [5].

It is important to emphasise that in Dirac's theory two states having the same value of the quantum number n and j but with values of l such that $l = j \pm 1/2$ have the same energy. The *parity* of the solutions is still given by $(-)^l$. Thus to each value of j correspond two series of $(2j + 1)$ solutions of opposite parity, except for $j = n - 1/2$ where there is only one series of solutions of parity $(-)^{n-1}$. It is also worth remarking that although the three separate contributions ΔE_1, ΔE_2 and ΔE_3 depend on l (see [5.15], [5.26] and [5.27]), the total energy shift ΔE_{nj} (given by [5.28]) does not! This is illustrated in Fig. 5.2, where we show the splitting of the $n = 2$ levels of atomic hydrogen due to each of the three terms H_1', H_2' and H_3', as well as the resulting degeneracy of the $2s_{1/2}$ and $2p_{1/2}$ levels. We shall see in Section 5.4 that this degeneracy of the levels with $l = j \pm 1/2$ is actually removed by small quantum electrodynamics effects,

[5] A similar notation with capital letters, such as $1S_{1/2}$, $2S_{1/2}$, $2P_{1/2}$, $2P_{3/2}$, etc., is also frequently used. We shall reserve capital letters for atomic systems with more than one electron.

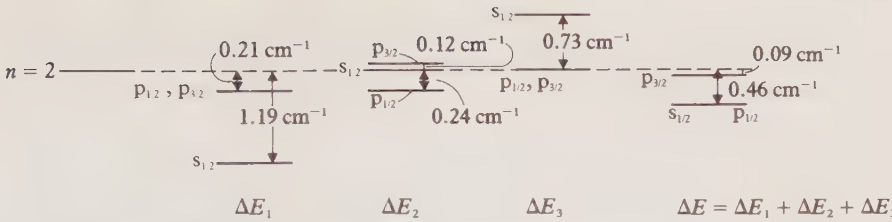

5.2 The contributions ΔE_1, ΔE_2, ΔE_3 to the splitting of the $n = 2$ level of hydrogen.

known as radiative corrections, which are responsible for additional energy shifts called Lamb shifts.

Another interesting point is that the three relativistic energy shifts ΔE_1, ΔE_2 and ΔE_3 we have obtained above have the same order of magnitude, and must therefore be treated together. This is a special feature of hydrogenic atoms. For many-electron atoms (and in particular for alkali atoms) we shall see in Chapter 7 that it is the spin–orbit effect (due here to the term H'_2) which is mainly responsible for the fine structure splitting.

According to [5.28], for any Z and $n \neq 1$, the energy difference between the two extreme components of a fine structure multiplet (corresponding respectively to the values $j_1 = n - 1/2$ and $j_2 = 1/2$) is given by

$$\delta E(j_1 = n - 1/2, j_2 = 1/2) = |E_n|(Z\alpha)^2 \frac{n-1}{n^2}$$

$$= \frac{\alpha^2 Z^4 (n-1)}{2n^4} \quad \text{a.u.}, \quad n \neq 1 \qquad [5.31]$$

We may also use [5.28] to obtain for any Z, $n \neq 1$ and $l \neq 0$ the energy separation between two levels corresponding respectively to $j_1 = l + 1/2$ and $j_2 = l - 1/2$. The result is

$$\delta E(j_1 = l + 1/2, j_2 = l - 1/2) = |E_n| \frac{(Z\alpha)^2}{nl(l+1)}$$

$$= \frac{\alpha^2 Z^4}{2n^3 l(l+1)} \quad \text{a.u.} \qquad [5.32]$$

For example, in the case of atomic hydrogen the splitting of the levels $j = 3/2$ and $j = 1/2$ for $n = 2$ and $n = 3$ is, respectively, 0.365 cm^{-1} (4.52×10^{-5} eV) and 0.108 cm^{-1} (1.34×10^{-5} eV), while the splitting of the levels $j = 5/2$ and $j = 3/2$ for $n = 3$ is 0.036 cm^{-1} (4.48×10^{-6} eV) as shown in Fig. 5.1.

Fine structure of spectral lines

The set of *spectral lines* due to the transitions $nlj \to n'l'j'$ between the fine structure components of the levels nl and $n'l'$ is known as a *multiplet* of lines.

Since the electric dipole operator $\mathbf{D} = -e\mathbf{r}$ does not depend on the spin, the selection rule derived in Chapter 4 for the quantum number l (in the dipole approximation) remains

$$\Delta l = \pm 1 \tag{5.33}$$

from which it follows that the selection rule with respect to the quantum number j is

$$\Delta j = 0, \pm 1 \tag{5.34}$$

Using [5.33] and [5.34], it is a simple matter to establish the character of the fine structure splitting of the hydrogenic atom spectral lines. For example, we see from Fig. 5.3 that the multiplet np–n's has two components. Thus each line of the Lyman series (lower state $n = 1$) is split by the fine structure into a pair of lines called a *doublet*, corresponding to the transitions

$$n\mathrm{p}_{1/2}\text{–}1\mathrm{s}_{1/2}, \qquad n\mathrm{p}_{3/2}\text{–}1\mathrm{s}_{1/2}$$

This is illustrated in Fig. 5.4 for the Lyman α line (upper state $n = 2$).

Referring to Fig. 5.3, we see that the multiplet np–n's has two components, while the multiplet nd–n'p has three components. Thus, in the case of the Balmer series (lower state $n = 2$) the following seven transitions are allowed:

$$\begin{array}{ll} n\mathrm{p}_{1/2}\text{–}2\mathrm{s}_{1/2}, & n\mathrm{p}_{3/2}\text{–}2\mathrm{s}_{1/2} \\ n\mathrm{s}_{1/2}\text{–}2\mathrm{p}_{1/2}, & n\mathrm{s}_{1/2}\text{–}2\mathrm{p}_{3/2} \\ n\mathrm{d}_{3/2}\text{–}2\mathrm{p}_{1/2}, & n\mathrm{d}_{3/2}\text{–}2\mathrm{p}_{3/2}, \\ \multicolumn{2}{c}{n\mathrm{d}_{5/2}\text{–}2\mathrm{p}_{3/2}} \end{array}$$

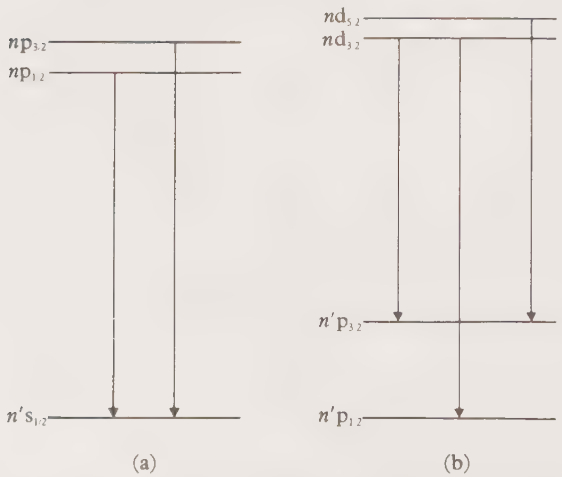

5.3 Allowed transitions in (a) the multiplet np –n's and (b) nd–n'p.

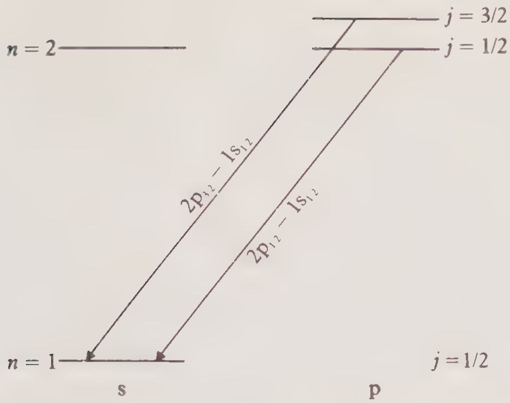

5.4 Allowed transitions between the $n = 2$ and $n = 1$ levels of atomic hydrogen giving rise to the Lyman alpha doublet (L_α).

However, since the levels $ns_{1/2}$ and $np_{1/2}$ coincide, as well as the levels $np_{3/2}$ and $nd_{3/2}$, each Balmer line only contains five distinct components. This is illustrated in Fig. 5.5 for the case of the fine structure of the H_α line, i.e. the red line of the Balmer series at 6563 Å, corresponding to the transition between the upper state $n = 3$ and the lower state $n = 2$.

Because the energy differences [5.31] or [5.32] rapidly decrease with increasing n, the fine structure splitting of a spectral line corresponding to a transition between two levels of different n is mainly due to the fine structure of the *lower* level, with additional (finer) fine structure arising from the smaller splitting of the upper level. For example, each line of the Balmer series essentially consists of a *doublet*, or more precisely of *two groups* of closely spaced lines. The distance between these two groups is approximately given by the fine structure splitting of the lower ($n = 2$) level (i.e. about 0.365 cm^{-1}) and this distance is constant for all the lines of the series. Within each of the two groups the magnitude of the (small) residual splitting due to the fine structure of the upper level rapidly falls off as n increases, i.e. as one goes to higher lines of the series. Similarly, each line of the Paschen series (lower state $n = 3$) consists of *three groups* of closely spaced lines, etc. Finally, we remark that for hydrogenic ions the fine structure splitting is more important than for hydrogen since the energy shift ΔE_{nj} given by [5.28] is proportional to Z^4.

Intensities of fine structure lines

Since the radial integrals in [4.85] are the same for both the transitions $np_{3/2}$–$n's_{1/2}$ and $np_{1/2}$–$n's_{1/2}$, it is easy to obtain from the angular parts of those integrals (that is from angular momentum considerations) the ratio of the two transition probabilities, which is found to be equal to 2 (Problem 5.1). More generally, the ratios of the transition probabilities for the most important special

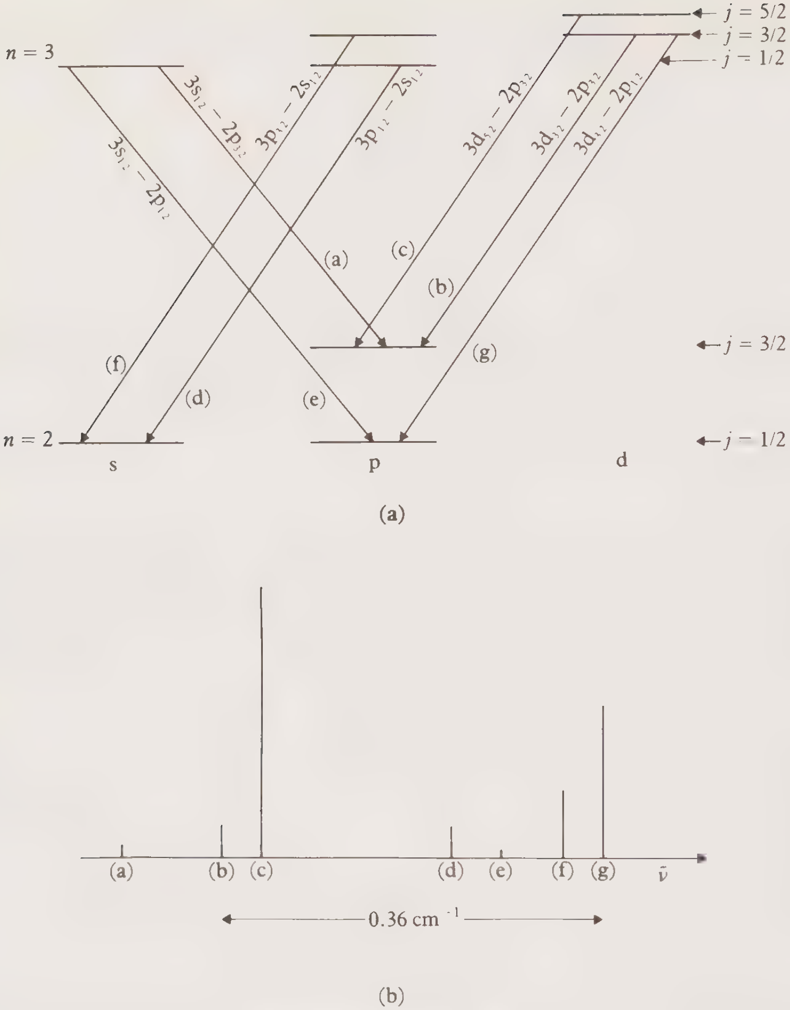

5.5 (a) Transitions contributing to the Balmer alpha (H_α) line between the $n = 3$ and $n = 2$ levels of atomic hydrogen.
(b) The relative intensities of the lines (a), (b)–(g). Note that (b) and (g) have the same upper level, so that the wave number difference between the lines is determined by the $2p_{1/2}$, $2p_{3/2}$ energy difference and is $0.36\ cm^{-1}$. In the same way, the wave number difference between lines (a) and (e) is also $0.36\ cm^{-1}$. We note that the lines (d) and (e) should coincide according to Dirac theory, as well as the lines (f) and (g).

cases are (Bethe and Salpeter, 1957)

$$\begin{aligned}\text{for}\quad &\text{sp transitions: } \mathrm{s}_{1/2}\text{–}\mathrm{p}_{3/2} : \mathrm{s}_{1/2}\text{–}\mathrm{p}_{1/2} = 2:1\\ &\text{pd transitions: } \mathrm{p}_{3/2}\text{–}\mathrm{d}_{5/2} : \mathrm{p}_{3/2}\text{–}\mathrm{d}_{3/2} : \mathrm{p}_{1/2}\text{–}\mathrm{d}_{3/2} = 9:1:5\\ &\text{df transitions: } \mathrm{d}_{5/2}\text{–}\mathrm{f}_{7/2} : \mathrm{d}_{5/2}\text{–}\mathrm{f}_{5/2} : \mathrm{d}_{3/2}\text{–}\mathrm{f}_{5/2} = 20:1:14\end{aligned} \qquad [5.35]$$

Under most circumstances the initial states are excited in proportion to their statistical weights, that is the $(2j + 1)$ degenerate levels corresponding to an initial state with a given value of j (but differing in $m_j = -j, -j + 1, \ldots +j$) are equally populated. In this case the ratios of line intensities are the same as those of the corresponding transition probabilities. The relative intensities of the fine structure components of the H_α line are shown in Fig. 5.5.

Comparison with experiment

The fine structure splitting of the spectral lines of atomic hydrogen and of hydrogenic ions (in particular He^+) has been the subject of many spectroscopic investigations. The experimental results are in good *semi-quantitative* agreement with the formula [5.28] obtained from the Dirac theory. Nevertheless, and in spite of the fact that precise optical measurements of fine structure are very difficult to perform, small deviations from the theoretical predictions of [5.28] were observed as early as 1934. In particular, detailed experimental studies of the H_α line of atomic hydrogen indicated that the energy separation of the $2s_{1/2}$ and $2p_{1/2}$ levels is not exactly zero, as predicted from the Dirac theory (see [5.28] or [5.30]) but is about 10 per cent of the fine structure splitting of the $n = 2$ levels. However, the Doppler broadening of the spectral lines prevented precise results being obtained from optical spectroscopy, and the situation remained ambiguous until the first measurements of Lamb and Retherford were published in 1947. Using new methods of microwave spectroscopy, Lamb and Retherford demonstrated in a decisive way the existence of an energy difference between the two levels $2s_{1/2}$ and $2p_{1/2}$. This 'Lamb shift', to which we have already alluded in the discussion following [5.30], will be considered in Section 5.4 after we have familiarised ourselves with the behaviour of hydrogenic atoms in external magnetic and electric fields.

5.2. THE ZEEMAN EFFECT

In 1896, P. Zeeman observed that the spectral lines of atoms were split in the presence of an external magnetic field. In order to explain this effect, we shall discuss in this section the interaction of hydrogenic atoms with *constant* magnetic fields, which can be taken to be uniform over atomic dimensions. The vector potential $\mathbf{A}$ can then be written as

$$\mathbf{A} = \tfrac{1}{2}(\boldsymbol{\mathcal{B}} \times \mathbf{r}) \qquad [5.36]$$

where $\mathcal{B}$ is the constant magnetic field, which satisfies the relation $\mathcal{B} = \nabla \times \mathbf{A}$. If $\mathcal{B}$ is directed along the Z axis, the components of $\mathbf{A}$ are $(-y\mathcal{B}_z/2, +x\mathcal{B}_z/2, 0)$.

The non-relativistic Schrödinger equation for a hydrogenic atom in the presence of a constant magnetic field is given by (see Appendix 6 and Section 4.1)

$$\left[-\frac{\hbar^2}{2m}\nabla^2 - \frac{Ze^2}{(4\pi\varepsilon_0)r} - \frac{i\hbar e}{m}\mathbf{A}\cdot\nabla + \frac{e^2}{2m}\mathbf{A}^2\right]\psi(\mathbf{r}) = E\psi(\mathbf{r}) \qquad [5.37]$$

where reduced mass effects have been neglected, $\mathbf{A}$ is given by [5.36] and we have used the fact that $\nabla\cdot\mathbf{A} = 0$.

The linear term in $\mathbf{A}$ becomes, in terms of $\mathcal{B}$

$$\begin{aligned}-\frac{i\hbar e}{m}\mathbf{A}\cdot\nabla &= -\frac{i\hbar e}{2m}(\mathcal{B}\times\mathbf{r})\cdot\nabla \\ &= -\frac{i\hbar e}{2m}\mathcal{B}\cdot(\mathbf{r}\times\nabla) \\ &= \frac{e}{2m}\mathcal{B}\cdot\mathbf{L} \qquad [5.38]\end{aligned}$$

where

$$\mathbf{L} = \mathbf{r}\times\mathbf{p} = -i\hbar(\mathbf{r}\times\nabla) \qquad [5.39]$$

is the orbital angular momentum of the electron. The quadratic term in $\mathbf{A}$ appearing in [5.37] can be reduced as follows:

$$\begin{aligned}\frac{e^2}{2m}\mathbf{A}^2 &= \frac{e^2}{8m}(\mathcal{B}\times\mathbf{r})^2 \\ &= \frac{e^2}{8m}[\mathcal{B}^2r^2 - (\mathcal{B}\cdot\mathbf{r})^2] \qquad [5.40]\end{aligned}$$

The relative magnitude of the two terms [5.38] and [5.40] can now be estimated. Assuming that the dimensions of the atomic system are of the order of a_0, the Bohr radius of hydrogen, the quadratic term is of the order $e^2a_0^2\mathcal{B}^2/8m$, while if we are dealing with states of low orbital angular momentum (say about $\hbar$) the linear term is approximately given by $e\hbar\mathcal{B}/2m$. The ratio of the quadratic to the linear term is then

$$\frac{ea_0^2\mathcal{B}}{4\hbar} \simeq \mathcal{B}10^{-6} \qquad [5.41]$$

where $\mathcal{B}$ is expressed in Tesla (T). In the laboratory, the fields encountered do not exceed 10 T, so that for most purposes the quadratic term is negligible.

The linear term [5.38] corresponds to the interaction energy of a magnetic field $\mathcal{B}$ with a magnetic dipole moment $\mathcal{M}$, if $\mathcal{M}$ is defined as the operator

$$\mathcal{M} = -\frac{e}{2m}\mathbf{L} = -\mu_B \mathbf{L}/\hbar \qquad [5.42]$$

where

$$\mu_B = \frac{e\hbar}{2m} \qquad [5.43]$$

is called the *Bohr magneton* and has the value $9.274\,08 \times 10^{-24}$ joule/tesla or m^2A. The interaction energy [5.38] then takes the form

$$H_1' = -\mathcal{M} \cdot \mathcal{B} \qquad [5.44]$$

It is useful to express H_1' in various units. For example

$$\begin{aligned} H_1' &= 2.13 \times 10^{-6}\, \mathcal{B} \cdot \mathbf{L} \text{ a.u.} \\ &= 0.4669\, \mathcal{B} \cdot \mathbf{L}/\hbar \text{ cm}^{-1} \end{aligned} \qquad [5.45]$$

where in both cases $\mathcal{B}$ is to be given in Tesla.

Until this point we have not taken into account the intrinsic magnetic moment of the electron, revealed by experiments of the Stern–Gerlach type (see Chapter 1). This intrinsic magnetic moment, due to the electron spin, is given by

$$\mathcal{M}_s = -g_s \frac{e}{2m}\mathbf{S} \qquad [5.46]$$

or

$$\mathcal{M}_s = -g_s \mu_B \mathbf{S}/\hbar \qquad [5.47]$$

where $\mathbf{S}$ is the spin operator of the electron and g_s its spin *gyromagnetic ratio*. Dirac's relativistic theory predicts for g_s the value $g_s = 2$ (see Appendix 7) which is in very good agreement with experiment [6]. The spin magnetic moment $\mathcal{M}_s$ gives rise to an additional interaction energy

$$H_2' = -\mathcal{M}_s \cdot \mathcal{B} = g_s \mu_B \mathcal{B} \cdot \mathbf{S}/\hbar \qquad [5.48]$$

The complete Schrödinger equation for a one-electron atom in a constant magnetic field, including the spin–orbit interaction, but neglecting the reduced mass effect, the relativistic kinetic energy correction, the Darwin term and the quadratic ($\mathbf{A}^2$) term, is (with $g_s = 2$)

$$\left[-\frac{\hbar^2}{2m}\nabla^2 - \frac{Ze^2}{(4\pi\varepsilon_0)r} + \xi(r)\mathbf{L} \cdot \mathbf{S} + \frac{\mu_B}{\hbar}(\mathbf{L} + 2\mathbf{S}) \cdot \mathcal{B}\right]\psi(\mathbf{r}) = E\psi(\mathbf{r}) \qquad [5.49]$$

[6] The corrections to the Dirac result $g_s = 2$ come from quantum electrodynamics, which yields a value $g_s = 2(1 + \alpha/2\pi + \cdots)$ in excellent agreement with the experimental result $g_s = 2 \times 1.001\,159\,657$.

where $\xi(r)$ is given by [5.18] and $\psi(\mathbf{r})$ is now a 'spin-orbital' with two components.

The nature of the solution depends on whether the magnetic interaction is greater or less than the spin–orbit interaction. We shall first discuss the former case (strong magnetic fields) and then analyse the so-called 'anomalous Zeeman effect' which corresponds to weak fields.

Strong fields

The fine structure splitting of the $n = 2$ level of hydrogenic atoms is $(0.365\, Z^4)$ cm^{-1} and decreases for larger n like n^{-3}. We see from [5.45] that the magnetic interaction energy will be greater than this for field strengths $\mathcal{B} > Z^4$ Tesla. By laboratory standards, these are very strong fields even for hydrogenic atoms with small Z, but such fields can occur in certain astrophysical situations, such as in some stars. In the strong field limit, we first solve the Schrödinger equation without the spin–orbit coupling, which can be subsequently treated as a perturbation. Taking $\mathcal{B}$ to be along the Z axis, we have

$$\left(-\frac{\hbar^2}{2m}\nabla^2 - \frac{Ze^2}{(4\pi\varepsilon_0)r}\right)\psi(\mathbf{r}) = \left[E - \frac{\mu_B\mathcal{B}_z}{\hbar}(L_z + 2S_z)\right]\psi(\mathbf{r}) \qquad [5.50]$$

The unperturbed hydrogenic spin-orbitals $\psi_{nlm_lm_s}$ defined by [5.9] are eigenfunctions of L_z and S_z and satisfy this equation if

$$E = E_n + \mu_B\mathcal{B}_z(m_l + 2m_s), \qquad m_s = \pm 1/2 \qquad [5.51]$$

The introduction of the magnetic field does not remove the degeneracy in l, but by providing a preferred direction in space, it does remove the degeneracy in m_l and m_s, splitting each level with a given n into equally spaced terms. This is illustrated in Fig. 5.6 for the case of a p level ($l = 1$). However, the energy of the states with $m_l = +1$ and $m_s = -1/2$ coincides with those with $m_l = -1$ and $m_s = +1/2$. In the strong-field limit we are considering here (no spin–orbit coupling) the orbital and spin angular momenta are constants of the motion and

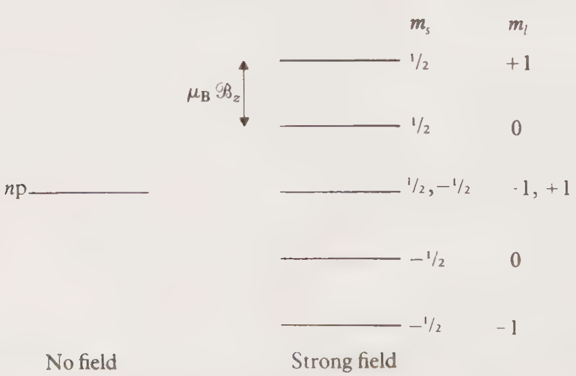

5.6 The splitting of a p level into five equally spaced levels by a strong magnetic field.

the eigenfunctions, written in Dirac notation, are of the form $|nlm_l sm_s\rangle$, with $s = 1/2$ and $m_s = \pm 1/2$.

The selection rules for electric dipole transitions require $\Delta m_s = 0$ and $\Delta m_l = 0, \pm 1$. Thus the spectral line corresponding to a transition $n \to n'$ is split into *three* components. The line corresponding to $\Delta m_l = 0$ has the original frequency $\nu_{nn'}$ and is called the π line, while the two lines with $\Delta m_l = \pm 1$ are called σ lines and correspond to frequencies

$$\nu_{nn'}^{\pm} = \nu_{nn'} \pm \nu_{\mathrm{L}} \qquad [5.52]$$

where

$$\nu_{\mathrm{L}} = \frac{\mu_{\mathrm{B}}\mathscr{B}_z}{h} \qquad [5.53]$$

is known as the *Larmor frequency*. This splitting is called the *normal Zeeman effect* and the three lines are said to form a *Lorentz triplet* (see Fig. 5.7). Apart from the case of very strong fields, Lorentz triplets can be observed in many-electron systems for which the total spin is zero, as in this case the spin–orbit coupling vanishes.

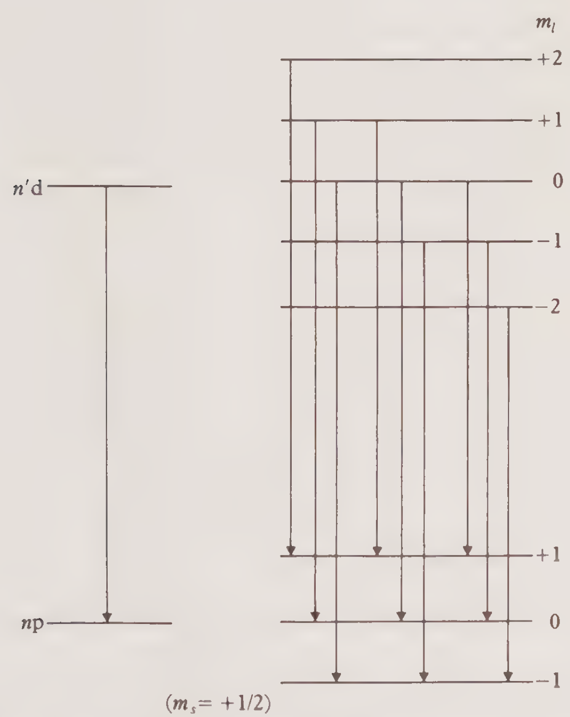

5.7 The normal Zeeman effect. In a strong magnetic field nine transitions are possible between the split levels consistent with $\Delta m_l = 0$ or ± 1 and $\Delta m_s = 0$. Of these, there are only three different frequencies and the lines form a Lorentz triplet. The frequencies of transitions associated with $m_s = -\frac{1}{2}$ are the same as those for $m_s = +\frac{1}{2}$.

The polarisation of the radiation in each of the emission lines has interesting properties. The transition rate for spontaneous emission of radiation described by a polarisation vector $\hat{\boldsymbol{\varepsilon}}$ is given by [4.70], namely

$$\begin{aligned} W^{\mathrm{s}}_{ab}\,\mathrm{d}\Omega &= \frac{1}{2\pi\hbar c^3}\left(\frac{e^2}{4\pi\varepsilon_0}\right)\omega_{ba}^3|\hat{\boldsymbol{\varepsilon}}\cdot\mathbf{r}_{ba}|^2\,\mathrm{d}\Omega \\ &= C(\omega_{ba})|\hat{\boldsymbol{\varepsilon}}\cdot\mathbf{r}_{ba}|^2\,\mathrm{d}\Omega \end{aligned} \qquad [5.54a]$$

where we have set

$$C(\omega_{ba}) = \frac{1}{2\pi\hbar c^3}\left(\frac{e^2}{4\pi\varepsilon_0}\right)\omega_{ba}^3 \qquad [5.54b]$$

The vector $\hat{\boldsymbol{\varepsilon}}$ can be expressed in terms of two independent vectors $\hat{\mathbf{e}}_1$ and $\hat{\mathbf{e}}_2$ as in [4.95], where $\hat{\mathbf{e}}_1$, $\hat{\mathbf{e}}_2$ and $\hat{\mathbf{k}}$ form a right-handed system of axes (see [4.96]). If we take (as can always be done) $\hat{\mathbf{e}}_2$ to lie in the (X, Y) plane and if (Θ, Φ) are the polar angles of $\hat{\mathbf{k}}$ (see Fig. 5.8), we have

$$\begin{aligned} &(\hat{e}_1)_x = \cos\Theta\cos\Phi; \quad &(\hat{e}_1)_y = \cos\Theta\sin\Phi; \quad &(\hat{e}_1)_z = -\sin\Theta \\ &(\hat{e}_2)_x = -\sin\Phi; \quad &(\hat{e}_2)_y = \cos\Phi; \quad &(\hat{e}_2)_z = 0 \end{aligned} \qquad [5.55]$$

Consider first the π line, with $\Delta m_l = 0$. From the discussion given in Section 4.5 we see that in this case $x_{ba} = y_{ba} = 0$ and we are only concerned with z_{ba}. The transition rate for emission in the solid angle $\mathrm{d}\Omega$ of a photon with

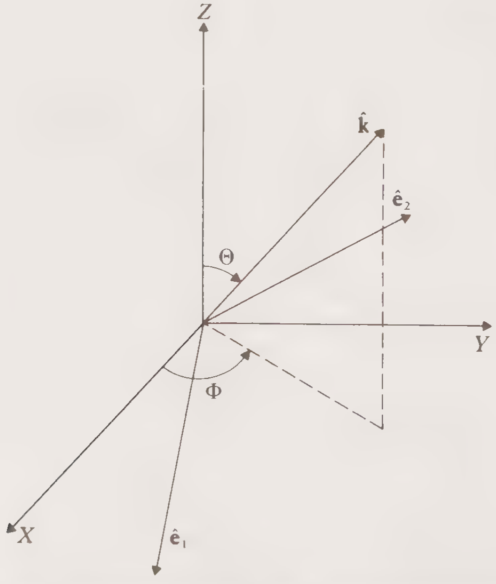

5.8 The unit vectors $\hat{\mathbf{e}}_1$, $\hat{\mathbf{e}}_2$ and $\hat{\mathbf{k}}$ form a right-handed set. The polar angles of $\hat{\mathbf{k}}$ are (Θ, Φ) and $\hat{\mathbf{e}}_2$ lies in the XY plane, $\hat{\mathbf{e}}_1$ pointing downwards.

polarisation $\hat{\mathbf{e}}_1$ is then

$$W^{s}_{ab}\, \mathrm{d}\Omega = C(\omega_{ba}) \sin^2 \Theta \, |z_{ba}|^2 \, \mathrm{d}\Omega \qquad [5.56]$$

and the rate is zero for emission of a photon with polarisation $\hat{\mathbf{e}}_2$. When the light is viewed longitudinally, so that $\hat{\mathbf{k}}$ is in the direction of the magnetic field (which is parallel to the Z axis), $\Theta = 0$ and the π line is absent. In transverse observation ($\Theta = \pi/2$), in a direction at right angles to the magnetic field, the π radiation is plane polarised with $\hat{\varepsilon} = \hat{\mathbf{e}}_1$ in the direction of the negative Z axis.

Let us now consider the case in which $\Delta m_l = m_l' - m_l = -1$ which corresponds to the amplitude (see [4.81]–[4.84])

$$\varepsilon^{\star}_{-1} I^{-1}_{n'l'm_l-1;nlm_l} = \frac{1}{\sqrt{2}}(\hat{\varepsilon}_x + i\hat{\varepsilon}_y)\frac{1}{\sqrt{2}}(x_{ba} - iy_{ba}) \qquad [5.57]$$

The transition rate for emission of a photon with polarisation $\hat{\varepsilon} = \hat{\mathbf{e}}_1$ is then

$$W^{s}_{ab}(1)\, \mathrm{d}\Omega = C(\omega_{ba}) \left| \frac{1}{\sqrt{2}} \cos\Theta\, \mathrm{e}^{i\Phi} \right|^2 \left| \frac{1}{\sqrt{2}}(x_{ba} - iy_{ba}) \right|^2 \mathrm{d}\Omega \qquad [5.58]$$

and that for polarisation $\hat{\varepsilon} = \hat{\mathbf{e}}_2$ is

$$W^{s}_{ab}(2)\, \mathrm{d}\Omega = C(\omega_{ba}) \left| \frac{i}{\sqrt{2}}\, \mathrm{e}^{i\Phi} \right|^2 \left| \frac{1}{\sqrt{2}}(x_{ba} - iy_{ba}) \right|^2 \mathrm{d}\Omega \qquad [5.59]$$

Summing over both independent polarisation directions, the transition rate for the line corresponding to $\Delta m_l = m_l' - m_l = -1$, which is known as the σ^+ line, is

$$W^{s}_{ab}(\sigma^+)\, \mathrm{d}\Omega = C(\omega_{ba}) \frac{1}{2}(1 + \cos^2\Theta) \left| \frac{1}{\sqrt{2}}(x_{ba} - iy_{ba}) \right|^2 \mathrm{d}\Omega \qquad [5.60]$$

In transverse observation $\Theta = \pi/2$ and the x and y components of $\hat{\mathbf{e}}_1$ vanish. In this case the σ^+ line is plane polarised with $\hat{\varepsilon} = \hat{\mathbf{e}}_2$, where $\hat{\mathbf{e}}_2$ lies in the (X, Y) plane. In contrast, in longitudinal observation along the direction of the magnetic field, we see from [4.102] that the radiation is left-hand circularly polarised, that is the emitted photon has helicity $+\hbar$.

In the same way, the transition rate for the σ^- line corresponding to $\Delta m_l = m_l' = +1$ is given by

$$W^{s}_{ab}(\sigma^-)\, \mathrm{d}\Omega = C(\omega_{ba}) \frac{1}{2}(1 + \cos^2\Theta) \left| \frac{1}{\sqrt{2}}(x_{ba} + iy_{ba}) \right|^2 \mathrm{d}\Omega \qquad [5.61]$$

The σ^- line is right-hand circularly polarised when viewed along the direction of the magnetic field and is plane polarised in transverse observation.

The preceding discussion of the polarisations of the σ and π components is illustrated in Fig. 5.9. It is easily shown (Problem 5.3) that in the transverse direction the intensity of the π component is twice that of each σ component.

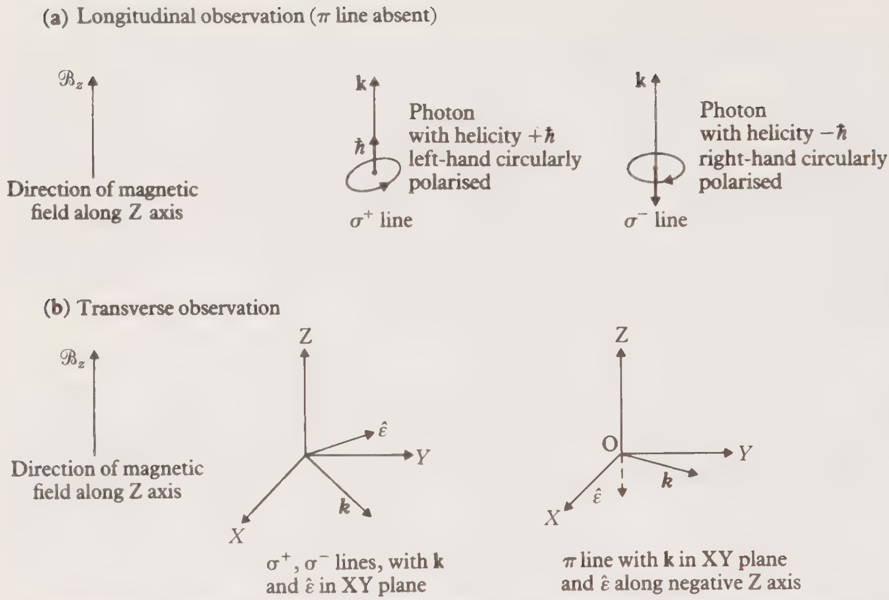

5.9 Polarisations of photons emitted in the direction of a magnetic field, or at right angles to a magnetic field.

The Paschen–Back effect

At field strengths for which the spin–orbit interaction is appreciable, but still small compared with the term in $\mathscr{B}$ in [5.49], it can be treated in first order perturbation theory. We see that the perturbation is just $\xi(r)\mathbf{L}\cdot\mathbf{S}$, and its contribution to the total energy is therefore

$$\begin{aligned}\Delta E &= \int_0^\infty \mathrm{d}r\, r^2[R_{nl}(r)]^2\xi(r)\left\langle l\frac{1}{2}m_l m_s\middle|\mathbf{L}\,.\,\mathbf{S}\middle|l\frac{1}{2}m_l m_s\right\rangle \\ &= \lambda_{nl}m_l m_s\,,\; l \neq 0 \end{aligned} \qquad [5.62]$$

while $\Delta E = 0$ for s-states ($l = 0$). The quantity λ_{nl} is given by

$$\begin{aligned}\lambda_{nl} &= \hbar^2\int_0^\infty \mathrm{d}r\, r^2[R_{nl}(r)]^2\xi(r) \\ &= -\frac{\alpha^2 Z^2}{n}E_n\frac{1}{l\left(l+\frac{1}{2}\right)(l+1)}\,,\; l\neq 0\end{aligned} \qquad [5.63]$$

The degeneracy in l is removed, as we expect. The energy difference between levels nlm_l and $n'l'm_l'$ when $m_s = m_s'$ is

$$\delta E = E_{n'} - E_n + \mu_B\mathscr{B}_z(m_l' - m_l) + (\lambda_{n'l'}m_l' - \lambda_{nl}m_l)m_s \qquad [5.64]$$

This expression gives the frequencies $\delta E/h$ of the observed lines, with

$\Delta m_l = m_l' - m_l$ restricted to the values 0, ± 1. The observed splitting in this case is known as the *Paschen–Back effect*.

Weak fields: the anomalous Zeeman effect

For historical reasons the case of a weak magnetic field is known as the *anomalous Zeeman effect*, although in fact this effect is the one most commonly encountered. In the early days of spectroscopy, before the electron spin was discovered, the normal Zeeman effect was predicted, on classical grounds, but the observations did not conform to the predictions and were said to be 'anomalous'. The explanation was finally given in terms of quantum mechanics and the electron spin.

When the interaction caused by the external magnetic field is small compared with the spin–orbit term, the unperturbed Hamiltonian can be taken to be

$$H_0 = -\frac{\hbar^2}{2m}\nabla^2 - \frac{Ze^2}{(4\pi\varepsilon_0)r} + \xi(r)\mathbf{L}\cdot\mathbf{S} \qquad [5.65]$$

The unperturbed wave functions are eigenfunctions of $\mathbf{L}^2$, $\mathbf{S}^2$, $\mathbf{J}^2$ and J_z, but not of L_z and S_z. They are therefore products of radial functions times the 'generalised spherical harmonics' (see Appendix 4)

$$\mathcal{Y}_{ls}^{jm_j} = \sum_{m_l,m_s} \langle lsm_lm_s|jm_j\rangle Y_{lm_l}(\theta,\phi)\chi_{s,m_s} \qquad [5.66]$$

where $\langle lsm_lm_s|jm_j\rangle$ are Clebsch–Gordan coefficients and $s = 1/2$.

Taking the magnetic field $\boldsymbol{\mathcal{B}}$ to be along the Z axis, the perturbation is

$$H' = \frac{\mu_B}{\hbar}(L_z + 2S_z)\mathcal{B}_z$$

$$= \frac{\mu_B}{\hbar}(J_z + S_z)\mathcal{B}_z \qquad [5.67]$$

The additional energy due to the magnetic interaction H' is thus

$$\Delta E = \mu_B\mathcal{B}_z m_j + \frac{\mu_B}{\hbar}\mathcal{B}_z \sum_{\text{spin}} \int d\Omega\, (\mathcal{Y}_{l,1/2}^{jm_j})^{\star} S_z \mathcal{Y}_{l,1/2}^{jm_j} \qquad [5.68]$$

where we have made use of the fact that $\mathcal{Y}_{l,1/2}^{jm_j}$ is a normalised eigenfunction of J_z belonging to the eigenvalue $m_j\hbar$.

Either of two methods can be used to evaluate the second term in [5.68].

1. The most straightforward procedure is to use the explicit expressions for the Clebsch–Gordan coefficients $\langle l1/2m_lm_s|jm_j\rangle$ given in Appendix 4. Setting $j = l \pm 1/2$, we have

$$\mathcal{Y}_{l,1/2}^{l+1/2,m_j} = \left(\frac{l + m_j + 1/2}{2l+1}\right)^{1/2} Y_{l,m_j-1/2}(\theta,\phi)\chi_{1/2,1/2}$$
$$+ \left(\frac{l - m_j + 1/2}{2l+1}\right)^{1/2} Y_{l,m_j+1/2}(\theta,\phi)\chi_{1/2,-1/2} \qquad [5.69a]$$

and

$$\mathcal{Y}_{l,1/2}^{l-1/2,m_j} = -\left(\frac{l - m_j + 1/2}{2l + 1}\right)^{1/2} Y_{l,m_j-1/2}(\theta, \phi)\chi_{1/2,1/2} + \left(\frac{l + m_j + 1/2}{2l + 1}\right)^{1/2} Y_{l,m_j+1/2}(\theta, \phi)\chi_{1/2,-1/2} \quad [5.69b]$$

from which one readily obtains

$$\sum_{\text{spin}} \int d\Omega\, (\mathcal{Y}_{l,1/2}^{l+1/2,m_j})^{\star} S_z \mathcal{Y}_{l,1/2}^{l+1/2,m_j} = \frac{m_j}{2l + 1}\hbar \quad [5.70a]$$

and

$$\sum_{\text{spin}} \int d\Omega\, (\mathcal{Y}_{l,1/2}^{l-1/2,m_j})^{\star} S_z \mathcal{Y}_{l,1/2}^{l-1/2,m_j} = -\frac{m_j}{2l + 1}\hbar \quad [5.70b]$$

2. The same result can be obtained by operator methods. A *vector operator* $\mathbf{V}$ has three components (V_x, V_y, V_z) along three orthogonal axes, where V_x, V_y and V_z are operators which transform under rotations like the components of a vector. Thus, if $V_u = \mathbf{V} \cdot \hat{\mathbf{u}}$ is the component of $\mathbf{V}$ along the unit vector $\hat{\mathbf{u}}$ which defines the axis Ou, and if the unit vector $\hat{\mathbf{u}}'$ defines the axis Ou' obtained from Ou by performing the rotation $\mathcal{R}$, the transform of V_u under the rotation $\mathcal{R}$ must be the component $V_{u'} = \mathbf{V} \cdot \hat{\mathbf{u}}'$ of $\mathbf{V}$ along $\hat{\mathbf{u}}'$. It may be shown that the components V_x, V_y, V_z of a vector operator $\mathbf{V}$ satisfy the commutation relations

$$\begin{aligned} &[\mathcal{J}_x, V_x] = 0, && [\mathcal{J}_y, V_x] = -i\hbar V_z, && [\mathcal{J}_z, V_x] = i\hbar V_y, \\ &[\mathcal{J}_x, V_y] = i\hbar V_z, && [\mathcal{J}_y, V_y] = 0, && [\mathcal{J}_z, V_y] = -i\hbar V_x, \\ &[\mathcal{J}_x, V_z] = -i\hbar V_y, && [\mathcal{J}_y, V_z] = i\hbar V_x, && [\mathcal{J}_z, V_z] = 0 \end{aligned} \quad [5.71]$$

The operators $\mathbf{L}$, $\mathbf{S}$ and $\mathbf{J}$ are examples of vector operators. Using [5.71] and the commutation relations for the components of $\mathbf{J}$, namely

$$[\mathcal{J}_x, \mathcal{J}_y] = i\hbar\mathcal{J}_z, \qquad [\mathcal{J}_y, \mathcal{J}_z] = i\hbar\mathcal{J}_x, \qquad [\mathcal{J}_z, \mathcal{J}_x] = i\hbar\mathcal{J}_y \quad [5.72]$$

it may be shown after some manipulation that a vector operator $\mathbf{V}$ satisfies the equations

$$\mathbf{J} \times \mathbf{V} + \mathbf{V} \times \mathbf{J} = 2i\hbar\mathbf{V} \quad [5.73]$$

and

$$[\mathbf{J}^2, [\mathbf{J}^2, \mathbf{V}]] = 2\hbar^2(\mathbf{J}^2\mathbf{V} + \mathbf{V}\mathbf{J}^2) - 4\hbar^2(\mathbf{V} \cdot \mathbf{J})\mathbf{J} \quad [5.74]$$

The matrix element of the left-hand side of the identity [5.74] with respect to states having the same value of j vanishes, so that

$$\langle lsjm_j|\mathbf{J}^2\mathbf{V} + \mathbf{V}\mathbf{J}^2|lsjm_j\rangle = 2\langle lsjm_j|(\mathbf{V} \cdot \mathbf{J})\mathbf{J}|lsjm_j\rangle \quad [5.75]$$

from which we have

$$j(j+1)\hbar^2\langle lsjm_j|\mathbf{V}|lsjm_j\rangle = \langle lsjm_j|(\mathbf{V}\cdot\mathbf{J})\mathbf{J}|lsjm_j\rangle \tag{5.76}$$

This relationship can also be obtained by using the Wigner–Eckart theorem discussed in Appendix 4.

Setting $\mathbf{V} = \mathbf{S}$ in [5.76] and taking the z component, we have

$$\begin{aligned} j(j+1)\hbar^2\langle lsjm_j|S_z|lsjm_j\rangle &= \langle lsjm_j|(\mathbf{S}\cdot\mathbf{J})J_z|lsjm_j\rangle \\ &= m_j\hbar\langle lsjm_j|\mathbf{S}\cdot\mathbf{J}|lsjm_j\rangle \end{aligned} \tag{5.77}$$

Since $\mathbf{S}\cdot\mathbf{J} = (\mathbf{J}^2 + \mathbf{S}^2 - \mathbf{L}^2)/2$, the matrix element of S_z is

$$\langle lsjm_j|S_z|lsjm_j\rangle = m_j\hbar\left[\frac{j(j+1) + s(s+1) - l(l+1)}{2j(j+1)}\right] \tag{5.78}$$

which agrees with [5.70] when $s = 1/2$ and $j = l \pm 1/2$. The energy shift due to the magnetic field is seen from [5.68] and [5.70] (or [5.78]) to be proportional to $\mu_B\mathcal{B}_z m_j$ and may be written as

$$\Delta E_{m_j} = g\mu_B\mathcal{B}_z m_j \tag{5.79}$$

where g is called the *Landé g factor* and is given by

$$g = 1 + \frac{j(j+1) + s(s+1) - l(l+1)}{2j(j+1)} \tag{5.80}$$

Since in our case $s = 1/2$ we have

$$\begin{aligned} \Delta E_{m_j} &= \frac{2l+2}{2l+1}\mu_B\mathcal{B}_z m_j, \qquad j = l + 1/2 \\ &= \frac{2l}{2l+1}\mu_B\mathcal{B}_z m_j, \qquad j = l - 1/2 \end{aligned} \tag{5.81}$$

The total energy of the level with quantum numbers n, j, m_j of a hydrogenic atom in a constant magnetic field is therefore

$$E_{n,j,m_j} = E_n + \Delta E_{n,j} + \Delta E_{m_j} \tag{5.82}$$

where E_n is the non-relativistic energy [3.29] [with $\mu = m$], $\Delta E_{n,j}$ is the fine structure correction [5.28] and ΔE_{m_j} is the correction due to the (weak) magnetic field.

The splitting of levels, δE, corresponding to the 'anomalous' Zeeman effect discussed above is illustrated in Fig. 5.10. We remark that since the splitting of the levels is not the same for each multiplet, there will be more lines in this case than the three lines (Lorentz triplet) corresponding to the normal Zeeman effect. This is shown in Fig. 5.11, where we display the allowed transitions (corresponding to $\Delta l = \pm 1$ and $\Delta m_j = 0, \pm 1$) between the $n = 2$ and $n = 1$ levels of atomic hydrogen occurring in the presence of a weak magnetic field.

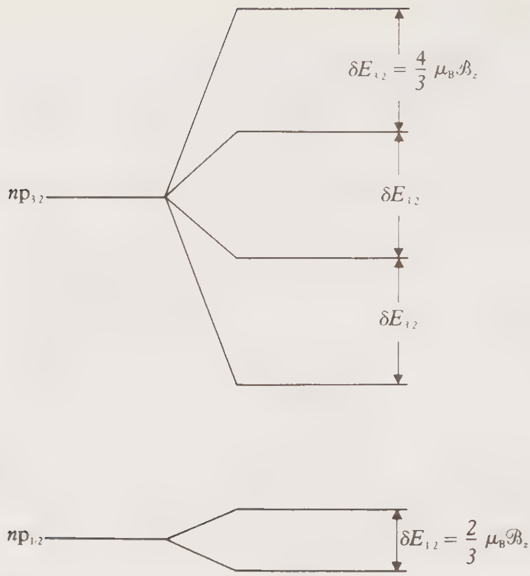

5.10 Splitting of $np_{3/2}$ and $np_{1/2}$ levels of atomic hydrogen in a weak magnetic field.

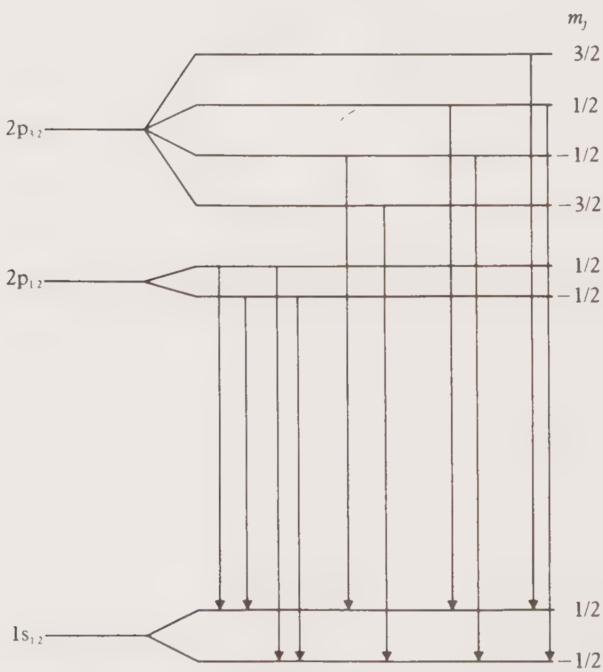

5.11 In electric dipole transitions between the $n = 2$ and $n = 1$ levels of hydrogen, in a weak magnetic field, four lines result from the $2p_{1/2} \rightarrow 1s_{1/2}$ transitions and six lines from the $2p_{3/2} \rightarrow 1s_{1/2}$ transitions.

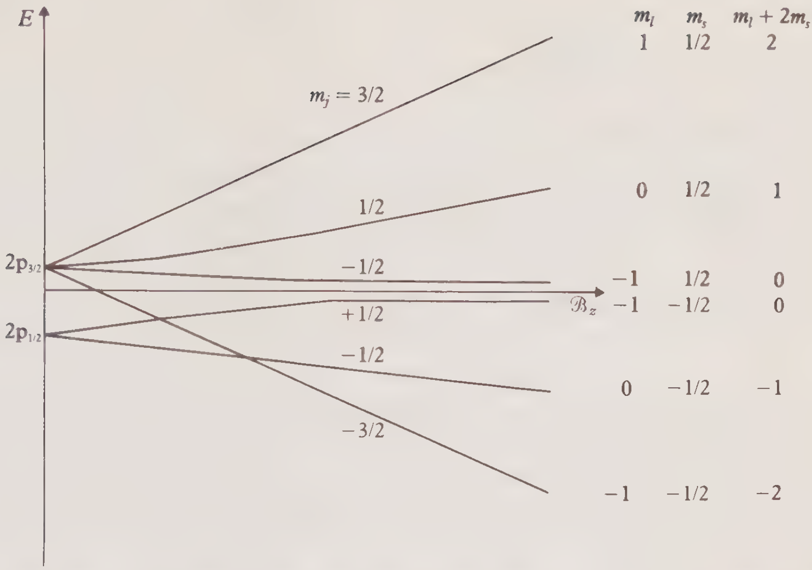

5.12 The energy of the levels of a hydrogen atom in a magnetic field are a smooth function of $\mathscr{B}_z$. For small $\mathscr{B}_z$, the splitting is uneven (the anomalous Zeeman effect), but for large $\mathscr{B}_z$, the splitting is even and only three lines are seen (Paschen–Back effect). A schematic diagram is shown for the 2p levels.

As the magnitude of the magnetic field $\mathscr{B}_z$ increases from the weak field to the strong field limit, the energy changes smoothly. This is depicted in Fig. 5.12 for the 2p states of atomic hydrogen.

5.3 THE STARK EFFECT

The effect of static electric fields on the spectrum of hydrogen and other atoms was studied by J. Stark and also by A. Lo Surdo in 1913. The splitting of spectral lines observed has become known as the *Stark effect*. We shall assume that the external electric field is constant over a region of atomic dimensions and is directed along the Z axis. We also suppose that the electric field strength $\mathscr{E}$ is large enough for fine structure effects to be unimportant [7]. The Hamiltonian H_0 for the unperturbed hydrogenic atom, given by [5.3] (we neglect reduced mass effects) is therefore modified by the addition of the perturbation

$$H' = e\mathscr{E}z \tag{5.83}$$

where we recall that $-e$ is the charge of the electron. Since H' does not depend on the electron spin we shall use for the zero-order wave functions the

[7] This is a correct assumption for electric field strengths usually encountered, which are of the order of 10^7 V/m. On the other hand, the treatment given here must be modified for electric fields $\mathscr{E} < 10^5$ V/m, since in this case the Stark splittings are of the same order of magnitude as the fine structure splittings studied in Section 5.1.

Schrödinger hydrogenic wave functions $\psi_{nlm}(\mathbf{r})$ where we have set $m \equiv m_l$ [3] in order to simplify the notation.

Linear Stark effect

Since the ground state (100) is non-degenerate, we see from [2.308] and [5.83] that the first-order correction to its energy is given by

$$\begin{aligned} E_{100}^{(1)} &= e\,\mathscr{E}\,\langle\psi_{100}|z|\psi_{100}\rangle \\ &= e\,\mathscr{E}\int|\psi_{100}(r)|^2 z\,\mathrm{d}\mathbf{r} \end{aligned} \tag{5.84}$$

Now our discussion at the end of Section 3.3 showed that the hydrogenic wave functions $\psi_{nlm}(\mathbf{r})$ have a *definite* parity (even when the orbital quantum number l is even, odd when l is odd). On the other hand the perturbation [5.83] is an *odd* operator under the parity operation since it changes sign when the coordinates are reflected through the origin. Thus we have

$$\langle\psi_{nlm}|z|\psi_{nlm}\rangle = 0 \tag{5.85}$$

since the matrix element $\langle\psi_{nlm}|z|\psi_{nlm}\rangle$ involves the product of the *even* function $|\psi_{nlm}(\mathbf{r})|^2$ times the odd function z under the parity operation. In particular, we see from [5.84] and [5.85] that $E_{100}^{(1)} = 0$, so that for the ground state there is no energy shift that is linear in the electric field $\mathscr{E}$. Remembering that a classical system having an electric dipole moment $\mathbf{D}$ will experience in an electric field $\boldsymbol{\mathscr{E}}$ an energy shift of magnitude $-\mathbf{D}\cdot\boldsymbol{\mathscr{E}}$, and noting that $-ez$ is the z component of the electric dipole moment operator in our case, we see that atomic hydrogen in the ground state cannot possess a permanent electric dipole moment (energy change proportional to $\mathscr{E}$).

Let us now examine the Stark effect on the first excited level ($n = 2$) of the hydrogen atom. Since we assume that $\mathscr{E}$ is large enough for fine structure effects to be neglected we may consider the unperturbed system in the $n = 2$ level to be fourfold degenerate, the four eigenfunctions

$$\psi_{200}, \qquad \psi_{210}, \qquad \psi_{211}, \qquad \psi_{21-1} \tag{5.86}$$

corresponding to the same unperturbed energy $E_{n=2} = -mc^2\alpha^2/8$ (see [3.30]). In principle we should therefore solve a homogeneous system [2.328] of four equations. However, we have already shown in our discussion of selection rules for electric dipole transitions (see Section 4.5) that matrix elements of the form $\langle nlm|z|n'l'm'\rangle$ vanish unless $m = m'$ and $l = l' \pm 1$. Thus the only non-vanishing matrix elements of the perturbation [5.83] are those connecting the 2s (200) and $2\mathrm{p}_0$ (210) states, and the linear homogeneous equations [2.328] reduce to a set of two equations which we write in matrix form as

$$\begin{pmatrix} -E^{(1)} & H'_{12} \\ H'_{21} & -E^{(1)} \end{pmatrix}\begin{pmatrix} c_1 \\ c_2 \end{pmatrix} = 0 \tag{5.87}$$

with

$$H'_{12} = H'_{21} = e\mathscr{E}\int \psi_{210}(\mathbf{r})z\psi_{200}(r)\,\mathrm{d}\mathbf{r} \qquad [5.88]$$

The reduction of the original homogeneous system of four equations to the two equations [5.87] may also be obtained easily by noting that (i) the operator H' commutes with L_z, the z component of the angular momentum, so that H' only connects states with the same value of the quantum number m and (ii) H' is odd under the parity operation.

The matrix element H'_{12} can be evaluated by using the hydrogenic wave functions given in Table 3.1 of Chapter 3. Since $z = r\cos\theta$, we have

$$\begin{aligned} H'_{12} &= e\mathscr{E}\frac{Z^3}{16\pi a_0^3}\int_0^\infty \mathrm{d}r\,r^3\left(\frac{Zr}{a_0}\right)\left(1-\frac{Zr}{2a_0}\right)\mathrm{e}^{-Zr/a_0}\int_0^\pi \mathrm{d}\theta\sin\theta\cos^2\theta\int_0^{2\pi}\mathrm{d}\phi \\ &= e\mathscr{E}\frac{Z^3}{8a_0^3}\frac{2}{3}\int_0^\infty \mathrm{d}r\,r^3\left(\frac{Zr}{a_0}\right)\left(1-\frac{Zr}{2a_0}\right)\mathrm{e}^{-Zr/a_0} \\ &= -3e\mathscr{E}a_0/Z \end{aligned} \qquad [5.89]$$

and $H'_{21} = H'_{12}$ since H'_{12} is real. Thus the two roots of the determinantal equation

$$\begin{vmatrix} -E^{(1)} & H'_{12} \\ H'_{12} & -E^{(1)} \end{vmatrix} = 0 \qquad [5.90]$$

are given by

$$E^{(1)} = \pm|H'_{12}| = \pm 3e\mathscr{E}a_0/Z \qquad [5.91]$$

Upon returning to [5.87] we see that for the lower root $E_1^{(1)} = -3e\mathscr{E}a_0/Z$ one has $c_1 = c_2$. The corresponding normalised eigenstate ψ_1 is given by

$$\psi_1 = \frac{1}{\sqrt{2}}(\psi_{200} + \psi_{210}) \qquad [5.92a]$$

The second root $E_2^{(1)} = +3e\mathscr{E}a_0/Z$ yields $c_1 = -c_2$ and a normalised eigenstate

$$\psi_2 = \frac{1}{\sqrt{2}}(\psi_{200} - \psi_{210}) \qquad [5.92b]$$

It should be emphasised that the states [5.92] are neither eigenstates of the parity operator, nor of $\mathbf{L}^2$, so that neither parity nor l is a 'good' quantum number in this case. On the other hand, m is a good quantum number because H' commutes with L_z (that is, the system is invariant under rotation about the Z axis). We also remark that the wave number shifts $\delta\tilde{\nu}$ corresponding to the energy correction $E^{(1)}$ are given by

$$\delta\tilde{\nu} = \pm\frac{3ea_0}{hc}\frac{\mathscr{E}}{Z} = \pm 12.8\left(\frac{\mathscr{E}}{Z}\right)10^{-7}\ \mathrm{cm}^{-1} \qquad [5.93]$$

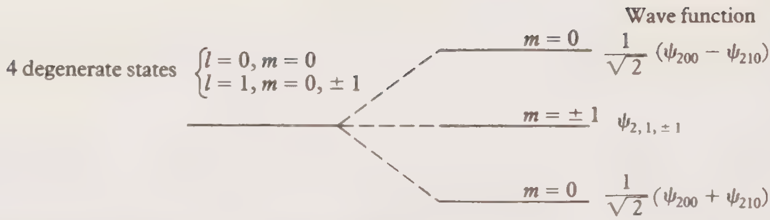

5.13 Splitting of the degenerate $n = 2$ levels of atomic hydrogen due to the linear Stark effect.

so that rather strong fields (of the order of 10^7 V/m in Stark's experiments) are required to demonstrate the effect.

The splitting of the degenerate $n = 2$ levels of atomic hydrogen due to the linear Stark effect is illustrated in Fig. 5.13. The degeneracy is partly removed by the perturbation, the energies of the $2p_{\pm 1}$ (i.e. 211 and $21-1$) states remaining unaltered. Thus the level $n = 2$ splits in a symmetrical way into *three* sublevels, one of which (corresponding to $m = \pm 1$) is twofold degenerate.

At this point it is worth recalling again that a classical system having an electric dipole moment $\mathbf{D}$ will experience in an electric field $\mathscr{E}$ an energy shift $-\mathbf{D} \cdot \mathscr{E}$. This suggests that the hydrogen atom in the *degenerate* unperturbed states $n = 2$ behaves as though it has a *permanent electric dipole moment* (independently of the value of $\mathscr{E}$), of magnitude $3ea_0$, which can be orientated in three different ways (that is, gives rise to spatial quantisation) in the presence of the field: one state (ψ_1) parallel to the field $\mathscr{E}$, one state (ψ_2) antiparallel to $\mathscr{E}$, and two states with no component along the field.

On the other hand, we found above that for the hydrogen ground state, which is *non-degenerate* and hence is an eigenstate of the *parity* operator, there is no energy shift linear in the electric field strength, and hence no permanent electric dipole moment. This conclusion may readily be generalised. Indeed, apart from tiny effects which we shall not consider here [8] all the systems studied in this book may be described by Hamiltonians which are unaffected by the parity operation (that is, the reflection of the coordinates of all the particles through the origin) and therefore any *non-degenerate* state of such systems has a definite parity (even or odd). Now for a system containing N particles of charges e_i ($i = 1, 2, \ldots N$) and coordinates $\mathbf{r}_i$, the electric-dipole moment operator

$$\mathbf{D} = \sum_{i=1}^{N} e_i \mathbf{r}_i \qquad [5.94]$$

is odd under the parity operation, so that its expectation value in a state of given parity is zero. As a result, *systems in non-degenerate states cannot have permanent electric dipole moments*. Note, however, that if we have a positive ion A^+ located at the position $\mathbf{r}_1$ and a negative ion B^- at the position $\mathbf{r}_2$, the system (A^+B^-)

[8] Parity non-conserving effects occur in the so-called *weak interactions*, which are responsible for weak decay processes of (elementary) particles, such as those observed in beta decay.

does possess an electric dipole moment. This does not contradict the previous argument since the configuration for which A^+ is at $\mathbf{r}_2$ and B^- at $\mathbf{r}_1$ has the same energy as the first arrangement and the system is necessarily degenerate. For the same reason, when atoms are bound together, the resulting molecules may possess permanent electric dipole moments [9].

Another remark concerns our use of degenerate perturbation theory for the treatment of the Stark effect on the $n = 2$ levels. As we know from our discussion in Section 5.1 there are small effects (fine structure, Lamb shift) which remove some of the degeneracies of this level, so that the situation will then correspond to a *near-degenerate* case. We shall not treat this problem in detail [10] but consider instead the simple model problem in which two unperturbed states $\psi_1^{(0)}$ and $\psi_2^{(0)}$ do not correspond exactly to the same unperturbed energy $E^{(0)}$ ($E_{n=2}$ in our case) but to energies given respectively by $E_1^{(0)} = E^{(0)} - \varepsilon$ and $E_2^{(0)} = E^{(0)} + \varepsilon$, which differ by a small amount 2ε. Instead of solving an equation of the type [5.87] we must now solve the matrix equation

$$\begin{pmatrix} E^{(0)} - \varepsilon - E & H'_{12} \\ H'_{21} & E^{(0)} + \varepsilon - E \end{pmatrix} \begin{pmatrix} c_1 \\ c_2 \end{pmatrix} = 0 \qquad [5.95]$$

where $H'_{12} = H'_{21}$ is given by [5.88]. Thus we have

$$E = E^{(0)} \pm [(H'_{12})^2 + \varepsilon^2]^{1/2} \qquad [5.96]$$

It is apparent from this result that for very weak fields (such that $|H'_{12}| \ll \varepsilon$ and the Stark splitting is small with respect to fine structure effects), there is no linear Stark effect. On the other hand, for strong field strengths $\mathscr{E}$ such that $|H'_{12}| \gg \varepsilon$ we retrieve the results found above by using degenerate perturbation theory (linear Stark effect). In what follows we shall continue to assume that the field strength $\mathscr{E}$ is large enough for the fine structure effects to be neglected.

The splitting of the $n = 3$ level due to the linear Stark effect may be treated in a way similar to the $n = 2$ case analysed above. It is found (Problem 5.4) that this level is split into *five* equally spaced levels, as shown in Fig. 5.14.

Also displayed in Fig. 5.14 are the radiative transitions between the levels $n = 2$ and $n = 3$ (corresponding to the spectral line H_α) of atomic hydrogen in the presence of an electric field. The selection rules with respect to the magnetic quantum number m are the same as those we obtained in Chapter 4 without an external field. That is

$$\Delta m = 0, \pm 1 \qquad [5.97]$$

The $\Delta m = 0$ transitions are said to correspond to π components, and the $\Delta m = \pm 1$ to σ components.

[9] The kind of degeneracy to which we have referred is often removed in an 'exact' calculation of molecular ground states. However, because the splittings involved are very small, in any experiment an average is taken over the ground and neighbouring states, of different parities, resulting in an effective permanent electric dipole moment.

[10] A comprehensive treatment may be found in Bethe and Salpeter (1957).

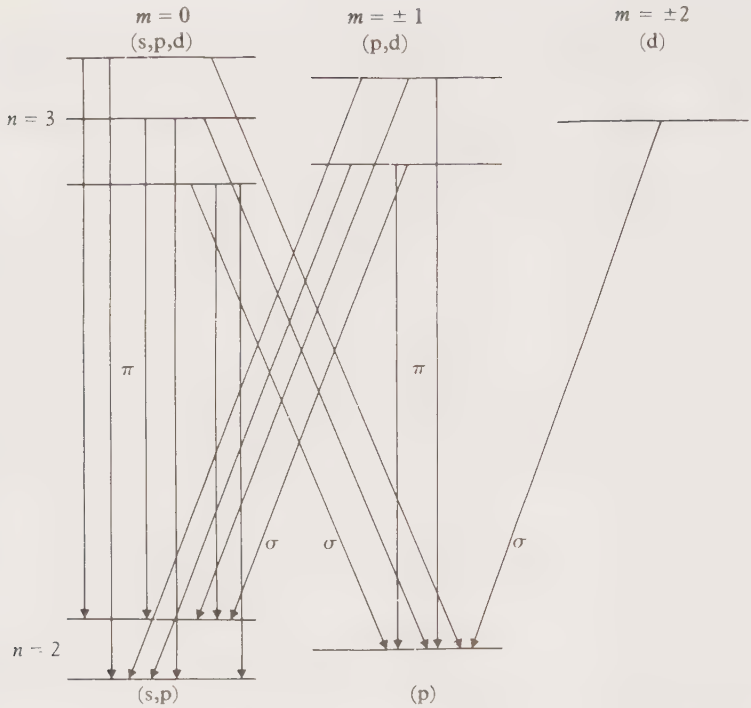

5.14 Splitting of the $n = 3$ and $n = 2$ levels of hydrogen due to the linear Stark effect. The various possible transitions are shown, those with $\Delta m = 0$ correspond to π lines and those with $\Delta m = \pm 1$ to σ lines.

On the other hand, since l is not a good quantum number in the presence of an external electric field, it is clear that the selection rules concerning l must be modified. In particular, because the operator [5.83] has a non-vanishing matrix element between the 2s and $2p_0$ states, these two states are 'mixed' by the perturbation H' with the result that the metastable 2s state is 'contaminated' by the unstable 2p state. Thus a radiative transition from the 2s state to the 1s state can be induced by an external electric field [11], so that the lifetime of the 2s state is considerably shortened by comparison with its value (1/7 s) in the absence of electric field.

In order to examine in more detail this process, which is called '*quenching* of the metastable 2s state', let us assume that at the initial time $t = 0$ the hydrogen atom is in the 2s (200) state. We then apply a constant electric field of strength $\mathscr{E}$ directed along the Z axis, and use the results [5.91] and [5.92] to write the time-dependent wave function of the atom at $t > 0$ as

$$\Psi(\mathbf{r}, t) = c_1\psi_1(\mathbf{r})e^{-(i/\hbar)(E_{n=2}-\Delta E)t} + c_2\psi_2(\mathbf{r})e^{-(i/\hbar)(E_{n=2}+\Delta E)t} \qquad [5.98]$$

[11] It is worth noting that this external electric field need not be a static field, as in the case studied here, but can also be a time-dependent (oscillating) field.

where $E_{n=2} = -mc^2\alpha^2/8$ and $\Delta E = |H'_{12}| = 3e\,\mathscr{E}\,a_0$ is the absolute value of the (first-order) energy shift. The coefficients c_1 and c_2 are easily found from the initial condition

$$\Psi(\mathbf{r}, t = 0) = \psi_{200}(r) \qquad [5.99]$$

Using [5.92] and [5.99], we find that $c_1 = c_2 = 2^{-1/2}$, so that

$$\begin{aligned}\Psi(\mathbf{r}, t) &= \frac{1}{\sqrt{2}}\,\psi_1(\mathbf{r})\mathrm{e}^{-(i/\hbar)(E_{n=2}-\Delta E)t} + \frac{1}{\sqrt{2}}\,\psi_2(\mathbf{r})\mathrm{e}^{-(i/\hbar)(E_{n=2}+\Delta E)t} \\ &= \left[\psi_{200}(r)\cos\left(\frac{\Delta E}{\hbar}\,t\right) + i\psi_{210}(\mathbf{r})\sin\left(\frac{\Delta E}{\hbar}\,t\right)\right]\mathrm{e}^{-(i/\hbar)E_{n=2}t}\end{aligned} \qquad [5.100]$$

Thus the atom oscillates between the 200 (2s) and 210 ($2\mathrm{p}_0$) states, with a period

$$T = \frac{\pi\hbar}{\Delta E} \qquad [5.101]$$

For example, in the case of an electric field of strength $\mathscr{E} = 10^7$ V/m, we find from [5.101] that $T \simeq 1.3 \times 10^{-12}$ s which is much shorter than the time $\tau \simeq 1.6 \times 10^{-9}$ s corresponding to the radiative transition 2p–1s (i.e. the lifetime of the 2p state in the absence of external field). As a result, the average population of both states 2s and $2\mathrm{p}_0$ is nearly equal during the entire decay time. This conclusion is easily seen to be true for initial conditions in which the atom is initially (at $t = 0$) in an arbitrary superposition of the 2s and $2\mathrm{p}_0$ states (Problem 5.5). Thus, in the presence of a strong electric field the radiative transitions 2s–1s and 2p–1s have the same transition probability per unit time, which is equal to $1/2\tau$. It is apparent from this discussion that in general, an external electric field will be able to induce n's – ns radiative transitions.

Quadratic Stark effect

We have shown above that for the ground state (100) of hydrogenic atoms there is no linear Stark effect. In order to investigate the effect of the perturbation [5.83] on that state we must therefore consider the second-order term of the perturbation series. Using [2.319] we see that in our case it reads

$$E_{100}^{(2)} = e^2\mathscr{E}^2 \sum_{\substack{n\neq 1\\ l,m}} \frac{|\langle\psi_{nlm}|z|\psi_{100}\rangle|^2}{E_1 - E_n} \qquad [5.102]$$

where the sum implies a summation over the discrete set together with an integration over the continuous set of hydrogenic eigenfunctions. It is clear from [5.102] that the ground state energy will be *lowered* by the quadratic Stark effect, since the energy differences $E_1 - E_n$ ($n \geq 2$) are always negative. In fact, we may readily obtain a lower limit for $E_{100}^{(2)}$ by replacing in [5.102] the energy

differences $E_1 - E_n$ by $E_1 - E_2$. That is,

$$E_{100}^{(2)} = -e^2 \mathscr{E}^2 \sum_{\substack{n \neq 1 \\ l,m}} \frac{|\langle \psi_{nlm}|z|\psi_{100}\rangle|^2}{E_n - E_1}$$
$$> -e^2 \mathscr{E}^2 \frac{1}{E_2 - E_1} \sum_{\substack{n \neq 1 \\ l,m}} |\langle \psi_{nlm}|z|\psi_{100}\rangle|^2 \qquad [5.103]$$

The summation on the right of [5.103] may now be performed as follows. We first note that because $\langle \psi_{100}|z|\psi_{100}\rangle = 0$ we may write

$$\sum_{\substack{n \neq 1 \\ l,m}} |\langle \psi_{nlm}|z|\psi_{100}\rangle|^2 = \sum_{n,l,m} |\langle \psi_{nlm}|z|\psi_{100}\rangle|^2$$
$$= \sum_{n,l,m} \langle \psi_{100}|z|\psi_{nlm}\rangle\langle \psi_{nlm}|z|\psi_{100}\rangle \qquad [5.104]$$

Using the completeness of the hydrogenic states, namely

$$\sum_{nlm} |\psi_{nlm}\rangle\langle\psi_{nlm}| = 1 \qquad [5.105]$$

we have

$$\sum_{n,l,m} \langle \psi_{100}|z|\psi_{nlm}\rangle\langle \psi_{nlm}|z|\psi_{100}\rangle = \langle \psi_{100}|z^2|\psi_{100}\rangle$$
$$= \langle z^2\rangle_{100} \qquad [5.106]$$

But

$$\langle z^2\rangle_{100} = \langle x^2\rangle_{100} = \langle y^2\rangle_{100} = \frac{1}{3}\langle r^2\rangle_{100} = \frac{a_0^2}{Z^2} \qquad [5.107]$$

so that from [5.103]–[5.107] and [3.29] we have

$$E_{100}^{(2)} > -\frac{8}{3}(4\pi\varepsilon_0)\frac{a_0^3}{Z^4}\mathscr{E}^2 \qquad [5.108]$$

It is possible to obtain in a straightforward way another estimate for $E_{100}^{(2)}$ (Problem 5.6):

$$E_{100}^{(2)} \approx -2(4\pi\varepsilon_0)\frac{a_0^3}{Z^4}\mathscr{E}^2 \qquad [5.109]$$

The exact evaluation of the expression [5.102] is more tedious and we shall not discuss it in detail here. One finds (Bethe and Salpeter, 1957) that

$$E_{100}^{(2)} = -2.25(4\pi\varepsilon_0)\frac{a_0^3}{Z^4}\mathscr{E}^2$$
$$= -3.71 \times 10^{-41}\left(\frac{\mathscr{E}^2}{Z^4}\right)\text{joule} \qquad [5.110]$$

It is worth noting that about one-third of the result [5.110] arises from the contribution of the continuum in the summation [5.102]. We also remark that the quadratic Stark effect given by [5.110] is generally very small, being approximately 0.02 cm^{-1} for atomic hydrogen in the case of a field strength $\mathscr{E} = 10^8$ volt/metre.

Upon differentiation of the expression [5.102] with respect to the electric field strength, we obtain for the magnitude of the dipole moment the result

$$D = -\frac{\partial E_{100}^{(2)}}{\partial \mathscr{E}} = \bar{\alpha}\mathscr{E} \qquad [5.111]$$

where

$$\bar{\alpha} = 2e^2 \sum_{\substack{n \neq 1 \\ l,m}} \frac{|\langle \psi_{nlm}|z|\psi_{100}\rangle|^2}{E_n - E_1} \qquad [5.112]$$

is called the *dipole polarisability* of the atom in the state (100). We see from [5.111] that D is proportional to $\mathscr{E}$, so that we have an *induced dipole moment*. We also note from [5.102] and [5.112] that

$$E_{100}^{(2)} = -\frac{1}{2}\bar{\alpha}\mathscr{E}^2 \qquad [5.113]$$

and the result [5.110] shows that

$$\begin{aligned} \bar{\alpha} &= 4.50(4\pi\varepsilon_0)\frac{a_0^3}{Z^4} \\ &= 7.42 \times 10^{-41}\, Z^{-4}\ \mathrm{F\ m^2} \end{aligned} \qquad [5.114]$$

The foregoing discussion of the quadratic Stark effect has been limited to the ground state of hydrogenic atoms, for which it is the first non-vanishing term of the perturbation series. Similar calculations may be carried out for excited states, where the quadratic Stark effect is a correction to the linear Stark effect studied above. This correction is in general quite small. For example, in the case of the H_α line, where the separation of the outermost components is about 200 cm^{-1} for a field strength of 4×10^7 volt/metre, the corresponding (red) shift due to the quadratic Stark effect is only 1 cm^{-1}.

Ionisation by a static electric field

So far we have used perturbation theory to study the energy shifts and the spectral lines of hydrogenic atoms in the presence of a static electric field. We shall now consider another effect due to the presence of an external electric field, namely the removal of the electron from the atom.

To see how this comes about, we first note that the total potential energy V of the electron is obtained by adding the potential energy $e\mathscr{E}z$ arising from the external field (see [5.83]) to the Coulomb potential $-Ze^2/(4\pi\varepsilon_0)r$ of the nucleus.

Thus

$$V = -\frac{Ze^2}{(4\pi\varepsilon_0)r} + e\,\mathscr{E}\,z \qquad [5.115]$$

A schematic drawing of V is shown in Fig. 5.15 as a function of z, for x and y fixed. It is apparent that the nucleus is not the only place at which V has a minimum, since V can become even more negative if z is negative enough, that is at large enough distances of the atom in the direction of the anode. Thus the potential V has two minima, one at the nucleus and the other at the anode, separated by a potential barrier. The electron, which is initially in a bound state of the atom, has therefore a finite probability of 'escaping' from the atom by means of the *tunnel effect*, and being accelerated toward the anode, so that ionisation will occur.

This possibility of ionisation by the electric field was first pointed out by J. Oppenheimer in 1928. Experimentally it can be observed when the external electric field is very strong and (or) for levels with high principal quantum number such that the radius of the electron orbit is large. It is then seen that the spectral lines are *weakened* because of the competition between the radiative transitions and the ionisation process. Moreover, in the presence of an external

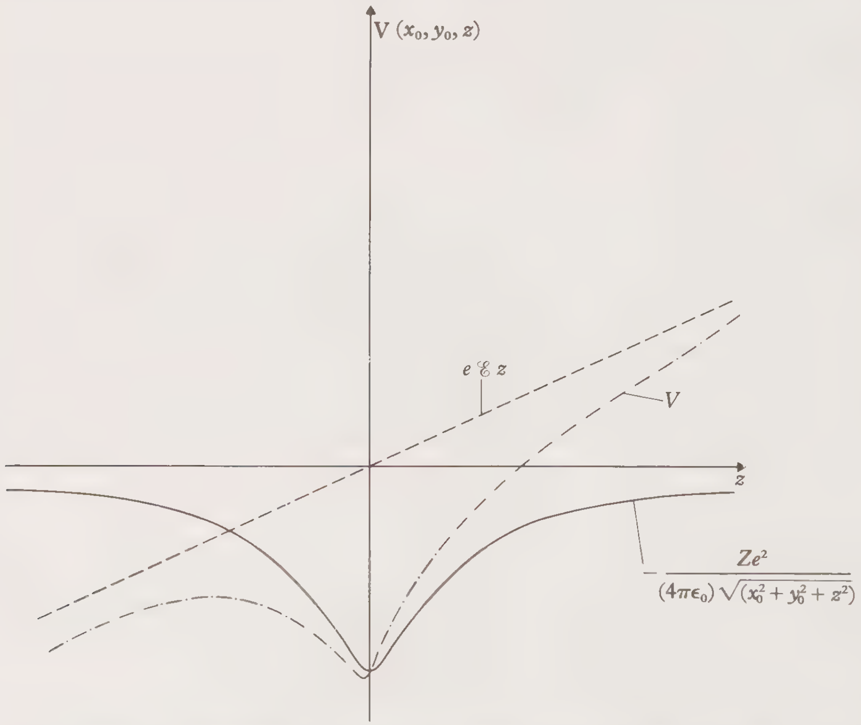

5.15 The potential V experienced by an electron interacting with a nucleus of charge (Ze), in a uniform electric field of strength $\mathscr{E}$, as a function of z, for $x = x_0$ and $y = y_0$ fixed.

electric field the lifetime of the discrete levels is decreased because of the 'tunnel effect', so that the width of the spectral lines is increased. This is known as *Stark broadening*. In particular, the ground state itself is no longer a stationary state, but becomes a metastable state when an external electric field is applied, and the perturbation series is found to diverge. However, if the electric field is not too strong, the ground state is stable on a very large time scale, and the predictions of the first few terms of the perturbation series agree very well with experiment.

5.4 THE LAMB SHIFT

We have seen in Section 5.1 that, according to the Dirac theory, energy levels of one-electron atoms with the same value of the quantum number j but different values of l should coincide. We also pointed out at the end of that section that in trying to resolve the fine structure of hydrogenic atoms by optical measurements, several investigators had reported small discrepancies between the observed spectra and the Dirac theory. In particular, W. V. Houston in 1937 and R. C. Williams in 1938 carried out experiments which were interpreted by S. Pasternack (1938) as showing that the $2s_{1/2}$ and $2p_{1/2}$ levels did not coincide, but that there existed a slight upward shift of the $2s_{1/2}$ level of about 0.03 cm^{-1}. However, the experimental attempts to obtain accurate information about the fine structure of atomic hydrogen (and in particular about the lines of the Balmer series) were frustrated by the broadening of the spectral lines due mainly to the Doppler effect. In fact other spectroscopists disagreed with the results of Houston and Williams, and found no discrepancy with the Dirac theory.

The question was settled in 1947 by W. E. Lamb and R. C. Retherford who performed a brilliant experiment which we shall now briefly describe. Instead of attempting to resolve the fine structure of hydrogen by investigating its optical spectrum, Lamb and Retherford used *microwave techniques* [12] to stimulate a direct *radio-frequency* transition between the $2s_{1/2}$ and $2p_{1/2}$ levels. As we noted in Section 4.5 there is no selection rule on the principal quantum number n for electric dipole transitions. In particular, these transitions can occur between levels having the *same* principal quantum number. This fact was pointed out as early as 1928 by Grotrian, who suggested that it should be possible with radio waves to induce such transitions among the excited states of the hydrogen atom. For example, in the case of the transition $2s_{1/2}-2p_{3/2}$, the energy separation $\delta E = 4.52 \times 10^{-5}$ eV $= 0.365$ cm^{-1} which we obtained in [5.32] corresponds to a wavelength of 2.74 cm or a frequency of 10949 MHz. Because the frequencies of radio waves are much smaller than those corresponding to optical lines (such as the H_α line), the Doppler broadening, which is proportional to the frequency (see [4.145]) is considerably reduced in radio-frequency experiments, and could in fact be neglected in the experiment of Lamb and Retherford. Of course, since the frequencies of radio waves are small, the transition rates for spontaneous emission, which are proportional to ν^3 (see [4.71]) are very small.

[12] A detailed account of microwave spectroscopy may be found in Townes and Schawlow (1955).

However, *stimulated* (induced) transitions can occur if the atoms are sent through a region where there is an electric field oscillating at the appropriate frequency corresponding to the transition to be studied. In the experiment of Lamb and Retherford such stimulated transitions are observed between the levels $2s_{1/2}$–$2p_{1/2}$ and $2s_{1/2}$–$2p_{3/2}$. Since the transition rates for stimulated absorption and emission are equal (see [4.43]), it is necessary that the two states between which the transitions are studied should be unequally populated.

The experimental method of Lamb and Retherford is based on the fact that the $2s_{1/2}$ level is *metastable*. Indeed, as we have seen in Chapter 4, the electric dipole transition from the state $2s_{1/2}$ to the ground state $1s_{1/2}$ is forbidden by the selection rule $\Delta l = \pm 1$. The most probable decay mechanism of the $2s_{1/2}$ state is two-photon emission, with a lifetime of 1/7 s. Thus, in the absence of perturbations, the lifetime of the $2s_{1/2}$ state is very long compared to that of the 2p states, which is about 1.6×10^{-9} s. In the apparatus of Lamb and Retherford, shown in Fig. 5.16, a beam of atomic hydrogen containing atoms in the metastable $2s_{1/2}$ state is produced by first dissociating molecular hydrogen in a tungsten oven (at a temperature of 2500 K where the dissociation is about 64 per cent complete), selecting a jet of atoms by means of slits, and bombarding this jet with a beam of electrons having a kinetic energy somewhat larger than 10.2 eV, which is the threshold energy for excitation of the $n = 2$ levels of atomic hydrogen. In this way a small fraction of hydrogen atoms (about one in 10^8) is excited to the $2s_{1/2}$, $2p_{1/2}$ and $2p_{3/2}$ states. The average velocity of the atomic beam is about 8×10^5 cm s^{-1}. Because of their long lifetime, the atoms in the metastable $2s_{1/2}$ state can easily reach a detector placed at a distance of about 10 cm from the region where they are produced. On the other hand the atoms which are excited in the $2p_{1/2}$ or $2p_{3/2}$ states quickly decay to the ground state $1s_{1/2}$ in 1.6×10^{-9} s, moving only about 1.3×10^{-3} cm in that time, so that they cannot reach the detector. This detector is a metallic surface (a tungsten ribbon), from which the atoms in the metastable state $2s_{1/2}$ can eject electrons by giving up their excitation energy. Atoms in the ground state are not detected, the measured electronic current being proportional to the number of metastable atoms reaching the detector. Now, if the beam containing the metastable $2s_{1/2}$ atoms passes through an 'interaction region' in which a radio-frequency field of the proper frequency is applied, the metastable atoms will undergo induced transitions to the $2p_{1/2}$ and $2p_{3/2}$ states, and decay to the

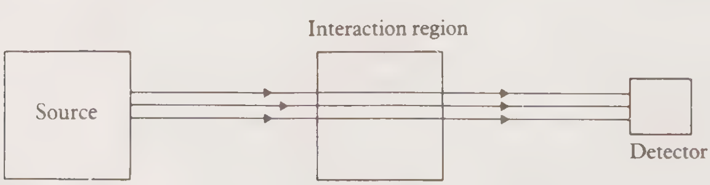

5.16 Schematic diagram of the Lamb–Retherford experiment. The source produces an atomic beam of hydrogen containing a small fraction of atoms in the $2s_{1/2}$ level. The beam is passed through a region of a radio-frequency electric field and a variable magnetic field and is detected by an apparatus which records only atoms in the $n = 2$ level.

ground state $1s_{1/2}$ in which they are not detected. As a result, there is a reduction of the number of metastable ($2s_{1/2}$) atoms registered by the detector at the (resonant) radio-frequencies corresponding to the frequencies of the $2s_{1/2}$–$2p_{1/2}$ and $2s_{1/2}$–$2p_{3/2}$ transitions. In the 'interaction region' the atomic beam also passes in a variable magnetic field. In this way Lamb and Retherford could separate not only the Zeeman components of the $2s_{1/2}$, $2p_{1/2}$ and $2p_{3/2}$ levels, but also reduce the probability of fortuitious disintegration of the $2s_{1/2}$ state due to Stark effect mixing of the $2s_{1/2}$ and the 2p levels caused by perturbing electric fields. Moreover, the use of a variable external magnetic field avoids the difficulty of producing a radio-frequency field with a variable frequency but a constant radio-frequency power. Instead, Lamb and Retherford could operate at a fixed frequency of the radio-frequency field and obtain the passage through the resonance by varying the magnetic field. The resonance frequency for zero magnetic field was found by extrapolation. In this way Lamb and Retherford found in 1947 that the $2s_{1/2}$ level lies above the $2p_{1/2}$ level by an amount of about 1000 MHz. Further experiments carried out by Lamb and his collaborators gave the very precise value (1057.77 ± 0.10) MHz for this energy difference, which is now called a 'Lamb shift'. We note that this value, which corresponds to 4.37462×10^{-6} eV or $0.0352834\ \mathrm{cm}^{-1}$, is about one-tenth of the fine structure splitting of the $n = 2$ term.

The need to explain the Lamb shift stimulated numerous theoretical developments which led Bethe, Tomonaga, Schwinger, Feynman and Dyson to fundamental revisions of physical concepts (such as the renormalisation of mass) and to the formulation of the theory of *quantum electrodynamics* (QED). In this theory, 'radiative corrections' to the Dirac theory are obtained by taking into account the interaction of the electron with the quantised electromagnetic field. These calculations are outside the scope of this book, and we only mention the following qualitative explanation of the Lamb shift given in 1948 by Welton. A quantised radiation field in its lowest energy state is not one with zero electromagnetic fields, but there exist zero-point oscillations similar to those we discussed for the case of the harmonic oscillator in Section 2.4. This means that even in the vacuum there are fluctuations in this zero-point radiation field which can act on the electron, causing it to execute rapid oscillatory motions so that its charge is 'smeared out' and the point electron effectively becomes a sphere of a certain radius. If the electron is bound by a non-uniform electric field, as in atomic systems, it will therefore experience a potential which is slightly different from that corresponding to its mean position. In particular, the electron in a one-electron atom is not so strongly attracted to the nucleus at short distances. As a result, s-states (which are most sensitive to short distance modifications because $|\psi(0)|^2 \neq 0$ for these states) are raised in energy with respect to other states, for which the corresponding modifications are much smaller.

The energy shifts for the $2s_{1/2}$, $2p_{1/2}$ and $2p_{3/2}$ levels with respect to the Dirac theory are illustrated in Fig. 5.17 for the case of atomic hydrogen. The theoretical value of 1057.91 MHz for the Lamb shift (the energy difference between the $2s_{1/2}$ and $2p_{1/2}$ levels) is in excellent agreement with the

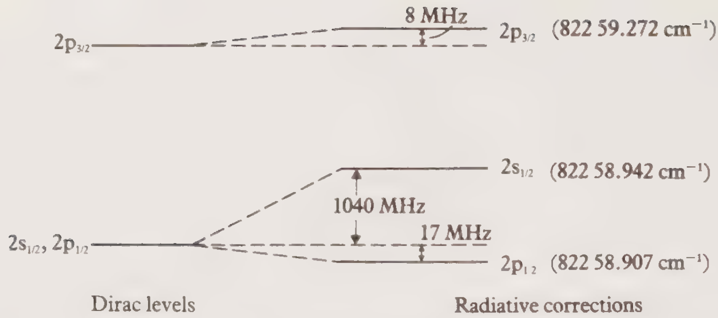

5.17 A diagram (not to scale) of the Lamb shift of the $n = 2$ levels of atomic hydrogen. The energies of the levels relative to the ground state are given to the right of the diagram in units of cm^{-1}.

experimental value (1057.77 ± 0.10) MHz obtained by Lamb *et al.* and with a more recent measurement by Robiscoe and Shyn giving the result (1057.90 ± 0.06) MHz. The Lamb shift has also been measured and calculated for other levels of atomic hydrogen and also for other hydrogenic systems such as deuterium, He^+, Li^{2+}, and so on.

5.5 HYPERFINE STRUCTURE AND ISOTOPE SHIFTS

Atomic nuclei have radii of the order of 10^{-4} Å (10^{-14} m) which are very small compared with typical distances of an electron from the nucleus (~1 Å). The nuclei are also much heavier (about 10^4 times) than electrons. It is therefore a very good approximation to consider the nuclei to be positive point charges of infinite mass. However, the high-precision experiments which can be carried out in atomic physics reveal the existence of tiny effects on the electronic energy levels, which cannot be explained if the nuclei are considered to be point charges of infinite mass. These effects, first observed by A. Michelson in 1891 and C. Fabry and A. Perot in 1897 are called *hyperfine effects*, because they produce shifts of the electronic energy levels which are usually much smaller than those corresponding to the fine structure studied in Section 5.1.

It is convenient to classify the hyperfine effects into those which give rise to *splittings* of the electronic energy levels, and those which slightly shift the energy levels, but without giving rise to splittings. The former are called *hyperfine structure* effects while the latter are known as *isotope shifts* (or isotope effects) since they can usually be detected only by examining their variation between two or more isotopes. We have already encountered examples of isotopic shifts in Chapters 1 and 3, when we studied the modification of the energy levels of hydrogenic atoms due to the fact that *the nuclear mass is finite* (reduced mass effect). In particular, we saw that the introduction of the reduced mass gives a very good account of the frequency difference between the spectral lines of 'ordinary' atomic hydrogen (proton + electron) and its heavy isotope, deuterium (deuteron + electron). Another isotope shift is the *volume effect*, which arises because the nuclear charge is distributed within a finite volume, so that

the potential felt by the electron is modified at short distances. We shall briefly consider this effect at the end of this section.

Let us now turn our attention to the *hyperfine structure effects*, which are responsible for splittings (extending over the range from 10^{-3} to $1\ \mathrm{cm}^{-1}$) of the energy levels of the atoms. These effects result from the fact that a nucleus may possess *electromagnetic multipole moments* (of higher order than the electric monopole) which can interact with the electromagnetic field produced at the nucleus by the electrons. By using general symmetry arguments of parity and time-reversal invariance it may be shown [13] that the number of possible multipole (2^k pole) nuclear moments is severely restricted. Indeed, the only non-vanishing nuclear multipole moments are the *magnetic moments* for *odd k* and the *electric moments* for *even k*, i.e. the magnetic dipole ($k = 1$), electric quadrupole ($k = 2$), magnetic octupole ($k = 3$), and so on. The most important of these moments are the *magnetic dipole moment* (associated with the nuclear spin) and the *electric quadrupole moment* (caused by the departure from a spherical charge distribution in the nucleus). We shall first examine the hyperfine structure due to the magnetic dipole interaction and then discuss briefly the electric quadrupole interaction.

Magnetic dipole hyperfine structure

In 1924 W. Pauli suggested that a nucleus has a total angular momentum $\mathbf{I}$ (called 'nuclear spin') and that hyperfine structure effects might be due to magnetic interactions between the nucleus and the moving electrons of the atom, dependent upon the orientation of this nuclear spin. The eigenvalues of the operator $\mathbf{I}^2$ will be written as $I(I+1)\hbar^2$, where I is the *nuclear spin quantum number* (also often called the spin of the nucleus) or in other words the maximum possible component of $\mathbf{I}$ (measured in units of $\hbar$) in any given direction. Now the nucleus is a compound structure of nucleons (protons and neutrons) which have an intrinsic spin 1/2 and may participate in orbital motion within the nucleus. Thus the nuclear spin is compounded from the spins of the nucleons, and can also contain an orbital component. The corresponding spin quantum number I may have integral or half-integral values. In the former case the nucleus is a *boson* (obeying Bose–Einstein statistics) while in the latter case it is a *fermion* (obeying Fermi-Dirac statistics). We shall also denote by $M_I\hbar$ the eigenvalues of the operator I_z, so that the possible values of M_I are $M_I = -I, -I+1, \ldots, I$.

As we pointed out above, a nucleus may possess 2^k-pole moments, with k odd for magnetic moments and k even for electric moments. Furthermore, it may be shown [13] that a nucleus of spin quantum number I cannot have a multipole moment of order 2^n, where n is greater than $2I$. We shall begin by considering the nucleus as a point dipole with a magnetic dipole moment $\boldsymbol{\mathcal{M}}_{\mathrm{N}}$ proportional to

[13] See for example Ramsey (1953).

the nuclear spin **I**. That is,

$$\boldsymbol{\mathcal{M}}_{\mathrm{N}} = g_I \mu_{\mathrm{N}} \mathbf{I}/\hbar \qquad [5.116]$$

where g_I is a dimensionless number (whose order of magntiude is unity) called the *nuclear g factor* or *nuclear Landé factor*. We note that g_I is positive if $\boldsymbol{\mathcal{M}}_{\mathrm{N}}$ lies along **I**. The quantity μ_{N} which appears in [5.116] is called the *nuclear magneton*; it is defined by

$$\mu_{\mathrm{N}} = \frac{e\hbar}{2M_{\mathrm{p}}} = \frac{m}{M_{\mathrm{p}}} \mu_{\mathrm{B}} \qquad [5.117]$$

where m is the mass of the electron, M_{p} the mass of the proton and μ_{B} the Bohr magneton. Thus the nuclear magneton μ_{N} is smaller than the Bohr magneton μ_{B} by the factor $m/M_{\mathrm{p}} = 1/1836.15$. The numerical value of the nuclear magneton is

$$\mu_{\mathrm{N}} = 5.05082 \times 10^{-27} \text{ joule/Tesla} \qquad [5.118]$$

It is worth noting that [5.116] is sometimes written in units of Bohr magnetons as

$$\boldsymbol{\mathcal{M}}_{\mathrm{N}} = g'_I \mu_{\mathrm{B}} \mathbf{I}/\hbar \qquad [5.119]$$

in which case

$$g'_I = \frac{\mu_{\mathrm{N}}}{\mu_{\mathrm{B}}} g_I = \frac{m}{M_{\mathrm{p}}} g_I = \frac{g_I}{1836.15} \qquad [5.120]$$

is a very small number. Since $I\hbar$ is the maximum component of **I** in a given direction, we may also write [5.116] as

$$\boldsymbol{\mathcal{M}}_{\mathrm{N}} = \left(\frac{\mathcal{M}_{\mathrm{N}}}{I}\right) \mathbf{I}/\hbar \qquad [5.121]$$

where $\mathcal{M}_{\mathrm{N}}$ is the value of the nuclear magnetic moment. In units of nuclear magnetons, we have

$$\mathcal{M}_{\mathrm{N}} = g_I I \qquad [5.122]$$

The values of the spin quantum number I, the nuclear Landé factor g_I and the nuclear magnetic moment $\mathcal{M}_{\mathrm{N}}$ are given in Table 5.1 for the nucleons and a few nuclei.

Let us consider a hydrogenic atom with a nucleus of charge Ze such that $Z\alpha \ll 1$, and a magnetic dipole moment $\boldsymbol{\mathcal{M}}_{\mathrm{N}}$. We shall write the Hamiltonian of this system as

$$H = H_0 + H'_{\mathrm{MD}} \qquad [5.123]$$

where the zero-order Hamiltonian H_0 now includes the Coulomb interaction $-Ze^2/(4\pi\varepsilon_0)r$ and the relativistic (fine structure) corrections discussed in

Table 5.1 Values of the spin, Landé factor and magnetic moment of the nucleons and some nuclei. The notation is such that ${}^a_bX$ represents a nucleus with a total of a nucleons, b of which are protons

Nucleus	*Spin* I	*Landé factor* g_I	*Magnetic moment* $\mathcal{M}_N$ *(in nuclear magnetons)*
proton p	1/2	5.5883	2.79278
neutron n	1/2	−3.8263	−1.91315
deuteron ${}^2_1D$	1	0.85742	0.85742
${}^3_2He$	1/2	−4.255	−2.1276
${}^4_2He$	0	—	0
${}^{12}_6C$	0	—	0
${}^{16}_8O$	0	—	0
${}^{39}_{19}K$	3/2	0.2609	0.3914
${}^{67}_{30}Zn$	5/2	0.35028	0.8757
${}^{85}_{37}Rb$	5/2	0.54108	1.3527
${}^{129}_{54}Xe$	1/2	−1.5536	−0.7768
${}^{133}_{55}Cs$	7/2	0.7369	2.579
${}^{199}_{80}Hg$	1/2	1.0054	0.5027
${}^{201}_{80}Hg$	3/2	−0.37113	−0.5567

Section 5.1 (which are of order $(Z\alpha)^2$, as seen from [5.29]) while H'_{MD} is a perturbative term due to the presence of the magnetic dipole moment $\mathcal{M}_N$. This term will clearly lead to even smaller corrections than those corresponding to the fine structure, since the magnetic moment of the nucleus is much smaller than that of the electron. We may therefore assume that we can deal with an isolated electronic level labelled by the total electronic angular momentum quantum number j. The zero-order wave functions (eigenfunctions of H_0) are separable in the electronic and nuclear variables and are eigenfunctions of $\mathbf{J}^2$, $\mathcal{J}_z$, $\mathbf{I}^2$ and I_z (where $\mathbf{J} = \mathbf{L} + \mathbf{S}$ is the total electronic angular momentum operator). Using the Dirac notation, we shall write them as $|\gamma j m_j I M_I\rangle$, where the symbol γ represents additional quantum numbers. These zero-order wave functions are $(2j + 1)(2I + 1)$-fold degenerate in m_j and M_I. We also remark that in the Pauli approximation (see Appendix 7) – which we shall adopt here – the zero-order wave functions are also eigenfunctions of $\mathbf{L}^2$ and $\mathbf{S}^2$, and will thus be written more explicitly as $|lsjm_jIM_I\rangle$.

We now examine the perturbation H'_{MD} due to the magnetic dipole moment $\mathcal{M}_N$ of the nucleus. The magnetic field due to this dipole moment will interact with both the orbital angular momentum $\mathbf{L}$ and the spin $\mathbf{S}$ of the atomic electron. We shall denote the former interaction by H'_1 and the second by H'_2, so that

$$H'_{MD} = H'_1 + H'_2 \qquad [5.124]$$

The term H'_1 is readily evaluated as follows. The vector potential $\mathbf{A}(\mathbf{r})$ due to a point dipole located at the origin is

$$\mathbf{A}(\mathbf{r}) = -\frac{\mu_0}{4\pi}\left[\mathcal{M}_N \times \nabla\left(\frac{1}{r}\right)\right]$$
$$= \frac{\mu_0}{4\pi}(\mathcal{M}_N \times \mathbf{r})\frac{1}{r^3} \qquad [5.125]$$

Neglecting for a moment the spin of the electron, the interaction term due to the presence of the vector potential $\mathbf{A}(\mathbf{r})$ is (see [4.22])

$$H'_1 = -\frac{i\hbar e}{m}\mathbf{A}\cdot\nabla \qquad [5.126]$$

Inserting [5.125] into [5.126] we obtain after a straightforward calculation (Problem 5.7)

$$H'_1 = \frac{\mu_0}{4\pi}\frac{2}{\hbar}\mu_B\frac{1}{r^3}\mathbf{L}\cdot\mathcal{M}_N$$
$$= \frac{\mu_0}{4\pi}\frac{2}{\hbar^2}g_I\mu_B\mu_N\frac{1}{r^3}\mathbf{L}\cdot\mathbf{I} \qquad [5.127]$$

where we have used [5.116] and we recall that $\mathbf{L} = \mathbf{r}\times\mathbf{p}$. We remark that the term H'_1 may be interpreted as the interaction of the nuclear dipole moment $\mathcal{M}_N$ with the magnetic field $-(\mu_0/4\pi)e\mathbf{L}/mr^3$ created at the nucleus by the rotation of the electronic charge. We also note that H'_1 has non-zero matrix elements only between states for which $l \neq 0$.

Next, we find the contribution H'_2 arising from the electron spin $\mathbf{S}$. The magnetic field associated with the vector potential [5.125] is

$$\mathcal{B} = \nabla\times\mathbf{A}$$
$$= -\frac{\mu_0}{4\pi}\left[\mathcal{M}_N\nabla^2\left(\frac{1}{r}\right) - \nabla(\mathcal{M}_N\cdot\nabla)\frac{1}{r}\right] \qquad [5.128]$$

The spin magnetic moment of the electron is $\mathcal{M}_s = -g_s\mu_B\mathbf{S}/\hbar$ so that the corresponding interaction energy is (with $g_s = 2$)

$$H'_2 = -\mathcal{M}_s\cdot\mathcal{B} = 2\mu_B\mathbf{S}\cdot\mathcal{B}/\hbar \qquad [5.129]$$

or

$$H'_2 = \frac{\mu_0}{4\pi}\left[\mathcal{M}_s\cdot\mathcal{M}_N\nabla^2\left(\frac{1}{r}\right) - (\mathcal{M}_s\cdot\nabla)(\mathcal{M}_N\cdot\nabla)\frac{1}{r}\right]$$
$$= -\frac{\mu_0}{4\pi}\frac{2}{\hbar^2}g_I\mu_B\mu_N\left[\mathbf{S}\cdot\mathbf{I}\,\nabla^2\left(\frac{1}{r}\right) - (\mathbf{S}\cdot\nabla)(\mathbf{I}\cdot\nabla)\frac{1}{r}\right] \qquad [5.130]$$

where we have used [5.116].

It is convenient to examine the term H'_2 separately for the two cases $r \neq 0$ and $r = 0$. Since the hydrogenic wave functions behave like r^l at the origin, the

expression of H_2' at $r = 0$ will only be relevant for states with $l = 0$ (s-states). We first note that since

$$\nabla^2\left(\frac{1}{r}\right) = -4\pi\,\delta(\mathbf{r}) \tag{5.131}$$

the first term in square brackets in [5.130] vanishes for $r \neq 0$. It is also a simple matter to show (Problem 5.8) that for $r \neq 0$

$$(\mathbf{S}\cdot\nabla)(\mathbf{I}\cdot\nabla)\frac{1}{r} = -\frac{1}{r^3}\left[\mathbf{S}\cdot\mathbf{I} - 3\frac{(\mathbf{S}\cdot\mathbf{r})(\mathbf{I}\cdot\mathbf{r})}{r^2}\right], \qquad r \neq 0 \tag{5.132}$$

Hence, using [5.130] and [5.132], we have

$$\begin{aligned} H_2' &= -\frac{\mu_0}{4\pi}\frac{2}{\hbar^2}g_I\mu_{\rm B}\mu_{\rm N}\frac{1}{r^3}\left[\mathbf{S}\cdot\mathbf{I} - 3\frac{(\mathbf{S}\cdot\mathbf{r})(\mathbf{I}\cdot\mathbf{r})}{r^2}\right] \\ &= \frac{\mu_0}{4\pi}\frac{1}{r^3}\left[\boldsymbol{\mathcal{M}}_s\cdot\boldsymbol{\mathcal{M}}_{\rm N} - 3\frac{(\boldsymbol{\mathcal{M}}_s\cdot\mathbf{r})(\boldsymbol{\mathcal{M}}_{\rm N}\cdot\mathbf{r})}{r^2}\right], \qquad r \neq 0 \end{aligned} \tag{5.133}$$

which represents the dipole–dipole interaction between the magnetic moments of the electron and the nucleus. Adding the results [5.127] and [5.133], the interaction between the nuclear magnetic dipole moment and an electron for which $l \neq 0$ is seen to be

$$H'_{\rm MD} = \frac{\mu_0}{4\pi}\frac{2}{\hbar^2}g_I\mu_{\rm B}\mu_{\rm N}\frac{1}{r^3}\left[\mathbf{L}\cdot\mathbf{I} - \mathbf{S}\cdot\mathbf{I} + 3\frac{(\mathbf{S}\cdot\mathbf{r})(\mathbf{I}\cdot\mathbf{r})}{r^2}\right], \qquad r \neq 0 \tag{5.134}$$

Let us now return to the expression [5.130] of H_2' and consider the case $r = 0$, which is important for s-states ($l = 0$). We have already seen that the first term in square brackets in [5.130] is porportional to $\delta(\mathbf{r})$. The second term in square brackets contains a similar term proportional to $\delta(\mathbf{r})$, as we now show. Indeed, for matrix elements involving spherically symmetric states (with $l = 0$) we remark that out of the expression (with $x_1 = x$, $x_2 = y$, $x_3 = z$)

$$(\mathbf{S}\cdot\nabla)(\mathbf{I}\cdot\nabla)\frac{1}{r} = \sum_{i=1}^{3}\sum_{j=1}^{3} S_i I_j \frac{\partial^2}{\partial x_i \partial x_j}\left(\frac{1}{r}\right) \tag{5.135}$$

all terms will vanish except those with $i = j$. Each of the matrix elements of

$$\frac{\partial^2}{\partial x_1^2}\left(\frac{1}{r}\right), \qquad \frac{\partial^2}{\partial x_2^2}\left(\frac{1}{r}\right), \qquad \frac{\partial^2}{\partial x_3^2}\left(\frac{1}{r}\right)$$

must have the same value, so that for $l = 0$

$$\begin{aligned} (\mathbf{S}\cdot\nabla)(\mathbf{I}\cdot\nabla)\frac{1}{r} &= \frac{1}{3}(\mathbf{S}\cdot\mathbf{I})\nabla^2\left(\frac{1}{r}\right) \\ &= -\frac{4\pi}{3}\mathbf{S}\cdot\mathbf{I}\,\delta(\mathbf{r}) \end{aligned} \tag{5.136}$$

From these equations and the fact that the term H'_1 does not contribute for states with $l = 0$, we deduce that the interaction between the nuclear magnetic dipole moment and an s electron is given by

$$H'_{\text{MD}} = \frac{\mu_0}{4\pi}\frac{2}{\hbar^2} g_I \mu_B \mu_N \frac{8\pi}{3} \delta(\mathbf{r})\mathbf{S} \cdot \mathbf{I}$$

$$= -\frac{\mu_0}{4\pi}\frac{8\pi}{3} \boldsymbol{\mathcal{M}}_{\text{S}} \cdot \boldsymbol{\mathcal{M}}_{\text{N}}\, \delta(\mathbf{r}), \qquad l = 0 \qquad [5.137]$$

This expression, which is proportional to $\delta(\mathbf{r})$, is called the *Fermi contact interaction*.

We now proceed to the calculation of the *first-order energy shifts* due to the perturbations [5.134] and [5.137]. We begin by considering the case $l \neq 0$, and write [5.134] more simply as

$$H'_{\text{MD}} = \frac{\mu_0}{4\pi}\frac{2}{\hbar^2} g_I \mu_B \mu_N \frac{1}{r^3} \mathbf{G} \cdot \mathbf{I} \qquad [5.138]$$

where

$$\mathbf{G} = \mathbf{L} - \mathbf{S} + 3\frac{(\mathbf{S} \cdot \mathbf{r})\mathbf{r}}{r^2} \qquad [5.139]$$

We have seen above that the zero-order wave functions $|lsjm_j IM_I\rangle$ are $(2j + 1)(2I + 1)$-fold degenerate in m_j and M_I. By analogy with the spin–orbit coupling discussed in Section 5.1, the diagonalisation of the perturbation is greatly simplified by introducing the total angular momentum of the atom (nucleus + electron)

$$\mathbf{F} = \mathbf{I} + \mathbf{J} \qquad [5.140]$$

We shall denote by $F(F + 1)\hbar^2$ the eigenvalues of the operator $\mathbf{F}^2$ and by $M_F\hbar$ those of F_z, with $M_F = -F, -F + 1, \ldots, +F$. From the rules concerning the addition of angular momenta, the possible values of the quantum number F are given by

$$F = |I - j|, |I - j| + 1, \ldots, I + j - 1, I + j \qquad [5.141]$$

Since F and M_F remain good quantum numbers under the application of the perturbation H'_{MD}, it is convenient to form new zero-order functions $|lsjIFM_F\rangle$ which are linear combinations of the functions $|lsjm_j IM_I\rangle$. The energy shift due to the perturbation [5.138] is then

$$\Delta E = \frac{\mu_0}{4\pi}\frac{2}{\hbar^2} g_I \mu_{\text{B}} \mu_{\text{N}} \left\langle lsjIFM_F \left| \frac{1}{r^3} \mathbf{G} \cdot \mathbf{I} \right| lsjIFM_F \right\rangle, \qquad l \neq 0 \qquad [5.142]$$

Using the identity [5.76] we can replace the matrix element of $\mathbf{G} \cdot \mathbf{I}$ taken between states with equal j by that of

$$\mathbf{G} \cdot \mathbf{I} = \frac{(\mathbf{G} \cdot \mathbf{J})(\mathbf{I} \cdot \mathbf{J})}{j(j + 1)\hbar^2} \qquad [5.143]$$

Moreover, since

$$\mathbf{F}^2 = \mathbf{I}^2 + 2\mathbf{I}\cdot\mathbf{J} + \mathbf{J}^2 \qquad [5.144]$$

so that

$$\mathbf{I}\cdot\mathbf{J} = \tfrac{1}{2}(\mathbf{F}^2 - \mathbf{I}^2 - \mathbf{J}^2) \qquad [5.145]$$

we have

$$\Delta E = \frac{C}{2}[F(F+1) - I(I+1) - j(j+1)] \qquad [5.146a]$$

with

$$C = \frac{\mu_0}{4\pi} 2g_I\mu_B\mu_N \frac{1}{j(j+1)\hbar^2}\left\langle \frac{1}{r^3}\mathbf{G}\cdot\mathbf{J}\right\rangle, \qquad l \neq 0 \qquad [5.146b]$$

and we have used the simplified notation $\langle\rangle$ for the expectation value.

The quantity $\langle r^{-3}\,\mathbf{G}\cdot\mathbf{J}\rangle$ is readily obtained as follows. We first note that since $\mathbf{L}\cdot\mathbf{r} = 0$, we may write

$$\begin{aligned}\mathbf{G}\cdot\mathbf{J} &= \left(\mathbf{L} - \mathbf{S} + 3\frac{(\mathbf{S}\cdot\mathbf{r})\mathbf{r}}{r^2}\right)\cdot(\mathbf{L}+\mathbf{S}) \\ &= \mathbf{L}^2 - \mathbf{S}^2 + 3\frac{(\mathbf{S}\cdot\mathbf{r})^2}{r^2}\end{aligned} \qquad [5.147]$$

It is easily shown (Problem 5.8) that

$$\mathbf{S}^2 - 3\frac{(\mathbf{S}\cdot\mathbf{r})^2}{r^2} = 0 \qquad [5.148]$$

so that $\mathbf{G}\cdot\mathbf{J} = \mathbf{L}^2$ and

$$\left\langle \frac{1}{r^3}\mathbf{G}\cdot\mathbf{J}\right\rangle = l(l+1)\hbar^2\left\langle\frac{1}{r^3}\right\rangle \qquad [5.149]$$

Thus we have

$$\begin{aligned}C &= \frac{\mu_0}{4\pi}2g_I\mu_B\mu_N\frac{l(l+1)}{j(j+1)}\left\langle\frac{1}{r^3}\right\rangle \\ &= \frac{\mu_0}{4\pi}2g_I\mu_B\mu_N\frac{l(l+1)}{j(j+1)}\frac{Z^3}{a_\mu^3 n^3 l(l+1/2)(l+1)}, \qquad l \neq 0\end{aligned} \qquad [5.150]$$

where we have used the expectation value of r^{-3} given by [3.73], and we recall that $a_\mu = a_0(m/\mu)$, μ being the reduced mass of the electron with respect to the nucleus.

Turning now to the case of s-states ($l = 0$), the first-order energy shift due to the perturbation [5.137] is

$$\Delta E = \frac{\mu_0}{4\pi}\frac{2}{\hbar^2}g_I\mu_B\mu_N\frac{8\pi}{3}\langle\delta(\mathbf{r})\mathbf{S}\cdot\mathbf{I}\rangle, \qquad l = 0 \qquad [5.151]$$

As $\mathbf{L} = 0$, we have $\mathbf{F} = \mathbf{I} + \mathbf{S}$, from which

$$\mathbf{S} \cdot \mathbf{I} = \tfrac{1}{2}(\mathbf{F}^2 - \mathbf{I}^2 - \mathbf{S}^2) \qquad [5.152]$$

and therefore

$$\Delta E = \frac{C_0}{2}[F(F+1) - I(I+1) - s(s+1)] \qquad [5.153a]$$

with

$$C_0 = \frac{\mu_0}{4\pi} 2g_I \mu_B \mu_N \frac{8\pi}{3} \langle \delta(\mathbf{r}) \rangle, \qquad l = 0 \qquad [5.153b]$$

Now

$$\begin{aligned} \langle \delta(\mathbf{r}) \rangle &= \int |\psi_{n00}(r)|^2 \, \delta(\mathbf{r}) \, d\mathbf{r} \\ &= |\psi_{n00}(0)|^2 \\ &= \frac{Z^3}{\pi a_\mu^3 n^3} \end{aligned} \qquad [5.154]$$

where we have used the result [3.60]. Thus

$$C_0 = \frac{\mu_0}{4\pi} \frac{16}{3} g_I \mu_B \mu_N \frac{Z^3}{a_\mu^3 n^3} \qquad [5.155]$$

Comparing [5.146] and [5.153], and recalling that $j = s$ for s-states, we see that for both cases $l \neq 0$ and $l = 0$ we have

$$\Delta E = \frac{C}{2}[F(F+1) - I(I+1) - j(j+1)] \qquad [5.156a]$$

with

$$C = \frac{\mu_0}{4\pi} 4g_I \mu_B \mu_N \frac{1}{j(j+1)(2l+1)} \frac{Z^3}{a_\mu^3 n^3} \qquad [5.156b]$$

Using atomic units and introducing the fine structure constant α, we may also write this result as

$$\Delta E = \frac{1}{2} \frac{m}{M_p} g_I \frac{Z^3 \alpha^2}{n^3} \left(\frac{\mu}{m} \right)^3 \frac{F(F+1) - I(I+1) - j(j+1)}{j(j+1)(2l+1)} \quad \text{a.u.} \qquad [5.157]$$

For a given nucleus having a spin quantum number I, a fine structure atomic energy level corresponding to fixed values of l and j is therefore split further into hyperfine components labelled by F. Since the energy correction does not depend on M_F, each of these hyperfine energy levels is $(2F + 1)$-fold degenerate. The possible values of F being $|I - j|, |I - j| + 1, \ldots I + j$ (see [5.141]), the number of hyperfine structure components corresponding to a fine structure

energy level is the smaller of the two numbers $(2j+1)$ and $(2I+1)$. These components are said to form a *hyperfine structure multiplet.* As an example, we shown in Fig. 5.18 a schematic drawing of the hyperfine structure splitting of the $n = 1$ and $n = 2$ levels of 'ordinary' hydrogen (H) and deuterium (D). For 'ordinary' hydrogen the spin of the nucleus is just the spin of the proton, $I = 1/2$, and since $j = 1/2, 3/2, \ldots$ we always have hyperfine *doublets*. On the other hand, for deuterium the spin of the nucleus is $I = 1$, so that we have doublets for $j = 1/2$ and triplets for the other values of j.

We remark from [5.156] that since the quantity C is independent of F the *energy difference* between two neighbouring hyperfine levels – called *hyperfine separation* – is just

$$\Delta E(F) - \Delta E(F-1) = CF \qquad [5.158]$$

and is thus proportional to F. This is an example of an *interval rule*. From [5.157] we also see that the energy separation δE between the two outermost components of the hyperfine multiplet (corresponding to the values $F_1 = I + j$ and $F_2 = |I - j|$ of the quantum number F) is given in atomic units by

$$\delta E = \frac{m}{M_p}\left(\frac{\mu}{m}\right)^3 g_I \frac{2Z^3\alpha^2}{n^3(j+1)(2l+1)} \times \begin{bmatrix} I + 1/2 & \text{for} \quad j \leqslant I \\ \dfrac{I(j+1/2)}{j} & \text{for} \quad j \geqslant I \end{bmatrix} \qquad [5.159]$$

The *hyperfine structure of spectral lines* resulting from the magnetic dipole interaction may be obtained (in a way similar to the fine structure discussed in Section 5.1) by combining the above results with the *selection rules* for electromagnetic transitions between energy levels. For *electric dipole transitions* the selection rules obtained in Section 5.1 ($\Delta l = \pm 1$ and $\Delta j = 0, \pm 1$) remain valid, and in addition it may be shown that the quantum number F obeys the selection rule

$$\Delta F = 0, \pm 1 \qquad [5.160]$$

the transition $F = 0 \rightarrow F = 0$ being excluded. Examples of allowed hyperfine transitions are shown in Fig. 5.19. We note that transitions between levels having the same value of j but different values of F can also take place. These transitions are in the microwave region and are generally weak, so that they are best observed by using stimulated emission techniques.

The hyperfine transitions, observed by optical or microwave spectroscopy, can be used to determine the spin I and magnetic dipole moment $\mathcal{M}_N = g_I I$ of the nucleus. Indeed, the maximum hyperfine multiplicity of levels with large enough j gives $(2I + 1)$ and the hyperfine separation allows the determination of the nuclear Landé factor g_I. Using the generalisation of the above equations for complex atoms (to be discussed in Chapter 8), the dipole magnetic moments of many nuclei have been obtained.

The hyperfine structure of the $1s_{1/2}$ ground state of 'ordinary' hydrogen (H) is of particular interest, because in this case very elaborate calculations can be

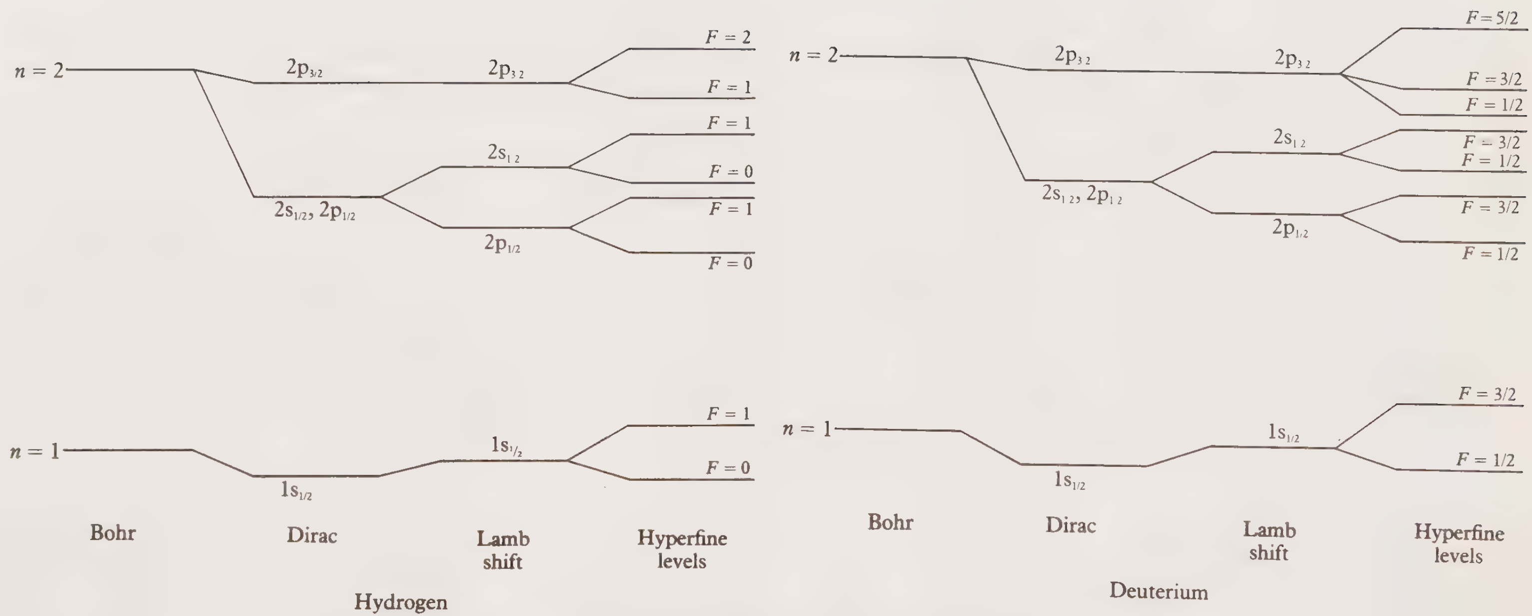

5.18 The splitting of the $n = 1$ and $n = 2$ levels of hydrogen and deuterium. The splittings are not to scale and are magnified from the left to the right of the diagram.

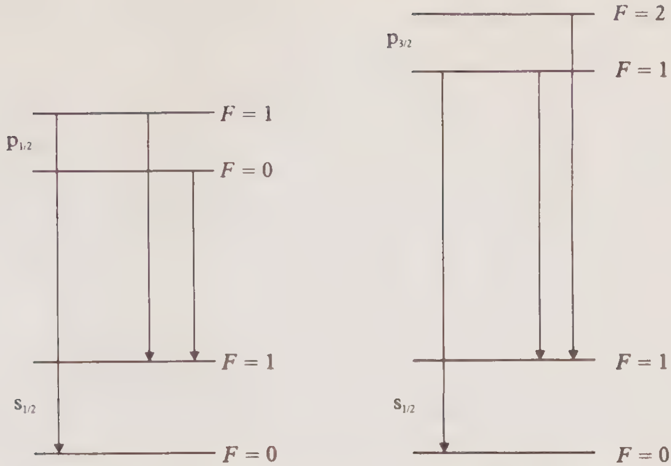

5.19 Allowed dipole transitions between n'p and ns levels of hydrogen. There is no restriction on n' and n, and the case $n' = n$ is allowed.

carried out and compared with extremely high precision measurements, performed by using atomic beam magnetic resonance methods [14]. Since the proton spin is $I = 1/2$ and the level $1s_{1/2}$ has a total electronic angular momentum quantum number $j = 1/2$, this level splits into two hyperfine components corresponding to the values $F = 0$ and $F = 1$, the state with $F = 0$ being the ground state (see Fig. 5.18). Using [5.159] we see that the energy difference between the two hyperfine levels is given in atomic units by

$$\delta E = \frac{4}{3} \frac{m}{M_{\mathrm{p}}} \left(\frac{\mu}{m}\right)^3 g_p \alpha^2 \qquad [5.161]$$

where $g_{\mathrm{p}} = 5.5883$ is the Landé factor of the proton. From this result we find that the frequency $\nu = \delta E/h$ of the transition between the two hyperfine levels (which is a magnetic dipole transition) is $\nu \simeq 1420$ MHz, the corresponding wavelength being $\lambda \simeq 21$cm. The experimental value of ν, obtained by Ramsey *et al.* in 1963 with the 'atomic hydrogen maser' [15] is one of the most accurately measured quantities in physics; it is given by

$$\nu = (1420\,405\,751.800 \pm 0.028) \text{ Hz} \qquad [5.162]$$

It is gratifying to note that the simple theory presented above agrees with this result within about 0.1 per cent. Much better agreement between theory and experiment can be obtained by including various corrections in the theoretical calculations. The most important of these is the introduction of the *anomalous magnetic moment of the electron*, according to which the spin gyromagnetic ratio g_s of the electron is slightly different from the value $g_s = 2$ predicted by the Dirac

[14] A detailed description of these methods may be found in Ramsey (1955).
[15] Masers are discussed in Chapter 14.

theory [6]. However, there is no theory at the present time that can account for all the significant figures given in [5.162]!

We also remark that the transition between the two hyperfine levels $F = 1$ and $F = 0$ of the ground state of hydrogen plays a very important role in *radio-astronomy*. Indeed, from the analysis of the intensity of the 21 cm radio-frequency radiation received, the astronomers have been able to learn a great deal about the distribution of neutral hydrogen atoms in interstellar space. We shall return in more detail to this question in Chapter 14.

Electric quadrupole hyperfine structure

A second important characteristic of the structure of a nucleus is the *electric quadrupole moment*. It is a symmetric, second-order tensor whose components Q_{ij} are defined in the following way. Let $\mathbf{R}_p$ be the coordinate of a proton with respect to the centre of mass of the nucleus, and let $X_{p1} = X_p, X_{p2} = Y_p, X_{p3} = Z_p$ be its Cartesian components. Then

$$Q_{ij} = \sum_p 3X_{pi}X_{pj} - \delta_{ij}R_p^2 \qquad (i, j = 1, 2, 3) \qquad [5.163]$$

where the sum is over all the protons in the nucleus. It is customary to define the *magnitude Q of the electric quadrupole moment* as the average value of the component $Q_{zz} \equiv Q_{33}$ in the state $|I, M_I = I\rangle$. That is

$$\begin{aligned} Q &= \langle I, M_I = I|Q_{zz}|I, M_I = I\rangle \\ &= \left\langle I, M_I = I \left| \sum_p 3Z_p^2 - R_p^2 \right| I, M_I = I \right\rangle \end{aligned} \qquad [5.164]$$

The quantity Q has the dimensions of an area and is often measured in barns (10^{-24} cm^2). For example, the deuteron has a electric quadrupole moment of magnitude $Q = 0.0028$ barns. It is clear from [5.164] that a nucleus whose charge distribution is spherically symmetric has no electric quadrupole moment, since then the average value of $3Z_p^2$ is equal to that of $R_p^2 = X_p^2 + Y_p^2 + Z_p^2$. In fact the value of Q gives a measure of the deviation from a spherical charge distribution in the nucleus. If the nuclear charge distribution is elongated along the direction of $\mathbf{I}$ (prolate), then $Q > 0$; on the other hand $Q < 0$ if the charge distribution is flattened (oblate).

The interaction energy H'_{EQ} between the electric quadrupole moment of the nucleus and the electrostatic potential V_e created by an electron at the nucleus was first obtained by H. Casimir. Provided I and j are both good quantum numbers, it is given in atomic units by [16]

$$H'_{EQ} = B\,\frac{\frac{3}{2}\mathbf{I}\cdot\mathbf{J}\,(2\mathbf{I}\cdot\mathbf{J} + 1) - \mathbf{I}^2\mathbf{J}^2}{2I(2I-1)j(2j-1)} \qquad [5.165]$$

[16] See for example Casimir (1963) or Ramsey (1953).

where the *quadrupole coupling constant* B is given by

$$B = Q\left\langle \frac{\partial^2 V_e}{\partial z^2} \right\rangle \qquad [5.166]$$

Here

$$\begin{aligned}\left\langle \frac{\partial^2 V_e}{\partial z^2} \right\rangle &= \left\langle j, m_j = j \left| \frac{\partial^2 V_e}{\partial z^2} \right| j, m_j = j \right\rangle \\ &= -\left\langle j, m_j = j \left| \frac{3z^2 - r^2}{r^5} \right| j, m_j = j \right\rangle \end{aligned} \qquad [5.167]$$

is the average gradient of the electric field produced by the electron at the nucleus.

The first-order energy shift due to the electric quadrupole interaction [5.165] is

$$\begin{aligned}\Delta E &= \langle jIFM_F | H'_{EQ} | jIFM_F \rangle \\ &= \frac{B}{4} \frac{\frac{3}{2}K(K+1) - 2I(I+1)j(j+1)}{I(2I-1)j(2j-1)}\end{aligned} \qquad [5.168]$$

where

$$K = F(F+1) - I(I+1) - j(j+1) \qquad [5.169]$$

Since $\langle \partial^2 V_e / \partial z^2 \rangle$ vanishes when the electron charge distribution is spherically symmetric, there is no quadrupole energy shift for s-states. We recall that the nuclei having no spin ($I = 0$) or a spin $I = 1/2$ have no electric quadrupole moment, so that the energy shift [5.168] also vanishes in this case.

Adding the electric quadrupole correction [5.168] to the magnetic dipole energy shift [5.156] we find that the total hyperfine structure energy correction is given by

$$\Delta E = \frac{C}{2} K + \frac{B}{4} \frac{\frac{3}{2}K(K+1) - 2I(I+1)j(j+1)}{I(2I-1)j(2j-1)} \qquad [5.170]$$

Because its dependence on the quantum number F is different from that of the magnetic dipole correction [5.156], we see that the electric quadrupole interaction causes a *departure from the interval rule* [5.158].

It is worth noting that the hyperfine energy levels obtained after the correction [5.170] has been applied are still independent of the quantum number M_F, and hence are $(2F + 1)$-fold degenerate. This degeneracy can be removed by applying an external magnetic field. We shall return to this *Zeeman effect in hyperfine structure* in Chapter 8.

Isotope shifts

We now consider briefly the *isotope shifts*, which do not give rise to splittings of the energy levels. As we pointed out above, these isotope shifts are caused by

two effects: the *mass effect* (due to the fact that the nuclear mass is finite) and the *volume effect* (arising from the distribution of the nuclear charge within a finite volume).

For one-electron atoms the mass effect is readily taken into account by the introduction of the *reduced mass* $\mu = mM/(m + M)$, as we saw in Chapters 1 and 3. For the case of atoms with more than one electron the finiteness of the nuclear mass gives rise to an additional energy shift called the *mass polarisation correction*, which will be examined in Chapter 6.

Pauli and Peierls first pointed out in 1931 that the difference in nuclear volume between isotopes can produce an isotope shift. Indeed, since the protons in the nucleus are distributed in a finite nuclear volume, the electrostatic potential inside the nucleus deviates from the $1/r$ law, and depends on the proton distribution within the nucleus. In order to obtain an estimate of this volume effect, let us consider a simple model of the nucleus, such that the nuclear charge is distributed in a uniform way within a sphere of radius

$$R = r_0 A^{1/3} \qquad [5.171]$$

where A is the mass number of the nucleus, and r_0 is a constant whose value is given approximately by $r_0 \simeq 1.2 \times 10^{-15}$ m. In this model, the electrostatic potential $V(r)$ due to the nucleus is easily shown to be (Problem 5.9)

$$V(r) = \begin{cases} \dfrac{Ze^2}{(4\pi\varepsilon_0)2R}\left(\dfrac{r^2}{R^2} - 3\right) & r \leqslant R \\ -\dfrac{Ze^2}{(4\pi\varepsilon_0)r} & r \geqslant R \end{cases} \qquad [5.172]$$

To simplify the problem further, we shall assume that the unperturbed Hamiltonian H_0 is the hydrogenic Hamiltonian [5.1] and that the perturbation H' is just the difference between the interaction [5.172] and the Coulomb interaction $-Ze^2/(4\pi\varepsilon_0)r$. Thus all other effects (such as the relativistic corrections) are neglected and we have

$$H' = \begin{cases} \dfrac{Ze^2}{(4\pi\varepsilon_0)2R}\left(\dfrac{r^2}{R^2} + \dfrac{2R}{r} - 3\right) & r \leqslant R \\ 0 & r \geqslant R \end{cases} \qquad [5.173]$$

The first-order energy shift due to this perturbation is

$$\begin{aligned} \Delta E &= \langle \psi_{nlm} | H' | \psi_{nlm} \rangle \\ &= \frac{Ze^2}{(4\pi\varepsilon_0)2R} \int_0^R |R_{nl}(r)|^2 \left(\frac{r^2}{R^2} + \frac{2R}{r} - 3\right) r^2 \, dr \end{aligned} \qquad [5.174]$$

where we have used [3.48] and the fact that the spherical harmonics are normalised on the unit sphere. Inside the small region $r \leqslant R$ we may write $R_{nl}(r) \simeq R_{nl}(0)$. Moreover, since $R_{nl}(0)$ vanishes except for s-states ($l = 0$), we

have, after a straightforward calculation (Problem 5.9)

$$\Delta E \simeq \frac{Ze^2}{4\pi\varepsilon_0}\frac{R^2}{10}|R_{n0}(0)|^2$$
$$\simeq \frac{Ze^2}{4\pi\varepsilon_0}\frac{2\pi}{5}R^2|\psi_{n00}(0)|^2, \qquad l = 0 \tag{5.175}$$

while $\Delta E \simeq 0$ for states with $l \neq 0$. Using [3.60] we have explicitly

$$\Delta E \simeq \frac{e^2}{4\pi\varepsilon_0}\frac{2}{5}R^2\frac{Z^4}{a_\mu^3 n^3}, \qquad l = 0 \tag{5.176}$$

The quantity which is measured experimentally is the difference δE of energy shifts between two isotopes, whose charge distributions have radii R and $R + \delta R$, respectively. We thus find to first order in δR

$$\delta E \simeq \frac{Ze^2}{4\pi\varepsilon_0}\frac{4\pi}{5}R^2|\psi_{n00}(0)|^2\frac{\delta R}{R}$$
$$\simeq \frac{Ze^2}{4\pi\varepsilon_0}\frac{4}{5}R^2\frac{Z^4}{a_\mu^3 n^3}\frac{\delta R}{R} \tag{5.177}$$

We note that the isotope with the larger radius has the higher energy value, and this is confirmed by experiment. We also see that δE increases when Z increases and n decreases, so that the most important volume effects occur for low-lying s-states (and in particular the ground state) of hydrogenic atoms with larger Z.

So far we have only considered 'ordinary' hydrogenic atoms (ions) containing a nucleus and an electron. As we pointed out in Chapter 3, there exist also 'exotic atoms' such as muonic atoms, in which a muon μ^- forms a bound system with a nucleus. We also noticed in Chapter 3 that since the mass of the muon μ^- is about 200 times larger than the electron mass, the Bohr radius associated with muonic atoms is much smaller than for 'ordinary' (electronic) atoms (see Table 3.2). We therefore expect that *hyperfine effects will be much larger for muonic atoms than for the corresponding ordinary atoms*. In particular, using the fact that the quantity a_μ is roughly 200 times smaller for a muonic atom than for an ordinary atom, we deduce from the foregoing discussion that the volume effect will be considerably magnified for muonic atoms, as we pointed out in Section 3.5.

Problems

5.1 Show that the ratio of the probabilities of the transitions in atomic hydrogen $n\text{p}_{3/2} \to n'\text{s}_{1/2}$ and $n\text{p}_{1/2} \to n'\text{s}_{1/2}$ is 2:1.

5.2 (a) Show that the Hamiltonian of a free electron in a uniform time-independent magnetic field $\boldsymbol{\mathcal{B}} = \mathcal{B}_z\hat{\mathbf{z}}$ is given by $H = H_{xy} + H_z$,

where

$$H_{xy} = \frac{1}{2m}(p_x^2 + p_y^2) + \frac{1}{2m}\omega_L^2(x^2 + y^2)$$

$$H_z = \frac{1}{2m}p_z^2 + \omega_L(L_z + 2S_z)$$

where $\omega_L = (\mu_B/\hbar)\mathcal{B}_z = 2\pi\nu_L$ is the Larmor angular frequency. It follows that the motion in the XY plane is harmonic.

(b) In neutrons' stars magnetic fields of the order of 10^8 T may occur. Find the energy separation between adjacent levels of the harmonic Hamiltonian H_{xy} (the Landau levels). What is the size of the region to which the motion in the XY plane is confined?

5.3 Show that in the limit of strong magnetic fields in transverse observation the intensity of the π Zeeman component is twice that of the σ.

5.4 Show that in the linear Stark effect the $n = 3$ level of a hydrogen atom is split into five equally spaced components, and obtain the level separation in electron-volts.

5.5 Suppose that at time $t = 0$ a hydrogen atom is in an arbitrary superposition of the 2s and $2p_0$ states. A constant electric field of strength 10^7 V/m is then applied along the Z axis. Show that during the lifetime of the $2p_0$ state (due to radiative decay to the 1s state), the average population of the 2s level is nearly the same as that of the $2p_0$ level.

5.6 Show that the second-order correction to the energy in perturbation theory can be written as

$$E_n^{(2)} = \frac{(H'^2)_{nn}}{E_n} - \frac{(H'_{nn})^2}{E_n} + \sum_{k\neq n} \frac{E_k|H'_{nk}|^2}{E_n(E_n - E_k)}$$

By neglecting the sum of the right-hand side obtain the approximation [5.109] for the quadratic Stark effect.

5.7 Verify that the expression [5.127] follows from [5.125] and [5.126].

5.8 Prove the relations [5.132] and [5.148].

5.9 Consider an electron in the electrostatic field of a nucleus of charge Ze, and of mass number A. If the nuclear charge is distributed uniformly within a sphere of radius $R = r_0 A^{1/3}$ where $r_0 \simeq 1.2 \times 10^{-15}$ m, show that the potential is given by [5.172], and verify that the first-order energy shift due to the perturbation [5.173] is given by [5.175].

6 Two-electron atoms

In this chapter we begin our study of many-electron atoms by considering the simplest ones, namely atoms (or ions) consisting of a nucleus of charge Ze and *two* electrons. These include the negative hydrogen ion H^- ($Z = 1$), the helium atom ($Z = 2$), the singly ionised lithium atom Li^+ ($Z = 3$), and so on. These systems deserve particular attention for two reasons. It is for these systems that we shall first study in detail the implications of the *Pauli exclusion principle*, which plays a central role in atomic and molecular physics. Secondly, it is for two-electron atoms that various approximations used in atomic structure calculations can be explained most easily and tested accurately.

We shall limit our discussion to the non-relativistic theory of two-electron atoms. After analysing in succession the space and spin symmetries and the role of the Pauli exclusion principle, we will discuss the level scheme of two-electron atoms and introduce the independent particle model, which is of great importance in studying many-electron systems. We then study in some detail the ground state and the lowest excited states of two-electron atoms, using perturbation theory and the variational method, and conclude this chapter with a brief survey of autoionising states.

6.1 THE SCHRÖDINGER EQUATION FOR TWO-ELECTRON ATOMS. PARA AND ORTHO STATES

Let us consider an atom (or ion) consisting of a nucleus of charge Ze and mass M and two electrons of mass m. As in the case of one-electron atoms, we shall begin our treatment by neglecting all but the Coulomb interactions between the particles, and by writing down the Schrödinger equation for the spatial part of the wave function describing the relative motion. The separation of the centre of mass motion is somewhat more complicated than for the case of one-electron atoms, since we are now dealing with a three-body problem. This separation is performed in Appendix 8 for the general case of an atom (ion) having N electrons. Denoting by $\mathbf{r}_1$ and $\mathbf{r}_2$ the relative coordinates of the two electrons with respect to the nucleus (see Fig. 6.1) we see from the equations [A8.12] and [A8.16] of Appendix 8 that the Schrödinger equation for the spatial part

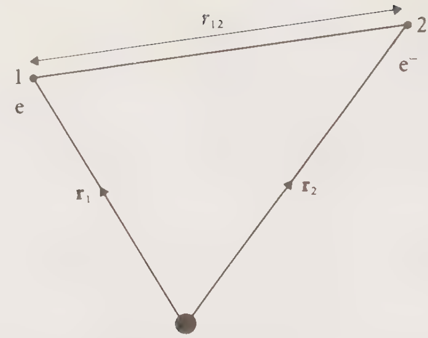

6.1 Coordinate system for two-electron atoms.

$\psi(\mathbf{r}_1, \mathbf{r}_2)$ of the wave function describing the relative motion is for a two-electron system

$$\left[-\frac{\hbar^2}{2\mu}\nabla^2_{r_1} - \frac{\hbar^2}{2\mu}\nabla^2_{r_2} - \frac{\hbar^2}{M}\nabla_{r_1}\cdot\nabla_{r_2} - \frac{Ze^2}{(4\pi\varepsilon_0)r_1} - \frac{Ze^2}{(4\pi\varepsilon_0)r_2} + \frac{e^2}{(4\pi\varepsilon_0)r_{12}}\right]\psi(\mathbf{r}_1, \mathbf{r}_2) = E\psi(\mathbf{r}_1, \mathbf{r}_2) \qquad [6.1]$$

where $\mu = mM/(m+M)$ is the reduced mass of an electron with respect to the nucleus and $r_{12} = |\mathbf{r}_1 - \mathbf{r}_2|$.

We shall first consider the case of an 'infinitely heavy' nucleus ($M = \infty$) so that (i) $\mu = m$ and (ii) the 'mass polarisation' term $(-\hbar^2/M)\nabla_{\mathbf{r}_1}\cdot\nabla_{\mathbf{r}_2}$ can be omitted. We shall work in atomic units (a.u.), in which the Hamiltonian is

$$H = -\frac{1}{2}\nabla^2_{r_1} - \frac{1}{2}\nabla^2_{r_2} - \frac{Z}{r_1} - \frac{Z}{r_2} + \frac{1}{r_{12}} \qquad [6.2]$$

and the Schrödinger equation for $\psi(\mathbf{r}_1, \mathbf{r}_2)$ becomes

$$\left[-\frac{1}{2}\nabla^2_{r_1} - \frac{1}{2}\nabla^2_{r_2} - \frac{Z}{r_1} - \frac{Z}{r_2} + \frac{1}{r_{12}}\right]\psi(\mathbf{r}_1, \mathbf{r}_2) = E\psi(\mathbf{r}_1, \mathbf{r}_2) \qquad [6.3]$$

We note that this equation is unchanged when the coordinates of the two electrons are interchanged. Thus, if we denote by P_{12} a permutation operator that interchanges the spatial coordinates of the two electrons, the wave functions

$$\psi(\mathbf{r}_2, \mathbf{r}_1) = P_{12}\psi(\mathbf{r}_1, \mathbf{r}_2) \qquad [6.4]$$

and $\psi(\mathbf{r}_1, \mathbf{r}_2)$ satisfy the same Schrödinger equation. Moreover, both functions $\psi(\mathbf{r}_1, \mathbf{r}_2)$ and $\psi(\mathbf{r}_2, \mathbf{r}_1)$ must be continuous, uniform and bounded. If $\psi(\mathbf{r}_1, \mathbf{r}_2)$ corresponds to a non-degenerate eigenvalue, $\psi(\mathbf{r}_1, \mathbf{r}_2)$ and $\psi(\mathbf{r}_2, \mathbf{r}_1)$ can only differ by a multiplicative factor λ,

$$\psi(\mathbf{r}_2, \mathbf{r}_1) = P_{12}\psi(\mathbf{r}_1, \mathbf{r}_2) = \lambda\psi(\mathbf{r}_1, \mathbf{r}_2) \qquad [6.5]$$

Applying the permutation operator P_{12} twice, we must obtain $\psi(\mathbf{r}_1, \mathbf{r}_2)$ again. Thus

$$\begin{aligned} P_{12}^2\psi(\mathbf{r}_1, \mathbf{r}_2) &= \lambda P_{12}\psi(\mathbf{r}_1, \mathbf{r}_2) \\ &= \lambda^2\psi(\mathbf{r}_1, \mathbf{r}_2) \\ &= \psi(\mathbf{r}_1, \mathbf{r}_2) \end{aligned} \tag{6.6}$$

so that $\lambda^2 = 1$, $\lambda = \pm 1$ and

$$\psi(\mathbf{r}_2, \mathbf{r}_1) = \pm\psi(\mathbf{r}_1, \mathbf{r}_2) \tag{6.7}$$

Wave functions which satisfy [6.7] with the plus sign (that is, whose spatial part remains unchanged upon permutating the spatial coordinates of the two electrons) are said to be *space-symmetric* and will be denoted by $\psi_+(\mathbf{r}_1, \mathbf{r}_2)$. On the other hand, wave functions satisfying [6.7] with the minus sign (that is, whose spatial part changes sign on interchanging the spatial coordinates of the two electrons) are said to be *space-antisymmetric* and will be written as $\psi_-(\mathbf{r}_1, \mathbf{r}_2)$. It is straightforward to show (Problem 6.1) that for degenerate eigenvalues the eigenfunctions of [6.3] can always be chosen so that [6.7] holds. Thus the eigenfunctions of a two-electron atom can be classified as being either space-symmetric or space-antisymmetric. The states described by space-symmetric wave functions are called *para* states; those corresponding to space-antisymmetric wave functions are known as *ortho* states.

6.2 SPIN WAVE FUNCTIONS AND THE ROLE OF THE PAULI EXCLUSION PRINCIPLE

Until now we have not taken into account the spin of the two electrons. In the case of one-electron atoms we have seen in Chapter 5 that the electron spin only affects the fine and hyperfine structure of the spectrum. On the contrary, for two-electron atoms, we shall see that spin effects directly influence the spectrum because of the requirements of the *Pauli exclusion principle*.

Since we are now dealing with the Hamiltonian [6.2] which is spin-independent, the atom can be completely described by specifying its spatial eigenfunction, together with the components of the electron spins in a given direction, which we choose as our Z axis. Thus the full eigenfunctions Ψ of the system must be products of the spatial eigenfunctions $\psi(\mathbf{r}_1, \mathbf{r}_2)$ satisfying the Schrödinger equation [6.3] times spin wave functions $\chi(1, 2)$ for the two-electron system. That is

$$\Psi(q_1, q_2) = \psi(\mathbf{r}_1, \mathbf{r}_2)\chi(1, 2) \tag{6.8}$$

where q_i denotes collectively the space and spin coordinates of electron i.

Spin wave functions

The spin wave functions $\chi(1, 2)$ are easily constructed from our knowledge of the spin wave functions $\chi_{1/2,m_s}(1)$ and $\chi_{1/2,m_s}(2)$ of the individual electrons. Let

us denote by $\mathbf{S}_1$ and $\mathbf{S}_2$ the spin operators of the two electrons, and by $(S_1)_z$ and $(S_2)_z$ the components of these operators along the Z direction. We also write the basic spin functions (see [2.209]) of the two electrons as $\alpha(1)$, $\beta(1)$ and $\alpha(2)$, $\beta(2)$, respectively. We emphasise that $\mathbf{S}_1$ only acts on $\alpha(1)$ and $\beta(1)$, while $\mathbf{S}_2$ operates only on $\alpha(2)$ and $\beta(2)$, so that the two operators $\mathbf{S}_1$ and $\mathbf{S}_2$ commute. The total spin is represented by the operator

$$\mathbf{S} = \mathbf{S}_1 + \mathbf{S}_2 \tag{6.9}$$

whose z component is

$$S_z = (S_1)_z + (S_2)_z \tag{6.10}$$

Because $\mathbf{S}_1^2 = \mathbf{S}_2^2 = 3/4$ (in a.u.) we have

$$\begin{aligned} \mathbf{S}^2 &= \mathbf{S}_1^2 + \mathbf{S}_2^2 + 2\mathbf{S}_1 \cdot \mathbf{S}_2 \\ &= \tfrac{3}{2} + 2\mathbf{S}_1 \cdot \mathbf{S}_2 \end{aligned} \tag{6.11}$$

Since there are no spin-dependent interactions each electron spin can be directed either up ($\uparrow$) or down ($\downarrow$) independently of the other, and we have four independent spin states each of which can be represented as the product of two individual spin functions. That is

$$\begin{aligned} \chi_1(1, 2) &= \alpha(1)\alpha(2) \uparrow \uparrow \\ \chi_2(1, 2) &= \alpha(1)\beta(2) \uparrow \downarrow \\ \chi_3(1, 2) &= \beta(1)\alpha(2) \downarrow \uparrow \\ \chi_4(1, 2) &= \beta(1)\beta(2) \downarrow \downarrow \end{aligned} \tag{6.12}$$

where the arrows illustrate the situation regarding the z components of the electron spins. Now

$$\begin{aligned} S_z\chi_1(1, 2) &= [(S_1)_z + (S_2)_z]\alpha(1)\alpha(2) \\ &= [(S_1)_z\alpha(1)]\alpha(2) + \alpha(1)[(S_2)_z\alpha(2)] \\ &= \tfrac{1}{2}\alpha(1)\alpha(2) + \tfrac{1}{2}\alpha(1)\alpha(2) \\ &= \chi_1(1, 2) \end{aligned} \tag{6.13}$$

Thus, if we write the eigenvalue equation for the operator S_z (in a.u.) as

$$S_z\chi = M_S\chi \tag{6.14}$$

we see that χ_1 is an eigenstate of S_z corresponding to the eigenvalue $M_S = +1$. Similarly, the spin states χ_2, χ_3 and χ_4 are easily shown to be eigenstates of S_z corresponding respectively to the values $M_S = 0$, 0 and -1 of the quantum number M_S [1]. Using [6.11] and the basic relations [2.206], the action of the operator $\mathbf{S}^2$ on the four spin functions [6.12] can also be studied (Problem 6.2).

[1] In what follows we shall use *capital* letters to denote the values of the quantum numbers for the *total* orbital angular momentum, total spin, etc.

Table 6.1 Values of $S_z\chi$ and $\mathbf{S}^2\chi$ (in a.u.) for the four two-electron spin functions [6.12]

Spin function χ	$S_z\chi$	$\mathbf{S}^2\chi$
$\chi_1 = \alpha(1)\alpha(2)\uparrow\uparrow$	χ_1	$2\chi_1$
$\chi_2 = \alpha(1)\beta(2)\uparrow\downarrow$	0	$\chi_2 + \chi_3$
$\chi_3 = \beta(1)\alpha(2)\downarrow\uparrow$	0	$\chi_2 + \chi_3$
$\chi_4 = \beta(1)\beta(2)\downarrow\downarrow$	$-\chi_4$	$2\chi_4$

The results are given in Table 6.1. If we write the eigenvalue equation for $\mathbf{S}^2$ (in a.u.) as

$$\mathbf{S}^2\chi = S(S+1)\chi \tag{6.15}$$

we see that both χ_1 and χ_4 are eigenstates of $\mathbf{S}^2$ corresponding to the eigenvalue $S(S+1) = 2$, that is to the value $S = 1$ of the quantum number S associated with the magnitude of the total spin. On the other hand, χ_2 and χ_3 are *not* eigenstates of $\mathbf{S}^2$.

Looking back at the four spin functions [6.12], we also see that both χ_1 and χ_4 are symmetric in the exchange of the labels of the two electrons, while neither χ_2 nor χ_3 is symmetric or antisymmetric. As we shall see below, it is essential to deal with two-electron spin functions which are either symmetric or antisymmetric in the interchange of the electron labels. Fortunately, it is easy to form linear combinations of χ_2 and χ_3 which are respectively symmetric and antisymmetric in the exchange of the electron labels 1 and 2. That is

$$\chi_+(1,2) = \frac{1}{\sqrt{2}}[\chi_2(1,2) + \chi_3(1,2)] \tag{6.16}$$

and

$$\chi_-(1,2) = \frac{1}{\sqrt{2}}[\chi_2(1,2) - \chi_3(1,2)] \tag{6.17}$$

where the subscripts + and − denote the symmetric and antisymmetric functions, respectively, and the factor $2^{-1/2}$ has been introduced so that both χ_+ and χ_- are normalised to unity. Using the results of Table 6.1, we see that the symmetric spin function χ_+ is an eigenstate of both operators $\mathbf{S}^2$ and S_z, with quantum numbers given by $S = 1$ and $M_S = 0$, respectively. The antisymmetric spin function χ_- is also an eigenstate of both $\mathbf{S}^2$ and S_z, with corresponding quantum numbers $S = 0$ and $M_S = 0$. In what follows, and by analogy with the one-electron case, we shall write the eigenstates common to both operators $\mathbf{S}^2$ and S_z as χ_{S,M_S}, so that in this new notation we have $\chi_{0,0} \equiv \chi_-$, $\chi_{1,1} \equiv \chi_1$, $\chi_{1,0} \equiv \chi_+$ and $\chi_{1,-1} \equiv \chi_4$.

The foregoing discussion shows that, starting with the four independent and normalised spin functions [6.12], we can construct four normalised and mutually orthogonal spin functions which are eigenstates of both operators $\mathbf{S}^2$ and S_z and possess a definite symmetry in the exchange of the two electrons.

These are the *antisymmetric spin function*

$$\chi_{0,0}(1, 2) = \frac{1}{\sqrt{2}}[\alpha(1)\beta(2) - \beta(1)\alpha(2)] \qquad [6.18]$$

three symmetric spin functions

$$\begin{aligned} \chi_{1,1}(1, 2) &= \alpha(1)\alpha(2) \\ \chi_{1,0}(1, 2) &= \frac{1}{\sqrt{2}}[\alpha(1)\beta(2) + \beta(1)\alpha(2)] \\ \chi_{1,-1}(1, 2) &= \beta(1)\beta(2) \end{aligned} \qquad [6.19]$$

The antisymmetric spin function [6.18] corresponding to the quantum numbers $S = 0$ and $M_S = 0$ is called a (spin) *singlet*, while the three symmetric spin states [6.19] corresponding to the total spin $S = 1$ and to the quantum numbers $M_S = 1, 0, -1$, respectively, are said to form a (spin) *triplet* (see Table 6.2).

Table 6.2 Values of the quantum numbers S and M_S for the antisymmetric spin function [6.18], and the three symmetric spin functions [6.19]. Each of these spin functions is a simultaneous eigenstate of the operators $\mathbf{S}^2$ and S_z, with eigenvalues given respectively (in a.u.) by $S(S + 1)$ and M_S. The antisymmetric spin function [6.18], corresponding to $S = 0$, $M_S = 0$ is a spin singlet, while the three symmetric spin states [6.19] corresponding to $S = 1$ and $M_S = 1, 0, -1$ are seen to form a spin triplet

Spin function	S	M_S
$\frac{1}{\sqrt{2}}[\alpha(1)\beta(2) - \beta(1)\alpha(2)]$	0	0
$\alpha(1)\alpha(2)$	1	1
$\frac{1}{\sqrt{2}}[\alpha(1)\beta(2) + \beta(1)\alpha(2)]$	1	0
$\beta(1)\beta(2)$	1	−1

The role of the Pauli exclusion principle

Let us now return to the equation [6.8]. At first sight, it would appear that by combining the four spin states [6.18] and [6.19] with the spatial eigenfunctions $\psi(\mathbf{r}_1, \mathbf{r}_2)$, we could obtain four times as many eigenstates $\Psi(q_1, q_2)$ for an atom (or ion) with two spin 1/2 electrons than if the electrons were spinless. However, this is not the case because, as we have seen in Chapter 2, *the Pauli exclusion principle requires that the total wave function $\Psi(q_1, q_2, \ldots q_N)$ of a system of N electrons must be antisymmetric*. In other words $\Psi(q_1, q_2, \ldots q_N)$ must change sign if all the coordinates (spatial as well as spin) of two electrons are interchanged. Hence, in our two-electron case, we see from [6.8] that in order to obtain total antisymmetric wave functions $\Psi(q_1, q_2)$ we must either multiply

symmetric spatial (para) wave functions $\psi_+(\mathbf{r}_1, \mathbf{r}_2)$ by the antisymmetric (singlet) spin state [6.18],

$$\Psi(q_1, q_2) = \psi_+(\mathbf{r}_1, \mathbf{r}_2) \frac{1}{\sqrt{2}} [\alpha(1)\beta(2) - \beta(1)\alpha(2)] \tag{6.20}$$

or multiply antisymmetric spatial (ortho) wave functions $\psi_-(\mathbf{r}_1, \mathbf{r}_2)$ by one of the three symmetric spin functions [6.19] belonging to the spin triplet,

$$\Psi(q_1, q_2) = \psi_-(\mathbf{r}_1, \mathbf{r}_2) \times \begin{cases} \alpha(1)\alpha(2) \\ \dfrac{1}{\sqrt{2}} [\alpha(1)\beta(2) + \beta(1)\alpha(2)] \\ \beta(1)\beta(2) \end{cases} \tag{6.21}$$

Thus para states must always be spin singlets, while ortho states must be spin triplets, so that the Pauli exclusion principle introduces a *coupling* between the *space* and *spin* variables of the electrons.

6.3 LEVEL SCHEME OF TWO-ELECTRON ATOMS

We shall prove in Chapter 8 that radiative transitions between singlet and triplet spin states (known as *intercombination lines*) are *forbidden* in the electric dipole approximation, provided that spin–orbit interactions can be neglected. This is the case for atoms or ions with low enough Z, so that the energy spectrum of two-electron atoms (or ions) with $Z \lesssim 40$ consists of *two nearly independent systems of levels*, one made of para (singlet) states and the other of ortho (triplet) states. As an example, we show in Fig. 6.2 the first few (lowest) energy levels of helium, divided into singlets ($S = 0$) and triplets ($S = 1$). Because intercombination lines are absent in practice in the helium spectrum, spectroscopists spoke for a long time of two different species of helium, *parahelium* and *orthohelium*; this terminology is still used now.

Let $\mathbf{L} = \mathbf{L}_1 + \mathbf{L}_2$ be the sum of the two orbital angular momentum operators of the electrons. Using atomic units ($\hbar = 1$), we shall denote by $L(L + 1)$ the eigenvalues of $\mathbf{L}^2$ and by M_L those of L_z, so that $M_L = -L, -L + 1, \ldots + L$. As seen from Fig. 6.2, the atomic energy levels, also called *terms* in spectroscopic language, are designated by symbols which generalise the ones we used for hydrogenic atoms. Thus each term is denoted as

$$^{2S+1}L$$

where a code letter is associated to the value of the total electronic orbital angular momentum quantum number L according to the correspondence

$$\begin{array}{lcccccc} L = & 0 & 1 & 2 & 3 & 4 & 5 \\ & \updownarrow & \updownarrow & \updownarrow & \updownarrow & \updownarrow & \updownarrow \\ & \mathrm{S} & \mathrm{P} & \mathrm{D} & \mathrm{F} & \mathrm{G} & \mathrm{H} \end{array}$$

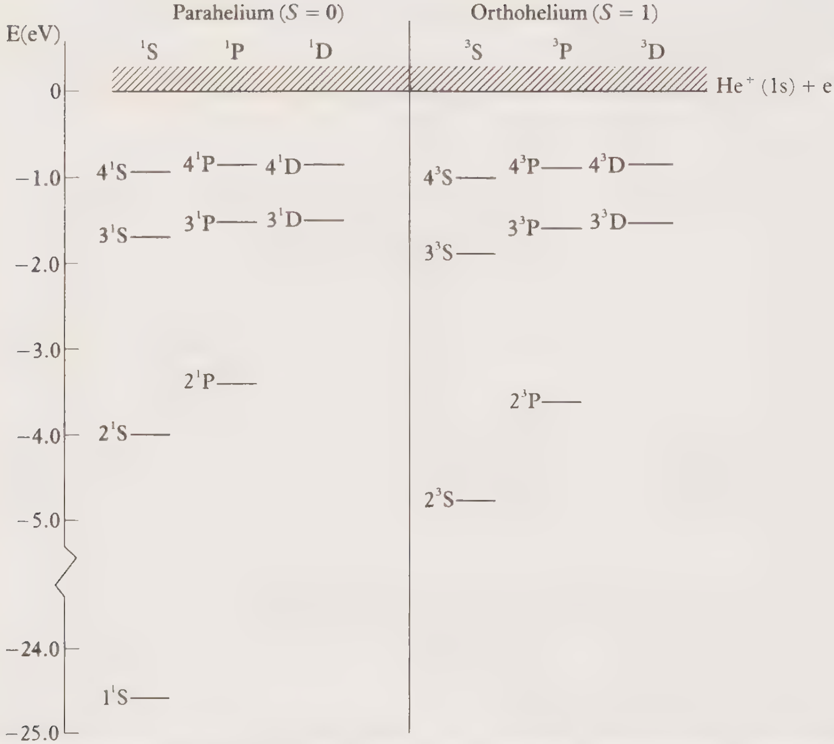

6.2 The experimental values of the lowest energy levels of helium. The energy scale is chosen so that $E = 0$ corresponds to the ionisation threshold. The configuration of each level is of the form 1s nl. The doubly excited states (for example 2s nl) are at positive energies on this scale, within the $He^+(1s) + e^-$ continuum.

and so on. In addition, a superscript to the left gives the value of the quantity $2S + 1$, or *multiplicity*, which is equal to 1 for singlet ($S = 0$) states and 3 for triplet ($S = 1$) states.

We remark that Fig. 6.2 does not exhibit the fine structure splitting of the levels, due to the relativistic interaction between the spin and orbital angular momentum (spin–orbit effect) and to the magnetic interaction between the spins of the two electrons (spin–spin effect). Calling $\mathbf{J} = \mathbf{L} + \mathbf{S}$ the total electronic angular momentum and denoting by $\mathcal{J}(\mathcal{J} + 1)$ and $M_{\mathcal{J}}$ the eigenvalues of the operators $\mathbf{J}^2$ and $\mathcal{J}_z$, respectively, it may be shown that the spin–orbit and spin–spin interactions partially remove the degeneracy of the triplet states by splitting them (except the ^{3}S states) into three closely spaced levels corresponding to the three possible values $\mathcal{J} = L + 1, L$ or $L - 1$ of the total angular momentum quantum number $\mathcal{J}$. We shall discuss this problem in Chapter 8.

It should be noted that Fig. 6.2 only represents the *discrete* part of the helium spectrum. A schematic diagram of the 'full' spectrum for the three-body system consisting of the He^{++} nucleus and two electrons is shown in Fig. 6.3. Choosing the origin of the energy scale in such a way that all three particles are

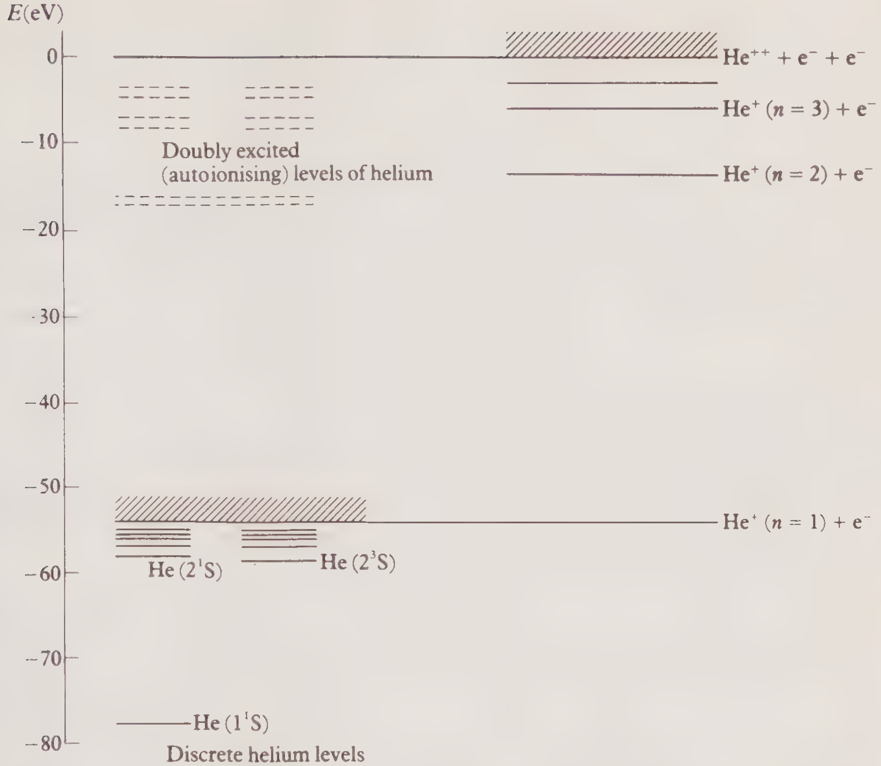

6.3 The ‘complete’ energy level spectrum of helium. The energy scale is relative to the threshold for the ionisation of both electrons and the zero of energy is 54 eV (the ground state energy of He^+), above the zero energy of the scale of Fig. 6.2.

unbound above $E = 0$, we see that the discrete levels of helium (displayed in more detail in Fig. 6.2) lie between the ground state value $E_0(\mathrm{He}) \simeq -79.0$ eV and the value $E_0(\mathrm{He}^+) \simeq -54.4$ eV of the ground state energy of the He^+ ion. Thus the ionisation potential numbers given in Fig. 6.2 correspond to the energy differences between the level $E_0(\mathrm{He}^+)$ and a given energy level of the helium atom. For example, the ionisation potential corresponding to the helium ground state is

$$\begin{aligned} I_P &= E_0(\mathrm{He}^+) - E_0(\mathrm{He}) \\ &\simeq 24.6 \text{ eV} \end{aligned} \qquad [6.22]$$

The spectrum of two-electron ions with $Z > 2$ is similar to that of helium which we have just discussed. On the other hand, the negative hydrogen ion H^-, for which $Z = 1$, constitutes an interesting special case. Indeed, as shown on Fig. 6.4, this ion has only *one* bound state. The corresponding ionisation potential is about 0.75 eV, so that the H^- ion is barely stable against dissociation into a neutral hydrogen atom and a free electron. We shall return

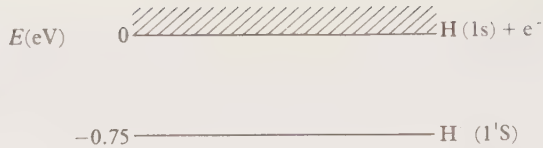

6.4 The ground state of the hydrogen negative ion.

below to the H system, which is of great importance in astrophysics, and also provides a stringent test of the approximation methods used in the analysis of two-electron systems.

6.4 THE INDEPENDENT PARTICLE MODEL

Before discussing in detail the ground state and various excited states of two-electron atoms, we shall develop in this section a simple approach which yields a qualitative understanding of the main features of their spectrum, and which will also pave the way for our study of many- electron atoms in Chapter 7.

We begin by rewriting the basic Hamiltonian [6.2] as

$$H = H_0 + H' \qquad [6.23]$$

where we choose our zero-order, 'unperturbed' Hamiltonian to be

$$H_0 = -\frac{1}{2}\nabla^2_{r_1} - \frac{Z}{r_1} - \frac{1}{2}\nabla^2_{r_2} - \frac{Z}{r_2} \qquad [6.24]$$

while the 'perturbation'

$$H' = \frac{1}{r_{12}} \qquad [6.25]$$

is the electron–electron interaction. We remark from [6.24] that H_0 is just the sum of two hydrogenic Hamiltonians, namely

$$H_0 = \hat{h}_1 + \hat{h}_2 \qquad [6.26]$$

where

$$\hat{h}_i = -\frac{1}{2}\nabla^2_{r_i} - \frac{Z}{r_i}, \qquad i = 1, 2 \qquad [6.27]$$

In what follows we shall denote by E_{n_i} the energy eigenvalues and by $\psi_{n_i l_i m_i}(\mathbf{r}_i)$ the corresponding normalised eigenfunctions of the hydrogenic Hamiltonian [6.27]. Thus

$$\hat{h}_i \psi_{n_i l_i m_i}(\mathbf{r}_i) = E_{n_i} \psi_{n_i l_i m_i}(\mathbf{r}_i) \qquad [6.28]$$

with

$$E_{n_i} = -\frac{1}{2}\frac{Z^2}{n_i^2} \qquad \text{(in a.u.)} \qquad [6.29]$$

Let us for the moment neglect the electron–electron repulsion term [6.25]. The Schrödinger equation [6.3] for the spatial part of the two-electron wave function then reduces to the 'zero-order' equation

$$H_0\psi^{(0)}(\mathbf{r}_1, \mathbf{r}_2) = E^{(0)}\psi^{(0)}(\mathbf{r}_1, \mathbf{r}_2) \qquad [6.30]$$

Using [6.26]–[6.29], we see that this equation is separable and that eigenfunctions of [6.30] can be written in the form of products of hydrogenic wave functions. In particular, for discrete states, we have

$$\psi^{(0)}(\mathbf{r}_1, \mathbf{r}_2) = \psi_{n_1l_1m_1}(\mathbf{r}_1)\psi_{n_2l_2m_2}(\mathbf{r}_2) \qquad [6.31]$$

the corresponding discrete energies being given (in a.u.) by

$$\begin{aligned} E^{(0)}_{n_1n_2} &= E_{n_1} + E_{n_2} \\ &= -\frac{Z^2}{2}\left(\frac{1}{n_1^2} + \frac{1}{n_2^2}\right) \end{aligned} \qquad [6.32]$$

We note that the wave function

$$\psi^{(0)}(\mathbf{r}_2, \mathbf{r}_1) = \psi_{n_2l_2m_2}(\mathbf{r}_1)\psi_{n_1l_1m_1}(\mathbf{r}_2) \qquad [6.33]$$

which differs from [6.31] only in an exchange of the electron labels, corresponds to the *same* energy $E^{(0)}_{n_1n_2}$. This particular case of degeneracy with respect to exchange of electron labels is called *exchange degeneracy*. According to the discussion of Section 6.2 the exact spatial wave functions of two-electron atoms must be either symmetric or antisymmetric with respect to the interchange of the coordinates $\mathbf{r}_1$ and $\mathbf{r}_2$ of the two electrons. The proper (zero-order) spatial wave functions of our simple independent-particle model must therefore be the symmetric (+) and antisymmetric (−) linear combinations

$$\psi^{(0)}_{\pm}(\mathbf{r}_1, \mathbf{r}_2) = \frac{1}{\sqrt{2}}\left[\psi_{n_1l_1m_1}(\mathbf{r}_1)\psi_{n_2l_2m_2}(\mathbf{r}_2) \pm \psi_{n_2l_2m_2}(\mathbf{r}_1)\psi_{n_1l_1m_1}(\mathbf{r}_2)\right] \qquad [6.34]$$

where the factor $2^{-1/2}$ guarantees that the functions $\psi^{(0)}_{\pm}$ are normalised. The functions $\psi^{(0)}_{+}$ are therefore approximations to the *para* wave functions, while the functions $\psi^{(0)}_{-}$ are approximations to the *ortho* wave functions. We see that the total orbital quantum number L can take the values $L = |l_1 - l_2|, \ldots l_1 + l_2$, the possible values of the quantum number M_L being $M_L = -L, -L + 1, \ldots, +L$. We also remark that in our crude model the two states $\psi^{(0)}_{\pm}$ correspond to the *same* energy $E^{(0)}_{n_1n_2}$. We shall see below that the electron–electron repulsion term $1/r_{12}$ removes this degeneracy.

An exception to [6.34] occurs for the case of the *ground state*, where both electrons are in the 1s state (that is, $n_1 = n_2 = 1$, $l_1 = l_2 = 0$, $m_1 = m_2 = 0$). The wave function $\psi^{(0)}_{-}$ for the ortho state is then seen to vanish, in agreement with the original formulation of the Pauli principle, according to which two electrons cannot be exactly in the same state. Indeed, the spatial quantum numbers for both electrons having the same values $n = 1$, $l = 0$ and $m = 0$, the spin quantum numbers of the two electrons must be different, so that the two

electrons must have antiparallel spin, and only the singlet (para) state is allowed. It is interesting to note that historically the argument was made the other way around, the experimental absence of the ground state triplet level of helium having provided key evidence that led Pauli to the discovery of the exclusion principle.

The normalised zero-order spatial wave function for the ground state of two-electron atoms is therefore given by the simple symmetric (para) wave function

$$\begin{aligned}\psi_0^{(0)}(r_1, r_2) &= \psi_{1s}(r_1)\psi_{1s}(r_2)\\ &= \frac{Z^3}{\pi}\, e^{-Z(r_1+r_2)}\end{aligned} \qquad [6.35]$$

where the subscript indicates that we are dealing with the ground state, and we have used the fact that the ground state wave function of the hydrogenic Hamiltonian [6.27] is

$$\psi_{100}(r_i) \equiv \psi_{1s}(r_i) = \left(\frac{Z^3}{\pi}\right)^{1/2} e^{-Zr_i} \qquad [6.36]$$

The ground state energy corresponding to [6.35] is (see [6.32])

$$E_0^{(0)} = E_{n_1=1,n_2=1}^{(0)} = -Z^2 \quad \text{a.u.} \qquad [6.37]$$

Thus for helium ($Z = 2$) we find from [6.37] that $E_0^{(0)} = -4$ a.u. ($= -108.8$ eV), which corresponds to an ionisation potential $I_P^{(0)} = 2$ a.u. ($= 54.4$ eV). The experimental values are $E_0^{\text{exp}} = -2.90$ a.u. ($= -79.0$ eV) and $I_P^{\text{exp}} = 0.90$ a.u. (=24.6 ev). As we should expect, our crude model gives an energy which is too low because we have neglected the repulsion term [6.25] between the two electrons, whose effect is clearly to raise the energy levels. It is also apparent that our simple independent particle approach should yield better results when Z is increased, since in that case the relative importance of the neglected term $1/r_{12}$ becomes smaller. For example, in the case of the C^{4+} ion, corresponding to $Z = 6$, the approximation [6.37] yields $E_0^{(0)} = -36$ a.u. ($\simeq -980$ eV) while the experimental value is $E_0^{\text{exp}} = -32.4$ a.u. ($\simeq -882$ eV). On the other hand, for the negative hydrogen ion H^- ($Z = 1$), the value $E_0^{(0)} = -1$ a.u. ($\simeq -27.2$ eV) is in gross disagreement with the observed value $E_0^{\text{exp}} = -0.528$ a.u. ($\simeq -14.4$ eV).

Let us now examine the predictions of our simple model concerning excited states. The energy spectrum corresponding to [6.32] is illustrated in Fig. 6.5(a) for the case of helium ($Z = 2$). Also shown for comparison in Fig. 6.5(b) is the experimental spectrum. We first remark that the energy levels $E_{n_1,n_2}^{(0)}$ corresponding to states for which *both* electrons are excited (that is, $n_1 \geqslant 2$ *and* $n_2 \geqslant 2$) are higher than the ground state energy of the He^+ ion ($E_0(He^+) = -2$ a.u. $\simeq -54.4$ eV) plus a free electron. These doubly excited states therefore lie in the continuum of our simplified spectrum (see

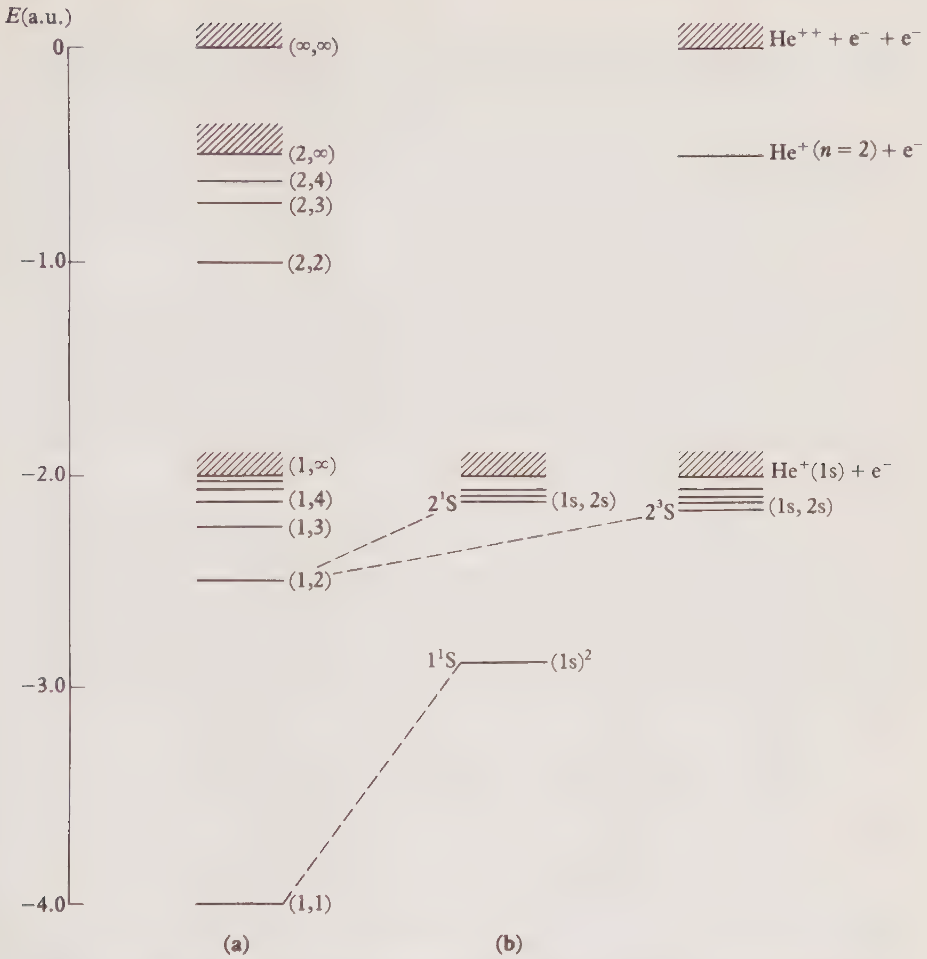

6.5 (a) The energy spectrum given by expression [6.32] with $Z = 2$. The levels are labelled by (n_1, n_2).

(b) The energy spectrum of helium.

Fig. 6.5(a)). Since the repulsion term $1/r_{12}$ can only raise the unperturbed energy levels $E^{(0)}_{n_1,n_2}$, the same property is also true for the actual He spectrum, and in fact it holds for all other He-like ions. We shall return at the end of this chapter to these discrete states embedded in the continuum. For the moment, however, we focus our attention on the *genuinely discrete states* of two-electron atoms, for which one of the two electrons remains in the ground state. The properly symmetrised zero-order spatial wave functions for these states are given (see [6.34]) by

$$\psi^{(0)}_{\pm}(\mathbf{r}_1, \mathbf{r}_2) = \frac{1}{\sqrt{2}}[\psi_{100}(\mathbf{r}_1)\psi_{nlm}(\mathbf{r}_2) \pm \psi_{nlm}(\mathbf{r}_1)\psi_{100}(\mathbf{r}_2)], \qquad n \geqslant 2 \quad [6.38]$$

and are therefore characterised by three quantum numbers (n, l, m) as in the case of one-electron atoms. The total orbital angular momentum quantum number L is given by $L = l$ and the values of M_L $(=m)$ are $M_L = -l, -l+1, \ldots l$. The energy levels corresponding to the wave functions [6.38] namely (see [6.32])

$$E^{(0)}_{1,n} = -\frac{Z^2}{2}\left(1 + \frac{1}{n^2}\right) \text{ a.u.}, \qquad n \geqslant 2 \qquad [6.39]$$

are degenerate in l and m. As pointed out above, they also exhibit the exchange degeneracy, according to which the para (+) and ortho (−) levels are degenerate in the 'zero-order' approximation [6.38]. The electron–electron repulsion term $1/r_{12}$, which is ignored in the very simple approach leading to [6.39], will clearly raise these energy levels, as may be seen from Fig. 6.5. As we shall show at the end of this section, the term $1/r_{12}$ is responsible for removing the exchange degeneracy between the para and ortho states.

For the special case of the negative hydrogen ion H^-, corresponding to $Z = 1$, the repulsive term $1/r_{12}$ has an even more drastic effect on the spectrum, as Fig. 6.6 illustrates. Indeed, all the excited states [6.39] which are present in the 'unperturbed' spectrum shown in Fig. 6.6(a) are lifted into the continuum when the electron–electron repulsion $1/r_{12}$ is taken into account (see Fig. 6.6(b)). This spectacular effect of the 'perturbation' $1/r_{12}$ is obviously due

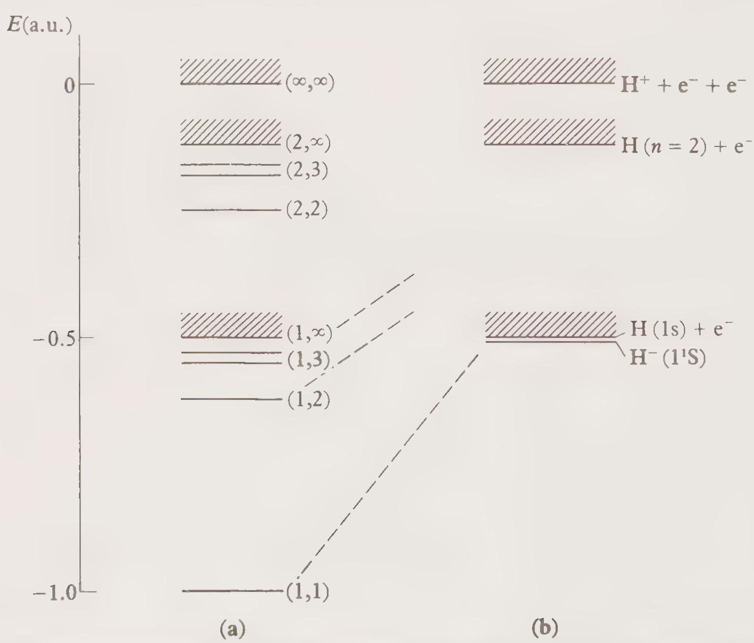

6.6 (a) The energy spectrum given by expression [6.32] with $Z = 1$. The levels are labelled by (n_1, n_2).
(b) The energy spectrum of H^-.

to the small value ($Z = 1$) of the nuclear charge. In what follows, when discussing the excited states of two-electron atoms, we shall assume implicitly that we are dealing with the case $Z \geqslant 2$.

So far we have used a very crude independent-particle approximation, in which the electron–electron repulsion term $1/r_{12}$ is completely omitted. While remaining within the convenient framework of the independent-particle model, we may improve our treatment by splitting the basic Hamiltonian [6.2] as

$$H = \tilde{H}_0 + \tilde{H}' \qquad [6.40]$$

where

$$\tilde{H}_0 = -\tfrac{1}{2}\nabla^2_{r_1} + V(r_1) - \tfrac{1}{2}\nabla^2_{r_2} + V(r_2) \qquad [6.41]$$

is the sum of the two individual Hamiltonians

$$h_i = -\tfrac{1}{2}\nabla^2_{r_i} + V(r_i) \qquad [6.42]$$

and

$$\tilde{H}' = \frac{1}{r_{12}} - \frac{Z}{r_1} - V(r_1) - \frac{Z}{r_2} - V(r_2) \qquad [6.43]$$

In the above formulae $V(r)$ is a central potential which should be chosen in such a way that the effect of the perturbation $\tilde{H}'$ is small. In Chapter 7 we shall study in detail this *central field approximation* for many-electron atoms, but for the moment we limit ourselves to simple qualitative considerations. Roughly speaking, the net effect of each electron on the motion of the other one is to screen somewhat the charge of the nucleus, so that a simple guess for $V(r)$ is

$$V(r) = -\frac{Z - S}{r} = -\frac{Z_e}{r} \qquad [6.44]$$

where S is a 'screening constant' and the quantity $Z_e = Z - S$ may be considered as an 'effective charge'. Since the potential [6.44] is a Coulomb interaction, the corresponding individual electron energies are given (in a.u.) by (see [6.29])

$$E_{n_i} = -\frac{1}{2}\frac{(Z - S)^2}{n_i^2} = -\frac{1}{2}\frac{Z_e^2}{n_i^2} \qquad [6.45]$$

and are independent of the quantum numbers l_i and m_i. Neglecting the perturbation $\tilde{H}'$, the total energy of the atom is just the sum of the individual electron energies [6.45]. In particular, the ground state energy E_0 is then given approximately (in a.u.) by

$$E_0 \simeq -(Z - S)^2 = -Z_e^2 \qquad [6.46]$$

the corresponding spatial part of the ground state wave function being (see [6.35])

$$\psi_0(r_1, r_2) = \frac{Z_e^3}{\pi} e^{-Z_e(r_1 + r_2)} \qquad [6.47]$$

In the next section we shall use the variational method to determine the 'optimum' value of the effective charge Z_e. Here we simply remark that the value $Z_e = 1.70$ would make the approximate expression [6.46] agree with the experimental value $E_0 = -2.903$ a.u. of the ground state energy of helium. Since $Z = 2$ in this case, the corresponding screening constant is $S = 0.30$. Thus, for the ground state of helium, we see that in this simple, 'average shielding' approximation, the screening effect of each electron on the other one is equivalent to about one-third of the electronic charge.

A better choice for the central potential $V(r)$ than the Coulomb form [6.44] is provided by an expression of the same type, but in which the 'screening constant' S varies with the distance r. Indeed, at small distances ($r \to 0$), the potential acting on an electron is essentially the Coulomb attraction $-Z/r$ of the nucleus, while for large r ($r \to \infty$), this potential is just the Coulomb field $-(Z - 1)/r$ due to a net charge $(Z - 1)$, namely the nuclear charge Z screened by the charge (-1) of the other electron. Thus we expect the quantity S in [6.44] to be in fact an increasing function of r, which takes on the values $S = 0$ at $r = 0$ and $S = 1$ at $r = \infty$. Since a potential of the form [6.44] where S is a function of r is no longer a Coulomb potential, the l degeneracy which is characteristic of the Coulomb field is removed. Thus the individual electron energies E_{nl} (where we have dropped the subscript i) are still degenerate with respect to the quantum number m, but now depend on both quantum numbers n and l. The principal quantum number n is defined as in the case of hydrogenic atoms, the number of nodes of the radial function being $n_r = n - l - 1$, with $n = 1, 2, \ldots$ and $l = 0, 1, \ldots n - 1$. Calling $u_{nlm}(\mathbf{r})$ an *individual electron orbital*, solution of the single-particle equation

$$[-\tfrac{1}{2}\nabla_r^2 + V(r)]u_{nlm}(\mathbf{r}) = E_{nl}u_{nlm}(\mathbf{r}) \qquad [6.48]$$

we see that $u_{nlm}(\mathbf{r})$ is just the product of a radial function and a spherical harmonic $Y_{lm}(\theta, \phi)$. It is important not to confuse the orbitals $u_{nlm}(\mathbf{r})$, whose radial part depends on $V(r)$ and is likely to be a complicated function, with a hydrogenic function $\psi_{nlm}(\mathbf{r})$, whose radial part corresponds to the particular choice $V(r) = -Z/r$, and which has been obtained in Chapter 3.

Let us now return to the Hamiltonian [6.41]. In terms of the individual electron orbitals $u_{nlm}(\mathbf{r})$, our new zero-order spatial wave functions, which are the properly symmetrised eigenstates of [6.41] are given by

$$\tilde{\psi}_0^{(0)}(r_1, r_2) = u_{100}(r_1)u_{100}(r_2) \qquad [6.49]$$

for the ground state and by

$$\tilde{\psi}_{\pm}^{(0)}(\mathbf{r}_1, \mathbf{r}_2) = \frac{1}{\sqrt{2}}[u_{100}(\mathbf{r}_1)u_{nlm}(\mathbf{r}_2) \pm u_{nlm}(\mathbf{r}_1)u_{100}(\mathbf{r}_2)], \quad n \geq 2 \quad [6.50]$$

for the genuinely discrete excited states. If we still neglect the perturbation $\tilde{H}'$, the total energy of the atom is just

$$\tilde{E}_{1s,nl}^{(0)} = E_{1s} + E_{nl} \qquad [6.51]$$

and the total orbital angular momentum quantum number is $L = l$. The para (+) and ortho (−) states [6.50] are still degenerate, but the degeneracy in l is removed. For a fixed value of n the (algebraic) value of E_{nl} is an increasing function of l. Indeed, electrons with a smaller value of l are more likely to penetrate at certain times the 'centrifugal barrier' (which is proportional to $l(l+1)/r^2$) and hence to feel the fully unscreened attractive Coulomb potential $-Z/r$ of the nucleus. We therefore expect that the energy of the atom will be an increasing function of L $(=l)$. That this is the case may be seen from Fig. 6.2. We note that in the central field approximation leading to [6.51] the energy of the atom is specified by the *electron configuration*, that is by the values of the quantum numbers n and l of the electrons. For the genuinely discrete states of two-electron atoms considered here, one electron remains in the ground state (that is, with $n = 1$ and $l = 0$) while the other, 'optically active' electron has the quantum numbers n and l. Following the convention used in spectroscopy the values of n and l are usually indicated by writing n as a number, and l as a letter, according to the code described in Chapter 3 (i.e. s for $l = 0$, p for $l = 1$, d for $l = 2$, etc.). If there are k electrons having the same values of n and l, this is denoted as $(nl)^k$. For example, in this notation the ground state [6.49] is characterised by the configuration $(1s)^2$ [also written $1s^2$], the first excited states [6.50] by the configurations (1s)(2s) [or 1s2s], (1s)(2p) [or 1s2p], and so on. It is of course understood that when we write for example (1s)(3s) this does not mean that electron 1 (say) is in the state 1s and electron 2 in the state 3s, since we know that properly symmetrised spatial wave functions must be used in order to obtain two-electron wave functions which are fully antisymmetric in the space and spin coordinates of the two electrons.

From our discussion of the wave functions of one-electron atoms it is also clear that for states of the excited electron corresponding to large values of n and l the orbitals $u_{nlm}(\mathbf{r})$ are concentrated at much larger values of r than the ground state orbital $u_{100}(r)$. We may then speak of an 'inner' (1s) electron with spatial quantum numbers (1, 0, 0) which is moving in the unscreened Coulomb field $-Z/r$ of the nucleus, and an 'outer' electron, which moves in the fully screened potential $-(Z-1)/r$. For such states of large n and l the 'zero-order' energy levels are then given approximately (in a.u.) by

$$E_n^{(0)} = -\frac{1}{2}Z^2 - \frac{1}{2}\frac{(Z-1)^2}{n^2} \qquad [6.52]$$

Apart from the addition constant $-Z^2/2$, we see that these energy levels are identical to those of a hydrogenic atom of nuclear charge $Z - 1$. This can be illustrated by drawing the energy levels of atomic hydrogen (shifted by the amount $-1/2$ a.u.) next to those of helium.

We shall not pursue further here the study of the central field approximation. From the above discussion it is clear that according to this approximation each electron moves independently of the other one in a net central potential $V(r)$ which represents the attraction of the nucleus plus some average central

repulsive potential due to the other electron. This basic idea, first expressed by Hartree in 1928, will be fully developed in the next chapter. It is also apparent from the foregoing discussion that the averaged repulsive effect of the other electron depends on its dynamical state, so that a single potential $V(r)$ cannot, even approximately, account for the entire energy spectrum of the atom.

To conclude this section we shall now give a simple, qualitative argument showing how the exchange degeneracy is removed when the electron–electron repulsion term $1/r_{12}$ is taken into account. Returning to the symmetrised zero–order spatial wave functions [6.38], we first observe that the space-antisymmetric (ortho) wave functions $\psi_-^{(0)}$ given by [6.38] vanish for $\mathbf{r}_1 = \mathbf{r}_2$, so that in ortho (spin triplet) states the two electrons tend to 'keep away' from each other and hence, on the average, have a relatively small repulsion energy. On the other hand, the space-symmetric (para) wave functions $\psi_+^{(0)}$ do not vanish for $\mathbf{r}_1 = \mathbf{r}_2$, so that in para (spin singlet) states the two electrons may be very close at certain times and experience on the average a stronger repulsion than in the corresponding ortho state having the same values of the quantum numbers (n, l, m). Therefore the electron-electron repulsion term $1/r_{12}$ is more effective in raising the energy of the atom in the para (spin singlet) states, from which we conclude that an ortho (triplet) state must lie lower than the corresponding para (singlet) state having the same values of (n, l, m). That this is indeed the case may be seen for example in Fig. 6.2. Thus, as pointed out in Section 6.2, the Pauli exclusion principle introduces a coupling between the space and spin variables of the electrons, which act as if they were moving under the influence of a force whose sign depends on the relative orientation of their spins. Such a force, which has no classical analogue, is known as an *exchange force*, and its effects will be studied in detail in Section 6.6.

It is worth stressing at this point that exchange forces are negligible between two electrons which always remain far apart. Indeed, in that case the wave functions of the two electrons have a vanishingly small overlap, and the two electrons may be considered as distinguishable. An example of this situation is provided by the electrons of two hydrogen atoms which are located at a large distance from each other. Similarly, for excited states of two-electron atoms with high values of both n and l, the 'outer' orbital has a very small overlap with the 'inner' (1s) orbital. The exchange force is then very small and the para and ortho levels are nearly degenerate, as may be seen from Fig. 6.2. On the other hand, for small values of n and l (in particular for S-states) the orbitals of the two electrons overlap significantly, and the energy difference between para (singlet) and ortho (triplet) states is appreciable as shown in Fig. 6.2.

The results we have obtained in this section thus show that in addition to their symmetry property (para or ortho), the spatial wave functions for the genuinely discrete states of two-electron atoms may be characterised by the three quantum numbers n, $l(=L)$ and $m(=M_L)$. The ground state is a para state and is non-degenerate. Excluding the negative hydrogen ion H^- (which has no other bound state than the ground state), the energy levels of the excited states are degenerate with respect to M_L and depend on n, on l and on S (with $S = 0$ for

para states, and $S = 1$ for ortho states). The energy levels or terms may therefore be labelled by the symbol

$$n^{2S+1}L$$

where the multiplicity $2S + 1$ takes on the values 1 or 3, and the code letters S, P, D, . . . correspond to $L = 0, 1, 2, \ldots$ as we have seen in Section 6.3. Thus in this notation the ground state is denoted by 1^1S and the following energy levels (by order of increasing energy) are 2^3S, 2^1S, 2^3P, 2^1P, and so on. In the following two sections we shall study successively the ground state 1^1S and various excited states by using perturbation theory and the variational method developed in Chapter 2.

6.5 THE GROUND STATE OF TWO-ELECTRON ATOMS

We have seen in the previous sections that the ground state wave function of two-electron atoms, $\Psi_0(q_1, q_2)$, is a para (spin singlet) state whose general expression in the non-relativistic approximation is

$$\Psi_0(q_1, q_2) = \psi_0(\mathbf{r}_1, \mathbf{r}_2) \frac{1}{\sqrt{2}} [\alpha(1)\beta(2) - \beta(1)\alpha(2)] \qquad [6.53]$$

where $\psi_0(\mathbf{r}_1, \mathbf{r}_2)$ is a space-symmetric function. We shall now focus our attention on this function and on the corresponding ground state energy E_0 of the Hamiltonian [6.2]. The motion of the nucleus and other small corrections will be briefly discussed at the end of this section. It is worth noting that the quantum mechanical treatment of the ground state of helium has been of great historical importance since the 'old quantum theory' was unable to deal successfully with the problem.

Perturbation theory

We shall first use the time-independent perturbation theory of Section 2.8. As in the beginning of the previous section, we split the Hamiltonian [6.2] as $H = H_0 + H'$, where the unperturbed Hamiltonian H_0, given by [6.24] is the sum of two hydrogenic Hamiltonians (see [6.26]–[6.27]) and where $H' = 1/r_{12}$ is the perturbation. The 'zero-order' approximation to the wave function $\psi_0(\mathbf{r}_1, \mathbf{r}_2)$ is then given by the simple wave function $\psi_0^{(0)}(r_1, r_2)$ of equation [6.35] and the corresponding 'zero-order' ground state energy is $E_0^{(0)} = -Z^2$ a.u.

According to [2.308] the first-order correction to the ground state energy is

$$E_0^{(1)} = \langle\psi_0^{(0)}|H'|\psi_0^{(0)}\rangle \qquad [6.54]$$

or, using [6.25] and [6.35],

$$E_0^{(1)} = \int |\psi_{1s}(r_1)|^2 \frac{1}{r_{12}} |\psi_{1s}(r_2)|^2 \, \mathrm{d}\mathbf{r}_1 \, \mathrm{d}\mathbf{r}_2 \qquad [6.55]$$

We note that in SI units this quantity reads

$$E_0^{(1)} = \int |\psi_{1s}(r_1)|^2 \frac{e^2}{(4\pi\varepsilon_0)r_{12}} |\psi_{1s}(r_2)|^2 \, d\mathbf{r}_1 \, d\mathbf{r}_2 \qquad [6.56]$$

and the integral on the right has a simple physical interpretation. Indeed, since $|\psi_{1s}(r_1)|^2$ is the probability density of finding the electron 1 at $\mathbf{r}_1$, we see that

$$\rho(r_1) = -e|\psi_{1s}(r_1)|^2 \qquad [6.57]$$

may be interpreted as the charge density due to electron 1. A similar interpretation may be given to the quantity $\rho(r_2) = -e|\psi_{1s}(r_2)|^2$. Thus the integral in [6.56] is just the electrostatic interaction energy of two overlapping spherically symmetric distributions of electricity, of charge density $\rho(r_1)$ and $\rho(r_2)$ respectively.

Let us now return to [6.55], which we write explicitly (see [6.35]–[6.36]) as

$$E_0^{(1)} = \frac{Z^6}{\pi^2} \int e^{-2Z(r_1+r_2)} \frac{1}{r_{12}} \, d\mathbf{r}_1 \, d\mathbf{r}_2 \qquad [6.58]$$

We shall calculate this integral by using a general procedure which is very useful in many atomic physics calculations. Using the generating function [2.168], we first expand $1/r_{12}$ in Legendre polynomials as

$$\begin{aligned} \frac{1}{r_{12}} &= \frac{1}{r_1} \sum_{l=0}^{\infty} \left(\frac{r_2}{r_1}\right)^l P_l(\cos\theta), \qquad r_1 > r_2 \\ &= \frac{1}{r_2} \sum_{l=0}^{\infty} \left(\frac{r_1}{r_2}\right)^l P_l(\cos\theta), \qquad r_1 < r_2 \end{aligned} \qquad [6.59]$$

where θ is the angle between the vectors $\mathbf{r}_1$ and $\mathbf{r}_2$ (see Fig. 6.7), so that

$$\cos\theta = \cos\theta_1 \cos\theta_2 + \sin\theta_1 \sin\theta_2 \cos(\phi_1 - \phi_2) \qquad [6.60]$$

Here (θ_1, ϕ_1) and (θ_2, ϕ_2) are the polar angles of the vectors $\mathbf{r}_1$ and $\mathbf{r}_2$, respectively. We can also write [6.59] in the more compact form

$$\frac{1}{r_{12}} = \sum_{l-0}^{\infty} \frac{(r_<)^l}{(r_>)^{l+1}} P_l(\cos\theta) \qquad [6.61]$$

where $r_<$ is the smaller and $r_>$ the larger of r_1 and r_2. Using the 'addition theorem' of the spherical harmonics (see [A4.23]) we have

$$\frac{1}{r_{12}} = \sum_{l=0}^{\infty} \sum_{m=-l}^{+l} \frac{4\pi}{2l+1} \frac{(r_<)^l}{(r_>)^{l+1}} Y_{lm}^{\star}(\theta_1, \phi_1) Y_{lm}(\theta_2, \phi_2) \qquad [6.62]$$

Let us substitute this expansion in [6.58] and use the fact that the spherical harmonics are orthonormal on the unit sphere (see [2.182]). Since the function $\exp[-2Z(r_1 + r_2)]$ which appears under the integral sign in [6.58] is spherically symmetric, and because $Y_{00} = (4\pi)^{-1/2}$, we obtain at once by integrating over

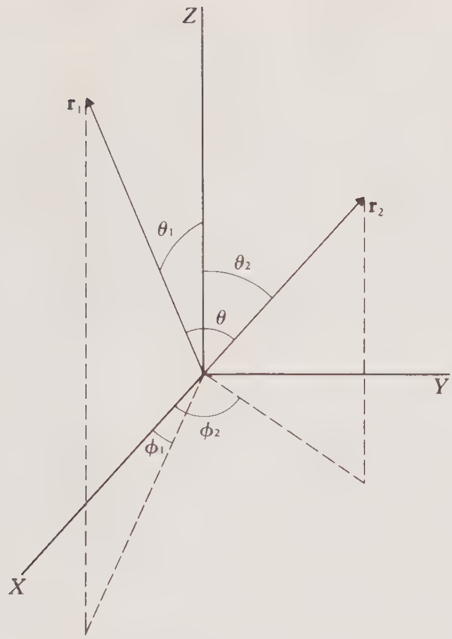

6.7 The polar coordinates of vectors $\mathbf{r}_1$ and $\mathbf{r}_2$.

the polar angles (θ_1, ϕ_1) and (θ_2, ϕ_2)

$$
\begin{aligned}
E_0^{(1)} &= \frac{Z^6}{\pi^2} \sum_{l=0}^{\infty} \sum_{m=-l}^{+l} \frac{(4\pi)^2}{2l+1} \int_0^\infty \mathrm{d}r_1 r_1^2 \int_0^\infty \mathrm{d}r_2 r_2^2\, \mathrm{e}^{-2Z(r_1+r_2)} \frac{(r_<)^l}{(r_>)^{l+1}} \\
&\quad \times \int \mathrm{d}\Omega_1 Y_{lm}^{\star}(\theta_1, \phi_1) Y_{00} \int \mathrm{d}\Omega_2 Y_{00} Y_{lm}(\theta_2, \phi_2) \\
&= \frac{Z^6}{\pi^2} \sum_{l=0}^{\infty} \sum_{m=-l}^{+l} \frac{(4\pi)^2}{2l+1} \int_0^\infty \mathrm{d}r_1 r_1^2 \int_0^\infty \mathrm{d}r_2 r_2^2\, \mathrm{e}^{-2Z(r_1+r_2)} \\
&\quad \times \frac{(r_<)^l}{(r_>)^{l+1}} \delta_{l,0}\, \delta_{m,0}
\end{aligned} \tag{6.63}
$$

Thus all the terms in this double sum vanish, except the first one, for which $l = m = 0$, and

$$
\begin{aligned}
E_0^{(1)} &= 16Z^6 \int_0^\infty \mathrm{d}r_1 r_1^2 \int_0^\infty \mathrm{d}r_2 r_2^2\, \mathrm{e}^{-2Z(r_1+r_2)} \frac{1}{r_>} \\
&= 16Z^6 \int_0^\infty \mathrm{d}r_1 r_1^2\, \mathrm{e}^{-2Zr_1} \left[\frac{1}{r_1} \int_0^{r_1} \mathrm{d}r_2 r_2^2\, \mathrm{e}^{-2Zr_2} \right. \\
&\quad \left. + \int_{r_1}^\infty \mathrm{d}r_2 r_2\, \mathrm{e}^{-2Zr_2} \right]
\end{aligned} \tag{6.64}
$$

The integrals are now straightforward, and yield the answer

$$E_0^{(1)} = \tfrac{5}{8}Z \qquad \text{a.u.} \tag{6.65}$$

which is a positive contribution to the energy, as expected. We also remark that $E_0^{(1)}$ is linear in Z [2], while the unperturbed energy $E_0^{(0)} = -Z^2$ a.u. is quadratic in Z, so that the ratio $|E_0^{(1)}/E_0^{(0)}|$ decreases like Z^{-1} when Z increases. This is in line with our comments in the previous section concerning the decrease in relative importance of the electron-electron repulsion term $1/r_{12}$ with increasing Z.

Adding the first-order correction [6.65] to our zero-order result $E_0^{(0)} = -Z^2$ a.u., we find for the ground state energy E_0 the approximate value

$$E_0 \simeq E_0^{(0)} + E_0^{(1)} = -Z^2 + \tfrac{5}{8}Z \quad \text{a.u.} \tag{6.66}$$

Both this 'first-order' result and the unperturbed energy $E_0^{(0)}$ are given in Table 6.3 for various two-electron atoms (ions), from the negative hydrogen ion H^- ($Z = 1$) to four times ionised carbon C^{4+} ($Z = 6$). The 'exact' [3] values E_0^{ex} are also tabulated. Except for H^-, the simple first-order perturbation approach yields quite good results. If we define ΔE, where

$$\Delta E = E_0^{ex} - (E_0^{(0)} + E_0^{(1)}) \tag{6.67}$$

Table 6.3 Values of the ground state energy E_0 of the Hamiltonian [6.2], for various two-electron atoms and ions (in atomic units)

	Ground state energy			
	Unperturbed $E_0^{(0)}$ (*equation* [6.37])	*First order* $E_0^{(0)} + E_0^{(1)}$ (*equation* [6.66])	*Simple variational* $\left(Z_e = Z - \frac{5}{16}\right)$ (*equation* [6.79])	*'Exact'*
H^-	−1	−0.375	−0.473	−0.528
He	−4	−2.750	−2.848	−2.904
Li^+	−9	−7.125	−7.222	−7.280
Be^{2+}	−16	−13.50	−13.60	−13.66
B^{3+}	−25	−21.88	−21.97	−22.03
C^{4+}	−36	−32.25	−32.35	−32.41

[2] The fact that $E_0^{(1)}$ is linear in Z may readily be understood by noting that each charge distribution in [6.56] contains a total charge $-e$ and extends over a region of space of linear dimension given approximately by $a = a_0/Z$. Their mutual interaction energy is therefore roughly given by $e^2/(4\pi\varepsilon_0)a = Ze^2/(4\pi\varepsilon_0)a_0$, which is indeed proportional to Z.

[3] The 'exact' results quoted in Table 6.3 are accurate values of the ground state energy E_0 of the Hamiltonian [6.2], obtained by using the Rayleigh–Ritz variational method with elaborate trial functions. Only a few of the presently available significant figures are given. Since these 'exact' values of E_0 must still be corrected for the motion of the nucleus, as well as relativistic and radiative corrections, they should not be confused with the experimental ground state energies E_0^{exp}.

as the difference between the 'exact' value E_0^{ex} and the first-order result [6.66], we see that the ratio $|\Delta E/E_0^{ex}|$ varies from about 5 per cent for He to 0.4 per cent for C^{4+}. It is interesting to note that this first-order perturbation treatment, carried out by Unsöld in 1927, was the first quantum mechanical calculation of the helium ground state. In view of the large discrepancies shown by the old quantum theory calculations, the relatively small difference of about 0.15 a.u. ($\simeq$4 eV) between his result and the experimental value was very promising.

The calculation of second and higher order corrections, $E_0^{(n)}$ ($n \geqslant 2$), is a much more difficult problem, to which we shall return further, after having discussed the Rayleigh–Ritz variational approach.

Variational method

We have seen in Section 2.8 that if H denotes the Hamiltonian of a quantum system, and ϕ a physically admissible trial function, the functional

$$E[\phi] = \frac{\langle\phi|H|\phi\rangle}{\langle\phi|\phi\rangle} \tag{6.68}$$

provides a variational principle for the discrete eigenvalues of the Hamiltonian. Moreover, it also yields a minimum principle for the ground state energy. That is,

$$E_0 \leqslant E[\phi] \tag{6.69}$$

For the case of two-electron atoms the Hamiltonian H (neglecting the motion of the nucleus and all but the Coulomb interactions) is given by [6.2]. Following the Rayleigh–Ritz variational method, we shall use trial functions ϕ depending on variational parameters, and carry out the variation $\delta E = 0$ with respect to these parameters.

It is apparent from the discussion of Section 6.4 that a basic defect of the 'zero-order' ground state wave function [6.35] (from which the first-order energy result [6.66] was obtained) is that each electron moves in the fully unscreened field of the nucleus. In order to take into account approximately the screening effect of each electron on the other one, we shall therefore choose a trial function of the form [6.47]. That is, (in a.u.)

$$\phi(r_1, r_2) = \frac{Z_e^3}{\pi} \mathrm{e}^{-Z_e(r_1+r_2)} \tag{6.70}$$

or

$$\phi(r_1, r_2) = \psi_{1s}^{Z_e}(r_1)\psi_{1s}^{Z_e}(r_2) \tag{6.71a}$$

where

$$\psi_{1s}^{Z_e}(r) = \left(\frac{Z_e^3}{\pi}\right)^{1/2} \mathrm{e}^{-Z_e r} \tag{6.71b}$$

and the 'effective charge' Z_e is considered as a variational parameter.

The first step of the calculation consists in evaluating the expression $E[\phi]$. Since our trial function [6.70] is normalised ($\langle\phi|\phi\rangle = 1$) we have from [6.68] and [6.2]

$$E[\phi] = \left\langle \phi \left| T_1 + T_2 - \frac{Z}{r_1} - \frac{Z}{r_2} + \frac{1}{r_{12}} \right| \phi \right\rangle \qquad [6.72]$$

where we have set $T_1 = -\nabla^2_{r_1}/2$ and $T_2 = -\nabla^2_{r_2}/2$. Using the equations [6.71] and the virial theorem (see [3.76]–[3.77]) we find that

$$\langle\phi|T_1|\phi\rangle = \langle\psi^{Z_e}_{1s}|T_1|\psi^{Z_e}_{1s}\rangle = \tfrac{1}{2}Z_e^2 \qquad [6.73]$$

and $\langle\phi|T_2|\phi\rangle = \langle\phi|T_1|\phi\rangle$. We also have from [3.71] and [6.71]

$$\left\langle \phi \left| \frac{1}{r_1} \right| \phi \right\rangle = \left\langle \psi^{Z_e}_{1s} \left| \frac{1}{r_1} \right| \psi^{Z_e}_{1s} \right\rangle = Z_e \qquad [6.74]$$

and $\langle\phi|1/r_2|\phi\rangle = \langle\phi|1/r_1|\phi\rangle$. The expression $\langle\phi|1/r_{12}|\phi\rangle$ has already been calculated when $Z_e = Z$, in which case it is identical to the first-order energy correction $E_0^{(1)}$ (see [6.54]–[6.58]). Using [6.65] we find that

$$\left\langle \phi \left| \frac{1}{r_{12}} \right| \phi \right\rangle = \frac{5}{8} Z_e \qquad [6.75]$$

Putting together the above results, we have

$$E[\phi] \equiv E(Z_e) = Z_e^2 - 2ZZ_e + \tfrac{5}{8}Z_e \qquad [6.76]$$

In the second step of the calculation, we shall now minimise $E(Z_e)$ with respect to the variational parameter Z_e. Hence we write

$$\frac{\partial E}{\partial Z_e} = 2Z_e - 2Z + \frac{5}{8} = 0 \qquad [6.77]$$

so that

$$Z_e = Z - \frac{5}{16} \qquad [6.78]$$

This 'optimum' value of Z_e corresponds to a 'screening constant' $S \simeq 0.31$. The lowest energy which can be obtained with a trial function of the form [6.70] is given by choosing $Z_e = Z - 5/16$ and substituting this value in [6.76], namely

$$E\left(Z_e = Z - \frac{5}{16}\right) = -Z^2 + \frac{5}{8}Z - \frac{25}{256} = -\left(Z - \frac{5}{16}\right)^2 \text{ a.u.} \qquad [6.79]$$

We remark that with the choice $Z_e = Z$ the expression [6.76] reduces to the first-order perturbation theory value [6.66], which is therefore equivalent to a 'non-optimum' variation calculation. The variational result [6.79], corresponding to the 'optimum' choice $Z_e = Z - 5/16$, is lower, and hence more accurate, than the first-order perturbation theory result [6.66]. This may be seen from Table 6.3, where the variational values obtained from [6.79] are given

for various two-electron atoms (ions). It is clear from this table that the variational results are remarkably good, given the simplicity of the trial function we have used. If we denote by ΔE the difference between the 'exact' [3] value E_0^{ex} and the variational result [6.79], we see that the relative error $|\Delta E/E_0^{\mathrm{ex}}|$ varies from about 2 per cent for He to less than 0.2 per cent for C^{4+}. This corresponds to a reduction by more than a factor of two with respect to the relative error made in the first-order perturbation calculation. For the delicate case of H the variational result is also a marked improvement over the first-order perturbation value, although the ground state energy of -0.473 a.u. given by our simple variational treatment still lies above the ground state energy of atomic hydrogen (-0.5 a.u.) and hence is not low enough to predict the existence of a stable bound state for H^-.

We now describe briefly how very accurate values of the non-relativistic ground state energy of two-electron atoms can be obtained by using the Rayleigh–Ritz variational method with elaborate trial functions. We first remark that for S-states ($L = 0$) the spatial wave function does not depend on the Euler angles which specify the orientation of the triangle formed by the nucleus and the two electrons. Thus spatial wave functions for S-states (and in particular for the ground state 1^1S) can only depend on the shape and size of this triangle, which is specified for example by the radial coordinates r_1 and r_2 of the two electrons and their relative distance $r_{12} = |\mathbf{r}_1 - \mathbf{r}_2|$. Another possible choice for the three variables describing this triangle is

$$\begin{aligned} s &= r_1 + r_2 & 0 &\leqslant s \leqslant \infty \\ t &= r_1 - r_2 & -\infty &\leqslant t \leqslant \infty \\ u &= r_{12} & 0 &\leqslant u \leqslant \infty \end{aligned} \qquad [6.80]$$

The coordinates [6.80] have been used by Hylleraas to construct trial functions of the type

$$\phi(s, t, u) = \mathrm{e}^{-ks} \sum_{l,m,n=0}^{N} c_{l,2m,n} s^l t^{2m} u^n \qquad [6.81]$$

where the coefficients $c_{l,2m,n}$ are linear variational parameters and k is a 'non-linear' variational parameter similar to the 'effective charge' Z_e used in our simple trial function [6.70]. We note that since the ground state is a para state (space-symmetric) the trial function [6.81] must be an even function of t. The number N which appears in [6.81] determines the maximum number of terms kept in the trial function. It is clear that for $N = 0$ the trial function [6.81] reduces to the simple form [6.70], so that $k = Z_e = Z - 5/16$ in that case.

The Hylleraas approach, which accounts explicitly for 'correlations' between the motion of the two electrons through the variable $u = r_{12}$, has been very successful in getting accurate values of the ground state energy E_0 of the Hamiltonian [6.2]. For example, with a trial wave function of the type [6.81] containing six linear parameters, Hylleraas obtained in the case of helium the value $E_0 = -2.903\,24$ a.u., which differs from the 'exact' value

$E_0^{\text{ex}} = -2.90372$ a.u. by only 0.00048 a.u. ($\simeq 0.013$ eV). By now, extensive variational calculations, using trial functions of a somewhat more general form [4] than [6.81], have been performed for a variety of two-electron atoms and ions. The corresponding 'exact' results are given in the last column of Table 6.3 for the systems H^- ($Z = 1$) through C^{4+} ($Z = 6$). It is worth stressing that the numbers quoted in that column do not contain all the significant figures which are presently available. For example, the value of E_0 for He is one of the most accurate theoretical numbers which have been calculated by quantum mechanical approximation methods, the result obtained by Frankowski and Pekeris being

$$E_0 = -2.903\,724\,377\,03 \quad \text{a.u.} \tag{6.82}$$

The very accurate Hylleraas-type ground state wave functions determined by the Rayleigh–Ritz variational method have also been used to calculate expectation values of various operators, oscillator strengths, transition probabilities, and so on. In many cases of practical interest, however, it is convenient to use less accurate, but more tractable wave functions, which do not involve explicitly the interelectronic coordinate r_{12}, and we shall now briefly describe how such wave functions may be obtained.

As we pointed out above, the spatial wave functions for S-states of two-electron atoms depend only on the shape and size of the triangle formed by the nucleus and the two electrons. Instead of using the three variables (r_1, r_2, r_{12}) or the Hylleraas coordinates (s, t, u), one can also choose the radial coordinates r_1 and r_2 of the two electrons, and the angle θ between the vectors $\mathbf{r}_1$ and $\mathbf{r}_2$. It is then natural to use for the ground state trial wave functions which are expansions in Legendre polynomials,

$$\phi(\mathbf{r}_1, \mathbf{r}_2) = \sum_{l=0}^{\lambda} F_l(r_1, r_2) P_l(\cos\theta) \tag{6.83}$$

where the subscript l refers of course to *relative* partial waves. This approach is known as the '*configuration interaction*' (CI) method [5]. The (symmetric) functions $F_l(r_1, r_2)$ are expanded in some convenient basis set, for example

$$F_l(r_1, r_2) = \mathrm{e}^{-k(r_1+r_2)} \sum_{i \leq j} c_{ij}^{(l)} r_1^l r_2^l (r_1^i r_2^j + r_1^j r_2^i) \tag{6.84}$$

[4] For example, Kinoshita has used trial functions which, in addition to the terms contained in [6.81], also include terms of the form $s^{h+1}(u/s)^i(t/u)^{2j}$. Schwartz has successfully tried functions of the type [6.81], but with some half-integer powers. Pekeris has also obtained extremely accurate results by using trial functions expressed in terms of the three perimetric coordinates $u = \varepsilon(r_2 + r_{12} - r_1)$, $v = \varepsilon(r_1 + r_{12} - r_2)$ and $w = 2\varepsilon(r_1 + r_2 - r_{12})$, with $\varepsilon = (-E_0)^{1/2}$.

[5] The name 'configuration interaction' (or 'configuration mixing') arises from the fact that a trial function of the form [6.83] may be written symbolically as

$$\phi = c_{10,10}(1s, 1s) + \sum_{nln'l'} c_{nl,n'l'}(nl, n'l').$$

Here (1s, 1s) is the $1s^2$ configuration obtained for the ground state in the independent particle approximation, and $(nl, n'l')$ represent configurations 'mixed' into the ground state because the electron–electron interaction $1/r_{12}$ has non-zero matrix elements between the $1s^2$ configuration and other ones.

where k is a non-linear variational parameter, and the coefficients $c_{ij}^{(l)}$ are linear variational parameters. If one sets $\lambda = 0$ in [6.83], so that the trial wave function is restricted to the pure relative s-wave ($l = 0$), only *radial* correlations between the positions of the two electrons are introduced in the wave function. In this way a *radial limit* for the ground state energy is approached when an increasing number of parameters is included in the function $F_0(r_1, r_2)$. For example, in helium this radial limit is about -2.879 a.u., and differs from the correct value of -2.904 a.u. by 0.025 a.u. (=0.68 eV). This difference is due to *radial* and *angular* correlations distributed among the higher relative partial waves in the expansion [6.83].

An important drawback of the CI approach is that the expansion [6.83] converges much less rapidly than the Hylleraas method, which makes explicit use of the interelectronic coordinate r_{12}. This is due to the fact that the expansion of r_{12} in Legendre polynomials $P_l(\cos\theta)$ converges very slowly. On the other hand, the calculation of matrix elements (such as those occurring for example in collision processes) is considerably simpler when use is made of CI wave functions instead of Hylleraas-type wave functions.

Before closing our discussion of variational wave functions for the ground state of two-electron atoms, we give two explicit examples of simple wave functions which represent improvements over the one-parameter 'screened hydrogenic' wave function [6.70], with $Z_e = Z - 5/16$. For helium, a useful wave function is that of Byron and Joachain,

$$\psi_0(r_1, r_2) = u_{1s}(r_1)u_{1s}(r_2) \qquad [6.85a]$$

where the 1s orbital $u_{1s}(r)$ is given by

$$u_{1s}(r) = (4\pi)^{-1/2}(A\mathrm{e}^{-\alpha r} + B\mathrm{e}^{-\beta r}) \qquad [6.85b]$$

with $A = 2.60505$, $B = 2.08144$, $\alpha = 1.41$ and $\beta = 2.61$. This (normalised) function is an analytical fit to the Hartree–Fock orbital, to be discussed in Chapter 7. The corresponding Hartree–Fock ground state energy is $E_0 = -2.86167$ a.u. For the negative hydrogen ion H^-, a convenient (normalised) wave function, obtained by Chandrasekhar, is given by

$$\psi_0(r_1, r_2) = \frac{1}{4\pi} N(\mathrm{e}^{-\alpha r_1 - \beta r_2} + \mathrm{e}^{-\beta r_1 - \alpha r_2}) \qquad [6.86]$$

with $N = 0.3948$, $\alpha = 1.039$ and $\beta = 0.283$. The wave function [6.86] yields an energy $E_0 = -0.514$ a.u. and therefore correctly predicts a bound state for the H^- system. Although the ionisation potential $I_\mathrm{P} = 0.014$ a.u. resulting from [6.86] is rather far from the correct value $I_\mathrm{P}^\mathrm{ex} = 0.028$ a.u., it is much better than the *negative* value $I_\mathrm{P} = -0.027$ a.u. corresponding to the simple variational function [6.70]. Wave functions of the type [6.86], with $\alpha \neq \beta$, are known as 'open shell' wave functions. We note that the values of α and β obtained in the present case imply that H^- can be viewed as a two-electron system in which one electron is weakly bound in the field of a polarised hydrogen atom.

Variation–perturbation method

Let us now return to the perturbation treatment which we started at the beginning of this section by calculating the first-order energy correction $E_0^{(1)}$. It is possible to obtain higher order corrections by using the variation–perturbation method discussed in Section 2.8. In order to display explicitly the Z dependence of the various orders of perturbation theory, it is convenient to choose Za_0 as our unit of length and $Z^2e^2/(4\pi\varepsilon_0)a_0 = Z^2$ a.u. as our unit of energy. Setting

$$\boldsymbol{\rho}_1 = Z\mathbf{r}_1, \qquad \boldsymbol{\rho}_2 = Z\mathbf{r}_2, \qquad \rho_{12} = |\boldsymbol{\rho}_1 - \boldsymbol{\rho}_2| \tag{6.87}$$

the Schrödinger equation [6.3] then becomes

$$(H_0 + \lambda H')\psi(\boldsymbol{\rho}_1, \boldsymbol{\rho}_2) = \varepsilon\psi(\boldsymbol{\rho}_1, \boldsymbol{\rho}_2) \tag{6.88}$$

where

$$H_0 = -\frac{1}{2}\nabla^2_{\rho_1} - \frac{1}{2}\nabla^2_{\rho_2} - \frac{1}{\rho_1} - \frac{1}{\rho_2}$$

$$H' = \frac{1}{\rho_{12}}, \qquad \lambda = Z^{-1}, \qquad \varepsilon = E/Z^2 \tag{6.89}$$

With this choice of units, the ground state energy $\varepsilon_0 = E_0/Z^2$, expanded in powers of λ, reads

$$\varepsilon_0 = \sum_{n=0}^{\infty} \varepsilon_0^{(n)} Z^{-n} \tag{6.90}$$

Following the procedure outlined in Section 2.8, approximate values of $\varepsilon_0^{(n)}$ may be obtained by using trial functions $\phi^{(1)}, \phi^{(2)}, \ldots$ in the functionals $F_1[\phi^{(1)}]$, $F_2[\phi^{(2)}]$, and so on. Table 6.4 shows the first few values of $\varepsilon_0^{(n)}$ $(2 \leqslant n \leqslant 10)$ calculated by Scherr and Knight from elaborate Hylleraas-type trial functions. The agreement between the values of $E_0 = Z^2\varepsilon_0$ obtained from

Table 6.4 Values of $\varepsilon_0^{(n)}$ (in a.u.) for the first few orders of perturbation theory, as obtained by Scherr and Knight. We recall that $\varepsilon_0^{(0)} = -1$ and $\varepsilon_0^{(1)} = 5/8$. The corresponding values of $E_0^{(n)}$ are given (in a.u.) by $E_0^{(n)} = \varepsilon_0^{(n)} Z^{2-n}$

Order n of Perturbation theory	*Value of* $\varepsilon_0^{(n)}$
2	−0.15766
3	0.00869
4	−0.00088
5	−0.00103
6	−0.00061
7	−0.00037
8	−0.00024
9	−0.00016
10	−0.00011

[6.90] and the results of Table 6.4 and those calculated from the Rayleigh–Ritz method (quoted in the last column of Table 6.3) is excellent. It is interesting to note that for the case of H it is necessary to include the values of $\varepsilon_0^{(n)}$ up to order $n = 7$ to obtain agreement with the correct result ($E_0 = -0.528$ a.u.) within 0.001 a.u. ($\simeq$0.027 eV).

Comparison with experiment

The extremely accurate result [6.82] is actually *lower* than the experimental value of the ground state of helium ! This, however, is not a paradox since [6.82] is only an upper limit to the exact *non-relativistic* value of E_0 corresponding to an *infinitely heavy nucleus* (i.e. the ground state of the Hamiltonian [6.2]). Before comparing theory and experiment several corrections must therefore be calculated, which we now discuss briefly.

We begin by considering the *motion of the nucleus*. From Appendix 8 and equation [6.1], we see that the Schrödinger equation in which this effect is ignored (i.e. in which one sets $M = \infty$) is then modified in *two* ways. Firstly, as in the case of one-electron atoms, the *reduced mass* $\mu = mM/(m + M)$ of the electron with respect to the nucleus replaces the mass m of the electron. Secondly, a 'mass polarisation' term $(-\hbar^2/M)\boldsymbol{\nabla}_{r_1} \cdot \boldsymbol{\nabla}_{r_2}$ appears in the Schrödinger equation.

The reduced mass correction is easily taken into account by using the method discussed in Chapters 1 and 3 for hydrogenic atoms. We introduce a new atomic unit of length $a_\mu = a_0 m/\mu$ and a new atomic unit of energy

$$\frac{e^2}{(4\pi\varepsilon_0)a_\mu} = \frac{e^2}{(4\pi\varepsilon_0)a_0}\frac{\mu}{m} \qquad [6.91]$$

which differs from the usual atomic energy unit $e^2/(4\pi\varepsilon_0)a_0$ by the factor μ/m. After having calculated the energy E_∞ corresponding to infinite nuclear mass ($M = \infty$) we may therefore obtain the value E_μ appropriate to the reduced mass μ by writing

$$E_\mu = \frac{\mu}{m} E_\infty \qquad [6.92]$$

Thus, as for one-electron atoms (see Chapters 1 and 3), the reduced mass effect modifies all the energy levels of the atom in the same manner, all the frequencies of the spectral lines being reduced by the factor $\mu/m \simeq 1 - m/M$. If we call ΔE_1 the reduced mass correction to be applied to the energy levels E_∞, we see that

$$\begin{aligned}\Delta E_1 &= E_\mu - E_\infty \\ &= E_\infty\left(\frac{\mu}{m} - 1\right) \\ &\simeq -\frac{m}{M} E_\infty \qquad [6.93]\end{aligned}$$

and we notice that ΔE_1 is positive. In particular, for the ground state of ^{4}He this correction reduces the ionisation potential I_P^∞ (corresponding to $M = \infty$) by an amount of about 27 cm^{-1}.

We now turn to the correction arising from the 'mass polarisation' term. Calling ΔE_2 that correction, and using first-order perturbation theory, we have (in a.u.)

$$\begin{aligned}\Delta E_2 &= -\frac{1}{M}\langle\psi_0|\nabla_{\mathbf{r}_1}\cdot\nabla_{\mathbf{r}_2}|\psi_0\rangle \\ &= \frac{1}{M}\langle\psi_0|\mathbf{p}_1\cdot\mathbf{p}_2|\psi_0\rangle\end{aligned} \tag{6.94}$$

where $\psi_0(\mathbf{r}_1, \mathbf{r}_2)$ is the spatial part of the ground state wave function, corresponding to the case $M = \infty$, and $\mathbf{p}_i$ is the momentum of electron i. We note that if ψ_0 is a simple product of individual orbitals $u_i(\mathbf{r}_i)$ $(i = 1, 2)$, then $\Delta E_2 = 0$, since the expectation value of the momentum, $\langle\mathbf{p}\rangle$, vanishes for a stationary bound (discrete) state. With an accurate Hylleraas-type variational wave function, it is found that for ^{4}He the correction ΔE_2 is about 4.8 cm^{-1}.

The discussion of the relativistic corrections and of the radiative corrections (Lamb shift) falls outside the scope of this book [6]. Calling ΔE_3 the former ones, and ΔE_4 the latter ones, we list in Table 6.5 the numerical values of these corrections for helium and several helium-like ions. Also given in Table 6.5 are the reduced mass correction ΔE_1 and the mass polarisation correction ΔE_2 discussed above. When subtracted from the non-relativistic ionisation potential I_P^∞ (corresponding to $M = \infty$), these four corrections yield the total theoretical ionisation potential I_P^{th}, which is seen from Table 6.5 to be in excellent agreement with experiment. Of particular interest is the comparison between the theoretical and experimental values of the ionisation potential for helium. From the work of Frankowski and Pekeris, and Schwartz, the theoretical value is

$$I_P^{\text{th}} = (198\,310.699 \pm 0.05) \quad \text{cm}^{-1} \tag{6.95}$$

while the experimental value obtained by Herzberg is

$$I_P^{\text{exp}} = (198\,310.82 \pm 0.15) \quad \text{cm}^{-1} \tag{6.96}$$

The fantastic agreement between [6.95] and [6.96] may be considered as one of the most striking triumphs of quantum mechanics.

6.6 EXCITED STATES OF TWO-ELECTRON ATOMS

We now turn to the study of the excited states of helium-like atoms. Disregarding for the moment the 'double excited states' (which will be considered in the next section), we shall analyse various 'genuinely discrete' excited states of two-electron atoms with $Z \geqslant 2$. For the sake of simplicity we shall neglect all

[6] A detailed account may be found in Bethe and Salpeter (1957).

Table 6.5 Values of the non-relativistic ionisation potential I_P^∞, the reduced mass correction ΔE_1, the mass polarisation correction ΔE_2, the relativistic corrections ΔE_3, the radiative corrections ΔE_4, the theoretical ionisation potential $I_P^{th} = I_P^\infty - (\Delta E_1 + \Delta E_2 + \Delta E_3 + \Delta E_4)$ and the experimental ionisation potential I_P^{exp} (in cm^{-1}) for various two-electron atoms and ions

	I_P^∞	ΔE_1	ΔE_2	ΔE_3	ΔE_4	I_P^{th}	I_P^{exp}
H^-	6090.644289	3.315791	3.928	0.304	0.0037	6083.092	6100 ± 100
He	198344.58014348	27.192711	4.785	0.562	1.341	198310.699	198 310.82 + 0.15
Li^+	610120.4882	47.7689	4.960	−19.69	7.83	610079.62	610079 ± 25
Be^{2+}	1241253.351	75.681	5.619	−114.52	27.1	1241259.5	1241225 ± 100
B^{3+}	2091806.533	104.436	6.046	−372.88	65.7	2092003.2	2091960 ± 200
C^{4+}	3161805.752	144.864	6.878	−919.00	132	3162441	3162450 ± 300

the small corrections (motion of the nucleus, relativistic and radiative corrections) mentioned at the end of the preceding section. Our starting point will therefore be the Schrödinger equation [6.3] and our discussion of Section 6.4 based on the independent particle model.

Perturbation theory

As in the case of the ground state, we shall first use perturbation theory. We again choose to split the Hamiltonian [6.2] as $H = H_0 + H'$, where the unperturbed Hamiltonian H_0 is given by [6.24] and $H' = 1/r_{12}$ is the perturbation. The properly symmetrised 'zero-order' spatial wave functions for the genuinely discrete excited states we are considering are therefore the wave functions $\psi_\pm^{(0)}(\mathbf{r}_1, \mathbf{r}_2)$ given by [6.38], the corresponding 'zero-order' energies being given by [6.39].

Since the energy levels [6.39] are degenerate with respect to l and m, and also exhibit the 'exchange degeneracy', we should in principle use degenerate perturbation theory. However, by using the expansion [6.62] of $1/r_{12}$ in spherical harmonics and the orthogonality property of the Y_{lm}, it is straightforward to prove that the matrix elements of H' between two degenerate zero-order wave functions $\psi_\pm^{(0)}$ corresponding to different l or m vanish. Moreover, since H' is invariant for a permutation of the spatial coordinates of the two electrons, it is clear that the matrix elements $\langle\psi_-^{(0)}|H'|\psi_+^{(0)}\rangle$ of H' between two degenerate zero-order wave functions corresponding respectively to a para and an ortho state vanish. Thus, from the point of view of degenerate perturbation theory, the wave functions [6.38] are already the correct 'zero-order' wave functions and we can use non-degenerate perturbation theory directly to calculate the first-order energy corrections. That is

$$E_\pm^{(1)} = \langle\psi_\pm^{(0)}|H'|\psi_\pm^{(0)}\rangle \qquad [6.97]$$

where the plus sign refers to para states and the minus sign to ortho states, as usual. Using the expression [6.38] of $\psi_\pm^{(0)}$ and the fact that $H' = 1/r_{12}$, we have

$$E_+^{(1)} = \mathcal{J} + K, \qquad E_-^{(1)} = \mathcal{J} - K \qquad [6.98]$$

where

$$\mathcal{J} = \int |\psi_{100}(\mathbf{r}_1)|^2 \frac{1}{r_{12}} |\psi_{nlm}(\mathbf{r}_2)|^2 \, d\mathbf{r}_1 \, d\mathbf{r}_2 \qquad [6.99]$$

and

$$K = \int \psi_{100}^*(\mathbf{r}_1)\psi_{nlm}^*(\mathbf{r}_2) \frac{1}{r_{12}} \psi_{100}(\mathbf{r}_2)\psi_{nlm}(\mathbf{r}_1) \, d\mathbf{r}_1 \, d\mathbf{r}_2 \qquad [6.100]$$

with $n \geqslant 2$.

The integral $\mathcal{J}$ is called the *Coulomb* (or *direct*) *integral*. By analogy with the discussion following [6.55], we see that it represents the Coulomb interaction

between the charge distributions of the two electrons. The integral K is known as the *exchange integral*; it is the matrix element of $1/r_{12}$ between two states such that the electrons have exchanged their quantum numbers. Using the fact that the hydrogenic functions $\psi_{nlm}(\mathbf{r})$ are given by $\psi_{nlm}(\mathbf{r}) = R_{nl}(r)Y_{lm}(\theta, \phi)$ (see [3.48]), together with the expansion [6.62] and the orthonormality property of the spherical harmonics, we have

$$\mathcal{J}_{nl} = \int_0^\infty \mathrm{d}r_2 r_2^2 R_{nl}^2(r_2) \int_0^\infty \mathrm{d}r_1 r_1^2 R_{10}^2(r_1) \frac{1}{r_>} \quad [6.101]$$

and

$$K_{nl} = \frac{1}{2l+1} \int_0^\infty \mathrm{d}r_2 r_2^2 R_{10}(r_2) R_{nl}(r_2) \int_0^\infty \mathrm{d}r_1 r_1^2 R_{10}(r_1) R_{nl}(r_1) \frac{(r_<)^l}{(r_>)^{l+1}} \quad [6.102]$$

where we recall that $r_<$ is the smaller and $r_>$ the larger of r_1 and r_2. In the above formulae we have explicitly indicated that the integrals $\mathcal{J}$ and K depend on n and l, but not on m. The first-order energy corrections [6.98] may therefore be written more explicitly as

$$E_{nl,\pm}^{(1)} = \mathcal{J}_{nl} \pm K_{nl} \quad [6.103]$$

and we remark that the independence of these energy shifts with respect to m can also be deduced from the fact that the perturbation $H' = 1/r_{12}$ commutes with L_z.

Adding the corrections [6.103] to the zero-order energies [6.39], we thus obtain the 'first-order' energy values

$$E_{nl,\pm} \simeq E_{1,n}^{(0)} + E_{nl,\pm}^{(1)} = -\frac{Z^2}{2}\left(1 + \frac{1}{n^2}\right) + \mathcal{J}_{nl} \pm K_{nl} \quad [6.104]$$

The integrals $\mathcal{J}_{nl}$ and K_{nl} can be evaluated explicitly (see for example Problem 6.4 for the case $n = 2, l = 0, 1$), but we shall use here only a couple of their general properties. First of all, it is obvious from [6.101] that $\mathcal{J}_{nl}$ must be positive. Furthermore, for $l = n - 1$ the radial wave function $R_{n,n-1}$ has no nodes, so that we deduce directly from [6.102] that $K_{n,n-1} > 0$. It turns out that in the general case one has $K_{nl} > 0$, so that we see from [6.104] that *an ortho* (spin triplet) *state has a lower energy than the corresponding para* (spin singlet) *state* having the same value of n and l. This conclusion is in accordance with our discussion at the end of Section 6.4. In fact, the role of the spin-dependent *exchange force* introduced at that point can be made explicit in the following way. We first note from [6.11] and [6.15] that the operator

$$\mathbf{S}_1 \cdot \mathbf{S}_2 = \tfrac{1}{2}\mathbf{S}^2 - \tfrac{3}{4} \quad [6.105]$$

yields the value $-3/4$ when acting on singlet spin states ($S = 0$) and $1/4$ when acting on triplet spin states ($S = 1$). The first-order energy correction [6.103]

can therefore by symbolically written as

$$E^{(1)}_{nl,\pm} = \mathcal{J}_{nl} - \tfrac{1}{2}(1 + 4\mathbf{S}_1 \cdot \mathbf{S}_2)K_{nl}$$
$$= \mathcal{J}_{nl} - \tfrac{1}{2}(1 + \boldsymbol{\sigma}_1 \cdot \boldsymbol{\sigma}_2)K_{nl} \qquad [6.106]$$

where we have introduced the $\boldsymbol{\sigma}_i$ operators, which are related to the spin operators $\mathbf{S}_i$ by

$$\mathbf{S}_i = \tfrac{1}{2}\boldsymbol{\sigma}_i \qquad \text{(in a.u.)} \qquad [6.107]$$

We see that in the sense specified by [6.106] the energy shifts $E^{(1)}_{nl,\pm}$ – and hence the first-order energy values [6.104] – depend explicitly upon the relative orientation of the electron spins, even though the Hamiltonian [6.2] does not contain spin-dependent terms. We also remark that the spin-dependent exchange force responsible for this effect is of the same order of magnitude as the electrostatic force. It is therefore much stronger than the spin-dependent forces arising from relativistic effects, such as the spin–orbit interaction which has been shown in Chapter 5 to yield corrections of order $(Z\alpha)^2$ to the energy levels. In fact, as Heisenberg first observed, the exchange force is strong enough to keep the electron spins aligned in certain solids, and hence is responsible for the phenomenon of *ferromagnetism*.

The splitting of the unperturbed energy levels predicted by the first-order expression [6.104] is illustrated schematically in Fig. 6.8 for the case $n = 2$. The effects of the Coulomb integrals $\mathcal{J}_{2l}$ and of the exchange integrals K_{2l} are displayed separately. We remark that $\mathcal{J}_{21} > \mathcal{J}_{20}$, so that the energy of the configuration 1s2s is lower than that of the configuration 1s2p, as we expect from the discussion following [6.51]. We also see from Fig. 6.8 that the triplet

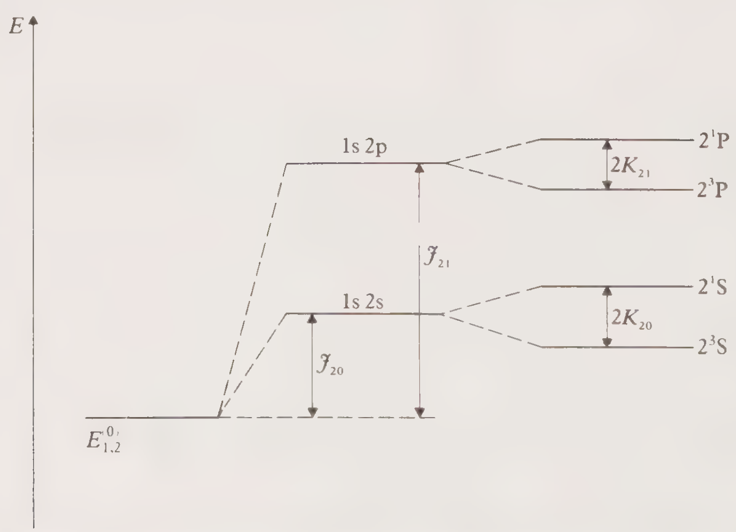

6.8 The splitting of the unperturbed helium level for $n = 2$ by the Coulomb integrals $\mathcal{J}_{2l}$ and the exchange integrals K_{2l}.

states lie below the singlet states corresponding to the same values of n and l, in agreement with the foregoing discussion.

Variational method

As we remarked in Section 2.8, the application of the Rayleigh–Ritz variational method to excited states of a quantum system is in general more difficult than for the ground state, because the trial wave function corresponding to an excited state must be orthogonal to the wave functions of all the eigenstates having a lower energy. However, we also noticed in Section 2.8 that an important simplification occurs when the Hamiltonian can be diagonalised simultaneously with a Hermitian operator A. Indeed, we saw that in that case a trial wave function entirely constructed from eigenfunctions of A corresponding to a given eigenvalue α_i is automatically orthogonal to all the eigenfunctions of A corresponding to eigenvalues α_j different from α_i; this trial wave function will therefore provide an upper bound for the lowest energy eigenvalue associated with the eigenvalue α_i.

We now apply these ideas to the case of two-electron atoms. Among the operators which can be diagonalised simultaneously with the Hamiltonian [6.2], we shall consider the permutation operator P_{12} (see [6.4]) as well as the operators $\mathbf{S}^2$ and $\mathbf{L}^2$. First of all, since para wave functions (which correspond to the eigenvalue $+1$ of P_{12} and to the value $S = 0$ of the total spin) are orthogonal to ortho wave functions (corresponding to the eigenvalue -1 of P_{12} and to the total spin $S = 1$), we can study separately the variational determination of the para and ortho energy levels, provided trial functions having the appropriate para or ortho symmetry are used in the variational principle. Moreover, because the eigenfunctions belonging to states with different values of L are orthogonal, we can consider a separate variational problem for each value of L by using trial functions which exhibit the angular dependence corresponding to a state of given L. In this way we see that a minimum principle for the lowest energy state belonging to a given L and S will always be obtained without imposing further orthogonality constraints on the trial function. Hence, if we adopt trial functions ϕ having the correct para or ortho symmetry and the appropriate angular dependence, we may use directly the Rayleigh–Ritz method – that is, substitute the trial function ϕ in the functional [6.68] – to obtain upper bounds for the energies of the states 2^3S, 2^1P, 2^3P, 3^1D, 3^3D, and so on. On the other hand, when calculating the energy of the 2^1S state by the variational method, one must explicitly constrain the trial function to be orthogonal to the wave function of the ground state 1^1S. Similarly, the trial wave function for the 3^1S state must be made orthogonal to the wave functions of both the 1^1S and 2^1S state, the trial wave function for the 3^1P state has to be made orthogonal to the wave function of the 2^1P state, and so on. It should be noted from our discussion at the end of Section 2.8 (see [2.380]) that even after the orthogonalisations have been performed we do not necessarily have upper bounds for the energies of these excited states, since the wave functions of the lower states are only known approximately.

As an illustration of the foregoing analysis we shall consider the lowest four excited states of helium. We begin by studying the 2^3S, 2^1P and 2^3P states, which can be treated by the 'standard' Rayleigh–Ritz variational procedure, without imposing additional orthogonality conditions; we then go on to discuss the 2^1S state, whose wave function must explicitly be orthogonalised to the wave function of the ground state.

The 2^3S state

This is the lowest ortho (space-antisymmetric) state, corresponding to the configuration 1s2s. On the basis of the independent-particle model discussed in Section 6.4 and of our first-order perturbation theory calculation, it is reasonable to adopt for the spatial part of the wave function a simple trial function which is the antisymmetrised product of an 'inner' (1s) orbital u_{1s} corresponding to the 'effective charge' Z_i and an 'outer' (2s) orbital v_{2s} corresponding to the effective charge Z_0. That is

$$\phi_{2^3S}(r_1, r_2) = N[u_{1s}(r_1)v_{2s}(r_2) - v_{2s}(r_1)u_{1s}(r_2)] \qquad [6.108a]$$

where

$$\begin{aligned} u_{1s}(r) &= e^{-Z_i r} \\ v_{2s}(r) &= (1 - Z_0 r/2)e^{-Z_0 r/2} \end{aligned} \qquad [6.108b]$$

and N is a normalisation constant. Upon substituting [6.108] into the functional [6.68], and varying the variational parameters Z_i and Z_0 to obtain the minimum energy, Eckart found the values $Z_i = 2.01$ and $Z_0 = 1.53$, which yield the energy $E_{2^3S} = -2.167$ a.u. $(= -58.97$ eV).

Very accurate results for the energy of the 2^3S state may be obtained by using elaborate Hylleraas-type variational functions depending on the three variables (r_1, r_2, r_{12}) or the Hylleraas coordinates $s = r_1 + r_2$, $t = r_1 - r_2$ and $u = r_{12}$. Of course the trial wave function $\phi(s, t, u)$ must now be space-antisymmetric, and hence has to be an odd function of t. The 'exact' value obtained in this way by Hylleraas and Undheim and more recently by Pekeris *et al.* (using generalised Hylleraas-type wave functions) is $E^{ex}_{2^3S} = -2.175$ a.u. $(= -59.19$ eV). The agreement between the Eckart result and this 'exact' value is seen to be good, considering the simplicity of the trial function [6.108].

The 2^1P and 2^3P states

Since the 2^1P and 2^3P states are respectively the lowest para and ortho states corresponding to the configuration 1s2p, simple trial wave functions for these states may be written as

$$\phi_{2^{1,3}P}(\mathbf{r}_1, \mathbf{r}_2) = N_\pm[u_{1s}(r_1)v_{2pm}(\mathbf{r}_2) \pm v_{2pm}(\mathbf{r}_1)u_{1s}(r_2)] \qquad [6.109a]$$

where the plus sign refers to the 2^1P state, the minus signs to the 2^3P state, $N_\pm$

are normalisation constants, and

$$u_{1s}(r) = e^{-Z_i r}$$
$$v_{2pm}(\mathbf{r}) = re^{-Z_0 r/2} Y_{1,m}(\hat{\mathbf{r}}), \qquad m = 1, 0, -1 \qquad [6.109b]$$

the symbol $\hat{\mathbf{r}}$ denoting the angular variables of $\mathbf{r}$. Substituting the trial functions [6.109] into the functional [6.68] and varying the parameters Z_i and Z_0 to obtain a minimum for the energy, Eckart found for the 2^1P state the values $Z_i = 2.00$ and $Z_0 = 0.97$, giving the energy $E_{2^1P} = -2.123$ a.u. ($= -57.77$ eV), which is in excellent agreement with the 'exact' result $E^{ex}_{2^1P} = -2.124$ a.u. ($= -57.80$ eV) of Pekeris. For the 2^3P state Eckart obtained for the variational parameters the optimum values $Z_i = 1.99$ and $Z_0 = 1.09$, the corresponding energy being $E_{2^3P} = -2.131$ a.u. ($= -57.99$ eV), in very good agreement with the 'exact' result $E^{ex}_{2^3P} = -2.133$ a.u. ($= -58.04$ eV). It should be noted that for both the 2^1P and 2^3P states the value of Z_0 is much closer to $Z - 1 = 1$ (corresponding to complete screening) than for the 2^3S state which we have studied previously.

The 2^1S state

Since the 2^1S state is a para (space-symmetric) state corresponding to the configuration 1s2s, one could attempt to construct a simple trial wave function, similar to the 2^3S wave function [6.108], but which would be space-symmetric instead of space-antisymmetric. That is,

$$\phi_{2^1S}(r_1, r_2) = N[u_{1s}(r_1)v_{2s}(r_2) + v_{2s}(r_1)u_{1s}(r_2)] \qquad [6.110a]$$

where u_{1s} is again an 'inner' (1s) orbital, v_{2s} an 'outer' (2s) orbital and N a normalisation constant. However, a trial wave function of the form [6.110a] is not necessarily orthogonal to the wave function of the ground state 1^1S. As we pointed out above, this orthogonality constraint must therefore be imposed explicitly. A simple variational wave function of the form [6.110a], which does satisfy the requirement of being orthogonal to the ground state wave function [6.85], is such that the orbitals $u_{1s}(r)$ and $v_{2s}(r)$ are given by

$$u_{1s}(r) = e^{-2r}$$
$$v_{2s}(r) = e^{-\tau_1 r} - Cre^{-\tau_2 r} \qquad [6.110b]$$

where the 'optimum' variational parameters, obtained by Byron and Joachain are given by $\tau_1 = 0.865$, $\tau_2 = 0.522$ and $C = 0.432\,784$. The corresponding energy is $E_{2^1S} = -2.143$ a.u. ($= -58.31$ eV) which is close to the 'exact' result $E^{ex}_{2^1S} = -2.146$ a.u. ($= -58.40$ eV) obtained by Pekeris.

Another variational approach which may be applied to the study of the 2^1S state consists in using the Hylleraas–Undheim theorem (see Section 2.8). A trial function is first chosen, which has the symmetry of a ^1S state, and contains a number of variational parameters. According to the Hylleraas–Undheim theorem, the *second* root of the determinantal equation [2.387] then provides an

upper bound for the energy of the 2^1S state. In this way very accurate results for the energy of the 2^1S state, and also for other excited states of helium, have been obtained.

6.7 DOUBLY EXCITED STATES OF TWO-ELECTRON ATOMS. AUGER EFFECT (AUTOIONISATION). RESONANCES

In the language of the independent particle model introduced in Section 6.4, the 'genuinely discrete' excited states which we have studied in the preceding section all correspond to *singly* excited states, for which one electron occupies the ground state (1s) orbital and one occupies an excited orbital. However, we noticed in Section 6.4 (see [6.34]) that there exist also *doubly excited states* of the Hamiltonian [6.24], in which both electrons occupy excited orbitals (for example $2s^2$, 2s2p, 3p4d, etc.). We remarked that all these states lie *above* the ionisation threshold and are therefore *discrete states embedded in the continuum.*

Let us now study the action of the perturbation $H' = 1/r_{12}$ on a given doubly excited state $|\alpha\rangle$, having an 'unperturbed' energy $E_\alpha^{(0)}$ and a corresponding zero-order wave function $\psi_\alpha^{(0)}$. Because of the presence of *continuum* energy levels in the neighbourhood of $E_\alpha^{(0)}$, an eigenfunction of the full Hamiltonian H in this energy region is

$$\Psi(E) \simeq a(E)\psi_\alpha^{(0)} + \int b(E, E')\psi(E')\,\mathrm{d}E' \qquad [6.111]$$

where $\psi(E')$ is a properly symmetrised continuum wave function describing the system made of a *free* electron of kinetic energy E' and a one-electron atom (ion). It is clear that the perturbation H' will cause the discrete state $\psi_\alpha^{(0)}$ to interact with the nearby continuum states. Hence, in addition to an *energy shift* of the discrete state, a *radiationless transition* from the doubly excited state to a state of an *ionised* configuration will occur. Such a transition is known as the *Auger effect* or *autoionisation*, and the doubly excited states (which are unstable against ionisation) are called *autoionising states.* Direct application of the Fermi Golden Rule (see [2.359]) shows that, to first order of perturbation theory, the transition rate for autoionisation is given by

$$W = \frac{2\pi}{\hbar}\,|\langle\psi(E)|H'|\psi_\alpha^{(0)}\rangle|^2\rho_\mathrm{f}(E) \qquad [6.112]$$

where $\rho_\mathrm{f}(E)$ is the density of final states corresponding to the continuum wave function $\psi(E)$, and the kinetic energy E of the free electron is specified by energy conservation. Not only helium-like atoms (ions) but all atoms or ions with two or more electrons possess such autoionising states.

As an example, let us consider the $(2s2p)^1P$ state of helium, in which the two electrons form a singlet spin state in the configuration 2s2p. This state can be excited from the ground state $(1s)^2\ ^1S$ by the absorption of (ultra-violet) radiation, since the selection rules $\Delta L = \pm 1$ and $\Delta S = 0$[7] are satisfied. Once

[7] These selection rules will be proved in Chapter 8.

excited, the $(2s2p)^1P$ state can decay via *radiative transitions* to bound states of He allowed by the selection rules (that is, ^1D and ^1S states, including of course the ground state). However, it can also decay via a *radiationless* (*autoionising*) *transition* into a free electron and a He^+ ion in the ground state, the kinetic energy of the free electron being determined by conservation of energy. Explicit calculations show that the autoionising transition (Auger effect) is much more probable than a radiative transition to a He bound state, and this is also true for the other doubly excited states of helium. As a result, spectral lines of emission spectra corresponding to doubly excited states of helium are very weak.

The presence of autoionising states in the continuum spectrum of two-electron atoms has several important consequences. Firstly, these states will show up in the *absorption spectrum* of the system. For example, if one analyses the absorption spectrum of helium corresponding to the photoionisation process

$$h\nu + \mathrm{He}(1^1S) \rightarrow e^- + \mathrm{He}^+ \qquad [6.113]$$

one observes that sharp *peaks* or *resonances*, superimposed on the smooth continuum absorption, occur in the neighbourhood of the energy of autoionising states. This is illustrated in Fig. 6.9, which shows the resonances in the helium continuum absorption spectrum obtained by Madden and Codling, who used an electron synchrotron to obtain a continuous photon source in the wavelength region around 200 Å. For example, the large peak shown in Fig. 6.9 appears at the energy corresponding to the 2s2p level. In the vicinity of the energy of an autoionising state, which we denote by the symbol He** (doubly excited He state), the reaction [6.113] may thus be viewed as proceeding

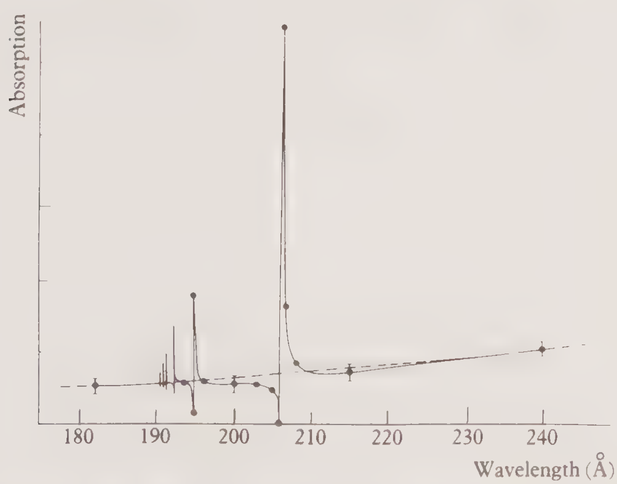

6.9 Resonances found in the continuous absorption spectrum of helium by R. B. Madden and K. Codling.

through the steps

$$h\nu + \mathrm{He}(1^1\mathrm{S}) \rightarrow \mathrm{He}^{\star\star} \rightarrow \mathrm{e}^- + \mathrm{He}^+ \qquad [6.114]$$

where the autoionising state $\mathrm{He}^{\star\star}$ corresponds to a temporarily bound or *resonant* state of the compound system $(\mathrm{e}^- + \mathrm{He}^+)$.

A second way in which the autoionising states of two electron atoms manifest themselves is in the *collisions of electrons* with the corresponding one-electron atom or ion. Consider for example the scattering of electrons by He^+ ions. If the incident electron has just the right kinetic energy, an autoionising state $\mathrm{He}^{\star\star}$ will be formed, and this compound state of the system $(\mathrm{e}^- + \mathrm{He}^+)$ will subsequently decay into a free electron and a He^+ ion. Thus the scattering event may be analysed in terms of the two-step process

$$\mathrm{e}^- + \mathrm{He}^+ \rightarrow \mathrm{He}^{\star\star} \rightarrow \mathrm{e}^- + \mathrm{He}^+ \qquad [6.115]$$

in which a resonant state of the $(\mathrm{e}^- + \mathrm{He}^+)$ system is temporarily obtained. As in the case of the absorption spectrum, a dramatic peak or *resonance* is then observed in the scattering cross-section. We shall return in Chapter 12 to the study of these resonances, which have become the subject of numerous investigations in recent years.

PROBLEMS

6.1 Prove that eigenfunctions $\psi(\mathbf{r}_1, \mathbf{r}_2)$ of the Schrödinger equation [6.3] corresponding to degenerate eigenvalues can always be chosen to be either space-symmetric $[\psi_+(\mathbf{r}_2, \mathbf{r}_1) = \psi_+(\mathbf{r}_1, \mathbf{r}_2)]$ or space-antisymmetric $[\psi_-(\mathbf{r}_2, \mathbf{r}_1) = -\psi_-(\mathbf{r}_1, \mathbf{r}_2)]$.

6.2 Study the action of the operator $\mathbf{S}^2 = 3/2 + 2\mathbf{S}_1 \cdot \mathbf{S}_2$ on the four spin functions [6.12] and obtain the results quoted in Table 6.1.

6.3 Calculate the average values of
(i) $r_1^2 + r_2^2$, (ii) $\delta(\mathbf{r}_1)$, (iii) $\delta(\mathbf{r}_{12})$
for the ground state of helium by using:
(a) the zero-order product of hydrogenic wave functions $\psi_0^{(0)}$ given by [6.35], with $Z = 2$;
(b) the simple 'screened' variational function given by [6.70], with $Z_e = 27/16$ (see [6.78]);
(c) the Hartree–Fock wave function [6.85].
Compare your results with the 'exact' values $\langle r_1^2 + r_2^2 \rangle = 2.39$, $\langle \delta(\mathbf{r}_1) \rangle = 1.81$ and $\langle \delta(\mathbf{r}_{12}) \rangle = 0.106$ (in a.u.).

6.4 Evaluate explicitly the Coulomb integral $\mathcal{J}_{nl}$ and the exchange integral K_{nl}, given respectively by [6.101] and [6.102] for the cases $n = 2$, $l = 0, 1$. Using [6.104], obtain the corresponding 'first-order' energy values for the energies of the 2^1S, 2^1P, 2^3S and 2^3P states of helium.

6.5 A helium atom is excited from the ground state to the autoionising state 2s4p by absorption of ultraviolet light. Assuming that the 2s electron

moves in the unscreened Coulomb field of the nucleus and the 4p electron in the fully screened Coulomb potential $-1/r$:

(a) Obtain the energy of this autoionising level and the corresponding wavelength of the ultraviolet radiation.

(b) Find the velocity of the electron emitted in the autoionising process in which the autoionising level 2s4p decays into a free electron and a He^+ ion in the ground state 1s.

7 Many-electron atoms

We have seen in the preceding chapter that Schrödinger's equation cannot be solved exactly for two-electron atoms or ions, so that approximation methods must be used. We also saw in Chapter 6 that very accurate results can be obtained for the energy levels and wave functions of helium-like atoms by performing variational calculations – such as those of the Rayleigh–Ritz type – in which elaborate trial functions containing a large number of variational parameters are used. Extended variational calculations of this kind have also been carried out for other light atoms (such as lithium, which contains three electrons) but this approach becomes increasingly tedious when the number of atomic electrons increases. We shall therefore develop in this chapter some general methods which, at the expense of simplifying assumptions, can be applied to study the structure of many-electron atoms and ions.

The starting point of all calculations on many-electron atoms is the *central field approximation*, which we have already discussed in the previous chapter for the case of two-electron atoms. The basic idea of this approximation is that each of the atomic electrons moves in an effective spherically symmetric potential $V(r)$ created by the nucleus and all the other electrons. We shall first discuss some general properties of this central potential, and show that a number of qualitative features of many-electron atoms – including the periodicity in the properties of the chemical elements – can be understood without a detailed knowledge of the form of this central field. Next, we turn to the problem of the determination of the potential $V(r)$, for which we first discuss the simple semi-classical method of Thomas and Fermi, and then the more precise Hartree–Fock or self-consistent field approach. We conclude this chapter by considering the corrections which must be applied to the central field approximation.

7.1 THE CENTRAL FIELD APPROXIMATION

Let us consider an atom or ion containing a nucleus of charge Ze and N electrons. A detailed treatment of this system should take into account:

1. The kinetic energy of the electrons and their potential energy in the electrostatic (Coulomb) attractive field of the nucleus (assumed to be point-like and infinitely massive).

2. The electrostatic (Coulomb) repulsion between the electrons.
3. The magnetic interactions of the electronic spins with their orbital motion (spin–orbit interactions).
4. Several small effects such as spin–spin interactions between the electrons, various relativistic effects, radiative corrections and nuclear corrections (due to the finite mass of the nucleus, its finite extension, nuclear magnetic dipole moments, etc.).

It is clear that such a detailed study of a many-electron atom is a very difficult task, in which approximations must be made. In what follows, we shall neglect all the 'small' effects mentioned in 4. The spin–orbit interactions (3 above) will be considered in Section 7.5 when we discuss the corrections to the central field approximation. Thus, keeping only the attractive Coulomb interactions between the electrons and the nucleus (which we assume to be infinitely heavy) and the Coulomb repulsions between the electrons, we write the Hamiltonian of the N-electron atom (ion) in the absence of external fields as

$$H = \sum_{i=1}^{N}\left(-\frac{\hbar^2}{2m}\nabla_{r_i}^2 - \frac{Ze^2}{(4\pi\varepsilon_0)r_i}\right) + \sum_{i<j-1}^{N}\frac{e^2}{(4\pi\varepsilon_0)r_{ij}} \qquad [7.1]$$

where $\mathbf{r}_i$ denotes the relative coordinate of the electron i with respect to the nucleus, $r_{ij} = |\mathbf{r}_i - \mathbf{r}_j|$ and the last summation is over all pairs of electrons. As in the previous chapter, it is convenient to use atomic units, so that the Hamiltonian [7.1] becomes

$$H = \sum_{i=1}^{N}\left(-\frac{1}{2}\nabla_{r_i}^2 - \frac{Z}{r_i}\right) + \sum_{i<j=1}^{N}\frac{1}{r_{ij}} \qquad [7.2]$$

and the Schrödinger equation for the N-electron atom wave function $\Psi(q_1, q_2, \dots q_N)$ reads

$$\left[\sum_{i=1}^{N}\left(-\frac{1}{2}\nabla_{r_i}^2 - \frac{Z}{r_i}\right) + \sum_{i<j=1}^{N}\frac{1}{r_{ij}}\right]\Psi(q_1, q_2, \dots q_N) = E\Psi(q_1, q_2, \dots q_N) \qquad [7.3]$$

where q_i denotes the ensemble of the (continuous) spatial coordinates $\mathbf{r}_i$ and (discrete) spin coordinates of electron i.

Since we are dealing with a system containing N indistinguishable particles, its Hamiltonian must be invariant under an interchange of the coordinates (spatial and spin) of any two particles. This is clearly the case for the Hamiltonian [7.2], which is independent of the spins of the electrons, and is symmetric in their spatial variables. Moreover, because electrons have spin 1/2 and hence are fermions, the *Pauli exclusion principle* requires that *the total wave function* $\Psi(q_1, q_2, \dots q_N)$ *be completely antisymmetric*, i.e. changes sign if the coordinates (spatial and spin) of any two electrons are interchanged.

The Hamiltonian [7.2] being independent of the spin of the electrons, the eigenfunction Ψ can be separated into a spatial part $\psi(\mathbf{r}_1, \mathbf{r}_2, \dots \mathbf{r}_N)$ and a spin

part $\chi(1, 2, \ldots N)$, as we did in Chapter 6 for the special case $N = 2$. Thus we may write

$$\Psi(q_1, q_2, \ldots q_N) = \psi(\mathbf{r}_1, \mathbf{r}_2, \ldots \mathbf{r}_N)\chi(1, 2, \ldots N) \qquad [7.4]$$

where the spatial part of the wave function satisfies the Schrödinger equation

$$\left[\sum_{i=1}^{N}\left(-\frac{1}{2}\nabla^2_{r_i} - \frac{Z}{r_i}\right) + \sum_{i<j=1}^{N}\frac{1}{r_{ij}}\right]\psi(\mathbf{r}_1, \mathbf{r}_2, \ldots \mathbf{r}_N) = E\psi(\mathbf{r}_1, \mathbf{r}_2, \ldots \mathbf{r}_N) \qquad [7.5]$$

We see that this equation is a partial differential equation in $3N$ dimensions involving the coordinates $\mathbf{r}_1, \mathbf{r}_2, \ldots \mathbf{r}_N$ of the electrons. Because of the presence of the terms $1/r_{ij}$, which express the mutual repulsion of the electrons, this equation is not separable. We have already encountered this situation in our study of helium-like atoms. However, in contrast to the case of two-electron atoms, where the term $1/r_{12}$ can be treated by perturbation theory, the term $\Sigma_{i<j}\, 1/r_{ij}$ which appears in [7.5] is in general too large to be treated as a perturbation. Indeed, even though for a fairly large value of Z any one of the terms $1/r_{ij}$ is small compared to Z/r_i, there are many $1/r_{ij}$ terms, and their total effect may become of the same size as that of the interaction between the electron i and the nucleus. Thus, if we want to apply perturbation theory in a meaningful way to the present problem, we must define a new 'unperturbed' Hamiltonian which is not just the sum of hydrogenic Hamiltonians $\Sigma_i(-(1/2)\nabla^2_{r_i} - Z/r_i)$, but which includes, at least approximately, the mutual repulsion between the electrons. On the other hand this unperturbed Hamiltonian should be sufficiently simple so that the corresponding Schrödinger equation is tractable.

The answer to this problem, proposed by Hartree and by Slater, is to use as our starting point the *central field approximation*. This approximation is based on an *independent particle model*, in which each electron moves in an *effective potential* which represents the attraction of the nucleus and the *average* effect of the repulsive interactions between this electron and the $(N - 1)$ other electrons. Moreover, since the overall effect of the $(N - 1)$ other electrons is to *screen* the central Coulomb attraction between an electron and the nucleus, it is clear that the inter-electron repulsion term $\Sigma_{i<j}\, 1/r_{ij}$ contains a large spherically symmetric component, which we shall write as $\Sigma_i S(r_i)$. A good approximation to the effective potential energy of an electron is therefore provided by a spherically symmetric potential $V(r)$ such that

$$V(r) = -\frac{Z}{r} + S(r) \qquad [7.6]$$

We may readily obtain the form of $V(r)$ at large and small distances. Indeed, let us first consider an electron i whose distance r_i from the nucleus is large compared to the distances r_j associated with the $(N - 1)$ other electrons. In this case we have $r_{ij} \simeq r_i$ and $1/r_{ij} \simeq 1/r_i$ so that the electron i moves in a potential

given approximately by

$$-\frac{Z}{r_i} + \sum_{j=1}^{N-1} \frac{1}{r_i} = -\frac{Z-N+1}{r_i} \qquad [7.7]$$

which corresponds to the Coulomb field of the nucleus, screened by the $(N - 1)$ other electrons. As the distance r_i diminishes, this screening effect becomes less pronounced. In fact, when the electron i is near the nucleus, so that $r_{ij} \simeq r_j$, the potential felt by this electron is given approximately by

$$-\frac{Z}{r_i} + \left\langle \sum_{j=1}^{N-1} \frac{1}{r_j} \right\rangle = -\frac{Z}{r_i} + C \qquad [7.8]$$

where the symbol $\langle\rangle$ denotes an average over the distances of the $(N - 1)$ other electrons, and C is a constant. Thus we see that in the limit $r_i \to 0$ the effective potential acting on the electron i is just the unscreened Coulomb potential $(-Z/r_i)$ due to the nucleus. We shall therefore require that the effective central potential $V(r)$ be such that

$$V(r) \to -\frac{Z}{r}, \qquad r \to 0 \qquad [7.9a]$$

$$V(r) \to -\frac{Z-N+1}{r}, \qquad r \to \infty \qquad [7.9b]$$

In particular, for a neutral atom (such that $Z = N$), we have

$$V(r) \to -\frac{1}{r}, \qquad r \to \infty \qquad [7.9c]$$

The determination of the effective potential at intermediate distances is a much more difficult problem, to which we shall return in Sections 7.3 and 7.4 where we discuss the Thomas–Fermi and Hartree–Fock methods, respectively. At this point, however, it is important to realise that for intermediate values of r the potential $V(r)$ – which represents the attraction of the nucleus plus the average repulsion of the other electrons – must depend on the details of the charge distribution of the electrons, or in other words on the dynamical state of the electrons. As a result, *the same effective potential $V(r)$ cannot account for the full spectrum of a complex atom (ion)*. However, if we restrict our attention to the ground state and the first excited states, it is reasonable to assume that a fixed central potential $V(r)$ can be used as a starting point. In fact, we shall see below that many important features concerning the structure of complex atoms or ions can be obtained by using only the information contained in equations [7.9], without a detailed knowledge of the central potential $V(r)$.

Let us now return to the Hamiltonian [7.2]. From the foregoing discussion it is clear that a meaningful separation of H into an unperturbed part and a perturbation may be achieved by writing

$$H = H_c + H_1 \qquad [7.10]$$

where

$$H_c = \sum_{i=1}^{N} \left(-\frac{1}{2} \nabla_{r_i}^2 + V(r_i) \right)$$
$$= \sum_{i=1}^{N} h_i, \qquad h_i = -\frac{1}{2} \nabla_{r_i}^2 + V(r_i) \qquad [7.11]$$

is the Hamiltonian corresponding to the central field approximation, and

$$H_1 = \sum_{i<j=1}^{N} \frac{1}{r_{ij}} - \sum_i \left(\frac{Z}{r_i} + V(r_i) \right)$$
$$= \sum_{i<j=1}^{N} \frac{1}{r_{ij}} - \sum_i S(r_i) \qquad [7.12]$$

is the remaining part of the full Hamiltonian [7.2] containing the remaining spherical and all the non-spherical part of the electronic repulsion. All we have done, of course, is to add and subtract the expression $\Sigma_i V(r_i)$ in [7.2], but the perturbation H_1 defined by [7.12] is now much smaller than the term $\Sigma_{i<j} 1/r_{ij}$ representing the full mutual repulsion between the electrons.

We shall therefore begin by neglecting the perturbation H_1 and concentrate our attention on the central field Hamiltonian H_c which, as seen from [7.6] and [7.10], contains the kinetic energy, the potential energy in the field of the nucleus, and the average (spherical) electron repulsion energy. The corresponding Schrödinger equation for the spatial part of the N-electron central field wave function $\psi_c(\mathbf{r}_1, \mathbf{r}_2, \ldots \mathbf{r}_N)$ then reads

$$H_c\psi_c = \sum_{i=1}^{N} \left[-\frac{1}{2} \nabla_{r_i}^2 + V(r_i) \right] \psi_c = E_c\psi_c \qquad [7.13]$$

and is separable into N equations, one for each electron. A solution of [7.13] may therefore be written as

$$\psi_c = u_{a_1}(\mathbf{r}_1) u_{a_2}(\mathbf{r}_2) \cdots u_{a_N}(\mathbf{r}_N) \qquad [7.14]$$

where the (normalised) individual electron orbitals $u_{a_1}(\mathbf{r}_1)$, $u_{a_2}(\mathbf{r}_2) \ldots$ are solutions of an equation having the form

$$[-\tfrac{1}{2} \nabla_r^2 + V(r)] u_{nlm_l}(\mathbf{r}) = E_{nl} u_{nlm_l}(\mathbf{r}) \qquad [7.15]$$

and the symbol a_i in [7.14] refers to the three quantum numbers $(n_i l_i m_{l_i})$ of electron i.

With the substitution $m_l \to m$, the equation [7.15] is identical to [6.48], which we already discussed in our study of two-electron atoms. Since the potential $V(r)$ is central, the one-electron or *central field orbitals* $u_{nlm_l}(\mathbf{r})$ are products of radial functions times spherical harmonics,

$$u_{nlm_l}(\mathbf{r}) = R_{nl}(r) Y_{lm_l}(\theta, \phi) \qquad [7.16]$$

where the radial functions satisfy the equation

$$-\frac{1}{2}\left(\frac{\mathrm{d}^2}{\mathrm{d}r^2}+\frac{2}{r}\frac{\mathrm{d}}{\mathrm{d}r}-\frac{l(l+1)}{r^2}\right)R_{nl}(r)+V(r)R_{nl}(r)=E_{nl}R_{nl}(r) \quad [7.17]$$

We recall that the principal quantum number n is defined to be $n = n_r + l + 1$, where n_r is the number of nodes of the radial function. The quantum numbers n, l and m_l can therefore take the values

$$\begin{aligned} n &= 1, 2, \ldots \\ l &= 0, 1, 2, \ldots n-1 \\ m_l &= -l, -l+1, \ldots +l \end{aligned} \quad [7.18]$$

As we already noted in connection with [6.48], the central field orbitals $u_{nlm}(\mathbf{r})$ should not be confused with the hydrogenic wave functions $\psi_{nlm}(\mathbf{r})$ of Chapter 3, since the radial functions $R_{nl}(r)$, solutions of [7.17] differ from the hydrogenic radial functions [3.53], which correspond to the particular choice $V(r) = -Z/r$.

Because the potential $V(r)$ in [7.15] is spherically symmetric, the energy eigenvalues E_{nl} do not depend on the quantum number m_l. However, in contrast to the hydrogenic case, the individual electron energies depend on both n and l. The total energy E_c in the central field approximation is of course the sum of the individual electron energies, namely

$$E_c = \sum_{i=1}^{N} E_{n_i l_i} \quad [7.19]$$

As in the case of two-electron atoms discussed in Chapter 6, we note that there is *exchange degeneracy*, since any spatial wave function obtained from [7.14] by a permutation of the electron coordinates is an equally good solution of [7.13] corresponding to the same energy [7.19].

Spin, the Pauli exclusion principle and Slater determinants

So far we have not introduced the spin of the electrons into our central field model. This is readily done by multiplying the one-electron spatial orbitals $u_{nlm_l}(\mathbf{r})$ by a spin-1/2 eigenfunction $\chi_{1/2,m_s}$, thus forming the (normalised) *spin orbitals*

$$\begin{aligned} u_{nlm_lm_s}(q) &= u_{nlm_l}(\mathbf{r})\chi_{1/2,m_s} \\ &= R_{nl}(r)Y_{lm_l}(\theta, \phi)\chi_{1/2,m_s} \end{aligned} \quad [7.20]$$

characterised by the *four* quantum numbers n, l, m_l and m_s. The three 'spatial' quantum numbers n, l and m_l can take the values given in [7.18], while the spin quantum number m_s is such that $m_s = \pm 1/2$. It is clear that the spin orbitals [7.20] satisfy the equations

$$[-\tfrac{1}{2}\nabla_r^2 + V(r)]u_{nlm_lm_s} = E_{nl}u_{nlm_lm_s} \quad [7.21]$$

Since the energy E_{nl} does not depend on the quantum numbers m_l and m_s, we see that each individual electron energy level is $2(2l + 1)$ times degenerate.

Our next task is to built up out of single-electron spin orbitals a total N-electron (central field) wave function $\Psi_c(q_1, q_2, \ldots q_N)$ which is antisymmetric in the (spatial and spin) coordinates of any two electrons, in order to satisfy the requirements of the *Pauli exclusion principle*. This may be accomplished in a simple way as follows. Let us designate the four quantum numbers (n, l, m_l, m_s) corresponding to given independent particle states in the atom by the single letters $\alpha, \beta, \ldots \nu$. The total wave function Ψ_c describing an atom in which one electron is in state α, another in state β, and so on may then be written as a $N \times N$ determinant,

$$\Psi_c(q_1, q_2, \ldots q_N) = \frac{1}{\sqrt{N!}} \begin{vmatrix} u_\alpha(q_1) & u_\beta(q_1) \cdots & u_\nu(q_1) \\ u_\alpha(q_2) & u_\beta(q_2) \cdots & u_\nu(q_2) \\ \vdots & & \\ u_\alpha(q_N) & u_\beta(q_N) \cdots & u_\nu(q_N) \end{vmatrix} \qquad [7.22]$$

which is known as a *Slater determinant*. This wave function is obviously antisymmetric because if we interchange the (spatial and spin) coordinates of two electrons (say q_1 and q_2) this is equivalent to interchanging two rows, so that the determinant changes sign. The eigenvalue E_c of the central field Hamiltonian H_c corresponding to a given Slater determinant is just the sum [7.19] of the energies of the N individual states which are present in the determinant.

We note that since a determinant vanishes when two columns (or rows) are equal, the Slater determinant [7.22] will vanish if two electrons have the same values of the four quantum numbers n, l, m_l and m_s. Within the framework of the independent-particle model, we may therefore state the exclusion principle in the form originally discovered by Pauli in 1925, namely that *no two electrons in an atom can have the same set of four quantum numbers*.

The $(N!)^{-1/2}$ factor appearing in [7.22] is a normalisation factor, arising from the fact that there are $N!$ permutations of the electron coordinates $q_1, q_2, \ldots q_N$. If we denote by P a permutation of the electron coordinates, we may rewrite the Slater determinant [7.22] as

$$\Psi_c(q_1, q_2, \ldots q_N) = \frac{1}{\sqrt{N!}} \sum_P (-1)^P P u_\alpha(q_1) u_\beta(q_2) \cdots u_\nu(q_N) \qquad [7.23]$$

where the symbol $(-1)^P$ is equal to $+1$ when P is an even permutation and to -1 when P is an odd permutation [1], and the sum is over all permutations P.

Let us now investigate the behaviour of the Slater determinant [7.22] under the inversion transformation $\mathbf{r}_i \to -\mathbf{r}_i$. Since a spin orbital [7.20] has parity $(-1)^l$, the Slater determinant has the well-defined parity

$$(-1)^{l_1}(-1)^{l_2} \cdots (-1)^{l_N} = (-1)^{\Sigma_i l_i} \qquad [7.24]$$

[1] We recall that a permutation P is said to be even or odd depending on whether the number of interchanges leading to it is even or odd.

and will therefore be even or odd under the inversion transformation, depending on whether the sum of the orbital angular momentum quantum numbers of the electrons, $\Sigma_i l_i$, is even or odd.

As a simple example, let us consider the ground state $(1s)^2\ {}^1S$ of helium. The spin orbitals for the two electrons are then given by

$$u_{100,1/2} = u_{100}(r)\chi_{1/2,1/2} = u_{100}(r)\alpha \quad \text{for} \quad m_s = +1/2 \qquad [7.25a]$$

and

$$u_{100,-1/2} = u_{100}(r)\chi_{1/2,-1/2} = u_{100}(r)\beta \quad \text{for} \quad m_s = -1/2 \qquad [7.25b]$$

where α and β are the spin functions defined by [2.209], and the orbital $u_{100}(r)$ is that introduced in Section 6.4. According to [7.22], the two-electron wave function $\Psi_c(q_1, q_2)$ describing the helium ground state in the central field approximation is

$$\Psi_c(q_1, q_2) = \frac{1}{\sqrt{2}}\begin{vmatrix} u_{100}(r_1)\alpha(1) & u_{100}(r_1)\beta(1) \\ u_{100}(r_2)\alpha(2) & u_{100}(r_2)\beta(2) \end{vmatrix}$$

$$= u_{100}(r_1)u_{100}(r_2)\frac{1}{\sqrt{2}}[\alpha(1)\beta(2) - \alpha(2)\beta(1)] \qquad [7.26]$$

in accordance with the results obtained in Chapter 6.

It is a simple matter to verify (Problem 7.1) that the central field Hamiltonian H_c commutes with both the total orbital angular momentum operator $\mathbf{L}$ and the total spin operator $\mathbf{S}$. That is,

$$[H_c, \mathbf{L}] = 0 \qquad [7.27a]$$

$$[H_c, \mathbf{S}] = 0 \qquad [7.27b]$$

where

$$\mathbf{L} = \sum_{i=1}^{N} \mathbf{L}_i \qquad [7.28a]$$

$$\mathbf{S} = \sum_{i=1}^{N} \mathbf{S}_i \qquad [7.28b]$$

Here $\mathbf{L}_i$ and $\mathbf{S}_i$ denote respectively the orbital angular momentum and the spin operator of the ith electron. As a consequence, it is possible to obtain eigenfunctions of H_c which are also eigenfunctions of the operators $\mathbf{L}^2$, $\mathbf{S}^2$, L_z and S_z, with eigenvalues given respectively by $L(L+1)\hbar^2$, $S(S+1)\hbar^2$, $M_L\hbar$ and $M_S\hbar$ ($\hbar = 1$ in a.u.). Such eigenfunctions will be denoted by $|\alpha LSM_LM_S\rangle$, where α is an index representing additional information (such as the radial part of the wave function, the parity, etc.). It is precisely this 'coupled representation' L, S, M_L, M_S which we used in Chapter 6 to discuss the two-electron problem. Now, in obtaining the Slater determinant [7.22] we used spin-orbitals $u_{nlm_lm_s}$ expressed in the n, l, m_l, m_s representation. As a result, a Slater determinant [7.22] is an eigenfunction of the operators L_z and S_z, but not

necessarily of $\mathbf{L}^2$ and $\mathbf{S}^2$, and we must in general construct *linear combinations of Slater determinants* to obtain an eigenfunction of $\mathbf{L}^2$, $\mathbf{S}^2$, L_z and S_z (see Problem 7.2). The helium ground state considered above is a simple case (with $L = S = 0$) for which a single Slater determinant is an eigenfunction of all four operators $\mathbf{L}^2$, $\mathbf{S}^2$, L_z and S_z.

Electron states in a central field. Configurations, shells and subshells

We have shown that within the framework of the central field approximation the energy levels E_c of an atom (ion) having N electrons are given by summing the individual electron energies E_{nl}, while the N-electron wave functions $\Psi_c(q_1, q_2, \ldots q_N)$ are obtained by forming Slater determinants (or linear combinations of them) with the individual spin orbitals $u_{nlm_lm_s}$. The problem of finding the eigenvalues and eigenfunctions of the central field Hamiltonian H_c is therefore reduced to the determination of the individual energy levels E_{nl} and the spin orbitals [7.20]. Since the spherical harmonics $Y_{l,m_l}(\theta, \phi)$ and the spin eigenfunctions $\chi_{1/2,m_s}$ are known, this problem in turn comes down to solving the radial equation [7.17] for an attractive potential $V(r)$ satisfying the conditions [7.9].

The order of the energy levels E_{nl} does not depend in a crucial way on the detailed form of the potential $V(r)$. If $V(r)$ were simply the Coulomb field $-Z/r$ of the nucleus, all the levels $l = 0, 1, \ldots n - 1$ corresponding to a given value of n would coincide. The screening due to the other electrons results in a raising of the energy levels, this effect being more pronounced as n and l increase, since in this case the orbitals are concentrated at larger values of r. Thus, for a fixed value of l the energy E_{nl} is an increasing function of n and for a given value of n it is an increasing function of l (the orbitals with larger l values being 'forced' out by the centrifugal barrier). If we restrict our attention to the ground and lowest excited states, the order of succession of the individual energy levels E_{nl} (which can be inferred from spectroscopic evidence) is nearly the same for all atoms, and is given in Table 7.1. It is worth noting that this sequence is different from that in hydrogen, where the energy levels depend only on n, and $E_{n+1} > E_n$. For example the 4s state, which has a higher energy than the 3d state in hydrogen, is depressed because of its low angular momentum, which causes this orbital to be large at small r, where it can feel the full nuclear attraction. We also see that as a rule the individual electron energy E_{nl} is an increasing function of the sum $n + l$.

In the central field approximation, the total energy [7.19] of the atom depends only on the number of electrons occupying each of the individual energy levels E_{nl}. Therefore, as we already noted in Section 6.4 for the particular case of two-electron atoms, this total energy is entirely determined by the *electron configuration*, that is by the distribution of the electrons with respect to the quantum numbers n and l. Thus the assignment of an electron configuration requires the enumeration of the values of n and l for all the electrons of the atom. We recall that in the usual spectroscopic notation the value of n is given as a

Table 7.1 The ordering of the individual energy levels E_{nl}. The energy increases from bottom to top, the brackets enclosing levels which have so nearly the same energy that their order can vary from one atom to another. Also given is the spectroscopic notation for the subshell (nl) and the maximum number $2(2l + 1)$ of the electrons allowed in a subshell

Quantum numbers n, l	*Spectroscopic notation for subshell* (nl)	*Maximum number of electrons allowed in the subshell* $= 2(2l + 1)$
⎡6,2	⎡6d	10
⎢5,3	⎢5f	14
⎣7,0	⎣7s	2
6,1	6p	6
⎡5,2	⎡5d	10
⎢4,3	⎢4f	14
⎣6,0	⎣6s	2
5,1	5p	6
⎡4,2	⎡4d	10
⎣5,0	⎣5s	2
4,1	4p	6
⎡3,2	⎡3d	10
⎣4,0	⎣4s	2
3,1	3p	6
3,0	3s	2
2,1	2p	6
2,0	2s	2
1,0	1s	2

number, that of l as a letter (s for $l = 0$, p for $l = 1$, and so on) and the number of electrons having given values of n and l as a numerical superscript (for example $(2s)^2$ or $2s^2$, $(3p)^4$ or $3p^4$, etc.).

Electrons having the same value of n and l are said to belong to the same *subshell* [2]. According to our foregoing discussion, there are $2(2l + 1)$ states having the same value of n and l but different values of m_l and m_s. Such states are called equivalent. In spectroscopic jargon the electrons having the same value of n and l (i.e. belonging to the same subshell) are known as *equivalent electrons*. Because of the Pauli exclusion principle there cannot be more than one electron in each individual state labelled by the quantum numbers (nlm_lm_s). Thus the maximum number of electrons in a subshell is $2(2l + 1)$, so that

For $l = 0$ (s electrons) this maximum number is 2
$l = 1$ (p electrons) this maximum number is 6
$l = 2$ (d electrons) this maximum number is 10
$l = 3$ (f electrons) this maximum number is 14
$l = 4$ (g electrons) this maximum number is 18
$l = 5$ (h electrons) this maximum number is 22

[2] Some authors use the word 'shell' (instead of 'subshell') to characterise electrons having the same values of n and l. We shall reserve the word 'shell' for electrons having only the same value of n, the principal quantum number.

In addition to the ordering of the energy levels E_{nl}, Table 7.1 also gives the spectroscopic notation of the corresponding subshells, and the maximum number of electrons allowed in each subshell. An assembly of $2(2l + 1)$ equivalent electrons is called a *closed* (or filled) *subshell.*

Electrons which have the same value of the principal quantum number n are said to belong to the same *shell.* Following a notation introduced in Chapter 1 for the hydrogenic atoms, and commonly used in discussing X-ray spectra of complex atoms, the value of the principal quantum number n is sometimes specified by a capital letter according to the correspondence

Value of n	1	2	3	4	5	6
	$\updownarrow$	$\updownarrow$	$\updownarrow$	$\updownarrow$	$\updownarrow$	$\updownarrow$
Code letter	K	L	M	N	O	P

The maximum number of electrons in a shell is $2n^2$, in which case we have a *closed* (or filled) *shell.*

Degeneracies

Since the assignment of an electron configuration requires only the enumeration of the values of n and l for all electrons, but not those of m_l and m_s, a given degeneracy g will be attached to a configuration. Let ν_i be the number of electrons occupying a given individual level $E_{n_i l_i}$ and $\delta_i = 2(2l_i + 1)$ be the degeneracy of that level. There are

$$d_i = \frac{\delta_i!}{\nu_i!(\delta_i - \nu_i)!} \qquad [7.29]$$

ways of distributing the ν_i electrons among the δ_i individual states corresponding to the level $E_{n_i l_i}$, and we note that $d_i = 1$ for a closed subshell (such that $\nu_i = \delta_i$). The *total* degeneracy or statistical weight g of the configuration is then obtained by forming the product of d_i with the degeneracies corresponding to the electrons of the other subshells.

As an example, let us consider the ground state of the carbon atom, which has the configuration $1s^2 2s^2 2p^2$. In this case:

for the two 1s electrons: $\nu = 2, \quad \delta = 2, \quad d = 1$

for the two 2s electrons: $\nu = 2, \quad \delta = 2, \quad d = 1$

for the two 2p electrons: $\nu = 2, \quad \delta = 6, \quad d = 15$

and the total degeneracy of the ground state configuration of carbon is $g = 15$.

7.2 THE PERIODIC SYSTEM OF THE ELEMENTS

We are now equipped with all the necessary information to discuss the electronic structure and the 'building up' (*aufbau*) of atoms. For the sake of simplicity we shall only consider the *ground state* of *neutral* atoms. The Z

electrons of an atom of atomic number (nuclear charge) Z then occupy the lowest individual energy levels in accordance with the requirements of the Pauli exclusion principle discussed above; the ordering of the individual levels is that displayed in Table 7.1. The *ground state configuration* of an atom is therefore obtained by distributing the Z electrons among a certain number f of subshells, the first $(f - 1)$ subshells being filled and the last one – corresponding to the highest energy – generally not, except for particular values of Z (2, 4, 10, 12, 18, etc.). The least tightly bound electrons, which are in the subshell of highest energy, and in insufficient numbers to form another closed subshell, are called *valence* electrons. In going from one atom having atomic number Z to the next one, with atomic number $Z + 1$, the number of electrons increases by one, the $(Z + 1)$ electrons occupying the lowest energy levels allowed by the exclusion principle. In this way the subshells are progressively filled. This is illustrated in Table 7.2 which gives the electron configuration of the ground state of neutral atoms. Also given in Table 7.2 are the ionisation potential and the ground term, the latter being written according to the Russell–Saunders notation

$$^{2S+1}L_{\mathcal{J}}$$

where $\mathcal{J}$ is the total angular momentum quantum number and the code letters S, P, D, . . . correspond to the values $L = 0, 1, 2, \ldots$ as described in Chapter 6. We shall return in detail in Section 7.5 to the assignment of the term values.

The table begins with hydrogen, which has the ground state configuration 1s. The ionisation potential, as we have learned in Chapter 3, is 13.6 eV and the ground term value is clearly $^2S_{1/2}$, since we have $L(=l) = 0$, $S(=s) = 1/2$ and $\mathcal{J}(=j) = 1/2$.

The next element, helium, has the ground state configuration $1s^2$ and was studied in detail in Chapter 6. Since $L = 0$ and $S = 0$ in this case, the ground term value is $^1S_0$. We see by looking at Table 7.2 that helium has the largest ionisation potential (24.59 eV). We also note that the two electrons of helium fill the K shell $(n = 1)$.

The third element, lithium, has the ground state configuration $1s^22s$ (abbreviated as [He]2s in the table) because the configuration $1s^3$ is forbidden by the exclusion principle. The ground term value of lithium is $^2S_{1/2}$, since we have one electron outside a closed shell. If the screening of the nuclear charge by the two inner 1s electrons were perfect, the outer electron would feel an effective charge $Z_e = 1$, the corresponding ionisation potential being then $13.6/4 = 3.4$ eV. In fact the screening is not perfect and, as a result, the ionisation potential is somewhat larger, being 5.39 eV.

With the next element, beryllium $(Z = 4)$ the 2s subshell is filled and the ground state configuration is $1s^22s^2$. Since we have a closed subshell as in helium, the ground term is $^1S_0$. The ionisation potential (9.32 eV) is larger than for lithium, because of the increase of the nuclear charge.

The 2p subshell becomes progressively filled beginning with boron $(Z = 5$, ground state configuration $1s^22s^22p)$ up to neon $(Z = 10$, ground state

Table 7.2 Electronic configuration, term value and ionisation potential of the atoms in their ground state

Z	*Element*		*Electronic configuration*†	*Term*†	*Ionisation potential* (eV)
1	H	hydrogen	1s	$^2S_{1/2}$	13.60
2	He	helium	$1s^2$	$^1S_0$	24.59
3	Li	lithium	[He]2s	$^2S_{1/2}$	5.39
4	Be	beryllium	[He]$2s^2$	$^1S_0$	9.32
5	B	boron	[He]$2s^22p$	$^2P_{1/2}$	8.30
6	C	carbon	[He]$2s^22p^2$	$^3P_0$	11.26
7	N	nitrogen	[He]$2s^22p^3$	$^4S_{3/2}$	14.53
8	O	oxygen	[He]$2s^22p^4$	$^3P_2$	13.62
9	F	fluorine	[He]$2s^22p^5$	$^2P_{3/2}$	17.42
10	Ne	neon	[He]$2s^22p^6$	$^1S_0$	21.56
11	Na	sodium	[Ne]3s	$^2S_{1/2}$	5.14
12	Mg	magnesium	[Ne]$3s^2$	$^1S_0$	7.65
13	Al	aluminium	[Ne]$3s^23p$	$^2P_{1/2}$	5.99
14	Si	silicon	[Ne]$3s^23p^2$	$^3P_0$	8.15
15	P	phosphorus	[Ne]$3s^23p^3$	$^4S_{3/2}$	10.49
16	S	sulphur	[Ne]$3s^23p^4$	$^3P_2$	10.36
17	Cl	chlorine	[Ne]$3s^23p^5$	$^2P_{3/2}$	12.97
18	Ar	argon	[Ne]$3s^23p^6$	$^1S_0$	15.76
19	K	potassium	[Ar]4s	$^2S_{1/2}$	4.34
20	Ca	calcium	[Ar]$4s^2$	$^1S_0$	6.11
21	Sc	scandium	[Ar]$4s^23d$	$^2D_{3/2}$	6.54
22	Ti	titanium	[Ar]$4s^23d^2$	$^3F_2$	6.82
23	V	vanadium	[Ar]$4s^23d^3$	$^4F_{3/2}$	6.74
24	Cr	chromium	[Ar]$4s3d^5$	$^7S_3$	6.77
25	Mn	manganese	[Ar]$4s^23d^5$	$^6S_{5/2}$	7.44
26	Fe	iron	[Ar]$4s^23d^6$	$^5D_4$	7.87
27	Co	cobalt	[Ar]$4s^23d^7$	$^4F_{9/2}$	7.86
28	Ni	nickel	[Ar]$4s^23d^8$	$^3F_4$	7.64
29	Cu	copper	[Ar]$4s3d^{10}$	$^2S_{1/2}$	7.73
30	Zn	zinc	[Ar]$4s^23d^{10}$	$^1S_0$	9.39
31	Ga	gallium	[Ar]$4s^23d^{10}4p$	$^2P_{1/2}$	6.00
32	Ge	germanium	[Ar]$4s^23d^{10}4p^2$	$^3P_0$	7.90
33	As	arsenic	[Ar]$4s^23d^{10}4p^3$	$^4S_{3/2}$	9.81
34	Se	selenium	[Ar]$4s^23d^{10}4p^4$	$^3P_2$	9.75
35	Br	bromine	[Ar]$4s^23d^{10}4p^5$	$^2P_{3/2}$	11.81
36	Kr	krypton	[Ar]$4s^23d^{10}4p^6$	$^1S_0$	14.00
37	Rb	rubidium	[Kr]5s	$^2S_{1/2}$	4.18
38	Sr	strontium	[Kr]$5s^2$	$^1S_0$	5.70
39	Y	yttrium	[Kr]$5s^24d$	$^2D_{3/2}$	6.38
40	Zr	zirconium	[Kr]$5s^24d^2$	$^3F_2$	6.84
41	Nb	niobium	[Kr]$5s4d^4$	$^6D_{1/2}$	6.88
42	Mo	molybdenum	[Kr]$5s4d^5$	$^7S_3$	7.10
43	Tc	technetium	[Kr]$5s^24d^5$	$^6S_{5/2}$	7.28
44	Ru	ruthenium	[Kr]$5s4d^7$	$^5F_5$	7.37
45	Rh	rhodium	[Kr]$5s4d^8$	$^4F_{9/2}$	7.46
46	Pd	palladium	[Kr]$4d^{10}$	$^1S_0$	8.34
47	Ag	silver	[Kr]$5s4d^{10}$	$^2S_{1/2}$	7.58
48	Cd	cadmium	[Kr]$5s^24d^{10}$	$^1S_0$	8.99
49	In	indium	[Kr]$5s^24d^{10}5p$	$^2P_{1/2}$	5.79
50	Sn	tin	[Kr]$5s^24d^{10}5p^2$	$^3P_0$	7.34
51	Sb	antimony	[Kr]$5s^24d^{10}5p^3$	$^4S_{3/2}$	8.64

Table 7.2(Cont.)

Z	*Element*		*Electronic configuration*†	*Term*†	*Ionisation potential* (eV)
52	Te	tellurium	$[Kr]5s^24d^{10}5p^4$	$^3P_2$	9.01
53	I	iodine	$[Kr]5s^24d^{10}5p^5$	$^2P_{3/2}$	10.45
54	Xe	xenon	$[Kr]5s^24d^{10}5p^6$	$^1S_0$	12.13
55	Cs	cesium	$[Xe]6s$	$^2S_{1/2}$	3.89
56	Ba	barium	$[Xe]6s^2$	$^1S_0$	5.21
57	La	lanthanum	$[Xe]6s^25d$	$^2D_{3/2}$	5.58
58	Ce	cerium	$[Xe](6s^24f5d)$	$(^1G_4)$	5.47
59	Pr	praseodymium	$[Xe](6s^24f^3)$	$(^4I_{9/2})$	5.42
60	Nd	neodymium	$[Xe]6s^24f^4$	$^5I_4$	5.49
61	Pm	promethium	$[Xe](6s^24f^5)$	$(^6H_{5/2})$	5.55
62	Sm	samarium	$[Xe]6s^24f^6$	$^7F_0$	5.63
63	Eu	europium	$[Xe]6s^24f^7$	$^8S_{7/2}$	5.67
64	Gd	gadolinium	$[Xe]6s^24f^75d$	$^9D_2$	6.14
65	Tb	terbium	$[Xe](6s^24f^9)$	$^6H_{15/2}$	5.85
66	Dy	dysprosium	$[Xe](6s^24f^{10})$	$(^5I_8)$	5.93
67	Ho	holmium	$[Xe](6s^24f^{11})$	$(^4I_{15/2})$	6.02
68	Er	erbium	$[Xe](6s^24f^{12})$	$(^3H_6)$	6.10
69	Tm	thulium	$[Xe]6s^24f^{13}$	$^2F_{7/2}$	6.18
70	Yb	ytterbium	$[Xe]6s^24f^{14}$	$^1S_0$	6.25
71	Lu	lutetium	$[Xe]6s^24f^{14}5d$	$^2D_{3/2}$	5.43
72	Hf	hafnium	$[Xe]6s^24f^{14}5d^2$	$^3F_2$	7.0
73	Ta	tantalum	$[Xe]6s^24f^{14}5d^3$	$^4F_{3/2}$	7.89
74	W	tungsten	$[Xe]6s^24f^{14}5d^4$	$^5D_0$	7.98
75	Re	rhenium	$[Xe]6s^24f^{14}5d^5$	$^6S_{5/2}$	7.88
76	Os	osmium	$[Xe]6s^24f^{14}5d^6$	$^5D_4$	8.7
77	Ir	iridium	$[Xe]6s^24f^{14}5d^7$	$(^4F_{9/2})$	9.1
78	Pt	platinum	$[Xe]6s4f^{14}5d^9$	$^3D_3$	9.0
79	Au	gold	$[Xe]6s4f^{14}5d^{10}$	$^2S_{1/2}$	9.23
80	Hg	mercury	$[Xe]6s^24f^{14}5d^{10}$	$^1S_0$	10.44
81	Tl	thallium	$[Xe]6s^24f^{14}5d^{10}6p$	$^2P_{1/2}$	6.11
82	Pb	lead	$[Xe]6s^24f^{14}5d^{10}6p^2$	$^3P_0$	7.42
83	Bi	bismuth	$[Xe]6s^24f^{14}5d^{10}6p^3$	$^4S_{3/2}$	7.29
84	Po	polonium	$[Xe]6s^24f^{14}5d^{10}6p^4$	$^3P_2$	8.42
85	At	astatine	$[Xe](6s^24f^{14}5d^{10}6p^5)$	$^2P_{3/2}$	9.5
86	Rn	radon	$[Xe]6s^24f^{14}5d^{10}6p^6$	$^1S_0$	10.75
87	Fr	francium	$[Rn]7s$	$^2S_{1/2}$	4.0
88	Ra	radium	$[Rn]7s^2$	$^1S_0$	5.28
89	Ac	actinium	$[Rn]7s^26d$	$^2D_{3/2}$	6.9
90	Th	thorium	$[Rn]7s^26d^2$	$^3F_2$	
91	Pa	protactinium	$[Rn](7s^25f^26d)$	$(^4K_{11/2})$	
92	U	uranium	$[Rn]7s^25f^36d$	$^5L_6$	4.0
93	Np	neptunium	$[Rn]7s^25f^46d$	$^6L_{11/2}$	
94	Pu	plutonium	$[Rn]7s^25f^6$	$^7F_0$	5.8
95	Am	americium	$[Rn]7s^25f^7$	$^8S_{7/2}$	6.0
96	Cm	curium	$[Rn]7s^25f^76d$	$^9D_2$	
97	Bk	berkelium	$[Rn]7s^25f^86d$	$^8H_{17/2}$	
98	Cf	californium	$[Rn]7s^25f^{10}$	$^5I_8$	
99	Es	einsteinium	$[Rn]7s^25f^{11}$	$^4I_{15/2}$	
100	Fm	fermium	$[Rn](7s^25f^{12})$	$(^3H_6)$	
101	Md	mendelevium	$[Rn](7s^25f^{13})$	$(^2F_{7/2})$	
102	No	nobelium	$[Rn](7s^25f^{14})$	$(^1S_0)$	
103	Lw	lawrencium	$[Rn]7s^25f^{14}6d)$	$(^2D_{3/2})$	

† Configurations and terms in parentheses are estimated.

configuration $1s^22s^22p^6$). Since the 2p individual energy level is somewhat higher than the 2s level, the ionisation potential of boron (8.30 eV) is smaller than that of beryllium. For neon the ionisation potential reaches the value of 21.56 eV, which is larger than any other one, except helium. We note that since the 2p subshell is closed for neon, its ground term value is $^1S_0$. In fact, neon has the maximum number of electrons allowed in the $n = 2$ (L) shell.

With $Z = 11$ (sodium) the eleventh electron must go into the 3s subshell. The ionisation potential of sodium (5.14 eV) is therefore much smaller than that of neon. From $Z = 11$ to $Z = 18$ the 3s and 3p subshells are progressively filled, the ground state configuration of argon ($Z = 18$) being $1s^22s^22p^63s^23p^6$.

The process of filling the $n = 3$ states is temporarily interrupted at $Z = 19$ (potassium). Indeed, looking at Table 7.1, we see that after the 3p subshell is filled the first departure from the ordering according to the lowest value of n occurs. The added electrons in potassium ($Z = 19$) and calcium ($Z = 20$) thus go into the 4s rather than the 3d subshell, the 3d level being energetically less favourable because of the screening by the argon core [Ar].

The filling of the 3d subshell is therefore deferred until scandium ($Z = 21$), which has the ground state configuration $1s^22s^2\,2p^63s^23p^64s^23d$ (or $[Ar]4s^23d$ in abbreviated notation). It is the first element of the so-called *first transition* or *iron group*, extending from $Z = 21$ to $Z = 30$ (zinc). It is worth noting that because the 4s and 3d states are very close in energy, a competition between these two states develops, and the process of filling is not so regular as for the previous subshells. Thus from scandium ($Z = 21$) to vanadium ($Z = 23$) the added electrons occupy successively the states $4s^23d$, $4s^23d^2$ and $4s^23d^3$, but chromium ($Z = 24$) has only one 4s electron, the state $4s3d^5$ being energetically more favourable than $4s^23d^4$. With manganese ($Z = 25$) the added electron goes into the 4s state left free in chromium, so that Mn has the ground state configuration $[Ar]4s^23d^5$. The 3d subshell then continues to be filled regularly with iron ($Z = 26$, ground state configuration $[Ar]4s^23d^6$), cobalt ($Z = 27$, ground state configuration $[Ar]4s^23d^7$) and nickel ($Z = 28$, ground state configuration $[Ar]4s^23d^8$), but this regularity is again broken with copper ($Z = 29$) which has only one 4s electron (as does chromium), its ground state configuration being $[Ar]4s3d^{10}$. The last element of the first transition or iron group, zinc ($Z = 30$) has the ground state configuration $[Ar]4s^23d^{10}$.

The elements of the first transition group have ground state configurations in which the outer electrons occupy states of the type $(n + 1)s^2nd^x$ or $(n + 1)s\, nd^{x+1}$ with $n = 3$. Two other sets of transition elements, the *second transition* or *palladium* group (from $Z = 39$ to $Z = 48$) and the *third transition* or *platinum* group (from $Z = 71$ to $Z = 80$) correspond to similar situations, but with $n = 4$ and $n = 5$, respectively. Here again a competition develops between the nd and the $(n + 1)$s levels, and irregularities in the filling of the subshells occur.

The *rare-earth* elements or *lanthanides* are the 14 elements, beginning with lanthanum ($Z = 57$) which correspond to the filling of the 4f subshell, the 4s subshell being already complete. We note that this filling of the 4f subshell is irregular, with a competition taking place between the 4f and 5d levels.

Analogous to the rare-earth elements are the *actinides*, beginning with actinium ($Z = 89$) in which the 5s subshell is complete and a competition occurs between the 5f and the 6d states.

The electron configurations of atoms with large values of Z are clearly difficult to explain on the basis of the simple qualitative arguments developed above. One reason, which we have already mentioned, is that various energy levels are very close in energy. Also, for large Z, relativisitic effects (such as spin–orbit coupling) become important and prevent the simple decoupling of the space and spin parts of the wave functions, which we have made here. We shall return to spin–orbit effects in Section 7.5.

Ionisation potentials

It is apparent from Table 7.2 and from Fig. 7.1 that in going from an element to the next one, the ionisation potential of the added electron does not vary in a monotonic way with Z. In particular, the ionisation potential is seen to reach maximum values for the *noble gases* (He, Ne, Ar, Kr, Xe) which have a full K shell or p subshell. It is smallest for the *alkalis* (Li, Na, K, Rb, Cs) whose electron configuration corresponds to that of a noble gas plus an s electron.

These features can be understood qualitatively by recalling that the electrons in the same subshell have equivalent spatial distributions, so that their screening of one another is rather small. For example, in the case of helium we saw in Section 6.4 that the screening constant corresponding to the shielding between the two 1s electrons is given approximately by $S \simeq 0.30$. As a result, the effective charge Z_e increases as Z increases during the filling of a subshell, and the ionisation potential is maximum for a closed subshell. On the other hand,

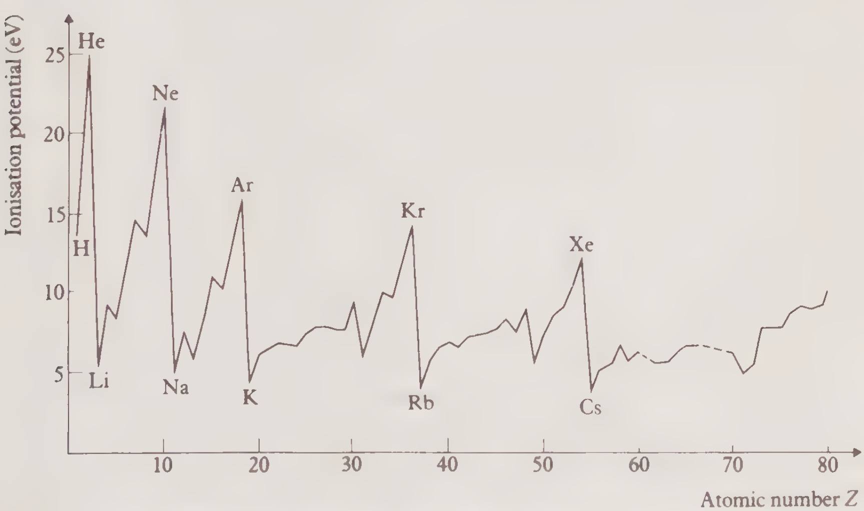

7.1 The ionisation potential as a function of the atomic number Z. The maxima occur at $Z = 2$ (He), $Z = 10$ (Ne), $Z = 18$ (Ar), $Z = 36$ (Kr), $Z = 54$ (Xe) and (not shown) $Z = 86$ (Rn).

when a subshell has been filled, the added electron must go into another state having a larger value of n or l, whose orbital is concentrated at larger r values, outside the closed subshells. Thus in this case the increase of the nuclear charge Z is more than compensated by the very effective screening of the inner electrons on the outer one, and the ionisation potential is significantly reduced.

Chemical properties and the Mendeleev classification of the elements

The chemical properties of an atom are related to the possible interactions of this atom with other ones, and in particular to its possibility of being bound with other atoms to form a molecule. At the low energies involved in chemical reactions, the interactions between atoms are mostly determined by the least tightly bound or *valence* electrons which, as we have seen, are in the 'outer' subshell. The key factors are the number of occupied electron states in this subshell, and the energy interval between this subshell and the next (empty) one. For example, an atom tends to be chemically *inert* if (i) its outer subshell is filled, and (ii) there is an appreciable energy difference between this subshell and the next higher one, so that it takes quite a lot of energy to perturb the atom. This is the case for the *noble gases* (He, Ne, Ar, Kr, Xe). On the other hand, the *alkalis* (Li, Na, K, Rb, Cs) which contain a single weakly bound s electron outside a 'noble gas' core are very active chemically, because they will frequently loose their valence electron in their interactions with other atoms. The *halogens* (F, Cl, Br, I) which have a p subshell lacking only one electron (that is a '*hole*' in their outer p subshell) will also exhibit a large chemical reactivity, because of their high electron *affinity* – their tendency to capture an electron in order to reach the more stable arrangement corresponding to completely filled subshells. In particular, a halogen (such as F) will readily combine with an alkali (such as Li) to form a F^- ion and a Li^+ ion, which bond together. This is an example of ionic bonding, which will be discussed in Chapter 9.

The rare gases, alkalis and halogens provide examples of *recurrences* (as Z increases) *of similar chemical properties*, due to regularities in the structure of the outer electron shells. These recurrences led Mendeleev in 1869 to classify the elements in a table, the *periodic table*, such that the elements of a same column (group) have comparable chemical properties and those of a same row are said to form a *period*. The atomic number Z of an element was then obtained by ordering the spaces in the table. It is worth noting that when Mendeleev proposed his periodic table in 1869 neither electrons nor nuclei were known, and that he also had the foresight to leave some empty spaces in his table, to be filled by elements not yet discovered. Mendeleev subdivided the set of elements into *seven* periods; this subdivision is still kept today and includes elements discovered later. A modern version of the Mendeleev, or periodic, table of the elements is given in Table 7.3. We see that each of the periods begins with an alkali element and ends with a noble gas atom, except for the seventh period,

Table 7.3 The periodic table of the elements

Period	IA	IIA	IIIB	IVB	VB	VIB	VIIB		VIIIB	VIIIB	IB	IIB	IIIA	IVA	VA	VIA	VIIA	Noble gases
1	1 H 1.008																	2 He 4.003
2	3 Li 6.939	4 Be 9.012											5 B 10.811	6 C 12.011	7 N 14.007	8 O 15.999	9 F 18.998	10 Ne 20.183
3	11 Na 22.990	12 Mg 24.312											13 Al 26.982	14 Si 28.086	15 P 30.974	16 S 32.064	17 Cl 35.453	18 Ar 39.948
4	19 K 39.102	20 Ca 40.08	21 Sc 44.956	22 Ti 47.90	23 V 50.942	24 Cr 51.996	25 Mn 54.938	26 Fe 55.847	27 Co 58.933	28 Ni 58.71	29 Cu 63.54	30 Zn 65.37	31 Ga 69.72	32 Ge 72.59	33 As 74.922	34 Se 78.96	35 Br 79.909	36 Kr 83.80
5	37 Rb 85.47	38 Sr 87.62	39 Y 88.905	40 Zr 91.22	41 Nb 92.906	42 Mo 95.94	43 Tc (99)	44 Ru 101.07	45 Rh 102.91	46 Pd 106.4	47 Ag 107.87	48 Cd 112.40	49 In 114.82	50 Sn 118.69	51 Sb 121.75	52 Te 127.60	53 I 126.90	54 Xe 131.30
6	55 Cs 132.91	56 Ba 137.34	57† La 138.91	72 Hf 178.49	73 Ta 180.95	74 W 183.85	75 Re 186.2	76 Os 190.2	77 Ir 192.2	78 Pt 195.09	79 Au 196.97	80 Hg 200.59	81 Tl 204.37	82 Pb 207.19	83 Bi 208.98	84 Po (210)	85 At (210)	86 Rn (222)
7	87 Fr (223)	88 Ra (226)	89‡ Ac (227)	104	105													

† Lanthanides	58 Ce 140.12	59 Pr 140.91	60 Nd 144.24	61 Pm (145)	62 Sm 150.35	63 Eu 151.96	64 Gd 157.25	65 Tb 158.92	66 Dy 162.50	67 Ho 164.93	68 Er 167.26	69 Tm 168.93	70 Yb 173.04	71 Lu 174.97
‡ Actinides	90 Th 232.04	91 Pa (231)	92 U 238.03	93 Np (237)	94 Pu 242	95 Am 243	96 Cm 247	97 Bk 249	98 Cf 251	99 Es (254)	100 Fm 253	101 Md 256	102 No 253	103 Lr 257

which is incomplete. We remark, parenthetically, that nothing in atomic structure prevents atoms with $Z > 100$ existing. The reason that such atoms are not observed naturally is that their *nuclei* undergo spontaneous fission, and are unstable.

To conclude our discussion, we emphasise once more the importance of the Pauli exclusion principle. Indeed, the variety which we find in the periodic table is basically a consequence of the Pauli principle. If it were not obeyed, all the electrons of an atom would be in the 1s subshell (which has the lowest energy), and all atoms would be more or less alike, with spherically symmetric charge distributions having very small radii.

7.3 THE THOMAS–FERMI MODEL OF THE ATOM

We now turn to a basic problem in the central field approximation, namely the determination of the central potential $V(r)$. This problem will be analysed by using two approaches. The elaborate Hartree–Fock method will be studied in the next section, while the simpler Thomas–Fermi model, which is based on *statistical* and *semi-classical* considerations, is discussed here.

The Fermi electron gas

Before we analyse the theory developed by Thomas and Fermi for the ground state of multielectron atoms, it is convenient to consider the simpler problem of the Fermi electron gas, that is a system consisting of a large number N of free electrons confined to a certain region of space [3]. We shall suppose that the N free electrons of our system are confined to a large cube of side L. Each of the electrons is therefore moving independently in a potential which is constant (we may take this constant to be zero) inside the cube, and is assumed to be infinite at the boundary. Thus, the spatial part of the wave function describing the motion of an electron satisfies the free particle Schrödinger equation [4]

$$-\frac{\hbar^2}{2m}\left(\frac{\partial^2}{\partial x^2}+\frac{\partial^2}{\partial y^2}+\frac{\partial^2}{\partial z^2}\right)\psi(\mathbf{r}) = E\psi(\mathbf{r}) \tag{7.30}$$

inside the cube, while $\psi = 0$ at the boundary.

Since the equation [7.30] is separable in Cartesian coordinates, we may use the results obtained in Section 2.4 for the one-dimensional infinite square well potential. Generalising these results to three dimensions, and moving the origin of our coordinate system from the centre of the box to one corner, we find that the eigenfunctions of [7.30] which vanish at the boundary (i.e. the wave functions for a spinless particle in a cubical box of side L) are given by

$$\psi_{n_x n_y n_z}(\mathbf{r}) = C\sin\left(\frac{n_x\pi}{L}x\right)\sin\left(\frac{n_y\pi}{L}y\right)\sin\left(\frac{n_z\pi}{L}z\right) \tag{7.31}$$

where $C = (8/L^3)^{1/2}$ is a normalisation constant and n_x, n_y, n_z are positive integers [5]. The corresponding allowed values of the energy E of an electron are (see [2.131])

$$\begin{aligned} E &= \frac{\pi^2\hbar^2}{2mL^2}(n_x^2+n_y^2+n_z^2) \\ &= \frac{\pi^2\hbar^2}{2mL^2}n^2 \end{aligned} \tag{7.32}$$

[3] A good example of a Fermi electron gas is provided by the conduction electrons in a metal. A detailed discussion may be found in Kittel (1976).

[4] In this section we shall use SI units.

[5] A zero set of values of (n_x, n_y, n_z) leads to the unacceptable trivial solution $\psi = 0$ everywhere, and negative values of n_x, n_y, n_z, do not yield different wave functions from those given by [7.31].

where

$$n^2 = n_x^2 + n_y^2 + n_z^2 \qquad [7.33]$$

We remark that each energy level [7.32] can in general be obtained from a number of different sets of values of (n_x, n_y, n_z), and is therefore usually degenerate.

Since electrons have spin 1/2, we must multiply the spatial part [7.31] of their wave function by the spin functions $\chi_{1/2,m_s}$, with $m_s = \pm 1/2$. The individual electron wave functions are therefore the spin orbitals

$$\psi_{n_x n_y n_z m_s} = \psi_{n_x n_y n_z}(\mathbf{r})\chi_{1/2,m_s} \qquad [7.34]$$

and the quantum states of an electron are specified by the three spatial quantum numbers $(n_x n_y n_z)$ *and* the spin quantum number m_s. We note that for each energy level [7.32] labelled by the quantum numbers $(n_x n_y n_z)$, there are two spin-orbitals, one corresponding to spin up ($m_s = +1/2$) and one to spin down ($m_s = -1/2$), so that the degeneracy of the individual energy levels [7.32] is multiplied by two.

Because the energy spacings are very small for any reasonable macroscopic box of side L, it is a good approximation to consider that the energy levels are distributed nearly continuously. We may then introduce the *density of states* or *density of orbitals* $D(E)$, which is defined as the number of electron quantum states (i.e. the number of spin orbitals) per unit energy range. Thus $D(E)\,\mathrm{d}E$ is the number of electron states for which the energy of an electron lies between E and $E + \mathrm{d}E$.

In order to obtain the quantity $D(E)$, we consider the space formed by the axes n_x, n_y and n_z (see Fig. 7.2). Since n_x, n_y and n_z are positive integers, we are interested only in the octant for which $n_x > 0$, $n_y > 0$ and $n_z > 0$. As seen from Fig. 7.2 each set of spatial quantum numbers (n_x, n_y, n_z) corresponds to a point

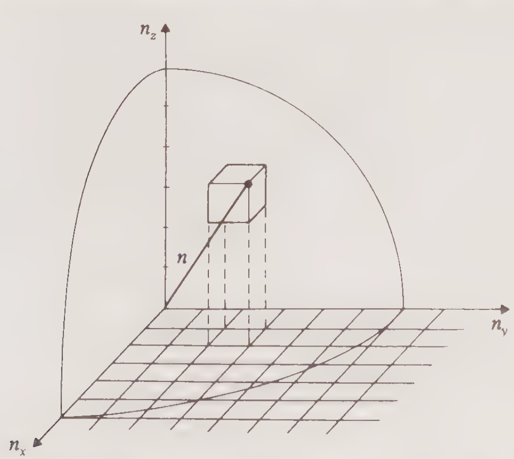

7.2 Three-dimensional n-space used in the calculation of $D(E)$. To each state (n_x, n_y, n_z) is associated a cube of unit volume. For fairly large values of (n_x, n_y, n_z) the total number of states within $n = (n_x^2 + n_y^2 + n_z^2)^{1/2}$ equals the volume of one octant of a sphere of radius n in n-space.

of a cubical lattice, and every elementary cube of the lattice has unit volume. Thus, for fairly large values of the quantum triplet (n_x, n_y, n_z), the total number of spatial orbitals for all energies up to a certain value E is closely equal to the volume of the octant of a sphere of radius $n = (n_x^2 + n_y^2 + n_z^2)^{1/2}$. The total number of individual electron states for energies up to E is therefore given approximately by

$$N_s = 2\,\frac{1}{8}\,\frac{4}{3}\,\pi n^3 = \frac{1}{3}\,\pi n^3 \qquad [7.35]$$

where the factor 2 is due to the two spin states per spatial orbital. Using [7.32] and setting $V = L^3$, we may also write this result as

$$N_s = \frac{1}{3\pi^2}\left(\frac{2m}{\hbar^2}\right)^{3/2} VE^{3/2} \qquad [7.36]$$

The number $D(E)\,\mathrm{d}E$ of electron states within the energy range $(E, E + \mathrm{d}E)$ is then obtained by differentiating [7.36], namely

$$\mathrm{d}N_s = D(E)\,\mathrm{d}E = \frac{1}{2\pi^2}\left(\frac{2m}{\hbar^2}\right)^{3/2} VE^{1/2}\,\mathrm{d}E \qquad [7.37]$$

so that

$$D(E) = \frac{\mathrm{d}N_s}{\mathrm{d}E} = \frac{1}{2\pi^2}\left(\frac{2m}{\hbar^2}\right)^{3/2} VE^{1/2} \qquad [7.38]$$

It may be shown that the above results remain valid for a volume of arbitrary shape, provided its minimum dimension is much larger than the average wavelength of the orbitals.

According to the Pauli exclusion principle, the total wave function describing the entire system of N electrons must be fully antisymmetric in the (spatial and spin) coordinates of the electrons, and will therefore be a Slater determinant constructed from the individual spin orbitals [7.34]. The corresponding total energy is the sum of the individual electron energies. Assuming that the system is in the *ground state* (i.e. our Fermi electron gas is at an absolute temperature $T = 0$), the lowest total energy is then obtained when the N electrons fill all the spin orbitals up to an energy E_F, called the *Fermi energy*, the remaining orbitals (with energies $E > E_F$) being vacant. This is illustrated in Fig. 7.3, which shows the density of states $D(E)$ as a function of E, the occupied orbitals corresponding to the ground state of the Fermi electron gas being represented by the shaded area.

The Fermi energy may be evaluated by requiring that the total number N of electrons in the system should be equal to

$$N = \int_0^{E_F} D(E)\,\mathrm{d}E \qquad [7.39]$$

In writing this equation we have used the fact that the system contains many electrons, so that the integral [7.39] is a good approximation to the correspond-

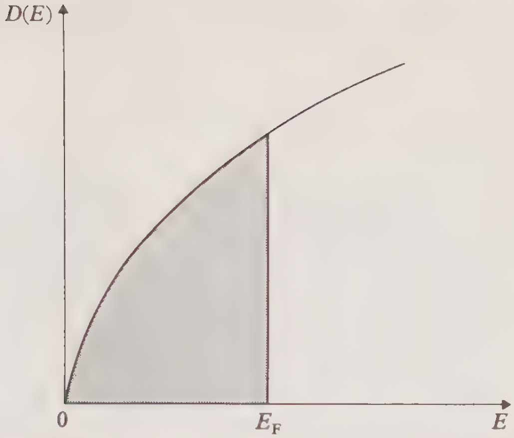

7.3 The density of states $D(E)$ as a function of the energy E. The occupied orbitals corresponding to the ground state of the Fermi electron gas are represented by the shaded area.

ing sum over discrete states. Moreover, since N is large, it does not matter whether the last level contains one or more electrons. Using the result [7.38], we have

$$N = \frac{1}{2\pi^2}\left(\frac{2m}{\hbar^2}\right)^{3/2} V \int_0^{E_F} E^{1/2}\,\mathrm{d}E$$

$$= \frac{1}{3\pi^2}\left(\frac{2m}{\hbar^2}\right)^{3/2} V E_F^{3/2} \qquad [7.40]$$

so that

$$E_F = \frac{\hbar^2}{2m}(3\pi^2\rho)^{2/3} \qquad [7.41]$$

where

$$\rho = \frac{N}{V} \qquad [7.42]$$

is the number of electrons per unit volume, i.e. the density of electrons. We note that the total energy of a Fermi electron gas in the ground state (at absolute zero) is

$$E_{tot} = \int_0^{E_F} E D(E)\,\mathrm{d}E$$

$$= \frac{1}{2\pi^2}\left(\frac{2m}{\hbar^2}\right)^{3/2} V \int_0^{E_F} E^{3/2}\,\mathrm{d}E$$

$$= \frac{1}{5\pi^2}\left(\frac{2m}{\hbar^2}\right)^{3/2} V E_F^{5/2}$$

$$= \frac{3}{5} N E_F \qquad [7.43]$$

where we have used [7.38] and [7.40]. The average electron energy at $T = 0$ K is therefore

$$\bar{E} = \frac{E_{\text{tot}}}{N} = \frac{3}{5} E_{\text{F}} \qquad [7.44]$$

It is also instructive to study the problem of the Fermi electron gas by imposing *periodic boundary conditions* on the (spatial) wave functions of the electrons, i.e. by requiring these wave functions to be periodic in x, y and z with period L. Instead of the standing waves [7.31] we then have *travelling* wave solutions of the Schrödinger equation [7.30], having the form

$$\psi_{\mathbf{k}}(\mathbf{r}) = \mathrm{e}^{i\mathbf{k}\cdot\mathbf{r}} \qquad [7.45]$$

As we already showed in Section 4.2, the allowed components of the wave vector $\mathbf{k}$ are then given by (see [4.50])

$$k_x = \frac{2\pi}{L} n_x, \qquad k_y = \frac{2\pi}{L} n_y, \qquad k_z = \frac{2\pi}{L} n_z \qquad [7.46]$$

where n_x, n_y and n_z are positive or negative integers, or zero. The number of spatial orbitals in the range $\mathrm{d}\mathbf{k} = \mathrm{d}k_x\, \mathrm{d}k_y\, \mathrm{d}k_z$ is $(L/2\pi)^3\, \mathrm{d}k_x\, \mathrm{d}k_y\, \mathrm{d}k_z$ and this number must be multiplied by 2 to take into account the two possible spin states. A unit volume of $\mathbf{k}$-space will therefore accommodate $V/4\pi^3$ electrons (with $V = L^3$). Thus, the individual electron states having energies up to $E = \hbar^2 k^2/2m$ will be contained within a sphere in $\mathbf{k}$-space, of radius k, the number N_{s} of these states being given by

$$\begin{aligned} N_{\text{s}} &= \frac{V}{4\pi^3} \frac{4}{3} \pi k^3 = \frac{1}{3\pi^2} V k^3 \\ &= \frac{1}{3\pi^2} \left(\frac{2m}{\hbar^2} \right)^{3/2} V E^{3/2} \end{aligned} \qquad [7.47]$$

in agreement with [7.36].

We have seen above that in the ground state of our Fermi electron gas the N electrons fill all the states up to the Fermi energy E_{F}. Thus in $\mathbf{k}$-space all states up to a maximum value of k equal to k_{F} are then filled, while the states for which $k > k_{\text{F}}$ are empty. In other words all occupied orbitals of a Fermi electron gas at 0 K fill a sphere in $\mathbf{k}$-space having radius k_{F}. This sphere, which is called the *Fermi sphere*, obviously contains

$$\frac{1}{3\pi^2} V k_{\text{F}}^3 = N \qquad [7.48]$$

orbitals, so that

$$k_{\text{F}} = (3\pi^2 \rho)^{1/3} \qquad [7.49]$$

At the surface of the Fermi sphere, known as the *Fermi surface*, the energy is the Fermi energy

$$E_F = \frac{\hbar^2}{2m} k_F^2 \qquad [7.50]$$

and we note that the result [7.41] follows upon substitution of [7.49] in [7.50]. It is also convenient to introduce the Fermi momentum p_F, velocity v_F and temperature T_F such that

$$E_F = \frac{p_F^2}{2m} = \frac{1}{2} m v_F^2 = kT_F \qquad [7.51]$$

where k is Boltzmann's constant.

The Thomas–Fermi theory for multielectron atoms and ions

The theory developed independently by Thomas and Fermi for the ground state of complex atoms (or ions) having a large number of electrons is based on *statistical* and *semi-classical* considerations. The N electrons of the system are treated as a Fermi electron gas in the ground state, confined to a region of space by a central potential $V(r)$ which vanishes at infinity. It is assumed that this potential is slowly varying over a distance which is large compared with the de Broglie wavelengths of the electrons, so that enough electrons are present in a volume where $V(r)$ is nearly constant, and the statistical approach used in studying the Fermi electron gas can be applied. In addition, since the number of electrons is large, many of them have high principal quantum numbers, so that semi-classical methods should be useful.

The aim of the Thomas–Fermi model is to provide a method of calculating the potential $V(r)$ and the electron density $\rho(r)$. These two quantities can first be related by using the following arguments. The total energy of an electron is written as $p^2/2m + V(r)$, and this energy cannot be positive, otherwise the electron would escape to infinity. Since the maximum kinetic energy of an electron in a Fermi electron gas at 0 K is the Fermi energy E_F, we write for the total energy of the most energetic electrons of the system the classical equation

$$E_{max} = E_F + V(r) \qquad [7.52]$$

It is clear that E_{max} must be independent of r, because if this were not the case electrons would migrate to that region of space where E_{max} is smallest, in order to lower the total energy of the system. Furthermore, we must have $E_{max} \leq 0$. We note from [7.50] and [7.52] that the quantity k_F is now a function of r. That is

$$k_F^2(r) = \frac{2m}{\hbar^2} \left[E_{max} - V(r) \right] \qquad [7.53]$$

Using [7.41] and [7.52] we then have

$$\rho(r) = \frac{1}{3\pi^2}\left(\frac{2m}{\hbar^2}\right)^{3/2}[E_{\max} - V(r)]^{3/2} \tag{7.54}$$

and we see that ρ vanishes when $V = E_{\max}$. In the classically forbidden region $V > E_{\max}$ we must set $\rho = 0$, since otherwise [7.52] would yield a negative value of the maximum kinetic energy E_F. Let us denote by

$$\phi(r) = -\frac{1}{e}V(r) \tag{7.55}$$

the electrostatic potential and by $\phi_0 = -E_{\max}/e$ a non-negative constant. Setting

$$\Phi(r) = \phi(r) - \phi_0 \tag{7.56}$$

we see that $\rho(r)$ and $\Phi(r)$ are related by

$$\rho(r) = \frac{1}{3\pi^2}\left(\frac{2m}{\hbar^2}\right)^{3/2}[e\Phi(r)]^{3/2} \qquad \Phi \geqslant 0 \tag{7.57a}$$

$$= 0 \qquad \Phi < 0 \tag{7.57b}$$

The equation $\Phi = 0$ (i.e. $\phi = \phi_0$ or $V = E_{\max}$) may be thought of as determining the 'boundary' $r = r_0$ of the atom (ion) in this model. Now, for a neutral atom ($N = Z$) the electrostatic potential $\phi(r)$ vanishes at the boundary, so that we shall set $\phi_0 = 0$ in that case. On the other hand $\phi_0 > 0$ for an ion.

A second relation between $\rho(r)$ and $\Phi(r)$ may be obtained as follows. The sources of the electrostatic potential $\phi(r)$ are:

(i) the point charge Ze of the nucleus, located at the origin;
(ii) the distribution of electricity due to the N electrons.

Treating the charge density $-e\rho(r)$ of the electrons as continuous, we may use Poisson's equation of electrostatics to write

$$\nabla^2\Phi(r) = \frac{1}{r}\frac{d^2}{dr^2}[r\Phi(r)] = \frac{e}{\varepsilon_0}\rho(r) \tag{7.58}$$

The equations [7.57a] and [7.58] are two simultaneous equations for $\rho(r)$ and $\Phi(r)$. Eliminating $\rho(r)$ from these equations, we find that for $\Phi \geqslant 0$

$$\frac{1}{r}\frac{d^2}{dr^2}[r\Phi(r)] = \frac{e}{3\pi^2\varepsilon_0}\left(\frac{2m}{\hbar^2}\right)^{3/2}[e\Phi(r)]^{3/2}, \qquad \Phi \geqslant 0 \tag{7.59}$$

On the other hand, when $\Phi < 0$ we see from [7.57b] and [7.58] that

$$\frac{d^2}{dr^2}[r\Phi(r)] = 0, \qquad \Phi < 0 \tag{7.60}$$

For $r \to 0$ the leading term of the electrostatic potential must be due to the nucleus, so that the boundary condition at $r = 0$ reads

$$\lim_{r \to 0} r\Phi(r) = \frac{Ze}{4\pi\varepsilon_0} \qquad [7.61]$$

On the other hand, since the N electrons of the system are assumed to be confined to a sphere of radius r_0, we must have the 'normalisation' condition

$$4\pi \int_0^{r_0} \rho(r)\, r^2\, \mathrm{d}r = N \qquad [7.62]$$

In order to simplify the above equations, it is convenient to introduce the new dimensionless variable x and the function $\chi(x)$ such that

$$r = bx, \qquad r\Phi(r) = \frac{Ze}{4\pi\varepsilon_0}\chi(x) \qquad [7.63]$$

where

$$b = \frac{(3\pi)^{2/3}}{2^{7/3}} a_0 Z^{-1/3} \simeq 0.8853\, a_0 Z^{-1/3} \qquad [7.64]$$

and $a_0 = (4\pi\varepsilon_0)\hbar^2/me^2$ is the first Bohr radius. The relation [7.57] then becomes

$$\rho = \frac{Z}{4\pi b^3}\left(\frac{\chi}{x}\right)^{3/2} \qquad \chi \geqslant 0 \qquad [7.65a]$$

$$= 0 \qquad \chi < 0 \qquad [7.65b]$$

and the important equation [7.59] may be written in dimensionless form as

$$\frac{\mathrm{d}^2\chi}{\mathrm{d}x^2} = x^{-1/2}\chi^{3/2} \qquad \chi \geqslant 0 \qquad [7.66]$$

This is known as the *Thomas–Fermi equation*. For negative χ we see from [7.60] and [7.63] that

$$\frac{\mathrm{d}^2\chi}{\mathrm{d}x^2} = 0 \qquad \chi < 0 \qquad [7.67]$$

In addition, the boundary condition at $r = 0$, expressed by [7.61] now reads

$$\chi(0) = 1 \qquad [7.68]$$

It is clear from [7.66] and [7.67] that $\chi(x)$ has at most one zero in the interval $(0, +\infty)$. Let x_0 be the position of this zero. From our above discussion we have $x_0 = r_0/b$, where r_0 is the 'boundary' of the system. We also note that $\chi > 0$ for $x < x_0$ and $\chi < 0$ for $x > x_0$. Moreover, the equation [7.67] has the solution $\chi = C(x - x_0)$, where C is a negative constant, which must be equal to $\chi'(x_0)$. As a result, the solution $\chi(x)$ is entirely determined if we know it for $\chi \geqslant 0$. We

also remark that for any finite x_0 the quantity $\chi'(x_0)$ must be different from zero, since otherwise both χ and χ' would vanish at $x = x_0$, and the equation [7.66] would yield the unacceptable trivial solution $\chi = 0$.

The Thomas–Fermi equation [7.66] is a 'universal' equation, which does not depend on Z, nor on physical constants such as $\hbar$, m or e which have been 'scaled out' by performing the change of variables [7.63]. We also note that it is a second-order, non-linear equation. Since the boundary condition at the origin [7.68] only specifies one constraint, there exist a whole family of solutions $\chi(x)$ satisfying the Thomas–Fermi equation [7.66] and the condition [7.68], which differ by their initial slope $\chi'(0)$. It is also clear from [7.66] that all these solutions must be concave upwards. As illustrated in Fig. 7.4, we can classify them into three categories:

1. a solution which is asymptotic to the x axis;
2. solutions which vanish for a finite value $x = x_0$;
3. solutions which never vanish and diverge for large x.

The physical meaning of the solutions belonging to the first two categories may be obtained by looking at the 'normalisation' condition [7.62]. Taking into account [7.63], [7.65] and [7.66], this condition reads

$$\begin{aligned} N &= Z \int_0^{x_0} x^{1/2} \chi^{3/2} \, dx \\ &= Z \int_0^{x_0} x \chi'' \, dx \\ &= Z[x\chi' - \chi]_0^{x_0} \end{aligned} \qquad [7.69]$$

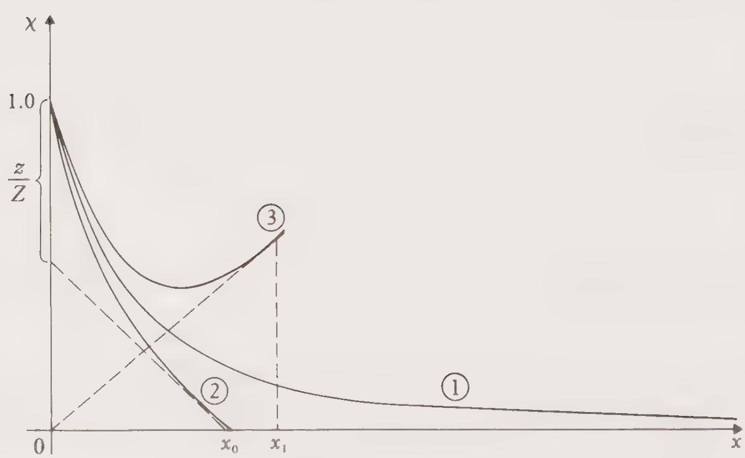

7.4 The three categories of solutions of the Thomas–Fermi equation: (1) neutral atom solution; (2) solution corresponding to a positive ion ($N < Z$); (3) solution corresponding to a neutral atom under pressure.

Using the boundary condition [7.68] and the fact that $\chi(x_0) = 0$, we then have

$$x_0 \chi'(x_0) = \frac{N-Z}{Z} \qquad [7.70]$$

Let us first consider *neutral atoms* for which $N = Z$. The condition [7.70] then requires that $\chi'(x_0) = 0$, so that χ' should vanish at the same point as χ. Since this condition cannot be satisfied for a finite value x_0 by non-trivial solutions, the point x_0 must be at infinity. As a consequence, the solution $\chi(x)$ corresponding to a neutral atom must be asymptotic to the x axis, namely

$$\chi(\infty) = 0 \qquad [7.71]$$

and is therefore the (unique) solution classified above in the first category. We remark that since $\chi(x)$ vanishes only at infinity, there is no 'boundary' to the neutral atom in the Thomas–Fermi model.

The Thomas–Fermi equation [7.66] and the boundary conditions [7.68] and [7.71] define a *universal function* $\chi(x)$ for all neutral atoms. Values of this function, obtained by numerical integration, are given in Table 7.4. We remark from this table that $\chi(x)$ is monotonically decreasing. It can be shown that the asymptotic form of $\chi(x)$ for large x is given by the function $144\,x^{\;\;3}$. At $x = 0$ one has $\chi'(0) = -1.588$ so that in the vicinity of the origin

$$\chi(x) \simeq 1 - 1.588x + \cdots \qquad [7.72]$$

Knowing the universal function $\chi(x)$, we can obtain the function $\Phi(r)$, and hence the electrostatic potential $\phi(r)$, the potential energy $V(r)$ and the density $\rho(r)$. Using [7.55], [7.56], [7.63], and remembering that $\phi_0 = 0$ for a neutral atom, we see that in the Thomas–Fermi model the central potential $V(r)$ is given for neutral atoms by

$$V(r) = -\frac{Ze^2}{(4\pi\varepsilon_0)r}\chi \qquad [7.73]$$

Table 7.4 Values of the function $\chi(x)$ for neutral atoms

x	$\chi(x)$	x	$\chi(x)$	x	$\chi(x)$	x	$\chi(x)$
0.00	1.000	0.9	0.453	3.4	0.135	9.0	0.0295
0.02	0.972	1.0	0.425	3.6	0.125	9.5	0.0268
0.04	0.947	1.2	0.375	3.8	0.116	10	0.0244
0.06	0.924	1.4	0.333	4.0	0.108	11	0.0204
0.08	0.902	1.6	0.298	4.5	0.0918	12	0.0172
0.1	0.882	1.8	0.268	5.0	0.0787	13	0.0147
0.2	0.793	2.0	0.242	5.5	0.0679	14	0.0126
0.3	0.721	2.2	0.220	6.0	0.0592	15	0.0109
0.4	0.660	2.4	0.201	6.5	0.0521	20	0.0058
0.5	0.607	2.6	0.185	7.0	0.0461	25	0.0035
0.6	0.561	2.8	0.171	7.5	0.0409	30	0.0023
0.7	0.521	3.0	0.158	8.0	0.0365	40	0.0011
0.8	0.485	3.2	0.146	8.5	0.0327	50	0.00063

As $r \to 0$, we have $V(r) \to -Ze^2/(4\pi\varepsilon_0)r$. More precisely, we deduce from [7.63], [7.72] and [7.73] that for small r

$$V(r) \simeq \frac{e^2}{4\pi\varepsilon_0}\left(-\frac{Z}{r} + 1.794\,\frac{Z^{4/3}}{a_0}\right) \qquad [7.74]$$

or, using atomic units

$$V(r) \simeq -\frac{Z}{r} + 1.794\,Z^{4/3} + \cdots \qquad [7.75]$$

The first term is the nuclear attraction while the second one, which is repulsive, arises from the contribution of the electrons. When $r \to \infty$, we see from [7.71] and [7.73] that $rV(r) \to 0$, so that the Thomas–Fermi potential [7.73] falls off more rapidly than $1/r$ for larger r. This behaviour is at variance with the result [7.9c] which we obtained in our discussion of the central field approximation. The reason is that the potential V discussed in Section 7.1 is the one felt by an atomic electron, while the Thomas–Fermi potential [7.73] is that experienced by an infinitesimal test charge. The difference between the two potentials is due to the statistical and semi-classical approximations made in the Thomas–Fermi model, the Thomas–Fermi result becoming exact in the limit when $\hbar$ and e tend to zero, while the number $N(=Z)$ of electrons becomes infinite.

Turning now to the electron density $\rho(r)$, we see from [7.65a] that it is similar for all atoms, except for a different length scale, which is determined by the quantity b (see [7.64]) and is proportional to $Z^{-1/3}$. As a result, the radial scale of $\rho(r)$ contracts according to $Z^{-1/3}$ when Z increases. We remark that for fixed Z the Thomas–Fermi method is inaccurate at both small $r(r < a_0/Z)$ and large $r(r \gg a_0)$, where it overestimates the electron density. Indeed, the Thomas–Fermi electron density [7.65a] diverges at the origin (as $r^{-3/2}$) and falls off like r^{-6} as $r \to \infty$, while the correct electron density should remain finite at $r = 0$, and decrease exponentially for large r. Thus the application of the Thomas–Fermi method is limited to 'intermediate' distances r between a_0/Z and a few times a_0. It is worth noting, however, that in complex atoms most of the electrons are to be found precisely in this spatial region. Thus we expect the Thomas–Fermi method to be useful in calculating quantities which depend on the 'average electron', such as the total energy of the atom. On the other hand, quantities which rely on the properties of the 'outer' electrons (such as the ionisation potential) are poorly given in the Thomas–Fermi model.

We have shown above that a neutral atom has no 'boundary' in the Thomas–Fermi model. Nevertheless, it is possible to define in this case an atomic 'radius' $R(\alpha)$ as the radius of a sphere centred at the origin and containing a given fraction $(1 - \alpha)$ of the Z electrons. We then have (see [7.62])

$$4\pi \int_0^{R(\alpha)} \rho(r)\, r^2\, \mathrm{d}r = (1 - \alpha)Z \qquad [7.76]$$

Making the change of variable

$$R(\alpha) = bX(\alpha) \qquad [7.77]$$

and taking into account [7.63], [7.65] and [7.66], we find for X the equation

$$\chi(X) - X\chi'(X) = \alpha \qquad [7.78]$$

which must be solved numerically. If the same value of α is adopted for all atoms, [7.78] becomes a 'universal' equation and X is the same for all atoms. Using [7.64] and [7.77] we see that the atomic radius $R(\alpha)$ is then proportional to $Z^{-1/3}$. On the other hand, if we set $\alpha = Z^{-1}$, then $R(Z^{-1}) = bX(Z^{-1})$ is the radius of a sphere containing all the atomic electrons except one. The quantity $R(Z^{-1})$ is found to be a slowly increasing function of Z, such that $4a_0 < R(Z^{-1}) < 6a_0$. Thus in both cases the atomic radius is nearly independent of Z. Similarly, the energy of the 'outer' electrons – and hence the ionisation potential of the atom – is almost independent of Z. As a consequence, the Thomas–Fermi model cannot account for the periodic properties of atoms as a function of Z, discussed in Section 7.2.

Let us now briefly discuss the two other categories of solutions (see Fig. 7.4) mentioned in our discussion of the Thomas–Fermi equation [7.66]. Returning to [7.69]–[7.70] we remark that solutions $\chi(x)$ which vanish at a finite value $x = x_0$ (that is, which belong to the second category) are such that $N \neq Z$, and hence correspond to *ions* of radius $r_0 = bx_0$. Moreover, since the slope of χ is negative at x_0 (see Fig. 7.4) the equation [7.70] implies that these ions must be *positive ions*, such that $Z > N$ [6]. Setting $z = Z - N$, so that ze is the net charge of the ion, we note from [7.70] that the quantity z/Z is readily obtained from the tangent to the curve χ at $x = x_0$, as shown in Fig. 7.4. Since $\chi(x_0) = 0$, the electron density $\rho(r)$ vanishes at $r = r_0 = bx_0$, as seen from [7.65]. On the other hand, looking at [7.55], [7.56] and [7.63], and remembering that $\phi_0 > 0$ for an ion, we see that the potential $V(r)$ remains finite at $r = r_0$.

The solutions of the Thomas–Fermi equation belonging to the third category (that is those which have no zero and diverge for large x) are more difficult to interpret. First of all, the electron density $\rho(r)$ does not vanish in this case, and one may consider that these solutions correspond to negative values of ϕ_0. As seen from Fig. 7.4, such solutions lie above the 'universal' curve of the neutral atom. Now the total charge inside a sphere of radius $r = bx$ is just

$$Ze - 4\pi e \int_0^r \rho(r')r'^2 \, \mathrm{d}r' = Ze[\chi(x) - x\chi'(x)] \qquad [7.79]$$

Thus, at the point $r_1 = bx_1$, where

$$\chi(x_1) - x_1\chi'(x_1) = 0 \qquad [7.80]$$

the total charge inside the sphere $r = r_1$ vanishes, and we note that the tangent to $\chi(x)$ at $x = x_1$ passes through the origin (see Fig. 7.4). For $x \leqslant x_1$, the curve $\chi(x)$ therefore corresponds to a neutral atom having a finite boundary at $r = r_1$,

[6] Negative ions cannot be handled by the Thomas–Fermi theory.

where the density $\rho(r)$ does not vanish. This may be interpreted as a representation of a *neutral atom under pressure* [7].

7.4 THE HARTREE–FOCK METHOD AND THE SELF-CONSISTENT FIELD

We shall now study a more elaborate approximation for complex atoms (ions), known as the *Hartree–Fock* or *self-consistent field* method. The starting point of this approach, formulated by Hartree in 1928, is the *independent particle model*, discussed in Section 7.1, according to which each electron moves in an effective potential which takes into account the attraction of the nucleus and the average effect of the repulsive interactions due to the other electrons. Each electron in a multielectron system is then described by its own wave function. By using intuitive arguments, Hartree was able to write down equations for the individual electron wave functions. He also proposed an original iterative procedure, based on the requirement of *self-consistency*, to solve his equations. We shall return shortly to this self-consistent procedure, which is a key feature of the theory of many-electron atoms discussed in this section.

As we shall show at the end of this section, the Hartree total wave function for the atom (ion) is not antisymmetric in the electron coordinates. The generalisation of the Hartree method which takes into account this antisymmetry requirement – imposed by the Pauli exclusion principle – was carried out in 1930 by Fock and Slater. It is this generalisation of Hartree's theory, known as the *Hartree–Fock* method, which we now discuss.

The Hartree–Fock equations

In the Hartree–Fock approach, it is assumed, in accordance with the independent particle approximation and the Pauli exclusion principle, that the N-electron wave function is a *Slater determinant* Φ, or in other words an antisymmetric product of individual electron spin–orbitals. The optimum Slater determinant is then obtained by using the *variational method* to determine the 'best' individual electron spin–orbitals. The Hartree–Fock method is therefore a particular case of the variational method, in which the trial function for the N-electron atom is a Slater determinant whose individual spin–orbitals are optimised. It should be noted that the N-electron atom wave function $\Psi(q_1, q_2, \ldots q_N)$, solution of the Schrödinger equation [7.3], can only be represented by an infinite sum of Slater determinants, so that the Hartree–Fock method may be considered as a first step in the determination of atomic wave functions and energies. We also remark that the application of the Hartree–Fock method is not confined to atoms (ions), but can also be made to other systems such as the electrons in a molecule or a solid.

[7] We are not considering ions under pressure, since in dealing with an ensemble of such ions, difficulties due to the presence of the Coulomb forces between ions would arise.

In what follows we shall limit our discussion to the *ground state* of an atom or ion having N electrons [8]. We start from the non-relativistic Hamiltonian [7.2], which we write (in a.u.) as

$$H = H_1 + H_2 \qquad [7.81]$$

where

$$H_1 = \sum_{i=1}^{N} \hat{h}_i, \qquad [7.82]$$

$$\hat{h}_i = -\frac{1}{2}\nabla_{r_i}^2 - \frac{Z}{r_i} \qquad [7.83]$$

and

$$H_2 = \sum_{i<j=1}^{N} \frac{1}{r_{ij}}, \qquad r_{ij} = |\mathbf{r}_i - \mathbf{r}_j| \qquad [7.84]$$

The first term of [7.81], H_1, is the sum of the N identical *one-body* Hamiltonians $\hat{h}_i$, each individual Hamiltonian $\hat{h}_i$ containing the kinetic energy operator of an electron and its potential energy due to the attraction of the nucleus. The second term, H_2, is the sum of $N(N-1)/2$ identical terms $1/r_{ij}$ which represent the *two-body* interactions between each pair of electrons.

Let us denote by E_0 the ground state energy of the system. According to the variational method (see Section 2.8) we have

$$E_0 \leqslant E[\Phi] = \langle\Phi|H|\Phi\rangle \qquad [7.85]$$

where Φ is a trial function which we assume to be normalised to unity,

$$\langle\Phi|\Phi\rangle = 1 \qquad [7.86]$$

In the Hartree–Fock method the trial function Φ is a Slater determinant, so that (see [7.22])

$$\Phi(q_1, q_2, \ldots q_N) = \frac{1}{\sqrt{N!}} \begin{vmatrix} u_\alpha(q_1) & u_\beta(q_1) & \cdots & u_\nu(q_1) \\ u_\alpha(q_2) & u_\beta(q_2) & \cdots & u_\nu(q_2) \\ \vdots & & & \\ u_\alpha(q_N) & u_\beta(q_N) & \cdots & u_\nu(q_N) \end{vmatrix} \qquad [7.87]$$

where we recall that each of the symbols $\alpha, \beta \ldots \nu$ represents a set of four quantum numbers (n, l, m_l, m_s). We require that all spin-orbitals be

[8] The derivation of the Hartree–Fock equations given here follows the treatment of Messiah (1968).

orthonormal, namely

$$\langle u_\mu | u_\lambda \rangle = \int u_\mu^\star(q) u_\lambda(q) \, dq = \delta_{\lambda\mu} \qquad [7.88]$$

where the symbol $\int dq$ implies an integration over the space coordinates and a summation over the spin coordinate. Since spin–orbitals corresponding to 'spin up' ($m_s = +1/2$) are automatically orthogonal to those corresponding to 'spin' down' ($m_s = -1/2$), the requirement [7.88] reduces to the condition that the space orbitals corresponding to the same spin function be orthonormal. We note that [7.88] ensures that the Slater determinant [7.87] satisfies the normalisation condition [7.86].

It is convenient to rewrite the Slater determinant [7.87] in the more compact form [7.23]. That is

$$\begin{aligned}\Phi(q_1, q_2, \ldots q_N) &= \frac{1}{\sqrt{N!}} \sum_P (-1)^P P u_\alpha(q_1) u_\beta(q_2) \cdots u_\nu(q_N) \\ &= \sqrt{N!} \mathscr{A} \Phi_H \qquad [7.89]\end{aligned}$$

where Φ_H is the simple product of spin–orbitals

$$\Phi_H(q_1, q_2, \ldots q_N) = u_\alpha(q_1) u_\beta(q_2) \cdots u_\nu(q_N) \qquad [7.90]$$

which will be referred to as a Hartree wave function. The operator which appears in [7.89] is the antisymmetrisation operator

$$\mathscr{A} = \frac{1}{N!} \sum_P (-1)^P P \qquad [7.91]$$

It is a simple matter to show that the operator $\mathscr{A}$ is Hermitian and that it is also a projection operator, namely

$$\mathscr{A}^2 = \mathscr{A} \qquad [7.92]$$

A further remark, which will be useful shortly, is that both operators H_1 and H_2 are invariant under permutations of the electron coordinates, and hence commute with $\mathscr{A}$,

$$[H_1, \mathscr{A}] = [H_2, \mathscr{A}] = 0 \qquad [7.93]$$

Let us now calculate the functional $E[\Phi]$. Using [7.81] and [7.85], we have

$$E[\Phi] = \langle \Phi | H_1 | \Phi \rangle + \langle \Phi | H_2 | \Phi \rangle \qquad [7.94]$$

The first expectation value $\langle \Phi | H_1 | \Phi \rangle$ is readily evaluated as follows. We first have

$$\begin{aligned}\langle \Phi | H_1 | \Phi \rangle &= N! \langle \Phi_H | \mathscr{A} H_1 \mathscr{A} | \Phi_H \rangle \\ &= N! \langle \Phi_H | H_1 \mathscr{A}^2 | \Phi_H \rangle \\ &= N! \langle \Phi_H | H_1 \mathscr{A} | \Phi_H \rangle \qquad [7.95]\end{aligned}$$

where we have used [7.89], [7.92] and [7.93]. Taking into account the fact that H_1 is the sum of one-body operators (see [7.82]) together with [7.88], [7.90] and

[7.91] we then find that

$$\langle\Phi|H_1|\Phi\rangle = \sum_{i=1}^{N}\sum_{P}(-1)^P\langle\Phi_{\rm H}|\hat{h}_i P|\Phi_{\rm H}\rangle$$
$$= \sum_{i=1}^{N}\langle\Phi_{\rm H}|\hat{h}_i|\Phi_{\rm H}\rangle$$
$$= \sum_{\lambda}\langle u_\lambda(q_i)|\hat{h}_i|u_\lambda(q_i)\rangle, \qquad \lambda = \alpha, \beta, \ldots \nu \tag{7.96}$$

where the sum on λ runs over the N individual quantum states (i.e. the N spin orbitals) occupied by the electrons.

Defining

$$I_\lambda = \langle u_\lambda(q_i)|\hat{h}_i|u_\lambda(q_i)\rangle \tag{7.97}$$

to be the average value of the individual Hamiltonian $\hat{h}_i$ relative to the spin orbital u_λ, we have

$$\langle\Phi|H_1|\Phi\rangle = \sum_\lambda I_\lambda \tag{7.98}$$

The second expectation value $\langle\Phi|H_2|\Phi\rangle$ can be calculated in a similar way. From [7.89], [7.92] and [7.93], we have

$$\begin{aligned}\langle\Phi|H_2|\Phi\rangle &= N!\langle\Phi_{\rm H}|\mathscr{A}H_2\mathscr{A}|\Phi_{\rm H}\rangle\\ &= N!\langle\Phi_{\rm H}|H_2\mathscr{A}^2|\Phi_{\rm H}\rangle\\ &= N!\langle\Phi_{\rm H}|H_2\mathscr{A}|\Phi_{\rm H}\rangle\end{aligned} \tag{7.99}$$

Using [7.91] and the fact that H_2 is the sum [7.84] of two-body operators, we obtain

$$\langle\Phi|H_2|\Phi\rangle = \sum_{i<j}\sum_{P}(-1)^P\left\langle\Phi_H\left|\frac{1}{r_{ij}}P\right|\Phi_{\rm H}\right\rangle$$
$$= \sum_{i<j}\left\langle\Phi_{\rm H}\left|\frac{1}{r_{ij}}(1-P_{ij})\right|\Phi_{\rm H}\right\rangle \tag{7.100}$$

where P_{ij} is an operator that interchanges the coordinates (spatial and spin) of the electrons i and j. Hence, taking into account [7.88] and [7.90], we find that

$$\langle\Phi|H_2|\Phi\rangle = \sum_{\substack{\lambda,\mu\\ \text{(all pairs)}}}\left[\left\langle u_\lambda(q_i)u_\mu(q_j)\left|\frac{1}{r_{ij}}\right|u_\lambda(q_i)u_\mu(q_j)\right\rangle - \left\langle u_\lambda(q_i)u_\mu(q_j)\left|\frac{1}{r_{ij}}\right|u_\mu(q_i)u_\lambda(q_j)\right\rangle\right] \tag{7.101}$$

where the sum over λ and μ runs over the $N(N-1)/2$ pairs of orbitals. We may also write [7.101] as

$$\langle\Phi|H_2|\Phi\rangle = \frac{1}{2}\sum_{\lambda}\sum_{\mu}\left[\left\langle u_\lambda(q_i)u_\mu(q_j)\left|\frac{1}{r_{ij}}\right|u_\lambda(q_i)u_\mu(q_j)\right\rangle - \left\langle u_\lambda(q_i)u_\mu(q_j)\left|\frac{1}{r_{ij}}\right|u_\mu(q_i)u_\lambda(q_j)\right\rangle\right]$$

$$\lambda,\ \mu = \alpha,\ \beta,\ \ldots\ \nu \qquad [7.102]$$

Let us define the *direct* term

$$\mathcal{J}_{\lambda\mu} = \left\langle u_\lambda(q_i)u_\mu(q_j)\left|\frac{1}{r_{ij}}\right|u_\lambda(q_i)u_\mu(q_j)\right\rangle \qquad [7.103]$$

which is the average value of the interaction $1/r_{ij}$ relative to the state $u_\lambda(q_i)u_\mu(q_j)$ such that electron i is in the spin orbital u_λ and electron j in the spin orbital u_μ. We also introduce the *exchange* term

$$K_{\lambda\mu} = \left\langle u_\lambda(q_i)u_\mu(q_j)\left|\frac{1}{r_{ij}}\right|u_\mu(q_i)u_\lambda(q_j)\right\rangle \qquad [7.104]$$

which is the matrix element of the interaction $1/r_{ij}$ between the two states $u_\lambda(q_i)u_\mu(q_j)$ and $u_\mu(q_i)u_\lambda(q_j)$ obtained by interchanging the electrons i and j. We note that both $\mathcal{J}_{\lambda\mu}$ and $K_{\lambda\mu}$ are real; they are also symmetric in λ and μ,

$$\mathcal{J}_{\lambda\mu} = \mathcal{J}_{\mu\lambda} \qquad K_{\lambda\mu} = K_{\mu\lambda} \qquad [7.105]$$

In terms of $\mathcal{J}_{\lambda\mu}$ and $K_{\lambda\mu}$, [7.102] reads

$$\langle\Phi|H_2|\Phi\rangle = \frac{1}{2}\sum_{\lambda}\sum_{\mu}[\mathcal{J}_{\lambda\mu} - K_{\lambda\mu}] \qquad [7.106]$$

Using [7.94], [7.98] and [7.106], the total energy $E[\Phi]$ is seen to be given by

$$E[\Phi] = \sum_{\lambda} I_\lambda + \frac{1}{2}\sum_{\lambda}\sum_{\mu}[\mathcal{J}_{\lambda\mu} - K_{\lambda\mu}] \qquad [7.107]$$

Having obtained the functional $E[\Phi]$, we now proceed to the second step of the calculation, which consists in expressing that $E[\Phi]$ is stationary with respect to variations of the spin orbitals $u_\lambda(\lambda = \alpha, \beta, \ldots \nu)$, subject to the N^2 conditions [7.88] imposed by the orthonormality requirement on the u_λ's. To satisfy these conditions we introduce N^2 Lagrange multipliers which we denote by $\varepsilon_{\lambda\mu}$ $(\lambda, \mu = \alpha, \beta, \ldots \nu)$. The variational equation then reads

$$\delta E - \sum_{\lambda}\sum_{\mu}\varepsilon_{\lambda\mu}\,\delta\langle u_\mu|u_\lambda\rangle = 0 \qquad [7.108]$$

It is readily seen from [7.108] that $\varepsilon_{\lambda\mu} = \varepsilon^{\star}_{\mu\lambda}$, so that the N^2 Lagrange multipliers may be considered as the elements of a Hermitian matrix.

It is convenient at this point to make a unitary transformation on the spin-orbitals u_λ, namely

$$u'_\lambda = \sum_\mu U_{\mu\lambda} u_\mu \tag{7.109}$$

where $U_{\mu\lambda}$ are the elements of a $N \times N$ unitary matrix. The new Slater determinant Φ' formed with the spin-orbitals u'_λ differs from the previous one only by a phase factor, since

$$\Phi' = (\det U)\Phi \tag{7.110}$$

and $|\det U| = 1$ because U is unitary. Moreover, the functional $E[\Phi] = \langle\Phi|H|\Phi\rangle$ is clearly unaffected by this unitary transformation. Since any Hermitian matrix can be diagonalised by a unitary transformation, we may always choose U in such a way that the matrix $\varepsilon_{\lambda\mu}$ of Lagrange multipliers will become a *diagonal* matrix having elements $E_\lambda\, \delta_{\lambda\mu}$. In what follows we shall assume that this diagonalisation has already been made from the outset, so that the variational equation [7.108] then reads

$$\delta E - \sum_\lambda E_\lambda\, \delta\langle u_\lambda|u_\lambda\rangle = 0 \tag{7.111}$$

Let us now vary with respect to the spin-orbitals u_λ. Proceeding as in Section 2.8, and using the expression [7.107] of $E[\Phi]$ together with the relations [7.83], [7.97], [7.103] and [7.104], we find for the N spin-orbitals $u_\alpha, u_\beta, \ldots u_\nu$ the system of integro-differential equations

$$\begin{gathered}\left[-\frac{1}{2}\nabla^2_{r_i} - \frac{Z}{r_i}\right] u_\lambda(q_i) + \left[\sum_\mu \int u^\star_\mu(q_j)\,\frac{1}{r_{ij}}\,u_\mu(q_j)\,\mathrm{d}q_j\right] u_\lambda(q_i) \\ - \sum_\mu \left[\int u^\star_\mu(q_j)\,\frac{1}{r_{ij}}\,u_\lambda(q_j)\,\mathrm{d}q_j\right] u_\mu(q_i) = E_\lambda u_\lambda(q_i) \\ \lambda, \mu = \alpha, \beta, \ldots \nu\end{gathered} \tag{7.112}$$

where the summation over μ extends over the N occupied spin-orbitals. We recall that the symbol $\int \mathrm{d}q_j$ implies an integration over the spatial coordinates $\mathbf{r}_j$ and a summation over the spin-coordinate of electron j. The equations [7.112] are known as the *Hartree–Fock equations*. Writing the spin-orbitals $u_\lambda(q_i)$ as

$$u_\lambda(q_i) = u_\lambda(\mathbf{r}_i)\chi_{1/2,m_s^\lambda} \tag{7.113}$$

and using the orthonormality property of the spin functions, namely

$$\langle\chi_{1/2,m_s^\lambda}|\chi_{1/2,m_s^\mu}\rangle = \delta_{m_s^\lambda, m_s^\mu} \tag{7.114}$$

we can also write the Hartree–Fock equations in a form that involves only the

spatial part of the spin-orbitals. That is,

$$\left[-\frac{1}{2}\nabla^2_{r_i} - \frac{Z}{r_i}\right]u_\lambda(\mathbf{r}_i) + \left[\sum_\mu \int u^\star_\mu(\mathbf{r}_j)\frac{1}{r_{ij}}u_\mu(\mathbf{r}_j)\,\mathrm{d}\mathbf{r}_j\right]u_\lambda(\mathbf{r}_i)$$
$$- \sum_\mu \delta_{m_s^\lambda, m_s^\mu}\left[\int u^\star_\mu(\mathbf{r}_j)\frac{1}{r_{ij}}u_\lambda(\mathbf{r}_j)\,\mathrm{d}\mathbf{r}_j\right]u_\mu(\mathbf{r}_i) = E_\lambda u_\lambda(\mathbf{r}_i)$$
$$\lambda, \mu = \alpha, \beta, \ldots \nu \qquad [7.115]$$

A more compact form of the Hartree–Fock equations may be written down in the following way. We define the *direct* operator

$$V^{\mathrm{d}}_\mu(q_i) = \int u^\star_\mu(q_j)\frac{1}{r_{ij}}u_\mu(q_j)\,\mathrm{d}q_j$$
$$= \int u^\star_\mu(\mathbf{r}_j)\frac{1}{r_{ij}}u_\mu(\mathbf{r}_j)\,\mathrm{d}\mathbf{r}_j \equiv V^{\mathrm{d}}_\mu(\mathbf{r}_i) \qquad [7.116]$$

which is just the electrostatic repulsion potential due to electron j, when the position of this electron is averaged over the orbital u_μ. We also define the *exchange* (non-local) operator $V^{\mathrm{ex}}_\mu(q_i)$ such that

$$V^{\mathrm{ex}}_\mu(q_i)f(q_i) = \left[\int u^\star_\mu(q_j)\frac{1}{r_{ij}}f(q_j)\,\mathrm{d}q_j\right]u_\mu(q_i) \qquad [7.117]$$

where $f(q_i)$ is an arbitrary function. In particular, when acting on a spin-orbital $u_\lambda(q_i)$, we see that the exchange operator V^{ex}_μ yields

$$V^{\mathrm{ex}}_\mu(q_i)\,u_\lambda(q_i) = \left[\int u^\star_\mu(q_j)\frac{1}{r_{ij}}u_\lambda(q_j)\,\mathrm{d}q_j\right]u_\mu(q_i)$$
$$= \delta_{m_s^\lambda, m_s^\mu}\left[\int u^\star_\mu(\mathbf{r}_j)\frac{1}{r_{ij}}u_\lambda(\mathbf{r}_j)\,\mathrm{d}\mathbf{r}_j\right]u_\mu(\mathbf{r}_i)\,\chi_{1/2, m_s^\mu}$$
$$= \delta_{m_s^\lambda, m_s^\mu}V^{\mathrm{ex}}_\mu(\mathbf{r}_i)u_\lambda(\mathbf{r}_i)\chi_{1/2, m_s^\mu} \qquad [7.118]$$

where the exchange operator $V^{\mathrm{ex}}_\mu(\mathbf{r}_i)$ only acts on the spatial coordinates, and is defined by

$$V^{\mathrm{ex}}_\mu(\mathbf{r}_i)f(\mathbf{r}_i) = \left[\int u^\star_\mu(\mathbf{r}_j)\frac{1}{r_{ij}}f(\mathbf{r}_j)\,\mathrm{d}\mathbf{r}_j\right]u_\mu(\mathbf{r}_i) \qquad [7.119]$$

$f(\mathbf{r}_i)$ being an arbitrary function. Using [7.116] and [7.117], the Hartree–Fock equations become

$$\left[-\frac{1}{2}\nabla^2_{r_i} - \frac{Z}{r_i} + \sum_\mu V^{\mathrm{d}}_\mu(\mathbf{r}_i) - \sum_\mu V^{\mathrm{ex}}_\mu(q_i)\right]u_\lambda(q_i) = E_\lambda u_\lambda(q_i) \qquad [7.120]$$

or

$$\left[-\frac{1}{2}\nabla_{r_i}^2 - \frac{Z}{r_i} + \mathcal{V}^{\mathrm{d}}(\mathbf{r}_i) - \mathcal{V}^{\mathrm{ex}}(q_i)\right] u_\lambda(q_i) = E_\lambda u_\lambda(q_i) \qquad [7.121]$$

where we have introduced the *direct* and *exchange* potentials

$$\mathcal{V}^{\mathrm{d}}(\mathbf{r}_i) = \sum_\mu V_\mu^{\mathrm{d}}(\mathbf{r}_i) \qquad [7.122a]$$

and

$$\mathcal{V}^{\mathrm{ex}}(q_i) = \sum_\mu V_\mu^{\mathrm{ex}}(q_i) \qquad [7.122b]$$

It is also interesting to write the Hartree–Fock equations in terms of the *density matrix*

$$\rho(q_i, q_j) = \sum_\mu u_\mu(q_i) u_\mu^\star(q_j) \qquad [7.123]$$

or the corresponding spinless density matrix

$$\rho(\mathbf{r}_i, \mathbf{r}_j) = \sum_\mu u_\mu(\mathbf{r}_i) u_\mu^\star(\mathbf{r}_j) \qquad [7.124]$$

The diagonal elements $\rho(q_i, q_i)$ and $\rho(\mathbf{r}_i, \mathbf{r}_i)$ of these density matrices will be denoted by $\rho(q_i)$ and $\rho(\mathbf{r}_i)$, respectively. We note that

$$\rho(\mathbf{r}) = \sum_\mu |u_\mu(\mathbf{r})|^2 \qquad [7.125]$$

gives the probability density of finding an electron at the point $\mathbf{r}$. In terms of the density matrices, we have

$$\mathcal{V}^{\mathrm{d}}(\mathbf{r}_i) = \int \rho(\mathbf{r}_j) \frac{1}{r_{ij}} \,\mathrm{d}\mathbf{r}_j \qquad [7.126]$$

and

$$\begin{aligned}\mathcal{V}^{\mathrm{ex}}(q_i) u_\lambda(q_i) &= \int \rho(q_i, q_j) \frac{1}{r_{ij}} u_\lambda(q_j)\,\mathrm{d}q_j \\ &= \delta_{m_s^\lambda, m_s^\mu}\left[\int \rho(\mathbf{r}_i, \mathbf{r}_j) \frac{1}{r_{ij}} u_\lambda(\mathbf{r}_j)\,\mathrm{d}\mathbf{r}_j\right] \chi_{1/2, m_s^\mu} \qquad [7.127]\end{aligned}$$

Finally, if we define the full Hartree–Fock potential as

$$\begin{aligned}\mathcal{V}(q_i) &= -\frac{Z}{r_i} + \sum_\mu V_\mu^{\mathrm{d}}(\mathbf{r}_i) - \sum_\mu V_\mu^{\mathrm{ex}}(q_i) \\ &= -\frac{Z}{r_i} + \mathcal{V}^{\mathrm{d}}(\mathbf{r}_i) - \mathcal{V}^{\mathrm{ex}}(q_i) \qquad [7.128]\end{aligned}$$

the Hartree–Fock equations take the (deceptively) simple form

$$\left[-\frac{1}{2}\nabla_{r_i}^2 + \mathcal{V}(q_i)\right] u_\lambda(q_i) = E_\lambda u_\lambda(q_i) \qquad [7.129]$$

Physical interpretation of the Hartree–Fock equations. Self-consistent field. Koopman's theorem

A striking feature of the Hartree–Fock equations [7.129] is that they look similar to individual Schrödinger eigenvalue equations for each of the spin orbitals u_λ. They are *not* genuine eigenvalue equations, however, since the Hartree–Fock potential $\mathcal{V}$ depends on the spin-orbitals themselves through the operators V_μ^{d} and V_μ^{ex}. In fact, to solve the system of Hartree–Fock integro-differential equations, one proceeds by *iteration*. Starting from approximate individual spin-orbitals [9] $u_\alpha^{(1)}, u_\beta^{(1)}, \ldots u_\nu^{(1)}$, one first calculates the corresponding approximate expression $\mathcal{V}^{(1)}$ of the Hartree–Fock potential. The Hartree–Fock equations are then solved with this potential $\mathcal{V}^{(1)}$ to obtain new spin-orbitals $u_\alpha^{(2)}, u_\beta^{(2)}, \ldots u_\nu^{(2)}$, which in turn yield a new potential $\mathcal{V}^{(2)}$. This procedure is then repeated until the final spin-orbitals give a potential $\mathcal{V}^{(n)}$ which is identical (within the desired approximation) to the potential $\mathcal{V}^{(n-1)}$ obtained from the preceding cycle. The Hartree–Fock potential determined in this way is known as the *self-consistent field* of the atom (ion).

Despite the fact that the Hartree–Fock equations [7.129] are not true eigenvalue equations, we shall now show that, when acting on the spin-orbital u_λ, the individual Hartree–Fock Hamiltonian

$$h_{\mathrm{HF}} = -\tfrac{1}{2}\nabla_{r_i}^2 + \mathcal{V}(q_i) \tag{7.130}$$

may be interpreted as the energy operator of an electron in the state u_λ. To obtain this result, which is in accord with our basic independent-particle approximation, we first note from [7.116] and [7.117] that

$$V_\lambda^{\mathrm{d}}(q_i)u_\lambda(q_i) = V_\lambda^{\mathrm{ex}}(q_i)u_\lambda(q_i) \tag{7.131}$$

Upon returning to the Hartree–Fock equations [7.120], we see that there is no self-energy ($\mu = \lambda$) contribution to the potential. It is therefore convenient to introduce the modified density matrix

$$\rho_\lambda(q_i, q_j) = \sum_{\mu \neq \lambda} u_\mu(q_i)u_\mu^\star(q_j) \tag{7.132}$$

and the corresponding modified spinless density matrix

$$\rho_\lambda(\mathbf{r}_i, \mathbf{r}_j) = \sum_{\mu \neq \lambda} u_\mu(\mathbf{r}_i)u_\mu^\star(\mathbf{r}_j) \tag{7.133}$$

whose diagonal elements will be denoted as $\rho_\lambda(q_i)$ and $\rho_\lambda(\mathbf{r}_i)$, respectively. We remark that

$$\rho_\lambda(\mathbf{r}) = \sum_{\mu \neq \lambda} |u_\mu(\mathbf{r})|^2 \tag{7.134}$$

is the probability density of finding an electron at $\mathbf{r}$ in one of the $(N-1)$ occupied states other than u_λ. We also define the modified direct and exchange

[9] Simple approximate spin-orbitals may be obtained by using screening arguments such as those discussed in Section 7.1. We shall also see below that the solutions of the Hartree equations can be used to provide a set of functions $u_\alpha^{(1)}, u_\beta^{(1)}, \ldots u_\nu^{(1)}$.

potentials

$$\mathcal{V}_\lambda^{\mathrm{d}}(\mathbf{r}_i) = \sum_{\mu \neq \lambda} V_\mu^{\mathrm{d}}(\mathbf{r}_i)$$
$$= \int \rho_\lambda(\mathbf{r}_j) \frac{1}{r_{ij}} \, \mathrm{d}\mathbf{r}_j \qquad [7.135]$$

and

$$\mathcal{V}_\lambda^{\mathrm{ex}}(q_i) = \sum_{\mu \neq \lambda} V_\mu^{\mathrm{ex}}(q_i) \qquad [7.136]$$

with

$$\mathcal{V}_\lambda^{\mathrm{ex}}(q_i) u_\lambda(q_i) = \int \rho_\lambda(q_i, q_j) \frac{1}{r_{ij}} u_\lambda(q_j) \, \mathrm{d}q_j$$
$$= \delta_{m_s^\lambda, m_s^\mu} \left[\int \rho_\lambda(\mathbf{r}_i, \mathbf{r}_j) \frac{1}{r_{ij}} u_\lambda(\mathbf{r}_j) \, \mathrm{d}\mathbf{r}_j \right] \chi_{1/2, m_s^\mu} \qquad [7.137]$$

so that the Hartree–Fock equations [7.121] now read

$$h_{\mathrm{HF}}\, u_\lambda(q_i) \equiv \left[-\frac{1}{2} \nabla_{r_i}^2 - \frac{Z}{r_i} + \mathcal{V}_\lambda^{\mathrm{d}}(\mathbf{r}_i) - \mathcal{V}_\lambda^{\mathrm{ex}}(q_i) \right] u_\lambda(q_i) = E_\lambda u_\lambda(q_i) \quad [7.138]$$

In addition to the kinetic energy term $-\nabla_{r_i}^2/2$ and the nuclear attraction term $-Z/r_i$, we see that the individual Hamiltonian h_{HF} contains a term $\mathcal{V}_\lambda^{\mathrm{d}}(\mathbf{r}_i)$ which represents the *average potential* due to the presence of the $(N-1)$ other electrons, and a (non-local) *exchange term* $\mathcal{V}_\lambda^{\mathrm{ex}}(q_i)$ which takes into account the exchange effects between the state u_λ and the $(N-1)$ other states occupied by the electrons. We may therefore interpret h_{HF} in [7.138] as the energy operator of the electron in the state u_λ.

According to this interpretation, the quantity E_λ has the meaning of a one-electron eigenvalue. To give a more precise significance to E_λ, we first remark that upon taking the scalar product of [7.112] with u_λ and using [7.97], [7.103] and [7.104] we find that

$$E_\lambda = I_\lambda + \sum_\mu [\mathcal{J}_{\lambda\mu} - K_{\lambda\mu}] \qquad [7.139]$$

Summing over λ, we then have

$$\sum_\lambda E_\lambda = \sum_\lambda I_\lambda + \sum_\lambda \sum_\mu [\mathcal{J}_{\lambda\mu} - K_{\lambda\mu}]$$
$$= \langle \Phi | H_1 | \Phi \rangle + 2 \langle \Phi | H_2 | \Phi \rangle \qquad [7.140]$$

where we have used [7.98] and [7.106]. We may also rewrite [7.140] as

$$E[\Phi] = \sum_\lambda E_\lambda - \langle \Phi | H_2 | \Phi \rangle \qquad [7.141]$$

and we see that the total energy is *not* the sum of the individual energies. This is because in summing the individual electron energies, each kinetic energy and each interaction energy with the nucleus is counted once, while the mutual

interaction energy, which has the average value $\langle\Phi|H_2|\Phi\rangle$ is counted twice. The total energy must therefore be obtained by subtracting $\langle\Phi|H_2|\Phi\rangle$ from the sum of individual energies as expressed in [7.141].

Let us now imagine that the electron λ is removed from the N-electron system. For example, if the original system was a neutral atom, we now have a positive ion with $(N - 1)$ electrons. If we assume that the orbitals of the $(N - 1)$-electron system are the same as these of the N-electron system, we see from [7.107] that the difference between the total energy of the two systems is

$$\begin{aligned} E_N - E_{N-1} &= I_\lambda + \sum_\mu [\mathcal{J}_{\lambda\mu} - K_{\lambda\mu}] \\ &= E_\lambda \end{aligned} \qquad [7.142]$$

Thus the quantity E_λ represents approximatively the energy required to remove an electron from the spin-orbital u_λ, or in other words the *ionisation energy* of electron λ. This result is known as *Koopman's theorem*. It is worth stressing that the identification of E_λ with the ionisation energy of the electron λ is not rigorous, since the readjustment of the orbitals of the $(N - 1)$ electron system, which occurs after the removal of an electron, has been ignored. We also remark that although E_N and E_{N-1} are upper bounds to the true ground state energy of the N-electron and the $(N - 1)$-electron systems (see [7.85]), the quantity E_λ is not an upper bound for the ionisation energy, since we have taken the difference of two upper bounds.

Properties of the Hartree–Fock potentials and spin-orbitals

Let us return to the Hartree–Fock equations [7.129]. We see that *for a given state* of the atom or ion (here the ground state), characterised by the occupied spin-orbitals, all the electrons move in the *same* Hartree–Fock potential. Moreover, for a given potential, two spin-orbitals u_λ and $u_{\lambda'}$ corresponding to different individual energies $E_\lambda \neq E_{\lambda'}$ are easily shown to be *orthogonal*. Indeed, if we take the scalar product of [7.112] with $u_{\lambda'}(q_i)$, we find that

$$\left\langle u_{\lambda'}(q_i)\left| -\frac{1}{2}\nabla^2_{r_i} - \frac{Z}{r_i}\right| u_\lambda(q_i)\right\rangle + \sum_\mu \left\langle u_{\lambda'}(q_i)u_\mu(q_j)\left|\frac{1}{r_{ij}}\right| u_\mu(q_j)u_\lambda(q_i)\right\rangle - \sum_\mu \left\langle u_{\lambda'}(q_i)u_\mu(q_j)\left|\frac{1}{r_{ij}}\right| u_\mu(q_i)u_\lambda(q_j)\right\rangle = E_\lambda\langle u_{\lambda'}(q_i)|u_\lambda(q_i)\rangle \qquad [7.143]$$

Similarly, from the Hartree–Fock equation satisfied by $u_{\lambda'}(q_i)$ and the fact that the Hamiltonian [7.2] is Hermitian, we deduce that

$$\left\langle u_{\lambda'}(q_i)\left| -\frac{1}{2}\nabla^2_{r_i} - \frac{Z}{r_i}\right| u_\lambda(q_i)\right\rangle + \sum_\mu \left\langle u_{\lambda'}(q_i)u_\mu(q_j)\left|\frac{1}{r_{ij}}\right| u_\lambda(q_i)u_\mu(q_j)\right\rangle - \sum_\mu \left\langle u_{\lambda'}(q_i)u_\mu(q_j)\left|\frac{1}{r_{ij}}\right| u_\mu(q_i)u_\lambda(q_j)\right\rangle = E_{\lambda'}\langle u_{\lambda'}(q_i)|u_\lambda(q_i)\rangle \qquad [7.144]$$

Hence, upon subtracting [7.144] from [7.143], we have

$$(E_\lambda - E_{\lambda'})\langle u_{\lambda'}(q_i)|u_\lambda(q_i)\rangle = 0 \qquad [7.145]$$

so that

$$\langle u_{\lambda'}|u_\lambda\rangle = 0, \qquad E_\lambda \neq E_{\lambda'} \qquad [7.146]$$

We shall now show that for atoms or ions with *closed subshells* (such as He, Li^+, Be, B^+, C^{2+}, Ne, etc.) the Hartree–Fock potential is *spherically symmetric*, so that the electron spatial orbitals are solutions of a *central field* problem. To see this we first note that in the case of closed subshells the N spin-orbitals (with N even) are obtained from $N' = N/2$ spatial orbitals. Each of these N' spatial orbitals occurs twice in the Slater determinant [7.87], once with spin 'up' (α) and once with spin 'down' (β). The simplest example is that of helium, where there is only one spatial orbital $u_{100} \equiv u_{1s}$ (see [7.26]).

In order to prove the above statement, we shall assume that the N' spatial orbitals are of the form

$$u_{nlm}(\mathbf{r}) = r^{-1}P_{nl}(r)Y_{lm}(\theta, \phi) \qquad [7.147]$$

where we have set

$$P_{nl}(r) = rR_{nl}(r) \qquad [7.148]$$

and we shall then show that the resulting Hartree–Fock potential $\mathcal{V}$ is spherically symmetric. Remembering that $\mathcal{V}$ contains the (central) nuclear attraction term $-Z/r_i$, the 'direct' potential $\mathcal{V}^{\mathrm{d}}$ and the 'exchange' potential $\mathcal{V}^{\mathrm{ex}}$ (see [7.128]) we first look at the direct potential $\mathcal{V}^{\mathrm{d}}$. Using [7.116], [7.122a], [7.147] and [7.148], the part of $\mathcal{V}^{\mathrm{d}}$ coming from a complete subshell $(n'l')$ is seen to be

$$\begin{aligned}\mathcal{V}^{\mathrm{d}}_{n'l'} &= 2\sum_{m'=-l'}^{+l'} \int |u_{n'l'm'}(\mathbf{r}_j)|^2 \frac{1}{r_{ij}}\,\mathrm{d}\mathbf{r}_j \\ &= 2\int |P_{n'l'}(r_j)|^2 \frac{1}{r_{ij}} \sum_{m'=-l'}^{+l'} |Y_{l'm'}(\theta_j, \phi_j)|^2\,\mathrm{d}r_j\,\mathrm{d}\Omega_j \end{aligned} \qquad [7.149]$$

where the factor of 2 arises from the two spin orientations, and $\mathrm{d}\Omega_j \equiv \sin\theta_j\,\mathrm{d}\theta_j\,\mathrm{d}\phi_j$. Using the addition theorem of the spherical harmonics (see equation [A4.23] of Appendix 4) we have

$$\sum_{m'=-l'}^{+l'} |Y_{l'm'}(\theta_j, \phi_j)|^2 = \frac{2l'+1}{4\pi} \qquad [7.150]$$

so that

$$\mathcal{V}^{\mathrm{d}}_{n'l'} = \frac{2(2l'+1)}{4\pi}\int |P_{n'l'}(r_j)|^2 \frac{1}{r_{ij}}\,\mathrm{d}r_j\,\mathrm{d}\Omega_j \qquad [7.151]$$

The integrals on the angular variables (θ_j, ϕ_j) can readily be performed by expanding the quantity $1/r_{ij}$ in spherical harmonics and using the fact that the

function $P_{n'l'}(r_j)$ does not depend on the angles. Writing (see [A4.25])

$$\frac{1}{r_{ij}} = \sum_{l=0}^{\infty} \sum_{m=-l}^{+l} \frac{4\pi}{2l+1} \frac{(r_<)^l}{(r_>)^{l+1}} Y^{\star}_{lm}(\theta_i, \phi_i) Y_{lm}(\theta_j, \phi_j) \qquad [7.152]$$

where $r_<$ is the smaller and $r_>$ the larger of r_i and r_j, and proceeding as in Section 6.5, we find that

$$\mathcal{V}^{\mathrm{d}}_{n'l'} = 2(2l'+1) \int_0^{\infty} |P_{n'l'}(r_j)|^2 \frac{1}{r_>} \mathrm{d}r_j \qquad [7.153]$$

This expression is clearly independent of the angles (θ_i, ϕ_i) of $\mathbf{r}_i$ so that $\mathcal{V}^{\mathrm{d}}_{n'l'}$ is *central*. For an atom or ion with closed subshells the direct potential $\mathcal{V}^{\mathrm{d}}$ is just the sum of spherically symmetric contributions of the form [7.153], coming from each subshell, so that $\mathcal{V}^{\mathrm{d}}$ itself is spherically symmetric.

Let us now turn to the exchange potential $\mathcal{V}^{\mathrm{ex}}$. Using [7.118] and [7.122b], we see that when acting upon a spin orbital $u_\lambda(q_i)$ whose spatial orbital is of the form [7.147], the part of $\mathcal{V}^{\mathrm{ex}}$ coming from a closed subshell $(n'l')$ gives

$$\mathcal{V}^{\mathrm{ex}}_{n'l'}[r_i^{-1} P_{nl}(r_i) Y_{lm}(\theta_i, \phi_i)] = \sum_{m'=-l'}^{+l'} \left[\int P^{\star}_{n'l'}(r_j) Y^{\star}_{l'm'}(\theta_j, \phi_j) \frac{1}{r_{ij}} \right.$$

$$\left. \times P_{nl}(r_j) Y_{lm}(\theta_j, \phi_j)\, \mathrm{d}r_j\, \mathrm{d}\Omega_j \right] r_i^{-1} P_{n'l'}(r_i) Y_{l'm'}(\theta_i, \phi_i) \qquad [7.154]$$

The expression on the right-hand side can now be evaluated by expanding $1/r_{ij}$ in spherical harmonics (see [7.152]) and using the formulae [A4.25] and [A4.40] of Appendix 4, together with the orthogonality relation [A4.32] for the Clebsch–Gordan coefficients. The result is (Problem 7.8)

$$\mathcal{V}^{\mathrm{ex}}_{n'l'}[r_i^{-1} P_{nl}(r_i) Y_{lm}(\theta_i, \phi_i)] = (2l'+1) \left\{ \sum_{L=|l-l'|}^{l+l'} \frac{1}{2L+1} |\langle ll'00|L0\rangle|^2 \right.$$

$$\left. \times \int_0^{\infty} P^{\star}_{n'l'}(r_j) \frac{(r_<)^L}{(r_>)^{L+1}} P_{nl}(r_j)\, \mathrm{d}r_j \right\} r_i^{-1} P_{n'l'}(r_i) Y_{lm}(\theta_i, \phi_i) \qquad [7.155]$$

Looking only at the angular dependence, we see that when acting on the spherical harmonic $Y_{lm}(\theta_i, \phi_i)$, the exchange operator $\mathcal{V}^{\mathrm{ex}}_{n'l'}$ gives back something proportional to $Y_{lm}(\theta_i, \phi_i)$, the proportionality factor being independent of the angles (θ_i, ϕ_i). The angular dependence of the exchange potential $\mathcal{V}^{\mathrm{ex}}$ (which is a sum of contributions of the form [7.155] arising from each subshell) is therefore such that it is equivalent to a central potential.

The above discussion shows that for atoms (ions) with closed subshells the central field approximation is exact within the framework of the Hartree–Fock method. The radial equations then read

$$\left[-\frac{1}{2} \frac{\mathrm{d}^2}{\mathrm{d}r_i^2} + \frac{l(l+1)}{2r_i^2} - \frac{Z}{r_i} + \mathcal{V}^{\mathrm{d}} - \mathcal{V}^{\mathrm{ex}} \right] P_{nl}(r_i) = E_{nl} P_{nl}(r_i) \qquad [7.156]$$

where

$$\mathcal{V}^{\mathrm{d}} = \sum_{n'l'} \mathcal{V}^{\mathrm{d}}_{n'l'}$$
$$= \sum_{n'l'} 2(2l' + 1) \int_0^\infty |P_{n'l'}(r_j)|^2 \frac{1}{r_>} \, \mathrm{d}r_j \qquad [7.157a]$$

and

$$\mathcal{V}^{\mathrm{ex}} P_{nl}(r_i) = \sum_{n'l'} \mathcal{V}^{\mathrm{ex}}_{n'l'} P_{nl}(r_i)$$
$$= \sum_{n'l'} \sum_{L=|l-l'|}^{l+l'} \frac{2l'+1}{2L+1} |\langle ll'00|L0\rangle|^2 \left[\int_0^\infty P^\star_{n'l'}(r_j) \right.$$
$$\left. \times \frac{(r_<)^L}{(r_>)^{L+1}} P_{nl}(r_j) \, \mathrm{d}r_j \right] P_{n'l'}(r_i) \qquad [7.157b]$$

where

$$r_> = \max(r_i, r_j)$$
$$r_< = \min(r_i, r_j)$$
$$|l - l'| \leqslant L \leqslant l + l' \qquad [7.157c]$$

For atoms (ions) having incomplete subshells, the Hartree–Fock potential $\mathcal{V}$ is no longer spherically symmetric. However, this departure from spherical symmetry is often small, since in many cases (in particular for the ground state) it arises from only *one* incomplete subshell. An approximate Hartree–Fock central field $\bar{\mathcal{V}}$ is then obtained by averaging $\mathcal{V}$ over spin directions and angles.

An example: the Be ground state

We shall illustrate the Hartree–Fock method by considering the ground state $1s^2 2s^2\ {}^1S$ of beryllium. In this case the Slater determinant [7.87] reads

$$\Phi(q_1, q_2, q_3, q_4) = \frac{1}{\sqrt{4!}} \begin{vmatrix} u_{1s\uparrow}(q_1) & u_{1s\downarrow}(q_1) & u_{2s\uparrow}(q_1) & u_{2s\downarrow}(q_1) \\ u_{1s\uparrow}(q_2) & u_{1s\downarrow}(q_2) & u_{2s\uparrow}(q_2) & u_{2s\downarrow}(q_2) \\ u_{1s\uparrow}(q_3) & u_{1s\downarrow}(q_3) & u_{2s\uparrow}(q_3) & u_{2s\downarrow}(q_3) \\ u_{1s\uparrow}(q_4) & u_{1s\downarrow}(q_4) & u_{2s\uparrow}(q_4) & u_{2s\downarrow}(q_4) \end{vmatrix} \qquad [7.158]$$

and the Hartree–Fock potential is given by (see [7.128])

$$\mathcal{V} = -\frac{4}{r_i} + V^{\mathrm{d}}_{1s\uparrow} + V^{\mathrm{d}}_{1s\downarrow} + V^{\mathrm{d}}_{2s\uparrow} + V^{\mathrm{d}}_{2s\downarrow}$$
$$- (V^{\mathrm{ex}}_{1s\uparrow} + V^{\mathrm{ex}}_{1s\downarrow} + V^{\mathrm{ex}}_{2s\uparrow} + V^{\mathrm{ex}}_{2s\downarrow}) \qquad [7.159]$$

where the notation is self-explanatory. Because we have complete (sub) shells, the spatial parts of $u_{1s\uparrow}$ and $u_{1s\downarrow}$ are the same, as are those of $u_{2s\uparrow}$ and $u_{2s\downarrow}$. We

may thus write

$$u_{1s\uparrow}(q) = u_{1s}(r)\alpha; \qquad u_{1s\downarrow}(q) = u_{1s}(r)\beta$$
$$u_{2s\uparrow}(q) = u_{2s}(r)\alpha; \qquad u_{2s\downarrow}(q) = u_{2s}(r)\beta \tag{7.160}$$

From the foregoing discussion, the Hartree–Fock equations for the functions $u_{1s}(r)$ and $u_{2s}(r)$ are the two coupled integro-differential equations

$$\left[-\frac{1}{2}\nabla_r^2 - \frac{4}{r} + V_{1s}^{d}(r) + 2V_{2s}^{d}(r) - V_{2s}^{ex}(r)\right]u_{1s}(r) = E_{1s}u_{1s}(r) \tag{7.161a}$$

and

$$\left[-\frac{1}{2}\nabla_r^2 - \frac{4}{r} + V_{2s}^{d}(r) + 2V_{1s}^{d}(r) - V_{1s}^{ex}(r)\right]u_{2s}(r) = E_{2s}u_{2s}(r) \tag{7.161b}$$

where

$$V_{1s}^{d}(r) = \int u_{1s}^{*}(r')\frac{1}{|\mathbf{r}-\mathbf{r}'|}u_{1s}(r')\,d\mathbf{r}' \tag{7.162a}$$

$$V_{1s}^{ex}(r)f(\mathbf{r}) = \left[\int u_{1s}^{*}(r')\frac{1}{|\mathbf{r}-\mathbf{r}'|}f(\mathbf{r}')\,d\mathbf{r}'\right]u_{1s}(r) \tag{7.162b}$$

with similar definitions for $V_{2s}^{d}(r)$ and $V_{2s}^{ex}(r)$ (see [7.116] and [7.119]). The individual electron energies E_{1s} and E_{2s} introduced in [7.161] are such that

$$E_{1s} = E_{1s\uparrow} = E_{1s\downarrow} \qquad E_{2s} = E_{2s\uparrow} = E_{2s\downarrow} \tag{7.163}$$

The spatial orbital $u_{1s}(r)$ is a solution corresponding to the lowest eigenvalue of [7.161a], whereas $u_{2s}(r)$ corresponds to the lowest eigenvalue of [7.161b], with the condition $\langle u_{1s}|u_{2s}\rangle = 0$. Writing the orbitals in the form [7.147], namely

$$u_{1s}(r) = r^{-1}P_{1s}(r)Y_{00}; \qquad u_{2s}(r) = r^{-1}P_{2s}(r)Y_{00} \tag{7.164}$$

with $Y_{00} = (4\pi)^{-1/2}$, the two coupled Hartree–Fock equations [7.161] become

$$\left[-\frac{1}{2}\frac{d^2}{dr^2} + \frac{l(l+1)}{2r^2} - \frac{4}{r} + V_{1s}^{d}(r) + 2V_{2s}^{d}(r) - V_{2s}^{ex}(r)\right]P_{1s}(r) = E_{1s}P_{1s}(r) \tag{7.165a}$$

and

$$\left[-\frac{1}{2}\frac{d^2}{dr^2} + \frac{l(l+1)}{2r^2} - \frac{4}{r} + V_{2s}^{d}(r) + 2V_{1s}^{d}(r) - V_{1s}^{ex}(r)\right]P_{2s}(r) = E_{2s}P_{2s}(r) \tag{7.165b}$$

It is worth stressing that the Hartree–Fock potential corresponding to an excited state of the atom is different from the ground state potential [7.159], so that the Hartree–Fock equations for the orbitals of the excited atom will be different from [7.161] or [7.165]. As a result, the excited state solutions of the

coupled equations [7.161] or [7.165] do *not* represent orbitals corresponding to low-lying excited states of the atom.

Solution of the Hartree–Fock equations

We have already indicated above that the solution of the Hartree–Fock equations proceeds by iteration, starting from approximate individual spin-orbitals, and subject to the requirement of self-consistency. At each step of the iteration the coupled equations must be solved numerically, the final result of the computations being numerical values of the radial Hartree–Fock orbitals.

For practical purposes, however, analytical fits to the (numerical) solutions of the Hartree–Fock equations are very useful. For example, we already encountered in Chapter 6 a simple analytical fit to the Hartree–Fock ground state orbital for helium (see [6.85]). More generally, a convenient basis set for analytic fits to Hartree–Fock spatial orbitals is provided by *Slater orbitals*, the general form of which is

$$\chi_{nlm}(\mathbf{r}) = Nr^{n-1}\mathrm{e}^{-\alpha r}Y_{lm}(\theta, \phi) \qquad [7.166]$$

where n is a positive integer, α is the 'orbital exponent', and N is a normalisation constant, given by

$$N = \frac{(2\alpha)^{n+1/2}}{[(2n)!]^{1/2}} \qquad [7.167]$$

Looking back at [3.48] and [3.53], and remembering that L_{n+l}^{2l+1} is a polynomial of degree $n - l - 1$, we see that the Slater orbitals [7.166] behave in the same way as hydrogenic wave functions for large r. However, in contrast to the hydrogenic radial functions [3.53], the Slater orbitals do not possess radial nodes. In terms of Slater orbitals $\chi_i(\mathbf{r})$, a Hartree–Fock spatial orbital $u(\mathbf{r})$ is then given by

$$u(\mathbf{r}) = \sum_{i=1}^{N} c_i \chi_i(\mathbf{r}) \qquad [7.168]$$

where the quantities c_i are given coefficients. For example, the Hartree–Fock spatial orbitals of the neon ground state are [10]

$$\begin{aligned} u_{1s} &= r^{-1}P_{1s}(r)Y_{00}(\theta, \phi) = 0.93717\,\chi_1 + 0.04899\,\chi_2 + 0.00058\,\chi_3 \\ &\quad - 0.00064\,\chi_4 + 0.00551\,\chi_5 + 0.01999\,\chi_6 \\ u_{2s} &= r^{-1}P_{2s}(r)Y_{00}(\theta, \phi) = -0.23093\,\chi_1 - 0.00635\,\chi_2 + 0.18620\,\chi_3 \\ &\quad + 0.66899\,\chi_4 + 0.30910\,\chi_5 - 0.13871\,\chi_6 \\ u_{2p} &= r^{-1}P_{2p}(r)Y_{10}(\theta, \phi) = 0.21799\,\chi_7 + 0.53338\,\chi_8 \\ &\quad + 0.32933\,\chi_9 + 0.01872\,\chi_{10} \end{aligned} \qquad [7.169]$$

[10] See Clementi and Roetti (1974).

where

$$\begin{aligned}
\chi_1 &= N_1 \exp(-9.48486\, r) Y_{00}(\theta, \phi); \\
\chi_2 &= N_2 \exp(-15.56590\, r) Y_{00}(\theta, \phi) \\
\chi_3 &= N_3\, r \exp(-1.96184\, r) Y_{00}(\theta, \phi); \\
\chi_4 &= N_4\, r \exp(-2.86423\, r) Y_{00}(\theta, \phi) \\
\chi_5 &= N_5\, r \exp(-4.82530\, r) Y_{00}(\theta, \phi); \\
\chi_6 &= N_6\, r \exp(-7.79242\, r) Y_{00}(\theta, \phi) \\
\chi_7 &= N_7\, r \exp(-1.45208\, r) Y_{10}(\theta, \phi); \\
\chi_8 &= N_8\, r \exp(-2.38168\, r) Y_{10}(\theta, \phi) \\
\chi_9 &= N_9\, r \exp(-4.48489\, r) Y_{10}(\theta, \phi); \\
\chi_{10} &= N_{10}\, r \exp(-9.13464\, r) Y_{10}(\theta, \phi)
\end{aligned} \qquad [7.170]$$

and the normalisation constants are given by [7.167].

The radial functions P_{1s}, P_{2s} and P_{2p} for neon are plotted in Fig. 7.5. The *radial density function* $D(r)$, defined as the probability per unit length of finding an electron at a distance r from the nucleus, is given by

$$\begin{aligned}
D(r) &= r^2 \int \rho(\mathbf{r})\, d\Omega \\
&= \sum_{nl} q_{nl} |P_{nl}(r)|^2
\end{aligned} \qquad [7.171]$$

where q_{nl} is the number of equivalent electrons in a subshell (nl). Thus, for the case of neon considered here we have

$$D(r) = 2|P_{1s}(r)|^2 + 2|P_{2s}(r)|^2 + 6|P_{2p}(r)|^2 \qquad [7.172]$$

This function is shown in Fig. 7.6.

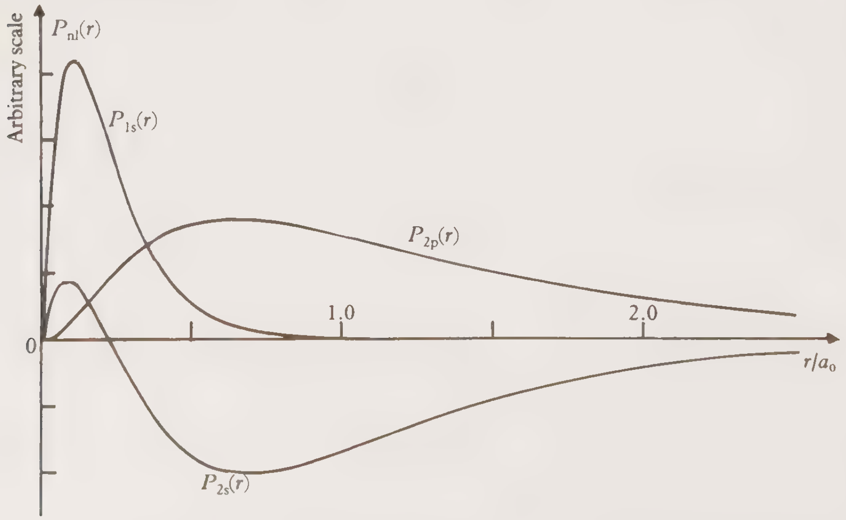

7.5 The radial functions $P_{1s}(r)$, $P_{2s}(r)$ and $P_{2p}(r)$ for neon.

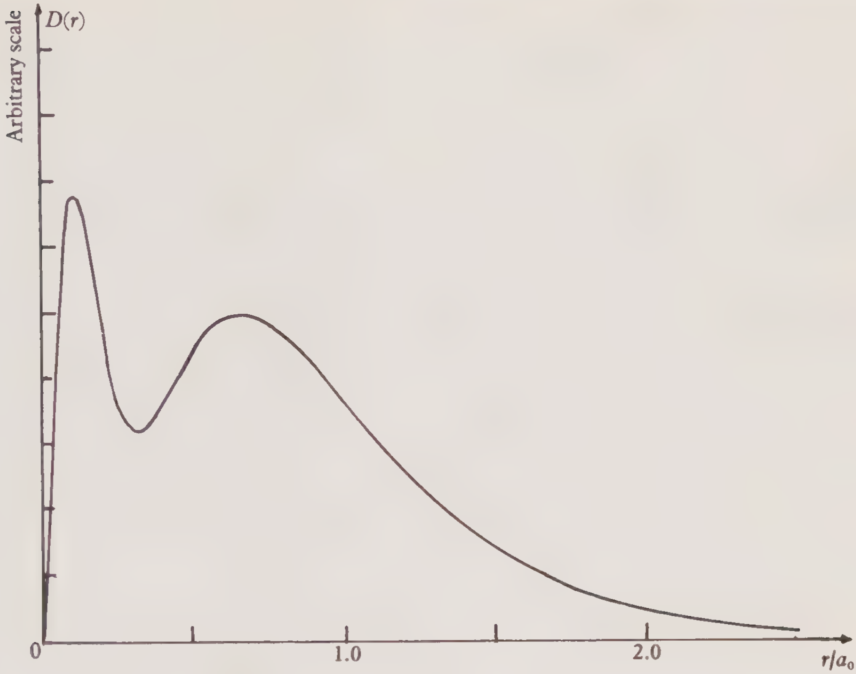

7.6 The radial density function $D(r)$ for neon.

The Hartree equations

Let us return to the Hartree–Fock equations [7.138]. If the exchange potential $\mathcal{V}_\lambda^{\text{ex}}$ is neglected in [7.138], one obtains the system of integro-differential equations

$$\left[-\frac{1}{2}\nabla_{r_i}^2 - \frac{Z}{r_i} + \mathcal{V}_\lambda^{\text{d}}(\mathbf{r}_i)\right]u_\lambda(q_i) = E_\lambda u_\lambda(q_i)$$

$$\lambda = \alpha, \beta, \ldots \nu \qquad [7.173]$$

or, more explicitly

$$\left[-\frac{1}{2}\nabla_{r_i}^2 - \frac{Z}{r_i} + \sum_{\mu\neq\lambda}\int u_\mu^\star(\mathbf{r}_j)\frac{1}{r_{ij}}u_\mu(\mathbf{r}_j)\,\mathrm{d}\mathbf{r}_j\right]u_\lambda(\mathbf{r}_i) = E_\lambda u_\lambda(\mathbf{r}_i) \qquad [7.174]$$

$$\lambda = \alpha, \beta, \ldots \nu$$

where we have used [7.113], [7.116] and [7.135]. These equations were originally obtained by Hartree from the independent particle approximation and the assumption that there is a charge density associated with each electron, which is equal to $-e$ times its position probability density. By making the central field approximation, which consists in replacing $\mathcal{V}_\lambda^{\text{d}}(\mathbf{r}_i)$ by its average $\bar{\mathcal{V}}_\lambda^{\text{d}}(r_i)$ taken over the angles of $\mathbf{r}_i$, one obtains for the radial functions $P_{nl}(r_i)$ the

radial Hartree equations

$$\left[-\frac{1}{2}\frac{\mathrm{d}^2}{\mathrm{d}r_i^2}+\frac{l(l+1)}{2r_i^2}-\frac{Z}{r_i}+\bar{\mathcal{V}}_\lambda^{\mathrm{d}}(r_i)\right]P_{nl}(r_i)=E_{nl}P_{nl}(r_i) \qquad [7.175]$$

From the derivation of the Hartree–Fock equations given above, it is apparent that the Hartree equations [7.173] can be obtained from the variational method by using as trial function the simple (*non*-antisymmetrised) product of spin-orbitals Φ_H given by [7.90] instead of the antisymmetrised product Φ given by the Slater determinant [7.87]. Thus *the Hartree trial function* Φ_H *does not satisfy the requirement of antisymmetry* imposed by the Pauli exclusion principle, so that the Hartree equations [7.173] lack the exchange potential $\mathcal{V}_\lambda^{\mathrm{ex}}$. Nevertheless, the weaker condition of the exclusion principle, according to which 'no two electrons in an atom may have the same set of quantum numbers' can be satisfied in Hartree's method by requiring that only one electron populates each quantum state. It is also worth noting that in contrast with the Hartree–Fock equations, where all the electrons move in the same Hartree–Fock potential for a given state of the system, the effective potential in the Hartree equations depends on the particular orbital u_λ considered. It follows that in general the Hartree orbitals are not mutually orthogonal.

As in the case of the Hartree–Fock equations discussed above, the system of Hartree equations can be solved by iteration, subject to the self-consistency requirement. Because of the absence of exchange terms, the Hartree equations are in fact much simpler to solve than the corresponding Hartree–Fock equations, so that the Hartree spin-orbitals can be used as a first approximation to start the iterative solution of the Hartree–Fock equations.

Correlation effects

We have seen above that the Hartree–Fock approach is a variational method in which the trial function for the N-electron atom (ion) is a Slater determinant, whose individual spin-orbitals are optimised. Let us call E_{HF} the Hartree–Fock energy of a given state, and Ψ_{HF} the corresponding Hartree–Fock wave function. It is clear that both E_{HF} and Ψ_{HF} are only approximations to the exact energy E_{exact} and the exact wave function Ψ_{ex} of the Hamiltonian [7.2]. The difference

$$E_{\mathrm{corr}}=E_{\mathrm{exact}}-E_{\mathrm{HF}} \qquad [7.176]$$

is known as the *correlation energy*. We emphasise that the quantity E_{exact} which appears in [7.176] is the exact energy of the *non-relativistic* Hamiltonian [7.2], and hence is not quite the same as the experimental energy. It should also be noted that a certain amount of correlation is already included in the Hartree–Fock wave function because of the fact that it is totally antisymmetric. One usually denotes by *correlation effects* the remaining electron correlations, not included in the Hartree–Fock wave function, which are responsible for the correlation energy [7.176].

Table 7.5 Values of E_{HF}, E_{exact}, E_{corr} (in a.u.) and of the ratio $E_{\mathrm{corr}}/E_{\mathrm{exact}}$ for the ground state of several atomic systems

Atomic system	E_{HF}	E_{exact}	E_{corr}	$E_{\mathrm{corr}}/E_{\mathrm{exact}}$
He	−2.862	−2.904	−0.042	0.014
Be	−14.573	−14.667	−0.094	0.006
B^+	−24.238	−24.349	−0.111	0.005
Ne	−128.55	−128.93	−0.38	0.003

Since the Hartree–Fock method is a variational one, the energy E_{HF} must lie above E_{exact} for the ground state, so that E_{corr} is always negative in this case. As an example, we give in Table 7.5 the values of E_{HF}, E_{exact}, E_{corr} and the relative error $E_{\mathrm{corr}}/E_{\mathrm{exact}}$ for the ground state of a few atomic systems. We see from this table that the error in the Hartree–Fock energy of an atom (ion) is only about 1 per cent. However, in particular regions of configuration space – which do not play an important role in the variational integral – the Hartree–Fock wave functions may be quite inaccurate. As a consequence, various matrix elements, such as those required to calculate transition rates or hyperfine structure effects, may sometimes be in serious error when evaluated with the Hartree–Fock wave functions.

Correlation effects can be studied by using *perturbation theory*, starting with the Hartree–Fock energies and wave functions as the 'zero-order' approximation. In particular, the *variation-perturbation method* has been applied successfully to obtain correlation energies for various atoms and ions. Alternatively, the variational method can be used with a trial function Φ which is a linear combination of Slater determinants,

$$\Phi = \sum_i c_i \Phi_i \qquad [7.177]$$

where the coefficients c_i are variational parameters. The various Slater determinants Φ_i differ in the choice of the spin-orbitals occupied by the electrons, and correspond therefore to different electronic configurations. This approach is known as the *configuration–interaction method*. It is clear that the configuration–interaction approach reduces to the Hartree–Fock method when only one Slater determinant is used in [7.177].

7.5 CORRECTIONS TO THE CENTRAL FIELD APPROXIMATION. L–S COUPLING AND j-j COUPLING

In the central field approximation, the non-relativistic Hamiltonian [7.2] of the N-electron atom (ion) is replaced by the Hamiltonian

$$H_c = \sum_{i=1}^{N} h_i, \qquad [7.178a]$$

where h_i is the individual Hamiltonian of electron i in the central field $V(r_i)$ (see

[7.11]). For example, if we choose the Hartree–Fock potential $\bar{\mathcal{V}}$ (that is, the Hartree–Fock potential $\mathcal{V}$, averaged for the case of atoms or ions with incomplete subshells) as our central field, then

$$h_i = -\tfrac{1}{2}\nabla_{r_i}^2 + \bar{\mathcal{V}} \qquad [7.178b]$$

Let us now consider the main corrections to the central field approximation. The first important correction to the central field Hamiltonian H_c is the term H_1, given by [7.12], which represents the *difference between the actual Coulomb interactions of the electrons and the average electron repulsion* contained in the central field V. In particular, if V is a (central) Hartree–Fock potential, the term H_1 leads to the correlation effects discussed at the end of the previous section. In this section, however, we shall also consider the corrections due to the *spin–orbit interactions* of the electrons. Working within the framework of the independent particle model, we write the spin–orbit correction term in a form which is an extension of (5.16)–(5.17). That is

$$H_2 = \sum_i \xi(r_i)\mathbf{L}_i \cdot \mathbf{S}_i \qquad [7.179]$$

where $\mathbf{L}_i = \mathbf{r}_i \times \mathbf{p}_i$ is the orbital angular momentum operator of electron i, $\mathbf{S}_i$ is its spin angular momentum, and the function $\xi(r_i)$ is given by

$$\xi(r_i) = \frac{1}{2m^2c^2}\frac{1}{r_i}\frac{\mathrm{d}V(r_i)}{\mathrm{d}r_i} \qquad [7.180]$$

It can be shown that the contribution to the sum [7.179] coming from closed subshells vanishes, so that the summation in [7.179] is only over electrons outside closed subshells.

Adding the corrections H_1 and H_2 to the central field Hamiltonian, we obtain the total Hamiltonian

$$\mathcal{H} = H_c + H_1 + H_2 \qquad [7.181]$$

Because this Hamiltonian describes an isolated atom, the *total parity* and the *total angular momentum* are constants of the motion. In the present case the total angular momentum is given by

$$\mathbf{J} = \mathbf{L} + \mathbf{S} = \sum_{i=1}^{N} \mathbf{J}_i \qquad [7.182]$$

where $\mathbf{L} = \Sigma_i\mathbf{L}_i$ is the total orbital angular momentum of the electrons, $\mathbf{S} = \Sigma_i\mathbf{S}_i$ is their total spin angular momentum, and

$$\mathbf{J}_i = \mathbf{L}_i + \mathbf{S}_i \qquad [7.183]$$

In order to discuss the effects of the terms H_1 and H_2, we shall use *perturbation theory*, starting from the eigenfunctions and eigenenergies of H_c as our zero-order approximation. As we have seen in Section 7.1, these unperturbed eigenfunctions and eigenenergies correspond to given electron configurations. In what follows we shall assume that the matrix elements of the

perturbation between two different electron configurations is small with respect to the energy intervals between unperturbed configuration energies. We can then study the effect of the perturbation on atomic states corresponding to a single configuration of the electrons.

The manner in which the perturbation calculation is to be carried out depends on the relative magnitude of the two perturbing terms H_1 and H_2. The case for which both perturbations H_1 and H_2 are of the same order of magnitude is difficult to handle because both terms must be treated on the same footing. This situation, which is known as *intermediate coupling*, will not be examined here [11]. Instead, we shall consider the two extreme situations for which $|H_1| \gg |H_2|$ and $|H_2| \gg |H_1|$. The first one is the most frequently encountered; it occurs for atoms (ions) with small and intermediate values of Z, and is called the *L–S (or Russell–Saunders) coupling case*. The second situation, which arises for atoms (ions) with large Z is known as the *j–j coupling case*. We shall first discuss L–S coupling, and then turn to j–j coupling.

L–S coupling

Since in this case the electrostatic energy correction H_1 is large in comparison with the spin–orbit term H_2, the *first step* of the perturbation calculation consists in neglecting H_2 and obtaining approximate eigenfunctions and eigenenergies of the Hamiltonian

$$H = H_c + H_1 \qquad [7.184]$$

In general, there are a number of degenerate states belonging to the same configuration, which differ by the values of the quantum numbers m_l and m_s of the individual electrons. The perturbation H_1 has the effect of removing – at least partly – this degeneracy. The energy levels of $H = H_c + H_1$ arising from a given unperturbed energy level E_c of H_c will thus be obtained by diagonalising the perturbation H_1 within the subspace of the degenerate states belonging to the eigenvalue E_c.

This diagonalisation is greatly simplified by taking into account the symmetry properties of the Hamiltonian $H = H_c + H_1$. Since the Hamiltonian does not contain spin–orbit energy terms, it commutes not only with the total angular momentum $\mathbf{J}$, but also separately with the total orbital angular momentum $\mathbf{L}$ (see Problem 7.9) and the total spin angular momentum $\mathbf{S}$ [12]. As a result, the eigenvalues of H can be characterised by the total orbital angular momentum quantum number L and the total spin quantum number S. Moreover, these energy eigenvalues are independent of the quantum numbers M_L and M_S, so

[11] The intermediate coupling case is treated for example in Condon and Shortley (1951) and Sobelman (1979) where a detailed account of the theory of atomic spectra can be found.

[12] It is worth noting that the use of antisymmetric wave functions (Slater determinants) couples the electron spins to the electrostatic energy (as we have seen in Section 6.6 in discussing the excited states of helium) despite the fact that $[H, \mathbf{S}] = 0$.

that each energy level of H labelled by a pair (LS) is $(2L + 1)(2S + 1)$ times degenerate with respect to M_L and M_S. As we already saw in Section 6.3, energy levels corresponding to definite values of L and S are called *terms* and are denoted as ^{2S+1}L, with the capital letters S, P, D, F, . . . corresponding to the values $L = 0, 1, 2, 3, \ldots$ We also recall that the number $2S + 1$ is called the *multiplicity* of the term. If the multiplicity $2S + 1$ equals 1 (that is, if $S = 0$) the term is called a singlet. If $2S + 1 = 2, 3, 4, \ldots$ we have respectively a doublet, a triplet, a quartet, and so on. The parity of the term may be indicated by the addition of the superscripts *e* (even) or *o* (odd), for example $^2\mathrm{P}^o$, $^3\mathrm{D}^e$, etc. Using the Dirac notation, the wave functions corresponding to a term will be denoted by $|\gamma LSM_LM_S>$, where γ refers to the configuration of H_c to which the level belongs.

Determination of the possible terms of a multielectron configuration in L–S coupling

In order to determine all the possible terms corresponding to a given configuration (that is, the possible values of L and S), the rules for the *addition of angular momenta* must be used. However, in combining the individual electron orbital angular momenta $\mathbf{L}_i$ to obtain $\mathbf{L}$ and the individual electron spin angular momenta $\mathbf{S}_i$ to obtain $\mathbf{S}$, one must not forget to reject the values of L and S corresponding to states forbidden by the Pauli exclusion principle.

We first note that for a *filled subshell*, that is a configuration containing the maximum number $2(2l + 1)$ of equivalent electrons (having the same values of n and l), there is only one possible term, namely the ^{1}S term. This is a direct consequence of the fact that $M_L = \Sigma_i m_{l_i} = 0$ (since m_{l_i} runs over all the possible values $0, \pm 1, \pm 2, \ldots \pm l$) and similarly $M_S = \Sigma_i m_{s_i} = 0$. As a result, we have $L = S = 0$ for a filled subshell.

Let us now consider the case of atoms (ions) with *incomplete subshells*. Since $L = S = 0$ for filled subshells, we only need to consider the electrons outside filled subshells ('optically active' electrons) to determine the possible values of L and S. Three cases must be considered:

Electrons belonging to different subshells (non-equivalent electrons)

In this case no two 'optically active' electrons can have the same set of quantum numbers, so that the Pauli exclusion principle is automatically satisfied. The allowed values of the quantum numbers L and S are therefore obtained by adding the individual orbital angular momenta $\mathbf{L}_i$ of the 'optically active' electrons to form $\mathbf{L}$ and the spin angular momenta $\mathbf{S}_i$ of these electrons to form $\mathbf{S}$. We recall that on adding two orbital angular momenta $\mathbf{L}_1$ and $\mathbf{L}_2$, with corresponding orbital angular quantum numbers l_1 and l_2 (such that $l_1(l_1 + 1)\hbar^2$ is the eigenvalue of $\mathbf{L}_1^2$ and $l_2(l_2 + 1)\hbar^2$ the eigenvalue of $\mathbf{L}_2^2$) the allowed values of the total orbital angular momentum quantum number L are

$$L = |l_1 - l_2|, |l_1 - l_2| + 1, \ldots l_1 + l_2 \tag{7.185}$$

Similarly, upon adding two spins $\mathbf{S}_1$ and $\mathbf{S}_2$, with spin quantum numbers s_1 and s_2, the allowed values of the total spin quantum number S are

$$S = |s_1 - s_2|, |s_1 - s_2| + 1, \ldots s_1 + s_2 \qquad [7.186]$$

Let us now consider two non-equivalent electrons, having orbital angular momentum quantum numbers l_1 and l_2, respectively. The allowed values of L are then given by [7.185]. Moreover, since $s_1 = s_2 = 1/2$, we have $S = 0, 1$. We illustrate these considerations by two examples:

***Configuration* np n′p**

We have $l_1 = l_2 = 1$ and $s_1 = s_2 = 1/2$, so that $L = 0, 1, 2$ and $S = 0, 1$. The possible terms are therefore

$$^1\mathrm{S},\ ^1\mathrm{P},\ ^1\mathrm{D},\ ^3\mathrm{S},\ ^3\mathrm{P},\ ^3\mathrm{D} \qquad [7.187]$$

***Configuration* np n′d**

Here $l_1 = 1$, $l_2 = 2$ and $s_1 = s_2 = 1/2$. Thus $L = 1, 2, 3$ and $S = 0, 1$. The possible terms are thus given by

$$^1\mathrm{P},\ ^1\mathrm{D},\ ^1\mathrm{F},\ ^3\mathrm{P},\ ^3\mathrm{D},\ ^3\mathrm{F} \qquad [7.188]$$

If there are more than two electrons, the addition of orbital angular momenta and spins is first performed for two electrons; the rules [7.185] and [7.186] are then used successively to add the orbital angular momentum and the spin of the third electron, the fourth electron, and so on. As an example, let us consider the configuration np n'p n''d. Adding first the orbital angular momenta and spins of the two electrons np and n'p, we find the terms listed in [7.187]. Now the third electron n''d has $l = 2$ and $s = 1/2$. Using [7.185] and [7.186] we see that the addition of the electron n''d to the term ^{1}S of [7.187] gives a term with $L = 2$ and $S = 1/2$, namely ^{2}D. In the same way, adding the n''d electron

to the term ^{1}P yields the terms ^{2}P, ^{2}D, ^{2}F

to the term ^{1}D yields the terms ^{2}S, ^{2}P, ^{2}D, ^{2}F, ^{2}G

to the term ^{3}S yields the terms ^{2}D, ^{4}D

to the term ^{3}P yields the terms ^{2}P, ^{2}D, ^{2}F, ^{4}P, ^{4}D, ^{4}F

to the term ^{3}D yields the terms ^{2}S, ^{2}P, ^{2}D, ^{2}F, ^{2}G, ^{4}S, ^{4}P, ^{4}D, ^{4}F, ^{4}G

These results may be summarised by writing that the terms we have obtained are

$$\begin{matrix} ^2\mathrm{S}, & ^2\mathrm{P}, & ^2\mathrm{D}, & ^2\mathrm{F}, & ^2\mathrm{G}, & ^4\mathrm{S}, & ^4\mathrm{P}, & ^4\mathrm{D}, & ^4\mathrm{F}, & ^4\mathrm{G} \\ 2 & 4 & 6 & 4 & 2 & & 2 & 3 & 2 & \end{matrix} \qquad [7.189]$$

where the number under the term symbol indicates the number of identical terms.

Electrons belonging to the same subshell (equivalent electrons)

The determination of the possible terms for equivalent 'optically active' electrons is more difficult. Indeed, in this case certain values of L and S are ruled out because of the Pauli exclusion principle.

The simplest case is that of two equivalent s electrons, corresponding to the configuration ns^2. As we have seen above in discussing closed subshells, we must have $M_L = M_S = 0$, which implies that the only possible term is ^{1}S. We note that if the Pauli principle were ignored, an additional term ^{3}S would appear.

Let us now consider the case of two equivalent p electrons, corresponding to the configuration $n\text{p}^2$. We have seen in Section 7.1 that the degeneracy (or statistical weight) of a configuration $n\text{p}^2$ is $g = 15$. The 15 possible states associated with the configuration $n\text{p}^2$ can be inferred directly from Table 7.6, where the possible quantum numbers m_{l_1}, m_{s_1}, m_{l_2}, m_{s_2} of the two electrons are given. In obtaining this table, we note that the states for which the two electrons have the same values of m_l and m_s (for example $m_{l_1} = m_{l_2} = 1$, $m_{s_1} = m_{s_2} = 1/2$) must be excluded because of the exclusion principle. Moreover, since the two electrons are indistinguishable, two pairs of values (m_{l_1}, m_{s_1}) and (m_{l_2}, m_{s_2}) which differ only by the electron label (1 or 2) only give one state. For example, $m_{l_1} = 1$, $m_{s_1} = 1/2$, $m_{l_2} = 0$, $m_{s_2} = -1/2$ yields the same state as $m_{l_1} = 0$, $m_{s_1} = -1/2$, $m_{l_2} = 1$, $m_{s_2} = 1/2$. We have also listed in Table 7.6 the values of the quantum numbers M_L and M_S, namely

$$M_L = m_{l_1} + m_{l_2}, \qquad M_S = m_{s_1} + m_{s_2} \qquad [7.190]$$

We shall now identify the possible terms corresponding to the 15 states listed in Table 7.6. We recall that in the case of the configuration $n\text{p}\,n'\text{p}$ (non-equivalent electrons) we had obtained the six possible terms given in [7.187]. For the present $n\text{p}^2$ configuration, however, the pairs (M_L, M_S) appearing in the two last columns of Table 7.6 are only compatible with a restricted number

Table 7.6 Possible quantum numbers for the configuration $n\text{p}^2$

Number	m_{l_1}	m_{s_1}	m_{l_2}	m_{s_2}	$M_L = m_{l_1} + m_{l_2}$	$M_S = m_{s_1} + m_{s_2}$
1	1	$\frac{1}{2}$	1	$-\frac{1}{2}$	2	0
2	1	$-\frac{1}{2}$	0	$\frac{1}{2}$	1	0
3	0	$\frac{1}{2}$	0	$-\frac{1}{2}$	0	0
4	0	$-\frac{1}{2}$	-1	$\frac{1}{2}$	-1	0
5	-1	$\frac{1}{2}$	-1	$-\frac{1}{2}$	-2	0
6	1	$\frac{1}{2}$	0	$\frac{1}{2}$	1	1
7	1	$-\frac{1}{2}$	0	$-\frac{1}{2}$	1	-1
8	0	$\frac{1}{2}$	-1	$\frac{1}{2}$	-1	1
9	0	$-\frac{1}{2}$	-1	$-\frac{1}{2}$	-1	-1
10	1	$\frac{1}{2}$	0	$-\frac{1}{2}$	1	0
11	1	$-\frac{1}{2}$	-1	$\frac{1}{2}$	0	0
12	0	$\frac{1}{2}$	-1	$-\frac{1}{2}$	-1	0
13	1	$\frac{1}{2}$	-1	$\frac{1}{2}$	0	1
14	1	$-\frac{1}{2}$	-1	$-\frac{1}{2}$	0	-1
15	1	$\frac{1}{2}$	-1	$-\frac{1}{2}$	0	0

of terms. Indeed, we first note that the pair ($M_L = 2, M_S = 1$) is missing so that the term ^{3}D is not present. On the other hand, the occurrence of the pairs ($M_L = 2, M_S = 0$) and ($M_L = -2, M_S = 0$) indicates that a term with $L = 2$ must exist. Since the term ^{3}D has just been ruled out, the term with $L = 2$ must be ^{1}D; it may be constructed with the states corresponding to the first five entries in Table 7.6. The states corresponding to the entries 6 to 14 are easily seen to correspond to a term ^{3}P. Finally, the last entry in the table, with $M_L = M_S = 0$, corresponds to a term ^{1}S. Hence, for the configuration $n\mathrm{p}^2$, there are only three possible terms, namely

$$ {}^1\mathrm{S},\ {}^1\mathrm{D},\ {}^3\mathrm{P} \qquad [7.191] $$

instead of the six terms [7.187] we found for the configuration $n\mathrm{p}n'\mathrm{p}$.

A similar analysis can be carried out for other configurations containing equivalent electrons. In Table 7.7 are given the possible terms for configurations $(nl)^k$, with $l = 0, 1, 2$. We note in particular from this table that the configurations $(nl)^k$ and $(nl)^{2(2l+1)-k}$ lead to the same possible terms. In other words, the possible terms corresponding to a configuration in which there are k electrons in a subshell are the same as those in which k electrons are missing (that is, there are k 'holes') in this subshell.

Equivalent and non-equivalent electrons

If a configuration contains a group of equivalent electrons together with a number of non-equivalent electrons, the possible terms of the group of equivalent electrons must first be determined. The overall possible terms are then obtained by using the ordinary rules of addition of angular momenta to add the

Table 7.7 The possible terms for electron configurations $(nl)^k$, with $l = 0, 1, 2$

Configuration							
ns			^{2}S				
$n\mathrm{s}^2$		^{1}S					
np	$n\mathrm{p}^5$		^{2}P				
$n\mathrm{p}^2$	$n\mathrm{p}^4$	^{1}S, ^{1}D		^{3}P			
$n\mathrm{p}^3$			^{2}P, ^{2}D		^{4}S		
$n\mathrm{p}^6$		^{1}S					
nd	$n\mathrm{d}^9$		^{2}D				
$n\mathrm{d}^2$	$n\mathrm{d}^8$	^{1}S, ^{1}D, ^{1}G		^{3}P, ^{3}F			
$n\mathrm{d}^3$	$n\mathrm{d}^7$		^{2}P, $\underset{2}{{}^2\mathrm{D}}$, ^{2}F, ^{2}G, ^{2}H		^{4}P, ^{4}F		
$n\mathrm{d}^4$	$n\mathrm{d}^6$	$\underset{2}{{}^1\mathrm{S}}$, $\underset{2}{{}^1\mathrm{D}}$, ^{1}F, $\underset{2}{{}^1\mathrm{G}}$, ^{1}I		$\underset{4}{{}^3\mathrm{P}}$, ^{3}D, $\underset{2}{{}^3\mathrm{F}}$, ^{3}G, ^{3}H		^{5}D	
$n\mathrm{d}^5$			^{2}S, ^{2}P, $\underset{3}{{}^2\mathrm{D}}$, $\underset{2}{{}^2\mathrm{F}}$, $\underset{2}{{}^2\mathrm{G}}$, ^{2}H, ^{2}I		^{4}P, ^{4}D, ^{4}F, ^{4}G		^{6}S
$n\mathrm{d}^{10}$		^{1}S					

non-equivalent electrons. Similarly, if a configuration contains two or more groups of equivalent electrons, the possible terms of each group must first be obtained, and the overall possible terms are then determined by using the ordinary rules for the addition of angular momenta.

Hund's rules

Before leaving the subject of the effect of the electrostatic interaction H_1, we mention the so-called *Hund's rules*, which have been established empirically for the ground state configuration and for configurations containing equivalent electrons. According to these rules:

1. The term with the largest possible value of S for a given configuration has the lowest energy; the energy of the other terms increases with decreasing S.
2. For a given value of S, the term having the maximum possible value of L has the lowest energy.

Fine structure of terms in L–S coupling. Multiplet splitting and the Lande interval rule

Having obtained the energy levels of the Hamiltonian [7.184], we now proceed to the *second step* of the perturbation calculation, which consists in taking into account the spin–orbit term H_2 given by [7.179]. We shall first examine how the additional perturbation H_2 further removes degeneracies. The total Hamiltonian $\mathcal{H} = H_c + H_1 + H_2$ does not commute with $\mathbf{L}$ and $\mathbf{S}$, but it does commute with $\mathbf{J} = \mathbf{L} + \mathbf{S}$. On the other hand, the energy of an isolated atom cannot depend on the orientation of the total angular momentum $\mathbf{J}$. As a result, the $(2L + 1)(2S + 1)$ degeneracy associated with a term ^{2S+1}L corresponding to given values of L and S is partly removed by the perturbation H_2. The term ^{2S+1}L splits into a number of *fine structure components*, characterised by the value of J, the total angular momentum quantum number, and written in the Russell–Saunders notation as $^{2S+1}L_J$. Because $|H_2| \ll |H_1|$ in L–S coupling, the energy separation between the fine structure components $^{2S+1}L_J$ of a term ^{2S+1}L is small with respect to the energy separation between terms. The various fine structure components are said to form a *multiplet*. Each fine structure term $^{2S+1}L_J$ is still $(2J + 1)$-fold degenerate with respect to M_J (where $M_J\hbar$ are the eigenvalues of J_z), the possible values of M_J for a given J being

$$M_J = -J, -J + 1, \ldots J - 1, J \qquad [7.192]$$

The degeneracy in M_J can only be removed if a preferred direction in space is introduced, for example if an external magnetic field is applied as in the Zeeman effect.

Using the rules of addition of angular momenta, the possible values of J corresponding to given values of L and S are

$$|L–S|, |L–S| + 1, \ldots L + S \qquad [7.193]$$

It is clear that the number of possible values of J is equal to the multiplicity $2S + 1$ if $L \geqslant S$, and to $2L + 1$ if $L < S$. It is worth noting that the word 'multiplicity' always denotes the number $2S + 1$, even in the case $L < S$, where the term ${}^{2S+1}L$ can only split into $2L + 1$ fine structure components. We also note that

$$\sum_{J=|L-S|}^{L+S} (2J + 1) = (2L + 1)(2S + 1) \qquad [7.194]$$

so that by counting all the fine structure states (including their multiplicity) we retrieve the $(2L + 1)(2S + 1)$ degeneracy attached to the term ${}^{2S+1}L$.

As a first example, we show in Fig. 7.7 the partial removal of degeneracies, due successively to the perturbations H_1 and H_2, for a configuration containing two non-equivalent optically active electrons $np\, n'p$. In this case the possible values of L, S, and J are given by

$$L = 0,\ 1,\ 2$$
$$S = 0,\ 1$$
$$J = 0,\ 1,\ 2,\ 3$$

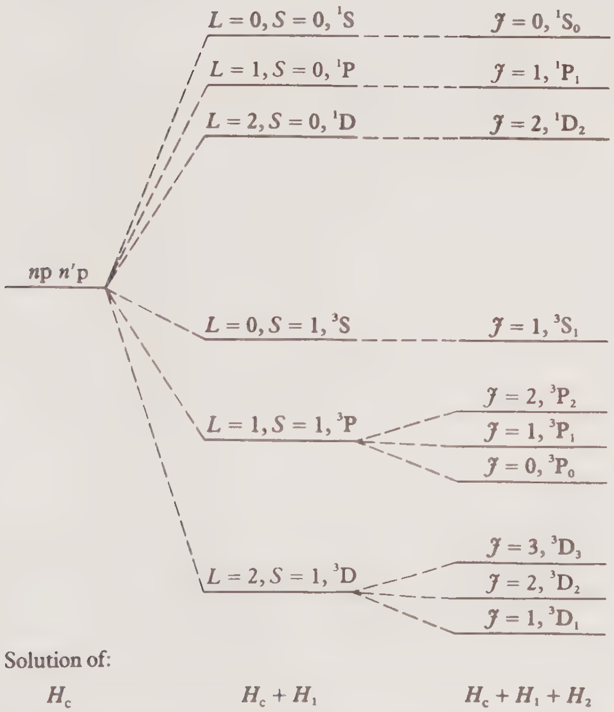

7.7 The splitting of the configuration $np\, n'p$ by the electrostatic perturbation H_1 and the spin–orbit perturbation H_2.

In the absence of the spin-orbit perturbation H_2 the possible terms ${}^{2S+1}L$ are given by [7.187]. When the effect of H_2 is included, the fine structure terms ${}^{2S+1}L_J$ are seen to be

$$ {}^1S_0,\ {}^1P_1,\ {}^1D_2,\ {}^3S_1,\ {}^3P_0,\ {}^3P_1,\ {}^3P_2,\ {}^3D_1,\ {}^3D_2,\ {}^3D_3 \qquad [7.195] $$

A second example is given in Fig. 7.8, where the case of a configuration containing two equivalent electrons np^2 is considered. This case is relevant in particular for the study of the ground state of the carbon atom, which has the configuration $1s^22s^22p^2$, the two 'optically active' electrons being the two 2p electrons. When the perturbation H_2 is taken into account the three terms obtained in [7.191] give rise to the five fine structure terms

$$ {}^1S_0,\ {}^1D_2,\ {}^3P_0,\ {}^3P_1,\ {}^3P_2 \qquad [7.196] $$

which are shown in Fig. 7.8. Both examples in Fig 7.7 and 7.8 also illustrate Hund's rules. Looking at Fig. 7.8 we also see that the 'true' ground state of the carbon atom is $1s^22s^22p^2\ {}^3P_0$.

In order to obtain the fine structure energy shifts due to the spin-orbit interaction, the perturbation H_2 must be diagonalised in the subspace of the wave functions $|\gamma LSM_LM_S\rangle$ which correspond to a given term, that is to a given energy level (γLS). By using the Wigner–Eckart theorem (see Appendix 4) it may be shown that the matrix elements of H_2 in that subspace are the same as those of the operator $\bar{A}\mathbf{L}\cdot\mathbf{S}$, where $\bar{A}$ is a constant, characteristic of the unperturbed level (γLS). Thus

$$ \langle\gamma LSM_LM_S|H_2|\gamma LSM'_LM'_S\rangle = \bar{A}\langle\gamma LSM_LM_S|\mathbf{L}\cdot\mathbf{S}|\gamma LSM'_LM'_S\rangle \qquad [7.197] $$

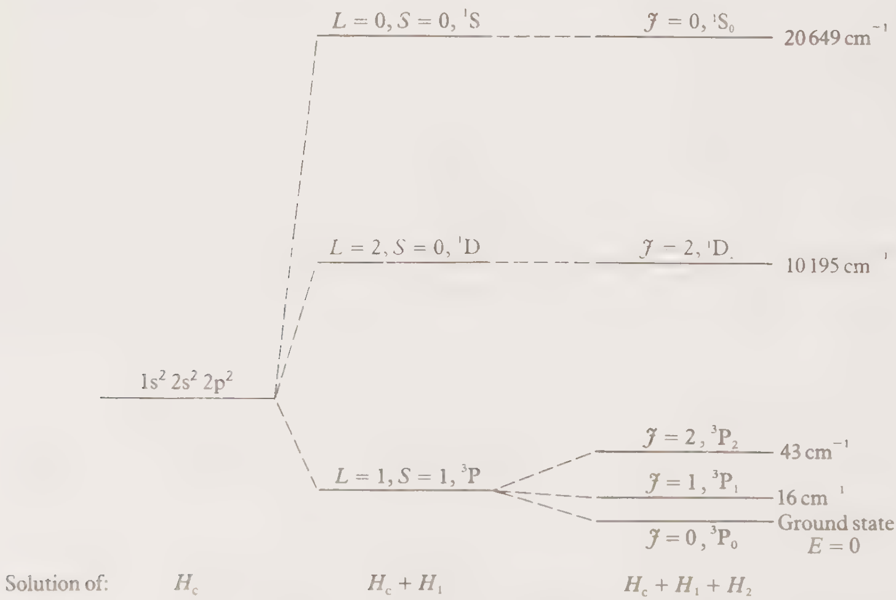

7.8 The splitting of the ground state configuration of carbon.

The perturbation H_2 is not diagonal in the subspace of the wave functions $|\gamma LSM_LM_S\rangle$. However, by proceeding as in Section 5.1, we can form linear combinations of the functions $|\gamma LSM_LM_S\rangle$ to obtain new 'unperturbed' functions $|\gamma LS\mathcal{J}M_\mathcal{J}\rangle$ which are eigenstates of $\mathbf{L}^2$, $\mathbf{S}^2$, $\mathbf{J}^2$ and $\mathcal{J}_z$ in that subspace. Since $\mathbf{J}^2 = \mathbf{L}^2 + 2\mathbf{L}\cdot\mathbf{S} + \mathbf{S}^2$, we then have (with $A = \bar{A}\hbar^2$)

$$\begin{aligned}\langle\gamma LS\mathcal{J}M_\mathcal{J}|H_2|\gamma LS\mathcal{J}M_\mathcal{J}\rangle &= \tfrac{1}{2}\bar{A}\langle\gamma LS\mathcal{J}M_\mathcal{J}|\mathbf{J}^2 - \mathbf{L}^2 - \mathbf{S}^2|\gamma LS\mathcal{J}M_\mathcal{J}\rangle \\ &= \tfrac{1}{2}A[\mathcal{J}(\mathcal{J}+1) - L(L+1) - S(S+1)] \quad [7.198]\end{aligned}$$

so that the unperturbed level (γLS) splits into $2S+1$ (if $L \geqslant S$) or $2L+1$ (if $L < S$), fine structure levels labelled by $\mathcal{J}$, as we have seen above. Moreover, we see from [7.198] that the energy separation between adjacent levels $E(\mathcal{J})$ and $E(\mathcal{J}-1)$ of a given multiplet (L and S fixed) is

$$\begin{aligned}E(\mathcal{J}) - E(\mathcal{J}-1) &= \tfrac{1}{2}A[\mathcal{J}(\mathcal{J}+1) - L(L+1) - S(S+1)] - \tfrac{1}{2}A[(\mathcal{J}-1)\mathcal{J} \\ &\quad - L(L+1) - S(S+1)] \\ &= A\mathcal{J} \qquad [7.199]\end{aligned}$$

and is therefore proportional to $\mathcal{J}$, the larger of the two $\mathcal{J}$ values characterising the pair of fine structure levels.

The result [7.199] is known as the *Landé interval rule*. It is well satisfied experimentally if the atom is well described by the L–S coupling case ($|H_2| \ll |H_1|$) and if in addition the perturbation H_2 only contains the spin–orbit interactions [13] as we have assumed here (see [7.199]). In that case the multiplets are called *regular multiplets*. When $A > 0$, we see from [7.198] that the multiplet component having the smallest possible value of $\mathcal{J}$ (that is, $\mathcal{J} = |L - S|$) has the lowest energy value; these multiplets are called *normal*. On the other hand, if $A < 0$, the multiplet component having the largest possible value of $\mathcal{J}$ (namely $\mathcal{J} = L + S$) has the lowest energy value; in this case one speaks of an *inverted* multiplet. The multiplets shown in Fig. 7.7 and 7.8 are regular, normal multiplets. It has been established empirically that normal multiplets occur if there is a single open subshell that is *less than half-filled*, while inverted multiplets arise if that subshell is *more than half-filled*. When the subshell is just half-filled, there is no multiplet splitting.

j–j Coupling

Let us now consider the case for which the spin–orbit energy H_2 is large with respect to the electrostatic energy correction H_1. In Section 5.1 we showed that the energy of the spin–orbit interaction is proportional to Z^4 (see [5.26]) while in Section 6.5 the first-order electrostatic correction $\langle 1/r_{12}\rangle$ was shown to be

[13] In some cases the fine structure of the levels may be very different because of the presence of other interactions, such as the spin–spin interactions between the electrons, mentioned at the beginning of Section 7.1.

proportional to Z. We therefore expect that the importance of the spin–orbit term H_2 relative to the electrostatic correction term will increase as Z is increased, so that j–j coupling could occur for atoms (ions) with large Z. In fact, j–j coupling is rarely found in pure form, although the atomic spectra of heavy atoms exhibit a structure which is close to that predicted by the j–j coupling scheme. The best examples of j–j coupling are provided by multiply charged ions the nuclei of which have high values of Z, since in these cases the relative importance of the electrostatic correction term H_1 is reduced because of the reduction in the number of electrons.

Since $|H_2| \gg |H_1|$ in the j–j coupling case, the *first step* of the perturbation calculation consists in neglecting H_1 and solving, approximately, the problem associated with the Hamiltonian

$$\tilde{H} = H_c + H_2 \qquad [7.200]$$

Now, from [7.11] and [7.179], we see that $\tilde{H}$ is just the sum of individual Hamiltonians. That is

$$\tilde{H} = \sum_{i=1}^{N} \tilde{h}_i \qquad [7.201]$$

where

$$\begin{aligned} \tilde{h}_i &= h_i + \xi(r_i)\mathbf{L}_i \cdot \mathbf{S}_i \\ &= -\frac{1}{2}\nabla_{r_i}^2 + V(r_i) + \xi(r_i)\mathbf{L}_i \cdot \mathbf{S}_i \end{aligned} \qquad [7.202]$$

The spin-orbit term $\xi(r_i)\mathbf{L}_i \cdot \mathbf{S}_i$ has the effect of partly removing the degeneracy of the individual electron energy levels E_{nl} (corresponding to the Hamiltonian h_i) by splitting each level E_{nl} with $l \neq 0$ into two components E_{nlj} having the total (individual) angular momentum quantum number $j = l \pm 1/2$. The corresponding individual wave functions are spin orbitals u_{nljm_j} labelled by the quantum numbers $(nljm_j)$ where m_j is the magnetic quantum number associated with the z component of the total angular momentum operator of an electron. Since m_j can take on the values

$$m_j = -j, -j+1, \ldots, j \qquad [7.203]$$

and the energy levels E_{nlj} do not depend on m_j, we see that each individual electron energy level E_{nlj} is $(2j+1)$-fold degenerate. When $j = l + 1/2$, this degeneracy is equal to $2l + 2$, and when $j = l - 1/2$, it is equal to $2l$. The energy levels $\tilde{E}$ associated with the Hamiltonian $\tilde{H}$ are obtained by summing the individual electron energies

$$\tilde{E} = \sum_{i=1}^{N} E_{n_i l_i j_i} \qquad [7.204]$$

and the corresponding wave functions are antisymmetrised products (Slater determinants) formed from the spin-orbitals $u_{n_i l_i j_i m_{j_i}}$. Each configuration of H_c

therefore yields a certain number of configurations of $\tilde{H}$, characterised by the values of the quantum numbers $(n_i l_i j_i)$ of the electrons.

In the *second step* of the perturbation calculation, the effect of the electrostatic correction term H_1 is taken into account. Each of the levels $\tilde{E}$ of $\tilde{H}$, characterised by a set of quantum numbers $(n_i l_i j_i)$ of the electrons, will now be split by the additional perturbation H_1 into a certain number of levels labelled by the values of the total angular momentum quantum number J of the system. Of course, as in the case of L–S coupling, each of these levels is still $(2J+1)$-fold degenerate with respect to M_J. A typical example of the splitting of levels in j–j coupling is shown in Fig. 7.9.

In the case of j–j coupling the notation for the spectral terms must specify the quantum numbers $(n_i l_i j_i)$ of each electron and the total angular momentum quantum number J. The values of the individual j_i's are usually written between parentheses, and J as a subscript. For example, one of the energy levels of the ground state configuration $6p^2$ of Pb, corresponding to the values $j_1 = 1/2$, $j_2 = 3/2$ and $J = 2$ is written as $6p^2\ (1/2, 3/2)_2$.

The possible values of J can be obtained by using methods similar to those we discussed above in order to obtain the possible terms in L–S coupling. In the case of non-equivalent electrons, it is sufficient to use the rule for addition of angular momenta. Let us consider for example the configuration $ns\, n'p$. For an s electron one has $j = 1/2$; while for a p electron $j = 1/2, 3/2$. Now, if $j_1 = 1/2$ and $j_2 = 1/2$, the possible values of J are $J = 0,1$, while for $j_1 = 1/2$ and $j_2 = 3/2$ the allowed values of J are $J = 1,2$. Thus the possible terms are

$$(1/2, 1/2)_0, \qquad (1/2, 1/2)_1, \qquad (1/2, 3/2)_1, \qquad (1/2, 3/2)_2 \qquad [7.205]$$

In the case of equivalent electrons, it is necessary to take into account the effect of the Pauli exclusion principle, just as in the case of L–S coupling. The possible terms for a configuration $(j)^k$, with $j = 1/2$, $3/2$ and $5/2$ are given in Table 7.8. It is worth noting that the total number of levels having a given value of J for a given electron configuration must be the same in L–S and j–j coupling.

Finally, we recall that the two cases of L–S and j–j coupling which we have discussed here are *extreme* cases. Many atoms are not described accurately by

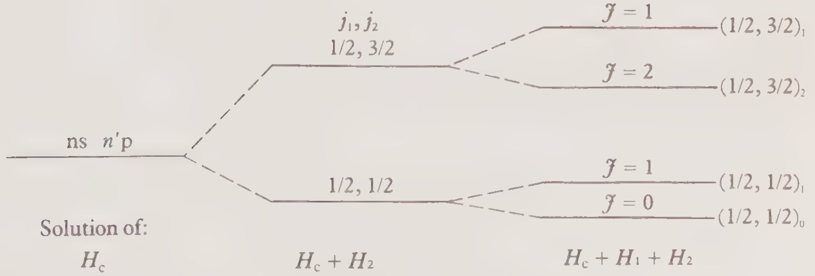

7.9 The splitting of levels in j–j coupling.

Table 7.8 The possible terms for configurations $(j)^k$, with $j = 1/2, 3/2, 5/2$

Configuration			J
	$(1/2)^1$		1/2
	$(1/2)^2$		0
$(3/2)^1$		$(3/2)^3$	3/2
	$(3/2)^2$		0, 2
$(5/2)^1$		$(5/2)^5$	5/2
$(5/2)^2$		$(5/2)^4$	0, 2, 4
	$(5/2)^3$		3/2, 5/2, 9/2

either of these schemes, and some form of *intermediate coupling* scheme must be devised. This is illustrated in Fig. 7.10 where we see that the energy levels of the configurations 2p3s of C and 3p4s of Si are well described by L–S coupling, and the levels 6p7s of Pb by j–j coupling, while the 4p5s levels of Ge and 5p6s levels of Sn are intermediate in character.

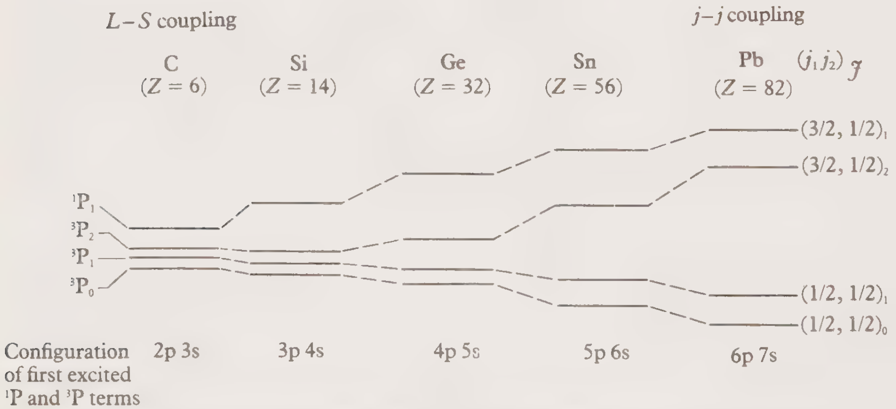

7.10 The splitting of levels in the first excited ^{1}P and ^{3}P terms of the carbon sequence.

PROBLEMS

7.1 Prove that the central field Hamiltonian H_c given by [7.11] commutes with the total orbital angular momentum $\mathbf{L}$ of the electrons.

7.2 Consider the wave functions of the 2^3S level of helium, which are given in the central field approximation by

$$\Psi_c(2^3S) = \phi_-(r_1, r_2)\begin{cases} \alpha(1)\alpha(2) & M_S = 1 \\ \dfrac{1}{\sqrt{2}}[\alpha(1)\beta(2) + \beta(1)\alpha(2)], & M_S = 0 \\ \beta(1)\beta(2) & M_S = -1 \end{cases}$$

with

$$\phi_-(r_1, r_2) = \frac{1}{\sqrt{2}}\,[u_{1s}(r_1)u_{2s}(r_2) - u_{2s}(r_1)u_{1s}(r_2)]$$

Write the three functions $\Psi_c(2^3S)$ in the form of Slater determinants (or a sum of Slater determinants) constructed with the spin-orbitals

$$u_{1s\uparrow} = u_{1s}(r)\alpha, \qquad u_{1s\downarrow} = u_{1s}(r)\beta$$
$$u_{2s\uparrow} = u_{2s}(r)\alpha, \qquad u_{2s\downarrow} = u_{2s}(r)\beta$$

7.3 (a) Show that the total energy of a neutral Thomas-Fermi atom can be written in terms of the electronic density $\rho(r)$ as

$$E = \kappa \int [\rho(r)]^{5/3}\,\mathrm{d}\mathbf{r} - \frac{Ze^2}{4\pi\varepsilon_0}\int \frac{\rho(r)}{r}\,\mathrm{d}\mathbf{r} + \frac{1}{2}\frac{e^2}{4\pi\varepsilon_0}\int \frac{\rho(r)\rho(r')}{|\mathbf{r} - \mathbf{r}'|}\,\mathrm{d}\mathbf{r}\,\mathrm{d}\mathbf{r}' \qquad [1]$$

with $\kappa = 3^{5/3}\pi^{4/3}/(10\,m)$. The first term on the right of [1] is the total kinetic energy of the electrons, the second term is the potential energy of their interaction with the nucleus, and the third term is the potential energy of their mutual interaction.

(b) Obtain the Thomas–Fermi equation [7.66] by minimising the expression [1], subject to the normalisation condition

$$4\pi \int_0^\infty \rho(r) r^2\,\mathrm{d}r = Z$$

7.4 Using the Thomas–Fermi model, obtain an estimate of the following quantities:
(a) average distance of an electron from the nucleus;
(b) average kinetic energy of an electron;
(c) total ionisation energy of the atom.

7.5 Obtain the two coupled equations [7.161] for the spatial orbitals $u_{1s}(r)$ and $u_{2s}(r)$ of the beryllium ground state.

7.6 Show that the Hartree–Fock and Hartree equations for the ground state orbital $u_{1s}(r)$ of helium are identical and given by

$$\left[-\frac{1}{2}\nabla_r^2 - \frac{2}{r} + \int |u_{1s}(r)|^2 \frac{1}{|\mathbf{r} - \mathbf{r}'|}\,\mathrm{d}\mathbf{r}'\right] u_{1s}(r) = E_{1s}u_{1s}(r)$$

Using the Hartree-Fock orbital [6.85b], evaluate the Hartree–Fock potential

$$\mathcal{V}(r) = -\frac{2}{r} + \int |u_{1s}(r)|^2 \frac{1}{|\mathbf{r} - \mathbf{r}'|}\,\mathrm{d}\mathbf{r}'$$

Plot $\mathcal{V}(r)$ and interpret your results in terms of screening.

7.7 Obtain a pair of Hartree–Fock coupled equations for the spatial orbitals $u_{1s}(r)$ and $u_{2s}(r)$ corresponding to the 2^3S ($M = 1$) wave function of helium. Prove that the orbitals $u_{1s}(r)$ and $u_{2s}(r)$ are orthogonal.

7.8 Prove equation [7.155].

7.9 Prove that $[H, \mathbf{L}] = 0$, where H is the Hamiltonian [7.2] and $\mathbf{L} = \Sigma_i \mathbf{L}_i$ is the total orbital angular momentum of the electrons.

7.10 Assuming that L–S coupling holds:

(a) List the possible spectral terms ^{2S+1}L which result from the following electronic configurations

(i) ns n's
(ii) ns n'p
(iii) ns n'd
(iv) nd^2
(v) np n'p n''p
(vi) np^3

(b) List the corresponding fine structure terms $^{2S+1}L_J$.

7.11 Assuming that j–j coupling holds, list the possible terms $(j_1, j_2)_J$ of the following electronic configurations

(a) np nd
(b) $(nl\ 3/2)^2$.

8 The interaction of many-electron atoms with electromagnetic fields

In the previous two chapters, we discussed the energy levels of atoms with more than one electron and now we describe some features of the spectra that result from transitions between these levels, and also how the levels are perturbed by external static electric and magnetic fields. For the most part, this is a straightforward generalisation of the material in Chapters 4 and 5, where the interaction of one-electron atoms with radiation and with static fields was discussed. The selection rules for electric dipole radiative transitions will be obtained and then we shall describe the simple spectra of the alkali metals and of the alkaline earths, which contain one and two optically active electrons respectively. We shall go on to discuss some general features of multiplets, the group of spectral lines arising from transitions between two terms and we then consider the interaction of atoms with static magnetic fields (the Zeeman effect) and with electric fields (the Stark effect). We conclude the chapter with an account of X-ray spectra.

8.1 SELECTION RULES

The selection rules for radiative transitions in a one-electron atom were obtained in Chapter 4. These will now be generalised for atoms containing any number of electrons. We shall consider only transitions in which a single photon is emitted or absorbed because, as explained earlier, in allowed transitions higher order processes make a negligible contribution. The photon field can be described by a vector potential $\mathbf{A}(\mathbf{r}, t)$ and the interaction energy between the radiation field and a number of atomic electrons, 1, 2, . . . N, with position vectors $\mathbf{r}_j$ is

$$-\sum_{j=1}^{N} \frac{i\hbar e}{m} \mathbf{A}(\mathbf{r}_j, t) \cdot \boldsymbol{\nabla}_j = \sum_{j=1}^{N} \frac{e}{m} \mathbf{A}(\mathbf{r}_j, t) \cdot \mathbf{p}_j \qquad [8.1]$$

where $N = Z$ for a neutral atom and $N \neq Z$ for an ion.

This is the generalisation of the linear term in [4.19]. The quadratic term in $\mathbf{A}$ can again be omitted since it contributes to two-photon and higher order processes. The treatment of Chapter 4 can be followed step-by-step. Making the electric dipole approximation, the transition probability is found to depend on a matrix element M_{ba} which can be expressed as a sum of contributions from each

electron (see [4.62])

$$M_{ba} = -\sum_{j=1}^{N} \frac{m\omega_{ba}}{\hbar}\, \hat{\boldsymbol{\varepsilon}} \cdot (\mathbf{r}_j)_{ba}$$

where $(\mathbf{r}_j)_{ba}$ is the matrix element of the position vector $\mathbf{r}_j$ between the two atomic states concerned.

Each atomic state is an eigenstate of $\mathbf{J}^2$ and $\mathcal{J}_z$, where $\mathbf{J} = \sum_{j=1}^{N} \mathbf{J}_j$ is the total angular momentum operator, with quantum numbers $\mathcal{J}$ and $M_{\mathcal{J}}$. It is also an eigenstate of the parity $\mathcal{P}$, but not necessarily of the total orbital angular momentum or the total spin angular momentum. The states can be further specified by a (non-angular momentum) label γ. The quantum numbers of the states a and b will be written

$$\begin{aligned} a &\rightarrow (\gamma, \mathcal{J}, M_{\mathcal{J}}) \\ b &\rightarrow (\gamma', \mathcal{J}', M'_{\mathcal{J}}) \end{aligned}$$

and M_{ba} can be written as

$$M_{ba} = -\sum_{j=1}^{N} \frac{m\omega_{ba}}{\hbar}\, \hat{\boldsymbol{\varepsilon}} \cdot \langle \gamma', \mathcal{J}', M'_{\mathcal{J}} | \mathbf{r}_j | \gamma, \mathcal{J}, M_{\mathcal{J}} \rangle \qquad [8.2]$$

We notice in passing that, since the electrons in the atom (ion) are indistinguishable,

$$M_{ba} = -N \frac{m\omega_{ba}}{\hbar}\, \hat{\boldsymbol{\varepsilon}} \cdot \langle \gamma', \mathcal{J}', M'_{\mathcal{J}} | \mathbf{r}_1 | \gamma, \mathcal{J}, M_{\mathcal{J}} \rangle \qquad [8.3]$$

It is convenient to introduce the total dipole moment operator of the atom as

$$\mathbf{D} = -\sum_{j=1}^{N} e\mathbf{r}_j \qquad [8.4]$$

so that

$$M_{ba} = \frac{m\omega_{ba}}{\hbar e}\, \hat{\boldsymbol{\varepsilon}} \cdot \langle \gamma', \mathcal{J}', M'_{\mathcal{J}} | \mathbf{D} | \gamma, \mathcal{J}, M_{\mathcal{J}} \rangle \qquad [8.5]$$

The transition rates for photon emission or absorption can be written in terms of $\mathbf{D}$, and for spontaneous emission of a photon of polarisation $\hat{\varepsilon}$ into a solid angle $\mathrm{d}\Omega$ in the direction (θ, ϕ), we have (see [4.70])

$$W^{s}_{ab}\, \mathrm{d}\Omega = \frac{1}{2\pi\hbar c^3} \frac{1}{4\pi\varepsilon_0} \omega^3_{ba} |\hat{\boldsymbol{\varepsilon}} \cdot \langle \gamma', \mathcal{J}', M'_{\mathcal{J}} | \mathbf{D} | \gamma, \mathcal{J}, M_{\mathcal{J}} \rangle|^2\, \mathrm{d}\Omega \qquad [8.6]$$

The dipole moment $\mathbf{D}$ is a vector operator (see Appendix 4) because, as can be verified easily, it obeys the following commutation relations with the total

angular momentum $\mathbf{J}$:

$$[\mathcal{J}_x, D_x] = [\mathcal{J}_y, D_y] = [\mathcal{J}_z, D_z] = 0$$

$$[\mathcal{J}_x, D_y] = i\hbar D_z; \qquad [\mathcal{J}_y, D_z] = i\hbar D_x$$

and

$$[\mathcal{J}_z, D_x] = i\hbar D_y \tag{8.7}$$

The spherical components D_q $(q = 0, \pm 1)$ of $\mathbf{D}$ are defined so that

$$\begin{aligned} D_1 &= -\frac{1}{\sqrt{2}}(D_x + iD_y) = |\mathbf{D}|\left(\frac{4\pi}{3}\right)^{1/2} Y_{1,1}(\alpha, \beta) \\ D_0 &= D_z = |\mathbf{D}|\left(\frac{4\pi}{3}\right)^{1/2} Y_{1,0}(\alpha, \beta) \\ D_{-1} &= \frac{1}{\sqrt{2}}(D_x - iD_y) = |\mathbf{D}|\left(\frac{4\pi}{3}\right)^{1/2} Y_{1,-1}(\alpha, \beta) \end{aligned} \tag{8.8}$$

where (α, β) are the polar angles of $\mathbf{D}$.

Similarly the spherical components of the polarisation vector $\hat{\varepsilon}$ are ε_q, where (see [4.81])

$$\varepsilon_1 = -\frac{1}{\sqrt{2}}(\hat{\varepsilon}_x + i\hat{\varepsilon}_y),\ \varepsilon_0 = \hat{\varepsilon}_z,\ \varepsilon_{-1} = \frac{1}{\sqrt{2}}(\hat{\varepsilon}_x - i\hat{\varepsilon}_y) \tag{8.9}$$

The scalar product $\hat{\varepsilon} \cdot \mathbf{D}$ can be expressed in spherical components as

$$\hat{\varepsilon} \cdot \mathbf{D} = \sum_{q=0,\pm 1} \varepsilon_q^{\star} D_q \tag{8.10}$$

Now the Wigner–Eckart theorem (Appendix 4) states that the matrix elements of a vector operator with respect to eigenstates of $\mathbf{J}^2$ and $\mathcal{J}_z$ only depends on $M_\mathcal{J}$, $M'_\mathcal{J}$ and q through the Clebsch–Gordan coefficient $\langle \mathcal{J} 1 M_\mathcal{J} q | \mathcal{J}' M'_\mathcal{J} \rangle$. We have

$$\langle \gamma', \mathcal{J}', M'_\mathcal{J} | D_q | \gamma, \mathcal{J}, M_\mathcal{J} \rangle = \frac{1}{\sqrt{2\mathcal{J}' + 1}} \langle \mathcal{J} 1 M_\mathcal{J} q | \mathcal{J}' M'_\mathcal{J} \rangle \langle \gamma' \mathcal{J}' \| \mathbf{D} \| \gamma \mathcal{J} \rangle \tag{8.11}$$

where the reduced matrix element $\langle \gamma' \mathcal{J}' \| \mathbf{D} \| \gamma \mathcal{J} \rangle$ is independent of q, $M_\mathcal{J}$, $M'_\mathcal{J}$.

The Clebsch–Gordan coefficient $\langle \mathcal{J} 1 M_\mathcal{J} q | \mathcal{J}' M'_\mathcal{J} \rangle$ vanishes unless:

$$\begin{aligned} &\text{(a)}\ M_\mathcal{J} + q = M'_\mathcal{J} \\ &\text{(b)}\ |\mathcal{J} - 1| \leqslant \mathcal{J}' \leqslant \mathcal{J} + 1 \\ &\text{(c)}\ \mathcal{J} + \mathcal{J}' \geqslant 1 \end{aligned} \tag{8.12}$$

The selection rules for electric dipole transitions are thus:

$$\Delta M_\mathcal{J} = 0, \pm 1 \tag{8.13a}$$

and

$$\Delta \mathcal{J} = 0, \pm 1, \tag{8.13b}$$

but

$$\mathcal{J} = 0 \leftrightarrow \mathcal{J}' = 0 \tag{8.13c}$$

is not allowed.

In addition, since under the parity operation **D** changes sign, and because the atomic states are eigenstates of parity, we see that the dipole matrix element vanishes unless the states a and b have opposite parity. This is known as *Laporte's Rule*.

It can be shown, by extending these arguments, that all matrix elements for multipole transitions, either electric or magnetic, are proportional to the Clebsch–Gordan coefficient $\langle \mathcal{J}\lambda M_{\mathcal{J}} q | \mathcal{J}' M'_{\mathcal{J}} \rangle$, where $\lambda = 1$ for dipole transitions, $\lambda = 2$ for quadrupole transitions and so on. For electric multipole transitions, the parity changes if λ is odd and does not change if λ is even, while for magnetic multipoles the parity changes for even λ and does not change for odd λ. Combining this parity rule with the properties of the Clebsch–Gordan coefficient the selection rules can be obtained (Problem 8.1) for any multipole.

L–S coupling

When the spin–orbit interaction is weak then, as we saw in the previous chapter, the Russell–Saunders, or L–S coupling, approximation is accurate, in which both the total orbital angular momentum and the total spin angular momentum are conserved. Since the operator **D** is independent of spin, we have

$$\langle \mathcal{J}', L', S', M'_{\mathcal{J}} | \mathbf{D} | \mathcal{J}, L, S, M_{\mathcal{J}} \rangle = \delta_{SS'} \langle \mathcal{J}', L', S', M'_{\mathcal{J}} | \mathbf{D} | \mathcal{J}, L, S, M_{\mathcal{J}} \rangle \tag{8.14}$$

The selection rules which hold in addition to those of [8.13] for electric dipole transitions are then:

$$\Delta L = 0, \pm 1 \qquad (L = 0 \leftrightarrow L' = 0 \text{ is not allowed}) \tag{8.15a}$$

$$\Delta S = 0 \tag{8.15b}$$

The most usual case is one in which the orbital of only one electron in the atom changes. If the orbital concerned has an angular momentum quantum number l_j, then our discussion of the one-electron atom shows that

$$\Delta l_j = \pm 1 \tag{8.15c}$$

The case $\Delta l_j = 0$ is not allowed because the parity of the atom must change. If two or more configurations are strongly mixed in a particular state, then more than one electron can make a transition simultaneously even though only one photon is being emitted or absorbed, but this is a rather uncommon circumstance and we shall not deal with it.

8.2 THE SPECTRA OF THE ALKALIS

As we have seen in Chapter 7, the structure of the ground states of the alkali metals (Li, Na, K, Rb, Cs, Fr) is that of a single valence electron moving in an s orbital outside a *core* consisting of a *closed (sub)shell* system. In lithium, the configuration of the core is $(1s)^2$, in sodium $(1s)^2(2s)^2(2p)^6$, in potassium $(1s)^2(2s)^2(2p)^6(3s)^2(3p)^6$, and in each case the total orbital angular momentum and the total spin angular momentum of the core are zero, designated as ${}^1S_0$. The cores of rubidium, caesium and francium are also ${}^1S_0$. Because the core is spherically symmetric, the valence electron of a neutral alkali atom ($N = Z$) moves in an effective *central* potential $V(r)$, which at large distances approaches the Coulomb potential

$$V(r) \underset{r\to\infty}{\longrightarrow} -\frac{e^2}{(4\pi\varepsilon_0)r} \qquad [8.16]$$

since the nuclear charge Ze is screened by the core which contains $(Z - 1)$ electrons. The lowest state of the valence electron has zero orbital angular momentum ($l = 0$) and the corresponding orbital is designated (n_0s), where, to satisfy the Pauli principle, $n_0 = 2$ for Li, 3 for Na, 4 for K and so on. For small r the potential $V(r)$ is always more attractive than $-e^2/(4\pi\varepsilon_0)r$, so that the binding energy of the orbital (n_0s) is always greater than that of the (n_0s) level of hydrogen. The excited states of the valence electron, moving with respect to the unexcited core, are designated (nl) with $n \geqslant n_0$. The binding energy of the orbital (nl) is again greater than that of the (nl) level of hydrogen. For highly excited states, for which the charge density of the orbital is almost entirely outside the region of the core, the orbitals approximate closely to true hydrogenic wave functions, and the energy levels are very close to those of hydrogen.

As $V(r)$ is not Coulombic at short distances, the energy levels are not degenerate in l, for a given n. Thus the (2s) level in lithium lies well below the (2p) level, and for sodium the (3s) level is below the (3p) level, which in turn is below the (3d) level (see Fig. 8.1). As the excitation increases and the levels become more hydrogenic in character, there is near degeneracy in l, for a given n. The valence electron is bound weakly compared with the core electrons. For each of the alkalis it requires about 5 eV to detach the valence electron, compared with over 20 eV for the least bound of the core electrons, and it follows that the optical spectrum is due to transitions involving the valence electron only, the core remaining inert. The term symbol of the ground state of an alkali can be written, omitting the core, as $(n_0s)^2S_{1/2}$ where the superscript denotes the multiplicity of the spin state $(2s + 1)$, in this case with $s = 1/2$, and the subscript is the total angular momentum quantum number. Excited states are of the form $(ns)^2S_{1/2}$, $(np)^2P_{1/2,3/2}$, $(nd)^2D_{3/2,5/2}$ and so on.

The gross structure of the alkali spectra can be obtained by combining the selection rules for a one-electron atom (see Chapter 4) with a knowledge of the energies of the levels (nl) of the valence electron. The energy levels can be

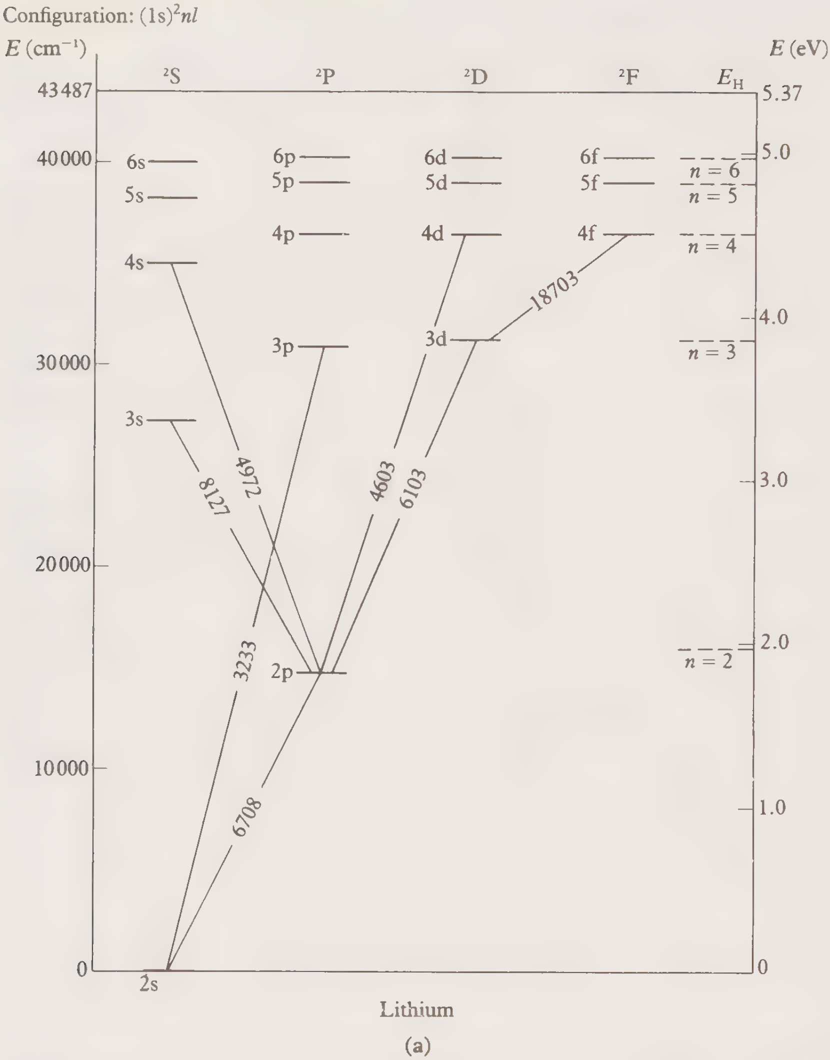

8.1 Grotrian diagrams of energy levels and transitions in (a) lithium and (b) sodium. Energies are shown relative to the ground state, with the horizontal line at the top of each diagram showing the ionisation potential of the ground state. The column headed E_H shows the corresponding positions of the levels of atomic hydrogen.

represented by the empirical formula

$$E_{nl} = -\frac{1}{2}\frac{1}{(n - \mu_{nl})^2} \text{ a.u.} \qquad [8.17]$$

The quantities μ_{nl} are known as *quantum defects*. To a good approximation μ_{nl} is (for a particular alkali) a function of l only; $\mu_{nl} \sim \alpha(l)$. Thus we can write the effective principal quantum number, in a form due to Rydberg, as

$$n^\star = n - \alpha(l) \qquad [8.18]$$

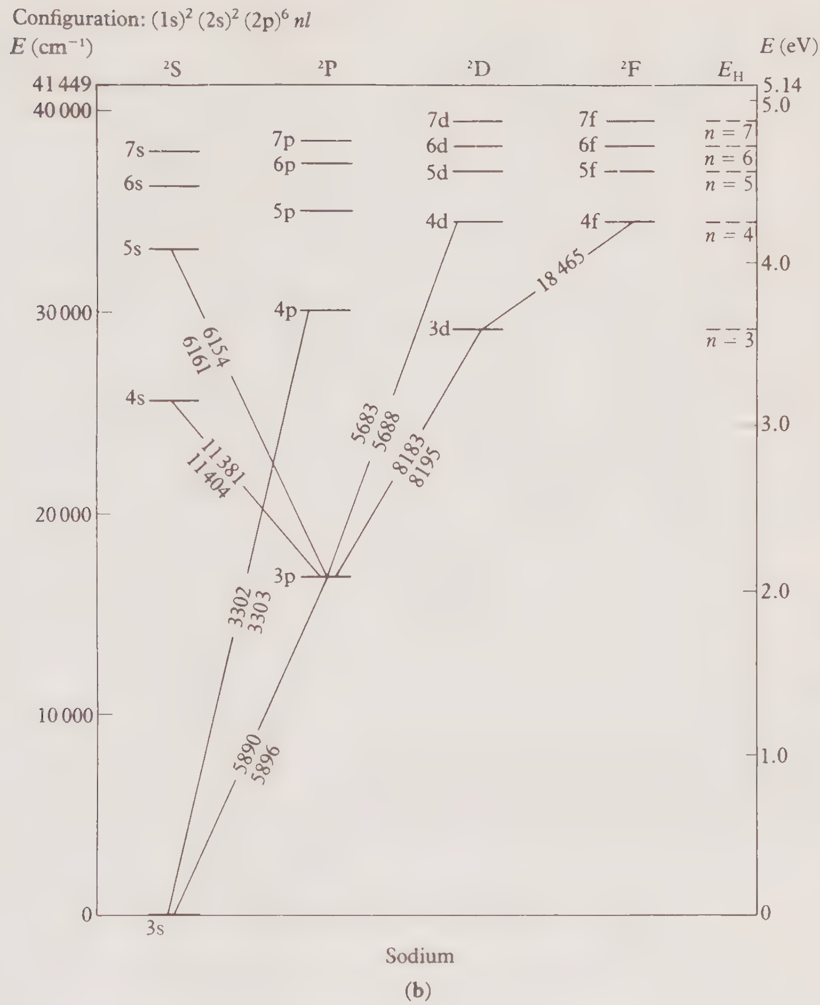

Fig. 8.1(*Cont.*)

for lithium, sodium and potassium. A small correction to this formula was made by Ritz, who wrote [1]

$$n^* = n - \alpha(l) - \beta(l)/n^2 \qquad [8.19]$$

For example, in the case of the p levels of lithium one has $\alpha(1) = 0.040$ and $\beta(1) = 0.024$. Some parameters of the energy levels of the alkalis are given in Table 8.1.

[1] Complete tables of the quantities n^* can be found in Kuhn (1970).

Table 8.1 Parameters of the energy levels of the alkalis

(a) *quantum defects* $\alpha(l)$

Atom $l =$	0	1	2	3
Li	0.40	0.04	0.00	0.00
Na	1.35	0.85	0.01	0.00
K	2.19	1.71	0.25	0.00
Rb	3.13	2.66	1.34	0.01
Cs	4.06	3.59	2.46	0.02

(b) Effective principal quantum numbers $n^\star$ for the $(n_0\mathrm{s})$ and $(n_0\mathrm{p})$ levels

Level	Li($n_0 = 2$)	Na($n_0 = 3$)	K($n_0 = 4$)	Rb($n_0 = 5$)	Cs($n_0 = 6$)
$(n_0\mathrm{s})^2\mathrm{S}_{1/2}$	1.588	1.626	1.771	1.805	1.869
$(n_0\mathrm{p})^2\mathrm{P}_{1/2}$	1.966	2.116	2.232	2.280	2.392
$(n_0\mathrm{p})^2\mathrm{P}_{3/2}$	1.966	2.117	2.235	2.293	2.362

(c) Ionisation potentials of the alkalis

	Li	Na	K	Rb	Cs
$\mathrm{I_P}$(eV)	5.39	5.14	4.34	4.18	3.89

Absorption spectra

The absorption spectra can be obtained by passing light through the vapour of the alkali metal. Except at very high temperatures, most atoms will be in the ground state, and the series of absorption lines correspond to transitions from the $(n_0\mathrm{s})$ ground state to the $(n\mathrm{p})$ levels, with frequencies

$$\nu = R\left[\left(\frac{1}{n^\star_{n_0\mathrm{s}}}\right)^2 - \left(\frac{1}{n^\star_{n\mathrm{p}}}\right)^2\right] \tag{8.20}$$

where R is the Rydberg constant. This series of lines is called the *principal series*.

Emission spectra

The *principal series* can be observed in emission as well as in absorption. By far the strongest line is that corresponding to the transition $n_0\mathrm{p} \rightarrow n_0\mathrm{s}$ and is called a *resonance line*. Because of spin–orbit coupling, which we shall discuss below, the resonance lines are doublets. The wavelengths of these lines are given in Table 8.2. Several other series of emission lines can be observed (see Fig. 8.1), including the *sharp series*, corresponding to $n\mathrm{s} \rightarrow n_0\mathrm{p}$ transitions, the *diffuse series*, which correspond to $n\mathrm{d} \rightarrow n_0\mathrm{p}$ and the *fundamental series*, which correspond to $n\mathrm{f} \rightarrow n_0\mathrm{d}$.

The emission spectra of positive ions with one valence electron outside an inert core can also be observed in a spark discharge. For instance the sequence of ions iso-electronic with lithium consists of LiI, BeII, BIII, CIV . . . where I stands for the neutral atom, II for a singly ionised atom and so forth. The energy

Table 8.2 The resonance lines of the alkali metals: Li, Na, K, Rb, Cs. The most prominent emission lines in the alkali spectra are the resonance lines corresponding to the transition $(n_0\text{p}) \to (n_0\text{s})$

Atom	*Frequency* (cm^{-1})	*Wavelength* (Å)
Li	14904	6708
Na†	16956	5896
	16973	5890
K	12985	7699
	13043	7665
Rb	12582	7946
	12817	7800
Cs	11179	8943
	11733	8521

† The yellow lines in this doublet are known as the Fraunhofer D-lines which occur in the spectrum of sunlight.

levels of such a sequence can be written as

$$E_{nl} = -\frac{1}{2}\frac{\tilde{Z}^2}{[n - \alpha(l)]^2} \text{ a.u.} \tag{8.21}$$

where $\tilde{Z} = Z - N + 1$, Z being the nuclear charge and N the number of electrons. The quantity $\tilde{Z}$ is therefore the net charge of the nucleus and the core electrons, and is equal to the Roman numeral in the symbols BeII, BIII, CIV, and so on. The quantum defect $\alpha(l)$ decreases smoothly during such a sequence so that for large Z the spectrum becomes hydrogenic.

Fine structure

All the energy levels of the valence electron in an alkali (except for those with $l = 0$) are split into two; one level corresponding to a total angular momentum quantum number $j = l + 1/2$ and the other to $j = l - 1/2$. The interaction causing this splitting is the spin–orbit interaction, which was discussed in Chapter 5 in connection with the hydrogen atom. The shift in energy due to this effect is given by (see Section 5.1)

$$\Delta E = \tfrac{1}{2}\lambda_{nl}[j(j + 1) - l(l + 1) - \tfrac{3}{4}] \tag{8.22}$$

The constant λ_{nl} is proportional to the expectation value of $r^{-1}\,\text{d}V(r)/\text{d}r$, $V(r)$ being the effective central potential in which the valence electron moves:

$$\lambda_{nl} = \frac{\hbar^2}{2m^2c^2}\left\langle \frac{1}{r}\frac{\text{d}V(r)}{\text{d}r} \right\rangle = \hbar^2\langle \xi(r) \rangle \tag{8.23}$$

Table 8.3 Spin–orbit splitting of the $(n_0\text{p})$ levels of the alkalis

Atom	Li	Na	K	Rb	Cs
n_0	2	3	4	5	6
ΔE	0.337	17.2	57.7	238	554 cm^{-1}
	0.42	21	72	295	687×10^{-4} eV

The magnitude of λ_{nl} can be estimated by using $V(r)$ as calculated by the Hartree–Fock method. It turns out to be much larger than for atomic hydrogen (about 50 times larger for the 3p level of sodium than for the 2p level of hydrogen), and the other relativistic corrections which are important for hydrogen are negligible. The observed splitting of the $(n_0\text{p})$ levels of the neutral alkali atoms are shown in Table 8.3. For a given atom the splitting decreases with increasing n and l, while along an iso-electronic sequence of positive ions the splitting increases with the charge $\tilde{Z}e$ on the (nucleus + core), behaving like $\tilde{Z}^4$ for large $\tilde{Z}$.

Using the Hartree–Fock potential λ_{nl} is found to be positive, and the level with $j = 3/2$ has greater energy than that with $j = 1/2$. This is found to be true for all terms of lithium, and for the lower lying states of the other alkalis, although quantitative agreement with the observed magnitude of the splitting is not good. For the ^{2}D terms of sodium and potassium and for many other higher terms, the normal order is inverted, this effect being due to exchange interactions between the valence and core electrons and other small interactions with the core.

The one-electron selection rules (see Chapter 4) require $\Delta l = \pm 1$ and $\Delta j = 0, \pm 1$ with $j = 0 \leftrightarrow j = 0$ forbidden. Thus the principal and sharp series of lines corresponding to $^2\text{P}_{3/2,1/2} \leftrightarrow {}^2\text{S}_{1/2}$ transitions are doublets, while the diffuse series $^2\text{D}_{5/2,3/2} \to {}^2\text{P}_{3/2,1/2}$ and the fundamental series $^2\text{F}_{7/2,5/2} \to {}^2\text{D}_{5/2,3/2}$ are triplets. The frequencies and wavelengths of the split resonance lines are given in Table 8.2.

8.3 HELIUM AND THE ALKALINE EARTHS

The energy levels of helium and two-electron ions were discussed in Chapter 6. In the absence of spin–orbit and other spin-dependent interactions, which are in fact exceedingly small, the total spin is a good quantum number, and the energy levels can be divided into singlet levels with $S = 0$ and triplet levels with $S = 1$.

The electric dipole operator cannot change the spin of an electron, and in the absence of spin-dependent forces, the selection rule $\Delta S = 0$ must hold. For helium and for helium-like ions with small nuclear charge Ze, the spin–orbit and spin–spin interactions are a small perturbation on the triplet states, but are not large enough to mix the triplet states with the singlet states to a detectable extent. Both the total orbital angular momentum L and the total spin S remain conserved to a very good approximation, and the system is a good example of

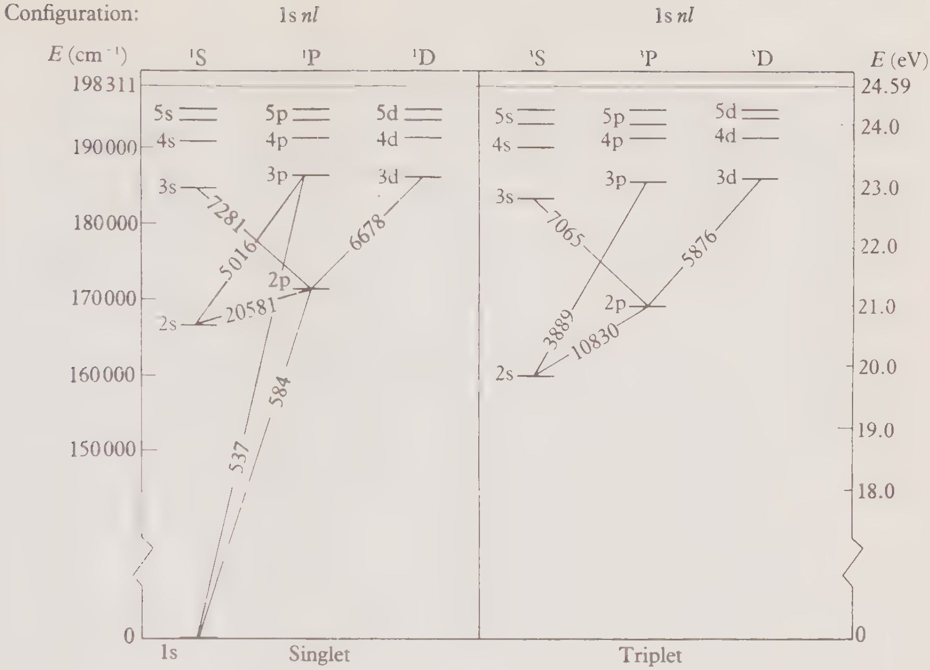

Helium

(a)

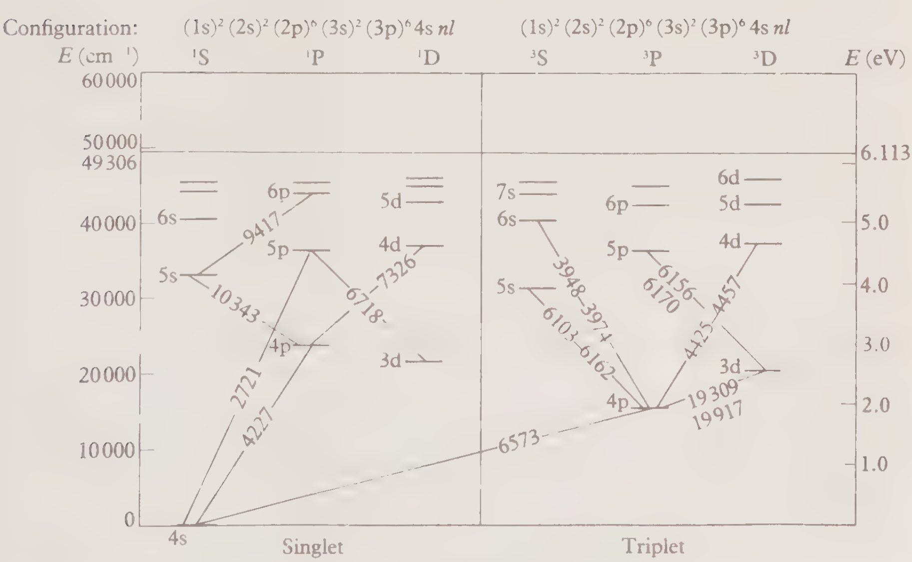

Calcium

(b)

8.2 Simplified Grotrian diagrams showing transitions in (a) helium (b) calcium. Wavelengths in angstom units are shown against the lines representing the transitions. For multiplets with substantial splitting the extreme wavelengths are shown against the lines. Energies in cm^{-1} or eV are given relative to the ground state and the horizontal line indicates the ionisation potential. Notice the intercombination line shown for calcium. Only a few of the transitions which have been identified are shown, for clarity.

L–S or Russell–Saunders coupling. For helium-like ions with large Z, L–S coupling becomes a less accurate approximation and lines corresponding to singlet to triplet transitions can be observed. These are called *intercombination lines* and are usually weak. A term diagram for helium is shown in Fig. 8.2. The terms of the singlet and triplet states can be written $(1sns)^1S_0$, $(1snp)^1P_1$, $(1snd)^1D_2$ . . . and $(1sns)^3S_1$, $(1snp)^3P_J$, $(1snd)^3D_J$. . . . In the triplet states, the possible values of J for a given $L \neq 0$ are $J = L$ and $J = L \pm 1$ while $J = 1$ when $L = 0$. Spin-orbit coupling, which removes the degeneracy in J, splits each level with $L \neq 0$ into three components.

Helium can also be found in states in which both electrons are excited, for example $(2s2p)^1P_1$. Such states can decay by dipole radiation, for example

$$(2s2p)^1P_1 \rightarrow (2s1s)^1S_0$$

but a competing process is energetically possible in which an electron is ejected

$$\mathrm{He}(2s2p) \rightarrow \mathrm{He}^+(1s) + e^-$$

This process is called *autoionisation* and was discussed at the end of Chapter 6. It is generally a very rapid process, with the result that doubly excited levels have a very short lifetime and the corresponding spectral lines are very broad and weak.

The fine structure of helium and two-electron ions

The spin–orbit coupling is of the form $A(\mathbf{L} \cdot \mathbf{S})$. The magnitude of the coupling A depends on the nuclear charge, and for helium it is so small that the magnetic interaction between the spins of the two electrons is comparable in magnitude, and in this case the Landé interval rule breaks down. The spin magnetic dipole moment of each electron is $-2\mu_B \mathbf{S}_i/\hbar$ $(i = 1, 2)$ and the interaction energy between them, when separated by a distance $r \neq 0$, is

$$V_S(r) = \frac{\mu_0}{4\pi}\frac{4\mu_B^2}{\hbar^2}\left[\frac{\mathbf{S}_1 \cdot \mathbf{S}_2}{r^3} - 3\frac{(\mathbf{S}_1 \cdot \mathbf{r})(\mathbf{S}_2 \cdot \mathbf{r})}{r^5}\right] \qquad [8.24]$$

The energy shift due to this interaction can be calculated by first-order perturbation theory. It clearly vanishes for singlet states. There is one further interaction of significance in helium, namely the interaction between the spin of one electron and the orbital motion of another, called the spin–other orbit interaction. This interaction is of the form $A'(\mathbf{L} \cdot \mathbf{S})$ and so obeys the interval rule (for given L and S)

$$\frac{E(J) - E(J - 1)}{J} = \text{constant} \qquad [8.25]$$

(although the sign of A' may be different from that of A). The constant A' does not increase as fast as A does with Z and the spin–other orbit interaction is small compared with the spin–own orbit interaction in the heavier atoms.

To bring out some of these points it is interesting to compute the fine structure of helium and two-electron ions approximately, following the treatment of Bethe and Salpeter (1957). We are concerned with triplet states of the configuration ($1snl$) with $l \neq 0$. Since the charge distribution of the electron in the (nl) orbit (with $l > 0$) is at greater distances from the nucleus than that for the (1s) electron, exchange can be neglected and the (nl) electron (labelled 2) can be considered to be moving in a Coulomb potential V due to the nucleus (of charge Ze) fully screened by the inner electron

$$V(r_2) = -(Z - 1)/r_2$$

Here and in what follows we use atomic units. Since the average value of r_2 is much larger than the average value of r_1, we can replace the inter-electron distance r in [8.24] by r_2. Then the energy due to the spin–spin interaction can be shown to be

$$\Delta E_{SS} = \langle nl|V_S(r_2)|nl\rangle = 2\alpha^2\mu_{\mathrm{B}}^2\left\langle\left(\frac{1}{r_2}\right)^3\right\rangle X = \frac{\alpha^2}{2}\left\langle\left(\frac{1}{r_2}\right)^3\right\rangle X \qquad [8.26]$$

where

$$\begin{aligned} X &= l/(2l+3) && \text{for } \mathcal{J} = l+1 \\ X &= -1 && \text{for } \mathcal{J} = l \\ X &= (l+1)/(2l-1) && \text{for } \mathcal{J} = l-1. \end{aligned}$$

The spin–orbit interaction is

$$\frac{1}{2}\alpha^2(Z-1)\left\langle\left(\frac{1}{r_2}\right)^3\right\rangle(\mathbf{L}_2\cdot\mathbf{S}_2) \qquad [8.27]$$

and the spin–other orbit interaction is

$$-\frac{1}{2}\alpha^2 2\left\langle\left(\frac{1}{r_2}\right)^3\right\rangle(\mathbf{L}_2\cdot\mathbf{S}_1) \qquad [8.28]$$

The two interactions [8.27] and [8.28] together provide an energy shift

$$\Delta E_{\mathrm{LS}} = \left\langle\left(\frac{1}{r_2}\right)^3\right\rangle\frac{1}{8}\alpha^2(Z-3)[\mathcal{J}(\mathcal{J}+1) - l(l+1) - S(S+1)] \qquad [8.29]$$

where $S = 1$ for the triplet levels.

The level shift ΔE_{LS} obeys the Landé rule. If only the spin–orbit interaction had been considered ($Z - 3$) would have been replaced by ($Z - 1$). For neutral helium with $Z = 2$, the multiplet is inverted by the spin–other orbit interaction, but the addition of the spin–spin interaction completely alters the ratio of the level shifts (see Fig. 8.3). This is true for two-electron ions with small Z. We have in a ^{3}P multiplet, $E(\mathcal{J} = 0) > E(\mathcal{J} = 1) > E(\mathcal{J} = 2)$ for helium; $E(\mathcal{J} = 0) > E(\mathcal{J} = 2) > E(\mathcal{J} = 1)$ for Li^+; while for $Z \geqslant 8$, $E(\mathcal{J} = 2) > E(\mathcal{J} = 1) > E(\mathcal{J} = 0)$. For large Z the spin–orbit interaction dominates and the order of the levels is normal.

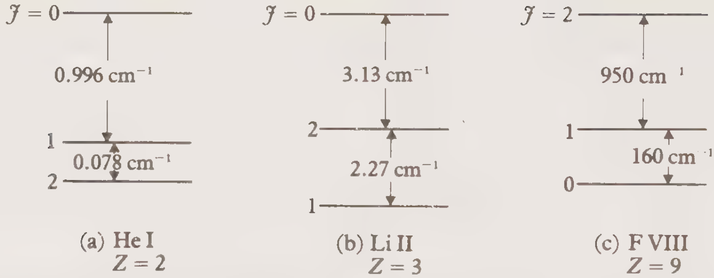

8.3 Diagram (not to scale) of the splitting of the 2^3P_J level in two-electron atoms. The experimental splitting is shown for He I and Li II and for F VIII.

The alkaline earths (Be, Mg, Ca, Sr, Ba, Zn, Cd, Hg)

Just as the spectra of the alkalis have a close connection with those of one-electron atoms, the spectra of the alkaline earths can be compared with those of helium and the two-electron ions. The alkaline earths have two valence electrons moving outside an inert closed (sub)shell core, with $L = 0$ and $S = 0$. For example the ground state of Be is $(1s)^2(2s)^2\ {}^1S_0$, and that of Mg is $(1s)^2(2s)^2(2p)^6(3s)^2\ {}^1S_0$. The energy required to ionise a valence electron is 9.3 eV for Be and 7.6 eV for Mg. As these electrons are more easily excited than core electrons, the optical spectrum is formed by transitions involving the valence electrons alone. As for helium, the energy levels are either singlet (total spin $S = 0$) or triplet (total spin $S = 1$) and the most prominent lines are the resonance lines between the lowest singlet states $(n_0sn_0p)^1P_1 \to (n_0s)^2\ {}^1S_0$. The spin–orbit interaction splits the triplet series into three levels, except for S terms. A term diagram for Ca is shown in Fig. 8.2; the triplet splitting is too small to be indicated.

8.4 ATOMS WITH SEVERAL OPTICALLY ACTIVE ELECTRONS. MULTIPLET STRUCTURE

The spectra of atoms with one and two valence electrons consist, as we have seen, of simple series and the same is largely true of the trivalent elements such as B and Al. Such simple series can be readily identified and analysed, but in the complex spectra of more complicated systems, series are much more difficult, and often impossible, to identify. To identify the terms involved in a given region of the spectrum, the multiplets of lines which arise from transitions between the members of two terms must be analysed. In Chapter 7 we have seen how single configurations are split by the electrostatic energy into a number of terms ${}^{2S+1}L_J$, which are degenerate in the total angular momentum J, for a given L and S. In L–S coupling the degeneracy in J is removed by the spin–orbit interaction, but L and S remain good quantum numbers. The relative spacing of the levels within a multiplet is given by the Landé interval rule [7.199]

$$E(L, S, J) - E(L, S, J - 1) = AJ \qquad [8.30]$$

Another aid to analysis of the observed spectra is the total splitting of the term, which is

$$E(L, S, \mathcal{J} = L + S) - E(L, S, \mathcal{J} = |L - S|) = AS(2L + 1), \qquad L \geq S$$
$$= AL(2S + 1), \qquad L < S \qquad [8.31]$$

For example, consider the triplet of lines which arise from the transition in Mg between the (3s4s) 4^3S_1 level and the (3s3p) $3^3P_{2,1,0}$ levels. The observed frequencies are 19286, 19326 and 19346 cm^{-1}. We see that (1/2) $[E(\mathcal{J} = 2) - E(\mathcal{J} = 1)] = 20$ cm^{-1} and $[E(\mathcal{J} = 1) - E(\mathcal{J} = 0)] = 20$ cm^{-1} which is consistent with the Landé rule [8.30] with $A = 20$. For heavy atoms on the other hand, L–S coupling breaks down and the Landé rule is not satisfied. An example is the corresponding transition in Hg, that is between the 7^3S_1 and $6^3P_{2,1,0}$ levels. The observed frequencies are 18307, 22938, 24705 cm^{-1}. From these data, (1/2) $[E(\mathcal{J} = 2) - E(\mathcal{J} = 1)] = 2315.5$ cm^{-1} and $[E(\mathcal{J} = 1) - E(\mathcal{J} = 0)] = 1767$ cm^{-1}. This time the two differences, which should be both equal to A, if L–S coupling were satisfied accurately, are far from equal.

In general, the heavy elements have spectra which do not conform to the interval rule, because of the mixing of states with different S. As we have seen the interval rule can be violated in other circumstances, notably in helium, where the spin–orbit coupling is not large compared with the spin–spin interaction.

The number of spectral lines arising from transitions between two terms is determined by the selection rules. Consider the group of lines arising from transitions between members of two triplet terms, for example $^3D_{1,2,3}$ and $^3F_{2,3,4}$ terms. The selection rules $\Delta S = 0$, $\Delta L = \pm 1$ are satisfied, and the rule $\Delta\mathcal{J} = 0, \pm 1$ allows the following six transitions:

$$^3D_1 \leftrightarrow {}^3F_2; \quad {}^3D_2 \leftrightarrow {}^3F_2; \quad {}^3D_2 \leftrightarrow {}^3F_3; \quad {}^3D_3 \leftrightarrow {}^3F_2;$$
$$^3D_3 \leftrightarrow {}^3F_3; \quad {}^3D_3 \leftrightarrow {}^3F_4$$

A particular example of a $^3D \to {}^3P$ transition in strontium is shown in Fig. 8.4 ($5^3D \to 5^3P$).

Intensities

The radial integrals in the matrix element of the electric dipole moment [8.5] are the same for each transition between members of two terms, so the relative intensity of the lines forming the multiplet depend only on angular momentum factors. These have been tabulated and may be consulted in Kuhn (1970) or Condon and Shortley (1951). It is found that in each multiplet the strongest lines are those for which $\Delta\mathcal{J} = \Delta L$, and if several lines satisfy this relation, the strength among these lines increases with $\mathcal{J}$. Under normal conditions of excitation, the number of atoms in each level of a term is proportioned to the statistical weight $(2\mathcal{J} + 1)$ of that level. This leads to the sum rule of Ornstein, Burger and Dorgelo, valid for L–S coupling, that the sum of the intensities of all

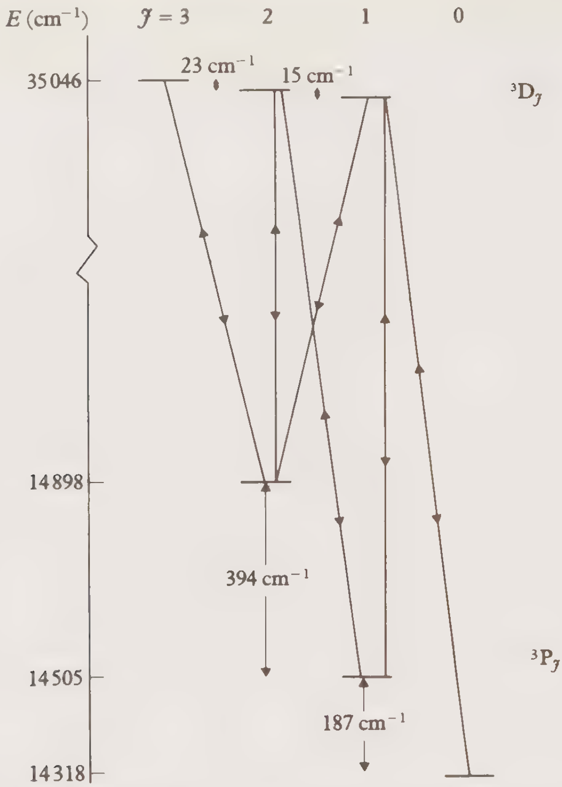

8.4 The transitions between the $(5s5d)^3D_J$ and the $(5s5p)^3P_J$ terms of strontium. The left-hand side shows the energies above the $(5s^2)^1S_0$ ground state in cm^{-1}.

the transitions from (or to) a given level of total angular momentum J in a multiplet is proportional to $(2J + 1)$. In some cases, this rule is sufficient to determine the relative strengths of the lines in a multiplet completely. For example in a ^3P_J to $^3S_1$ multiplet, the intensities of the three lines are in the ratio 5:3:1. In other cases, where both terms are split this is not so. An example is the $^3D_J \rightarrow {}^3F_J$ multiplet for which the sum rules provide only four equations, so the relative intensities between the six lines cannot be completely determined. On the other hand in a doublet system such as $^2D_{3/2,5/2} \leftrightarrow {}^2F_{5/2,7/2}$, the relative intensities for the three lines can be found as follows. Let a, b, c be the intensities of the lines $^2D_{3/2} \leftrightarrow {}^2F_{5/2}$, $^2D_{5/2} \leftrightarrow {}^2F_{5/2}$, $^2D_{5/2} \leftrightarrow {}^2F_{7/2}$. Applying the sum rule to each of the ^2D levels, we find

$$a = 4\lambda$$
$$b + c = 6\lambda$$

Similarly applying the rule to the ^2F levels we find

$$a + b = 6\mu$$
$$c = 8\mu$$

where λ and μ are constants of proportionality. Solving we find that $a:b:c$ is 14:1:20.

Displaced terms

For the most part, we have considered situations in which only one electron in an atom is excited, the remaining electrons being in the ground state of the positive ion. In practice, lines can be observed which correspond to situations in which more than one electron is in an excited state, and we have already shown how some of these excited states are subject to autoionisation. Frequently, regular series of lines can be observed which are associated with a particular state of the excited ion. For example in Be, there is a doubly excited configuration $(1s)^2(2p)^2$, which gives rise to singlet and triplet series of lines corresponding to transitions $(1s)^2 2pns \rightarrow (1s)^2(2p)^2$. The series limit $(n \rightarrow \infty)$, is at a higher energy than the series limit for the regular series $(1s)^2 2snp \rightarrow (1s)^2(2s)^2$, so the terms are said to be *displaced*. Transitions between the regular and displaced terms are possible. For example in Be, there is a line at 14 320 cm^{-1}, corresponding to the transition

$$(1s)^2(2p)^2\ {}^1D_2 \rightarrow (1s)^2(2s2p)\ {}^1P_1$$

and another at 28 944 cm^{-1} corresponding to

$$(1s)^2(2p)^2\ {}^1S_0 \rightarrow (1s)^2(2s2p)\,{}^1P_1$$

Similarly, triplet transitions can be observed forming a multiplet of lines between the $(2p)^2\ {}^3D_J$ and the $(2s2p)^3P_J$ terms (see Fig. 8.5).

Hyperfine structure

We saw in Chapter 5, in the case of a one-electron atom, that the magnetic interaction between the nucleus and an electron splits an atomic term specified by the total electronic angular momentum **J** into a number of hyperfine levels characterised by the value of the quantum number of the total angular momentum of the whole atom, including the nucleus. The many-electron case is similar. The total angular momentum **F** of the atom is the sum of **J** and the angular momentum of the nucleus **I**,

$$\mathbf{F} = \mathbf{I} + \mathbf{J} \tag{8.32}$$

Each atomic level is an eigenstate of $\mathbf{F}^2$ and of F_z with quantum numbers F and M_F respectively. The eigenfunctions $|F, M_F\rangle$ satisfy

$$\begin{aligned} F^2|F, M_F\rangle &= F(F+1)\hbar^2|F, M_F\rangle \\ F_z|F, M_F\rangle &= M_F\hbar|F, M_F\rangle \end{aligned} \tag{8.33}$$

By examining the equations [5.142] and [5.143], we see that in the one-electron atom, the magnetic dipole interaction between the nucleus and the atom can be

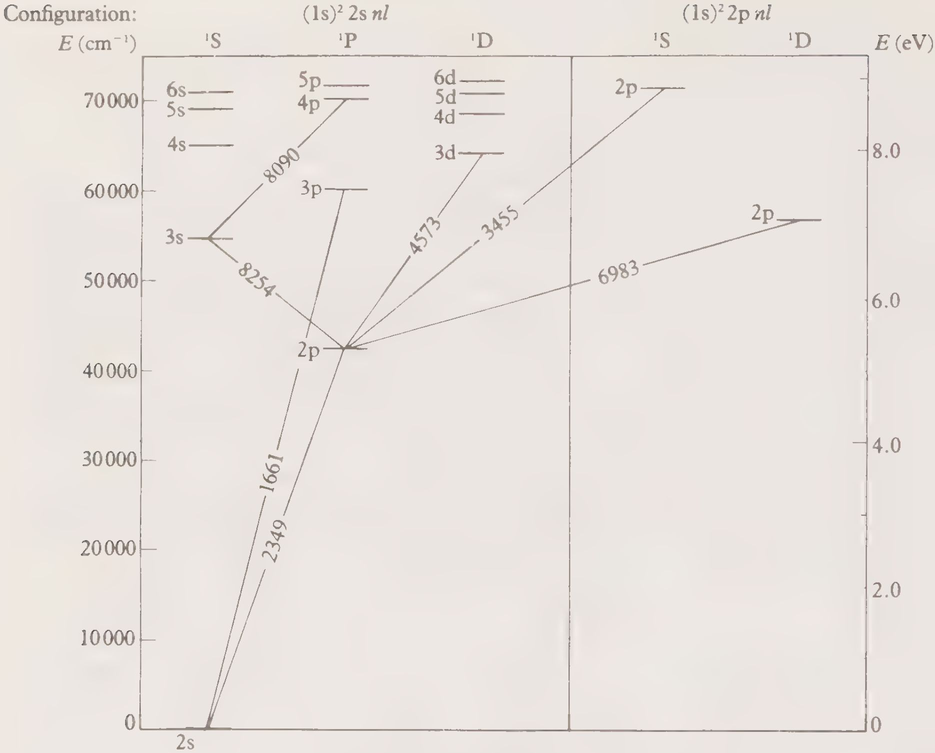

Beryllium – singlet transitions

(a)

8.5 Grotrian diagram for transitions in beryllium (a) singlet (b) triplet energies are shown relative to the $(1s)^2(2s)^2\ {}^1S$ ground state. Only a selection of transitions are shown, for sake of clarity. The numbers against the lines show the wavelength in angstroms. The 'displaced terms' are shown on the right-hand side of each diagram.

taken to be proportioned to $(\mathbf{I}\cdot\mathbf{J})$, where the constant of proportionality depends only on the quantum numbers $\mathcal{J}$, L and S. We shall assume this to be true for the many-electron case as well, so that the energy shift of each term will be determined by an interaction of the form

$$H' = \bar{C}(\mathbf{I}\cdot\mathbf{J}) \qquad [8.34]$$

where $\bar{C}$ depends on $\mathcal{J}$, L and S, and is known as the *hyperfine structure constant*. Since

$$\mathbf{I}\cdot\mathbf{J} = \tfrac{1}{2}(\mathbf{F}^2 - \mathbf{I}^2 - \mathbf{J}^2) \qquad [8.35]$$

the energy shift of a particular term is (with $C = \bar{C}\hbar^2$)

$$\Delta E = \frac{C}{2}[F(F+1) - I(I+1) - \mathcal{J}(\mathcal{J}+1)] \qquad [8.36]$$

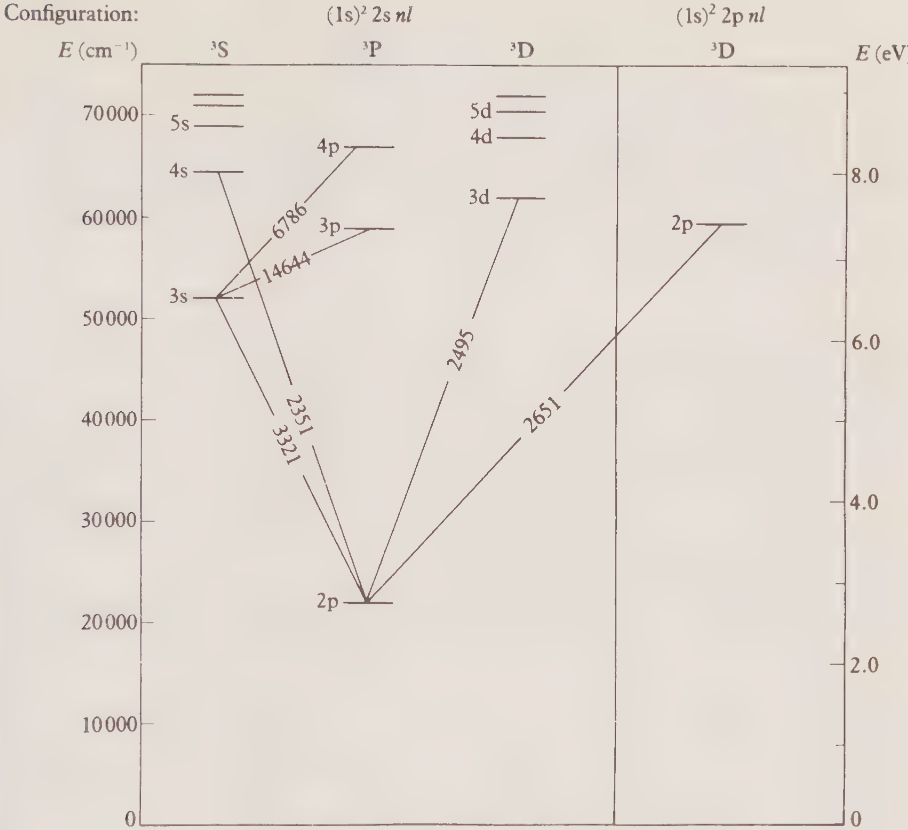

Beryllium – triplet transitions

(b)

Fig. 8.5(*Cont.*)

The possible values of F are from $|I - \mathcal{J}|$ to $(I + \mathcal{J})$, so the number of levels differing in F is $(2I + 1)$ if $I \leqslant \mathcal{J}$, or $(2\mathcal{J} + 1)$ if $\mathcal{J} < I$. For example, if $\mathcal{J} = 2$ and $I = 3/2$, the term will be split into four components with $F = 1/2, 3/2, 5/2, 7/2$. The energy difference between levels is given by the interval rule

$$\Delta E(F + 1) - \Delta E(F) = C(F + 1) \qquad [8.37]$$

Some values of the hyperfine splitting for a number of levels are given in Table 8.4. Transitions between different hyperfine levels corresponding to the same term can be measured by radio-frequency methods. The measurements can be made to great precision and for this reason can be used as time standards. In SI units the fundamental unit of time, the second, is defined in terms of the frequency of the transition between the levels with $F = 4$, $M_F = 0$ and $F = 3$,

Table 8.4 Hyperfine structure of selected levels

Atom	I	*Term*	F	$[\Delta E(F+1) - \Delta E(F)]^{\dagger}$	$C^{\dagger}$
H	1/2	$(1s)^2S_{1/2}$	0	1420.4057518	1420.406
^{3}He	1/2	$(1s2s)^1S_{1/2}$	1/2	6739.70	4212.31
^{67}Zn	5/2	$(4s4p)^3P_2$	1/2	7810.865	521.24
^{133}Cs	7/2	$(6s)^2S_{1/2}$	3	9192.631770	2298.2

† Energy splittings and C are given in MHz.

$M_F = 0$ of the ground state of ^{133}Cs. The frequency is assigned the value 9192.631770 MHz.

The selection rules for electric dipole transitions between different terms must be supplemented by the rules $\Delta F = 0, \pm 1$ with the transition $F = 0 \leftrightarrow F' = 0$ forbidden. The analysis of the hyperfine structure of particular transitions offers a method of determining the spin of the nucleus, and historically this has been of great importance.

Since the level shifts are small, of the order of 10^{-5} of the energy difference between the ground and first excited states of the atom, other effects may be of comparable magnitude. For example, the value of the constant C is different for different isotopes of the same element. For a given isotope, there is a further small interaction, which depends on F, and which is of experimental importance. This arises because the nucleus is not a point charge and so has a charge distribution which can be specified in terms of multipole moments (see Chapter 5). Being in a parity eigenstate, the nucleus can have no permanent electric dipole moment, but can possess an electric quadrupole moment. The interaction between this quadrupole moment and the electronic charge distribution leads to a further very small F-dependent shift, which can be detected by departures from the interval rule [8.37]. This was discussed in Chapter 5 for one-electron atoms. For the generalisation to the many-electron atom case, reference may be made to Kuhn (1970).

8.5 INTERACTION WITH MAGNETIC FIELDS. THE ZEEMAN EFFECT

In the absence of external fields, there is no preferred direction in space and the energy of an isolated system, such as an atom, cannot depend on which direction we choose as the Z axis. As a consequence, the energy of an atom does not depend on $M_J\hbar$, the eigenvalues of J_z, and the atomic energy levels are $(2J+1)$-fold degenerate. This degeneracy is removed by external magnetic fields which destroy the isotropy of the situation. In Chapter 5 we studied the interaction of a one-electron atom with a static magnetic field of magnitude $\mathscr{B}$ and we shall now extend the treatment to a multielectron atom. The interaction energy between each electron and the field will be of the same form as

before (see [5.49]) and is, for the ith electron,

$$H'_i = \frac{\mu_B}{\hbar} \boldsymbol{\mathcal{B}} \cdot (\mathbf{L}_i + 2\mathbf{S}_i) \qquad [8.38]$$

where $\mathbf{L}_i$ and $\mathbf{S}_i$ are the orbital and spin angular momenta of the electron, and μ_B is the Bohr magneton. The total interaction energy between the field and an atom containing N electrons is obtained by summing over i:

$$H' = \sum_{i=1}^{N} H'_i = \frac{\mu_B}{\hbar} \boldsymbol{\mathcal{B}} \cdot (\mathbf{L} + 2\mathbf{S}) \qquad [8.39]$$

where $\mathbf{L}$ is the total orbital angular momentum of the atom, $\mathbf{L} = \sum_i \mathbf{L}_i$, and $\mathbf{S}$ is the total spin angular momentum, $\mathbf{S} = \sum_i \mathbf{S}_i$. This interaction is of exactly the same form as for the one-electron atom, and the matrix elements we worked out in Chapter 5 can be used here, provided the atom is described by the L–S (Russell–Saunders) coupling scheme.

As before, there are three cases, depending on whether the perturbation H' is much greater than the spin–orbit interaction, $\bar{A}(\mathbf{L} \cdot \mathbf{S})$, comparable with it, or (the most usual case) much less than it. In the strong field case, the spin–orbit energy can be ignored so that the atomic wave function becomes a simultaneous eigenfunction of $\mathbf{L}^2$, L_z, $\mathbf{S}^2$ and S_z. As a result, one has (with $\boldsymbol{\mathcal{B}} = \mathcal{B}_z \hat{\mathbf{z}}$)

$$\Delta E = \mu_B (M_L + 2M_S)\mathcal{B}_z \qquad [8.40]$$

In the intermediate case (the Paschen–Back effect), the spin–orbit interaction is now introduced as a perturbation, and we have (with $A = \bar{A}\hbar^2$)

$$\langle L, S, M_L, M_S | \bar{A}\mathbf{L} \cdot \mathbf{S} | L, S, M_L, M_S \rangle = AM_L M_S \qquad [8.41]$$

The level shift is the sum of [8.40] and [8.41], namely

$$\Delta E = \mu_B (M_L + 2M_S)\mathcal{B}_z + AM_L M_S \qquad [8.42]$$

Finally, in the weak field case (the anomalous Zeeman effect), we first take into account the spin–orbit interaction and subsequently treat the interaction with the external field as a perturbation. The degeneracy in J is removed by the interaction $\bar{A}(\mathbf{L} \cdot \mathbf{S})$ and the atom is in an eigenstate of $\mathbf{J}^2$, $\mathbf{L}^2$, $\mathbf{S}^2$ and J_z. The magnetic interaction is treated as a small perturbation and

$$\Delta E = \frac{\mu_B}{\hbar} \mathcal{B}_z \langle JLSM_J | L_z + 2S_z | JLSM_J \rangle \qquad [8.43]$$

This matrix element was evaluated in Section 5.2 for one-electron atoms, with the result [5.79]–[5.80]. In an identical way, one has in the present case

$$\Delta E = g_J \mu_B \mathcal{B}_z M_J \qquad [8.44]$$

where g_J is the Landé factor

$$g_J = 1 + \frac{J(J+1) + S(S+1) - L(L+1)}{2J(J+1)} \qquad [8.45]$$

The transition from the weak to the strong field limits is continuous, and an example was shown in Fig. 5.12 for the $2p_{1/2}$ and $2p_{3/2}$ levels of hydrogen.

The Zeeman effect in hyperfine structure

The degeneracy of the hyperfine levels, corresponding to $(2F + 1)$ values of M_F, can be removed by the application of a magnetic field. If a nucleus possesses a magnetic moment $\mathcal{M}_N$ there is an additional interaction of the form $-(\mathcal{M}_N \cdot \mathcal{B})$. We write (see [5.116])

$$\mathcal{M}_N = g_I \mu_N \mathbf{I}/\hbar \qquad [8.46]$$

where $\mathbf{I}$ is the nuclear spin, μ_N is the nuclear magneton and g_I is the nuclear g factor. The total interaction of an atom with a magnetic field in the Z direction of strength $\mathcal{B}_z$, is

$$H' = \left(\frac{\mu_B}{\hbar}\right)\mathcal{B}_z(L_z + 2S_z) - g_I\left(\frac{\mu_N}{\hbar}\right)\mathcal{B}_z I_z \qquad [8.47]$$

We shall take the case of L–S coupling, and we can again identify a number of limiting cases. The first of these is the weak field case in which H' is smaller than the hyperfine interaction $\bar{C}(\mathbf{I}\cdot\mathbf{J})$. In this case, the atom is in an eigenstate of $\mathbf{F}^2$, $\mathbf{J}^2$, $\mathbf{I}^2$ and F_z and the energy shift is

$$\Delta E = \langle F, \mathcal{J}, I, M_F|H'|F, \mathcal{J}, I, M_F\rangle \qquad [8.48]$$

By methods similar to those given in Chapter 5, it can be shown that

$$\Delta E = g_F \mu_B \mathcal{B}_z M_F \qquad [8.49]$$

where g_F is a Landé factor given by

$$g_F = g_{\mathcal{J}}\frac{F(F+1) + \mathcal{J}(\mathcal{J}+1) - I(I+1)}{2F(F+1)} - g_I'\frac{F(F+1) + I(I+1) - \mathcal{J}(\mathcal{J}+1)}{2F(F+1)} \qquad [8.50]$$

Here $g_{\mathcal{J}}$ is the Landé factor in the absence of a nuclear magnetic moment [8.45] and (see [5.120])

$$g_I' = \frac{\mu_N}{\mu_B} g_I \qquad [8.51]$$

Since $\mu_N/\mu_B = (m/M_p) \simeq 1/1836$, g_I' is small and can be neglected.

The second case arises when the magnetic interaction is larger than the hyperfine interaction $\bar{C}(\mathbf{I}\cdot\mathbf{J})$. This is the Back–Goudsmit effect and the theory can be developed in a similar way to that of the Paschen--Back effect. The interaction $\bar{C}(\mathbf{I}\cdot\mathbf{J})$ is first omitted. In this case the atom is in an eigenstate of $\mathbf{J}^2$, $\mathcal{J}_z$ and of $\mathbf{I}^2$, I_z which is $(2\mathcal{J}+1)\times(2I+1)$-fold degenerate in $M_{\mathcal{J}}$ and M_I. The magnetic interaction causes a level shift

$$\Delta E = (M_{\mathcal{J}} g_{\mathcal{J}} - M_I g_I')\mu_B \mathcal{B}_z \qquad [8.52]$$

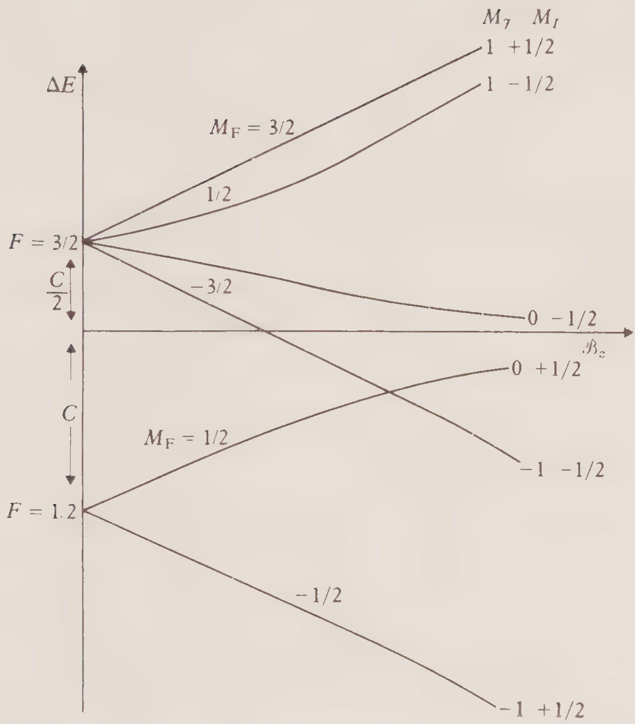

8.6 Behaviour of the hyperfine splitting as a function of $\mathcal{B}_z$ for $I = 1/2, J = 1$ (arbitrary scale). In the weak field case to the left of the diagram the states are classified by F, I, J, M_F and in the strong field case to the right by I, J, M_J and M_I, (see equations [8.49] and [8.53] respectively). To connect the strong and weak field limits we must remember that $M_F = M_I + M_J$, always and levels with the same M_F or M_J never intersect each other. If the field strength increases even further, then the spin-orbit coupling breaks down and the states are classified by L, S, I, M_L, M_I, M_S (this is the extreme Paschen–Back effect).

Introducing now the hyperfine interaction $\bar{C}(\mathbf{I} \cdot \mathbf{J})$ as a perturbation, the hyperfine interaction level shift becomes (with $C = \bar{C}\hbar^2$)

$$\Delta E = (M_J g_J - M_I g'_I)\mu_B \mathcal{B}_z + C M_I M_J \qquad [8.53]$$

As in the Zeeman effect, the energy of the hyperfine levels is a smooth function of $\mathcal{B}_z$ and a diagram of a particular case where $J = 1$ and $I = 1/2$ is shown in Fig. 8.6.

8.6 THE QUADRATIC STARK EFFECT

In Chapter 5 we discussed the influence of a static electric field on the hydrogen atom. Since the excited energy levels of hydrogen are degenerate in l, the perturbation mixes states of opposite parity and produces level shifts linear in the field strength. For other atoms, the linear effect vanishes and the level shifts are quadratic in the field strength. The interaction energy between N electrons

at positions (x_i, y_i, z_i) and a uniform electric field of strength $\mathscr{E}$ directed parallel to the Z axis is

$$H' = e\sum_{i=1}^{N} \mathscr{E} z_i$$
$$= -\mathscr{E} D_z \qquad [8.54]$$

where $\mathbf{D}$ is the electric dipole moment defined by [8.4] and D_z its component along the Z axis.

The matrix elements of $\mathbf{D}$ with respect to atomic states of definite parity vanishes, so that the first order level shift also vanishes

$$\Delta E = -\mathscr{E}\langle \gamma LSJM_J|D_z|\gamma LSJM_J\rangle = 0 \qquad [8.55]$$

where γ denotes the configuration, and we have assumed L–S coupling.

The second-order perturbation theory gives (see [2.319])

$$\Delta E = \mathscr{E}^2 \sum_{\gamma' L' S' J' M_J'}{}' \frac{|\langle \gamma LSJM_J|D_z|\gamma' L' S' J' M_J'\rangle|^2}{E_{\gamma LSJ} - E_{\gamma' L' S' J'}} \qquad [8.56]$$

where the symbol Σ' means that the state $|\gamma LSJM_J\rangle$ is excluded from the sum. The intermediate states $|\gamma' L' S' J' M_J'\rangle$ must have opposite parity from the state $|\gamma LSJM_J\rangle$. The matrix element of D_z is diagonal in M_J and also in S, so that $M_J' = M_J$ and $S' = S$. The selection rules for the matrix element of a component of the electric dipole operator require that $J' = J \pm 1$ or $J' = J$. The dependence of the matrix elements on M_J is then given by [8.11] (with $q = 0$). It is entirely contained in the Clebsh–Gordan coefficient $\langle J\,1M_J0|J'M_J\rangle$. We have (see Table A4.1)

$$\langle J1M_J0|J+1, M_J\rangle = \left[\frac{(J+1)^2 - M_J^2}{(2J+1)(J+1)}\right]^{1/2}$$

$$\langle J1M_J0|J, M_J\rangle = \left[\frac{M_J^2}{J(J+1)}\right]^{1/2} \qquad [8.57]$$

$$\langle J1M_J0|J-1, M_J\rangle = -\left[\frac{J^2 - M_J^2}{J(2J+1)}\right]^{1/2}$$

From these expressions, we see that ΔE is of the form

$$\Delta E = \mathscr{E}^2(A + BM_J^2) \qquad [8.58]$$

where A and B depend on (γ, L, S, J). In contrast to the Zeeman effect, the degeneracy in M_J is not completely removed, because levels with $M_J = \pm|M_J|$ have the same energy.

In the sum in [8.56], the most important contribution is from the nearest level of opposite parity to the level γ. For example, in sodium, the shift in the ground state energy is very small because the nearest levels of opposite parity are the

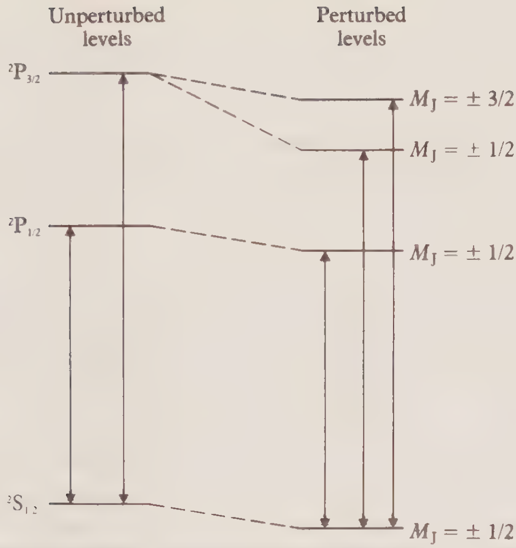

8.7 Schematic diagram of the splitting of the D lines of sodium due to an electric field (the Stark effect).

$2^2P_{1/2}$ and $2^2P_{3/2}$ levels and the corresponding energy differences $E_{\gamma LSJ} - E_{\gamma' L'S'J'}$ are large. In fact the ground state energy is lowered and the energy shift in cm^{-1} is $7.8 \times 10^{-11} \mathscr{E}^2$ where $\mathscr{E}$ is given in kV/m. The energy shifts of the $2^2P_{1/2}$ and $2^2P_{3/2}$ levels are about twice as large, since these are perturbed both by the ground state and by the ^2D levels which lie closer. The two D lines are split into three by the field (see Fig. 8.7).

Apart from producing a level shift, the electric field has the effect of mixing states of opposite parity. A perturbed ^2P_J wave function, for example, now contains a small admixture of the ^2D_J function. As a consequence, lines are observed in the presence of an electric field that would normally be forbidden, for example the series $n^2S \rightarrow n'^2D$ and $n^2S \rightarrow n'^2S$.

8.7 X-RAY SPECTRA

The valence electrons in heavy neutral atoms move in an effective field, which at large distances approaches the Coulomb field due to a unit charge (in units of e). The binding energies of these electrons are always of the same order of magnitude as the binding energy of atomic hydrogen – a few electron-volts. In contrast, the electrons in the inner shells, K, L, M . . . with principal quantum numbers $n = 1, 2, 3, \ldots$, move in a potential field dominated by the charge of the nucleus (Ze). The nuclear charge is screened to some extent by the other electrons, and to a good approximation this can be represented by taking the effective potential in which the inner electrons move as a Coulomb potential due to a charge $(Z - \sigma_n)e$, where $\sigma_n \ll Z$. The energy levels in such a field are just

those of a one-electron atom, and

$$E_n = -\frac{1}{2}\frac{(Z - \sigma_n)^2}{n^2} \text{ a.u.} \qquad [8.59]$$

In contrast to the valence electrons, the binding energy of a K shell electron increases smoothly with increasing Z. To a fair approximation, $\sigma_1 = 2$. Thus for Fe with $Z = 26$, $|E_1| = 288$ a.u. $= 7.8$ keV, for Cs with $Z = 55$ $|E_1| = 1404$ a.u. $= 38.2$ keV and for Pb with $Z = 82$ $|E_1| = 3200$ a.u. $=$ 87 keV. Similarly for the L shell, $n = 2$, an approximation for σ_2 is $\sigma_2 = 9.4$, and, for example, the binding energy of a L shell electron for Pb is 17.9 keV.

By bombarding a substance with fast electrons, some atoms become ionised through the ejection of an inner shell electron. Suppose a vacancy is created in the K shell in this way. Subsequently an electron from a higher shell, L, M, . . . , will make a radiative transition filling the vacancy. The energy of the photon emitted will be in the range from a few keV to a few hundred keV, and so lies in the X-ray region [2] which may be taken to be in the range of wavelengths from 0.1 to 10 A (see Fig. 1.9). The emission spectrum which results is a line spectrum, forming a simple series. The lines originating from a K shell vacancy are called the K_α, K_β, K_γ . . . lines and correspond to the $L \to K$, $M \to K$, $N \to K$ . . . transitions. The K_α line is the strongest. The early experiments of Moseley in 1913 and 1914 established that the square root of the frequency of the K_α line is a linear function of atomic number (see Fig. 1.20). Historically this was of considerable importance because it was consistent with the energy formula [8.59], which had been predicted by Bohr's model of a one-electron system, published in 1913. A similar series of lines, labelled L_α, L_β in order of increasing frequency, arises from transitions which fill a vacancy in the L shell.

The spin–orbit interaction splits the energy levels of the shells (other than the K shell). In the L shell, the electrons with $l = 0$ have the greatest binding energy, those with $l = 1, j = 1/2$ come next, and then those with $l = 1$ and $j = 3/2$. The three levels are labelled L_I, L_{II} and L_{III} respectively. The energy splitting between the sublevels is large, because spin–orbit coupling is proportional to $(Z - \sigma_2)^4$ (see [5.26]) and the doublet $K_{\alpha 1}$ and $K_{\alpha 2}$, which corresponds to the transitions $L_{III} \to K$ and $L_{II} \to K$ can be resolved. For example the wavelengths of the $K_{\alpha 1}$ and $K_{\alpha 2}$ lines in ^{26}Fe are 1.9360 Å and 1.9321 Å respectively. A typical X-ray term diagram (including the K, L and M shells) is shown in Fig. 8.8.

X-rays can be absorbed by ionising atoms through the photoelectric effect (see Chapter 4). The cross-section for this process decreases smoothly with increasing frequency, until sufficient energy is reached to ionise an electron from the L_{III} shell. At this point, the cross-section increases sharply. Similar 'absorption edges' occur as successively sufficient energy is available to ionise electrons from the L_{II}, L_I and finally the K shell. This is illustrated in Fig. 8.9 for absorption in lead.

[2] The wavelength λ, expressed in Å, is given by $\lambda \sim 12.4/E$, where the energy E is in keV.

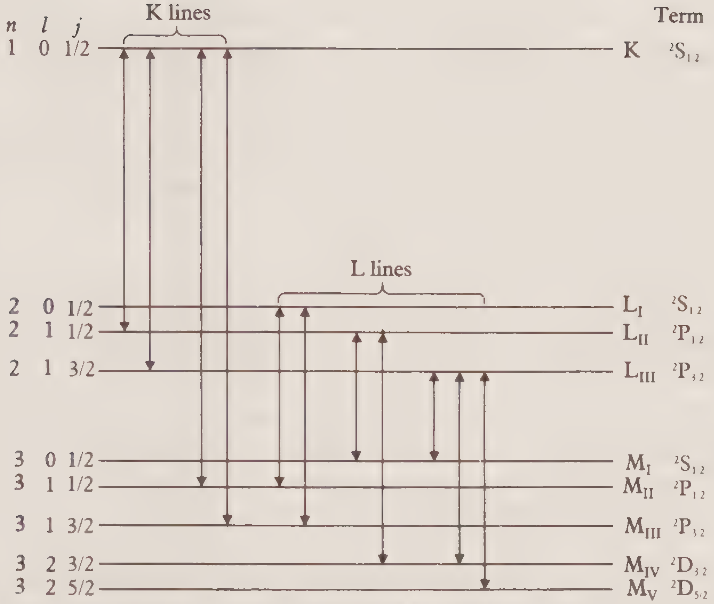

8.8 X-ray term diagram (not to scale). The allowed transitions are determined from the usual selection rules $\Delta l = \pm 1$, $\Delta j = 0, \pm 1$.

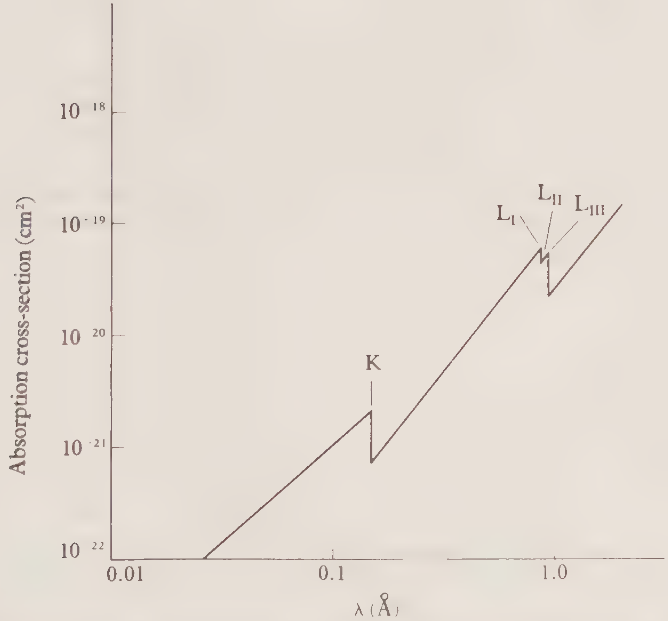

8.9 The cross-section for the absorption of X-rays by lead atoms shown as a function of the wavelength.

PROBLEMS

8.1 Write down the selection rules for: (a) electric multipole transitions of order $\lambda = 1, 2, 3$ and 4; (b) magnetic multipole transitions of order $\lambda = 1, 2, 3$ and 4.

8.2 Using Table 8.1 calculate the energies of the ten lowest levels of Li, Na, K and Cs, expressing the results both in eV and in cm^{-1}. Find the frequencies of the resonance line in each case and compare the answer with the experimental values given in Table 8.2.

8.3 Use expression [3.73] together with [8.29] to estimate the energy splitting of the $2^3P_{\mathcal{J}}(1s2p)$, $3^3P_{\mathcal{J}}(1s3p)$ and $3^3D_{\mathcal{J}}(1s3d)$ levels of HeI, CV, and Na X by the spin–orbit interactions, expressing the answer in cm^{-1}. Using the selection rules discuss the splitting of the spectral lines in the transitions from the $2^3P_{\mathcal{J}}$ levels to the lowest triplet state and from the $3^3D_{\mathcal{J}}$ levels to the $2^3P_{\mathcal{J}}$ levels.
(Hint: The effective charge to be used in [3.73] is equal to the Roman numeral in the designation of the ions.)

8.4 Measurements made on the line spectrum of the neutral carbon atom show that a certain excited term consists of three fine structure levels having energies above the ground state given (in cm^{-1}) by 60 333, 60 353 and 60 393.

(a) With the help of the Landé interval rule, identify the values of L, S and $\mathcal{J}$ for these fine structure levels.

(b) The ground state term of carbon, $1s^2 2s^2 2p^2\ {}^3P$ is split into three fine structure levels, with $\mathcal{J} = 0, 1, 2$ (see Fig. 7.8). The levels with $\mathcal{J} = 1$ and $\mathcal{J} = 2$ are 16 and 43 cm^{-1}, respectively, above the level $\mathcal{J} = 0$. Discuss the multiplet structure of the lines arising from dipole transitions between the excited term considered in (a) (which has opposite parity to the ground state) and the ground state term. Write down the corresponding wavelengths.

8.5 (a) Find how many separate lines occur in the multiplet arising from the ${}^2P_{3/2} \rightarrow {}^2S_{1/2}$ and ${}^2P_{1/2} \rightarrow {}^2S_{1/2}$ transitions of an alkali placed in a weak magnetic field.

(b) Find the relative intensities of the lines in transverse observation.

9 Molecular structure

Bound systems of electrons and more than one nucleus are known as molecules. In this chapter, we shall discuss the structure of molecules, concentrating on the simplest diatomic systems which contain just two nuclei. We shall start by discussing the general nature of molecular structure, showing how the rotational, vibrational and electronic motions can be treated independently. Following an analysis of the rotational and vibrational motions, we shall discuss the electronic structure of diatomic molecules, showing how chemical bonding (or binding) comes about. Finally, we shall indicate how the more complicated polyatomic molecules can be treated.

9.1 GENERAL NATURE OF MOLECULAR STRUCTURE

The description of molecular structure is considerably more complicated than that of isolated atoms, but fortunately the problem is greatly simplified because *the mass of the electrons is much smaller than that of the nuclei*, while the forces to which the electrons and the nuclei are submitted are of comparable intensity. As a result, the motion of the nuclei is much slower than that of the electrons, and the nuclei occupy nearly fixed positions within the molecule. This can be shown quite directly by observing the diffraction pattern in neutron scattering by molecules. The neutrons, having no charge, do not interact with the electrons, but interact strongly, through the nuclear force, with each of the nuclei within the molecule. For example, in the simplest neutral diatomic molecule H_2, formed by the association of two hydrogen atoms, the equilibrium spacing of the two protons is 0.74 Å, while in the molecule O_2 formed from two oxygen atoms, the internuclear spacing is 1.21 Å. In the methane molecule CH_4, composed of a single carbon atom and four hydrogen atoms, the carbon nucleus lies at the centre of a regular tetrahedron, with the protons at the vertices (see Fig. 9.1).

Evidence from X-ray diffraction and molecular spectra shows that when atoms associate to form molecules, the tightly bound inner shells of electrons are nearly undisturbed, and remain localised about each nucleus. The outer electrons, on the other hand, are distributed throughout the molecule, and it is the charge distribution of these *valence* electrons that provides the binding force. The order of magnitude of the separation of energy levels for the

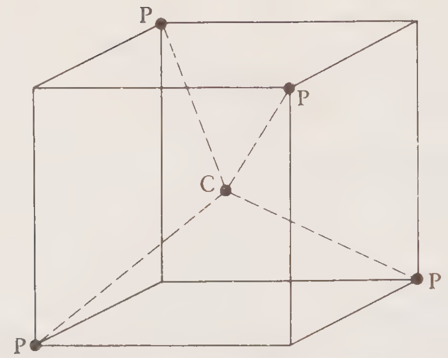

9.1 The methane molecule CH_4. The carbon nucleus lies at the centre of a regular tetrahedron inscribed in a cube with the protons at alternate vertices. The distance between the carbon nucleus and a proton (the bond length) is 2.067 a.u. (1.094 Å).

electronic motion of the valence electrons can be estimated by using the following argument. Let a be a typical average distance of the nuclei in a molecule. From the uncertainty principle, the magnitude of the momentum of the valence electrons is of the order of $\hbar/a$, so that a rough estimate of their kinetic energy – and hence of the magnitude E_e of the electronic energies – is given by

$$E_e \simeq \frac{\hbar^2}{ma^2} \qquad [9.1]$$

where m is the mass of the electron. Since $a \simeq 1$ Å we see that E_e is of the order of a few eV, which is similar to the binding energy of the outer electrons in isolated atoms. The result [9.1] clearly gives also an estimate of the energy separation between low-lying electronic energy levels of the molecule. The corresponding line spectra are observed in the ultra violet and visible regions.

Let us now consider the nuclear motions. These can be classified into *translations* and *rotations* of the entire (quasi-rigid) equilibrium arrangement, and internal *vibrations* of the nuclei about their equilibrium position. The translational motion can be separated by introducing the centre of mass, which moves as a free particle in the absence of external fields. In what follows we shall assume that the separation of the centre of mass has been performed, and we shall only consider the vibrational and rotational motions of the nuclei. To estimate the vibrational energy, we can use the following classical argument. If the electrons are bound to the molecule by a force of magnitude F, the nuclei must be bound by an equal and opposite force. Taking this force to be simple harmonic, with a force constant k, the angular frequency of the electronic motion will be $\omega_e = (k/m)^{1/2}$ and that of the vibrational nuclear motion will be $\omega_N = (k/M)^{1/2}$, where M is of the order of a typical nuclear mass. The ratio of the energy of the vibrational motion to that of the electronic motion is thus $\hbar\omega_N/\hbar\omega_e \simeq (m/M)^{1/2}$ and the energy E_v associated with a low mode of

vibration is given approximately by

$$E_v \simeq \left(\frac{m}{M}\right)^{1/2} E_e \qquad [9.2]$$

The ratio m/M being in the range 10^{-3} to 10^{-5}, we see from [9.2] that E_v is roughly a hundred times smaller than E_e, so that typical vibrational transitions lie in the infra-red (see Fig. 9.2). For example, the natural vibrational wave number of the molecule HCl is at approximately $3000\ \text{cm}^{-1}$. The vibrational motion of the nuclei also produces a 'first-order' splitting of the electronic lines.

To estimate the rotational energy E_r, we consider the simple case of a diatomic molecule, with each of the two nuclei having the same mass M and being a distance a apart, as shown in Fig. 9.3. The moment of inertia of the molecule is then $I = Ma^2/2$. Using the result [2.193] which we obtained in Chapter 2 for the rigid rotator, we see that the order of magnitude of the energy associated with a fairly low mode of rotation is

$$E_r \simeq \frac{\hbar^2}{Ma^2} \simeq \frac{m}{M} E_e \qquad [9.3]$$

where we have used [9.1]. Thus the rotational molecular energies are smaller than electronic energies by a factor of the order of m/M, and smaller than

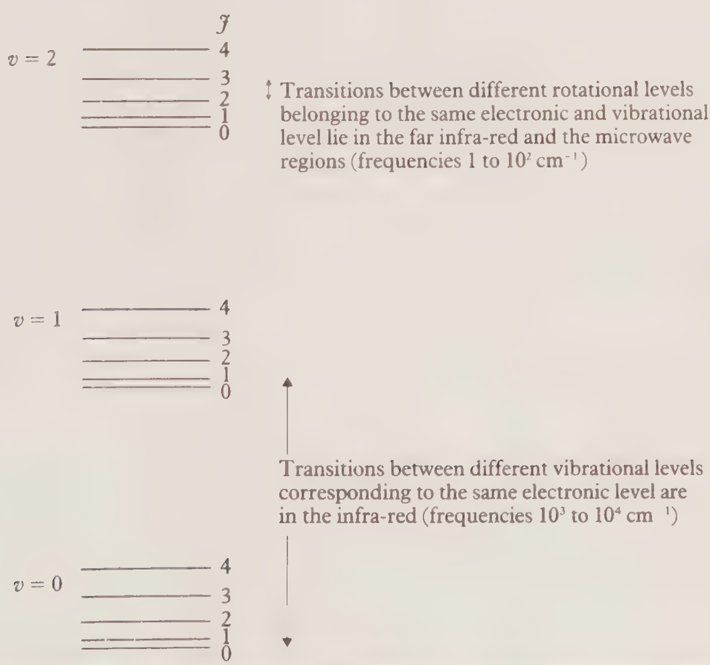

9.2 Schematic diagram of the energy levels of a diatomic molecule belonging to the same electronic level. The vibrational levels are labelled by the quantum number v and the rotational levels by the quantum number $\mathcal{J}$.

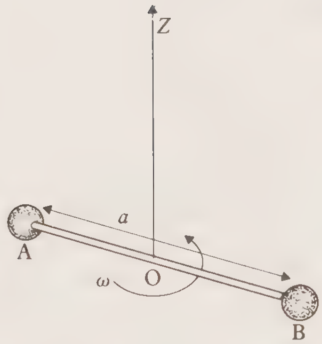

9.3 Rotation of a diatomic molecule composed of two nuclei A and B, each of the same mass M, a distance a apart. The rotation is of angular frequency ω about an axis OZ through the centre of mass. The classical energy of rotation is $E = \frac{1}{2}I\omega^2$, where the moment of inertia I is given by $I = \frac{1}{2}Ma^2$.

vibrational energies by a factor of the order of $(m/M)^{1/2}$. The rotational motion leads to a 'second-order' splitting of the line spectrum, the spacing being of the order of 0.001 eV, which is very small compared with the 'first-order' splitting of ~0.1 eV produced by the vibrational motion. Transitions between rotational levels, belonging to the same electronic and vibrational level, are observed in the far infra-red and the microwave regions at wave numbers of 1 to 10^2 cm^{-1}.

Because of the small ratio of the electronic mass to the nuclear mass ($m/M \simeq 10^{-3}$–10^{-5}), and since the period of a motion is of the order of h divided by its energy, we see from [9.1]–[9.3] that the nuclear periods are much longer than the electronic periods. Thus the electronic and nuclear motions can essentially be treated independently, and it is a good approximation to determine the electronic states at each value of the internuclear separation by treating the nuclei as fixed. The charge distribution of the electrons is then a function of the nuclear positions and determines the nuclear motion. In the next paragraphs we shall use these qualitative ideas to develop a mathematical formalism for diatomic molecules.

9.2 THE BORN–OPPENHEIMER SEPARATION FOR DIATOMIC MOLECULES

To see how the ideas of the previous paragraph translate into the language of quantum mechanics, we shall consider a diatomic molecule composed of nuclei A and B, of masses M_A and M_B, together with a number N of electrons. The internuclear coordinate will be denoted by $\mathbf{R}$ and the position vectors of the electrons with respect to O, the centre of mass of A and B, by $\mathbf{r}_1, \mathbf{r}_2, \ldots \mathbf{r}_N$ (see Fig. 9.4). We shall also write the position vectors of A and B with respect to O as $\mathbf{R}_A$ and $\mathbf{R}_B$, respectively, so that $\mathbf{R} = \mathbf{R}_B - \mathbf{R}_A$. The time-independent Schrödinger equation for the system (neglecting spin interactions) is

$$[T_N + T_e + V]\psi(\mathbf{R}; \mathbf{r}_1, \mathbf{r}_2, \ldots \mathbf{r}_N) = E\psi(\mathbf{R}; \mathbf{r}_1, \mathbf{r}_2, \ldots \mathbf{r}_N) \qquad [9.4]$$

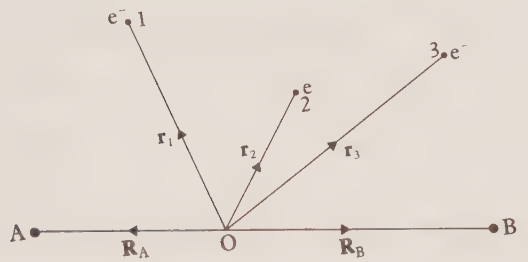

9.4 Coordinate system for a diatomic molecule. The nuclei are at A and B, with position vectors $\mathbf{R}_A$, $\mathbf{R}_B$ with respect to O the centre of mass. The position vectors of the electrons with respect to O are denoted by $\mathbf{r}_1, \mathbf{r}_2, \mathbf{r}_3 \ldots$.

where T_N is the kinetic energy operator for the nuclei, T_e is the kinetic energy operator for the electrons and V is the total potential energy of the system. Explicitly T_N and T_e are given respectively by [1]

$$T_N = -\frac{\hbar^2}{2\mu} \nabla_R^2 \qquad [9.5]$$

and

$$T_e = \sum_{i=1}^{N} \left(-\frac{\hbar^2}{2m} \nabla_{r_i}^2 \right) \qquad [9.6]$$

where

$$\mu = \frac{M_A M_B}{M_A + M_B} \qquad [9.7]$$

is the reduced mass of A and B.

The potential energy V consists of the sum of the Coulomb interactions between all pairs of particles, i.e. of the electrostatic interactions between the electrons and the nuclei, between the electrons themselves, and between the two nuclei. Denoting respectively by $Z_A e$ and $Z_B e$ the charges of the nuclei A and B, we therefore have

$$\begin{aligned} V(\mathbf{R}; \mathbf{r}_1, \mathbf{r}_2, \ldots \mathbf{r}_N) = &- \sum_{i=1}^{N} \frac{Z_A e^2}{(4\pi\varepsilon_0)\,|\mathbf{r}_i - \mathbf{R}_A|} - \sum_{i=1}^{N} \frac{Z_B e^2}{(4\pi\varepsilon_0)\,|\mathbf{r}_i - \mathbf{R}_B|} \\ &+ \sum_{\substack{i,j=1 \\ (i>j)}}^{N} \frac{e^2}{(4\pi\varepsilon_0)\,|\mathbf{r}_i - \mathbf{r}_j|} + \frac{Z_A Z_B e^2}{(4\pi\varepsilon_0)\,R} \end{aligned} \qquad [9.8]$$

[1] In obtaining the equation [9.4], we have assumed that the mass m of an electron can be neglected compared with the reduced mass μ of the two nuclei A and B, so that O (the centre of mass of A and B) can be treated as being a fixed centre so far as the electrons are concerned.

The time-independent Schrödinger equation for the electrons moving in the field of nuclei *fixed* at the positions $\mathbf{R}_A$ and $\mathbf{R}_B$ is

$$(T_e + V)\Phi_q(\mathbf{R}; \mathbf{r}_1, \mathbf{r}_2, \ldots \mathbf{r}_N) = E_q(\mathbf{R})\Phi_q(\mathbf{R}; \mathbf{r}_1, \mathbf{r}_2, \ldots \mathbf{r}_N) \quad [9.9]$$

This is known as the *electronic wave equation*. The eigenvalues $E_q(\mathbf{R})$ and the wave functions Φ_q for each electronic state q depend parametrically on the internuclear coordinate $\mathbf{R}$, which is held fixed during the calculation. The wave functions Φ_q form a complete set at each value of $\mathbf{R}$ and can be taken to be orthonormal, i.e.

$$\int d\mathbf{r}_1 \, d\mathbf{r}_2 \cdots d\mathbf{r}_N \Phi_q^\star(\mathbf{R}; \mathbf{r}_1, \mathbf{r}_2, \ldots \mathbf{r}_N)\Phi_p(\mathbf{R}; \mathbf{r}_1, \mathbf{r}_2, \ldots \mathbf{r}_N) = \delta_{qp} \quad [9.10]$$

Since the set of wave functions Φ_q is complete, the exact wave function for the molecule, ψ, can be expanded as

$$\psi(\mathbf{R}; \mathbf{r}_1, \mathbf{r}_2, \ldots \mathbf{r}_N) = \sum_q F_q(\mathbf{R})\Phi_q(\mathbf{R}; \mathbf{r}_1, \mathbf{r}_2, \ldots \mathbf{r}_N) \quad [9.11]$$

The expansion coefficients $F_q(\mathbf{R})$ are wave functions representing the nuclear motion when the electronic system is in the state q. Equations for $F_q(\mathbf{R})$ are found by inserting ψ into the Schrödinger equation [9.4] and projecting the equation with the functions Φ_s ($s = 1, 2, \ldots$). That is,

$$\sum_q \int d\mathbf{r}_1 \, d\mathbf{r}_2 \cdots d\mathbf{r}_N \, \Phi_s^\star[T_N + T_e + V - E]F_q(\mathbf{R})\Phi_q = 0,$$

$$s = 1, 2, \ldots \quad [9.12]$$

Using the equation [9.9] satisfied by the functions Φ_q and the orthonormality property [9.10], the coupled equations for $F_q(\mathbf{R})$ reduce to the form

$$\sum_q \left[\int d\mathbf{r}_1 \, d\mathbf{r}_2 \cdots d\mathbf{r}_N \Phi_s^\star T_N \Phi_q F_q(\mathbf{R})\right] + [E_s(\mathbf{R}) - E]F_s(\mathbf{R}) = 0$$

$$s = 1, 2, \ldots \quad [9.13]$$

Since both Φ_q and F_q depend on $\mathbf{R}$, the action of the operator T_N on the product $\Phi_q F_q$ gives

$$T_N(\Phi_q F_q) = -\frac{\hbar^2}{2\mu}[F_q(\nabla_R^2\Phi_q) + 2(\boldsymbol{\nabla}_R F_q \cdot \boldsymbol{\nabla}_R \Phi_q) + \Phi_q(\nabla_R^2 F_q)] \quad [9.14]$$

The *Born–Oppenheimer approximation* consists of neglecting $|\boldsymbol{\nabla}_R \Phi_q|$ with respect to $|\boldsymbol{\nabla}_R F_q|$ for values of R near the equilibrium value R_0. In this case the equations [9.13] uncouple and $F_s(\mathbf{R})$ satisfies the *nuclear wave equation*

$$\left[-\frac{\hbar^2}{2\mu}\nabla_R^2 + E_s(\mathbf{R}) - E\right]F_s(\mathbf{R}) = 0 \qquad s = 1, 2, \ldots \quad [9.15]$$

The accuracy of this approximation can be checked in any particular case, once the functions Φ_q are known. The omitted terms are not important for many molecular *structure* problems, but they are responsible for *inelastic transitions* between electronic states ($s \to s'$) occurring in atom–atom *collisions*, which will be studied in Chapter 13.

9.3 THE ROTATION AND VIBRATION OF DIATOMIC MOLECULES

The above equation [9.15] is of the form of a Schrödinger equation for a particle of mass μ, in a potential well $E_s(\mathbf{R})$. If the electrons are in states of zero orbital angular momentum $E_s(\mathbf{R})$ is a function of the radial variable R only, and throughout this section we shall assume that this is the case. As in the case of the hydrogen atom, studied in Chapter 3, the wave function $F_s(\mathbf{R})$ is the product of a radial function depending on the radial variable R, and an angular function which depends on the polar angles Θ and Φ of the vector $\mathbf{R}$. This angular function must be an eigenfunction of $\mathbf{J}^2$ and $\mathcal{J}_z$, where $\mathbf{J}$ is the angular momentum operator of the molecule and Z is the direction of quantisation. The simultaneous eigenfunctions of $\mathbf{J}^2$ and $\mathcal{J}_z$ are the spherical harmonics $Y_{\mathcal{J},M_{\mathcal{J}}}(\Theta, \Phi)$, with eigenvalues $\mathcal{J}(\mathcal{J}+1)\hbar^2$ and $M_{\mathcal{J}}\hbar$, respectively. For the particular case in which the electrons have zero angular momentum the energy of the system cannot depend on the value of $M_{\mathcal{J}}$, so that each level is $(2\mathcal{J}+1)$-fold degenerate. However, the energy does depend on the *rotational* quantum number $\mathcal{J}$, and also on an additional quantum number v,which plays the role of the radial (or principal) quantum number, and will be shown shortly to be associated with the *vibrational* motion of the nuclei. For a given electronic state, the states labelled by the rotational quantum number $\mathcal{J}$ and the vibrational quantum number v are called *rovibronic states*. Thus, for a given value of the electronic quantum number s, we write

$$F_s(\mathbf{R}) = R^{-1}\mathcal{F}^s_{v,\mathcal{J}}(R)Y_{\mathcal{J},M_{\mathcal{J}}}(\Theta, \Phi) \qquad [9.16]$$

Substituting [9.16] into [9.15], we find that the functions $\mathcal{F}^s_{v,\mathcal{J}}(R)$ satisfy the radial equation

$$\left[-\frac{\hbar^2}{2\mu}\left(\frac{d^2}{dR^2} - \frac{\mathcal{J}(\mathcal{J}+1)}{R^2}\right) + E_s(R) - E_{s,v,\mathcal{J}}\right]\mathcal{F}^s_{v,\mathcal{J}}(R) = 0 \qquad [9.17]$$

The general form of $E_s(R)$ for a bound state is shown in Fig. 9.5. As $R \to 0$, $E_s(R)$ is dominated by the Coulomb repulsion between the nuclei A and B, while as $R \to \infty$, $E_s(R)$ tends to a constant energy $E_s(\infty)$ which is the sum of the energies of the two isolated atoms from which the molecule is composed. If there is a stable bound state, $E_s(R)$ will exhibit a minimum at some distance R_0. For a given 'potential' $E_s(R)$ there is no difficulty in solving [9.17] numerically, but since the nuclear motion is generally confined to a small region of R close to R_0 it is often convenient to expand $E_s(R)$ about R_0 in order to obtain an analytic

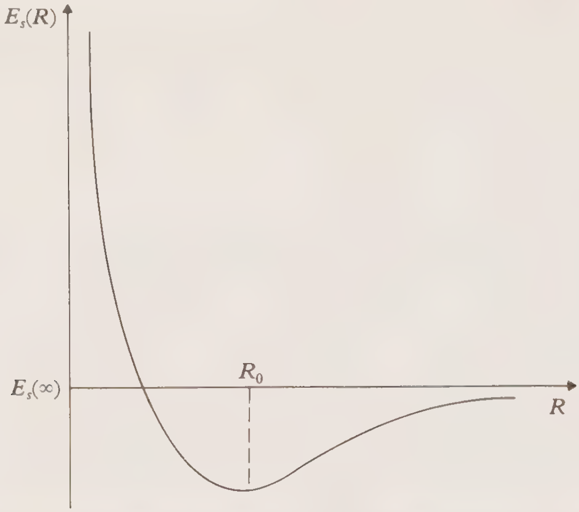

9.5 The general form of the electronic energy $E_s(R)$ for a bound state of a diatomic molecule.

approximation to the function $\mathscr{F}^s_{v,\mathcal{J}}(R)$. That is,

$$E_s(R) = E_s(R_0) + (R - R_0)\left.\frac{\mathrm{d}E_s}{\mathrm{d}R}\right|_{R=R_0} + \frac{1}{2}(R - R_0)^2\left.\frac{\mathrm{d}^2E_s}{\mathrm{d}R^2}\right|_{R=R_0} + \cdots \tag{9.18}$$

Since $E_s(R)$ has a minimum at $R = R_0$, the second term on the right of [9.18] vanishes. Neglecting terms of third and higher order in $(R - R_0)$, we may represent the potential well $E_s(R)$ approximately by the parabolic approximation

$$E_s(R) \simeq E_s(R_0) + \tfrac{1}{2}k(R - R_0)^2 \tag{9.19}$$

where

$$k = \left.\frac{\mathrm{d}^2E_s}{\mathrm{d}R^2}\right|_{R=R_0} \tag{9.20}$$

At the same time, we can approximate the rotational energy E_r by evaluating it at the equilibrium distance R_0. That is

$$\begin{aligned} E_r &= \frac{\hbar^2}{2\mu R_0^2}\mathcal{J}(\mathcal{J}+1) \\ &= \frac{\hbar^2}{2I_0}\mathcal{J}(\mathcal{J}+1) \\ &= B\mathcal{J}(\mathcal{J}+1) \qquad \mathcal{J} = 0, 1, 2, \ldots \end{aligned} \tag{9.21}$$

where $I_0 = \mu R_0^2$ is the moment of inertia for the reduced mass μ and the equilibrium distance R_0, and $B = \hbar^2/2I_0$ is called the *rotational constant* of the molecule.

Using [9.17]–[9.21] we see that the total energy $E_{s,v,\mathcal{J}}$ is the sum of the electronic energy $E_s(R_0)$, the rotational energy E_r and a vibrational energy E_v,

$$E_{s,v,\mathcal{J}} \equiv E_{s,v,r} = E_s(R_0) + E_v + E_r \qquad [9.22]$$

where E_v is an eigenvalue of the equation

$$\left[-\frac{\hbar^2}{2\mu}\frac{d^2}{dR^2} + \frac{1}{2}k(R - R_0)^2 - E_v\right]\psi_v = 0 \qquad [9.23]$$

corresponding to simple harmonic motion, with a force constant k. From Section 2.4 the eigenvalues E_v are given by

$$E_v = \hbar\omega_0(v + \tfrac{1}{2}) = h\nu_0(v + \tfrac{1}{2}), \qquad v = 0, 1, 2, \ldots \qquad [9.24]$$

with $\omega_0 = (k/\mu)^{1/2}$ and $\nu_0 = \omega_0/2\pi$. The corresponding eigenfunctions ψ_v are the harmonic oscillator wave functions which we studied in Section 2.4.

In real systems, the function $E_s(R)$ is only represented accurately by the parabolic approximation [9.19] for small values of $(R - R_0)$, so that the vibrational energy E_v is only well represented by [9.24] for small values of the vibrational quantum number v. In general, for large values of v, the levels tend to become more closely spaced, as shown in Fig. 9.6. When the energy exceeds the depth of the well, the molecule dissociates, so that there are only a finite number of vibrational levels associated with each electronic level.

A better representation of the potential well $E_s(R)$ than the parabolic approximation [9.19] is given by $E_s(R) = E_s(\infty) + V(R)$, $V(R)$ being an empirical potential due to P. M. Morse, which has the form

$$V(R) = D_e[e^{-2\alpha(R-R_0)} - 2e^{-\alpha(R-R_0)}] \qquad [9.25]$$

where R_0, D_e and α are constants for a given molecule. Table 9.1 gives the values of R_0, D_e and α for a few molecules. We see from [9.25] that the Morse potential is attractive at large distances and has a minimum equal to $-D_e$ at the equilibrium distance R_0, so that we must have

$$D_e = E_s(\infty) - E_s(R_0) \qquad [9.26]$$

At short distances, where the nuclei come close together, the potential [9.25] exhibits a strong repulsion. The constant α appearing in the Morse potential can be related to the 'force constant' k introduced above (see [9.19]–[9.20]) by expanding $V(R)$ in powers of $(R - R_0)$. That is

$$V(R) = D_e[-1 + \alpha^2(R - R_0)^2 + \cdots] \qquad [9.27]$$

so that, by comparing with [9.19] and using [9.26], we have

$$D_e\alpha^2 = \tfrac{1}{2}k \qquad [9.28]$$

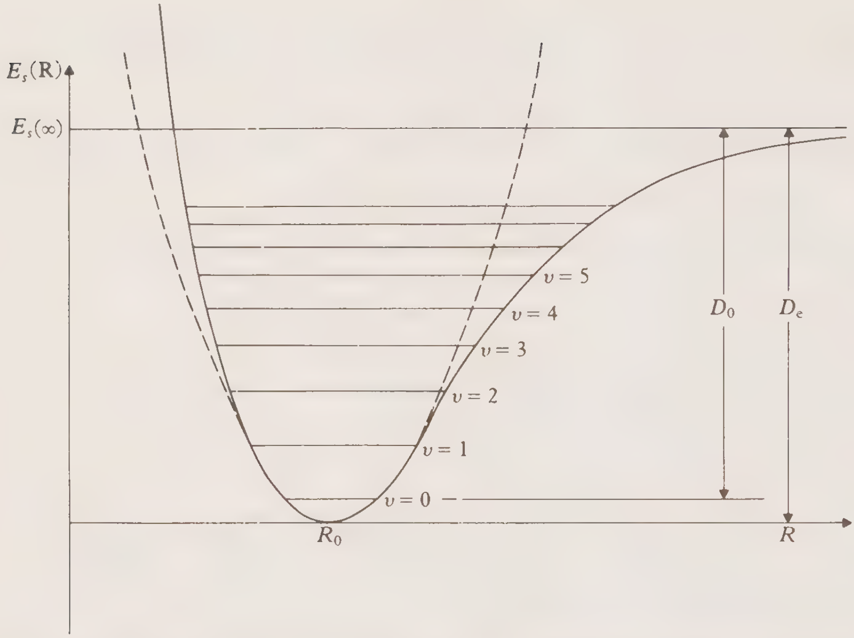

9.6 Vibrational energy levels of a diatomic molecule. The dashed line shows the parabolic approximation to the potential well, which is accurate in the region close to R_0, the equilibrium separation.

The lower energy levels in the potential $D_e + V(R)$, where $V(R)$ is the Morse potential [9.25] are given quite accurately by the expression,

$$E_v = \hbar\omega_0[(v + \tfrac{1}{2}) - \beta(v + \tfrac{1}{2})^2] \qquad [9.29]$$

where β is a small number ($\beta \ll 1$). The quantity $\beta\omega_0$ is known as the *anharmonicity constant* and is found to be given by

$$\beta\omega_0 = \frac{\hbar\omega_0^2}{4D_e} \qquad [9.30]$$

It is interesting to note that because of the zero-point energy ($v = 0$) of $\sim\hbar\omega_0/2$, the dissociation energy of the molecule in the electronic state s is not exactly $E_s(\infty) - E_s(R_0)$, but is given by $E_s(\infty) - E_s(R_0) - \hbar\omega_0/2$ (see Fig. 9.6).

Table 9.1 Values of the constants R_0, D_e and α for a few typical molecules

Molecule	R_0(Å)	D_e(eV)	αR_0
H_2	0.742	4.75	1.44
I_2	2.66	1.56	4.95
HCl	1.27	4.62	2.38

In terms of D_e and ω_0, the dissociation energy is therefore given by

$$D_0 = D_e - \hbar\omega_0/2 \qquad [9.31]$$

In Table 9.2 we list the equilibrium distance R_0, the dissociation energy D_0, the fundamental vibrational frequency $\nu_0 = \omega_0/2\pi$ and the fundamental rotational constant $\hbar^2/(2\mu R_0^2)$ for a few typical diatomic molecules.

Centrifugal distortion

So far we have approximated the rotational energy E_r by the simple 'rigid rotator' expression [9.21] evaluated at the equilibrium distance R_0, so that there is no coupling between the rotational and vibrational motions. In a more accurate treatment, we should solve the radial equation [9.17] directly. Adopting the Morse potential [9.23] for $E_s(R) - E_s(\infty)$, this equation reads

$$\left[-\frac{\hbar^2}{2\mu}\frac{\mathrm{d}^2}{\mathrm{d}R^2} + V_{\text{eff}}(R) - \bar{E}_{s,v,\mathcal{J}}\right]\mathcal{F}^s_{v,\mathcal{J}}(R) = 0 \qquad [9.32]$$

where $\bar{E}_{s,v,\mathcal{J}} = E_{s,v,\mathcal{J}} - E_s(\infty)$ and the effective interaction

$$V_{\text{eff}}(R) = V(R) + \frac{\hbar^2}{2\mu}\frac{\mathcal{J}(\mathcal{J}+1)}{R^2}, \qquad \mathcal{J} = 0, 1, 2, \ldots \qquad [9.33]$$

is the sum of the Morse potential [9.25] and the *centrifugal distortion* term $\hbar^2\mathcal{J}(\mathcal{J}+1)/(2\mu R^2)$. It is clear that if we set $R = R_0$ in this centrifugal term we retrieve our earlier results. We also remark that for values of $\mathcal{J}$ which are not too large, the shape of $V_{\text{eff}}(R)$ is similar to that of $V(R)$. If we are interested in the lower energy levels we may expand $V_{\text{eff}}(R)$ about its minimum V_0 at $R = R_1$. Keeping terms up to order $(R - R_1)^4$, we have

$$V_{\text{eff}}(R) = V_0 + \tfrac{1}{2}\tilde{k}(R - R_1)^2 + c_1(R - R_1)^3 + c_2(R - R_1)^4 \qquad [9.34]$$

Table 9.2 The equilibrium distance R_0, dissociation energy $D_0 = D_e - \hbar\omega_0/2$, fundamental vibrational frequency $\nu_0 = \omega_0/2\pi$, fundamental rotational constant $B = \hbar^2/2\mu R_0^2 = \hbar^2/2I_0$ and magnitude $|D|$ of the electric dipole moment for some diatomic molecules

Molecule	R_0(Å)	D_0(eV)	$\tilde{\nu}_0$(cm^{-1})†	$\tilde{B}$ (cm^{-1})†	$10^{30}\,\|D\|$ (Cm)
H_2^+	1.06	2.65	2297	29.8	—
H_2	0.742	4.48	4395	60.8	—
O_2	1.21	5.08	1580	1.45	—
Cl_2	1.99	2.48	565	0.244	—
N_2	1.09	9.75	2360	2.01	—
CO	1.13	9.60	2170	1.93	0.40
NO	1.15	5.3	1904	1.70	0.50
LiH	1.60	2.5	1406	7.51	19.4
HCl	1.28	4.43	2990	10.6	3.53
NaCl	2.36	4.22	365	0.190	28.1

† Note that for both quantities $\tilde{\nu}_0$ and $\tilde{B}$ the values have been converted in units of cm^{-1}; $\tilde{\nu}_0 = \nu_0/c$; $\tilde{B} = B/hc$.

where the new force constant $\bar{k}$ and the coefficients c_1 and c_2 can be expressed in terms of the rotational quantum number $\mathcal{J}$ and of the constants D_e, α and R_0 of the Morse potential [9.25].

It is important to notice that the value R_1 for which $V_{\text{eff}}(R)$ has its minimum only coincides with R_0 if $\mathcal{J} = 0$. A simple approximation for R_1 may be obtained by setting $c_1 = c_2 = 0$ and $\bar{k} = k$ in [9.34], and solving the equation $\mathrm{d}V_{\text{eff}}(R)/\mathrm{d}R = 0$ by iteration. Using [9.28], we then have (Problem 9.4)

$$R_1 \simeq R_0 + \frac{\hbar^2}{2\mu} \frac{\mathcal{J}(\mathcal{J}+1)}{\alpha^2 R_0^3 D_e} \tag{9.35}$$

which shows that the molecule 'stretches' because of the rotational motion.

Returning to the effective potential [9.34] and treating the c_1 and c_2 terms as perturbations it may be shown that the energy eigenvalues of [9.32] are given to second order in $(v + 1/2)$ and $\mathcal{J}(\mathcal{J} + 1)$ by

$$\begin{aligned} \bar{E}_{s,v,\mathcal{J}} = {} & -D_e + \hbar\omega_0 \left[\left(v + \frac{1}{2}\right) - \beta\left(v + \frac{1}{2}\right)^2 \right] + \frac{\hbar^2}{2\mu R_0^2} \mathcal{J}(\mathcal{J}+1) \\ & - a(v + \tfrac{1}{2})\mathcal{J}(\mathcal{J}+1) - b\mathcal{J}^2(\mathcal{J}+1)^2 \end{aligned} \tag{9.36}$$

where

$$\begin{aligned} a &= \frac{3\hbar^3\omega_0}{4\mu\alpha R_0^3 D_e}\left(1 - \frac{1}{\alpha R_0}\right) \\ b &= \frac{\hbar^4}{4\mu^2\alpha^2 R_0^6 D_e} \end{aligned} \tag{9.37}$$

and we recall that $D_e = E_s(\infty) - E_s(R_0)$. The first three terms on the right of [9.36] are identical to those discussed above in the absence of centrifugal distortion; they are respectively the potential depth $(-D_e)$, the harmonic and anharmonic vibration terms, and the rigid rotator energy. The two additional terms are respectively a *rotation–vibration coupling* term (which is negative because for higher values of v the average internuclear distance is larger than R_0 due to the anharmonicity) and a *correction to the rigid rotator energy* [9.21], which is also negative since larger values of $\mathcal{J}$ lead to an increase in the average distance between the nuclei, as seen from [9.35].

9.4 ELECTRONIC STRUCTURE OF DIATOMIC MOLECULES

In this section we shall discuss the electronic wave functions of the simplest diatomic molecules. Our discussion will be based on the electronic wave equation [9.9], where we recall that all but the Coulomb interactions are neglected in the electronic Hamiltonian $H = T_e + V$. As a preliminary, we first consider some important symmetry properties possessed by diatomic molecules.

Symmetry properties

Let us return to the Hamiltonian [7.2] which approximately describes an N-electron atom by taking into account all the Coulomb interactions, but neglecting spin–orbit and other corrections such as spin–spin and hyperfine structure effects. The three components of the total electronic orbital angular momentum $\mathbf{L}$ commute with the Hamiltonian [7.2] and so does $\mathbf{L}^2$. Taking the Z axis in an arbitrary direction, the atomic eigenfunctions of [7.2] can be constructed to be simultaneous eigenfunctions of H, $\mathbf{L}^2$ and L_z. Thus, both the total electronic orbital quantum number L and the quantum number M_L are conserved when the atom is described by the (approximate) Hamiltonian [7.2]. As we have seen in Chapter 7, the fact that L is (approximately) a 'good quantum number' plays a central role in the classification of atomic energy levels (or terms).

In contrast, the internuclear axis of a diatomic molecule picks out a particular direction in space. If this direction is taken as the Z axis, then L_z commutes with the electronic molecular Hamiltonian $H = T_e + V$ of equation [9.9] (in which spin-dependent interactions have been neglected), but L_x, L_y and $\mathbf{L}^2$ do not. This is due to the fact that the electronic Hamiltonian $H = T_e + V$ of a diatomic molecule is invariant under rotations about the internuclear line (the Z axis), but not under rotations about the X or Y axes. The same result can also be obtained by examining the commutators $[H, L_x]$, $[H, L_y]$ and $[H, L_z]$ directly (Problem 9.5).

The electronic eigenfunctions Φ_s of a diatomic molecule can thus be constructed to be simultaneous eigenfunctions of H and L_z. That is,

$$\begin{aligned} L_z\Phi_s &= M_L\hbar\Phi_s, \qquad & M_L &= 0, \pm 1, \pm 2, \ldots \\ &= \pm\Lambda\hbar\Phi_s, \qquad & \Lambda &= 0, 1, 2, \ldots \end{aligned} \tag{9.38}$$

where

$$\Lambda = |M_L| \tag{9.39}$$

is the absolute value (in a.u.) of the projection of the total electronic angular momentum on the internuclear axis. The azimuthal part of the wave functions Φ_s is therefore of the form $(2\pi)^{-1/2}\exp(\pm i\Lambda\phi)$. By analogy with the spectroscopic notation S, P, D, F, ... used for atoms, it is customary to associate code letters with the values of Λ according to the correspondence:

Value of Λ	0	1	2	3	
	$\updownarrow$	$\updownarrow$	$\updownarrow$	$\updownarrow$	
Code letter	Σ	Π	Δ	Φ	, ...

If we are dealing with individual electrons, we shall use the notation $\lambda = |m_l|$ and the correspondence:

Value of λ	0	1	2	3	
	$\updownarrow$	$\updownarrow$	$\updownarrow$	$\updownarrow$	
Code letter	σ	π	δ	ϕ	, ...

The electronic Hamiltonian for a diatomic molecule is also invariant under reflections in all planes containing the internuclear line. The (XZ) plane is such a plane, and reflection of the coordinates of the electrons in this plane corresponds to the operation $y_i \to -y_i$. If A_y is the operator that performs this reflection, then

$$[A_y, H] = 0 \qquad [9.40]$$

In addition, since $L_z = -i\hbar(x\partial/\partial y - y\partial/\partial x)$, we have

$$A_y L_z = -L_z A_y \qquad [9.41]$$

It follows immediately that if $\Lambda \neq 0$ the action of the operator A_y on a wave function corresponding to the eigenvalue $\Lambda\hbar$ of L_z converts this wave function into another one corresponding to the eigenvalue $-\Lambda\hbar$, and that both eigenfunctions have the same energy. The electronic terms such that $\Lambda \neq 0$ (that is, the Π, Δ, Φ, . . . terms) are thus *doubly degenerate*, each value of the energy corresponding to two states which differ by the direction of the projection of the orbital angular momentum along the molecular axis. In fact, this twofold degeneracy is only approximate and it is possible to show that the interaction between the electronic and rotational motions leads to a splitting of the terms with $\Lambda \neq 0$ into two nearby levels, which is called Λ-*doubling*.

Let us now return to the relations [9.40]–[9.41] and consider the case $\Lambda = 0$ corresponding to the Σ states. These states are non-degenerate, so that the wave function of a Σ term can only be multiplied by a constant in a reflection through a plane containing the molecular axis. We also note that when $\Lambda = 0$ simultaneous eigenfunctions of H, L_z and A_y can be constructed. Since $A_y^2 = 1$ the eigenfunctions of A_y have eigenvalues ± 1. To completely specify Σ states of diatomic molecules, one therefore distinguishes Σ^+ states, for which the wave function is left unchanged upon reflection in a plane containing the nuclei, from Σ^- states, for which it changes sign in performing that operation.

In the special case of a *homonuclear* diatomic molecule, namely a diatomic molecule containing identical nuclei (such as H_2, N_2, O_2, . . .) there is an extra symmetry since in addition to the axis of symmetry provided by the internuclear axis, there is a *centre of symmetry* at the midpoint of the distance between the two nuclei [2]. Choosing this point as the origin of the coordinates, the Hamiltonian is invariant under an inversion of the coordinates of all electrons with respect to that origin, namely in the operation $\mathbf{r}_i \to -\mathbf{r}_i$. Since the operator which effects this transformation also commutes with L_z, we may then classify electronic terms having a given value of Λ according to their parity. The electronic wave functions therefore split into two sets: those that are even, i.e. remain unaltered by the operation $\mathbf{r}_i \to -\mathbf{r}_i$, and those that are odd, i.e. change sign in that

[2] The symmetry discussed in this paragraph only depends on the two nuclear *charges* being the same. The two nuclei can therefore have different mass, that is they can be two isotopes of the same species such as the proton and the deuteron, or ^{16}O and ^{18}O, and so on.

operation. The former are denoted by a subscript g and are called *gerade* states, while the latter are denoted by a subscript u and are called *ungerade* states. The subscripts g or u are added to the term symbol, so that for homonuclear diatomic molecules we have Σ_g, Σ_u, Π_g, Π_u, . . . states. We note that a homonuclear diatomic molecule has four non-degenerate Σ states: Σ_g^+, Σ_u^+, Σ_g^-, Σ_u^-.

The two transformations we have considered ($y_i \to -y_i$ and $\mathbf{r}_i \to -\mathbf{r}_i$) are carried out keeping the internuclear coordinate $\mathbf{R}$ fixed. We now turn to the question of the behaviour of the electronic wave function of a homonuclear diatomic molecule if the two identical nuclei are interchanged, so that $\mathbf{R} \to -\mathbf{R}$ and

$$\Phi_s(\mathbf{R}; \mathbf{r}_1, \mathbf{r}_2, \ldots \mathbf{r}_N) \to \Phi_s(-\mathbf{R}; \mathbf{r}_1, \mathbf{r}_2, \ldots \mathbf{r}_N) \qquad [9.42]$$

This operation can be achieved by first rotating the molecule as a whole through 180° about the Y axis, followed by a reflection in the (XZ) plane ($y_i \to -y_i$) and then the inversion $\mathbf{r}_i \to -\mathbf{r}_i$ about the centre of symmetry. The first rotation cannot alter the electronic part of the wave function because this is only a function of the *relative* position of the electrons and the nuclei. The net effect of the two reflections is to change the sign of the wave function for the Σ_u^+, Σ_g^- levels and to leave the sign of the Σ_g^+ and Σ_u^- wave functions unaltered.

Spin

Let us denote by $\mathbf{S}$ the resultant of the individual electron spins, and as usual $S(S + 1)\hbar^2$ are the eigenvalues of $\mathbf{S}^2$. As in the case of atoms, each electronic term of the molecule is also characterised by the value of S. Provided fine structure effects (spin–orbit coupling) are neglected, there is a degeneracy of order $2S + 1$ associated with S. Just as for atoms, the quantity $2S + 1$ is called the *multiplicity* of the term and is written as a (left) superscript, so that the term symbol is written ${}^{2S+1}\Lambda$, with the code letters for $\Lambda = 0, 1, 2, \ldots$ discussed above. For example, the symbol ${}^3\Delta$ denotes a term such that $\Lambda = 2$ and $S = 1$.

It is worth noting that the ground state (often labelled by the symbol X) of most diatomic molecules is such that $S = 0$ and exhibits maximum symmetry. Thus, in most cases it is a ${}^1\Sigma^+$ state (written as $X^1\Sigma^+$) for a heteronuclear molecule and a ${}^1\Sigma_g^+$ state (written as $X^1\Sigma_g^+$) for a homonuclear molecule [3].

So far we have not taken into account the spin of the nuclei. Hyperfine structure interactions due to the coupling between the nuclear spins and the orbital motion and spin of the electrons have very little effect on the molecular energies. However, *symmetry* effects related to the spin of the nuclei have an important influence on the structure of homonuclear molecules, as we shall see in detail in Section 10.5.

[3] Exceptions occur for the molecules O_2 and NO, for which the ground states $X^3\Sigma_g^-$ and $X^2\Pi$, respectively.

Intersection of potential curves and the von Neumann–Wigner non-crossing rule

The electronic terms or potential curves $E_s(R)$ of a diatomic molecule depend only on the internuclear distance R, and it is important to investigate the behaviour of these potential curves as R varies. We shall analyse below a few low-lying potential curves of simple molecular systems such as H_2^+ and H_2. Before we do this, however, we shall consider the important question of the intersection of two potential curves.

Let us denote by $E_1(R)$ and $E_2(R)$ two different electronic potential curves, and suppose that at the internuclear distance R_c the values $E_1(R_c)$ and $E_2(R_c)$ are *close*, but distinct (see Fig. 9.7). The energies $E_1^{(0)} = E_1(R_c)$ and $E_2^{(0)} = E_2(R_c)$ are eigenvalues of the Hamiltonian $H_0 = H(R_c)$ describing the motion of the electrons in the field of the two nuclei located a distance R_c apart. The corresponding orthonormal electronic eigenfunctions will be denoted by $\Phi_1^{(0)}$ and $\Phi_2^{(0)}$ and are assumed to be real.

Let us see if the two potential curves $E_1(R)$ and $E_2(R)$ can be made to intersect by modifying the internuclear distance from R_c to $R_c + \Delta R$. The Hamiltonian now becomes $H \equiv H(R_c + \Delta R) = H_0 + H'$, where $H' = \Delta R \partial H_0/\partial R_c$ is a small perturbation. Setting $H'_{ij} = \langle \Phi_i^{(0)} | H' | \Phi_j^{(0)} \rangle$, $i,j = 1,2$, and referring to the equation [2.329] we deduce that in order for $E_1(R)$ and $E_2(R)$ to be equal at the point $R = R_c + \Delta R$ we must require that the two equations

$$E_1^{(0)} - E_2^{(0)} + H'_{11} - H'_{22} = 0 \qquad [9.43a]$$

$$H'_{12} = 0 \qquad [9.43b]$$

are simultaneously satisfied. Remembering that we only have *one* parameter (ΔR) at our disposal, we must distinguish two cases:

1. The matrix element H'_{12} vanishes identically. It is then possible for the

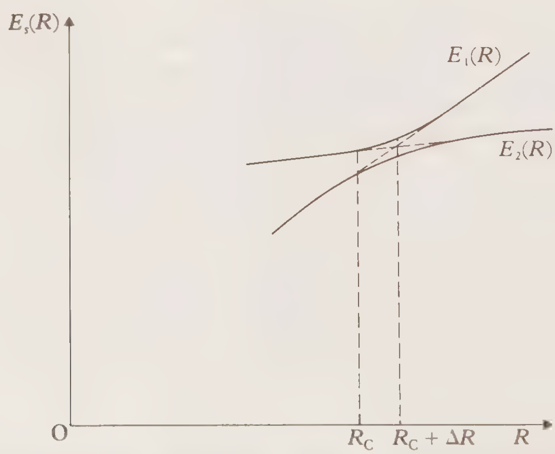

9.7 The non-crossing role of von Neumann and Wigner. Two potential curves $E_1(R)$ and $E_2(R)$ cannot cross if the states 1 and 2 have the same symmetry.

crossing to occur if, for a certain value of ΔR (i.e. of R) the equation [9.43a] is satisfied. Remembering that the operator H' (or H) commutes with the symmetry operators of the molecule, we see that this case will happen if the two functions $\Phi_1^{(0)}$ and $\Phi_2^{(0)}$ have *different symmetries* (for example if they correspond to two electronic terms having different values of Λ, different parities g and u, different multiplicities, or to terms Σ^+ and Σ^-).

2. If $\Phi_1^{(0)}$ and $\Phi_2^{(0)}$ have the *same symmetry*, then H'_{12} will in general be non-zero. Except for accidental crossing which would occur if, by coincidence, the two equations [9.43] were satisfied at the same value of R, it is in general impossible to find a single value of ΔR (i.e. of R) for which the two conditions are satisfied simultaneously. Thus we conclude that in general *two electronic curves belonging to the same symmetry species cannot cross*. This result is known as the non-crossing rule of von Neumann and Wigner and is illustrated in Fig. 9.7 [4].

The hydrogen molecular ion

The simplest of all molecules is the hydrogen molecular ion, H_2^+, which is composed of two protons and one electron. The Schrödinger equation for the electronic motion is in this case

$$\left[-\frac{\hbar^2}{2m}\nabla_r^2 - \frac{e^2}{(4\pi\varepsilon_0)r_A} - \frac{e^2}{(4\pi\varepsilon_0)r_B} + \frac{e^2}{(4\pi\varepsilon_0)R} - E_s\right]\Phi_s = 0 \qquad [9.44]$$

where R is the internuclear separation, and $\mathbf{r}_A$, $\mathbf{r}_B$ and $\mathbf{r}$ are the position vectors of the electron with respect to the protons A and B, and to the midpoint of the internuclear line, respectively (see Fig. 9.8). The vectors $\mathbf{r}_A$, $\mathbf{r}_B$ and $\mathbf{r}$ are not independent since $\mathbf{r}_A = \mathbf{r} + \mathbf{R}/2$ and $\mathbf{r}_B = \mathbf{r} - \mathbf{R}/2$.

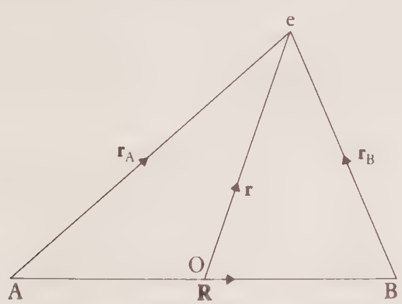

9.8 A coordinate system for the hydrogen molecular ion H_2^+.

From this point, it is convenient to work in atomic units (see Appendix 11) and in these units the Schrödinger equation [9.44] reads

[4] It should be noted that the proof of the von Neumann–Wigner non-crossing rule assumes that the Born–Oppenheimer approximation can be made. If this is not the case the non-crossing rule may break down, the concept of potential energy curves becoming meaningless.

$$\left(-\frac{1}{2}\nabla_r^2 - \frac{1}{r_A} - \frac{1}{r_B} + \frac{1}{R} - E_s\right)\Phi_s = 0 \qquad [9.45]$$

This Schrödinger electronic equation for the hydrogen molecular ion is sufficiently simple so that it is possible to obtain numerical solutions to any desired degree of accuracy, as we shall see below. This is important because it provides a test of approximate methods, which have to be used for more complicated systems. However, we will first develop the approximate method of the linear combination of atomic orbitals (LCAO) because it gives considerable physical insight into the nature of the solution.

When the two protons A and B are far apart, the electron must be attached to one of them. If the system is in the ground state, and the electron is attached to proton A we might expect the wave function to be (we drop the label s)

$$\Phi(\mathbf{R}; \mathbf{r}) = \psi_{1s}(r_A) \qquad [9.46]$$

where $\psi_{1s}(r) = \pi^{-1/2}\exp(-r)$ is the normalised ground state wave function for atomic hydrogen (written in atomic units). Clearly such a wave function does not have the required symmetry about the midpoint of the internuclear line, but we can construct the linear combinations

$$\Phi_g(\mathbf{R}; \mathbf{r}) = \frac{1}{\sqrt{2}}[\psi_{1s}(r_A) + \psi_{1s}(r_B)] \qquad [9.47a]$$

and

$$\Phi_u(\mathbf{R}; \mathbf{r}) = \frac{1}{\sqrt{2}}[\psi_{1s}(r_A) - \psi_{1s}(r_B)] \qquad [9.47b]$$

which are even and odd under reflection in the midpoint of AB, respectively. The first one is therefore of σ_g character and the second one is a σ_u wave function. Although these functions are only expected to be accurate in the asymptotic region of large R, we can use them as trial functions in the variational expression [2.361], namely

$$E_{g,u}(R) = \frac{\int \Phi_{g,u}^{\star} H \Phi_{g,u}\, d\mathbf{r}}{\int |\Phi_{g,u}|^2\, d\mathbf{r}} \qquad [9.48]$$

Let us first work out the denominator of this expression:

$$\begin{aligned} D &= \int |\Phi_{g,u}|^2\, d\mathbf{r} \\ &= \frac{1}{2}\int [|\psi_{1s}(r_A)|^2 + |\psi_{1s}(r_B)|^2 \pm 2\psi_{1s}(r_A)\psi_{1s}(r_B)]\, d\mathbf{r} \end{aligned} \qquad [9.49]$$

Since $\mathbf{R}$ is fixed, $\int d\mathbf{r} = \int d\mathbf{r}_A = \int d\mathbf{r}_B$ and, as $\psi_{1s}(r)$ is normalised to unity, we

have

$$D = 1 \pm I(R) \qquad [9.50]$$

where $I(R)$ is the overlap integral

$$I(R) = \int \psi_{1s}(r_A)\psi_{1s}(r_B)\,d\mathbf{r} \qquad [9.51]$$

This expression can be evaluated by using the integrals given in Appendix 9, with the result

$$I(R) = \left(1 + R + \frac{1}{3}R^2\right)e^{-R} \qquad [9.52]$$

The numerator of [9.48] is equal to

$$N = H_{AA} \pm H_{AB} \qquad [9.53]$$

where

$$H_{AA} = \int \psi_{1s}(r_A)H\psi_{1s}(r_A)\,d\mathbf{r}_A$$

$$H_{AB} = \int \psi_{1s}(r_A)H\psi_{1s}(r_B)\,d\mathbf{r}_B \qquad [9.54]$$

Using the Schrödinger equation satisfied by $\psi_{1s}(r)$, which is

$$\left(-\frac{1}{2}\nabla^2 - \frac{1}{r} - E_{1s}\right)\psi_{1s}(r) = 0 \qquad [9.55]$$

where $E_{1s} = -0.5$ a.u. is the ground state of atomic hydrogen, and making use of the integrals of Appendix 9, we find that

$$H_{AA} = E_{1s} + \frac{1}{R}(1 + R)e^{-2R}$$

and

$$H_{AB} = \left(E_{1s} + \frac{1}{R}\right)I(R) - (1 + R)e^{-R} \qquad [9.56]$$

Putting the various terms together, the expression [9.48] for the energies $E_g(R)$ and $E_u(R)$ becomes

$$E_{g,u}(R) = E_{1s} + \frac{1}{R}\,\frac{(1 + R)e^{-2R} \pm (1 - \frac{2}{3}R^2)e^{-R}}{1 \pm (1 + R + \frac{1}{3}R^2)e^{-R}} \qquad [9.57]$$

The functions $E_g(R) - E_{1s}$ and $E_u(R) - E_{1s}$ are plotted in Fig. 9.9. The function $E_g(R)$ corresponding to the symmetrical (gerade) wave function exhibits a minimum at $R_0 = 2.49$ a.u. (1.32 Å) and it is found that $D_e = E_{1s} - E_g(R_0) = 0.065$ a.u. $= 1.77$ eV. As a result, this curve represents

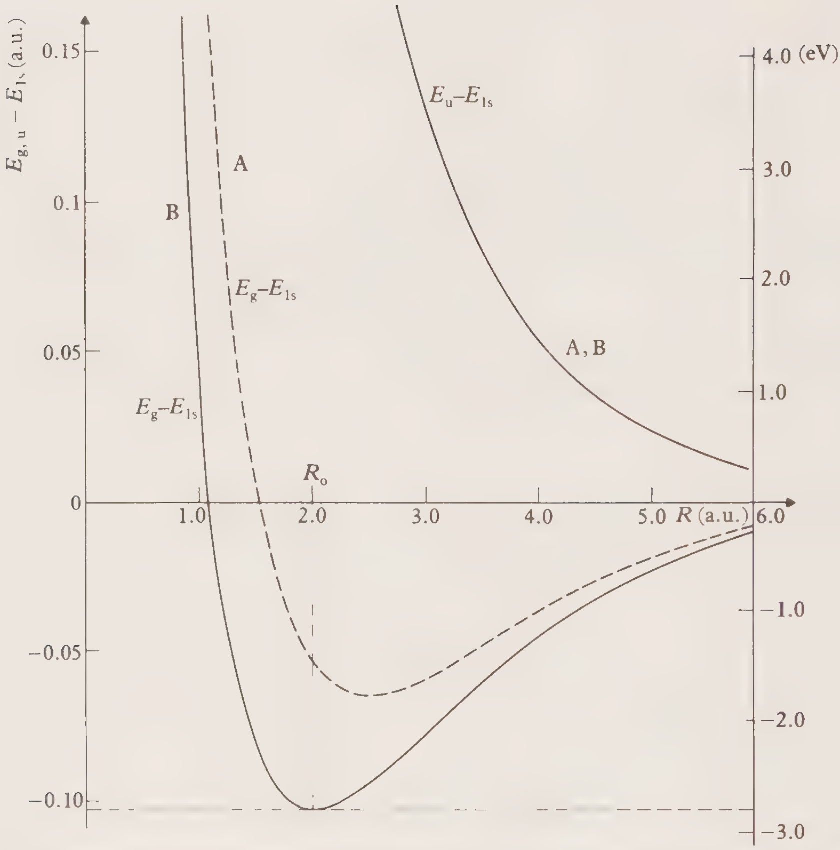

9.9 The lowest electronic potential energy curves of H_2^+. The dashed lines labelled A, show $(E_g(R) - E_{1s})$ and $(E_u(R) - E_{1s})$ calculated using the simple LCAO wave functions of [9.47], while the solid curves labelled B show the exact values of the same quantities calculated from equations [9.61] to [9.64].

an attraction leading to the formation of a stable molecular ion. The corresponding molecular orbital Φ_g given by [9.47a] is said to be a *bonding* molecular orbital. In the present case it is an approximation to the ground state (that is, the lowest σ_g state) and is designated $\sigma_g 1s$.

In contrast, we see from Fig. 9.9 that the function $E_u(R)$ has no minimum and is repulsive at all distances; a molecule in this state will immediately dissociate into a proton and a hydrogen atom in the 1s state. The corresponding molecular orbital Φ_u (see (9.47b)) is called an *antibonding* orbital, and is denoted in the present case by $\sigma_u^\star 1s$, where the superscript ($\star$) indicates that we are dealing with an antibonding orbital.

It is worth noting that the term H_{AB}, in which the matrix element of the Hamiltonian H between atomic orbitals centred on the protons A and B is evaluated, plays a vital role in obtaining bonding for the $\sigma_g 1s$ state. If this term

were ignored, the two functions $E_g(R)$ and $E_u(R)$ would coincide, the resulting curve being repulsive at all distances.

The electron probability density in the states Φ_g and Φ_u is given by $|\Phi_g|^2$ and $|\Phi_u|^2$, respectively, so that the corresponding charge densities are $\rho_g = -e|\Phi_g|^2$ and $\rho_u = -e|\Phi_u|^2$ (or $\rho_g = -|\Phi_g|^2$ and $\rho_u = -|\Phi_u|^2$ in atomic units). If the charge density ρ_g is evaluated at points between A and B along the internuclear line, it is found to be greater (in absolute value) than the sum of the densities due to two isolated H atoms with their protons placed at A and B, normalised so that half an electron is associated with each proton. It is this *excess of negative charge* between the protons which causes the binding (or bonding). On the other hand, if the charge density ρ_u corresponding to the antibonding case is evaluated, a *deficiency of negative charge* is found between the protons. This is clearly seen in Fig. 9.10 where the wave functions Φ_g and Φ_u as well as the absolute value of the charge densities ρ_g and ρ_u are plotted along the internuclear line.

The *exact* binding energy of H_2^+ is a little greater than the result obtained above, with $D_e = E_{1s} - E_g(R_0) = 0.103$ a.u. $= 2.79$ eV, and the true equilibrium distance is $R_0 = 1.06$ Å. The principal failing of the approximate wave function $\Phi_g(\mathbf{R}; \mathbf{r})$ given by [9.47a] is that at small separations Φ_g should approach the wave function of $He^+(1s)$, the ground state of the positive helium ion with nuclear charge $Z = 2$, and in the approximation [9.47a] it does not. This defect can be remedied by using orbitals of variable charge, such as

$$u_{1s}(Z^\star, r) = \left(\frac{Z^{\star 3}}{\pi}\right)^{1/2} e^{-Z^\star r} \qquad [9.58]$$

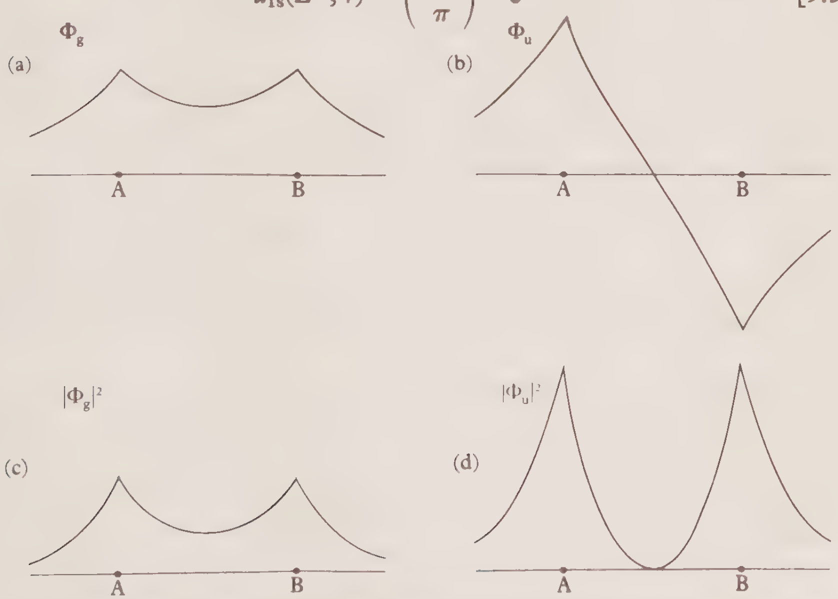

9.10 Wave functions Φ_g and Φ_u and charge densities $|\Phi_g|^2$, $|\Phi_u|^2$ for the hydrogen molecular ion H_2^+, plotted along the internuclear line to an arbitrary scale. The points A and B represent the positions of the two protons.

with $Z^\star$ a function of R, and by determining $Z^\star$ at each R with the help of the Rayleigh–Ritz variational method (see Chapter 2). We also note that at large R a dipole moment is induced in a hydrogen atom by the electrostatic field of a proton. This interaction gives rise to a potential proportional to R^{-4}. With the approximate wave functions discussed so far this effect is not taken into account, and the energy $E_{g,u}(R) - E_{1s}$ decreases exponentially (see [9.57]). This feature is not important for bound-state calculations, but as we shall see in Chapter 13 it plays an important role in elastic ion–atom scattering.

The exact solution

As we pointed out above, it is also possible to obtain accurate numerical solutions of the Schrödinger electronic equation [9.45] for the hydrogen molecular ion. The equation is first written in terms of confocal elliptic coordinates (ξ, η, ϕ), where

$$\begin{aligned} \xi &= \frac{1}{R}(r_A + r_B), \qquad 1 \leqslant \xi \leqslant \infty \\ \eta &= \frac{1}{R}(r_A - r_B), \qquad -1 \leqslant \eta \leqslant +1 \end{aligned} \tag{9.59}$$

and ϕ is the azimuthal angle with respect to the internuclear line, chosen as the Z-axis. Using the fact that in these new coordinates the Laplacian operator ∇^2 is

$$\begin{aligned} \nabla^2 = \frac{4}{R^2(\xi^2 - \eta^2)} \Bigg\{ & \frac{\partial}{\partial \xi}\left[(\xi^2 - 1)\frac{\partial}{\partial \xi}\right] + \frac{\partial}{\partial \eta}\left[(1 - \eta^2)\frac{\partial}{\partial \eta}\right] \\ & + \frac{\xi^2 - \eta^2}{(\xi^2 - 1)(1 - \eta^2)}\frac{\partial^2}{\partial \phi^2}\Bigg\} \end{aligned} \tag{9.60}$$

the Schrödinger equation [9.45] becomes

$$\begin{aligned} & \frac{\partial}{\partial \xi}\left[(\xi^2 - 1)\frac{\partial \Phi_s}{\partial \xi}\right] + \frac{\partial}{\partial \eta}\left[(1 - \eta^2)\frac{\partial \Phi_s}{\partial \eta}\right] + \left(\frac{1}{\xi^2 - 1} + \frac{1}{1 - \eta^2}\right)\frac{\partial^2 \Phi_s}{\partial \phi^2} \\ & \quad + 2R^2\left[\frac{1}{4}\left(E_s - \frac{1}{R}\right)(\xi^2 - \eta^2) + \frac{1}{R}\xi\right]\Phi_s = 0 \end{aligned} \tag{9.61}$$

An eigenfunction solution of this equation can be found in the form of the product

$$\Phi_s(\xi, \eta, \phi) = F(\xi)G(\eta)e^{im\phi}, \qquad m = 0, \pm 1, \pm 2, \ldots \tag{9.62}$$

where the functions $F(\xi)$ and $G(\eta)$ are the normalisable solutions of the equations

$$\frac{d}{d\xi}\left[(\xi^2 - 1)\frac{dF}{d\xi}\right] + \left[\frac{R^2}{2}\left(E_s - \frac{1}{R}\right)\xi^2 + 2R\xi - \frac{m^2}{\xi^2 - 1} + \mu\right]F(\xi) = 0 \tag{9.63}$$

and

$$\frac{d}{d\eta}\left[(1-\eta^2)\frac{dG}{d\eta}\right]-\left[\frac{R^2}{2}\left(E_s-\frac{1}{R}\right)\eta^2+\frac{m^2}{1-\eta^2}+\mu\right]G(\eta)=0 \quad [9.64]$$

μ being a separation constant. Each electronic term is therefore characterised by three quantum numbers, namely $\lambda = |m|$ and the quantum numbers n_ξ and n_η giving respectively the number of zeros of the functions $F(\xi)$ and $G(\eta)$. As a result of this complete separation of variables, it is worth noting that two potential curves corresponding to the same λ but different values of the couple (n_ξ, n_η) are allowed to cross.

These equations [9.61]–[9.64] can be solved numerically for the ground state and excited states. The accurate values of the quantities $E_g - E_{1s}$ and $E_u - E_{1s}$ obtained in this way for the states σ_g 1s and $\sigma_u^\star$ 1s are shown in Fig. 9.9. A similar treatment can be applied to any one-electron diatomic molecular ion (containing two nuclei A and B and one electron), whether homonuclear or heteronuclear.

Molecular hydrogen H_2

In much the same way as atomic wave functions are built in the Hartree–Fock method from one-electron atomic orbitals, electronic wave functions for molecular systems containing several electrons can be constructed from one-electron molecular orbitals. This approach is known as the Hund–Mulliken or *molecular orbital* (MO) method. It will be illustrated below for several diatomic molecules, starting with the neutral hydrogen molecule H_2, where the two-electron wave function will be built by using the one-electron molecular orbitals obtained for H_2^+. As in the case of the helium atom discussed in Chapter 6, the character of the two-electron wave function depends on the total electronic spin quantum number S. In fact, as we shall see shortly, the spin plays a key role as to whether bonding or antibonding takes place.

Molecular orbital treatment

Labelling the two electrons in H_2 as 1 and 2 and using the coordinate system of Fig. 9.11, we shall now build the lowest states of H_2 from the H_2^+ orbitals Φ_g

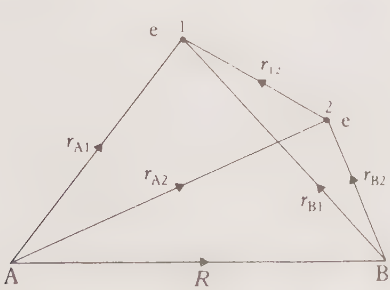

9.11 A coordinate system for the hydrogen molecule H_2.

and Φ_u discussed above. As shown in Chapter 6 (see [6.18]–[6.19]) the spin wave functions for the two-electron system must either be singlet ($S = 0$),

$$\chi_{0,0}(1, 2) = \frac{1}{\sqrt{2}}[\alpha(1)\beta(2) - \beta(1)\alpha(2)] \tag{9.65}$$

or triplet ($S = 1$),

$$\begin{aligned} \chi_{1,1}(1, 2) &= \alpha(1)\alpha(2) \\ \chi_{1,0}(1, 2) &= \frac{1}{\sqrt{2}}[\alpha(1)\beta(2) + \beta(1)\alpha(2)] \\ \chi_{1,-1}(1, 2) &= \beta(1)\beta(2) \end{aligned} \tag{9.66}$$

Since the overall wave function must be antisymmetric in the electrons, the spatial wave function corresponding to the singlet case must be symmetrical, while the spatial wave function for the triplet case must be antisymmetrical. Four combinations can be formed, namely

$$\Phi_A(1, 2) = \Phi_g(1)\Phi_g(2)\chi_{0,0}(1, 2) \tag{9.67a}$$

$$\Phi_B(1, 2) = \Phi_u(1)\Phi_u(2)\chi_{0,0}(1, 2) \tag{9.67b}$$

$$\Phi_C(1, 2) = \frac{1}{\sqrt{2}}[\Phi_g(1)\Phi_u(2) + \Phi_g(2)\Phi_u(1)]\chi_{0,0}(1, 2) \tag{9.67c}$$

$$\Phi_D(1, 2) = \frac{1}{\sqrt{2}}[\Phi_g(1)\Phi_u(2) - \Phi_g(2)\Phi_u(1)]\chi_{1,M_S}(1, 2) \qquad M_S = 0, \pm 1 \tag{9.67d}$$

Both Φ_A and Φ_B represent $^1\Sigma_g^+$ states, while Φ_C corresponds to a $^1\Sigma_u^+$ term and Φ_D to $^3\Sigma_u^+$ states.

The wave function Φ_A describes two electrons having opposite spins each occupying the bonding orbital Φ_g. By analogy with the He atom we expect this wave function to yield the lowest energy of the four combinations, and to be therefore an approximation to the *ground state* wave function of H_2. In order to study this problem in more detail, we start from the electronic wave equation for the two electrons in the field of the two (fixed) protons, namely

$$(H - E_s)\Phi_s = 0 \tag{9.68}$$

where the electronic Hamiltonian H is given (in atomic units) by

$$H = -\frac{1}{2}\nabla_1^2 - \frac{1}{2}\nabla_2^2 - \frac{1}{r_{A1}} - \frac{1}{r_{A2}} - \frac{1}{r_{B1}} - \frac{1}{r_{B2}} + \frac{1}{r_{12}} + \frac{1}{R} \tag{9.69}$$

and may be written as

$$H = H_0(1) + H_0(2) + \left(\frac{1}{r_{12}} + \frac{1}{R}\right) \tag{9.70}$$

with

$$H_0(i) = -\frac{1}{2}\nabla_i^2 - \frac{1}{r_{Ai}} - \frac{1}{r_{Bi}} \quad i = 1, 2 \tag{9.71}$$

The exact one-electron molecular orbitals satisfy the equation

$$H_0(i)\Phi_{g,u} = \left(E_{g,u} - \frac{1}{R}\right)\Phi_{g,u} \qquad [9.72]$$

and we shall normalise them to unity (for all R), namely

$$\int |\Phi_{g,u}|^2 \, d\mathbf{r} = 1 \qquad [9.73]$$

The lowest energy, obtained by using the wave function Φ_A (given by [9.67a]) in the Rayleigh–Ritz variational expression [2.361] is then

$$\begin{aligned} E_A &= \int \Phi_A^\star H\Phi_A \, d\mathbf{r}_1 \, d\mathbf{r}_2 \\ &= 2E_g(R) - \frac{1}{R} + \int d\mathbf{r}_1 \, d\mathbf{r}_2 \, \frac{|\Phi_g(1)\Phi_g(2)|^2}{r_{12}} \end{aligned} \qquad [9.74]$$

The 'exact' molecular orbitals Φ_g (or elaborate variational forms) can be used in this expression, but it is illuminating to use the simple LCAO form [9.47a]. In this case the equilibrium distance for H_2 can be computed to be $R_0 = 1.5$ a.u. (0.8 Å), and the corresponding energy difference $D_e = 2E_{1s} - E_A(R_0)$ is found to be 0.098 a.u. (2.68 eV). The experimental values are $R_0 = 1.4$ a.u. (0.74 Å) and $D_e = 0.175$ a.u. (4.75 eV).

Using [9.47a] and writing out the approximate wave function [9.67a] in full, we have

$$\begin{aligned} \Phi_A = \frac{1}{2} [&\psi_{1s}(r_{A1})\psi_{1s}(r_{B2}) + \psi_{1s}(r_{A2})\psi_{1s}(r_{B1}) \\ &+ \psi_{1s}(r_{A1})\psi_{1s}(r_{A2}) + \psi_{1s}(r_{B1})\psi_{1s}(r_{B2})]\chi_{0,0}(1, 2) \end{aligned} \qquad [9.75]$$

or

$$\Phi_A = \Phi_A^{cov} + \Phi_A^{ion} \qquad [9.76]$$

where

$$\Phi_A^{cov} = \frac{1}{2} [\psi_{1s}(r_{A1})\psi_{1s}(r_{B2}) + \psi_{1s}(r_{A2})\psi_{1s}(r_{B1})]\chi_{0,0}(1, 2) \qquad [9.77]$$

and

$$\Phi_A^{ion} = \frac{1}{2} [\psi_{1s}(r_{A1})\psi_{1s}(r_{A2}) + \psi_{1s}(r_{B1})\psi_{1s}(r_{B2})]\chi_{0,0}(1, 2) \qquad [9.78]$$

The function Φ_A^{cov} represents the situation in which one electron is associated with each nucleus. In the separated atom limit, this function yields two isolated neutral hydrogen atoms in the ground state: H(1s) + H(1s). The type of bonding associated with this function is called *covalent bonding* and Φ_A^{cov} is said to be the covalent part of Φ_A. On the other hand, the function Φ_A^{ion} corresponds to the situation in which both electrons are attached to one nucleus. In the separated atom limit, this function represents a proton and a negative hydrogen

ion H^-. Functions like Φ_A^{ion} which represent an unequal division of charge between the nuclei are said to be of ionic character and the type of bonding corresponding to such functions is called *ionic bonding*. It is worth noting that each term of the function [9.78] yields a very poor representation of the bound state of H^- [5] and in any case the probability of this configuration of the system is not large. For this reason, the wave function Φ_A given by [9.75] is expected to be a poor approximation for large internuclear separations R.

A better approximation to the electronic ground state wave function of H_2 can be obtained by using in the Rayleigh–Ritz variational principle a trial function Φ_T which is a mixture of Φ_A (see [9.67a]) and Φ_B (see [9.67b]), both of which have the correct symmetry $^1\Sigma_g^+$. That is,

$$\Phi_T = \Phi_A + \lambda\Phi_B \tag{9.79}$$

The parameter λ can be determined by the variational method. We first obtain the energy as a function of λ (for a fixed value of R):

$$E(\lambda) = \frac{\int d\mathbf{r}_1\, d\mathbf{r}_2\, \Phi_T^* H \Phi_T}{\int d\mathbf{r}_1\, d\mathbf{r}_2\, \Phi_T^* \Phi_T} \tag{9.80}$$

and then require that $\partial E/\partial\lambda = 0$. The equilibrium distance is found to be $R_0 = 1.42$ a.u. (0.749 Å) and the quantity $D_e = 2E_{1s} - E(R_0)$ is given by 0.147 a.u. (4.00 eV), a considerable improvement over our former result. It is worth noting that the wave function Φ_T can be written in the form of a linear combination of covalent and ionic terms, namely

$$\Phi_T = (1 - \lambda)\Phi_A^{cov} + (1 + \lambda)\Phi_A^{ion} \tag{9.81}$$

The ratio of the ionic to the covalent part of the wave function is given by $q = (1 + \lambda)/(1 - \lambda)$, and is displayed in Fig. 9.12 as a function of R. We see from this figure that the maximum value of q is about 0.2 at $R_0 \simeq 1.5$ a.u. (0.8 Å) and that $q \to 0$ as $R \to \infty$.

The Heitler–London or valence bond method

An alternative approach, due to Heitler and London, is to approximate the wave function for H_2 by using orbitals based on the separated atom wave functions, just as we did for H_2^+. In this approximation, the trial wave function to be used in the Rayleigh–Ritz variational principle is Φ_A^{cov} (the covalent part of Φ_A) which is given by [9.77]. The corresponding triplet function is

$$\Phi_D^{cov} = \frac{1}{2}[\psi_{1s}(r_{A1})\psi_{1s}(r_{B2}) - \psi_{1s}(r_{A2})\psi_{1s}(r_{B1})]\chi_{1,M_S}, \quad M_S = 0, \pm 1 \tag{9.82}$$

and this function has the symmetry $^3\Sigma_u^+$.

[5] See our discussion of H^- in Chapter 6, Section 6.5.

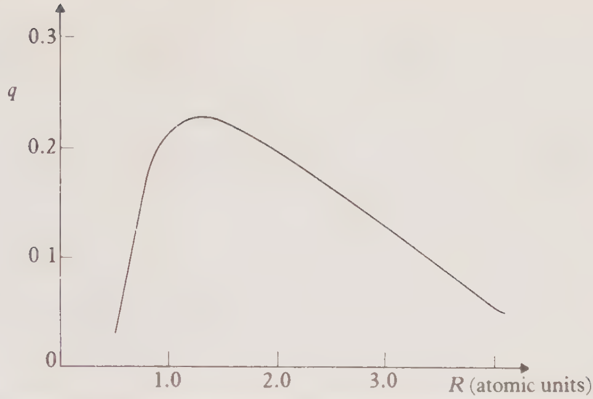

9.12 The ratio λ of the ionic to the covalent part of the wave function for the hydrogen molecule H_2, as a function of nuclear separation R.

Substituting Φ_A^{cov} (which corresponds to the *gerade* state ${}^1\Sigma_g^+$) and Φ_D^{cov} (which corresponds to the *ungerade* state ${}^3\Sigma_u^+$) in the Rayleigh–Ritz variational principle [2.361], we find that the corresponding gerade (g) and ungerade (u) expressions of the energy are given by

$$E_{g,u} = 2E_{1s} + \frac{\mathcal{J}}{1 \pm I^2} \pm \frac{K}{1 \pm I^2} + \frac{1}{R} \qquad [9.83]$$

where the upper signs are taken for g and the lower ones for u. The quantity I is the overlap integral defined by [9.51], namely

$$I = \int \psi_{1s}(r_{A1})\psi_{1s}(r_{B1})\,d\mathbf{r}_1 = \int \psi_{1s}(r_{A2})\psi_{1s}(r_{B2})\,d\mathbf{r}_2 \qquad [9.84]$$

while $\mathcal{J}$ and K are defined as

$$\mathcal{J} = \int d\mathbf{r}_1\,d\mathbf{r}_2\,|\psi_{1s}(r_{A1})|^2|\psi_{1s}(r_{B2})|^2\left(\frac{1}{r_{12}} - \frac{1}{r_{A2}} - \frac{1}{r_{B1}}\right) \qquad [9.85]$$

and

$$K = \int d\mathbf{r}_1\,d\mathbf{r}_2\,\psi_{1s}(r_{A1})\psi_{1s}(r_{B2})\left(\frac{1}{r_{12}} - \frac{1}{r_{A2}} - \frac{1}{r_{B1}}\right)\psi_{1s}(r_{A2})\psi_{1s}(r_{B1}) \qquad [9.86]$$

The expression $\mathcal{J}$ is known as the *Coulomb integral* and represents the interaction between the charge densities $|\psi_{1s}(r_{A1})|^2$ and $|\psi_{1s}(r_{B2})|^2$, while K is called the *exchange integral*. It is found that K is negative, so that the ${}^1\Sigma_g^+$ state is lower than the state ${}^3\Sigma_u^+$. With the wave function Φ_A^{cov} used for the ${}^1\Sigma_g^+$ state, the equilibrium distance is given by $R_0 = 1.6$ a.u. (0.87 Å) and one has $D_e = 2E_{1s} - E(R_0) = 0.115$ a.u. (3.14 eV), which is better than the result 0.098 a.u. (2.68 eV) obtained above from the simple MO wave function Φ_A. In Fig. 9.13 we show the computed energy curves for the attractive ground state $X^1\Sigma_g^+$ and the repulsive state ${}^3\Sigma_u^+$.

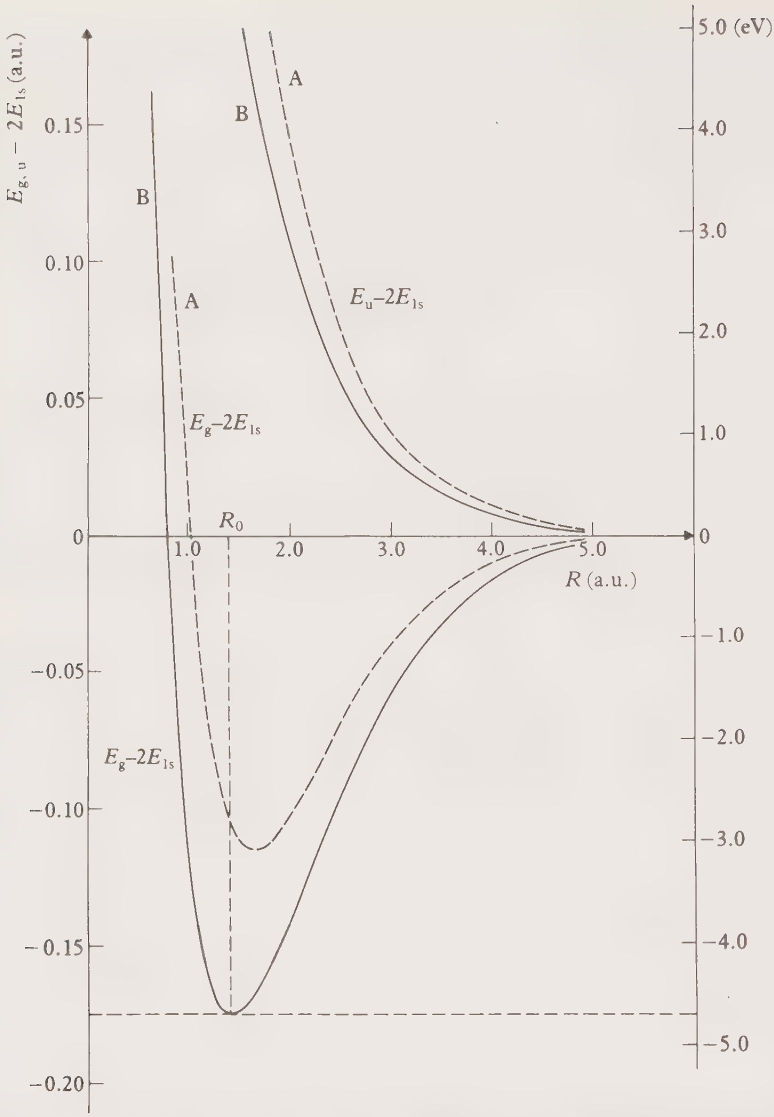

9.13 The lowest electronic potential energy curves of H_2. The curves A are in the Heitler and London approximation, and the curves B show the accurate values for the ground state X $^1\Sigma_g^+$ and the repulsive state $^3\Sigma_u^+$.

If we add to the Heitler–London wave function [9.77] an extra term of the form $\mu\Phi_A^{\text{ion}}$ to represent ionic bonding (where the parameter μ is determined from the variational principle), the resulting energy is identical with that obtained from the improved MO wave function [9.79]. When applied to more complicated systems, it is generally true that the MO method, using 'mixed' wave functions of the type [9.79], provides similar results to the valence-bond method, improved with additional variationally determined terms. When

unimproved, the two approximations are distinct, and the MO approximation is, in general, the better one. This, however, is not true for the H_2 molecule since in this case the nuclear charges ($Z_A = Z_B = 1$) are not large enough to dominate the electron–electron interaction.

To conclude our study of the electronic structure of H_2^+ and H_2, we illustrate in Fig. 9.14 the relationship between the energy levels of these two systems. From the examination of this figure it is clear that

$$I_P(H_2) + D_0(H_2^+) = I_P(H) + D_0(H_2) \qquad [9.87]$$

where I_P are ionisation potentials and D_0 dissociation energies.

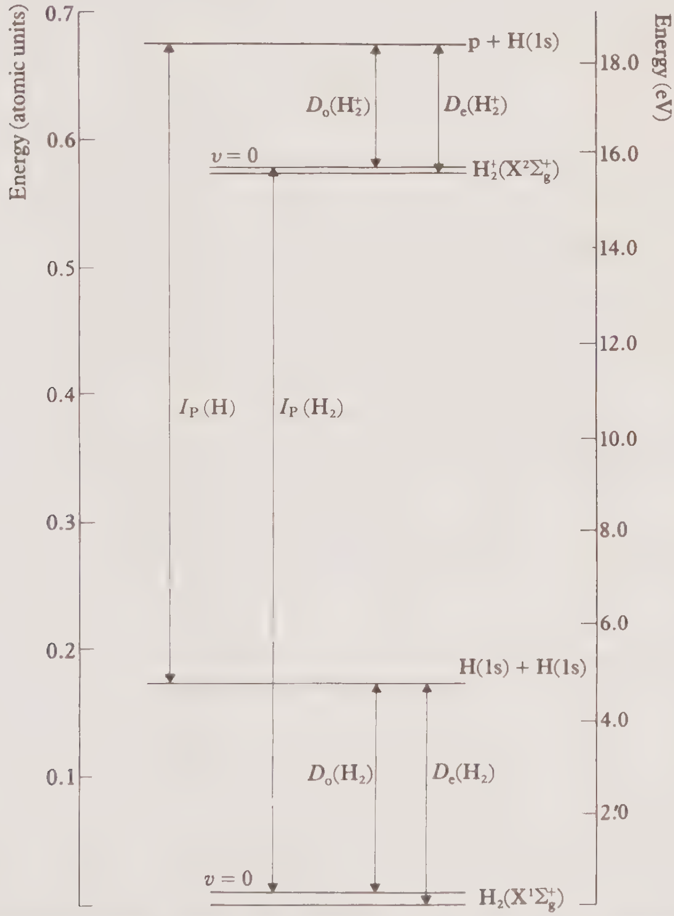

9.14 Relationships between the ground state energies of H_2, H_2^+ and H. The chemical dissociation energies and spectroscopic dissociation energies denoted by D_0 and D_e, respectively, differ by the zero-point vibrational energy $\frac{1}{2}\hbar\omega_0$. The ionisation potentials of the hydrogen atom and hydrogen molecule are denoted by $I_P(H)$ and $I_P(H_2)$.

Homonuclear diatomic molecules

We shall now discuss the electronic structure of more complicated molecules, and in particular their bonding properties. In general, to obtain a bound state of a molecule the negative charge density between the nuclei must be in excess of what would be expected if the charge distribution were due to two non-interacting atoms. The charge density depends on the overlap of the atomic wave functions centred on each nucleus, and only the wave functions of the electrons in the outer shells of the atoms will contribute to the overlap appreciably. The contributing electrons are known as *valence electrons*.

We begin by considering homonuclear diatomic molecules. Using the Hund–Mulliken molecular orbital approach, the full electronic wave function can be built from one-electron MOs. These in turn can be constructed in the LCAO approximation from atomic orbitals. For example, using one atomic orbital centred on each atom, the MOs are given by

$$\Phi_{g,u}(i) = N_{g,u}[u_a(\mathbf{r}_{Ai}) \pm u_b(\mathbf{r}_{Bi})] \qquad [9.88]$$

where $N_{g,u}$ is a normalisation factor and u_a, u_b are atomic orbitals.

In order to analyse the nature of the MOs of a diatomic molecule, and in particular their behaviour when the internuclear distance varies, it is useful to draw a *correlation diagram*, which exhibits the qualitative features of the relative energies of the orbitals as a function of R. In establishing correlation diagrams it is convenient to subtract out the Coulomb repulsion between the nuclei. These diagrams therefore give both the *separated atom* limit ($R \to \infty$) and the *united atom* limit ($R \to 0$), with the intermediate region corresponding to $R \simeq R_0$, the equilibrium internuclear separation.

A simple example of a correlation diagram showing the lowest orbitals of a homonuclear diatomic molecule is displayed in Fig. 9.15. We see that this diagram represents a unique correspondence in going from the atomic orbitals of the united atom to the MOs of the molecule, and finally to the atomic orbitals of the separated atoms. The correspondence is based on the following features:

1. Molecular orbitals having a given value of λ (the component of the orbital angular momentum along the internuclear axis) must connect with atomic orbitals having the same value of λ (i.e. the same value of $|m|$).
2. The parity of the wave function (g or u) must be preserved as R varies from 0 to ∞.
3. The von Neumann–Wigner non-crossing rule must be obeyed, so that energy curves corresponding to orbitals having the same symmetry do not cross [6] as we let R vary from 0 to ∞.

A simple illustration of the two first conditions given above is provided by the H_2^+ problem we have already studied. We recall that in this case the exact

[6] As we pointed out after the equation [9.64], there is an exception to this rule for one-electron systems (such as H_2^+) where a complete separation of variables can be made, so that quantum numbers other than λ are well defined for intermediate values of R.

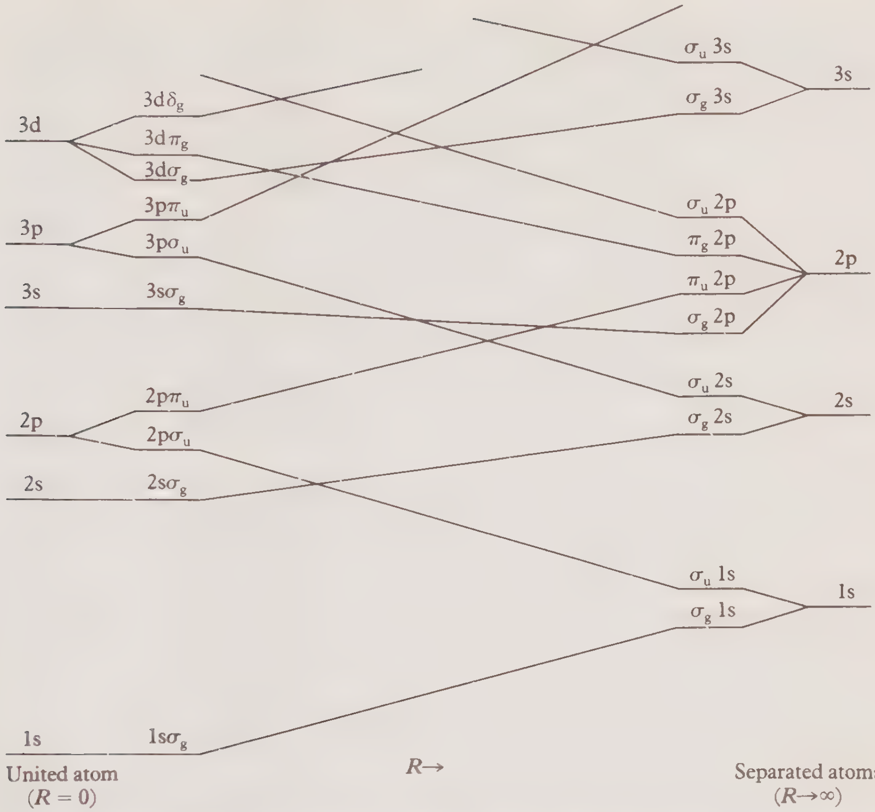

9.15 A diagram showing the correlation between united atom and separated atom states for homonuclear diatomic molecules. The diagram is not to scale and the actual energies of the united and separated atoms vary from molecule to molecule.

ground state orbital Φ_g must approach for large R the orbital of atomic hydrogen in the 1s state. For small R, Φ_g must go over to the lowest state of He^+, also a 1s state. On the other hand, the exact lowest repulsive orbital Φ_u also correlates with H(1s) at large R, while as $R \to 0$ it must approach a wave function of He^+ with odd parity. The component of the angular momentum along the internuclear line (the Z axis) is $\lambda = 0$, and the lowest lying state of He^+ with odd parity and such that $\lambda = 0$ (that is, $m = 0$) is the $2p_0$ state. Thus Φ_u must go over to the $2p_0$ wave function in the united atom limit ($R \to 0$).

It should be noted that molecular orbitals can either be labelled by the separated or the united atom limits. For example, the lowest odd orbital Φ_u can be designated in the separated atom limit as $\sigma_u^\star 1s$ (as was done above) or in the united atom limit as $2p\sigma_u^\star$. We recall that the repulsive (or antibonding) orbitals are distinguished from the attractive (or bonding) orbitals by the addition of an asterisk.

From spatial MOs, $\Phi(i)$ for each electron, spin-orbitals $\Phi(i)\alpha(i)$ or $\Phi(i)\beta(i)$ can be formed, and a completely antisymmetric many-electron wave function is

given by the Slater determinant of these spin-orbitals. For example, the $^1\Sigma_g^+$ wave function Φ_A for H_2, given in [9.67a], can be written in determinantal form as

$$\Phi_A = \frac{1}{\sqrt{2}}\begin{vmatrix} \Phi_g(1)\alpha(1) & \Phi_g(1)\beta(1) \\ \Phi_g(2)\alpha(2) & \Phi_g(2)\beta(2) \end{vmatrix} \qquad [9.89]$$

In this case, both electrons can be in the bonding orbital Φ_g which is $\sigma 1s$ in character. However, in the three-electron system He_2^+, the Pauli principle only allows two electrons to be in the $\sigma 1s$ orbital, and the third one must go into the next level $\sigma^\star 1s$, so that the molecule has the configuration $(\sigma 1s)^2(\sigma^\star 1s)$. The combination of one bonding and one antibonding orbital, with the same separated atom limit, leads to a small net repulsion. In the present case, with two bonding and one antibonding orbitals, the net effect is a weakly bound state.

The four-electron system He_2 must have the configuration $(\sigma 1s)^2(\sigma^\star 1s)^2$ with two electrons bonding and two antibonding. The net effect is a repulsion and there is no stable ground state. It should be noted that excited states such as $(\sigma 1s)^2(\sigma^\star 1s)(\sigma 2s)$ can exist as stable bound states.

Next in complexity is the lithium molecule Li_2. Atomic lithium has the configuration $(1s)^2(2s)$. The two K shell electrons play a small role in the molecular structure, and the bonding is due to the 2s valence electron. The ground state has the configuration $(\sigma 2s)^2$. Continuing up the periodic table, the molecule Be_2 must be $(\sigma 2s)^2(\sigma^\star 2s)^2$ and this state is not bound. The boron atom has a configuration $(1s)^2(2s)^2(2p)$ and bonding results from a $(\sigma 2p)^2$ molecular configuration. The next case, carbon, with an atomic configuration $(1s)^2(2s)^2(2p)^2$ is interesting in that the molecule C_2 contains two separate bonding orbitals $(\sigma_g 2p)$ and $(\pi_u 2p)$.

Lastly we consider the case of oxygen. Atomic oxygen has the configuration $(1s)^2(2s)^2(2p)^4$. Three of the p electrons in each atom can form the bonding orbitals $(\sigma_g 2p)^2(\pi 2p_x)^2(\pi 2p_y)^2$. The remaining pair of electrons must be associated with antibonding orbitals $(\pi^\star 2p)$. It turns out that one electron goes into the $(\pi^\star 2p_x)$ and one into the $(\pi^\star 2p_y)$ orbital.

Pairing and valency

In order to form a bonding orbital, the electron from one atom must usually form a singlet spin state with the electron taken from the second atom, as in H_2. The triplet state, on the other hand, leads to a repulsion. Now consider what happens when a hydrogen atom is brought up to a helium atom. Both the electrons in the helium atom are in the 1s level, and are in a singlet state with $S = 0$, one electron with spin $m_s = +1/2$ and one with $m_s = -1/2$. The electron on the hydrogen atom cannot exchange with the electron of opposite spin in the helium atom, for if this happened, we would have two electrons in the same spin state in the 1s orbital, which would violate the Pauli principle.

The electron in the hydrogen atom can only exchange with the electron of the same spin in the helium atom. In this case, the corresponding spatial part of the wave function is antisymmetric and the orbital is antibonding. To see this in more detail, we can form a trial function, of the Heitler–London type, by taking two electrons to be in the 1s orbital of helium, v_{1s}, and one electron to be in the 1s orbital of atomic hydrogen, u_{1s}. The Slater determinant for the three-electron system is

$$\Phi = N \begin{vmatrix} v_{1s}(1)\alpha(1) & v_{1s}(1)\beta(1) & u_{1s}(1)\alpha(1) \\ v_{1s}(2)\alpha(2) & v_{1s}(2)\beta(2) & u_{1s}(2)\alpha(2) \\ v_{1s}(3)\alpha(3) & v_{1s}(3)\beta(3) & u_{1s}(3)\alpha(3) \end{vmatrix} \tag{9.90}$$

where N is a normalisation factor. Substituting [9.90] into the variational expression [2.361] of the energy, we find that

$$E(R) = \mathcal{J} - K \tag{9.91}$$

where $\mathcal{J}$ is the direct integral

$$\mathcal{J} = N^2 \int d\mathbf{r}_1\, d\mathbf{r}_2\, d\mathbf{r}_3\; v_{1s}(1)v_{1s}(2)u_{1s}(3)Hv_{1s}(1)v_{1s}(2)u_{1s}(3) \tag{9.92}$$

and K is the exchange integral

$$K = N^2 \int d\mathbf{r}_1\, d\mathbf{r}_2\, d\mathbf{r}_3\; v_{1s}(1)v_{1s}(2)u_{1s}(3)Hv_{1s}(3)v_{1s}(2)u_{1s}(1) \tag{9.93}$$

The only exchange is between electrons 1 and 3, which have the same spin, and the effect is to introduce a repulsion, so that a stable molecule of HHe does not exist. The two electrons on the helium atom are said to be *paired*. Only unpaired electrons contribute to chemical bonding, and the number of unpaired outer shell electrons is equal to the valency of the atom. As all the electrons in a closed subshell atom are paired, such atoms are chemically inert. A chemical bond is formed from two unpaired electrons, one from each atom. The two bonding electrons are themselves in a singlet state, and therefore cannot form a bond with a third electron. Each bond uses up a different pair of electrons, and since each pair is in a singlet state, stable molecules generally are in states with overall spin $S = 0$, although exceptions to this rule occur, as in the case of O_2, where the two electrons in antibonding orbitals are in a relative triplet state and the total spin of O_2 is $S = 1$.

Heteronuclear diatomic molecules

The molecular orbital method can equally well be applied to heteronuclear molecules, formed from two dissimilar atoms. We now form the molecular orbital by taking a linear combination of atomic orbitals, one from each atom

$$\Phi(i) = \lambda u_a(\mathbf{r}_{Ai}) + \mu v_b(\mathbf{r}_{Bi}) \tag{9.94}$$

Unlike the homonuclear case there is no reflection symmetry about the mid-point of the internuclear line, and the orbitals cannot be classified as g or u. Another difference is that the separated atom classification of the configurations is less convenient, and the orbitals can either be designated by the united atom configuration, for example $1s\sigma$, $1s\sigma^\star$, $2p\pi$, etc, or just labelled $1\sigma, 2\sigma, 3\sigma, \ldots$ $1\pi, 2\pi, 3\pi, \ldots$ in order of increasing energy within the $\sigma, \pi, \ldots$ levels. In general, the energy of the atomic levels must be close to each other, otherwise the overlap between the atomic wave functions is small and no bonding orbital can be formed.

A correlation diagram for heteronuclear molecules such that the nuclear charges are not too different is shown in Fig. 9.16, while a diagram showing the energy splittings near the equilibrium distance is shown in Fig. 9.17. It should be emphasised that the very simple approximation to a molecular orbital in which only one orbital is taken from each atom (see [9.94]) cannot be expected to be very precise, and in general accurate approximations will require the combination of many atomic orbitals or other basis functions.

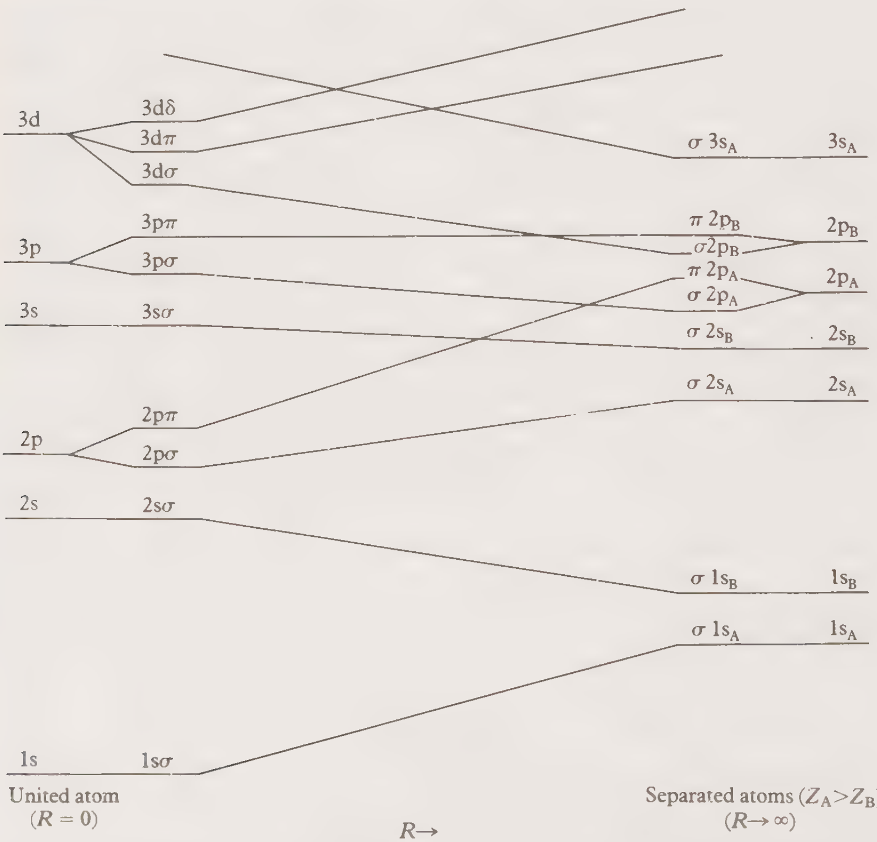

9.16 A correlation diagram for heteronuclear diatomic molecules. As in Fig. 9.15, the diagram is not to scale and the actual energies vary from molecule to molecule.

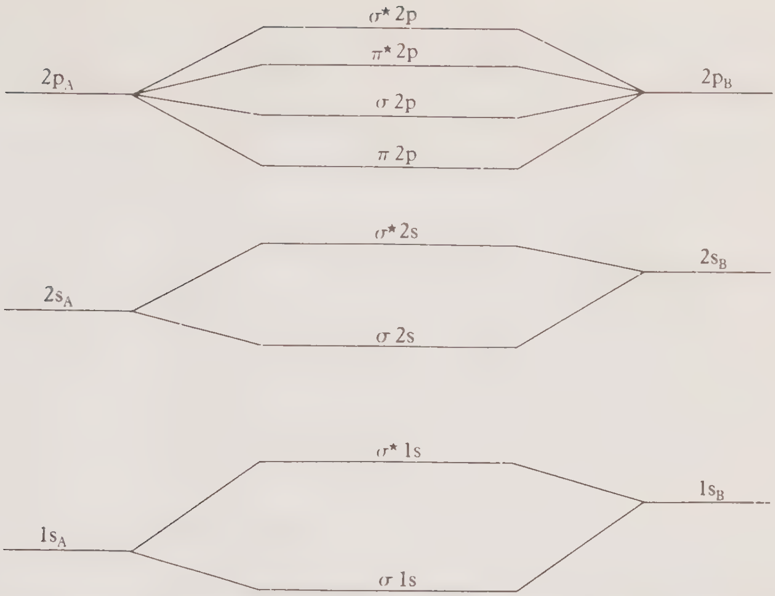

9.17 Energy levels of a diatomic molecule composed of two atoms A and B, where A is more electronegative than B. The energies of the molecular orbitals at equilibrium separation R_0 are shown in the middle with the energies of the atomic levels on either side. The diagram is not to scale.

In order to illustrate some of these points, we shall now consider the examples of the LiH, HCl and NaCl molecules.

Lithium hydride LiH

In this system, which is one for which detailed calculations have been made, we have four electrons. An isolated lithium atom has the ground state configuration $(1s)^2 2s$, and ground state atomic hydrogen is of course in the 1s state. The lowest lying molecular orbital is designated 1σ, and in accordance with the inert nature of the inner shells of atoms, it is practically identical with the 1s atomic orbital of the K shell of lithium.

It would be natural to suppose that the next highest molecular orbital would be a 2σ composed of the 2s atomic orbital of lithium and the 1s orbital of hydrogen. In fact this is not quite correct, as it turns out that a lower energy is obtained from the variational method if a linear combination of the 2s and $2p_z$ atomic orbitals of lithium is used in place of just the 2s orbital. This phenomenon, which occurs when ns and np atomic orbitals are very close in energy, arises because the linear combination of a symmetrical s function $f_0(r)$ with a p function, such as $f_1(r) \cos \theta$, provides an asymmetric charge distribution (see Fig. 9.18) which leads to a large electron density in the region between the atoms. This combination of orbitals corresponding to different values of the angular momentum is called a *hybrid orbital* (a sp hybrid in the present case) and

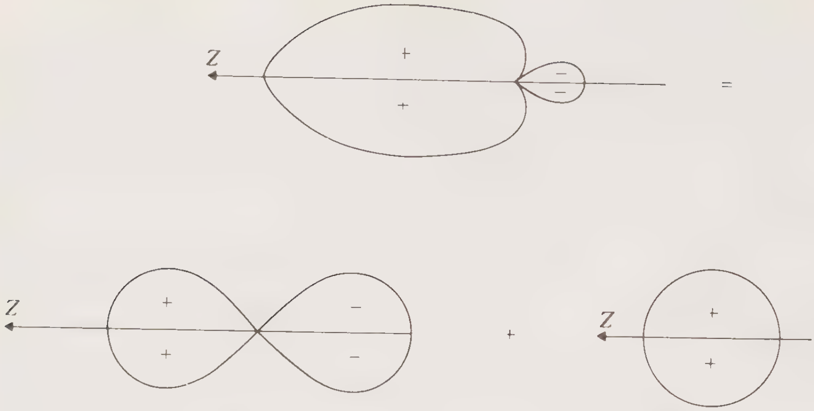

9.18 Charge distribution of a hybridised (s + p_z) orbital.

this phenomenon is known as *hybridisation*. In the separated atom limit the 2σ orbital approaches the 1s orbital of atomic hydrogen.

The ground state of the molecule, which has two electrons in each of the 1σ and 2σ orbitals, becomes $Li^+ + H^-$ in the separated atom limit, with two electrons in the 1s orbital of Li^+ and two in the 1s orbital of H^-. At the equilibrium distance, $R_0 = 1.6$ Å, excess *negative* charge is still associated with the proton. As a consequence, the molecule has a permanent electric dipole moment. It is interesting to remark that other hydrides such as BH, NH and HF also possess permanent electric dipole moments, but of opposite sign.

Hydrogen chloride HCl

In the chlorine atom the K and L shells are completely full and these play no part in chemical activity. The valence shell with $n = 3$ has the configuration $(3s)^2(3p)^5$. The 3s electrons do not mix significantly with the 1s orbital of hydrogen, as the energies are not sufficiently commensurate. This leaves the $3p_x$, $3p_y$ and $3p_z$ orbitals to be considered. Of these only $3p_z$ can contribute to a σ orbital and the bonding orbital is thus a mixture of the $3p_z$ orbital of chlorine with the 1s orbital of hydrogen. This time the coefficient of the $3p_z$ atomic orbital of chlorine is larger than that of the 1s orbital of atomic hydrogen, so that the wave function represents $H^+ + Cl^-$ and the dipole moment has the polarity associated with the redistribution of charge. The bonding is *ionic* in character.

Sodium chloride NaCl

Particularly good examples of ionic bonding are given by the compounds of an alkali atom and a halogen. The alkalis (Li, Na, K, Rb, Cs) consist of a single

valence electron moving outside closed shells. This single electron is easily detached leaving a stable closed shell singly charged positive ion. On the other hand, the halogens (F, Cl, Br, I) have a single vacancy, or hole, in an otherwise closed shell. These atoms are strongly electronegative, and readily combine with an electron to form a stable closed shell singly charged negative ion. In the case of sodium, with the configuration $(1s)^2(2s)^2(2p)^6 3s$, and chlorine, with the configuration $(1s)^2(2s)^2(2p)^6(3s)^2(3p)^5$, it is necessary to supply 1.49 eV to convert (Na + Cl) to the ionic state ($Na^+ + Cl^-$), at infinite separation, but because of the Coulomb attraction between the ions, at separations less than about 18 a.u. the ionic system ($Na^+ + Cl^-$) has a lower energy than the atomic system (Na + Cl).

At small separations where the electron densities overlap, the interaction between the closed shell Na^+ and Cl^- systems is similar to that between the inert gases, He + He for example, and is strongly repulsive. It can be empirically represented by the potential $A \exp(-cR)$. The variation with the internuclear separation R, of the energy of the ($Na^+ + Cl^-$) system relative to the sum of the energies of the isolated neutral atoms is given by

$$E_s(R) = E_s(\infty) - \frac{1}{R} + Ae^{-cR} \qquad [9.95]$$

where atomic units have been used, and $E_s(\infty) = 0.0548$ a.u. (1.49 eV). The function $E_s(R)$ is displayed in Fig. 9.19. It has a minimum at an equilibrium distance R_0 determined by the constants A and c in the repulsive potential.

A simple ionic model of sodium chloride (NaCl) is obtained by viewing the molecule as a combination of Na^+ and Cl^- ions bound by the Coulomb attraction and with an energy $E_s(R_0)$, the energy at the minimum of [9.95]. To establish the accuracy of this model, we need to find A and c, from which R_0, $E_s(R_0)$ and the dissociation energy D_0 can be computed. The chemically measured dissociation energy D_0 is 4.22 eV and this can be compared with the computed value of D_0. The rotational and vibrational spectrum of the molecule can be used to find A and c. First, from the rotational spectrum, the moment of inertia of the molecule can be obtained (see [9.21]) and this gives the equilibrium distance R_0 which is found to have the value 4.38 a.u. Then, from the vibrational spectrum, the fundamental wave number $\tilde{\nu}_0 = \omega_0/(2\pi c)$ can be determined (see [9.24]), which in turn yields the force constant k. The value of $\tilde{\nu}_0$ (see Table 9.3) is 364.6 cm^{-1}. Having obtained R_0 and $\tilde{\nu}_0$, the constants A and c can be calculated by using the equation [9.19]. The quantity $D_e = E_s(\infty) - E_s(R_0)$ and the dissociation energy $D_0 = D_e - \hbar\omega_0/2$ can then be determined. Using the calculated values, the dissociation energy $\mathbf{D}_0$ is found (Problem 9.7) to be 3.85 eV, which is about 10 per cent less than the measured value (by chemical means) of 4.22 eV.

The ionic model can be further confirmed by computing the electric dipole moment and comparing this with the experimental value. The model can be refined in various ways, the most important of which is to take into account the long range attractive interaction between the Na^+ and Cl^- ions due to their

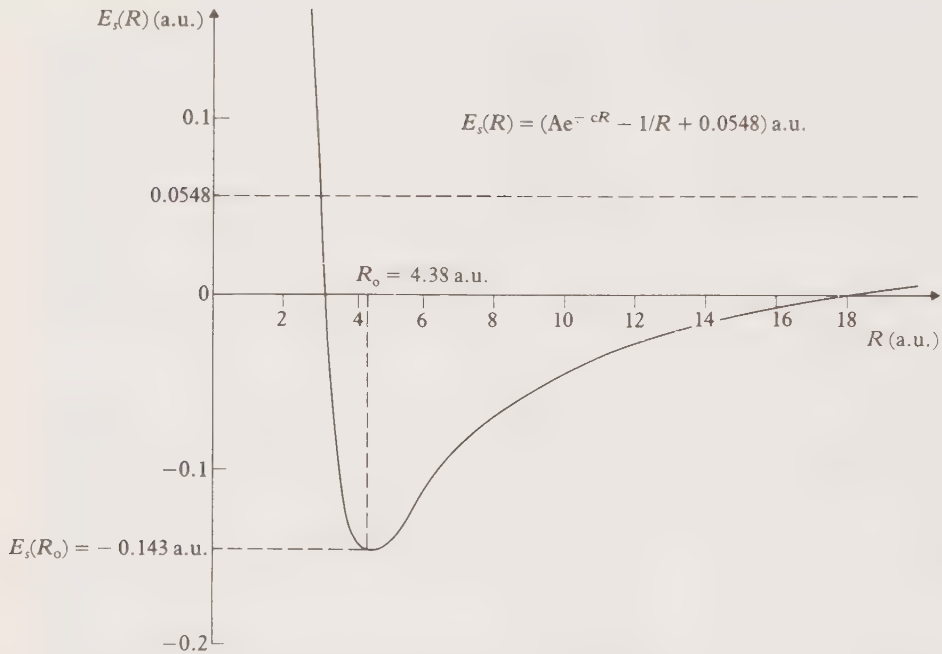

9.19 Potential energy curve for NaCl.

polarisability (see Chapter 12). This very simple model of the ionic bond can be applied to the other alkali halides and the properties of a number of these molecules are shown in Table 9.3.

9.5 THE STRUCTURE OF POLYATOMIC MOLECULES

Just as for diatomic molecules, the Born–Oppenheimer separation can be made for polyatomic molecules, and the motion divided into rotational, vibrational

Table 9.3 Some properties of selected alkali halide molecules

Molecules	R_0(Å)	$\bar{\nu}_0$(cm^{-1})	$10^{29} \cdot \lvert D \rvert$(C m)†	D_0(eV)
Li F	1.564	910.3	2.11	5.99
Li Cl	2.021	641.0	2.38	4.85
Na Cl	2.361	364.6	3.00	4.22
Na Br	2.502	298.5	3.04	3.74
K Cl	2.667	279.8	3.42	4.37
K Br	2.821	219.2	3.54	3.92
Rb Cl	2.787	223.3	3.51	4.31
Cs Cl	2.906	214.2	3.47	4.59

† In many texts electric dipole moments are given in units of debyes, where 1 debye ≡ $10^{-29} \times 0.336$ coulomb-metres.

and electronic modes. The rotational motion may be treated approximately by supposing that the nuclei are fixed at their equilibrium position, so that the molecule forms a rigid body. If the molecules possesses an n-fold symmetry axis, with $n \geq 3$, then two of the three principal moments of inertia [7] of the rigid body are equal, and the molecule is called a *symmetrical top*. For example, the ammonia molecule NH_3, which has a threefold symmetry axis, is a symmetrical top. The rotational energy levels of symmetrical tops are not difficult to obtain [8] and we shall briefly discuss the corresponding spectra in the next chapter. If all three principal moments of inertia of a molecule are equal (as in the case of methane, CH_4) the molecule is called a *spherical top*. It is then a simple matter to show that the rotational energy levels are given by an expression which has the same form as the result [9.21] we obtained for the rotational energy levels of a (rigid) diatomic molecule. On the other hand, for *asymmetric top* molecules (such as water, H_2O) having three different principal moments of inertia, no simple treatment of the rotational motion is possible and the energy levels and wave functions must be computed numerically.

The vibrational motion of a polyatomic molecule can be discussed by supposing that the nuclei execute small oscillations about their equilibrium positions. The *normal modes* of vibration can then be determined by the usual methods of classical mechanics, described for example by Goldstein (1962). Each normal mode is associated with a characteristic frequency ν_i and the corresponding quantised normal-mode energy is

$$\begin{aligned} E_{v_i} &= h\nu_i\left(v_i + \frac{1}{2}\right) \\ &= \hbar\omega_i\left(v_i + \frac{1}{2}\right) \end{aligned} \qquad [9.96]$$

where $v_i = 0, 1, 2, \ldots$ and $\omega_i = 2\pi\nu_i$. The total vibrational energy is the sum of the individual vibrational energies associated with each normal mode, namely

$$E = \sum_i \hbar\omega_i\left(v_i + \frac{1}{2}\right) \qquad [9.97]$$

In general, the vibrational spectrum of a molecule with many degrees of freedom is extremely complex and the treatment of this problem is beyond the scope of this book [9]. In the next chapter, however, we shall consider in some detail a particularly interesting vibrational motion, which is responsible for the inversion spectrum of the ammonia molecule NH_3.

[7] The principal moments of inertia are defined for example in Goldstein (1962).
[8] See for example Pauling and Wilson (1935).
[9] A comprehensive account of the rotational and vibrational spectra of polyatomic molecules may be found in Herzberg (1945).

Electronic structure

The general principles of the molecular orbital approach can be applied to the electronic structure of polyatomic molecules. The molecular orbitals, as before, can be built from atomic orbitals corresponding to each centre (LCAO approximation). Except for very simple molecules containing a few centres and a few electrons, molecular orbital theory must be built up on a semi-empirical basis, but in the simple cases elaborate calculations are possible, using modern computers, in which energy levels and wave functions are obtained *ab initio* [10].

The water molecule H_2O

As a simple example, let us consider the water molecule H_2O. From spectroscopic measurements, it is known that the oxygen nucleus, O, and the two protons p_1 and p_2 form an isosceles triangle, with the p_1Op_2 angle equal to 105° (see Fig. 9.20). The two protons are about twice as far apart (1.6 Å) as they are in the hydrogen molecule H_2 (0.7 Å), so that the important bonds are between the oxygen atom and each hydrogen atom. From our discussion of O_2, we expect that the bonding orbitals will be constructed from two of the 2p orbitals of atomic oxygen. If the plane of the molecule is the (XY) plane, we can, from linear combinations of the $2p_x$ and $2p_y$ orbitals of oxygen, construct orbitals v_1 and v_2 which are directed along the lines Op_1 and Op_2, respectively. If the hydrogenic 1s orbitals centred on the protons p_1 and p_2 are denoted respectively by u_1 and u_2 then suitable LCAO molecular orbitals will be of the form

$$\begin{aligned} \Phi_A &= v_1 + \lambda u_1 \\ \Phi_B &= v_2 + \lambda u_2 \end{aligned} \qquad [9.98]$$

The full wave function for the two valence electrons coming from the oxygen atom and the two electrons from the hydrogen atoms can then be written as a

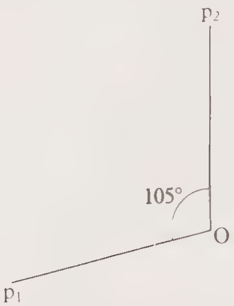

9.20 The water molecule. The bond angle with no hybridisation would be 90°.

[10] A detailed treatment of the electronic structure of polyatomic molecules is given by Pilar (1968).

Slater determinant, namely

$$\Phi = N \begin{vmatrix} \Phi_A(1)\alpha(1) & \Phi_A(1)\beta(1) & \Phi_B(1)\alpha(1) & \Phi_B(1)\beta(1) \\ \Phi_A(2)\alpha(2) & \Phi_A(2)\beta(2) & \Phi_B(2)\alpha(2) & \Phi_B(2)\beta(2) \\ \Phi_A(3)\alpha(3) & \Phi_A(3)\beta(3) & \Phi_B(3)\alpha(3) & \Phi_B(3)\beta(3) \\ \Phi_A(4)\alpha(4) & \Phi_A(4)\beta(4) & \Phi_B(4)\alpha(4) & \Phi_B(4)\beta(4) \end{vmatrix} \qquad [9.99]$$

where N is a normalisation constant.

Calculations based on wave functions of this kind show that the equilibrium angle p_1Op_2 is about 90°. The hybridisation of the 2s and 2p oxygen orbitals accounts for the slightly greater angle found experimentally. The orbitals Φ_A and Φ_B give rise to charge distributions which are localised along the lines Op_1 and Op_2. This localisation is the physical basis of the directional character of a chemical bond. If the hydrogen atom with nucleus p_1 were replaced by a different atom, then the wave function in the region between the oxygen atom and the proton p_2 would be hardly altered, so that we can speak of a characteristic O—H bond, associated with a molecular orbital of the type Φ_A or Φ_B.

The methane, ethylene and acetylene molecules

As a further example, we shall now look at the methane molecule, CH_4. The carbon atom in the ground state has the configuration $(1s)^2(2s)^2(2p)^2$, but there is an excited state with the configuration $(1s)^2(2s)(2p)^3$ which is very close in energy and it is from this state that carbon bonds most readily. The orbitals are hybridised by forming linear combinations of the 2s, $2p_x$, $2p_y$ and $2p_z$ orbitals, which consist in this case of one 2s orbital and three 2p orbitals, and are therefore called sp^3 hybrids. Four combinations can be constructed:

$$\begin{aligned} \Phi_1 &= v_{2s} + v_{2p_x} + v_{2p_y} + v_{2p_z} \\ \Phi_2 &= v_{2s} + v_{2p_x} - v_{2p_y} - v_{2p_z} \\ \Phi_3 &= v_{2s} - v_{2p_x} + v_{2p_y} - v_{2p_z} \\ \Phi_4 &= v_{2s} - v_{2p_x} - v_{2p_y} + v_{2p_z} \end{aligned} \qquad [9.100]$$

Since the functions v_{2p_x}, v_{2p_y} and v_{2p_z} are proportional to x, y and z respectively, and v_{2s} is spherically symmetric and positive Φ_1 has a maximum in the direction defined by a vector with Cartesian coordinates (1, 1, 1). Similarly, Φ_2, Φ_3 and Φ_4 have maxima in the directions (1, −1, −1), (−1, 1, −1) and (−1, −1, 1) respectively. The angles between each pair of directions are 109.6° and CH_4 forms a tetrahedral structure, as shown in Fig. 9.1.

Carbon is particularly rich in different structures, which arise because other types of directional bonds are possible. For example, sp^2 hybrid orbitals which are linear combinations of only v_{2s}, v_{2p_x} and v_{2p_y} orbitals can be formed, namely

$$\begin{aligned} \Phi_1 &= v_{2s} + \sqrt{2}\, v_{2p_x} \\ \Phi_2 &= v_{2s} + \sqrt{3/2}\, v_{2p_y} - \sqrt{1/2}\, v_{2p_x} \\ \Phi_3 &= v_{2s} - \sqrt{3/2}\, v_{2p_y} - \sqrt{1/2}\, v_{2p_x} \end{aligned} \qquad [9.101]$$

Here the bonds lie in a plane, with an angle of 120° between each bond. This structure is found in ethylene C_2H_4 (see Fig. 9.21(a)). The four protons and the two carbon atoms lie in a plane, the four C—H bonds and one of the C—C bonds being of the type considered in [9.101]. For such bonds the component of the orbital angular momentum in the bond direction is zero, and by analogy with the terminology used in the theory of diatomic molecules these bonds are called σ bonds. The remaining pair of valence electrons are associated with the $2p_z$ orbitals in the carbon atom, the Z axis being perpendicular to the plane of

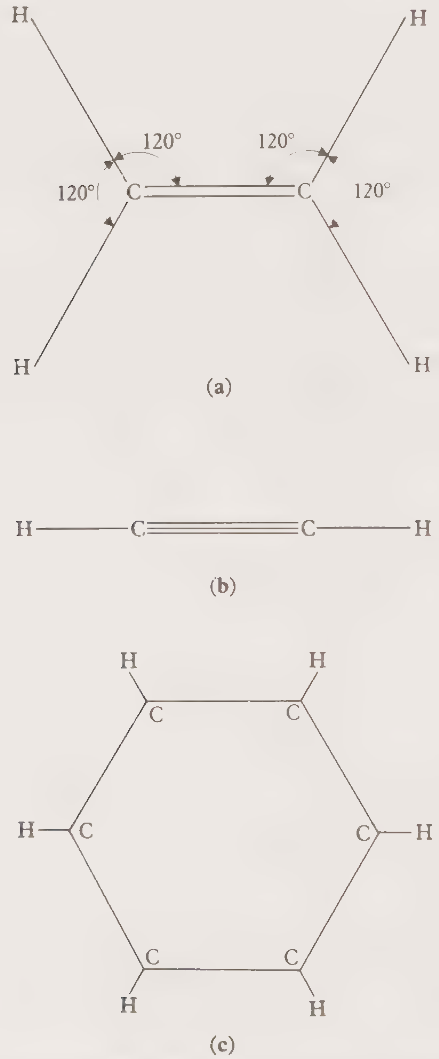

9.21 Three carbon–hydrogen bond structures: (a) Ethylene C_2H_4; (b) Acetylene C_2H_2; (c) Benzene C_6H_6.

the molecule. This pair is said to form a π bond, the component of the angular momentum in the bond direction being $\pm\hbar$.

Yet another possibility occurs in acetylene C_2H_2, which is a linear molecule arranged as shown in Fig. 9.21(b). In this case one can form two hybrid orbitals consisting of the 2s orbital and only one 2p (for example $2p_x$) carbon orbital. These sp hybrid orbitals are given by

$$\begin{aligned}\Phi_1 &= v_{2s} + v_{2p_x}\\ \Phi_2 &= v_{2s} - v_{2p_x}\end{aligned} \qquad [9.102]$$

This gives rise to σ bonds linking the hydrogen atoms with the carbon atom, and to a single σ bond linking the two carbon atoms. The angle between these bonds is 180°. The remaining four electrons form a pair of π bonds between the carbon atoms.

The benzene molecule and non-localised orbitals

In the molecules we have been discussing, the bonds are localised and provide a directed interaction between a pair of atoms within a molecule. A single bond contains a pair of electrons in a relative singlet spin configuration, and the most important bonds are designated σ, in which the magnitude of the component of the orbital angular momentum of each electron in the bond direction is zero, or π in which this component has the magnitude $|\hbar|$. The σ bond are usually stronger and more localised than π bonds, and we have also seen that hybridised bonds are stronger than simple bonds. Although this description is successful for many molecules, it must be extended and a new concept of *non-localised* bonds introduced for others. A typical example is benzene (C_6H_6). The six carbon atoms lie in a plane, which we shall take to be the (XY) plane, and form a regular hexagon, while the six hydrogen atoms also lie in this plane, as shown in Fig. 9.21(c). We can assume that three out of the four $n = 2$ electrons of carbon form sp^2 hybrid orbitals, as in the case of ethylene, the combinations of atomic orbitals being given by [9.101]. A linear combination of one of these functions with the 1s orbital of atomic hydrogen forms a σ C—H bond, while the other two combine with the corresponding orbitals on the neighbouring carbon atoms to form C—C bonds which are also σ in character. The remaining atomic carbon orbitals are $2p_z$, and there is one of these per atom. Because of the symmetry of the structure, there is no unique way of associating these $2p_z$ orbitals in pairs, forming localised π bonds. We could form all possible combinations of localised bonds, and use the variational method to determine the coefficients of each term, but a useful alternative is to construct a non-localised orbital by combining all the six atomic orbitals directly. The ground state is represented by the completely symmetrical combination

$$\begin{aligned}\Phi = N[&u_{2p_z}(1) + u_{2p_z}(2) + u_{2p_z}(3) + u_{2p_z}(4)\\ &+ u_{2p_z}(5) + u_{2p_z}(6)]\end{aligned} \qquad [9.103]$$

where N is a normalisation factor. This orbital forms a π bond, which is associated with the whole benzene ring and which is not localised to a pair of atoms. The six equivalent electrons are free to move round the ring, with the result that benzene has a very large diamagnetic susceptibility resulting from the magnetic field created by this current loop.

A qualitative understanding of chemical bonding in the hydrocarbons can be achieved in the way we have sketched for methane, ethylene, acetylene and benzene. In the case of the simpler structures, quantitative results confirming these ideas have been obtained by performing elaborate *ab initio* numerical calculations, based on the variational method.

PROBLEMS

9.1 The moment of inertia of $H^{79}Br$ is 3.30×10^{-47} kg m^2. Calculate the energies of the first five excited rotational levels of the molecule in eV and the corresponding wave numbers ($\tilde{\nu} = E/hc$) in units of cm^{-1}. Find the internuclear distance in atomic units and in angstroms.

9.2 The wave number $\tilde{\nu}_0$ of the fundamental vibrational motion of the molecule $H^{79}Br$ is 2650 cm^{-1}. Calculate (a) the energy of the lowest and first excited states in electron-volts; (b) the corresponding periodic times; (c) the force constant in SI units.

9.3 Find the energy of dissociation D_0 of the deuterium molecule D_2, given that the energy of dissociation of H_2 is 4.48 eV and that the energy of the lowest vibrational level of H_2 is 0.26 eV.

9.4 When a diatomic molecule rotates it stretches, so that the internuclear distance is increased to R_1 where R_1 is given approximately by [9.35]. Prove this result as indicated in the text.

9.5 If H is the electronic Hamiltonian of a diatomic molecule and $\mathbf{L}$ is the total orbital angular momentum of the electrons, show directly that $[H, L_z] = 0$ and $[H, L_x] \neq 0$, $[H, L_y] \neq 0$, where the Z axis is along the internuclear line. The Hamiltonian is given by $H = T_e + V$, where T_e and V are defined by [9.6] and [9.8] respectively.

9.6 Obtain the overlap function D and the matrix elements H_{AA}, H_{AB} for the hydrogen molecular ion from [9.49] and [9.54], by using the variable charge orbital of [9.58] in place of the hydrogenic functions $\psi_{1s}(r_A)$, $\psi_{1s}(r_B)$. Evaluate the integrals using the results of Appendix 9. Using a calculator, plot how $E_g(R)$ varies with the effective charge $Z^\star$ at the equilibrium distance $R_0 = 1.06$ Å.

9.7 Using $R_0 = 2.36$ Å and $\tilde{\nu}_0 = 364.6$ cm^{-1} determine the constants A and c in the potential [9.95] representing the energy of $Na^{35}Cl$. Calculate the depth of the well D_e and hence the dissociation energy D_0. Calculate the electric dipole moment of NaCl assuming a simple ionic model.

9.8 Repeat the calculation of the dissociation energy D_0 and the dipole moment for the molecules LiF, KF and KI using the following data:

$$\begin{array}{llll} \text{LiF:} & R_0 = 1.564\ \text{Å} & \quad & \tilde{\nu}_0 = 910.3\ \text{cm}^{-1} \\ \text{KF:} & R_0 = 2.172\ \text{Å} & \quad & \tilde{\nu}_0 = 426.0\ \text{cm}^{-1} \\ \text{KI:} & R_0 = 3.048\ \text{Å} & \quad & \tilde{\nu}_0 = 186.5\ \text{cm}^{-1} \end{array}$$

The ionisation energy of Li is 5.39 eV and that of K is 4.34 eV. The electron affinity of F is 3.45 eV and that of I is 3.08 eV.
(Note $E_s(\infty)$ of [9.95] is the difference between the ionisation energy of the alkali and the electron affinity of the halogen.)

10 Molecular spectra

Transitions between the energy levels of a molecular system can take place with the emission or absorption of radiation. The molecular spectra are more complicated than those of atoms, and in this chapter we shall only analyse some of the simpler features of the rotational, vibrational and electronic spectra. For the most part we shall confine the discussion to diatomic molecules, pointing out in some cases how extensions to polyatomic systems can be made. In the last section, however, we shall examine in some detail the inversion spectrum of the ammonia molecule NH_3, which as we shall see in Chapter 14 is of great interest in the construction of the *maser*.

10.1 ROTATIONAL ENERGY LEVELS OF DIATOMIC MOLECULES

In Section 9.3 we obtained an expression for the energy levels of a diatomic molecule which is in a Σ state, that is for a state in which the electrons have a zero component of orbital angular momentum along the internuclear line. We found (see [9.22]) that

$$E_{s,v,r} = E_s(R_0) + E_v + E_r \qquad [10.1]$$

where $E_s(R_0)$ is the electronic energy, E_v the vibrational energy and E_r the rotational energy.

Let us now consider the situation in which the electrons have non-zero orbital angular momentum, assuming that L–S coupling is small so that the spins of the electrons need not be considered. The total orbital angular momentum of the electrons will be denoted by $\mathbf{L}$ and the orbital angular momentum of the nuclei by $\mathbf{N}$. The total angular momentum $\mathbf{J}$ is then

$$\mathbf{J} = \mathbf{L} + \mathbf{N} \qquad [10.2]$$

Since $\mathbf{N} = \mathbf{R} \times \mathbf{P}$, where $\mathbf{R}$ is the internuclear position vector and $\mathbf{P}$ is the relative (linear) momentum of the two nuclei (see [A2.12]), we must have that

$$\mathbf{N} \cdot \mathbf{R} = 0 \qquad [10.3]$$

This implies that the projection of $\mathbf{J}$ on the internuclear line, $\mathcal{J}_R = (\mathbf{J} \cdot \mathbf{R})/R$ must be equal to the projection of $\mathbf{L}$ along this line, L_R (see Fig. 10.1). It has already been shown in Chapter 9 that the electronic wave function of a diatomic

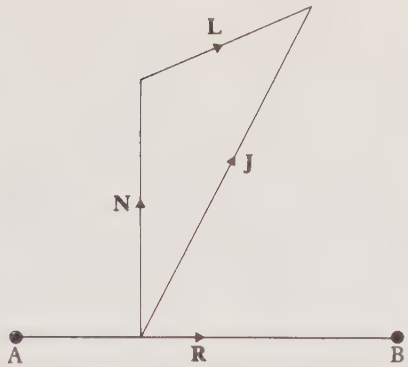

10.1 The anguiar momentum of a diatomic molecule with no coupling between the electronic and the orbital motion. Since the angular momentum **N** of the nuclei A and B is at right angles to the internuclear line AB, the components of the electronic orbital angular momentum **L** and the total angular momentum **J** along AB are equal ($L_R = \mathcal{J}_R$).

molecule is an eigenfunction of L_R (which was previously called L_z because we took the internuclear line as the Z axis) belonging to the eigenvalues $\pm\Lambda\hbar$. Since $\mathbf{J}^2$ and $\mathcal{J}_z$ (with the Z axis fixed in space) are always conserved, the eigenfunctions of the Hamiltonian for the diatomic molecule can be labelled by $\mathcal{J}$, $M_{\mathcal{J}}$, Λ, s, sn, where s denotes the electronic states and sn the sign of L_R (when $\Lambda \neq 0$).

The radial equation for the nuclear wave function (which satisfied [9.17] in the case $L = 0$) in general reads

$$\left[-\frac{\hbar^2}{2\mu}\frac{d^2}{dR^2} + \frac{\langle \mathbf{N}^2\rangle}{2\mu R^2} + E_s(R) - E\right]\mathcal{F}(R) = 0 \qquad [10.4]$$

where $\langle \mathbf{N}^2\rangle$ denotes the expectation value of $\mathbf{N}^2$ with respect to the simultaneous eigenfunctions of $\mathbf{J}^2$, $\mathcal{J}_z$, L_R and sn. Thus

$$\begin{aligned}\langle \mathbf{N}^2\rangle &= \langle(\mathbf{J} - \mathbf{L})^2\rangle \\ &= \hbar^2\mathcal{J}(\mathcal{J} + 1) - 2\langle \mathbf{J}\cdot\mathbf{L}\rangle + \langle \mathbf{L}^2\rangle\end{aligned} \qquad [10.5]$$

We note that since the system is in an eigenstate of L_R, the expectation value of a component of **L** in a direction perpendicular to **R** must vanish, and since $\mathcal{J}_R = L_R$, we have

$$\langle \mathbf{J}\cdot\mathbf{L}\rangle = \langle \mathcal{J}_R L_R\rangle = \Lambda^2\hbar^2 \qquad [10.6]$$

Evaluating the rotational energy at the equilibrium distance $R = R_0$, we have

$$E_r = \frac{1}{2\mu R_0^2}\left[\mathcal{J}(\mathcal{J} + 1)\hbar^2 + \langle \mathbf{L}^2\rangle - 2\Lambda^2\hbar^2\right] \qquad [10.7]$$

The term $(\langle \mathbf{L}^2\rangle - 2\Lambda^2\hbar^2)$ depends only on the electronic state and can therefore be included with the electronic energy $E_s(R_0)$. Thus we write

$$E_{s,v,r} = E_s'(R_0) + E_v + B\mathcal{J}(\mathcal{J} + 1) \qquad [10.8]$$

where

$$E'_s(R_0) = E_s(R_0) + \frac{1}{2\mu R_0^2}(\langle \mathbf{L}^2 \rangle - 2\Lambda^2\hbar^2) \qquad [10.9]$$

and $B = \hbar^2/2\mu R_0^2$. The form of the rotational energy $B\mathcal{J}(\mathcal{J}+1)$ is the same as for the case $\Lambda = 0$, but with the important difference that the possible values of $\mathcal{J}$ are such that $\mathcal{J} \geqslant \Lambda$. This arises because the component of $\mathbf{J}$ along the internuclear line is $\mathcal{J}_R = \pm\Lambda\hbar$ and the magnitude of $\mathbf{J}$ must be equal or greater than its component in any direction, $|\mathbf{J}| \geqslant \mathcal{J}_R$.

The rotational energy can be discussed from a slightly different point of view. In our treatment in the previous paragraph, the approximation in which we fixed R at its equilibrium value was made at the last stage; but instead we could have started by considering the molecule to behave, as far as rotations are concerned, like a completely rigid body. In the principal axis system (Goldstein, 1962) the kinetic energy of a rigid rotating body is

$$T = \frac{1}{2I_a}\mathcal{J}_a^2 + \frac{1}{2I_b}\mathcal{J}_b^2 + \frac{1}{2I_c}\mathcal{J}_c^2 \qquad [10.10]$$

where I_a, I_b and I_c are the moments of inertia about axes a, b and c and $\mathcal{J}_a, \mathcal{J}_b, \mathcal{J}_c$ are the components of the angular momentum about these axes. It should be noted that the axes a, b, c form a system fixed in the rotating body, and the corresponding operators obey slightly different commutation relations from the components of $\mathbf{J}$ in a coordinate system fixed in space.

A diatomic molecule is axially symmetrical about the internuclear line, which can be taken as the axis c. Then $I_a = I_b$ and the system forms a symmetrical top, with energy

$$T = \frac{1}{2I_a}(\mathcal{J}_a^2 + \mathcal{J}_b^2) + \frac{1}{2I_c}\mathcal{J}_c^2 \qquad [10.11]$$

The component $\mathcal{J}_c$ is along the internuclear line, $\mathcal{J}_c = \mathcal{J}_R$, and, as we have seen, $\mathcal{J}_R = \Lambda\hbar$. As usual, the operator $\mathbf{J}^2$ has eigenvalues $\mathcal{J}(\mathcal{J}+1)\hbar^2$, so that the rotational energy is given by

$$E_r = \frac{\hbar^2}{2I_a}\mathcal{J}(\mathcal{J}+1) + \left(\frac{1}{2I_c} - \frac{1}{2I_a}\right)\Lambda^2\hbar^2 \qquad [10.12]$$

The moment of inertia of the molecule about the axis a, which is perpendicular to the internuclear line and goes through the centre of mass is $I_a = \mu R_0^2$, while I_c is the moment of inertia about the internuclear line, and depends on the electronic state. It is seen that the expression [10.12] is equivalent to the result [10.7] which we have previously obtained, since the term in $\Lambda^2\hbar^2$ can be included in the electronic energy.

In the approximation in which the nuclei are considered to be fixed at their equilibrium positions, a *polyatomic molecule* also behaves like a rigid body with the rotational kinetic energy given by [10.10]. We have seen in Section 9.5 that

if there is an n-fold symmetry axis, with $n \geqslant 3$, then two of the three principal moments of inertia are the same, and the molecule is called a *symmetrical top*. In this case the rotational energy levels are again given by an expression like [10.12].

The rotational spectrum

In the electric dipole approximation, which was discussed in Chapter 4, the transition amplitude for emission or absorption of radiation was shown to be proportional to the matrix element of the electric dipole operator $\mathbf{D}$. For a molecule this operator is given by

$$\mathbf{D} = e\left(\sum_i Z_i \mathbf{R}_i - \sum_j \mathbf{r}_j\right) \qquad [10.13]$$

where the first sum is over the positions $\mathbf{R}_i$ and charges $Z_i e$ of all the nuclei and the second sum is over the positions $\mathbf{r}_j$ of the electrons.

On the other hand, we have seen in the previous chapter that in the simplest approximation the couplings between the electronic, vibrational and rotational motions can be neglected. Disregarding spin, the complete molecular wave function Ψ_α corresponding to a given state α is then the product of an electronic wave function Φ_s, a vibrational wave function ψ_v (times R^{-1}) and a rotational wave function $\phi_{\mathcal{J},M_{\mathcal{J}},\Lambda}$. The diagonal elements of $\mathbf{D}$ are thus given by

$$\mathbf{D}_{\alpha\alpha} = \langle \Psi_\alpha | \mathbf{D} | \Psi_\alpha \rangle, \qquad \alpha \equiv (s, v, \mathcal{J}, M_{\mathcal{J}}, \Lambda) \qquad [10.14]$$

and are equal to the *permanent electric dipole moment* in the state α. This quantity always vanishes for non-degenerate levels of atoms, because these are eigenstates of the parity operator. However, for heteronuclear molecules in which an excess of charge is associated with one of the nuclei, $D_{\alpha\alpha}$ has a finite value (see Section 5.3). In symmetrical homonuclear diatomic molecules, such as H_2, O_2, N_2, . . . , the permanent electric dipole moment vanishes. Since the rotational and vibrational motions preserve the symmetry of the molecule, the matrix elements of $\mathbf{D}$ between different rotational or vibrational states must vanish for symmetrical homonuclear molecules, unless the electronic state changes. As a result symmetrical molecules possess no purely rotational or vibrational spectrum, without an electronic transition. In contrast, molecules which possess a permanent electric dipole moment such as HCl exhibit spectra corresponding to rotational and vibrational transitions, without change in the electronic state.

The selection rules for a rotational transition are, if $\Lambda = 0$

$$\begin{aligned} \Delta\mathcal{J} &= \pm 1 \\ \Delta M_{\mathcal{J}} &= 0, \pm 1 \end{aligned} \qquad [10.15]$$

If $\Lambda \neq 0$, the first selection rule must be replaced by $\Delta\mathcal{J} = 0, \pm 1$. This is due to the fact that although the photon absorbed or emitted carries one unit of angular momentum, the nuclear rotation can change, with no change in $\mathcal{J}$, if the

electronic angular momentum makes an equal and opposite change. Symmetry considerations require that the electric dipole moment of a diatomic molecule is directed along the internuclear line, and this leads to the additional selection rule $\Delta\Lambda = 0$. If no change in vibrational state occurs then we must have $\Delta\mathcal{J} = \pm 1$.

The pure rotational spectrum of a diatomic molecule consists of lines in the far infra-red or the microwave region, the frequencies of these lines being given by

$$\begin{aligned} h\nu_{\mathcal{J}+1,\mathcal{J}} &= E_r(\mathcal{J}+1) - E_r(\mathcal{J}) \\ &= 2B(\mathcal{J}+1) \end{aligned} \qquad [10.16]$$

where $\mathcal{J} \geqslant \Lambda$. Figure 10.2 illustrates the rotational spectrum of HCl. The constant B can be obtained with an accuracy of up to 1 part in 10^9 from the observed spectra, and this allows the equilibrium distance R_0 to be determined. The intensity of the line is proportional to the permanent electric dipole moment in the particular electronic state concerned.

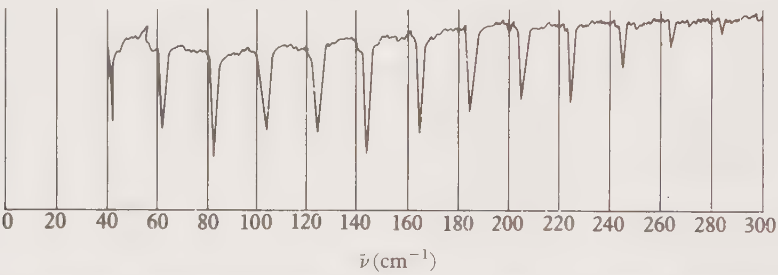

10.2 The rotational absorption spectrum of gaseous HCl. From [10.16] we see that the spacing in frequency between the absorption lines, (corresponding to transitions from $\mathcal{J} \to \mathcal{J}+1$), is constant and equal to $2B/h$. For HCl $\tilde{B} = (B/hc) = 10.59\ \mathrm{cm}^{-1}$ and the spacing in terms of the wave number $\tilde{\nu}$ is $2\tilde{B} = 21.18\ \mathrm{cm}^{-1}$.

10.2 VIBRATIONAL–ROTATIONAL SPECTRA OF DIATOMIC MOLECULES

Vibrational transitions can occur, due to the interaction with the radiation field, if the matrix element

$$\mathbf{D}_{v'v} = \int \psi_{v'}^{*}\mathbf{D}(R)\psi_v\,\mathrm{d}R \qquad [10.17]$$

does not vanish. In this expression $\mathbf{D}(R)$ is the matrix element of the electric dipole moment expressed as a function of the internuclear distance R, and ψ_v, $\psi_{v'}$ are vibrational wave functions, which are simple harmonic oscillator wave functions in the first approximation (see Section 9.3).

If $\mathbf{D}$ is independent of R, the integral [10.17] vanishes because of the orthogonality of ψ_v and $\psi_{v'}$ when $v \neq v'$. On the other hand, if $\mathbf{D}$ depends on R,

we may expand it as

$$\mathbf{D}(R) = \mathbf{D}(R_0) + (R - R_0) \left. \frac{\mathrm{d}\mathbf{D}}{\mathrm{d}R} \right|_{R=R_0} + \cdots \qquad [10.18]$$

and we can neglect the higher order terms in first approximation since the amplitude of the vibrational motion is small compared with R_0. In this approximation the selection rule depends on the integral

$$I(v', v) = \int \psi_{v'}^{*}(R - R_0)\psi_v \, \mathrm{d}R \qquad [10.19]$$

The harmonic oscillator wave functions ψ_v are given (see Section 2.4) by

$$\psi_v(x) = N_v \mathrm{e}^{-\alpha^2 x^2/2} H_v(\alpha x) \qquad [10.20]$$

where N_v is a normalisation constant, $x = R - R_0$ and $\alpha^2 = \mu\omega_0/\hbar$, ω_0 being the angular frequency of the oscillator. Using the result [A3.15] of Appendix 3 we see that the integral [10.19] vanishes unless $v' = v \pm 1$. We note that this selection rule may also be derived immediately by using the recurrence relation for the Hermite polynomials. Using [2.147],

$$2(\alpha x)H_v(\alpha x) = 2vH_{v-1}(\alpha x) + H_{v+1}(\alpha x) \qquad [10.21]$$

it follows at once that the integral [10.19] vanishes unless

$$\Delta v = v' - v = \pm 1 \qquad [10.22]$$

Since the potential well is only approximately described by a simple harmonic oscillator, transitions with $\Delta v = v' - v = \pm 2, \pm 3, \ldots$ can occur, but these transitions are usually weaker, by at least an order of magnitude.

Because the absorption of a photon requires the molecule to take up one unit of angular momentum, vibrational transitions are accompanied by a change in rotational state, which is subject to the same selection rules as for the pure rotational spectrum. For a molecule in a Σ state (with $\Lambda = 0$), the transitions between two rovibronic levels $(v, \mathcal{J})$ and $(v', \mathcal{J}')$, with vibrational quantum numbers v and $v' = v + 1$, fall into two sets according to whether $\Delta\mathcal{J} = +1$ or $\Delta\mathcal{J} = -1$ (see Fig. 10.3). The first set is called the *R branch*. Using the simple linear harmonic oscillator expression [9.24] for the vibrational energy and the rigid rotator formula [9.21] for the rotational energy, we find that the corresponding frequencies ν^{R} are given by

$$\begin{aligned} h\nu^{\mathrm{R}} &= E(v+1, \mathcal{J}+1) - E(v, \mathcal{J}) \\ &= 2B(\mathcal{J}+1) + \hbar\omega_0, \qquad \mathcal{J} = 0, 1, 2, \ldots \end{aligned} \qquad [10.23]$$

The second set is known as the *P branch*. In the same approximation (linear harmonic oscillator, rigid rotator), its frequencies, ν^{P} are such that

$$\begin{aligned} h\nu^{\mathrm{P}} &= E(v+1, \mathcal{J}-1) - E(v, \mathcal{J}) \\ &= -2B\mathcal{J} + \hbar\omega_0, \qquad \mathcal{J} = 1, 2, 3, \ldots \end{aligned} \qquad [10.24]$$

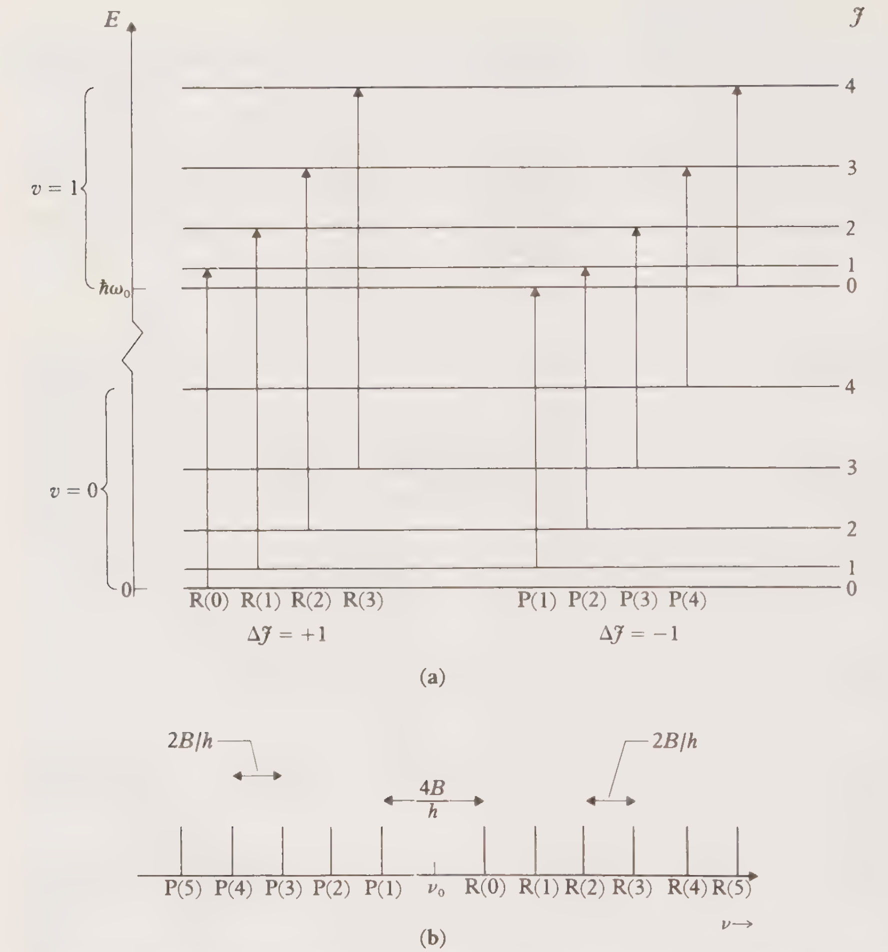

10.3 (a) Energy level diagram of the lowest vibrational–rotational levels in a diatomic molecule showing the absorptive transitions from the band with $v = 0$ to the band with $v = 1$. The band spectrum contains two branches: the R branch with $\Delta \mathcal{J} = +1$ and the P branch with $\Delta \mathcal{J} = -1$. The lines in each branch are labelled by the $\mathcal{J}$ value of the lower level.
(b) A spectrogram showing the lines corresponding to the transitions shown in (a). It is assumed that the rotational constants of the $v = 0$ and $v = 1$ are the same so that the lines are equally spaced in frequency, except for a gap corresponding to the vibrational frequency ν_0.

Both branches make up what is called a *vibrational–rotational band*. These bands are in the infra-red part of the spectrum. We note that according to [10.23] and [10.24] such bands contain lines whose frequencies are equally spaced by $2B/h$, except that there is a gap of $4B/h$ at the vibrational frequency $\nu_0 = \omega_0/2\pi$. This is illustrated in Fig. 10.3(b) and in Fig. 10.4, the latter showing the absorption spectrum of HCl. We see that a measurement of the position of the gap determines ω_0, while a measurement of the spacing of the lines determines $B(= \hbar^2/2\mu R_0^2)$ which is inversely proportional to the moment

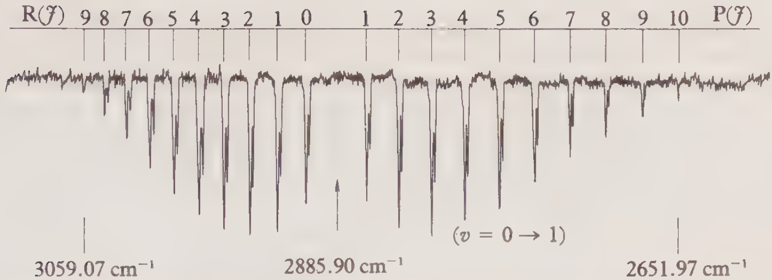

10.4 Absorption spectrum of HCl. The double peaks exist because naturally occurring chlorine is a mixture of the two isotopes ^{35}Cl(75.5 per cent) and ^{37}Cl(24.5 per cent). The position of the central gap in the spectrum determines $\bar{\nu}_0 = 2885.9\ \mathrm{cm}^{-1}$, ($\hbar\omega_0 = 0.369$ eV) and the spacing determines the rotational constant $\bar{B} = B/hc = 10.59\ \mathrm{cm}^{-1}$ ($B = 1.31 \times 10^{-3}$ eV). (By courtesy of R. Colin.)

of inertia $I_0 = \mu R_0^2$ of the molecule. Except for very heavy molecules, most molecules in a gas at room temperature are in the vibrational ground state with $v = 0$, so the most easily observed transitions are between the levels with $v = 0$ and $v = 1$. This band is called the fundamental band.

In actual spectra the difference in frequencies between adjacent lines is not quite constant, as in the simple model we have just described. This may be seen from Table 10.1, which displays the observed frequencies of a band in the spectrum of HCl. This departure from constancy is due to the fact that the rotational constant B is not quite the same in each of the vibrational states, so that we must consider two constants B_v and B_{v+1}. In this case the frequency of the lines is a quadratic function of $\mathcal{J}$, and the second differences of the frequencies are constant. From the first and second differences both B_v and B_{v+1} can be calculated. We also note from Table 10.1 that the central line in the spectrum which should be at $2885.9\ \mathrm{cm}^{-1}$ is missing. The corresponding gap makes the identification of the P and R branches lines easy. In practice, the

Table 10.1 Wave numbers of the central lines in the rotational–vibrational band ($v = 0 \leftrightarrow 1$) of HCl

	$\bar{\nu}$ (cm^{-1})	A (cm^{-1})
R(5)	2997.78	
R(4)	2980.90	16.88
R(3)	2963.24	17.66
R(2)	2944.89	18.55
R(1)	2925.78	19.11
R(0)	2906.25	19.53
$\bar{\nu}_0$	missing at 2885.90	—
P(1)	2865.09	—
P(2)	2843.56	21.53
P(3)	2821.49	22.07
P(4)	2798.78	22.71
P(5)	2775.79	22.99
P(6)	2752.03	23.76

A = Wave number difference between neighbouring lines.

departure from simple harmonic motion in vibrational–rotational spectra can be observed and the anharmonicity constant (see [9.29]) can also be calculated.

If the molecule is not in a Σ state, so that Λ is not zero, transitions with $\Delta \mathcal{J} = 0$ are allowed. This gives rise to a further branch of the vibrational–rotational spectrum, called the *Q branch*. The frequencies ν^{Q} corresponding to the lines in this branch are given by a quadratic function of $\mathcal{J}$ if B_{v+1} and B_v are unequal, and reduce to the single frequency

$$\begin{aligned} h\nu^{Q} &= E(v+1, \mathcal{J}) - E(v, \mathcal{J}) \\ &= \hbar\omega_0 \end{aligned} \qquad [10.25]$$

if $B_{v+1} = B_v$.

Raman scattering

So far, the main experimental technique for obtaining information about the properties of atoms and molecules that we have considered is the observation of the emission or absorption of radiation. Important additional methods involve the scattering of electrons or of radiation by atomic systems. We shall study electron scattering in Chapter 12, while here we discuss briefly some characteristics of the scattering of radiation by an atom or a molecule.

The scattering of radiation by an atomic system must be at least a second-order process. In step 1, a photon of energy $\hbar\omega$ is absorbed, exciting the atom (or molecule) from a state a to a state n, and in step 2 the atomic system emits a photon of energy $\hbar\omega'$ and is de-excited from the state n to a final state b. Alternatively, the two steps can occur in reverse order, the photon of energy $\hbar\omega'$ being emitted first and the photon of energy $\hbar\omega$ being absorbed subsequently (see Fig. 10.5).

If the final state b of the system is the same as the initial state a, the emitted radiation has the same frequency as the incident radiation. This process is called *Rayleigh scattering* and was first discussed within the framework of classical physics by Lord Rayleigh. If the final state of the atom is different from the initial state, the scattering is inelastic, and by conservation of energy the angular frequency ω' of the emitted radiation is given by

$$\hbar\omega' = \hbar\omega + (E_a - E_b) \qquad [10.26]$$

The inelastic scattering process is called *Raman* scattering (or the *Raman effect*) after C. V. Raman who discovered the effect experimentally. The theory of both Rayleigh and Raman scattering may be developed in a straightforward way

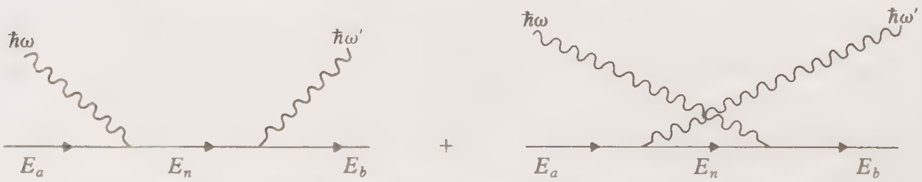

10.5 The two second-order terms in scattering of photons by atomic systems.

by solving the coupled equations [4.25] to second order. In particular, the differential cross-section for Raman scattering is found to be

$$\frac{d\sigma}{d\Omega} = r_0^2 \omega \omega'^3 \left| \sum_n \left(\frac{m}{e^2}\right) \left\{ \frac{(\hat{\boldsymbol{\varepsilon}}' \cdot \mathbf{D}_{bn})(\hat{\boldsymbol{\varepsilon}} \cdot \mathbf{D}_{na})}{E_n - E_a - \hbar\omega} + \frac{(\hat{\boldsymbol{\varepsilon}} \cdot \mathbf{D}_{bn})(\hat{\boldsymbol{\varepsilon}}' \cdot \mathbf{D}_{na})}{E_n - E_a + \hbar\omega'} \right\} \right|^2 \qquad [10.27]$$

where

$$r_0 = \left(\frac{e^2}{4\pi\varepsilon_0}\right)\frac{1}{mc^2} = 2.82 \times 10^{-15} \text{ m} \qquad [10.28]$$

is the '*classical radius of the electron*', $\mathbf{D}_{ij}$ is the matrix element of the electric dipole moment $\mathbf{D}$ between the states i and j of the atomic system, while $\hat{\boldsymbol{\varepsilon}}$ and $\hat{\boldsymbol{\varepsilon}}'$ are the polarisation vectors of the photons in the initial and final states; the sum over n which occurs in [10.27] is over all possible intermediate states. If the energy of the incident photons is such that $\hbar\omega = E_n - E_a$, where E_n is the energy of one of the intermediate states, the first term in the cross-section formula [10.27] becomes infinite. This is due to the fact that in obtaining the

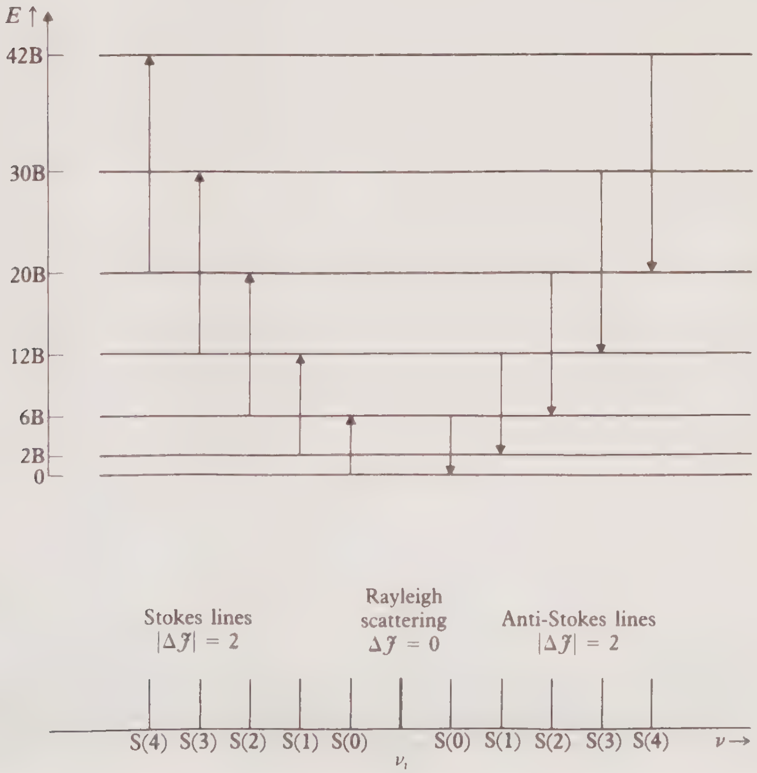

10.6 A Raman spectrum for rotational transitions. The scattered light contains a line at the incident frequency ν_i due to Rayleigh scattering $\Delta J = 0$, and equally spaced lines on either side due to Raman scattering with $|\Delta J| = 2$. Transitions with $|\Delta J| = 2$ are often called the S branch and are numbered by the J value of the lower level.

result [10.27] the width of the energy level E_n has been neglected. If we allow for the finite width Γ_n of this level by replacing E_n by $E_n - i\Gamma_n/2$ (see Section 4.6), the correct behaviour of the cross-section in the region $\hbar\omega \simeq E_n - E_a$ is found.

By the usual electric dipole selection rules, the intermediate state n must have opposite parity to each of the states a and b. Thus Raman scattering does not change the parity of the atom or molecule, and the selection rules are given by

$$\Delta \mathcal{J} = 0, \pm 2 \qquad [10.29]$$

If the initial state a of the atomic system is the ground state, the final state b must have higher energy, so that $\omega' < \omega$. In this case the observed spectral line is called a *Stokes line*. If the initial state a of the atomic system is an excited state the final state b may have higher or lower energy. In the latter case $\omega' > \omega$ and the corresponding spectral line is known as an *anti-Stokes* line.

For Raman scattering to occur with appreciable strength, the intermediate states n should have closely spaced energies E_n which are also close to E_a and (or) E_b, since in this case the energy denominators in [10.27] are small. This condition is met by the rotational–vibrational levels in molecules. We note that the Raman effect does not require the existence of a permanent electric dipole moment, but rather than an electric dipole moment should be developed under the influence of the radiation field. For this reason, Raman lines are observed for symmetrical molecules like H_2, O_2, . . . which exhibit no pure rotational and vibrational spectra without a change in electronic state. A schematic energy level diagram for the rotational Raman spectrum is shown in Fig. 10.6, together with the corresponding spectrogram.

10.3 ELECTRONIC SPECTRA OF DIATOMIC MOLECULES

Molecular spectra for which changes in the electronic as well as in the vibrational and rotational states of the molecule occur are called *electronic spectra*. The energy differences between electronic levels being much larger than those corresponding to transitions without a change in the electronic state, the lines associated with electronic spectra lie in the *visible* or the *ultra-violet* part of the spectrum. When observed with small dispersion, electronic spectra usually appear to consist of more or less broad *bands*, and one speaks of *electronic band spectra*. As an example, we show in Fig. 10.7 various bands (photographed in

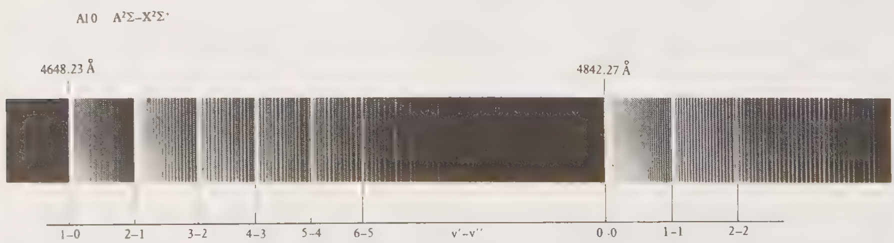

10.7 Electronic band spectra photographed in emission in transitions from an excited state to the ground state of the molecule AlO. (By courtesy of R. Colin.)

emission) corresponding to the transition $A^2\Sigma^+ \rightarrow X^2\Sigma^+$ between the excited electronic state $A^2\Sigma^+$ and the ground state $X^2\Sigma^+$ of the AlO molecule. When spectrographs of larger resolving power are used, one finds that most of the bands exhibit a *fine structure* in the sense that they consist of many closely spaced individual lines. This is illustrated in Fig. 10.8, which shows the fine structure of a particular band of the electronic emission spectrum of the BeI molecule.

In order to understand the basic features of electronic spectra, we return to [10.1] which expresses the fact that the total energy $E_{s,v,r}$ of the molecule may be written (approximately) as the sum of the electronic energy E_s, the vibrational energy E_v and the rotational energy E_r. Thus the emitted or absorbed frequencies of the various spectral lines corresponding to the transitions between two electronic states are given by

$$\nu = \frac{(E_{s'} + E_{v'} + E_{r'}) - (E_s + E_v + E_r)}{h} \qquad [10.30]$$

where the primed letters refer to the upper electronic state. We may also write [10.30] as

$$\nu = \nu_{s's} + \nu_{v'v} + \nu_{r'r} \qquad [10.31a]$$

with

$$\nu_{s's} = \frac{E_{s'} - E_s}{h}, \qquad \nu_{v'v} = \frac{E_{v'} - E_v}{h}, \qquad \nu_{r'r} = \frac{E_{r'} - E_r}{h} \qquad [10.31b]$$

For a *given electronic transition* (s, s' fixed) the quantity $\nu_{s's}$ is a *constant*, which is positive since we have assumed that $E_{s'} > E_s$. On the other hand, $\nu_{v'v}$ and $\nu_{r'r}$ can vary and need not be positive. A given *band* corresponds to fixed values of both $\nu_{s's}$ and $\nu_{v'v}$ and all possible (allowed) values of $\nu_{r'r}$, while the *band system* of a given electronic transition ($\nu_{s's}$ fixed) is obtained by letting both $\nu_{v'v}$ and $\nu_{r'r}$ take all possible values. Thus $\nu_{v'v}$ characterises the *vibrational* or *band structure* of the spectrum, and $\nu_{r'r}$ its *rotational* structure, that is the *fine structure* of the band.

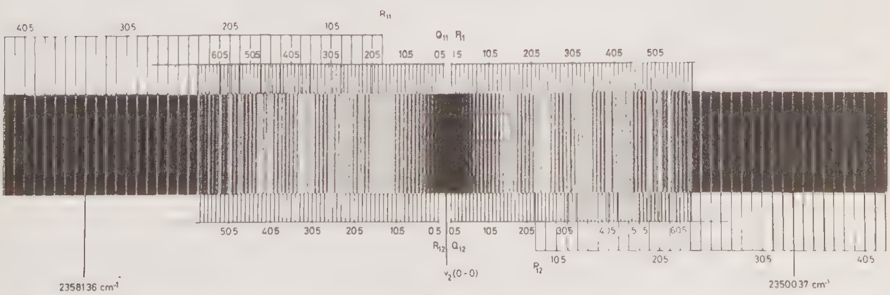

10.8 The fine structure of the 0–0 emission band of BeI, arising from the electronic transition $A^2\Pi_{1/2} - X^2\Sigma^+$. (By courtesy of R. Colin.)

Vibrational structure of electronic spectra

Let us neglect for the moment the fine structure due to the rotation of the molecule. Keeping only the first two terms on the right of (10.31a) and using for the vibrational energy levels the simple linear harmonic oscillator expression [9.24], we find that for a given electronic transition ($\nu_{s's}$ fixed) the frequencies ν of the transitions ($s'v' \to sv$) are such that

$$h\nu = h\nu_{s's} + \hbar\omega_0'(v' + \tfrac{1}{2}) - \hbar\omega_0(v + \tfrac{1}{2}) \qquad [10.32]$$

where ω_0 and ω_0' are the vibrational constants of the lower and upper electronic states, respectively. A more precise expression may be obtained by taking into account the anharmonicity of the vibrational motion. In terms of the anharmonicity constant introduced in [9.29], we have

$$\begin{aligned} h\nu = h\nu_{s's} &+ \hbar\omega_0'(v' + \tfrac{1}{2}) - \hbar\beta'\omega_0'(v' + \tfrac{1}{2})^2 \\ &- \hbar\omega_0(v + \tfrac{1}{2}) + \hbar\beta\omega_0(v + \tfrac{1}{2})^2 \end{aligned} \qquad [10.33]$$

which is known as the *Deslandres formula.*

It is customary to record the frequencies of the transitions ($s'v' \to sv$) between pairs of vibrational levels v and v' (for a given pair of electronic states s and s') in a *Deslandres table.* The rows of such a table are labelled by the vibrational quantum number v of the lower level and the columns by the vibrational quantum number v' of the upper level. A set of bands having the same v (or v') is called a v (or v') *progression*. At thermal energies (corresponding to room temperature) gases are primarily in the ground electronic state, with $v = 0$, and the absorption spectrum only contains the corresponding $v = 0$ progressions. Finally, a group of bands having the same value of $v' - v$ is called a band *sequence*; it occurs along the diagonal of the Deslandres table.

Rotational structure of electronic spectra

Let us consider a given electronic band, corresponding to fixed values of (s, v) and (s' v'). The rotational energies E_r and $E_{r'}$ are characterised by the quantum numbers $\mathcal{J}$ and $\mathcal{J}'$, respectively. If the transition occurs between two Σ states, then the selection rule is $\Delta\mathcal{J} = \pm 1$. On the other hand, if one or both of the electronic states have $\Lambda \neq 0$ (where we recall that Λ is the absolute value of the projection of the orbital angular momentum on the internuclear axis) the selection rules are $\Delta\mathcal{J} = 0, \pm 1$ and $\Delta\Lambda = 0, \pm 1$. Moreover, in the absence of spin–orbit coupling we have $\Delta S = 0$, while for transitions between Σ states we have $\Sigma^+ \leftrightarrow \Sigma^+$ and $\Sigma^- \leftrightarrow \Sigma^-$. For homonuclear molecules, we have the additional selection rule g $\leftrightarrow$ u which only allows transitions between gerade and ungerade states. There is no selection rule for the vibrational quantum number since the harmonic oscillator wave functions ψ_v and ψ_v' which enter into [10.19] belong to different wells.

As a result of the selection rule $\Delta \mathcal{J} = 0, \pm 1$, the band divides into P, Q and R branches, the Q branch being absent for transitions between two Σ states, where $\Delta \mathcal{J} = \pm 1$. The frequencies of the rotational lines are given by

$$\begin{aligned} h\nu^{\mathrm{P}} &= h\nu + B'\mathcal{J}(\mathcal{J} - 1) - B\mathcal{J}(\mathcal{J} + 1) \\ h\nu^{\mathrm{Q}} &= h\nu + B'\mathcal{J}(\mathcal{J} + 1) - B\mathcal{J}(\mathcal{J} + 1) \\ h\nu^{\mathrm{R}} &= h\nu + B'(\mathcal{J} + 1)(\mathcal{J} + 2) - B\mathcal{J}(\mathcal{J} + 1) \end{aligned} \qquad [10.34]$$

where $h\nu$ is either given by the Deslandres formula [10.33] or – if the simple linear harmonic oscillator approximation is made – by [10.32]. In these formulae, the lower level in each case has angular momentum $\mathcal{J}$, while the upper level has angular momentum $\mathcal{J} - 1$, $\mathcal{J}$ or $\mathcal{J} + 1$ for the P, Q and R branches, respectively.

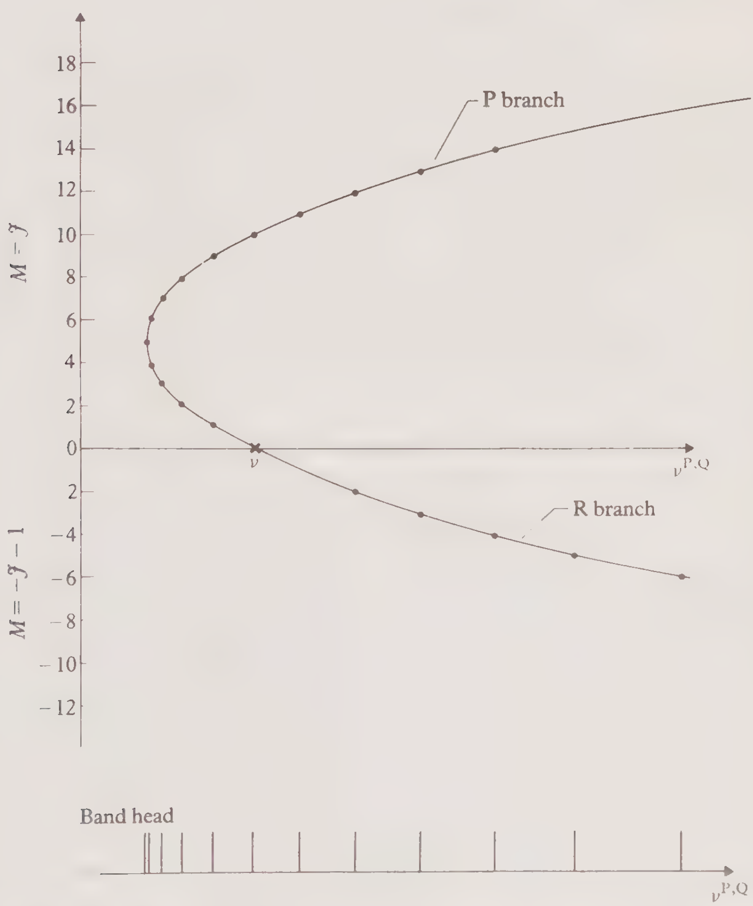

10.9 A Fortrat parabola for a $\Sigma \to \Sigma$ transition in a diatomic molecule, (no Q branch). The spectrogram beneath shows the position of the band head.

In contrast to the vibrational–rotational expressions [10.23]–[10.24], which are linear in J, or [10.25] which is independent of J, the formulae [10.34] for the rotational structure of electronic bands are *parabolic* in J. This is due to the fact that the rotational constants B and B' are in general different in the lower and upper levels. Plots of J against the frequencies of the rotational lines are called Fortrat diagrams. A typical example of a *Fortrat parabola* is shown in Fig. 10.9. We see that since $B \neq B'$ the lines are not equally spaced. In the example shown the lines become closely spaced at the low frequency ('red end') of the band, and form what is known as a *band head* at the minimum frequency. As one goes to higher frequencies the intervals between the lines increase, and the intensity of the band falls off gradually. This is called *band degradation* . In other cases the band head can be at the highest frequency and the band degrades towards lower frequencies.

The Franck–Condon principle

We have seen in Chapter 9 that there is little interaction between the electronic and nuclear motions in a molecule, the nuclear periods being much longer than the electronic ones. Thus an electronic transition can be considered as taking place 'instantaneously' on the time scale of vibrations, or in other words at a nearly *constant* value of the internuclear separation R. The heavy nuclei do not change their positions or momenta during the electronic transition, but only *after* it has occurred. Referring to Fig. 10.10, in which the potential energy curves of two electronic states A and B are shown with their associated vibrational levels, we see that an electronic transition between the states A and B is accurately represented by a *vertical line*, that is a line of constant R. This is known as the *Franck–Condon principle*.

The Franck–Condon principle can be combined with our discussion of the linear harmonic oscillator wave functions in Section 2.4 to understand the *intensity distribution* among the bands of a band system. Indeed, if the molecule is in the lowest vibrational state of a given electronic state, the probability distribution function for R is large only near the equilibrium separation of that electronic state. On the other hand, in excited vibrational states this probability distribution becomes larger at the classical turning points, that is at the extreme ends of the classical vibrational motions. Thus, looking again at Fig. 10.10, we see for example that an electronic (absorption) transition from the ground ($v = 0$) vibrational level of the (lower) electronic state A will lead to the point P_1 on the upper electronic curve B, corresponding to the vibrational level $v' = 6$. As a result, the band $v = 0 \rightarrow v' = 6$ will be the most intense member of the progression starting from the $v = 0$ vibrational level of the electronic state A. Similarly, we see from Fig. 10.10 that an (emission) electronic transition from the $v' = 0$ state of B will lead to the point P_2 on the lower electronic state, corresponding to $v = 7$. When both vibrational levels v and v' are excited states, the most favoured transitions will be those that can occur at constant R with the nuclei in the electronic states A and B at the classical end points of their

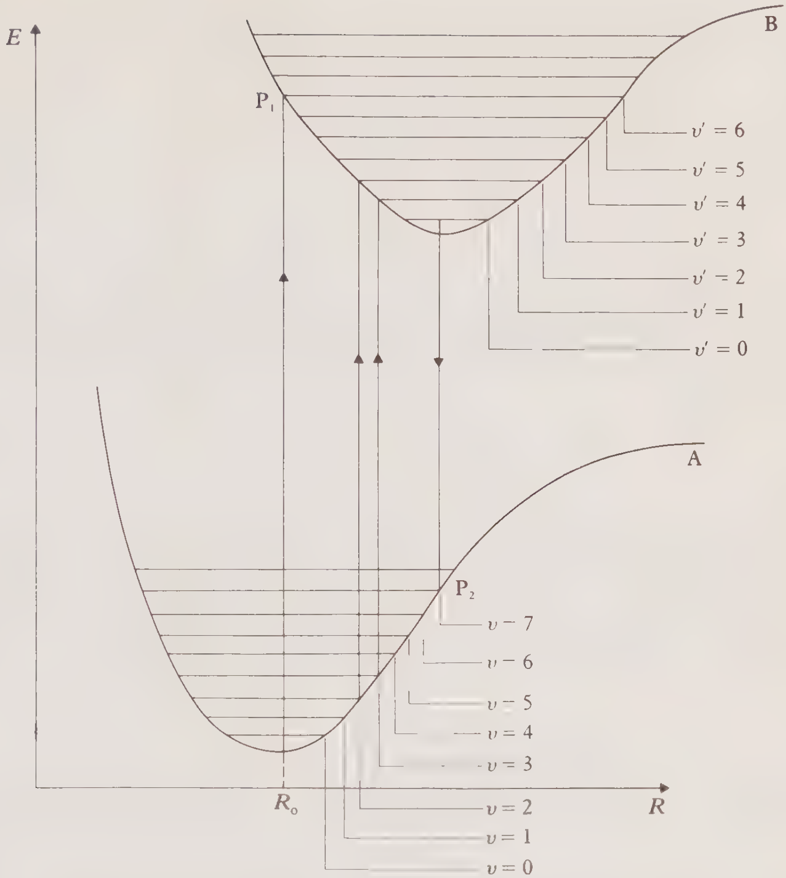

10.10 Electronic transitions illustrating the Franck–Condon principle.

vibrational motion. Examples in Fig. 10.10 are shown by the vertical lines from $v = 2$ to $v' = 2$ and $v = 3$ to $v' = 1$.

The above qualitative considerations can be expressed more precisely as follows. The total wave function Ψ_α of the molecule in a given state α (neglecting spin) is the product $\Phi_s R^{-1} \psi_v \phi_{\mathcal{J},M_\mathcal{J},\Lambda}$ and the transition amplitude is proportional to the matrix element of the electric dipole operator [10.13] between two wave functions Ψ_α and $\Psi_{\alpha'}$. That is

$$\langle \Psi_{\alpha'} | \mathbf{D} | \Psi_\alpha \rangle = e \int \mathrm{d}\mathbf{R}\, R^{-2} \int \mathrm{d}\mathbf{r}\, \Phi_{s'}^{\star} \psi_{v'}^{\prime\star} \phi_{\mathcal{J}'}^{\prime\star}{}_{,M_{\mathcal{J}}',\Lambda'}$$
$$\times \left(\sum_{i=1}^{2} Z_i \mathbf{R}_i - \sum_j \mathbf{r}_j \right) \Phi_s \psi_v \phi_{\mathcal{J},M_\mathcal{J},\Lambda} \qquad [10.35]$$

where $\mathbf{R} = \mathbf{R}_1 - \mathbf{R}_2$ and the symbol $\int \mathrm{d}\mathbf{r}$ denotes an integration over all the coordinates of the electrons. Because of the orthogonality of the electronic wave

functions Φ_s and $\Phi_{s'}$, the first term in [10.35] containing only nuclear coordinates vanishes, so that

$$\langle \Psi_{\alpha'} | \mathbf{D} | \Psi_\alpha \rangle = \int \psi_{v'}'^{\star} \phi_{\mathcal{J}', M_{\mathcal{J}}', \Lambda'}'^{\star} \mathbf{D}_{\text{el}}(R) \psi_v \phi_{\mathcal{J}, M_{\mathcal{J}}, \Lambda} R^{-2} \mathrm{d}\mathbf{R} \qquad [10.36]$$

where

$$\mathbf{D}_{\text{el}}(R) = -e \int \Phi_{s'}^{\star} \left(\sum_j \mathbf{r}_j \right) \Phi_s \, \mathrm{d}\mathbf{r} \qquad [10.37]$$

is the electronic part of the matrix element of the electric dipole operator $\mathbf{D}$. The Franck–Condon principle amounts to assuming that $\mathbf{D}_{\text{el}}(R)$ is independent of R, so that the transition amplitude [10.36] is proportional to the *Franck–Condon factor*

$$f_{v'v} = \int \psi_{v'}'^{\star} \psi_v \, \mathrm{d}R \qquad [10.38]$$

This quantity is just the *overlap* integral between vibrational wave functions ψ_v and $\psi_{v'}'$ in *different* electronic states. Thus we see that the most intense transitions will be those for which the overlap between ψ_v (determined from the electronic potential in the lower state) and $\psi_{v'}'$ (obtained from the electronic potential for the upper state) is a maximum, in accordance with our foregoing qualitative discussion.

Dissociation and predissociation

In addition to the discrete molecular transitions which we have considered thus far, *continuous* molecular spectra are frequently observed, both in emission and absorption. These spectra result from transitions in which at least one of the states is a *dissociative state*. For example, we show in Fig. 10.11 two electronic absorption transitions leading to the *dissociation* of a molecule.

It may also happen that an excited state B is coupled by internal perturbations (such as spin–orbit effects) or external ones (such as collisions) to a dissociative state D. In this case the excited state B can either decay to a lower electronic state A by a radiative transition (spontaneous emission of radiation) or be transferred to the dissociative state D by a *radiationless transition* due to the coupling between the states B and D. The latter process is called *predissociation* and is illustrated in Fig. 10.12. We remark that it is similar to autoionisation and to the Auger effect discussed in previous chapters for atoms. The effect of predissociation is to weaken and broaden the emission lines from the excited state.

Fluorescence and phosphorescence

Molecules which absorb radiation in the near ultra-violet and visible range may re-emit it at a longer wavelength. This phenomenon is known as *fluorescence* and

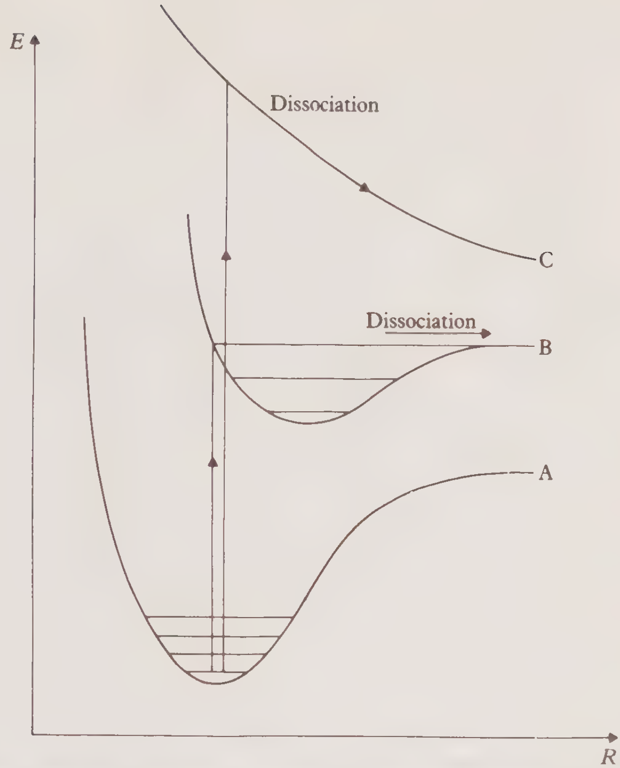

10.11 Electronic transitions leading to dissociation. A transition from level A to level C leads to dissociation because C is repulsive. The curve B exhibits a minimum, but the transition shown leads to a level with sufficient energy to surmount the barrier.

is illustrated in Fig. 10.13(a). First, absorption transitions occur from a lower electronic state to some vibrational levels of an upper electronic state, these absorption transitions being governed by the Franck–Condon principle. For example, we have shown in Fig. 10.13(a) a transition leading from the lowest vibrational level of the ground electronic state of the molecule (which we take to be a singlet state and denote by ^1X) to an excited vibrational level of an upper electronic state ^1A. The molecule may then lose vibrational energy through collisions with other molecules (thermal decay) and reach the lowest vibrational state $v' = 0$ of the excited electronic level ^1A. This process is often more rapid than spontaneous emission of radiation, so that when the molecule finally re-emits radiation, it is from the vibrational level $v' = 0$. As a result, the emitted radiation is at a lower frequency than the incident one.

The fluorescence phenomenon which we have just discussed involves a spontaneous emission between two electronic states of the *same multiplicity*. A

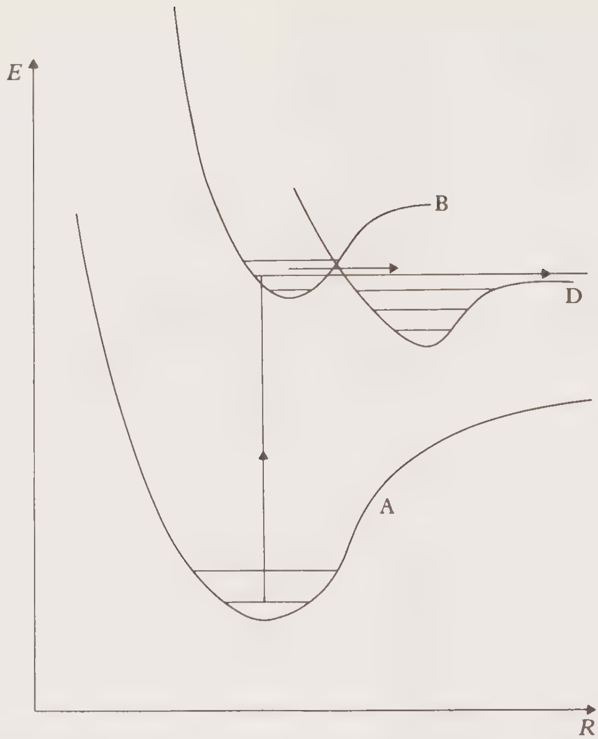

10.12 Predissociation. A transition from A to B leads to a bound vibrational level, but a further transition is made to a dissociating level of D.

related process, known as *phosphorescence*, involves the spontaneous emission from an excited electronic state to a lower one of *different multiplicity*. For example, let us assume that a molecule first undergoes an absorption transition from a singlet ground state ^1X to a singlet excited state ^1A, as in the case of fluorescence studied above. Thermal degradation of the vibrational energy then occurs via collisions with other molecules. Suppose now that the state ^1A is coupled to a triplet state ^3A of similar energy, as shown in Fig. 10.13(b). Instead of going down the vibrational ladder of the state ^1A, the molecule may then undergo an *intersystem crossing* and be transferred by a radiationless transition into the triplet state ^3A. After the crossing has occurred, thermal decay will proceed within the ^3A well, until the molecule has reached the lowest vibrational level of the ^3A state. This triplet state may now decay to the ground (singlet) state ^1X by a radiative transition called *phosphorescent emission*. Indeed, although electric dipole transitions between the excited ^3A state and the ground state ^1X are spin-forbidden because of the selection rule $\Delta S = 0$, radiative transitions $^3A \rightarrow {}^1X$ may not be absolutely forbidden, and may occur slowly through

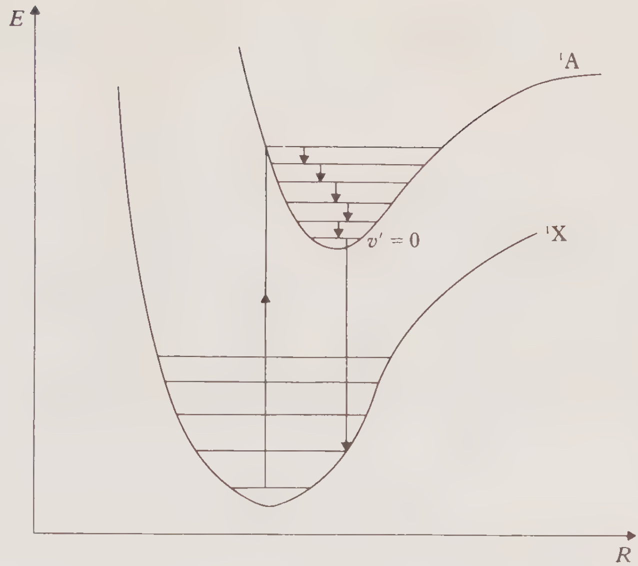

(a)

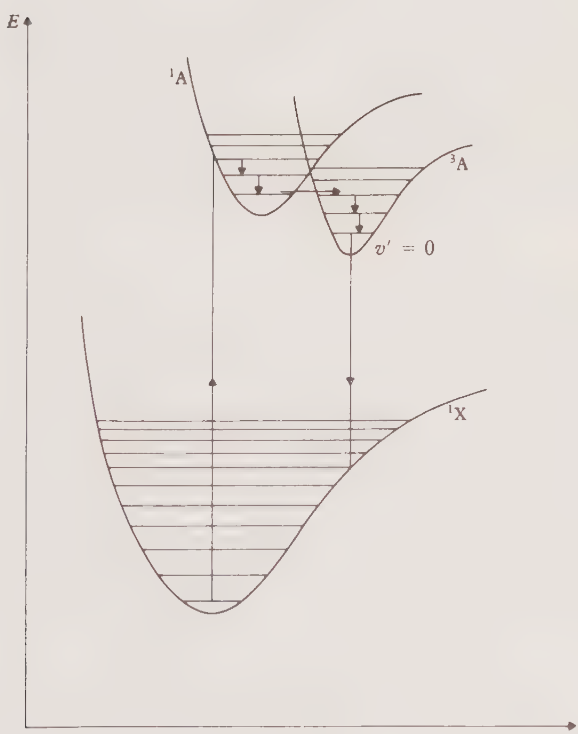

(b)

10.13 (a) Fluorescence. (b) Phosphorescence.

spin–orbit interactions. As a result, phosphorescent emission may take place for seconds or even longer after the incident radiation (responsible for the initial absorption process $^1X \to {}^1A$) has been switched off.

10.4 THE ELECTRONIC SPIN AND HUND'S CASES

In our discussion of the spectra of diatomic molecules to this point, we have not taken into account the coupling between the spin of the electrons and the orbital angular momentum. For light molecules (as for light atoms) this coupling is small, and of course the L–S coupling vanishes in any case for singlet states ($S = 0$) and for Σ states ($\Lambda = 0$). More generally, the molecular angular momenta may couple together in various ways: L–S, $\mathcal{J}$–L, $\mathcal{J}$–S, N–S, . . . where

$$\mathbf{J} = \mathbf{L} + \mathbf{N} + \mathbf{S} \tag{10.39}$$

denotes the total angular momentum (excluding nuclear spin) and we recall that $\mathbf{N}$ is the orbital angular momentum of the nuclei, which is perpendicular to the internuclear axis of a diatomic molecule.

The coupling schemes were first systematically studied by Hund, who considered five limiting cases, known as Hund's cases (a), (b), (c), (d) and (e). Hund's cases are idealisations, but they represent good approximations to the actual states of many molecules. The relative strength of the couplings determines which case applies, and therefore also the fine structure of the spectra. We shall only consider here two of Hund's cases [1].

Hund's case (a)

In this case the electronic orbital angular momentum $\mathbf{L}$ is coupled by the strong axial internuclear field to the molecular axis. Moreover, the spin–orbit (L–S) coupling is sufficiently strong also to constrain the total spin $\mathbf{S}$ to interact strongly with the axial field of the molecule, while the interaction of the nuclear rotation with the electronic motion (orbital and spin) is very small. Thus only the projections of $\mathbf{L}$ and $\mathbf{S}$ on the internuclear axis are well-defined quantities. We have seen previously that the magnitude of the projection of $\mathbf{L}$ on the internuclear axis is $\Lambda\hbar$. It is customary to denote the projection of the total spin $\mathbf{S}$ on the molecular axis by $\Sigma\hbar$ [2]; the quantum number Σ can therefore take on

[1] A detailed account of Hund's five cases may be found, for example, in Herzberg (1950).
[2] The quantum number Σ used here should not be confused with the symbol Σ describing the electronic terms with $\Lambda = 0$!

the $2S + 1$ values $-S$, $-S + 1$, $\ldots$ $+S$. Both Λ and Σ are thus 'good quantum numbers' in Hund's cases (a). Defining

$$\Omega = |\Lambda + \Sigma| \qquad [10.40]$$

it follows that Ω is also a good quantum number, which can take on the values $|\Lambda - S|$, $|\Lambda - S| + 1$, $\ldots$ $\Lambda + S$ (see Fig. 10.14(a)). Hence, for a given value of Λ an electronic term splits into $2S + 1$ terms which can be labelled by the value of Ω, written as a lower subscript. To each set of quantum numbers Λ and Ω corresponds a series of rotational levels with different values of $\mathcal{J}$, where $\mathcal{J}$ must be such that $\mathcal{J} \geqslant \Omega$. For example, in a $^3\Pi$ state, with $\Lambda = 1$ and $S = 1$, the allowed values of Ω are $\Omega = 0, 1, 2$. The electronic level $^3\Pi$ splits into three levels, denoted by $^3\Pi_0$, $^3\Pi_1$ and $^3\Pi_2$, the magnitude of the splitting being determined by the spin–orbit interaction. Each of these three levels gives rise to a series of rotational levels, as shown in Fig. 10.15.

In order to obtain the energies of the rotational levels, we notice that the total angular momentum **J** is obtained by adding to **N** (the orbital angular

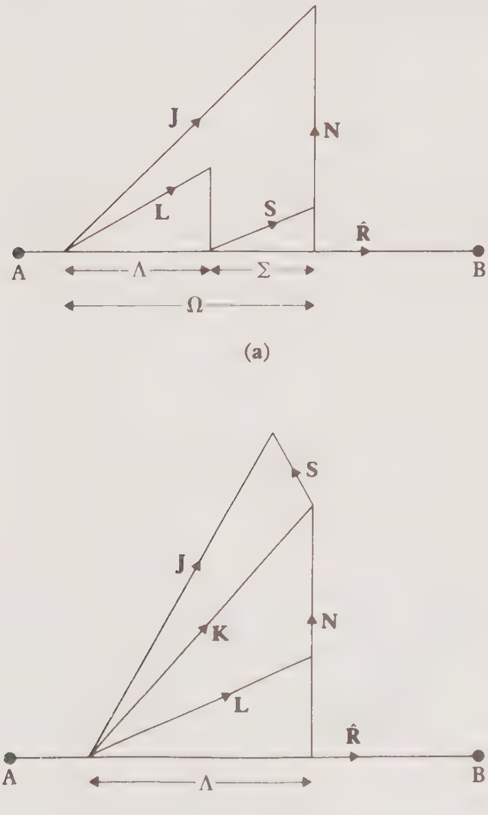

10.14 Angular momentum vectors in Hund's cases (a) and (b).

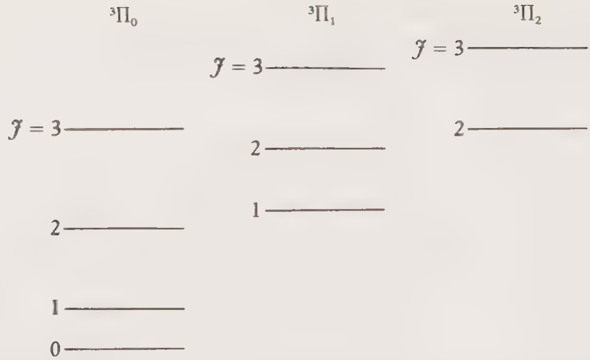

10.15 Spin orbit splitting of a $^3\Pi_\Omega$ level. Note $\Omega = 0$, 1 or 2 and $\mathcal{J} \geqslant \Omega$. The electronic energy of a multiplet term is given by $A\,\Lambda\Sigma$ where A is a constant and Λ and Σ are the projections of **L** and **S** on the internuclear line.

momentum of the nuclear motion) the vector $\mathbf{\Omega} = \Omega\hbar\hat{\mathbf{R}}$, where $\hat{\mathbf{R}}$ is a unit vector along the molecular axis. That is

$$\mathbf{J} = \mathbf{N} + \mathbf{\Omega} \tag{10.41}$$

The rotational energies are given as in Section 10.1 (see [10.5] and [10.7]) by

$$E_r = B\langle \mathbf{N}^2 \rangle/\hbar^2 \tag{10.42}$$

where $B = \hbar^2/2\mu R_0^2$. Using [10.41] and [10.42] and remembering that **N** and $\mathbf{\Omega}$ are at right angles, we then have

$$E_r = B[\mathcal{J}(\mathcal{J} + 1) - \Omega^2] \tag{10.43}$$

Hund's case (b)

Here the electron spin **S** is either very weakly coupled or not coupled at all to the molecular axis. This decoupling takes place in particular for Σ states ($\Lambda = 0$) where the spin–orbit coupling is absent; it may also occur even if $\Lambda \neq 0$ provided the spin–orbit interaction is weak; this situation happens in particular in light molecules, for example in some of the first row hydrides. In this case the orbital angular momentum **L** may still couple to the molecular axis, with a projection determined by Λ, which is therefore a good quantum number. On the other hand, since the spin **S** is decoupled from the molecular axis, we note that Ω is not a good quantum number in the present case. Writing $\mathbf{\Lambda} = \Lambda\hbar\hat{\mathbf{R}}$, we first neglect **S** and form the resultant of $\mathbf{\Lambda}$ and **N**, which is denoted by **K** (see Fig. 10.14(b)). That is,

$$\mathbf{K} = \mathbf{\Lambda} + \mathbf{N} \tag{10.44}$$

so that **K** is the total angular momentum apart from spin. The corresponding quantum number K can take on the integral values $\Lambda, \Lambda + 1, \Lambda + 2, \ldots$, and

the rotational energy of the molecule – neglecting spin – is given by

$$E_r^0 = BK(K+1) \tag{10.45}$$

The total angular momentum $\mathbf{J}$ is obtained by coupling $\mathbf{K}$ and $\mathbf{S}$, namely

$$\mathbf{J} = \mathbf{K} + \mathbf{S} \tag{10.46}$$

so that the possible values of the quantum number $\mathcal{J}$ are $|K - S|, |K - S| + 1, \ldots, K + S$. Thus, except if $K < S$, each level corresponding to a given K splits into $2K + 1$ components. The simplest type of Hund's case (b) molecules are in $^2\Sigma$ states, with $S = 1/2$. The additional energy due to the coupling between $\mathbf{K}$ and $\mathbf{S}$ is then of the form

$$E_r' = \gamma\langle \mathbf{K} \cdot \mathbf{S}\rangle \tag{10.47}$$

where γ is a small coupling constant. Now, using [10.46], we have

$$\langle \mathbf{K} \cdot \mathbf{S}\rangle = \tfrac{1}{2}[\mathcal{J}(\mathcal{J}+1) - K(K+1) - S(S+1)]\hbar^2$$

so that

$$\begin{aligned} E_r' &= \frac{\gamma}{2} K\hbar^2, & \mathcal{J} &= K + \frac{1}{2} \\ &= -\frac{\gamma}{2}(K+1)\hbar^2, & \mathcal{J} &= K - \frac{1}{2} \end{aligned} \tag{10.48}$$

and the total rotational energy, including the electron spin interaction is given by

$$\begin{aligned} E_r &= E_r^0 + E_r' \\ &= BK(K+1) + \frac{\gamma}{2} K\hbar^2, & \mathcal{J} &= K + \frac{1}{2} \\ &= BK(K+1) - \frac{\gamma}{2}(K+1)\hbar^2, & \mathcal{J} &= K - \frac{1}{2} \end{aligned} \tag{10.49}$$

Spin uncoupling. Λ-doubling

As we pointed out above, Hund's coupling cases are idealisations, to which many molecules approximately conform. However, deviations from these idealisations may occur, which represent a partial *uncoupling* or *decoupling* of some of the angular momenta. This uncoupling may increase as $\mathcal{J}$ increases, since the electrons may not follow the nuclear motion. Thus a molecule may fall approximately in one coupling case for low $\mathcal{J}$, but in another case for high $\mathcal{J}$, while for intermediate rotational states one has *intermediate coupling*.

A common example of intermediate coupling is provided by the transition from Hund's case (a) to (b). For low $\mathcal{J}$, the spin $\mathbf{S}$ is coupled to the molecular

axis, according to the coupling scheme (a). However, as $\mathcal{J}$ increases and the rotational frequency becomes larger, **S** uncouples from the molecular axis (spin uncoupling) and eventually couples with **K**, as in Hund's case (b).

Another type of uncoupling, produced by an interaction between the rotational and electronic motions, is that which decouples the electronic orbital angular momentum **L** from the molecular axis. This uncoupling has the effect of splitting the two otherwise degenerate levels corresponding to $\Lambda \neq 0$, and is known as *Λ-doubling*.

10.5 THE NUCLEAR SPIN

The coupling between the spins of the nuclei and the magnetic fields, due to the orbital motion and the spin of the electrons, makes no significant contribution to the molecular energies. Despite this fact, the nuclear spin has a large influence upon the spectrum of molecules containing *identical* nuclei, because of symmetry considerations. A particularly interesting case is that of *homonuclear diatomic* molecules, which have two identical nuclei. Neglecting the very small coupling of the nuclear spins with the rest of the molecule, we can write the total wave function Ψ_{tot} of a homonuclear diatomic molecule as

$$\Psi_{tot} = \Psi(\mathbf{R}, q)\chi_N(1, 2) \qquad [10.50]$$

where χ_N is the spin function of the two nuclei. The part of the wave function not depending on the nuclear spin, Ψ, is a function of the internuclear coordinate **R** and of the spatial and spin coordinates of the electrons, which we denote collectively by q. The total wave function Ψ_{tot} must of course be antisymmetric with respect to the interchange of any pair of electrons, in order to satisfy the Pauli exclusion principle. In addition, however, since the two nuclei 1 and 2 are *identical* in a homonuclear diatomic molecule, the total function Ψ_{tot} must be either *symmetric* or *antisymmetric* under the interchange $1 \leftrightarrow 2$ of the identical nuclei. According to our discussion of Section 2.7, the symmetrical case arises when the nuclei are *bosons* which have zero or integer spin (for example $^{16}O_2$, $^{14}N_2$) and the antisymmetrical case occurs when the nuclei are *fermions*, having half-integer spin (for example $^1H_2$, $^{19}F_2$, $^{127}I_2$).

On interchanging the nuclei 1 and 2, we see that $\Psi(\mathbf{R}, q) \to \Psi(-\mathbf{R}, q)$ while $\chi_N(1, 2) \to \chi_N(2, 1)$. Under these transformations, the factors Ψ and χ_N must each be either symmetrical or antisymmetrical, and we denote the corresponding functions by Ψ^S, Ψ^A, and χ_N^S, χ_N^A, respectively. Thus, when the nuclei are bosons, the total wave function Ψ_{tot} must be of the form $\Psi^S\chi_N^S$ or $\Psi^A\chi_N^A$, while for fermions, Ψ_{tot} must have the form $\Psi^S\chi_N^A$ or $\Psi^A\chi_N^S$.

Let us consider first the functions Ψ, which, neglecting spin–orbit coupling, can be written in the form of the product:

$$\Psi = \Phi_s\chi_{el}R^{-1}\psi_v\phi_{\mathcal{J}, M_{\mathcal{J}}, \Lambda} \qquad [10.51]$$

where Φ_s is the spatial part of the wave function for the orbital motion of the

electrons, χ_{el} is the spin function of the electrons, and ψ_v and $\phi_{\mathcal{J} M_{\mathcal{J}},\Lambda}$ are the nuclear vibrational and rotational wave functions, respectively. The function Φ_s is even or odd under the operation $\mathbf{R} \to -\mathbf{R}$. Indeed, we saw in Section 9.4 that for Σ states ($\Lambda = 0$) the levels Σ_g^+ and Σ_u^- are even while Σ_g^- and Σ_u^+ are odd. Moreover, if the degeneracy of the levels with $\Lambda \neq 0$ ($\Pi, \Delta, \ldots$) is removed by magnetic interactions (Λ-doubling) then one has levels Π_g^+, Π_u, Δ_g^+, Δ_u^- ... which are even, and levels Π_g^-, Π_u^+, Δ_g^-, Δ_u^+, ... which are odd. The second factor, χ_{el}, is clearly unaffected by the operation $\mathbf{R} \to -\mathbf{R}$, since it does not depend on the nuclear coordinates. The vibrational wave function ψ_v depends only on the magnitude R of the vector $\mathbf{R}$, and so is also unaltered when $\mathbf{R} \to -\mathbf{R}$. The rotational wave functions $\phi_{\mathcal{J},M_{\mathcal{J}},\Lambda}$, however, may be either even (if $\mathcal{J} = 0, 2, 4, \ldots$) or odd (if $\mathcal{J} = 1, 3, 5$) under the transformation $\mathbf{R} \to -\mathbf{R}$. The overall symmetrical (S) or antisymmetrical (A) character of the function Ψ is therefore given as follows:

	g+	g−	u+	u−
$\mathcal{J}$ even	S	A	A	S
$\mathcal{J}$ odd	A	S	S	A

We now turn to the nuclear spin function χ_N. According to the rules of addition of angular momenta, the spins $\mathbf{I}$ of the two nuclei form a resultant $\mathbf{T}$, which is the total nuclear spin of the molecule. The corresponding total nuclear spin quantum number T can therefore take on any one of the $2I + 1$ values $T = 0, 1, \ldots 2I - 1, 2I$, where I is the spin quantum number of the individual nuclei.

We begin by looking at the simple case of spinless nuclei, for which $I = T = 0$ (for example $^{16}O_2$). In this case χ_N is a constant and hence trivially symmetric in the interchange of the nuclei $1 \leftrightarrow 2$. Since the total wave function Ψ_{tot} has to be symmetrical, it follows that only even rotational levels can occur if the electronic wave function is even, and only odd rotational levels are present if the electronic wave function is odd. For example, the ground electronic state of $^{16}O_2$ is a $^3\Sigma_g^-$ state; its (g−) character requires that $\mathcal{J}$ should be odd. As a consequence, the ground state of the molecule is a $\mathcal{J} = 1$ state. Moreover, in the rotational Raman spectrum of molecules like $^{16}O_2$, half of the expected levels are missing. Also, in transitions between electronic Σ states of homonuclear diatomic molecules with spin-zero nuclei (say $\Sigma_g^+ \to \Sigma_u^+$ or $\Sigma_g \to \Sigma_u$) alternative lines in the rotational fine structure are missing, since $\Delta\mathcal{J} = \pm 1$ and transitions between symmetrical (S) and antisymmetrical (A) states are forbidden. If the nuclei are not identical, for example if one of the ^{16}O nuclei of the $^{16}O_2$ molecule is replaced by the isotope ^{17}O, then the missing transitions are restored. The appearance of these 'missing' lines is an important tool for determining the existence of isotopes like ^{17}O and ^{18}O.

Let us now analyse the case of the 'ordinary' hydrogen molecule $^1H_2$, which contains two protons. Since the spin of the proton is $I = \frac{1}{2}$, the total nuclear spin quantum number T can take on the values $T = 0$ or $T = 1$. When $T = 0$

the nuclear spin function is the singlet function

$$\chi_{\mathrm{N}}^{\mathrm{A}}(1, 2) = \frac{1}{\sqrt{2}}[\alpha(1)\beta(2) - \beta(1)\alpha(2)] \qquad [10.52]$$

which is antisymmetrical (A) with respect to the interchange $1 \leftrightarrow 2$ of the two protons. For $T = 1$ we have the triplet of nuclear spin functions

$$\chi_{\mathrm{N}}^{\mathrm{S}}(1, 2) = \begin{cases} \alpha(1)\alpha(2) \\ \dfrac{1}{\sqrt{2}}[\alpha(1)\beta(2) + \beta(1)\alpha(2)] \\ \beta(1)\beta(2) \end{cases} \qquad [10.53]$$

which are symmetric (S) with respect to the interchange of the two protons. Transitions between the $T = 0$ and $T = 1$ states occur extremely rarely, because such transitions could result only from very small perturbations involving the nuclear spins. Thus one can consider molecular hydrogen as consisting of two distinct species, namely *para hydrogen* for which $T = 0$ (antisymmetrical case) and *ortho hydrogen* where $T = 1$ (symmetrical case). Remembering that the electronic ground state of the hydrogen molecule is a Σ_g^+ state, and that the total function Ψ_{tot} must be antisymmetric in the interchange of the two protons, we see that in this state para hydrogen can only have rotational levels $J = 0, 2, 4 \ldots$ while ortho hydrogen can only possess rotational levels with odd values $J = 1, 3, 5, \ldots$. In statistical equilibrium, at room temperature, three times as many hydrogen molecules will be in $T = 1$ (ortho) states as in $T = 0$ (para) states. As a consequence, the alternate lines in the rotational fine structure show a 3 : 1 ratio of intensities. On cooling to temperatures of the order of 20 K, at which hydrogen is liquid, the molecules of para hydrogen are concentrated in their lowest allowed rotational state, $J = 0$, while those of ortho hydrogen go over to their lowest allowed rotational state $J = 1$. Since the coupling between the $T = 0$ and $T = 1$ states is extremely small, the ortho hydrogen molecules will remain in the $J = 1$ state for a long period of time. Eventually, after some months, the molecules will all be found in the $J = 0$ state of para hydrogen. If now the hydrogen is allowed to warm to room temperature, hydrogen gas will be obtained in the pure para form.

Finally, let us consider the general case of two identical nuclei with spin quantum number $I \neq 0$. The possible values of the Z component of spin of each nucleus are $M_I = -I, -I + 1, \ldots I - 1, I$; $(2I + 1)$ values in all. The total number of combinations of $M_I(1)$ and $M_I(2)$ is therefore $(2I + 1)^2$. Out of these, all the $2I + 1$ spin functions of the form $\chi_{M_I}(1)\,\chi_{M_I}(2)$ are symmetrical. One-half of the remaining $(2I + 1)^2 - (2I + 1)$ functions can be combined in symmetrical states

$$\chi_{\mathrm{N}}^{\mathrm{S}}(1, 2) = \frac{1}{\sqrt{2}}[\chi_{M_I}(1)\chi_{M_I'}(2) + \chi_{M_I'}(1)\chi_{M_I}(2)], \qquad M_I \neq M_I' \qquad [10.54]$$

and one-half in antisymmetrical states,

$$\chi_N^A(1, 2) = \frac{1}{\sqrt{2}} [\chi_{M_I}(1)\, \chi_{M_I'}(2) - \chi_{M_I'}(1)\, \chi_{M_I}(2)], \qquad M_I \neq M_I' \quad [10.55]$$

The total number of symmetrical states is then

$$2I + 1 + \tfrac{1}{2}[(2I + 1)^2 - (2I + 1)] = (2I + 1)(I + 1) \qquad [10.56]$$

and the total number of antisymmetrical states is

$$\tfrac{1}{2}[(2I + 1)^2 - (2I + 1)] = (2I + 1)I \qquad [10.57]$$

As a result, the ratio of intensities in the lines of the rotational fine structure of homonuclear diatomic molecules with nuclei of spin quantum number I is $(I + 1)/I$; for bosons this represents the relative statistical weights of the states Ψ^S to the states Ψ^A, while for fermions it represents the relative statistical weights of the states Ψ^A to the states Ψ^S. The observation of this alternation of strong and weak lines provides an important method for the determination of nuclear spins.

10.6 THE INVERSION SPECTRUM OF AMMONIA

The ammonia molecule NH_3 has the form of a pyramid, whose summit is occupied by the nitrogen atom, while the basis is an equilateral triangle formed by the three hydrogen atoms (see Fig. 10.16). At equilibrium, the distance NH is $d = 1.014$ Å, the distance of the nitrogen atom from the plane of the hydrogen is $z_0 = 0.38$ Å and the angle α between a NH bond and the threefold axis of symmetry of the molecule is $\alpha = 67°58'$.

There are many degrees of freedom in this system, involving electronic, vibrational and rotational motions, and resulting in a variety of energy levels and various quantum numbers to specify them. In this section, however, we shall assume that the NH_3 molecule is in its lowest electronic state and analyse a particular vibrational motion which is associated with the *inversion* of the molecule. To see how this comes about, let us consider one of the possible

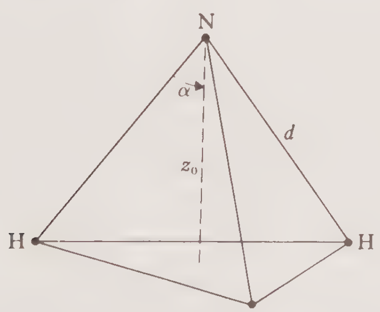

10.16 Schematic diagram of the ammonia molecule.

vibrational motions of the NH_3 molecule, analogous to the movement of an umbrella which is being opened and closed, and during which the angle α oscillates around its equilibrium position. Neglecting all other degrees of freedom, the potential energy of the system is then a function $V(z)$ of the algebraic distance z between the plane of the hydrogens and the nitrogen atom. The curve $V(z)$ is sketched in Fig. 10.17(a). Because the system is symmetric with respect to the plane $z = 0$ it is clear that the potential $V(z)$ must be an *even* function of z. The two minima of $V(z)$ correspond to symmetrical configurations of the molecule such that the nitrogen atom is located respectively above and below the plane of the hydrogen atoms (see Fig. 10.17(b)) at the equilibrium positions $z = \pm z_0 = \pm 0.38$ Å. We shall refer to these two configurations as the 'up' and 'down' configurations, respectively. The molecule can vibrate in the manner indicated above in either of the two potential wells, with the nitrogen atom on one side of the plane of the hydrogen atoms. The wave number corresponding to this vibrational motion is $\tilde{\nu} = 950\ \text{cm}^{-1}$, which is in the infra-red region.

As seen from Fig. 10.17(a), the potential $V(z)$ forms a barrier about $z = 0$. This barrier is due to the Coulomb repulsion between the nitrogen nucleus and the three protons. If it were of infinite height, the nitrogen atom would never be able to penetrate the plane of the hydrogens and be found on the other side of this plane. However, the barrier has a finite height $V_0 = 2072\ \text{cm}^{-1}$, so that there is a certain probability that the molecule will *invert* during the course of its vibrations, that is make transitions between the 'up' and 'down' configurations. It is important to emphasise that in the ground state ($v = 0$) as well as in the first excited state ($v = 1$) of the vibrational mode considered here, the energy of the molecule is lower than the potential height. As a result, the inversion of the molecule NH_3 in the vibrational states $v = 0$ and $v = 1$ is a classically forbidden (or hindered) motion which can only take place because of the quantum mechanical *tunnel effect*.

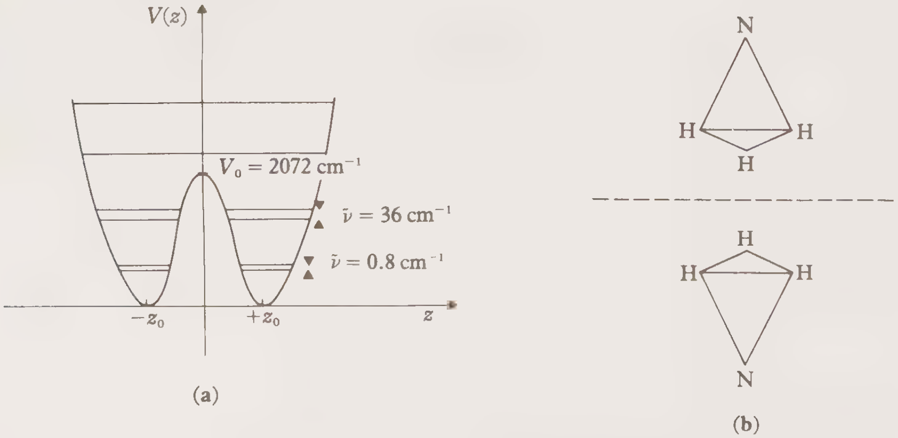

10.17 The potential well (a) for the inversion motion (b) of ammonia.

In order to understand the characteristics of this tunnelling motion let us write the one-dimensional Schrödinger equation for the motion along the Z axis, namely

$$-\frac{\hbar^2}{2m}\frac{d^2\psi(z)}{dz^2} + V(z)\psi(z) = E\psi(z) \qquad [10.58]$$

where m is an effective mass [3]. If the potential barrier between the two wells were of infinite height, the two wells would be totally 'disconnected' and the energy spectrum would consist of the same set of energy eigenvalues in each well. Thus, each energy eigenvalue of the system would be doubly degenerate, and the eigenfunctions corresponding to a given energy would be linear combinations of the (normalised) 'up' and 'down' wave functions $\hat{\psi}_u(z)$ and $\hat{\psi}_d(z)$ which vanish identically for $z \leqslant 0$ and $z \geqslant 0$, respectively. A pair of wave functions $\hat{\psi}_u$ and $\hat{\psi}_d$ is shown in Fig. 10.18(a) for the case of the lowest ($v = 0$) vibrational state.

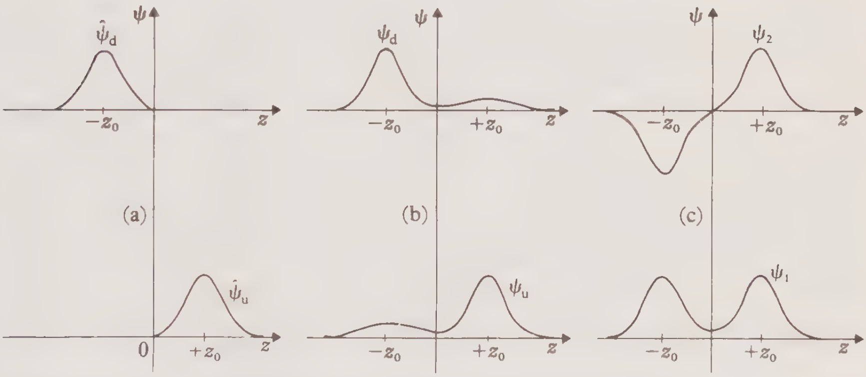

10.18 The wave functions (a) $\hat{\psi}_u$ and $\hat{\psi}_d$; (b) ψ_u and ψ_d; (c) ψ_1 and ψ_2.

In the real situation, with a finite barrier, there is a 'coupling' between the two wells which allows the inversion motion to occur. As a result, the degeneracy is removed, and the energy levels are split into *doublets* (see Problem 10.5). In the simple model considered here, the separation between the pair of energy levels forming a doublet depends only on the nature of the potential barrier and on the vibrational state of the molecule. As indicated in Fig. 10.17(a), the two energy levels forming the lowest ($v = 0$) doublet are separated by about 9.84×10^{-5} eV ($0.8\ \text{cm}^{-1}$), while the next ($v = 1$) lowest pair of levels are about 4.4×10^{-3} eV ($36\ \text{cm}^{-1}$) apart. We note that the inversion wave numbers $\tilde{\nu}(v = 0) = 0.8\ \text{cm}^{-1}$ and $\tilde{\nu}(v = 1) = 36\ \text{cm}^{-1}$ are much smaller than the wave

[3] Assuming that the distance between the hydrogen atoms remains constant during the motion, the effective mass m is then the reduced mass $m = 3M_HM_N/(3M_H + M_N)$, where M_H is the mass of the hydrogen atom and M_N that of the nitrogen atom.

number $\tilde{\nu} = 950\ \text{cm}^{-1}$ corresponding to the vibrational motion, since inversion is considerably inhibited by the presence of the potential barrier.

In what follows we shall focus our attention on the lowest doublet ($v = 0$) which we shall treat as a two-level system. It is clear from the above discussion that since the potential barrier is finite we do not have rigorous 'up' and 'down' eigenfunctions $\hat{\psi}_u(z)$ and $\hat{\psi}_d(z)$ vanishing identically for $z \leqslant 0$ and $z \geqslant 0$, respectively. Instead, we define the corresponding (normalised) wave functions $\psi_u(z)$ and $\psi_d(z)$ to be those for which the nitrogen atom is *most probably* located above or below the plane of the hydrogen. These wave functions are sketched in Fig. 10.18(b). It is important to realise that because the two wells are coupled, the functions ψ_u and ψ_d are *not* energy eigenfunctions, and are not orthogonal to each other. Indeed, the true energy eigenfunctions must be either symmetric or antisymmetric with respect to the inversion operation $z \to -z$. In terms of ψ_u and ψ_d, the normalised energy eigenfunctions are therefore given by

$$\psi_1 = \frac{1}{\sqrt{2}}(\psi_u + \psi_d) \qquad [10.59a]$$

and

$$\psi_2 = \frac{1}{\sqrt{2}}(\psi_u - \psi_d) \qquad [10.59b]$$

The symmetric wave function ψ_1 corresponds to the lowest energy E_1 of the doublet, while the antisymmetric wave function ψ_2 corresponds to the higher energy E_2. Both functions ψ_1 and ψ_2 are shown in Fig. 10.18(c).

Having obtained the energy eigenfunctions $\psi_1(z)$ and $\psi_2(z)$ we may write the general time-dependent wave function of our two-level problem as (see [2.85])

$$\Psi(z, t) = c_1\psi_1(z)e^{-(i/\hbar)E_1 t} + c_2\psi_2(z)e^{-(i/\hbar)E_2 t} \qquad [10.60]$$

where

$$E_2 = E_1 + \Delta E \qquad [10.61]$$

and $\Delta E = 9.84 \times 10^{-5}$ eV is the energy splitting of the doublet. Let us assume that at time $t = 0$ the wave function describing the system is ψ_u, so that the nitrogen atom is most probably to be found above the plane of the hydrogen at that time. Using [10.59] and [10.60], we then have

$$\Psi(z, 0) = c_1\psi_1(z) + c_2\psi_2(z) = \psi_u(z) = \frac{1}{\sqrt{2}}[\psi_1(z) + \psi_2(z)] \qquad [10.62]$$

so that

$$c_1 = c_2 = \frac{1}{\sqrt{2}} \qquad [10.63]$$

Substituting [10.63] into [10.60] and using [10.61], we see that the function

$\Psi(z, t)$ will evolve in time according to

$$\Psi(z, t) = \frac{1}{\sqrt{2}}[\psi_1(z)e^{-(i/\hbar)E_1 t} + \psi_2(z)e^{-(i/\hbar)E_1 t}\, e^{-(i/\hbar)\Delta E t}]$$

$$= \frac{1}{\sqrt{2}}[\psi_1(z) + \psi_2(z)\, e^{-2\pi i \nu t}]\, e^{-(i/\hbar)E_1 t} \qquad [10.64]$$

where we have written $\Delta E = h\nu$. At the time $t = 1/2\nu$ the wave function [10.64] is given by

$$\Psi(z, t = 1/2\nu) = \frac{1}{\sqrt{2}}[\psi_1(z) - \psi_2(z)]e^{-(i/\hbar)E_1 t}$$

$$= \psi_d(z)e^{-(i/\hbar)E_1 t} \qquad [10.65]$$

so that

$$|\Psi(z, t = 1/2\nu)|^2 = |\psi_d(z)|^2 \qquad [10.66]$$

and the nitrogen atom is most probably to be found under the plane of the hydrogen at $t = 1/2\nu$. Since the energy difference $\Delta E = h\nu \simeq 9.84 \times 10^{-5}$ eV corresponds to a frequency $\nu \simeq 23\,800$ MHz, we see that the time required for the NH_3 molecule to invert is $t = 1/2\nu \simeq 2.1 \times 10^{-11}$ s.

The existence of the energy doublets of the ammonia molecule was first inferred from the analysis of its infra-red vibrational–rotational and pure rotational spectra. However, radiative transitions between the two states forming a doublet can also occur, the corresponding lines being in the microwave region. In 1934, the progress made in radio-frequency techniques allowed C. E. Cleeton and N. H. Williams to observe directly a peak in the absorption spectrum at a wavelength $\lambda \simeq 1.25$ cm which corresponds to the inversion frequency $\nu \simeq 23\,800$ MHz of the lowest doublet. The experiment of Cleeton and Williams opened the new field of microwave spectroscopy [4], and eventually made possible the development of the *maser*. Of course, it should be realised that, in common with all molecular vibrational motions, the inversion spectrum of NH_3 contains a fine and hyperfine structure due respectively to the rotational motion and to magnetic and quadrupole interactions involving the nuclei.

PROBLEMS

10.1 Show that the ratio of the number of molecules in the rotational level $\mathcal{J}$ to that in the lowest level, in a gas at temperature T, is $R = (2\mathcal{J} + 1) \exp[(E_0 - E_{\mathcal{J}})/kT]$ where $E_{\mathcal{J}} = B\mathcal{J}(\mathcal{J} + 1)$. Make a graph of this expression as a function of $\mathcal{J}$ for $H^{35}Cl$ at room temperature. Show that

[4] A comprehensive treatment of microwave spectroscopy may be found in Townes and Schawlow (1955).

$R(J)$ has a maximum and obtain the relative intensities of absorption lines in a pure rotational spectrum. $\tilde{B} = B/hc = 10.6\ \text{cm}^{-1}$ for HCl.

10.2 Find the ratio of the number of molecules in the first vibrational level to the number in the lowest level, in a gas at temperature T. For (a) $H^{35}Cl$ and (b) $D^{35}Cl$ calculate this ratio at 300 K, 1500 K and 3000 K. $\tilde{\nu}_0 = 2990\ \text{cm}^{-1}$ for $H^{35}Cl$.

10.3 In the fundamental band of $^{12}C^{16}O$ the spacing of the lines is found to be constant with the value $3.86\ \text{cm}^{-1}$. The band is centred on a missing line at $2170.21\ \text{cm}^{-1}$. Calculate the rotational constant $\tilde{B}$, the internuclear separation R_0 and the force constant of the vibrational motion.

10.4 In the $^{14}N_2$ molecule the ground state $X^1\Sigma_g^+$ and the excited state $b'\ ^1\Sigma_u^+$ have the following constants:

	$\tilde{\nu}_0$	$(\beta\tilde{\nu}_0)$	$\tilde{B}$
X	2359.6	14.456	2.010
b′	751.7	4.82	1.145

where all values are given in units of cm^{-1} and $\tilde{\nu}_0 = \nu_0/c$, $(\beta\tilde{\nu}_0) = \beta\nu_0/c$ and $\tilde{B} = B/hc$.

The wave number of the electronic transition is $\tilde{\nu}_{s's} = \nu_{s's}/c = 103678.9\ \text{cm}^{-1}$.

(a) Construct a Deslandres table for the transitions between the vibrational states $v' = 0, 1, 2, 3, 4, 5$ and $v = 0, 1, 2, 3, 4, 5$.

(b) Calculate the wave numbers of the first few members of the R and P branches for the transition $v' = 0$ to $v = 0$.

(c) Draw the Fortrat parabola by using the variable $m = -J - 1$ for the R branch and $m = J$ for the P branch. Determine whether the band is shaded to the red or to the violet and find the position of the band head.

10.5 Consider the one-dimensional Schrödinger equation [10.58] which describes the inversion motion of ammonia. Compare the solutions in two cases:

(a) An infinite barrier separating two wells, so that

$$\begin{aligned} V(z) &= \infty \qquad & z < -L,\ -a < z < a,\ z > L \\ V(z) &= 0 \qquad & -L < z < -a,\ a < z < L \end{aligned}$$

(b) A finite barrier separating the two wells:

$$\begin{aligned} V(z) &= \infty \qquad & z < -L \quad \text{and} \quad z > -L \\ V(z) &= V_0 \qquad & -a < z < a \\ V(z) &= 0 \qquad & -L < z < -a \quad \text{and} \quad a < z < L. \end{aligned}$$

Show that the (degenerate) energy levels of case (a) are each split into two non-degenerate levels in case (b).

11 Atomic collisions: basic concepts and potential scattering

Atomic collisions phenomena are of fundamental importance in atomic and molecular physics and play also an important role in other fields such as astrophysics, chemistry, plasma physics and laser physics. Basically, these phenomena involve collisions between an 'elementary particle' (photon, electron, . . .) and an atomic system (atom, ion, molecule) or between two atomic systems. We have already discussed in previous chapters various photon–atom (molecule) collision processes, such as the photoelectric effect, the Compton effect and Raman scattering. In the next chapter, we shall study electron–atom collisions while Chapter 13 is devoted to atom (ion)–atom collisions. However, before analysing these complex collision processes, we shall introduce in this chapter various basic definitions, and discuss in some detail the simple problem of the quantum theory of scattering by a centre of force [1].

11.1 TYPES OF COLLISIONS, CHANNELS, THRESHOLDS AND CROSS-SECTIONS

Let us consider a typical atomic collision experiment [2] which is illustrated schematically in Fig. 11.1. A homogeneous, well-collimated beam of mono-energetic particles A is directed towards a target containing the scatterers B. We shall assume that the experimental conditions have been chosen in such a way that each target scatterer acts as if it were alone [3]. After the collision between a beam particle A and a target particle B, some or all the particles emerging from the interaction region are registered by detectors, which are placed outside the path of the incident beam, so that undeflected particles are not recorded. Several

[1] More detailed accounts of the atomic scattering theory discussed in Chapters 11, 12 and 13 can be found in the books of Bransden (1970) and Joachain (1979).

[2] The type of experiment shown in Fig. 11.1 in which a beam of particles is scattered by a stationary target is not the only possible kind. It is often more convenient to study the scattering of one beam of particles by another, for example, and more complicated experiments are concerned with two or more successive scattering processes.

[3] Single scattering conditions can be achieved by making the target sufficiently thin. Coherent scattering as in electron diffraction by crystals will not be considered here.

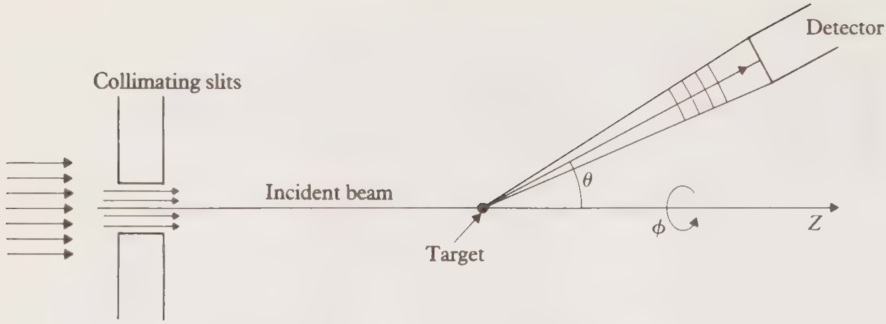

11.1 Schematic diagram of a scattering experiment.

processes can occur:

1. The two particles A and B are scattered without change in their internal structure. That is,

$$\mathrm{A} + \mathrm{B} \rightarrow \mathrm{A} + \mathrm{B} \tag{11.1}$$

   This is known as *elastic scattering*.
2. The two particles A and (or) B undergo a change of their internal quantum state during the collision. For example

$$\mathrm{A} + \mathrm{B} \rightarrow \mathrm{A} + \mathrm{B}' \tag{11.2}$$

   where B′ denotes an excited state of the particle B. Such processes are called *inelastic collisions*.
3. The composite system (A + B) splits into two particles C and D, different from A and B,

$$\mathrm{A} + \mathrm{B} \rightarrow \mathrm{C} + \mathrm{D} \tag{11.3}$$

   or into more than two particles:

$$\mathrm{A} + \mathrm{B} \rightarrow \mathrm{C}_1 + \mathrm{C}_2 + \cdots \mathrm{C}_n \tag{11.4}$$

   These collision processes are known as *reactions*.

Channels

A channel is a possible mode of fragmentation of the composite system (A + B) during the collision. It is characterised by the number and the nature of the fragments into which the system (A + B) can be decomposed. In elastic collisions the two colliding particles A and B remain in the initial channel, while inelastic collisions or reactions are processes leading from a given initial channel to a different final channel. A channel is said to be *open* if the corresponding collision is allowed by known conservation laws (such as energy conservation); otherwise it is said to be closed.

Thresholds

Let us consider a general reaction of the type [11.4], and denote by w_A, w_B, w_1, w_2, . . . w_n the internal energies of the particles A, B, C_1, C_2, . . . C_n. Working in the *centre of mass* (CM) *system* (in which the centre of mass of the composite system (A + B) is at rest) we write the energy conservation law as

$$T_i + w_A + w_B = T_f + w_1 + w_2 \cdots w_n \qquad [11.5]$$

where T_i and T_f are the initial and final kinetic energies, respectively. This relation may also be written as

$$T_f = T_i + Q_{if} \qquad [11.6]$$

where

$$Q_{if} = w_A + w_B - (w_1 + w_2 + \cdots w_n) \qquad [11.7]$$

is the change in internal energy which has occurred.

A necessary condition for the reaction to take place is that $T_f \geqslant 0$. As a result, if $Q_{if} \geqslant 0$ the reaction is always allowed from the point of view of energy conservation (it can be forbidden by other conservation laws) and is called *exothermic*. On the other hand, if $Q_{if} < 0$, the reaction is said to be *endothermic*. It can only occur if

$$T_i \geqslant T_i^t \qquad [11.8]$$

where $T_i^t = -Q_{if}$ is known as the *threshold* of the reaction (in the CM system). In the *laboratory system* – where the target particle B is at rest before the collision, the corresponding threshold energy $(T_i^t)_L$ is given by (see [A2.9])

$$(T_i^t)_L = \frac{m_A + m_B}{m_B} T_i^t \qquad [11.9]$$

where m_A and m_B are the masses of the particles A and B, respectively.

In order to illustrate the notions of channels and thresholds introduced above, let us consider the scattering of electrons by hydrogen atoms initially in the ground state 1s. We shall take the mass of the proton to be infinite with respect to the electron mass, so that the centre of mass and laboratory systems coincide. For incident electron energies $E(= T_i)$ below the threshold energy for excitation of the $n = 2$ levels of hydrogen (that is for $E < 10.2$ eV) the only open final channel corresponds to the elastic scattering process:

$$e^- + H(1s) \rightarrow e^- + H(1s)$$

For incident electron energies E ranging between the $n = 2$ excitation threshold (10.2 eV) and the ionisation threshold at 13.6 eV, the inelastic channels $e^- + H^\star$ – where $H^\star$ denotes an excited hydrogen atom – open successively, corresponding to the inelastic collisions

$$e^- + H(1s) \rightarrow e^- + H^\star$$

Finally, if $E \geqslant 13.6$ eV, the ionisation channel ($H^+ + 2e^-$) becomes open, corresponding to the ionisation reaction

$$e^- + H(1s) \rightarrow H^+ + 2e^-$$

Cross-sections

The results of collision experiments are usually expressed in terms of quantities called *cross-sections*. Generalising the definition given in Appendix 1 for the simple case of scattering by a centre of force, we shall define *the cross-section for a certain type of event in a given collision as the ratio of the number of events of this type per unit time and per unit scatterer, to the flux of the incident particles with respect to the target.* Cross-sections are independent of the incident flux so that we may choose this number to be one, and cross-sections can also be defined as *transition probabilities per unit time, per unit target scatterer and per unit flux of the incident particles with respect to the target* [4].

Consider for example the reaction [11.3]. Let N_A be the flux of incident particles relative to the target (defined as the number of particles A crossing per unit time a unit area placed at right angles to the direction of the incident beam and at rest with respect to the target) and let n_B be the number of particles B within the target interacting with the incident beam. Calling N_{tot}^{C} the total number of particles C which, together with the particles D, have been produced per unit time in the collision between the beam particles A and the target particles B, we have

$$N_{tot}^{C} = N_A n_B \sigma_{tot}^{C} \qquad [11.10]$$

where σ_{tot}^{C} is the total cross-section for the reaction [11.3]. Total cross-sections for elastic scattering, inelastic scattering and reactions of the type [11.4] may be defined in a similar way. Finally, if we denote by N_{tot} the total number of particles A which have interacted per unit time with target scatterers, we may define a total (complete) cross-section σ_{tot} by the relation

$$N_{tot} = N_A n_B \sigma_{tot} \qquad [11.11]$$

If only elastic scattering between the particles A and B can occur, then σ_{tot} is just equal to the total elastic cross-section σ_{tot}^{el}. However, when other channels than the elastic one are open, then σ_{tot} is the sum of the total cross-sections corresponding to each of the open channels.

It is apparent from the foregoing discussion that total cross-sections have the dimensions of an area. Since in atomic units (a.u.) the unit of length is the first Bohr radius $a_0 \simeq 5.29 \times 10^{-11}$ m, it is convenient to express atomic cross-sections in units of $a_0^2 = 2.80 \times 10^{-21}$ m^2. Units of $\pi a_0^2 = 8.80 \times 10^{-21}$ m^2 are also often used for atomic total cross-sections.

[4] This is the same definition as that used for the absorption and stimulated emission of radiation in Chapter 4.

In order to define *differential* cross-sections, we must choose a coordinate system or reference framework. Two convenient choices are the *laboratory* system and *centre of mass* system which have been introduced above. Experiments are often, but not always [5], performed in the laboratory system, while calculations are usually carried out in the CM system, where the three degrees of freedom attached to the centre of mass of the system (A + B) may be ignored. The relationship between the laboratory and centre of mass differential cross-sections is established in Appendix 2 for the simple case of elastic scattering. The results obtained in Appendix 2 can be generalised in a straightforward way (Problem 11.1) to inelastic collisions and reactions involving two particles (complex or not) in the initial or final states.

11.2 POTENTIAL SCATTERING. GENERAL FEATURES

In this and the next three sections, we shall study the simplest collision problem, which is the *non-relativistic scattering of a spinless particle by a potential* $V(\mathbf{r})$. From our discussion in Section 2.7 it is apparent that this problem is equivalent to that of the elastic collision between two structureless particles, treated in their centre of mass system.

The stationary state wave function for scattering

We start from the Schrödinger equation

$$\left[-\frac{\hbar^2}{2m}\nabla^2 + V(\mathbf{r})\right]\Psi(\mathbf{r}, t) = i\hbar\frac{\partial}{\partial t}\Psi(\mathbf{r}, t) \qquad [11.12]$$

where m denotes the mass of the particle. The potential is taken to be real and independent of the time, in which case the equation [11.12] has stationary solutions of the form

$$\Psi(\mathbf{r}, t) = \psi(\mathbf{r})e^{-iEt/\hbar} \qquad [11.13]$$

where $\psi(\mathbf{r})$ is a solution of the time-independent Schrödinger equation

$$\left[-\frac{\hbar^2}{2m}\nabla^2 + V(\mathbf{r})\right]\psi(\mathbf{r}) = E\psi(\mathbf{r}) \qquad [11.14]$$

and E, the energy of the particle, has the well-defined value

$$E = \frac{p^2}{2m} = \frac{\hbar^2k^2}{2m} = \frac{1}{2}mv^2 \qquad [11.15]$$

[5] Crossed beam experiments in which two beams, inclined at a certain angle, interact, are neither in the centre of mass nor the laboratory systems, but the measured quantities are easily transformed to one of the standard reference systems.

Here

$$p = |\mathbf{p}_i| = |\mathbf{p}_f|, \qquad k = |\mathbf{k}_i| = |\mathbf{k}_f|, \qquad v = |\mathbf{v}_i| = |\mathbf{v}_f| \qquad [11.16]$$

are respectively the magnitudes of the initial (or final) momentum, wave vector and velocity of the particle, with

$$\mathbf{p}_i = \hbar\mathbf{k}_i = m\mathbf{v}_i, \qquad \mathbf{p}_f = \hbar\mathbf{k}_f = m\mathbf{v}_f \qquad [11.17]$$

It is convenient to introduce the reduced potential

$$U(\mathbf{r}) = \frac{2m}{\hbar^2} V(\mathbf{r}) \qquad [11.18]$$

so that [11.14] may be rewritten as

$$[\nabla^2 + k^2 - U(\mathbf{r})]\psi(\mathbf{r}) = 0 \qquad [11.19]$$

In what follows we shall assume that the potential vanishes faster than $1/r$ for large r. In this case, the scattering wave function (which we denote by $\psi_{\mathbf{k}_i}$) satisfies at large r the free-particle Schrödinger equation

$$(\nabla^2 + k^2)\psi(\mathbf{r}) = 0 \qquad [11.20]$$

and in this region we can write

$$\psi_{\mathbf{k}_i}(\mathbf{r}) \underset{r\to\infty}{\sim} \psi_{\text{inc}}(\mathbf{r}) + \psi_{\text{sc}}(\mathbf{r}) \qquad [11.21]$$

where ψ_{inc} represents the incident beam of particles and ψ_{sc} represents the scattered particles. Since the incident particles are monoenergetic and are travelling in the direction $\hat{\mathbf{k}}_i$, which we take to be parallel to the Z axis, the incident beam can be represented by the plane wave

$$\psi_{\text{inc}}(\mathbf{r}) = A\exp(\mathrm{i}\mathbf{k}_i \cdot \mathbf{r}) = A\exp(ikz) \qquad [11.22]$$

where A is an arbitrary normalisation constant. Since the number of particles per unit volume is $|\psi_{\text{inc}}|^2 = A^2$ and each particle has the velocity $v = \hbar k/m$, the incident flux F is

$$F = v|A|^2 \qquad [11.23]$$

A plane wave is of infinite extent in a transverse direction, but in any real experiment the beam is collimated and has a finite transverse extension. However the transverse dimensions of the beam, which may be of the order of 1 cm to 1 mm, are sufficiently large for the corresponding uncertainty in momentum to be negligible and for the wave function to be described accurately by a plane wave over the scattering region (which, for atoms, is of the order $\sim 10^{-8}$ cm).

Far from the scatterer, the scattered wave function must represent an outward flow of particles from the scattering centre. It has the form of an *outgoing* spherical wave, the amplitude of which depends on the direction of $\mathbf{r}$

and on the energy E (i.e. on k). We write

$$\psi_{\text{sc}}(\mathbf{r}) = Af(k, \theta, \phi)\frac{e^{ikr}}{r} \qquad [11.24]$$

where (θ, ϕ) are the polar angles of $\mathbf{r}$, with respect to the Z axis (the incident direction) and f is known as the *scattering amplitude*. The function ψ_{sc} is an asymptotic solution (large r) of the free-particle Schrödinger equation, so that in the large r region the wave function $\psi_{\mathbf{k}_i}(\mathbf{r})$ must satisfy the asymptotic boundary condition

$$\psi_{\mathbf{k}_i}(\mathbf{r}) \underset{r\to\infty}{\sim} A\left[e^{i\mathbf{k}_i\cdot\mathbf{r}} + f(k, \theta, \phi)\frac{e^{ikr}}{r}\right] \qquad [11.25]$$

The cross-section

Using the general definition of cross-sections, given in Section 11.1, we introduce a *differential cross-section*, $d\sigma/d\Omega$. We imagine that the detector subtends at the scattering centre a small solid angle $d\Omega$ and is placed in the direction (θ, ϕ) at a distance r. Then $d\sigma/d\Omega$ is defined as the ratio of the outgoing flux of particles passing through the area $r^2\, d\Omega$ to the incident flux. The detector is placed outside the incident beam, so that only scattered particles are recorded and the corresponding flux can be calculated from ψ_{sc} alone.

The probability current density $\mathbf{j}$ has been obtained in Section 2.2 (see [2.50]). For a stationary state, it is given by

$$\mathbf{j} = \frac{\hbar}{2mi}\left[\psi^\star(\nabla\psi) - (\nabla\psi^\star)\psi\right] \qquad [11.26]$$

The gradient operator in spherical coordinates is

$$\nabla = \frac{\partial}{\partial r}\hat{\mathbf{r}} + \frac{1}{r}\frac{\partial}{\partial\theta}\hat{\boldsymbol{\theta}} + \frac{1}{r\sin\theta}\frac{\partial}{\partial\phi}\hat{\boldsymbol{\phi}} \qquad [11.27]$$

so that the radial current is given by

$$\mathbf{j}\cdot\hat{\mathbf{r}} = \frac{\hbar}{2mi}\left(\psi^\star\frac{\partial\psi}{\partial r} - \frac{\partial\psi^\star}{\partial r}\psi\right) \qquad [11.28]$$

If we substitute the expression [11.24] for ψ_{sc} into [11.28], we find that at large r the corresponding radial current, $\mathbf{j}_{\text{sc}}\cdot\hat{\mathbf{r}}$, is

$$\mathbf{j}_{\text{sc}}\cdot\hat{\mathbf{r}} = |A|^2 v|f(k, \theta, \phi)|^2/r^2 \qquad [11.29]$$

where terms of higher order in $1/r$ have been neglected. The outgoing flux per unit solid angle is just $(j_{\text{sc}}r^2\, d\Omega)/d\Omega$, so that the differential cross-section is

$$\frac{d\sigma}{d\Omega} = |f(k, \theta, \phi)|^2 \qquad [11.30]$$

where we have used [11.23] for the incident flux.

The total cross-section for elastic scattering is obtained by integrating over all solid angles, namely

$$\sigma_{\text{tot}} = \int \frac{\mathrm{d}\sigma}{\mathrm{d}\Omega}\,\mathrm{d}\Omega$$
$$= \int_0^{\pi} \sin\theta\,\mathrm{d}\theta \int_0^{2\pi} \mathrm{d}\phi\,\frac{\mathrm{d}\sigma}{\mathrm{d}\Omega} \qquad [11.31]$$

We notice that the cross-section is determined by the amplitude of the asymptotic wave function, which corresponds to the experimental conditions because any detector will be placed at a very large distance from the scattering region, compared with atomic dimensions.

The optical theorem

Since the total number of particles entering the scattering region per unit time must be balanced by the number leaving it per unit time, we must have

$$r^2 \int (\mathbf{j}\cdot\hat{\mathbf{r}})\,\mathrm{d}\Omega = 0 \qquad [11.32]$$

where the integration is over all angles and $\mathbf{j}\cdot\hat{\mathbf{r}}$ is the complete radial current, rather than the outgoing current $\mathbf{j}_{\text{sc}}\cdot\hat{\mathbf{r}}$. The complete radial current is computed by substituting [11.21] into [11.28], which gives up to terms of order $(1/r^3)$

$$\mathbf{j}\cdot\hat{\mathbf{r}} = |A|^2 \frac{\hbar}{2mi}\left[\mathrm{e}^{-ikr\cos\theta} + f^{\star}(k,\theta,\phi)\frac{\mathrm{e}^{-ikr}}{r}\right]$$
$$\times\left[ik\cos\theta\,\mathrm{e}^{ikr\cos\theta} + f(k,\theta,\phi)ik\frac{\mathrm{e}^{ikr}}{r}\right] + \text{c.c.} \qquad [11.33]$$

where c.c. denotes the complex conjugate and we have used the fact that $z = r\cos\theta$. By inserting this expression into [11.32], one finds (Problem 11.2)

$$\operatorname{Im} f(k, \theta = 0) = \frac{k}{4\pi}\int |f|^2\,\mathrm{d}\Omega$$

or, using [11.30]

$$\sigma_{\text{tot}} = \frac{4\pi}{k}\operatorname{Im} f(k, \theta = 0) \qquad [11.34]$$

This relation is known as the *optical theorem* and expresses *conservation of the probability flux*.

11.3 THE METHOD OF PARTIAL WAVES

We now turn to the problem of calculating the scattering amplitude, from which the cross-section can be found from [11.30]. We shall first consider the case of a *central* potential $V(r)$, which depends only on the magnitude r of the

vector $\mathbf{r}$. As we have seen in Section 2.6 the Hamiltonian operator

$$H = -\frac{\hbar^2}{2m}\nabla^2 + V(r) \qquad [11.35]$$

then commutes with the operators $\mathbf{L}^2$ and L_z, and the Schrödinger equation [11.14] is separable in spherical polar coordinates. In addition, the problem also possesses symmetry about the incident direction (which coincides with our Z axis), so that the wave function $\psi_{\mathbf{k}_i}$ – and hence the scattering amplitude and the differential cross-section – is independent of the azimuthal angle ϕ. The wave function $\psi_{\mathbf{k}_i}$ may therefore be expanded in a series of Legendre polynomials (which form a complete set in the interval $-1 \leqslant \cos\theta \leqslant +1$) as

$$\psi_{\mathbf{k}_i}(k, r, \theta) = \sum_{l=0}^{\infty} R_l(k, r) P_l(\cos\theta) \qquad [11.36]$$

The radial equations

The equations satisfied by the radial functions $R_l(k, r)$ can be found as in Section 2.6. We have

$$\left[\frac{\mathrm{d}^2}{\mathrm{d}r^2} + \frac{2}{r}\frac{\mathrm{d}}{\mathrm{d}r} - \frac{l(l+1)}{r^2} - U(r) + k^2\right] R_l(k, r) = 0 \qquad [11.37]$$

where $U(r)$ is given by [11.18]. For the special case of the Coulomb interaction, these are the same equations as we found in [3.6]; but in that case, we were looking for solutions of negative energy. As shown in Section 2.6, the equations [11.37] can be simplified by introducing the new radial functions

$$u_l(k, r) = rR_l(k, r) \qquad [11.38]$$

which satisfy the equations

$$\left[\frac{\mathrm{d}^2}{\mathrm{d}r^2} - \frac{l(l+1)}{r^2} - U(r) + k^2\right] u_l(k, r) = 0 \qquad [11.39]$$

There is no loss of generality in assuming $u_l(k, r)$ to be real since both the real and imaginary parts of a complex $u_l(k, r)$ would separately satisfy the radial equations [11.39].

For potentials which are less singular than r^{-2} at the origin, the radial function $u_l(k, r)$ can be expanded in a power series,

$$u_l(k, r) = \sum_n a_n r^n \qquad [11.40]$$

and the examination of the indicial equation [6] shows that there are two solutions, one *regular* at the origin, which behaves like

$$u_l(k, r) \underset{r\to 0}{\sim} r^{l+1} \qquad [11.41a]$$

[6] Series solutions of differential equations are described in Mathews and Walker (1973).

and one *irregular*, such that

$$u_l(k, r) \underset{r\to 0}{\sim} r^{-l} \qquad [11.41b]$$

In order to describe a physical scattering situation, the wave function $\psi_{\mathbf{k}_i}$ must be finite everywhere, so that we must choose for $u_l(k, r)$ the regular solution which behaves like r^{l+1} at the origin. It is clear from [11.38] that the corresponding regular radial function $R_l(k, r)$ behaves like r^l as $r \to 0$.

Let us now examine the behaviour of the functions $R_l(k, r)$ or $u_l(k, r)$ for large r. We shall assume that the potential may be neglected when r is larger than a given value a. In this *external region* $r > a$ the equation [11.37] then reduces to the free particle equation

$$\left[\frac{\mathrm{d}^2}{\mathrm{d}\rho^2} + \frac{2}{\rho}\frac{\mathrm{d}}{\mathrm{d}\rho} + \left(1 - \frac{l(l+1)}{\rho^2}\right)\right] R_l(\rho) = 0 \qquad [11.42]$$

where we have set $\rho = kr$. This equation is known as the *spherical Bessel differential equation*. The general solution of this equation is a linear combination of the spherical Bessel function

$$j_l(\rho) = \left(\frac{\pi}{2\rho}\right)^{1/2} \mathcal{J}_{l+1/2}(\rho) \qquad [11.43]$$

and the spherical Neumann function

$$n_l(\rho) = (-1)^{l+1}\left(\frac{\pi}{2\rho}\right)^{1/2} \mathcal{J}_{-l-1/2}(\rho) \qquad [11.44]$$

where $\mathcal{J}_\nu(\rho)$ is a Bessel function of order ν. We have already encountered the spherical Bessel functions j_l in Section 2.6 when we discussed the expansion of a plane wave in Legendre polynomials, and we shall return to this point shortly. We recall here for convenience the expressions of the first three spherical Bessel functions, and also give the first three spherical Neumann functions, namely

$$\begin{aligned}
j_0(\rho) &= \frac{\sin\rho}{\rho} \\
n_0(\rho) &= -\frac{\cos\rho}{\rho} \\
j_1(\rho) &= \frac{\sin\rho}{\rho^2} - \frac{\cos\rho}{\rho} \\
n_1(\rho) &= -\frac{\cos\rho}{\rho^2} - \frac{\sin\rho}{\rho} \\
j_2(\rho) &= \left(\frac{3}{\rho^3} - \frac{1}{\rho}\right)\sin\rho - \frac{3}{\rho^2}\cos\rho \\
n_2(\rho) &= -\left(\frac{3}{\rho^3} - \frac{1}{\rho}\right)\cos\rho - \frac{3}{\rho^2}\sin\rho
\end{aligned} \qquad [11.45]$$

The behaviour of the functions j_l and n_l for small ρ is given by

$$j_l(\rho) \underset{\rho\to 0}{\sim} \frac{\rho^l}{(2l+1)!!}\left[1 - \frac{\rho^2/2}{1!(2l+3)} + \frac{(\rho^2/2)^2}{2!(2l+3)(2l+5)} - \cdots\right] \tag{11.46a}$$

and

$$n_l(\rho) \underset{\rho\to 0}{\sim} -\frac{(2l-1)!!}{\rho^{l+1}}\left[1 - \frac{\rho^2/2}{1!(1-2l)} + \frac{(\rho^2/2)^2}{2!(1-2l)(3-2l)} - \cdots\right] \tag{11.46b}$$

where

$$(2l-1)!! = 1.3.5\cdots(2l-1); \qquad (2l-1)!! = 1 \quad \text{for} \quad l = 0$$

Thus the spherical Bessel function j_l, which is proportional to ρ^l as $\rho \to 0$, is a regular solution of [11.42]. On the other hand, the function n_l, which has a pole of order $(l+1)$ at $\rho = 0$ is an irregular solution of [11.42].

For ρ somewhat larger than $l(l+1)$ one may use the asymptotic formulae

$$j_l(\rho) \underset{\rho\to\infty}{\to} \frac{1}{\rho}\sin(\rho - l\pi/2) \tag{11.47a}$$

and

$$n_l(\rho) \underset{\rho\to\infty}{\to} -\frac{1}{\rho}\cos(\rho - l\pi/2) \tag{11.47b}$$

Let us now return to the radial functions $R_l(k, r)$ and $u_l(k, r)$. We see that in the external region $r > a$, $R_l(k, r)$ must be a linear combination of $j_l(kr)$ and $n_l(kr)$

$$R_l(k, r) = \frac{u_l(k, r)}{r} = B_l(k)j_l(kr) + C_l(k)n_l(kr) \tag{11.48}$$

where $B_l(k)$ and $C_l(k)$ are real 'constants of integration' which are independent of r. Using the asymptotic formulae [11.47], we see that

$$\begin{aligned} R_l(k, r) &= \frac{u_l(k, r)}{r} \\ &\underset{r\to\infty}{\sim} B_l(k)\frac{\sin(kr - l\pi/2)}{kr} - C_l(k)\frac{\cos(kr - l\pi/2)}{kr} \end{aligned} \tag{11.49}$$

It is convenient to set

$$A_l(k) = [B_l^2(k) + C_l^2(k)]^{1/2} \tag{11.50a}$$

and

$$\tan \delta_l(k) = -C_l(k)/B_l(k) \qquad [11.50b]$$

so that we obtain for $R_l(k, r)$ the simple asymptotic behaviour

$$R_l(k, r) = \frac{u_l(k, r)}{r} \underset{r\to\infty}{\sim} \frac{A_l(k)}{kr} \sin[kr - l\pi/2 + \delta_l(k)] \qquad [11.51]$$

It may be shown (Problem 11.3) that this expression is valid for all potentials which vanish faster than r^{-1} when $r \to \infty$. Using [11.48] and [11.50b], we see that for $r > a$ the radial function can be written as

$$R_l(k, r) = \frac{u_l(k, r)}{r} = B_l(k)[j_l(kr) - \tan \delta_l(k) n_l(kr)] \qquad [11.52]$$

The quantities $\delta_l(k)$ which are called *phase shifts*, display the influence of the interaction. Indeed, in the complete absence of interaction the free particle equation [11.42] holds for all r and the boundary condition at $r = 0$ excludes the irregular solution n_l in [11.48], thus forcing us to set $C_l = 0$. As a result, the corresponding free particle radial functions R_l^0 are proportional to $j_l(kr)$, in agreement with the expansion [2.260] of a plane wave in Legendre polynomials,

$$Ae^{ikz} = Ae^{ikr\cos\theta} = A \sum_{l=0}^{\infty} (2l + 1) i^l j_l(kr) P_l(\cos\theta) \qquad [11.53]$$

where A is an arbitrary normalisation constant as in [11.22]. The asymptotic behaviour of R_l^0 is then

$$R_l^0(k, r) = r^{-1} u_l^0(k, r) \underset{r\to\infty}{\sim} A_l(kr)^{-1} \sin(kr - l\pi/2) \qquad [11.54]$$

To relate the scattering amplitude to the phase shifts, we use [11.53] to write the asymptotic form of $\psi_{\mathbf{k}_i}(\mathbf{r})$, given by [11.25] as

$$\psi_{\mathbf{k}_i}(\mathbf{r}) \underset{r\to\infty}{\sim} A\left[\sum_{l=0}^{\infty} (2l + 1) i^l (kr)^{-1} \sin(kr - l\pi/2) P_l(\cos\theta) + f(k, \theta)\frac{e^{ikr}}{r}\right]$$

$$= A\left[\frac{e^{ikr}}{r}\left\{f(k, \theta) - \sum_{l=0}^{\infty}\left(\frac{i}{2k}\right)(2l + 1)P_l(\cos\theta)\right\}\right.$$

$$\left. + \frac{e^{-ikr}}{r}\left\{\sum_{l=0}^{\infty} (-1)^l\left(\frac{i}{2k}\right)(2l + 1)P_l(\cos\theta)\right\}\right] \qquad [11.55]$$

On the other hand, the asymptotic form of $\psi_{\mathbf{k}_i}(\mathbf{r})$ can be written from [11.51] and

[11.36] as

$$\psi_{\mathbf{k}_i}(\mathbf{r}) \underset{r\to\infty}{\sim} \sum_{l=0}^{\infty} (kr)^{-1} A_l(k) P_l(\cos\theta) \frac{1}{2i}$$

$$\times \{\exp[i(kr - l\pi/2 + \delta_l)] - \exp[-i(kr - l\pi/2 + \delta_l)]\} \quad [11.56]$$

On equating the coefficients of e^{-ikr} in [11.55] and [11.56] we find that

$$A_l(k) = A(2l + 1)i^l \exp[i\delta_l(k)] \quad [11.57]$$

Next, by matching the coefficients of e^{ikr} and using [11.57], we have

$$f(k, \theta) = \frac{1}{2ik} \sum_{l=0}^{\infty} (2l + 1)\{\exp[2i\delta_l(k)] - 1\} P_l(\cos\theta) \quad [11.58]$$

which is the desired result. We remark that the scattering amplitude is independent of the choice of the 'normalisation constants' $A_l(k)$.

Turning now to the differential cross-section, we have from [11.30] and [11.58]

$$\frac{d\sigma}{d\Omega} = |f(k, \theta)|^2$$

$$= \frac{1}{k^2} \sum_{l=0}^{\infty} \sum_{l'=0}^{\infty} (2l + 1)(2l' + 1) \exp\{i[\delta_l(k) - \delta_{l'}(k)]\}$$

$$\times \sin\delta_l(k) \sin\delta_{l'}(k) P_l(\cos\theta) P_{l'}(\cos\theta) \quad [11.59]$$

and the total cross-section is given by

$$\sigma_{\text{tot}}(k) = 2\pi \int_0^{\pi} \frac{d\sigma}{d\Omega}(k, \theta) \sin\theta \, d\theta$$

$$= \frac{4\pi}{k^2} \sum_{l=0}^{\infty} (2l + 1) \sin^2\delta_l(k) \quad [11.60]$$

where we have used the result [2.171]. We may also write [11.60] as

$$\sigma_{\text{tot}}(k) = \sum_{l=0}^{\infty} \sigma_l(k) \quad [11.61]$$

where each partial wave cross-section $\sigma_l(k)$ is given by

$$\sigma_l(k) = \frac{4\pi}{k^2} (2l + 1) \sin^2 \delta_l(k) \quad [11.62]$$

The maximum contribution of each partial wave to the total cross-section is

$$\sigma_l^{\max}(k) = \frac{4\pi}{k^2} (2l + 1) \quad [11.63]$$

and occurs when $\delta_l(k) = (n + 1/2)\pi$, $n = 0, \pm 1, \pm 2, \ldots$ In contrast, when $\delta_l(k) = n\pi$ at a certain value of k there is no contribution to the scattering from the partial wave of order l at that value of k. We also note that the *optical theorem* [11.34] follows by comparing [11.58] with [11.60] and using the fact that $P_l(1) = 1$.

It is clear that the method of partial waves is most useful when only a small number of partial waves contribute to the scattering. This situation occurs at *low incident energies*. Indeed, the 'effective (reduced) potential' which occurs in the radial equations [11.37] or [11.39] is

$$U_{\text{eff}}(r) = U(r) + \frac{l(l+1)}{r^2} \qquad [11.64]$$

Thus, as l increases, the centrifugal barrier term $l(l + 1)/r^2$ becomes more important and the incident particle needs more energy to overcome this repulsion and to probe the interaction region where the potential acts. Hence at low energies we expect that only a few partial waves will be required in the partial wave expansion.

In order to obtain an estimate of the number of partial waves which are needed for a given value of the incident energy, we note that the first and most important maximum of the free radial wave function $j_l(kr)$ occurs approximately at $r_0 \simeq l/k$ while for small r, $j_l(kr)$ is small, and behaves like r^l as $r \to 0$. Thus, if the potential has a 'range' a (that is, it acts in a region $r < a$), and if $a \ll l/k$, the function j_l will remain small in the scattering region, and the corresponding phase shift will be negligible. It is then reasonable to cut off the partial wave expansion at a value $l_{\max} \simeq ka$. Hence, if ka is small only a small number of phase shifts must be calculated.

We must also come to the above conclusion by using a simple (non-rigorous) semi-classical argument. If a potential vanishes beyond a certain distance a, then according to classical mechanics an incident particle having an impact parameter b will be deflected or not according to whether $b < a$ or $b > a$ (see Fig. 11.2). Now the impact parameter is given by

$$b = \frac{L}{p} \qquad [11.65]$$

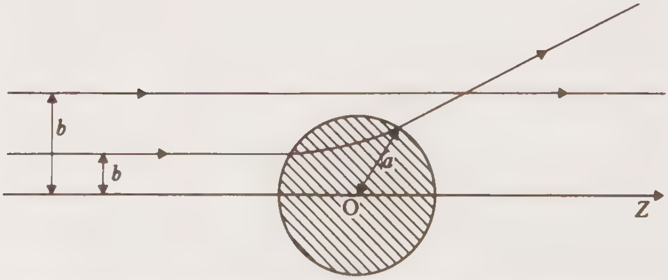

11.2 Classical scattering of a particle with impact parameter b, by a potential of finite range a. If $b > a$ no scattering occurs.

where p and L are the magnitudes of the particle momentum and orbital angular momentum, respectively. Thus, according to classical mechanics, particles with orbital angular momentum

$$L > pa \tag{11.66a}$$

are not scattered. Let us now assume that the quantity ka is somewhat larger than unity, so that the reduced de Broglie wavelength $\lambda\!\!\!^{-} = \lambda/2\pi = k^{-1}$ of the particle is small with respect to a and we are in a semi-classical situation. We may then write $L \simeq \hbar l$ and since $p = \hbar k$, we see that scattering is again expected to be small in angular momentum states for which

$$l > ka \tag{11.66b}$$

The phase shifts

Before we turn to the problem of the actual determination of the phase shifts, we shall discuss a few of their key properties [7]. First of all, the relation between the phase shifts and the interaction potential may be analysed by considering the scattering first by a reduced potential $U(r)$ and then by a different reduced potential $\bar{U}(r)$. The radial equations are (see [11.39])

$$\left[\frac{\mathrm{d}^2}{\mathrm{d}r^2} - \frac{l(l+1)}{r^2} - U(r) + k^2\right]u_l(k, r) = 0 \tag{11.67a}$$

and

$$\left[\frac{\mathrm{d}^2}{\mathrm{d}r^2} - \frac{l(l+1)}{r^2} - \bar{U}(r) + k^2\right]\bar{u}_l(k, r) = 0 \tag{11.67b}$$

We shall adopt a normalisation such that in the external region $r > a$

$$\begin{aligned} R_l(k, r) &= r^{-1}u_l(k, r) = j_l(kr) - \tan\delta_l(k)n_l(kr) \\ &\underset{r\to\infty}{\sim} \frac{1}{kr}[\sin(kr - l\pi/2) + \tan\delta_l(k)\cos(kr - l\pi/2)] \end{aligned} \tag{11.68}$$

with similar relations for $\bar{R}_l$ and $\bar{u}_l$, in which $\tan\delta_l$ is replaced by $\tan\bar{\delta}_l$.

The Wronskian of the two solutions u_l and $\bar{u}_l$ is defined as

$$W(u_l, \bar{u}_l) = u_l\bar{u}_l' - u_l'\bar{u}_l \tag{11.69}$$

where the prime denotes a derivative with respect to r. Premultiplying [11.67a] by $\bar{u}_l$, [11.67b] by u_l, subtracting term by term, and using [11.69], we have

$$\frac{\mathrm{d}}{\mathrm{d}r}W(u_l, \bar{u}_l) = -(U - \bar{U})u_l\bar{u}_l \tag{11.70}$$

[7] Further properties of the phase shifts are given by Bransden (1970) and Joachain (1979).

Upon integration over the variable r from 0 to ∞, we obtain

$$\begin{aligned}\tan \delta_l(k) - \tan \bar{\delta}_l(k) &= -k \int_0^\infty \bar{u}_l(k, r)[U(r) - \bar{U}(r)]u_l(k, r)\, \mathrm{d}r \\ &= -k \int_0^\infty \bar{R}_l(k, r)[U(r) - \bar{U}(r)]R_l(k, r)r^2\, \mathrm{d}r\end{aligned} \qquad [11.71]$$

where we have used the fact that $u_l(k, 0) = \bar{u}_l(k, 0) = 0$, together with [11.68].

We note from [11.71] that if the difference $(U - \bar{U})$ is small, so that $u_l\bar{u}_l \simeq (u_l)^2$, the difference $(\delta_l - \bar{\delta}_l)$ has the opposite sign to that of $(U - \bar{U})$. Moreover, by constructing a series of 'comparison potentials' between U and $\bar{U}$, this result remains true for all $(U - \bar{U})$. If we adopt an *absolute definition* of phase shifts by requiring that $\delta_l = 0$ if $U = 0$, we see from [11.71] that if the potential is everywhere repulsive (positive for all r) then $\delta_l < 0$. On the other hand, a potential which is everywhere attractive (negative for all r) yields phase shifts with $\delta_l > 0$. By choosing $\bar{U} = 0$ we also deduce from [11.71] the important integral representation

$$\tan \delta_l = -k \int_0^\infty j_l(kr)U(r)R_l(k, r)r^2\, \mathrm{d}r \qquad [11.72]$$

which is valid provided the radial function, R_l, is normalised according to [11.68].

In order to compute the phase shifts, the radial equations [11.37] or [11.39] are solved (in general by numerical methods) in the internal region $(r < a)$ subject to the boundary conditions at the origin discussed above. We then require both R_l and $\mathrm{d}R_l/\mathrm{d}r$ to be continuous at $r = a$. An equivalent procedure consists in requiring that the logarithmic derivative $[R_l^{-1}(\mathrm{d}R_l/\mathrm{d}r)]$ is continuous at $r = a$. Since the radial wave function R_l is given in the external region by [11.52], and denoting by

$$\gamma_l = [R_l^{-1}(\mathrm{d}R_l/\mathrm{d}r)]_{r=a} \qquad [11.73]$$

the value of the logarithmic derivative of the internal solution at $r = a$, we have

$$\gamma_l(k) = \frac{k[j_l'(ka) - \tan \delta_l(k)\, n_l'(ka)]}{j_l(ka) - \tan \delta_l(k)\, n_l(ka)} \qquad [11.74]$$

where

$$j_l'(ka) = \left[\frac{\mathrm{d}j_l(\rho)}{\mathrm{d}\rho}\right]_{\rho=ka}; \quad n_l'(ka) = \left[\frac{\mathrm{d}n_l(\rho)}{\mathrm{d}\rho}\right]_{\rho=ka}$$

Thus

$$\tan \delta_l(k) = \frac{kj_l'(ka) - \gamma_l(k)j_l(ka)}{kn_l'(ka) - \gamma_l(k)n_l(ka)} \qquad [11.75]$$

The behaviour of the phase shifts at *low energies* is readily obtained by using the properties of the functions $j_l(\rho)$ and $n_l(\rho)$ for small values of ρ. For example, if we define the quantity

$$\hat{\gamma}_l = \lim_{k \to 0} \gamma_l(k) \qquad [11.76]$$

it may be shown that provided

$$a\hat{\gamma}_l \neq -(l+1) \qquad [11.77]$$

the quantity $\tan \delta_l(k)$ behaves like k^{2l+1} as $k \to 0$. Except for the s wave ($l = 0$) contribution which in general tends towards a non-zero constant, all partial cross-sections $\sigma_l(l \geqslant 1)$ then vanish as k^{4l} when $k \to 0$. Thus the scattering is *isotropic* at very low energies and $\sigma_{tot} = \sigma_0$. Defining the *scattering length* α as

$$\alpha = -\lim_{k \to 0} \frac{\tan \delta_0(k)}{k} \qquad [11.78]$$

the scattering amplitude is such that

$$f \underset{k \to 0}{\to} -\alpha \qquad [11.79]$$

while the differential cross-section is given by

$$\frac{d\sigma}{d\Omega} \underset{k \to 0}{\to} \alpha^2 \qquad [11.80]$$

and the total cross-section becomes

$$\sigma_{tot} \underset{k \to 0}{\to} 4\pi\alpha^2 \qquad [11.81]$$

Let us now examine the behaviour of the phase shifts at *high energies*. For fixed l and large k we expect that the importance of the potential will become vanishingly small, so that the radial function R_l will approach the corresponding free spherical wave j_l. Hence, using [11.72] we may write $\tan \delta_l \simeq (\tan \delta_l)_{B1}$, where

$$(\tan \delta_l)_{B1} = -k \int_0^\infty [j_l(kr)]^2 U(r) r^2 \, dr \qquad [11.82]$$

is called the *first Born approximation* to $\tan \delta_l$.

Examples

As a first example of the determination of the phase shifts, let us consider a *square well* potential

$$U(r) = \begin{cases} -U_0 \quad (U_0 > 0), & r < a \\ 0, & r > a \end{cases} \qquad [11.83]$$

In the internal region $r < a$ the radial equation [11.37] becomes

$$\left[\frac{d^2}{dr^2} + \frac{2}{r}\frac{d}{dr} - \frac{l(l+1)}{r^2} + \kappa^2\right] R_l(k, r) = 0 \qquad [11.84]$$

where we have set $\kappa = (k^2 + U_0)^{1/2}$. Upon comparison with [11.42] we see that the regular solution of [11.84] is

$$R_l(k, r) = D_l(k) j_l(\kappa r) \qquad [11.85]$$

where $D_l(k)$ is a normalisation constant. In the external region $r > a$, the radial wave function R_l is given by [11.52], so we find that $\tan \delta_l(k)$ is given by [11.75], with

$$\gamma_l(k) = \frac{\kappa j_l'(\kappa a)}{j_l(\kappa a)} \qquad [11.86]$$

For example, in the case of s wave ($l = 0$) scattering, we have

$$\tan \delta_0 = \frac{k \tan(\kappa a) - \kappa \tan(ka)}{\kappa + k \tan(ka) \tan(\kappa a)} \qquad [11.87]$$

and

$$\delta_0 = -ka + \tan^{-1}\left[\frac{k}{\kappa} \tan \kappa a\right] \qquad [11.88]$$

where we have used the fact that $j_0(\rho) = (\sin \rho)/\rho$ and $n_0(\rho) = -(\cos \rho)/\rho$. We see from [11.78] and [11.87] that the scattering length is given by

$$\alpha = \left[1 - \frac{\tan(\lambda_0 a)}{\lambda_0 a}\right] a \qquad [11.89]$$

where $\lambda_0 = \sqrt{U_0}$. We note that for weak couplings ($\lambda_0 a \ll 1$) the phase shift $\delta_0(k)$ tends to zero as $k \to 0$ and the scattering length α is negative. When $\lambda_0 a$ reaches the value $\pi/2$ such that the potential is nearly able to bind an s wave bound state, the phase shift $\delta_0(k)$ tends to $\pi/2$ as $k \to 0$. The scattering length then becomes infinite and the s wave cross-section diverges like k^{-2} at $k = 0$, thus providing an example of a 'zero-energy resonance'. If $\lambda_0 a$ is just above $\pi/2$, then $\delta_0(k)$ will tend to π as $k \to 0$. Repeating this argument, it is seen that if λ_0 is increased in such a way that the potential can support n bound s states, then the s wave phase shift is such that

$$\lim_{k \to 0} \delta_0(k) = n\pi \qquad [11.90]$$

Moreover, when $\lambda_0 a = (2n + 1)\pi/2$, so that the potential is about to support its $(n + 1)$th bound s state, we have

$$\lim_{k \to 0} \delta_0(k) = \left(n + \frac{1}{2}\right)\pi \qquad [11.91]$$

A similar study can also be carried out for higher angular momenta ($l > 0$). In particular, it may be shown that

$$\lim_{k \to 0} \delta_l(k) = n_l \pi \qquad [11.92]$$

where n_l is the number of bound states of angular momentum $l > 0$ which can be supported by the potential. The results [11.90]–[11.92] turn out to be true for more general interactions than the square well considered here; they are examples of *Levinson's theorem.*

Another simple, but interesting example is the '*hard sphere*' potential

$$U(r) = \begin{cases} +\infty, & r < a \\ 0, & r > a \end{cases} \qquad [11.93]$$

Since in this case the particle cannot penetrate into the region $r < a$, the boundary condition is simply that the 'external' radial function [11.52] must vanish at $r = a$. Thus

$$\tan \delta_l = \frac{j_l(ka)}{n_l(ka)} \qquad [11.94]$$

and in this case γ_l is infinite. Using [11.46] we see that in the low-energy limit ($ka \ll 1$)

$$\tan \delta_l \simeq - \frac{(ka)^{2l+1}}{(2l + 1)!!(2l - 1)!!} \qquad [11.95]$$

so that $|\tan \delta_l|$ quickly decreases as l increases. In fact the low-energy scattering is always dominated by the s wave ($l = 0$), the corresponding phase shift being

$$\delta_0 = -ka \qquad [11.96]$$

As $k \to 0$, the differential cross-section is isotropic and given by $d\sigma/d\Omega = a^2$, and the total cross-section at zero energy becomes

$$\sigma_{\text{tot}} \underset{k \to 0}{\longrightarrow} 4\pi a^2 \qquad [11.97]$$

which is four times the classical value.

At high energies ($ka \gg 1$), we may use the asymptotic formulae [11.47] to obtain from [11.94] the approximate expressions of the phase shifts. That is,

$$\delta_l \simeq -ka + \tfrac{1}{2} l\pi \qquad [11.98]$$

It is worth noting that because of the singular nature of the 'hard sphere' potential [11.93] the phase shifts [11.98] do not vanish as $k \to \infty$, but tend to $-\infty$ in that limit. Using [11.60] we write the total cross-section as

$$\sigma_{\text{tot}} \simeq \frac{4\pi}{k^2} \sum_{l=0}^{l_{\max}} (2l + 1) \sin^2\left(\frac{1}{2} l\pi - ka\right) \qquad [11.99]$$

Taking $l_{\max} = ka$ in accordance with our general discussion of the partial wave method, and pairing successive terms in [11.99], we have

$$\sigma_{\text{tot}} \simeq \frac{4\pi}{k^2}\left\{\left[\sin^2(ka) + \sin^2\left(ka - \frac{1}{2}\pi\right)\right]\right.$$
$$\left. + 2\left[\sin^2\left(ka - \frac{1}{2}\pi\right) + \sin^2(ka - \pi)\right] + \cdots\right\}$$
$$\simeq \frac{4\pi}{k^2}\sum_{l=0}^{l_{\max}}(l) = 2\pi a^2 \qquad [11.100]$$

This result is twice the classical value, which at first sight is surprising since we have $ka \gg 1$. However, because the 'hard sphere' potential has a sudden discontinuity at $r = a$ the scattering can never be treated classically. A detailed study of this problem shows that at high energies half of the total cross-section arises from 'diffraction' or 'shadow' scattering which is produced by interference between the incident wave and the outgoing scattered wave, and occurs within a narrow diffraction peak in the forward direction.

Resonances

In general the phase shifts – and therefore also the cross sections – vary slowly as a function of the incident energy and of the strength of the potential. However, in certain cases it may happen that a phase shift δ_l will vary rapidly in a certain energy interval, causing a dramatic change in the corresponding partial cross-section σ_l in that energy range.

In order to study this problem, we first use [11.75] to write $\exp(2i\delta_l)$ in the form

$$e^{2i\delta_l} = e^{2i\xi_l}\frac{\gamma_l - r_l + is_l}{\gamma_l - r_l - is_l} \qquad [11.101]$$

where γ_l is the logarithmic derivative of the internal solution R_l at $r = a$ (see [11.73]) and the real quantities ξ_l, r_l and s_l are defined by

$$e^{2i\xi_l} = -\frac{j_l(ka) - in_l(ka)}{j_l(ka) + in_l(ka)} \qquad [11.102a]$$

and

$$r_l + is_l = k\frac{j_l'(ka) + in_l'(ka)}{j_l(ka) + in_l(ka)} \qquad [11.102b]$$

Since the quantity $(\gamma_l - r_l + is_l)/(\gamma_l - r_l - is_l)$ is of unit modulus, it may be written as $\exp(2i\rho_l)$, where

$$\rho_l = \arg(\gamma_l - r_l + is_l)$$
$$= \tan^{-1}\frac{s_l}{\gamma_l - r_l} \qquad [11.103]$$

and therefore we see from [11.101] that the phase shift δ_l can be decomposed as

$$\delta_l = \xi_l + \rho_l \qquad [11.104]$$

The first term ξ_l on the right of this equation has an interesting significance. Indeed, by comparing [11.94] and [11.102a], we see that the quantity ξ_l corresponds to 'hard sphere' scattering by a potential of 'range' a. The function ξ_l does not depend on the shape and depth of the potential. On the other hand, the term ρ_l does depend on the details of the potential through the logarithmic derivative γ_l.

The quantities ξ_l, r_l and s_l vary, in general, slowly and smoothly with the incident particle energy. On the other hand, the logarithmic derivative γ_l, and hence the contribution ρ_l to the phase shift, may in certain cases [8] vary rapidly in a small energy interval of width Γ about a given energy value E_r. For example, if ρ_l increases rapidly through an odd multiple of $\pi/2$ when the energy passes through the value E_r (see Fig. 11.3(a)), we may write $\rho_l \simeq \delta_l^r$ in the energy interval $(E_r - \Gamma/2, E_r + \Gamma/2)$, with

$$\delta_l^r = \tan^{-1} \frac{\Gamma}{2(E_r - E)} \qquad [11.105]$$

In that energy interval the phase shift [11.104] is therefore given approximately by $\delta_l \simeq \xi_l + \delta_l^r$, and will also rapidly increase through an odd multiple of $\pi/2$. This behaviour is called a *resonance*, with E_r being the *resonance energy* and Γ the *width* of the resonance. In the vicinity of the resonance energy $E = E_r$, [11.101] may be written as

$$e^{2i\delta_l} \simeq e^{2i\xi_l} \frac{E - E_r - i\Gamma/2}{E - E_r + i\Gamma/2} \qquad [11.106]$$

Let us call f_l the contribution of the l-th partial wave to the scattering amplitude. From [11.58] and [11.106] we see that in the energy interval $(E_r - \Gamma/2, E_r + \Gamma/2)$ we have

$$f_l \simeq \frac{2l+1}{k} \left[e^{i\xi_l} \sin \xi_l + e^{2i\xi_l} \frac{\Gamma/2}{E_r - E - i\Gamma/2} \right] P_l(\cos\theta) \qquad [11.107]$$

Thus, near the resonance energy $E = E_r$, the quantity f_l will be dominated by the second term on the right of [11.107]. In what follows we shall assume for the sake of simplicity that the 'hard sphere' scattering in the lth partial wave (due to ξ_l) can be completely neglected, together with the contribution of other partial waves to the scattering amplitude [11.58] In that (idealised) case, which corresponds to a *pure resonance* the full scattering amplitude can be written in

[8] A simple example is that of low-energy scattering by a strongly attractive square well, which is treated in detail in Joachain (1979).

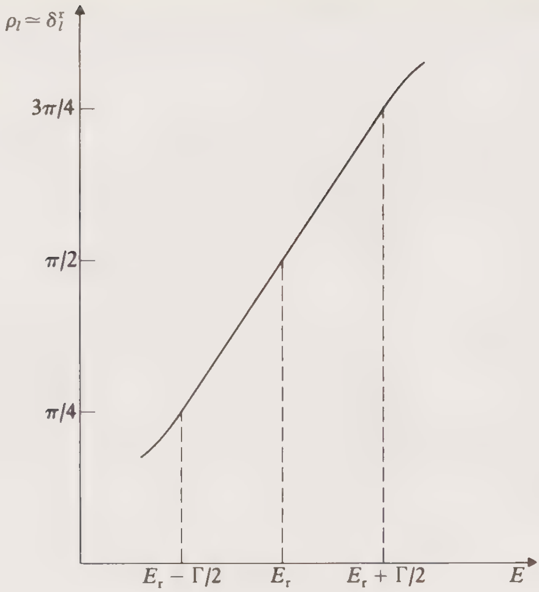

(a)

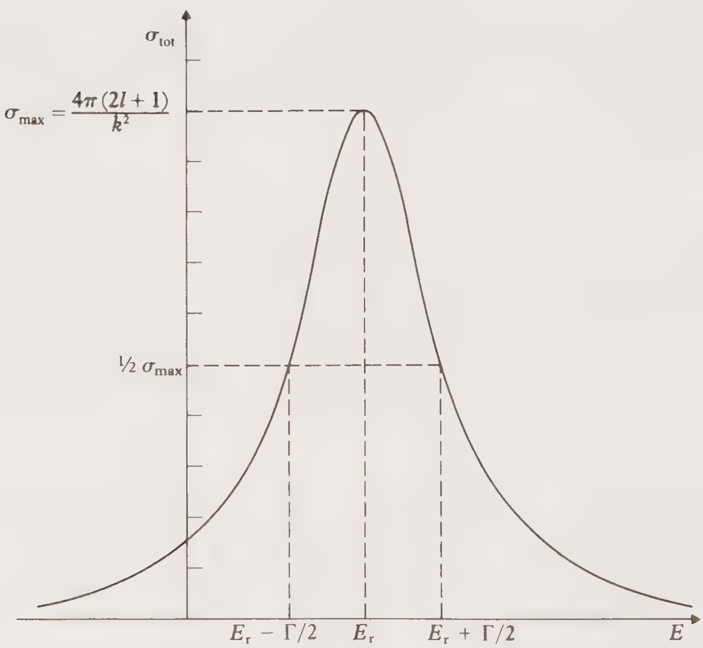

(b)

11.3 (a) Rapid increase of the phase shift through $\pi/2$ at a narrow resonance. The energy scale is expanded to show only a narrow range of energies about E_r.
(b) Total cross-section at a resonance.

the vicinity of $E = E_r$ as

$$f \simeq \frac{2l+1}{k} \frac{\Gamma/2}{E_r - E - i\Gamma/2} P_l(\cos\theta) \qquad [11.108]$$

and the corresponding differential cross-section is

$$\frac{d\sigma}{d\Omega} \simeq \frac{(2l+1)^2}{k^2} \frac{\Gamma^2/4}{(E_r - E)^2 + \Gamma^2/4} P_l^2(\cos\theta) \qquad [11.109]$$

We see that for any scattering angle θ the 'pure resonance' differential cross-section [11.109] exhibits a sharp peak of width Γ about the resonance energy $E = E_r$. It is also apparent that near $E = E_r$ the shape of the angular distribution does not depend on the energy, but only on the value of the angular momentum quantum number l. Integrating [11.109] over the scattering angle, we obtain the 'pure resonance' total cross-section

$$\sigma_{tot} \simeq \sigma_l = \frac{4\pi(2l+1)}{k^2} \frac{\Gamma^2/4}{(E - E_r)^2 + \Gamma^2/4} \qquad [11.110]$$

which is called the (one-level) *Breit–Wigner formula*, and is illustrated in Fig. 11.3(b). We note that at $E = E_r$, σ_{tot} reaches its maximum value and this is identical with σ_l^{max} given by [11.63]. The shape of σ_l is the characteristic *Lorentz shape* which we already encountered in Chapter 4.

It is worth stressing that the above discussion of a 'pure resonance' represents an idealisation. Within the framework of potential scattering, it is often necessary to take into account the effect of 'hard sphere' scattering in the lth partial wave, and the contribution of the other (non-resonant) partial waves to the scattering amplitude. Moreover, in actual atomic collision processes, where resonance phenomena are of great interest, the complex (many-body) structure of the particles involved in the collision must also be taken into account. We shall return to this point in the next chapter, where the narrow resonances observed in the scattering of electrons by atoms will be discussed.

The physical significance of a narrow resonance can be inferred by examining the amplitude of the radial wave function inside the interaction region. Let us consider for example the simple case of a strongly attractive square well. If we normalise the radial wave $u_l(k, r)$ outside the well to unit amplitude, namely

$$u_l(k, r) = \sin(kr - \tfrac{1}{2}l\pi + \delta_l), \qquad r \geq a \qquad [11.111]$$

then near $E = E_r$ the corresponding 'internal' wave function, obtained by requiring that the function u_l and its first derivative be continuous at $r = a$, is given by [9]

$$u_l(k, r) \simeq \frac{(2l-1)!!}{(ka)^l} \frac{\Gamma/2}{[(E - E_r)^2 + \Gamma^2/4]^{1/2}} (\kappa r) j_l(\kappa r) \qquad [11.112]$$

[9] See for example Joachain (1979).

where $\kappa = (k^2 + U_0)^{1/2}$. We see from [11.112] that the probability of finding the scattered particle within the potential well is much larger near the resonance energy $E = E_r$, so that in this case the particle is *nearly bound* in the well. Thus the resonance may be considered as a *metastable state*, whose *lifetime* τ, which is much longer than a typical collision time, can be related to the resonance width Γ by using the uncertainty relation [2.23]. Thus, with $\Delta t \simeq \tau$ and $\Delta E \simeq \Gamma$, we have

$$\tau \simeq \frac{\hbar}{\Gamma} \qquad [11.113]$$

11.4 THE INTEGRAL EQUATION OF POTENTIAL SCATTERING

Let us return to the Schrödinger equation [11.19], which we rewrite as

$$(\nabla^2 + k^2)\psi(k, \mathbf{r}) = U(\mathbf{r})\psi(k, \mathbf{r}) \qquad [11.114]$$

where we have indicated explicitly the k dependence of the wave function. The general solution of this equation may be written as

$$\psi(k, \mathbf{r}) = \Phi(k, \mathbf{r}) + \int G_0(k, \mathbf{r}, \mathbf{r}')U(\mathbf{r}')\psi(k, \mathbf{r}')\,\mathrm{d}\mathbf{r}' \qquad [11.115]$$

where $\Phi(k, \mathbf{r})$ is a solution of the homogeneous equation

$$[\nabla^2 + k^2]\Phi(k, \mathbf{r}) = 0 \qquad [11.116]$$

and $G_0(k, \mathbf{r}, \mathbf{r}')$ is a *Green's function* such that

$$[\nabla^2 + k^2]G_0(k, \mathbf{r}, \mathbf{r}') = \delta(\mathbf{r} - \mathbf{r}') \qquad [11.117]$$

The Green's function

In order to determine the Green's function $G_0(k, \mathbf{r}, \mathbf{r}')$, we first use the integral representation [2.32] of the delta function, so that

$$\delta(\mathbf{r} - \mathbf{r}') = (2\pi)^{-3} \int \mathrm{e}^{i\mathbf{k}'\cdot(\mathbf{r}-\mathbf{r}')}\,\mathrm{d}\mathbf{k}' \qquad [11.118]$$

and we write

$$G_0(k, \mathbf{r}, \mathbf{r}') = (2\pi)^{-3} \int \mathrm{e}^{i\mathbf{k}'\cdot\mathbf{r}} g_0(k, \mathbf{k}', \mathbf{r}')\,\mathrm{d}\mathbf{k}' \qquad [11.119]$$

Substituting [11.118] and [11.119] in [11.117], we find that

$$g_0(k, \mathbf{k}', \mathbf{r}') = \frac{\mathrm{e}^{-i\mathbf{k}'\cdot\mathbf{r}'}}{k^2 - k'^2} \qquad [11.120]$$

giving

$$G_0(k, \mathbf{r}, \mathbf{r}') = -(2\pi)^{-3} \int \frac{e^{i\mathbf{k}'\cdot(\mathbf{r}-\mathbf{r}')}}{k'^2 - k^2} \mathrm{d}\mathbf{k}' \qquad [11.121]$$

The integrand in [11.121] has poles at $k' = \pm k$, so that a well-defined prescription is required to avoid these singularities. This may be done by using the boundary condition [11.25]. Upon comparison of [11.25] and [11.115], we first note that the free wave $\Phi(k, \mathbf{r})$ is just the incident plane wave $A \exp(i\mathbf{k}_i \cdot \mathbf{r})$. In what follows it will be convenient to choose the normalisation constant to be $A = 1$ and write the corresponding incident plane wave as

$$\Phi_{\mathbf{k}_i}(\mathbf{r}) = e^{i\mathbf{k}_i\cdot\mathbf{r}} \qquad [11.122]$$

Comparison of [11.115] with [11.25] also shows that the Green's function $G_0(k, \mathbf{r}, \mathbf{r}')$ must be determined in such a way that it leads to an outgoing spherical wave for large r. This particular Green's function will be denoted by $G_0^{(+)}(k\ \mathbf{r}, \mathbf{r}')$.

Setting $\mathbf{R} = \mathbf{r} - \mathbf{r}'$ and performing the angular integrations in [11.121] with $\mathbf{R}$ as the polar axis, we find that

$$G_0(k, R) = -\frac{1}{4\pi^2 R} \int_{-\infty}^{+\infty} \frac{k' \sin k'R}{k'^2 - k^2} \mathrm{d}k' \qquad [11.123]$$

where we have used the fact that the integrand is an even function of k', so that the integral may be extended from $-\infty$ to $+\infty$. We may also write [11.123] as

$$G_0(k, R) = \frac{i}{16\pi^2 R}(I_1 - I_2) \qquad [11.124a]$$

where

$$I_1 = \int_{-\infty}^{+\infty} e^{ik'R}\left(\frac{1}{k' - k} + \frac{1}{k' + k}\right)\mathrm{d}k' \qquad [11.124b]$$

and

$$I_2 = \int_{-\infty}^{+\infty} e^{-ik'R}\left(\frac{1}{k' - k} + \frac{1}{k' + k}\right)\mathrm{d}k' \qquad [11.124c]$$

We can give a meaning to the integrals I_1 and I_2 by regarding them as contour integrals in the complex k' plane. Suppose, for example, that we avoid the poles at $k' = \pm k$ by choosing the path P shown in Fig. 11.4 (a). The integral I_1 can then be evaluated by writing

$$I_1 = \oint_C e^{ik'R}\left(\frac{1}{k' - k} + \frac{1}{k' + k}\right)\mathrm{d}k' \qquad [11.125]$$

where the contour C consists of the path P plus an infinite semicircle C_1 in the upper-half k' plane (see Fig. 11.4(b)). Since $\exp(ik'R)$ vanishes on C_1, the

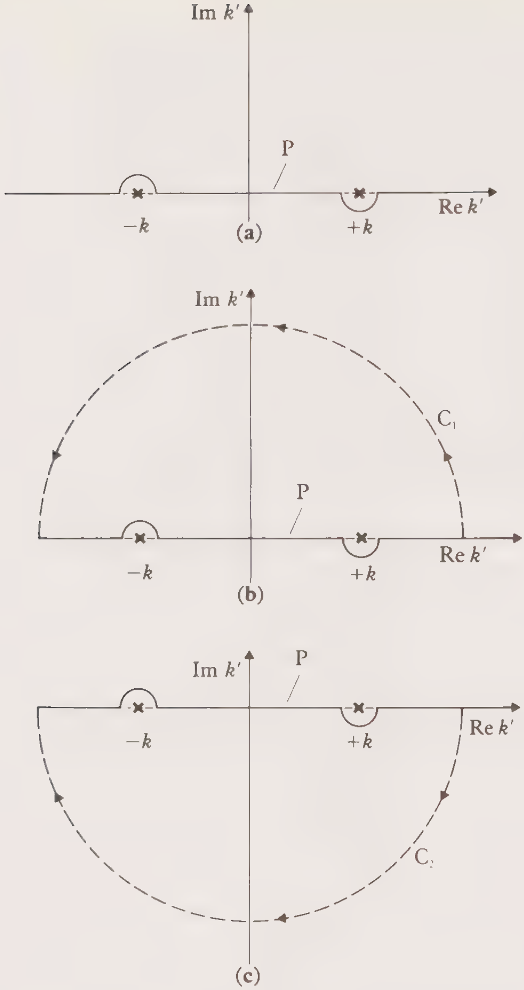

11.4 (a) The path P avoiding the poles at $k' = \pm k$.
(b) Contour (P + C_1) for calculating the integral I_1.
(c) Contour (P + C_2) for calculating the integral I_2.

contribution to I_1 from the infinite semicircle C_1 is equal to zero, and the integral [11.125] is equal to its value along the path P. Using the Cauchy theorem [10], we then obtain for the integral I_1, evaluated along the path P, the value $I_1 = 2\pi i \exp(ikR)$.

The integral I_2 can be evaluated in a similar way by closing the contour with an infinite semicircle C_2 in the lower-half k' plane as shown in Fig. 11.4(c). Using again the Cauchy theorem, we find that I_2, evaluated along the path P, is

[10] The Cauchy theorem is discussed for example in Byron and Fuller (1969).

given by $I_2 = -2\pi i \exp(ikR)$. Thus by choosing the path P to avoid the poles at $k' = \pm k$, we see that $I_1 - I_2 = 4\pi i \exp(ikR)$. Returning to [11.124] and remembering that $\mathbf{R} = \mathbf{r} - \mathbf{r}'$, we therefore obtain a Green's function

$$G_0^{(+)}(k, \mathbf{r}, \mathbf{r}') = -\frac{1}{4\pi}\frac{e^{ik|\mathbf{r}-\mathbf{r}'|}}{|\mathbf{r}-\mathbf{r}'|} \qquad [11.126]$$

which exhibits the required purely outgoing wave behaviour (of the form $\exp(ikr)/r$) when r is large. It is easy to verify that any other choice of integration contour which avoids the poles at $k' = \pm k$ in a way different from the path P shown in Fig. 11.5(a) leads to an *incoming* wave behaviour (of the form $\exp(-ikr)/r$) in addition to or in place of the outgoing wave behaviour obtained above.

We remark that the choice of the path P is equivalent to keeping the integration path along the real axis, and shifting the two poles slightly so that the poles are now at

$$k' = \pm(k + i\varepsilon'), \qquad \varepsilon' \to 0^+$$

We can then write

$$G_0^{(+)}(k, \mathbf{r}, \mathbf{r}') = -(2\pi)^{-3} \lim_{\varepsilon\to 0^+} \int \frac{e^{i\mathbf{k}'\cdot(\mathbf{r}-\mathbf{r}')}}{k'^2 - k^2 - i\varepsilon}\, d\mathbf{k}' \qquad [11.127]$$

where we have written $\varepsilon = 2k\varepsilon'$ and neglected terms in ε'^2.

Using $G_0^{(+)}$ given by [11.126], the final form of the integral equation [11.115] is (with $\psi(k, \mathbf{r}) \equiv \psi_{\mathbf{k}_i}(\mathbf{r})$)

$$\psi_{\mathbf{k}_i}(\mathbf{r}) = e^{i\mathbf{k}_i\cdot\mathbf{r}} - \frac{1}{4\pi}\int \frac{e^{ik|\mathbf{r}-\mathbf{r}'|}}{|\mathbf{r}-\mathbf{r}'|}\, U(\mathbf{r}')\psi_{\mathbf{k}_i}(\mathbf{r}')\, d\mathbf{r}' \qquad [11.128]$$

This is equivalent to the original Schrödinger equation [11.19], together with the boundary condition [11.25], which is satisfied automatically.

To verify the asymptotic behaviour of $\psi_{\mathbf{k}_i}(\mathbf{r})$, we note that for r large and $r' \ll r$,

$$|\mathbf{r} - \mathbf{r}'| \underset{r\to\infty}{\longrightarrow} r - \hat{\mathbf{r}}\cdot\mathbf{r}' + \cdots \qquad [11.129]$$

so that

$$\frac{e^{ik|\mathbf{r}-\mathbf{r}'|}}{|\mathbf{r}-\mathbf{r}'|} \underset{r\to\infty}{\longrightarrow} \frac{e^{ikr}}{r} e^{-i\mathbf{k}_f\cdot\mathbf{r}'} + \cdots \qquad [11.130]$$

where terms of higher order in $1/r$ have been neglected, and we have introduced the final wave vector $\mathbf{k}_f = k\hat{\mathbf{r}}$, which points in the direction of the detector and has spherical polar coordinates (k, θ, ϕ). Thus, using [11.128] and [11.130], we have

$$\psi_{\mathbf{k}_i}(\mathbf{r}) \underset{r\to\infty}{\longrightarrow} e^{i\mathbf{k}_i\cdot\mathbf{r}} - \frac{1}{4\pi}\frac{e^{ikr}}{r}\int e^{-i\mathbf{k}_f\cdot\mathbf{r}'} U(\mathbf{r}')\psi_{\mathbf{k}_i}(\mathbf{r}')\, d\mathbf{r}' \qquad [11.131]$$

Upon comparison with [11.25], we see that $\psi_{\mathbf{k}_i}$ exhibits the desired asymptotic behaviour, with $A = 1$, and we obtain for the scattering amplitude the integral representation

$$f = -\frac{1}{4\pi} < \Phi_{\mathbf{k}_f}|U|\psi_{\mathbf{k}_i} > = -\frac{1}{4\pi} \int \mathrm{e}^{-i\mathbf{k}_f\cdot\mathbf{r}'}\, U(\mathbf{r}')\psi_{\mathbf{k}_i}(\mathbf{r}')\mathrm{d}\mathbf{r}' \quad [11.132]$$

where we have introduced the plane wave $\Phi_{\mathbf{k}_f}$ corresponding to the final wave vector $\mathbf{k}_f$,

$$\Phi_{\mathbf{k}_f}(\mathbf{r}) = \mathrm{e}^{i\mathbf{k}_f\cdot\mathbf{r}} \quad [11.133]$$

The integral equation [11.128] can also be analysed in partial waves. Assuming that we are dealing with a central potential, and expanding the scattering wave function $\psi_{\mathbf{k}_i}$ in Legendre polynomials as in [11.36], it can be shown (Problem 11.10) that each radial function $R_l(k, r)$, normalised according to [11.68], satisfies the radial integral equation

$$R_l(k, r) = j_l(kr) + \int_0^\infty G_l(k, r, r')U(r')R_l(k, r')r'^2\,\mathrm{d}r' \quad [11.134]$$

where the radial Green's function $G_l(k, r, r')$ is given by

$$G_l(k, r, r') = kj_l(kr_<)n_l(kr_>) \quad [11.135]$$

Here $r_<$ and $r_>$ denote respectively the lesser and the greater of r and r'. By analysing the behaviour of the radial integral equation as $r \to \infty$ and comparing with [11.68], the expression [11.72] for $\tan\delta_l$ can be re-derived.

11.5 THE BORN APPROXIMATION

Approximation methods are clearly necessary in order to analyse complicated processes such as those occurring in atomic collisions, where exact solutions are not available. Whenever possible, it is useful to first discuss approximate treatments within the framework of potential scattering, where their interpretation is simpler and their accuracy can be checked easily. In this section we shall concentrate our attention on one of these approximation methods, the *Born series*, which is a perturbation expansion of the scattering wave function, or the scattering amplitude, in powers of the interaction potential. In particular, we shall study in some detail the first term of this expansion, known as the (first) Born approximation, since a generalised version of it will be used in the next two chapters to analyse electron–atom and atom–atom collisions.

The Born series

Let us attempt to solve the integral equation [11.128] by iteration, starting from the incident plane wave $\Phi_{\mathbf{k}_i}(\mathbf{r})$ as our 'zero-order' approximation. We obtain in

this way the sequence of functions

$$\psi_0(\mathbf{r}) = \Phi_{\mathbf{k}_i}(\mathbf{r}) = e^{i\mathbf{k}_i\cdot\mathbf{r}} \tag{11.136a}$$

$$\psi_1(\mathbf{r}) = \Phi_{\mathbf{k}_i}(\mathbf{r}) + \int G_0^{(+)}(k, \mathbf{r}, \mathbf{r}')U(\mathbf{r}')\psi_0(\mathbf{r}')\,d\mathbf{r}' \tag{11.136b}$$

$$\vdots$$

$$\psi_n(\mathbf{r}) = \Phi_{\mathbf{k}_i}(\mathbf{r}) + \int G_0^{(+)}(k, \mathbf{r}, \mathbf{r}')U(\mathbf{r}')\psi_{n-1}(\mathbf{r}')\,d\mathbf{r}' \tag{11.136c}$$

Assuming for the moment that this sequence converges towards the exact wave function $\psi_{\mathbf{k}_i}$, we may write for $\psi_{\mathbf{k}_i}(\mathbf{r})$ the *Born series*

$$\psi_{\mathbf{k}_i}(\mathbf{r}) = \Phi_{\mathbf{k}_i}(\mathbf{r}) + \int G_0^{(+)}(k, \mathbf{r}, \mathbf{r}')U(\mathbf{r}')\Phi_{\mathbf{k}_i}(\mathbf{r}')\,d\mathbf{r}' + \int G_0^{(+)}(k, \mathbf{r}, \mathbf{r}')U(\mathbf{r}')G_0^{(+)}(k, \mathbf{r}', \mathbf{r}'')U(\mathbf{r}'')\Phi_{\mathbf{k}_i}(\mathbf{r}'')\,d\mathbf{r}'\,d\mathbf{r}'' + \cdots \tag{11.137}$$

which is clearly a perturbation expansion in powers of the interaction potential. Upon substitution of the series [11.137] into the integral representation [11.132] of the scattering amplitude, we obtain the *Born series for the scattering amplitude*. That is,

$$f = -\frac{1}{4\pi}\langle\Phi_{\mathbf{k}_f}|U + UG_0^{(+)}U + UG_0^{(+)}UG_0^{(+)}U + \cdots|\Phi_{\mathbf{k}_i}\rangle \tag{11.138}$$

The first term of this series, namely

$$f_{B1} = -\frac{1}{4\pi}\langle\Phi_{\mathbf{k}_f}|U|\Phi_{\mathbf{k}_i}\rangle \tag{11.139}$$

is called the *(first) Born approximation to the scattering amplitude.*

Working in partial waves, we may also solve the radial integral equations [11.134] by iteration, starting from the zero-order approximation $R_l^{(0)}(k, r) = j_l(kr)$. Upon substitution in [11.72] we then generate a Born series for $\tan\delta_l$ whose first term is just the first Born approximation [11.82] to $\tan\delta_l$.

The problem of the convergence of the Born series is a difficult one, which lies outside the scope of this book. Roughly speaking, we may obtain a crude sufficient condition of convergence by requiring that the time τ_1 spent by the particle in the 'range' a of the potential should be small with respect to a 'characteristic' time τ_2 necessary for the potential to have a significant effect. The time τ_1 is given approximately by $\tau_1 \sim a/v$, where v is the velocity of the particle. On the other hand, if $|V_0|$ denotes a typical strength of the potential (which may be attractive or repulsive) and $|U_0| = 2m|V_0|/\hbar^2$ the corresponding strength of the reduced potential, we may take $\tau_2 \simeq \hbar/|V_0| = 2m/(\hbar|U_0|)$. If

we require that $\tau_1 \ll \tau_2$, we must have

$$\frac{|V_0|a}{\hbar v} = \frac{|U_0|a}{2k} \ll 1 \qquad [11.140]$$

The first Born approximation

Let us now study in more detail the first Born approximation [11.139]. Using the explicit expressions of $\Phi_{\mathbf{k}_i}(\mathbf{r})$ and $\Phi_{\mathbf{k}_f}(\mathbf{r})$ given respectively by [11.122] and [11.133], we have

$$\begin{aligned} f_{B1} &= -\frac{1}{4\pi}\int e^{i(\mathbf{k}_i-\mathbf{k}_f)\cdot\mathbf{r}}U(\mathbf{r})\,d\mathbf{r} \\ &= -\frac{1}{4\pi}\int e^{i\boldsymbol{\Delta}\cdot\mathbf{r}}U(\mathbf{r})\,d\mathbf{r} \end{aligned} \qquad [11.141]$$

where we have introduced the wave-vector transfer

$$\boldsymbol{\Delta} = \mathbf{k}_i - \mathbf{k}_f \qquad [11.142]$$

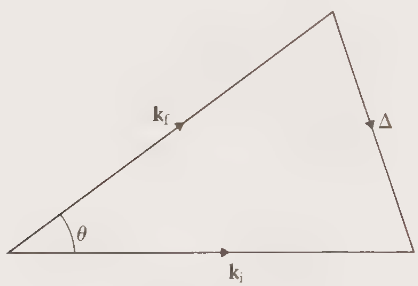

11.5 The vectors $\mathbf{k}_i$, $\mathbf{k}_f$ and Δ.

which is shown in Fig. 11.5, together with the vectors $\mathbf{k}_i$ and $\mathbf{k}_f$ and the scattering angle θ. The *momentum transfer* is given by $\hbar\boldsymbol{\Delta}$ and is of course identical to $\boldsymbol{\Delta}$ in systems of units (such as atomic units) where $\hbar = 1$. It is apparent from Fig. 11.5 that since $k = |\mathbf{k}_i| = |\mathbf{k}_f|$ the magnitude of the vector $\boldsymbol{\Delta}$ is given by

$$\Delta = 2k \sin\frac{\theta}{2} \qquad [11.143]$$

We see from [11.141] that the first Born scattering amplitude is proportional to the Fourier transform of the potential, and we also see that the first Born differential cross-section

$$\left(\frac{d\sigma}{d\Omega}\right)_{B1} = |f_{B1}|^2 \qquad [11.144]$$

remains unchanged when the sign of the potential is reversed.

Let us consider the particular case of *central* potentials. We may then easily perform the angular integrations in [11.141] and obtain (Problem 11.11)

$$f_{B1} = -\frac{1}{\Delta}\int_0^\infty r \sin(\Delta r)U(r)\, dr \qquad [11.145]$$

We see that this quantity is real and depends on k (i.e. on the energy) and on the scattering angle θ only via the magnitude Δ of the wave-vector transfer. The corresponding total cross-section in first Born approximation is given by

$$\begin{aligned}\sigma_{tot}^{B1} &= 2\pi\int_0^\pi |f_{B1}|^2 \sin\theta\, d\theta \\ &= \frac{2\pi}{k^2}\int_0^{2k} |f_{B1}(\Delta)|^2\, \Delta\, d\Delta\end{aligned} \qquad [11.146]$$

where we have used the fact that $\sin\theta\, d\theta = \Delta\, d\Delta/k^2$. It is interesting to note from [11.146] that

$$\lim_{k\to\infty} [k^2\sigma_{tot}^{B1}(k)] = 2\pi\int_0^\infty |f_{B1}(\Delta)|^2\Delta\, d\Delta \qquad [11.147]$$

Since the right-hand side of [11.147] is independent of k, we see that σ_{tot}^{B1} is proportional to k^{-2} as k becomes large. Because $E = \hbar^2k^2/2m$, we may also write

$$\sigma_{tot}^{B1} \underset{E\to\infty}{\sim} AE^{-1} \qquad [11.148]$$

where A is a constant. Thus σ_{tot}^{B1} tends to zero as E^{-1} at high energies.

As an illustration of this discussion, we consider the Yukawa (or 'screened Coulomb') reduced potential

$$\begin{aligned}U(r) &= U_0\frac{e^{-\alpha r}}{r} \\ &= U_0\frac{e^{r/a}}{r}, \qquad a = \alpha^{-1}\end{aligned} \qquad [11.149]$$

The integral [11.145] is then straightforward, and yields

$$f_{B1} = -\frac{U_0}{\alpha^2 + \Delta^2} \qquad [11.150]$$

The first Born differential cross-section

$$\left(\frac{d\sigma}{d\Omega}\right)_{B1} = \frac{U_0^2}{(\alpha^2 + \Delta^2)^2} \qquad [11.151]$$

is plotted in Fig. 11.6 as a function of the scattering angle θ, for various values of ka. We see that for large ka the differential cross-section [11.151] is essentially

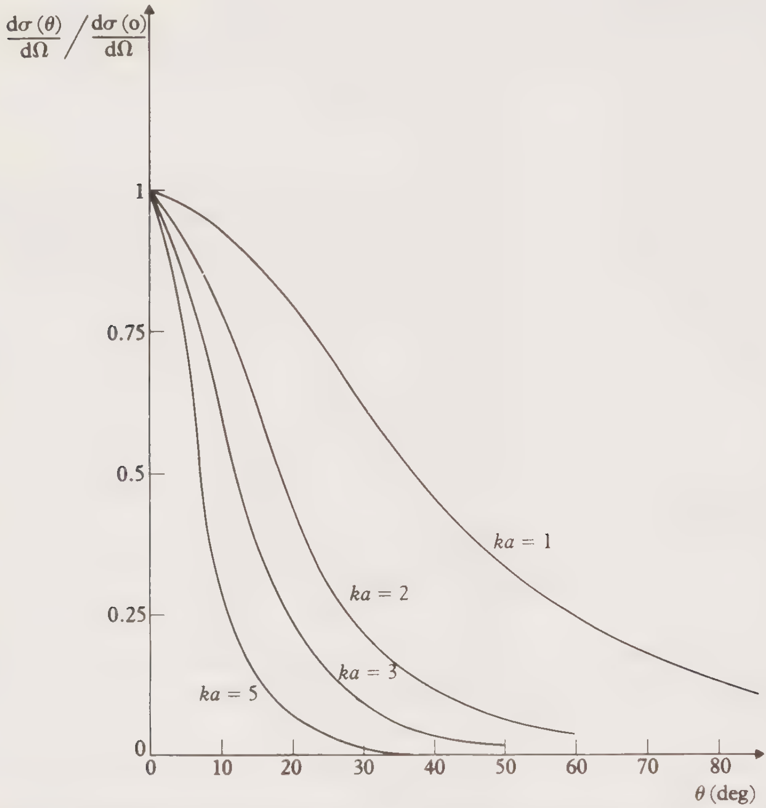

11.6 The angular distribution for scattering by a Yukawa potential in first Born approximation, for various values of *ka*.

concentrated within a forward cone of angular aperture $\delta\theta \simeq (ka)^{-1}$. This behaviour is a direct consequence of [11.141] and of the fact that the Fourier transform of a function $U(r)$ which is negligible for $r > a$ is appreciable only for values of Δ such that $\Delta \lesssim a^{-1}$, i.e. (see [11.143]) corresponding to scattering angles

$$\theta \lesssim \frac{1}{ka} \qquad [11.152]$$

The Coulomb potential

It is interesting to examine what happens in the above formulae when we let α tend to zero. The 'screened Coulomb' reduced potential [11.149] then becomes the reduced Coulomb potential

$$U(r) = \frac{U_0}{r} \qquad [11.153]$$

The first Born scattering amplitude [11.150] now reads

$$(f_{B1})_c = -\frac{U_0}{\Delta^2} \qquad [11.154]$$

and the corresponding first Born differential cross-section is

$$\left(\frac{d\sigma_{B1}}{d\Omega}\right)_c = \frac{U_0^2}{\Delta^4} \qquad [11.155]$$

where the subscript c refers to Coulomb scattering.

In order to relate this result with our discussion of classical Coulomb scattering in Appendix 1, we recall that the Coulomb interaction potential between two particles having electric charges q_A and q_B, respectively, is

$$V(r) = \frac{q_A q_B}{(4\pi\varepsilon_0)r} \qquad [11.156]$$

so that the corresponding reduced potential $U(r) = (2m/\hbar^2)V(r)$ is given by [11.153], with

$$U_0 = \frac{2m}{\hbar^2}\frac{q_A q_B}{(4\pi\varepsilon_0)} \qquad [11.157]$$

From this we see that [11.155] may also be written as

$$\left(\frac{d\sigma_{B1}}{d\Omega}\right)_c = \left(\frac{q_A q_B}{4\pi\varepsilon_0}\right)^2 \frac{1}{16E^2 \sin^4(\theta/2)} \qquad [11.158]$$

which is identical to the *Rutherford formula* [A1.33] obtained in Appendix 1 by using classical Newtonian mechanics. A detailed discussion of the Rutherford formula [11.158] is given in Appendix 1 and will therefore not be reproduced here.

It is a remarkable feature of Coulomb scattering that an *exact* quantum mechanical treatment of the Coulomb potential [11.156] also yields the Rutherford formula [11.158] for the differential cross-section $d\sigma_c/d\Omega$! However, the exact Coulomb *scattering amplitude* f_c (such that $d\sigma_c/d\Omega = |f_c|^2$) differs from the first Born result [11.154] by a phase factor. It is found that [9]

$$f_c(\theta) = -\frac{\gamma}{2k\sin^2(\theta/2)}\frac{\Gamma(1+i\gamma)}{\Gamma(1-i\gamma)}\exp\{-i\gamma\log[\sin^2(\theta/2)]\} \qquad [11.159]$$

where Γ denotes the gamma function and

$$\gamma = \frac{q_A q_B}{(4\pi\varepsilon_0)\hbar v} = \frac{q_A q_B m}{(4\pi\varepsilon_0)\hbar^2 k} \qquad [11.160]$$

11.6 ABSORPTION PROCESSES AND SCATTERING BY A COMPLEX POTENTIAL

Until now we have considered the scattering of a spinless particle by a *real* potential $V(\mathbf{r})$, a problem which is equivalent to the elastic scattering between two structureless particles. However, we have seen in Section 11.1 that when a particle collides with a target, non-elastic scattering may occur. This means that there may be one, several, or an infinite number of *open channels* in addition to the elastic one. As far as the elastic scattering is concerned, the presence of such non-elastic processes can be viewed as absorption from the incident beam, and taken into account by introducing a *complex* or '*optical*' potential of the form

$$V = V_R - iV_I \qquad [11.161]$$

The continuity equation [2.52] now reads

$$\nabla \cdot \mathbf{j} = -\frac{2}{\hbar} V_I |\Psi|^2 \qquad [11.162]$$

Hence, for $V_I > 0$, we have local *absorption* of the incident beam, the total number N_{abs} of particles which are 'absorbed' per unit time within the volume V being

$$N_{\text{abs}} = \frac{2}{\hbar} \int_V V_I |\Psi|^2 \, \mathrm{d}\mathbf{r} \qquad [11.163]$$

Let us consider the particular case of a *central*, complex potential $V(r) = V_R(r) - iV_I(r)$. Our discussion of the partial wave method is then easily generalised. The radial function $R_l(k, r)$, which is now complex, is the regular solution of [11.37], with the asymptotic form [11.51], where δ_l may now be complex. Let us write [11.51] as

$$R_l(k, r) \underset{r \to \infty}{\sim} \frac{A_l(k)}{2ikr} \mathrm{e}^{i\delta_l(k)} [-\mathrm{e}^{-i(kr - l\pi/2)} + S_l(k) \mathrm{e}^{i(kr - l\pi/2)}] \qquad [11.164]$$

where

$$S_l(k) = \exp[2i\delta_l(k)] \qquad [11.165]$$

If absorption takes place, the intensity of the outgoing wave must be reduced, leaving the incoming wave unaltered, and on the other hand if no absorption takes place, the intensity of the outgoing wave will remain the same as that of the incoming wave. For these reasons we must have

$$|S_l(k)| \leqslant 1 \qquad [11.166]$$

This suggests that we introduce *complex phase shifts*

$$\delta_l(k) = \text{Re}\, \delta_l(k) + i \,\text{Im}\, \delta_l(k) \qquad [11.167]$$

so that

$$S_l(k) = \eta_l(k)\exp[2i \text{ Re } \delta_l(k)] \tag{11.168}$$

where the quantity

$$\eta_l(k) = \exp[-2 \text{ Im } \delta_l(k)] \tag{11.169}$$

is called the 'inelasticity' or 'absorption' factor. It is clear from the above equations that Im $\delta_l \geqslant 0$, so that

$$0 \leqslant \eta_l(k) \leqslant 1 \tag{11.170}$$

and we note that the particular case $\eta_l = 1$ (i.e. Im $\delta_l = 0$) corresponds to pure elastic scattering.

The calculation of the elastic scattering amplitude f_{el} proceeds as in Section 11.3, and we find that (Problem 11.13)

$$\begin{aligned} f_{el} &= \frac{1}{2ik} \sum_{l=0}^{\infty} (2l + 1)[S_l(k) - 1]P_l(\cos\theta) \\ &= \frac{1}{2ik} \sum_{l=0}^{\infty} (2l + 1)[\eta_l(k)e^{2i\text{Re}\,\delta_l(k)} - 1]P_l(\cos\theta) \end{aligned} \tag{11.171}$$

The elastic differential cross-section is given by

$$\frac{d\sigma_{el}}{d\Omega} = |f_{el}|^2 \tag{11.172}$$

and the total elastic cross-section is

$$\begin{aligned} \sigma_{tot}^{el} &= \frac{\pi}{k^2} \sum_{l=0}^{\infty} (2l + 1)|\eta_l e^{2i\text{Re}\,\delta_l} - 1|^2 \\ &= \sum_{l=0}^{\infty} \sigma_l^{el} \end{aligned} \tag{11.173}$$

where

$$\sigma_l^{el} = \frac{\pi}{k^2}(2l + 1)|\eta_l e^{2i\text{Re}\cdot\delta_l} - 1|^2 \leqslant \frac{4\pi(2l + 1)}{k^2} \tag{11.174}$$

We can also obtain a total absorption cross-section σ_{tot}^{abs} (also called 'inelastic' or 'reaction' cross-section) by computing the ratio of the net ingoing flux divided by the incident flux. The result is (Problem 11.13)

$$\begin{aligned} \sigma_{tot}^{abs} &= \frac{\pi}{k^2} \sum_{l=0}^{\infty} (2l + 1)(1 - \eta_l^2) \\ &= \sum_{l=0}^{\infty} \sigma_l^{abs} \end{aligned} \tag{11.175}$$

where

$$\sigma_l^{\text{abs}} = \frac{\pi}{k^2}(2l+1)(1-\eta_l^2) \leqslant \frac{\pi(2l+1)}{k^2} \tag{11.176}$$

As we noted above, pure elastic scattering in the lth partial wave corresponds to $\eta_l = 1$, in which case $\sigma_l^{\text{abs}} = 0$. On the other hand, non-elastic scattering (corresponding to $0 \leqslant \eta_l < 1$) is always accompanied by elastic scattering.

The total (complete) cross-section including both elastic and non-elastic processes is given by

$$\begin{aligned}\sigma_{\text{tot}} &= \sigma_{\text{tot}}^{\text{el}} + \sigma_{\text{tot}}^{\text{abs}} \\ &= \frac{2\pi}{k^2}\sum_{l=0}^{\infty}(2l+1)[1-\eta_l\cos(2\text{Re}\,\delta_l)] \\ &= \sum_{l=0}^{\infty}\sigma_l \end{aligned} \tag{11.177}$$

where

$$\sigma_l = \frac{2\pi}{k^2}(2l+1)[1-\eta_l\cos(2\text{Re}\,\delta_l)] \leqslant \frac{4\pi(2l+1)}{k^2} \tag{11.178}$$

Upon comparison of [11.171] and [11.177], we see that the *optical theorem* [11.34] may be generalised to read

$$\sigma_{\text{tot}} = \frac{4\pi}{k}\,\text{Im}\,f_{\text{el}}(k, \theta = 0) \tag{11.179}$$

where σ_{tot} is the *total* (complete) cross-section and $\text{Im}\,f_{\text{el}}(k, \theta = 0)$ is the imaginary part of the *elastic* scattering amplitude in the forward direction. This generalised version of the optical theorem plays an important role in the analysis of complex collision processes.

PROBLEMS

11.1 Consider a reaction of the type A + B → C + D. Let m_A, m_B, m_C, m_D be the masses of the particles A, B, C and D, and w_A, w_B, w_C, w_D be their internal energies. Using the methods of Appendix A2, show that the centre of mass and laboratory differential cross-sections for observation of the particle C in a given direction are related by

$$\frac{d\sigma_C}{d\Omega_L}(\theta_L, \phi_L) = \frac{(1+\tau_C^2+2\tau_C\cos\theta)^{3/2}}{|1+\tau_C\cos\theta|}\frac{d\sigma_C}{d\Omega}(\theta, \phi)$$

where the subscript L refers to laboratory quantities, and

$$\tau_C = \left(\frac{m_A m_C}{m_B m_D}\frac{T_i}{T_i + Q_{if}}\right)^{1/2}$$

The quantity T_i is the initial centre of mass kinetic energy and Q_{if} is the change in internal energy which as occurred in the collision, namely

$$Q_{if} = w_A + w_B - (w_C + w_D).$$

11.2 Prove the optical theorem [11.34] by inserting the expression [11.33] into the equation [11.32], which expresses the conservation of the probability flux.

11.3 Prove that the asymptotic form [11.51] holds provided $r|V(r)| \to 0$ as $r \to \infty$.
(Hint: Write solutions of the radial equation [11.39] for large r in the form

$$u_l(k, r) = F_l(k, r)e^{\pm ikr}$$

where F_l is a slowly varying function of r. Obtain an equation for F_l and show that if $r|V(r)| \to 0$ as $r \to \infty$, then F_l is independent of r in the limit $r \to \infty$.)

11.4 Consider a repulsive (reduced) potential of the form $U(r) = A/r^2$ $(A > 0)$.
(a) Obtain the phase shifts δ_l and show that $\delta_l \simeq -\pi A/2(2l + 1)$ when l is large.
(b) Discuss the angular distribution. Is the differential cross-section finite in the forward direction? Is the total cross-section finite? (Hint: For given ν and large ρ one has $j_\nu(\rho) \sim \sin(\rho - \nu\pi/2)/\rho$.)

11.5 Consider an attractive (reduced) potential of the form $U(r) = A/r^2$ $(A < 0)$. How must the treatment of Problem 11.4 be modified? Show that the radial equation [11.39] has physically acceptable solutions only if $A > -1/4$.

11.6 Suppose that in an elastic scattering experiment between two structureless particles the centre of mass differential cross-section may be represented by an expression of the type

$$\frac{d\sigma}{d\Omega} = A + BP_1(\cos\theta) + CP_2(\cos\theta) + \cdots$$

Express the coefficients A, B and C in terms of the phase shifts δ_l. (Hint: Use the orthogonality relation [2.171] of the Legendre polynomials and the recurrence relation [2.170].)

11.7 Using the first two partial waves ($l = 0, 1$), discuss the low-energy scattering by an attractive square well potential of reduced strength U_0 and range a. Plot the phase shifts, the partial wave cross-sections and the total cross-section as a function of ka for $0 \leqslant ka \leqslant 1$ and (a) $U_0 a^2 = 1$, (b) $U_0 a^2 = 10$.

11.8 Find the total cross-section for low-energy (s-wave) scattering by a potential barrier such that

$$U(r) = \begin{cases} U_0(>0), & r < a \\ 0, & r > a \end{cases}$$

Derive the 'hard sphere' zero energy result [11.97] as a particular case.

11.9 Using the first Born approximation [11.82] for $\tan \delta_l$, find the $l = 0$ phase shift for scattering by
(a) the Yukawa (or 'screened Coulomb') potential $U(r) = U_0 \exp(-\alpha r)/r$
(b) the 'polarisation' potential $U(r) = U_0/(r^2 + d^2)^2$, where d is a constant.

11.10 Obtain the radial integral equations [11.134] and the expression [11.72] for $\tan \delta_l$ by analysing the integral equation [11.128] in partial waves. (Hint: Use the expansions [A4.26] and [A4.27] and the addition theorem [A4.23] of the spherical harmonics.)

11.11 Show that for the case of central potentials the expression [11.141] of the first Born amplitude can be reduced to [11.145].

11.12 Obtain in first Born approximation the scattering amplitude, the differential and the total cross-sections for scattering by the following (reduced) potentials
(a) Exponential potential: $U(r) = U_0 \exp(-\alpha r)$
(b) Gaussian potential: $U(r) = U_0 \exp(-\alpha^2 r^2)$
(c) Square well $U(r)\begin{cases} = U_0, & r < a \\ = 0, & r > a \end{cases}$
(d) 'Polarisation' potential $U(r) = U_0/(r^2 + d^2)^2$.

Discuss the angular distributions and compare your results with those obtained in the text for the Yukawa potential $U(r) = U_0 \exp(-\alpha r)/r$. Verify that $\sigma_{\text{tot}}^{\text{B1}} \sim AE^{-1}$ as $E \to \infty$, and find the coefficient A in each case.

11.13 Prove equations [11.171] and [11.175].

12 Electron-atom collisions

With the help of the results obtained in the last chapter, for scattering of a beam of particles by a potential, we are now ready to discuss electron scattering by atoms, or by ions. In order to explain how cross-sections for elastic and inelastic scattering can be calculated, we shall, for the most part, take the simple example of electron scattering by atomic hydrogen; but the methods used for hydrogen can be generalised, and both experimental and theoretical studies have been carried out for many elements in the periodic table. As we remarked earlier, a knowledge of electron scattering cross-sections is required for many important applications in astrophysics, plasma physics and so on, but electron scattering is also important in determining the structure of complex atoms, or ions, since an electron beam can excite atoms from the ground state to levels that would be forbidden in excitation by photons. In addition, the global properties of atoms, such as the charge density, can be inferred from the measured cross-sections for high energy electron scattering. We shall first discuss elastic scattering, in which the energy of the target atom does not change, and then go on to consider the excitation of discrete atomic levels and finally ionisation, in which one or more electrons are ejected from the target. Although corresponding experiments have been made for the scattering of electrons by molecules, because of the extra molecular degrees of freedom – rotational and vibrational – and because of the complicated nature of the molecular electronic wave function, the interpretation of these data is usually very complicated and beyond the scope of this book.

12.1 ELECTRON SCATTERING: GENERAL PRINCIPLES

An electron scattering experiment can be carried out as shown schematically in Fig. 11.1. The apparatus consists of an electron gun with electrostatic focusing and collimating devices, a target containing the atoms to be studied and apparatus to detect and analyse the scattered electrons. The whole apparatus must be enclosed in a high vacuum, often at pressures of 10^{-6} to 10^{-9} Torr, requiring the most advanced vacuum technology. Since the energy range spanned by experiments is very large, from a few electron-volts to several MeV, the detailed design of the electron source may differ considerably from experiment to experiment. In general, the electron gun contains a heated

filament (the cathode) which produces electrons by thermionic emission. The electrons are accelerated to an anode containing an aperture through which the beam is produced (see Fig. 12.1). The intensity of the beam is controlled by applying a voltage, negative with respect to the cathode, to a cylindrical electrode called a *Wehnelt cylinder* which surrounds the cathode except for a hole through which the beam passes. The Wehnelt cylinder acts as a converging 'lens' focusing the beam, and further *electrostatic lenses* can be added to produce a collimated beam in the region of interaction.

When studying scattering from the atoms of a monoatomic gas, such as helium, or argon, the target can consist of a cell containing a sample of the gas itself. This technique cannot be used when scattering by charged ions is to be investigated, or for neutral atoms which would normally occur bound in molecular form. In these cases a beam of target atoms, or ions, is produced and scattering takes place at the intersection of the atomic and electron beams. In the case of charged ions, the beam can be controlled and focused by passing it through suitable electrostatic fields, but for neutral atoms the procedure is different. Let us consider the example of hydrogen (see Fig. 12.2). By heating hydrogen in a furnace, consisting of a tungsten tube, to 3000 K, over 90 per cent of molecular hydrogen is dissociated to atomic hydrogen. If the hydrogen atoms are allowed to escape through a suitably shaped small nozzle, a jet of atomic hydrogen is produced, which can provide densities of up to 10^{14} atoms/m^3 in the interaction region. It should be noted that the velocities of the atoms are usually negligible compared with the electron beam velocities, so the collision can be treated as being between the moving electrons and a stationary target. To eliminate background effects, the atomic beam can be modulated by passing it through a slit in a rotating disc, thereby chopping the beam at a frequency of say

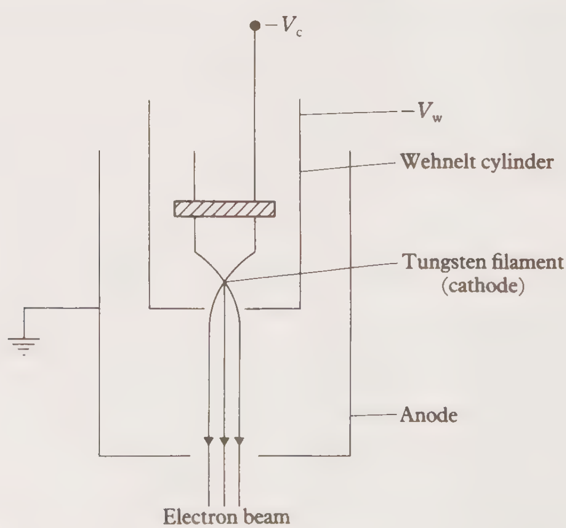

12.1 Schematic diagram of an electron gun. The potentials (with respect to the anode) on the cathode and the Wehnelt cylinder are denoted by $-V_c$ and $-V_w$, respectively.

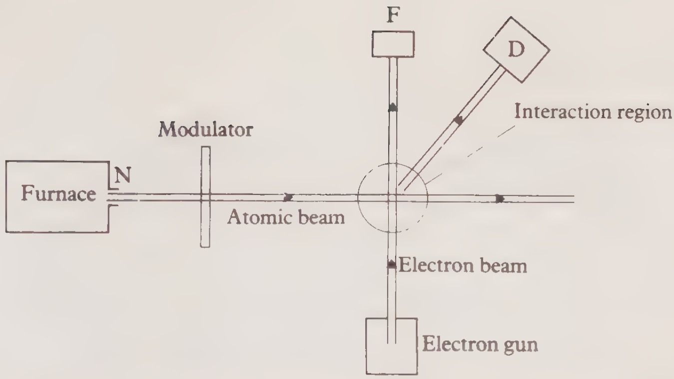

12.2 Diagram of an apparatus to measure electron scattering by atomic hydrogen. The atomic beam is produced by dissociating H_2 in a furnace at 3000 K. A jet of atomic hydrogen escapes through a nozzle N and passes through a modulator before reaching the interaction region, where it is intersected by an electron beam. The electron beam is monitored by collection in a Faraday cup F and the scattered electrons are detected and analysed at D.

100 Hz. Only the signal in the detector varying with this frequency represents scattering by the atomic beam, and any other signal represents scattering by impurity atoms.

The electrons scattered from the interaction region at a certain angle must be analysed and measured. The velocity of the electrons can be measured, or selected, by deflecting their paths by electrostatic fields of known characteristics. The velocity of selected electrons can be detected using electron multipliers and the scattered current measured. The electron multiplier is a device containing multiple electrodes called dynodes, such that the secondary electrons ejected when the beam falls on the first electrode are accelerated towards the second electrode, producing further secondary electrons, which are in turn accelerated towards a third electrode and so on. Larger fluxes of electrons are measured by collecting the electrons in a small metal container called a Faraday cup and amplifying the current produced electronically. Some results of an experiment by J. F. Williams and B. A. Willis, using an experimental arrangement of the general kind described, are shown in Fig. 12.3.

Theoretical description

We will now develop the theoretical description of non-relativistic electron scattering by atomic hydrogen. The spatial part $\psi(\mathbf{r}_1, \mathbf{r}_2)$ of the wave function of the scattered and target electrons satisfies the Schrödinger equation

$$\left[-\tfrac{1}{2}\nabla_1^2 - \tfrac{1}{2}\nabla_2^2 - \frac{1}{r_1} - \frac{1}{r_2} + \frac{1}{|\mathbf{r}_1 - \mathbf{r}_2|} - E_{\text{tot}}\right]\psi(\mathbf{r}_1, \mathbf{r}_2) = 0 \qquad [12.1]$$

where atomic units have been used for convenience, and $\mathbf{r}_1$ and $\mathbf{r}_2$ are the position vectors of the electrons, taking the proton to be at the origin of the

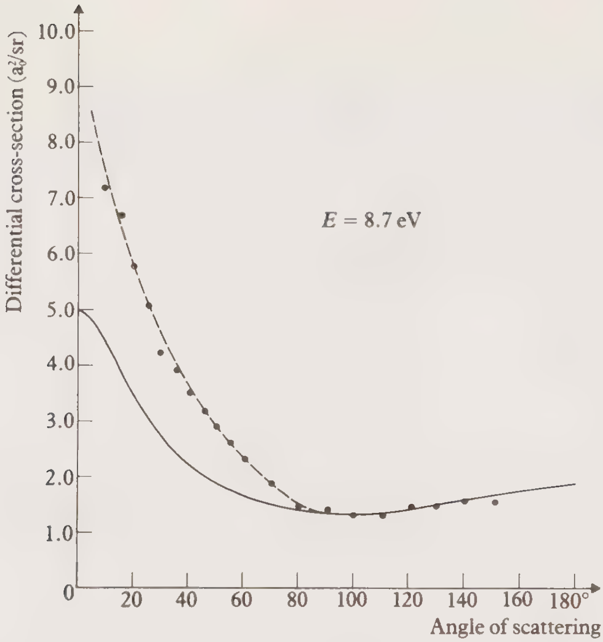

(a)

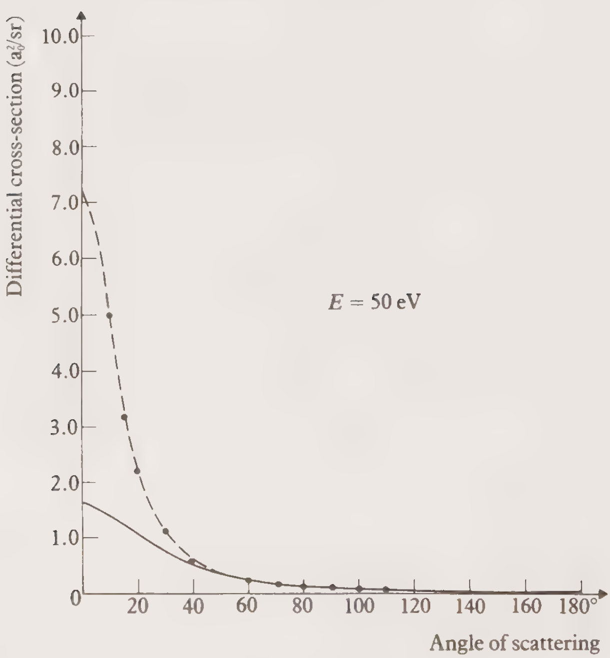

(b)

12.3 Cross-sections for the elastic scattering of electrons by atomic hydrogen. (a) At 8.7 eV (b) At 50 eV (c) At 100 eV • Data points
—— Static-exchange approximation
--------- Polarised orbital approximation using the potential [12.48].

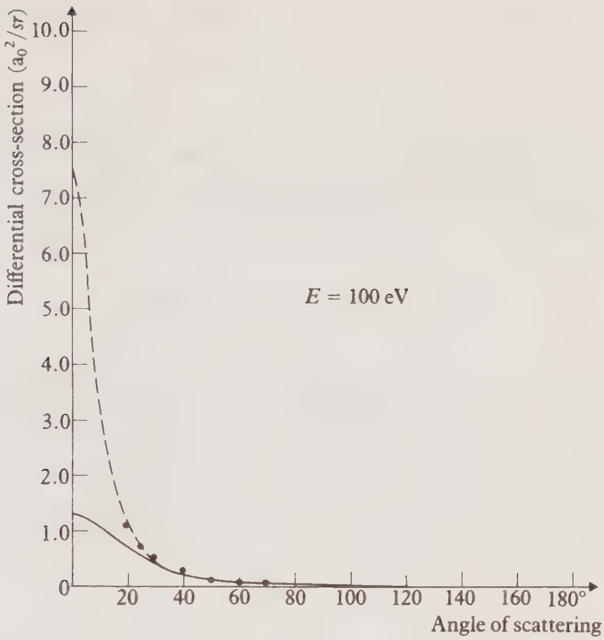

(c)

12.3(Cont.)

coordinate system. The infinite nuclear mass approximation is used, so that the proton can be considered to be at rest.

As explained in Chapter 6, the spatial part of the wave function must either be symmetrical $\psi_+(\mathbf{r}_1, \mathbf{r}_2)$ or antisymmetrical $\psi_-(\mathbf{r}_1, \mathbf{r}_2)$ under the interchange of the two electrons. The symmetrical spatial function corresponds to a singlet spin state $S = 0$ and the antisymmetrical spatial function to a triplet spin state $S = 1$. The functions ψ_+ and ψ_- can be determined independently, just as in the case of the helium atom.

Let us now consider the *boundary conditions* to be satisfied by $\psi_\pm(\mathbf{r}_1, \mathbf{r}_2)$, for the particular case in which the target hydrogen atom is initially in the ground (1s) state described by the hydrogenic wave function $\psi_{100}(\mathbf{r})$. The total energy of the system E_{tot} is given by

$$E_{\text{tot}} = E_1 + \tfrac{1}{2}k_1^2 \qquad [12.2]$$

where $E_1 = -\frac{1}{2}$ a.u. ($\simeq -13.6$ eV) is the ground state energy of atomic hydrogen and $\frac{1}{2}k_1^2$ is the kinetic energy of the incident electron. If the incident energy is insufficient to excite the hydrogen atom to the $n = 2$ level, the wave function, for $r_1 \gg r_2$, must represent electron 1 moving with respect to a ground state hydrogen atom containing electron 2, and we have

$$\psi_\pm(\mathbf{r}_1, \mathbf{r}_2) \underset{r_1\to\infty}{\sim} F_1^\pm(\mathbf{r}_1)\psi_{100}(\mathbf{r}_2) \qquad [12.3]$$

Because of the symmetry of the wave function, we must also have

$$\psi_{\pm}(\mathbf{r}_1, \mathbf{r}_2) \underset{r_2\to\infty}{\sim} \pm F_1^{\pm}(\mathbf{r}_2)\psi_{100}(\mathbf{r}_1) \tag{12.4}$$

The wave function for the free electron $F_1^{+}(\mathbf{r})$ must contain an incident plane wave and an outgoing spherical wave, and hence satisfies the boundary condition [11.25]. Taking, as before, the direction of incidence along the Z axis and the normalisation constant A (see [11.25]) to be unity, we write

$$F_1^{\pm}(\mathbf{r}_1) \underset{r_1\to\infty}{\sim} e^{ik_1z_1} + f_1^{\pm}(k_1, \theta, \phi)\frac{e^{ik_1r_1}}{r_1} \tag{12.5}$$

The differential cross-sections for scattering in the singlet and triplet spin states are then determined by the scattering amplitudes f_1^{+} and f_1^{-}, respectively. If the target atoms and the beam electrons are orientated at random (unpolarised), three times as many collisions occur in the triplet states as in the singlet state. The differential cross-section $d\sigma_{11}/d\Omega$ for the elastic scattering process $1 \to 1$, averaged over the four possible initial spin states is then

$$\frac{d\sigma_{11}}{d\Omega} = \tfrac{1}{4}|f_1^{+}|^2 + \tfrac{3}{4}|f_1^{-}|^2 \tag{12.6}$$

Since the system is symmetrical about the Z axis, $f_1^{\pm}$ and $d\sigma_{11}/d\Omega$ depend only on θ, and not on ϕ.

Before discussing ways in which the amplitudes $f_1^{\pm}$ might be calculated, let us consider the boundary conditions at higher energies, at which it is energetically possible to excite one or more higher levels. To simplify our notation, we will represent the three quantum numbers nlm of a hydrogenic level by the label q, where $q = 1$ for the ground state, so that each level q corresponds to a wave function ψ_q and an energy E_q. By conservation of energy, the kinetic energy of an electron which emerges from the scattering region after exciting the level q, is given by

$$\tfrac{1}{2}k_q^2 = E_{\text{tot}} - E_q = \tfrac{1}{2}k_1^2 + (E_1 - E_q) \tag{12.7}$$

and for 'open' channels $k_q^2 \geqslant 0$.

In the asymptotic region $r_1 \gg r_2$, there must be terms in the wave function representing a free electron of energy $\tfrac{1}{2}k_q^2$ moving with respect to the target in level q, and in place of [12.3], the asymptotic form of $\psi_{\pm}(\mathbf{r}_1, \mathbf{r}_2)$ is

$$\psi_{\pm}(\mathbf{r}_1, \mathbf{r}_2) \underset{r_1\gg r_2}{\sim} \sum_{q=1}^{N} F_q^{\pm}(\mathbf{r}_1)\psi_q(\mathbf{r}_2) \tag{12.8}$$

where the sum runs over the N open channels. In every open channel q, there must be spherical outgoing waves representing a current of electrons emerging from the scattering region, but only in the entrance, or incidence, channel does the plane wave representing the initial electron of energy $\tfrac{1}{2}k_1^2$ occur. The

generalisation of [12.5] is therefore

$$F_q^{\pm}(\mathbf{r}_1) \underset{r_1\to\infty}{\sim} e^{ik_1z_1}\,\delta_{q1} + f_q^{\pm}(k_1, \theta, \phi)\,\frac{e^{ik_qr_1}}{r_1} \qquad [12.9]$$

Calculating the flux of outgoing electrons with energies $\frac{1}{2}k_q^2$, along the lines indicated in Section 11.2, and dividing by the incident flux which is equal to k_1, the differential cross-section for excitation of the level q, from the level 1 is, for unpolarised beam electrons and target atoms

$$\frac{d\sigma_{q1}}{d\Omega} = \frac{k_q}{k_1}\left[\frac{1}{4}|f_q^+|^2 + \frac{3}{4}|f_q^-|^2\right] \qquad [12.10]$$

The exact wave functions $\psi_\pm$ can be written for all r_1 and r_2 in the form

$$\psi_\pm(\mathbf{r}_1, \mathbf{r}_2) = \sum_{q=1}^{N}\left[F_q^{\pm}(\mathbf{r}_1)\psi_q(\mathbf{r}_2) \pm F_q^{\pm}(\mathbf{r}_2)\psi_q(\mathbf{r}_1)\right] + \chi_N^{\pm}(\mathbf{r}_1, \mathbf{r}_2) \quad [12.11]$$

where $\chi_N^{\pm}$ are called the closed channel wave functions. Since for $r_1 \gg r_2$, or $r_2 \gg r_1$ there must be no electron flux associated with $\chi_N^{\pm}$, we must have

$$r_1\chi_N^{\pm} \to 0 \text{ as } r_1 \to \infty; \qquad r_2\chi_N^{\pm} \to 0 \text{ as } r_2 \to \infty \qquad [12.12]$$

If the incident energy is increased beyond the ionisation threshold, which for hydrogen is at $\frac{1}{2}k_1^2 = 13.6$ eV, the level q represents a continuum hydrogenic state with positive energy E_q. For these ionised states, q becomes a continuous index $q \equiv (E_q, l, m)$ and the sums over q in [12.8] or [12.11] must include an integration over the continuous range of q. We shall return to this later when discussing ionisation.

12.2 ELASTIC SCATTERING

The scattering amplitudes $f_1^{\pm}$ for elastic scattering can be calculated in one of several simple approximations which we shall now describe.

The static-exchange method

A procedure, analogous to the Hartree–Fock method for bound states described in Chapter 7, is to represent the wave functions $\psi_\pm(\mathbf{r}_1, \mathbf{r}_2)$ by the symmetrised products:

$$\psi_\pm(\mathbf{r}_1, \mathbf{r}_2) = [F_1^{\pm}(\mathbf{r}_1)\psi_1(\mathbf{r}_2) \pm F_1^{\pm}(\mathbf{r}_2)\psi_1(\mathbf{r}_1)] \qquad [12.13]$$

This is clearly an approximate wave function, as the true wave function must contain a closed channel component, as well as a component arising from any other open channels. To obtain an equation for the function $F_1^{\pm}(\mathbf{r}_1)$, we notice that the projections of the Schrödinger equation [12.1] onto the complete set of

orthonormal hydrogenic functions ψ_q must all vanish:

$$\int \psi_q^\star(\mathbf{r}_2)\left[-\tfrac{1}{2}\nabla_1^2 - \tfrac{1}{2}\nabla_2^2 - \frac{1}{r_1} - \frac{1}{r_2} + \frac{1}{|\mathbf{r}_1 - \mathbf{r}_2|} - E_{\text{tot}}\right]\psi_\pm(\mathbf{r}_1, \mathbf{r}_2)\, d\mathbf{r}_2 = 0,$$

$$q = 1, 2, \ldots \qquad [12.14]$$

With the approximate wave function [12.13], we can satisfy one of these condition, by requiring the projection onto the ground state function ψ_1 to vanish:

$$\int \psi_1^\star(\mathbf{r}_2)\left[-\tfrac{1}{2}\nabla_1^2 - \tfrac{1}{2}\nabla_2^2 - \frac{1}{r_1} - \frac{1}{r_2} + \frac{1}{|\mathbf{r}_1 - \mathbf{r}_2|} - E_{\text{tot}}\right]$$
$$\times \{F_1^\pm(\mathbf{r}_1)\psi_1(\mathbf{r}_2) \pm F_1^\pm(\mathbf{r}_2)\psi_1(\mathbf{r}_1)\}\, d\mathbf{r}_2 = 0 \qquad [12.15]$$

This equation can also be obtained from the variational principle of Section 2.8 by requiring that $\delta I = 0$ under the variations $F_1^\pm \rightarrow F_1^\pm + \delta F_1^\pm$, $F_1^{\pm\star} \rightarrow F_1^{\pm\star} + \delta F_1^{\pm\star}$, where

$$I = \int \psi_\pm^\star\, (H - E_{\text{tot}})\psi_\pm\, d\mathbf{r}_1\, d\mathbf{r}_2 \qquad [12.16]$$

and $\psi_\pm$ is given by [12.13] (see Problem 12.2)

Using [12.15] and the Schrödinger equation satisfied by the hydrogen atom wave functions ψ_q, namely

$$\left[-\tfrac{1}{2}\nabla^2 - \frac{1}{r} - E_q\right]\psi_q(\mathbf{r}) = 0 \qquad [12.17]$$

the functions $F_1^\pm$ are found to satisfy the equation

$$(\nabla_1^2 + k_1^2)F_1^\pm(\mathbf{r}_1) = 2V_{11}(\mathbf{r}_1)F_1^\pm(\mathbf{r}_1)$$
$$\pm 2\int K_{11}(\mathbf{r}_1, \mathbf{r}_2)F_1^\pm(\mathbf{r}_2)\, d\mathbf{r}_2 \qquad [12.18]$$

The *direct potential* V_{11} is simply the *static potential*, i.e. the electrostatic interaction between the incident electron and the target hydrogen atoms, averaged over the target state ψ_1. That is,

$$V_{11}(\mathbf{r}_1) = \left\langle \psi_1 \left| -\frac{1}{r_1} + \frac{1}{|\mathbf{r}_1 - \mathbf{r}_2|} \right| \psi_1 \right\rangle = -\frac{1}{r_1} + \int \frac{|\psi_1(\mathbf{r}_2)|^2}{|\mathbf{r}_1 - \mathbf{r}_2|}\, d\mathbf{r}_2 \qquad [12.19]$$

The first term is the interaction with the nucleus, and the second term, with the electronic charge density of the atom. Using the explicit form of the hydrogen atom wave function, $\psi_1 = \pi^{-1/2} \exp(-r_2)$, and the expansion [A4.24], we have

$$V_{11}(r_1) = -(1 + 1/r_1)\exp(-2r_1) \qquad [12.20]$$

The *exchange potential* K_{11} is non-local and is given by the expression

$$K_{11}(\mathbf{r}_1, \mathbf{r}_2) = \psi_1^{\star}(\mathbf{r}_1)\psi_1(\mathbf{r}_2)\left[\frac{1}{|\mathbf{r}_1 - \mathbf{r}_2|} - (E_{\text{tot}} - 2E_1)\right] \qquad [12.21]$$

In Chapter 7, it was shown that the exchange potential for bound states was important and could not be neglected. The same is true at low energies in the scattering problem, but because the function $F_1^{\pm}(\mathbf{r}_2)$ oscillate like $\exp(i\mathbf{k}_l \cdot \mathbf{r}_2)$, the integral $\int K_{11}(\mathbf{r}_1, \mathbf{r}_2)F_1^{\pm}(\mathbf{r}_2)\,d\mathbf{r}_2$ decreases rapidly with increasing energy. At high energies, where the Born approximation is accurate, the exchange potential can be neglected to a good approximation, but at low energies the exchange term must be retained.

At low energies, except near the inelastic thresholds where resonance phenomena can occur (see below), the static-exchange approximation gives a fair description of elastic scattering. The cross-section calculation proceeds by expanding the function $F_1^{\pm}$ in Legendre polynomials (see [11.36] and [11.38])

$$F_1^{\pm}(\mathbf{r}_1) = \sum_{l=0}^{\infty} r_1^{-1}u_l^{\pm}(r_1)P_l(\cos\theta_1) \qquad [12.22]$$

The radial functions $u_l^{\pm}$ satisfy the equations

$$\left(\frac{d^2}{dr_1^2} - \frac{l(l+1)}{r_1^2} + k_1^2\right)u_l^{\pm}(r_1) = 2V_{11}(r_1)u_l^{\pm}(r_1) \pm 2\int_0^{\infty} K_l(r_1, r_2)u_l^{\pm}(r_2)\,dr_2 \qquad [12.23]$$

where

$$K_l(r_1, r_2) = 4r_1r_2e^{-(r_1+r_2)}\left[\frac{r_<^l}{r_>^{l+1}} - \delta_{l0}(E_{\text{tot}} - 2E_1)\right](2l+1), \qquad [12.24]$$

$r_>$ and $r_<$ being the greater or the lesser of r_1 and r_2. These equations can be solved numerically to find the elastic scattering phase shifts. The expansion in partial waves is rapidly convergent and at low energies (<10 eV) only the terms with $l = 0$, 1 and 2 are significant. The differential cross-section in this approximation is shown in Fig. 12.3(a) compared with the experimental data.

High energies. The Born approximation

At energies for which exchange scattering can be neglected, $F_1^- = F_1^+ = F_1$ is a wave function for scattering by the static potential V_{11}. For any atom, the potential corresponding to [12.19] can be written down by recognising that $|\psi_1(\mathbf{r}_2)|^2$ is the electron density $\rho(\mathbf{r}_2)$, and in general, for an atom with nuclear charge Z

$$V_{11}(\mathbf{r}_1) = -\frac{Z}{r_1} + \int \frac{\rho(\mathbf{r}_2)}{|\mathbf{r}_1 - \mathbf{r}_2|}\,d\mathbf{r}_2 \qquad [12.25]$$

For sufficiently high energies, the elastic scattering amplitude is given by the Born approximation. From [11.141] we have with $U = 2V_{11}$ (in a.u.)

$$f_{B1} = -\frac{1}{2\pi}\int e^{i\boldsymbol{\Delta}\cdot\mathbf{r}_1} V_{11}(\mathbf{r}_1)\, d\mathbf{r}_1 \tag{12.26}$$

where $\boldsymbol{\Delta}$ is the momentum transfer with $\Delta = 2k_1 \sin\theta/2$ (see [11.143]).

To reduce the scattering amplitude f_{B1}, given by [12.26] in the Born approximation, to a more useful form, let us consider the integral

$$\begin{aligned} I &= \int e^{i\boldsymbol{\Delta}\cdot\mathbf{r}}(e^{-\lambda r}/r)\, d\mathbf{r} \\ &= \int_0^\infty r^2\, dr \int_{-1}^{+1} d(\cos\theta) \int_0^{2\pi} d\phi\, e^{i\Delta r\cos\theta}(e^{-\lambda r}/r) \end{aligned} \tag{12.27}$$

where $\boldsymbol{\Delta}$ has been taken as the Z axis. Integrating over $\cos\theta$ and ϕ we find

$$\begin{aligned} I &= \frac{4\pi}{\Delta}\int_0^\infty \sin(\Delta r)e^{-\lambda r}\, dr \\ &= \frac{4\pi}{(\lambda^2 + \Delta^2)} \end{aligned} \tag{12.28}$$

Taking the limit $\lambda \to 0$ we obtain the *Bethe integral*

$$\int \frac{e^{i\boldsymbol{\Delta}\cdot\mathbf{r}}}{r}\, d\mathbf{r} = \frac{4\pi}{\Delta^2} \tag{12.29}$$

Inserting the expression [12.25] for V_{11} into [12.26], and using [12.29], we find

$$f_{B1} = \frac{2}{\Delta^2}[Z - \mathcal{F}(\boldsymbol{\Delta})] \tag{12.30}$$

where $\mathcal{F}(\boldsymbol{\Delta})$ is a *form factor* called the *X-ray scattering factor* [1], defined as

$$\mathcal{F}(\boldsymbol{\Delta}) = \int e^{i\boldsymbol{\Delta}\cdot\mathbf{r}}\rho(\mathbf{r})\, d\mathbf{r} \tag{12.31}$$

The differential cross-section is, correspondingly,

$$\left(\frac{d\sigma}{d\Omega}\right)_{B1} = |f_{B1}|^2 = \frac{4}{\Delta^4}|Z - \mathcal{F}(\boldsymbol{\Delta})|^2 \tag{12.32}$$

In the case of atomic hydrogen $Z = 1$ and $\rho(r) = \exp(-2r)/\pi$, giving

$$\mathcal{F}_H(\Delta) = [1 + (\Delta/2)^2]^{-2} \tag{12.33a}$$

[1] The term X-ray scattering factor is used because the function $\mathcal{F}(\boldsymbol{\Delta})$ was first defined in the theory of X-ray scattering by atoms.

and

$$\left(\frac{d\sigma}{d\Omega}\right)_{B1} = 4\,\frac{(\Delta^2 + 8)^2}{(\Delta^2 + 4)^4} \qquad [12.33b]$$

For helium, ($Z = 2$), the density ρ can be evaluated using the approximate wave function [6.70],

$$\psi_{He}(r_1, r_2) = \frac{Z_e^3}{\pi}\, e^{-Z_e(r_1+r_2)} \qquad [12.34]$$

where the variational parameter Z_e has the value $Z_e = 27/16$ [see (6.78)]. We see immediately from [7.125] that

$$\rho(r) = 2\left(\frac{Z_e^3}{\pi}\right)e^{-2Z_e r} \qquad [12.35]$$

and correspondingly

$$\mathscr{S}_{He}(\Delta) = 2\left[1 + \left(\frac{\Delta}{2Z_e}\right)^2\right]^{-2} \qquad [12.36]$$

In general, it can be shown that $\mathscr{S}(\mathbf{\Delta}) \to Z$ as $\Delta \to 0$ and that $\mathscr{S}(\mathbf{\Delta})$ is usually a monotonically decreasing function of Δ as $\Delta \to \infty$.

Measurements of the differential scattering amplitudes as a function of $\mathbf{\Delta}$, at energies for which the Born approximation is accurate, determine $\mathscr{S}(\mathbf{\Delta})$, and, by inverting the Fourier transform [12.31], the density $\rho(\mathbf{r})$ can be calculated. By comparing the values of $\rho(\mathbf{r})$ obtained in this way with those calculated from Hartree–Fock wave functions, the importance of correlation in atomic wave functions can be established.

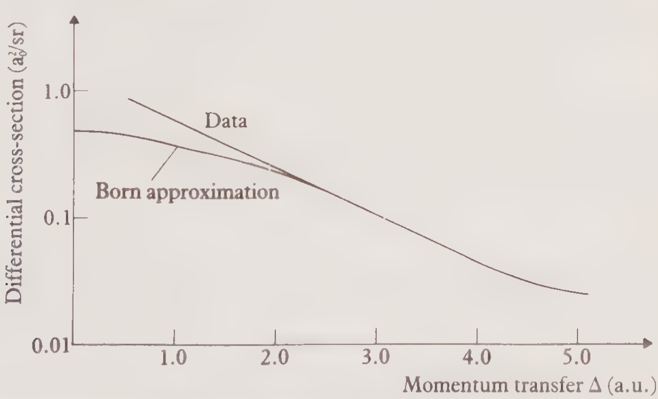

12.4 The elastic scattering differential cross-section for electron scattering by helium at 0.5 keV compared with the Born approximation.

To verify whether the Born approximation can be expected to be accurate, the experimental data at various angles and energies are analysed to check that $d\sigma/d\Omega$ is a function of Δ only, and not of k_1^2 or θ separately. For sufficiently high energies the Born approximation is accurate, except for angles near the forward

direction ($\theta = 0°$), where the distortion of the target wave function in the field of the incident electron is important. The velocity above which the Born approximation is accurate increases with the strength of the interaction, and so for a neutral atom increases with Z. For example, for helium the Born approximation is certainly accurate by incident energies of 500 eV, provided $\theta \gtrsim 15°$. Corresponding accuracies with a neon target are obtained above 12 keV, while for krypton energies above 40 keV are required. As an example the cross-section for electron scattering by helium at $E = 0.5$ keV is shown in Fig. 12.4.

The close coupling approximation

The static-exchange approximation based on the approximate wave functions [12.13] can be improved in several ways. The principal physical effects omitted in this approximation are the distortion of the target atom during the collision, and (above the lowest inelastic threshold) the loss of flux from the elastic scattering channel into other channels. Both these effects can be taken into account, approximately, by including additional configurations in the approximate wave functions. Taking N terms each similar in form to [12.13], an improved wave function can be written as

$$\psi_{\pm}(\mathbf{r}_1, \mathbf{r}_2) = \sum_{q=1}^{N} \{F_q^{\pm}(\mathbf{r}_1)\psi_q(\mathbf{r}_2) \pm F_q^{\pm}(\mathbf{r}_2)\psi_q(\mathbf{r}_1)\} \qquad [12.37]$$

The equations satisfied by the channel functions F_q are obtained from [12.14] with $q = 1, 2, \ldots N$. It is found that

$$(\nabla_1^2 + k_q^2)F_q^{\pm}(\mathbf{r}_1) = 2\sum_{q'=1}^{N} V_{qq'}(\mathbf{r}_1)F_{q'}^{\pm}(\mathbf{r}_1) \pm 2\sum_{q'=1}^{N} \int K_{qq'}(\mathbf{r}_1, \mathbf{r}_2)F_{q'}^{\pm}(\mathbf{r}_2)\, d\mathbf{r}_2$$

$$q = 1, 2, \ldots N \qquad [12.38]$$

These are a set of N coupled equations which must be solved by imposing the boundary conditions [12.9]. The direct potentials $V_{qq'}$ are (compare with [12.19])

$$V_{qq'}(\mathbf{r}_1) = \left\langle \psi_q \left| -\frac{1}{r_1} + \frac{1}{|\mathbf{r}_1 - \mathbf{r}_2|} \right| \psi_{q'} \right\rangle = -\frac{1}{r_1}\delta_{qq'} + \int \frac{\psi_q^{\star}(\mathbf{r}_2)\psi_{q'}(\mathbf{r}_2)}{|\mathbf{r}_1 - \mathbf{r}_2|}\, d\mathbf{r}_2 \qquad [12.39]$$

and the corresponding exchange potentials are

$$K_{qq'}(\mathbf{r}_1, \mathbf{r}_2) = \psi_q^{\star}(\mathbf{r}_1)\psi_{q'}(\mathbf{r}_2)\left[\frac{1}{|\mathbf{r}_1 - \mathbf{r}_2|} - (E_{\text{tot}} - E_q - E_{q'})\right] \qquad [12.40]$$

The approximation represented by [12.37] is called the *close coupling* approximation, because it assumes that the N states $q = 1, 2 \ldots N$ are closely coupled together and that the influence of the states with $q > N$ is small. To reduce the

equations [12.38] to radial form a decomposition into partial wave amplitudes can be made, but we shall not pursue this here. It is sufficient to note that detailed calculations based on this approximation can in suitable cases give a very good description of the scattering of electrons by light atoms.

The optical potential

An alternative approach to elastic scattering, which goes beyond the static exchange approximation, is to define an effective or *optical potential* $V_{\rm opt}^{\pm}$ such that the exact channel functions $F_1^{\pm}(\mathbf{r}_1)$ for elastic scattering satisfy the potential scattering equation (in a.u.)

$$[\nabla_1^2 + k_1^2 - 2V_{\rm opt}^{\pm}]F_1^{\pm}(\mathbf{r}_1) = 0 \qquad [12.41]$$

In the lowest (static-exchange) approximation $V_{\rm opt}^{\pm} \simeq V_{11} \pm K_{11}$ and contains both the direct potential V_{11} and the *non-local* exchange potential K_{11}. The distortion of the target atom during the collision modifies the effective potential, and the most important effect is to add to V_{11} potentials which are of 'long range' and decrease with r_1 like r_1^{-2n}, $n = 2, 3, \ldots$. The potential of longest range is the most important and is due to the dipole induced in the target by the incident charge. This effect is easiest to calculate at very low energies, for which the kinetic energy of the incident electron can be neglected in the first approximation. The Schrödinger equation for a hydrogen atom placed in the field of a *fixed* charge (-1) situated at the position $\mathbf{r}_1$ is

$$[H_0 + V(\mathbf{r}_1, \mathbf{r}_2)]\Phi(\mathbf{r}_1, \mathbf{r}_2) = E(\mathbf{r}_1)\Phi(\mathbf{r}_1, \mathbf{r}_2) \qquad [12.42]$$

with

$$V(\mathbf{r}_1, \mathbf{r}_2) = -\frac{1}{r_1} + \frac{1}{|\mathbf{r}_1 - \mathbf{r}_2|} \qquad [12.43]$$

and where H_0 is the Hamiltonian for the hydrogen atom

$$H_0 = -\tfrac{1}{2}\nabla_2^2 - \frac{1}{r_2} \qquad [12.44]$$

Both Φ and the eigenvalue E depend on $\mathbf{r}_1$ parametrically. Let us consider the solution of [12.42] which, as $r_1 \to \infty$, becomes equal to the unperturbed hydrogen ground state wave function $\psi_1(r_2) \equiv \psi_{100}(r_2)$. Thus

$$\Phi(\mathbf{r}_1, \mathbf{r}_2) \to \psi_{100}(r_2); \qquad E(\mathbf{r}_1) \to E_1 \quad \text{as} \quad r_1 \to \infty$$

Applying perturbation theory (see Section 2.8) up to second order, we have

$$E(\mathbf{r}_1) = E_1 + E_1^{(1)}(\mathbf{r}_1) + E_1^{(2)}(\mathbf{r}_1) \qquad [12.45]$$

The first-order correction $E_1^{(1)}$ is

$$E_1^{(1)} = \langle\psi_{100}|V(\mathbf{r}_1, \mathbf{r}_2)|\psi_{100}\rangle \qquad [12.46]$$

and we see that $E_1^{(1)} = V_{11}(r_1)$, the direct static interaction between an electron and a ground state hydrogen atom, given by [12.20].

The second-order term is

$$E_1^{(2)}(\mathbf{r}_1) = \sum_{\substack{nlm \\ (n\neq 1)}} \frac{|\langle\psi_{100}|V(\mathbf{r}_1, \mathbf{r}_2)|\psi_{nlm}\rangle|^2}{E_1 - E_n}$$

$$= \sum_{q'\neq 1} \frac{|V_{1q'}(\mathbf{r}_1)|^2}{E_1 - E_{q'}} \qquad [12.47]$$

where in the last line we have used the notation of [12.39]. The sum over (nlm) includes an integration over the continuum states of atomic hydrogen.

The direct part of the optical potential V_{opt} can then be identified at low energies with $E(\mathbf{r}_1) - E_1$. Adding the exchange potential $K_{11}(\mathbf{r}_1, \mathbf{r}_2)$, we have

$$V_{\text{opt}}^{\pm}(\mathbf{r}_1) = V_{11}(r_1) + V_{\text{pol}}(\mathbf{r}_1) \pm K_{11}(\mathbf{r}_1, \mathbf{r}_2) \qquad [12.48]$$

where the *polarisation* or *distortion potential* $V_{\text{pol}}(\mathbf{r}_1)$ is equal to $E_1^{(2)}(\mathbf{r}_1)$ and is given by [12.47]. Since the exchange part of $V_{\text{opt}}^{\pm}$ is non-local, the explicit form of [12.41] reads

$$[\nabla^2 + k_1^2 - 2V_{11}(r_1) - 2V_{\text{pol}}(\mathbf{r}_1)]F_1^{\pm}(\mathbf{r}_1)$$

$$= \pm 2\int K_{11}(\mathbf{r}_1, \mathbf{r}_2)F_1^{\pm}(\mathbf{r}_2)\,\mathrm{d}\mathbf{r}_2 \qquad [12.49]$$

We easily see from [12.47] that since $(E_1 - E_n) < 0$ for all $n(n \neq 1)$, $V_{\text{pol}} = E_1^{(2)}$ is negative and represents an attractive potential.

For large r_1, using the expansion [A4.24], we have

$$V(\mathbf{r}_1, \mathbf{r}_2) \underset{r_1\to\infty}{\sim} \frac{1}{r_1}\sum_{l=1}^{\infty}\left(\frac{r_2}{r_1}\right)^l P_l(\cos\theta_{12}) \qquad [12.50]$$

where θ_{12} is the angle between $\mathbf{r}_1$ and $\mathbf{r}_2$. The term decreasing most slowly when r_1 is large is that with $l = 1$, which decreases like r_1^{-2}. Correspondingly, the long range behaviour of V_{pol} from [12.47] and [12.50] is

$$V_{\text{pol}} \underset{r_1\to\infty}{\sim} -\frac{\bar{\alpha}}{2r_1^4} \qquad [12.51]$$

where $\bar{\alpha}$ is the *dipole polarisability* of the target atom, which is given in a.u. by (see [5.112])

$$\bar{\alpha} = 2\sum_{\substack{n\neq 1 \\ l,m}} \frac{|\langle\psi_{nlm}|z_2|\psi_{100}\rangle|^2}{E_n - E_1} \qquad [12.52]$$

Angular momentum conservation restricts the sum over intermediate states to p_0 states ($l = 1$, $m = 0$). For atomic hydrogen $\bar{\alpha} = 4.5$ a.u. The size of $\bar{\alpha}$ is largely determined by how close the lowest lying p state is to the ground state. For the rare gases, the polarisabilities are small (for example $\bar{\alpha} = 1.38$ a.u. for

helium) while for the alkalis where the level n_0p is very close to the ground state n_0s, the polarisabilities are very large ($\bar{\alpha} \simeq 140$ a.u. for sodium).

By studying the coupled equations [12.38] it can be shown that for large r_1 the interaction of longest range is given by [12.51] not just at very low energies but at all energies. Above the first inelastic threshold the optical potentials develop an imaginary part to account for *absorption* (loss of flux) from the incident channel (see Section 11.6), but the purely real potential [12.48] often gives a good account of elastic scattering at all energies.

At high energies the effect of the polarisation potential is to enhance the scattering in the forward direction, as observed in the experiments (see Fig. 12.3). At sufficiently high energies, the exchange interaction can be dropped and the direct interaction ($V_{11} + V_{\text{pol}}$) can be inserted into the expression for the Born approximation.

The asymptotic (large r_1) form of V_{pol} given by [12.51] is modified at small values of r_1. Since, except for hydrogen, it is difficult to calculate V_{pol} from perturbation formulae like [12.47], semi-empirical expressions are often used, for example

$$V_{\text{pol}}(r_1) = -\frac{\bar{\alpha}}{2(r_1^2 + d^2)^2} \qquad [12.53]$$

which depends on a constant d, of the order of magnitude of the radius of the atom. A more detailed account of the optical potential theory may be found in Joachain (1979).

12.3 EXCITATION OF ATOMS TO DISCRETE LEVELS

To illustrate how cross-sections for inelastic scattering can be determined, we shall again take the case of electron scattering by atomic hydrogen. The simplest approximate wave function must contain both the incident channel and the final channel of interest. If the target atom is initially in the ground state, and the final state of interest is labelled by q ($\neq 1$), the simplest approximate wave function is (compare with [12.37])

$$\begin{aligned}\psi_{\pm}(\mathbf{r}_1, \mathbf{r}_2) = {} & [F_1^{\pm}(\mathbf{r}_1)\psi_1(\mathbf{r}_2) \pm F_1^{\pm}(\mathbf{r}_2)\psi_1(\mathbf{r}_1)] \\ & + [F_q^{\pm}(\mathbf{r}_1)\psi_q(\mathbf{r}_2) \pm F_q^{\pm}(\mathbf{r}_2)\psi_q(r_1)]\end{aligned} \qquad [12.54]$$

A pair of coupled equations of the form [12.38] with $N = 2$, determines the unknown functions $F_1^{\pm}, F_q^{\pm}$. Solving these equations numerically, subject to the boundary conditions [12.9], allows the determination of the scattering amplitudes $f_q^{\pm}$ and the differential cross-sections by [12.10]. This *two-state approximation* can be extended to a many-state close-coupling approximation by using [12.37] and [12.38] with $N > 2$. For hydrogen the optically allowed transition 1s → 2p is the largest excitation cross-section, and a three-state approximation including the 1s, 2s and 2p states provides reasonably accurate cross-sections for this transition (see Fig. 12.5).

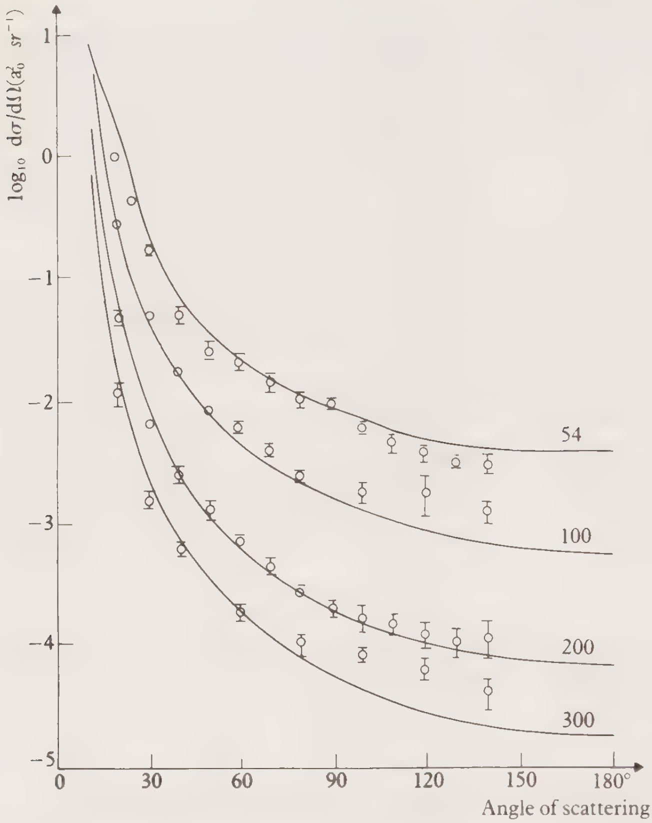

12.5 The cross-section for excitation of the (2s + 2p) levels of hydrogen by electron impact at 54, 100, 200 and 300 eV. The solid line is the result of a three-state close-coupling approximation.

The Born approximation

We saw that experiments on elastic scattering, at energies which are sufficiently high for the Born approximation to be accurate, provide a way of measuring the charge densities of atoms (and indeed of molecules). Equally important information can be obtained from excitation experiments at high energies.

At sufficiently high energies, exchange effects are small and the exchange potentials in [12.38] can be neglected. In the Born approximation, the lowest order wave function is set equal to the unperturbed function

$$\psi_{\pm}(\mathbf{r}_1, \mathbf{r}_2) \simeq \psi_0(\mathbf{r}_1, \mathbf{r}_2) = \exp(i\mathbf{k}_i \cdot \mathbf{r}_1)\psi_{100}(\mathbf{r}_2) \qquad [12.55]$$

with $\mathbf{k}_i = k_1\hat{\mathbf{z}}$. Hence the lowest order channel functions $F_q^{\pm}$ are given by

$$F_q^{\pm}(\mathbf{r}_1) \equiv F_q(\mathbf{r}_1) = \delta_{q1} \exp(i\mathbf{k}_i \cdot \mathbf{r}_1) \qquad [12.56]$$

Inserting this lowest order approximation into the right-hand side of [12.38],

and neglecting the exchange potentials, we have

$$(\nabla_1^2 + k_q^2)F_q(\mathbf{r}_1) \simeq 2V_{q1}(\mathbf{r}_1)\exp(i\mathbf{k}_i \cdot \mathbf{r}_1) \qquad [12.57]$$

where, since $F_q^+ = F_q^-$ in this approximation, the superscripts $\pm$ have been dropped. The solution of this equation, with the boundary condition [12.9], can be obtained with the help of the Green's function [11.126]. We have

$$F_q(\mathbf{r}_1) = -\frac{1}{2\pi}\int \frac{e^{ik_q|\mathbf{r}_1 - \mathbf{r}_1'|}}{|\mathbf{r}_1 - \mathbf{r}_1'|} V_{q1}(\mathbf{r}_1')e^{i\mathbf{k}_i\cdot\mathbf{r}_1'}\,d\mathbf{r}_1' \qquad [12.58]$$

In the limit of large r_1, this becomes

$$F_q(\mathbf{r}_1) \underset{r_1\to\infty}{\sim} -\frac{1}{2\pi}\frac{e^{ik_q r_1}}{r_1}\int e^{-i\mathbf{k}_q\cdot\mathbf{r}_1'}V_{q1}(\mathbf{r}_1')e^{i(\mathbf{k}_i\cdot\mathbf{r}_1')}\,d\mathbf{r}_1' \qquad [12.59]$$

where $\mathbf{k}_q$ is a vector in the direction of $\mathbf{r}_1$ with magnitude k_q. Comparing this expression with the asymptotic form [12.9], we obtain the scattering amplitude f_q in the Born approximation as

$$f_q = -\frac{1}{2\pi}\int e^{i\boldsymbol{\Delta}\cdot\mathbf{r}_1'}V_{q1}(\mathbf{r}_1')\,d\mathbf{r}_1' \qquad [12.60]$$

where the momentum transfer $\boldsymbol{\Delta}$ is now given by

$$\boldsymbol{\Delta} = \mathbf{k}_i - \mathbf{k}_q \qquad [12.61]$$

The amplitudes [12.60] can be transformed using the Bethe integral [12.29] to obtain for the case of excitation ($q \neq 1$)

$$f_q = -\frac{2}{\Delta^2}\int \psi_q^\star(\mathbf{r})\,e^{i\boldsymbol{\Delta}\cdot\mathbf{r}}\,\psi_1(\mathbf{r})\,d\mathbf{r} \qquad [12.62]$$

where we have used [12.39]. It is convenient to introduce the *inelastic form factor* $\mathcal{S}_{qq'}$, which corresponds to the integral [12.31] in the theory of elastic scattering

$$\mathcal{S}_{qq'}(\boldsymbol{\Delta}) = \int \psi_q^\star(\mathbf{r})e^{i\boldsymbol{\Delta}\cdot\mathbf{r}}\psi_{q'}(\mathbf{r})\,d\mathbf{r} \qquad [12.63]$$

so that we have

$$f_q = -\frac{2}{\Delta^2}\mathcal{S}_{q1}(\boldsymbol{\Delta}) \qquad [12.64]$$

In the case of scattering by a neutral atom, with nuclear charge Z, the generalisation of $\mathcal{S}_{qq'}$ is easily seen to be

$$\mathcal{S}_{qq'}(\boldsymbol{\Delta}) = \sum_{i=1}^{Z}\int d\mathbf{r}_1\int d\mathbf{r}_2 \ldots \int d\mathbf{r}_Z\,\psi_q^\star e^{i\boldsymbol{\Delta}\cdot\mathbf{r}_i}\psi_{q'} \qquad [12.65]$$

In general, $\mathcal{S}_{q1}(\boldsymbol{\Delta})$ depends on both the magnitude and the direction of $\boldsymbol{\Delta}$; but it can be shown that $\Sigma_m|\mathcal{S}_{q1}(\Delta)|^2$ depends only on Δ (the magnitude of Δ), where the sum is over the magnetic quantum number of the final state $q \equiv (nlm)$.

The differential cross-section in the Born approximation is given by [2]

$$\frac{\mathrm{d}\sigma_{q1}}{\mathrm{d}\Omega} = \frac{k_q}{k_1}|f_q|^2 \tag{12.66}$$

where f_q is given by [12.64]. The total cross-section summed over the magnetic quantum number of the final state $q \equiv (nlm)$ can be defined as

$$\sigma_{\bar{q}1}(k_1) = 2\pi \sum_m \frac{k_q}{k_1}\int_{-1}^{+1} \mathrm{d}(\cos\theta)|f_q|^2 \tag{12.67}$$

where $\bar{q} \equiv (nl)$ labels the final state. Since $\Sigma_m|f_q|^2$ depends only on Δ, and because from [12.61],

$$\Delta^2 = k_1^2 + k_q^2 - 2k_1k_q\cos\theta \tag{12.68}$$

we can write [12.67] in the alternative form, using [12.64]

$$\sigma_{\bar{q}1}(k_1) = \frac{8\pi}{k_1^2}\int_{\Delta_{\min}}^{\Delta_{\max}} \frac{1}{\Delta^3}\sum_m |\mathscr{G}_{q1}(\mathbf{\Delta})|^2\,\mathrm{d}\Delta \tag{12.69}$$

where $\Delta_{\max} = (k_1 + k_q)$ and $\Delta_{\min} = (k_1 - k_q)$. When the change of energy of the target atom $(E_q - E_1)$ is small compared with the incident energy $(k_1^2/2)$, we can write

$$\Delta_{\max} \simeq 2k_1 \quad \text{and} \quad \Delta_{\min} \simeq (E_q - E_1)/k_1 \tag{12.70}$$

In order to see the connection between cross-sections for transitions induced by electron impact with the radiative transitions, studied in Chapter 4, we introduce a *generalised oscillator strength*

$$\mathscr{F}_{qq'}(\mathbf{\Delta}) = (E_q - E_{q'})\frac{2}{\Delta^2}|\mathscr{G}_{qq'}(\mathbf{\Delta})|^2, \qquad q \neq q' \tag{12.71}$$

so that

$$\sigma_{\bar{q}1}(k_1) = \frac{4\pi}{k_1^2}\left(\frac{1}{E_q - E_1}\right)\int_{\Delta_{\min}}^{\Delta_{\max}} \mathscr{F}_{\bar{q}1}(\Delta)\frac{\mathrm{d}\Delta}{\Delta} \tag{12.72}$$

where

$$\mathscr{F}_{\bar{q}1}(\Delta) = \sum_m \mathscr{F}_{q1}(\mathbf{\Delta}) \tag{12.73}$$

From [12.63], by expanding the exponential, we have for small Δ

$$\mathscr{G}_{qq'}(\mathbf{\Delta}) = \langle\psi_q|1 + i(\mathbf{\Delta}\cdot\mathbf{r}) + \cdots|\psi_{q'}\rangle \tag{12.74}$$

When $q \neq q'$, ψ_q and $\psi_{q'}$ are orthogonal, and the first term is zero. In the limit of

[2] It may be shown that the first Born approximation for direct excitation at high energies is accurate at small values of the momentum transfer Δ, but not at large values of Δ. However, since the differential cross-section is only large for small Δ, the total (integrated) excitation cross-section is represented accurately by the first Born approximation at sufficiently high energies.

small Δ we then have

$$\mathcal{S}_{qq'}(\mathbf{\Delta}) \simeq i\Delta\langle\psi_q|z|\psi_{q'}\rangle \tag{12.75}$$

where z is the component of $\mathbf{r}$ in the direction $\mathbf{\Delta}$. From [12.71] and [12.75] we can find the form of the generalised oscillator strength for small $\mathbf{\Delta}$

$$\mathcal{F}_{qq'}(\mathbf{\Delta}) \simeq 2(E_q - E_{q'})|\langle\psi_q|z|\psi_{q'}\rangle|^2 \tag{12.76a}$$

$$\simeq 2(E_q - E_{q'})|z_{qq'}|^2 \tag{12.76b}$$

where we have introduced the notation used in Section 4.6, namely $z_{qq'} = \langle\psi_q|z|\psi_{q'}\rangle$. The right-hand side of [12.76] is identical with the optical oscillator strength $f_{qq'}$ defined in Section 4.6, and we may write

$$\lim_{\Delta\to 0} \mathcal{F}_{qq'}(\mathbf{\Delta}) = f_{qq'} \tag{12.77}$$

This result which we have proved here for atomic hydrogen is in fact true for any atom, for which the general expression [12.65] for $\mathcal{S}_{qq'}$ is used in the definition of the generalised oscillator strength [12.71]. Measurements of the differential cross-section for an inelastic transition as a function of Δ, $\mathrm{d}\sigma_{\bar{q}1}/\mathrm{d}\Delta$ enable $\mathcal{F}_{\bar{q}1}(\Delta)$ to be determined for a range of Δ, since

$$\frac{\mathrm{d}\sigma_{\bar{q}1}}{\mathrm{d}\Delta} = \frac{4\pi}{k_1^2}\left(\frac{1}{E_q - E_1}\right)\frac{\mathcal{F}_{\bar{q}1}(\Delta)}{\Delta} \tag{12.78}$$

This range does not extend to $\Delta = 0$, since the minimum value of Δ is given by [12.70]. However as the incident energy increases, $\Delta_{\min}$ decreases and the experimental data can be extrapolated to determine the optical oscillator strength $f_{\bar{q}1} = \Sigma_m f_{q1}$. As an example, the data for the excitation of the 2^1 P level of helium from the ground state is shown in Fig. 12.6. The relationship [12.77] between optical excitation and electron excitation implies that in the high energy limit the electron impact cross-sections for optically allowed transitions are much larger than those for optically forbidden transitions.

The high energy behaviour of total inelastic cross sections can be determined by noticing that (see Fig. 12.6) the generalised oscillator strength, and hence the differential cross-section, decreases rapidly beyond a certain value of Δ. If this value of Δ is denoted by $\bar{\Delta}$, we see from [12.72] that the total cross-section $\sigma_{\bar{q}1}$ is given approximately by

$$\sigma_{\bar{q}1}(k_1) = \frac{4\pi}{k_1^2}\frac{1}{E_q - E_1}\int_{\Delta_{\min}}^{\bar{\Delta}} \frac{\mathcal{F}_{\bar{q}1}(\Delta)}{\Delta}\,\mathrm{d}\Delta \tag{12.79}$$

From [12.65] and [12.71] and by expanding the exponential $\exp(i\mathbf{\Delta}\cdot\mathbf{r}_i)$, we have

$$\mathcal{F}_{q1}(\Delta) = 2(E_q - E_1)\left|i\left\langle\psi_q\left|\sum_{i=1}^{Z} z_i\right|\psi_1\right\rangle - \frac{\Delta}{2}\left\langle\psi_q\left|\sum_{i=1}^{Z} z_i^2\right|\psi_1\right\rangle + \cdots\right|^2 \tag{12.80}$$

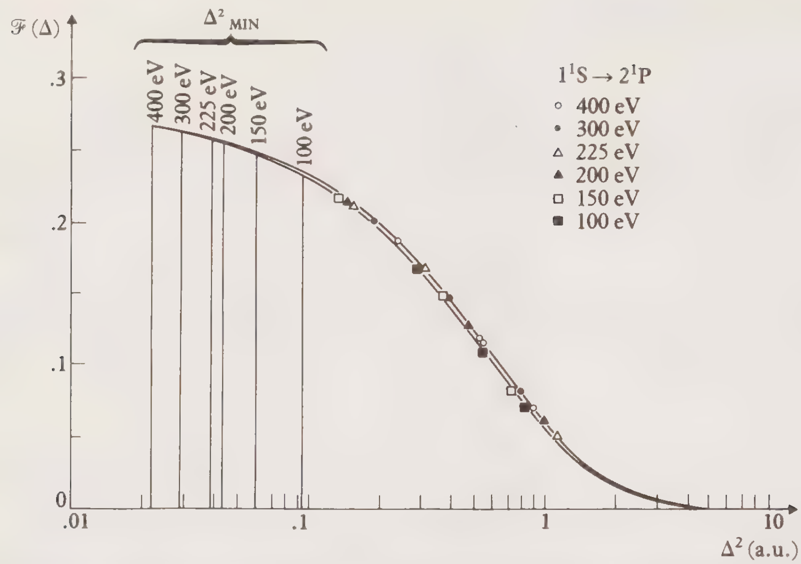

12.6 Generalised oscillator strength in atomic units for excitation of helium to the 2^1P level from the ground state.

In the case of optically allowed transitions the dipole term

$$\left\langle \psi_q \left| \sum_{i=1}^{Z} z_i \right| \psi_1 \right\rangle$$

does not vanish and is much larger than the quadrupole and higher multipole terms. In this case, $\mathcal{F}_{q1}(\Delta) \simeq \mathcal{F}_{q1}(0)$ and from [12.73], [12.79] and [12.80]

$$\sigma_{\bar{q}1}(k_1) = \frac{8\pi}{k_1^2} \sum_m \left| \left\langle \psi_q \left| \sum_{i=1}^{Z} z_i \right| \psi_1 \right\rangle \right|^2 \log\left(\frac{\bar{\Delta}}{\Delta_{\min}} \right) \qquad [12.81]$$

Using [12.70], we note that the high energy cross-section decreases like $E^{-1} \log E$, where $E = \frac{1}{2}k_1^2$.

If the dipole term vanishes, as in s → s or s → d transitions, we see from [12.73], [12.79] and [12.80] that the high energy cross-section decreases like E^{-1}, and

$$\sigma_{\bar{q}1}(k_1) \simeq \frac{\pi}{k_1^2} \sum_m \left| \left\langle \psi_q \left| \sum_{i=1}^{Z} z_i^2 \right| \psi_1 \right\rangle \right|^2 \bar{\Delta}^2 \qquad [12.82]$$

The expressions [12.81] and [12.82] are due to H. A. Bethe, and the *Bethe approximation* has been successfully used to analyse the *stopping power* of materials [3]. At high energies the dipole transitions dominate (whether for discrete excitation, or ionisation) and the energy loss per m of an electron of non-relativistic velocity v passing through a material containing N atoms per

[3] See for example Richtmyer, Kennard and Cooper (1969).

m^3, each of atomic number Z, is given approximately (in SI units) by

$$\frac{\mathrm{d}E}{\mathrm{d}x} = -\frac{NZe^4}{4\pi\varepsilon_0^2\, mv^2}\log\left(\frac{mv^2}{C}\right) \qquad [12.83]$$

where C is an empirical constant, which has the significance of a mean excitation energy.

12.4 IONISATION

Experimental studies of ionisation have been carried out with both neutral atoms and positive ions as targets. The related process of electron detachment from negative ions has also been measured in some cases, such as for the reaction

$$e^- + H^- \rightarrow H + 2e^-$$

In general, ionisation cross-sections increase from the ionisation threshold I, reach a maximum at an incident energy E from three to seven times I, and finally decrease like $E^{-1}\log E$. Two particular cases, the ionisation of Na^+ and of Ne^+ are shown in Fig. 12.7. Superimposed on this smooth variation is a fine structure which is due to the excitation of autoionising levels. For example, in the case of ionisation of neutral helium from the ground state, as well as direct ionisation, the reaction can proceed in two steps:

$$\begin{array}{l} e^- + He(1s^2) \rightarrow He(2s2p) + e^- \\ \qquad\qquad\qquad\qquad\quad \searrow \\ \qquad\qquad\qquad\qquad\qquad He^+(1s) + e^- \end{array}$$

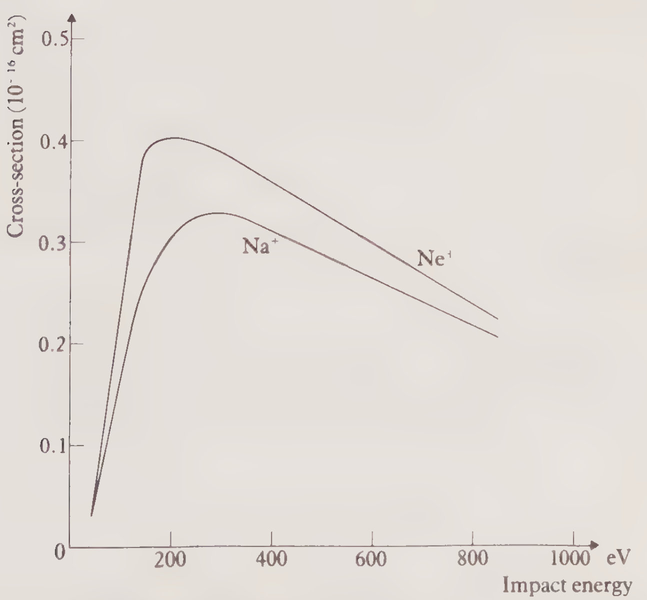

12.7 The cross-section for ionisation of Na^+ and Ne^+ by electron impact.

The (2s2p) ^{1}P level of helium is just one of a number of possible doubly excited intermediate states. The threshold for exciting this particular level is approximately 60 eV. The doubly excited state is long-lived compared with a characteristic collision time, and decays producing He^+ in the ground state and an ejected electron with a kinetic energy of about 36 eV.

Following the production of an inner shell vacancy in a heavy atom, a radiationless transition can occur in which an electron is ejected. As we saw earlier, this process is called the *Auger effect* and can lead to multiple ionisation. Consider for example the reaction

$$
\begin{array}{l}
\mathrm{e}^- + \mathrm{Ar} \rightarrow \mathrm{Ar}_\mathrm{L}^+ + \mathrm{e}^- + \mathrm{e}^- \\
\qquad\qquad\qquad\quad \searrow \\
\qquad\qquad\qquad\qquad \mathrm{Ar}^{2+} + \mathrm{e}^-
\end{array}
$$

In the first step, one of the L shell electrons is ionised and in the second step a second electron is ejected through an Auger rearrangement. The simultaneous direct ionisation of two or more electrons from many-electron atoms is possible, but the cross-sections are smaller than for the ionisation of a single electron. For a heavy atom or ion, it is possible to study ionisation in which an electron is ejected from a particular inner shell. This inner shell ionisation is the mechanism which produces the vacancies allowing the emission of X-rays in an X-ray tube, but useful ionisation cross-sections cannot be obtained from observations on such tubes as the targets are thick and complicated multiple scattering occurs.

Calculations of ionisation cross-sections are difficult for several reasons. At low energies, near to threshold, excitation cross-sections can be computed using a close-coupling approach, but this cannot be extended in any straightforward way to ionisation. At higher energies, the Born approximation can be formulated, but this does not take into account the long range Coulomb interaction between the scattered and ejected electrons which is certainly important at moderate energies. Since the scattered and ejected electrons are indistinguishable, the Born approximation, in which these electrons are not treated on an equal footing, is difficult to put on a completely logical basis. Despite these remarks, for sufficiently high energies, the *total* ionisation cross-section can be calculated accurately in the Born approximation.

In the Born approximation, the amplitude for the ionisation of atomic hydrogen in the ground state is again given by [12.62]. This time the wave function ψ_q must represent a state of positive energy, and the label q can be replaced by $\mathbf{q}$ where $\mathbf{q}$ is the momentum of the ejected electron in atomic units.

The wave functions $\psi_{\mathbf{q}}$ can be normalised so that (see [2.35])

$$\int \psi^*_{\mathbf{q}'}(\mathbf{r})\psi_{\mathbf{q}}(\mathbf{r})\,\mathrm{d}\mathbf{r} = \delta(\mathbf{q} - \mathbf{q}') \qquad [12.84]$$

The scattering amplitude $f_{\mathbf{q}}(k_1, \theta)$ depends not only on k_1 and on the angle θ of the scattered electron, but also on the magnitude and direction of $\mathbf{q}$, and the

differential cross-section from ionisation in which the ejected electron has momentum between $\mathbf{q}$ and $\mathbf{q} + d\mathbf{q}$ is

$$\frac{d^2\sigma}{d\Omega\, d\mathbf{q}} = \frac{k_{\mathbf{q}}}{k_1} |f_{\mathbf{q}}(k_1, \theta)|^2 \qquad [12.85]$$

Energy conservation requires that

$$\frac{1}{2} k_1^2 + E_1 = \frac{1}{2} k_{\mathbf{q}}^2 + \frac{1}{2} q^2 \qquad [12.86]$$

so that the maximum momentum of the ejected electron is

$$q_{\max} = (k_1^2 + 2E_1)^{1/2} \qquad [12.87]$$

The total cross-section is obtained by integrating over all the angles and energies of ejection, as well as the angle of scattering giving

$$\sigma_{\text{ION}}(k_1) = 2\pi \int_{-1}^{+1} d(\cos\theta) \int_0^{q_{\max}} q^2\, dq \int d\Omega(\hat{\mathbf{q}})\, \frac{k_q}{k_1} |f_{\mathbf{q}}(k_1, \theta)|^2 \qquad [12.88]$$

The evaluation of the cross-section is complicated and we shall not describe it. The details may be consulted in Bransden (1970). The computed and experimental cross-sections are shown in Fig. 12.8 and it is seen that above 200 eV the Born approximation agrees with the data.

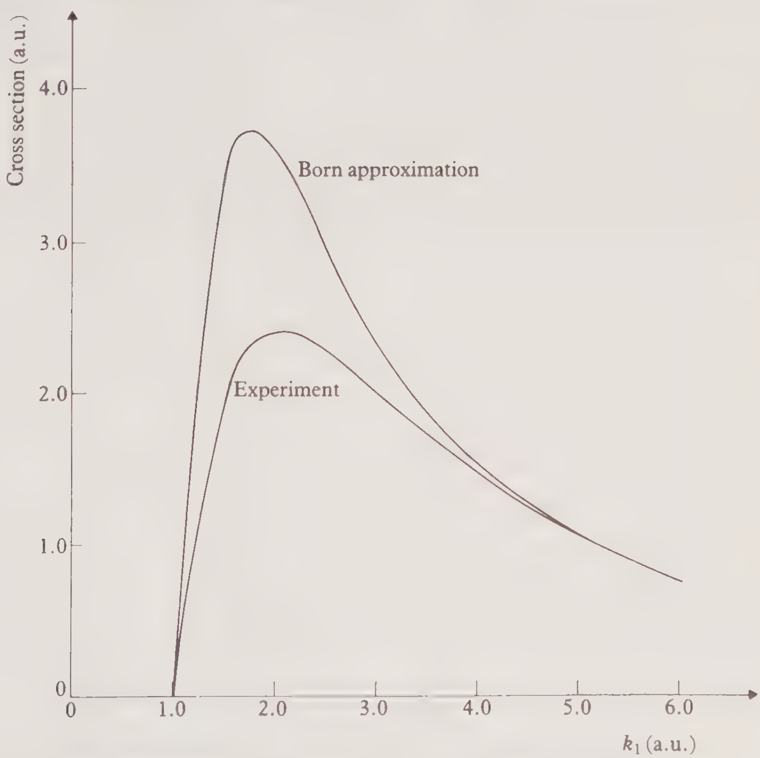

12.8 The cross-section for ionisation of atomic hydrogen by electron impact.

12.5 RESONANCE PHENOMENA

In the last section, and earlier in Chapter 6, we have referred to autoionising levels of atoms, which are metastable excited states and which decay, ejecting an electron of positive energy. The simplest example of a neutral atom possessing such levels is helium, and we have seen in Section 6.7 that there is a doubly excited state of the form $(2s2p)^1P$ with an energy of 60.1 eV above the ground state. This level can decay either by ejecting an electron or through radiation:

$$\begin{array}{l} He(2s2p) \rightarrow He^+(1s) + e^- \\ \qquad\qquad\quad \searrow \\ \qquad\qquad\quad\;\; He(2s1s) + h\nu \end{array}$$

These processes are in competition, but the probability of radiationless decay or 'autoionisation' is much greater than for radiative decay. Because of the finite lifetime of this level, the energy E_r of the level is not sharp, but has a width, in this case $\sim$0.17 eV.

Although originally doubly excited levels were discovered spectroscopically by observing emission lines, which because of the competitive radiationless decay are weak and broad, these levels can be seen most clearly in energy loss experiments. In such experiments a primary beam of high energy electrons is passed through a target containing helium and the energy spectrum of the emerging electrons is measured. In the data of S. M. Silverman and E. N. Lassettre shown in Fig. 12.9, obtained with a primary beam of 500 eV, two peaks are seen at 60.0 and 63.5 eV above the helium ground state.

Using perturbation theory or a variational method, it is possible to calculate the energies of doubly excited states. In helium there are sequences of excited states of the form $(2sns)^1S$, $(2sns)^3S$, $(2snp)^1P$, $(2snp)^3P$. In a sequence of levels, such as $(2sns)$, as n increases the energy of the system increases until

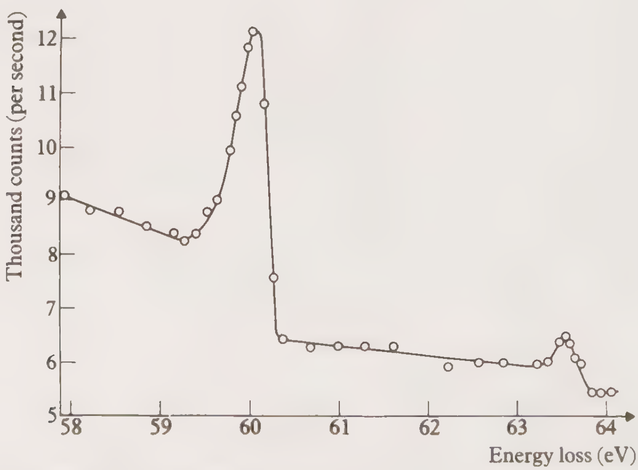

12.9 The energy loss spectrum of 500 eV electrons incident on helium.

eventually a situation is reached in which one electron occupies the 2s level of He^+ and the other electron is free. It follows that these levels can be found in electron scattering by He^+, at incident energies just below the threshold for exciting the $n = 2$ level of He^+. Since the lifetime of each level is of the order 10^{-14} s or less, the doubly excited atoms occur only as intermediate states in the elastic scattering process

$$e^- + He^+(1s) \rightarrow He^\star \rightarrow e^- + He^+(1s)$$

We saw in Chapter 11 that in potential scattering if the potential well possesses metastable levels so that the incident particle is temporarily captured, then the scattering amplitude shows a resonance behaviour, which can be represented by the Breit–Wigner formula [11.110]. This situation is called a *shape resonance* because it depends on the shape of the potential well. The transient formation of a doubly excited state during an electron-atom collision, also gives rise to a resonance, called *a Feshbach resonance*. The $(2sns)^1S$ sequence of levels causes a corresponding sequence of resonances below the $n = 2$ threshold in the $l = 0$ singlet partial wave. In the same way ^3S levels cause resonances in the triplet $l = 0$ partial wave, and $^{1,3}P$ levels cause resonances in the $l = 1$ partial waves. Similar sequences of levels with configurations 3s*n*s, 3s*n*p and so on, give rise to resonances just below then $n = 3$ threshold. In general the smooth variation of the elastic scattering cross-section, predicted by the static-exchange approximation, for example, is interrupted over a narrow range of energies below each inelastic threshold, where anomalous behaviour due to the resonant sequences can be expected.

The positions and widths Γ of some levels in helium are shown in Table 12.1. The widths are in general very small, and often smaller than the energy resolution of a detector in an electron scattering experiment. For this reason, it is difficult to observe a resonant profile in an electron scattering experiment.

Table 12.1 Resonance energies and widths of some doubly excited helium states, based on the $n = 2$ level

^1S			^3S		
E_r(eV)	Γ(eV)	*Configuration*	E_r(eV)	Γ(eV)	*Configuration*
57.84	0.12	$2s^2$	62.62	2×10^{-4}	2s3s
62.13	0.007	$2p^2$	63.76	7×10^{-6}	2p3p
62.97	0.036	2s3s	63.95	9×10^{-5}	2s4s

^1P			^3P		
E_r(eV)	Γ(eV)	*Configuration*	E_r(eV)	Γ(eV)	*Configuration*
60.19	4.4×10^{-2}	2s2p	58.30	1×10^{-2}	2s2p
62.82	1.4×10^{-2}	2s3p − 2p3s	63.15	3×10^{-3}	2s3p + 2p3s
63.88	8.7×10^{-3}	2s3p + 2p3s	63.94	8×10^{-5}	2s3p − 2p3s

E_r = Energies of the doubly excited levels above the ground state of He.
Γ = Level widths.

When the selection rules allow, the sequence of autoionising levels can be excited by photon absorption, as we saw in Chapter 6.

Resonances also occur below thresholds in the scattering of electrons by neutral atoms. The unstable resonant states are states of the corresponding negative ion. For example, in electron scattering by atomic hydrogen, the resonant states are doubly excited states of H^- and these occur in sequences below the thresholds for excitation of H. A few of these levels, with the corresponding widths are given in Table 12.2.

There is no mechanism to produce Feshbach resonances in the static-exchange or polarisation approximations. However, the resonances occurring below the $n = 2$ threshold are predicted by a close-coupling approximation in which the 1s, 2s and 2p levels of the target occur. To obtain the resonances below the $n = 3$ threshold, a close-coupling wave function can be employed, but this time the $n = 3$ levels of the target must be included. It is easy to see why this should be the case. Consider the 1s+2s+2p close-coupling wave function, which from [12.37] is explicitly

$$\begin{aligned}\psi_{\pm}(\mathbf{r}_1, \mathbf{r}_2) = {} & F_1^{\pm}(\mathbf{r}_1)\psi_{100}(\mathbf{r}_2) \pm F_1^{\pm}(\mathbf{r}_2)\psi_{100}(\mathbf{r}_1) \\ & + [F_2^{\pm}(\mathbf{r}_1)\psi_{200}(\mathbf{r}_2) \pm F_2^{\pm}(\mathbf{r}_2)\psi_{200}(\mathbf{r}_1) \\ & + \sum_{m=-1}^{+1} \{F_{3m}^{\pm}(\mathbf{r}_1)\psi_{21m}(\mathbf{r}_2) \pm F_{3m}^{\pm}(\mathbf{r}_2)\psi_{21m}(\mathbf{r}_1)\}]\end{aligned} \qquad [12.89]$$

where ψ_{nlm} is a hydrogenic function. Below the $n = 2$ threshold, $F_1^{\pm}$ satisfies the elastic scattering conditions [12.5] and $F_2^{\pm}(\mathbf{r})$, $F_{3m}^{\pm}(\mathbf{r}) \to 0$ as $r \to \infty$.

If the open elastic scattering channel wave function is omitted, retaining the terms in square brackets, we obtain a configuration–interaction wave function describing bound states (since this part of the wave function is bounded). The configurations that are mixed are all of the form 2snl and 2pnl. In the absence of the open channel, the equations [12.38] are eigenvalue equations and possess bounded solutions for $F_2^{\pm}$ and $F_{3m}^{\pm}$ only at discrete energies, that is for discrete *negative* values of k_q^2. (Notice that because of the degeneracy of the 2s and 2p levels of hydrogen $k_2^2 = k_3^2$.) If these discrete negative values are denoted by

Table 12.2 Resonance energies and widths of some doubly excited states of the hydrogen negative ion H

	E_r(eV)	Γ(eV)		E_r(eV)	Γ(eV)
^{1}S	9.56	0.05	^{1}P	10.18	—
	10.18	0.002		10.20	—
^{3}S	10.15	0.2×10^{-4}	^{3}P	9.73	—
	10.20	—		10.20	—

E_r = Energy of the doubly excited levels in terms of the energy of an electron scattered from the ground state of H. The threshold for excitation of the $n = 2$ levels of H is 10.24 eV.
Γ = Level widths.

$-\lambda_i^2$, resonances might be expected at incident energies in the open channel of

$$\left(\frac{1}{2}k_1^2\right)_i = -\frac{1}{2}\lambda_i^2 + (E_2 - E_1) \qquad [12.90]$$

where $E_1 = -0.5$ a.u. and $E_2 = -0.125$ a.u. are the energies of the $n = 1$ and $n = 2$ levels of H.

When the coupling to the open channel is taken into account by solving the set of equations [12.38] for all the functions F_1, F_2 and F_{3m}, resonances indeed do appear, of Breit Wigner form, in the elastic scattering amplitude. The coupling to the open channel gives the resonances a finite width, and also provides *level shifts* Δ_i so the resonances occur at energies $(\frac{1}{2}k_1^2)_i + \Delta_i$, where $\Delta_i \ll (\frac{1}{2}k_1)_i^2$.

Resonance phenomena are not confined to the simple two- and three-electron systems that we have considered, but are found frequently in low-energy electron scattering both by atoms and by molecules. Because of the strong overall Coulomb attraction, there are generally many more resonant states in electron scattering by highly charged ions than by neutral atoms and the magnitude of the cross-section in certain energy regions can be dominated by their presence.

PROBLEMS

12.1 By calculating the radial current using [12.9] show that the differential cross-section for inelastic scattering is given by [12.10].

12.2 Use the variational method with trial functions given by [12.13] to obtain [12.15]. Start from the functional I defined by [12.16] and require $\delta I = 0$ under independent variations of $F_1^{\pm}$ and $F_1^{\pm\star}$, subject to the conditions $\delta F^{\pm} \to 0$ as $r \to \infty$ and $\delta(F^{\pm\star}) \to 0$ as $r \to \infty$ (Hint: When $F_1^{\pm}$ and $F_1^{\pm\star}$ are varied independently $\delta F^{\pm}$ and $\delta(F^{+\star})$ are independent arbitrary quantities of the first order.)

12.3 Show that the direct potential $V_{11}(r_1)$ given by [12.20] can be obtained from [12.19] using $\psi_1(r_2) = \pi^{-1/2}\exp(-r_2)$.

12.4 Evaluate the direct potential V_{11} for electron scattering by helium:

$$V_{11}(r_1) = \int d\mathbf{r}_2 \int d\mathbf{r}_3 |\psi_{\mathrm{He}}(r_2, r_3)|^2 \left[-\frac{2}{r_1} + \frac{1}{|\mathbf{r}_1 - \mathbf{r}_2|} + \frac{1}{|\mathbf{r}_1 - \mathbf{r}_3|}\right]$$

where

$$\psi_{\mathrm{He}}(r_2, r_3) = \frac{Z_e^3}{\pi}\exp[-Z_e(r_2 + r_3)], \qquad Z_e = 27/16$$

(see [6.70])

12.5 Using the result [12.26], calculate the elastic scattering differential cross-section for electron scattering by helium at 500 eV in the Born

approximation (a) using V_{11} as the effective potential (b) using $V_{11} + V_{\text{pol}}$ as the effective potential, where V_{pol} is given by [12.53] with $\bar{\alpha} = 1.38$ a.u. and $d = 1.0$ a.u.

12.6 Show that the total cross-section for elastic scattering of electrons by the ground state of atomic hydrogen is given in first Born approximation (in a.u.) by

$$\sigma_{\text{tot}} = \pi \frac{7k_1^4 + 18k_1^2 + 12}{3(1 + k_1^2)^3}$$

which shows that $\sigma_{\text{tot}} \sim k_1^{-2}$ in the limit of high energies. (Start from [12.33b]).

12.7 Show that $\Sigma_m \, [\mathcal{G}_{q1}(\mathbf{\Delta})|^2$ depends only on the magnitude of $\mathbf{\Delta}$, where $\mathcal{G}_{q1}$ is defined by [12.63] in which $q' = 1$. Treat the case of excitation of atomic hydrogen where q is an excited state with quantum numbers nlm and 1 is the ground state (1s).

12.8 Although it is difficult to calculate the Born approximation amplitude for ionisation of atomic hydrogen using an exact continuum hydrogenic function, if this function is replaced by the plane wave $\psi_q(\mathbf{r}) = (2\pi)^{-3/2} \exp(i\mathbf{q} \cdot \mathbf{r})$ it is straightforward to obtain the differential cross-section. Compute the differential cross-section for ionisation of hydrogen in this approximation using [12.62] and [12.85].

13 Atom-atom collisions

In Chapters 9 and 10, we discussed in some detail the properties of diatomic molecules, which are the bound states of two atoms or ions. We shall now turn to the case in which one atom is scattered by another. Such processes occur naturally in an assembly of atoms, such as in a gas, but can also be studied experimentally by allowing two beams of atoms to interact and studying the distribution of the reaction products. A schematic diagram of one such experiment is shown in Fig. 13.1.

Under all conditions elastic scattering occurs, in which atom A is scattered from atom B, without any change in internal energy of either A or B

$$A + B \rightarrow A + B$$

Several other processes may also be possible. Indeed, provided enough energy is available, either or both A and B can be left in an excited state after the collision,

$$\begin{aligned} A + B &\rightarrow A' + B \\ &\rightarrow A + B' \\ &\rightarrow A' + B' \end{aligned}$$

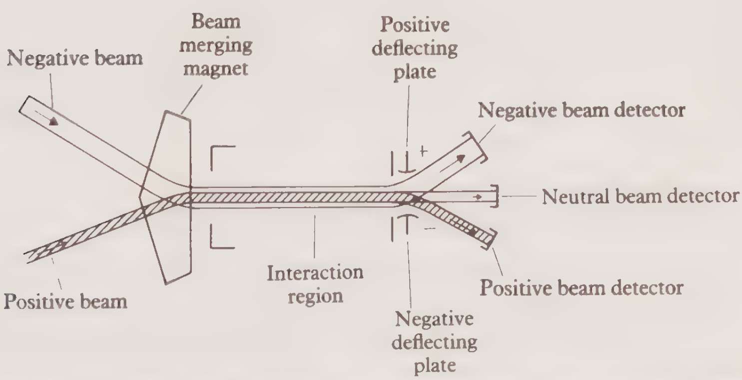

13.1 A schematic diagram of an apparatus to measure the neutral atoms produced in a reaction between ions of opposite charge: $A^+ + B^- \rightarrow A + B$. Since low energy beams of charged particles are difficult to prepare because of space charge and other effects, small relative velocities between the ions are achieved in this method by merging two beams each at energies of a few keV (see Problem 13.1)

Another process is one in which one, or more, electrons are transferred from one atom to the other. For example,

$$A + B \to A^- + B^+$$

This is known as charge exchange, or charge transfer. A further possibility is an ionisation process, in which one or more electrons are ejected. That is,

$$\begin{aligned} A + B &\to A^+ + B + e^- \\ &\to A + B^+ + e^- \\ &\to A^{++} + B + 2e^-, \quad \text{etc.} \end{aligned}$$

A simple system which exhibits several of these phenomena is that composed of two hydrogen atoms. For example, a typical excitation process is

$$H(1s) + H(1s) \to H(1s) + H(2p)$$

and a charge exchange reaction is

$$H(1s) + H(1s) \to p + H^-(1s^2)$$

Unfortunately, the simplest systems such as (p + H), (H + H), (H + He) are often the most difficult to study experimentally because hydrogen exists naturally in molecular form H_2. However, it is now known how to prepare beams of atomic hydrogen, and this has allowed data to be obtained for these systems.

We shall start by discussing elastic scattering, and then go on to describe the interesting process of charge exchange, for the p + H (1s) system. In Chapter 9, we saw that if the Born–Oppenheimer separation is made, the motion of the nuclei of the two interacting atoms is determined by an effective potential, which can be represented approximately by the Morse potential [9.25]. Provided the atoms are moving slowly with respect to the electrons we can continue to make the Born–Oppenheimer separation, and to describe the elastic scattering by an effective potential. The potential obtained in Chapter 9, while accurate at small distances of separation of the atoms is not sufficiently accurate at large distances and we shall see, in the next paragraph, how to calculate the long-range interactions which determine the elastic scattering at low velocities.

13.1 LONG-RANGE INTERACTIONS BETWEEN ATOMS

In analysing the most important interactions at large distances between atoms or ions, there are three cases to be considered. First, if we are dealing with the scattering of one positive ion by another, the dominant interaction is Coulombic and, at large r

$$V(r) \sim \frac{Z_A Z_B e^2}{(4\pi\varepsilon_0)r} \qquad [13.1a]$$

where $(Z_A e)$ and $(Z_B e)$ are the net charges on each ion. In this chapter it is

convenient to use atomic units, so that the potential [13.1a] becomes

$$V(r) \sim \frac{Z_A Z_B}{r} \tag{13.1b}$$

The second case arises in the interaction of a positive ion of net charge Z_A and a neutral atom B. The positive charge induces an electric dipole moment in the neutral atom, and the interaction at large distances can be calculated as we did in Chapter 12, when we derived the interaction of an electron with a neutral atom, using second-order perturbation theory. The potential behaves at large r as

$$V(r) \sim -\frac{(Z_A)^2 \bar{\alpha}_B}{2r^4} \qquad \text{(in atomic units)} \tag{13.2}$$

where $\bar{\alpha}_B$ is the dipole polarisability of the neutral atom B.

Finally, we consider the forces between two neutral atoms. For simplicity, we take the example of two hydrogen atoms, the first composed of a proton situated at A and electron 1 and the second of a proton situated at B and electron 2. The coordinate system is shown in Fig. 13.2. The internuclear distance AB is R, and is taken as the Z axis. The distances of electron 1 from A and B are denoted by r_{1A}, r_{1B} and, similarly, r_{2A} and r_{2B} denote the distances of electron 2 from A and B, respectively. The distance between the two electrons is r_{12}. The Hamiltonian for the system in the adiabatic approximation, in which the internuclear distance R is fixed, is

$$H = H_A + H_B + V(1, 2) \tag{13.3}$$

where H_A is the Hamiltonian of the atom $(A + e_1^-)$, H_B is that for the atom $(B + e_2^-)$ and $V(1, 2)$ is the interaction energy between the two atoms. In atomic units, we have

$$H_A = -\frac{1}{2}\nabla^2_{r_{1A}} - \frac{1}{r_{1A}} \tag{13.4a}$$

$$H_B = -\frac{1}{2}\nabla^2_{r_{2B}} - \frac{1}{r_{2B}} \tag{13.4b}$$

and

$$V(1, 2) = \left(\frac{1}{R} + \frac{1}{r_{12}} - \frac{1}{r_{1B}} - \frac{1}{r_{2A}}\right) \tag{13.4c}$$

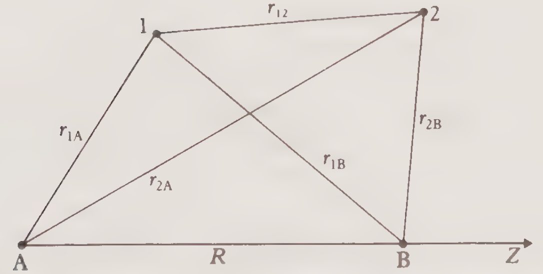

13.2 A coordinate system for calculating the long-range interaction between two hydrogen atoms.

Two points should be noticed. First, because we are interested in large distances of separation R, $V(1, 2)$ is small and can be treated as a perturbation. Second, since exchange effects arising from the identity of the two electrons are of short range, we can (for large R), ignore the antisymmetry of the wave function. Although these long-range forces are important for scattering, the binding forces considered in Chapter 9 are greater in magnitude by a factor of 10^3, which is why, even for states of large vibrational excitation, the long-range forces play no significant role in the bound state problem.

Let the Cartesian coordinates of electron 1, with respect to A as origin be x_{1A}, y_{1A}, z_{1A}, and of electron 2, with respect to B as origin be x_{2B}, y_{2B}, z_{2B}. Then, as we are taking the Z direction to be along AB,

$$\begin{aligned} r_{12} &= [(x_{2B} - x_{1A})^2 + (y_{2B} - y_{1A})^2 + (z_{2B} - z_{1A} + R)^2]^{1/2} \\ r_{1B} &= [x_{1A}^2 + y_{1A}^2 + (z_{1A} - R)^2]^{1/2} \\ r_{2A} &= [x_{2B}^2 + y_{2B}^2 + (z_{2B} + R)^2]^{1/2} \end{aligned} \qquad [13.5]$$

Each of the terms $1/r_{12}$, $1/r_{1B}$ and $1/r_{2A}$ can be expanded in a Taylor series in powers of $1/R$. Thus

$$\begin{aligned} \frac{1}{r_{1B}} &= \frac{1}{R}\left[1 + \left\{\frac{x_{1A}^2 + y_{1A}^2 + z_{1A}^2 - 2Rz_{1A}}{R^2}\right\}\right]^{-1/2} \\ &= \frac{1}{R}\left[1 - \frac{1}{2}\left\{\frac{x_{1A}^2 + y_{1A}^2 + z_{1A}^2 - 2Rz_{1A}}{R^2}\right\}\right. \\ &\qquad \left. + \frac{3}{8}\left\{\frac{x_{1A}^2 + y_{1A}^2 + z_{1A}^2 - 2Rz_{1A}}{R^2}\right\}^2 - \cdots\right] \\ &= \frac{1}{R}\left[1 + \frac{z_{1A}}{R} - \frac{x_{1A}^2 + y_{1A}^2 - 2z_{1A}^2}{2R^2} + \cdots\right] \end{aligned} \qquad [13.6]$$

In the same way, we have

$$\frac{1}{r_{2A}} = \frac{1}{R}\left[1 - \frac{z_{2B}}{R} - \frac{x_{2B}^2 + y_{2B}^2 - 2z_{2B}^2}{2R^2} + \cdots\right] \qquad [13.7]$$

and

$$\begin{aligned} \frac{1}{r_{12}} = \frac{1}{R}\Bigg[1 &- \frac{(z_{2B} - z_{1A})}{R} \\ &- \frac{(x_{2B} - x_{1A})^2 + (y_{2B} - y_{1A})^2 - 2(z_{2B} - z_{1A})^2}{2R^2} + \cdots\Bigg] \end{aligned} \qquad [13.8]$$

The expansion of $V(1, 2)$ in powers of $1/R$ is obtained by combining [13.4c] with [13.6], [13.7] and [13.8]. The terms in $1/R$ and $1/R^2$ are seen to cancel, so

that for large R

$$V(1, 2) = \frac{1}{R^3}(x_{1A}x_{2B} + y_{1A}y_{2B} - 2z_{1A}z_{2B}) \qquad [13.9]$$

This long-range interaction has the form of the interaction energy of two dipoles, the first composed of proton A and electron 1, with electric dipole moment $\mathbf{D}_1 = -\mathbf{r}_{1A}$ (in atomic units), and the second of proton B and electron 2 with dipole moment $\mathbf{D}_2 = -\mathbf{r}_{2B}$. The energy of interaction is

$$V = \frac{1}{R^3}\left\{\mathbf{D}_1 \cdot \mathbf{D}_2 - 3\,\frac{(\mathbf{D}_1 \cdot \mathbf{R})(\mathbf{D}_2 \cdot \mathbf{R})}{R^2}\right\} \qquad [13.10]$$

which on taking $\mathbf{R}$ as the Z axis, reduces to [13.9].

The perturbation energy

The energy of the unperturbed system in which both hydrogen atoms are in the ground state is $(2E_{1s})$, and the unperturbed wave function is $\psi_{1s}(r_{1a})\psi_{1s}(r_{2B})$, which satisfies the equation

$$(H_A + H_B - 2E_{1s})\psi_{1s}(r_{1A})\psi_{1s}(r_{2B}) = 0 \qquad [13.11]$$

The total energy of the system, allowing for the perturbation $V(1, 2)$ can be written as

$$E = 2E_{1s} + E^{(1)} + E^{(2)} + \cdots \qquad [13.12]$$

where $E^{(n)}$ is calculated from nth order perturbation theory, and $V(1, 2)$ is given by the large-R expression [13.9].

The first-order correction,

$$E^{(1)} = \int d\mathbf{r}_{1A} \int d\mathbf{r}_{2B}\, \psi^{\star}_{1s}(r_{1A})\psi^{\star}_{1s}(r_{2B})V(1, 2)\psi_{1s}(r_{1A})\psi_{1s}(r_{2B}) \qquad [13.13]$$

is immediately seen to vanish, because the matrix elements of the angular dependent terms, such as x_{1A}, y_{1A}, z_{1A} are zero when taken between spherically symmetric wave functions such as $\psi_{1s}(r_{1A})$. The first non-vanishing perturbation correction is $E^{(2)}$, which is given by (see [2.319])

$$E^{(2)} = \sum_{j \neq 0} \frac{\langle \psi_0 | V | \psi_j \rangle \langle \psi_j | V | \psi_0 \rangle}{E_0 - E_j} \qquad [13.14]$$

where $\psi_0 = \psi_{1s}(r_{1A})\psi_{1s}(r_{2B})$ and ψ_j are the wave functions of the intermediate states. In our case the ψ_j are of the form $\psi_{nlm}(r_{1A})\psi_{n'l'm'}(r_{2B})$, with n and $n' \neq 1$. The energy denominator is (in atomic units) given by $(E_0 - E_j) = (-1 + 1/2n^2 + 1/2n'^2)$, with both n and n' greater than 1, so that $(E_0 - E_j)$ is always negative. The numerator is positive and behaves like $1/R^6$, so that the long-range interaction between two hydrogen atoms is

$$E^{(2)}(R) = -\frac{C_W}{R^6} \qquad [13.15]$$

where C_W is a positive constant known as the van der Waals constant. The same procedure can be carried through for any pair of neutral atoms and [13.15] may be shown to give the general form of the long-range (van der Waals) interaction, although of course the quantity C_w varies from system to system.

The long-range force is always attractive, but when $R \to 0$, the force is ultimately repulsive in character as we saw in Chapter 9. This has suggested the introduction of empirical potentials to describe atom–atom scattering. One of the most widely used of these is the Lennard–Jones potential, which has the form

$$V(R) = C\left[\frac{1}{2}\left(\frac{R_0}{R}\right)^{12} - \left(\frac{R_0}{R}\right)^{6}\right] \qquad [13.16]$$

where C and R_0 are constants. The constant C can be related to C_W (the van der Waals constant), but both C and R_0 are usually treated as empirical constants to be determined from the data on atom–atom scattering.

13.2 THE CLASSICAL APPROXIMATION

With some exceptions, the motion of the nuclei in atom–atom scattering can be treated by classical Newtonian mechanics. The reason that classical theory can be employed, rather than the quantum scattering theory we used in Chapter 12 when discussing electron scattering, is that the wavelength associated with a moving atom is often very small compared with the size of the interaction region. The potential $V(R)$ is smoothly varying and only changes slowly over distances of the order of an atomic unit ($a_0 \simeq 0.53 \times 10^{-10}$ m). If the wavelength of the atom is small compared with this distance, a well-defined wave packet can be formed which will follow the classical path. The wavelength of a particle of mass M and velocity v is (in the non-relativistic case)

$$\lambda = \frac{h}{Mv} \qquad [13.17]$$

The lightest atom is hydrogen, so that in all cases $M > 1836m$, where m is the mass of the electron. Using atomic units with $m = 1$, $\hbar = 1$, we see that $\lambda < 1$ if $v > (2\pi/1836)$ a.u. Since 1 a.u. of velocity $= 2.19 \times 10^6$ m s^{-1}, we expect classical conditions to hold provided the velocity of the scattered atom is greater than 7.5×10^3 m s^{-1} which corresponds, for hydrogen, to an energy of 0.29 eV.

A further condition to be satisfied arises from Heisenberg's uncertainty principle. If classical mechanics is to hold the uncertainty in the angle through which the scattered atom is deflected must be small compared with the angle of scattering. Let us consider for example the situation illustrated in Fig. 13.3, which shows the path of a particle of mass M, scattered by a centre of force situated at the origin O. The initial motion of the particle is parallel to the Z axis, and the initial velocity is $\mathbf{v}$. The classical trajectory is determined by the impact parameter b, which is defined as the perpendicular distance between the

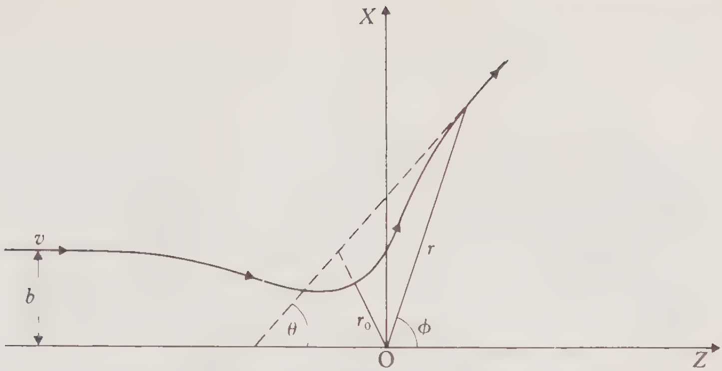

13.3 The classical path of a particle scattered by a centre of force situated at O.

Z axis and the initial straight line path. The particle has an angular momentum L about O, given by

$$L = bMv = bp \tag{13.18}$$

Looked at from the viewpoint of quantum mechanics, the scattered particle is represented by a narrow wave packet, which has a certain width Δx in the x direction and a corresponding uncertainty in the x component of the momentum Δp_x. By the uncertainty principle Δx and Δp_x must satisfy

$$\Delta x \, \Delta p_x \geqslant \hbar \tag{13.19}$$

Now the impact parameter b will also be uncertain by an amount Δb, which is of the same order as Δx, the width of the wave packet, so we must have

$$\Delta b \simeq \hbar/\Delta p_x \tag{13.20}$$

The uncertainty in the transverse momentum in turn gives rise to a corresponding uncertainty $\Delta\phi$ in the angular coordinate ϕ of the particle, such that

$$\Delta\phi = \frac{\Delta p_x}{p} \tag{13.21}$$

Combining [13.20] and [13.21], we have

$$\Delta b \simeq \hbar/(p\,\Delta\phi) \tag{13.22}$$

The angle of scattering θ will also be uncertain by the quantity $\Delta\phi$, and if the scattering angle is to be well defined we must ensure that

$$\theta \gg \Delta\phi \tag{13.23}$$

and simultaneously, for the impact parameter to be well defined, we must ensure that $b \gg \Delta b$.

Combining the two conditions gives

$$\theta \gg \frac{\hbar}{Mv\,\Delta b} \gg \frac{\hbar}{Mvb} \tag{13.24}$$

or since $Mvb = L$, we must have

$$\theta \gg \theta_c = \frac{\hbar}{L} \qquad [13.25]$$

where θ_c is referred to as the *critical angle*.

Even at thermal velocities ($v = 10^5$ cm/s), the important values of L are of the order of $10^3\ \hbar$, and it follows that classical conditions apply, provided the angle of scattering is greater than a few milliradians. At higher energies, the critical angle is correspondingly smaller. In contrast, for electron scattering, because the mass of the electron is $\sim$ (1/1836) of the proton mass, for given values of b and v, the angular momentum of an electron is (1/1836) times the angular momentum of a proton. It follows that small values of L are important in electron scattering and the conditions for classical mechanics to be valid are not satisfied.

13.3 THE ELASTIC SCATTERING OF ATOMS AT LOW VELOCITIES

Except at very small angles, and apart from some small interference effects that we will discuss briefly later, the considerations of the previous paragraph show that the elastic scattering of one atom by another can be determined by purely Newtonian mechanics. We have derived in Appendix 1 the classical cross-section for the scattering of a beam of particles. Using the results [A1.11] and [A1.12] and working in the centre of mass system, the angle of deflection is given by

$$\Theta = \pi - 2\int_{r_0}^{\infty} \frac{L}{Mr^2}\left[\frac{2}{M}(E - V(r)) - \frac{L^2}{M^2r^2}\right]^{-1/2} \mathrm{d}r \qquad [13.26]$$

where r_0 is the distance of closest approach, L is the angular momentum, and $E = Mv^2/2$, M being the reduced mass of the two colliding atoms. The angle of scattering θ is defined to lie in the interval $0 \leqslant \theta \leqslant \pi$. If Θ already lies in this interval we have $\theta = |\Theta|$ otherwise we take θ to be given by

$$\begin{aligned} &\theta = |\Theta| - 2\pi m \\ \text{or}\qquad &\theta = -\{|\Theta| - 2\pi m\} \end{aligned} \qquad [13.27]$$

where m is an integer chosen so that θ lies in the correct interval. The relationship [13.26] can be inverted so L can be expressed as a function of θ. The differential cross-section is then

$$\frac{\mathrm{d}\sigma}{\mathrm{d}\Omega} = \frac{1}{M^2v^2}\,\frac{L}{\sin\theta}\left|\frac{\mathrm{d}L}{\mathrm{d}\theta}\right| \qquad [13.28]$$

Although there is one value of θ corresponding to a given value of L, there may be several values of L, corresponding to a given value of θ. If these values are L_i, $i = 1, 2, \ldots$ the cross-section is obtained by summing the different

contributions:

$$\frac{d\sigma}{d\Omega} = \frac{1}{M^2 v^2} \sum_i \frac{L_i}{\sin\theta} \left| \frac{dL_i}{d\theta} \right| = \sum_i \frac{d\sigma_i}{d\Omega} \qquad [13.29]$$

When contributions to one scattering angle arise from different classical paths, quantum effects may be exhibited in the differential cross-section, which arise from interference between the wave packets of the particles following the different paths. It can be shown that the correct expression under these circumstances is

$$\frac{d\sigma}{d\Omega} = \left| \sum_i \left(\frac{d\sigma_i}{d\Omega} \right)^{1/2} e^{i\chi_i} \right|^2 \qquad [13.30]$$

where χ_i is the phase associated with the ith path. This phase can be calculated using semi-classical methods.

Deflection functions corresponding to potentials like the Lennard–Jones potential [13.16], have the general form shown in Fig. 13.4. At large values of the impact parameter (large L), the scattered particle is influenced by the outer part of the potential which is attractive. These glancing collisions contribute to the small angle scattering. We see from Fig. 13.4 that several values of L contribute to particular values of θ. For example, at the angle θ_0 the three values L_1, L_2 and L_3 all contribute. Another interesting feature is that at the point where Θ has a minimum, $d\Theta/dL$ vanishes, and $d\sigma/d\Omega$ becomes unbounded. The angle at which this occurs is known as the *rainbow angle*. Among the

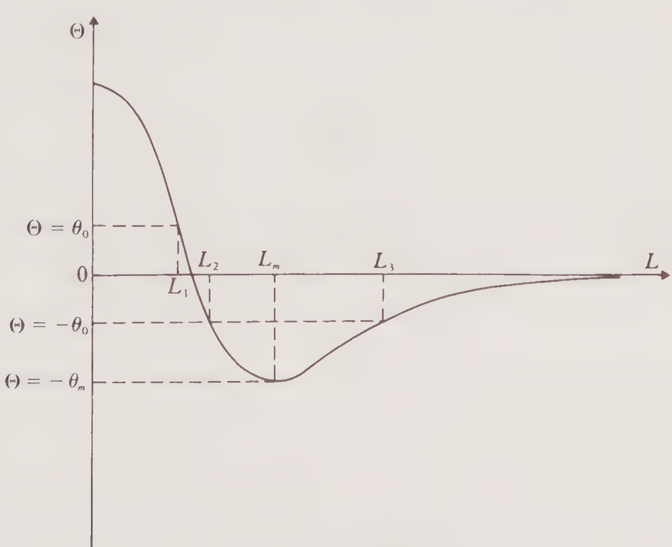

13.4 Schematic diagram of the deflection angle Θ as a function of angular momentum for a particle scattered by a Lennard–Jones potential. Note that the deflection angle Θ can be positive or negative, but that the angle of scattering θ is always positive ($0 \leqslant \theta \leqslant \pi$).

various phenomena that can happen we shall describe two: the behaviour of the small angle cross-section, and the behaviour of the cross-section close to the rainbow angle.

Small angle scattering

Let us discuss the scattering at small angles from a potential of the form

$$V(r) = -A/r^s, \; A > 0 \tag{13.31}$$

From [13.26], we write the expression for Θ in the form,

$$\Theta = \pi - 2b \int_{r_0}^{\infty} \frac{\mathrm{d}r}{r^2\left[1 - \dfrac{b^2}{r^2} - \dfrac{V(r)}{E}\right]^{1/2}} \tag{13.32}$$

where $b = L/Mv$ is the impact parameter and $E = Mv^2/2$, v being the magnitude of the incident velocity. It is convenient to change the variable of integration to $x = r_0/r$, so that

$$\Theta = \pi - 2\frac{b}{r_0} \int_0^1 \frac{\mathrm{d}x}{\left[1 - \dfrac{V(r_0/x)}{E} - \dfrac{x^2 b^2}{r_0^2}\right]^{1/2}} \tag{13.33}$$

The equation which determines the distance of closest approach is (see equation [A1.10] of Appendix 1)

$$\frac{b^2}{r_0^2} = 1 - \frac{V(r_0)}{E} \tag{13.34}$$

and we can use this to eliminate b^2, so that

$$\Theta = \pi - 2\int_0^1 \left[\left\{\frac{1 - V(r_0/x)/E}{1 - V(r_0)/E}\right\} - x^2\right]^{-1/2} \mathrm{d}x \tag{13.35}$$

For small angle scattering b is large, $V(r) = V(r_0/x)$ is small and $r_0 \simeq b$. Expanding the expression in curly brackets to lowest order in V, using the result

$$\int_0^1 \frac{\mathrm{d}x}{\sqrt{1 - x^2}} = \frac{\pi}{2}$$

and setting $r_0 = b$, we obtain

$$\Theta = \frac{1}{E}\int_0^1 \frac{V(b) - V(b/x)}{(1 - x^2)^{3/2}}\,\mathrm{d}x \tag{13.36}$$

With the potential [13.31], the result [13.36] can be expressed as

$$\Theta = -\frac{A}{E} b^{-s} F(s) \tag{13.37a}$$

where

$$F(s) = \int_0^1 \frac{1 - x^s}{(1 - x^2)^{3/2}}\, \mathrm{d}x \qquad [13.37b]$$

The corresponding differential cross-section is given by

$$\frac{\mathrm{d}\sigma}{\mathrm{d}\Omega} = g(s)\left(\frac{A}{E\theta}\right)^{2/s} \frac{1}{\theta \sin\theta}, \qquad [13.38a]$$

where $\theta = |\Theta|$ and

$$g(s) = s^{-1}[F(s)]^{2/s} \qquad [13.38b]$$

For the important cases where $s = 4$ and $s = 6$, we have $F(4) = 3\pi/4$ and $F(6) = 15\pi/16$, respectively.

The condition for the validity of the result [13.38] is $\theta \ll 1$ rad. On the other hand for classical conditions to apply we see from [13.25] that we must also have $\theta \gg \theta_c$, where the critical angle θ_c is of the order of a few milliradians.

Experiments can be analysed to determine s and A by plotting log $[\theta \sin\theta\, \mathrm{d}\sigma/\mathrm{d}\Omega]$ against log θ. An example of such a plot is shown in Fig. 13.5. Generally the experiments verify the van der Waals $1/r^6$ law for the interaction at large distances between neutral atoms.

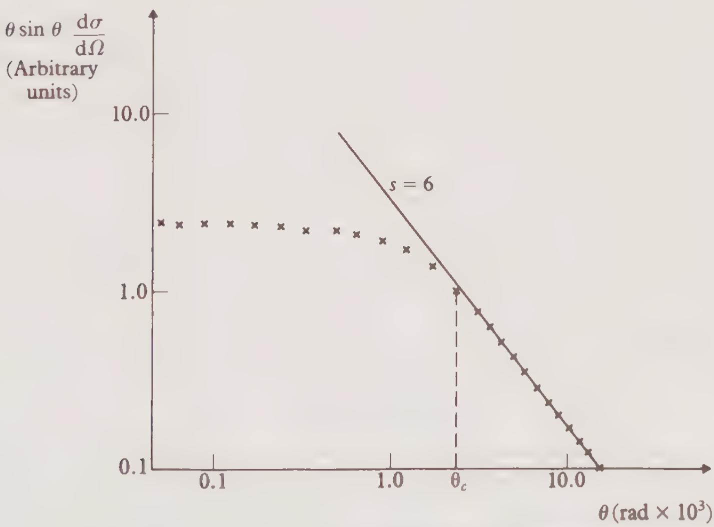

13.5 Log–log plot of $\theta \sin\theta\, \mathrm{d}\sigma/\mathrm{d}\Omega$ vs θ for the elastic scattering of potassium atoms by xenon atoms. The straight line corresponds to the classical cross-section for the potential $V(r) = -A/r^s$ with $s = 6$. The experimental data of Helbing and Pauly deviate from the classical result at very small angles ($\theta < \theta_c$) as expected (see text). For $\theta < \theta_c$ agreement can be obtained with the data by calculating the cross-section using quantum methods. Notice from [13.38] that the shape of the classical cross-section is independent of the velocity of the atoms in the beams.

Rainbow scattering

Rainbow scattering takes its name from the corresponding optical phenomenon, Referring to Fig. 13.4, we see that at the angle $-\theta_m$ the quantity $\mathrm{d}L/\mathrm{d}\Theta$ is singular. In the region near $-\theta_m$ the deflection function can be expanded as

$$\Theta = -\theta_m + (L - L_m)\frac{\mathrm{d}\Theta}{\mathrm{d}L}\bigg|_{L_m} + \frac{1}{2}(L - L_m)^2\frac{\mathrm{d}^2\Theta}{\mathrm{d}L^2}\bigg|_{L_m} + \cdots \qquad [13.39]$$

Since $\mathrm{d}\Theta/\mathrm{d}L = 0$ at $L = L_m$, we find that

$$\Theta \simeq -\theta_m + B(L - L_m)^2 \qquad [13.40]$$

where B is a constant.

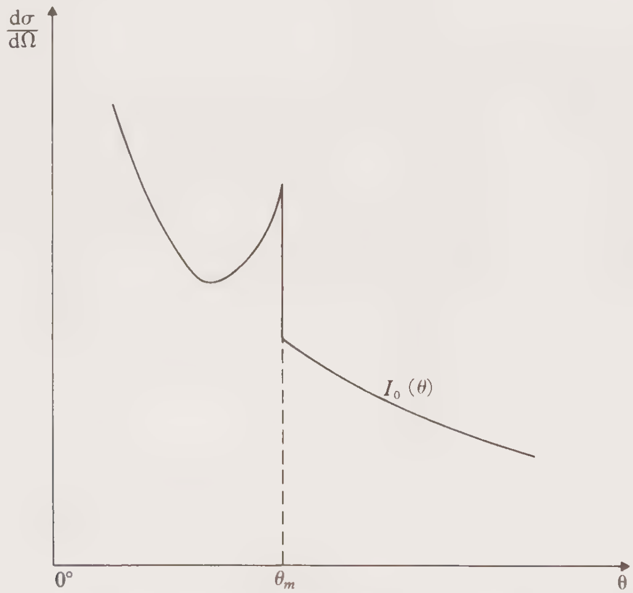

13.6 Schematic diagram of the differential cross-section for the elastic scattering of one atom by another showing the classical rainbow effect of equation [13.44].

The differential cross-section for $\theta > \theta_m$ is given by

$$\frac{\mathrm{d}\sigma}{\mathrm{d}\Omega} = I_0(\theta) \qquad [13.41]$$

where $I_0(\theta)$ is a smooth function arising from small values of L, corresponding to positive values of Θ, with $\theta = \Theta$ (see Fig. 13.4). For $\theta < \theta_m$ there will be additional contributions to the differential cross-section arising from $L_2 \simeq L_m - x$ and $L_3 \simeq L_m + x$. These contributions are evaluated by noting from [13.40] that

$$\frac{\mathrm{d}\Theta}{\mathrm{d}L} \simeq 2B(L - L_m) \qquad [13.42]$$

so that for $\theta < \theta_m$ the differential cross-section is given by

$$\frac{d\sigma}{d\Omega} = I_0(\theta) + \sum_{i-2}^{3} \frac{1}{M^2 v^2} \frac{L_i}{\sin \theta_m} \left| \frac{1}{2B(L_i - L_m)} \right| \qquad [13.43]$$

Using [13.40] this expression can also be written as

$$\frac{d\sigma}{d\Omega} = I_0(\theta) + \frac{1}{M^2 v^2} \frac{L_m}{\sin \theta_m} \left[\frac{1}{B(\theta_m - \theta)} \right]^{1/2}, \qquad \theta < \theta_m \qquad [13.44]$$

The general shape of the cross-section is shown in Fig. 13.6.

Measurement of the position of the rainbow angle provides further information about the shape of the interatomic potential. Since the rainbow effect is due to contributions from two classical trajectories, with $L = L_m \pm x$, interference phenomena are predicted by quantum theory.

In practice the cross-section oscillates for $\theta < \theta_m$, and tends smoothly to $I_0(\theta)$ for $\theta > \theta_m$ and the singularity at $\theta = \theta_m$ is removed. An example of rainbow scattering observed in the experiments of Barwig *et al.* is shown in Fig. 13.7.

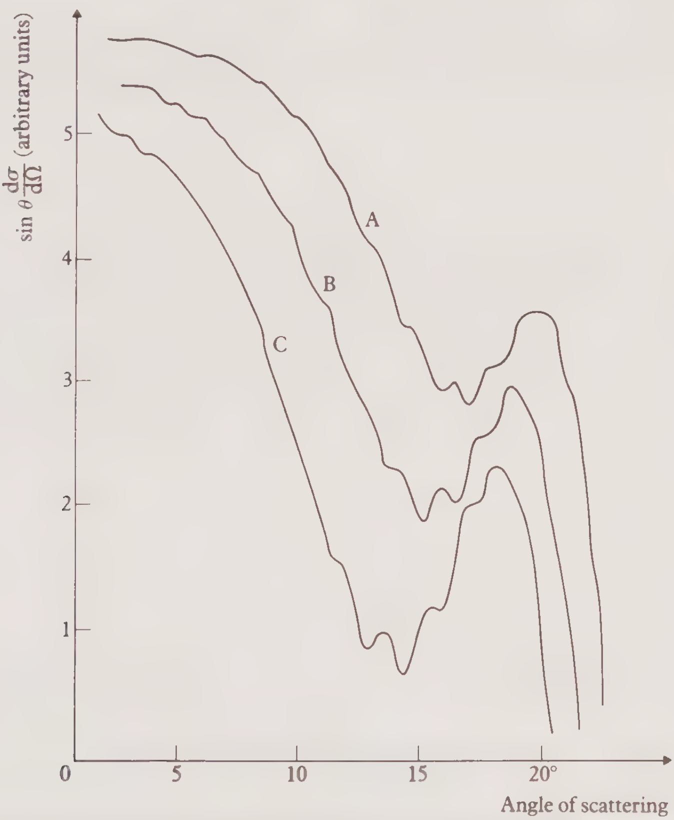

13.7 The differential cross-section for the elastic scattering of sodium atoms by krypton atoms measured by Barwig, Buck, Hundhausen and Pauly for relative velocities of (A), 767 m/s (B) 817 m/s (C) 870 m/s. Quantum mechanical interference effects are seen in the region of the rainbow angle. At smaller angles ($\theta < 2°$), the cross-section follows the $\theta^{7/3}$ law, for scattering by the potential $V(r) = -A/r^6$ (see equation [13.38]).

13.4 ELECTRONIC EXCITATION AND CHARGE EXCHANGE

In this section we will discuss the processes in which an atom is excited during a collision, or in which an electron is transferred from one atom to another. We will treat the case in which the kinetic energy of the relative motion of two atoms is very large compared with the change in electronic energy of either atom. Under these circumstances the motion of the nuclei of the atom is unaltered by the changes in the atomic wave functions. This motion is determined by a classical trajectory, as we have discussed in the previous paragraph. The motion of the electrons cannot be treated classically, but must be found from the solution of a Schrödinger equation. To make these remarks more definite, let us consider a system containing just one electron and two protons, as we did in Chapter 9, when we discussed the ion H_2^+. When the two protons (labelled A and B) are a great distance apart, each of them will be following an undeflected rectilinear path, as shown in Fig. 13.8. We take a system of coordinates in which the centre of mass, the mid-point of AB, is at rest. The relative velocity of A and B will be taken to be $\mathbf{v}$, and the initial motion is parallel to the Z axis and is defined by the impact parameter b.

The position vector of A relative to B is denoted by $\mathbf{R}$. Knowing the effective potential $V_{\text{eff}}(R)$ between the two protons, Newton's equations of motion can be solved to obtain $\mathbf{R}$ as a function of time, for each value of the impact parameter

$$\mathbf{R} = \mathbf{R}(b, t) \qquad [13.45]$$

As the energy of the scattered particle increases, the angle of deflection, for a given value of the impact parameter, gets smaller and smaller. This can be seen from [13.26]. In practice, at proton energies above ~1 keV, this means that the departure of the paths of A and B from straight lines can be ignored, except for nearly head-on collisions ($b \simeq 0$). Since the most important contributions to excitation, or charge transfer, arise from values of b of order a_0, we can make the straight line approximation. In this case the Cartesian components of $\mathbf{R}$, (X_R, Y_R, Z_R) are

$$\begin{aligned} X_R &= b \\ Y_R &= 0 \\ Z_R &= vt \end{aligned} \qquad [13.46]$$

The zero time is chosen so that $t = 0$ at the point of closest approach ($R = b$).

When the velocity of a proton (in the laboratory system) is one atomic unit (2.19×10^6 m/s) it possesses a kinetic energy $E = 25$ keV. For energies smaller than this, the velocity of the incident proton is less than the velocity of the electron in the ground state of hydrogen. As the proton energy decreases the adiabatic conditions described in Chapter 9 are approached. On the other hand for $E > 25$ keV, the incident proton has a velocity greater than the orbital velocity of the target electron and the collision is said to be fast. It should be

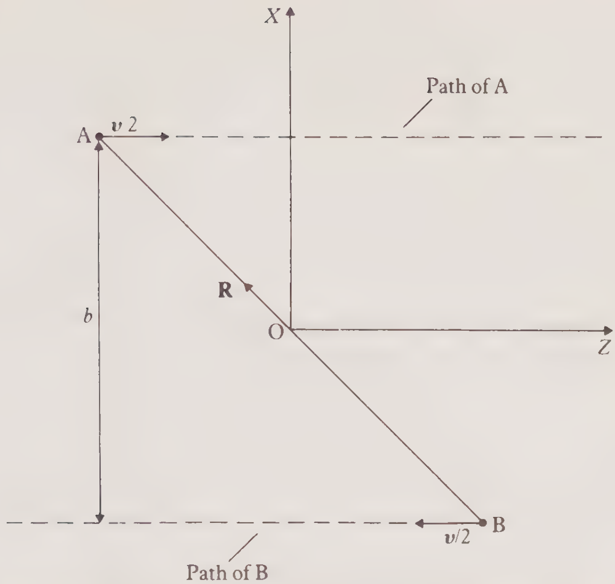

13.8 System of two protons, A and B, moving along rectilinear paths with a relative velocity **v**. The mid-point of AB is chosen as the origin of the coordinate system. Relative to O, A has the velocity **v**/2 and B has the velocity −**v**/2. The two protons are taken to move in the *XZ* plane.

remembered that if we consider the scattering of an ion of mass M atomic mass units, a velocity of one atomic unit corresponds to $E = 25M$ keV. It follows that the heavy ions produced at MeV energies in electrostatic accelerators may still have small velocities, given by $v = (E/25M)^{1/2}$ a.u. where E is in keV.

To discuss the motion of the electron we can introduce the coordinates of Fig. 13.9, similar to those we used to describe the hydrogen molecular ion H_2^+

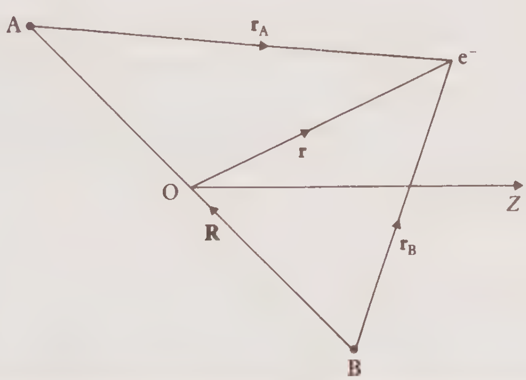

13.9 A coordinate system for the discussion of an $H^+ + H$ collision. Note that the position vector **r** of the electron can be in any direction whereas the vector **R** lies in the plane of motion of A and B, which has been taken to be the *XZ* plane (see Fig. 13.8).

in Chapter 9. The Hamiltonian operator for the electron is (in atomic units)

$$H(t) = -\frac{1}{2}\nabla_r^2 - \frac{1}{r_A} - \frac{1}{r_B} + \frac{1}{R} \qquad [13.47]$$

It is time-dependent since

$$\begin{aligned} \mathbf{r}_A &= -\tfrac{1}{2}\mathbf{R} + \mathbf{r} \\ \mathbf{r}_B &= +\tfrac{1}{2}\mathbf{R} + \mathbf{r} \end{aligned} \qquad [13.48]$$

and $\mathbf{R}$ is a function of t through equations [13.46]. The time-dependent Schrödinger equation for the electron reads

$$\left[H(t) - i\frac{\partial}{\partial t}\right]\Psi(\mathbf{r}, t) = 0 \qquad [13.49]$$

Consider the capture process into the ground state. The reaction is

$$\mathrm{p} + \mathrm{H}(1\mathrm{s}) \rightarrow \mathrm{H}(1\mathrm{s}) + \mathrm{p}$$

so that before the collision has taken place ($t \rightarrow -\infty$) the wave function must be of the form

$$\Psi(\mathbf{r}, t) \sim \psi_{1s}(\mathbf{r}_B)e^{-iE_{1s}t} \qquad [13.50]$$

while after the collision ($t \rightarrow +\infty$) Ψ must contain a mixture of $\psi_{1s}(\mathbf{r}_B)$, in which the electron remains attached to B, and $\psi_{1s}(\mathbf{r}_A)$, in which it emerges bound to A. If only these two possibilities are taken into account, then for large positive t, we expect that

$$\Psi(\mathbf{r}, t) \sim a(b, t)\psi_{1s}(\mathbf{r}_B)e^{-iE_{1s}t} + c(b, t)\psi_{1s}(\mathbf{r}_A)e^{-iE_{1s}t} \qquad [13.51]$$

The asymptotic forms [13.50] and [13.51] do not allow for the change in momentum of the electron when it is transferred from B to A. This will be discussed below.

The amplitudes $a(b, t)$ and $c(b, t)$ depend on the time and the impact parameter. With a normalised hydrogen atom wave function ψ_{1s}, the probability of elastic scattering is

$$P_{el} = |a(b, t = \infty)|^2 \qquad [13.52]$$

and that of charge exchange is given by

$$P_{CE} = |c(b, t = \infty)|^2 \qquad [13.53]$$

The total cross-section for charge exchange scattering is obtained by integrating over all impact parameters. Since the system is axially symmetric about the

Z axis, the number of incident particles with impact parameter between b and $b + \mathrm{d}b$ is $N2\pi b\,\mathrm{d}b$, where N is the number of particles crossing unit area per unit time in the incident beam. The total number of particles captured per second is

$$\int_0^\infty N2\pi b\,|c(b, t = \infty)|^2\,\mathrm{d}b$$

and by definition this is the product of the cross-section σ_{CE} and the incident flux N. We have then

$$\sigma_{\mathrm{CE}} = 2\pi \int_0^\infty |c(b, t = \infty)|^2 b\,\mathrm{d}b \qquad [13.54]$$

Actually at large t the wave functions [13.50] and [13.51] are only correct at low velocities. This is because an electron bound to the proton A(B) has momentum $\mathbf{p} = \mathbf{v}/2(\mathbf{p} = -\mathbf{v}/2)$ relative to the origin and a kinetic energy $E = m(v/2)^2/2$. A free electron with this momentum and energy would have the wave function

$$\psi = \mathrm{e}^{i\mathbf{p}\cdot\mathbf{r}}\,\mathrm{e}^{-iEt} \qquad [13.55]$$

The proper forms of the unperturbed wave function at large $|t|$ are therefore given by

$$\Psi \underset{t\to-\infty}{\sim} \psi_{1s}(r_{\mathrm{B}})\mathrm{e}^{-iE_{1s}t}\mathrm{e}^{-i\mathbf{v}\cdot\mathbf{r}/2}\mathrm{e}^{-iv^2t/8}$$

and

$$\Psi \underset{t\to+\infty}{\sim} a(b, t)\psi_{1s}(r_{\mathrm{B}})\mathrm{e}^{-iE_{1s}t}\mathrm{e}^{-i\mathbf{v}\cdot\mathbf{r}/2}\mathrm{e}^{-iv^2t/8}$$
$$+ c(b, t)\psi_{1s}(r_{\mathrm{A}})\mathrm{e}^{-iE_{1s}t}\mathrm{e}^{+i\mathbf{v}\cdot\mathbf{r}/2}\mathrm{e}^{-iv^2t/8} \qquad [13.56]$$

These extra factors are very important at all except the smallest velocities, and should be included certainly above energies of 10 keV. Since the additional factors are of unit modulus, the coefficients a and c have the same significance as before, and the cross-section is given by [13.54].

Slow collisions

When the relative velocity of the protons is small we can try to construct an approximate wave function out of the adiabatic molecular orbitals, discussed in Chapter 9. The two orbitals of lowest energy for the H_2^+ molecular ion are the σ_g 1s and $\sigma_u^\star$ 1s, with wave functions $\Phi_g(R; \mathbf{r})$ and $\Phi_u(R; \mathbf{r})$ respectively. As we pointed out in Chapter 9, these functions can be calculated exactly, although we confined our discussion to the LCAO approximation. Thus at large distances of

separation R we have

$$\frac{1}{\sqrt{2}}[\Phi_g(R;\mathbf{r}) + \Phi_u(R;\mathbf{r})] \to \psi_{1s}(r_A) \qquad [13.57a]$$

$$\frac{1}{\sqrt{2}}[\Phi_g(R;\mathbf{r}) - \Phi_u(R;\mathbf{r})] \to \psi_{1s}(r_B) \qquad [13.57b]$$

so that at large R the combination $2^{-1/2}[\Phi_g + \Phi_u]$ leads to a situation in which the electron is attached to proton A, and the combination $2^{-1/2}[\Phi_g - \Phi_u]$ to the situation in which the electron is attached to B.

If the velocity is so low that the momentum of the electron relative to the origin O can be ignored, the exponential factors [13.55] can be replaced by unity. A wave function $\Psi(\mathbf{r}, t)$ can be formed in this approximation by taking a linear combination of the terms (a) and (b) in (13.57). That is

$$\Psi(\mathbf{r}, t) \simeq \frac{1}{\sqrt{2}}[\Phi_g(R;\mathbf{r}) - \Phi_u(R;\mathbf{r})]e^{-iE_{1s}t}a(b, t)$$
$$+ \frac{1}{\sqrt{2}}[\Phi_g(R;\mathbf{r}) + \Phi_u(R;\mathbf{r})]e^{-iE_{1s}t}c(b, t) \qquad [13.58]$$

This wave function can be written as the sum of two terms each of which has a definite parity under the reflection $\mathbf{r} \to -\mathbf{r}$, namely

$$\Psi(\mathbf{r}, t) = \Psi^+(\mathbf{r}, t) + \Psi^-(\mathbf{r}, t) \qquad [13.59a]$$

where

$$\Psi^+(\mathbf{r}, t) = \Phi_g(R;\mathbf{r})e^{-iE_{1s}t}A^+(b, t)$$
$$\Psi^-(\mathbf{r}, t) = \Phi_u(R;\mathbf{r})e^{-iE_{1s}t}A^-(b, t) \qquad [13.59b]$$

and $A^{\pm}(b, t)$ are new amplitudes defined as

$$A^{\pm}(b, t) = \pm\frac{1}{\sqrt{2}}[a(b, t) \pm c(b, t)] \qquad [13.60]$$

Because the operation $\mathbf{r} \to -\mathbf{r}$ commutes with the operator $(H - i\partial/\partial t)$, the states of definite parity propagate independently, and, just as in the bound state case, the functions containing Φ_g and Φ_u do not mix. Since Ψ^+ and Ψ^- are only approximations, they do not satisfy the equations

$$\left(H - i\frac{\partial}{\partial t}\right)\Psi^{\pm} = 0 \qquad [13.61]$$

exactly, but we can impose the conditions that

$$\int [\Phi_g(R;\mathbf{r})e^{-iE_{1s}t}]^{\star}\left(H - i\frac{\partial}{\partial t}\right)\Psi^+(\mathbf{r}, t)\, d\mathbf{r} = 0 \qquad [13.62a]$$

and

$$\int [\Phi_u(R;\, \mathbf{r})e^{-iE_{1s}t}]^\star \left(H - i\frac{\partial}{\partial t}\right)\Psi^-(\mathbf{r},\, t)\, \mathrm{d}\mathbf{r} = 0 \qquad [13.62b]$$

The adiabatic functions $\Phi_{g,u}$ satisfy

$$H\Phi_{g,u} = E_{g,u}(R)\Phi_{g,u} \qquad [13.63]$$

where $E_{g,u}(R)$ are the electronic potentials, discussed in Chapter 9. In addition, these functions are normalised, so that

$$\int |\Phi_{g,u}(R;\, \mathbf{r})|^2\, \mathrm{d}\mathbf{r} = 1 \qquad [13.64]$$

Using [13.63] and [13.64], the equations [13.62] reduce to

$$\begin{aligned} i\dot{A}^+(b,\, t) &= (E_g(R) - E_{1s})A^+(b,\, t) \\ i\dot{A}^-(b,\, t) &= (E_u(R) - E_{1s})A^-(b,\, t) \end{aligned} \qquad [13.65]$$

where we have made the approximation that

$$\int [\Phi^\star_{g,u}(R;\, \mathbf{r})\, \frac{\mathrm{d}}{\mathrm{d}t}\, \Phi_{g,u}(R;\, \mathbf{r})]\mathrm{d}\mathbf{r}$$

can be ignored. As

$$\frac{\mathrm{d}}{\mathrm{d}t}\,[\Phi_{g,u}] = \frac{\mathrm{d}R}{\mathrm{d}t}\,\frac{\mathrm{d}}{\mathrm{d}R}\,[\Phi_{g,u}] \qquad [13.66]$$

and $\mathrm{d}R/\mathrm{d}t = vt/R$, this is consistent with the small velocity approximation.

To satisfy the boundary conditions $a(b,\, t = -\infty) = 1$ and $c(b,\, t = -\infty) = 0$ we must take from [13.60]

$$A^\pm(b,\, t = -\infty) = \pm\frac{1}{\sqrt{2}} \qquad [13.67]$$

The solutions of [13.65] satisfying these conditons are

$$A^\pm(b,\, t) = \pm\frac{1}{\sqrt{2}}\, \exp\left(i\int_{-\infty}^{t} [E_{g,u}(R) - E_{1s}]\, \mathrm{d}t'\right) \qquad [13.68]$$

where E_g is associated with A^+, and E_u with A^-. The probability amplitude for charge exchange $c(b,\, t = +\infty)$ is then

$$\begin{aligned} c(b,\, t = +\infty) &= \frac{1}{\sqrt{2}}\,[A^+(b,\, t = +\infty) + A^-(b,\, t = +\infty)] \\ &= \frac{1}{2}\left\{\exp\left(i\int_{-\infty}^{\infty} [E_g(R) - E_{1s}]\, \mathrm{d}t\right)\right. \\ &\qquad \left. - \exp\left(i\int_{-\infty}^{\infty} [E_u(R) - E_{1s}]\, \mathrm{d}t\right)\right\} \end{aligned} \qquad [13.69]$$

and the probability of charge exchange is given by

$$P_{\text{CE}} = |c(b, t = +\infty)|^2 = \sin^2\left\{\frac{1}{2}\int_{-\infty}^{+\infty} [E_{\text{g}}(R) - E_{\text{u}}(R)]\,\text{d}t\right\} \quad [13.70]$$

We see that for a fixed impact parameter, $|c(b, t = +\infty)|^2$ will oscillate between 0 and 1, as the incident energy is varied.

To obtain the probability $P_{\text{CE}}(\theta)$ of charge exchange as a function of the scattering angle θ we have to relax the assumption that the trajectory of the protons is a straight line. If we assume an effective potential between the incident proton and the target, for example the average of the potentials $(E_{\text{g}}(R) - E_{1\text{s}})$ and $(E_{\text{u}}(R) - E_{1\text{s}})$, the classical trajectory on which the protons move can be calculated. The impact parameter b is then a function of the scattering angle θ, $b = b(\theta)$, and

$$P_{\text{CE}}(\theta) = |c(b(\theta), t = +\infty)|^2 \quad [13.71]$$

In terms of the differential cross-sections for elastic scattering, $\text{d}\sigma_{\text{el}}/\text{d}\Omega$ and charge exchange, $\text{d}\sigma_{\text{CE}}/\text{d}\Omega$, we may also write

$$P_{\text{CE}}(\theta) = \frac{\text{d}\sigma_{\text{CE}}/\text{d}\Omega}{\text{d}\sigma_{\text{el}}/\text{d}\Omega + \text{d}\sigma_{\text{CE}}/\text{d}\Omega} \quad [13.72]$$

where

$$\frac{\text{d}\sigma_{\text{el}}}{\text{d}\Omega} = \frac{\text{d}\sigma}{\text{d}\Omega}|a(b(\theta), t = +\infty)|^2 \quad [13.73\text{a}]$$

$$\frac{\text{d}\sigma_{\text{CE}}}{\text{d}\Omega} = \frac{\text{d}\sigma}{\text{d}\Omega}|c(b(\theta), t = +\infty)|^2 \quad [13.73\text{b}]$$

and $\text{d}\sigma/\text{d}\Omega$ is the classical differential cross-section for scattering by the effective potential. The expressions [13.71] and [13.72] are in fact identical because of the relation

$$|a(b, t = +\infty)|^2 + |c(b, t = +\infty)|^2 = 1 \quad [13.74]$$

which can be verified from [13.60] and [13.68] and simply expresses the conservation of probability.

The experiments of Lockwood and Everhart demonstrate the oscillation of $P_{\text{CE}}(\theta)$ as a function of energy and are shown in Fig. 13.10. The maximum and minimum of the oscillations are near 0.8 and 0.2, rather than 1 and 0, as predicted by the simple two-state model. This is because more than just the $\sigma_{\text{g}}1\text{s}$ and $\sigma_{\text{u}}^{\star}1\text{s}$ levels of H_2^+ are important and there is, even at the lower energies, strong coupling to the level $\pi_{\text{u}}2\text{p}$. This is not surprising because in the united atom limit, the $\sigma_{\text{u}}^{\star}1\text{s}$ level approaches the 2p_0 level of He^+ and the $\pi_{\text{u}}2\text{p}$ level approaches the $2\text{p}_{\pm 1}$ level of He^+ and both levels have the same energy in this limit. When the approximate function [13.58] is improved to account for the

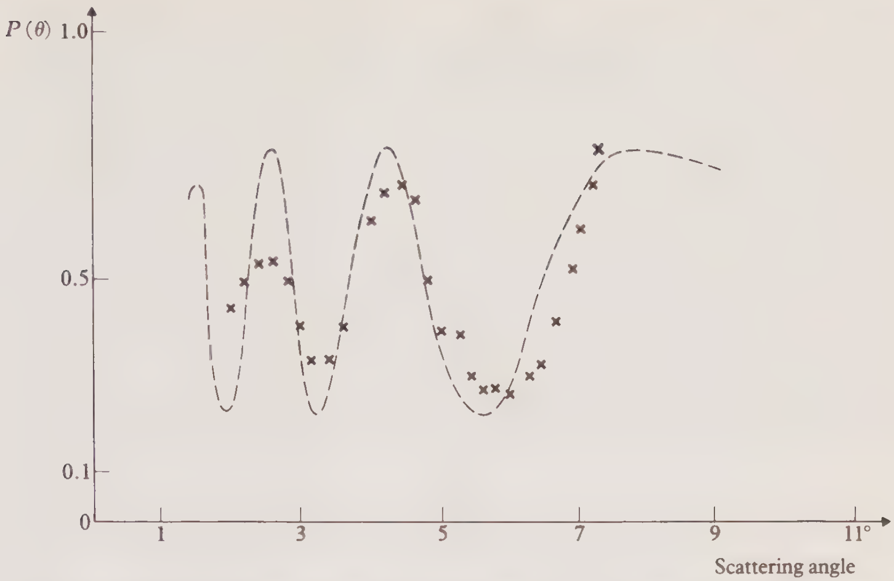

13.10 The probability of charge exchange in the collision of 250 eV protons with hydrogen atoms, measured as a function of scattering angle by Lockwood and Everhart. The dashed line shows the results of a theoretical coupled channel calculation retaining the $\sigma_g 1s$, $\sigma_u 1s$ and $\pi_u 2p$ levels of the H_2^+ system. If only the $\sigma_g 1s$ and $\sigma_u 1s$ levels are employed in a two-channel calculation, the theoretical results oscillate between 0 and 1 (see text).

$\pi_u 2p$ and other channels, very satisfactory agreement can be obtained with the experimental results [1]. From the calculated amplitudes for the $\pi_u 2p$ level, the probability of direct excitation of the 2p level of the atom ($B + e^-$) can be calculated and also the probability of capture into the 2p level of ($A + e^-$).

The homonuclear case is particularly simple because the equations divide into two classes, one for each parity state of the system. However, the technique of representing the wave function approximately by combinations of adiabatic molecular orbitals has been applied successfully to heteronuclear systems, such as p + He, He^+ + H, etc.

Heavy ion excitation

The simple theory of the last paragraph has had an unexpected and surprising success in interpreting what at first glance would seem to be very complicated processes concerning the slow collisions of heavy ions, such as Ne + Ne^+. In collisions of this kind, it is found that excitation of an inner K shell electron, producing a vacancy, can be detected by the subsequent emission of X-rays when an outer shell electron makes a transition into the vacant level, or by the

[1] See McDowell and Coleman (1970) or Bransden (1970).

emission of 'Auger electrons'. The latter process is a radiationless mechanism in which an outer electron fills the K shell vacancy, giving up its energy to a second electron which is ejected. Fano and Litchen realised that because of the large nuclear charge in a heavy ion, the K shell electrons could be considered as moving in the field of the two nuclei only, hardly influenced by the remaining electrons. The correlation diagram for the homonuclear system, composed of a K shell electron and the two nuclei, is the same as for H_2^+, and the system before the collision is composed of equal proportions of the $\sigma_u^\star 1s$ and $\sigma_g 1s$ molecular orbitals. The $\sigma_u^\star 1s$ orbital becomes degenerate with the $\pi_u 2p$ orbital in the united atom limit and at small separations the electron can be *promoted* easily from the $\sigma_u^\star 1s$ to the $\pi_u 2p$ orbital. The cross-section for this excitation process can be calculated by scaling the corresponding cross-section for the proton–hydrogen atom system. This is possible because the Schrödinger equation for an electron moving in the field of two identical charges Z, is (in atomic units)

$$\left[-\frac{1}{2}\nabla^2 - \frac{Z}{|\mathbf{r}-\mathbf{R}/2|} - \frac{Z}{|\mathbf{r}+\mathbf{R}/2|}\right]\Psi(\mathbf{r}, t) = i\frac{\partial}{\partial t}\Psi(\mathbf{r}, t) \qquad [13.75]$$

If we make the substitutions

$$\mathbf{r}' = Z\mathbf{r},\ \mathbf{R}'(t') = Z\mathbf{R}(t),\ t' = Z^2 t \qquad [13.76]$$

we regain the equation for the p–H system, namely

$$\left[-\frac{1}{2}\nabla^2 - \frac{1}{|\mathbf{r}'-\mathbf{R}'/2|} - \frac{1}{|\mathbf{r}'+\mathbf{R}'/2|}\right]\Psi(\mathbf{r}', t') = i\frac{\partial}{\partial t'}\Psi(\mathbf{r}', t') \qquad [13.77]$$

In fact all lengths scale from [13.76] as

$$l' \to Zl \qquad [13.78a]$$

and the velocities scale as

$$v' \to v/Z \qquad [13.78b]$$

The cross-section $\sigma(Z, v)$ for excitation of a particular level, for a system with nuclear charge Z, is related to that for excitation of the corresponding level in the p–H system, by

$$\sigma(Z, v) = Z^{-2}\sigma(1, v/Z) \qquad [13.79]$$

In fact, for the heavier systems, Z may be replaced by an effective charge to allow for the partial screening of the nuclear charge by the other electrons.

In Fig. 13.11 it is shown how the measured X-ray emission probability as function of impact parameter is correlated with the computed $\sigma_u^\star 1s \to \pi_u 2p$ transition probability, using the one-electron model.

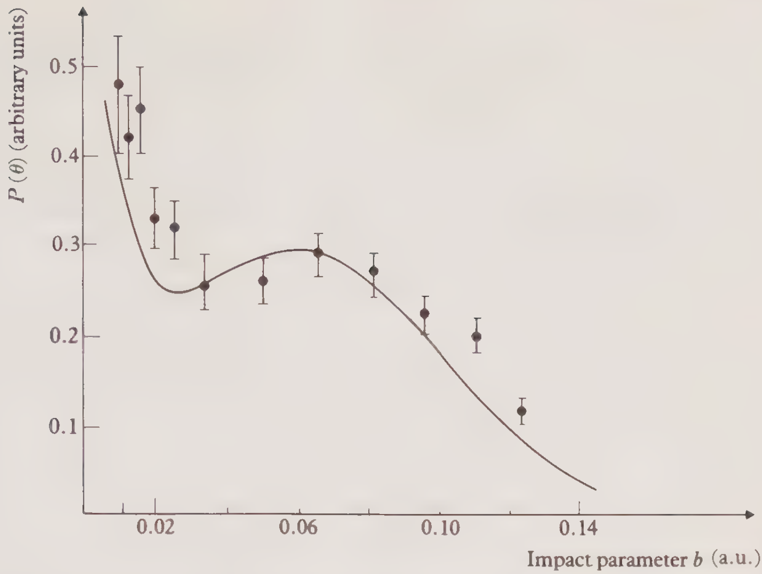

13.11 The data points show the measured probability of X-ray emission in a Ne^+–Ne collision of 363 keV as a function of impact parameter. The solid curve shows the probability for excitation of the K shell electron into a 2p level calculated using the theory outlined in the text. (The data is due to Sackmann, Lutz and Briggs)

Atom–atom collisions at high velocities

When the velocity of the incident atom or ion is large compared with the orbital velocities of the electrons in the target atom, excitation cross-sections can be obtained from the first Born approximation, along the lines discussed for electron scattering in Chapter 12. We can use the classical description of the heavy particle motion, as in the previous paragraphs of this chapter, and the resulting total cross-sections for excitation are the same as those found from the usual full wave-mechanical treatment of the first Born approximation.

Unfortunately, charge exchange processes cannot be evaluated by first-order perturbation theory at high velocities. This is because in the high velocity limit, the total cross-section is given by the second, rather than the first, Born approximation, and at most velocities of experimental interest, it is likely that several higher order terms are important. The methods that have been evolved for discussing such processes are beyond the scope of this book. Above energies of ~ 100 keV in the case of proton impact, the charge exchange cross-section decreases like v^{-12} (at still higher energies like v^{-11}), and charge exchange becomes very small compared with excitation, which decreases like $v^{-2} \log v$ for an $s \to p$ transition, and like v^{-2} for an $s \to s$ transition.

To illustrate the calculation of an excitation cross-section at high velocities, we shall again take the simple example of the proton–hydrogen atom system. The wave function for the electron satisfies the time-dependent Schrödinger equation [13.49], and the Hamiltonian is given by [13.47]. Since we are going to

omit the rearrangement channel, in which the electron is bound to the incident proton A, it is convenient to fix the origin of the coordinate system at the proton B, and to take $\mathbf{r}_B$ and t (see Fig. 13.9) as independent variables, with $\mathbf{r}_A$ given by

$$\mathbf{r}_A(t) = \mathbf{r}_B - \mathbf{R}(t) \tag{13.80}$$

where $\mathbf{R}(t)$ is again determined (in the straight line approximation) by [13.46].

The wave function $\Psi(\mathbf{r}_B, t)$ can be expanded in terms of a complete set of hydrogenic wave functions centred on proton B:

$$\Psi(\mathbf{r}_B, t) = \sum_j a_j(b, t)\psi_j(\mathbf{r}_B)e^{-iE_jt} \tag{13.81}$$

Equations for the amplitudes a_j which are functions of the impact parameter b as well as the time t, can be obtained by inserting the expansion [13.81] into the Schrödinger equation [13.49]. We find that

$$\sum_j i\dot{a}_j(b, t)\psi_j(\mathbf{r}_B)e^{-iE_jt} = \sum_j \left(\frac{1}{R} - \frac{1}{r_A}\right)a_j(b, t)\psi_j(\mathbf{r}_B)e^{-iE_jt} \tag{13.82}$$

where we have made use of the Schrödinger equation satisfied by the hydrogenic wave functions, namely

$$\left(-\frac{1}{2}\nabla^2_{r_B} - \frac{1}{r_B} - E_j\right)\psi_j(\mathbf{r}_B) = 0 \tag{13.83}$$

Multiplying by $\psi_k^\star(\mathbf{r}_B)$, integrating over $\mathbf{r}_B$, and using the orthonormality property

$$\int \psi_k^\star(\mathbf{r}_B)\psi_j(\mathbf{r}_B)\,d\mathbf{r}_B = \delta_{kj} \tag{13.84}$$

we find the set of coupled equations (compare with equations [2.336])

$$i\dot{a}_k(b, t) = \sum_j V_{kj}(t)e^{i(E_k-E_j)t}a_j(b, t) \tag{13.85}$$

where

$$V_{kj}(t) = \int \psi_k^\star(\mathbf{r}_B)\left(\frac{1}{R} - \frac{1}{r_A}\right)\psi_j(\mathbf{r}_B)\,d\mathbf{r}_B \tag{13.86}$$

A coupled channel approximation can be obtained by retaining a number of terms on the right-hand side of [13.85] and solving the resulting equations numerically. A first-order perturbation solution is found as follows. If the system was originally in the state labelled i, then

$$a_j(b, t) \to \delta_{ij} \qquad \text{as} \qquad t \to -\infty \tag{13.87}$$

If the perturbation is small, all the a_j apart from a_i will remain small as time evolves, and a_i will remain close to 1. The coupled equations [13.85] can then be approximated by

$$i\dot{a}_k(b, t) = V_{ki}(t)e^{i(E_k-E_i)t} \tag{13.88}$$

with the solution (for $k \neq i$)

$$a_k(b, t) = -i \int_{-\infty}^{t} V_{ki}(t') e^{i(E_k - E_i)t'} \, dt' \qquad [13.89]$$

The probability of finding the system after the collision in the state k is given by

$$P_k = |a_k(b, t = +\infty)|^2 \qquad [13.90]$$

and the corresponding cross-section is found by integrating over all impact parameters, namely

$$\sigma_k = 2\pi \int_0^{\infty} |a_k(b, t = +\infty)|^2 b \, db \qquad [13.91]$$

As an example, let us consider the excitation of the 2s level of atomic hydrogen from the 1s level by proton impact. Then

$$V_{2s,1s}(t) = \int \psi_{2s}^{\star}(r_B) \left(\frac{1}{R} - \frac{1}{|\mathbf{r}_B - \mathbf{R}|} \right) \psi_{1s}(r_B) \, d\mathbf{r}_B \qquad [13.92]$$

The term in $1/R$ vanishes because of the orthogonality of the functions ψ_{1s} and ψ_{2s}, and the result of the integration is (Problem 13.5)

$$V_{2s,1s}(t) = -\frac{2^{3/2}}{27}(2 + 3R)e^{-3R/2} \qquad [13.93]$$

where $R = (b^2 + v^2t^2)^{1/2}$. Since $V_{2s,1s}(t)$ is even in t, we find that

$$a_{2s}(b, t = +\infty) = -i \frac{2^{5/2}}{27} \int_0^{\infty} [2 + 3R(t)] e^{-3R(t)/2} \cos(3t/8) \, dt \qquad [13.94]$$

The integral over t can be done analytically in terms of Bessel functions, but the final integration over b to obtain the cross-section must be done numerically.

The cross-section for the excitation of the sum of the 2s and 2p levels of atomic hydrogen has been measured and the experimental data are shown in Fig. 13.12, together with the results of the first Born approximation and those of a more elaborate coupled channel calculation. The experimental data are not absolute, but have been normalised to the coupled channel calculation at 200 keV. It is seen that the first Born approximation gives a fair representation of the data above 100 keV, and becomes quite accurate above 200 keV.

It is straightforward to generalise the above results for excitation in any atom (ion)–atom collision. The equation [13.89] still holds and we have

$$a_k(b, t = +\infty) = -i \int_{-\infty}^{+\infty} V_{ki}(t) e^{i(E_k - E_i)t} \, dt \qquad [13.95]$$

where E_i and E_k are the unperturbed atomic energies in the initial and final

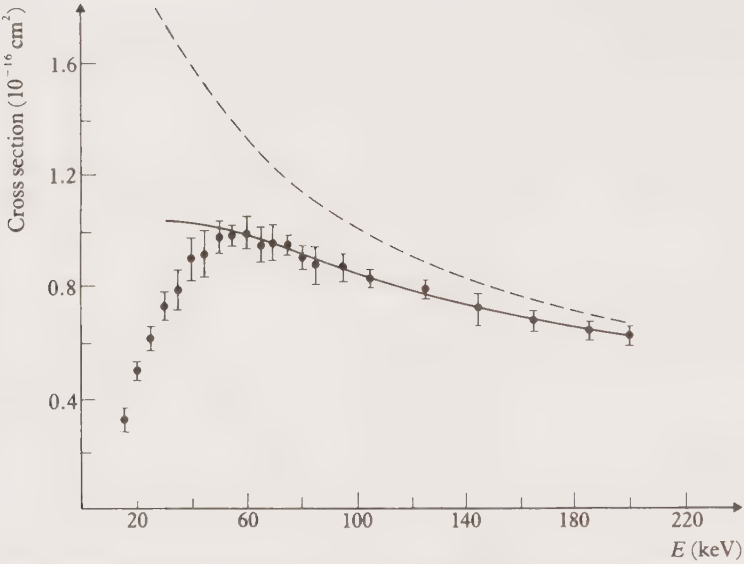

13.12 The cross-section for the excitation of the sum of the 2s and 2p levels of atomic hydrogen by proton impact measured by Park, Alday and George. The solid line shows the results of a coupled channel calculation and the dashed line is the Born approximation. The coupled channel calculation did not allow for charge exchange, and as this process becomes important at energies less than 60 keV, this calculation fails at low energies.

state, respectively, and

$$V_{ki}(t) = \int \psi_k^\star V \psi_i \, d\mathbf{r}_1 \, d\mathbf{r}_2 \cdots d\mathbf{r}_N \qquad [13.96]$$

Here V is the full interaction potential between the two colliding systems, ψ_i and ψ_k are the unperturbed atomic wave functions and the integration is over the coordinates of all the N electrons in the system. Such calculations have been carried out for a variety of atom (ion)–atom excitation collisions.

PROBLEMS

13.1 The relative energy of ions, in two beams inclined at an angle θ, travelling at speeds v_1 and v_2, is $E_R = \frac{1}{2}\mu v_R^2$, where μ is the reduced mass and $\mathbf{v}_R$ is the relative velocity, with

$$v_R = (v_1^2 + v_2^2 - 2v_1v_2 \cos\theta)^{1/2}$$

In the merged beam experiment illustrated in Fig. 13.1, $\theta = 0$. If the ions in each beam have the same mass M, show that the relative energy is approximately $(\Delta E)^2/8E$, where $\Delta E = E_1 - E_2$, $E = \frac{1}{2}(E_1 + E_2)$ and $E_i = (M/2)v_i^2$. If $E_1 = 5.1$ keV and $E_2 = 5.0$ keV, find E_R and calculate v_R in metres per second, for the case that the ions concerned are protons.

13.2 An approximation to the long-range interaction between two neutral hydrogen atoms can be obtained by neglecting the energies $E_j (j \neq 0)$ in the denominator of the expression [13.14] for $E^{(2)}(R)$. Show that if this is done, and if V is given by [13.9], then the long-range interaction is given by [13.15], where C_W has the approximate value of 6 a.u.

13.3 If classical mechanics is employed, the total cross-section for elastic scattering does not exist if the potential is of the form $V(r) = -A/r^s$. If $s > 1$, an effective total cross-section can be defined as

$$\sigma_T = 2\pi \int_{\theta_0}^{\pi} \left(\frac{d\sigma}{d\Omega}\right) \sin\theta \, d\theta,$$

where θ_0 is some lower limit, determined by the geometry of the particular experiment in view. Using the small angle approximation [13.38], find σ_T for the inverse sixth power potential ($s = 6$).

13.4 In Section 13.4, the probability for charge exchange in the reaction

$$p + H(1s) \to H(1s) + p$$

was calculated using a two-state approximation based on molecular orbitals. At higher energies an atomic expansion is more appropriate and in a two-state approximation (see [13.56])

$$\Psi(\mathbf{r}, t) = a(b, t)\psi_{1s}(r_B) e^{-iE_{1s}t} e^{-i\mathbf{v}\cdot\mathbf{r}/2} e^{-iv^2t/8} + c(b, t)\psi_{1s}(r_A) e^{-iE_{1s}t} e^{+i\mathbf{v}\cdot\mathbf{r}/2} e^{-iv^2t/8}$$

By writing down equations analogous to [13.62], find the equations which are satisfied by $a(b, t)$ and $c(b, t)$ and obtain the charge exchange probability $P_{CE} = |c(b, t = +\infty)|^2$.

13.5 By using the explicit forms of the hydrogenic 1s and 2s wave functions, obtain the result [13.93] for $V_{2s,1s}$ starting from [13.92]. Generalise this expression to the case in which a fully stripped ion of charge Z_A is incident on a one-electron ion of nuclear charge Z_B.

14 Some applications of atomic physics

The importance of atomic and molecular physics to other branches of science and to modern technology scarcely needs emphasis. Almost the whole of astrophysics is based upon the interpretation of the spectrum of electromagnetic radiation reaching the earth from other parts of space, and this interpretation rests on our fundamental knowledge of atomic and molecular structure outlined in earlier parts of this book. Among the many offshoots of the subject are the development of laser technology on the one hand, and of quantum chemistry on the other. In another direction, a knowledge of the cross-sections for many atomic processes is critical in assessing the feasibility of many of the proposed methods of power generation using nuclear fusion. Clearly anything like a survey of these many topics would be impossible within the confines of a single volume; but in this chapter, the elementary principles behind a few important techniques and applications of atomic physics will be discussed.

14.1 MAGNETIC RESONANCE AND THE MEASUREMENT OF THE GYROMAGNETIC RATIOS

The overall angular momentum of an atom, arising from both the orbital and the spin angular momenta of the electrons, can either be zero as for closed shell atoms, or non-zero, as for the ground state of atomic hydrogen ($j = s = \frac{1}{2}$; $l = 0$). When the total angular momentum $\mathbf{J}$ is non-zero, an atom possesses a permanent magnetic dipole moment $\boldsymbol{\mathcal{M}}$ given by (see Chapters 1 and 5)

$$\boldsymbol{\mathcal{M}} = -g\mu_B(\mathbf{J}/\hbar) \qquad [14.1]$$

where μ_B is the Bohr magneton, and g is the gyromagnetic ratio. The magnetic moment can be measured in a Stern–Gerlach experiment. An important consequence of the existence of permanent magnetic dipole moments is the *paramagnetism* observed when the magnetic moments of the atoms in a solid are partially aligned by a magnetic field.

If a single atom is placed in a uniform, constant, magnetic field directed along the Z axis, of magnitude $\mathcal{B}_z$, the system has stationary states, which are eigenstates of $\mathbf{J}^2$ and J_z and which have energies,

$$E_m = \mu_B g m \mathcal{B}_z, \qquad [14.2]$$

We denote by $j(j+1)\hbar^2$ the eigenvalues of $\mathbf{J}^2$ and by $m\hbar$ those of $\mathcal{J}_z$; m can take any one of the $(2j+1)$ values $-j, -j+1, \ldots j-1, j$. The nuclear magnetic moments also contribute, in principle, to the total magnetic energy; but since the nuclear moments are several orders of magnitude smaller than the atomic moments, this contribution is entirely unimportant.

The time dependence of the wave function in one of the stationary states is, as usual,

$$\Psi_m(t) = A \exp(-iE_m t/\hbar) \qquad [14.3]$$

which can be written as

$$\Psi_m(t) = A \exp(-i\omega_0 m t) \qquad [14.4]$$

where ω_0 is given by

$$\omega_0 = g\mu_B \mathcal{B}_z/\hbar = g\omega_L = g 2\pi\nu_L \qquad [14.5]$$

ν_L being the Larmor frequency defined in [5.53]. Classically, a magnetic dipole placed in a constant magnetic field precesses about the direction of the field with the angular frequency ω_0.

We now consider the response of the system to an additional weak oscillating magnetic field, $\mathcal{B}_x \cos \omega t$, directed along the X axis. It will be shown that when the angular frequency ω of this second field is close to the angular frequency ω_0, the system is strongly disturbed and there is a large probability of a transition from the initial state. This is called paramagnetic resonance (or electron spin resonance, ESR) and detection of the resonant frequency affords an accurate method of measuring gyromagnetic ratios.

In the presence of both components of the magnetic field, the Schrödinger equation is,

$$H\Psi(t) = i\hbar \frac{\partial}{\partial t} \Psi(t), \qquad [14.6]$$

where

$$H = -\boldsymbol{\mathcal{M}} \cdot \boldsymbol{\mathcal{B}} = \frac{\mu_B g}{\hbar}(\mathcal{J}_z \mathcal{B}_z + \mathcal{J}_x \mathcal{B}_x \cos \omega t) \qquad [14.7]$$

To simplify the discussion, consider a case (such as atomic hydrogen) for which $j = \frac{1}{2}$, so that $\mathbf{J}$ can be written in terms of the Pauli spin matrices $\sigma_x, \sigma_y, \sigma_z$ with

$$\mathbf{J} = \frac{\hbar}{2} \boldsymbol{\sigma} \qquad [14.8]$$

The wave function is now a two-component spinor,

$$\Psi(t) = \begin{pmatrix} a_+(t) \\ a_-(t) \end{pmatrix} \qquad [14.9]$$

where $|a_+(t)|^2$ is proportional to the probability of finding the system in the state with $m = +\frac{1}{2}$, and $|a_-(t)|^2$ to the corresponding probability that the system is in the state with $m = -\frac{1}{2}$. Since the system must be found in one of these two states the wave function can be normalised so that, for all t,

$$|a_+(t)|^2 + |a_-(t)|^2 = 1$$

When the perturbation $\mathcal{B}_x \cos \omega t$ is absent, the unperturbed eigenfunctions are

$$\Psi_{1/2} = \begin{pmatrix} \exp(-i\omega_0 t/2) \\ 0 \end{pmatrix}; \ \Psi_{-1/2} = \begin{pmatrix} 0 \\ \exp(i\omega_0 t/2) \end{pmatrix} \qquad [14.10]$$

If the system was originally in the $m = \frac{1}{2}$ state, and the perturbation was switched on at time $t = 0$, we can calculate the probability of finding the system in the $m = -\frac{1}{2}$ state at some later time t. Since we shall be interested in large values of t, we cannot use the perturbation theory described in Chapter 2 and employed in Chapters 4 and 5. Instead, we shall proceed by using the explicit forms of the Pauli matrices to write the Schrödinger equation as a pair of coupled equations for $a_\pm(t)$. That is,

$$\frac{\mu_B g}{2}\left[\begin{pmatrix} 1 & 0 \\ 0 & -1 \end{pmatrix}\mathcal{B}_z + \begin{pmatrix} 0 & 1 \\ 1 & 0 \end{pmatrix}\mathcal{B}_x \cos \omega t\right]\begin{pmatrix} a_+ \\ a_- \end{pmatrix} = i\hbar \frac{\partial}{\partial t}\begin{pmatrix} a_+ \\ a_- \end{pmatrix} \qquad [14.11]$$

In terms of $\omega_0 = \mu_B g \mathcal{B}_z/\hbar$ and $\bar{\omega}_0 = \mu_B g \mathcal{B}_x/\hbar$, we have,

$$\begin{aligned} i\dot{a}_+ &= \tfrac{1}{2}\omega_0\, a_+ + \tfrac{1}{2}\bar{\omega}_0 \cos(\omega t)\, a_- \\ i\dot{a}_- &= -\tfrac{1}{2}\omega_0\, a_- + \tfrac{1}{2}\bar{\omega}_0 \cos(\omega t)\, a_+ \end{aligned} \qquad [14.12]$$

A phase transformation

$$A_+ = a_+ e^{i\omega_0 t/2}, \qquad A_- = a_- e^{-i\omega_0 t/2} \qquad [14.13]$$

removes the secular terms in $\pm\frac{1}{2}\omega_0$ giving

$$\begin{aligned} i\dot{A}_+ &= \tfrac{1}{2}\bar{\omega}_0 \cos(\omega t)\, e^{+i\omega_0 t} A_- \\ i\dot{A}_- &= \tfrac{1}{2}\bar{\omega}_0 \cos(\omega t)\, e^{-i\omega_0 t} A_+ \end{aligned} \qquad [14.14]$$

These equations cannot be solved exactly, but an accurate approximation can be obtained by recognising that in the products $\cos(\omega t) \exp(\pm i\omega_0 t)$ terms in $\exp[\pm i(\omega - \omega_0)t]$ will be much more important than those in $\exp[\pm i(\omega + \omega_0)t]$. This is because the latter terms oscillate extremely rapidly and on the average make little contribution to $\dot{A}_+$ or $\dot{A}_-$. Dropping these terms, we find the approximate equations:

$$\begin{aligned} i\dot{A}_+ &= \tfrac{1}{4}\bar{\omega}_0 \exp[i(\omega_0 - \omega)t]\, A_- \\ i\dot{A}_- &= \tfrac{1}{4}\bar{\omega}_0 \exp[-i(\omega_0 - \omega)t] A_+ \end{aligned} \qquad [14.15]$$

Exact resonance

It is easy to verify that in the case of exact resonance $\omega = \omega_0$, the equations [14.15] have the general solution,

$$\begin{aligned} A_+ &= \lambda \cos(\bar{\omega}_0 t/4) + \mu \sin(\bar{\omega}_0 t/4) \\ A_- &= i\mu \cos(\bar{\omega}_0 t/4) - i\lambda \sin(\bar{\omega}_0 t/4) \end{aligned} \qquad [14.16]$$

where λ and μ are constants, which are determined by the initial conditions.

Suppose that at $t = 0$ the system is in the state with $m = \frac{1}{2}$; then $A_+(0) = a_+(0) = 1$; $A_-(0) = a_-(0) = 0$ so that $\lambda = 1$ and $\mu = 0$. Thus the probabilities $P(+ \to +)$ and $P(+ \to -)$ for finding the system in levels with $m = +\frac{1}{2}$ or $m = -\frac{1}{2}$ at time t, are

$$\begin{aligned} P(+ \to +) &= |A_+(t)|^2 = \cos^2(\bar{\omega}_0 t/4) \\ P(+ \to -) &= |A_-(t)|^2 = \sin^2(\bar{\omega}_0 t/4) \end{aligned} \qquad [14.17]$$

Both $P(+ \to +)$ and $P(+ \to -)$ range between 0 and 1; but $P(+ \to +) + P(+ \to -) = 1$, always.

In the same way, if at $t = 0$, the system is the state with $m = -\frac{1}{2}$ so that $A_+(0) = a_+(0) = 0$; $A_-(0) = a\ (0) = 1$, the probabilities $P(- \to +)$ and $P(- \to -)$ for finding the system in the levels with $m = +\frac{1}{2}$ and $m = -\frac{1}{2}$ after time t are

$$\begin{aligned} P(- \to +) &= \sin^2(\bar{\omega}_0 t/4) \\ P(- \to -) &= \cos^2(\bar{\omega}_0 t/4) \end{aligned} \qquad [14.18]$$

It should be noticed that, in conformity with time reversal invariance,

$$P(- \to +) = P(+ \to -) \qquad [14.19]$$

General solution

It is possible to solve equations [14.15] exactly, even when $\omega \neq \omega_0$. The general solution is (see Problem 14.1)

$$\begin{aligned} A_+ &= p e^{i\eta_+ t} + q e^{i\eta_- t} \\ A_- &= -\frac{4}{\bar{\omega}_0}[p\eta_+ e^{i\eta_+ t} + q\eta_- e^{i\eta_- t}]\, e^{i(\omega - \omega_0)t} \end{aligned} \qquad [14.20]$$

where p and q are constants of integration (different from λ and μ!) and η_+ are given by

$$\eta_\pm = \tfrac{1}{2}[(\omega_0 - \omega) \pm \sqrt{(\omega_0 - \omega)^2 + (\bar{\omega}_0)^2/4}] \qquad [14.21]$$

With the boundary conditions at $t = 0$, $A_+(0) = 1$; $A_-(0) = 0$, we find that

$$p = \frac{\eta_-}{\eta_- - \eta_+}, \qquad q = \frac{-\eta_+}{\eta_- - \eta_+} \qquad [14.22]$$

The probabilities $P\ (+ \to +)$ and $P\ (+ \to -)$ become

$$P(+ \to +) = \cos^2(\omega_R t/2) + \frac{(\omega_0 - \omega)^2}{(\omega_0 - \omega)^2 + (\bar{\omega}_0)^2/4} \sin^2(\omega_R t/2)$$

$$P(+ \to -) = \frac{\bar{\omega}_0^2/4}{(\omega_0 - \omega)^2 + \bar{\omega}_0^2/4} \sin^2(\omega_R t/2). \qquad [14.23]$$

The frequency ω_R is known as the Rabi 'flopping frequency' and is

$$\omega_R = (\eta_+ - \eta_-) = \sqrt{(\omega_0 - \omega)^2 + \bar{\omega}_0^2/4} \qquad [14.24]$$

Under the conditions in which $\mathcal{B}_x \ll \mathcal{B}_z$ and $\bar{\omega}_0 \ll \omega_0$, the probability that the system will be found in the second channel with $m = -\frac{1}{2}$ will remain small unless ω is close to ω_0. If the oscillating magnetic field $\mathcal{B}_x \cos \omega t$ is applied for a time T which is short ($\bar{\omega}_0 T \ll 1$), equations [14.15] can be solved by first-order perturbation theory and it is left as an exercise (Problem 14.2) to obtain this solution and compare it with [14.20].

Resonance occurs when the frequency of the oscillating field ω is such that $\hbar\omega$ is equal to the difference in energy of the two Zeeman levels of the system, ΔE. In our spin-$\frac{1}{2}$ case:

$$\Delta E = \hbar\omega_0 = \mu_B g \mathcal{B}_z. \qquad [14.25]$$

In general, for atoms with non-zero angular momentum, resonance can be produced by matching the frequency of the applied field to the frequency of a transition between particular Zeeman sublevels, and the theory can be generalised to treat a system of $(2j + 1)$ equations rather than the pair of equations treated here.

The Rabi molecular beam apparatus

A molecular beam experiment, which is much more accurate than the Stern–Gerlach experiment discussed in Chapter 1 has been devised by Rabi to measure magnetic moments of atoms, based on paramagnetic resonance. A schematic diagram is shown in Fig. 14.1. A beam of atoms from an oven is passed through a system of three magnets M1, M2 and M3. We shall suppose that the atoms have total angular momentum one-half (examples of which are silver, the alkalis, or copper), although the principle of the experiment is the same for other non-zero values of the angular momentum. The magnets M1 and M3 produce inhomogeneous fields as in the Stern–Gerlach experiment, identical in magnitude but opposite in sign. If the field gradient in M1 is positive upwards, those atoms with $\mathcal{J}_z = +\frac{1}{2}\hbar$ will be deflected downwards, and those with $\mathcal{J}_z = -\frac{1}{2}\hbar$ will be deflected upwards. If a slit S2 is placed, as shown, only two trajectories are possible from the source (slit S1) into the region to the right of S2. The trajectory B1 will contain atoms with $\mathcal{J}_z = +\frac{1}{2}\hbar$ and B2 will contain

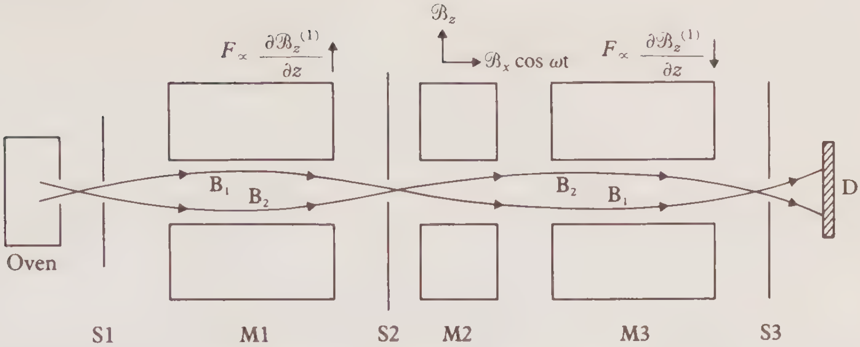

14.1 Schematic diagram of a molecular beam resonance apparatus.

those with $\mathcal{J}_z = -\frac{1}{2}\hbar$. Since the magnet M3 has an equal and opposite effect on the two trajectories, the atoms in B1 and B2 will be brought together at the slit S3 and detected at D. Now let us see what happens if the magnet M2 is switched on, which produces a large uniform static field in the Z direction, $\mathcal{B}_z$, and a small oscillating field, $\mathcal{B}_x \cos \omega t$, in the X direction. When ω is close to the resonance angular frequency ω_0, some of the atoms in the beam B1 will have their spin direction changed from $\mathcal{J}_z = \frac{1}{2}\hbar$ to $\mathcal{J}_z = -\frac{1}{2}\hbar$. These atoms will now be deflected downwards in the magnet M3 and miss the slit S3. Similarly, atoms in the beam B2 which make transitions from $\mathcal{J}_z = -\frac{1}{2}\hbar$ to $\mathcal{J}_z = +\frac{1}{2}\hbar$ will also miss the slit. The net effect is that as ω approaches the resonant angular frequency, the intensity of the beam entering the detector drops sharply. Under the conditions $\omega_0 \gg \bar{\omega}_0$, the resonance region is very narrow and well defined, and since frequencies can be measured very accurately, this method can provide correspondingly accurate values for atomic magnetic moments and gyromagnetic ratios.

Paramagnetic resonance and nuclear magnetic resonance in bulk samples

It is also possible to detect resonance phenomena in bulk samples of materials. Let us consider the case of a material composed of atoms of total angular momentum one-half. In the absence of a magnetic field, the two states of each atom with $\mathcal{J}_z = m\hbar$, $m = \pm\frac{1}{2}$ have the same energy, and in a bulk sample as many atoms have $m = \frac{1}{2}$ as have $m = -\frac{1}{2}$. If the sample is placed in a uniform magnetic field $\mathcal{B}_z$, directed along the Z axis, then those atoms with $m = \frac{1}{2}$ possess energy (see [14.2])

$$E_+ = \mu_B g \mathcal{B}_z/2 \qquad [14.26]$$

and those with $m = -\frac{1}{2}$ have the lower energy,

$$E_- = -\mu_B g \mathcal{B}_z/2 \qquad [14.27]$$

In thermal equilibrium, the ratio of the number of atoms per unit volume with $m = \frac{1}{2}$, N_+, to the number with $m = -\frac{1}{2}$, N_-, is

$$\frac{N_+}{N_-} = \frac{\exp[-E_+/kT]}{\exp[-E_-/kT]} \qquad [14.28]$$

Let $N = N_+ + N_-$ be the number of atoms per unit volume. Then

$$N_+ = N \frac{\exp[-\mu_B g \mathcal{B}_z/2kT]}{\exp[\mu_B g \mathcal{B}_z/2kT] + \exp[-\mu_B g \mathcal{B}_z/2kT]}$$

$$N_- = N \frac{\exp[+\mu_B g \mathcal{B}_z/2kT]}{\exp[\mu_B g \mathcal{B}_z/2kT] + \exp[-\mu_B g \mathcal{B}_z/2kT]} \qquad [14.29]$$

The atoms with $m = \frac{1}{2}$ contribute a magnetic moment in the Z direction of magnitude $(-\mu_B g/2)$ and those with $m = -\frac{1}{2}$ contribute a magnetic moment $(+\mu_B g/2)$, so that the magnitude of the net magnetic moment per unit volume is

$$\begin{aligned} \mathcal{M} &= N_+(-\mu_B g/2) + N_-(\mu_B g/2) \\ &= \left(\frac{\mu_B g}{2}\right) N \frac{\exp[\mu_B g \mathcal{B}_z/2kT] - \exp[-\mu_B g \mathcal{B}_z/2kT]}{\exp[\mu_B g \mathcal{B}_z/2kT] + \exp[-\mu_B g \mathcal{B}_z/2kT]} \end{aligned} \qquad [14.30]$$

Now if a small field $\mathcal{B}_x \cos \omega t$ is applied in the X direction, when ω is close to the resonant frequency transitions are induced between the two states with $m = \frac{1}{2}$ and $m = -\frac{1}{2}$. If these two levels were equally populated, these transitions could not be detected, but since the number of atoms in the state of lower energy is greater than the number in the state of higher energy, more transitions occur which absorb energy from the external field than transitions which feed energy into the external field. This net loss of energy at resonance is small, but can be detected in various ways. For example the oscillating magnetic field may be produced by a coil which is placed in a bridge circuit (see Fig. 14.2). At resonance, the energy loss to the medium gives rise to an apparent change in the self-induction of the coil, which can be detected by the bridge.

The technique of paramagnetic resonance is important to industry and research, to give information about the constituents of a sample. If these are known, the apparatus can serve as a magnetometer to measure small fields $\mathcal{B}_x$.

Although the magnetic moments of nuclei are smaller than those of atoms by a factor of the order of m/M_p (where m is the mass of the electron, and M_p that of the proton) and nuclear paramagnetism is too small to be observed directly, nuclear magnetic resonance experiments are perfectly possible and are, in fact, of great importance. A substance is chosen for which the total angular momentum due to the electrons is zero, for otherwise the nuclear effect would be completely masked. The experiment can then be performed in exactly the

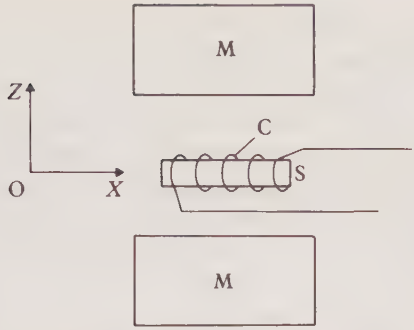

14.2 Paramagnetic resonance apparatus. The specimen S is placed between the poles M of a magnet producing a uniform static field in the Z direction. A small oscillating field in the X direction is produced by the coil C.

same way as for paramagnetic substances, with the resonant frequency being determined by the strength of the static field $\mathcal{B}_z$, where now (see [14.5])

$$\omega_0 = g\mu_N \mathcal{B}_z/\hbar \qquad [14.31]$$

and μ_N is the nuclear magneton

$$\mu_N = \mu_B m/M_p = e\hbar/2M_p \qquad [14.32]$$

For a field of strength 0.5 T, the resonant frequency of a proton ($g = 5.588$) is 21.3 MHz, which is in the radio-frequency region. The frequencies associated with paramagnetic resonance are about 2000 times higher and are in the microwave region, for which wave guide techniques must be employed.

Chemical shifts

Nuclear magnetic resonance has proved to be an important tool in the structural analysis of molecules. This is possible because there is a small dependence of resonant frequency on the local environment of a nucleus in a molecule. The effect of the external magnetic field on the electrons in a molecule is to induce currents which themselves create a magnetic field in opposition to the applied field. The effective magnetic field at the nucleus $\mathcal{B}_z^E$ is less than the applied field $\mathcal{B}_z$, and correspondingly the observed resonance frequency ω_0^E is slightly less than ω_0. This shielding effect is small, the resonance frequency changing in many cases by only a few parts in a million, but it is specific to the local environment of a nucleus. For example, the resonant frequency for a proton in an OH group is different from that of a proton in an NH_2 group, which is in turn different from that of a proton in a CH_3 group. These chemical shifts offer an excellent method of chemical analysis of a sample. Still more information can be obtained by examining the relative intensity of the resonant lines and from fine structure effects, which arise from the interactions between neighbouring nuclei in a molecule.

14.2 MASERS AND LASERS

In this section, we shall examine in outline how the phenomenon of stimulated emission, discussed in Chapter 4, can be used to construct amplifiers or generators of electromagnetic radiation. Suppose 1 and 2 are two levels, with energies E_1, E_2 ($E_2 > E_1$), out of the infinite number of levels of a particular material. Consider a beam of electromagnetic radiation of intensity I and angular frequency, $\omega = (E_2 - E_1)/\hbar$ passing through this material. The rate of change of the energy density because of absorption from the beam is

$$\frac{d\rho_a}{dt} = -N_1(\hbar\omega)W_{21} \qquad [14.33]$$

where N_1 is the number of atoms in the lower energy level per unit volume and W_{21} is the transition rate per atom for absorption. Similarly, the rate of change of the energy density because of stimulated emission is

$$\frac{d\rho_s}{dt} = N_2(\hbar\omega)W_{12} \qquad [14.34]$$

where N_2 is the number of atoms in the upper energy level per unit volume, and W_{12} is the transition rate per atom for stimulated emission. In Chapter 4, it was shown that W_{12} and W_{21} are equal and both are proportional to the intensity I of the incident radiation. The cross-section σ, defined as

$$\sigma = (\hbar\omega)W_{12}/I \qquad [14.35]$$

is characteristic of the particular pair of levels, (see [4.39]), but independent of the intensity of the beam of radiation. In terms of σ, we can write the net rate of change of energy per unit volume traversed by the beam as

$$\frac{d\rho}{dt} = \sigma I(N_2 - N_1) \qquad [14.36]$$

If the beam is of cross-sectional area A, and is travelling parallel to the z axis, this relation can be written in the form (see [4.11])

$$\frac{dI}{dz} = \sigma I(N_2 - N_1) \qquad [14.37]$$

We see that if $N_1 > N_2$ the incident radiation is absorbed as it traverses the material, but if $N_2 > N_1$ the radiation is amplified. Spontaneous emission will also increase the number of transitions from the upper level 2 to the lower level 1, but the corresponding transition rate is independent of the intensity I, and provided I is sufficiently large this contribution can be ignored.

Under thermal equilibrium, we know that for non-degenerate levels

$$\frac{N_2}{N_1} = \exp[-(E_2 - E_1)/kT] \qquad [14.38]$$

where k is Boltzmann's constant and T the temperature. Since $E_2 > E_1$ it follows that $N_2 < N_1$ and the material acts as an absorber. To achieve amplification a *population inversion* must be arranged with $N_2 > N_1$, and the substance cannot be in thermal equilibrium.

When amplification is achieved in the microwave region, we speak of a *maser* (microwave amplification by stimulated emission of radiation) and for radiation of higher frequencies we use the term *laser* (light amplification by stimulated emission of radiation).

To increase the gain of the amplifier and to act as a generator, the material can be placed between two plane mirrors (see Fig. 14.3), or in the case of a maser inside a resonant cavity. If one of the mirrors is partially transparent, an output beam can be formed. If the power generated within the material, by stimulated emission, is greater than the sum of the power output and the power losses, then the laser acts as an oscillator and the intensity of the radiation between the mirrors increases exponentially. This increase in intensity will be limited finally by the ability of the 'pumping' mechanism producing the inverted population to keep up the number of atoms in the upper level. The laser oscillations can be started by a single photon resulting from spontaneous emission from the upper to the lower level. In applications, masers are frequently used as amplifiers, but more usually lasers are employed as oscillators generating radiation.

The characteristic properties of a beam generated by a laser are (a) monochromaticity (b) directionality (c) spatial coherence (d) brightness (e) temporal coherence. The monochromaticity is a consequence of the fact that only light arising from a transition between a single pair of levels is amplified. The output of a laser is a parallel beam which emerges perpendicular to the plane of the mirrors in an arrangement such as that illustrated in Fig. 14.3. This is because only electromagnetic waves propagating in this direction will be reflected back and forth between the mirrors. Waves with any other direction of propagation will be lost to the system. This directionality also accounts for the brightness of a laser beam. The power output of a normal light source is usually spread out into a large solid angle, but in a laser it is concentrated into a narrow unidirectional beam.

In Chapter 4 we saw that, in stimulated emission, at each transition one photon is added to a mode containing N photons. The extra photon is completely in phase with the incident photons and has the same polarisation. It

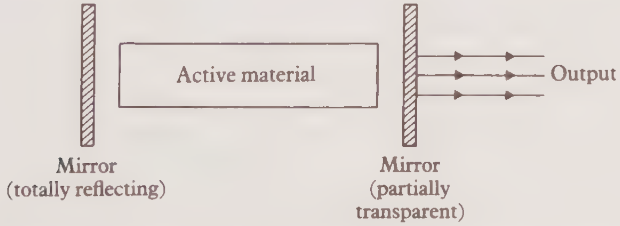

14.3 Schematic diagram of a laser in which the active material is confined between plane parallel mirrors.

follows that if laser action is initiated by a single photon, at each transition one extra photon will be produced and after N transitions, all $(N + 1)$ photons will be in phase and contribute to the same mode of the electromagnetic radiation. This is in contrast to a normal light source, where the dominant process is spontaneous emission, so that the phases and polarisations associated with each photon are different. There are two independent concepts of coherence – spatial coherence and temporal coherence. If the phase difference between two points on a wave front, normal to the direction of propagation, is zero at all times, the wave is said to exhibit perfect spatial coherence. If the active material in a laser is homogeneous, the output beam exhibits spatial coherence over its whole cross-sectional area. It is in fact effectively a single plane wave of the form $\mathscr{E} = \mathscr{E}_0 \sin(\mathbf{k} \cdot \mathbf{r} - \omega t)$, with a single angular frequency and with all points on the wave front in phase. Temporal coherence relates to the duration of the output wave, and the coherence time is the interval over which the output is represented by the same plane wave. The stability of the laser determines the coherence time; it can be extremely long compared with the periodic time of the radiation. Coherence times of up to 10^{-3} s can be achieved, which allows the observation of interference effects between the beams of light originating from two different lasers. In contrast, using conventional sources, interference can only be observed by splitting and recombining the light from one source.

Methods for obtaining a population inversion

We have seen that the key to laser (or maser) action is to obtain a population inversion between two levels of energy E_1 and E_2, with $E_2 > E_1$, so that more atoms are in the level 2 than in the level 1. Historically, the first method was beam separation which was used by C. H. Townes in 1954 in the ammonia maser. We shall describe this in some detail below. The technique used is analogous to the Stern-Gerlach method for separating beams of atoms possessing magnetic dipole moments, but in this case it is a separation of electric dipoles that is achieved. An alternative is to use a 'pumping' technique. In the three-level laser (Fig. 14.4) we look for three levels in an atom such that $E_3 > E_2 > E_1$, with a fast decay between levels 3 and 2 and a slow decay between 2 and 1. Incident radiation of angular frequency $\omega_{31} = (E_3 - E_1)/\hbar$ is used to raise as many

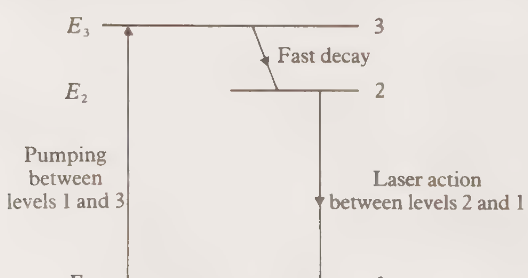

14.4 The three-level laser.

atoms as possible from the level 1 to the level 3 [1]. If level 3 decays rapidly to level 2, a population inversion can be obtained between levels 2 and 1. An example is the ruby laser. A ruby is a crystalline alumina (Al_2O_3), which contains Cr^{3+} ions. These Cr^{3+} ions are excited by green light ($\lambda = 5500$ Å) to a number of closely spaced levels. Interaction, with the crystal lattice, de-excites these levels by a non-radiative process to a metastable level 2, which possesses a particularly long life of the order of 10^{-3} s. Laser action can be initiated between the levels 2 and 1, resulting in red light ($\lambda = 6943$ Å).

Except in special cases, such as the ruby, it is difficult to produce a population inversion between a ground state and an excited state, because initially all the atoms are likely to be in the ground state, and we have to get more than half the atoms into level 2 before a population inversion can be achieved. An easier approach is to use a four-level system (see Fig. 14.5) and attempt to create a population inversion between two excited levels. We start with all the atoms in the ground state 1, and none in the excited states 2, 3 and 4 ($E_2 < E_3 < E_4$). Level 4 is chosen so that it has a fast decay to level 3, and pumping between levels 1 and 4 immediately produces a population inversion between levels 3 and 2. As level 2 begins to fill up by stimulated emission at the frequency $(E_3 - E_2)/h$, the population inversion will decrease. To minimise this, level 2 is chosen so that it has a fast decay to the ground state.

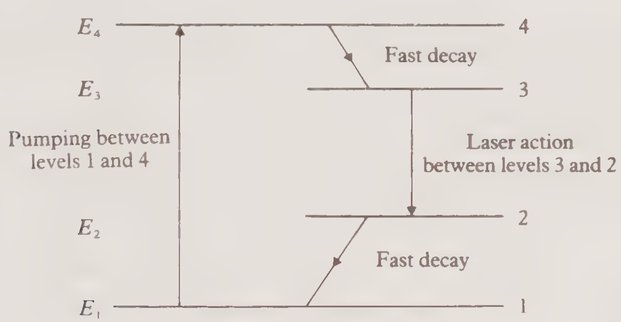

14.5 The four-level laser.

A gas laser presents an example of a multi-level system, which can be pumped by an electrical discharge, rather than by incident radiation. An important case is the He–Ne laser, in which the active material is a mixture of helium and neon gases at low pressure. The energy levels concerned are shown in Fig. 14.6. In an electrical discharge, the helium atoms are raised to the 2^1S and 2^3S levels which are metastable. The ground state of neon has the configuration $(1s)^2(2s)^2(2p)^6$ and the lowest excited states are of the form $(1s)^2(2s)^2(2p)^5(nl)$. Of these, the $nl = 4s$ and $nl = 5s$ are coincident in energy with the 2^3S and 2^1S helium levels

[1] Note that a population inversion cannot be obtained between levels 3 and 1, because when the number of atoms N_3 in level 3 equals the number N_1 in level 1, absorption will be balanced by stimulated emission and the material will become transparent at the frequency ω_{31}.

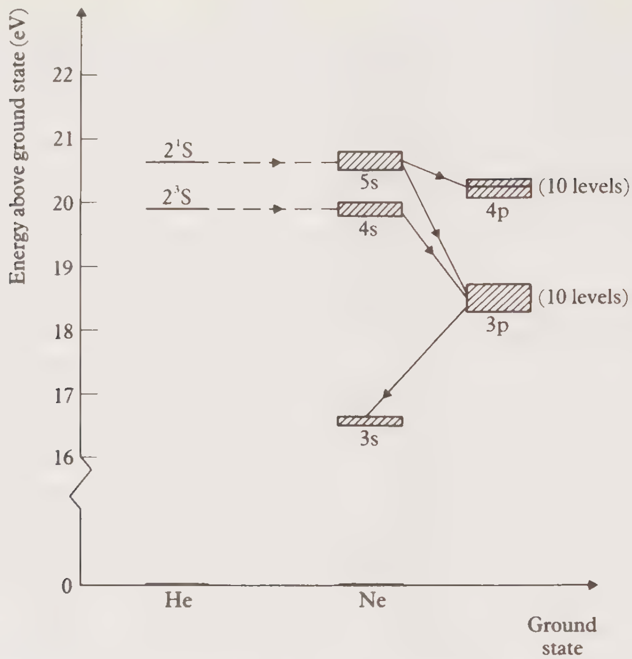

14.6 The energy levels of the He–Ne laser. The neon configuration concerned is $(1s)^2(2s)^2(2p)^5\,nl$; each configuration giving rise to a number of levels within the shaded regions. Note that in many textbooks, the (3s), (4s) and (5s) level are labelled (1s), (2s) and (3s), while the (3p) and (4p) levels are labelled (2p) and (3p). This alternative notation is due to Paschen.

respectively. Because of this, in collisions between the excited helium atoms and ground state neon atoms, there is a high probability that neon atoms will be excited to these levels, the helium atoms reverting to the ground state. The selection rules allow transitions to the lower lying neon 3p and 4p levels. Furthermore, the lifetimes of the 4s and 5s neon levels are of the order 10^{-7} s which is about ten times longer than the lifetimes of the 3p and 4p levels. The He–Ne mixture forms a four-level system, which can show laser action between the 4s or 5s levels and the 3p and 4p levels of neon. Each of the neon levels consists of several sublevels, and out of the various possible transitions the strongest are: (a) between the 5s and 4p levels at $\lambda = 33\,900$ Å; (b) between the 5s and 3p levels at $\lambda = 6330$ Å; and (c) between the 4s and 3p levels at 11 500 Å. The wavelength of the light generated in a He–Ne laser depends on the reflectivity of the mirrors between which the gas is placed (see Fig. 14.7). Oscillation will take place at the wavelength for which this reflectivity is a maximum.

A great many systems can be devised to show maser or laser action, in some desired region of the spectrum. Space does not permit us to describe the technical details of these devices, nor the important applications of laser light; those interested should consult the specialised literature for example the books by Svelto (1976) or Thorp (1969).

(a)

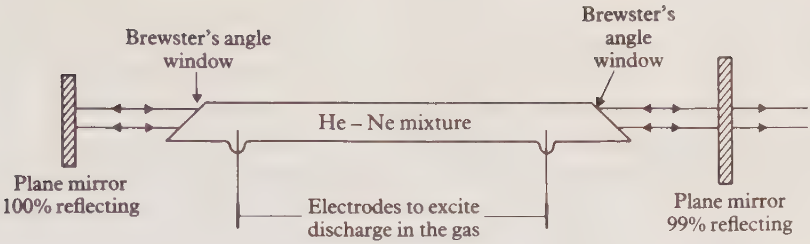

(b)

14.7 (a) Schematic diagram of a He–Ne laser. Notice the ends of the glass tube containing the gas are inclined at Brewster's angle ($\tan(\theta) = n$). The wave with the polarisation vector in the place of incidence is then transmitted through the ends of the tube without partial reflection and the output beam is consequently polarised in this plane.
(b) A photograph of an actual He–Ne laser.

The ammonia maser

It is of interest to discuss in a little more detail the concepts behind the first maser to be constructed: the ammonia maser built by Townes in 1954. In Chapter 10, we saw that the ammonia molecule NH_3 has two configurations, one in which the nitrogen atom is above the plane containing the three hydrogen atoms, and one in which it is on the other side. If the plane of the hydrogen atoms is the (XY) plane, then the wave function for the configuration when the nitrogen atom is above this plane (positive z coordinate) will be denoted by ψ_u and the wave function when the nitrogen atom is below the plane will be denoted by ψ_d. Because the potential barrier between the two configurations is finite, ψ_u and ψ_d are not energy eigenfunctions, but there are two closely spaced levels, with energies E_1, E_2 and corresponding eigenfunctions ψ_1 and ψ_2, such that

$$\psi_1 = \frac{1}{\sqrt{2}}(\psi_u + \psi_d)$$

$$\psi_2 = \frac{1}{\sqrt{2}}(\psi_u - \psi_d) \qquad [14.39]$$

The energy splitting is given by

$$\Delta E = E_2 - E_1 = 9.84 \times 10^{-5} \text{ eV} \qquad [14.40]$$

corresponding to a frequency of 23 800 MHz which is in the microwave region. Of course the ammonia molecule has many other levels, but maser action is

sought between just these two particular levels. The necessary coupling with the electromagnetic field takes place because the molecule possesses an electric dipole moment. In the configuration u(up) this moment is of magnitude D and is directed in the negative z direction, while in the configuration d(down), it is of the same magnitude but in the opposite direction.

Because the energy separation of the levels is so small a normal population in thermal equilibrium contains very nearly equal numbers of ammonia molecules in each of the energy eigenstates labelled E_1 and E_2. However, by passing a beam of ammonia molecules through an inhomogeneous electric field (see Fig. 14.8) a separation of the molecules in the two levels can be achieved, just as in a Stern–Gerlach magnet a separation is achieved between levels with different components of a magnetic dipole. To see this, consider a static electric field directed in the positive z direction of magnitude $\mathscr{E}$. The additional energy in configuration ψ_u is $+D\mathscr{E}$ and in configuration ψ_d is $-D\mathscr{E}$. This additional interaction alters the eigenenergies of the E_1 and E_2 levels slightly, which become (see Problem 14.3)

$$\begin{aligned} E_1' &= E_1 - (D\mathscr{E})^2/\Delta E \\ E_2' &= E_2 + (D\mathscr{E})^2/\Delta E \end{aligned} \qquad [14.41]$$

The force on the molecule in the z direction F_z depends on which of the states 1 or 2 is concerned, since

$$(F_z)_{1,2} = -\frac{\partial}{\partial z}(E_{1,2}') = \pm 2\left(\frac{D^2}{\Delta E}\right)\mathscr{E}\left(\frac{\partial \mathscr{E}}{\partial z}\right) \qquad [14.42]$$

In a uniform field, the force vanishes but in an inhomogeneous field with $\partial\mathscr{E}/\partial z > 0$ the molecules in the 2 level are deflected in the negative z direction and those in the 1 level in the positive z direction.

Having obtained a population entirely in the state of higher energy E_2, maser action is obtained by stimulated emission of the transition from the level 2 to the level 1 [2], which is reinforced by passing the beam through a cavity tuned to the

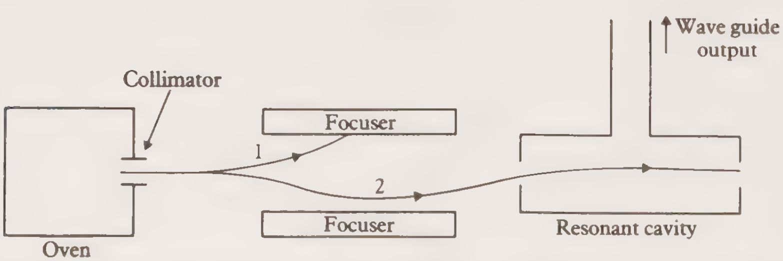

14.8 The ammonia maser. Molecules produced by the oven are collimated, selected into the upper level 2 by the inhomogeneous focusing field, and then passed through the maser cavity. The whole apparatus is placed in an evacuated vessel.

[2] Remember that the transition probability for spontaneous emission is proportional to ω^3, and is negligible at microwave and radio-frequencies.

required frequency. In the cavity, let us assume the electric field is varying with time like

$$\mathscr{E} = \mathscr{E}_0 \cos(\omega t) \quad [14.43]$$

and is directed in the z direction. The wave function of an individual molecule under the influence of this field will be a time-dependent mixture of the stationary levels ψ_1 and ψ_2 and we can write

$$\Psi(t) = A_1(t)\psi_1 e^{-iE_1t/\hbar} + A_2(t)\psi_2 e^{-iE_2t/\hbar} \quad [14.44]$$

From the time-dependent Schrödinger equation, we find in a manner with which we are now familiar, that the amplitudes satisfy the equations

$$\begin{aligned} i\hbar\dot{A}_1(t) &= \langle\psi_1|H'|\psi_2\rangle e^{i(E_1-E_2)t/\hbar}A_2(t) \\ i\hbar\dot{A}_2(t) &= \langle\psi_2|H'|\psi_1\rangle e^{-i(E_1-E_2)t/\hbar}A_1(t) \end{aligned} \quad [14.45]$$

Since

$$\langle\psi_1|H'|\psi_2\rangle = \langle\psi_2|H'|\psi_1\rangle = D\mathscr{E} = D\mathscr{E}_0 \cos(\omega t) \quad [14.46]$$

we can write [14.45] in the form

$$\begin{aligned} i\dot{A}_1(t) &= \tfrac{1}{2}\bar{\omega}_0 \cos(\omega t) \exp(-i\omega_0 t)A_2(t) \\ i\dot{A}_2(t) &= \tfrac{1}{2}\bar{\omega}_0 \cos(\omega t) \exp(i\omega_0 t)A_1(t) \end{aligned} \quad [14.47]$$

where

$$\hbar\omega_0 = E_2 - E_1 = \Delta E \quad [14.48]$$

and

$$\hbar\bar{\omega}_0 = 2D\mathscr{E}_0 \quad [14.49]$$

These equations are precisely of the form [14.14] and provided $\mathscr{E}_0$ is small, and the molecules enter the cavity in the upper level, the solution [14.23] will apply, and at resonance we find the solution [14.17], which in the present case reads

$$\begin{aligned} P_{2\to1}(t) &= |A_1(t)|^2 = \sin^2(\bar{\omega}_0 t/4) \\ P_{2\to2}(t) &= |A_2(t)|^2 = \cos^2(\bar{\omega}_0 t/4) \end{aligned} \quad [14.50]$$

From [14.50] we see that every ammonia molecule will make the transition from the upper to the lower level, giving up energy to the microwave field, if the time of transit of the cavity T is given by

$$\frac{\bar{\omega}_0 T}{4} = \frac{\pi}{2} \quad [14.51]$$

Of course not all the molecules entering the cavity will have the same velocity, but if the most probable velocity in the direction of motion is v, then the length

of the cavity L, should be adjusted so that

$$L = vT = \frac{2\pi v}{\bar{\omega}_0} \qquad [14.52]$$

More generally if $P_{2\to1}(T)$ is the probability that the transition $2 \to 1$ occurs while a molecule transverses the cavity, the power supplied to the microwave field is

$$W = N\,\Delta E P_{2\to1}(T) \qquad [14.53]$$

where N is the number of molecules entering the cavity per second. The power lost from the microwave field in the cavity is

$$W_L = W_{OUT} + W_{AB} \qquad [14.54]$$

where W_{OUT} is the power output and W_{AB} is the power absorbed by the walls:

$$W_{AB} = \frac{\omega_0 E}{Q}. \qquad [14.55]$$

Here E is the total energy of the field and Q is a constant known as the cavity quality factor. The power output can similarly be written as

$$W_{OUT} = \frac{\omega_0 E}{Q_1} \qquad [14.56]$$

where Q_1 is a quality factor determined by the coupling between the cavity and the output wave guide.

The total energy in the field within the cavity is given by

$$E = \tfrac{1}{8}\varepsilon_0(\mathscr{E}_0)^2 V \qquad [14.57]$$

where V is the cavity volume. If $W_{OUT} \ll W_{AB}$, the condition for the system to act as an oscillator is

$$W = W_L \simeq W_{AB} \qquad [14.58]$$

from which we see that

$$N = \frac{\varepsilon_0\omega_0(\mathscr{E}_0)^2 V}{8Q\Delta E P_{2\to1}(T)} \qquad [14.59]$$

If $(\bar{\omega}_0 T)$ is small, so that from [14.50] $P_{2\to1}(T) \approx (\bar{\omega}_0 T/4)^2$ this condition becomes

$$N = \frac{\hbar v^2 \varepsilon_0 V}{2D^2 L^2 Q} \qquad [14.60]$$

The mean velocity of molecules from an oven of temperature Θ, is

$$v = \left(\frac{3k\Theta}{M}\right)^{1/2} \qquad [14.61]$$

where M is the mass of the molecule and k is Boltzmann's constant. For an oven temperature of 300 K, $v \simeq 10^3$ m/s and with typical values of the other parameters, N is required to be about 10^{13} molecules per second, which can be achieved easily.

The actual magnitude $\mathscr{E}_0$ of the field in the cavity can be obtained from [14.59] if the Rabi flopping formula [14.23] is used for $P_{2\to 1}(T)$, rather than the small T approximation. In this case, we find

$$\frac{8ND^2}{\hbar\,\omega_R^2}\sin^2\left(\frac{\omega_R T}{2}\right) = \frac{\varepsilon_0 V}{Q} \qquad [14.62]$$

where ω_R is given by

$$\omega_R^2 = (\omega_0 - \omega)^2 + \left(\frac{D\mathscr{E}_0}{\hbar}\right)^2 \qquad [14.63]$$

This is an equation which can be solved numerically to find $\mathscr{E}_0$, both in the case of resonance $\omega = \omega_0$ and for frequencies ω away from resonance.

Power outputs of about $10^{\ 10}$ watts can be obtained with a line width as small as $10^{\ 2}$ Hz, which makes the ammonia maser an excellent frequency standard. For more details of construction and performance reference may be made to Thorp (1969).

Lasers and spectroscopy

The decades since the discovery of the laser have witnessed a revolution in spectroscopy. Unlike other sources of light, laser light is *coherent* and very nearly *monochromatic*. The line width which can be achieved is often smaller than the line widths of the atomic or molecular system to be investigated, and this allows studies with a much higher resolution than could be obtained with a conventional spectrometer using a diffraction grating technique. In the simple examples we discussed, the laser light was produced at certain fixed frequencies. Many thousands of such frequencies extending from the far ultra-violet to the microwave region are now available. However, to be really useful as a spectroscopic light source the laser must be *tunable* in some region of the spectrum.

Two methods of tuning have been developed. In the first, the frequency of the line can be altered by changing the physical conditions of the material. In the case of gas lasers this can be achieved by using the Zeeman effect, and for solid-state lasers by placing the active material under pressure. In the second method, an active material is chosen which has many closely spaced energy levels acting effectively as a continuum. The frequency at which the laser action takes place is then determined within a certain range by the characteristics of the optical resonators, which can be tuned. In particular, the active medium of *dye lasers* consists of solutions of certain organic dye compounds in liquids such as methyl alcohol or water. Electronic states of dye molecules are made up of

vibrational levels and rotational levels, the resulting rotational lines being unresolved because of the Doppler broadening. Thus the rotational levels act as a continuum of levels between the vibrational levels. Laser action can occur at a fluorescent frequency, and dye lasers, pumped for example by light from a ruby laser, can be tuned over a large part of the visible spectrum.

Although the total power emitted from a laser is not high, the light is produced in a narrow beam and at one frequency, and the brightness of the light at that frequency is many orders of magnitude greater than can be obtained from a conventional source. In fact, it is easy to obtain power densities of the order of 10^{20} W/m^2, which is high enough to ionise any material on to which light is focused.

Because of the strong fields which can be attained, non-linear optical effects can be studied which are due to processes in which two or more photons are simultaneously emitted or absorbed. The material studied can be in the form of an atomic or molecular beam, since the high power density of the laser beam produces a sufficiently large number of transitions. This has the great advantage that the Doppler broadening can be eliminated by making the atomic or molecular beam intersect the laser beam at right angles. In two-photon spectroscopy the linear Doppler broadening

$$\nu - \nu_0 = \mp \nu_0 \frac{v_x}{c} \qquad [14.64]$$

discussed in Chapter 4 (see [4.142]) can also be eliminated in the following way. If two photons of the same frequency, but travelling in opposite directions are absorbed in a single process by a moving gas atom or molecule, the linear Doppler shift of one photon, as seen from the atom, is equal and opposite to that of the second photon. The net linear Doppler shift in this case therefore vanishes, and measurements can be made with a resolution down to the natural line widths.

As one of the many examples which illustrate the power of laser techniques, let us consider a particularly interesting measurement of the excitation of the 2s level of atomic hydrogen from the ground state carried out in 1978 by Hänsch, Lee, Wallenstein and Wieman. They succeeded in detecting the Doppler-free two-photon 1s–2s line and in resolving the hyperfine doublet for the $F = 1 \rightarrow 1$ and $F = 0 \rightarrow 0$ transitions. They also compared the frequency of the 1s–2s transition in hydrogen and deuterium to that of the Balmer β line ($n = 4 \rightarrow n = 2$) at 4861 Å in order to obtain a value of the Lamb shift for the 1s state.

14.3 CONTROLLED THERMONUCLEAR FUSION

According to Einstein's law of equivalence of mass and energy, $E = mc^2$, the release of energy in an exothermic reaction implies a reduction of mass of the system. For example, a reduction of mass of 1 amu corresponds to a release of

energy of 931.5 MeV. In exothermic chemical reactions (such as burning wood or fossil fuels) the mass reduction is tiny, and the energies released never exceed a few electron-volts per reaction. In contrast, in exothermic nuclear reactions the reduction in mass, and hence the energy released per reaction, is much larger, so that despite high capital cost nuclear reactors provide a competitive source of energy.

As seen from Fig. 14.9 the binding energy per nucleon in a nucleus, plotted as a function of the mass number A, has a maximum near $A = 60$ (in the region of iron and nickel). This means that the energy can be obtained either by splitting heavy nuclei (fission) or by compounding light nuclei (fusion). Present-day nuclear reactors are based on the fission of heavy nuclei such as ^{235}U and have the well-publicised disadvantages that the supplies of the nuclear fuel are limited and that the fission products are radioactive, presenting a safety hazard. For this reason, over the last few decades, much effort has been spent in trying to develop alternative energy sources without such severe disadvantages, and in particular nuclear reactors based on fusion reactions [3].

The main obstacle to producing a fusion reaction is overcoming the Coulomb barrier arising from the electrostatic interaction between the two nuclei. To bring two nuclei of charge $Z_A e$ and $Z_B e$ close enough for a nuclear fusion reaction to take place with a sizable probability, that is to a separation of the order $R \simeq 5 \times 10^{-15}$ m, requires a kinetic energy E larger that the Coulomb

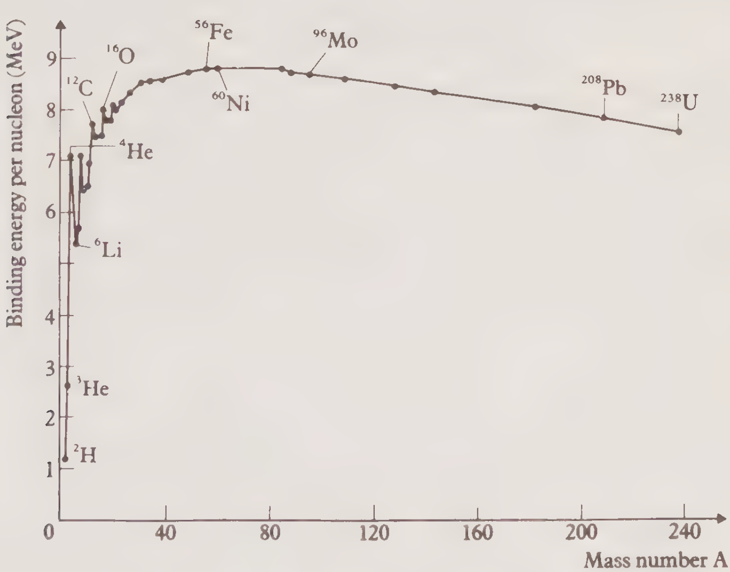

14.9 The binding energy per nucleon as a function of mass number A.

[3] An introduction to the subject of controlled thermonuclear fusion can be found in the book by Hagler and Kristiansen (1977).

barrier E_B, where

$$E_B = \frac{e^2}{4\pi\varepsilon_0}\frac{Z_A Z_B}{R}$$

$$\simeq 150\, Z_A Z_B \text{ keV} \qquad [14.65]$$

In fact, this estimate is too conservative, since the reaction can take place at much lower energies with sufficient probability by quantum mechanical tunnelling through the barrier. Because of this dependence on charge, the only practicable fusion reactions are those involving isotopes of hydrogen ($Z_A = Z_B = 1$). In addition, we see from Fig. 14.9 that the nuclei having small values of A release the most energy per nucleon. Possible reactions are

$$\mathrm{D} + \mathrm{D} \rightarrow \mathrm{T}(1.01 \text{ MeV}) + \mathrm{p}(3.03 \text{ MeV}) \qquad [14.66a]$$

$$\mathrm{D} + \mathrm{D} \rightarrow {}^3\mathrm{He}(0.82 \text{ MeV}) + \mathrm{n}(2.45 \text{ MeV}) \qquad [14.66b]$$

$$\mathrm{D} + \mathrm{T} \rightarrow {}^4\mathrm{He}(3.52 \text{ MeV}) + \mathrm{n}(14.06 \text{ MeV}) \qquad [14.66c]$$

where p denotes a proton, n a neutron, D (deuterium) is the isotope of hydrogen with $A = 2$ and T (tritium) the hydrogen isotope with $A = 3$. Deuterium occurs naturally in water, with an abundance of about 1 part in 6500, and so constitutes a fuel available in virtually unlimited amounts, at little cost. For this reason, the first two reactions [14.66] would appear to be promising, but this is outweighed by the much higher cross-section of the D–T reaction [14.66c] at low relative kinetic energies (see Fig. 14.10). Moreover, the D–T process

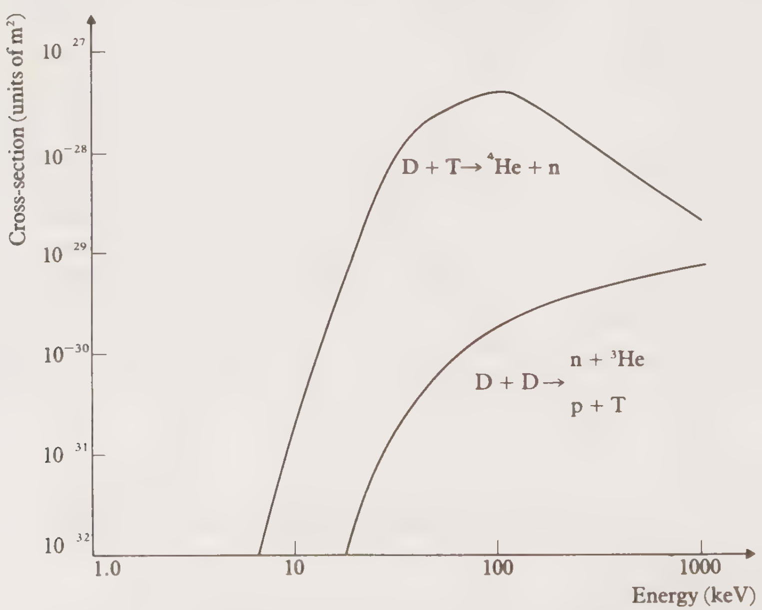

14.10 The cross-sections for the D–T and D–D reactions.

[14.66c] produces more energy per reaction. Unfortunately, tritium is not naturally occurring, being radioactive with a half-life of about 12.4 years; it must be produced artificially and carefully controlled.

The concept of a fusion reactor

In a fusion reactor based on the D–T reaction [14.66c], energy released in the form of the kinetic energy of neutrons must be converted to heat, used to raise steam to drive the turbines of a power station (see Fig. 14.11). This can be achieved by absorbing the neutrons in a lithium blanket, with the advantage of breeding tritium through the exothermic reaction

$$n + {}^{6}\mathrm{Li} \rightarrow \mathrm{T}(2.7\ \mathrm{MeV}) + {}^{4}\mathrm{He}(2.1\ \mathrm{MeV}) \qquad [14.67]$$

The isotope ^{6}Li constitutes about 7.5 per cent of natural lithium, which is readily available from commonly occurring minerals.

To obtain the energy output necessary to drive a power station of 100 MW, about 10^{21} D–T reactions are required per second. Such reaction rates require average kinetic energies of the order of 10 keV, corresponding to temperatures $T \simeq 10^8$ K. At such temperatures, the D–T mixture is completely ionised and forms a *plasma* containing D and T nuclei and electrons. No reactor vessel could withstand direct contact with a plasma at 10^8 K, so that means must be devised to keep the plasma away from the walls of the reactor. The thermonuclear power density produced in such a plasma is given by

$$P_{\mathrm{th}} = n_{\mathrm{D}} n_{\mathrm{T}} \langle \sigma v \rangle E \qquad [14.68]$$

where n_{D} and n_{T} denote the density of the deuterium and tritium ions, respectively, σ is the D–T cross-section at the relative velocity v, E is the energy output per reaction (17.58 MeV) and the symbol $\langle\ \rangle$ denotes an average over the Maxwellian distribution of velocities in the plasma.

Unfortunately, even if completely thermally insulated from the walls of the reactor vessel, a plasma heated to such temperatures will loose energy, mainly through *bremsstrahlung*, This is the radiation that occurs because the electrons in

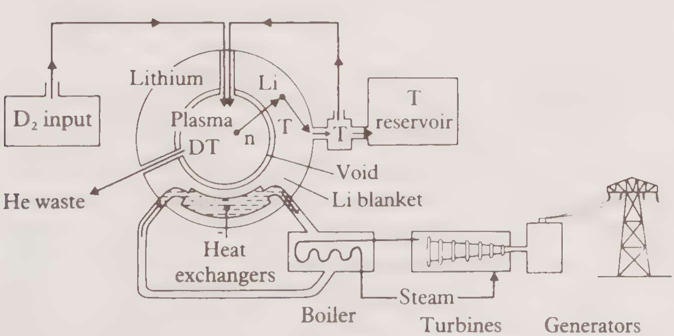

14.11 Conceptual design of a fusion reactor power station.

the plasma are accelerated in the Coulomb field of the nuclei. The *bremsstrahlung* power radiated per unit volume is

$$P_{br} = 1.7 \times 10^{-38}\, n^2 T_e^{1/2}\ \mathrm{W/m^3} \tag{14.69}$$

where $n = n_D + n_T$ is the ion density (which is equal to the electron density n_e) and T_e is the electron temperature, expressed in eV (that is, the electron kinetic temperature, with 1 eV $\simeq 1.2 \times 10^4$ K, see Appendix 11). For the fuel to burn, the thermonuclear power density P_{th} must be larger than the power density P_{br} of the radiation loss. Since P_{th} increases much more rapidly with temperature than P_{br}, there is an ignition temperature T_{ign} which is about 4 keV for the D–T reaction.

Thus far we have assumed that the plasma is in a steady-state condition, and remains perfectly confined. In practice, it is only possible to confine the plasma for a certain time interval τ, during which sufficient energy must be produced to (i) heat the plasma, (ii) overcome the energy losses and (iii) supply heat to a power station. These requirements impose a condition on both the confinement time τ and the ion density n. Assuming that the fusion energy produced can be utilised with an efficiency of about 30 per cent, this condition is

$$n\tau > 10^{20}\ \mathrm{m^{-3}\ s} \tag{14.70}$$

at a kinetic temperature $T \simeq 10$ keV. This relation is called the *Lawson criterion*.

Magnetic and inertial confinement

Two main approaches to the problem of producing a D–T plasma satisfying the Lawson criterion are being investigated. In the first, called *magnetic confinement*, a low-density plasma with $n \simeq 10^{20}$ m^{-3} occupying a volume $V \simeq 10$ m^3 is contained by magnetic fields. To satisfy the Lawson criterion, the confinement time should be at least $\tau \simeq 1$ s. Promising results have been obtained by using Tokamak machines (see Fig. 14.12), in which the plasma is contained within a torus by a combination of poloidal and toroidal magnetic fields. The toroidal field is produced by external coil windings, while the poloidal field is due to a current, maintained in the plasma by making the torus the secondary winding of a transformer. The experiment starts by introducing a mixture of neutral deuterium and tritium gas, which is then ionised by a radio-frequency discharge. The plasma so formed is a good conductor and can be heated by the same current used to generate the poloidal magnetic field. The parameters of some existing and future Tokamak machines are given in Table 14.1.

In the second method, known as *inertial confinement*, it is hoped to use a D–T pellet of high density $n \simeq 10^{30}$ m^{-3}, contained in a metal casing of a few millimetres diameter. This pellet must then be heated to fusion temperatures in such a short time that the nuclei can fuse and release energy before the plasma expands appreciably. Thus, in this approach, the plasma is confined by the inertia of the nuclei. According to the Lawson criterion [14.70], the confine-

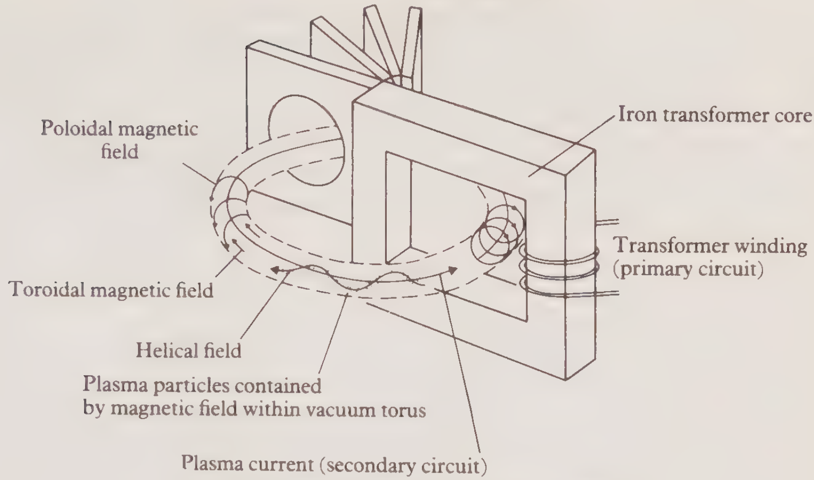

14.12 A schematic diagram of a Tokamak machine.

Table 14.1 Basic parameters of various Tokamak machines

Device	*Country*	R(m)	r(m)	$\mathcal{B}_t$(T)	I(MA)
		Existing			
DITE	UK	1.12	0.23	2.8	0.2
PLT	USA	1.30	0.40	3.5	0.6
T-10	USSR	1.50	0.37	3.5	0.4
		Under construction			
TFTR	USA	2.48	0.85	5.2	2.5
JET	EEC	2.96	1.25† 2.10	2.8	3.8

R: major radius of the torus
r: minor radius of the torus
$\mathcal{B}_t$: toroidal magnetic field
I: plasma current
† The JET machine will have a toroid with an elliptical cross-section; the lengths of the semi-minor and semi-major axes are given in the table.

ment time has to be of the order of $\tau \sim 10^{-10}$ s. It is envisaged that the pellets will be dropped one at a time into the reactor vessel, where they will be heated by pulses of intense electromagnetic radiation or high-energy particles. Experiments are in progress in which the intense radiation is produced by numbers of high powered lasers acting simultaneously (laser fusion). Alternative design studies are based on current accelerator technology. It is suggested that heavy ions (e.g. Cs^+, Xe^+, U^+) could be accelerated to high energy ($\simeq$20 GeV) and accumulated in a storage ring. Subsequently, the stored ions could be bunched and split into a number of beams which are fired simultaneously at the pellet.

Atomic processes

Although atomic and molecular processes play an important role in both the magnetic and inertial confinement approaches, we shall only discuss here by way of illustration some of the processes which are important in Tokamak experiments. In this case, atomic and molecular phenomena play an important role in various domains, such as the energy balance in the plasma, the interactions between the plasma and the wall of the reactor vessel, the heating of the plasma, and plasma diagnostics. A few of these phenomena will now be discussed.

Energy balance and impurities

In a fusion reactor the fundamental energy producing reaction rates are characterised by cross-sections which are of the order of 10^{-30} m^2. In contrast, the cross-sections for atomic collision processes, such as those discussed in Chapters 12 and 13, are of the order of 10^{-21} m^2. This implies that although the energies involved in atomic processes are much smaller than those of nuclear reactions, great care must be exercised if the atomic processes are not to dominate. A striking example of the importance of reducing energy losses through atomic mechanisms was provided by the early experiments with the Zeta machine in England in the 1950s. It was found that most of the energy input designed to heat the plasma was lost by ionising and exciting impurity atoms such as oxygen, followed by the emission of radiation from these impurities.

In a Tokamak machine it is necessary to keep the proportion of impurity ions – particularly those of high nuclear charge Z – as small as possible. This is because the power loss through *bremsstrahlung* radiation in electron–ion scattering is proportional to Z^2. If n_Z is the density of impurity ions of nuclear charge Z, the power density radiated from a D–T plasma by *bremsstrahlung* due to impurities is (compare with [14.69])

$$P_{\mathrm{br}}^{\mathrm{I}} = 1.7 \times 10^{-38}\, n_e n_Z Z^2 T_e^{1/2} \ \mathrm{W/m^3} \qquad [14.71]$$

where n_e is the electron density and T_e is the electron kinetic temperature, expressed in eV. Not all this power is lost to the plasma since radiation at the higher wavelengths is reabsorbed. However, the dimensions of the plasmas formed in the present machines are such that the plasma is transparent to radiation of wavelength $\lambda < 10$ Å, and the major part of the radiated power $P_{\mathrm{br}}^{\mathrm{I}}$ will be precisely in this wavelength region.

In considering the energy balance of a Tokamak machine the power density $P_{\mathrm{br}}^{\mathrm{I}}$ lost because of *bremsstrahlung* due to impurities must be added to the power density loss P_{br} arising from electron–hydrogen ion scattering. An ideally confined plasma will ignite if $P_{\mathrm{th}} > P_{\mathrm{br}} + P_{\mathrm{br}}^{\mathrm{I}}$. This is illustrated in Fig. 14.13, where the conditions for ignition are shown assuming the addition to the hydrogen plasma of 0.1 per cent and 1 per cent of completely ionised iron

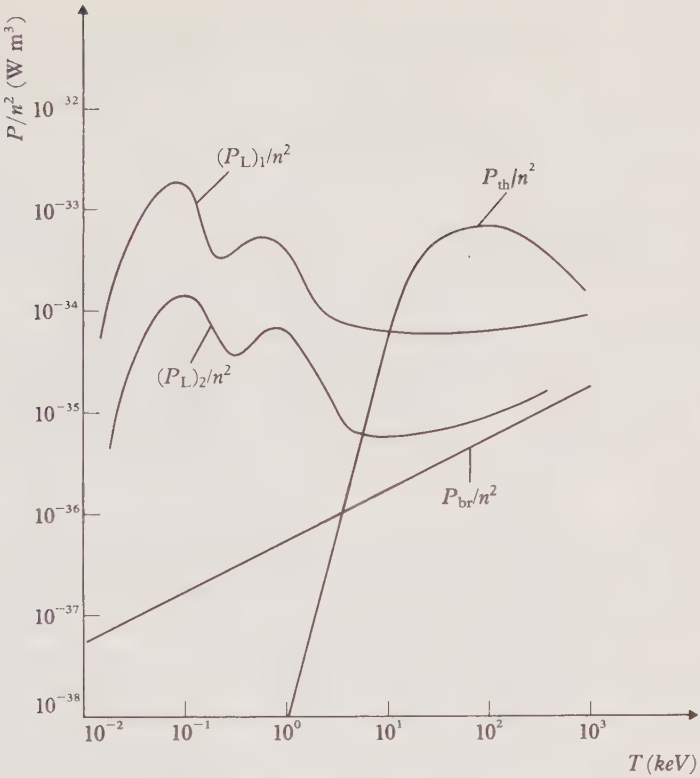

14.13 Conditions for ignition in a fusion reactor:
P_{th} = Power density produced by fusion.
P_{br} = Power density lost by *bremsstrahlung* from the D–T plasma.
$(P_L)_1 = P_{br} + P^I_{br}$(1 per cent) = Total power density lost when 1 per cent impurity ions of Fe are present in the plasma.
$(P_L)_2 = P_{br} + P^I_{br}$(0.1 per cent) = Total power density lost when 0.1 per cent impurity ions of Fe are present in the plasma
For ignition the plasma must be in the region in which $P_{th} > P_L$, where $P_L = P_{br} + P^I_{br}$ is the total power lost.

atoms. It is seen that in the first case the temperature for ignition is raised only slightly, but with 1 per cent of iron impurities the ignition temperature will be approximately doubled.

The presence of impurities can alter the conditions for ignition in other ways. During the heating process, when the plasma is still cold, the impurity atoms may become excited rather than ionised, and in this case power loss through line radiation will occur. Indeed, as we saw, the line radiation was responsible for the failure of the earlier machines to achieve the desired temperatures. It is also worth mentioning that in obtaining the Lawson criterion [14.70] it is assumed that the D–T plasma is 'clean'. The presence of impurities which significantly contribute to the energy loss will have the effect of changing the Lawson criterion for both the temperature and the value of $n\tau$.

How do the impurities arise? Because of the confining magnetic field the plasma does not touch the wall of the torus and is therefore thermally insulated from the surroundings. However, there will be certainly some un-ionised hydrogen molecules near the torus wall. At the edge of the plasma, these molecules become ionised by electron impact,

$$e^- + H_2 \rightarrow H_2^+ + 2e^-$$

and further collisions between the H_2^+ ions and electrons lead to dissociation,

$$e^- + H_2^+ \rightarrow H + H^+ + e^-$$

producing neutral hydrogen atoms with kinetic energies which are typically larger than 5 eV. Being neutral these atoms escape from the plasma and on impact with the torus wall cause sputtering of the materials (for example Fe and Mo used in the construction). In addition, the wall surface may contain occluded impurity gases such as O_2 or CO which will also be released in the plasma region.

Since the impurities originate near the edge of the plasma, methods have been devised to 'scrape' the edge to remove the unwanted ions. In the *divertor* concept, the outer edge of the plasma is diverted through a special chamber by means of a perturbing magnetic field. The plasma which enters the divertor is neutralised by collision with a solid target, and the neutralised atoms are pumped out of the machine. This method is expensive and the divertor is difficult to construct, so that alternative methods are being sought. One of these is to interpose a layer of cool (~20 eV) plasma between the hot plasma and the wall. Because the energy of particles in the cool plasma is small, sputtering at the wall should be reduced. Those heavy atoms which are sputtered into the cool plasma will help to keep it at a low temperature by losing radiative energy. The success of this concept depends critically on the cross-sections for various atomic collisions, some of which have not yet been measured. A particular process of interest is charge exchange (see Chapter 13) between hydrogen ions and partially ionised Fe, and also with ions of other materials used in the construction of the reactor vessel.

Plasma heating and neutral beam injection

As we mentioned earlier, the cold plasma formed by ionising neutral hydrogen with a radio-frequency discharge is heated by generating a large axial current along the torus. Unfortunately the resistivity of the plasma decreases with temperature, so that the maximum practical temperature that can be reached by this 'ohmic heating' is limited, perhaps to 3 keV. The electric current generated when the torus forms the secondary winding of a transformer is in the first place due to the motion of the light particles – the electrons. The slowly moving ions are then heated by elastic collisions with the rapidly moving electrons. Because elastic scattering cross-sections are Z-dependent, the presence of impurity ions increases the resistivity of the plasma and so enhances the ohmic heating power.

However, since the stored energy in the transformer is limited, the decrease in current due to an increase in resistivity outweighs the increased heating efficiency and overall the presence of even light ion (C^{n+} and O^{n+}) impurities is harmful.

To raise the temperature of the plasma to the ignition point some form of additional heating must be provided. Among several suggestions, we shall consider heating by injecting fast neutral atoms of deuterium. To heat the plasma it is clear that the injected atoms must have more energy than the particles of the plasma. Neutral atoms must be employed so that the confining magnetic field can be penetrated, and the energy deposited in the central region of the plasma. Once the neutral atoms have entered the plasma, ionisation must occur so that the fast ions are trapped in the confining field long enough for a transfer of energy to take place by collisions between the injected particles and those of the plasma.

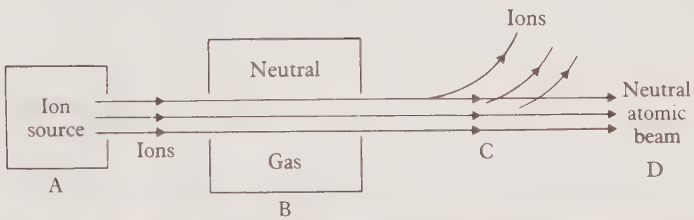

14.14 Neutral beam injection. The ions produced in the source A are partially neutralised by charge exchange in the chamber B. The remaining charged ions are removed by a field at C and the neutral beam D enters the plasma.

To produce the injected beam, an ion source capable of yielding pulses of D^+ ions at 100 keV is first constructed. The D^+ beam is neutralised by passing it through a gas target containing molecular deuterium (D_2) where charge exchange takes place (see Fig. 14.14)

$$D^+ + D_2 \rightarrow D + D_2^+$$

The cross-section for this reaction is small at 100 keV, and this makes the neutralisation rather inefficient. Another suggestion is to form the negative ion D^- and use the 'detachment' reaction

$$D^- + D_2 \rightarrow D + e^- + D_2$$

to form a neutral beam. This reaction has a large cross-section, but the formation of a beam containing a large current of D^- is difficult.

Inside the plasma, the neutral atoms are ionised through the processes

$$\begin{aligned} D + D^+ &\rightarrow D^+ + D \\ D + T^+ &\rightarrow D^+ + T \end{aligned} \qquad [14.72a]$$

$$\begin{aligned} D + D^+ &\rightarrow D^+ + D^+ + e^- \\ D + T^+ &\rightarrow D^+ + T^+ + e^- \end{aligned} \qquad [14.72b]$$

$$e^- + D \rightarrow D^+ + 2e^- \qquad [14.72c]$$

As we saw in Chapters 12 and 13, the cross-sections for these processes have been measured for H and H^+, and the cross-sections for D or T are the same at the same relative velocity. The charge exchange cross-sections for [14.72a] are of the order of 10^{-19} m^2 at beam energies of 10 keV and at this energy are by far the most important processes. At 100 keV, the cross-section for charge exchange has dropped to 10^{-21} m^2 and the cross-section for the ionisation processes [14.72b] are ten times larger. The electron ionisation reaction [14.72c] is of little importance at these energies.

An important limitation to the efficiency of neutral beam heating arises from the presence of fully ionised carbon and oxygen impurities, which as we have seen arise from occluded gas in the torus walls and which are present in concentrations of up to 1 per cent. Charge exchange between the neutral beam and those impurities produces carbon and oxygen ions in highly excited states. Because the energy of C^{5+} in the $n = 6$ level is the same as that of atomic hydrogen in the ground state, there is an energy balance between the electronic energies in the reaction

$$C^{6+} + D(1s) \rightarrow C^{5+}(n = 6) + D^+$$

which enhances the cross-section for this reaction. Similarly, there is an electronic energy balance in the reaction

$$O^{8+} + D(1s) \rightarrow O^{7+}(n = 8) + D^+$$

Detailed dynamical factors make the most likely level into which capture takes place rather lower than those required for energy balance ($n = 4$ or 5 for C^{5+} and $n = 5$, 6, or 7 for O^{7+}), but nevertheless, the carbon and oxygen ions are formed in highly excited states from which line radiation takes place, impairing the heating efficiency.

Diagnostics

An important area of application of atomic physics is in providing diagnostic information about the plasma parameters, such as the density and temperature of the plasma, the concentration of impurity ions, and the depth of penetration of the neutral beam injected for heating. For instance, we have seen that a neutral beam of atomic deuterium D can produce O^{7+} ions in levels with say $n = 6$. Other processes in which O^{7+} ions are formed typically lead to low states of excitation, $n = 2$ or 3. Locating the depth of the plasma from which radiation characteristic of the $n = 6$ level of O^{7+} arises then shows how far in the plasma the neutral beam penetrates before being ionised.

While information on the energy levels of neutral atoms is plentiful, the spectra of ionised species are often not so well known. This constitutes a limitation to both diagnostic procedures in reactors and in astrophysics, where a knowledge of the fine structure of transitions in multiply ionised species is frequently required. A recently developed technique, called *beam foil spectroscopy* has greatly added to our understanding of these spectra. It makes use of

the fact that if a high energy beam of singly ionised particles, produced by an accelerator, is passed through a thin foil (often of carbon), the emerging beam contains a mixture of atoms in many different states of excitation and ionisation. The observation of the line radiation along the emerging beam provides a powerful source of spectroscopic and lifetime information for multiply charged ions, which would be otherwise unavailable.

Fusion technology

Despite huge efforts in several countries the success of the quest for controlled thermonuclear energy is still far from assured, although the progress achieved has been significant. Further development of both the magnetic confinement and inertial confinement approaches requires the integration of techniques drawn from both nuclear and atomic physics with those of plasma physics and of large-scale engineering. As we have seen, nearly all aspects of atomic physics are concerned, including spectroscopy, collision physics and laser physics.

14.4 ASTROPHYSICS

Our knowledge of celestial objects such as the sun, the comets, the stars and the galaxies is mainly based on the analysis of the electromagnetic radiation [4] which arrives to us from these objects. At most wavelengths, the electromagnetic radiation coming from outer space is absorbed by the earth's atmosphere, except for three *windows*, or wavelength bands, through which ground-based astronomers can look at the universe.

The first window covers the optical or *visible* region (between 4000 and 7000 Å) and has been the source of most astronomical knowledge until recent times. The second window, in the *radio-frequency* region, extends from wavelengths of a few millimetres up to 100 m. Its existence was revealed in 1931 by K. Jansky, who discovered radio waves coming from the Milky Way. This discovery opened up the new field of radioastronomy, where many remarkable discoveries about the universe – such as pulsars, quasars and the universal block body radiation at 3 K – have been made during the past few decades. The third window is located in the *infra-red* region, between the long wavelength (red) end of the visible spectrum, at approximately 7000 Å, to about 1 mm. However, in contrast to the visible and the radio-frequency windows, the infra-red window is only partially transparent; it is opaque at many wavelengths, but contains a few transparent bands which have yielded interesting information about objects from which the radiation of visible wavelengths is absorbed by dust.

Astronomers began to be liberated from the difficulties of ground-based observation when instruments were first flown to high altitudes aboard balloons

[4] The cosmic ray particles, meteorites, etc. entering the earth's atmosphere also provide astronomical information.

and aircraft. More recently, instruments aboard artificial satellites have been able to record the emissions of celestial objects in all regions of the electromagnetic spectrum. For example, an ultra-violet telescope satellite, called Copernicus, was launched in 1968 and provided the first observations of extra-terrestrial objects in the far ultra-violet region, while the 'Einstein X-ray Observatory', launched in 1978, has yielded exciting new data about violent processes occurring in the Universe, such as supernovae explosions.

We shall now discuss briefly a few topics closely connected with the phenomena studied in this book [5].

Stellar spectra

The first spectroscopic study of a star was made in 1802 by W. H. Wollaston, who observed that the sun emitted a continuous spectrum interrupted by dark lines. In 1811, J. von Fraunhofer, using a diffraction grating, counted about six hundred of these lines, now called Fraunhofer lines, in the solar spectrum. The origin of the dark lines remained unexplained until G. R. Kirchhoff and R. G. Bunsen discovered that heated gas vapours emit spectra composed of bright lines characteristic of the elements from which the spectrum is emitted. Furthermore, Kirchhoff also showed that when continuum light is transmitted through a gas vapour, dark lines are observed at precisely the same wavelengths as the bright emission lines from the same gas (see Chapter 1). For example, sunlight passing through sodium vapour yields two dark lines at the same wavelengths at which heated sodium vapour emits two characteristic bright lines (the D lines). From these observations, Kirchhoff deduced that the gas vapour had *absorbed* its characteristic wavelengths, and in this way he could interpret the Fraunhofer lines of the solar spectrum as *absorption lines* of elements present in the atmosphere of the sun. Since that time, thousands of dark absorption lines have been catalogued in the sun's spectrum. By comparing them with the spectral lines emitted by chemical elements in laboratory experiments on earth, more than sixty elements have been identified in the sun [6].

More generally, stellar spectra mainly consist of dark absorption lines superimposed on a continuous spectrum. In the interior of the star, where temperatures are very high, the atoms and ions undergo violent collisions, thus emitting many spectral lines which overlap because of collision broadening. The radiation emitted from the star's opaque surface, or *photosphere* is therefore continuous. The atoms present in the cooler atmosphere of the star absorb their characteristic wavelengths, thus giving rise to the observed dark lines. The *chemical composition* of the star's atmosphere can therefore be deduced by analysing the dark lines in the star's spectrum.

[5] A general introduction to modern astronomy can be found in the book by Jastrow and Thompson (1977).

[6] It is interesting to note that helium was discovered in 1868 through an unidentified dark line in the solar spectrum, before being discovered on earth in 1895.

Spectral classes. The Harvard classification system

When the absorption spectra of stars were first studied, it was soon realised that stars could be categorised into several different types, called *spectral classes*. At the beginning of the century, the 'Harvard classification system' was proposed, in which the stars were classified according to the strength of the hydrogen lines in their spectra. Letters of the alphabet were used to identify the classes, with class A corresponding to the stars having the strongest hydrogen lines, class B the next strongest, and so on. At that time it was thought that the amount of hydrogen in the star decreased from class A to B, and so on. Today we know that the stars are nearly uniform in composition, being composed mainly of hydrogen and helium. As we shall see below the differences in their absorption spectra are due primarily to their *surface temperature* so that the spectral classes correspond in fact to different surface temperatures. However, the Harvard identification has been kept, and when the classes are arranged in order of decreasing temperature, the letters that designate each group form the sequence O B A F G K M. Astronomy students remember this sequence by using the mnemonic 'Oh Be A Fine Girl (Guy) Kiss Me'. Table 14.2 relates this classification to the range of temperatures involved, and also describes the main characteristics of the spectra. Each class is subdivided into 10 subclasses, for instance B is divided into B0, B1, . . . B9 corresponding to smaller distinctions which do not merit the creation of a separate class.

Table 14.2 Characteristics of the spectral classes of stars

Spectral class (Harvard classification)	*Temperature range* (K)	*Main characteristics of the spectrum*
0	30000–50000	Lines of ionised helium
B	10000–30000	Lines of neutral helium
A	7500–10000	Very strong hydrogen lines
F	6000–7500	Ionised calcium lines. Many metal lines (manganese, iron, titanium, strontium)
G	4500–6000	Very large number of metal lines. Strong ionised calcium lines, ionised and neutral iron
K	3500–4500	Large number of neutral metal lines
M	2000–3500	Band spectra of molecules, particularly of the tightly bound titanium oxide molecule

The differences between the various stellar spectra can be understood in terms of ordinary atomic physics. The strength of a particular absorption line of a given element depends on the number of atoms of this element which are present in the required initial level a. This number will be depleted by inelastic and ionising collisions with electrons, and on the other hand will be enhanced by recombination between ions and electrons. Both of these processes depend on the temperature and on the electron and atom densities in the atmosphere of a

star. Assuming that the stellar atmosphere is in a steady state, N. M. Saha obtained, in 1920, an equation relating the rate coefficients for ionisation with that for recombination, from which the line strengths can be deduced and expressed as a function of temperature and density. The temperatures and densities at which line strengths are at a maximum vary from element to element. Table 14.3 lists the temperature at which the absorption lines of various elements are most prominent. At high temperatures, (O stars), most atoms are heavily ionised (that is, their outer electrons are missing) and only the lines of systems such as He^+, which is tightly bound, are seen. As the temperature decreases, the lines of metal atoms appear (F, G, K stars), and finally at still lower temperatures, molecular band spectra can be identified.

Table 14.3 The temperature at which lines of certain elements have maximum strength

Atomic species	T(K)
He^+	35 000
He	14 000
H	10 000
Fe	7000
Ca^+	5500
Na	4000

Stellar abundances

Making a reasonable initial guess about the surface temperature of a particular star, and with a knowledge of the relative intensities of absorption lines, the relative abundances of the elements can be deduced. From these values of the temperature and abundances, a theoretical spectrum can be calculated and compared with the observed spectrum. The initial values can then be adjusted until consistency is obtained. It is found that the relative abundances of the elements in most stars are nearly the same and the values that have been determined are shown in Table 14.4.

Colour and spectral type

Assuming that stars radiate like black bodies, the spectral distribution of the energy emitted is given by Planck's distribution law [1.30], the wavelength λ_{max} at which the distribution has a maximum being given by Wien's law [1.19]. The hottest stars (O and B stars) radiate most energy in the ultra-violet region, and only a small fraction in the visible region, mostly towards the blue end of the spectrum. As a result these stars appear blue–white. The A-type stars radiate a bigger fraction of energy in the visible part of the spectrum, and so appear white. Stars of lower temperature radiate more energy at lower frequencies. Thus F stars appear yellow–white, G stars appear yellow, K stars orange, and

Table 14.4 Relative abundance of various elements in normal star atmospheres

Element	Relative abundance (per cent) by number of atoms	Relative abundance (per cent) by mass
H	90.8	70
He	9	27
C, N, O, Ne	~0.1	~2
Na, Mg, Al, Si, Ca, Fe	~0.01	~1

finally M stars have a reddish hue. Our sun, being a G star having a surface temperature of about 6000 K, has a spectral distribution peaking at approximately $\lambda_{max} \simeq 4800$ Å (see Problem 14.4) as shown in Fig. 14.15.

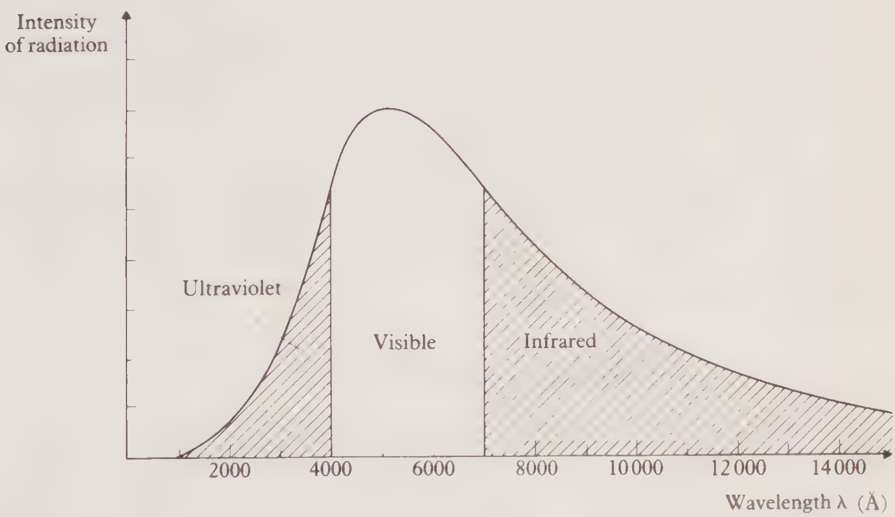

14.15 The spectral distribution of radiation from the sun corresponding to a surface temperature of about 6000 K.

Doppler shift and radial velocities

From the analysis of the spectrum of a star, its *radial velocity*, that is its velocity along the line of sight, can be inferred. Indeed, by comparing the stellar spectral lines of a given element with those of a reference spectrum taken in the laboratory, the Doppler shift can be determined, which in turn provides the value of the radial velocity. If a star is moving towards the observer lines are

shifted towards the shorter wavelengths (blue shift) while if a star is moving away from the observer the wavelengths are longer (red shift).

Line shapes

Additional information about the state of the stellar atmosphere can be obtained by analysing the *shape* of the observed spectral lines. As we saw in Chapter 4, all spectral lines have finite widths. Apart from the natural line width, we discussed *Doppler broadening* and *collisional broadening* (also known as *pressure broadening*). Natural line widths are very small and are entirely outweighed in stellar spectra by collisional and Doppler broadening. In the stellar atmosphere, the Doppler broadening is caused by the random thermal motion of the atoms or ions, and in this context the effect is often called *thermal broadening*. While this effect depends entirely on temperature, collisional broadening also depends on the density. Each effect can be distinguished because, as we saw in Chapter 4, collision broadening determines the wings of a spectral line, while Doppler broadening determines the central region. This allows separate information to be obtained about the density and the temperature.

Another source of Doppler broadening arises from the rotation of a star about its axis. This produces an effect called *rotational broadening*, which can be distinguished from other Doppler broadening mechanisms and which can yield an estimate of the frequency of rotation.

Finally, in some stars the magnetic field is sufficiently large for the Zeeman effect to produce detectable changes in the appearance of the lines. Since the magnetic field varies from point to point on the stellar surface, the Zeeman components usually cannot be resolved, but produce a characteristic *magnetic broadening*. However, for some stars having a very large field (of the order of several tesla), the lines can be resolved and the magnetic field strengths determined accurately.

The 21 cm line of atomic hydrogen

In Chapter 5, we learned that a hydrogen atom in the ground state exhibits hyperfine structure, splitting the two levels with $F = 0$ and $F = 1$. The difference in energy between these levels corresponds to a frequency of about 1420 MHz (see [5.162]) or a wavelength of $\lambda \simeq 21$ cm. Radiation of this frequency can be detected by radio-frequency techniques and its observation can be used to map the concentration of atomic hydrogen in our galaxy. It is found that the spiral arms of the galaxy contain the greatest concentration of hydrogen atoms and the different arms can be identified by making use of the Doppler shift, since each arm possesses a different radial velocity with respect to the earth. In contrast to atomic hydrogen, molecular hydrogen does not emit 21 cm radiation and the technique fails to reveal regions in which the concentration of hydrogen is so large that the formation of molecules is appreciable. Fortunately in these regions of high density, there exist concentra-

tions of CO molecules which have a characteristic emission line at the shorter wavelength of 2.6 mm and this, too, can be detected and used in mapping the galaxy.

The interstellar medium and collision processes

In these few brief paragraphs, we have explained how a whole range of spectroscopic measurements from the ultra-violet region to the radio-frequency region provides the basic information about the structure of both stars and the interstellar medium. New information is now coming from the X-ray and γ-ray parts of the spectrum as a result of high altitude and satellite measurements. In order to interpret the results obtained, mathematical models must be built which describe the physical processes occurring in various layers of a star, or in the clouds of the interstellar medium. For this purpose, a new range of atomic and molecular physics is required, and in particular the collision physics discussed in previous chapters. For example, it has been discovered that the interstellar medium contains many molecules (in small concentrations) of surprising complexity. In dense interstellar clouds containing particle densities of about 10^{10} particles/m^3, typical molecular abundances are (relative to hydrogen) CH^4 – 10^{-6}; CH – 10^{-8}; CN – 10^{-8}; OH – 10^{-6}, CO – 10^{-4}, while of the more complicated systems the concentration of CH_3OH is 10^{-7}, that of CH_3HCO is 10^{-9}, and so on. These molecules are presumably formed in collision processes, some radiative, such as

$$C^+ + H \rightarrow CH^+ + h\nu$$

and many of a radiationless character, for example

$$CH + O \rightarrow HCO^+ + e^-$$

or

$$CH + O \rightarrow H + CO$$

Dozens or even hundreds of possible reactions must be evaluated before a proper understanding of the physical conditions allowing the formation of large molecules can be understood.

In general the solution of the problems posed by the wealth of spectral information from outer space gathered by modern instrumentation requires the astrophysicist to apply all the principles of atomic and molecular physics that we have studied in this book to systems with physical conditions far removed from those that can be created in terrestrial laboratories, and this can be done with great success.

PROBLEMS

14.1 Obtain the general solution [14.20] of equations [14.15], by eliminating A_- from the coupled equations to form a single second-order differential equation for A_+.

14.2 Solve equations [14.15] in first-order perturbation theory by taking $A_+(t) \simeq 1$ for all t and integrating the equation for $A_-(t)$ for times $0 \leq t \leq T$, where T is the duration of the perturbation. Find the probability $P(T)$ that a transition has occurred from the level with $m = \frac{1}{2}$ to that with $m = -\frac{1}{2}$.

14.3 Obtain the result [14.41] for the shifted eigenenergies of the ammonia molecule in a static electric field. Use the fact that with the electric fields generated in the laboratory, one always has $D\mathscr{E} \ll \Delta E$.

14.4 The surface temperature of the sun, assumed to be a black body, is approximately 6000 K.

(a) At what wavelength $\lambda_{\max}$ does the spectral distribution of the sun peak?

(b) What fraction of the sun's energy is radiated in the visible range of the electromagnetic spectrum (4000 Å $< \lambda <$ 7000 Å) (Hint: use the result

$$\int_0^\infty \frac{x^3}{e^x - 1}\, dx = \frac{\pi^4}{15}$$

and integrate Planck's distribution law numerically.)

Appendices

I Classical scattering by a central potential

In this appendix we show how particles are scattered from a central potential $V(r)$ using classical Newtonian mechanics, and we obtain the Rutherford scattering formula [1.58] for the scattering of a beam of particles by a repulsive Coulomb potential.

The path of a particle in the field of a central potential is confined to a plane (see Goldstein, 1962), which we can take to be the (XZ) plane. Let us introduce plane polar coordinates (r, ϕ), defined by (see Fig. A1.1)

$$\begin{aligned} r^2 &= x^2 + z^2 \\ r\cos\phi &= z \end{aligned} \qquad \text{[A1.1]}$$

In the scattering problem we are considering r is arbitrarily large before and after the collision event.

The kinetic energy of the particle which is being scattered is given by

$$T = \tfrac{1}{2}m(\dot{r}^2 + r^2\dot{\phi}^2) \qquad \text{[A1.2]}$$

where m is the mass of the particle and we have used the notation $\dot{r} \equiv \mathrm{d}r/\mathrm{d}t$ and $\dot{\phi} \equiv \mathrm{d}\phi/\mathrm{d}t$. When the particle is at any position, the component of its velocity

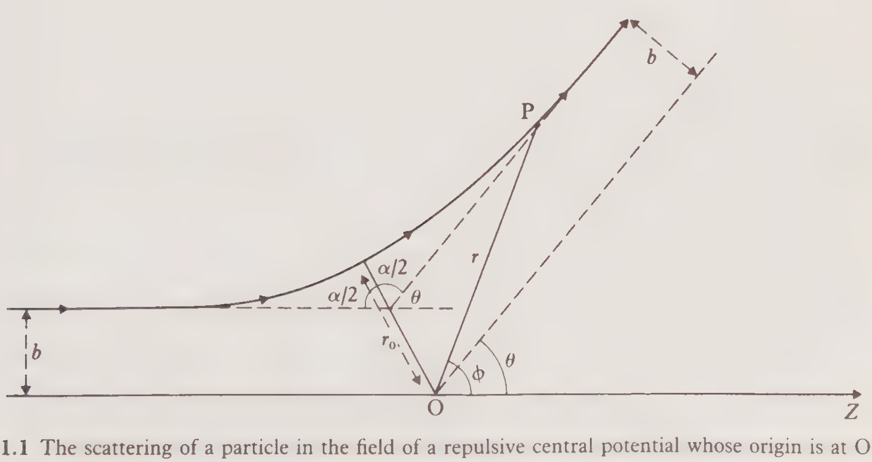

A1.1 The scattering of a particle in the field of a repulsive central potential whose origin is at O.

perpendicular to $\mathbf{r}$ is $r\dot{\phi}$ and its angular momentum about the centre of force at O is therefore

$$L = mr^2\dot{\phi} \tag{A1.3}$$

Because the potential is central the angular momentum must remain constant along any trajectory. In particular, we have

$$L = mvb \tag{A1.4}$$

where b is the impact parameter of the particle (see Fig. A1.1) and v the magnitude of its initial velocity. The total energy E is also constant, and is equal to $mv^2/2$. Thus, since $E = T + V$, we have

$$\begin{aligned} E &= \tfrac{1}{2}m(\dot{r}^2 + r^2\dot{\phi}^2) + V(r) \\ &= \tfrac{1}{2}m\left(\dot{r}^2 + \frac{L^2}{m^2r^2}\right) + V(r) = \tfrac{1}{2}mv^2 \end{aligned} \tag{A1.5}$$

and we note that

$$\dot{r} = \pm\left\{\frac{2}{m}[E - V(r)] - \frac{L^2}{m^2r^2}\right\}^{1/2} \tag{A1.6}$$

To find an equation for the trajectory, or orbit, we write

$$\begin{aligned} \frac{\mathrm{d}\phi}{\mathrm{d}r} &= \frac{\mathrm{d}\phi}{\mathrm{d}t}\frac{\mathrm{d}t}{\mathrm{d}r} \\ &= \frac{L}{mr^2}\left\{\frac{2}{m}[E - V(r)] - \frac{L^2}{m^2r^2}\right\}^{-1/2} \end{aligned} \tag{A1.7}$$

from which, upon integrating over r, we have

$$\phi - \phi_0 = \int_{r_0}^{r} \frac{L}{mr^2}\left\{\frac{2}{m}[E - V(r)] - \frac{L^2}{m^2r^2}\right\}^{-1/2} \mathrm{d}r \tag{A1.8}$$

where we have chosen the constant of integration so that $\phi = \phi_0$ at $r = r_0$. The value of r_0 is conveniently taken to be the distance of closest approach, which is found from the equation

$$\dot{r} = 0 \tag{A1.9}$$

It is therefore the largest root of the equation

$$E - V(r) - \frac{L^2}{2mr^2} = 0 \tag{A1.10}$$

Having obtained r_0 from [A1.10], the orbit can be found by performing the integral in [A1.8].

The deflection function

Let us consider a particle incident upon a centre of force. We assume that the central force acting on it falls to zero at large distances. Thus, when the particle is very far from the centre of force, it will move along a straight line trajectory. As it approaches the centre of force, it experiences an attractive or repulsive interaction and is therefore deflected from its original straight line path. After the particle has passed the centre of force, the force acting on it will ultimately vanish, so that its orbit will again approach a straight line (see Fig. A1.1). In general the final direction of motion is different from the incident one, and the particle is said to have been *scattered* by the centre of force. Because of the symmetry of the orbit about the point ($r = r_0$, $\phi = \phi_0$), the angle between the asymptotes to the orbit (see Fig. A1.1) is given by

$$\begin{aligned}\alpha &= 2[\phi(r = \infty) - \phi(r = r_0)] \\ &= 2\int_{r_0}^{\infty} \frac{L}{mr^2}\left\{\frac{2}{m}[E - V(r)] - \frac{L^2}{m^2r^2}\right\}^{-1/2} \mathrm{d}r \qquad \text{[A1.11]}\end{aligned}$$

The *deflection function* Θ is then defined as

$$\Theta = \pi - \alpha \qquad \text{[A1.12]}$$

For central potentials, there is axial symmetry about the Z axis, and it is convenient to introduce an *angle of scattering* θ, which is defined so that $0 \leqslant \theta \leqslant \pi$. To obtain θ, we first form the quantity

$$\Phi = |\Theta| - 2\pi n \qquad \text{[A1.13]}$$

where n is 0 or an integer, chosen so that $0 \leqslant \Phi \leqslant 2\pi$. Then

$$\begin{aligned}\theta &= \Phi && \text{if} \quad \Phi \leqslant \pi \\ &= 2\pi - \Phi && \text{if} \quad \pi \leqslant \Phi \leqslant 2\pi \qquad \text{[A1.14]}\end{aligned}$$

Cross-sections

Let us now consider a uniform *beam* of non-interacting, monoenergetic particles incident upon a target made of n scattering centres. We shall assume that the target particles are far enough apart so that each collision process involves only one of them. We also suppose that the target is sufficiently thin so that multiple scattering by several scatterers may be neglected. The beam particles, of mass m, approach the target from infinity with an initial velocity of magnitude v and whose direction is parallel to the Z axis (see Fig. A1.2). Let N be the number of incident particles crossing per unit time a unit area perpendicular to the beam, so that N represents the flux of incident particles. Let $\mathrm{d}N'$ be the number of incident particles scattered per unit time in a small solid angle $\mathrm{d}\Omega$ centred about a direction $\Omega \equiv (\theta, \phi)$ having polar angles (θ, ϕ) with respect to the Z axis.

Under the experimental conditions described above the number $\mathrm{d}N'$ of incident particles emerging per unit time in the solid angle $\mathrm{d}\Omega$ is proportional to

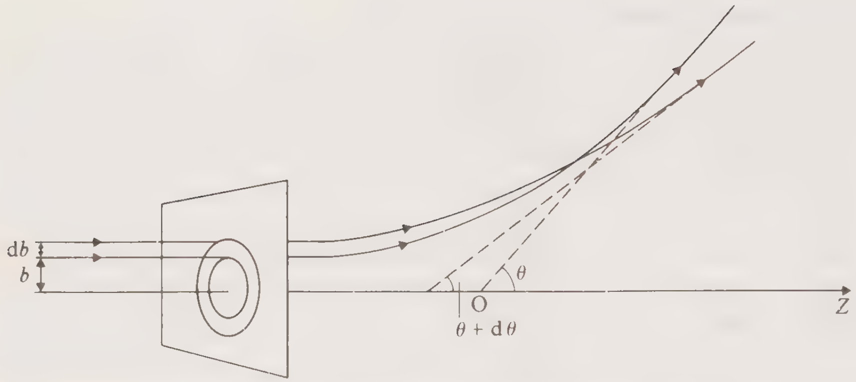

A1.2 The number of particles scattered with impact parameters between b and $b + \mathrm{d}b$ is equal to $2\pi b \mathrm{d}b N$ where N is the incident flux. These particles are scattered with scattering angles between θ and $\theta + \mathrm{d}\theta$.

N, n and $\mathrm{d}\Omega$, so that one can write

$$\mathrm{d}N' = Nn\sigma(\theta, \phi)\,\mathrm{d}\Omega \qquad [A1.15]$$

The proportionality factor $\sigma(\theta, \phi)$, which is also often written as

$$\sigma(\theta, \phi) \equiv \frac{\mathrm{d}\sigma}{\mathrm{d}\Omega}(\theta, \phi) \qquad [A1.16]$$

is called the *differential scattering cross-section*. From this definition we see that $\mathrm{d}\sigma/\mathrm{d}\Omega$ is the ratio of the number $\mathrm{d}N'$ of particles scattered into the solid angle $\mathrm{d}\Omega$ per unit time per unit scatterer and per unit solid angle, to the flux of incident particles with respect to the target. It is also clear from [A1.15] that $\sigma(\theta, \phi)\,\mathrm{d}\Omega$ has the dimensions of an area.

The total scattering cross-section is obtained by integrating the differential cross-section over all scattering angles. That is

$$\begin{aligned}\sigma_{\text{tot}} &= \int \frac{\mathrm{d}\sigma}{\mathrm{d}\Omega}(\theta, \phi)\,\mathrm{d}\Omega \\ &= \int_0^{2\pi} \mathrm{d}\phi \int_0^{\pi} \mathrm{d}\theta \sin\theta \frac{\mathrm{d}\sigma}{\mathrm{d}\Omega}(\theta, \phi) \qquad [A1.17]\end{aligned}$$

It is worth noting that in defining the above cross-sections we have considered the simple case of *elastic* collisions of particles with scattering centres. A general definition of cross-sections, which applies to elastic collisions as well as other types of collisions is given in Chapter 11.

Let us now consider the classical scattering of a beam of particles by a centre of force, assuming that the force is central and vanishes for large r. The position of each incident particle can then be specified by giving its cylindrical coordinates (b, ϕ, z), where b is the impact parameter and ϕ the azimuthal angle. Since the particles do not all have the same impact parameter b or angular

momentum $L = mvb$, they will in general be scattered differently. Indeed, each value of L (or b) defines a deflection function Θ and a corresponding angle of scattering θ. Thus the particles scattered at angles between θ and $\theta + d\theta$, independently of ϕ, are those having an angular momentum between L and $L + dL$ or an impact parameter between b and $b + db$. In other words they are the particles falling on the ring of area $2\pi b\, db$ shown on Fig. A1.2. Now, since N is the flux of incident particles, the number of particles passing per unit time through the ring is $N2\pi b\, db$, and the number of particles per unit time having angular momentum between L and $L + dL$ is $N2\pi L dL/m^2v^2$. This is the same as the number dN' of particles scattered per unit time within the solid angle $d\Omega$, so that

$$dN' = N2\pi b\, db = \frac{N2\pi L dL}{m^2v^2} \qquad \text{[A1.18]}$$

The differential scattering cross-section has been defined above (see [A1.15]) to be the ratio $dN'/(Nn\, d\Omega)$, where n is the number of scattering centres. Since $n = 1$ and $d\Omega = 2\pi \sin\theta\, d\theta$ in the present case, we have

$$\frac{d\sigma}{d\Omega} = \frac{b}{\sin\theta}\left|\frac{db}{d\theta}\right| \qquad \text{[A1.19]}$$

or

$$\frac{d\sigma}{d\Omega} = \frac{1}{m^2v^2}\frac{L}{\sin\theta}\left|\frac{dL}{d\theta}\right| \qquad \text{[A1.20]}$$

If more than one value of b (or L) contributes to a given value of θ, the differential cross-section is the sum over all values of b (or L) that contribute, namely

$$\frac{d\sigma}{d\Omega} = \sum_i \frac{b_i}{\sin\theta}\left|\frac{db_i}{d\theta}\right| \qquad \text{[A1.21]}$$

or

$$\frac{d\sigma}{d\Omega} = \frac{1}{m^2v^2}\sum_i \frac{L_i}{\sin\theta}\left|\frac{dL_i}{d\theta}\right| \qquad \text{[A1.22]}$$

In order to use the above formulae [A1.19]–[A1.22] one must first find b (or L) as a function of θ from [A1.8] and [A1.11]–[A1.14]. There are only a few potentials for which this can be done analytically; in the other cases numerical methods must be employed.

Rutherford scattering

The most famous example of a potential for which an exact solution can be obtained is the *Coulomb potential*. As shown in Chapter 1, the solution for this case helped Rutherford to interpret his experiments, which established the existence of the nucleus and therefore provided the evidence for the nuclear model of the atom.

The scattering potential is that produced by a fixed charge q_B acting on incident particles having a charge q_A, namely

$$V(r) = \frac{q_A q_B}{(4\pi\varepsilon_0)r} \qquad \text{[A1.23]}$$

and we shall treat the repulsive case for which $q_A q_B > 0$. According to [A1.10], the distance of closest approach r_0 is the largest root of the equation

$$E - \frac{q_A q_B}{(4\pi\varepsilon_0)r} - \frac{L^2}{2mr^2} = 0 \qquad \text{[A1.24]}$$

Setting

$$A = \frac{q_A q_B}{(4\pi\varepsilon_0)2E}, \qquad B = \frac{1}{2mE} \qquad \text{[A1.25]}$$

we find that

$$\begin{aligned} r_0 &= A + (A^2 + BL^2)^{1/2} \\ &= A + (A^2 + b^2)^{1/2} \end{aligned} \qquad \text{[A1.26]}$$

From [A1.11] and [A1.12] the deflection function is given by

$$\Theta = \pi - 2\int_{r_0}^{\infty} \frac{L}{mr^2} \left\{\frac{2}{m}[E - V(r)] - \frac{L^2}{m^2r^2}\right\}^{-1/2} \mathrm{d}r \qquad \text{[A1.27]}$$

which we may also write as

$$\begin{aligned} \Theta &= \pi - 2\int_{r_0}^{\infty} \frac{b}{r^2}\left[1 - \frac{2A}{r} - \frac{b^2}{r^2}\right]^{-1/2} \mathrm{d}r \\ &= \pi - 2\int_{r_0}^{\infty} \frac{b}{r}[r^2 - 2Ar - b^2]^{-1/2}\, \mathrm{d}r \end{aligned} \qquad \text{[A1.28]}$$

The integral on the right-hand side of this equation is a standard one (see for example Dwight, 1961) and we have

$$\begin{aligned} \Theta &= 2\cos^{-1}\left[\frac{1}{[1 + 4A^2/b^2]^{1/2}}\right] \\ &= 2\tan^{-1}\frac{A}{b} \end{aligned} \qquad \text{[A1.29]}$$

This relation can be inverted to obtain b in terms of the deflection function Θ or, using [A1.13]–[A1.14], in terms of the scattering angle θ. That is

$$b = A\cot\frac{\theta}{2} \qquad \text{[A1.30]}$$

We note that the trajectory of the particle may be readily obtained by performing the required (indefinite) integral in [A1.8] by a method similar to

the one we have used to calculate the definite integral in [A1.27]. One finds that

$$\frac{1}{r} = \frac{A}{b^2}(\varepsilon \cos \phi - 1) \qquad \text{[A1.31]}$$

where $\varepsilon = (1 + b^2/A^2)^{1/2}$. This is the equation of a hyperbola, with the centre of force being at the exterior focus.

The treatment of the attractive case ($q_A q_B < 0$) is similar to the one given above for the repulsive case. The quantity A is now negative, and one finds for the same value of $|A|$ a deflection angle Θ having the opposite sign of the one obtained above. The trajectory is then a hyperbola with the centre of force at the interior focus.

Let us now return to [A1.30]. Since we know the relation between b and θ, we may directly obtain the differential cross-section $\mathrm{d}\sigma/\mathrm{d}\Omega$. Thus, using [A1.19] and [A1.30], we find that

$$\frac{\mathrm{d}\sigma_c}{\mathrm{d}\Omega} = \left(\frac{A}{2}\right)^2 \frac{1}{\sin^4(\theta/2)} \qquad \text{[A1.32]}$$

or (see [A1.25])

$$\frac{\mathrm{d}\sigma_c}{\mathrm{d}\Omega} = \left(\frac{q_A q_B}{4\pi\varepsilon_0}\right)^2 \frac{1}{16\,E^2 \sin^4(\theta/2)} \qquad \text{[A1.33]}$$

where the subscript c refers to the Coulomb potential. This is the *Rutherford formula* for the differential cross-section corresponding to Coulomb scattering. The result [A1.33] is identical to that obtained from the quantum theory of Coulomb scattering. This coincidence is confined to the Coulomb potential and no other potential provides exactly the same cross-section in quantum theory and in classical theory.

The Rutherford formula [A1.33] for scattering by a Coulomb potential exhibits other remarkable features. Indeed, the differential cross-section [A1.33] does not depend on the *sign* of the potential. Moreover, since the energy E and the scattering angle θ enter into separate factors, $\mathrm{d}\sigma_c/\mathrm{d}\Omega$ is scaled at *all* angles by the factor $(q_A q_B/16\pi\varepsilon_0 E)^2$, so that the angular distribution is independent of the energy. We also note that at fixed θ the differential cross-section is proportional to E^{-2}. Finally, $\mathrm{d}\sigma_c/\mathrm{d}\Omega$ is infinite in the forward direction ($\theta = 0$), where it diverges like θ^{-4}. As a result, the total cross-section $\int(\mathrm{d}\sigma_c/\mathrm{d}\Omega)\,\mathrm{d}\Omega$ is not defined for pure Coulomb scattering. When considering real scattering processes, we must remember that all Coulomb potentials will be modified at large distances because of the screening effect of the charges in other atoms and molecules. As a result of this screening, the *quantum mechanical* differential cross-section becomes finite in the forward direction, and the corresponding total cross-section is then defined. It is worth noting that in *classical mechanics* the total cross-section does not exist for any potential that does not vanish strictly beyond a certain distance.

2 The laboratory and centre of mass systems

Let us consider a non-relativistic collision between a 'beam' particle A of mass m_A and a 'target' particle B of mass m_B. The *laboratory system* (L) is the framework in which the target particle B is at rest before the collision. In what follows we shall use the subscript L to denote quantities in the laboratory system. The *centre of mass* (CM) *system* is the coordinate system in which the centre of mass of the composite system (A + B) is at rest. Denoting by $\mathbf{v}_A$ and $\mathbf{v}_B$ the velocities of particles A and B in the CM system, and by $\mathbf{p}_A = m_A\mathbf{v}_A$ and $\mathbf{p}_B = m_B\mathbf{v}_B$ their CM momenta, we have

$$\mathbf{p}_A + \mathbf{p}_B = 0 \qquad \text{[A2.1]}$$

Observations are often [1] made in the laboratory system, while *calculations* are frequently performed in the CM system, since the three degrees of freedom attached to the centre of mass of the system (A + B) may then be ignored. In this appendix we shall study the kinematical problem of passing from one frame of reference to the other.

Let us choose the incident direction as our Z axis in both laboratory and CM systems. Calling $\hat{\mathbf{z}}$ the unit vector along this axis, we write the velocity of the centre of mass in the laboratory system as

$$\mathbf{V}_L = V_L\hat{\mathbf{z}} \qquad \text{[A2.2]}$$

We suppose that no external forces are present, so that the centre of mass keeps its uniform rectilinear motion and the laboratory and CM systems are in uniform translational motion of velocity $\mathbf{V}_L$ with respect to each other. Since the collision is non-relativistic, the velocity $\mathbf{v}_L$ of a particle in the laboratory system is therefore related to its velocity $\mathbf{v}$ in the CM system by

$$\mathbf{v}_L = \mathbf{v} + \mathbf{V}_L \qquad \text{[A2.3]}$$

We shall choose the X and Y axes of the CM system to be parallel to the corresponding axes in the laboratory system. Then, if $\mathbf{v}$ points in the direction (θ, ϕ) in the CM system and $\mathbf{v}_L$ in the direction (θ_L, ϕ_L) in the laboratory system

[1] Important exceptions are crossed beam, colliding beam or merged beam experiments, in which the 'target' consists of a beam of particles B.

(see Fig. A2.1) we have

$$\begin{aligned} v_L \cos\theta_L &= v\cos\theta + V_L \\ v_L \sin\theta_L &= v\sin\theta \\ \phi_L &= \phi \end{aligned} \qquad [A2.4]$$

Eliminating v_L from the first two of these equations, we find that

$$\tan\theta_L = \frac{\sin\theta}{\cos\theta + \tau} \qquad [A2.5]$$

where

$$\tau = \frac{V_L}{v} \qquad [A2.6]$$

Since the particle B is at rest before the collision in the laboratory system, the total momentum $\mathbf{P}_L$ in that system is equal to the momentum $(\mathbf{p}_A)_L$ of the incident particle A,

$$\mathbf{P}_L = (\mathbf{p}_A)_L \qquad [A2.7]$$

and the initial kinetic energy $(T_i)_L$ in the laboratory system is given by

$$(T_i)_L = \frac{(p_A)_L^2}{2m_A} = \frac{P_L^2}{2m_A} \qquad [A2.8]$$

The corresponding initial kinetic energy T_i available in the CM system is obtained by subtracting from $(T_i)_L$ the kinetic energy of the centre of mass in the laboratory system. Using the fact that the centre of mass moves in the laboratory system as a free particle of mass $M = m_A + m_B$, momentum $\mathbf{P}_L$ and

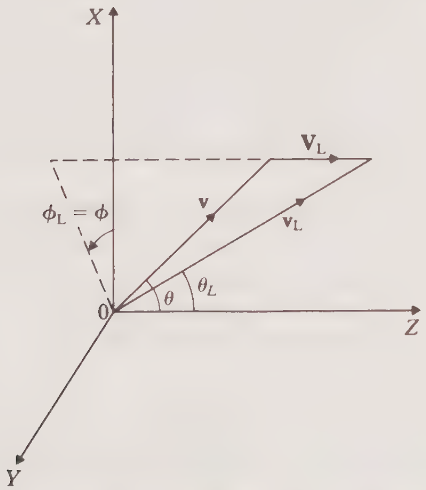

A2.1 Illustration of the velocities $\mathbf{v}$, $\mathbf{v}_L$ and $\mathbf{V}_L$ and the angles (θ, ϕ) and (θ_L, ϕ_L).

energy $P_L^2/2M$, we have

$$T_i = (T_i)_L - \frac{P_L^2}{2M}$$

$$= \frac{m_B}{m_A + m_B}(T_i)_L \qquad \text{[A2.9]}$$

and we also note that the centre of mass velocity V_L in the laboratory system is given by

$$V_L = \frac{(p_A)_L}{m_A + m_B} = \frac{m_A}{m_A + m_B}(v_A)_L$$

$$= \left[\frac{2m_A T_i}{m_B(m_A + m_B)}\right]^{1/2} \qquad \text{[A2.10]}$$

It is also clear that before the collision the magnitudes of the CM velocities of the particles A and B are given by

$$v_A = (v_A)_L - V_L = \frac{m_B}{m_A + m_B}(v_A)_L \qquad \text{[A2.11a]}$$

$$v_B = V_L = \frac{m_A}{m_A + m_B}(v_A)_L \qquad \text{[A2.11b]}$$

We remark that since the centre of mass always moves as a free particle, 'unaffected' by the collision process, it is the initial kinetic energy available in the CM system, T_i, which physically characterises the collision. For example, in electron–atom scattering, where m_A, the electron mass, is much smaller than m_B, the mass of the atom, we deduce from [A2.9] and [A2.10] that $T_i \simeq (T_i)_L$ and $V_L \simeq 0$. Thus in this case the laboratory and CM systems nearly coincide and almost all the initial kinetic energy in the laboratory system is available in the centre of mass system. On the contrary if we consider a collision between two atoms having the same mass ($m_A = m_B$) we see that $V_L = (v_A)_L/2$ and $T_i = (T_i)_L/2$, so that only one-half of the initial laboratory kinetic energy $(T_i)_L$ is transformed into CM kinetic energy, the second half being 'dissipated' in the motion of the centre of mass.

A useful expression of T_i may be obtained in the following way. We first define the *relative momentum* $\mathbf{p}$ of two particles 1 and 2 having masses m_1 and m_2 and momenta $\mathbf{p}_1$ and $\mathbf{p}_2$ by the relation

$$\mathbf{p} = \frac{m_2\mathbf{p}_1 - m_1\mathbf{p}_2}{m_1 + m_2} \qquad \text{[A2.12]}$$

Using this definition, and evaluating the momenta of the colliding particles A and B successively in the centre of mass and in the laboratory system, we find that the *initial relative momentum* of the two particles A and B is given by

$$\mathbf{p}_i = \mathbf{p}_A = -\mathbf{p}_B \qquad \text{[A2.13]}$$

or

$$\mathbf{p}_i = \frac{m_B}{m_A + m_B} (\mathbf{p}_A)_L \qquad [A2.14]$$

As a result, the initial kinetic energy T_i available in the CM system may be written as

$$T_i = \frac{p_A^2}{2m_A} + \frac{p_B^2}{2m_B} = \frac{p_i^2}{2\mu} = \frac{1}{2}\mu v_i^2 \qquad [A2.15]$$

where

$$\mu = \frac{m_A m_B}{m_A + m_B} \qquad [A2.16]$$

is the reduced mass of the two particles A and B, $\mathbf{v}_i = (\mathbf{v}_A)_L$ is the initial relative velocity, of magnitude v_i, and we have used the fact that $\mathbf{p}_i = \mu(\mathbf{v}_A)_L = \mu\mathbf{v}_i$

Elastic scattering

Thus far we have focused our attention on the initial situation, before the collision has occurred. The above analysis may also be repeated to obtain the relationships between the final centre of mass and laboratory quantities, that is *after* the collision has taken place. As an example, we shall consider the case of an *elastic scattering process*

$$A + B \rightarrow A + B \qquad [A2.17]$$

in which the particles are simply scattered without any change in their internal structure [2]. This process is represented in Fig. A2.2(a) in the laboratory system,while in Fig. A2.2(b) it is described in the centre of mass system.

Let $\mathbf{v}'_A$ and $\mathbf{v}'_B$ be respectively the CM velocities of particles A and B after the collision, while $\mathbf{p}'_A = m_A\mathbf{v}'_A$ and $\mathbf{p}'_B = m_B\mathbf{v}'_B$ are the corresponding CM momenta. Similarly, we shall write the final laboratory velocities as $(\mathbf{v}'_A)_L$ and $(\mathbf{v}'_B)_L$, the corresponding momenta being $(\mathbf{p}'_A)_L = m_A(\mathbf{v}'_A)_L$ and $(\mathbf{p}'_B)_L = m_B(\mathbf{v}'_B)_L$. From momentum conservation we have in the laboratory system

$$\mathbf{P}_L = (\mathbf{p}_A)_L = (\mathbf{p}'_A)_L + (\mathbf{p}'_B)_L \qquad [A2.18]$$

while in the centre of mass system

$$\mathbf{p}_A + \mathbf{p}_B = \mathbf{p}'_A + \mathbf{p}'_B = 0 \qquad [A2.19]$$

We also note from [A2.12] that the final relative momentum is

$$\mathbf{p}_f = \mathbf{p}'_A = -\mathbf{p}'_B \qquad [A2.20]$$

[2] The generalisation to inelastic collisions $A + B \rightarrow A' + B'$ or reactions $A + B \rightarrow C + D$ (see Problem 11.1) is straightforward; it may be found for example in Joachain (1979), where the case of relativistic collisions is also discussed.

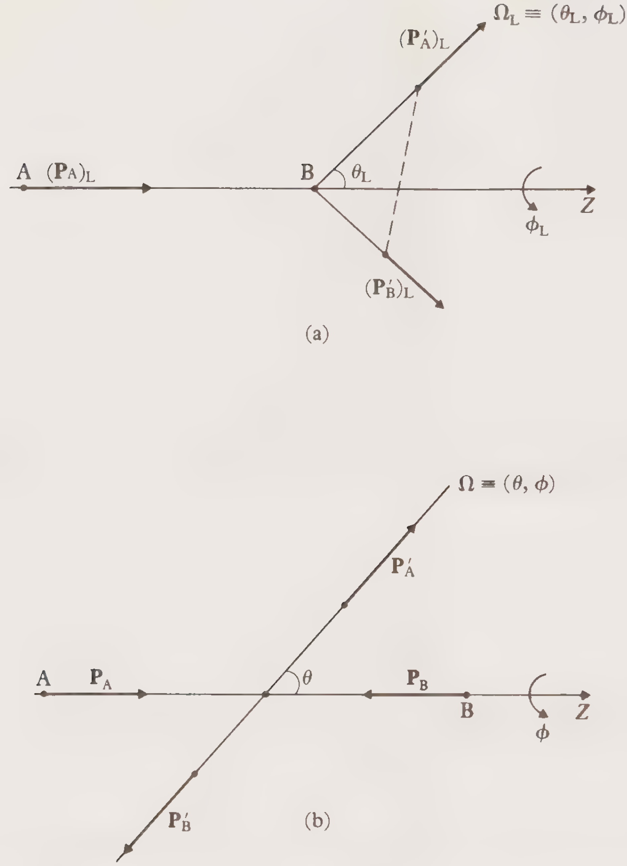

A2.2 An elastic collision A + B → A + B (a) in the laboratory system and (b) in the centre of mass system.

or

$$\mathbf{p}_f = \frac{m_B(\mathbf{p}'_A)_L - m_A(\mathbf{p}'_B)_L}{m_A + m_B} \qquad \text{[A2.21]}$$

The final kinetic energy in the laboratory system is

$$(T_f)_L = \frac{(p'_A)^2_L}{2m_A} + \frac{(p'_B)^2_L}{2m_B} \qquad \text{[A2.22]}$$

and the corresponding quantity in the centre of mass system is

$$T_f = (T_f)_L - \frac{P^2_L}{2M}$$

$$= \frac{(p'_A)^2}{2m_A} + \frac{(p'_B)^2}{2m_B} = \frac{p_f^2}{2\mu} \qquad \text{[A2.23]}$$

where μ is the reduced mass [A2.16]. Conservation of energy implies that for the elastic scattering event considered here we must have

$$T_i = T_f \quad \text{or} \quad p_i = p_f \qquad \text{[A2.24]}$$

Let us now consider the velocities of the particles. We see from [A2.13], [A2.20] and [A2.24] that for an elastic collision

$$\begin{aligned} v'_A &= v_A \\ v'_B &= v_B \end{aligned} \qquad \text{[A2.25]}$$

so that the magnitude of the CM velocities is unchanged. The initial and final velocities of the two particles are given in Table A2.1 in both the laboratory and centre of mass system.

From the definition [A1.15] of the differential cross-section, given in Appendix 1, we know that the same number dN'_A of particles A are emitted into the solid angle $d\Omega$ about the direction (θ, ϕ) in the CM system as are emitted into $d\Omega_L$ about (θ_L, ϕ_L) in the laboratory system. Thus the laboratory and CM differential cross-sections are related by

$$\frac{d\sigma}{d\Omega_L}(\theta_L, \phi_L)\, d\Omega_L = \frac{d\sigma}{d\Omega}(\theta, \phi)\, d\Omega$$

or

$$\frac{d\sigma}{d\Omega_L}(\theta_L, \phi_L) \sin\theta_L\, d\theta_L\, d\phi_L = \frac{d\sigma}{d\Omega}(\theta, \phi) \sin\theta\, d\theta\, d\phi \qquad \text{[A2.26]}$$

Using the last of equations [A2.4], we have immediately $d\phi_L = d\phi$. Moreover, using [A2.5] and [A2.6] we have

$$\tan\theta_L = \frac{\sin\theta}{\cos\theta + \tau_A} \qquad \text{[A2.27]}$$

where

$$\tau_A = \frac{V_L}{v_A} = \frac{m_A}{m_B} \qquad \text{[A2.28]}$$

for the elastic scattering case considered here. We may also write

$$\cos\theta_L = \frac{\cos\theta + \tau_A}{(1 + 2\tau_A \cos\theta + \tau_A^2)^{1/2}} \qquad \text{[A2.29]}$$

so that the elastic laboratory and CM differential cross-sections are related by

$$\frac{d\sigma}{d\Omega_L}(\theta_L, \phi_L) = \frac{(1 + \tau_A^2 + 2\tau_A \cos\theta)^{3/2}}{|1 + \tau_A \cos\theta|} \frac{d\sigma}{d\Omega}(\theta, \phi) \qquad \text{[A2.30]}$$

Finally, by integrating the differential cross-section over all scattering angles,

Table A2.1 The initial and final velocities of the particles A and B for an elastic collision $A + B \rightarrow A + B$. The spherical polar coordinates of a velocity $\mathbf{v}$ are denoted by (v, θ, ϕ)

	Initial velocities (before collision)		*Final velocities (after collision)*	
	A	B	A	B
In the laboratory system (L)	$(\mathbf{v}_A)_L = (v_A)_L\hat{\mathbf{z}}$	0	$(\mathbf{v}'_A)_L \equiv [(v'_A)_L, \theta_L, \phi_L]$	$(\mathbf{v}'_B)_L \equiv [(v'_B)_L, (\theta_B)_L, (\phi_B)_L]$
In the centre of mass system (CM)	$(\mathbf{v}_A)_L - \mathbf{V}_L = [(v_A)_L - V_L]\hat{\mathbf{z}}$	$-\mathbf{V}_L = -V_L\hat{\mathbf{z}}$	$\mathbf{v}'_A \equiv (v_A, \theta, \phi)$	$\mathbf{v}'_B \equiv (v_B, \pi - \theta, \phi + \pi)$
	$= v_A\hat{\mathbf{z}}$	$= -v_B\hat{\mathbf{z}}$		

we obtain the total cross-section σ_{tot}. Using [A2.26] we see that

$$\sigma_{tot} = \int \frac{d\sigma}{d\Omega_L}(\theta_L, \phi_L)\, d\Omega_L = \int \frac{d\sigma}{d\Omega}(\theta, \phi)\, d\Omega \qquad [A2.31]$$

so that the total cross-section is independent of the reference frame.

In Appendix 1 we discussed the scattering of a beam of particles A by fixed scattering centres B, or in other words by infinitely massive target scatterers B. These results can easily be extended to the realistic case of target scatterers B which have a finite mass m_B, and hence can recoil. Indeed, it is shown in Section 2.7 that the problem of two particles interacting through a potential $V(\mathbf{r})$ which depends only on their relative coordinate is entirely equivalent, in the CM system, to the problem of a 'relative' particle moving in the potential $V(\mathbf{r})$, the mass of the 'relative' particle being the reduced mass μ of the two particles. This reduction of a two-body problem to an equivalent one-body problem in the CM system is valid in both classical and quantum mechanics. In particular, the results obtained in Appendix 1 for classical scattering of a beam of particles by a central potential can be used directly for the classical scattering of two particles A and B interacting via a central force, provided the mass m is replaced by the reduced mass $\mu = m_A m_B/(m_A + m_B)$ and the scattering angle θ, energy E, velocities, etc. are understood to be the centre of mass quantities. For example, since the initial kinetic energy available in the CM system is given by $v_i^2/2$, the Rutherford differential cross-section [A1.33] becomes

$$\frac{d\sigma_c}{d\Omega} = \left(\frac{q_A q_B}{4\pi\varepsilon_0}\right)^2 \frac{1}{4\mu^2 v_i^4} \frac{1}{\sin^4(\theta/2)} \qquad [A2.32]$$

where $v_i = (v_A)_L$ is the initial relative velocity of the two colliding particles. The result [A2.32] is the Rutherford differential cross-section for Coulomb scattering of a particle A of charge q_A by a particle B of charge q_B, written in the CM system. The corresponding laboratory differential cross-section may be obtained by using the relation [A2.30].

3 Evaluation of integrals by using generating functions

In this appendix we shall show how generating functions may be used to evaluate various integrals involving harmonic oscillator or hydrogenic wave functions.

Harmonic oscillator

We have seen in Section 2.4 that the Hermite polynomials $H_n(\xi)$ can be expressed in terms of a generating function $G(\xi, s)$ as

$$G(\xi, s) = e^{-s^2+2s\xi} = \sum_{n=0}^{\infty} \frac{H_n(\xi)}{n!} s^n \qquad \text{[A3.1]}$$

This generating function is useful in many calculations, and in particular for the evaluation of various integrals involving the harmonic oscillator wave functions

$$\psi_n(x) = N_n e^{-\alpha^2x^2/2} H_n(\alpha x) \qquad \text{[A3.2]}$$

As a first example, we shall normalise the wave functions $\psi_n(x)$, i.e. find the normalisation constant N_n such that

$$\int_{-\infty}^{+\infty} |\psi_n(x)|^2 \, dx = \frac{|N_n|^2}{\alpha} \int_{-\infty}^{+\infty} e^{-\xi^2} H_n^2(\xi) \, d\xi = 1 \qquad \text{[A3.3]}$$

where we have set $\xi = \alpha x$. For this purpose, we consider the two generating functions $G(\xi, s)$ and

$$G(\xi, t) = e^{-t^2+2t\xi} = \sum_{m=0}^{\infty} \frac{H_m(\xi)}{m!} t^m \qquad \text{[A3.4]}$$

and use [A3.1] and [A3.4] to write

$$\int_{-\infty}^{+\infty} e^{-\xi^2} G(\xi, s) G(\xi, t) \, d\xi = \sum_{n=0}^{\infty} \sum_{m=0}^{\infty} \frac{s^n t^m}{n!m!} \int_{-\infty}^{+\infty} e^{-\xi^2} H_n(\xi) H_m(\xi) \, d\xi \qquad \text{[A3.5]}$$

Using the fact that

$$\int_{-\infty}^{+\infty} e^{-x^2} \, dx = \sqrt{\pi} \qquad \text{[A3.6]}$$

we see that the integral on the left-hand side of [A3.5] is simply

$$\int_{-\infty}^{+\infty} e^{-\xi^2} e^{-s^2+2s\xi} e^{-t^2+2t\xi} d\xi = \sqrt{\pi} e^{2st}$$

$$= \sqrt{\pi} \sum_{n=0}^{\infty} \frac{(2st)^n}{n!} \qquad [A3.7]$$

Equating the coefficients of equal powers of s and t on the right-hand sides of [A3.5] and [A3.7], we find that

$$\int_{-\infty}^{+\infty} e^{-\xi^2} H_n^2(\xi)\, d\xi = \sqrt{\pi} 2^n n! \qquad [A3.8]$$

and

$$\int_{-\infty}^{+\infty} e^{-\xi^2} H_n(\xi) H_m(\xi)\, d\xi = 0, \qquad n \neq m \qquad [A3.9]$$

From [A3.3] and [A3.8] we see that apart from an arbitrary phase factor the normalisation constant N_n is given by

$$N_n = \left(\frac{\alpha}{\sqrt{\pi} 2^n n!} \right)^{1/2} \qquad [A3.10]$$

The second result [A3.9] implies that

$$\int_{-\infty}^{+\infty} \psi_m(x) \psi_n(x)\, dx = 0, \qquad n \neq m \qquad [A3.11]$$

so that the (real) harmonic oscillator wave functions $\psi_n(x)$ and $\psi_m(x)$ are orthogonal if $n \neq m$, in agreement with the fact that they correspond to non-degenerate energy eigenvalues $E_n \neq E_m$

As a second example, we calculate the integral

$$x_{nm} = \int_{-\infty}^{+\infty} \psi_n(x) x \psi_m(x)\, dx = \frac{N_n N_m}{\alpha^2} \int_{-\infty}^{+\infty} e^{-\xi^2} \xi H_n(\xi) H_m(\xi)\, d\xi \quad [A3.12]$$

Using again the two generating functions $G(\xi, s)$ and $G(\xi, t)$ given respectively by [A3.1] and [A3.4], we now look at the quantity

$$\int_{-\infty}^{+\infty} e^{-\xi^2} \xi G(\xi, s) G(\xi, t)\, d\xi = \sum_{n=0}^{\infty} \sum_{m=0}^{\infty} \frac{s^n t^m}{n! m!} \int_{-\infty}^{+\infty} e^{-\xi^2} \xi H_n(\xi) H_m(\xi)\, d\xi$$

[A3.13]

The integral on the left-hand side is simply

$$\int_{-\infty}^{+\infty} e^{-\xi^2} \xi e^{-s^2+2s\xi} e^{-t^2+2t\xi} d\xi = \sqrt{\pi}(s+t) e^{2st}$$

$$= \sqrt{\pi} \sum_{n=0}^{\infty} \frac{2^n}{n!} (s^{n+1} t^n + s^n t^{n+1}) \quad [A3.14]$$

Upon comparison of the coefficients of equal powers of s and t on the right-hand sides of [A3.13] and [A3.14], and using our previous result [A3.10], we find that

$$x_{nm} = \begin{cases} 0 \quad , & m \neq n \pm 1 \\ \dfrac{1}{\alpha}\left(\dfrac{n+1}{2}\right)^{1/2}, & m = n+1 \\ \dfrac{1}{\alpha}\left(\dfrac{n}{2}\right)^{1/2}, & m = n-1 \end{cases} \qquad \text{[A3.15]}$$

Hydrogenic atom

A similar method may be used to evaluate certain integrals involving the radial hydrogenic wave functions (see [3.47])

$$R_{nl}(r) = N_{nl} e^{-\rho/2} \rho^l L_{n+l}^{2l+1}(\rho), \qquad \rho = \frac{2Z}{na_\mu} r \qquad \text{[A3.16]}$$

Suppose, for example, that we want to evaluate integrals of the type

$$I^{\alpha}_{pq,p'q'} = \int_0^\infty e^{-\rho} \rho^\alpha L_q^p(\rho) L_{q'}^{p'}(\rho)\, d\rho \qquad \text{[A3.17]}$$

Using the generating function [3.45] for the associated Laguerre polynomials,

$$U_p(\rho, s) = \frac{(-s)^p e^{-\rho s/(1-s)}}{(1-s)^{p+1}} = \sum_{q=p}^{\infty} \frac{L_q^p(\rho)}{q!} s^q \qquad \text{[A3.18]}$$

and a similar expression for $U_{p'}(\rho, t)$, we have

$$\int_0^\infty e^{-\rho} \rho^\alpha U_p(\rho, s) U_{p'}(\rho, t)\, d\rho = \sum_{q=p}^{\infty} \sum_{q'=p'}^{\infty} \frac{s^q t^{q'}}{q!(q')!} I^{\alpha}_{pq,p'q'} \qquad \text{[A3.19]}$$

The integral on the left-hand side is just

$$\begin{aligned} &\int_0^\infty e^{-\rho} \rho^\alpha \frac{(-s)^p e^{-\rho s/(1-s)}}{(1-s)^{p+1}} \frac{(-t)^{p'} e^{-\rho t/(1-t)}}{(1-t)^{p'+1}}\, d\rho \\ &= \frac{(-1)^{p+p'} s^p t^{p'}}{(1-s)^{p+1}(1-t)^{p'+1}} \int_0^\infty e^{-\rho[1+s/(1-s)+t/(1-t)]} \rho^\alpha\, d\rho \\ &= \frac{(-1)^{p+p'} s^p t^{p'}}{(1-s)^{p+1}(1-t)^{p'+1}} \frac{\Gamma(\alpha+1)}{\left(1 + \dfrac{s}{1-s} + \dfrac{t}{1-t}\right)^{\alpha+1}} \end{aligned} \qquad \text{[A3.20]}$$

where Γ is Euler's gamma function and we have used the fact that

$$\int_0^\infty e^{-\beta x} x^\alpha\, dx = \frac{\Gamma(\alpha+1)}{\beta^{\alpha+1}} \qquad \text{[A3.21]}$$

The required integral $I^{\alpha}_{pq,p'q'}$ may therefore be obtained by expanding the result [A3.20] as a power series in s and t and comparing the coefficients with those of the series on the right of [A3.19].

As a simple illustration of the method, we shall normalise the radial hydrogenic eigenfunctions. We see from [3.51] that for this purpose we need the integral

$$I^{p+1}_{pq,pq} = \int_0^{\infty} e^{-\rho}\rho^{p+1}[L^p_q(\rho)]^2 \, d\rho \qquad \text{[A3.22]}$$

with $p = 2l + 1$ and $q = n + l$. Using the generating functions $U_p(\rho, s)$ and $U_p(\rho, t)$ we therefore have in this case

$$\int_0^{\infty} e^{-\rho}\rho^{p+1}U_p(\rho, s)U_p(\rho, t) \, d\rho = \sum_{q=p}^{\infty}\sum_{q'=p}^{\infty} \frac{s^q t^{q'}}{q!(q')!} I^{p+1}_{pq,pq'} \qquad \text{[A3.23]}$$

and also

$$\begin{aligned}
\int_0^{\infty} e^{-\rho}\rho^{p+1}U_p(\rho, s)U_p(\rho, t) \, d\rho &= \frac{(st)^p}{(1-s)^{p+1}(1-t)^{p+1}} \\
&\quad \times \int_0^{\infty} e^{-\rho[1+s/(1-s)+t/(1-t)]} \rho^{p+1} \, d\rho \\
&= \frac{(p+1)!\,(st)^p\,(1-s)(1-t)}{(1-st)^{p+2}} \\
&= (p+1)!(1-s-t+st) \\
&\quad \times \sum_{k=0}^{\infty} \frac{(p+k+1)!}{k!(p+1)!}(st)^{p+k} \qquad \text{[A3.24]}
\end{aligned}$$

where we have used the binomial theorem to expand the quantity $(1 - st)^{-p-2}$. Upon comparison of the right-hand sides of [A3.23] and [A3.24], we see that the required integral $I^{p+1}_{pq,pq}$ is equal to $(q!)^2$ times the coefficient of $(st)^q$ in the series [A3.24]. Thus

$$\begin{aligned}
I^{p+1}_{pq,pq} &= (q!)^2(p+1)!\left[\frac{(q+1)!}{(q-p)!(p+1)!} + \frac{q!}{(q-p-1)!(p+1)!}\right] \\
&= \frac{(q!)^3(2q-p+1)}{(q-p)!} \qquad \text{[A3.25]}
\end{aligned}$$

and remembering that $p = 2l + 1$ and $q = n + l$, we finally have

$$\int_0^{\infty} e^{-\rho}\rho^{2l}[L^{2l+1}_{n+l}(\rho)]^2\rho^2 \, d\rho = \frac{2n[(n+l)!]^3}{(n-l-1)!} \qquad \text{[A3.26]}$$

which is the result quoted in [3.52].

4 Angular momentum – useful formulae and results

In this appendix, we collect, for the most part without proof, useful relations and results concerned with angular momentum. A good elementary treatment of angular momentum can be found in the texts by Powell and Crasemann (1962) and Merzbacher (1970) while a more advanced and complete treatment can be found in the monographs of Edmonds (1957), and Rose (1957).

Angular momentum operators

In Chapter 2, we discussed the representation of the components of the orbital angular momentum $\mathbf{L}$ by differential operators, starting from the expression $\mathbf{L} = \mathbf{r} \times \mathbf{p}$. We also outlined the theory of particles of spin one-half, for which the components of the spin angular momentum $\mathbf{S}$ were represented by 2×2 matrices. We shall obtain a general matrix representation for the Cartesian components $\mathcal{J}_x$, $\mathcal{J}_y$ and $\mathcal{J}_z$ of the angular momentum operator $\mathbf{J}$, which will include the particular cases such that the angular momentum is purely of orbital or of spin type.

The operators $\mathcal{J}_x$, $\mathcal{J}_y$ and $\mathcal{J}_z$ are *defined* as linear self-adjoint operators satisfying the commutation relations

$$[\mathcal{J}_x, \mathcal{J}_y] = i\hbar\mathcal{J}_z \text{ (and cyclicly)} \qquad \text{[A4.1]}$$

Since $\mathbf{J}^2 = \mathcal{J}_x^2 + \mathcal{J}_y^2 + \mathcal{J}_z^2$ commutes with each component, simultaneous eigenfunctions ψ_{jm} of $\mathbf{J}^2$ and one component, say $\mathcal{J}_z$, can be found, with

$$\begin{aligned} \mathbf{J}^2\psi_{jm} &= j(j+1)\hbar^2\psi_{jm} \\ \mathcal{J}_z\psi_{jm} &= m\hbar\psi_{jm} \end{aligned} \qquad \text{[A4.2]}$$

We may normalise the ψ_{jm} to unity, in which case the orthonormality relations

$$\langle\psi_{j'm'}|\psi_{jm}\rangle = \delta_{jj'}\,\delta_{mm'} \qquad \text{[A4.3]}$$

are satisfied, and $\mathcal{J}_z$ is represented by a diagonal matrix with elements

$$\langle\psi_{j'm'}|\mathcal{J}_z|\psi_{jm}\rangle = \delta_{jj'}\,\delta_{mm'}m\hbar \qquad \text{[A4.4]}$$

In this matrix representation, the eigenfunctions ψ_{jm} are, in fact, column vectors.

The eigenvalues, which we have written for later convenience in the form $j(j+1)\hbar^2$ and $m\hbar$, are real as $\mathbf{J}^2$ and $\mathcal{J}_z$ are self-adjoint. They can be determined by the following argument, which we give in outline only.

Let us define the raising and lowering operators $\mathcal{J}_\pm$ as

$$\mathcal{J}_\pm = \mathcal{J}_x \pm i\mathcal{J}_y \qquad [A4.5]$$

where $\mathcal{J}_+ = \mathcal{J}_-^\dagger$; $\mathcal{J}_- = \mathcal{J}_+^\dagger$. We note the relations

$$[\mathcal{J}_z, \mathcal{J}_\pm] = \pm\hbar\mathcal{J}_\pm \qquad [A4.6]$$

$$[\mathbf{J}^2, \mathcal{J}_\pm] = 0 \qquad [A4.7]$$

$$\mathcal{J}_+\mathcal{J}_- = \mathbf{J}^2 - \mathcal{J}_z^2 + \hbar\mathcal{J}_z; \quad \mathcal{J}_-\mathcal{J}_+ = \mathbf{J}^2 - \mathcal{J}_z^2 - \hbar\mathcal{J}_z \qquad [A4.8]$$

From the commutation relation [A4.6], we have

$$\begin{aligned}\mathcal{J}_z\{\mathcal{J}_\pm\psi_{jm}\} &= \mathcal{J}_\pm\mathcal{J}_z\psi_{jm} \pm \hbar\mathcal{J}_\pm\psi_{jm} \\ &= (m \pm 1)\hbar\{\mathcal{J}_\pm\psi_{jm}\}\end{aligned} \qquad [A4.9]$$

so that $(\mathcal{J}_\pm\psi_{jm})$ are eigenfunctions of $\mathcal{J}_z$ belonging to the eigenvalues $(m \pm 1)$. Because of [A4.7], these functions are simultaneously eigenfunctions of $\mathbf{J}^2$, belonging to the eigenvalue $j(j+1)\hbar^2$.

For any wave function ϕ, $\langle\phi|\mathbf{J}^2|\phi\rangle \geq \langle\phi|\mathcal{J}_z^2|\phi\rangle$, and setting $\phi = \psi_{jm}$, we find

$$j(j+1) \geq m_j^2 \qquad [A4.10]$$

By operating with $\mathcal{J}_+$ or $\mathcal{J}_-$ repeatedly, sequences of eigenfunctions of $\mathcal{J}_z$ can be constructed, namely $(\mathcal{J}_+)^n\psi_{jm}$, $(\mathcal{J}_-)^{n'}\psi_{jm}$, with eigenvalues $(m+n)\hbar$ and $(m-n')\hbar$ respectively. In view of [A4.10], for each j there must be a maximum eigenvalue of $\mathcal{J}_z$, say $\lambda\hbar$, and also a minimum eigenvalue, say $\lambda'\hbar$, such that $\lambda - \lambda'$ = an integer (or zero). If $\mathcal{J}_+$ is applied to $\psi_{j\lambda}$, we must have $\mathcal{J}_+\psi_{j\lambda} = 0$, for otherwise the sequence would not terminate and $\lambda\hbar$ would not be the maximum eigenvalue. Using [A4.8], we have

$$\mathcal{J}_-\mathcal{J}_+\psi_{j\lambda} = \{j(j+1) - \lambda^2 - \lambda\}\hbar^2\psi_{j\lambda} = 0 \qquad [A4.11]$$

with the solution $\lambda = j$. In the same way $\mathcal{J}_-\psi_{j\lambda'} = 0$, from which we find $\lambda' = -j$. Since $(\lambda - \lambda')$ is an integer (or zero), $(2j)$ is an integer (or zero) and j must be one of the integers or half-integers, $j = 0, \frac{1}{2}, 1, 3/2, 2, \ldots$. For a given value of j, m can take the $(2j+1)$ values $-j, -j+1, \ldots j-1, j$.

To find the matrix elements of $\mathcal{J}_x$ and $\mathcal{J}_y$, or equivalently of $\mathcal{J}_+$ and $\mathcal{J}_-$, we note that

$$\mathcal{J}_+\psi_{jm} = N\psi_{jm+1} \qquad [A4.12]$$

where N is a constant. Since both ψ_{jm} and ψ_{jm+1} are normalised to unity, we have from [A4.3]

$$\begin{aligned}N^2 &= \langle\mathcal{J}_+\psi_{jm}|\mathcal{J}_+\psi_{jm}\rangle = \langle\psi_{jm}|\mathcal{J}_-\mathcal{J}_+|\psi_{jm}\rangle \\ &= \hbar^2(j(j+1) - m(m+1))\end{aligned} \qquad [A4.13]$$

where we have used [A4.8]. Adopting the convention that N is real and positive, we then obtain

$$N = \hbar \sqrt{j(j+1) - m(m+1)} \qquad \text{[A4.14]}$$

From [A4.12], the matrix representing $\mathcal{J}_+$ in the basis of eigenfunctions ψ_{jm} is

$$\langle \psi_{j'm'} | \mathcal{J}_+ | \psi_{jm} \rangle = \sqrt{j(j+1) - m(m+1)}\,\hbar\, \delta_{jj'}\, \delta_{m'm+1} \qquad \text{[A4.15]}$$

In a similar way, we find

$$\langle \psi_{j'm'} | \mathcal{J}_- | \psi_{jm} \rangle = \sqrt{j(j+1) - m(m-1)}\,\hbar\, \delta_{jj'}\, \delta_{m'm-1} \qquad \text{[A4.16]}$$

As we saw in Chapter 2, if $\mathbf{J}$ is a pure orbital angular momentum ($\mathbf{L}$), the wave function must be single valued as a function of position, and this excludes the half-integral values of j. For a spin angular momentum or when $\mathbf{J}$ is the sum of an orbital and a spin angular momentum, both the integral and half-integral values are allowed.

Spherical harmonics and Legendre polynomials

In Chapter 2 we introduced the spherical harmonics $Y_{lm}(\theta, \phi)$, which are the simultaneous eigenfunctions of the orbital angular momentum operators $\mathbf{L}^2$ and L_z,

$$\mathbf{L}^2 Y_{lm} = l(l+1)\hbar^2 Y_{lm}; \qquad L_z Y_{lm} = m\hbar Y_{lm} \qquad \text{[A4.17]}$$

where $l = 0, 1, 2, \ldots$ and $m = -l, -l+1, \ldots l-1, l$. They satisfy the orthonormality relation

$$\int Y^{\star}_{l'm'}(\theta, \phi) Y_{lm}(\theta, \phi)\, \mathrm{d}\Omega = \delta_{ll'}\, \delta_{mm'}; \qquad (\mathrm{d}\Omega = \sin\theta\, \mathrm{d}\theta\, \mathrm{d}\phi) \qquad \text{[A4.18]}$$

and the closure relation

$$\sum_{l=0}^{\infty} \sum_{m=-l}^{l} Y^{\star}_{lm}(\theta, \phi) Y_{lm}(\theta', \phi') = \delta(\Omega - \Omega') \qquad \text{[A4.19]}$$

where

$$\delta(\Omega - \Omega') = \frac{1}{\sin\theta}\, \delta(\theta - \theta')\, \delta(\phi - \phi')$$

If the operators $L_\pm$ are defined as $L_\pm = L_x \pm iL_y$ (see [A4.5]) we have

$$L_\pm = \hbar e^{\pm i\phi}\left[\pm \frac{\partial}{\partial\theta} + i \cot\theta \frac{\partial}{\partial\phi} \right] \qquad \text{[A4.20]}$$

and

$$L_\pm Y_{lm} = \hbar \sqrt{l(l+1) - m(m\pm 1)}\; Y_{lm\pm 1} \qquad \text{[A4.21]}$$

in agreement with the general results of [A4.15] and [A4.16].

In the special case $m = 0$, the spherical harmonics are given by

$$Y_{l0} = \sqrt{\frac{2l+1}{4\pi}}\, P_l(\cos\theta) \qquad \text{[A4.22]}$$

where the functions $P_l(\cos\theta)$ are the Legendre polynomials defined in Section 2.5.

Let $\mathbf{r}_1$ and $\mathbf{r}_2$ be two vectors having polar angles (θ_1, ϕ_1) and (θ_2, ϕ_2) respectively, and let θ be the angle between them. It can be shown that

$$P_l(\cos\theta) = \frac{4\pi}{2l+1} \sum_{m=-l}^{+l} Y^{\star}_{lm}(\theta_1, \phi_1) Y_{lm}(\theta_2, \phi_2) \qquad \text{[A4.23]}$$

which is known as the addition (or biaxial) theorem of the spherical harmonics. From the generating function [2.168] of the Legendre polynomials, we see that

$$\frac{1}{|\mathbf{r}_1 - \mathbf{r}_2|} = \sum_{l=0}^{\infty} \frac{(r_<)^l}{(r_>)^{l+1}} P_l(\cos\theta) \qquad \text{[A4.24]}$$

which, using [A4.23], may also be written as

$$\frac{1}{|\mathbf{r}_1 - \mathbf{r}_2|} = \sum_{l=0}^{\infty} \sum_{m=-l}^{+l} \frac{4\pi}{2l+1} \frac{(r_<)^l}{(r_>)^{l+1}} Y^{\star}_{lm}(\theta_1, \phi_1) Y_{lm}(\theta_2, \phi_2) \qquad \text{[A4.25]}$$

It can also be shown (Mathews and Walker, 1973) that

$$\frac{\exp[ik|\mathbf{r}_1 - \mathbf{r}_2|]}{|\mathbf{r}_1 - \mathbf{r}_2|} = ik \sum_{l=0}^{\infty} (2l+1) j_l(kr_<)[j_l(kr_>) + i n_l(kr_>)] P_l(\cos\theta) \qquad \text{[A4.26]}$$

where j_l and n_l are spherical Bessel and Neumann functions respectively. Finally, we quote the formula giving the expansion of a plane wave in Legendre polynomials, namely

$$e^{i\mathbf{k}\cdot\mathbf{r}} = \sum_{l=0}^{\infty} (2l+1) i^l j_l(kr) P_l(\cos\theta) \qquad \text{[A4.27]}$$

where θ is the angle between the vectors $\mathbf{k}$ and $\mathbf{r}$.

Addition of angular momenta. The Clebsch–Gordan coefficients

Consider a system described by two angular momenta $\mathbf{J}_1$ and $\mathbf{J}_2$, such that the components of $\mathbf{J}_1$ commute with the components of $\mathbf{J}_2$. For example, $\mathbf{J}_1$ and $\mathbf{J}_2$ could be the angular momenta of different particles, or the orbital and spin angular momenta of a single particle. The normalised simultaneous eigenfunctions of $\mathbf{J}_1^2$ and $\mathcal{J}_{1z}$ corresponding to eigenvalues $j_1(j_1+1)\hbar^2$ and $m_1\hbar$ will be denoted by $\psi_{j_1 m_1}$ and similarly, the normalised eigenfunctions of $\mathbf{J}_2^2$ and $\mathcal{J}_{2z}$ corresponding to eigenvalues $j_2(j_2+1)\hbar^2$ and $m_2\hbar$ will be denoted by $\psi_{j_2 m_2}$. The simultaneous eigenfunctions of $\mathbf{J}_1^2, \mathcal{J}_{1z}, \mathbf{J}_2^2$ and $\mathcal{J}_{2z}$ are then given by the product

functions

$$\psi_{j_1 m_1; j_2 m_2} = \psi_{j_1 m_1} \times \psi_{j_2 m_2} \qquad \text{[A4.28]}$$

and for a given j_1 and j_2, there are $(2j_1 + 1) \times (2j_2 + 1)$ of these functions.

Now consider the total angular momentum

$$\mathbf{J} = \mathbf{J}_1 + \mathbf{J}_2 \qquad \text{[A4.29]}$$

Since $\mathbf{J}^2, \mathcal{J}_z, \mathbf{J}_1^2$ and $\mathbf{J}_2^2$ all commute, these operators possess a set of simultaneous eigenfunctions, which we shall write as $\Phi^{jm}_{j_1 j_2}$ where

$$\begin{aligned} \mathbf{J}^2 \Phi^{jm}_{j_1 j_2} &= j(j+1)\hbar^2 \Phi^{jm}_{j_1 j_2} \\ \mathcal{J}_z \Phi^{jm}_{j_1 j_2} &= m\hbar \Phi^{jm}_{j_1 j_2} \end{aligned} \qquad \text{[A4.30]}$$

For a given j, there are $(2j + 1)$ values of m with $-j \leqslant m \leqslant j$ and j can take any of the values $|j_1 - j_2|, |j_1 - j_2| + 1, \ldots (j_1 + j_2)$. Again there are $(2j_1 + 1) \times (2j_2 + 1)$ of the functions $\Phi^{jm}_{j_1 j_2}$, which can be related to the function [A4.28] by a unitary transformation:

$$\Phi^{jm}_{j_1 j_2} = \sum_{m_1 m_2} \langle j_1 j_2 m_1 m_2 | jm \rangle \psi_{j_1 m_1;\, j_2 m_2} \qquad \text{[A4.31]}$$

The coefficients $\langle j_1 j_2 m_1 m_2 | jm \rangle$ are called Clebsch–Gordan coefficients. These coefficients vanish unless $m = m_1 + m_2$ and $|j_1 - j_2| \leqslant j \leqslant j_1 + j_2$, and possess the following important properties:
Orthonormality relations

$$\sum_{m_1 m_2} \langle j_1 j_2 m_1 m_2 | jm \rangle \langle j_1 j_2 m_1 m_2 | j'm' \rangle = \delta_{jj'}\, \delta_{mm'}$$

$$\sum_{j,m} \langle j_1 j_2 m_1 m_2 | jm \rangle \langle j_1 j_2 m_1' m_2' | jm \rangle = \delta_{m_1 m_1'} \delta_{m_2 m_2'} \qquad \text{[A4.32]}$$

Symmetry properties

$$\begin{aligned} \langle j_1 j_2 m_1 m_2 | jm \rangle &= (-1)^{j_1 + j_2 - j} \langle j_2 j_1 m_2 m_1 | jm \rangle \\ &= (-1)^{j_1 + j_2 - j} \langle j_1 j_2 - m_1 - m_2 | j - m \rangle \\ &= (-1)^{j_1 - m_1} \left(\frac{2j+1}{2j_2+1} \right)^{1/2} \langle j_1 j m_1 - m | j_2 - m_2 \rangle \end{aligned} \qquad \text{[A4.33]}$$

In Table A4.1, the coefficients $\langle j_1 j_2 m_1 m_2 | jm \rangle$ are tabulated for the cases $j_2 = \frac{1}{2}$ and $j_2 = 1$. By using the symmetry relations, all the coefficients with any one of j_1, j_2 or j equal to $\frac{1}{2}$, or to 1, can be found.

Useful notations

When adding two orbital angular momenta $\mathbf{L}_1$ and $\mathbf{L}_2$, we shall write [A4.31] in the explicit position representation as

$$\mathcal{Y}^{lm}_{l_1 l_2}(\theta_1 \phi_1;\, \theta_2 \phi_2) = \sum_{m_1 m_2} \langle l_1 l_2 m_1 m_2 | lm \rangle\, Y_{l_1 m_1}(\theta_1, \phi_1) Y_{l_2 m_2}(\theta_2, \phi_2) \qquad \text{[A4.34]}$$

Table A4.1 Clebsch–Gordan coefficients for $j_2 = \frac{1}{2}$ and $j_2 = 1$

$\langle j_1 \tfrac{1}{2} m_1 m_2 | jm \rangle$

j	$m_2 = \frac{1}{2}$	$m_2 = -\frac{1}{2}$
$j_1 + \frac{1}{2}$	$\left(\dfrac{j_1 + m + \frac{1}{2}}{2j_1 + 1}\right)^{1/2}$	$\left(\dfrac{j_1 - m + \frac{1}{2}}{2j_1 + 1}\right)^{1/2}$
$j_1 - \frac{1}{2}$	$-\left(\dfrac{j_1 - m + \frac{1}{2}}{2j_1 + 1}\right)^{1/2}$	$\left(\dfrac{j_1 + m + \frac{1}{2}}{2j_1 + 1}\right)^{1/2}$

$\langle j_1 1 m_1 m_2 | jm \rangle$

j	$m_2 = 1$	$m_2 = 0$	$m_2 = -1$
$j_1 + 1$	$\left[\dfrac{(j_1 + m)(j_1 + m + 1)}{(2j_1 + 1)(2j_1 + 2)}\right]^{1/2}$	$\left[\dfrac{(j_1 - m + 1)(j_1 + m + 1)}{(2j_1 + 1)(j_1 + 1)}\right]^{1/2}$	$\left[\dfrac{(j_1 - m)(j_1 - m + 1)}{(2j_1 + 1)(2j_1 + 2)}\right]^{1/2}$
j_1	$-\left[\dfrac{(j_1 + m)(j_1 - m + 1)}{2j_1(j_1 + 1)}\right]^{1/2}$	$\left[\dfrac{m^2}{j_1(j_1 + 1)}\right]^{1/2}$	$\left[\dfrac{(j_1 - m)(j_1 + m + 1)}{2j_1(j_1 + 1)}\right]^{1/2}$
$j_1 - 1$	$\left[\dfrac{(j_1 - m)(j_1 - m + 1)}{2j_1(2j_1 + 1)}\right]^{1/2}$	$-\left[\dfrac{(j_1 - m)(j_1 + m)}{j_1(2j_1 + 1)}\right]^{1/2}$	$\left[\dfrac{(j_1 + m + 1)(j_1 + m)}{2j_1(2j_1 + 1)}\right]^{1/2}$

where $\mathcal{Y}_{l_1 l_2}^{lm}$ is a simultaneous eigenfunction of $\mathbf{L}_1^2$, $\mathbf{L}_2^2$, $\mathbf{L}^2$ and L_z, and $\mathbf{L} = \mathbf{L}_1 + \mathbf{L}_2$. Similarly, when adding an orbital angular momentum $\mathbf{L}$ with a spin angular momentum $\mathbf{S}$, so that $\mathbf{J} = \mathbf{L} + \mathbf{S}$ we shall often write

$$\mathcal{Y}_{ls}^{jm}(\theta, \phi) = \sum_{m_l m_s} \langle l s m_l m_s | jm \rangle Y_{l m_l}(\theta, \phi)\, \chi_{s m_s} \qquad \text{[A4.35]}$$

where $\chi_{s m_s}$ is a spin wave function.

When taking matrix elements of operators with respect to the eigenfunctions $\Phi_{j_1 j_2}^{jm}$, $\mathcal{Y}_{ls}^{jm}$ . . . , we shall frequently use the Dirac notation in which eigenvectors are written in the form $\Phi_{j_1 j_2}^{jm} \to |j_1 j_2 jm\rangle$. We then write

$$\langle \Phi_{j_1 j_2}^{jm} | A | \Phi_{j_1' j_2'}^{j'm'} \rangle = \langle j_1 j_2 jm | A | j_1' j_2' j' m' \rangle \qquad \text{[A4.36]}$$

and

$$\int \mathrm{d}\Omega_1 \int \mathrm{d}\Omega_2\, \mathcal{Y}_{l_1 l_2}^{lm*}(\theta_1 \phi_1;\, \theta_2 \phi_2) A \mathcal{Y}_{l_1' l_2'}^{l'm'}(\theta_1 \phi_1;\, \theta_2 \phi_2)$$
$$= \langle l_1 l_2 lm | A | l_1' l_2' l' m' \rangle \qquad \text{[A4.37]}$$

where A is an operator. The defining relation of the Clebsch–Gordan coefficients [A4.31] can then be written as

$$|j_1 j_2 jm\rangle = \sum_{m_1 m_2} \langle j_1 j_2 m_1 m_2 | jm \rangle |j_1 m_1\rangle \times |j_2 m_2\rangle \qquad \text{[A4.38]}$$

Integrals of products of spherical harmonics

It can be shown that the product $Y_{l_1m_1}(\theta, \phi)Y_{l_2m_2}(\theta, \phi)$ can be expressed as a series by

$$Y_{l_1m_1}(\theta, \phi)Y_{l_2m_2}(\theta, \phi) = \sum_{l=|l_1-l_2|}^{l_1+l_2} \sum_{m=-l}^{l} \left[\frac{(2l_1+1)(2l_2+1)}{4\pi(2l+1)}\right]^{1/2} \times \langle l_1l_200|l0\rangle\langle l_1l_2m_1m_2|lm\rangle Y_{lm}(\theta, \phi) \quad \text{[A4.39]}$$

This enables us to evaluate the integral of a product of three spherical harmonics. Using [2.181b] and the orthonormality property [A4.18] we have

$$\int Y_{l_1m_1}(\theta, \phi)Y_{l_2m_2}(\theta, \phi)Y_{l_3m_3}(\theta, \phi)\, d\Omega = (-1)^{m_3}\left[\frac{(2l_1+1)\,(2l_2+1)}{4\pi(2l_3+1)}\right]^{1/2} \langle l_1l_200|l_30\rangle\langle l_1l_2m_1m_2|l_3 -m_3\rangle \quad \text{[A4.40]}$$

Scalar and vector operators

A scalar operator $\mathscr{S}$ is one for which the expectation values $\langle\phi|\mathscr{S}|\phi\rangle$ are unaltered by a rotation of the coordinate system. It can be shown (Powell and Crasemann, 1962; Merzbacher, 1970) that for an operator to be scalar it must commute with all components of the total angular momentum operator $\mathbf{J}$:

$$[\mathscr{S}, \mathbf{J}] = 0 \quad \text{[A4.41]}$$

from which it follows that if ψ_{jm} is a simultaneous eigenfunction of $\mathbf{J}^2$ and $\mathscr{J}_z$ belonging to the quantum numbers j and m, then $\langle\psi_{jm}|\mathscr{S}|\psi_{j'm'}\rangle$ vanishes unless $j = j'$ and $m = m'$, and

$$\mathscr{S}\psi_{jm} = \lambda\psi_{jm} \quad \text{[A4.42]}$$

where λ is an eigenvalue of $\mathscr{S}$. Since $\mathscr{J}_+\psi_{jm} = N\psi_{jm+1}$ and as $[\mathscr{J}_+, \mathscr{S}] = 0$, we must also have

$$\mathscr{S}\psi_{jm+1} = \lambda\psi_{jm+1} \quad \text{[A4.43]}$$

so the eigenvalue λ is independent of m (but it does depend on j).

In general, wave functions depend on other quantum numbers in addition to angular momentum quantum numbers (for example, principal quantum numbers). Denoting these other quantum numbers collectively by α, we see that

$$\langle\phi_{\alpha jm}|\mathscr{S}|\phi_{\alpha'j'm'}\rangle \equiv \langle\alpha jm|\mathscr{S}|\alpha'j'm'\rangle = \lambda_{j\alpha\alpha'}\delta_{jj'}\delta_{mm'} \quad \text{[A4.44]}$$

This is the simplest example of the fact that matrix elements of operators having well-defined properties under rotations depend upon the magnetic quantum numbers through a 'geometrical' factor (equal in the present case to $\delta_{mm'}$) which is independent of the dynamics of the system.

In this book, we are mainly concerned with *vector operators*, of which the components transform like the components of a vector under rotations. The condition for an operator $\mathbf{V}$ with components V_x, V_y, V_z to be a vector operator is that it satisfies the commutation relations [5.71]. It is useful to define the spherical components of $\mathbf{V}$ as

$$V_1 = -\frac{1}{\sqrt{2}}(V_x + iV_y); \qquad V_0 = V_z; \qquad V_{-1} = \frac{1}{\sqrt{2}}(V_x - iV_y) \quad \text{[A4.45]}$$

The set of three operators V_q ($q = -1, 0, +1$) satisfies the commutation relations (which follow from [5.71])

$$\begin{aligned} [J_z, V_q] &= q\hbar V_q \\ [J_+, V_q] &= [(1-q)(2+q)]^{1/2}\hbar V_{q+1} \\ [J_-, V_q] &= [(1+q)(2-q)]^{1/2}\hbar V_{q-1} \end{aligned} \qquad \text{[A4.46]}$$

where $V_q = 0$ if $q \neq 0, \pm 1$. The operators V_q are special cases of *irreducible tensor operators* T_q^k of rank k, which form a set of $(2k + 1)$ operators with q running over the values $-k, -k + 1, \ldots k - 1, k$, and satisfying the commutation relations

$$\begin{aligned} [J_z, T_q^k] &= q\hbar T_q^k \\ [J_+, T_q^k] &= [(k-q)(k+q+1)]^{1/2}\hbar T_{q+1}^k \\ [J_-, T_q^k] &= [(k+q)(k-q+1)]^{1/2}\hbar T_{q-1}^k \end{aligned} \qquad \text{[A4.47]}$$

For such operators, the matrix elements between eigenfunctions ψ_{jm} and $\psi_{j'm'}$ depend on m and m' only through a factor which can be shown to be equal to the Clebsch–Gordan coefficient $\langle jkmq|j'm'\rangle$. Thus

$$\langle \alpha' j' m' | T_q^k | \alpha j m \rangle = \frac{1}{\sqrt{2j'+1}} \langle jkmq|j'm'\rangle \langle \alpha' j' \| T^k \| \alpha j \rangle \quad \text{[A4.48]}$$

where the reduced matrix element $\langle \alpha' j' \| T^k \| \alpha j \rangle$ is a number depending on $\alpha\alpha' jj'$ but not on m and m'. This result is called the *Wigner–Eckart theorem*. It should be noticed that the appearance of the factor $(2j' + 1)^{-1/2}$ on the right-hand side of [A4.48] is conventional; it could be absorbed into the reduced matrix element.

The application of the Wigner–Eckart theorem to a scalar operator $\mathcal{S} = T_0^0$ reproduces the result [A4.44]. For vector operators we have $V_q \equiv T_q^1$. As an example of a vector operator we can take the total angular momentum, $\mathbf{J}$. Then definining J_q by using [A4.45] with J in place of V we have,

$$\langle \alpha' j' m' | J_q | \alpha j m \rangle = \frac{1}{\sqrt{2j'+1}} \langle j1mq|j'm'\rangle \langle \alpha' j' \| J_q \| \alpha j \rangle \qquad \text{[A4.49]}$$

Setting $q = 0$ and noting that $J_0 \equiv J_z$, we find by using Table A4.1 that

$$\langle \alpha' j' \| J \| \alpha j \rangle = \sqrt{j(j+1)}\hbar \, \delta_{jj'} \, \delta_{\alpha\alpha'} \qquad \text{[A4.50]}$$

It follows from [A4.48] that if **V** is any vector operator then

$$\langle \alpha' j' m' | \mathbf{V} | \alpha j m \rangle = C \langle \alpha' j' m' | \mathbf{J} | \alpha j m \rangle \qquad \text{[A4.51]}$$

where C is independent of m and m'. For the case $j' = j$, $\alpha' = \alpha$, C can be found by writing

$$\langle \alpha j m | \mathbf{V} \cdot \mathbf{J} | \alpha j m \rangle = \sum_{m'} \langle \alpha j m | \mathbf{V} | \alpha j m' \rangle \cdot \langle \alpha j m' | \mathbf{J} | \alpha j m \rangle \qquad \text{[A4.52]}$$

where we have used the closure property

$$\sum_{m'} | \alpha j m' \rangle \langle \alpha j m' | = 1 \qquad \text{[A4.53]}$$

Thus

$$\begin{aligned} \langle \alpha j m | \mathbf{V} \cdot \mathbf{J} | \alpha j m \rangle &= C \sum_{m'} \langle \alpha j m | \mathbf{J} | \alpha j m' \rangle \cdot \langle \alpha j m' | \mathbf{J} | \alpha j m \rangle \\ &= C \langle \alpha j m | \mathcal{J}^2 | \alpha j m \rangle \\ &= C j(j+1)\hbar^2 \end{aligned} \qquad \text{[A4.54]}$$

Using [A4.51], we then obtain the useful equation

$$\begin{aligned} j(j+1)\hbar^2 \langle \alpha j m' | \mathbf{V} | \alpha j m \rangle &= \langle \alpha j m | \mathbf{V} \cdot \mathbf{J} | \alpha j m \rangle \langle \alpha j m' | \mathbf{J} | \alpha j m \rangle \\ &= \langle \alpha j m' | (\mathbf{V} \cdot \mathbf{J}) \mathbf{J} | \alpha j m \rangle \end{aligned} \qquad \text{[A4.55]}$$

which relates the expectation values of the components of **V** to those of the components of **J**.

5 Hydrogenic wave functions in momentum space

We have seen in Section 2.1 that the wave function in momentum space, $\phi(\mathbf{p})$, is defined as the Fourier transform of the ordinary wave function $\psi(\mathbf{r})$ in position space. That is,

$$\phi(\mathbf{p}) = (2\pi\hbar)^{-3/2} \int e^{-i\mathbf{p}\cdot\mathbf{r}/\hbar}\psi(\mathbf{r})\, d\mathbf{r} \qquad [A5.1]$$

The wave function $\psi(\mathbf{r})$ may be deduced from $\phi(\mathbf{p})$ by the inverse Fourier transform

$$\psi(\mathbf{r}) = (2\pi\hbar)^{-3/2} \int e^{i\mathbf{p}\cdot\mathbf{r}/\hbar}\phi(\mathbf{p})\, d\mathbf{p} \qquad [A5.2]$$

In what follows we shall use atomic units (see Appendix 11), the unit of length being a_0 and the unit of momentum being $p_0 = \hbar/a_0$. In these units equations [A5.1] and [A5.2] become simply

$$\phi(\mathbf{p}) = (2\pi)^{-3/2} \int e^{-i\mathbf{p}\cdot\mathbf{r}}\psi(\mathbf{r})\, d\mathbf{r} \qquad [A5.3]$$

and

$$\psi(\mathbf{r}) = (2\pi)^{-3/2} \int e^{i\mathbf{p}\cdot\mathbf{r}}\phi(\mathbf{p})\, d\mathbf{p} \qquad [A5.4]$$

We note that if $\psi(\mathbf{r})$ is normalised to unity, i.e.

$$\int |\psi(\mathbf{r})|^2\, d\mathbf{r} = 1 \qquad [A5.5]$$

we have from [A5.4]

$$\int d\mathbf{r}\, \psi^\star(\mathbf{r})\psi(\mathbf{r}) = (2\pi)^{-3} \int d\mathbf{r} \int d\mathbf{p} \int d\mathbf{p}' e^{i(\mathbf{p}-\mathbf{p}')\cdot\mathbf{r}}\phi^\star(\mathbf{p}')\phi(\mathbf{p}) = 1 \qquad [A5.6]$$

and since

$$(2\pi)^{-3} \int \mathrm{d}\mathbf{r}\ \mathrm{e}^{i(\mathbf{p}-\mathbf{p}')\cdot\mathbf{r}} = \delta(\mathbf{p}-\mathbf{p}') \qquad [A5.7]$$

we see that

$$\int \mathrm{d}\mathbf{p} \int \mathrm{d}\mathbf{p}'\ \delta(\mathbf{p}-\mathbf{p}')\phi^{\star}(\mathbf{p}')\phi(\mathbf{p}) = 1 \qquad [A5.8]$$

Using the definition [2.28] of the Dirac δ-function, this last equation reduces to

$$\int |\phi(\mathbf{p})|^2\ \mathrm{d}\mathbf{p} = 1 \qquad [A5.9]$$

so that the wave function $\phi(\mathbf{p})$ is also normalised to unity.

Before using [A5.3] for a direct calculation of hydrogenic wave functions in momentum space, it is instructive to rewrite the Schrödinger equation itself in momentum space, namely as an equation involving $\phi(\mathbf{p})$ directly. Neglecting for the moment the reduced mass effect, we begin by considering an electron (of mass $m = 1$ in a.u.) in an arbitrary real potential $V(\mathbf{r})$. The corresponding time-independent Schrödinger equation in position space reads

$$\left[\frac{p^2}{2} + V(\mathbf{r})\right]\psi(\mathbf{r}) = E\psi(\mathbf{r}) \qquad [A5.10]$$

We assume that $E < 0$, so that we are considering only the bound states. Premultiplying both sides by $(2\pi)^{-3/2}\exp(-i\mathbf{p}\cdot\mathbf{r})$ and integrating over all space, we find by using [A5.3] that

$$\frac{p^2}{2}\phi(\mathbf{p}) + (2\pi)^{-3/2}\int \mathrm{e}^{-i\mathbf{p}\cdot\mathbf{r}}V(\mathbf{r})\psi(\mathbf{r})\ \mathrm{d}\mathbf{r} = E\phi(\mathbf{p}) \qquad [A5.11]$$

Making use of [A5.4] and introducing the quantity

$$\tilde{V}(\mathbf{p}-\mathbf{p}') = (2\pi)^{-3}\int \mathrm{e}^{-i(\mathbf{p}-\mathbf{p}')\cdot\mathbf{r}}V(\mathbf{r})\ \mathrm{d}\mathbf{r} \qquad [A5.12]$$

we see that [A5.10] reduces to

$$\left[\frac{p^2}{2} - E\right]\phi(\mathbf{p}) = -\int \tilde{V}(\mathbf{p}-\mathbf{p}')\phi(\mathbf{p}')\ \mathrm{d}\mathbf{p}' \qquad [A5.13]$$

which is the required Schrödinger equation in momentum space (in a.u.). We note that it is an integral equation for $\phi(\mathbf{p})$.

If the potential $V(\mathbf{r})$ is central (i.e. depends only on $r = |\mathbf{r}|$) the 'potential' $\tilde{V}(\mathbf{p}-\mathbf{p}')$ in momentum space may be simplified by setting $\mathbf{q} = \mathbf{p}' - \mathbf{p}$ and performing the integral in [A5.12] in spherical polar coordinates, with the polar

axis in the direction of the vector $\mathbf{q}$. That is,

$$\tilde{V}(\mathbf{p}-\mathbf{p}') = (2\pi)^{-3}\int_0^\infty \mathrm{d}r r^2 \int_0^\pi \mathrm{d}\theta \sin\theta \int_0^{2\pi} \mathrm{d}\phi\, \mathrm{e}^{iqr\cos\theta} V(r)$$

$$= (2\pi)^{-2}\int_0^\infty \mathrm{d}r r^2 V(r) \int_0^\pi \mathrm{d}\theta \sin\theta\, \mathrm{e}^{iqr\cos\theta}$$

$$= (2\pi^2 q)^{-1}\int_0^\infty \mathrm{d}r\, r \sin(qr) V(r) \qquad [A5.14]$$

Thus we see that when $V(\mathbf{r})$ is central the quantity $\tilde{V}$ is real and depends only on q, i.e. on $|\mathbf{p}-\mathbf{p}'|$. It is worth noting that the result [A5.14] may also be obtained by using the expansion of a plane wave in Legendre polynomials (see [2.260]), i.e.

$$\mathrm{e}^{i\mathbf{q}\cdot\mathbf{r}} = \sum_{l=0}^{\infty} (2l+1) i^l j_l(qr) P_l(\cos\theta) \qquad [A5.15]$$

so that [A5.12] becomes

$$\tilde{V}(\mathbf{p}-\mathbf{p}') = (2\pi)^{-2}\sum_{l=0}^{\infty}(2l+1)\, i^l \int_0^\infty \mathrm{d}r r^2 j_l(qr) V(r)$$

$$\times \int_0^\pi \mathrm{d}\theta \sin\theta\, P_l(\cos\theta) \qquad [A5.16]$$

Since

$$\int_0^\pi \mathrm{d}\theta \sin\theta\, P_l(\cos\theta) P_{l'}(\cos\theta) = \frac{2}{2l+1}\,\delta_{ll'} \qquad [A5.17]$$

and $P_0 = 1$, we see that all the terms of the sum on the right of [A5.16] vanish, except the first one (for which $l = 0$). Hence $\tilde{V}(\mathbf{p}-\mathbf{p}')$ reduces to

$$\tilde{V}(|\mathbf{p}-\mathbf{p}'|) = (2\pi^2)^{-1}\int_0^\infty \mathrm{d}r r^2 j_0(qr) V(r) \qquad [A5.18]$$

which agrees with [A5.14] since $j_0(qr) = \sin(qr)/qr$.

For a central potential $V(r)$ the Schrödinger equation [A5.10] admits solutions of the form $\psi(\mathbf{r}) = R_{E,l}(r) Y_{lm}(\theta, \phi)$. Similarly, if we denote by (p, θ_p, ϕ_p) the polar coordinates of the momentum $\mathbf{p}$, solutions of the Schrödinger equation in momentum space [A5.13] exist of the form

$$\phi(\mathbf{p}) = F_{E,l}(p) Y_{lm}(\theta_p, \phi_p) \qquad [A5.19]$$

This may be checked directly by returning to the definition [A5.3] of $\phi(\mathbf{p})$, substituting in it $\psi(\mathbf{r}) = R_{E,l}(r) Y_{lm}(\theta, \phi)$ and using the expansion of a plane

wave in spherical harmonics (see [2.261]). Explicitly, we have

$$\phi(\mathbf{p}) = (2\pi)^{-3/2} 4\pi \sum_{l'=0}^{\infty} \sum_{m'=-l'}^{+l'} (-i)^{l'} Y_{l'm'}(\theta_p, \phi_p)$$
$$\times \int_0^\infty \mathrm{d}r r^2 j_{l'}(pr) R_{E,l'}(r) \int_0^\pi \mathrm{d}\theta \sin\theta \int_0^{2\pi} \mathrm{d}\phi\, Y^{\star}_{l'm'}(\theta, \phi) Y_{lm}(\theta, \phi) \quad [A5.20]$$

Using the orthonormality of the spherical harmonics, we see that [A5.20] reduces to [A5.19], with

$$F_{E,l}(p) = N_l \int_0^\infty r^2 j_l(pr) R_{E,l}(r)\, \mathrm{d}r \quad [A5.21]$$

N_l being a normalisation constant. We note that $F_{E,l}$ does not depend on the magnetic quantum number m. The quantity $|pF_{E,l}(p)|^2$ is called the *momentum distribution function*. The probability that the absolute value of the momentum lies between p and $p + \mathrm{d}p$ (independently of the direction) is given by $|pF_{E,l}(p)|^2\, \mathrm{d}p$ and we have

$$\int_0^\infty p^2 |F_{E,l}(p)|^2\, \mathrm{d}p = 1 \quad [A5.22]$$

A one-dimensional integral equation for $F_{E,l}(p)$ may readily be obtained from the Schrödinger equation in momentum space [A5.13] by using [A5.19] and expanding $\tilde{V}(|\mathbf{p} - \mathbf{p}'|)$ in Legendre polynomials. That is,

$$\tilde{V}(|\mathbf{p} - \mathbf{p}'|) = \sum_{l=0}^{\infty} T_l(p, p') P_l(x) \quad [A5.23]$$

with $x = \mathbf{p} \cdot \mathbf{p}'/pp'$ and

$$T_l(p, p') = \frac{2l+1}{2} \int_{-1}^{+1} P_l(x) \tilde{V}(|\mathbf{p} - \mathbf{p}'|)\, \mathrm{d}x \quad [A5.24]$$

The result is

$$\left[\frac{p^2}{2} - E\right] F_{E,l}(p) = -\int_0^\infty p'^2 K_l(p, p') F_{E,l}(p')\, \mathrm{d}p' \quad [A5.25]$$

where

$$K_l(p, p') = 2\pi \int_{-1}^{+1} \tilde{V}([p^2 + p'^2 - 2pp'x]^{1/2}) P_l(x)\, \mathrm{d}x \quad [A5.26]$$

is a symmetric kernel in p and p'.

Before we examine the particular case of the Coulomb potential, it is interesting to look at a screened Coulomb interaction which we write (in a.u.) as

$$V(r) = -\frac{Z}{r}\mathrm{e}^{-\alpha r}, \qquad \alpha > 0 \tag{A5.27}$$

Using [A5.14], the corresponding potential $\tilde{V}$ in momentum space is easily obtained,

$$\tilde{V}(q) = -\frac{Z}{2\pi^2}\frac{1}{q^2+\alpha^2} \tag{A5.28}$$

where $q = |\mathbf{p} - \mathbf{p}'|$. The Coulomb potential $V(r) = -Z/r$ (in a.u.) may be considered as a limiting case of [A5.27] for which $\alpha \to 0$. Letting α tend to zero in [A5.28] we obtain

$$\tilde{V}(q) = -\frac{Z}{2\pi^2}\frac{1}{q^2} \tag{A5.29}$$

We note that this expression is singular at $q = 0$. By comparing [A5.28] and [A5.29] we see that this singularity may be traced to the 'infinite range' of the Coulomb potential, which in turn is due to the fact that the photon has zero mass.

Using the expression [A5.29] for $\tilde{V}(q)$, the kernel $K_l(p, p')$ given by [A5.26] becomes

$$\begin{aligned} K_l(p, p') &= -\frac{Z}{\pi}\frac{1}{2pp'}\int_{-1}^{+1}\frac{1}{(p^2+p'^2)/2pp' - x}P_l(x)\,\mathrm{d}x \\ &= -\frac{Z}{\pi}\frac{1}{2pp'}Q_l\left(\frac{p^2+p'^2}{2pp'}\right) \end{aligned} \tag{A5.30}$$

where Q_l is the Legendre function of the second kind, such that

$$Q_l(z) = \frac{1}{2}\int_{-1}^{+1}\frac{1}{z-x}P_l(x)\,\mathrm{d}x \tag{A5.31}$$

The first few functions $Q_l(z)$ are given by

$$\begin{aligned} Q_0(z) &= \frac{1}{2}\log\left(\frac{z+1}{z-1}\right) \\ Q_1(z) &= \frac{z}{2}\log\left(\frac{z+1}{z-1}\right) - 1 \\ Q_2(z) &= \frac{1}{4}(3z^2-1)\log\left(\frac{z+1}{z-1}\right) - \frac{3z}{2}, \quad \text{etc.} \end{aligned} \tag{A5.32}$$

Substituting [A5.30] in [A5.25], we then obtain for the case of the Coulomb

potential the one-dimensional integral equation

$$\left[\frac{p^2}{2} - E\right]F_{E,l}(p) = \frac{Z}{\pi p}\int_0^\infty p' Q_l\left(\frac{p^2 + p'^2}{2pp'}\right)F_{E,l}(p')\,\mathrm{d}p' \qquad \text{[A5.33]}$$

This equation has been solved by Fock. For $E < 0$ it has discrete eigenvalues E_n which are of course identical to those which we obtained in Chapter 3 by solving the Schrödinger equation in position space. By analogy with the radial hydrogenic wave functions $R_{nl}(r)$, we shall denote the 'radial' hydrogenic momentum space wave functions by $F_{nl}(p)$ instead of $F_{E,l}(p)$.

The 'radial' functions $F_{nl}(p)$, corresponding to the hydrogen atom, obtained either by performing directly the Fourier transformation (see [A5.3] and [A5.21]) or by solving the radial momentum space equation [A5.33] and normalised according to [A5.22], are given (in a.u.) by

$$F_{nl}(p) = \left[\frac{2}{\pi}\frac{(n-l-1)!}{(n+l)!}\right]^{1/2} n^2 2^{2l+2} l!$$
$$\times \frac{n^l p^l}{(n^2p^2+1)^{l+2}} C^{l+1}_{n-l-1}\left(\frac{n^2p^2-1}{n^2p^2+1}\right) \qquad \text{[A5.34]}$$

where $C_N^\alpha(\alpha)$ denotes the Gegenbauer polynomial, defined by the relation

$$(1 - 2xs + s^2)^{-\alpha} = \sum_{N=0}^{\infty} C_N^\alpha(x)s^N, \qquad |s| < 1 \qquad \text{[A5.35]}$$

For other hydrogenic atoms corresponding to a nucleus of charge Z the expressions for $F_{nl}(p)$ are identical, provided that p is expressed in units of Zp_0. The reduced mass effect is also easily taken into account by using 'reduced' units such that $p_0 = \hbar/a_0$ is replaced by $p_\mu = \hbar/a_\mu$, with $a_\mu = a_0(m/\mu)$ and μ being the reduced mass.

Let us write down the first few radial momentum space wave functions explicitly. Using the fact that

$$\begin{aligned} C_0^\alpha(x) &= 1, \\ C_1^\alpha(x) &= 2\alpha x, \\ C_2^\alpha(x) &= 2\alpha(\alpha+1)x^2 - \alpha \end{aligned} \qquad \text{[A5.36]}$$

we find that

$$F_{10}(p) = \frac{2^{5/2}}{\sqrt{\pi}}\frac{1}{(p^2+1)^2}$$

$$F_{20}(p) = \frac{32}{\sqrt{\pi}}\frac{4p^2-1}{(4p^2+1)^3}$$

$$F_{21}(p) = \frac{128}{\sqrt{3\pi}} \frac{p}{(4p^2 + 1)^3}$$

$$F_{30}(p) = \frac{108\sqrt{2}}{\sqrt{3\pi}} \frac{81p^4 - 30p^2 + 1}{(9p^2 + 1)^4}$$

$$F_{31}(p) = \frac{864}{\sqrt{3\pi}} \frac{p(9p^2 - 1)}{(9p^2 + 1)^4}$$

$$F_{32}(p) = \frac{5184}{\sqrt{15\pi}} \frac{p^2}{(9p^2 + 1)^4} \qquad \text{[A5.37]}$$

We note that in contrast with the position space hydrogenic radial functions $R_{nl}(r)$, which fall off *exponentially* at large r, the radial momentum space wave functions $F_{nl}(p)$ behave like *inverse powers* of p for large p. In particular, we see that for s-states ($l = 0$) they decrease like p^{-4} at large p, for p-states ($l = 1$) they fall off like p^{-5}, etc. More generally, since the argument of the Gegenbauer polynomial in [A5.34] is just $+1$ when $p \to \infty$, we see that $F_{nl}(p)$ is proportional to $p^{-(l+4)}$ when p is large.

When p tends to zero the argument of the Gegenbauer polynomial in [A5.34] is -1 and we may use the fact that

$$\begin{aligned} C_N^{\alpha}(-1) &= (-1)^N C_N^{\alpha}(1) \\ &= (-1)^N \frac{(2\alpha + N - 1)!}{(2\alpha - 1)!N!} \end{aligned} \qquad \text{[A5.38]}$$

to deduce that for s states ($l = 0$)

$$F_{n0}(0) = (-1)^{n-1} 4\left(\frac{2}{\pi}\right)^{1/2} n^{5/2} \qquad \text{[A5.39]}$$

For $l \neq 0$ we see from [A5.34] that F_{nl} vanishes in the limit $p \to 0$.

We recall that in all the expressions of $F_{nl}(p)$ written above the variable p is expressed in units of Zp_0. If we want to use other units, we should simply make the substitution $p \to p/Zp_0$ in [A5.34] and recall that the normalisation condition [A5.22] introduces an extra factor of $(Zp_0)^{-3/2}$ in $F_{nl}(p)$. For example, the wave function $F_{10}(p)$ then becomes

$$F_{10}(p) = \frac{2^{5/2}}{\sqrt{\pi}} (Zp_0)^{5/2} \frac{1}{(p^2 + Z^2p_0^2)^2} \qquad \text{[A5.40]}$$

Wave functions in momentum space are particularly useful to evaluate matrix elements involving various functions of p. For example, let us evaluate the average value of p^2 when the hydrogenic atom is in the ground state. We then have

$$\begin{aligned} \langle p^2 \rangle_{100} &= \int_0^{\infty} p^2 |pF_{10}(p)|^2 \, \mathrm{d}p \\ &= (Zp_0)^2 = (Z\hbar/a_0)^2 \end{aligned} \qquad \text{[A5.41]}$$

where we have used [A5.40]. For a general hydrogenic state $\phi_{nlm}(\mathbf{p}) = F_{nl}(p)Y_{lm}(\theta_p, \phi_p)$ one finds from [A5.34] that

$$\langle p^2 \rangle_{nlm} = (Zp_0/n)^2 = (Z\hbar/na_0)^2 \qquad \text{[A5.42]}$$

In order to include the reduced mass effect we just have to replace a_0 by $a_\mu = a_0(m/\mu) = 4\pi\varepsilon_0\hbar^2/\mu e^2$. The average value of the kinetic energy operator $T = p^2/2\mu$ is therefore given by

$$\begin{aligned} \langle T \rangle_{nlm} &= \frac{1}{2\mu}(Z\hbar/na_\mu)^2 \text{ a.u.} \\ &= \frac{e^2}{(4\pi\varepsilon_0)a_\mu} \frac{Z^2}{2n^2} \end{aligned} \qquad \text{[A5.43]}$$

in agreement with the result [3.76] of Chapter 3 and with the virial theorem proved in Section 3.4.

6 The Hamiltonian for a charged particle in an electromagnetic field

We start from Lagrange's equations of motion (Goldstein, 1962)

$$\frac{\mathrm{d}}{\mathrm{d}t}\left(\frac{\partial L}{\partial \dot{q}_i}\right) - \frac{\partial L}{\partial q_i} = 0 \quad i = 1, 2, \ldots \tag{A6.1}$$

where q_i are generalised coordinates and L is the Lagrangian function. For a conservative system, $L = T - V$, where T is the kinetic energy and V is the potential energy. Since the electromagnetic field is not conservative, a generalisation is required. We have to find L such that [A6.1] provides the equation of motion of a particle of mass m, charge q and velocity $\mathbf{v}$ in an electromagnetic field specified by the electric field $\boldsymbol{\mathscr{E}}(\mathbf{r}, t)$ and the magnetic field $\boldsymbol{\mathscr{B}}(\mathbf{r}, t)$ and subject to the Lorentz force

$$\begin{aligned}\mathbf{F} &= q(\boldsymbol{\mathscr{E}} + \mathbf{v} \times \boldsymbol{\mathscr{B}}) \\ &= q\left[-\boldsymbol{\nabla}\phi - \frac{\partial \mathbf{A}}{\partial t} + \mathbf{v} \times (\boldsymbol{\nabla} \times \mathbf{A})\right]\end{aligned} \tag{A6.2}$$

where $\phi(\mathbf{r}, t)$ and $\mathbf{A}(\mathbf{r}, t)$ are respectively the scalar and vector electromagnetic potentials.

This can be achieved if we take L to be

$$L = \frac{1}{2} mv^2 - q\phi + q\mathbf{v} \cdot \mathbf{A} \tag{A6.3}$$

and work in a Cartesian system of coordinates, so that $q_1 = x$, $q_2 = y$ and $q_3 = z$. It is then easily shown that the equation [A6.1] reduces to the equation of motion

$$m\ddot{\mathbf{r}} = \mathbf{F} \tag{A6.4}$$

where the force $\mathbf{F}$ is given by [A6.2].

The generalised momenta are defined as

$$p_i = \frac{\partial L}{\partial \dot{q}_i} \tag{A6.5}$$

Using the Lagrangian L given by [A6.3], one finds that $p_1 = p_x$, $p_2 = p_y$ and $p_3 = p_z$, where p_x, p_y and p_z are the components of the vector $\mathbf{p}$, given by

$$\mathbf{p} = m\mathbf{v} + q\mathbf{A} \qquad \text{[A6.6]}$$

The Hamiltonian H is defined by

$$H = \sum_{i=1}^{3} p_i \dot{q}_i - L \qquad \text{[A6.7]}$$

and in terms of $\mathbf{p}$, $\mathbf{A}$ and ϕ we have

$$H = \frac{1}{2m}(\mathbf{p} - q\mathbf{A})^2 + q\phi \qquad \text{[A6.8]}$$

7 The Dirac equation and relativistic corrections to the Schrödinger equation

In our discussion of atomic structure and of the interaction of atoms with external electromagnetic fields, we have introduced various interactions which are approximations to a complete relativistic theory and which could not be derived, without additional assumptions, from the non-relativistic Schrödinger equation for an atom interacting with an electromagnetic field. In this appendix, we shall show how the spin-dependent interactions as well as other terms in the Hamiltonian can be derived from Dirac's relativistic theory of the electron. Although the theory we shall discuss provides a highly accurate description of atomic structure, it is still an approximation to a fully self-consistent relativistic theory, because it does not allow for interactions in which the number of particles in a system changes. These interactions are characteristic of relativistic field theory, and are needed to provide a description of processes such as those in which photons turn into electron–positron pairs, or the reverse process, in which electron–positron pairs annihilate into photons.

The Schrödinger relativistic equation or Klein–Gordon equation

At the time when he was developing his non-relativistic wave equation, Schrödinger also proposed a relativistic generalisation of it, which is known as the *Schrödinger relativistic equation* or *Klein–Gordon equation*.

Free particle

We begin by considering the case of a free particle. The relativistic relationship between the energy E and momentum $\mathbf{p}$ of a free particle of rest mass m is

$$E^2 = m^2c^4 + \mathbf{p}^2c^2 \qquad \text{[A7.1]}$$

Adopting for E and $\mathbf{p}$ the substitutions (see [2.11])

$$E \to i\hbar\frac{\partial}{\partial t}, \qquad \mathbf{p} \to -i\hbar\nabla \qquad \text{[A7.2]}$$

and operating on a wave function $\Psi(\mathbf{r}, t)$, we obtain the Schrödinger relativistic

equation (or Klein–Gordon equation) for a free particle, namely

$$-\hbar^2 \frac{\partial^2 \Psi}{\partial t^2} = m^2c^4\Psi - \hbar^2c^2\nabla^2\Psi \qquad [A7.3]$$

It is worth noting that this is a second order differential equation with respect to the time.

If the wave function Ψ is taken to have a single component, this equation describes a free particle with no internal degrees of freedom, and is a suitable equation for the description of a free particle of spin-zero.

Charged particle in an electromagnetic field

If the spinless particle has an electric charge q, and it is placed in an external electromagnetic field described by a vector potential $\mathbf{A}$ and a scalar potential ϕ, we can make the replacements (see Appendix 6)

$$\mathbf{p} \rightarrow \mathbf{p} - q\mathbf{A}, \qquad E \rightarrow E - q\phi \qquad [A7.4]$$

so that [A7.1] is replaced by

$$(E - q\phi)^2 = m^2c^4 + c^2(\mathbf{p} - q\mathbf{A})^2 \qquad [A7.5]$$

Using the substitutions [A7.2], we then obtain the Klein–Gordon equation for a spinless particle of charge q in an electromagnetic field,

$$\left(i\hbar \frac{\partial}{\partial t} - q\phi\right)^2 \Psi = m^2c^4\Psi + c^2(-i\hbar\nabla - q\mathbf{A})^2\Psi \qquad [A7.6]$$

In order to investigate the non-relativistic limit of this equation, we introduce the new function $X(\mathbf{r}, t)$ which is related to Ψ by

$$X(\mathbf{r}, t) = \Psi(\mathbf{r}, t)e^{imc^2t/\hbar} \qquad [A7.7]$$

and satisfies the equation

$$-\hbar^2 \frac{\partial^2 X}{\partial t^2} + 2i\hbar(mc^2 - q\phi)\frac{\partial X}{\partial t} - \left[q\phi(2mc^2 - q\phi) + i\hbar q\frac{\partial \phi}{\partial t}\right]X$$
$$= c^2[-\hbar^2\nabla^2 + 2i\hbar q\mathbf{A}\cdot\nabla + i\hbar q(\nabla\cdot\mathbf{A}) + q^2\mathbf{A}^2]X \qquad [A7.8]$$

In the limit in which $|q\phi| \ll mc^2$, $|(\hbar/2mc^2)\partial\phi/\partial t| \ll |\phi|$ and $|(\hbar^2/2mc^2)\partial^2 X/\partial t^2| \ll |\hbar\partial X/\partial t|$, this equation reduces to the non-relativistic Schrödinger equation for a spinless particle in an electromagnetic field, namely

$$i\hbar\frac{\partial X}{\partial t} = \left[\frac{1}{2m}(-i\hbar\nabla - q\mathbf{A})^2 + q\phi\right]X \qquad [A7.9]$$

This is the equation we used in Chapter 4 (see [4.17]) with $q = -e$ and $q\phi = V(r) = -Ze^2/(4\pi\varepsilon_0)r$.

The Dirac equation

To describe a particle of spin-1/2, we require a wave function having two components which allow for the two spin states, the z-component S_z of the spin angular momentum taking on the values $m_s\hbar$, where $m_s = \pm 1/2$. However, since all spin-1/2 particles are associated with particles of the same mass and spin, but of opposite charge, known as antiparticles, we expect to need a four-component wave function. This was unknown when Dirac put forward his equation, and it was one of the great achievements of theoretical physics that Dirac was able to predict the existence of the positron, the anti-particle of the electron, from his theory.

Dirac started by looking for a wave equation of the form

$$i\hbar \frac{\partial}{\partial t} \Psi = H\Psi \qquad \text{[A7.10]}$$

which like the (non-relativistic) Schrödinger equation [2.46] is *linear* in $\partial/\partial t$, and not quadratic like the Klein–Gordon equation. Since in a relativistic theory the spatial [1] coordinates (x_1, x_2, x_3) must enter on the same footing as $x_0 = ct$, the equation [A7.10] – and hence the Hamiltonian H – is expected to be linear in the space derivatives $\partial/\partial x_k$ $(k = 1, 2, 3)$. The wave function in [A7.10] is assumed to contain N components Ψ_i $(i = 1, 2, \ldots N)$ and hence may be written in the form of a column matrix as

$$\Psi = \begin{pmatrix} \Psi_1 \\ \Psi_2 \\ \cdot \\ \cdot \\ \cdot \\ \Psi_N \end{pmatrix} \qquad \text{[A7.11]}$$

Free particle

Let us first consider the case of a free particle. The Hamiltonian must then be independent of $\mathbf{r}$ and t (since there are no forces) and the simplest candidate, linear in the momentum and mass terms, may be written in the form

$$H = c\boldsymbol{\alpha} \cdot \mathbf{p} + \beta mc^2 \qquad \text{[A7.12]}$$

where $\mathbf{p} = -i\hbar\boldsymbol{\nabla}$ according to the correspondence rule [A7.2]. The three components $(\alpha^1, \alpha^2, \alpha^3)$ of $\boldsymbol{\alpha}$ as well as the quantity β are independent of $\mathbf{r}$, t, $\mathbf{p}$ and E, but need not commute with each other.

Substituting [A7.12] into [A7.10] and remembering that $E = i\hbar\partial/\partial t$, we obtain the Dirac wave equation

$$(E - c\boldsymbol{\alpha} \cdot \mathbf{p} - \beta mc^2)\Psi = 0 \qquad \text{[A7.13]}$$

[1] It is convenient to denote the Cartesian coordinates of a point by (x_1, x_2, x_3) in this appendix, rather than by (x, y, z) which we have used elsewhere.

or

$$i\hbar \frac{\partial}{\partial t} \Psi = -i\hbar c \boldsymbol{\alpha} \cdot \nabla \Psi + \beta mc^2 \Psi \qquad \text{[A7.14]}$$

More explicitly, we may write [A7.14] as

$$i\hbar \frac{\partial}{\partial t} \Psi_i = -i\hbar c \sum_{j=1}^{N} \sum_{k=1}^{3} \alpha_{ij}^k \frac{\partial}{\partial x_k} \Psi_j + \sum_{j=1}^{N} \beta_{ij} mc^2 \Psi_j,$$

$$i = 1, 2, \ldots N \qquad \text{[A7.15]}$$

where α_{ij}^1, α_{ij}^2, α_{ij}^3 and β_{ij} *form* $N \times N$ matrices. The equations [A7.15] are a set of N coupled equations for the N components Ψ_i of Ψ.

We require the Hamiltonian H to be Hermitian, $H = H^\dagger$, and for this reason the matrices α^1, α^2, α^3 and β must also be Hermitian

$$\boldsymbol{\alpha} = \boldsymbol{\alpha}^\dagger, \qquad \beta = \beta^\dagger \qquad \text{[A7.16]}$$

Further conditions to be satisfied by $\boldsymbol{\alpha}$ and β follow from the requirement that each component of Ψ must separately satisfy the Klein–Gordon equation [A7.3], which we rewrite as

$$[E^2 - \mathbf{p}^2 c^2 - m^2 c^4]\Psi = 0 \qquad \text{[A7.17]}$$

Multiplying [A7.13] on the left by the operator $[E + c\boldsymbol{\alpha} \cdot \mathbf{p} + \beta\, mc^2]$, we obtain the second order equation

$$\left\{E^2 - c^2\left[\sum_{k=1}^{3} (\alpha^k)^2 p_k^2 + \sum_{\substack{k \\ (k<l)}} \sum_{l} (\alpha^k \alpha^l + \alpha^l \alpha^k) p_k p_l\right]\right.$$

$$\left. - mc^3\left[\sum_{k=1}^{3} (\alpha^k \beta + \beta \alpha^k) p_k\right] - m^2 c^4 \beta^2\right\}\Psi = 0 \qquad \text{[A7.18]}$$

where p_k ($k = 1, 2, 3$) denote the Cartesian components of $\mathbf{p}$. Comparing [A7.18] with [A7.17], we see that each component Ψ_i satisfies the Klein–Gordon equation provided that

$$\begin{aligned} (\alpha^1)^2 = (\alpha^2)^2 = (\alpha^3)^2 = \beta^2 = 1, \\ [\alpha^1, \alpha^2]_+ = [\alpha^2, \alpha^3]_+ = [\alpha^3, \alpha^1]_+ = 0, \\ [\alpha^1, \beta]_+ = [\alpha^2, \beta]_+ = [\alpha^3, \beta]_+ = 0 \end{aligned} \qquad \text{[A7.19]}$$

where $[\mathrm{A}, \mathrm{B}]_+$ denotes the anti-commutator

$$[\mathrm{A}, \mathrm{B}]_+ = \mathrm{AB} + \mathrm{BA}. \qquad \text{[A7.20]}$$

It can be shown that the minimum dimensions for the matrices α^1, α^2, α^3 and β required to satisfy the conditions [A7.16] and [A7.19] are 4×4. Correspondingly, the wave function Ψ must have at least four components ($N = 4$) and in view of our expectation that four components are required to accommodate a

description of a particle and antiparticle each of spin 1/2, we shall assume that $N = 4$. The solution of equations [A7.16] and [A7.19] is not unique, but it can be shown that any set of matrices satisfying these conditions will provide the same physical results. A representation of the matrices α^1, α^2, α^3 and β which is particularly useful for studying the non-relativistic limit of the Dirac equation is given by

$$\boldsymbol{\alpha} = \begin{pmatrix} 0 & \boldsymbol{\sigma} \\ \boldsymbol{\sigma} & 0 \end{pmatrix} \qquad \beta = \begin{pmatrix} I & 0 \\ 0 & -I \end{pmatrix} \tag{A7.21}$$

where I is the unit two-by-two matrix while σ_1, σ_2 and σ_3 are the three Pauli two-by-two spin matrices, namely (see [2.216])

$$\sigma_1 = \begin{pmatrix} 0 & 1 \\ 1 & 0 \end{pmatrix}, \qquad \sigma_2 = \begin{pmatrix} 0 & -i \\ i & 0 \end{pmatrix}, \qquad \sigma_3 = \begin{pmatrix} 1 & 0 \\ 0 & -1 \end{pmatrix} \tag{A7.22}$$

Using the properties [2.217] of $\boldsymbol{\sigma}$, the relations [A7.16] and [A7.19] are easily shown to be satisfied.

Charged particle in an electromagnetic field

To obtain the Dirac equation for a particle of charge q in an electromagnetic field $(\mathbf{A}, \phi)$ we make the usual replacements [A7.4] in [A7.13] and obtain

$$[(E - q\phi) - c\boldsymbol{\alpha} \cdot (p - q\mathbf{A}) - \beta mc^2]\Psi = 0 \tag{A7.23}$$

or

$$i\hbar \frac{\partial}{\partial t} \Psi = [-i\hbar c\boldsymbol{\alpha} \cdot \boldsymbol{\nabla} - cq\boldsymbol{\alpha} \cdot \mathbf{A} + q\phi + \beta mc^2]\Psi \tag{A7.24}$$

Upon comparison with [A7.10], we see that the Dirac Hamiltonian in the presence of an external electromagnetic field $(\mathbf{A}, \phi)$ is given by

$$H = c\boldsymbol{\alpha} \cdot (\mathbf{p} - q\mathbf{A}) + q\phi + \beta mc^2 \tag{A7.25}$$

Adjoint equation. Continuity equation. Probability and current densities

We have seen above that the wave function Ψ may be considered as a column matrix of the form [A7.11], with four components $\Psi_i (i = 1, \ldots 4)$. We can define $\Psi^\dagger$ to be a row matrix with components Ψ_i^*, namely

$$\Psi^\dagger = (\Psi_1^* \quad \Psi_2^* \quad \Psi_3^* \quad \Psi_4^*) \tag{A7.26}$$

Using [A7.24], [A7.25] and the fact that $\boldsymbol{\alpha}$, β and $\mathbf{p}$ are Hermitian, we see that $\Psi^\dagger$ satisfies the adjoint equation

$$\begin{aligned} -i\hbar \frac{\partial}{\partial t} \Psi^\dagger &= \Psi^\dagger H \\ &= (i\hbar c\boldsymbol{\nabla} - cq\mathbf{A})\Psi^\dagger \cdot \boldsymbol{\alpha} + q\phi\Psi^\dagger + mc^2\Psi^\dagger\beta \end{aligned} \tag{A7.27}$$

The quantity

$$\rho(\mathbf{r}, t) = \Psi^\dagger\Psi = \sum_{i=1}^{4} |\Psi_i|^2 \qquad [A7.28]$$

is clearly positive and can be interpreted as a *position probability density*, in the same way that $|\Psi|^2$ is the position probability density for the non-relativistic Schrödinger equation [2.46]. By multiplying [A7.24] on the left by $\Psi^\dagger$ and [A7.27] on the right by Ψ, and taking the difference of the two results, it is found that

$$\frac{\partial \rho}{\partial t} + \nabla \cdot (\Psi^\dagger c\boldsymbol{\alpha}\Psi) = 0 \qquad [A7.29]$$

If we interpret the vector

$$\mathbf{j}(\mathbf{r}, t) = \Psi^\dagger c\boldsymbol{\alpha}\Psi \qquad [A7.30]$$

as a *probability current density*, the equation [A7.29] takes the form of a continuity equation,

$$\frac{\partial \rho}{\partial t} + \nabla \cdot \mathbf{j} = 0 \qquad [A7.31]$$

and we see that $c\boldsymbol{\alpha}$ can be interpreted as a velocity operator.

Stationary solutions

Let us assume that $\mathbf{A}$ and ϕ are time-independent. We may then look for stationary solutions of the Dirac equation which we write as

$$\Psi(\mathbf{r}, t) = \chi(\mathbf{r})e^{-iEt/\hbar} \qquad [A7.32]$$

From [A7.24] and [A7.32] we obtain the time-independent equation

$$E\chi(\mathbf{r}) = [-i\hbar c\boldsymbol{\alpha} \cdot \nabla - cq\boldsymbol{\alpha} \cdot \mathbf{A} + q\phi + \beta mc^2]\chi(\mathbf{r}) \qquad [A7.33]$$

The four-component spinor $\chi(\mathbf{r})$ can be expressed in terms of two 2-component spinors $\psi(\mathbf{r})$ and $\eta(\mathbf{r})$ by writing

$$\chi(\mathbf{r}) \equiv \begin{pmatrix} \psi(\mathbf{r}) \\ \eta(\mathbf{r}) \end{pmatrix} \qquad [A7.34]$$

Using the representation [A7.21] of the matrices $\boldsymbol{\alpha}$ and β, the 2-component spinors ψ and η are found to satisfy the two coupled equations

$$E\psi(\mathbf{r}) = c(-i\hbar\nabla - q\mathbf{A}) \cdot \boldsymbol{\sigma}\eta(\mathbf{r}) + (q\phi + mc^2)\psi(\mathbf{r}) \qquad [A7.35a]$$

$$E\eta(\mathbf{r}) = c(-i\hbar\nabla - q\mathbf{A}) \cdot \boldsymbol{\sigma}\psi(\mathbf{r}) + (q\phi - mc^2)\eta(\mathbf{r}) \qquad [A7.35b]$$

These equations will be used below to study the non-relativistic limit of the Dirac equation.

Central field. Spin angular momentum. Total angular momentum

Consider a Dirac particle in a central field (such that $\mathbf{A} = 0$ and ϕ is spherically symmetric). Let $V(r) = q\phi(r)$ be the corresponding potential energy. The Dirac Hamiltonian [A7.25] is then

$$H = c\boldsymbol{\alpha} \cdot \mathbf{p} + \beta mc^2 + V(r) \qquad \text{[A7.36]}$$

We saw in Chapter 2 that in the non-relativistic Schrödinger theory every component of the orbital angular momentum $\mathbf{L} = \mathbf{r} \times \mathbf{p}$, as well as $\mathbf{L}^2$, commutes with the (non-relativistic) Hamiltonian $H = p^2/2m + V(r)$ of a spinless particle in a central field. As a result, simultaneous eigenstates of the operators H, $\mathbf{L}^2$ and L_z exist in Schrödinger's theory, with eigenvalues given respectively by E, $l(l+1)\hbar^2$ and $m\hbar$. In Dirac's theory, however, neither the components of $\mathbf{L}$, nor $\mathbf{L}^2$, commute with the Dirac Hamiltonian [A7.36]. Instead, one can readily show that

$$[\mathbf{L}, H] = i\hbar c\boldsymbol{\alpha} \times \mathbf{p} \qquad \text{[A7.37]}$$

Let us now consider the operator

$$\mathbf{S} = \frac{\hbar}{2}\boldsymbol{\Sigma} \qquad \text{[A7.38]}$$

where $\boldsymbol{\Sigma} \equiv (\Sigma^1, \Sigma^2, \Sigma^3)$, the Σ^k being 4×4 matrices given by

$$\boldsymbol{\Sigma} = \begin{pmatrix} \boldsymbol{\sigma} & 0 \\ 0 & \boldsymbol{\sigma} \end{pmatrix} \qquad \text{[A7.39]}$$

It follows from the properties [2.217] of the Pauli spin matrices that the three Cartesian components of $\mathbf{S}$ satisfy the commutation relations [2.194]. Moreover, for any state Ψ,

$$\mathbf{S}^2\Psi = s(s+1)\hbar^2\Psi, \qquad s = \tfrac{1}{2} \qquad \text{[A7.40]}$$

and the two possible eigenvalues of $S_i (i = 1, 2, 3)$ are $\pm\hbar/2$. We shall therefore refer to the operator [A7.38] as the *spin angular momentum* operator. We remark that any component of $\mathbf{S}$ commutes with any component of $\mathbf{L}$. Moreover, using [2.217] we have

$$[\mathbf{S}, H] = -i\hbar c\boldsymbol{\alpha} \times \mathbf{p} \qquad \text{[A7.41]}$$

where H is the Dirac Hamiltonian [A7.36]

We can now define a *total angular momentum* operator as the sum of the orbital and spin angular momentum operators,

$$\mathbf{J} = \mathbf{L} + \mathbf{S} \qquad \text{[A7.42]}$$

We note that the three Cartesian components of $\mathbf{J}$ satisfy the commutation relations [2.223]. In addition, using the results [A7.37] and [A7.41], we see that every component of $\mathbf{J}$ commutes with the Dirac Hamiltonian H given by [A7.36]. Making use of [2.120c], we also remark that $\mathbf{J}^2$ commutes with H. We

shall denote the eigenvalues of $\mathbf{J}^2$ by $j(j+1)\hbar^2$ and those of $\mathcal{J}_3(\equiv\mathcal{J}_z)$ by $m_j\hbar$. Thus, in Dirac's theory, simultaneous eigenstates of the Hamiltonian [A7.36] and of the operators $\mathbf{J}^2$ and $\mathcal{J}_z$ can be found, with eigenvalues given respectively by E, $j(j+1)\hbar^2$ and $m_j\hbar$.

The non-relativistic limit

Let us return to the system of equations [A7.35] for stationary states. In order to investigate its non-relativistic limit, we write

$$E = E' + mc^2 \tag{A7.43}$$

Substituting [A7.43] into [A7.35], we find that

$$E'\psi(\mathbf{r}) = c(-i\hbar\boldsymbol{\nabla} - q\mathbf{A})\cdot\boldsymbol{\sigma}\eta(\mathbf{r}) + q\phi\psi(\mathbf{r}) \tag{A7.44a}$$

$$(E' + 2mc^2)\eta(\mathbf{r}) = c(-i\hbar\boldsymbol{\nabla} - q\mathbf{A})\cdot\boldsymbol{\sigma}\psi(\mathbf{r}) + q\phi\eta(\mathbf{r}) \tag{A7.44b}$$

This pair of equations is still exact, but in the non-relativistic limit both $|E'|$ and $|q\phi|$ are small in comparison with mc^2. The equation [A7.44b] can then be solved approximately to give

$$\eta(\mathbf{r}) = \frac{1}{2mc}(-i\hbar\boldsymbol{\nabla} - q\mathbf{A})\cdot\boldsymbol{\sigma}\psi(\mathbf{r}) \tag{A7.45}$$

and we see that η is smaller than ψ by a factor of order p/mc (i.e. v/c, where v is the magnitude of the velocity). The two-component spinors ψ and η are known in this case as the *large* and *small components*, respectively.

The Pauli equation

Substituting [A7.45] into [A7.44a], we find that

$$E'\psi(\mathbf{r}) = \frac{1}{2m}[(-i\hbar\boldsymbol{\nabla} - q\mathbf{A})\cdot\boldsymbol{\sigma}]^2\psi(\mathbf{r}) + q\phi\psi(\mathbf{r}) \tag{A7.46}$$

The identity [2.218] – where $\mathbf{A}$ and $\mathbf{B}$ are vector operators whose components commute with those of $\boldsymbol{\sigma}$ – can be used to reduce the first term on the right hand side of [A7.46]. That is,

$$\frac{1}{2m}[(-i\hbar\boldsymbol{\nabla} - q\mathbf{A})\cdot\boldsymbol{\sigma}]^2\psi = \frac{1}{2m}(-i\hbar\boldsymbol{\nabla} - q\mathbf{A})^2\psi - \frac{q\hbar}{2m}\boldsymbol{\sigma}\cdot(\boldsymbol{\nabla}\times\mathbf{A})\psi \tag{A7.47}$$

Now $\boldsymbol{\nabla}\times\mathbf{A} = \boldsymbol{\mathcal{B}}$, where $\boldsymbol{\mathcal{B}}$ is the magnetic field, so that [A7.46] becomes

$$E'\psi(\mathbf{r}) = \left[\frac{1}{2m}(-i\hbar\boldsymbol{\nabla} - q\mathbf{A})^2 - \frac{q\hbar}{2m}(\boldsymbol{\sigma}\cdot\boldsymbol{\mathcal{B}}) + q\phi\right]\psi(\mathbf{r}) \tag{A7.48}$$

This equation is known as the *Pauli equation*. It differs from the non-relativistic form of the Klein–Gordon equation for spinless particles in predicting an interaction between the external magnetic field $\mathcal{B}$ and the spin $\mathbf{S} = \hbar\boldsymbol{\sigma}/2$ of the particle [2]. We emphasize that the Pauli equation [A7.48] is an equation for a two-component spinor wave function ψ.

To apply the Pauli equation to an electron, we put $q = -e$, where e is the magnitude of the electronic charge. We then have

$$E'\psi(\mathbf{r}) = \left[\frac{1}{2m}(-i\hbar\boldsymbol{\nabla} + e\mathbf{A})^2 + \frac{e\hbar}{2m}(\boldsymbol{\sigma}\cdot\mathcal{B}) - e\phi\right]\psi(\mathbf{r}) \qquad [A7.49]$$

The term $e\hbar(\boldsymbol{\sigma}\cdot\mathcal{B})/2m$ on the right of this equation corresponds to an interaction $-\mathcal{M}_s\cdot\mathcal{B}$ between the magnetic field $\mathcal{B}$ and an intrinsic magnetic moment $\mathcal{M}_s$ of the electron, due to its spin, with

$$\mathcal{M}_s = -\mu_B\boldsymbol{\sigma} = -g_s\mu_B\mathbf{S}/\hbar = -g_s\frac{e}{2m}\mathbf{S} \qquad [A7.50]$$

Here

$$\mu_B = \frac{e\hbar}{2m} \qquad [A7.51]$$

is the Bohr magneton and the spin gyromagnetic ratio g_s has the value $g_s = 2$. We see that the Dirac theory not only predicts the existence of an intrinsic magnetic moment for the electron, but it also gives essentially its correct value $\mathcal{M}_s = -(e/m)\mathbf{S}$ (apart from very small corrections coming from quantum electrodynamics). The Pauli equation is used in Chapter 5 to analyse the Zeeman effect for one-electron atoms.

Higher order corrections for one-electron atoms and ions

We have shown above that to lowest order in v/c, the Dirac theory is equivalent to the two-component Pauli theory. We shall now investigate higher order corrections for the case of an electron in the Coulomb field of a nucleus, so that $\mathbf{A} = 0$ and $q\phi = -e\phi = V(r) = -Ze^2/(4\pi\varepsilon_0)r$. The Dirac equation can be solved exactly in that case [see for example Messiah (1968) or Schiff (1968)] but here we shall only display the corrections of order $(v/c)^2$ which are needed in our discussion of fine structure effects in Chapter 5.

Let us return to the system of equations [A7.44]. Solving [A7.44b] for $\eta(\mathbf{r})$, we obtain

$$\eta(\mathbf{r}) = \frac{1}{E' + 2mc^2 - V(r)}c(-i\hbar\boldsymbol{\sigma}\cdot\boldsymbol{\nabla})\psi(\mathbf{r}) \qquad [A7.52]$$

[2] We recall that the spin operator $\mathbf{S} = \hbar\boldsymbol{\Sigma}/2$ introduced in [A7.38] acts on four-component Dirac wave functions. In order to simplify the notation we also denote by $\mathbf{S}$ the spin operator $\hbar\boldsymbol{\sigma}/2$ acting on two-component Pauli wave functions.

Substituting in [A7.44a], we find

$$E'\psi(\mathbf{r}) = c^2(i\hbar\boldsymbol{\sigma}\cdot\boldsymbol{\nabla})\frac{1}{E' + 2mc^2 - V(r)}(i\hbar\boldsymbol{\sigma}\cdot\boldsymbol{\nabla})\psi(\mathbf{r}) + V(r)\psi(\mathbf{r}) \tag{A7.53}$$

Expanding $[E' + 2mc^2 - V(r)]^{-1}$ in powers of $[E' - V(r)]/2mc^2$, we have to lowest order

$$[E' + 2mc^2 - V(r)]^{-1} \simeq \frac{1}{2mc^2}\left[1 - \frac{E' - V(r)}{2mc^2}\right] \tag{A7.54}$$

so that [A7.53] becomes

$$\begin{aligned} E'\psi(\mathbf{r}) = & -\frac{\hbar^2}{2m}\left[1 - \frac{E' - V(r)}{2mc^2}\right](\boldsymbol{\sigma}\cdot\boldsymbol{\nabla})^2\psi(\mathbf{r}) \\ & -\frac{\hbar^2}{4m^2c^2}[\boldsymbol{\sigma}\cdot\boldsymbol{\nabla}V(r)][\boldsymbol{\sigma}\cdot\boldsymbol{\nabla}\psi(\mathbf{r})] + V(r)\psi(\mathbf{r}) \end{aligned} \tag{A7.55}$$

Now, using the identity [2.218], we have $(\boldsymbol{\sigma}\cdot\boldsymbol{\nabla})^2 = \nabla^2$ and

$$(\boldsymbol{\sigma}\cdot\boldsymbol{\nabla}V)(\boldsymbol{\sigma}\cdot\boldsymbol{\nabla}\psi) = (\boldsymbol{\nabla}V)\cdot(\boldsymbol{\nabla}\psi) + i\boldsymbol{\sigma}\cdot[(\boldsymbol{\nabla}V)\times(\boldsymbol{\nabla}\psi)] \tag{A7.56}$$

Moreover, since $V(r)$ is spherically symmetric,

$$\boldsymbol{\nabla}V(r) = \frac{dV}{dr}\hat{\mathbf{r}} \tag{A7.57a}$$

$$(\boldsymbol{\nabla}V)\cdot(\boldsymbol{\nabla}\psi) = \frac{dV}{dr}\frac{\partial\psi}{\partial r} \tag{A7.57b}$$

and

$$i\boldsymbol{\sigma}\cdot[(\boldsymbol{\nabla}V)\times(\boldsymbol{\nabla}\psi)] = -\frac{2}{\hbar^2}\frac{1}{r}\frac{dV}{dr}\mathbf{L}\cdot\mathbf{S} \tag{A7.57c}$$

where we have used the fact that $\mathbf{L} = \mathbf{r}\times\mathbf{p} = \mathbf{r}\times(-i\hbar\boldsymbol{\nabla})$ and $\mathbf{S} = \hbar\boldsymbol{\sigma}/2$.

Collecting the various terms, we obtain

$$\begin{aligned} E'\psi(\mathbf{r}) = & \left[-\frac{\hbar^2}{2m}\nabla^2 + V(r) + \frac{\hbar^2}{2m}\frac{E' - V(r)}{2mc^2}\nabla^2 + \frac{1}{2m^2c^2}\frac{1}{r}\frac{dV}{dr}\mathbf{L}\cdot\mathbf{S}\right. \\ & \left. -\frac{\hbar^2}{4m^2c^2}\frac{dV}{dr}\frac{\partial}{\partial r}\right]\psi(\mathbf{r}) \end{aligned} \tag{A7.58}$$

Since $\mathbf{p} = -i\hbar\boldsymbol{\nabla}$ and $E' - V(r) \simeq p^2/2m$, the third term on the right hand side can be written as

$$\frac{\hbar^2}{2m}\frac{E' - V(r)}{2mc^2}\nabla^2 \simeq -\frac{p^4}{8m^3c^2} \tag{A7.59}$$

and is a *relativistic correction* (of order v^2/c^2) *to the kinetic energy* term $-\hbar^2\nabla^2/2m \equiv p^2/2m$. The fourth term is the *spin-orbit interaction* which is readily shown to be of order v^2/c^2 times the potential energy $V(r)$. The last term on the right-hand side of [A7.58] is a relativistic correction (or order v^2/c^2) to the potential energy which gives rise to some difficulty because it is non-Hermitian. The origin of the trouble is that if the original Dirac four-component wave function is normalised to unity, namely

$$\int (\psi^\dagger\psi + \eta^\dagger\eta)\,\mathrm{d}\mathbf{r} = 1 \qquad \text{[A7.60]}$$

then the two-component spinor ψ only satisfies the normalisation condition approximately. Darwin has shown that the normalisation of ψ can be obtained correctly by replacing the last term in [A7.58] by the symmetrical combination (which is Hermitian)

$$\frac{1}{2}\left[\left(-\frac{\hbar^2}{4m^2c^2}\frac{dV(r)}{dr}\frac{\partial}{\partial r}\right) + \left(-\frac{\hbar^2}{4m^2c^2}\frac{dV(r)}{dr}\frac{\partial}{\partial r}\right)^\dagger\right] = \frac{\hbar^2}{8m^2c^2}\nabla^2 V(r) \qquad \text{[A7.61]}$$

For a one-electron atom (ion) $V(r) = -Ze^2/(4\pi\varepsilon_0)r$ and we have

$$\nabla^2 V(r) = 4\pi\left(\frac{Ze^2}{4\pi\varepsilon_0}\right)\delta(\mathbf{r}) \qquad \text{[A7.62]}$$

so that the Darwin term [A7.61] is then given by

$$\frac{\hbar^2}{8m^2c^2}\nabla^2 V(r) = \frac{\pi\hbar^2}{2m^2c^2}\left(\frac{Ze^2}{4\pi\varepsilon_0}\right)\delta(\mathbf{r}) \qquad \text{[A7.63]}$$

and we see that it only contributes to the energy of the states with $l = 0$.

Using the above results, we may write down the final form of the wave equation for one-electron atoms (ions), with relativistic corrections through order (v^2/c^2). That is,

$$H\psi(\mathbf{r}) = E'\psi(\mathbf{r}) \qquad \text{[A7.64]}$$

where

$$H = \frac{p^2}{2m} + V(r) - \frac{p^4}{8m^3c^2} + \frac{1}{2m^2c^2}\frac{1}{r}\frac{dV}{dr}\mathbf{L}\cdot\mathbf{S} + \frac{\pi\hbar^2}{2m^2c^2}\left(\frac{Ze^2}{4\pi\varepsilon_0}\right)\delta(\mathbf{r}) \qquad \text{[A7.65]}$$

and $V(r) = -Ze^2/(4\pi\varepsilon_0)r$. It is the Hamiltonian [A7.65] which is the starting point of our discussion of the fine structure of hydrogenic atoms in Chapter 5.

8 Separation of the centre of mass coordinates for an *N*-electron atom

Let us consider an atom or ion containing a nucleus of mass M and charge Ze and N electrons of mass m and charge $(-e)$. We denote by $\mathbf{R}_0$ the coordinates of the nucleus with respect to a fixed origin O, and by $\mathbf{R}_1, \mathbf{R}_2, \ldots \mathbf{R}_N$ those of the electrons. In the absence of external field, and neglecting all but the Coulomb interactions, the non-relativistic Hamiltonian operator of this system is given by

$$H = T + V \qquad [A8.1]$$

where the kinetic energy operator T reads

$$T = -\frac{\hbar^2}{2M}\nabla^2_{R_0} + \sum_{i=1}^{N}\left(-\frac{\hbar^2}{2m}\nabla^2_{R_i}\right) \qquad [A8.2]$$

and the potential energy V is the sum of the Coulomb interactions between the $(N+1)$ particles of the system.

In order to separate the motion of the centre of mass, we change our coordinates from $(\mathbf{R}_0, \mathbf{R}_1, \ldots \mathbf{R}_N)$ to $(\mathbf{R}, \mathbf{r}_1, \ldots \mathbf{r}_N)$ where

$$\mathbf{R} = \frac{1}{M + Nm}(M\mathbf{R}_0 + m\mathbf{R}_1 + \cdots m\mathbf{R}_N) \qquad [A8.3]$$

is the coordinate of the centre of mass and

$$\mathbf{r}_i = \mathbf{R}_i - \mathbf{R}_0, \qquad i = 1, 2, \ldots N \qquad [A8.4]$$

are the relative coordinates of the electrons with respect to the nucleus. It is apparent from [A8.3] and [A8.4] that

$$\boldsymbol{\nabla}_{R_0} = \frac{M}{M + Nm}\boldsymbol{\nabla}_R - \sum_{i=1}^{N}\boldsymbol{\nabla}_{r_i} \qquad [A8.5]$$

and

$$\boldsymbol{\nabla}_{R_i} = \frac{m}{M + Nm}\boldsymbol{\nabla}_R + \boldsymbol{\nabla}_{r_i} \qquad [A8.6]$$

Hence

$$\nabla^2_{R_0} = \left(\frac{M}{M + Nm}\right)^2\nabla^2_R - \frac{2M}{M + Nm}\sum_{i=1}^{N}\boldsymbol{\nabla}_R\cdot\boldsymbol{\nabla}_{r_i} + \left(\sum_{i=1}^{N}\boldsymbol{\nabla}_{r_i}\right)^2 \qquad [A8.7]$$

and

$$\nabla^2_{R_i} = \left(\frac{m}{M + Nm}\right)^2 \nabla^2_R + \frac{2m}{M + Nm} \boldsymbol{\nabla}_R \cdot \boldsymbol{\nabla}_{r_i} + \nabla^2_{r_i} \qquad [A8.8]$$

Substituting the expressions [A8.7] and [A8.8] in [A8.2], we find that the kinetic energy operator becomes in the new coordinates

$$T = -\frac{\hbar^2}{2(M + Nm)} \nabla^2_R - \frac{\hbar^2}{2\mu} \sum_{i=1}^{N} \nabla^2_{r_i} - \frac{\hbar^2}{M} \sum_{i>j} \boldsymbol{\nabla}_{r_i} \cdot \boldsymbol{\nabla}_{r_j} \qquad [A8.9]$$

where

$$\mu = \frac{mM}{m + M} \qquad [A8.10]$$

is the reduced mass of the electron with respect to the nucleus. The Hamiltonian [A8.1] may therefore be written as

$$H = -\frac{\hbar^2}{2(M + Nm)} \nabla^2_R - \frac{\hbar^2}{2\mu} \sum_{i=1}^{N} \nabla^2_{r_i} - \frac{\hbar^2}{M} \sum_{i>j} \boldsymbol{\nabla}_{r_i} \cdot \boldsymbol{\nabla}_{r_j} + V(\mathbf{r}_1, \mathbf{r}_2, \ldots \mathbf{r}_N) \qquad [A8.11]$$

The only term involving the coordinate $\mathbf{R}$ in [A8.11] is the first one, which represents the kinetic energy operator of the centre of mass. The second term represents the sum of the kinetic energy operators of the N electrons, each of them having their mass m replaced by the reduced mass μ because of the motion of the nucleus. The nuclear motion is also responsible for the existence of the third term, which is often called the *mass polarisation* term. We note that this term is only present if $N \geqslant 2$. Finally, the potential energy term V is readily expressed in terms of the relative coordinates as

$$V(\mathbf{r}_1, \mathbf{r}_2, \ldots \mathbf{r}_N) = -\sum_{i=1}^{N} \frac{Ze^2}{(4\pi\varepsilon_0)r_i} + \sum_{i>j} \frac{e^2}{(4\pi\varepsilon_0)r_{ij}} \qquad [A8.12]$$

with $r_{ij} = |\mathbf{r}_i - \mathbf{r}_j|$.

The time-independent Schrödinger equation for the spatial part of the wave function corresponding to the total ($(N + 1)$ particle) system reads

$$H\psi_{\text{tot}}(\mathbf{R}, \mathbf{r}_1, \mathbf{r}_2, \ldots, \mathbf{r}_N) = E_{\text{tot}}\psi_{\text{tot}}(\mathbf{R}, \mathbf{r}_1, \mathbf{r}_2, \ldots, \mathbf{r}_N) \qquad [A8.13]$$

where the Hamiltonian H is given by [A8.11] and E_{tot} is the total energy of the system. Since H is made up of a term involving only the centre of mass coordinate $\mathbf{R}$ and other terms which involve only the relative coordinates $(\mathbf{r}_1, \mathbf{r}_2, \ldots, \mathbf{r}_N)$, the Schrödinger equation [A8.13] possesses a complete set of eigensolutions of the form

$$\psi_{\text{tot}}(\mathbf{R}, \mathbf{r}_1, \mathbf{r}_2, \ldots, \mathbf{r}_N) = U(\mathbf{R})\psi(\mathbf{r}_1, \mathbf{r}_2, \ldots, \mathbf{r}_N) \qquad [A8.14]$$

where the functions $U(\mathbf{R})$ and $\psi(\mathbf{r}_1, \mathbf{r}_2, \ldots, \mathbf{r}_N)$ satisfy respectively the

time-independent Schrödinger equations

$$-\frac{\hbar^2}{2(M + Nm)} \nabla_R^2 U(\mathbf{R}) = E_{\mathrm{CM}} U(\mathbf{R}) \qquad \text{[A8.15]}$$

and

$$\left[-\frac{\hbar^2}{2\mu} \sum_{i=1}^{N} \nabla_{r_i}^2 - \frac{\hbar^2}{M} \sum_{i>j} \boldsymbol{\nabla}_{r_i} \cdot \boldsymbol{\nabla}_{r_j} + V(\mathbf{r}_1, \mathbf{r}_2, \ldots, \mathbf{r}_N) \right] \psi(\mathbf{r}_1, \mathbf{r}_2, \ldots \mathbf{r}_N)$$

$$= E\psi(\mathbf{r}_1, \mathbf{r}_2, \ldots \mathbf{r}_N) \qquad \text{[A8.16]}$$

with

$$E_{\mathrm{tot}} = E_{\mathrm{CM}} + E \qquad \text{[A8.17]}$$

Equation [A8.15] shows that the centre of mass moves as a *free* particle having a mass $(M + Nm)$ equal to the total mass of the system and a kinetic energy E_{CM}. On the other hand, equation [A8.16] describes the *relative* motion, which is the problem of physical interest in the study of atomic structure.

9 Evaluation of two-centre integrals

The integrals required in the discussion of the hydrogen molecular ion can all be obtained from the basic integral

$$\mathcal{J} = \int \frac{e^{-pr_A} e^{-qr_B}}{r_A r_B} d\mathbf{r} \qquad [A9.1]$$

where $\mathbf{r}$, $\mathbf{r}_A$ and $\mathbf{r}_B$ are defined in Fig. 9.8.

This integral is most easily evaluated by introducing confocal elliptic coordinates defined by (see [9.59])

$$\begin{aligned} \xi &= \frac{1}{R}(r_A + r_B), \qquad 1 \leqslant \xi \leqslant \infty \\ \eta &= \frac{1}{R}(r_A - r_B), \qquad -1 \leqslant \eta \leqslant 1 \end{aligned} \qquad [A9.2]$$

and ϕ, the azimuthal angle about the Z axis. We recall that the quantity R which appears in [A9.2] is the internuclear separation. The volume element $d\mathbf{r}$, expressed in terms of the confocal elliptic coordinates (ξ, η, ϕ), is given by

$$d\mathbf{r} = \frac{R^3}{8}(\xi^2 - \eta^2)\, d\xi\, d\eta\, d\phi \qquad [A9.3]$$

so that

$$\mathcal{J} = \frac{R}{2} \int_1^{\infty} d\xi \int_{-1}^{+1} d\eta \int_0^{2\pi} d\phi\, e^{-a\xi - b\eta} \qquad [A9.4]$$

where

$$\begin{aligned} a &= \frac{R}{2}(p + q) \\ b &= \frac{R}{2}(p - q) \end{aligned} \qquad [A9.5]$$

The integral [A9.4] is now elementary and is given by

$$\mathcal{J} = \frac{\pi R}{ab} e^{-a}(e^{b} - e^{-b})$$

$$= \frac{4\pi}{R} \frac{1}{p^2 - q^2} (e^{-qR} - e^{-pR}) \qquad \text{[A9.6]}$$

The other relevant integrals are obtained by differentiating the above result with respect to p and q. That is,

$$K = \int \frac{e^{-pr_\mathrm{A}} e^{-qr_\mathrm{B}}}{r_\mathrm{A}} \mathrm{d}\mathbf{r} = -\frac{\partial}{\partial q}\mathcal{J}$$

$$= \frac{4\pi}{R}\left[\frac{R}{p^2 - q^2} e^{-qR} + \frac{2q}{(p^2 - q^2)^2}(e^{-pR} - e^{-qR})\right] \qquad \text{[A9.7]}$$

and

$$L = \int e^{-pr_\mathrm{A}} e^{-qr_\mathrm{B}} \, \mathrm{d}\mathbf{r} = -\frac{\partial}{\partial p} K$$

$$= \frac{8\pi}{R(p^2 - q^2)^2}\left[R(pe^{-qR} + qe^{-pR}) + \frac{4pq}{p^2 - q^2}(e^{-pR} - e^{-qR})\right] \qquad \text{[A9.8]}$$

In the particular case $p = q$, we have

$$\mathcal{J} = \frac{2\pi}{p} e^{-pR} \qquad \text{[A9.9]}$$

$$K = \frac{\pi}{p^2}(1 + pR)e^{-pR} \qquad \text{[A9.10]}$$

and

$$L = \frac{\pi}{p^3}\left(1 + pR + \frac{1}{3}p^2R^2\right)e^{-pR} \qquad \text{[A9.11]}$$

10 Solutions to selected problems

CHAPTER 1

1.1 (a) $v = 4.55 \times 10^7$ m s^{-1}
(b) $e/m = 1.65 \times 10^{11}$ C kg^{-1}.

1.3 The value of λ_{max} is obtained by solving the equation $\mathrm{d}\rho(\lambda)/\mathrm{d}\lambda = 0$, where $\rho(\lambda)$ is given by [1.30]. Setting $x = hc/\lambda kT$, it is found that the maximum of $\rho(\lambda)$ occurs at a value x_0 of x such that $x_0 = 5(1 - \mathrm{e}^{-x_0})$. This equation is conveniently solved by writing $x_0 = 5 - \varepsilon$, so that $\varepsilon \simeq (e^5/5 - 1)^{-1} = 0.03486$ and $x_0 = 4.965$. Thus $\lambda_{\text{max}} = hc/(4.965k)$, and from the values of h, c and k given in Appendix 11 one finds $b = 2.898 \times 10^{-3}$ mK.

1.4
$$\rho_{\text{tot}} = \int_0^\infty \rho(\lambda)\, \mathrm{d}\lambda = 8\pi hc \int_0^\infty \lambda^{-5}(\mathrm{e}^{hc/\lambda kT} - 1)^{-1}\, \mathrm{d}\lambda$$
$$= 8\pi hc(kT/hc)^4 \int_0^\infty x^3(\mathrm{e}^x - 1)^{-1}\, \mathrm{d}x$$

where we have written $x = hc/\lambda kT$. Thus, using the result

$$\int_0^\infty x^3(\mathrm{e}^x - 1)^{-1}\, \mathrm{d}x = \pi^4/15,$$

we get

$$\rho_{\text{tot}} = aT^4, \qquad a = \frac{8\pi^5}{15}\frac{k^4}{h^3c^3}$$

1.5 (a) $\lambda_t = 5391$ Å
(b) Maximum kinetic energy $\frac{1}{2}mv_{\text{max}}^2 = 3.90$ eV; stopping voltage $V_0 = 3.90$ V.

1.7 (a) $\Delta\lambda = \lambda_{\mathrm{c}}(1 - \cos 30°) = 0.00325$ Å
(b) $\phi = 15°$
(c) $T_2 = 80$ eV.

1.9 $E_1 = 7.6$ GeV.

1.10 (a) The maximum momentum transferred to the atomic electron (of mass m) is $\Delta p = m(2v)$ where $v = 2.2 \times 10^7$ ms^{-1} is the velocity of the α particle. Thus $\Delta p = 4.0 \times 10^{-23}$ kg ms^{-1}.

(b) $\theta_{\max} = \Delta p/p = m(2v)/M_\alpha v = 2.7 \times 10^{-4}$ radians.

1.11 (a) From [1.59] we have $r_0 = 2.3 \times 10^{-14}$ m.

(b) From [A1.25] and [A1.30] $\theta = 2 \cot^{-1}\left(\dfrac{2b}{r_0}\right) = 16.5°$.

1.12 Using [1.59], departures from Rutherford scattering occur if the CM energy of the α particle is larger than 16.7 MeV, i.e. if its laboratory energy $E > 17.8$ MeV.

1.15 $\Delta\lambda = 1.8$ Å.

1.18 $P_2P_3 = 2P_1P_2 = 2|\mathcal{M}_z| \dfrac{\partial \mathcal{B}_z}{\partial z} \dfrac{L(L/2 + l)}{Mv^2}$

$$= 2\mu_B \frac{\partial \mathcal{B}_z}{\partial z} \frac{L(L/2 + l)}{3kT} = 0.078 \text{ m.}$$

CHAPTER 2

2.1 From [2.13]

$$\psi(x) = (2\pi\hbar)^{-1/2} C \int_{p_0-\gamma}^{p_0+\gamma} e^{ip_x x/\hbar} \, dp_x$$

$$= 2\left(\frac{\hbar}{2\pi}\right)^{1/2} C \, \frac{\sin(\gamma x/\hbar)}{x} \, e^{ip_0 x/\hbar}$$

Using the result

$$\int_{-\infty}^{\infty} \frac{\sin^2 y}{y^2} \, dy = \pi,$$

we find $C = 1/\sqrt{2\gamma}$. The function $|\psi(x)|$ has a maximum at $x = 0$ and falls to zero at $x = \pm \pi\hbar/\gamma$. Taking $\Delta x = 2\pi\hbar/\gamma$, and $\Delta p_x = 2\gamma$ we find $\Delta x \, \Delta p_x = 4\pi\hbar$ so that $\Delta x \, \Delta p_x > \hbar$.

2.2 From the uncertainty principle $\Delta p \gtrsim \hbar/\Delta r$. Making the assumption $\Delta p \simeq \hbar/\Delta r = \hbar/r$, we obtain

$$E = \frac{\hbar^2}{2m}\frac{1}{r^2} - \left(\frac{e^2}{4\pi\varepsilon_0}\frac{1}{r}\right).$$

The radius at which E is a minimum is given by the condition $dE/dr = 0$, from which we find

$$r = \frac{(4\pi\varepsilon_0)\hbar^2}{me^2} = a_0.$$

The corresponding lowest value is

$$E_0 = -\frac{e^4 m}{(4\pi\varepsilon_0)^2 2\hbar^2} = -13.6 \text{ eV}.$$

It is interesting, but not significant, that the particular choice $\Delta r = r$ and $\Delta p = p$, together with the assumption $\Delta r\, \Delta p = \hbar$, gives the *exact* value of E_0. The correct order of magnitude would have been obtained with any reasonable choice for Δr and Δp, with $\Delta r\, \Delta p \geqslant \hbar$.

2.5 From [2.56] $i\hbar(\mathrm{d}/\mathrm{d}t)\langle \mathbf{r}\rangle = \langle[\mathbf{r}, H]\rangle$. We take each of the Cartesian coordinates in turn, thus

$$i\hbar \frac{\mathrm{d}}{\mathrm{d}t}\langle x\rangle = \langle [x, H]\rangle$$

Now,

$$\begin{aligned}[x, H] &= x\left\{-\frac{\hbar^2}{2m}\left(\frac{\partial^2}{\partial x^2} + \frac{\partial^2}{\partial y^2} + \frac{\partial^2}{\partial z^2}\right) + V(x, y, z)\right\} \\ &\quad - \left\{-\frac{\hbar^2}{2m}\left(\frac{\partial^2}{\partial x^2} + \frac{\partial^2}{\partial y^2} + \frac{\partial^2}{\partial z^2}\right) + V(x, y, z)\right\}x \\ &= -\frac{\hbar^2}{2m}\left\{x\frac{\partial^2}{\partial x^2} - \frac{\partial^2}{\partial x^2}x\right\} \\ &= \frac{\hbar^2}{m}\frac{\partial}{\partial x}\end{aligned}$$

Since $p_x = -i\hbar(\partial/\partial x)$, we have $(\mathrm{d}/\mathrm{d}t)\langle x\rangle = (1/m)\langle p_x\rangle$, and similarly with y and z, which proves the result. The result $(\mathrm{d}\langle \mathbf{p}\rangle/\mathrm{d}t) = -\langle \boldsymbol{\nabla} \cdot V\rangle$ can be proved in a similar way.

2.6 (a) From [2.65]

$$\int \Phi^\star (AB)^\dagger \Psi \,\mathrm{d}\mathbf{r} = \int (AB\Phi)^\star \Psi \,\mathrm{d}\mathbf{r} = \int (B\Phi)^\star A^\dagger \Psi \,\mathrm{d}\mathbf{r}$$

$$= \int \Phi^\star B^\dagger (A^\dagger \Psi)\,\mathrm{d}\mathbf{r}. \quad \text{Hence} \quad (AB)^\dagger = B^\dagger A^\dagger.$$

(b) Using the result (a), we find (i) and (ii) are not Hermitian while (iii), (iv) and (v) are Hermitian.

2.7 (a) $$\Psi(x, t) = \frac{1}{\sqrt{2}} \mathrm{e}^{i\alpha_1}\psi_1(x)\mathrm{e}^{-iE_1 t/\hbar} + \frac{1}{\sqrt{3}} \mathrm{e}^{i\alpha_2}\psi_2(x)\mathrm{e}^{-iE_2 t/\hbar} + \frac{1}{\sqrt{6}} \mathrm{e}^{i\alpha_3}\psi_3(x)\mathrm{e}^{-iE_3 t/\hbar}$$

(b) Probability $= 1/3$

(c) $\langle x\rangle$ and $\langle p_x\rangle$ are time-dependent; $E = \langle H\rangle$ is time-independent.

2.10 (a) $P_n = \dfrac{960}{\pi^6 n^6}$, n odd

$= 0$, n even

(b) $E = \langle H \rangle = 5\hbar^2/4ma^2$

2.16 Since $\mathbf{L}$ and $\mathbf{S}$ operate in different spaces all the components of $\mathbf{L}$ commute with all the components of $\mathbf{S}$ and hence $[\mathbf{L}^2, \mathbf{S}^2] = 0$. Now $\mathbf{J}^2 = \mathbf{L}^2 + \mathbf{S}^2 + 2\mathbf{L}\cdot\mathbf{S}$ so that since $\mathbf{L}^2$ commutes with all the components of $\mathbf{L}$ and $\mathbf{S}^2$ commutes with all the components of $\mathbf{S}$, one has $[\mathbf{L}^2, \mathbf{J}^2] = [\mathbf{S}^2, \mathbf{J}^2] = 0$. Since $J_z = L_z + S_z$, we have $[\mathbf{L}^2, J_z] = [\mathbf{S}^2, J_z] = 0$. Finally since $\mathbf{J}$ satisfies the commutation relations [2.223], it follows that $\mathbf{J}^2$ commutes with all its components and $[\mathbf{J}^2, J_z] = 0$, from which $[(\mathbf{L}\cdot\mathbf{S}), J_z] = 0$.

2.17 Using the orthogonality properties of $P_l(\cos\theta)$ we have

$$\left(\frac{2}{2l+1}\right) c_l j_l(kr) = \int_{-1}^{+1} \mathrm{d}(\cos\theta) \mathrm{e}^{ikr\cos\theta} P_l(\cos\theta)$$

Integrating by parts we find

$$\left(\frac{2}{2l+1}\right) c_l j_l(kr) = \left[\frac{\mathrm{e}^{ikr\cos\theta}}{ikr} P_l(\cos\theta)\right]_{\cos\theta=-1}^{\cos\theta=1}$$

$$- \int_{-1}^{+1} \mathrm{d}(\cos\theta) \frac{\mathrm{e}^{ikr\cos\theta}}{ikr} \frac{\mathrm{d}P_l(\cos\theta)}{\mathrm{d}(\cos\theta)}$$

For large r, the second term on the right-hand side is of order r^{-2} (which can be seen by integrating by parts a second time), so that

$$\left(\frac{2}{2l+1}\right) c_l \frac{1}{kr} \sin(kr - \tfrac{1}{2}l\pi) = \frac{1}{ikr}(\mathrm{e}^{ikr} - (-1)^l \mathrm{e}^{-ikr}).$$

Hence we find $c_l = (2l+1)i^l$.

2.20 (b) The first excited level is twofold degenerate with $n_x = 1$, $n_y = 0$ and $n_x = 0$, $n_y = 1$. The determinantal equation [2.329] becomes

$$\begin{vmatrix} \langle 1|\lambda xy|1\rangle - E^{(1)} & \langle 1|\lambda xy|2\rangle \\ \langle 2|\lambda xy|1\rangle & \langle 2|\lambda xy|2\rangle - E^{(1)} \end{vmatrix} = 0$$

Using equation [A3.15], $\langle 1|\lambda xy|1\rangle = \langle 2|\lambda xy|2\rangle = 0$ and $\langle 1|\lambda xy|2\rangle = \langle 2|\lambda xy|1\rangle = \lambda(2\alpha^2)^{-1}$, where $\alpha^2 = (mk/\hbar^2)^{1/2}$, and we find $E^{(1)} = \pm\lambda(2\alpha^2)^{-1}$. Hence to first order in λ the first excited level splits into two levels with energies $E = 2\hbar(k/m)^{1/2} \pm \lambda(2\alpha^2)^{-1}$.

2.21 Since $H'_{ba}(t) = -q\mathcal{E}(t)\langle\psi_b|x|\psi_a\rangle$, it follows from [A3.15] that the only non-vanishing matrix element is H'_{10}. From [2.343] and [2.344] we find

$$P_{10}(t = +\infty) = \frac{q^2\mathcal{E}_0^2}{2m\hbar\omega}\left|\int_0^\infty \mathrm{e}^{i\omega t}\mathrm{e}^{-t/\tau}\,\mathrm{d}t\right|^2$$

where $\omega = (k/m)^{1/2}$. Thus

$$P_{10}(t = +\infty) = \frac{q^2\mathscr{E}_0^2}{2m\hbar\omega} \frac{\tau^2}{(\tau\omega)^2 + 1}$$

CHAPTER 3

3.2 (a) $r \geqslant 2a_0$

(b) Probability is $13e^{-4} = 0.238$.

3.3 (a) Yes, since ψ_{100}, ψ_{200} and ψ_{322} have even parity.

(b) $P_{100} = 2/7, P_{200} = 9/14, P_{322} = 1/14$. For other states the probability is zero.

(c) Using atomic units,

$$\begin{aligned}\langle H \rangle &= (2/7)E_{n=1} + (9/14)E_{n=2} + (1/14)E_{n-3} \\ &= -0.227 \\ \langle \mathbf{L}^2 \rangle &= 6(1/14) = 0.43 \\ \langle L_z \rangle &= 2(1/14) = 0.14.\end{aligned}$$

3.4 Let us assume that the decay occurs at $t = 0$. At times $t \leqslant 0$, the wave function of the system is (in a.u.)

$$\Psi(\mathbf{r}, t) = \psi_{1s}^{Z=1}(r)e^{-iE_{1s}t}$$

where

$$\psi_{1s}^{Z=1}(r) = \frac{1}{\sqrt{\pi}} e^{-r}$$

is the ground state wave function for the tritium atom ($Z = 1$). At times $t \geqslant 0$, we have

$$\Psi(\mathbf{r}, t) = \sum_k c_k \psi_k^{Z-2}(\mathbf{r})\, e^{\ iE_k t}$$

where $\psi_k^{Z\ 2}$ are hydrogenic wave functions for $Z = 2$ (^{3}He). Thus the probability of finding the ^{3}He ion in the state ψ_k^{Z-2} at $t \geqslant 0$ is $P_k = |c_k|^2$, where

$$c_k = \langle \psi_k^{Z=2} | \psi_{1s}^{Z=1} \rangle$$

As a result, we have that

(a) $c_{1s} = \int \psi_{1s}^{Z=2}(r)\psi_{1s}^{Z=1}(r)\, d\mathbf{r} = \dfrac{16\sqrt{2}}{27}$ and

$$P_{1s} = |c_{1s}|^2 = \frac{512}{729} = 0.702$$

(b) Total probability for excitation and ionisation $= 1 - P_{1s} = 0.298$.

(c) $P_{2s} = |c_{2s}|^2 = \int \psi_{2s}^{Z=2}(r)\psi_{1s}^{Z=1}(r)\,d\mathbf{r} = 0.25$

(d) For states with $l \neq 0$ the coefficients c_k vanish since $\psi_{1s}^{Z=1}$ is spherically symmetric, and $P_k = 0$.

3.5 The perturbation H' is the potential energy of the electron in the gravitational field of the proton. That is,

$$H' = -G\frac{mM_p}{r}$$

where G is the gravitational constant, m is the electron mass and M_p the proton mass. The energy shift ΔE due to H' is given to first order in perturbation theory by

$$\Delta E = \langle\psi_{1s}|H'|\psi_{1s}\rangle = \frac{1}{\pi a_\mu^3}\int e^{-2r/a_\mu}\left(-\frac{GmM_p}{r}\right)d\mathbf{r}$$

$$= -\frac{GmM_p}{a_\mu}, \qquad a_\mu = \frac{4\pi\varepsilon_0\hbar^2}{\mu e^2}$$

On the other hand, since $E_{1s} = -(e^2/4\pi\varepsilon_0)(1/2a_\mu)$, we have

$$\frac{\Delta E}{E_{1s}} = \frac{8\pi\varepsilon_0 GmM_p}{e^2} \simeq 8.8 \times 10^{-40}.$$

CHAPTER 4

4.1 The total number of photons radiated per second are:
(a) 5×10^{25} (b) 5×10^{23} (c) 3×10^{18} (d) 5×10^{14};
The corresponding fluxes and densities are:
(a) 4×10^{22} photons/(m^2 s); 1.3×10^{14} photons/m^3
(b) 4×10^{20} photons/(m^2 s); 1.3×10^{12} photons/m^3
(c) 2.4×10^{15} photons/(m^2 s); 0.8×10^{7} photons/m^3
(d) 4×10^{11} photons/(m^2 s); 1.3×10^{3} photons/m^3.

4.4 (a) To obtain [4.69], we assume the radiation is randomly orientated, with a uniform distribution of polarisation vectors. The average required is

$$A = \frac{1}{4\pi}\int \cos^2\theta\, d\Omega_\varepsilon$$

where $d\Omega_\varepsilon$ is an element of solid angle about the direction of $\hat{\boldsymbol{\varepsilon}}$.

Taking $\mathbf{r}_{ba}$ to be fixed in space as axis,

$$A = \frac{1}{4\pi}\int_{-1}^{+1} \cos^2\theta \, d(\cos\theta) \int_0^{2\pi} d\phi = \frac{1}{3}.$$

(b) In considering the transition rate for spontaneous emission [4.70] or [4.71] let us choose the Z axis to be the direction of emission of the photon. The two independent polarisation vectors can then be taken to be $\hat{\boldsymbol{\varepsilon}}_1 = \hat{\mathbf{x}}$ and $\hat{\boldsymbol{\varepsilon}}_2 = \hat{\mathbf{y}}$, unit vectors along the X and Y axes. The sum over polarisation directions is proportional to

$$|\hat{\boldsymbol{\varepsilon}}_1 \cdot \mathbf{r}_{ba}|^2 + |\hat{\boldsymbol{\varepsilon}}_2 \cdot \mathbf{r}_{ba}|^2 = |\mathbf{r}_{ba}|^2(\cos^2\theta_1 + \cos^2\theta_2)$$

where θ_1 is the angle between $\mathbf{r}_{ba}$ and the X axis and θ_2 is the angle between $\mathbf{r}_{ba}$ and the Y axis. If the polar angles of $\mathbf{r}_{ba}$ are θ and ϕ, $\cos\theta_1 = \sin\theta\cos\phi$, $\cos\theta_2 = \sin\theta\sin\phi$ and $\cos^2\theta_1 + \cos^2\theta_2 = \sin^2\theta$. We now have to integrate over all directions of emission, which is equivalent to keeping the direction of emission fixed and integrating over all orientations of $\mathbf{r}_{ba}$. We have

$$\int d\Omega \sin^2\theta = \int_{-1}^{+1} d(\cos\theta)(1 - \cos^2\theta) \int_0^{2\pi} d\phi = 8\pi/3$$

from which we find the result [4.71].

4.5 We assume that each of the degenerate levels a are populated with an equal probability, in which case the transition rate per atom for absorption is obtained by averaging over the g_a initial states and summing over the g_b final states, so that

$$B_{ba} = \frac{1}{g_a}\sum_a \sum_b W_{ba}/\rho$$

Similarly for stimulated emission, since $\bar{W}_{ab} = W_{ba}$

$$B_{ab} = \frac{1}{g_b}\sum_b \sum_a W_{ba}/\rho$$

from which, $g_a B_{ba} = g_b B_{ab}$ (the principle of detailed balance). Hence equation [4.75] becomes,

$$\frac{g_b}{g_a} B_{ab}\rho N_a = (A_{ab} + B_{ab}\rho)N_b$$

Combining this with Boltzmann's relation, which in the case of degenerate levels is,

$$\frac{N_a}{N_b} = \frac{g_a}{g_b} e^{\hbar\omega_{ba}/kT},$$

and using the Planck distribution law [4.77] for ρ, the expression [4.79b] for A_{ab} is found.

4.6 The explicit expressions for $\mathscr{A}$ are

$$\mathscr{A}(l, m; l+1, m; 0) = \left(\frac{3}{4\pi}\right)^{1/2}\left[\frac{(l+1)^2 - m^2}{(2l+1)(2l+3)}\right]^{1/2}$$

$$\mathscr{A}(l, m; l-1, m; 0) = \left(\frac{3}{4\pi}\right)^{1/2}\left[\frac{l^2 - m^2}{(2l-1)(2l+1)}\right]^{1/2}$$

$$\mathscr{A}(l, m; l+1, m \pm 1; \pm 1) = +\left(\frac{3}{4\pi}\right)^{1/2}\left[\frac{(l \pm m + 1)(l \pm m + 2)}{2(2l+1)(2l+3)}\right]^{1/2}$$

$$\mathscr{A}(l, m; l-1, m \pm 1; \pm 1) = -\left(\frac{3}{4\pi}\right)^{1/2}\left[\frac{(l \mp m)(l \mp m - 1)}{2(2l-1)(2l+1)}\right]^{1/2}$$

4.7 The sums $\Sigma_{m'}|\mathscr{A}(l, m; l', m'; m'-m)|^2$ can be performed using the explicit forms of $\mathscr{A}$ found in Problem 4.6. The absorption rate from a level (nlm) to the $(2l'+1)$ degenerate levels $(n'l'm')$ is given by [4.63] and [4.82], as

$$W_{ba} = \frac{4\pi}{c\hbar^2}\left(\frac{e^2}{4\pi\varepsilon_0}\right)\sum_{m'}|\varepsilon^\star_{m'-m} I^{m'-m}_{n'l'm';nlm}|^2$$

$$= \frac{4\pi}{c\hbar^2}\left(\frac{e^2}{4\pi\varepsilon_0}\right)\sum_{m'}|\varepsilon^\star_{m'-m} I^{m'-m}_{n'l'm';nlm}|$$

Now
$$|\varepsilon^\star_q|^2 = \left|\sqrt{\frac{4\pi}{3}}\,Y_{1,q}(\hat{\varepsilon})\right|^2$$

and for unpolarised isotropic light, the average of $|\varepsilon^\star_q|^2$ is

$$\mathrm{Av}|\varepsilon^\star_q|^2 = \frac{1}{4\pi}\int \mathrm{d}\Omega\, |\varepsilon^\star_q|^2 = \frac{1}{3}$$

We have

$$W_{ba} = \frac{4\pi}{c\hbar^2}\left(\frac{e^2}{4\pi\varepsilon_0}\right)\frac{1}{3}\sum_{m'}|I^{m'-m}_{n'l'm';nlm}|^2$$

$$= \frac{4\pi}{3c\hbar^2}\left(\frac{e^2}{4\pi\varepsilon_0}\right)\left[\int_0^\infty R_{n'l'}(r)R_{nl}(r)r^3\,\mathrm{d}r\right]^2$$

$$\times \frac{1}{2l+1}\begin{cases} l+1, & \text{if } l' = l+1 \\ l\ \ \ \ \ , & \text{if } l' = l-1 \end{cases}$$

which is independent of m. In the same way, it follows that the lifetime of a level nlm is independent of m.

4.10 In the electric dipole approximation, the left-hand side of the required relation is

$$\text{left-hand side} = \frac{4\pi^2}{c\hbar}\left(\frac{e^2}{4\pi\varepsilon_0}\right)\left[\sum_b \omega_{ba}|\hat{\varepsilon}\cdot\mathbf{r}_{ba}|^2 - \sum_b{}' \omega_{ab}|\hat{\varepsilon}\cdot\mathbf{r}_{ba}|^2\right]$$

where $\hbar\omega_{ba} = (E_b - E_a)$. Averaging over all directions of polarisation gives a factor of 1/3, and using the definition of the oscillator strength [4.111] we find

$$\text{left-hand side} = \frac{4\pi^2}{c\hbar}\left(\frac{e^2}{4\pi\varepsilon_0}\right)\frac{1}{3}\frac{3\hbar}{2m}\left(\sum_b + \sum_b{}'\right) f_{ba}$$

Since

$$\left(\sum_b + \sum_b{}'\right) f_{ba} = \sum_k f_{ka} = 1$$

the result follows.

CHAPTER 5

5.1 The wave functions for the $np_{3/2}$, $np_{1/2}$ and $n's_{1/2}$ levels of atomic hydrogen are

$$\psi(np_{3/2}) = R_{n1}(r)\sum_{m_s}\left\langle 1\,\frac{1}{2}\,m_l m_s\middle|\frac{3}{2}\,m\right\rangle Y_{1,m_l}\chi_{1/2m_s}$$

$$\psi(np_{1/2}) = R_{n1}(r)\sum_{m_s}\left\langle 1\,\frac{1}{2}\,m_l m_s\middle|\frac{1}{2}\,m\right\rangle Y_{1,m_l}\chi_{1/2m_s}$$

$$\psi(n's_{1/2}) = R_{n'0}(r)\chi_{1/2m_s'}$$

The selection rules require that $m_s' = m_s$. Taking the case $m_s = 1/2$ the possible transitions from the states of the $np_{3/2}$ level to the $n's_{1/2}$ level and the corresponding transition rates are given (apart from an overall constant) in the following table

Initial states				Transition rate
q	m_l	m_s	m	
1	1	1/2	3/2	$A^2\left\lvert\left\langle 1\,\frac{1}{2}\,1\,\frac{1}{2}\middle\vert\frac{3}{2}\,\frac{3}{2}\right\rangle\right\rvert^2 = A^2$
0	0	1/2	1/2	$A^2\left\lvert\left\langle 1\,\frac{1}{2}\,0\,\frac{1}{2}\middle\vert\frac{3}{2}\,\frac{1}{2}\right\rangle\right\rvert^2 = \frac{2}{3}A^2$
−1	−1	1/2	−1/2	$A^2\left\lvert\left\langle 1\,\frac{1}{2}\,-1\,\frac{1}{2}\middle\vert\frac{3}{2}\,-\frac{1}{2}\right\rangle\right\rvert^2 = \frac{1}{3}A^2$

where $A = CI^q_{n'00,n1m}$, C being a constant and $I^q_{n'00,n1m}$ is given by [4.85] and has the same value in each case. The transition rates for the case $m_s = -1/2$ are the same as for $m_s = +1/2$, so that the total rate is $4A^2$. For transitions from the states of the $np_{1/2}$ level the possible transition

rates are, for $m_s = m_s' = 1/2$

Initial states				Transition rate
q	m_l	m_s	m	
0	0	1/2	1/2	$A^2\left\lvert\left\langle 1\frac{1}{2}0\frac{1}{2}\middle\vert\frac{1}{2}\frac{1}{2}\right\rangle\right\rvert^2 = \frac{A^2}{3}$
-1	-1	1/2	$-1/2$	$A^2\left\lvert\left\langle 1\frac{1}{2}-1\frac{1}{2}\middle\vert\frac{1}{2}-\frac{1}{2}\right\rangle\right\rvert^2 = \frac{2A^2}{3}$

where A has the same value as before. The total rate from both the $m_s = 1/2$ and $m_s = -1/2$ states is thus $2A^2$ and the ratio of the transition rate $np_{3/2} \to n's_{1/2}$ to the transition rate $np_{1/2} \to n's_{1/2}$ is 2:1.

5.3 From [5.56] and [5.60] the transition rates for the π and $\sigma^{\pm}$ lines are (using [4.85], [4.40])

$$W_{ab}^s(\pi) = C(\omega_{ba}) \sin^2 \Theta \langle l1m0|l'm'\rangle^2 A$$

$$W_{ab}^s(\sigma^{\pm}) = C(\omega_{ba})\tfrac{1}{2}(1 + \cos^2 \Theta)\langle l1m \mp 1|l'm'\rangle A$$

where $A = \dfrac{2l+1}{2l'+1}\langle l100|l'0\rangle^2\left[\displaystyle\int_0^\infty drr^3R_{n'l'}(r)R_{nl}(r)\right]^2$

and $l - l' = \pm 1$.

Each of the $(2l' + 1)$ states of the initial level will be, in general, populated equally, so the intensities of the π and $\sigma^{\pm}$ lines are

$$I(\pi) = \frac{\hbar\omega_{ba}}{2l'+1}\sum_{m'} W_{ab}^s(\pi)$$

$$I(\sigma^{\pm}) = \frac{\hbar\omega_{ba}}{2l'+1}\sum_{m'} W_{ab}^s(\sigma^{\pm})$$

Using the orthogonality relation for the Clebsch–Gordan coefficients [A4.32], together with [A4.33], we see that

$$\sum_{m'}\langle l1m0|l'm'\rangle^2 = \sum_{m'}\langle l1m \mp 1|l'm'\rangle^2 = \tfrac{1}{3}(2l'+1)$$

It follows that with $\Theta = \pi/2$

$$I(\pi):I(\sigma^+):I(\sigma^-) = 2:1:1$$

A similar argument shows that in the anomalous Zeeman effect the average intensity of the π lines is twice that of the σ^+ (or σ^-) lines (see Problem 8.5).

CHAPTER 6

6.3 The following table summarises the results (in a.u.)

	'Zero-order' wave function $\psi_0^{(0)}$ ([6.35])	Screened variat. function [6.70] with $Z_e = 27/16$	Hartree–Fock wave function [6.85]	'Exact' (variat.) wave function
Energy	-2.750	-2.848	-2.862	-2.904
$\langle r_1^2 + r_2^2 \rangle$	1.50	2.11	2.37	2.39
$\langle \delta(\mathbf{r}_1) \rangle$	2.55	1.53	1.80	1.81
$\langle \delta(\mathbf{r}_{12}) \rangle$	0.318	0.191	0.188	0.106

Note the improvement in going from the zero-order wave function $\psi_0^{(0)}$ to the Hartree–Fock wave function. Nevertheless, the Hartree–Fock wave function provides a poor value (too large by almost a factor of two) of $\langle \delta(\mathbf{r}_{12}) \rangle$. This is to be expected since the Hartree–Fock wave function is an independent particle wave function, and $\delta(\mathbf{r}_{12})$ probes the region $\mathbf{r}_1 = \mathbf{r}_2$ where the electrostatic repulsion term $1/r_{12}$ is most important.

6.5 (a) $E_{2s2p} = \left(-\dfrac{1}{2} - \dfrac{1}{32}\right)$ a.u. $= -0.53125$ a.u. $\simeq -14.5$ eV; $\lambda = 192$ Å;

(b) $v = 1.71$ a.u. $= 3.75 \times 10^6$ m s^{-1}

CHAPTER 7

7.1 $$H_c = \sum_{i=1}^{N} h_i, \qquad h_i = -\frac{1}{2}\nabla_{r_i}^2 + V(r_i)$$

Since the angular part of $\nabla_{r_i}^2$ is proportional to $\mathbf{L}_i^2$, we have $[\nabla_i^2, \mathbf{L}_i] = 0$. Moreover, we know from Problem 2.12 that $\mathbf{L}_i$ commutes with any function of r_i. Therefore $\mathbf{L}_i$ commutes with h_i, and hence $\mathbf{L} = \Sigma_i \mathbf{L}_i$ commutes with H_c.

7.2 $$\Phi_{2^3S}(M_S = 1) = \frac{1}{\sqrt{2}} \begin{vmatrix} u_{1s\uparrow}(1) & u_{2s\uparrow}(1) \\ u_{1s\uparrow}(2) & u_{2s\uparrow}(2) \end{vmatrix}$$

$$\Phi_{2^3S}(M_S = 0) = \frac{1}{\sqrt{2}} \left\{ \frac{1}{\sqrt{2}} \begin{vmatrix} u_{1s\uparrow}(1) & u_{2s\downarrow}(1) \\ u_{1s\uparrow}(2) & u_{2s\downarrow}(2) \end{vmatrix} + \frac{1}{\sqrt{2}} \begin{vmatrix} u_{1s\downarrow}(1) & u_{2s\uparrow}(1) \\ u_{1s\downarrow}(2) & u_{2s\uparrow}(2) \end{vmatrix} \right\}$$

$$\Phi_{2^3S}(M_S = -1) = \frac{1}{\sqrt{2}} \begin{vmatrix} u_{1s\downarrow}(1) & u_{2s\downarrow}(1) \\ u_{1s\downarrow}(2) & u_{2s\downarrow}(2) \end{vmatrix}$$

7.4 (a) $Z^{-1/3}$ a.u.
(b) $Z^{4/3}$ a.u.
(c) $Z^{7/3}$ a.u.

7.7 From Problem 7.2, we have

$$\Phi_{2^3S}(M_S = 1) = \frac{1}{\sqrt{2}} \begin{vmatrix} u_{1s\uparrow}(1) & u_{2s\uparrow}(1) \\ u_{1s\uparrow}(2) & u_{2s\uparrow}(2) \end{vmatrix}$$

with $u_{1s\uparrow} = u_{1s}(r)\alpha, \qquad u_{2s\uparrow} = u_{2s}(r)\alpha$

The coupled Hartree–Fock equations for $u_{1s}(r)$ and $u_{2s}(r)$ are

$$\left[-\frac{1}{2}\nabla^2 - \frac{2}{r} + V^{\mathrm{d}}_{2s} - V^{\mathrm{ex}}_{2s}\right] u_{1s}(r) = E_{1s} u_{1s}(r) \tag{1}$$

and

$$\left[-\frac{1}{2}\nabla^2 - \frac{2}{r} + V^{\mathrm{d}}_{1s} - V^{\mathrm{ex}}_{1s}\right] u_{2s}(r) = E_{2s} u_{2s}(r) \tag{2}$$

with

$$V^{\mathrm{d}}_{1s}(r) = \int u_{1s}(r') \frac{1}{|\mathbf{r} - \mathbf{r}'|} u_{1s}(r') \,\mathrm{d}\mathbf{r}'$$

$$V^{\mathrm{ex}}_{1s}(r) f(\mathbf{r}) = \left[\int u_{1s}(r') \frac{1}{|\mathbf{r} - \mathbf{r}'|} f(\mathbf{r}') \,\mathrm{d}\mathbf{r}'\right] u_{1s}(r)$$

and similar relations for V^{d}_{2s} and V^{ex}_{2s}. Taking the scalar product of (1) with u_{2s}, we have

$$\left\langle u_{2s} \left| -\frac{1}{2}\nabla^2 - \frac{2}{r} + V^{\mathrm{d}}_{2s} - V^{\mathrm{ex}}_{2s} \right| u_{1s} \right\rangle = E_{1s} \langle u_{2s} | u_{1s} \rangle \tag{3}$$

Similarly, taking the scalar product of (2) with u_{1s} and using the fact that the operators are Hermitian, we find that

$$\left\langle u_{2s} \left| -\frac{1}{2}\nabla^2 - \frac{2}{r} + V^{\mathrm{d}}_{1s} - V^{\mathrm{ex}}_{1s} \right| u_{1s} \right\rangle = E_{2s} \langle u_{2s} | u_{1s} \rangle \tag{4}$$

Subtracting (4) from (3) and remembering that

$$(V^{\mathrm{d}}_{1s} - V^{\mathrm{ex}}_{1s}) u_{1s} = 0, \qquad (V^{\mathrm{d}}_{2s} - V^{\mathrm{ex}}_{2s}) u_{2s} = 0$$

we see that

$$\langle u_{2s} | u_{1s} \rangle = 0.$$

7.10 (a) (i) ^{1}S; ^{3}S

(ii) ^{1}P; ^{3}P

(iii) ^{1}D; ^{3}D

(iv) ^{1}S; ^{1}D; ^{1}G; ^{3}P; ^{3}F

(v)	^{2}S;	^{2}P;	^{2}D;	^{2}F:	^{4}S;	^{4}P;	^{4}D;	^{4}F
	2	6	4	2		3	2	

(vi) ^{2}P; ^{2}D; ^{4}S

(b) (i) $^1S_0$; $^3S_1$
(ii) $^1P_1$; $^3P_0$; $^3P_1$; $^3P_2$
(iii) $^1D_2$; $^3D_1$; $^3D_2$; $^3D_3$
(iv) $^1S_0$; $^1D_2$; $^1G_4$; $^3P_0$, $^3P_1$, $^3P_2$; $^3F_2$, $^3F_3$, $^3F_4$,
(v) $^2S_{1/2}$; $^2P_{1/2}$, $^2P_{3/2}$; $^2D_{3/2}$, $^2D_{5/2}$; $^2F_{5/2}$, $^2F_{7/2}$; $^4S_{3/2}$; $^4P_{1/2}$, $^4P_{3/2}$, $^4P_{5/2}$; $^4D_{1/2}$, $^4D_{3/2}$, $^4D_{5/2}$, $^4D_{7/2}$; $^4F_{3/2}$, $^4F_{5/2}$, $^4F_{7/2}$, $^4F_{9/2}$
(vi) $^2P_{1/2}$, $^2P_{3/2}$; $^2D_{3/2}$, $^2D_{5/2}$; $^4S_{3/2}$.

7.11 (a) We have $j_1 = 1/2, 3/2$ for a p electron and $j_2 = 3/2, 5/2$ for a d electron. For the configuration np nd the possible values of J and terms $(j_1 j_2)_J$ are then given by

$j_1 j_2$	J	Terms $(j_1 j_2)_J$
1/2 3/2	1, 2	$(1/2\ 3/2)_1$, $(1/2\ 3/2)_2$
1/2 5/2	2, 3	$(1/2\ 5/2)_2$, $(1/2\ 5/2)_3$
3/2 3/2	0, 1, 2, 3	$(3/2\ 3/2)_0$, $(3/2\ 3/2)_1$, $(3/2\ 3/2)_2$, $(3/2\ 3/2)_3$
3/2 5/2	1, 2, 3, 4	$(3/2\ 5/2)_1$, $(3/2\ 5/2)_2$, $(3/2\ 5/2)_3$, $(3/2\ 5/2)_4$

(b) For the configuration $(nl\ 3/2)^2$ the only allowed values of J are $J = 0, 2$ and the terms are

$$(3/2\ 3/2)_0,\ (3/2\ 3/2)_2$$

CHAPTER 8

8.1 (a) $\Delta M_J = \pm 1, 0$ for all λ and
$|\Delta J| = \lambda, \lambda - 1, \ldots 0$ with $J + J' > \lambda$
For odd λ the parity changes while for even λ the parity does not change.
(b) The rules for M_J and J are the same as for (a) but for odd λ the parity does not change, while for even λ the parity changes.

8.4 (a) The intervals between adjacent levels are 20 cm^{-1} and 40 cm^{-1}. Thus, if J is the total angular momentum quantum number of the highest level of the multiplet, the Landé interval rule gives $40 = AJ$ and $20 = A(J - 1)$. Hence $J = 2$, and the two other levels have $J = 1$ and $J = 0$. Since $J = 0$ is possible, $|L - S| = 0$ from which $L = S$. From [8.31] we then see that $L = S = 1$. The three fine structure levels of the multiplet are therefore $^3P_0$, $^3P_1$, $^3P_2$.
(b) Since both the ground state term and the excited term are ^3P, we have $\Delta L = \Delta S = 0$. The allowed transitions are given by $\Delta J = 0, \pm 1$, with $J = 0 \to J' = 0$ forbidden. Thus there are six lines

J	J'	λ
$J = 2$	to $J' = 2$	$\lambda = 1657.0$ Å
1	1	$= 1657.4$ Å
2	1	$= 1658.1$ Å
1	0	$= 1657.9$ Å
1	2	$= 1656.3$ Å
0	1	$= 1656.9$ Å

8.5 (a) From [8.45] the Landé factors are

$$^2P_{3/2},\ g_{\mathcal{J}} = 4/3; \qquad ^2P_{1/2},\ g_{\mathcal{J}} = 2/3; \qquad ^2S_{1/2}, \qquad g_{\mathcal{J}} = 2$$

The possible angular frequencies are $\omega^{\mathcal{J}} = \omega_0^{\mathcal{J}} + \Delta\omega_0^{\mathcal{J}}$ where $\omega_0^{\mathcal{J}}$ is the frequency in the absence of the magnetic field and

$$\Delta\omega^{\mathcal{J}} = \frac{\mu_B \mathcal{B}_z}{\hbar}(g_{\mathcal{J}'} M'_{\mathcal{J}} - g_{\mathcal{J}} M_{\mathcal{J}})$$

where the prime denotes the upper level b.
For $^2P_{1/2} \rightarrow {}^2S_{1/2}$ we find separate lines in order of increasing frequency

$M_{\mathcal{J}'}$	$M_{\mathcal{J}}$	$g_{\mathcal{J}'} M'_{\mathcal{J}} - g_{\mathcal{J}} M_{\mathcal{J}}$	Type of line	q
$-1/2$	$1/2$	$-4/3$	σ^+	-1
$1/2$	$1/2$	$-2/3$	π	0
$-1/2$	$-1/2$	$2/3$	π	0
$1/2$	$-1/2$	$4/3$	σ^-	$+1$

For $^2P_{3/2} \rightarrow {}^2S_{1/2}$ we find

$M_{\mathcal{J}'}$	$M_{\mathcal{J}}$	$g_{\mathcal{J}'} M'_{\mathcal{J}} - g_{\mathcal{J}} M_{\mathcal{J}}$	Type of line	q
$-1/2$	$1/2$	$-5/3$	σ^+	-1
$-3/2$	$-1/2$	-1	σ^+	-1
$1/2$	$1/2$	$-1/3$	π	0
$-1/2$	$-1/2$	$1/3$	π	0
$3/2$	$1/2$	1	σ^-	$+1$
$1/2$	$-1/2$	$5/3$	σ^-	$+1$

(b) The transition rates for π and σ lines are from [8.6] (compare with [5.56] and [5.60])

$$W^s_{ab}(\pi) = \tilde{C}(\omega_{ba}) \sin^2\Theta\, |\langle\gamma'\mathcal{J}'M'_{\mathcal{J}}|D_0|\gamma\mathcal{J}M_{\mathcal{J}}\rangle|^2$$

$$W^s_{ab}(\sigma^{\pm}) = \tilde{C}(\omega_{ba})\tfrac{1}{2}(1 + \cos^2\Theta)|\langle\gamma'\mathcal{J}'M'_{\mathcal{J}}|D_{\mp 1}|\gamma\mathcal{J}M_{\mathcal{J}}\rangle|^2$$

where $\tilde{C}(\omega_{ba}) = e\ {}^2C(\omega_{ba})$ and $\Theta = \pi/2$ for transverse observation. Assuming the upper levels are equally populated, the relative intensities of the lines are given by [8.11], through the factors $\sin^2\Theta\ |\langle\mathcal{J}1M_{\mathcal{J}}0|\mathcal{J}'M_{\mathcal{J}'}\rangle|^2$ for the π lines and $\frac{1}{2}(1 + \cos^2\Theta)$ $|\langle\mathcal{J}1M_{\mathcal{J}} \pm 1|\mathcal{J}'M_{\mathcal{J}'}\rangle|^2$ for the $\sigma^{\pm}$ lines
With $\Theta = \pi/2$, we find by using Table A4.1 that
(i) the intensities of all the lines in the $^2P_{1/2} \rightarrow {}^2S_{1/2}$ transition are equal
(ii) the intensities of the lines in the $^2P_{3/2} \rightarrow {}^2S_{1/2}$ transition are in the ratios 1:3:4:4:3:1.
Note that (see Problem 5.3) the average intensity of the π lines is twice the average intensity of the σ^+ or of the σ^- lines.

CHAPTER 9

9.1 The energies of these five levels are: 2.1×10^{-3}; 6.3×10^{-3}; 12.6×10^{-3}; 21×10^{-3}; 31.5×10^{-3} eV and the corresponding wave numbers are: 16.9; 50.8; 101.5; 169.2; 253.8 cm^{-1}. The internuclear distance is 1.43 Å or 2.71 a.u.

9.2 (a) 0.164 eV and 0.493 eV (b) 2.5×10^{-14} s and 0.84×10^{-14} s. (c) 4.12×10^2 N/m.

9.3 The depth of the potential well in H_2 is $D_e = D_0 + \hbar\omega_0/2 = (4.48 + 0.26)$ eV and this is the same for the D_2 molecule. The force constant for the vibrational motion k is the same for H_2 and D_2, hence the zero-point energy for $D_2 = 0.26 \times (M_p/M_D)^{1/2} = 0.18$ eV (see [9.24]). Hence for D_2, $D_0 = 4.48 + 0.26 - 0.18 = 4.56$ eV.

9.4 From [9.34], with $\bar{k} \simeq k$ and $c_1 = c_2 = 0$, we have

$$\frac{\mathrm{d}V_{\text{eff}}}{\mathrm{d}R} \simeq k(R - R_1) \tag{a}$$

and from [9.33]

$$\frac{\mathrm{d}V_{\text{eff}}}{\mathrm{d}R} = \frac{\mathrm{d}V(R)}{\mathrm{d}R} - \frac{\hbar^2}{\mu}\frac{\mathcal{J}(\mathcal{J}+1)}{R^3} \tag{b}$$

Equating (a) and (b) at the point $R = R_0$, for which $\mathrm{d}V(R)/\mathrm{d}R = 0$ we find

$$R_1 = R_0 + \frac{\hbar^2}{k\mu}\frac{\mathcal{J}(\mathcal{J}+1)}{R_0^3}$$

from which [9.35] follows on substituting for k using [9.28].

9.7 Using the reduced mass $\mu = 2.3042 \times 10^{-26}$ kg and $\tilde{\nu}$ we calculate the force constant k. Converting to atomic units this is $k = 0.0698$ a.u. From [9.95], at $R = R_0$

$$\frac{\partial E_s}{\partial R} = 0 \quad \text{or} \quad \left(\frac{1}{R_0^2} - cA\mathrm{e}^{-cR_0}\right) = 0 \tag{1}$$

which gives $A = \mathrm{e}^{cR_0}/cR_0^2$. Now

$$k = \left.\frac{\partial^2 E_s}{\partial R^2}\right|_{R=R_0} = -\frac{2}{R_0^3} + Ac^2\mathrm{e}^{-cR_0} \tag{2}$$

From (1) and (2) and using the computed value of k, we find $c = 1.837$ a.u. (or 3.47 Å^{-1}). Finally from (1) $A = 98.9$ a.u. (or 2692 eV) and $E_s(R_0) = -0.142$ a.u. (or -3.87 eV), giving $D_0 = (3.87 - 0.02)$ eV $= 3.85$ eV.

CHAPTER 10

10.1 The ratio is given by Boltzmann's distribution $R = (g_J/g_0)\exp(E_0 - E_J)/kT$ where g_J is the degeneracy of the Jth level. Since each rotational level is $(2J + 1)$-fold degenerate the result follows. By differentiating we find that $R(J)$ has a maximum at $J \simeq (kT/2B)^{1/2}$. The intensity of an absorption line is proportional to the number of molecules in the *lower* level and hence is proportional to $R(J)$.

10.2 Unlike rotational levels, vibrational levels are not degenerate so that $R = \exp[(E_0 - E_v)/kT]$. For $v = 1$ we have $R = \exp(-\hbar\omega_0/kT)$.

10.3 $\tilde{B} = 1.93\ \text{cm}^{-1}$; $R_0 = 1.12$ Å; $k = 1.9 \times 10^3$ N/m.

10.4 (a) The Deslandres table is constructed from [10.33]

(b) The wave number of the $v' = 0$ to $v = 0$ transition is $\tilde{\nu} = \tilde{\nu}_{s's} - 801.54\ \text{cm}^{-1} = 102\,877.3\ \text{cm}^{-1}$

(c) To draw the Fortrat parabola and calculate the positions of the lines of each branch we use [10.34] with

$$\begin{aligned}(\tilde{\nu}^{\mathrm{P}} - \tilde{\nu}) &= 1.145\, J(J - 1) - 2.010\, J(J + 1)\\ &= 1.145\, m(m - 1) - 2.010\, m(m + 1)\end{aligned}$$

with $m = 0, 1, 2, 3 \ldots$ and $(\tilde{\nu}^{\mathrm{R}} - \tilde{\nu})$ is given by the same formula with $m = -1, -2, -3 \ldots$.
The $R(1)$ line forms the band head at $(\tilde{\nu} + 2.29\ \text{cm}^{-1}) = 102\,879.6\ \text{cm}^{-1}$ and the band is shaded to the red.

CHAPTER 11

11.6 Starting from [11.59], we have

$$\int_{-1}^{1} P_L(\cos\theta)\frac{d\sigma}{d\Omega}\, d(\cos\theta) = \frac{1}{k^2}\sum_{l=0}^{\infty}\sum_{l'=0}^{\infty}(2l + 1)(2l' + 1)\, e^{i(\delta_l - \delta_{l'})}$$

$$\times \sin\delta_l \sin\delta_{l'} \int_{-1}^{+1} P_L(\cos\theta)P_l(\cos\theta)P_{l'}(\cos\theta)\, d(\cos\theta)$$

Evaluating this expression with $L = 0$, we find

$$A = \frac{\sigma_{\text{tot}}}{4\pi} = \frac{1}{k^2}\sum_{l=0}^{\infty}(2l + 1)\sin^2\delta_l$$

Similarly, with $L = 1$, we have

$$B = \frac{6}{k^2}\sum_{l=0}^{\infty}(l + 1)\sin\delta_l \sin\delta_{l+1}\cos(\delta_{l+1} - \delta_l)$$

and with $L = 2$, one obtains

$$C = \frac{5}{k^2} \sum_{l=0}^{\infty} \left[\frac{l(l+1)(2l+1)}{(2l+1)(2l+3)} \sin^2 \delta_l \right.$$

$$\left. + \frac{3(l+1)(l+2)}{2l+3} \sin \delta_l \sin \delta_{l+2} \cos(\delta_{l+2} - \delta_l) \right]$$

11.8 Proceeding as in the case of the square well [11.83], but with U_0 replaced by $-U_0$, we find that

$$\delta_0 = -ka + \tan^{-1}\left(\frac{k}{K} \tanh Ka\right), \qquad K = (U_0 - k^2)^{1/2}$$

Hence, for $k \to 0$, we have

$$\delta_0 = ka\left[\frac{\tanh(\lambda_0 a)}{\lambda_0 a} - 1\right], \qquad \lambda_0 = \sqrt{U_0}$$

and therefore, at zero energy

$$\sigma_{\text{tot}} = \sigma_0 = 4\pi a^2 \left[\frac{\tanh(\lambda_0 a)}{\lambda_0 a} - 1\right]^2$$

As $U_0 \to \infty$, this zero-energy cross-section becomes $\sigma_{\text{tot}} = 4\pi a^2$, in agreement with the result [11.97] obtained for the 'hard sphere' potential.

11.9 (a) $\tan \delta_0 = -\frac{1}{k} \int_0^\infty \sin^2(kr)\, U(r)\, \mathrm{d}r$

$$= -\frac{U_0}{k} \int_0^\infty \sin^2(kr) \frac{\mathrm{e}^{-\alpha r}}{r} \mathrm{d}r = -\frac{U_0}{4k} \log\left(1 + \frac{4k^2}{\alpha^2}\right)$$

(b) $\tan \delta_0 = -\frac{U_0}{k} \int_0^\infty \sin^2(kr) \frac{1}{(r^2 + d^2)^2} \mathrm{d}r$

$$= -\frac{\pi U_0}{8kd^3} [1 - (1 + 2kd)\mathrm{e}^{-2kd}]$$

11.12 (a) $f_{\mathrm{B1}} = -U_0 \frac{2\alpha}{(\alpha^2 + \Delta^2)^2}$

$$\sigma_{\text{tot}}^{\mathrm{B1}} = \frac{16\pi U_0^2}{3} \frac{16k^4 + 12\alpha^2 k^2 + 3\alpha^4}{\alpha^4(\alpha^2 + 4k^2)^3}$$

$$\sigma_{\text{tot}}^{\mathrm{B1}} \underset{E\to\infty}{\sim} AE^{-1}, \qquad A = \frac{2\pi\hbar^2 U_0^2}{3m\alpha^4}$$

$$\text{(b)}\quad f_{\mathrm{B1}} = -U_0\,\frac{\pi^{1/2}}{4\alpha^3}\,\mathrm{e}^{-\Delta^2/4\alpha^2}$$

$$\sigma_{\mathrm{tot}}^{\mathrm{B1}} = \frac{\pi^2 U_0^2}{8\alpha^4 k^2}\,[1 - \mathrm{e}^{-2k^2/\alpha^2}]$$

$$\sigma_{\mathrm{tot}}^{\mathrm{B1}} \underset{E\to\infty}{\sim} AE^{-1}, \qquad A = \frac{\pi^2\hbar^2 U_0^2}{16m\alpha^4}$$

$$\text{(c)}\quad f_{\mathrm{B1}} = -\frac{U_0}{\Delta^3}\,(\sin\Delta a - \Delta a\cos\Delta a)$$

$$\sigma_{\mathrm{tot}}^{\mathrm{B1}} = 8\pi U_0^2 a^6 F(x)$$

where

$$F(x) = \frac{1}{4x^2}\left(1 - \frac{1}{x^2} + \frac{\sin 2x}{x^3} - \frac{\sin^2 x}{x^4}\right)$$

and $x = 2ka$

$$\sigma_{\mathrm{tot}}^{\mathrm{B1}} \underset{E\to\infty}{\sim} AE^{-1}, \qquad A = \frac{\pi\hbar^2 a^4 U_0^2}{4m}$$

$$\text{(d)}\quad f_{\mathrm{B1}} = -\frac{\pi U_0}{4d}\,\mathrm{e}^{-\Delta d}$$

$$\sigma_{\mathrm{tot}}^{\mathrm{B1}} = \frac{\pi^3 U_0^2}{32 d^4 k^2}\,[1 - (4kd + 1)\mathrm{e}^{-4kd}]$$

$$\sigma_{\mathrm{tot}}^{\mathrm{B1}} \underset{E\to\infty}{\sim} AE^{-1}, \qquad A = \frac{\pi^3\hbar^2 U_0^2}{64 m d^4}$$

CHAPTER 12

12.3 In atomic units $\psi_1(r) = \mathrm{e}^{-r}/\sqrt{\pi}$, so that

$$V_{11}(r_1) = -\frac{1}{r_1} + \frac{1}{\pi}\int_0^\infty r_2^2\,\mathrm{d}r_2 \int_{-1}^{-1} \mathrm{d}(\cos\theta_2) \times \int_0^{2\pi} \mathrm{d}\phi_2\,\mathrm{e}^{-2r_2}\,\frac{1}{|\mathbf{r}_1 - \mathbf{r}_2|}$$

Taking $\mathbf{r}_1$ as the polar axis for the integration over $\mathbf{r}_2$, and expanding

$$\frac{1}{|\mathbf{r}_1 - \mathbf{r}_2|} = \sum_{l=0}^{\infty} \frac{r_<^l}{r_>^{l+1}}\,P_l(\cos\theta_2)$$

where $r_<$ and $r_>$ are respectively the lesser and greater of r_1 and r_2, we find

$$V_{11}(r_1) = -\frac{1}{r_1} + 4\int_0^\infty r_2^2\, e^{-2r_2}\left(\frac{1}{r_>}\right) dr_2$$
$$= -\frac{1}{r_1} + \frac{4}{r_1}\int_0^{r_1} r_2^2\, e^{-2r_2}\, dr_2 + 4\int_{r_1}^\infty r_2\, e^{-2r_2}\, dr_2$$

The integration is elementary and we find

$$V_{11}(r_1) = -\left(1 + \frac{1}{r_1}\right)\exp(-2r_1)$$

12.4 Using the approximate wave function for helium

$$\psi(r_2, r_3) = \left(\frac{Z_e^3}{\pi}\right)\exp[-Z_e(r_2 + r_3)], \quad \text{we have}$$

$$V_{11}(r_1) = -\frac{2}{r_1} + \left(\frac{Z_e^3}{\pi}\right)^2 \int d\mathbf{r}_2 \int d\mathbf{r}_3 \exp[-2Z_e(r_2 + r_3)]$$
$$\times\left(\frac{1}{|\mathbf{r}_1 - \mathbf{r}_2|} + \frac{1}{|\mathbf{r}_1 - \mathbf{r}_3|}\right)$$

Proceeding as in Problem 12.3, we find

$$V_{11}(r_1) = -2\left(Z_e + \frac{1}{r_1}\right)\exp(-2Z_e r_1)$$

12.5 Using $f_s = -\dfrac{1}{2\pi}\displaystyle\int e^{i\boldsymbol{\Delta}\cdot\mathbf{r}}V_{11}(r)\, d\mathbf{r}$

with V_{11} equal to the static potential obtained in Problem 12.4 we find

$$f_s = 4\left[\frac{8Z_e^2 + \Delta^2}{(4Z_e^2 + \Delta^2)^2}\right]$$

For the polarisation potential, we have

$$f_{\text{pol}} = \frac{1}{2\pi}\int e^{i\boldsymbol{\Delta}\cdot\mathbf{r}}\frac{\bar{\alpha}}{2(r^2 + d^2)^2}\, d\mathbf{r}$$
$$= \frac{\pi\bar{\alpha}}{4d}\, e^{-d\Delta}$$

The total amplitude in the Born approximation is $f = f_s + f_{\text{pol}}$ and the cross-section is $d\sigma/d\Omega = |f|^2$. On substituting the numerical values comparison can be made with the data shown in Fig. 12.4.

CHAPTER 13

13.1 (a) $E_R = 0.247$ eV (b) $v_R = 0.97 \times 10^4$ m/s

13.2 Making the approximation $E_j = 0$, $j \neq 0$, we have

$$E^{(2)}(R) = \frac{1}{E_0} \sum_{j \neq 0} \langle \psi_0 | V | \psi_j \rangle \langle \psi_j | V | \psi_0 \rangle$$

where the sum over j runs over all excited states of the two hydrogenic systems centred at A and B. The sum can now be extended to cover the ground state term ($j = 0$), since, as in [13.13], the ground state matrix element $\langle \psi_0 | V | \psi_0 \rangle$ vanishes. This allows us to use the closure relation $\Sigma_j | \psi_j \rangle \langle \psi_j | = 1$, giving

$$E^{(2)}(R) = \frac{1}{E_0} \langle \psi_0 | V^2 | \psi_0 \rangle$$

and from [13.9]

$$E^{(2)}(R) = \frac{1}{R^6} \langle \psi_0 | x_{1A}^2 x_{2B}^2 + y_{1A}^2 y_{2B}^2 + 4 z_{1A}^2 z_{2B}^2 | \psi_0 \rangle$$

all other terms vanishing because ψ_0 is spherically symmetrical. It follows immediately that

$$E^{(2)}(R) = -\frac{C_W}{R^6}$$

with

$$C_W = 6\left(\frac{4\pi}{3}\right)^2 \left[\int_0^\infty r^4 |\psi_{1s}(r)|^2 \, dr\right]^2 = 6 \text{ a.u.}$$

This may be compared with the exact value of $C_W = 6.499$ a.u.

13.3 From [13.38]

$$\begin{aligned} \sigma_T &= 2\pi \int_{\theta_0}^{\pi} g(s) \left(\frac{A}{E}\right)^{2/s} \left(\frac{1}{\theta}\right)^{1+2/s} d\theta \\ &\simeq 2\pi g(s) \left(\frac{A}{E}\right)^{2/s} \left(\frac{s}{2}\right) \theta_0^{-2/s} \end{aligned}$$

(since the scattering is concentrated at small angles, the contribution from the upper limit of the integral can be neglected).

Now $g(6) = \dfrac{1}{6}\left[\dfrac{15\pi}{16}\right]^{1/3}$, so that

$$\sigma_T(E, \theta_0) = \pi \left[\frac{15\pi}{16} \frac{A}{E\theta_0}\right]^{1/3}$$

13.4 Proceeding as in the MO case, the equation comparable to [13.62] is

$$\int \mathrm{d}\mathbf{r}[\psi_{1s}(r_B)\mathrm{e}^{-iE_{1s}t}\mathrm{e}^{-i\mathbf{v}\cdot\mathbf{r}/2}\mathrm{e}^{-iv^2t/8}]^\star\left(H - i\frac{\partial}{\partial t}\right)\Psi(\mathbf{r}, t) = 0$$

$$\int \mathrm{d}\mathbf{r}[\psi_{1s}(r_A)\mathrm{e}^{-iE_{1s}t}\mathrm{e}^{+i\mathbf{v}\cdot\mathbf{r}/2}\mathrm{e}^{-iv^2t/8}]^\star\left(H - i\frac{\partial}{\partial t}\right)\Psi(\mathbf{r}, t) = 0 \qquad [A]$$

A little calculation shows that the unperturbed functions satisfy

$$\left[-\frac{1}{2}\nabla_r^2 - \frac{1}{r_{A,B}} - i\frac{\partial}{\partial t}\right]\{\psi_{1s}(r_{A,B})\mathrm{e}^{-iE_{1s}t}\mathrm{e}^{\pm i\mathbf{v}\cdot\mathbf{r}/2}\mathrm{e}^{-iv^2t/8}\} = 0$$

Using this result we find, from [A], coupled equations for the amplitudes $a(b, t)$ and $c(b, t)$:

$$i[\dot{a}(b, t) + N\dot{c}(b, t)] = Pa(b, t) + Qc(b, t)$$

$$i[N^\star\dot{a}(b, t) + \dot{c}(b, t)] = \bar{Q}a(b, t) + Pc(b, t) \qquad [B]$$

where

$$N(t) = \int \psi_{1s}(r_B)\psi_{1s}(r_A)\mathrm{e}^{i\mathbf{v}\cdot\mathbf{r}}\,\mathrm{d}\mathbf{r}$$

$$P(t) = \int |\psi_{1s}(r_B)|^2\left(\frac{1}{R} - \frac{1}{r_A}\right)\mathrm{d}\mathbf{r} = \int |\psi_{1s}(r_A)|^2\left(\frac{1}{R} - \frac{1}{r_B}\right)\mathrm{d}\mathbf{r}$$

$$Q(t) = \int \psi_{1s}(r_B)\psi_{1s}(r_A)\mathrm{e}^{i\mathbf{v}\cdot\mathbf{r}}\left(\frac{1}{R} - \frac{1}{r_B}\right)\mathrm{d}\mathbf{r}$$

$$\bar{Q}(t) = \int \psi_{1s}(r_A)\psi_{1s}(r_B)\mathrm{e}^{-i\mathbf{v}\cdot\mathbf{r}}\left(\frac{1}{R} - \frac{1}{r_A}\right)\mathrm{d}\mathbf{r}$$

Using [13.48], it is easy to show that $N = N^\star$ and $Q = Q^\star = \bar{Q}$, and the equations [B] can be written in the form

$$i\dot{a}(b, t) = \left(\frac{P - NQ}{1 - N^2}\right)a(b, t) + \left(\frac{Q - NP}{1 - N^2}\right)c(b, t)$$

$$i\dot{c}(b, t) = \left(\frac{Q - NP}{1 - N^2}\right)a(b, t) + \left(\frac{P - NQ}{1 - N^2}\right)c(b, t)$$

A solution with $a(b, t = -\infty) = 1$, $c(b, t = -\infty) = 0$, can now be obtained, and the charge exchange probability is given (compare with [13.70]) by

$$P_{\mathrm{CE}} = |c(b, t = +\infty)|^2 = \sin^2\left\{\int_{\infty}^{\infty}\left(\frac{Q - NP}{1 - N^2}\right)\mathrm{d}t\right\}$$

CHAPTER 14

14.4 (a) From [1.19], $\lambda_{max} = 4830$ Å

(b) The fraction of the sun's energy radiated in the visible range is

$$f = \frac{\displaystyle\int_{\lambda_1}^{\lambda_2} \lambda^{-5}[\exp(hc/\lambda kT) - 1]^{-1}\, d\lambda}{\displaystyle\int_0^{\infty} \lambda^{-5}[\exp(hc/\lambda kT) - 1]^{-1}\, d\lambda}$$

where $\lambda_1 = 4000$ Å and $\lambda_2 = 7000$ Å. Writing $x = hc/\lambda kT$, we have

$$f = \frac{\displaystyle\int_{x_1}^{x_2} x^3(e^x - 1)^{-1}\, dx}{\displaystyle\int_0^{\infty} x^3(e^x - 1)^{-1}\, dx}$$

with $x_1 = 3.426$ and $x_2 = 5.995$. The denominator is exactly $\pi^4/15$ and the numerator can be evaluated by numerical integration, yielding the result $f \simeq 0.38$.

11 Fundamental constants, atomic units and conversion factors

The physical constants listed in Table A11.1 are mainly taken from 'The 1973 Least-Squares Adjustment of the Fundamental Constants' by E. R. Cohen and B. N. Taylor, in *J. Phys. Chem. Ref. Data* **2**, 663 (1973) and from 'The 1973 Table of the Fundamental Physical Constants', by E. R. Cohen, in *Atomic Data and Nuclear Data Tables*, **18**, 587 (1976), where critical discussions of errors may be found.

We recall that the quantities ε_0 and μ_0 are related by the formula

$$\varepsilon_0 \mu_0 c^2 = \kappa^2 \qquad \text{[A11.1]}$$

where c is the velocity of light in vacuum and κ is a coefficient depending on the system of units. In the rationalised MKSA (SI) units used in this book one has

$$\kappa = 1, \qquad \mu_0 = 4\pi \times 10^{-7}\ \text{H m}^{-1},$$

$$\varepsilon_0 = \frac{1}{\mu_0 c^2} = 8.85419 \times 10^{-12}\ \text{F m}^{-1} \qquad \text{[A11.2]}$$

The Gaussian (mixed) system of units uses electric units of the electrostatic CGS system, and magnetic units of the electromagnetic CGS system. In the Gaussian system of units one therefore has

$$\kappa = c, \qquad \varepsilon_0 = \frac{1}{4\pi}, \qquad \mu_0 = 4\pi \qquad \text{[A11.3]}$$

The quantum mechanical equations of atomic and molecular physics are considerably simplified if Hartree's atomic units (a.u.) are used. These units are defined in Table A11.2

We note that since $m = e = \hbar = a_0 = 1$ in a.u., while $\alpha = 1/137.036$ is dimensionless, one has in particular (with $\kappa = 1$)

$$\begin{aligned} c &= \alpha^{-1}\ \text{a.u.} = 137.036\ \text{a.u.} \\ \varepsilon_0 &= 1/4\pi \text{ in a.u.} \\ \mu_0 &= 4\pi/c^2 = 4\pi\alpha^2 \text{ in a.u.} \end{aligned} \qquad \text{[A11.4]}$$

We also give in Table A11.3 a few important conversion factors.

Table A11.1 Fundamental constants

Quantity	*Symbol*	*Value*
Planck's constant	h	6.62618×10^{-34} J s
	$\hbar = \dfrac{h}{2\pi}$	1.05459×10^{-34} J s
Velocity of light in vacuum	c	2.99792×10^{8} m s^{-1}
Elementary charge (absolute value of electron charge)	e	1.60219×10^{-19} C
Permeability of free space	μ_0	$4\pi \times 10^{-7}$ H m^{-1} $= 1.25664 \times 10^{-6}$ H m^{-1}
Permittivity of free space	$\varepsilon_0 = \dfrac{1}{\mu_0 c^2}$	8.85419×10^{-12} F m^{-1}
Gravitational constant	G	6.672×10^{-11} N m^2 kg^{-2}
Fine structure constant	$\alpha = \dfrac{e^2}{4\pi\varepsilon_0\hbar c}$	$\dfrac{1}{137.036} = 7.29735 \times 10^{-3}$
Avogadro's number	N_A	6.02205×10^{23} mol^{-1}
Faraday's constant	$F = N_A e$	9.64846×10^{4} C mol^{-1}
Boltzmann's constant	k	1.38066×10^{-23} J K^{-1}
Gas constant	$R = N_A k$	8.31441 J mol^{-1} K^{-1}
Atomic mass unit	a.m.u. $= \dfrac{1}{12} M_{^{12}C}$	1.66057×10^{-27} kg
Electron mass	m or m_e	9.10953×10^{-31} kg $= 5.48580 \times 10^{-4}$ a.m.u.
Proton mass	M_p	1.67265×10^{-27} kg $= 1.007276$ a.m.u.
Neutron mass	M_n	1.67492×10^{-27} kg $= 1.008665$ a.m.u.
Ratio of proton to electron mass	M_p/m	1836.15
Electron charge to mass ratio	$\lvert e\rvert/m$	1.75880×10^{11} C kg^{-1}
Compton wavelength of electron	$\lambda_c = \dfrac{h}{mc}$	2.42631×10^{-12} m
Classical radius of electron	$r_0 = \dfrac{e^2}{4\pi\varepsilon_0 mc^2}$	2.81794×10^{-15} m
Bohr radius for atomic hydrogen (with infinite nuclear mass)	$a_0 = \dfrac{4\pi\varepsilon_0\hbar^2}{me^2}$	5.29177×10^{-11} m
Non-relativistic ionisation potential of atomic hydrogen for infinite nuclear mass	$I_P^H(\infty) = \dfrac{e^2}{8\pi\varepsilon_0 a_0} = \dfrac{1}{2}\alpha^2 mc^2$	2.17991×10^{-18} J $= 13.6058$ eV
Rydberg's constant for infinite nuclear mass	$\tilde{R}(\infty) = \dfrac{me^4}{8\varepsilon_0^2 h^3 c} = \dfrac{\alpha}{4\pi a_0}$	1.09737×10^{7} m^{-1}
Rydberg's constant for atomic hydrogen	R_H	1.09678×10^{7} m^{-1}
Bohr magneton	$\mu_B = \dfrac{e\hbar}{2m}$	9.27408×10^{-24} J T^{-1}
Nuclear magneton	$\mu_N = \dfrac{e\hbar}{2M_p}$	5.05082×10^{-27} J T^{-1}
Electron magnetic moment	$\mathcal{M}_e$	9.28483×10^{-24} J T^{-1} $= 1.00116\ \mu_B$
Proton magnetic moment	$\mathcal{M}_p$	1.41062×10^{-26} J T^{-1} $= 2.79285\ \mu_N$
Neutron magnetic moment	$\mathcal{M}_n$	-0.96630×10^{-26} J T^{-1} $= -1.91315\ \mu_N$

Table A11.2 Atomic units

Quantity	*Unit*	*Physical significance*	*Value*
Mass	m or m_e	Electron mass	9.10953×10^{-31} kg
Charge	e	Absolute value of electron charge	1.60219×10^{-19} C
Angular momentum	$\hbar$	Planck's constant divided by (2π)	1.05459×10^{-34} J s
Length	a_0	Bohr radius for atomic hydrogen (with infinite nuclear mass)	5.29177×10^{-11} m
Velocity	$v_0 = \alpha c$	Magnitude of electron velocity in first Bohr orbit	2.18769×10^{6} m s^{-1}
Momentum	$p_0 = mv_0$	Magnitude of electron momentum in first Bohr orbit	1.99288×10^{-24} kg m s^{-1}
Time	$\dfrac{a_0}{v_0}$	Time required for electron in first Bohr orbit to travel one Bohr radius	2.41889×10^{-17} s
Frequency	$\dfrac{v_0}{2\pi a_0}$	Angular frequency of electron in first Bohr orbit (v_0/a_0) divided by (2π)	6.57968×10^{15} s^{-1}
Energy	$\dfrac{e^2}{4\pi\varepsilon_0 a_0} = \alpha^2 mc^2$	Twice the ionisation potential of atomic hydrogen (with infinite nuclear mass)	4.35981×10^{-18} J $= 27.2116$ eV
Wave number	$\dfrac{\alpha}{2\pi a_0} = 2\tilde{R}(\infty)$	Twice the Rydberg constant, i.e. twice the wave number corresponding to the ionisation potential of atomic hydrogen (with infinite nuclear mass)	2.19474×10^{7} m^{-1}

Table A11.3 Conversion factors

1 Å (angström) = 0.1 nm = 10^{-10} m = 10^{-8} cm

1 fm (femtometer or Fermi) = 10^{-6} nm = 10^{-15} m

λ (in Å) × $\tilde{\nu}$ (in cm^{-1}) = 10^8 (from $\lambda\tilde{\nu} = 1$)

$a_0 = 5.29177 \times 10^{-11}$ m = 0.529177 Å

$a_0^2 = 2.80028 \times 10^{-21}$ m^2

$\pi a_0^2 = 8.79735 \times 10^{-21}$ m^2

1 Hz = 1 s^{-1}

1 electron mass (m_e) = 0.511003 MeV/c^2

1 proton mass (M_p) = 938.280 MeV/c^2

1 a.m.u. = 1/12 $M_{^{12}C}$ = 1.66057×10^{-27} kg = 931.502 MeV/c^2

1 J = 10^7 erg = 0.239 cal = 6.24146×10^{18} eV

1 cal = 4.184 J = 2.611×10^{19} eV

1 eV = 1.60219×10^{-19} J = 1.60219×10^{-12} erg

1 MeV = 1.60219×10^{-13} J = 1.60219×10^{-6} erg

1 eV corresponds to:
a frequency of 2.41797×10^{14} Hz (from $E = h\nu$)
a wavelength of 1.23985×10^{-6} m = 12398.5 Å (from $E = hc/\lambda$)
a wave number of 8.06548×10^5 m^{-1} = 8065.48 cm^{-1} (from $E = hc\tilde{\nu}$)
a temperature of 1.16045×10^4 K (from $E = kT$)

1 cm^{-1} corresponds to
an energy of 1.23985×10^{-4} eV
a frequency of 2.99792×10^{10} Hz

1 atomic unit of energy = 27.2116 eV corresponds to
a frequency of 6.57968×10^{15} Hz
a wavelength of 4.55633×10^{-8} m = 455.633 Å
a wave number of 2.19475×10^7 m^{-1} = 219475 cm^{-1}
a temperature of 3.15777×10^5 K

1 a.m.u. corresponds to an energy of 931.502 MeV = 1.49244×10^{-10} J

$kT = 8.61735 \times 10^{-5}$ eV at $T = 1$ K

$hc = 1.23985 \times 10^{-6}$ eV × m = 12398.5 eV × Å

$\hbar c = 1.97329 \times 10^{-7}$ eV × m = 1973.29 eV × Å

ΔE (in eV) × Δt (in s) = 6.58218×10^{-16} eV × s (from $\Delta E \Delta t = \hbar$)

References

Bashkin, S. and Stoner, J. O. (1975) *Atomic Energy Levels and Grotrian Diagrams*. North-Holland, Amsterdam.

Bethe, H. A. and Salpeter, E. E. (1957) *Quantum Mechanics of One- and Two-Electron Atoms*. Springer-Verlag, Berlin.

Borse, H. and Motz, L. (Eds.) (1966) *The World of the Atom*. Basic Books Inc., New York.

Bransden, B. H. (1970) *Atomic Collision Theory*. Benjamin, New York.

Burcham, W. E. (1979) *Elements of Nuclear Physics*. Longman, London.

Byron, F. W. and Fuller, R. W. (1969) *Mathematics of Classical and Quantum Physics*. Addison-Wesley, Reading, Massachusetts.

Casimir, H. B. C. (1963) *On the Interaction Between Atomic Nuclei and Electrons*. Freeman, San Francisco.

Clementi, E. and Roetti, C. (1974) *Atomic Data and Nuclear Data Tables* Vol. 14, Nos 3–4. Academic Press, New York.

Condon, E. U. and Shortley, G. H. (1951) *Theory of Atomic Spectra*. Cambridge University Press, London.

Dicke, R. H. and Wittke, J. P. (1960) *Introduction to Quantum Mechanics*. Addison-Wesley, Reading, Massachusetts.

Duffin, W. J. (1968) *Advanced Electricity and Magnetism for Undergraduates*. McGraw-Hill, London.

Dwight, H. B. (1961) *Tables of Integrals and Other Mathematical Data*. MacMillan, London.

Edmonds, A. R. (1957) *Angular Momentum in Quantum Mechanics*. Princeton Univ. Press, Princeton, New Jersey.

Goldstein, H. (1962) *Classical Mechanics*. Addison-Wesley, Reading, Massachusetts.

Hagler, M. O. and Kristiansen, M. (1977) *An Introduction to Controlled Thermonuclear Fusion*. Lexington Books, Lexington, Massachusetts.

Herzberg, G. (1945) *Infrared and Raman Spectra of Polyatomic Molecules*. Van Nostrand, New York.

Herzberg, G. (1950) *Spectra of Diatomic Molecules* 2nd Edn. Van Nostrand, New York.

Jackson, J. D. (1975) *Classical Electrodynamics* 2nd Edn. Wiley, New York.

Jastrow, R. and Thompson, M. H. (1977) *Astronomy: Fundamentals and Frontiers* 3rd Edn. Wiley, New York.

Joachain, C. J. (1979) *Quantum Collision Theory* 2nd Edn. North-Holland, Amsterdam.

Kittel, C. (1958) *Elementary Statistical Physics*. Wiley, New York.

Kittel, C. (1976) *Introduction to Solid State Physics* 5th Edn. Wiley, New York.

Knight, D. M. (1967) *Atoms and Elements: a Study of Theories of Matter in England in the 19th Century*. Hutchinson, London.

Kuhn, H. G. (1970) *Atomic Spectra* 2nd Edn. Longman, London.

McDowell, M. R. C. and Coleman, J. P. (1970) *Introduction to the Theory of Ion-Atom Collisions*. North-Holland, Amsterdam.

Mathews, J. and Walker, R. L. (1973) *Mathematical Methods of Physics* World Student Series Edn. Benjamin, New York.

Merzbacher, E. (1970) *Quantum Mechanics* 2nd Edn. Wiley, New York.

Messiah A. (1968) *Quantum Mechanics*. North-Holland, Amsterdam.

Morse, P. M. (1966) *Thermal Physics*. Benjamin, New York.

Pauling, L. and Wilson, E. B. (1935) *Introduction to Quantum Mechanics*. McGraw-Hill, New York.

Pilar, F. L. (1968) *Elementary Quantum Chemistry*. McGraw-Hill, New York.

Powell, J. L. and Crasemann, B. (1961) *Quantum Mechanics*. Addison-Wesley, Reading, Massachusetts.
Ramsey, N. F. (1953) *Nuclear Moments*. Wiley, New York.
Ramsey, N. F. (1955) *Molecular Beams*. Oxford University Press, London.
Richtmyer, F. K., Kennard, E. H. and Cooper, J. N. (1969) *Introduction to Modern Physics* 6th Edn. McGraw-Hill, New York.
Rose, M. E. (1957) *Elementary Theory of Angular Momentum*. Wiley, New York.
Sakurai, J. J. (1967) *Advanced Quantum Mechanics*. Addison-Wesley, Reading, Massachusetts.
Schiff, L. I. (1968) *Quantum Mechanics* 3rd Edn. McGraw-Hill, New York.
Sobelman, I. I. (1979) *Atomic Spectra and Radiative Transitions*. Springer-Verlag, Berlin.
Svelto, O. (1976) *Principles of Lasers*. Plenum Press, New York.
Taylor, E. F. and Wheeler, J. A. (1966) *Spacetime Physics*. Freeman, San Francisco.
Thorp, J. S. (1969) *Masers and Lasers*. Macmillan, London.
Townes, C. H. and Schawlow, A. L. (1955) *Microwave Spectroscopy*. McGraw-Hill, New York.

Index

DATE DUE

ILL 722 8655			
DD 4-9-95			
ill: 7957136			
d: 7/20/02			
JUL 2 2 REC'D			
GAYLORD			P